

**Ongoing Face Recognition  
Vendor Test (FRVT)**  
**Part 1: Verification**

Patrick Grother  
Mei Ngan  
Kayee Hanaoka  
*Information Access Division  
Information Technology Laboratory*

This publication is available free of charge from:  
<https://www.nist.gov/programs-projects/face-recognition-vendor-test-frvt-ongoing>

2019/07/05

## ACKNOWLEDGMENTS

The authors are grateful to Wayne Salamon and Greg Fiumara at NIST for robust software infrastructure, particularly that which leverages [Berkeley DB Btrees](#) for storage of images and templates, and [Open MPI](#) for parallel execution of algorithms across our computers. Thanks also to Brian Cochran at NIST for providing highly available computers and network-attached storage.

## DISCLAIMER

Specific hardware and software products identified in this report were used in order to perform the evaluations described in this document. In no case does identification of any commercial product, trade name, or vendor, imply recommendation or endorsement by the National Institute of Standards and Technology, nor does it imply that the products and equipment identified are necessarily the best available for the purpose.

## FRVT STATUS

**This report** is a draft NIST Interagency Report, and is open for comment. It is the sixteenth edition of the report since the first was published in June 2017. Prior editions of this report are maintained on the FRVT website, and may contain useful information about older algorithms and datasets no longer used in FRVT.

**FRVT remains open:** All [four tracks](#) of the FRVT remain open to new algorithm submissions indefinitely. This report will be updated as new algorithms are evaluated, as new datasets are added, and as new analyses are included. Comments and suggestions should be directed to [frvt@nist.gov](mailto:frvt@nist.gov).

### Changes since June 2019:

- ▷ This report adds results for algorithms from 18 developers submitted in early June 2019. These are from CTBC Bank, Deep Glint, Thales Cogent, Ever AI Paravision, Gorilla Technology, Imagus, Incode, Kneron, N-Tech Lab, Neurotechnology, Notiontag Technologies, Star Hybrid, Videonetics, Vigilant Solutions, Winsense, Anke Investments, CEIEC, and DSK. Nine of these are new participants.
- ▷ Several other algorithms have been submitted and are being evaluated. Results will be released in the next report, scheduled for August 1. That report will include results for new datasets.
- ▷ Older algorithms from Everai, Thales Cogent, Gorilla Technology, Incode, Neurotechnology, N-Tech Lab and Vigilant Solutions have been retired, per the policy to list only two algorithms per developer.

### Changes since April 2019:

- ▷ This report adds results for nine algorithms from nine developers submitted in early June 2019. These are from Tencent Deepsea, Hengrui, Kedacom, Moontime, Guangzhou Pixel, Rank One Computing, Synesis, Sensetime and Vocord.
- ▷ Another 23 algorithms have been submitted and are being evaluated. Results will be released in the next report, scheduled for July 3.
- ▷ Older algorithms for Rank One, Synesis, and Vocord have been retired, per the policy to list only two algorithms per developer.

### Changes since February 2019:

- ▷ This report adds results for 49 algorithms from 42 developers submitted in early March 2019.
- ▷ This report omits results for algorithms that we retired. We retired for three reasons: 1. The developer submitted a new algorithm, and we only list two. 2. The algorithm needs a GPU, and we no longer allow GPU-based algorithms. 3. Inoperable algorithms.
- ▷ Previous results for retired algorithms are available in older editions of this report linked [here](#).
- ▷ The mugshot database used from February 2017 to January 2019 has been replaced with an extract of the mugshot database documented in NIST Interagency Report 8238, November 2018. The new mugshot set is described in section [2.3](#) and is adopted because:
  - ▷▷ It has much better identity label integrity, so that false non-match rates are substantially lower than those reported in FRVT 1:1 reports to date - see Figure [30](#).
  - ▷▷ It includes images collected over a 17 year period such that ageing can be much better characterized - - see Figure [110](#).
- ▷ Using the new mugshot database, Figure [110](#) shows accuracy for four demographic groups identified in the biographic metadata that accompanies the data: black females, black males, white females and white males.

- ▷ The report adds Figure 9 with results for the twenty human-difficult pairs used in the May 2018 paper *Face recognition accuracy of forensic examiners, superrecognizers, and face recognition algorithms* by Phillips et al. [1].
- ▷ The report uses an update to the wild image database that corrects some ground truth labels.
- ▷ Some results for the child exploitation database are not complete. They are typically updated less frequently than for other image sets.

## Contents

<b>ACKNOWLEDGMENTS</b>	<b>1</b>
<b>DISCLAIMER</b>	<b>1</b>
<b>1 METRICS</b>	<b>22</b>
1.1 CORE ACCURACY . . . . .	22
<b>2 DATASETS</b>	<b>23</b>
2.1 CHILD EXPLOITATION IMAGES . . . . .	23
2.2 VISA IMAGES . . . . .	23
2.3 MUGSHOT IMAGES . . . . .	23
2.4 WILD IMAGES . . . . .	24
<b>3 RESULTS</b>	<b>24</b>
3.1 TEST GOALS . . . . .	24
3.2 TEST DESIGN . . . . .	25
3.3 FAILURE TO ENROLL . . . . .	27
3.4 RECOGNITION ACCURACY . . . . .	31
3.5 GENUINE DISTRIBUTION STABILITY . . . . .	119
3.5.1 EFFECT OF BIRTH PLACE ON THE GENUINE DISTRIBUTION . . . . .	119
3.5.2 EFFECT OF AGEING . . . . .	131
3.5.3 EFFECT OF AGE ON GENUINE SUBJECTS . . . . .	141
3.6 IMPOSTOR DISTRIBUTION STABILITY . . . . .	155
3.6.1 EFFECT OF BIRTH PLACE ON THE IMPOSTOR DISTRIBUTION . . . . .	155
3.6.2 EFFECT OF AGE ON IMPOSTORS . . . . .	385

## List of Tables

1 ALGORITHM SUMMARY . . . . .	14
2 ALGORITHM SUMMARY . . . . .	15
3 ALGORITHM SUMMARY . . . . .	16
4 FALSE NON-MATCH RATE . . . . .	17
5 FALSE NON-MATCH RATE . . . . .	18
6 FALSE NON-MATCH RATE . . . . .	19
7 FAILURE TO ENROL RATES . . . . .	28
8 FAILURE TO ENROL RATES . . . . .	29
9 FAILURE TO ENROL RATES . . . . .	30

## List of Figures

1 PERFORMANCE SUMMARY: FNMR VS. TEMPLATE SIZE TRADEOFF . . . . .	20
2 PERFORMANCE SUMMARY: FNMR VS. TEMPLATE TIME TRADEOFF . . . . .	21
3 EXAMPLE IMAGES . . . . .	24
(A) VISA . . . . .	24
(B) MUGSHOT . . . . .	24
(C) WILD . . . . .	24
4 PERFORMANCE ON 20 HUMAN-DIFFICULT PAIRS . . . . .	32
5 PERFORMANCE ON 20 HUMAN-DIFFICULT PAIRS . . . . .	33
6 PERFORMANCE ON 20 HUMAN-DIFFICULT PAIRS . . . . .	34
7 PERFORMANCE ON 20 HUMAN-DIFFICULT PAIRS . . . . .	35

8	PERFORMANCE ON 20 HUMAN-DIFFICULT PAIRS . . . . .	36
9	PERFORMANCE ON 20 HUMAN-DIFFICULT PAIRS . . . . .	37
10	ERROR TRADEOFF CHARACTERISTIC: VISA IMAGES . . . . .	38
11	ERROR TRADEOFF CHARACTERISTIC: VISA IMAGES . . . . .	39
12	ERROR TRADEOFF CHARACTERISTIC: VISA IMAGES . . . . .	40
13	ERROR TRADEOFF CHARACTERISTIC: VISA IMAGES . . . . .	41
14	ERROR TRADEOFF CHARACTERISTIC: VISA IMAGES . . . . .	42
15	ERROR TRADEOFF CHARACTERISTIC: VISA IMAGES . . . . .	43
16	ERROR TRADEOFF CHARACTERISTIC: VISA IMAGES . . . . .	44
17	ERROR TRADEOFF CHARACTERISTIC: VISA IMAGES . . . . .	45
18	ERROR TRADEOFF CHARACTERISTIC: VISA IMAGES . . . . .	46
19	ERROR TRADEOFF CHARACTERISTIC: VISA IMAGES . . . . .	47
20	ERROR TRADEOFF CHARACTERISTIC: VISA IMAGES . . . . .	48
21	ERROR TRADEOFF CHARACTERISTIC: VISA IMAGES . . . . .	49
22	ERROR TRADEOFF CHARACTERISTIC: VISA IMAGES . . . . .	50
23	ERROR TRADEOFF CHARACTERISTIC: VISA IMAGES . . . . .	51
24	ERROR TRADEOFF CHARACTERISTIC: MUGSHOT IMAGES . . . . .	52
25	ERROR TRADEOFF CHARACTERISTIC: MUGSHOT IMAGES . . . . .	53
26	ERROR TRADEOFF CHARACTERISTIC: MUGSHOT IMAGES . . . . .	54
27	ERROR TRADEOFF CHARACTERISTIC: MUGSHOT IMAGES . . . . .	55
28	ERROR TRADEOFF CHARACTERISTIC: MUGSHOT IMAGES . . . . .	56
29	ERROR TRADEOFF CHARACTERISTIC: MUGSHOT IMAGES . . . . .	57
30	ERROR TRADEOFF CHARACTERISTIC: MUGSHOT IMAGES . . . . .	58
31	ERROR TRADEOFF CHARACTERISTIC: WILD IMAGES . . . . .	59
32	ERROR TRADEOFF CHARACTERISTIC: WILD IMAGES . . . . .	60
33	ERROR TRADEOFF CHARACTERISTIC: WILD IMAGES . . . . .	61
34	ERROR TRADEOFF CHARACTERISTIC: WILD IMAGES . . . . .	62
35	ERROR TRADEOFF CHARACTERISTIC: WILD IMAGES . . . . .	63
36	ERROR TRADEOFF CHARACTERISTIC: WILD IMAGES . . . . .	64
37	ERROR TRADEOFF CHARACTERISTICS: CHILD EXPLOITATION IMAGES . . . . .	65
38	ERROR TRADEOFF CHARACTERISTICS: CHILD EXPLOITATION IMAGES . . . . .	66
39	ERROR TRADEOFF CHARACTERISTICS: CHILD EXPLOITATION IMAGES . . . . .	67
40	CMC CHARACTERISTICS: CHILD EXPLOITATION IMAGES . . . . .	68
41	CMC CHARACTERISTICS: CHILD EXPLOITATION IMAGES . . . . .	69
42	CMC CHARACTERISTICS: CHILD EXPLOITATION IMAGES . . . . .	70
43	FALSE MATCH RATES WITHIN AND ACROSS DEMOGRAPHIC GROUPS . . . . .	71
44	FALSE MATCH RATES WITHIN AND ACROSS DEMOGRAPHIC GROUPS . . . . .	72
45	FALSE MATCH RATES WITHIN AND ACROSS DEMOGRAPHIC GROUPS . . . . .	73
46	FALSE MATCH RATES WITHIN AND ACROSS DEMOGRAPHIC GROUPS . . . . .	74
47	FALSE MATCH RATES WITHIN AND ACROSS DEMOGRAPHIC GROUPS . . . . .	75
48	FALSE MATCH RATES WITHIN AND ACROSS DEMOGRAPHIC GROUPS . . . . .	76
49	FALSE MATCH RATES WITHIN AND ACROSS DEMOGRAPHIC GROUPS . . . . .	77
50	SEX AND RACE EFFECTS: MUGSHOT IMAGES . . . . .	78
51	SEX AND RACE EFFECTS: MUGSHOT IMAGES . . . . .	79
52	SEX AND RACE EFFECTS: MUGSHOT IMAGES . . . . .	80
53	SEX AND RACE EFFECTS: MUGSHOT IMAGES . . . . .	81
54	SEX AND RACE EFFECTS: MUGSHOT IMAGES . . . . .	82
55	SEX AND RACE EFFECTS: MUGSHOT IMAGES . . . . .	83
56	SEX AND RACE EFFECTS: MUGSHOT IMAGES . . . . .	84
57	SEX EFFECTS: VISA IMAGES . . . . .	85
58	SEX EFFECTS: VISA IMAGES . . . . .	86
59	SEX EFFECTS: VISA IMAGES . . . . .	87
60	SEX EFFECTS: VISA IMAGES . . . . .	88
61	SEX EFFECTS: VISA IMAGES . . . . .	89
62	SEX EFFECTS: VISA IMAGES . . . . .	90
63	SEX EFFECTS: VISA IMAGES . . . . .	91
64	SEX EFFECTS: VISA IMAGES . . . . .	92

65	SEX EFFECTS: VISA IMAGES . . . . .	93
66	SEX EFFECTS: VISA IMAGES . . . . .	94
67	SEX EFFECTS: VISA IMAGES . . . . .	95
68	SEX EFFECTS: VISA IMAGES . . . . .	96
69	FALSE MATCH RATE CALIBRATION: MUGSHOT IMAGES . . . . .	97
70	FALSE MATCH RATE CALIBRATION: MUGSHOT IMAGES . . . . .	98
71	FALSE MATCH RATE CALIBRATION: MUGSHOT IMAGES . . . . .	99
72	FALSE MATCH RATE CALIBRATION: MUGSHOT IMAGES . . . . .	100
73	FALSE MATCH RATE CALIBRATION: MUGSHOT IMAGES . . . . .	101
74	FALSE MATCH RATE CALIBRATION: MUGSHOT IMAGES . . . . .	102
75	FALSE MATCH RATE CALIBRATION: MUGSHOT IMAGES . . . . .	103
76	FALSE MATCH RATE CALIBRATION: VISA IMAGES . . . . .	104
77	FALSE MATCH RATE CALIBRATION: VISA IMAGES . . . . .	105
78	FALSE MATCH RATE CALIBRATION: VISA IMAGES . . . . .	106
79	FALSE MATCH RATE CALIBRATION: VISA IMAGES . . . . .	107
80	FALSE MATCH RATE CALIBRATION: VISA IMAGES . . . . .	108
81	FALSE MATCH RATE CALIBRATION: VISA IMAGES . . . . .	109
82	FALSE MATCH RATE CALIBRATION: VISA IMAGES . . . . .	110
83	FALSE MATCH RATE CALIBRATION: VISA IMAGES . . . . .	111
84	FALSE MATCH RATE CALIBRATION: VISA IMAGES . . . . .	112
85	FALSE MATCH RATE CALIBRATION: VISA IMAGES . . . . .	113
86	FALSE MATCH RATE CALIBRATION: VISA IMAGES . . . . .	114
87	FALSE MATCH RATE CALIBRATION: VISA IMAGES . . . . .	115
88	FALSE MATCH RATE CALIBRATION: VISA IMAGES . . . . .	116
89	FALSE MATCH RATE CALIBRATION: VISA IMAGES . . . . .	117
90	FALSE MATCH RATE CONCENTRATION: VISA IMAGES . . . . .	118
91	EFFECT OF COUNTRY OF BIRTH ON FNMR . . . . .	120
92	EFFECT OF COUNTRY OF BIRTH ON FNMR . . . . .	121
93	EFFECT OF COUNTRY OF BIRTH ON FNMR . . . . .	122
94	EFFECT OF COUNTRY OF BIRTH ON FNMR . . . . .	123
95	EFFECT OF COUNTRY OF BIRTH ON FNMR . . . . .	124
96	EFFECT OF COUNTRY OF BIRTH ON FNMR . . . . .	125
97	EFFECT OF COUNTRY OF BIRTH ON FNMR . . . . .	126
98	EFFECT OF COUNTRY OF BIRTH ON FNMR . . . . .	127
99	EFFECT OF COUNTRY OF BIRTH ON FNMR . . . . .	128
100	EFFECT OF COUNTRY OF BIRTH ON FNMR . . . . .	129
101	EFFECT OF COUNTRY OF BIRTH ON FNMR . . . . .	130
102	ERROR TRADEOFF CHARACTERISTIC: MUGSHOT IMAGES . . . . .	132
103	ERROR TRADEOFF CHARACTERISTIC: MUGSHOT IMAGES . . . . .	133
104	ERROR TRADEOFF CHARACTERISTIC: MUGSHOT IMAGES . . . . .	134
105	ERROR TRADEOFF CHARACTERISTIC: MUGSHOT IMAGES . . . . .	135
106	ERROR TRADEOFF CHARACTERISTIC: MUGSHOT IMAGES . . . . .	136
107	ERROR TRADEOFF CHARACTERISTIC: MUGSHOT IMAGES . . . . .	137
108	ERROR TRADEOFF CHARACTERISTIC: MUGSHOT IMAGES . . . . .	138
109	ERROR TRADEOFF CHARACTERISTIC: MUGSHOT IMAGES . . . . .	139
110	ERROR TRADEOFF CHARACTERISTIC: MUGSHOT IMAGES . . . . .	140
111	EFFECT OF SUBJECT AGE ON FNMR . . . . .	142
112	EFFECT OF SUBJECT AGE ON FNMR . . . . .	143
113	EFFECT OF SUBJECT AGE ON FNMR . . . . .	144
114	EFFECT OF SUBJECT AGE ON FNMR . . . . .	145
115	EFFECT OF SUBJECT AGE ON FNMR . . . . .	146
116	EFFECT OF SUBJECT AGE ON FNMR . . . . .	147
117	EFFECT OF SUBJECT AGE ON FNMR . . . . .	148
118	EFFECT OF SUBJECT AGE ON FNMR . . . . .	149
119	EFFECT OF SUBJECT AGE ON FNMR . . . . .	150
120	EFFECT OF SUBJECT AGE ON FNMR . . . . .	151

121	EFFECT OF SUBJECT AGE ON FNMR	152
122	EFFECT OF SUBJECT AGE ON FNMR	153
123	WORST CASE REGIONAL EFFECT FNMR	156
124	IMPOSTOR DISTRIBUTION SHIFTS FOR SELECT COUNTRY PAIRS	158
125	ALGORITHM 3DIVI-003 CROSS REGION FMR	159
126	ALGORITHM ADERA-001 CROSS REGION FMR	160
127	ALGORITHM ALCHERA-000 CROSS REGION FMR	161
128	ALGORITHM ALCHERA-001 CROSS REGION FMR	162
129	ALGORITHM ALLGOVISION-000 CROSS REGION FMR	163
130	ALGORITHM AMPLIFIEDGROUP-001 CROSS REGION FMR	164
131	ALGORITHM ANKE-003 CROSS REGION FMR	165
132	ALGORITHM ANYVISION-002 CROSS REGION FMR	166
133	ALGORITHM ANYVISION-004 CROSS REGION FMR	167
134	ALGORITHM AWARE-003 CROSS REGION FMR	168
135	ALGORITHM AWARE-004 CROSS REGION FMR	169
136	ALGORITHM AYONIX-000 CROSS REGION FMR	170
137	ALGORITHM BM-001 CROSS REGION FMR	171
138	ALGORITHM CAMVI-002 CROSS REGION FMR	172
139	ALGORITHM CAMVI-003 CROSS REGION FMR	173
140	ALGORITHM CEIEC-001 CROSS REGION FMR	174
141	ALGORITHM CEIEC-002 CROSS REGION FMR	175
142	ALGORITHM COGENT-003 CROSS REGION FMR	176
143	ALGORITHM COGENT-004 CROSS REGION FMR	177
144	ALGORITHM COGNITEC-000 CROSS REGION FMR	178
145	ALGORITHM COGNITEC-001 CROSS REGION FMR	179
146	ALGORITHM CYBEREXTRUDER-001 CROSS REGION FMR	180
147	ALGORITHM CYBEREXTRUDER-002 CROSS REGION FMR	181
148	ALGORITHM CYBERLINK-001 CROSS REGION FMR	182
149	ALGORITHM CYBERLINK-002 CROSS REGION FMR	183
150	ALGORITHM DAHUA-001 CROSS REGION FMR	184
151	ALGORITHM DAHUA-002 CROSS REGION FMR	185
152	ALGORITHM DEEPLINT-001 CROSS REGION FMR	186
153	ALGORITHM DEEPSEA-001 CROSS REGION FMR	187
154	ALGORITHM DERMALOG-005 CROSS REGION FMR	188
155	ALGORITHM DERMALOG-006 CROSS REGION FMR	189
156	ALGORITHM DIGITALBARRIERS-002 CROSS REGION FMR	190
157	ALGORITHM EVERAI-002 CROSS REGION FMR	191
158	ALGORITHM GLORY-000 CROSS REGION FMR	192
159	ALGORITHM GLORY-001 CROSS REGION FMR	193
160	ALGORITHM GORILLA-002 CROSS REGION FMR	194
161	ALGORITHM GORILLA-003 CROSS REGION FMR	195
162	ALGORITHM HIK-001 CROSS REGION FMR	196
163	ALGORITHM HR-000 CROSS REGION FMR	197
164	ALGORITHM HR-001 CROSS REGION FMR	198
165	ALGORITHM ID3-003 CROSS REGION FMR	199
166	ALGORITHM ID3-004 CROSS REGION FMR	200
167	ALGORITHM IDEMIA-003 CROSS REGION FMR	201
168	ALGORITHM IDEMIA-004 CROSS REGION FMR	202
169	ALGORITHM IIT-000 CROSS REGION FMR	203
170	ALGORITHM IMAGUS-000 CROSS REGION FMR	204
171	ALGORITHM IMPERIAL-000 CROSS REGION FMR	205
172	ALGORITHM IMPERIAL-001 CROSS REGION FMR	206
173	ALGORITHM INCODE-003 CROSS REGION FMR	207
174	ALGORITHM INCODE-004 CROSS REGION FMR	208
175	ALGORITHM INNOVATRICS-004 CROSS REGION FMR	209
176	ALGORITHM INNOVATRICS-005 CROSS REGION FMR	210

177 ALGORITHM INTELLIVISION-001 CROSS REGION FMR . . . . .	211
178 ALGORITHM IQFACE-000 CROSS REGION FMR . . . . .	212
179 ALGORITHM ISITYOU-000 CROSS REGION FMR . . . . .	213
180 ALGORITHM ISYSTEMS-001 CROSS REGION FMR . . . . .	214
181 ALGORITHM ISYSTEMS-002 CROSS REGION FMR . . . . .	215
182 ALGORITHM ITMO-005 CROSS REGION FMR . . . . .	216
183 ALGORITHM ITMO-006 CROSS REGION FMR . . . . .	217
184 ALGORITHM KAKAO-001 CROSS REGION FMR . . . . .	218
185 ALGORITHM KAKAO-002 CROSS REGION FMR . . . . .	219
186 ALGORITHM KEDACOM-000 CROSS REGION FMR . . . . .	220
187 ALGORITHM LOOKMAN-002 CROSS REGION FMR . . . . .	221
188 ALGORITHM LOOKMAN-004 CROSS REGION FMR . . . . .	222
189 ALGORITHM MEGVII-001 CROSS REGION FMR . . . . .	223
190 ALGORITHM MEGVII-002 CROSS REGION FMR . . . . .	224
191 ALGORITHM MEIYA-001 CROSS REGION FMR . . . . .	225
192 ALGORITHM MICROFOCUS-001 CROSS REGION FMR . . . . .	226
193 ALGORITHM MICROFOCUS-002 CROSS REGION FMR . . . . .	227
194 ALGORITHM MT-000 CROSS REGION FMR . . . . .	228
195 ALGORITHM NEUROTECHNOLOGY-005 CROSS REGION FMR . . . . .	229
196 ALGORITHM NEUROTECHNOLOGY-006 CROSS REGION FMR . . . . .	230
197 ALGORITHM NODEFLUX-000 CROSS REGION FMR . . . . .	231
198 ALGORITHM NODEFLUX-001 CROSS REGION FMR . . . . .	232
199 ALGORITHM NOTIONTAG-000 CROSS REGION FMR . . . . .	233
200 ALGORITHM NTECHLAB-006 CROSS REGION FMR . . . . .	234
201 ALGORITHM NTECHLAB-007 CROSS REGION FMR . . . . .	235
202 ALGORITHM PIXELALL-002 CROSS REGION FMR . . . . .	236
203 ALGORITHM PSL-001 CROSS REGION FMR . . . . .	237
204 ALGORITHM PSL-002 CROSS REGION FMR . . . . .	238
205 ALGORITHM RANKONE-006 CROSS REGION FMR . . . . .	239
206 ALGORITHM RANKONE-007 CROSS REGION FMR . . . . .	240
207 ALGORITHM REALNETWORKS-002 CROSS REGION FMR . . . . .	241
208 ALGORITHM REALNETWORKS-003 CROSS REGION FMR . . . . .	242
209 ALGORITHM REMARKAI-000 CROSS REGION FMR . . . . .	243
210 ALGORITHM REMARKAI-001 CROSS REGION FMR . . . . .	244
211 ALGORITHM SAFFE-001 CROSS REGION FMR . . . . .	245
212 ALGORITHM SAFFE-002 CROSS REGION FMR . . . . .	246
213 ALGORITHM SENSETIME-001 CROSS REGION FMR . . . . .	247
214 ALGORITHM SENSETIME-002 CROSS REGION FMR . . . . .	248
215 ALGORITHM SHAMAN-000 CROSS REGION FMR . . . . .	249
216 ALGORITHM SHAMAN-001 CROSS REGION FMR . . . . .	250
217 ALGORITHM SIAT-002 CROSS REGION FMR . . . . .	251
218 ALGORITHM SIAT-004 CROSS REGION FMR . . . . .	252
219 ALGORITHM SMILART-002 CROSS REGION FMR . . . . .	253
220 ALGORITHM SMILART-003 CROSS REGION FMR . . . . .	254
221 ALGORITHM STARHYBRID-001 CROSS REGION FMR . . . . .	255
222 ALGORITHM SYNESIS-004 CROSS REGION FMR . . . . .	256
223 ALGORITHM SYNESIS-005 CROSS REGION FMR . . . . .	257
224 ALGORITHM TECH5-001 CROSS REGION FMR . . . . .	258
225 ALGORITHM TECH5-002 CROSS REGION FMR . . . . .	259
226 ALGORITHM TEVIAN-003 CROSS REGION FMR . . . . .	260
227 ALGORITHM TEVIAN-004 CROSS REGION FMR . . . . .	261
228 ALGORITHM TIGER-002 CROSS REGION FMR . . . . .	262
229 ALGORITHM TIGER-003 CROSS REGION FMR . . . . .	263
230 ALGORITHM TONGYI-005 CROSS REGION FMR . . . . .	264
231 ALGORITHM TOSHIBA-002 CROSS REGION FMR . . . . .	265
232 ALGORITHM TOSHIBA-003 CROSS REGION FMR . . . . .	266
233 ALGORITHM VCOG-002 CROSS REGION FMR . . . . .	267

234 ALGORITHM VD-001 CROSS REGION FMR . . . . .	268
235 ALGORITHM VERIDAS-001 CROSS REGION FMR . . . . .	269
236 ALGORITHM VERIDAS-002 CROSS REGION FMR . . . . .	270
237 ALGORITHM VIDEONETICS-001 CROSS REGION FMR . . . . .	271
238 ALGORITHM VIGILANTSOLUTIONS-006 CROSS REGION FMR . . . . .	272
239 ALGORITHM VION-000 CROSS REGION FMR . . . . .	273
240 ALGORITHM VISIONBOX-000 CROSS REGION FMR . . . . .	274
241 ALGORITHM VISIONBOX-001 CROSS REGION FMR . . . . .	275
242 ALGORITHM VISIONLABS-006 CROSS REGION FMR . . . . .	276
243 ALGORITHM VISIONLABS-007 CROSS REGION FMR . . . . .	277
244 ALGORITHM VOCORD-006 CROSS REGION FMR . . . . .	278
245 ALGORITHM VOCORD-007 CROSS REGION FMR . . . . .	279
246 ALGORITHM WINSENSE-000 CROSS REGION FMR . . . . .	280
247 ALGORITHM YISHENG-004 CROSS REGION FMR . . . . .	281
248 ALGORITHM YITU-003 CROSS REGION FMR . . . . .	282
249 ALGORITHM 3DIVI-003 CROSS COUNTRY FMR . . . . .	283
250 ALGORITHM ADERA-001 CROSS COUNTRY FMR . . . . .	284
251 ALGORITHM ALCHERA-000 CROSS COUNTRY FMR . . . . .	285
252 ALGORITHM ALCHERA-001 CROSS COUNTRY FMR . . . . .	286
253 ALGORITHM ALLGOVISION-000 CROSS COUNTRY FMR . . . . .	287
254 ALGORITHM AMPLIFIEDGROUP-001 CROSS COUNTRY FMR . . . . .	288
255 ALGORITHM ANKE-003 CROSS COUNTRY FMR . . . . .	289
256 ALGORITHM ANYVISION-002 CROSS COUNTRY FMR . . . . .	290
257 ALGORITHM ANYVISION-004 CROSS COUNTRY FMR . . . . .	291
258 ALGORITHM AWARE-003 CROSS COUNTRY FMR . . . . .	292
259 ALGORITHM AWARE-004 CROSS COUNTRY FMR . . . . .	293
260 ALGORITHM AYONIX-000 CROSS COUNTRY FMR . . . . .	294
261 ALGORITHM BM-001 CROSS COUNTRY FMR . . . . .	295
262 ALGORITHM CAMVI-002 CROSS COUNTRY FMR . . . . .	296
263 ALGORITHM CAMVI-003 CROSS COUNTRY FMR . . . . .	297
264 ALGORITHM CEIEC-001 CROSS COUNTRY FMR . . . . .	298
265 ALGORITHM CEIEC-002 CROSS COUNTRY FMR . . . . .	299
266 ALGORITHM COGENT-003 CROSS COUNTRY FMR . . . . .	300
267 ALGORITHM COGNITEC-000 CROSS COUNTRY FMR . . . . .	301
268 ALGORITHM COGNITEC-001 CROSS COUNTRY FMR . . . . .	302
269 ALGORITHM CYBEREXTRUDER-001 CROSS COUNTRY FMR . . . . .	303
270 ALGORITHM CYBEREXTRUDER-002 CROSS COUNTRY FMR . . . . .	304
271 ALGORITHM CYBERLINK-001 CROSS COUNTRY FMR . . . . .	305
272 ALGORITHM DAHUA-001 CROSS COUNTRY FMR . . . . .	306
273 ALGORITHM DAHUA-002 CROSS COUNTRY FMR . . . . .	307
274 ALGORITHM DEEPSEA-001 CROSS COUNTRY FMR . . . . .	308
275 ALGORITHM DERMALOG-005 CROSS COUNTRY FMR . . . . .	309
276 ALGORITHM DERMALOG-006 CROSS COUNTRY FMR . . . . .	310
277 ALGORITHM DIGITALBARRIERS-002 CROSS COUNTRY FMR . . . . .	311
278 ALGORITHM EVERAI-002 CROSS COUNTRY FMR . . . . .	312
279 ALGORITHM GLORY-000 CROSS COUNTRY FMR . . . . .	313
280 ALGORITHM GLORY-001 CROSS COUNTRY FMR . . . . .	314
281 ALGORITHM GORILLA-002 CROSS COUNTRY FMR . . . . .	315
282 ALGORITHM HIK-001 CROSS COUNTRY FMR . . . . .	316
283 ALGORITHM HR-000 CROSS COUNTRY FMR . . . . .	317
284 ALGORITHM HR-001 CROSS COUNTRY FMR . . . . .	318
285 ALGORITHM ID3-003 CROSS COUNTRY FMR . . . . .	319
286 ALGORITHM ID3-004 CROSS COUNTRY FMR . . . . .	320
287 ALGORITHM IDEMIA-003 CROSS COUNTRY FMR . . . . .	321
288 ALGORITHM IDEMIA-004 CROSS COUNTRY FMR . . . . .	322
289 ALGORITHM IIT-000 CROSS COUNTRY FMR . . . . .	323
290 ALGORITHM IMPERIAL-000 CROSS COUNTRY FMR . . . . .	324

291 ALGORITHM IMPERIAL-001 CROSS COUNTRY FMR . . . . .	325
292 ALGORITHM INCODE-003 CROSS COUNTRY FMR . . . . .	326
293 ALGORITHM INNOVATRICS-004 CROSS COUNTRY FMR . . . . .	327
294 ALGORITHM INNOVATRICS-005 CROSS COUNTRY FMR . . . . .	328
295 ALGORITHM INTELLIVISION-001 CROSS COUNTRY FMR . . . . .	329
296 ALGORITHM IQFACE-000 CROSS COUNTRY FMR . . . . .	330
297 ALGORITHM ISITYOU-000 CROSS COUNTRY FMR . . . . .	331
298 ALGORITHM ISYSTEMS-001 CROSS COUNTRY FMR . . . . .	332
299 ALGORITHM ISYSTEMS-002 CROSS COUNTRY FMR . . . . .	333
300 ALGORITHM ITMO-005 CROSS COUNTRY FMR . . . . .	334
301 ALGORITHM ITMO-006 CROSS COUNTRY FMR . . . . .	335
302 ALGORITHM KAKAO-001 CROSS COUNTRY FMR . . . . .	336
303 ALGORITHM KEDACOM-000 CROSS COUNTRY FMR . . . . .	337
304 ALGORITHM LOOKMAN-002 CROSS COUNTRY FMR . . . . .	338
305 ALGORITHM LOOKMAN-004 CROSS COUNTRY FMR . . . . .	339
306 ALGORITHM MEGVII-001 CROSS COUNTRY FMR . . . . .	340
307 ALGORITHM MEGVII-002 CROSS COUNTRY FMR . . . . .	341
308 ALGORITHM MEIYA-001 CROSS COUNTRY FMR . . . . .	342
309 ALGORITHM MICROFOCUS-001 CROSS COUNTRY FMR . . . . .	343
310 ALGORITHM MICROFOCUS-002 CROSS COUNTRY FMR . . . . .	344
311 ALGORITHM MT-000 CROSS COUNTRY FMR . . . . .	345
312 ALGORITHM NEUROTECHNOLOGY-005 CROSS COUNTRY FMR . . . . .	346
313 ALGORITHM NODEFLUX-001 CROSS COUNTRY FMR . . . . .	347
314 ALGORITHM NTECHLAB-006 CROSS COUNTRY FMR . . . . .	348
315 ALGORITHM PSL-001 CROSS COUNTRY FMR . . . . .	349
316 ALGORITHM PSL-002 CROSS COUNTRY FMR . . . . .	350
317 ALGORITHM RANKONE-006 CROSS COUNTRY FMR . . . . .	351
318 ALGORITHM REALNETWORKS-002 CROSS COUNTRY FMR . . . . .	352
319 ALGORITHM REMARKAI-000 CROSS COUNTRY FMR . . . . .	353
320 ALGORITHM REMARKAI-001 CROSS COUNTRY FMR . . . . .	354
321 ALGORITHM SAFFE-001 CROSS COUNTRY FMR . . . . .	355
322 ALGORITHM SAFFE-002 CROSS COUNTRY FMR . . . . .	356
323 ALGORITHM SENSETIME-001 CROSS COUNTRY FMR . . . . .	357
324 ALGORITHM SENSETIME-002 CROSS COUNTRY FMR . . . . .	358
325 ALGORITHM SHAMAN-000 CROSS COUNTRY FMR . . . . .	359
326 ALGORITHM SHAMAN-001 CROSS COUNTRY FMR . . . . .	360
327 ALGORITHM SIAT-002 CROSS COUNTRY FMR . . . . .	361
328 ALGORITHM SIAT-004 CROSS COUNTRY FMR . . . . .	362
329 ALGORITHM SMILART-002 CROSS COUNTRY FMR . . . . .	363
330 ALGORITHM SMILART-003 CROSS COUNTRY FMR . . . . .	364
331 ALGORITHM TECH5-001 CROSS COUNTRY FMR . . . . .	365
332 ALGORITHM TECH5-002 CROSS COUNTRY FMR . . . . .	366
333 ALGORITHM TEVIAN-003 CROSS COUNTRY FMR . . . . .	367
334 ALGORITHM TEVIAN-004 CROSS COUNTRY FMR . . . . .	368
335 ALGORITHM TIGER-002 CROSS COUNTRY FMR . . . . .	369
336 ALGORITHM TIGER-003 CROSS COUNTRY FMR . . . . .	370
337 ALGORITHM TOSHIBA-002 CROSS COUNTRY FMR . . . . .	371
338 ALGORITHM TOSHIBA-003 CROSS COUNTRY FMR . . . . .	372
339 ALGORITHM VCOG-002 CROSS COUNTRY FMR . . . . .	373
340 ALGORITHM VD-001 CROSS COUNTRY FMR . . . . .	374
341 ALGORITHM VERIDAS-001 CROSS COUNTRY FMR . . . . .	375
342 ALGORITHM VERIDAS-002 CROSS COUNTRY FMR . . . . .	376
343 ALGORITHM VIGILANTSOLUTIONS-006 CROSS COUNTRY FMR . . . . .	377
344 ALGORITHM VION-000 CROSS COUNTRY FMR . . . . .	378
345 ALGORITHM VISIONBOX-000 CROSS COUNTRY FMR . . . . .	379
346 ALGORITHM VISIONBOX-001 CROSS COUNTRY FMR . . . . .	380
347 ALGORITHM VISIONLABS-006 CROSS COUNTRY FMR . . . . .	381

348 ALGORITHM YISHENG-004 CROSS COUNTRY FMR . . . . .	382
349 ALGORITHM YITU-003 CROSS COUNTRY FMR . . . . .	383
350 IMPOSTOR COUNTS FOR CROSS COUNTRY FMR CALCULATIONS . . . . .	384
351 ALGORITHM 3DIVI-003 CROSS AGE FMR . . . . .	386
352 ALGORITHM ADERA-001 CROSS AGE FMR . . . . .	387
353 ALGORITHM ALCHERA-000 CROSS AGE FMR . . . . .	388
354 ALGORITHM ALCHERA-001 CROSS AGE FMR . . . . .	389
355 ALGORITHM ALLGOVISION-000 CROSS AGE FMR . . . . .	390
356 ALGORITHM AMPLIFIEDGROUP-001 CROSS AGE FMR . . . . .	391
357 ALGORITHM ANKE-003 CROSS AGE FMR . . . . .	392
358 ALGORITHM ANKE-004 CROSS AGE FMR . . . . .	393
359 ALGORITHM ANYVISION-002 CROSS AGE FMR . . . . .	394
360 ALGORITHM ANYVISION-004 CROSS AGE FMR . . . . .	395
361 ALGORITHM AWARE-003 CROSS AGE FMR . . . . .	396
362 ALGORITHM AWARE-004 CROSS AGE FMR . . . . .	397
363 ALGORITHM AYONIX-000 CROSS AGE FMR . . . . .	398
364 ALGORITHM BM-001 CROSS AGE FMR . . . . .	399
365 ALGORITHM CAMVI-002 CROSS AGE FMR . . . . .	400
366 ALGORITHM CAMVI-003 CROSS AGE FMR . . . . .	401
367 ALGORITHM CEIEC-001 CROSS AGE FMR . . . . .	402
368 ALGORITHM CEIEC-002 CROSS AGE FMR . . . . .	403
369 ALGORITHM COGENT-003 CROSS AGE FMR . . . . .	404
370 ALGORITHM COGENT-004 CROSS AGE FMR . . . . .	405
371 ALGORITHM COGNITEC-000 CROSS AGE FMR . . . . .	406
372 ALGORITHM COGNITEC-001 CROSS AGE FMR . . . . .	407
373 ALGORITHM CTBCBANK-000 CROSS AGE FMR . . . . .	408
374 ALGORITHM CYBEREXTRUDER-001 CROSS AGE FMR . . . . .	409
375 ALGORITHM CYBEREXTRUDER-002 CROSS AGE FMR . . . . .	410
376 ALGORITHM CYBERLINK-001 CROSS AGE FMR . . . . .	411
377 ALGORITHM CYBERLINK-002 CROSS AGE FMR . . . . .	412
378 ALGORITHM DAHUA-001 CROSS AGE FMR . . . . .	413
379 ALGORITHM DAHUA-002 CROSS AGE FMR . . . . .	414
380 ALGORITHM DEEPLINT-001 CROSS AGE FMR . . . . .	415
381 ALGORITHM DEEPSEA-001 CROSS AGE FMR . . . . .	416
382 ALGORITHM DERMALOG-005 CROSS AGE FMR . . . . .	417
383 ALGORITHM DERMALOG-006 CROSS AGE FMR . . . . .	418
384 ALGORITHM DIGITALBARRIERS-002 CROSS AGE FMR . . . . .	419
385 ALGORITHM DSK-000 CROSS AGE FMR . . . . .	420
386 ALGORITHM EVERAI-002 CROSS AGE FMR . . . . .	421
387 ALGORITHM GLORY-001 CROSS AGE FMR . . . . .	422
388 ALGORITHM GORILLA-002 CROSS AGE FMR . . . . .	423
389 ALGORITHM GORILLA-003 CROSS AGE FMR . . . . .	424
390 ALGORITHM HIK-001 CROSS AGE FMR . . . . .	425
391 ALGORITHM HR-000 CROSS AGE FMR . . . . .	426
392 ALGORITHM HR-001 CROSS AGE FMR . . . . .	427
393 ALGORITHM ID3-003 CROSS AGE FMR . . . . .	428
394 ALGORITHM ID3-004 CROSS AGE FMR . . . . .	429
395 ALGORITHM IDEMIA-003 CROSS AGE FMR . . . . .	430
396 ALGORITHM IDEMIA-004 CROSS AGE FMR . . . . .	431
397 ALGORITHM IIT-000 CROSS AGE FMR . . . . .	432
398 ALGORITHM IMAGUS-000 CROSS AGE FMR . . . . .	433
399 ALGORITHM IMPERIAL-000 CROSS AGE FMR . . . . .	434
400 ALGORITHM IMPERIAL-001 CROSS AGE FMR . . . . .	435
401 ALGORITHM INCODE-003 CROSS AGE FMR . . . . .	436
402 ALGORITHM INCODE-004 CROSS AGE FMR . . . . .	437
403 ALGORITHM INNOVATRICS-004 CROSS AGE FMR . . . . .	438
404 ALGORITHM INNOVATRICS-005 CROSS AGE FMR . . . . .	439

405 ALGORITHM INTELLIVISION-001 CROSS AGE FMR . . . . .	440
406 ALGORITHM IQFACE-000 CROSS AGE FMR . . . . .	441
407 ALGORITHM ISITYOU-000 CROSS AGE FMR . . . . .	442
408 ALGORITHM ISYSTEMS-001 CROSS AGE FMR . . . . .	443
409 ALGORITHM ISYSTEMS-002 CROSS AGE FMR . . . . .	444
410 ALGORITHM ITMO-005 CROSS AGE FMR . . . . .	445
411 ALGORITHM ITMO-006 CROSS AGE FMR . . . . .	446
412 ALGORITHM KAKAO-001 CROSS AGE FMR . . . . .	447
413 ALGORITHM KAKAO-002 CROSS AGE FMR . . . . .	448
414 ALGORITHM KEDACOM-000 CROSS AGE FMR . . . . .	449
415 ALGORITHM LOOKMAN-002 CROSS AGE FMR . . . . .	450
416 ALGORITHM LOOKMAN-004 CROSS AGE FMR . . . . .	451
417 ALGORITHM MEGVII-001 CROSS AGE FMR . . . . .	452
418 ALGORITHM MEGVII-002 CROSS AGE FMR . . . . .	453
419 ALGORITHM MEIYA-001 CROSS AGE FMR . . . . .	454
420 ALGORITHM MICROFOCUS-001 CROSS AGE FMR . . . . .	455
421 ALGORITHM MICROFOCUS-002 CROSS AGE FMR . . . . .	456
422 ALGORITHM MT-000 CROSS AGE FMR . . . . .	457
423 ALGORITHM NEUROTECHNOLOGY-006 CROSS AGE FMR . . . . .	458
424 ALGORITHM NODEFLUX-001 CROSS AGE FMR . . . . .	459
425 ALGORITHM NOTIONTAG-000 CROSS AGE FMR . . . . .	460
426 ALGORITHM NTECHLAB-006 CROSS AGE FMR . . . . .	461
427 ALGORITHM NTECHLAB-007 CROSS AGE FMR . . . . .	462
428 ALGORITHM PIXELALL-002 CROSS AGE FMR . . . . .	463
429 ALGORITHM PSL-001 CROSS AGE FMR . . . . .	464
430 ALGORITHM PSL-002 CROSS AGE FMR . . . . .	465
431 ALGORITHM RANKONE-006 CROSS AGE FMR . . . . .	466
432 ALGORITHM RANKONE-007 CROSS AGE FMR . . . . .	467
433 ALGORITHM REALNETWORKS-002 CROSS AGE FMR . . . . .	468
434 ALGORITHM REALNETWORKS-003 CROSS AGE FMR . . . . .	469
435 ALGORITHM REMARKAI-000 CROSS AGE FMR . . . . .	470
436 ALGORITHM REMARKAI-001 CROSS AGE FMR . . . . .	471
437 ALGORITHM SAFFE-001 CROSS AGE FMR . . . . .	472
438 ALGORITHM SAFFE-002 CROSS AGE FMR . . . . .	473
439 ALGORITHM SENSETIME-001 CROSS AGE FMR . . . . .	474
440 ALGORITHM SENSETIME-002 CROSS AGE FMR . . . . .	475
441 ALGORITHM SHAMAN-000 CROSS AGE FMR . . . . .	476
442 ALGORITHM SHAMAN-001 CROSS AGE FMR . . . . .	477
443 ALGORITHM SIAT-002 CROSS AGE FMR . . . . .	478
444 ALGORITHM SIAT-004 CROSS AGE FMR . . . . .	479
445 ALGORITHM SMILART-002 CROSS AGE FMR . . . . .	480
446 ALGORITHM SMILART-003 CROSS AGE FMR . . . . .	481
447 ALGORITHM STARHYBRID-001 CROSS AGE FMR . . . . .	482
448 ALGORITHM SYNESIS-004 CROSS AGE FMR . . . . .	483
449 ALGORITHM SYNESIS-005 CROSS AGE FMR . . . . .	484
450 ALGORITHM TECH5-001 CROSS AGE FMR . . . . .	485
451 ALGORITHM TECH5-002 CROSS AGE FMR . . . . .	486
452 ALGORITHM TEVIAN-003 CROSS AGE FMR . . . . .	487
453 ALGORITHM TEVIAN-004 CROSS AGE FMR . . . . .	488
454 ALGORITHM TIGER-002 CROSS AGE FMR . . . . .	489
455 ALGORITHM TIGER-003 CROSS AGE FMR . . . . .	490
456 ALGORITHM TONGYI-005 CROSS AGE FMR . . . . .	491
457 ALGORITHM TOSHIBA-002 CROSS AGE FMR . . . . .	492
458 ALGORITHM TOSHIBA-003 CROSS AGE FMR . . . . .	493
459 ALGORITHM VCOG-002 CROSS AGE FMR . . . . .	494
460 ALGORITHM VD-001 CROSS AGE FMR . . . . .	495

461 ALGORITHM VERIDAS-001 CROSS AGE FMR . . . . .	496
462 ALGORITHM VERIDAS-002 CROSS AGE FMR . . . . .	497
463 ALGORITHM VIDEONETICS-001 CROSS AGE FMR . . . . .	498
464 ALGORITHM VIGILANTSOLUTIONS-006 CROSS AGE FMR . . . . .	499
465 ALGORITHM VION-000 CROSS AGE FMR . . . . .	500
466 ALGORITHM VISIONBOX-000 CROSS AGE FMR . . . . .	501
467 ALGORITHM VISIONBOX-001 CROSS AGE FMR . . . . .	502
468 ALGORITHM VISIONLABS-006 CROSS AGE FMR . . . . .	503
469 ALGORITHM VISIONLABS-007 CROSS AGE FMR . . . . .	504
470 ALGORITHM VOCORD-006 CROSS AGE FMR . . . . .	505
471 ALGORITHM VOCORD-007 CROSS AGE FMR . . . . .	506
472 ALGORITHM WINSENSE-000 CROSS AGE FMR . . . . .	507
473 ALGORITHM YISHENG-004 CROSS AGE FMR . . . . .	508
474 ALGORITHM YITU-003 CROSS AGE FMR . . . . .	509

Developer		Short	Seq.	Validation	Config <sup>1</sup>	Template		GPU	Comparison Time (ns) <sup>3</sup>	
Name		Name	Num.	Date	Data (KB)	Size (B)	Time (ms) <sup>2</sup>		Genuine	Impostor
1	3DiVi	3divi	003	2018-10-09	191636	124 4096 ± 0	89 650 ± 90	No	23 627 ± 11	26 623 ± 32
2	Adera Global PTE Ltd	aderा	001	2019-06-17	0	112 2560 ± 0	497 ± 0	No	65 1604 ± 71	66 1649 ± 56
3	Alchera	alchera	000	2019-03-01	258450	65 2048 ± 0	80 587 ± 13	No	91 3189 ± 32	91 3031 ± 142
4	Alchera	alchera	000	2019-03-01	174013	63 2048 ± 0	85 627 ± 11	No	94 3342 ± 81	93 3243 ± 47
5	AllGoVision	allgovision	000	2019-03-01	172509	76 2048 ± 0	51 384 ± 8	No	123 29903 ± 406	124 29735 ± 194
6	Amplified Group	amplifiedgroup	001	2019-03-01	0	27 866 ± 2	393 ± 0	No	127 57803 ± 4210	127 56365 ± 1196
7	Anke Investments	anke	003	2019-02-27	340160	101 2056 ± 0	117 811 ± 23	No	9 425 ± 28	11 437 ± 32
8	Anke Investments	anke	004	2019-06-27	349388	100 2056 ± 0	84 625 ± 1	No	24 633 ± 22	28 632 ± 34
9	AnyVision	anyvision	002	2018-01-31	662659	37 1024 ± 0	21 248 ± 0	No	128 74069 ± 188	128 74019 ± 198
10	AnyVision	anyvision	004	2018-06-15	401001	33 1024 ± 0	43 355 ± 1	No	72 1891 ± 51	70 1829 ± 85
11	Aware	aware	003	2018-10-19	377729	115 3108 ± 0	113 783 ± 10	No	57 1392 ± 42	60 1334 ± 80
12	Aware	aware	004	2019-03-01	427829	109 2084 ± 0	128 900 ± 10	No	54 1279 ± 50	59 1287 ± 100
13	Ayonix	ayonix	000	2017-06-22	58505	38 1036 ± 0	18 ± 2	No	22 621 ± 23	28 620 ± 26
14	Bitmain	bitmain	001	2018-10-17	287734	14 64 ± 0	59 444 ± 88	No	71 1887 ± 31	72 1877 ± 26
15	Camvi Technologies	camvitech	002	2018-10-19	236278	35 1024 ± 0	100 677 ± 7	No	21 612 ± 26	23 603 ± 20
16	Camvi Technologies	camvitech	003	2019-03-01	285657	29 1024 ± 0	108 750 ± 3	No	18 571 ± 23	20 565 ± 26
17	China Electronics Import-Export Corp	ceiec	001	2019-03-01	159618	36 1024 ± 0	37 314 ± 3	No	121 22831 ± 108	121 22813 ± 120
18	China Electronics Import-Export Corp	ceiec	002	2019-06-12	269063	62 2048 ± 0	82 612 ± 17	No	81 2188 ± 57	80 2301 ± 56
19	Gemalto Cogent	cogent	003	2019-03-01	698290	28 973 ± 0	130 952 ± 0	No	111 12496 ± 75	111 11822 ± 163
20	Gemalto Cogent	cogent	004	2019-06-14	722919	56 1983 ± 0	129 941 ± 28	No	114 14448 ± 56	114 15882 ± 81
21	Cognitec Systems GmbH	cognitec	000	2018-10-19	474759	89 2052 ± 0	18 224 ± 1	No	98 3835 ± 108	97 3782 ± 83
22	Cognitec Systems GmbH	cognitec	001	2019-03-01	476809	95 2052 ± 0	33 297 ± 17	No	100 4253 ± 59	99 4102 ± 167
23	CTBC Bank Co. Ltd	ctbcbank	000	2019-06-28	257208	66 2048 ± 0	71 568 ± 43	No	96 3551 ± 87	100 4805 ± 209
24	Cyberextruder	cyberex	001	2017-08-02	121211	9 256 ± 0	127 893 ± 25	No	43 1083 ± 16	47 1079 ± 19
25	Cyberextruder	cyberex	002	2018-01-30	168909	60 2048 ± 0	68 532 ± 6	No	70 1803 ± 14	69 1779 ± 22
26	Cyberlink Corp	cyberlink	001	2019-03-01	222009	98 2052 ± 0	57 425 ± 29	No	77 2051 ± 32	77 2060 ± 31
27	Cyberlink Corp	cyberlink	002	2019-06-12	222311	91 2052 ± 0	92 656 ± 22	No	82 2264 ± 71	89 2649 ± 195
28	Dahua Technology Co. Ltd	dahua	001	2018-10-19	283642	83 2048 ± 0	46 363 ± 6	No	6 367 ± 10	7 354 ± 16
29	Dahua Technology Co. Ltd	dahua	002	2019-03-01	526452	64 2048 ± 0	86 628 ± 7	No	11 461 ± 23	13 454 ± 20
30	Deepglint	deepglint	001	2019-06-21	569802	121 4096 ± 0	102 721 ± 4	No	97 3680 ± 35	96 3517 ± 182
31	Tencent Deepsea Lab	deepsea	001	2019-06-03	147497	30 1024 ± 0	87 630 ± 7	No	59 1401 ± 37	62 1467 ± 50
32	Dermalog	dermalog	005	2018-02-02	0	2 128 ± 0	6 130 ± 11	No	14 499 ± 22	16 500 ± 22
33	Dermalog	dermalog	006	2018-10-18	0	3 128 ± 0	6 532 ± 12	No	15 506 ± 23	14 459 ± 23
34	Digital Barriers	barriers	002	2019-03-01	83002	102 2056 ± 0	15 209 ± 11	No	113 13409 ± 228	113 13267 ± 206
35	DSK	dsk	000	2019-06-28	11967	18 512 ± 0	35 304 ± 47	No	107 7152 ± 115	107 7134 ± 111
36	Ever AI	everai	002	2019-03-01	561727	125 4096 ± 0	109 758 ± 0	No	26 644 ± 14	27 624 ± 35
37	Ever AI	everai	002	2019-07-01	539802	120 4096 ± 0	99 674 ± 4	No	31 699 ± 20	32 713 ± 47
38	Glory Ltd	glory	000	2018-06-06	0	15 418 ± 0	8 165 ± 2	No	106 7003 ± 84	105 6978 ± 71
39	Glory Ltd	glory	001	2018-06-08	0	53 1726 ± 0	53 393 ± 2	No	110 9607 ± 128	110 9539 ± 182
40	Gorilla Technology	gorilla	002	2018-10-17	93869	43 1132 ± 0	40 322 ± 14	No	88 2715 ± 68	88 2585 ± 84
41	Gorilla Technology	gorilla	003	2019-06-19	94409	42 1132 ± 0	42 334 ± 25	No	89 2840 ± 42	90 2865 ± 87
42	Hikvision	hik	001	2019-03-01	667866	47 1408 ± 0	90 651 ± 0	No	13 488 ± 19	13 477 ± 22
43	Hengrui AI Technology Ltd	hr	000	2019-03-01	284600	101 2057 ± 0	8 600 ± 2	No	115 16747 ± 238	115 16627 ± 220
44	Hengrui AI Technology Ltd	hr	001	2019-06-04	346156	106 2057 ± 0	93 665 ± 3	No	117 17816 ± 260	117 17878 ± 464

## Notes

- 1 The configuration size does not capture static data included in libraries. We do not count these because some algorithms include common ancillary libraries for image processing (e.g. openCV) or numerical computation (e.g. blas).
- 2 The median template creation times are measured on Intel® Xeon® CPU E5-2630 v4 @ 2.20GHz processors or, for GPU-enabled implementations, NVidia Tesla K40.
- 3 The comparison durations, in nanoseconds, are estimated using std::chrono::high\_resolution\_clock which on the machine in (2) counts 1ns clock ticks. Precision is somewhat worse than that however. The ± value is the median absolute deviation times 1.48 for Normal consistency.

Table 1: Summary of algorithms and properties included in this report. The red superscripts give ranking for the quantity in that column.

	Developer	Short	Seq.	Validation	Config <sup>1</sup>	Template		GPU	Comparison Time (ns) <sup>3</sup>	
	Name	Name	Num.	Date	Data (KB)	Size (B)	Time (ms) <sup>2</sup>		Genuine	Impostor
45	ID3 Technology	id3	003	2018-10-05	265951	<sup>11</sup> 264 ± 0	<sup>38</sup> 316 ± 19	No	<sup>56</sup> 1330 ± 25	<sup>61</sup> 1354 ± 28
46	ID3 Technology	id3	004	2019-03-01	171526	<sup>10</sup> 264 ± 0	<sup>72</sup> 541 ± 11	No	<sup>45</sup> 1135 ± 23	<sup>52</sup> 1156 ± 32
47	Idemia	Idemia	003	2018-10-19	427244	<sup>14</sup> 352 ± 0	<sup>47</sup> 368 ± 6	No	<sup>105</sup> 6654 ± 75	<sup>101</sup> 4835 ± 90
48	Idemia	Idemia	004	2019-03-01	406924	<sup>13</sup> 352 ± 0	<sup>30</sup> 306 ± 5	No	<sup>103</sup> 5592 ± 518	<sup>104</sup> 5533 ± 426
49	Institute of Information Technologies	ittvision	000	2019-03-01	237317	<sup>34</sup> 1024 ± 0	<sup>14</sup> 197 ± 8	No	<sup>62</sup> 1537 ± 81	<sup>58</sup> 1282 ± 20
50	Imagus Technology Pty Ltd	imus	000	2019-06-19	183453	<sup>78</sup> 2048 ± 0	<sup>58</sup> 425 ± 24	No	<sup>46</sup> 1145 ± 25	<sup>68</sup> 1718 ± 63
51	Imperial College London	imperial	000	2019-03-01	370120	<sup>71</sup> 2048 ± 0	<sup>95</sup> 669 ± 1	No	<sup>79</sup> 2130 ± 32	<sup>76</sup> 2052 ± 100
52	Imperial College London	imperial	001	2019-03-01	370260	<sup>81</sup> 2048 ± 0	<sup>97</sup> 671 ± 0	No	<sup>78</sup> 2090 ± 28	<sup>78</sup> 2062 ± 74
53	Incode Technologies Inc	incode	003	2019-03-01	170632	<sup>123</sup> 4096 ± 0	<sup>50</sup> 384 ± 11	No	<sup>74</sup> 1928 ± 44	<sup>71</sup> 1876 ± 81
54	Incode Technologies Inc	incode	004	2019-06-12	260224	<sup>61</sup> 2048 ± 0	<sup>63</sup> 479 ± 23	No	<sup>73</sup> 1913 ± 60	<sup>84</sup> 2443 ± 114
55	Innovatrics	innova	004	2018-10-19	0	<sup>40</sup> 1076 ± 0	<sup>52</sup> 391 ± 0	No	<sup>109</sup> 8573 ± 274	<sup>108</sup> 7929 ± 244
56	Innovatrics	innova	005	2019-03-01	0	<sup>41</sup> 1076 ± 0	<sup>78</sup> 577 ± 1	No	<sup>116</sup> 16880 ± 194	<sup>116</sup> 17232 ± 385
57	Intellivision	intellivision	001	2017-10-10	43692	<sup>104</sup> 2056 ± 0	<sup>2</sup> 62 ± 2	No	<sup>85</sup> 2573 ± 91	<sup>87</sup> 2544 ± 38
58	iQIYI Inc	iqface	000	2019-03-01	268819	<sup>129</sup> 4750 ± 32	<sup>69</sup> 538 ± 26	No	<sup>131</sup> 636433 ± 38446	<sup>131</sup> 632654 ± 85615
59	Is It You	isityou	000	2017-06-26	48010	<sup>130</sup> 19200 ± 0	<sup>5</sup> 113 ± 5	No	<sup>129</sup> 237517 ± 1318	<sup>129</sup> 237374 ± 1279
60	Innovation Systems	isystems	001	2018-06-12	274621	<sup>57</sup> 2048 ± 0	<sup>31</sup> 291 ± 9	No	<sup>17</sup> 557 ± 16	<sup>19</sup> 564 ± 22
61	Innovation Systems	isystems	002	2018-10-18	358984	<sup>74</sup> 2048 ± 0	<sup>120</sup> 822 ± 8	No	<sup>33</sup> 749 ± 31	<sup>29</sup> 632 ± 28
62	ITMO University	itmo	005	2018-10-19	482155	<sup>128</sup> 4173 ± 0	<sup>110</sup> 759 ± 1	No	<sup>112</sup> 13214 ± 164	<sup>112</sup> 12576 ± 257
63	ITMO University	itmo	006	2019-03-01	599187	<sup>111</sup> 2121 ± 0	<sup>118</sup> 814 ± 1	No	<sup>122</sup> 26154 ± 148	<sup>122</sup> 26217 ± 260
64	Kakao Corp	kakao	001	2019-03-01	107616	<sup>32</sup> 1024 ± 0	<sup>49</sup> 379 ± 1	No	<sup>38</sup> 930 ± 22	<sup>42</sup> 948 ± 38
65	Kakao Corp	kakao	002	2019-06-19	479406	<sup>84</sup> 2048 ± 0	<sup>106</sup> 747 ± 6	No	<sup>68</sup> 1720 ± 62	<sup>67</sup> 1715 ± 83
66	Kedacom International Pte	kedacom	000	2019-06-03	245292	<sup>12</sup> 292 ± 0	<sup>64</sup> 506 ± 3	No	<sup>27</sup> 684 ± 14	<sup>30</sup> 682 ± 16
67	Kneron Inc	kenron	003	2019-07-01	58366	<sup>69</sup> 2048 ± 0	<sup>29</sup> 281 ± 3	No	<sup>102</sup> 5237 ± 63	<sup>103</sup> 5274 ± 99
68	Lookman Electroplast Industries	lookman	002	2018-06-13	138200	<sup>24</sup> 548 ± 0	<sup>9</sup> 173 ± 1	No	<sup>20</sup> 610 ± 19	<sup>24</sup> 612 ± 22
69	Lookman Electroplast Industries	lookman	004	2019-06-03	244775	<sup>23</sup> 548 ± 0	<sup>68</sup> 507 ± 5	No	<sup>36</sup> 871 ± 29	<sup>41</sup> 878 ± 29
70	Megvii/Face++	megvii	001	2018-06-15	1361523	<sup>82</sup> 2048 ± 0	<sup>74</sup> 543 ± 0	No	<sup>101</sup> 5228 ± 32	<sup>102</sup> 5252 ± 60
71	Megvii/Face++	megvii	002	2018-10-19	1809564	<sup>127</sup> 4100 ± 0	<sup>88</sup> 644 ± 0	No	<sup>126</sup> 50630 ± 183	<sup>126</sup> 47591 ± 716
72	Xiamen Meiya Pico Information Co. Ltd	meiya	001	2019-03-01	280055	<sup>87</sup> 2049 ± 0	<sup>83</sup> 622 ± 12	No	<sup>108</sup> 8356 ± 615	<sup>109</sup> 8134 ± 97
73	MicroFocus	microfocus	001	2018-06-13	104524	<sup>8</sup> 256 ± 0	<sup>23</sup> 264 ± 18	No	<sup>1</sup> 215 ± 8	<sup>1</sup> 217 ± 10
74	MicroFocus	microfocus	002	2018-10-17	96288	<sup>6</sup> 256 ± 0	<sup>23</sup> 259 ± 18	No	<sup>4</sup> 337 ± 34	<sup>2</sup> 230 ± 25
75	Moontime Smart Technology	mt	000	2019-06-03	372169	<sup>85</sup> 2049 ± 0	<sup>103</sup> 724 ± 12	No	<sup>67</sup> 1678 ± 47	<sup>65</sup> 1614 ± 85
76	Neurotechnology	neurotech	005	2019-03-01	270450	<sup>7</sup> 256 ± 0	<sup>55</sup> 399 ± 0	No	<sup>238</sup> 238 ± 10	<sup>3</sup> 237 ± 7
77	Neurotechnology	neurotech	006	2019-06-26	525541	<sup>19</sup> 512 ± 0	<sup>101</sup> 678 ± 56	No	<sup>16</sup> 513 ± 14	<sup>18</sup> 535 ± 26
78	Nodeflux	nodeflux	000	2019-03-01	347079	<sup>59</sup> 2048 ± 0	<sup>73</sup> 542 ± 1	No	<sup>93</sup> 3283 ± 51	<sup>95</sup> 3285 ± 56
79	Nodeflux	nodeflux	001	2019-03-01	262553	<sup>73</sup> 2048 ± 0	<sup>20</sup> 247 ± 1	No	<sup>92</sup> 3242 ± 81	<sup>91</sup> 3255 ± 93
80	NotionTag Technologies Private Limited	notiontag	000	2019-06-12	92753	<sup>25</sup> 584 ± 0	<sup>75</sup> 548 ± 64	No	<sup>125</sup> 44672 ± 269	<sup>125</sup> 44593 ± 358
81	N-Tech Lab	ntech	006	2019-03-01	7901590	<sup>114</sup> 2600 ± 0	<sup>107</sup> 749 ± 1	No	<sup>41</sup> 1055 ± 93	<sup>40</sup> 844 ± 48
82	N-Tech Lab	ntech	007	2019-06-25	2509686	<sup>116</sup> 3348 ± 0	<sup>115</sup> 792 ± 3	No	<sup>49</sup> 1209 ± 59	<sup>56</sup> 1267 ± 65
83	Guangzhou Pixel Solutions Co. Ltd	pixelall	002	2019-06-06	0	<sup>113</sup> 2560 ± 0	<sup>13</sup> 191 ± 1	No	<sup>30</sup> 1223 ± 56	<sup>54</sup> 1230 ± 47
84	Panasonic R+D Center Singapore	psl	001	2018-10-12	382035	<sup>105</sup> 2056 ± 0	<sup>114</sup> 785 ± 16	No	<sup>3</sup> 298 ± 13	<sup>4</sup> 292 ± 14
85	Panasonic R+D Center Singapore	psl	002	2019-02-28	804934	<sup>92</sup> 2052 ± 0	<sup>126</sup> 888 ± 9	No	<sup>64</sup> 1590 ± 48	<sup>48</sup> 1133 ± 78
86	Rank One Computing	rankone	006	2019-02-27	0	<sup>5</sup> 165 ± 0	<sup>16</sup> 210 ± 1	No	<sup>10</sup> 443 ± 26	<sup>9</sup> 395 ± 22
87	Rank One Computing	rankone	007	2019-06-03	0	<sup>4</sup> 165 ± 0	<sup>19</sup> 245 ± 5	No	<sup>28</sup> 688 ± 20	<sup>22</sup> 601 ± 16
88	Realnetworks Inc	realnetworks	002	2019-02-28	95328	<sup>55</sup> 1848 ± 0	<sup>22</sup> 250 ± 2	No	<sup>55</sup> 1285 ± 17	<sup>55</sup> 1247 ± 42

Notes

1 The configuration size does not capture static data included in libraries. We do not count these because some algorithms include common ancillary libraries for image processing (e.g. openCV) or numerical computation (e.g. blas).

2 The median template creation times are measured on Intel®Xeon®CPU E5-2630 v4 @ 2.20GHz processors or, for GPU-enabled implementations, NVidia Tesla K40.

3 The comparison durations, in nanoseconds, are estimated using std::chrono::high\_resolution\_clock which on the machine in (2) counts 1ns clock ticks. Precision is somewhat worse than that however. The ± value is the median absolute deviation times 1.48 for Normal consistency.

Table 2: Summary of algorithms and properties included in this report. The red superscripts give ranking for the quantity in that column.

	Developer	Short	Sq.	Validation	Config <sup>1</sup>	Template		GPU	Comparison Time (ns) <sup>3</sup>	
	Name	Name	Num.	Date	Data (KB)	Size (B)	Time (ms) <sup>2</sup>		Genuine	Impostor
89	Realnetworks Inc	realnetworks	003	2019-06-12	95334	54 1848 ± 0	11 177 ± 10	No	61 1516 ± 29	63 1522 ± 60
90	KanKan Ai	remarkai	000	2019-03-01	240152	58 2048 ± 0	121 829 ± 7	No	37 873 ± 4	39 835 ± 35
91	KanKan Ai	remarkai	001	2019-03-01	241857	94 2052 ± 0	122 831 ± 6	No	51 1229 ± 20	38 805 ± 56
92	Saffe Ltd	saffe	001	2018-10-19	85973	45 1280 ± 0	28 281 ± 1	No	53 1274 ± 19	57 1277 ± 26
93	Saffe Ltd	saffe	002	2019-03-01	260622	77 2048 ± 0	119 817 ± 11	No	32 717 ± 7	33 714 ± 29
94	Sensetime Group Ltd	sensetime	002	2018-10-19	531783	88 2052 ± 0	104 725 ± 3	No	84 2546 ± 102	82 2371 ± 45
95	Sensetime Group Ltd	sensetime	002	2018-10-19	531783	96 2052 ± 0	116 797 ± 3	No	87 2713 ± 90	81 2301 ± 25
96	Shaman Software	shaman	000	2017-12-05	0	122 4096 ± 0	91 653 ± 16	No	7380 ± 25	8 379 ± 31
97	Shaman Software	shaman	001	2018-01-13	0	118 4096 ± 0	32 294 ± 2	No	29 635 ± 19	12 441 ± 25
98	Shenzhen Inst. Adv. Integrated Tech. CAS	SIAT	002	2018-06-13	486842	97 2052 ± 0	79 579 ± 0	No	34 769 ± 13	35 750 ± 13
99	Shenzhen Inst. Adv. Integrated Tech. CAS	SIAT	004	2019-03-01	940063	126 4100 ± 0	96 670 ± 0	No	99 4013 ± 45	98 3782 ± 173
100	Smilart	smilart	002	2018-02-06	111826	31 1024 ± 0	10 176 ± 16	No	119 18784 ± 136	119 18795 ± 151
101	Smilart	smilart	003	2018-06-18	67339	17 512 ± 0	12 180 ± 12	No	58 1395 ± 74	44 1027 ± 66
102	Star Hybrid Limited	starhybrid	001	2019-06-19	100509	67 2048 ± 0	45 358 ± 82	No	42 1075 ± 51	46 1078 ± 53
103	Synesis	synesis	004	2019-03-01	270628	80 2048 ± 0	109 735 ± 15	No	8424 ± 14	10 430 ± 22
104	Synesis	synesis	005	2019-06-06	146509	72 2048 ± 0	17 211 ± 9	No	19 599 ± 23	21 581 ± 32
105	Tech5 SA	tech5	001	2018-10-19	636346	119 4096 ± 0	66 522 ± 5	No	44 1087 ± 34	36 799 ± 44
106	Tech5 SA	tech5	002	2019-03-01	1150887	46 1280 ± 0	111 780 ± 10	No	60 1406 ± 120	45 1048 ± 57
107	Tevian	tevian	003	2018-10-19	791725	86 2049 ± 0	56 404 ± 15	No	5350 ± 11	6 338 ± 25
108	Tevian	tevian	004	2019-03-01	863474	68 2048 ± 0	63 506 ± 30	No	12 474 ± 31	326 ± 20
109	TigerIT Americas LLC	tiger	002	2018-06-13	341638	103 2056 ± 0	54 393 ± 20	No	80 2135 ± 29	79 2137 ± 38
110	TigerIT Americas LLC	tiger	003	2018-10-16	426164	99 2056 ± 0	60 458 ± 21	No	76 2031 ± 35	75 2029 ± 38
111	TongYi Transportation Technology	tongyi	005	2019-06-12	1140701	110 2089 ± 0	7 165 ± 1	No	120 18924 ± 65	120 20158 ± 103
112	Toshiba	toshiba	002	2018-10-19	813606	50 1560 ± 0	71 541 ± 0	No	98 3521 ± 369	85 2449 ± 124
113	Toshiba	toshiba	003	2019-03-01	984125	51 1560 ± 0	70 540 ± 0	No	83 2390 ± 41	83 2407 ± 81
114	China University of Petroleum	upc	001	2019-06-05	0	39 1052 ± 0	76 551 ± 15	No	90 3114 ± 44	92 3165 ± 97
115	VCognition	vcog	002	2017-06-12	3229434	131 61504 ± 5	44 357 ± 25	No	130 296154 ± 3077	130 296436 ± 4183
116	Visidon	visidon	001	2019-02-26	170262	90 2052 ± 0	39 316 ± 6	No	52 1258 ± 38	50 1148 ± 109
117	Veridas Digital Authentication Solutions S.L.	veridas	001	2019-03-01	196540	70 2048 ± 0	98 671 ± 21	No	104 5748 ± 20	106 7111 ± 148
118	Veridas Digital Authentication Solutions S.L.	veridas	000	2019-03-01	193466	22 512 ± 0	94 669 ± 20	No	69 1733 ± 81	73 1934 ± 44
119	Videonetics Technology Pvt Ltd	videonetics	001	2019-06-19	30875	16 512 ± 0	24 262 ± 3	No	47 1153 ± 38	49 1142 ± 65
120	Vigilant Solutions	vigilant	006	2019-03-01	343048	49 1548 ± 0	123 841 ± 8	No	39 939 ± 32	31 711 ± 37
121	Vigilant Solutions	vigilant	007	2019-06-27	255600	48 1548 ± 0	62 493 ± 6	No	35 803 ± 35	37 800 ± 40
122	Beijing Vion Technology Inc	vion	000	2018-10-19	228219	93 2052 ± 0	41 333 ± 1	No	124 39839 ± 3561	123 26830 ± 2241
123	Vision-Box	visionbox	000	2019-02-26	176501	79 2048 ± 0	34 304 ± 7	No	66 1648 ± 57	53 1192 ± 42
124	Vision-Box	visionbox	001	2019-03-01	256869	75 2048 ± 0	131 983 ± 7	No	48 1161 ± 22	51 1154 ± 20
125	VisionLabs	visionlabs	006	2019-03-01	353044	21 512 ± 0	26 270 ± 0	No	30 698 ± 19	34 734 ± 28
126	VisionLabs	visionlabs	007	2019-06-12	357204	20 512 ± 0	27 272 ± 0	No	40 965 ± 41	43 972 ± 31
127	Vocord	vocord	006	2019-03-01	559457	26 768 ± 0	128 886 ± 1	No	78 2020 ± 72	74 1969 ± 62
128	Vocord	vocord	007	2019-06-06	587489	52 1664 ± 0	112 780 ± 2	No	86 2593 ± 83	86 2526 ± 59
129	Winsense Co. Ltd	winsense	000	2019-06-17	270819	44 1280 ± 0	30 283 ± 1	No	63 1551 ± 31	64 1532 ± 42
130	Zhuhai Yisheng Electronics Technology	yisheng	004	2018-06-12	486351	117 3704 ± 0	48 378 ± 12	No	29 693 ± 137	17 526 ± 34
131	Shanghai Yitu Technology	yitu	003	2019-03-01	1525719	108 2082 ± 0	124 860 ± 0	No	118 18305 ± 71	118 18286 ± 62

## Notes

- 1 The configuration size does not capture static data included in libraries. We do not count these because some algorithms include common ancillary libraries for image processing (e.g. openCV) or numerical computation (e.g. blas).
- 2 The median template creation times are measured on Intel® Xeon® CPU E5-2630 v4 @ 2.20GHz processors or, for GPU-enabled implementations, NVidia Tesla K40.
- 3 The comparison durations, in nanoseconds, are estimated using std::chrono::high\_resolution\_clock which on the machine in (2) counts 1ns clock ticks. Precision is somewhat worse than that however. The ± value is the median absolute deviation times 1.48 for Normal consistency.

Table 3: Summary of algorithms and properties included in this report. The red superscripts give ranking for the quantity in that column.

	Algorithm	FALSE NON-MATCH RATE (FNMR)									
		CONSTRAINED, COOPERATIVE					LESS CONSTRAINED, NON-COOP.				
		Name	VISAMC	VISA	VISA	MUGSHOT	WILD	CHILD EXP			
	FMR	0.0001	1E-06	0.0001	1E-05	0.0001	0.0001	0.01			
1	3divi-003	0.0318	88	0.0588	89	0.0097	79	0.0389	86	0.0867	85
2	adera-001	0.1021	103	0.1757	103	0.0368	102	0.1823	109	0.1965	100
3	alchera-000	0.0165	59	0.0243	50	0.0086	75	0.0125	46	0.0370	48
4	alchera-001	0.0183	63	0.0299	63	0.0078	70	0.0142	53	0.0372	49
5	allgvision-000	0.0346	90	0.0527	86	0.0210	94	0.0232	75	0.0607	79
6	amplifiedgroup-001	0.5034	122	0.5848	122	0.2999	123	0.6973	121	0.4250	114
7	anke-003	0.0131	44	0.0213	42	0.0056	46	0.0094	21	0.0302	20
8	anke-004	0.0080	21	0.0154	27	0.0031	18	0.0073	9	0.0288	14
9	anyvision-002	0.0660	98	0.0898	95	0.0387	103	0.0928	102	0.2227	102
10	anyvision-004	0.0267	83	0.0385	77	0.0081	71	0.0258	77	0.0470	66
11	aware-003	0.0793	100	0.1161	100	0.0288	100	0.1028	103	0.3180	111
12	aware-004	0.0690	99	0.0949	98	0.0257	97	0.0837	100	0.0516	72
13	ayonix-000	0.4351	119	0.4872	117	0.2299	120	0.6150	119	0.3635	112
14	bm-001	0.7431	127	0.9494	128	0.6188	128	0.9586	125	0.9935	118
15	camvi-002	0.0125	39	0.0221	46	0.0049	40	0.0089	19	0.0288	13
16	camvi-003	0.0184	64	0.0320	68	0.0062	52	0.0134	50	0.0300	18
17	ceiec-001	0.0328	89	0.0475	83	0.0163	89	0.0295	81	0.0847	82
18	ceiec-002	0.0161	57	0.0193	38	0.0124	87	0.0122	44	0.0465	65
19	cogent-003	0.0091	22	0.0188	37	0.0032	19	0.0098	26	0.0406	55
20	cogent-004	0.0064	13	0.0116	18	0.0024	14	0.0096	23	0.0379	50
21	cognitec-000	0.0116	34	0.0177	33	0.0036	23	0.0118	41	0.0953	89
22	cognitec-001	0.0126	40	0.0185	36	0.0047	37	0.0120	43	0.0598	78
23	ctbcbank-000	0.0168	60	0.0250	55	0.0064	53	0.0146	56	1.0000	126
24	cyberextruder-001	0.1972	111	0.2547	110	0.0755	112	0.4686	117	0.1747	97
25	cyberextruder-002	0.0811	101	0.1336	102	0.0265	98	0.1465	107	0.1000	90
26	cyberlink-001	0.0131	43	0.0210	41	0.0050	41	0.0439	90	0.0318	32
27	cyberlink-002	0.0114	33	0.0195	39	0.0044	32	0.0101	27	0.0298	17
28	dahua-001	0.0250	78	0.0466	82	0.0108	84	0.0228	73	0.0457	64
29	dahua-002	0.0129	41	0.0157	29	0.0090	77	0.0116	40	0.0323	34
30	deepglint-001	0.0040	6	0.0062	5	0.0014	7	0.0047	4	0.0278	5
31	deepsea-001	0.0136	46	0.0215	44	0.0071	66	0.0142	54	0.0347	43
32	dermalog-005	0.1526	109	0.1823	105	0.0658	110	0.2580	112	0.0855	84
33	dermalog-006	0.0253	79	0.0369	75	0.0172	92	0.0171	62	0.0623	80
34	digitalbarriers-002	0.3360	116	0.3690	115	0.0968	115	0.0877	101	0.0436	59
35	dsk-000	0.1526	108	0.2169	107	0.0765	113	0.3787	116	0.2201	101
36	everai-002	0.0104	30	0.0159	30	0.0041	30	0.0063	6	0.0294	15
37	everai-paravision-003	0.0034	2	0.0050	3	0.0011	3	0.0036	2	0.0278	6
38	glory-000	0.1094	104	0.1286	101	0.0514	107	0.2179	110	0.4762	116
39	glory-001	0.0902	102	0.1082	99	0.0410	104	0.1642	108	0.4261	115
40	gorilla-002	0.0256	80	0.0413	78	0.0076	69	0.0478	93	0.0507	70
41	gorilla-003	0.0165	58	0.0291	60	0.0053	43	0.0205	69	0.0359	46
42	hik-001	0.0096	26	0.0125	19	0.0036	25	0.0093	20	0.0271	1
43	hr-000	0.0265	82	0.0434	79	0.0112	86	0.0340	83	0.1902	99
44	hr-001	0.0044	7	0.0072	8	0.0019	10	0.0073	10	0.0303	21
45	id3-003	0.0361	91	0.0757	92	0.0104	83	0.0292	80	0.0848	83
46	id3-004	0.0198	68	0.0344	70	0.0084	73	0.0238	76	-	-
47	idemia-003	0.0222	71	0.0316	67	0.0082	72	0.0188	65	0.0578	77
48	idemia-004	0.0160	56	0.0244	52	0.0065	54	0.0199	68	0.0309	27
49	iit-000	0.1516	107	0.1981	106	0.0620	109	0.0828	99	-	-
50	imagus-000	0.0642	96	0.0882	93	0.0330	101	0.0497	94	0.1158	91
51	imperial-000	0.0067	15	0.0108	16	0.0022	13	0.0080	14	0.0281	8
52	imperial-001	0.0094	25	0.0154	28	0.0033	20	0.0072	8	0.0276	3
53	incode-003	0.0142	49	0.0249	54	0.0054	44	0.0448	91	0.0318	31
54	incode-004	0.0077	19	0.0132	21	0.0034	21	0.0096	24	0.0313	29
55	innovatrics-004	0.0194	66	0.0292	61	0.0068	61	0.0344	84	0.0454	62
56	innovatrics-005	0.0230	73	0.0353	72	0.0085	74	0.0398	88	0.0301	19
57	intellivision-001	0.1335	106	0.2205	108	0.0417	105	0.1090	105	0.2445	103
58	iqface-000	0.0091	23	0.0143	24	0.0043	31	0.0075	13	0.0381	51
59	isityou-000	0.5682	124	0.7033	124	0.4145	126	1.0000	127	1.0000	122
60	isystems-001	0.0149	53	0.0245	53	0.0067	59	0.0138	52	0.0524	75

Table 4: FNMR is the proportion of mated comparisons below a threshold set to achieve the FMR given in the header on the fourth row. FMR is the proportion of impostor comparisons at or above that threshold. The light grey values give rank over all algorithms in that column. The green column applies to “matched-covariates” i.e. impostors of the same sex, age group, and country of birth. The pink column uses only same-sex impostors; All others are zero effort. The pink column includes effects of extended ageing, and is the most important. Missing entries for visa, mugshot and wild images generally mean the algorithm did not run to completion. For child exploitation, missing entries arise because NIST executes those runs only infrequently.

	Algorithm	FALSE NON-MATCH RATE (FNMR)									
		CONSTRAINED, COOPERATIVE					LESS CONSTRAINED, NON-COOP.				
		Name	VISAMC	VISA	VISA	MUGSHOT	WILD	CHILD EXP			
	FMR	0.0001	1E-06	0.0001	1E-05	0.0001	0.01				
61	isystems-002	0.0118	35	0.0182	35	0.0066	55	0.0111	34	0.0516	73
62	itmo-005	0.0182	62	0.0345	71	0.0067	60	0.0181	63	0.0433	57
63	itmo-006	0.0125	38	0.0220	45	0.0046	34	0.0149	57	0.0329	37
64	kakao-001	0.4553	121	0.5532	121	0.2034	119	0.6580	120	1.0000	131
65	kakao-002	0.0625	95	0.1779	104	0.0168	91	0.0791	98	1.0000	124
66	kedacom-000	0.0055	9	0.0081	10	0.0027	15	0.0111	36	0.2511	105
67	kneron-003	0.0542	93	0.0902	96	0.0218	95	0.0346	85	0.3053	110
68	lookman-002	0.0297	85	0.0547	88	0.0102	82	0.0339	82	0.2640	108
69	lookman-004	0.0074	18	0.0099	13	0.0037	26	0.0124	45	0.2516	106
70	megvii-001	0.0157	54	0.0244	51	0.0045	33	0.0392	87	0.0916	87
71	megvii-002	0.0104	29	0.0145	25	0.0036	24	0.0225	71	0.0692	81
72	meiya-001	0.0171	61	0.0275	59	0.0066	57	0.0159	61	0.0363	47
73	microfocus-001	0.4482	120	0.5524	120	0.2309	121	0.7256	122	0.2567	107
74	microfocus-002	0.3605	117	0.5057	118	0.1566	118	0.5783	118	0.1582	96
75	mt-000	0.0100	28	0.0170	31	0.0047	36	0.0074	12	0.0326	36
76	neurotechnology-005	0.0141	48	0.0300	64	0.0051	42	0.0108	32	0.0332	38
77	neurotechnology-006	0.0098	27	0.0136	22	0.0040	29	0.0105	30	0.0303	22
78	nodeflux-000	1.0000	130	1.0000	130	1.0000	130	1.0000	130	1.0000	128
79	nodeflux-001	1.0000	131	1.0000	131	1.0000	131	1.0000	131	1.0000	129
80	notiontag-000	0.6669	125	0.7885	125	0.3222	125	0.3715	115	0.1807	98
81	ntechlab-006	0.0078	20	0.0111	17	0.0021	12	0.0112	37	0.0275	2
82	ntechlab-007	0.0056	10	0.0076	9	0.0018	9	0.0073	11	0.0276	4
83	pixelall-002	0.0193	65	0.0340	69	0.0066	56	0.0127	48	0.0342	42
84	psl-001	0.0549	94	0.0927	97	0.0198	93	0.0096	22	0.0431	56
85	psl-002	0.0107	31	0.0180	34	0.0048	39	0.0089	18	0.0295	16
86	rankone-006	0.0242	75	0.0460	81	0.0070	63	0.0119	42	0.0538	76
87	rankone-007	0.0197	67	0.0366	74	0.0057	48	0.0113	38	0.0450	60
88	realnetworks-002	0.0248	77	0.0358	73	0.0099	80	0.0513	95	0.0334	39
89	realnetworks-003	0.0259	81	0.0372	76	0.0100	81	0.0541	96	0.0335	41
90	remarkai-000	0.0147	52	0.0257	57	0.0062	51	0.0102	28	0.0304	23
91	remarkai-001	0.0144	50	0.0256	56	0.0061	50	0.0102	29	0.0308	26
92	saffe-001	0.4339	118	0.5261	119	0.2340	122	0.7539	124	0.3887	113
93	saffe-002	0.0119	36	0.0206	40	0.0054	45	0.0107	31	0.0308	25
94	sensetime-001	0.0063	12	0.0092	11	0.0030	17	0.0130	49	1.0000	121
95	sensetime-002	0.0068	16	0.0098	12	0.0035	22	0.0143	55	0.9999	119
96	shaman-000	0.9297	129	0.9774	129	0.9128	129	0.9990	126	0.9575	117
97	shaman-001	0.3346	115	0.4616	116	0.1360	117	0.2368	111	0.1498	95
98	siat-002	0.0091	24	0.0126	20	0.0039	28	0.0109	33	0.0520	74
99	siat-004	0.0067	14	0.0099	14	0.0028	16	0.0152	59	1.0000	120
100	smilart-002	0.2440	114	0.3532	114	0.0821	114	-	-	0.700	34
101	smilart-003	0.6944	126	0.8836	126	0.1088	116	0.0695	97	0.1190	92
102	starhybrid-001	0.0108	32	0.0138	23	0.0058	49	0.0081	15	0.0350	44
103	synesis-004	0.0310	86	0.0480	84	0.0166	90	0.0476	92	0.1319	93
104	synesis-005	0.0147	51	0.0226	48	0.0073	68	0.0153	60	0.0334	40
105	tech5-001	0.0130	42	0.0176	32	0.0037	27	0.0218	70	0.0938	88
106	tech5-002	0.0046	8	0.0063	6	0.0009	2	0.0113	39	0.0310	28
107	tevian-003	0.0217	70	0.0298	62	0.0067	58	0.0230	74	0.0456	63
108	tevian-004	0.0228	72	0.0304	65	0.0069	62	0.0226	72	0.0394	53
109	tiger-002	0.0658	97	0.0889	94	0.0227	96	0.1083	104	0.0512	71
110	tiger-003	0.0313	87	0.0602	91	0.0087	76	0.0188	66	0.0482	68
111	tongyi-005	0.0073	17	0.0146	26	0.0019	11	0.0187	64	0.0399	54
112	toshiba-002	0.0134	45	0.0222	47	0.0048	38	0.0097	25	0.0434	58
113	toshiba-003	0.0125	37	0.0214	43	0.0047	35	0.0085	17	0.0282	9
114	upc-001	0.0234	74	0.0519	85	0.0071	65	0.0291	79	0.0314	30
115	vcog-002	0.7522	128	0.9033	127	0.5040	127	-	-	0.752	39
116	vd-001	0.0243	76	0.0452	80	0.0093	78	0.0271	78	0.1389	94
117	veridas-001	0.1998	113	0.2724	111	0.0742	111	0.2987	114	0.0501	69
118	veridas-002	0.1733	110	0.2257	109	0.0528	108	0.2617	113	0.0450	61
119	videonetcs-001	0.5483	123	0.6446	123	0.3063	124	0.7517	123	0.2986	109
120	vigilantsolutions-006	0.1264	105	0.3221	112	0.0136	88	0.0150	58	0.0321	33

Table 5: FNMR is the proportion of mated comparisons below a threshold set to achieve the FMR given in the header on the fourth row. FMR is the proportion of impostor comparisons at or above that threshold. The light grey values give rank over all algorithms in that column. The green column applies to “matched-covariates” i.e. impostors of the same sex, age group, and country of birth. The pink column uses only same-sex impostors; All others are zero effort. The pink column includes effects of extended ageing, and is the most important. Missing entries for visa, mugshot and wild images generally mean the algorithm did not run to completion. For child exploitation, missing entries arise because NIST executes those runs only infrequently.

Algorithm Name	FALSE NON-MATCH RATE (FNMR)						
	CONSTRAINED, COOPERATIVE				LESS CONSTRAINED, NON-COOP.		
	VISAMC	VISA	VISA	MUGSHOT	WILD	CHILD EXP	
FMR	0.0001	1E-06	0.0001	1E-05	0.0001	0.01	
121 vigilantsolutions-007	0.0202	69	0.0307	66	0.0070	64	0.0136 51 0.0306 24 -
122 vion-000	0.0419	92	0.0590	90	0.0288	99	0.0422 89 0.2479 104 0.876 48
123 visionbox-000	0.0293	84	0.0541	87	0.0110	85	0.0197 67 0.0476 67 -
124 visionbox-001	0.0159	55	0.0270	58	0.0072	67	0.0111 35 0.0389 52 -
125 visionlabs-006	0.0037	3	0.0066	7	0.0012	4	0.0041 3 0.0285 11 -
126 visionlabs-007	0.0038	4	0.0048	2	0.0012	6	0.0036 1 0.0286 12 0.371 3
127 vocord-006	0.0062	11	0.0102	15	0.0016	8	0.0082 16 0.0282 10 -
128 vocord-007	0.0039	5	0.0053	4	0.0012	5	0.0061 5 0.0280 7 0.847 46
129 winsense-000	0.0140	47	0.0228	49	0.0056	47	0.0125 47 0.0352 45 -
130 yisheng-004	0.1988	112	0.3329	113	0.0475	106	0.1147 106 0.0908 86 0.715 36
131 yitu-003	0.0015	1	0.0026	1	0.0003	1	0.0066 7 0.0325 35 -

Table 6: FNMR is the proportion of mated comparisons below a threshold set to achieve the FMR given in the header on the fourth row. FMR is the proportion of impostor comparisons at or above that threshold. The light grey values give rank over all algorithms in that column. The green column applies to “matched-covariates” i.e. impostors of the same sex, age group, and country of birth. The pink column uses only same-sex impostors; All others are zero effort. The pink column includes effects of extended ageing, and is the most important. Missing entries for visa, mugshot and wild images generally mean the algorithm did not run to completion. For child exploitation, missing entries arise because NIST executes those runs only infrequently.

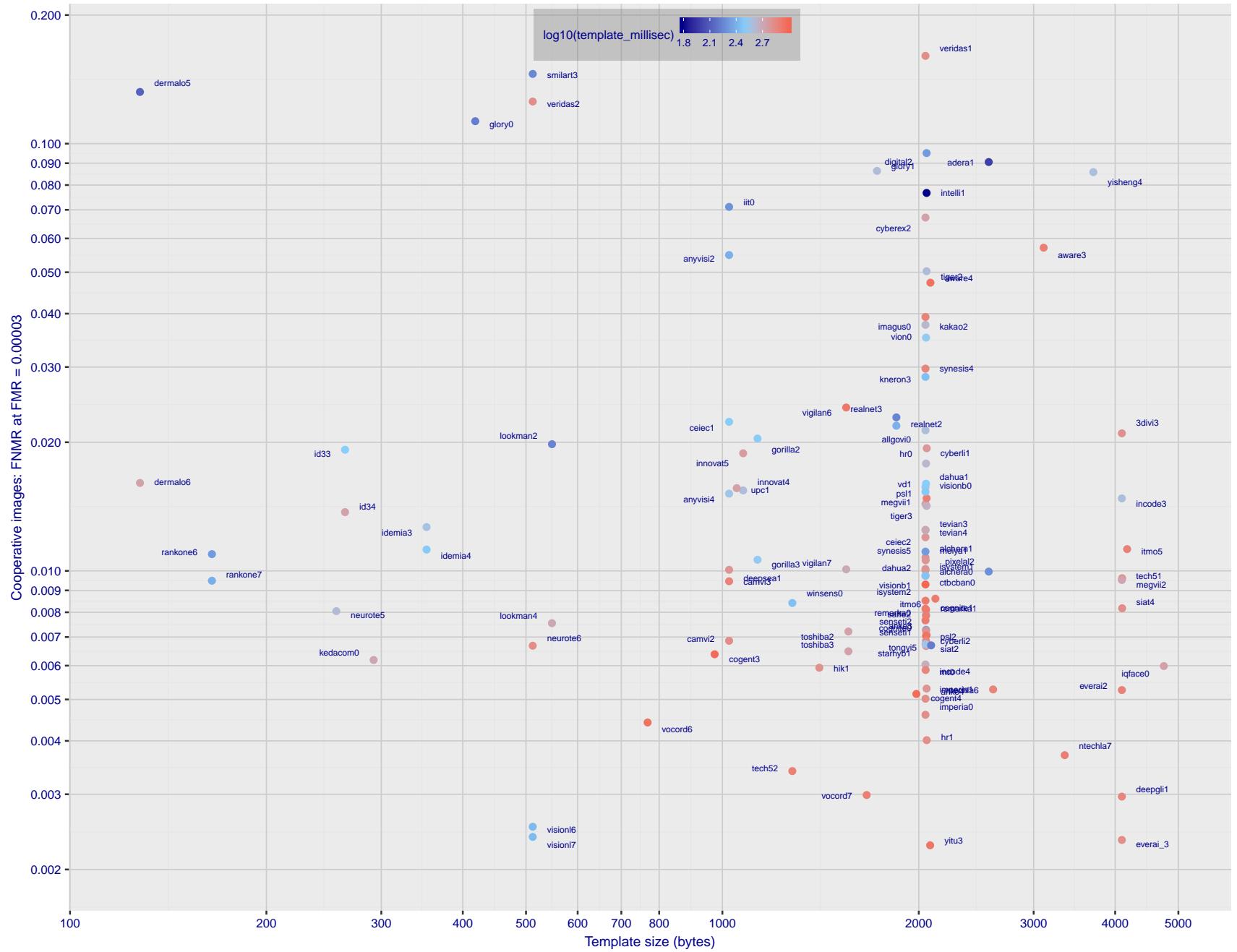


Figure 1: The points show false non-match rates (FNMR) versus the size of the encoded template. FNMR is the geometric mean of FNMR values for visa and mugshot images (from Figs. 23 and 30) at a false match rate (FMR) of 0.0001. The color of the points encodes template generation time - which spans at least one order of magnitude. Durations are measured on a single core of a c. 2016 Intel Xeon E5-2630 v4 running at 2.20GHz. Algorithms with poor FNMR are omitted.

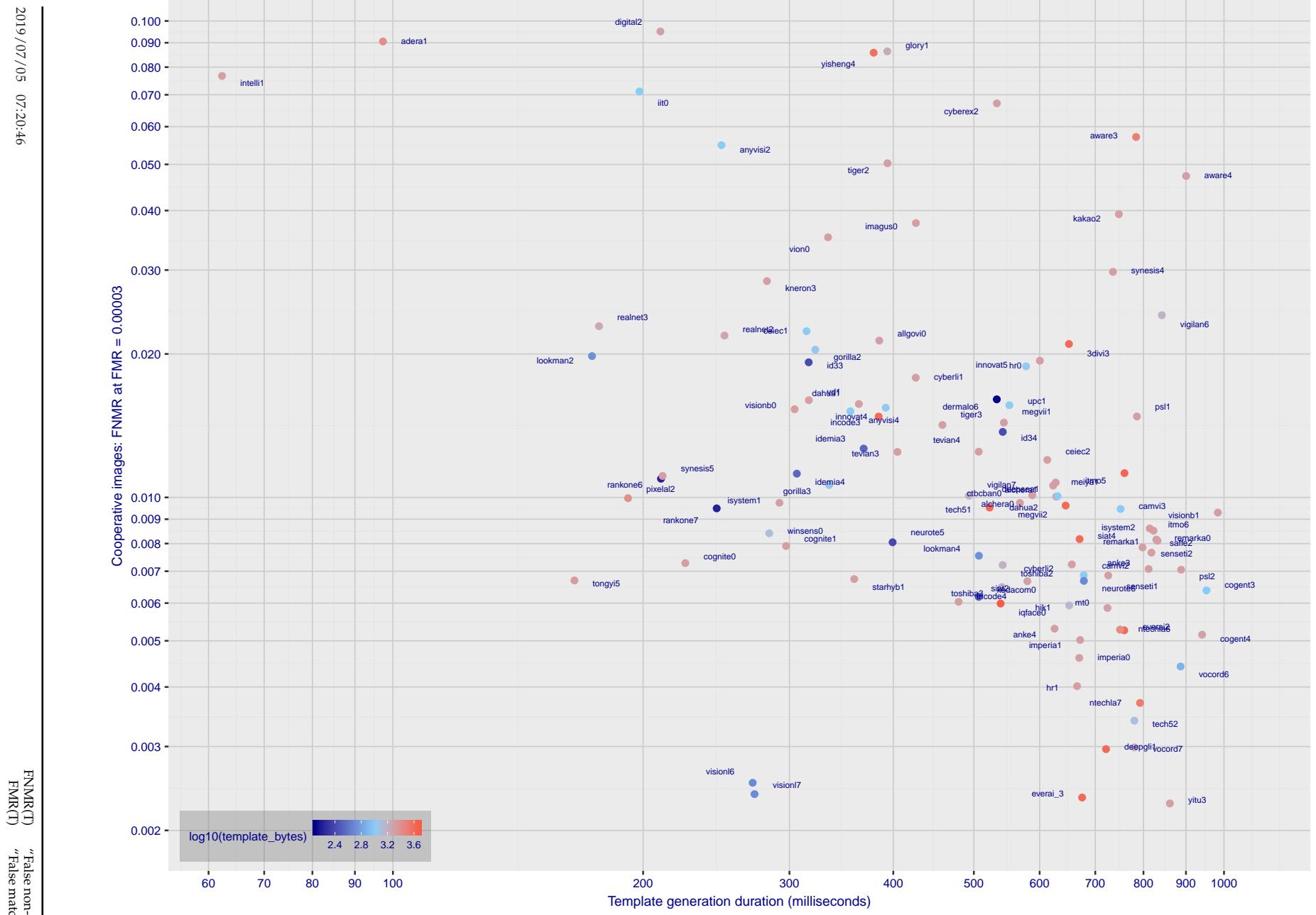


Figure 2: The points show false non-match rates (FNMR) versus the duration of the template generation operation. FNMR is the geometric mean of FNMR values for visa and mugshot images (from Figs. 23 and 30) at a false match rate (FMR) of 0.0001. Template generation time is a median estimated over 640 x 480 pixel portraits. It is measured on a single core of a c. 2016 Intel Xeon CPU E5-2630 v4 running at 2.20GHz. The color of the points encodes template size - which span two orders of magnitude. Algorithms with poor FNMR are omitted.

# 1 Metrics

## 1.1 Core accuracy

Given a vector of N genuine scores,  $u$ , the false non-match rate (FNMR) is computed as the proportion below some threshold, T:

$$\text{FNMR}(T) = 1 - \frac{1}{N} \sum_{i=1}^N H(u_i - T) \quad (1)$$

where  $H(x)$  is the unit step function, and  $H(0)$  taken to be 1.

Similarly, given a vector of N impostor scores,  $v$ , the false match rate (FMR) is computed as the proportion above T:

$$\text{FMR}(T) = \frac{1}{N} \sum_{i=1}^N H(v_i - T) \quad (2)$$

The threshold, T, can take on any value. We typically generate a set of thresholds from quantiles of the observed impostor scores,  $v$ , as follows. Given some interesting false match rate range,  $[\text{FMR}_L, \text{FMR}_U]$ , we form a vector of K thresholds corresponding to FMR measurements evenly spaced on a logarithmic scale

$$T_k = Q_v(1 - \text{FMR}_k) \quad (3)$$

where  $Q$  is the quantile function, and  $\text{FMR}_k$  comes from

$$\log_{10} \text{FMR}_k = \log_{10} \text{FMR}_L + \frac{k}{K} [\log_{10} \text{FMR}_U - \log_{10} \text{FMR}_L] \quad (4)$$

Error tradeoff characteristics are plots of FNMR(T) vs. FMR(T). These are plotted with  $\text{FMR}_U \rightarrow 1$  and  $\text{FMR}_L$  as low as is sustained by the number of impostor comparisons, N. This is somewhat higher than the “rule of three” limit  $3/N$  because samples are not independent, due to re-use of images.

## 2 Datasets

### 2.1 Child exploitation images

- ▷ The number of images is on the order of  $10^4$ .
- ▷ The number of subjects is on the order of  $10^3$ .
- ▷ The number of subjects with two images on the order of  $10^3$ .
- ▷ The images are operational. They are taken from ongoing investigations of child exploitation crimes. The images are arbitrarily unconstrained. Pose varies considerably around all three axes, including subject lying down. Resolution varies very widely. Faces can be occluded by other objects, including hair and hands. Lighting varies, although the images are intended for human viewing. Mis-focus is rare. Images are given to the algorithm without any cropping; faces may occupy widely varying areas.
- ▷ The images are usually large from contemporary cameras. The mean interocular distance (IOD) is 70 pixels.
- ▷ The images are of subjects from several countries, due to the global production of this imagery.
- ▷ The images are of children, from infancy to late adolescence.
- ▷ All of the images are live capture, none are scanned. Many have been cropped.
- ▷ When these images are input to the algorithm, they are labelled as being of type "EXPLOITATION" - see Table 4 of the FRVT API.

### 2.2 Visa images

- ▷ The number of images is on the order of  $10^5$ .
- ▷ The number of subjects is on the order of  $10^5$ .
- ▷ The number of subjects with two images on the order of  $10^4$ .
- ▷ The images have geometry in reasonable conformance with the ISO/IEC 19794-5 Full Frontal image type. Pose is generally excellent.
- ▷ The images are of size 252x300 pixels. The mean interocular distance (IOD) is 69 pixels.
- ▷ The images are of subjects from greater than 100 countries, with significant imbalance due to visa issuance patterns.
- ▷ The images are of subjects of all ages, including children, again with imbalance due to visa issuance demand.
- ▷ Many of the images are live capture. A substantial number of the images are photographs of paper photographs.
- ▷ When these images are input to the algorithm, they are labelled as being of type "ISO" - see Table 4 of the FRVT API.

### 2.3 Mugshot images

- ▷ The number of images is on the order of  $10^6$ .
- ▷ The number of subjects is on the order of  $10^6$ .
- ▷ The number of subjects with two images on the order of  $10^6$ .



Figure 3: The figure gives simulated samples of image types used in this report.

- ▷ The images have geometry in reasonable conformance with the ISO/IEC 19794-5 Full Frontal image type.
  - ▷ The images are of variable sizes. The median IOD is 105 pixels. The mean IOD is 113 pixels. The 1-st, 5-th, 10-th, 25-th, 75-th, 90-th and 99-th percentiles are 34, 58, 70, 87, 121, 161 and 297 pixels.
  - ▷ The images are of subjects from the United States.
  - ▷ The images are of adults.
  - ▷ The images are all live capture.
  - ▷ When these images are input to the algorithm, they are labelled as being of type "mugshot" - see Table 4 of the FRVT API.

## 2.4 Wild images

- ▷ The number of images is on the order of  $10^5$ .
  - ▷ The number of subjects is on the order of  $10^3$ .
  - ▷ The number of subjects with two images on the order of  $10^3$ .
  - ▷ The images include many photojournalism-style images. Images are given to the algorithm using a variable but generally tight crop of the head. Resolution varies very widely. The images are very unconstrained, with wide yaw and pitch pose variation. Faces can be occluded, including hair and hands.
  - ▷ The images are of adults.
  - ▷ All of the images are live capture, none are scanned.
  - ▷ When these images are input to the algorithm, they are labelled as being of type "WILD" - see Table 4 of the FRVT API.

### 3 Results

### 3.1 Test goals

- ▷ To state overall accuracy.
  - ▷ To compare algorithms.

### 3.2 Test design

**Method:** For visa images:

- ▷ The comparisons are of visa photos against visa photos.
- ▷ The number of genuine comparisons is on the order of  $10^4$ .
- ▷ The number of impostor comparisons is on the order of  $10^{10}$ .
- ▷ The comparisons are fully zero-effort, meaning impostors are paired without attention to sex, age or other covariates. However, later analysis is conducted on subsets.
- ▷ The number of persons is on the order of  $10^5$ .
- ▷ The number of images used to make 1 template is 1.
- ▷ The number of templates used to make each comparison score is two corresponding to simple one-to-one verification.

For mugshot images:

- ▷ The comparisons are of mugshot photos against mugshot photos.
- ▷ The number of genuine comparisons is on the order of  $10^6$ .
- ▷ The number of impostor comparisons is on the order of  $10^8$ .
- ▷ The impostors are paired by sex, but not by age or other covariates.
- ▷ The number of persons is on the order of  $10^6$ .
- ▷ The number of images used to make 1 template is 1.
- ▷ The number of templates used to make each comparison score is two corresponding to simple one-to-one verification.

**Method:** For wild images:

- ▷ The comparisons are of wild photos against wild photos.
- ▷ The number of genuine comparisons is on the order of  $10^6$ .
- ▷ The number of impostor comparisons is on the order of  $10^7$ .
- ▷ The comparisons are fully zero-effort, meaning impostors are paired without attention to sex, age or other covariates.
- ▷ The number of persons is on the order of  $10^4$ .
- ▷ The number of images used to make 1 template is 1.
- ▷ The number of templates used to make each comparison score is two corresponding to simple one-to-one verification.

For child exploitation images:

- ▷ The comparisons are of unconstrained child exploitation photos against others of the same type.

- ▷ The number of genuine comparisons is on the order of  $10^4$ .
- ▷ The number of impostor comparisons is on the order of  $10^7$ .
- ▷ The comparisons are fully zero-effort, meaning impostors are paired without attention to sex, age or other covariates.
- ▷ The number of persons is on the order of  $10^3$ .
- ▷ The number of images used to make 1 template is 1.
- ▷ The number of templates used to make each comparison score is two corresponding to simple one-to-one verification.
- ▷ We produce two performance statements. First, is a DET as used for visa and mugshot images. The second is a cumulative match characteristic (CMC) summarizing a simulated one-to-many search process. This is done as follows.
  - We regard  $M$  enrollment templates as items in a gallery.
  - These  $M$  templates come from  $M > N$  individuals, because multiple images of a subject are present in the gallery under separate identifiers.
  - We regard the verification templates as search templates.
  - For each search we compute the rank of the highest scoring mate.
  - This process should properly be conducted with a 1:N algorithm, such as those tested in NIST IR 8009. We use the 1:1 algorithms in a simulated 1:N mode here to a) better reflect what a child exploitation analyst does, and b) to show algorithm efficacy is better than that revealed in the verification DETs.

### 3.3 Failure to enroll

	Algorithm Name	Failure to Enrol Rate <sup>1</sup>							
		CHILD-EXPLOIT	MUGSHOT	VISA	WILD				
1	3divi-003	0.1806	43	0.0007	92	0.0006	86	0.0294	104
2	adera-001	0.1928	44	0.0003	66	0.0005	83	0.0505	114
3	alchera-000	-	131	0.0004	82	0.0014	112	0.0038	75
4	alchera-001	-	131	0.0004	81	0.0014	111	0.0038	74
5	allgovision-000	-	131	0.0026	116	0.0052	129	0.0131	96
6	amplifiedgroup-001	-	131	0.0189	131	0.0279	135	0.1390	126
7	anke-003	-	131	0.0001	46	0.0004	59	0.0006	48
8	anke-004	-	131	0.0001	47	0.0004	67	0.0006	53
9	anyvision-002	0.4866	57	0.0070	126	0.0090	131	0.1146	122
10	anyvision-004	0.1660	40	0.0001	55	0.0004	64	0.0080	87
11	aware-003	0.3314	53	0.0016	111	0.0013	108	0.0745	119
12	aware-004	-	131	0.0002	58	0.0005	73	0.0014	65
13	ayonix-000	0.0000	3	0.0113	128	0.0137	133	0.1194	123
14	bm-001	0.0000	9	0.0000	29	0.0000	14	0.0000	11
15	camvi-002	0.0000	4	0.0000	19	0.0000	21	0.0000	17
16	camvi-003	-	131	0.0000	2	0.0000	2	0.0000	1
17	ceiec-001	-	131	0.0029	119	0.0023	119	0.0068	83
18	ceiec-002	0.2482	50	0.0036	120	0.0031	124	0.0081	88
19	cogent-003	-	131	0.0001	44	0.0004	62	0.0009	61
20	cogent-004	0.0000	7	0.0000	4	0.0000	5	0.0000	3
21	cognitec-000	0.6342	60	0.0007	93	0.0007	92	0.0388	111
22	cognitec-001	-	131	0.0008	97	0.0010	95	0.0185	100
23	ctcbank-000	-	131	0.0011	103	0.0019	116	0.0868	121
24	cyberextruder-001	0.5338	58	0.0024	114	0.0029	123	0.0597	117
25	cyberextruder-002	0.2672	51	0.0027	117	0.0028	122	0.0335	109
26	cyberlink-001	-	131	0.0073	127	0.0005	75	0.0008	55
27	cyberlink-002	0.1463	39	0.0004	75	0.0004	71	0.0007	54
28	dahua-001	0.0000	17	0.0000	28	0.0000	30	0.0000	26
29	dahua-002	-	131	0.0024	115	0.0022	118	0.0009	58
30	deepglint-001	0.0000	11	0.0000	13	0.0000	15	0.0000	12
31	deepsea-001	0.0000	10	0.0000	6	0.0000	7	0.0000	5
32	dermalog-005	0.1796	41	0.0013	107	0.0041	126	0.0163	98
33	dermalog-006	0.1797	42	0.0013	106	0.0041	127	0.0163	99
34	digitalbarriers-002	-	131	0.0028	118	0.0027	121	0.0071	84
35	dsk-000	-	131	0.0000	10	0.0000	11	0.0000	8
36	everai-002	-	131	0.0002	61	0.0004	45	0.0004	44
37	everai-paravision-003	-	131	0.0002	57	0.0004	52	0.0004	42
38	glory-000	0.0000	8	0.0053	124	0.0013	109	0.1565	127
39	glory-001	0.0000	13	0.0051	123	0.0010	96	0.1651	128
40	gorilla-002	0.1347	35	0.0003	74	0.0004	72	0.0117	92
41	gorilla-003	0.1347	34	0.0003	73	0.0004	70	0.0043	78
42	hik-001	-	131	0.0000	23	0.0000	25	0.0000	21
43	hr-000	-	131	0.0003	69	0.0008	93	0.0034	73
44	hr-001	-	131	0.0001	39	0.0004	53	0.0003	38
45	id3-003	0.3032	52	0.0016	112	0.0011	106	0.0317	107
46	id3-004	-	131	0.0015	110	0.0011	105	-	131
47	idemia-003	0.0481	20	0.0000	31	0.0004	46	0.0042	77
48	idemia-004	-	131	0.0000	34	0.0004	49	0.0003	39
49	iit-000	-	131	0.0007	91	0.0011	100	0.0836	120
50	imagus-000	-	131	0.0010	102	0.0012	107	0.0347	110
51	imperial-000	-	131	0.0000	15	0.0000	17	0.0000	14
52	imperial-001	-	131	0.0000	26	0.0000	28	0.0000	24
53	incode-003	-	131	0.0004	86	0.0007	89	0.0014	64
54	incode-004	-	131	0.0004	85	0.0007	88	0.0014	63
55	innovatrics-004	0.1170	33	0.0000	37	0.0004	66	0.0041	76
56	innovatrics-005	-	131	0.0000	38	0.0004	65	0.0006	49
57	intellivision-001	0.5495	59	0.0048	122	0.0042	128	0.1358	124
58	iqface-000	0.0000	12	0.0000	22	0.0000	24	0.0000	20
59	isityou-000	0.4714	56	0.0023	113	0.0010	98	0.0663	118
60	isystems-001	0.1421	37	0.0010	100	0.0007	90	0.0128	94

Table 7: FTE is the proportion of failed template generation attempts. Failures can occur because the software throws an exception, or because the software electively refuses to process the input image. This would typically occur if a face is not detected. FTE is measured as the number of function calls that give EITHER a non-zero error code OR that give a “small” template. This is defined as one whose size is less than 0.3 times the median template size for that algorithm. This second rule is needed because some algorithms incorrectly fail to return a non-zero error code when template generation fails.

<sup>1</sup>The effects of FTE are included in the accuracy results of this report by regarding any template comparison involving a failed template to produce a low similarity score. Thus higher FTE results in higher FNMR and lower FMR.

	Algorithm Name	Failure to Enrol Rate <sup>1</sup>							
		CHILD-EXPLOIT	MUGSHOT	VISA	WILD				
61	isystems-002	0.1421	38	0.0010	101	0.0007	91	0.0128	95
62	itmo-005	0.1353	36	0.0005	88	0.0002	32	0.0075	85
63	itmo-006	-	131	0.0004	84	0.0004	63	0.0006	52
64	kakao-001	-	131	0.0002	62	0.0005	77	0.0310	105
65	kakao-002	-	131	0.0002	63	0.0005	81	0.0310	106
66	kedacom-000	-	131	0.0000	12	0.0000	13	0.0000	10
67	kneron-003	-	131	0.0044	121	0.0016	115	0.1823	129
68	lookman-002	-	131	0.0000	21	0.0000	23	0.0000	19
69	lookman-004	-	131	0.0000	18	0.0000	20	0.0000	16
70	megvii-001	0.0274	19	0.0007	94	0.0004	51	0.0152	97
71	megvii-002	0.0274	18	0.0054	125	0.0004	50	0.0126	93
72	meiya-001	-	131	0.0004	87	0.0010	99	0.0025	70
73	microfocus-001	0.0791	31	0.0008	96	0.0016	114	0.0220	103
74	microfocus-002	0.0791	30	0.0008	95	0.0016	113	0.0220	102
75	mt-000	-	131	0.0002	60	0.0004	68	0.0004	40
76	neurotechnology-005	-	131	0.0004	78	0.0004	55	0.0018	66
77	neurotechnology-006	0.1068	32	0.0004	79	0.0004	56	0.0018	67
78	nodeflux-000	-	131	0.0001	48	0.0002	33	0.0003	34
79	nodeflux-001	-	131	0.0001	49	0.0002	34	0.0003	35
80	notiontag-000	-	131	0.0000	16	0.0000	18	0.0000	15
81	ntechlab-006	-	131	0.0000	30	0.0004	43	0.0003	33
82	ntechlab-007	0.0682	29	0.0001	40	0.0004	47	0.0005	47
83	pixelall-002	-	131	0.0000	9	0.0000	10	0.0001	31
84	psl-001	0.0000	14	0.0000	27	0.0000	29	0.0000	25
85	psl-002	-	131	0.0000	11	0.0000	12	0.0000	9
86	rankone-006	-	131	0.0000	25	0.0000	27	0.0000	23
87	rankone-007	-	131	0.0003	68	0.0004	69	0.0043	79
88	realnetworks-002	-	131	0.0004	77	0.0003	37	0.0004	41
89	realnetworks-003	-	131	0.0004	76	0.0003	36	0.0004	43
90	remarkai-000	-	131	0.0000	3	0.0000	3	0.0000	29
91	remarkai-001	-	131	0.0000	17	0.0000	19	0.0000	30
92	saffe-001	0.0000	15	0.0000	14	0.0000	16	0.0000	13
93	saffe-002	-	131	0.0000	24	0.0000	26	0.0000	22
94	sensetime-001	0.0631	28	0.0000	33	0.0004	58	0.0003	36
95	sensetime-002	0.3345	54	0.0011	104	0.0005	84	0.0218	101
96	shaman-000	0.0000	5	0.0000	20	0.0000	22	0.0000	18
97	shaman-001	0.0000	1	0.0000	1	0.0000	1	0.0000	27
98	siat-002	0.0616	25	0.0000	36	0.0004	61	0.0048	81
99	siat-004	-	131	0.0000	35	0.0004	60	0.0003	37
100	smilart-002	0.2422	47	0.0003	72	0.0011	102	0.0575	116
101	smilart-003	-	131	0.0014	108	0.0013	110	0.0555	115
102	starhybrid-001	-	131	0.0009	99	0.0023	120	0.0044	80
103	synesis-004	-	131	0.0164	130	0.0035	125	0.0485	113
104	synesis-005	-	131	0.0001	45	0.0005	74	0.0021	68
105	tech5-001	0.0000	2	0.0004	80	0.0003	39	0.0409	112
106	tech5-002	-	131	0.0001	43	0.0003	35	0.0000	28
107	tevian-003	0.2430	49	0.0003	65	0.0005	85	0.0076	86
108	tevian-004	-	131	0.0002	59	0.0005	82	0.0057	82
109	tiger-002	0.0619	26	0.0001	52	0.0004	57	0.0082	90
110	tiger-003	0.0619	27	0.0001	50	0.0004	54	0.0082	89
111	tongyi-005	-	131	0.0000	5	0.0000	6	0.0000	4
112	toshiba-002	0.0000	16	0.0000	8	0.0000	9	0.0000	7
113	toshiba-003	-	131	0.0001	53	0.0001	31	0.0002	32
114	upc-001	-	131	0.0003	64	0.0003	41	0.0011	62
115	vd-001	-	131	0.0004	83	0.0009	94	0.0024	69
116	veridas-001	-	131	0.0001	51	0.0005	78	0.0006	50
117	veridas-002	-	131	0.0001	54	0.0005	80	0.0006	51
118	videonetics-001	-	131	0.0015	109	0.0010	97	0.0112	91
119	vigilantsolutions-006	-	131	0.0001	42	0.0004	48	0.0005	46
120	vigilantsolutions-007	-	131	0.0001	41	0.0004	44	0.0005	45

Table 8: FTE is the proportion of failed template generation attempts. Failures can occur because the software throws an exception, or because the software electively refuses to process the input image. This would typically occur if a face is not detected. FTE is measured as the number of function calls that give EITHER a non-zero error code OR that give a “small” template. This is defined as one whose size is less than 0.3 times the median template size for that algorithm. This second rule is needed because some algorithms incorrectly fail to return a non-zero error code when template generation fails.

<sup>1</sup>The effects of FTE are included in the accuracy results of this report by regarding any template comparison involving a failed template to produce a low similarity score. Thus higher FTE results in higher FNMR and lower FMR.

	Algorithm Name	Failure to Enrol Rate <sup>1</sup>					
		CHILD-EXPLOIT	MUGSHOT	VISA	WILD		
121	vion-000	0.6388	61	0.0130	129	0.0078	130
122	visionbox-000	-	131	0.0005	90	0.0011	104
123	visionbox-001	-	131	0.0005	89	0.0011	103
124	visionlabs-006	-	131	0.0003	71	0.0005	79
125	visionlabs-007	0.1939	45	0.0003	70	0.0005	76
126	vocord-006	-	131	0.0003	67	0.0003	40
127	vocord-007	0.0000	6	0.0001	56	0.0004	42
128	winsense-000	-	131	0.0000	7	0.0000	8
129	yisheng-004	0.4279	55	0.0013	105	0.0006	87
130	yitu-003	-	131	0.0009	98	0.0000	4
						0.0000	2

Table 9: FTE is the proportion of failed template generation attempts. Failures can occur because the software throws an exception, or because the software electively refuses to process the input image. This would typically occur if a face is not detected. FTE is measured as the number of function calls that give EITHER a non-zero error code OR that give a “small” template. This is defined as one whose size is less than 0.3 times the median template size for that algorithm. This second rule is needed because some algorithms incorrectly fail to return a non-zero error code when template generation fails.

<sup>1</sup>The effects of FTE are included in the accuracy results of this report by regarding any template comparison involving a failed template to produce a low similarity score. Thus higher FTE results in higher FNMR and lower FMR.

### 3.4 Recognition accuracy

Core algorithm accuracy is stated via:

▷ **Cooperative subjects**

- The summary table of Figure 6;
- The visa image DETs of Figure 23;
- The mugshot DETs of Figure 30;
- The mugshot ageing profiles of Figure 110;
- The human-difficult pairs of Figure 9

▷ **Non-cooperative subjects**

- The photojournalism DET of Figure 36
- The child-exploitation DET of Figure 39;
- The child-exploitation CMC of Figure 41.

Figure 89 shows dependence of false match rate on algorithm score threshold. This allows a deployer to set a threshold to target a particular false match rate appropriate to the security objectives of the application.

Figure 75 likewise shows FMR(T) but for mugshots, and specially four subsets of the population.

Note that in both the mugshot and visa sets false match rates vary with the ethnicity, age, and sex, of the enrollee and impostor - see section 3.6. For example figure 49 summarizes FMR for impostors paired from four groups black females, black males, white females, white males.

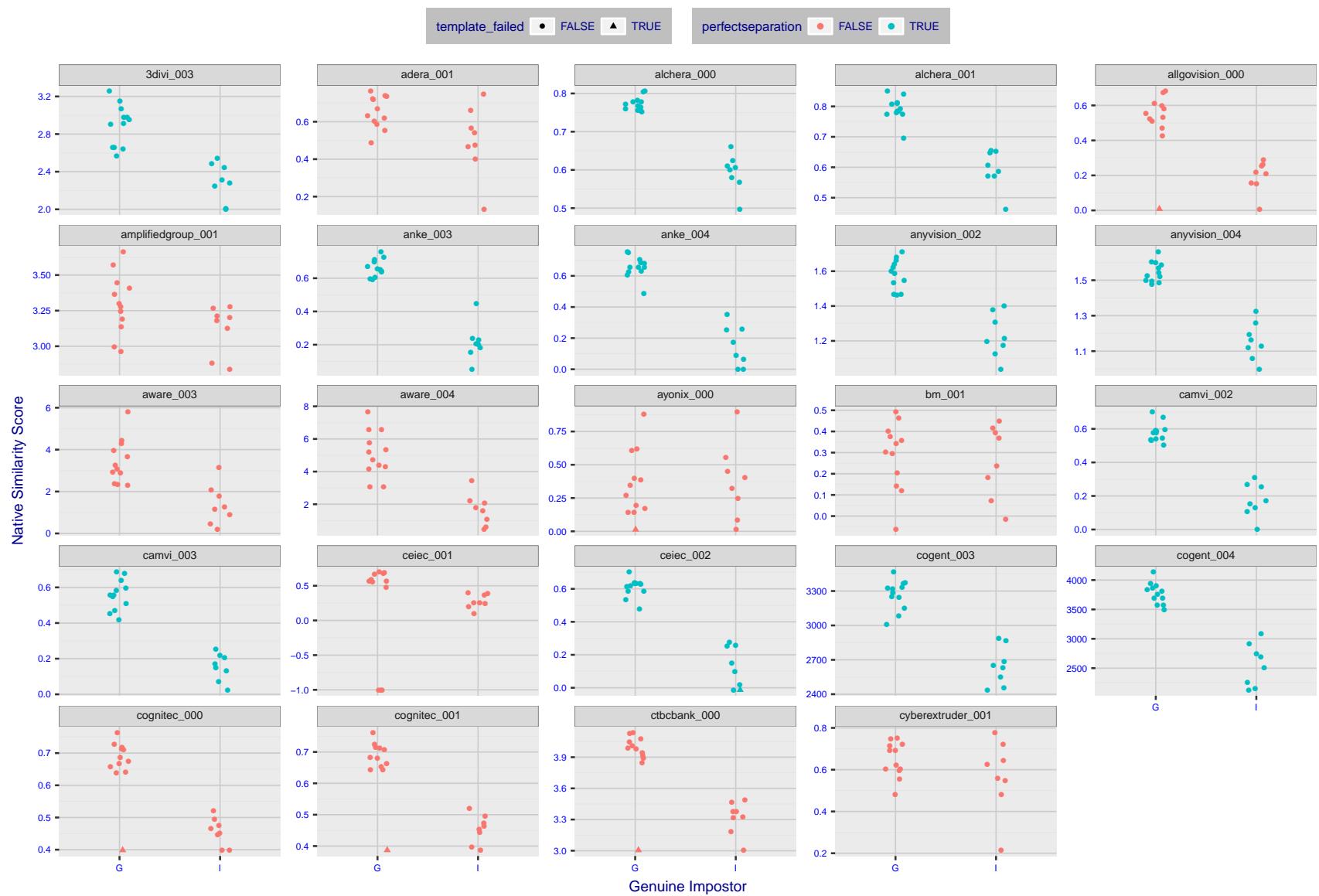


Figure 4: The Figure shows, in blue, algorithms that correctly separate the 12 genuine and 8 impostor pairs used in the May 2018 paper [Face recognition accuracy of forensic examiners, superrecognizers, and face recognition algorithms](#) (Phillips et al. [1]). In red are algorithms that are imperfect. Some algorithms fail only because they failed to make a template e.g. due to face detection failure (shown as a triangle). Others fail because the pairs were selected for that study because they had been difficult for three leading algorithms used in FRVT 2006. Caution: Given the small sample size ( $n=20$ ) the figure may change substantially if larger or different sets were used.

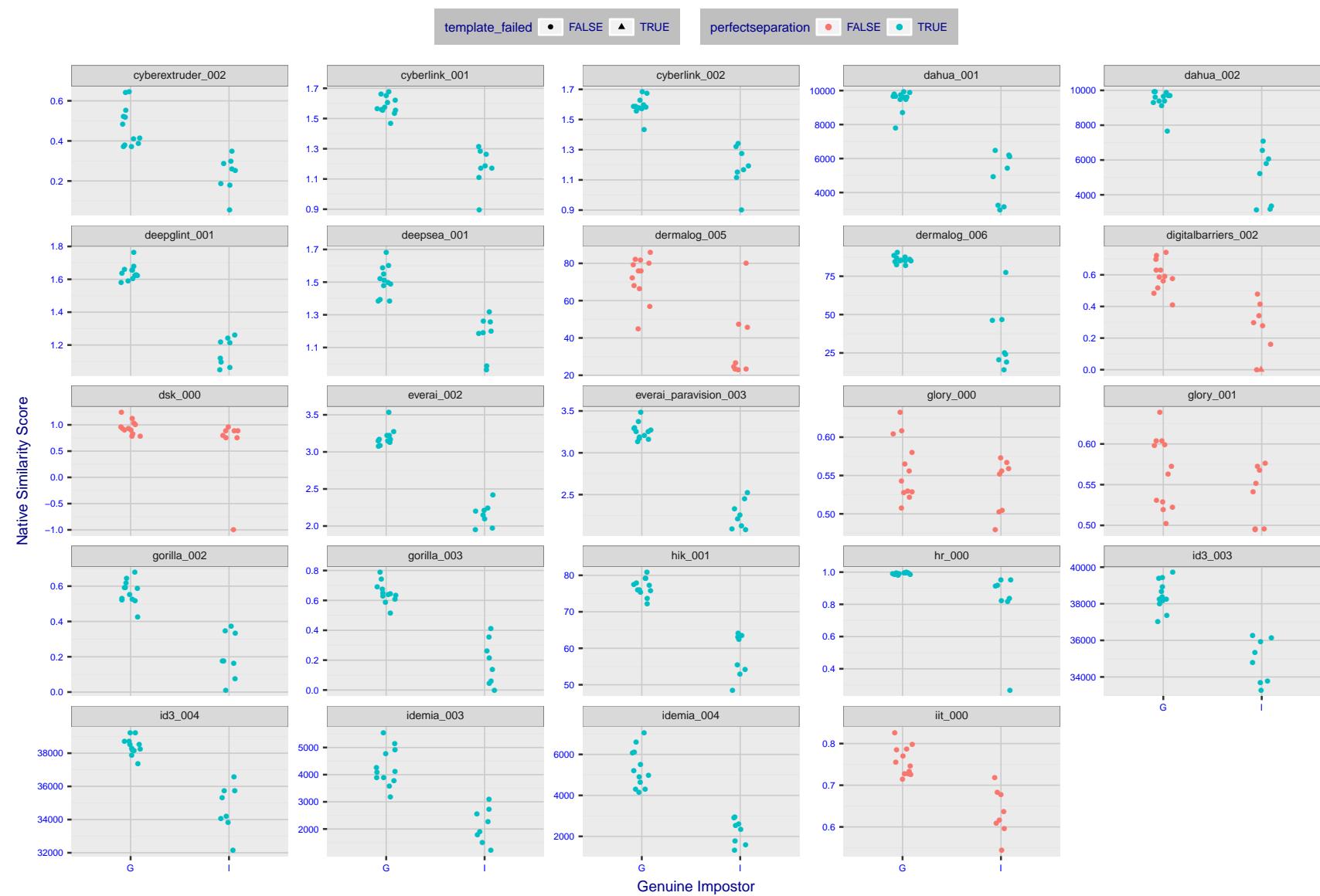


Figure 5: The Figure shows, in blue, algorithms that correctly separate the 12 genuine and 8 impostor pairs used in the May 2018 paper [Face recognition accuracy of forensic examiners, superrecognizers, and face recognition algorithms](#) (Phillips et al. [1]). In red are algorithms that are imperfect. Some algorithms fail only because they failed to make a template e.g. due to face detection failure (shown as a triangle). Others fail because the pairs were selected for that study because they had been difficult for three leading algorithms used in FRVT 2006. Caution: Given the small sample size ( $n=20$ ) the figure may change substantially if larger or different sets were used.

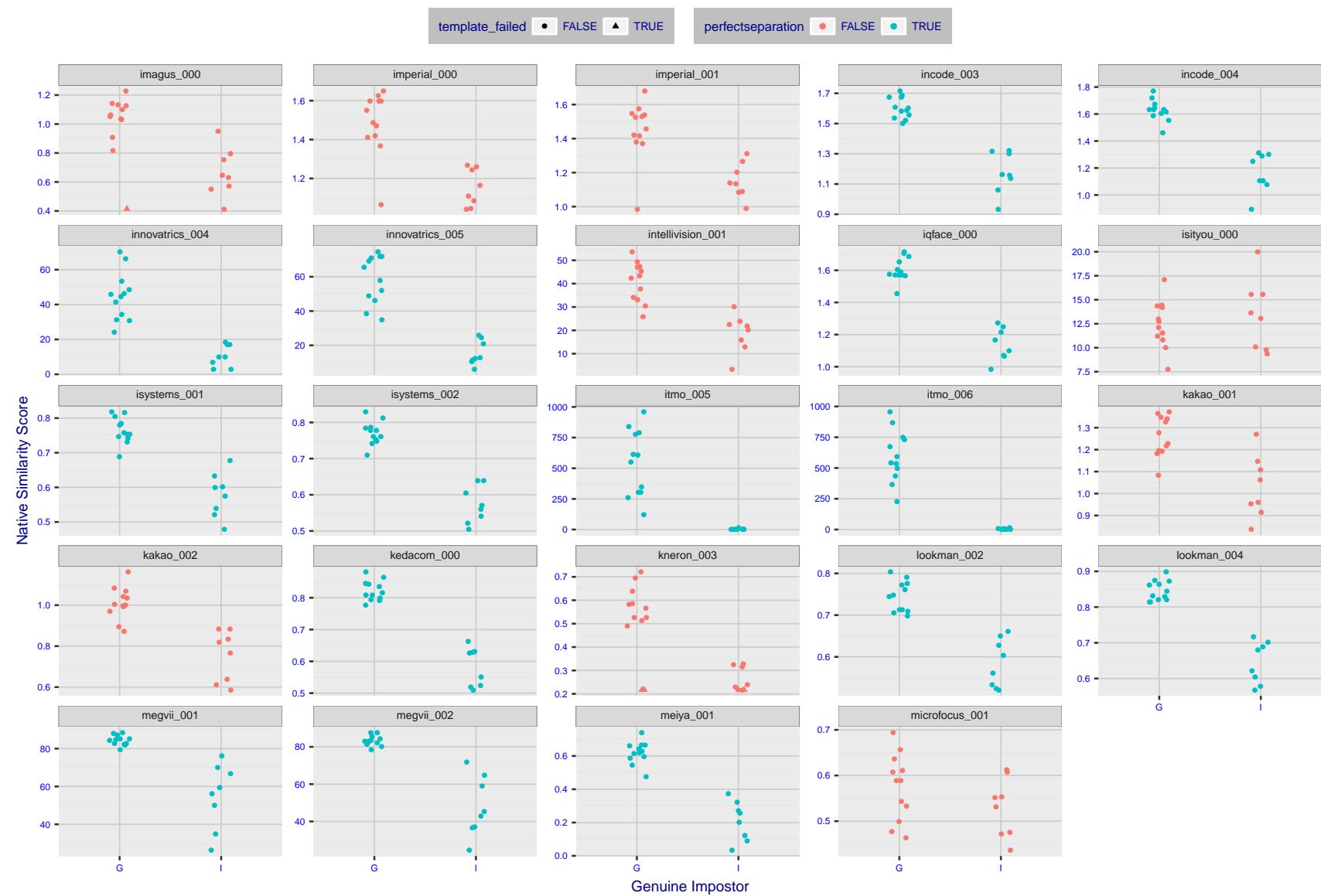


Figure 6: The Figure shows, in blue, algorithms that correctly separate the 12 genuine and 8 impostor pairs used in the May 2018 paper [Face recognition accuracy of forensic examiners, superrecognizers, and face recognition algorithms](#) (Phillips et al. [1]). In red are algorithms that imperfect. Some algorithms fail only because they failed to make a template e.g. due to face detection failure (shown as a triangle). Others fail because the pairs were selected for that study because they had been difficult for three leading algorithms used in FRVT 2006. Caution: Given the small sample size ( $n=20$ ) the figure may change substantially if larger or different sets were used.

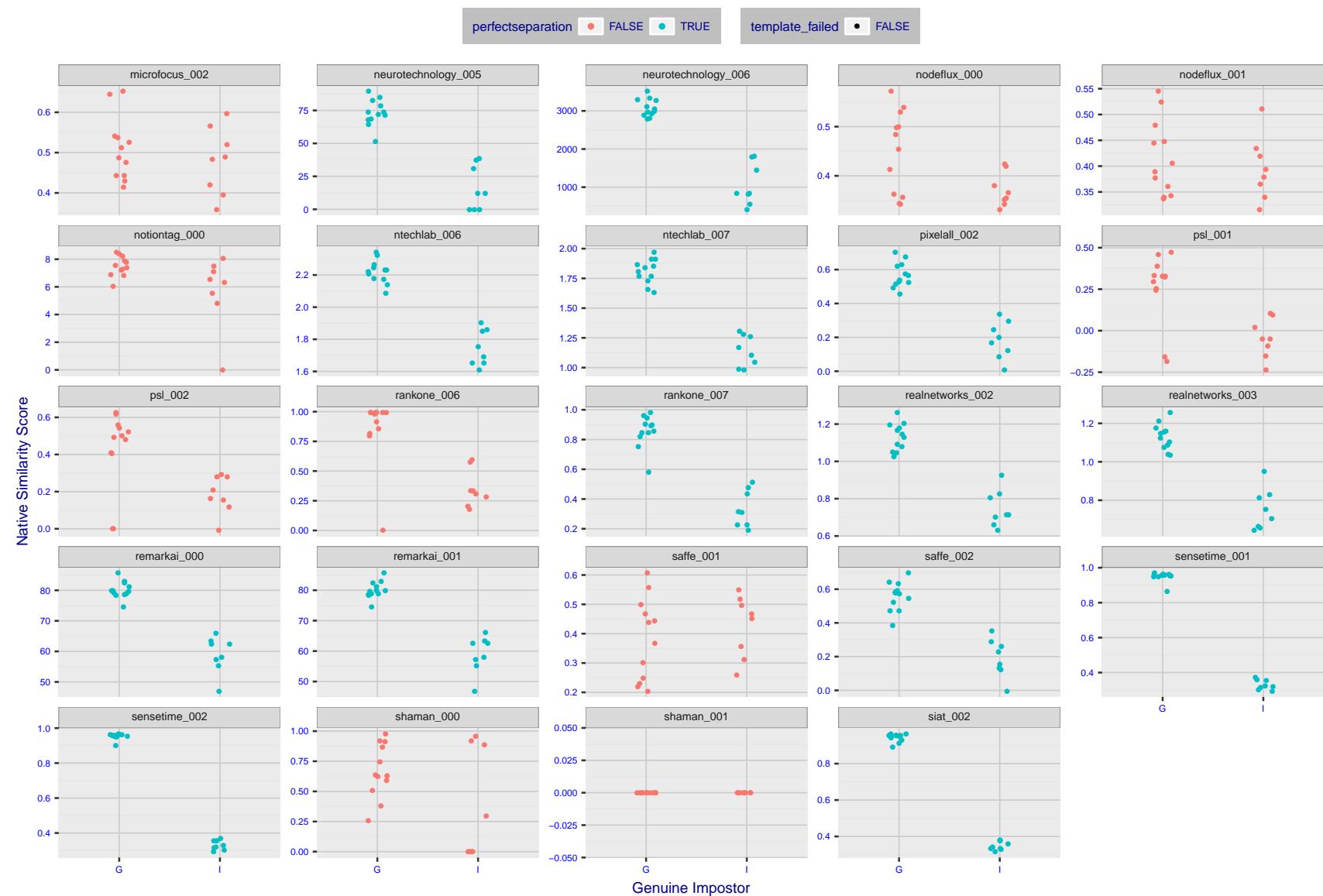


Figure 7: The Figure shows, in blue, algorithms that correctly separate the 12 genuine and 8 impostor pairs used in the May 2018 paper Face recognition accuracy of forensic examiners, superrecognizers, and face recognition algorithms (Phillips et al. [1]). In red are algorithms that are imperfect. Some algorithms fail only because they failed to make a template e.g. due to face detection failure (shown as a triangle). Others fail because the pairs were selected for that study because they had been difficult for three leading algorithms used in FRVT 2006. Caution: Given the small sample size ( $n=20$ ) the figure may change substantially if larger or different sets were used.

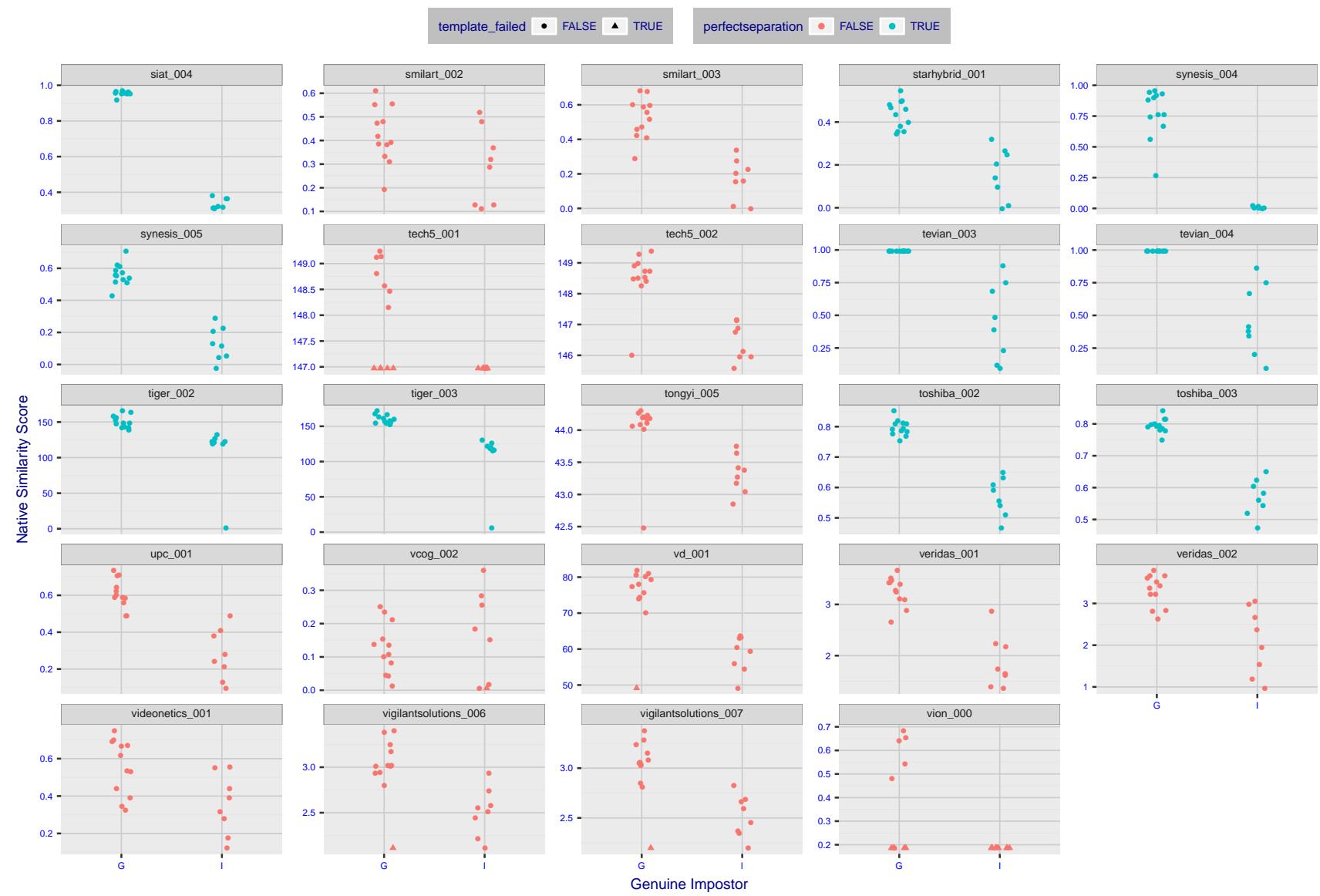


Figure 8: The Figure shows, in blue, algorithms that correctly separate the 12 genuine and 8 impostor pairs used in the May 2018 paper [Face recognition accuracy of forensic examiners, superrecognizers, and face recognition algorithms](#) (Phillips et al. [1]). In red are algorithms that are imperfect. Some algorithms fail only because they failed to make a template e.g. due to face detection failure (shown as a triangle). Others fail because the pairs were selected for that study because they had been difficult for three leading algorithms used in FRVT 2006. Caution: Given the small sample size ( $n=20$ ) the figure may change substantially if larger or different sets were used.

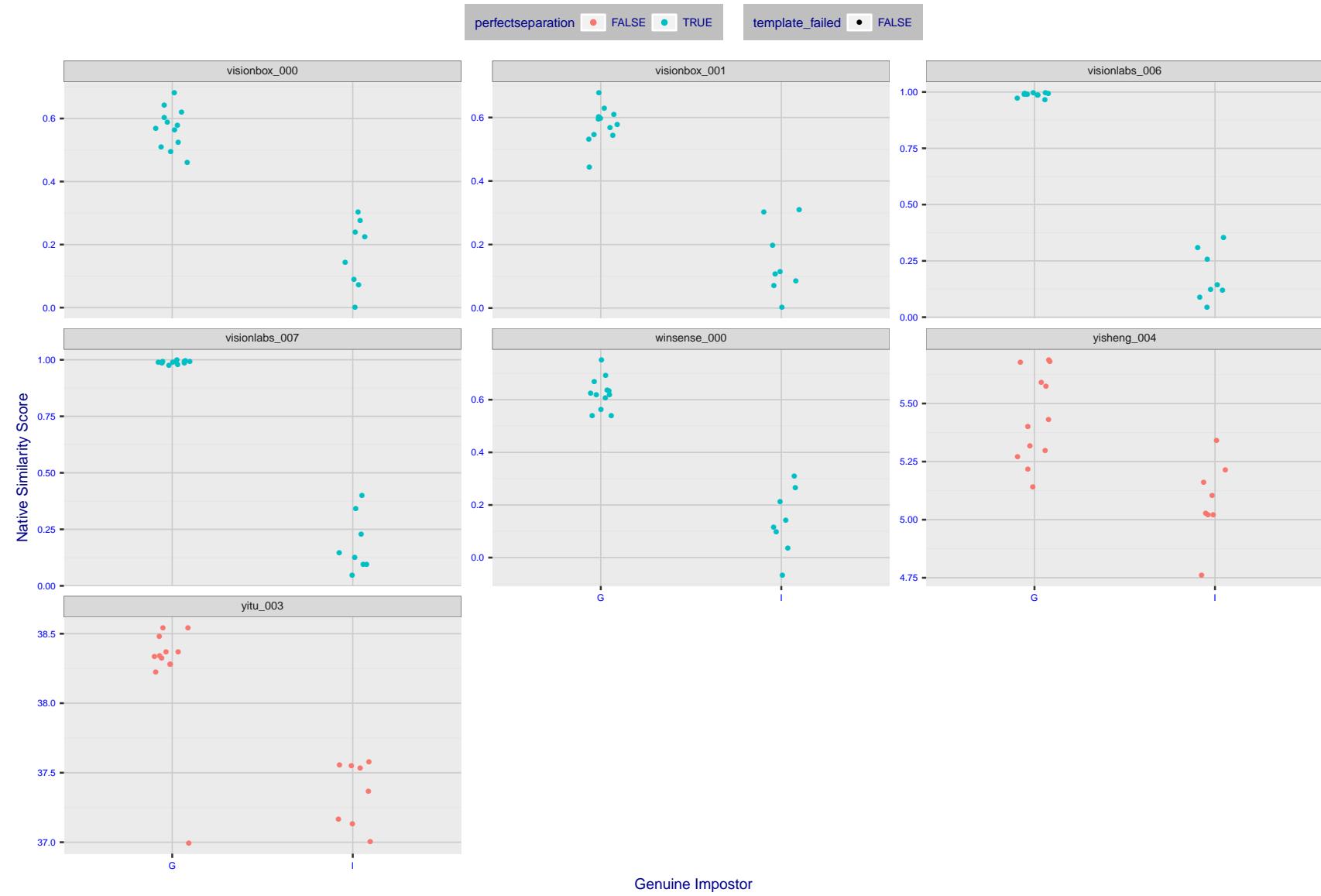


Figure 9: The Figure shows, in blue, algorithms that correctly separate the 12 genuine and 8 impostor pairs used in the May 2018 paper [Face recognition accuracy of forensic examiners, superrecognizers, and face recognition algorithms](#) (Phillips et al. [1]). In red are algorithms that are imperfect. Some algorithms fail only because they failed to make a template e.g. due to face detection failure (shown as a triangle). Others fail because the pairs were selected for that study because they had been difficult for three leading algorithms used in FRVT 2006. Caution: Given the small sample size ( $n=20$ ) the figure may change substantially if larger or different sets were used.

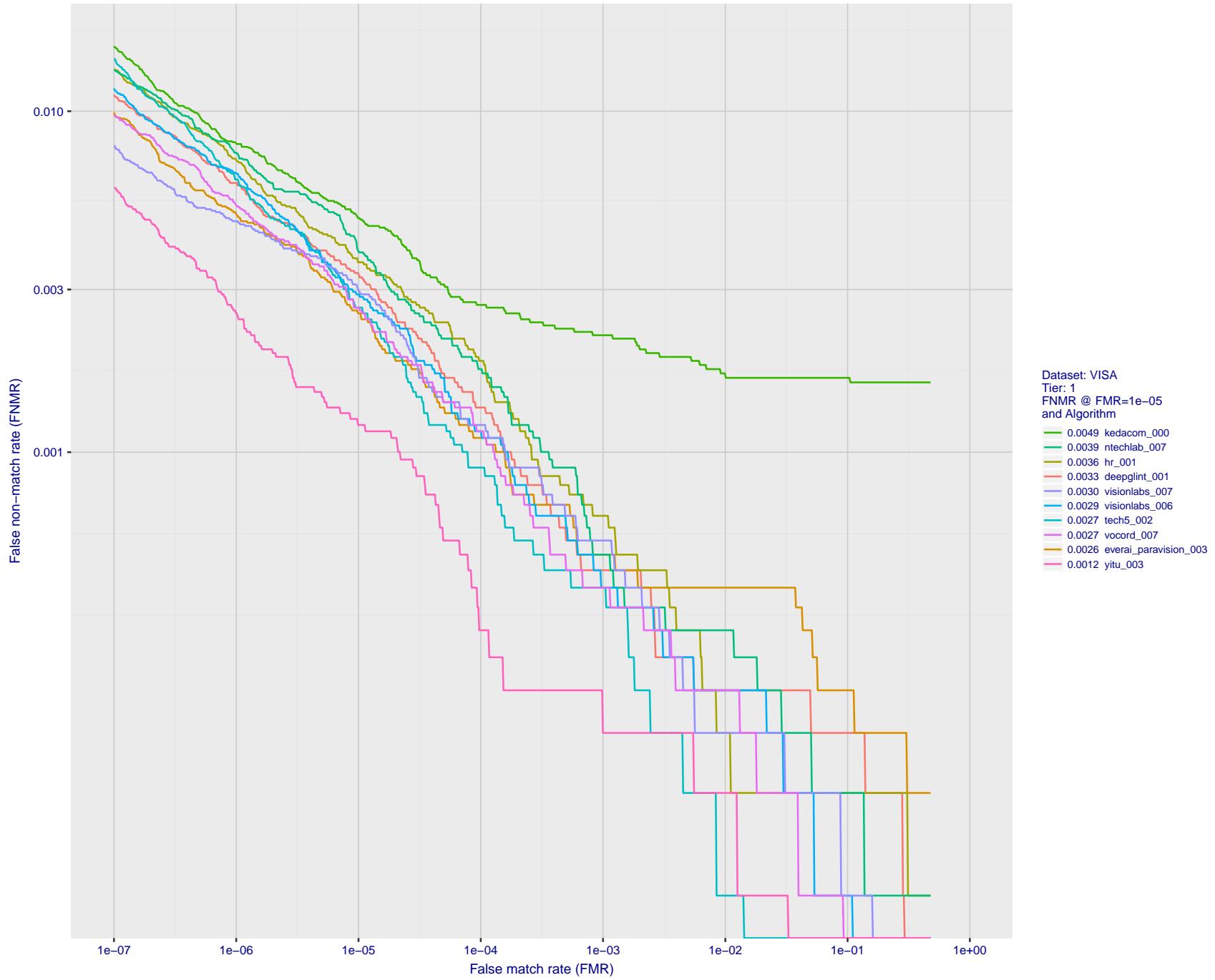


Figure 10: For the visa images, detection error tradeoff (DET) characteristics showing false non-match rate vs. false match rate plotted parametrically on threshold,  $T$ . The scales are logarithmic in order to show many decades of FMR.

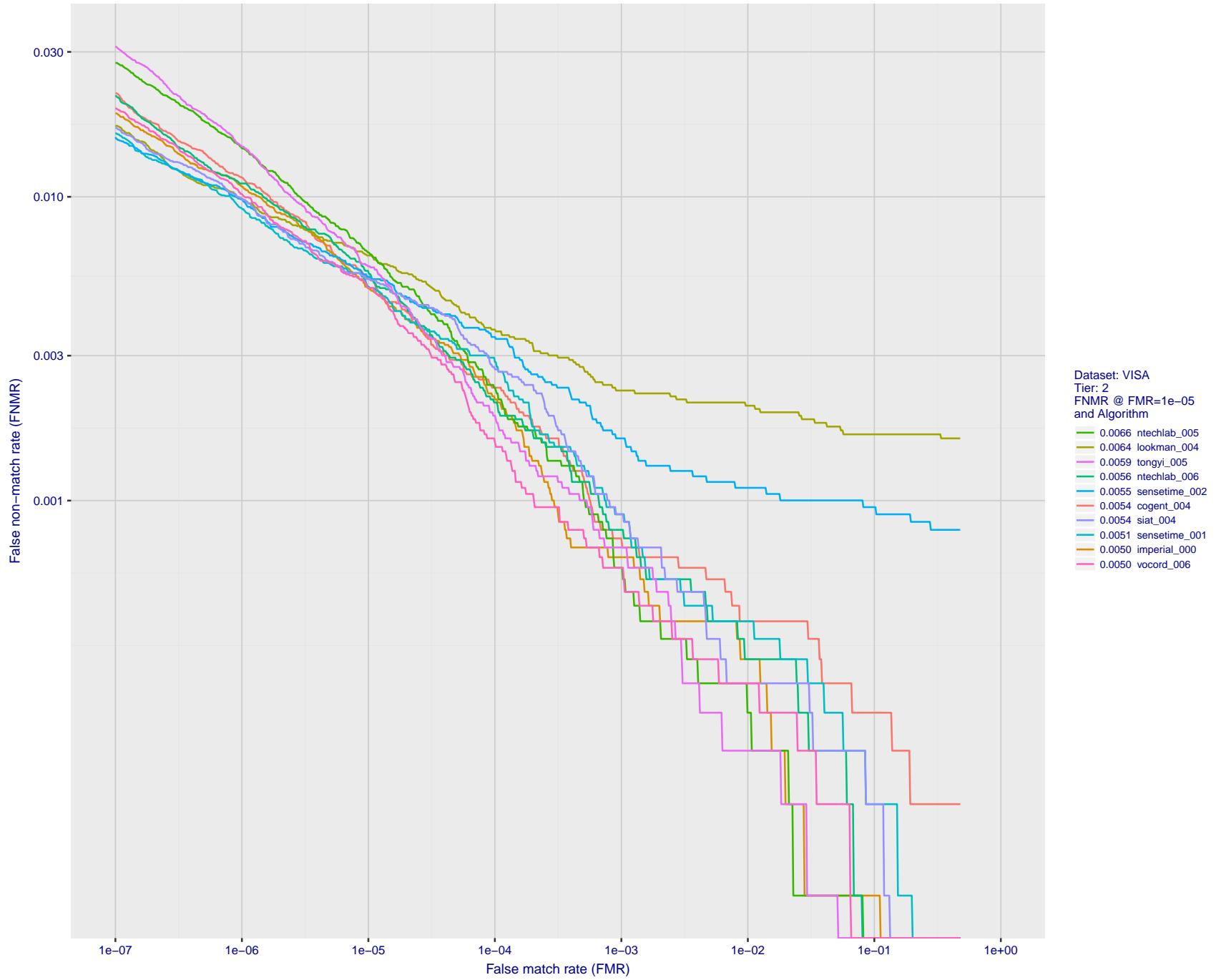


Figure 11: For the visa images, detection error tradeoff (DET) characteristics showing false non-match rate vs. false match rate plotted parametrically on threshold,  $T$ . The scales are logarithmic in order to show many decades of FMR.

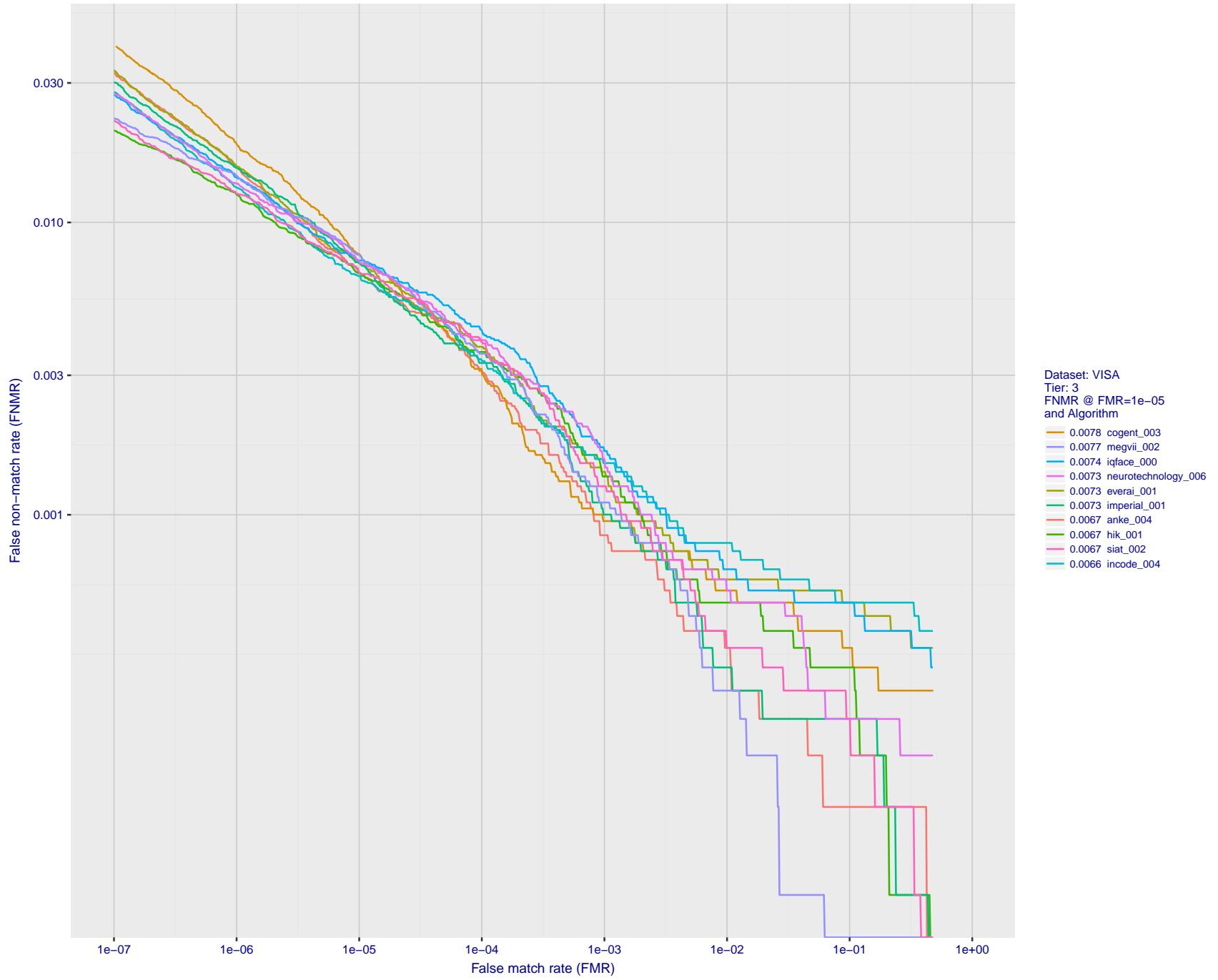


Figure 12: For the visa images, detection error tradeoff (DET) characteristics showing false non-match rate vs. false match rate plotted parametrically on threshold,  $T$ . The scales are logarithmic in order to show many decades of FMR.

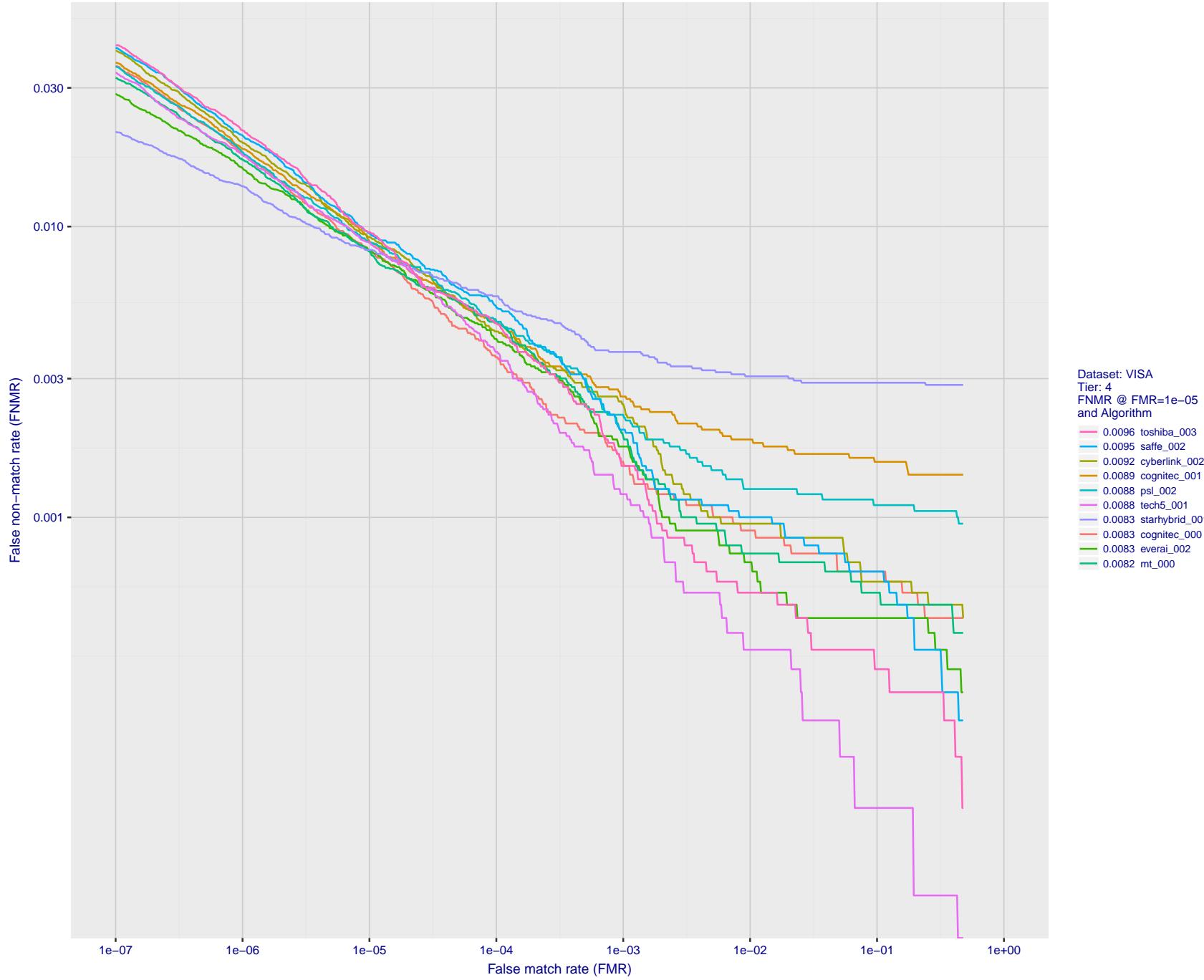


Figure 13: For the visa images, detection error tradeoff (DET) characteristics showing false non-match rate vs. false match rate plotted parametrically on threshold,  $T$ . The scales are logarithmic in order to show many decades of FMR.

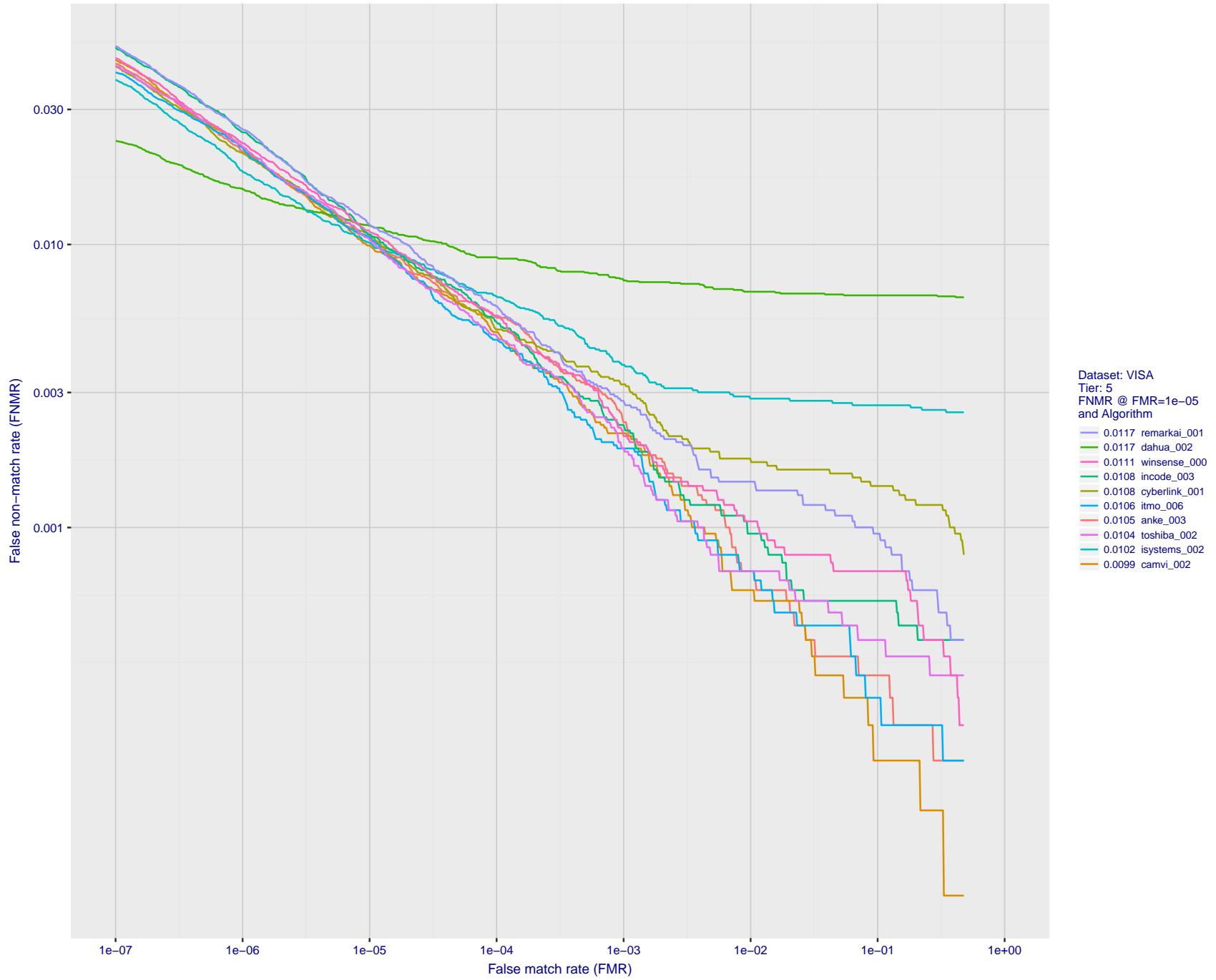


Figure 14: For the visa images, detection error tradeoff (DET) characteristics showing false non-match rate vs. false match rate plotted parametrically on threshold,  $T$ . The scales are logarithmic in order to show many decades of FMR.

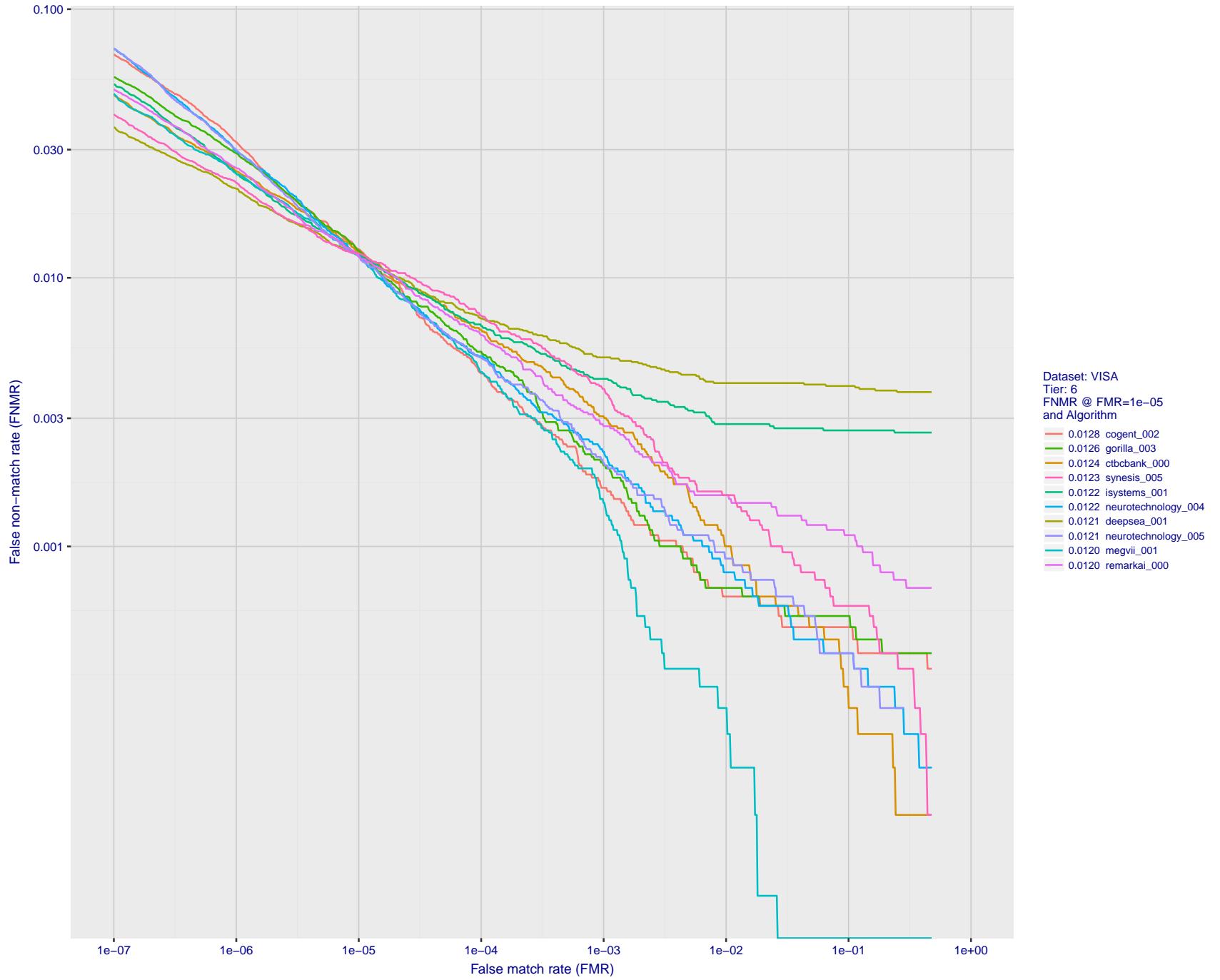


Figure 15: For the visa images, detection error tradeoff (DET) characteristics showing false non-match rate vs. false match rate plotted parametrically on threshold,  $T$ . The scales are logarithmic in order to show many decades of FMR.

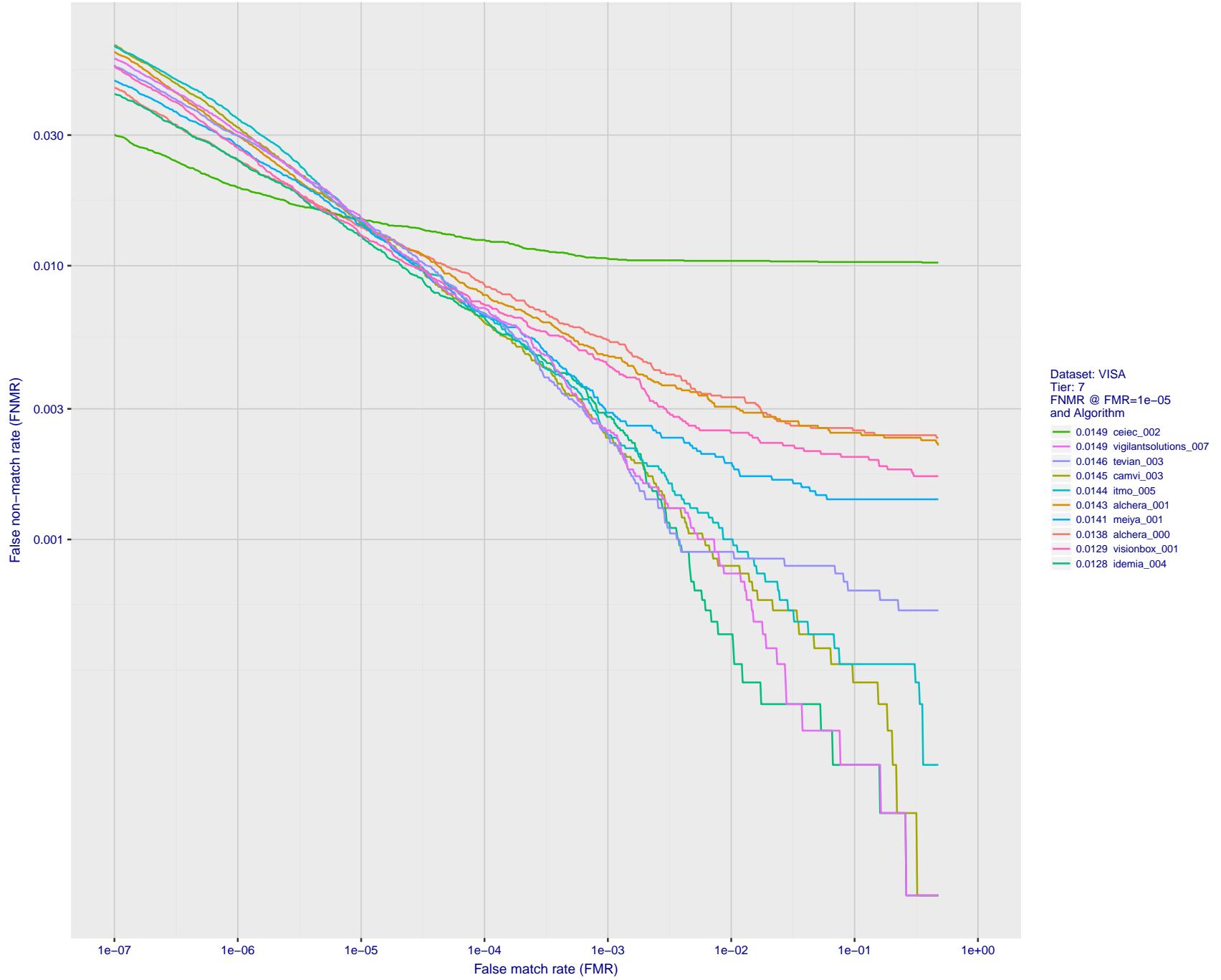


Figure 16: For the visa images, detection error tradeoff (DET) characteristics showing false non-match rate vs. false match rate plotted parametrically on threshold,  $T$ . The scales are logarithmic in order to show many decades of FMR.

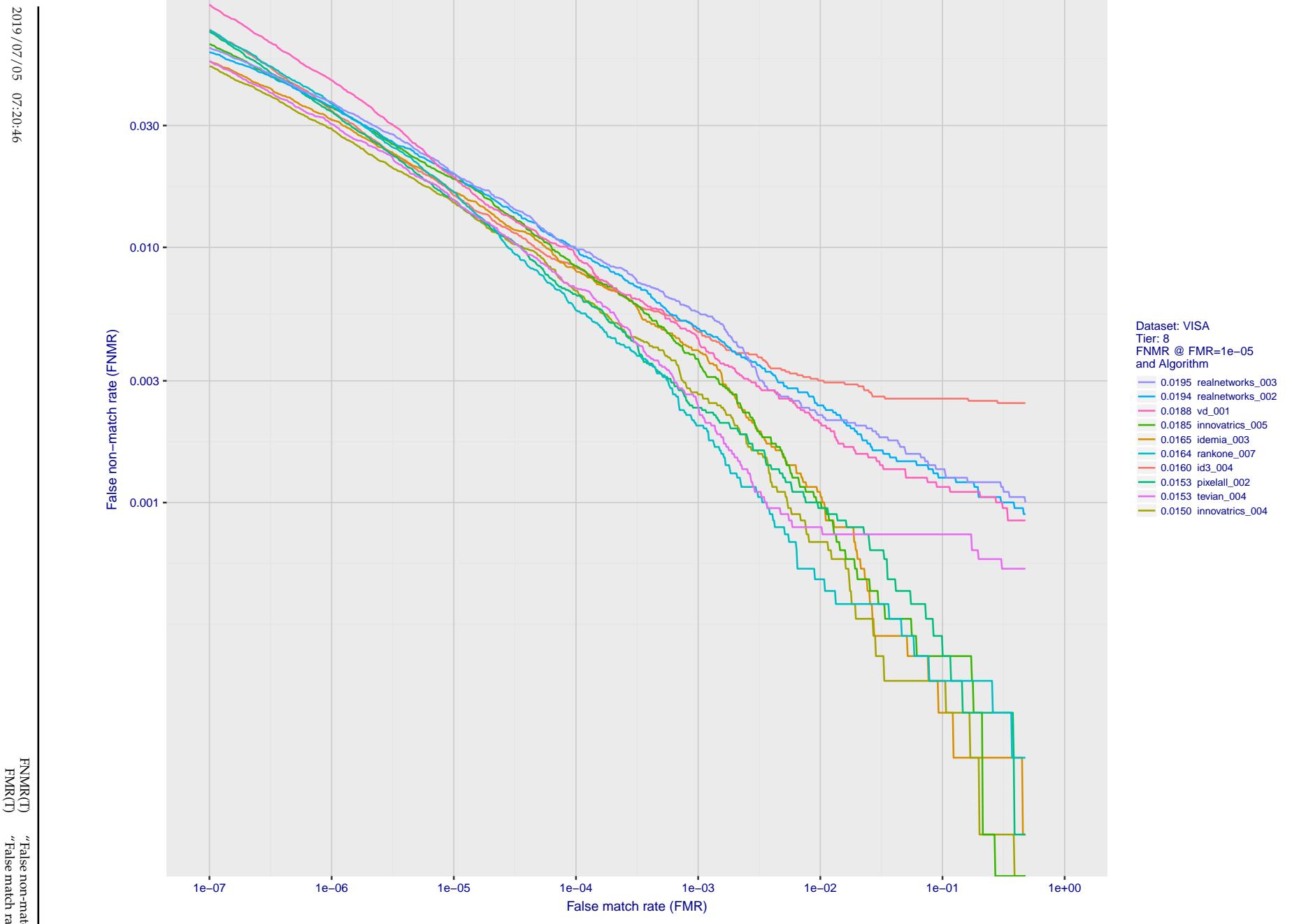


Figure 17: For the visa images, detection error tradeoff (DET) characteristics showing false non-match rate vs. false match rate plotted parametrically on threshold,  $T$ . The scales are logarithmic in order to show many decades of FMR.

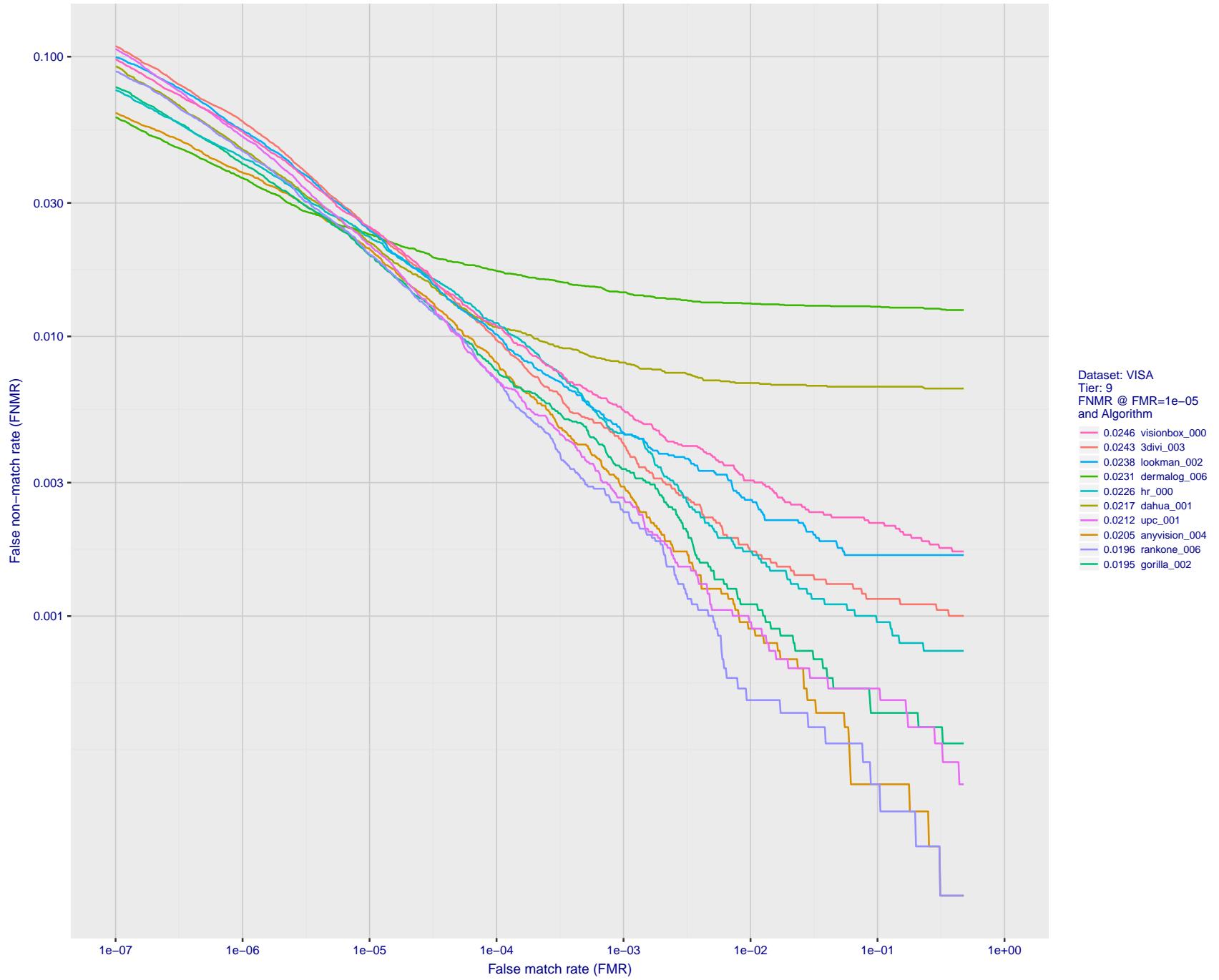


Figure 18: For the visa images, detection error tradeoff (DET) characteristics showing false non-match rate vs. false match rate plotted parametrically on threshold,  $T$ . The scales are logarithmic in order to show many decades of FMR.

2019/07/05 07:20:46

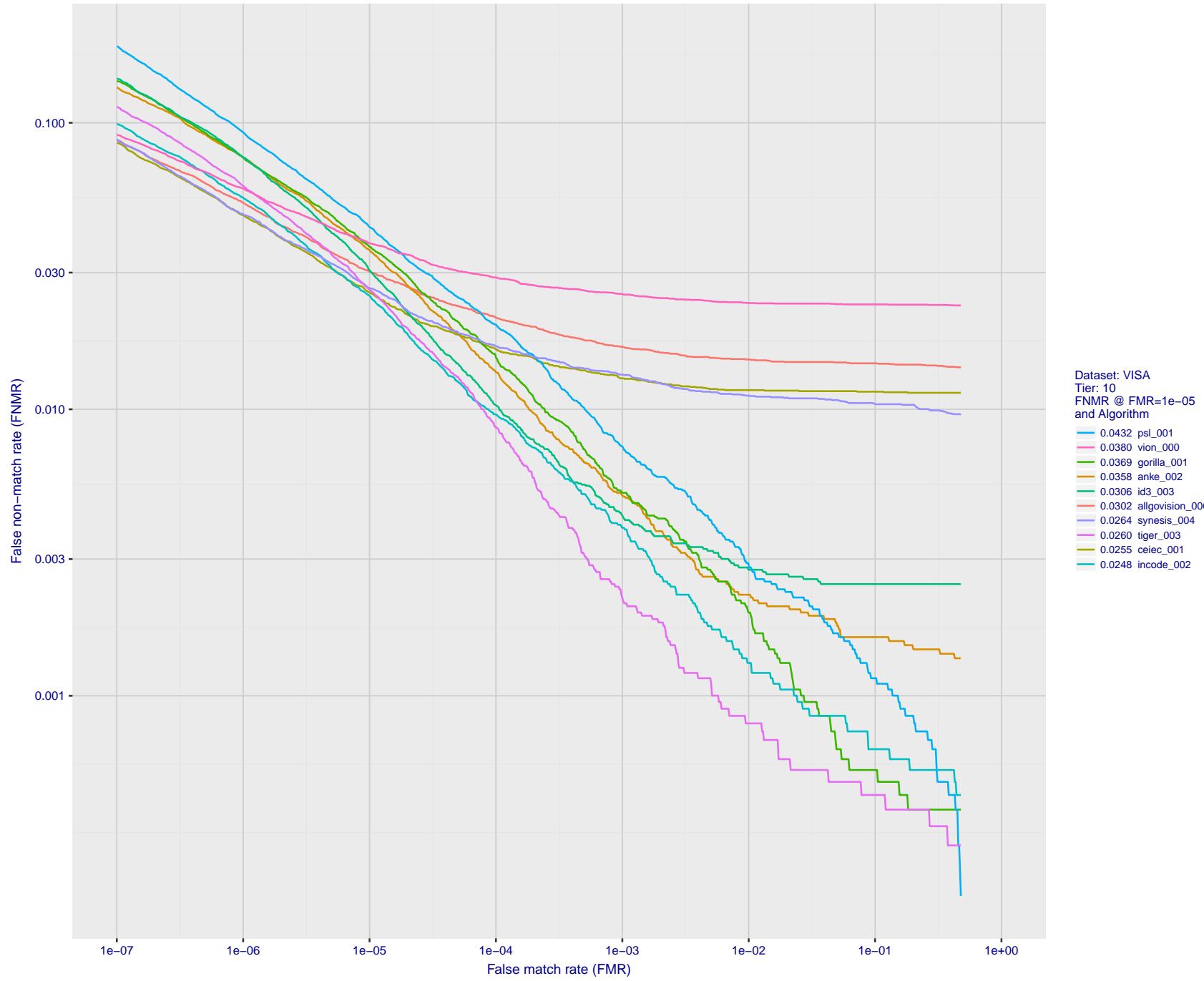


Figure 19: For the visa images, detection error tradeoff (DET) characteristics showing false non-match rate vs. false match rate plotted parametrically on threshold,  $T$ . The scales are logarithmic in order to show many decades of FMR.

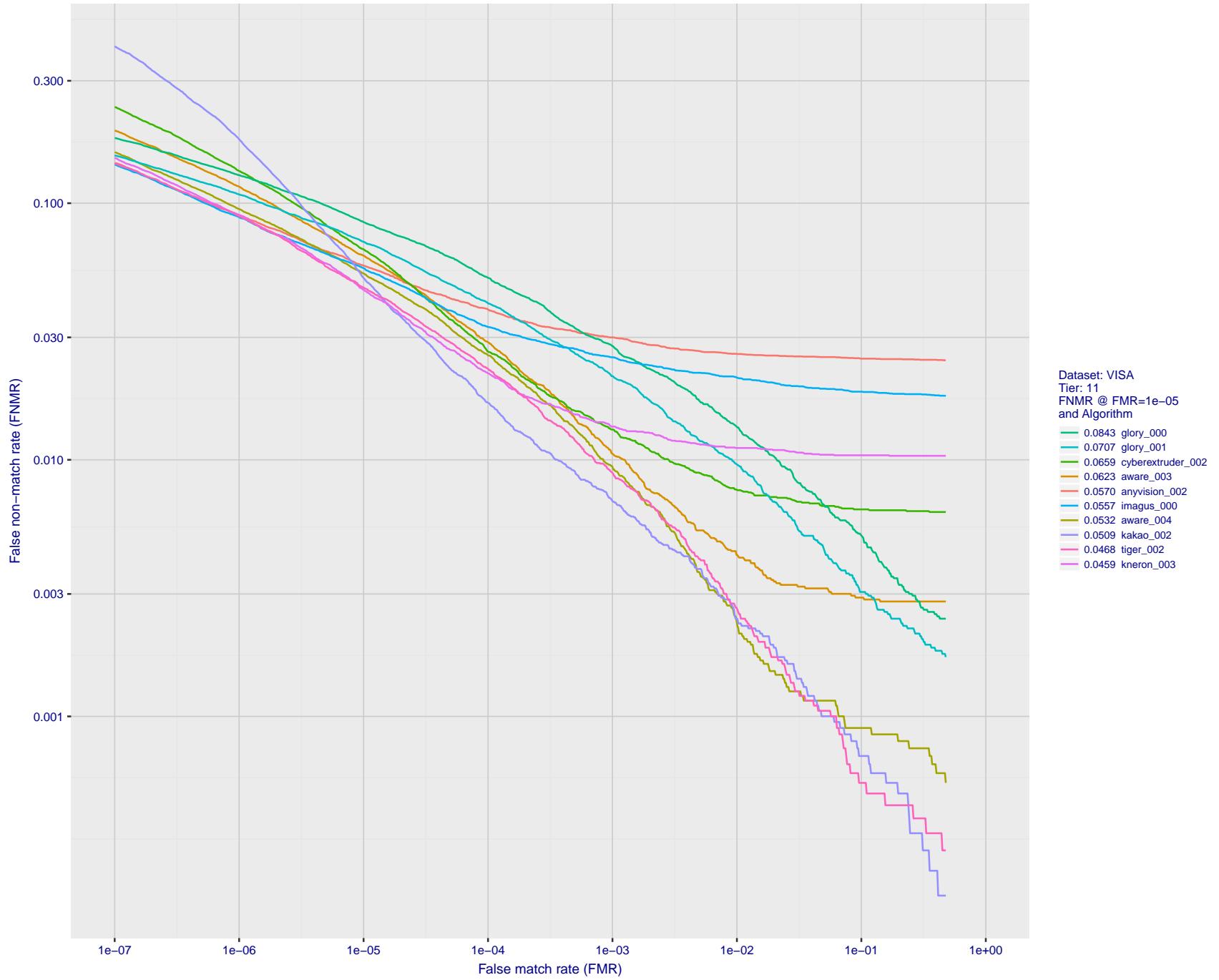


Figure 20: For the visa images, detection error tradeoff (DET) characteristics showing false non-match rate vs. false match rate plotted parametrically on threshold,  $T$ . The scales are logarithmic in order to show many decades of FMR.

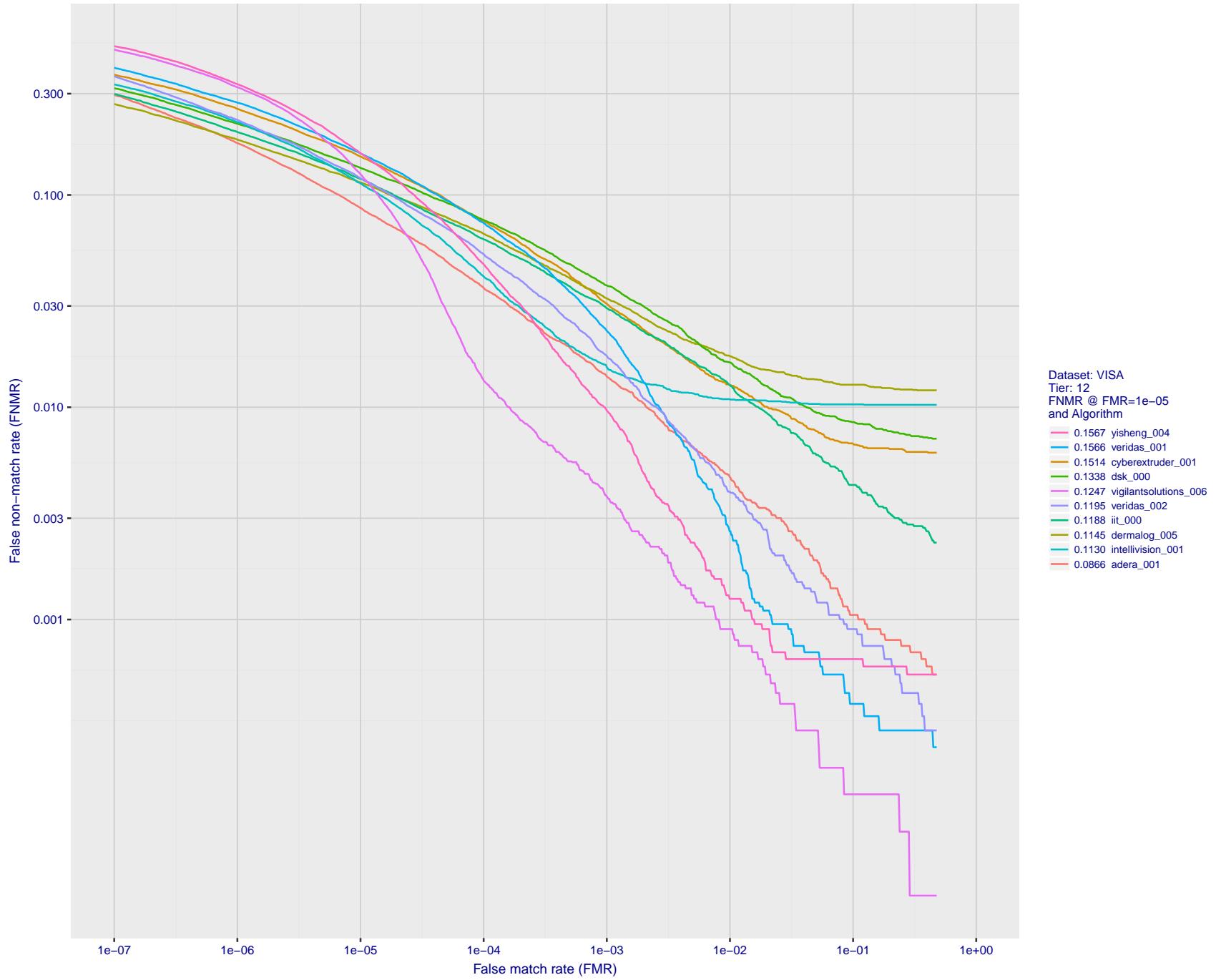


Figure 21: For the visa images, detection error tradeoff (DET) characteristics showing false non-match rate vs. false match rate plotted parametrically on threshold,  $T$ . The scales are logarithmic in order to show many decades of FMR.

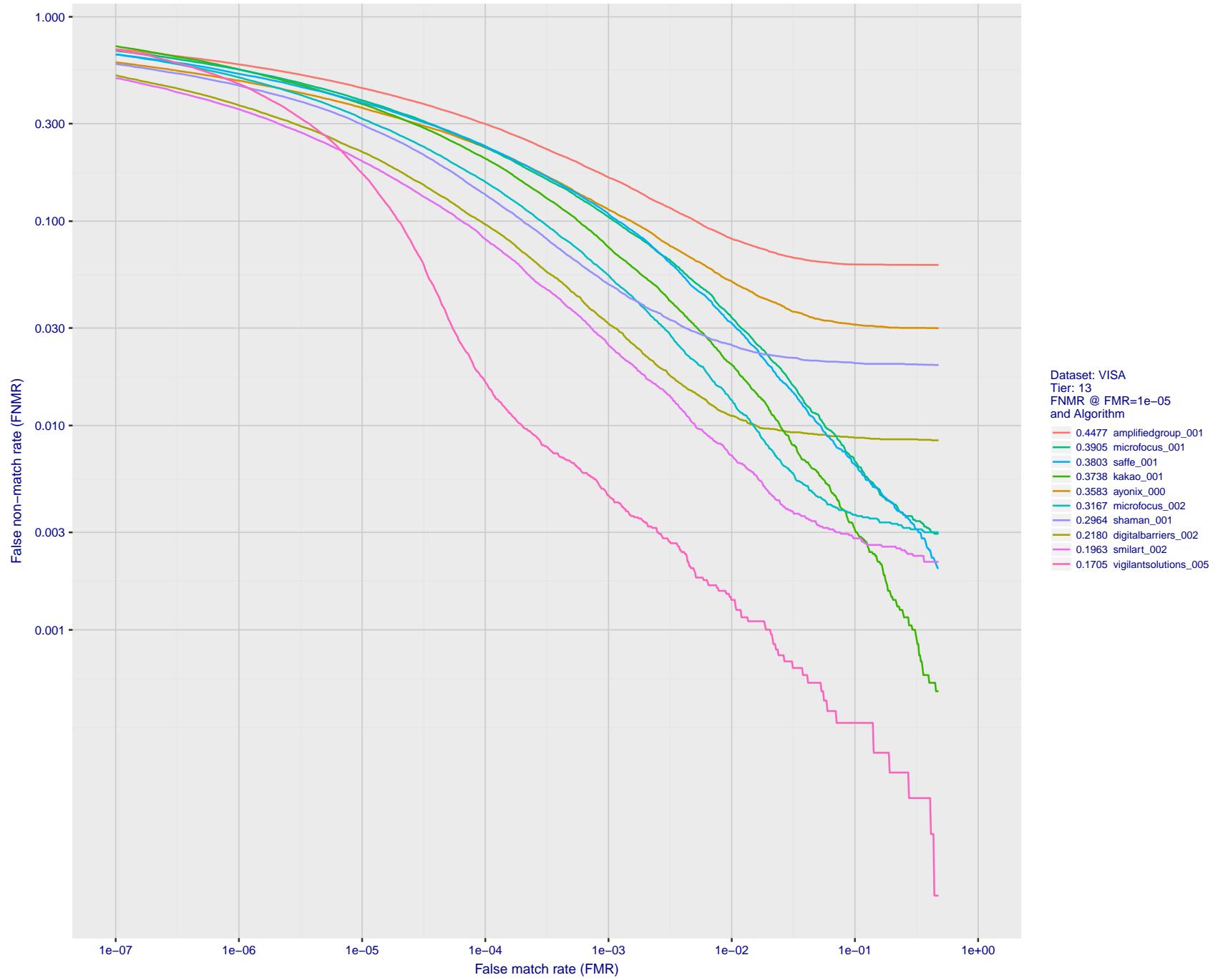


Figure 22: For the visa images, detection error tradeoff (DET) characteristics showing false non-match rate vs. false match rate plotted parametrically on threshold,  $T$ . The scales are logarithmic in order to show many decades of FMR.

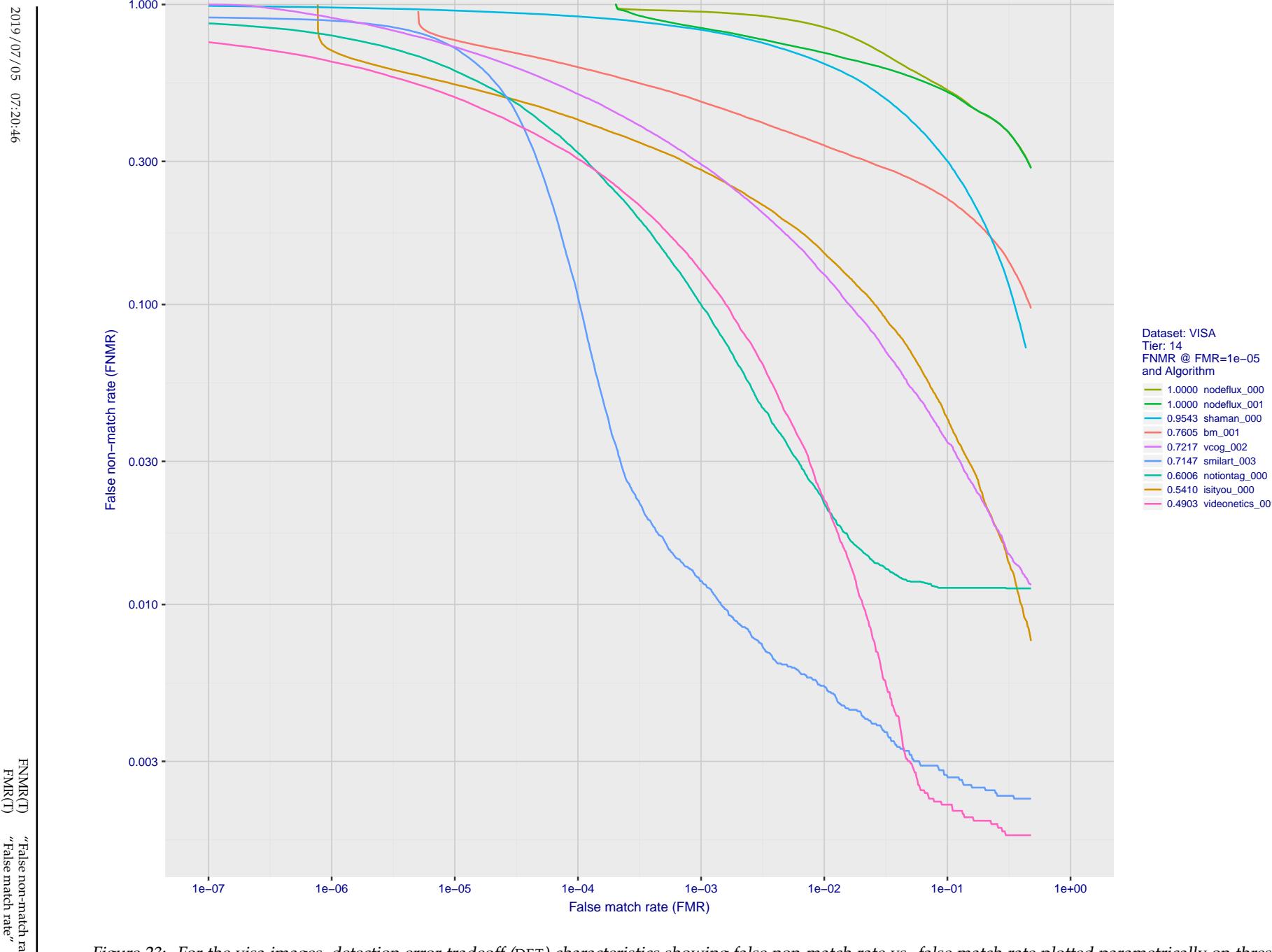


Figure 23: For the visa images, detection error tradeoff (DET) characteristics showing false non-match rate vs. false match rate plotted parametrically on threshold,  $T$ . The scales are logarithmic in order to show many decades of FMR.

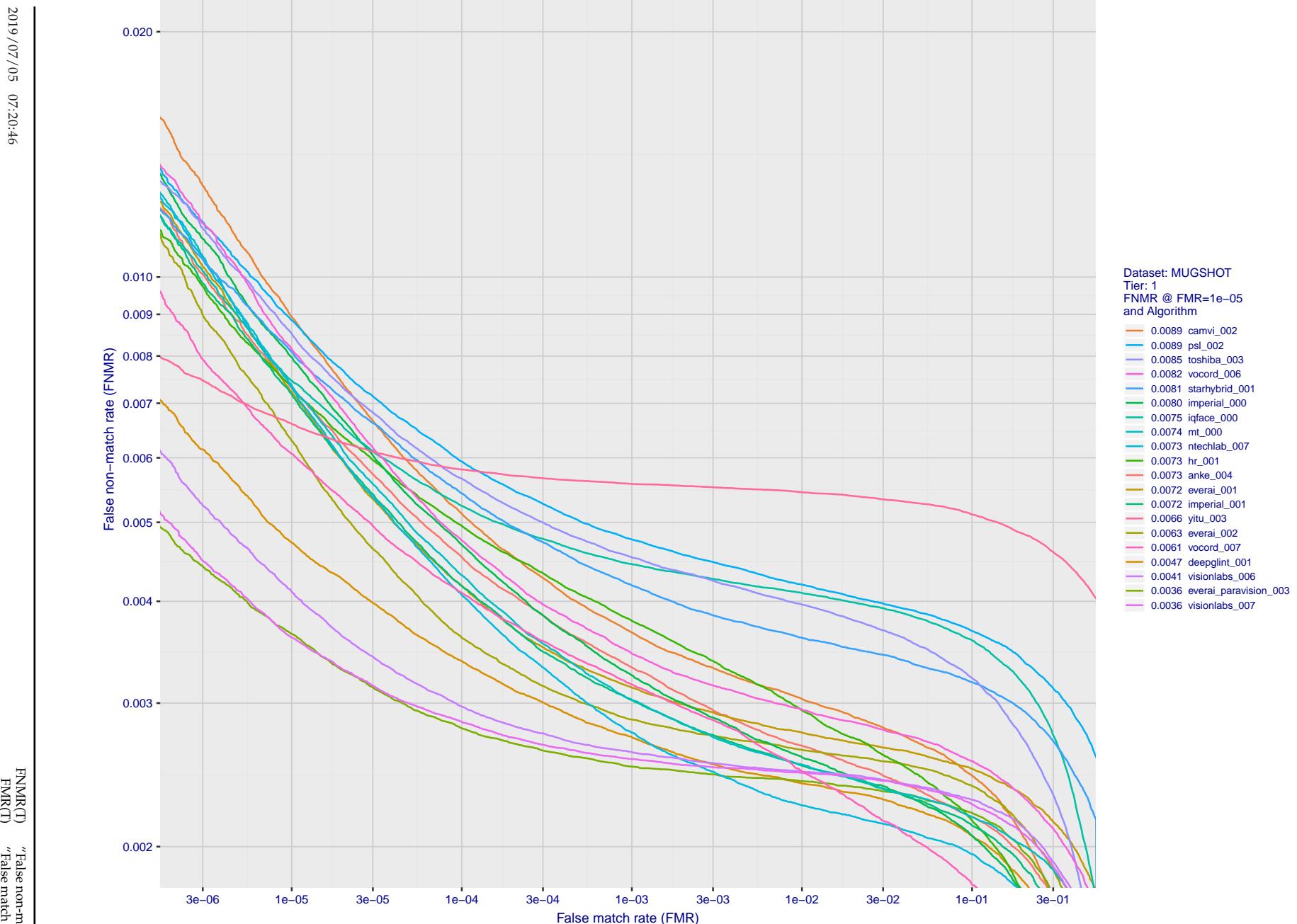


Figure 24: For the mugshot images, detection error tradeoff (DET) characteristics showing false non-match rate vs. false match rate plotted parametrically on threshold, T. The scales are logarithmic in order to show decades of FMR.

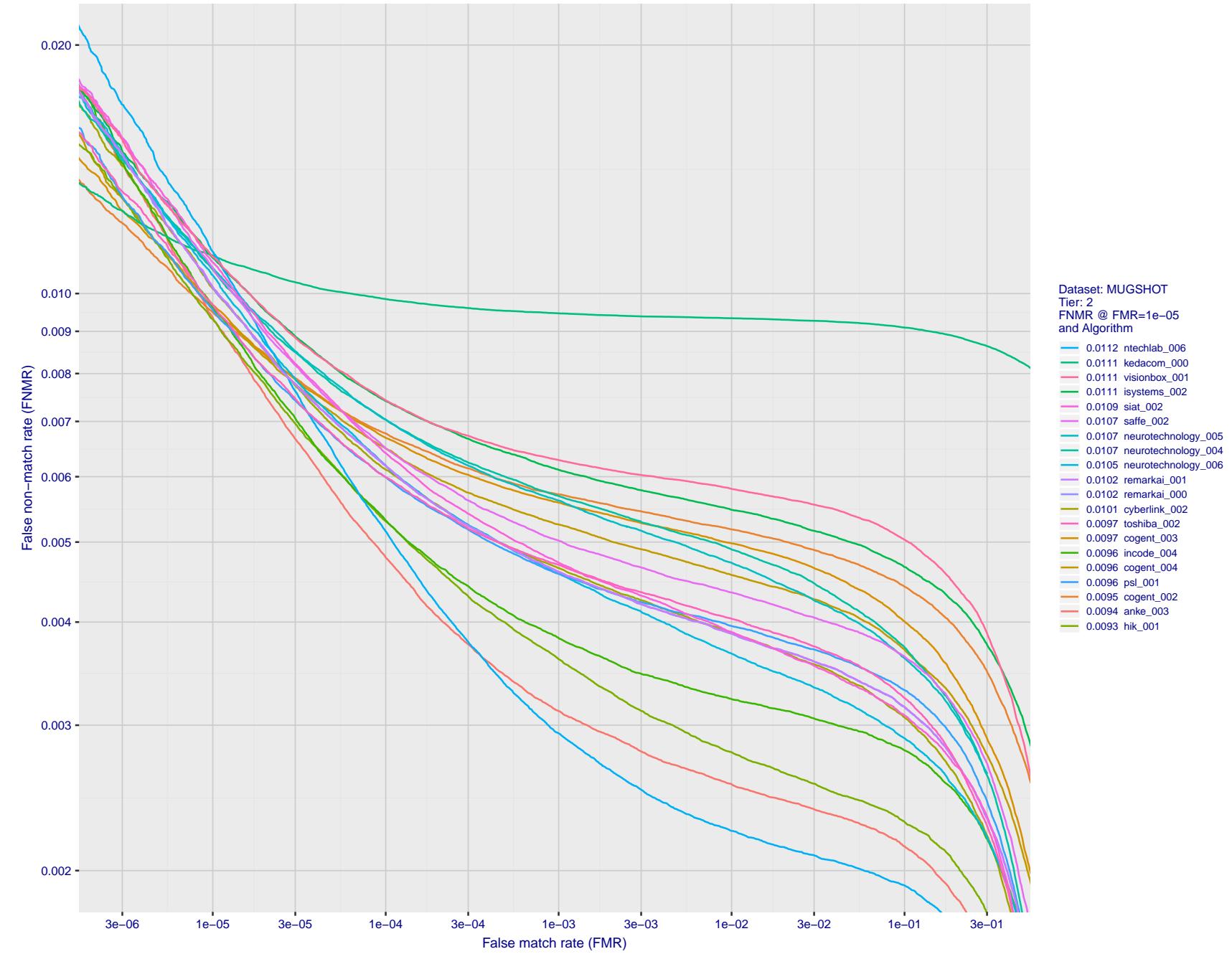


Figure 25: For the mugshot images, detection error tradeoff (DET) characteristics showing false non-match rate vs. false match rate plotted parametrically on threshold,  $T$ . The scales are logarithmic in order to show decades of FMR.

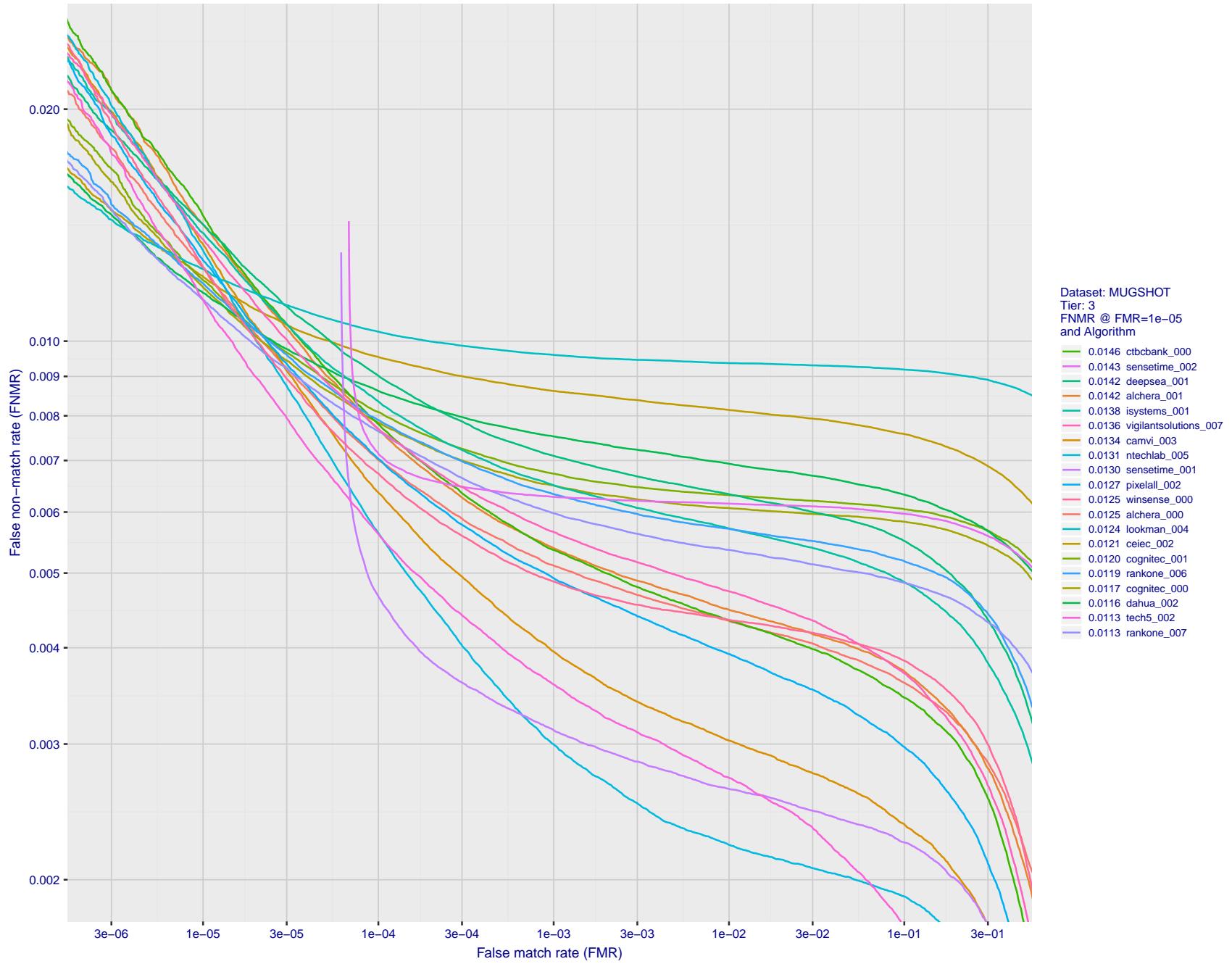


Figure 26: For the mugshot images, detection error tradeoff (DET) characteristics showing false non-match rate vs. false match rate plotted parametrically on threshold,  $T$ . The scales are logarithmic in order to show decades of FMR.

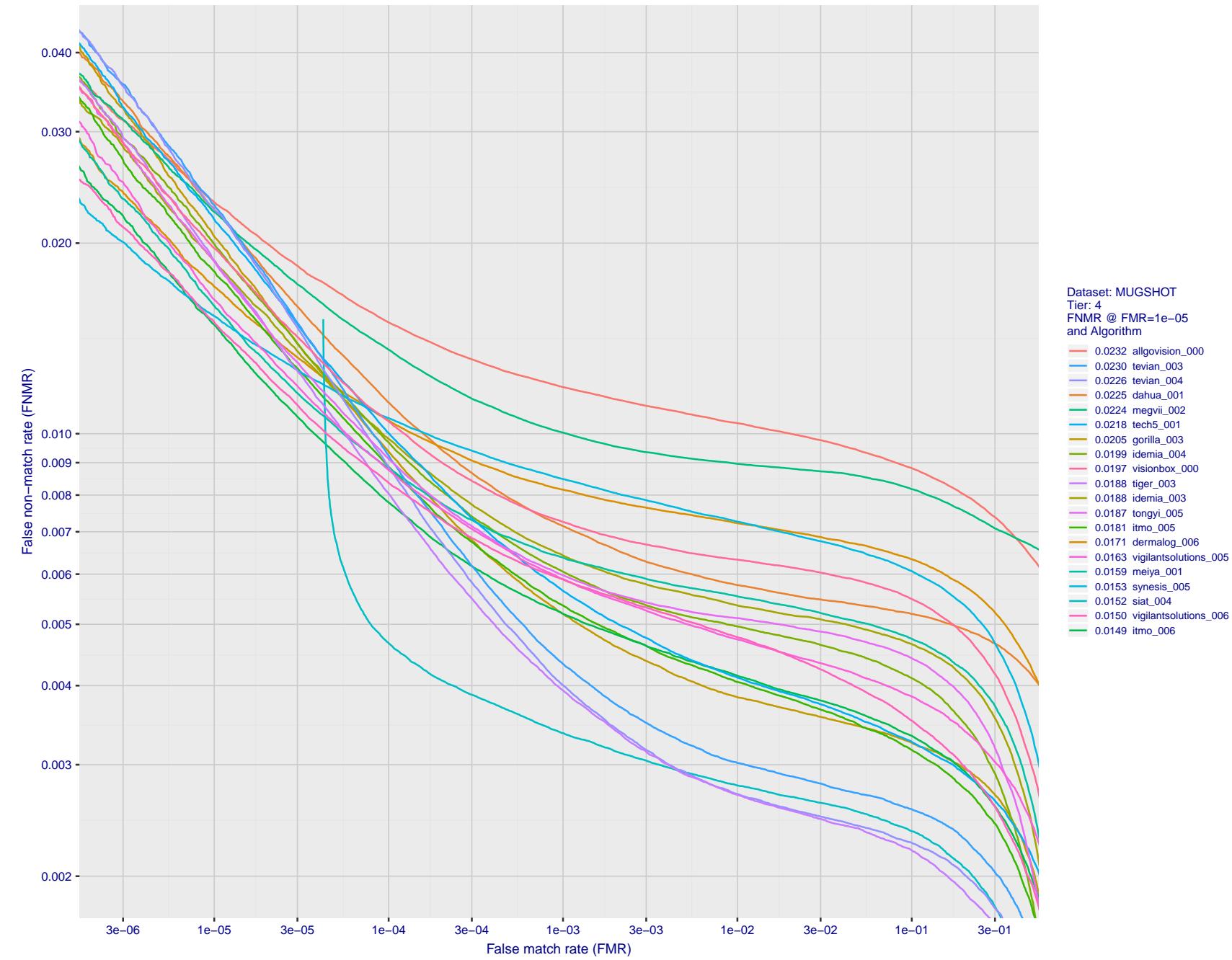


Figure 27: For the mugshot images, detection error tradeoff (DET) characteristics showing false non-match rate vs. false match rate plotted parametrically on threshold,  $T$ . The scales are logarithmic in order to show decades of FMR.

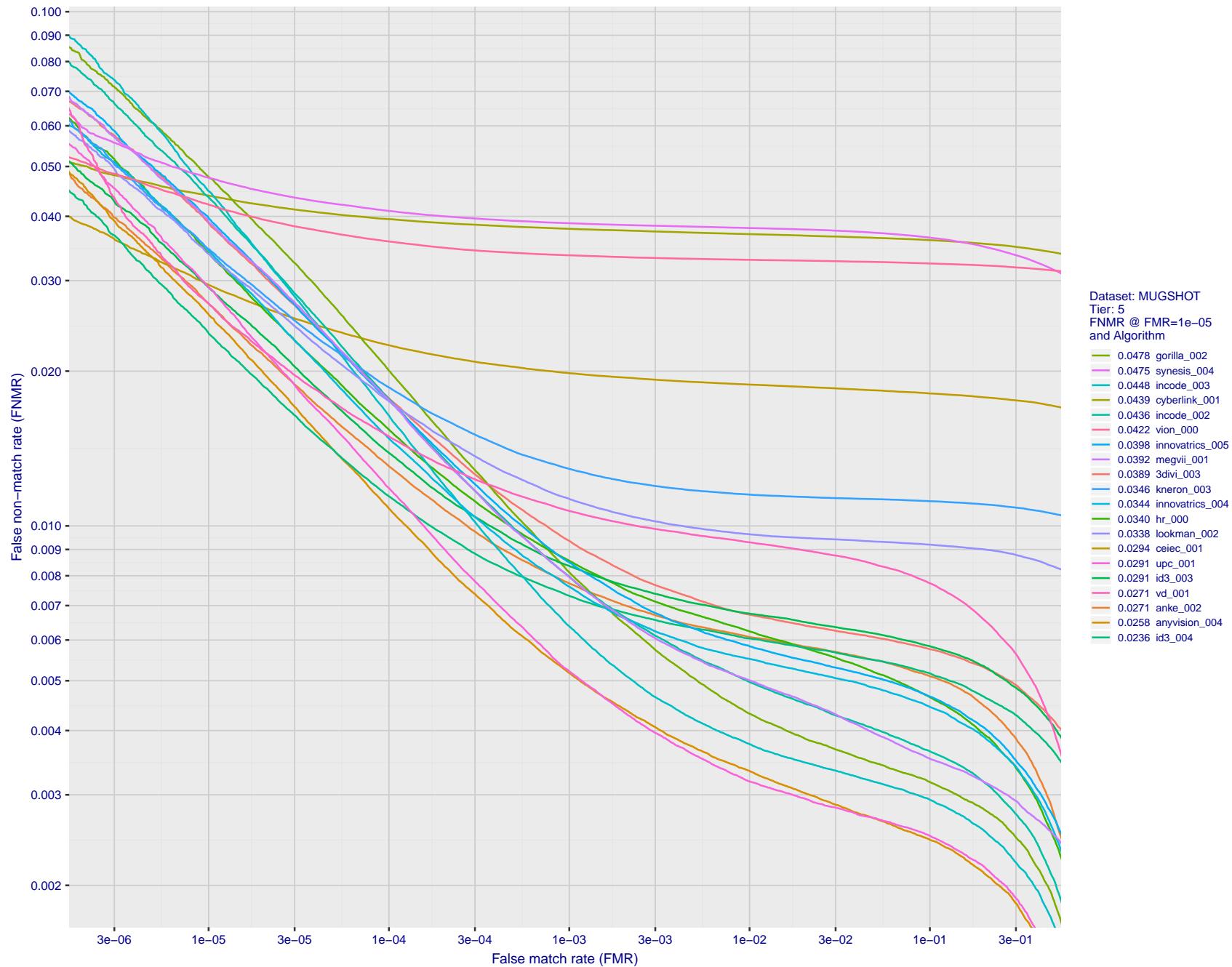


Figure 28: For the mugshot images, detection error tradeoff (DET) characteristics showing false non-match rate vs. false match rate plotted parametrically on threshold,  $T$ . The scales are logarithmic in order to show decades of FMR.

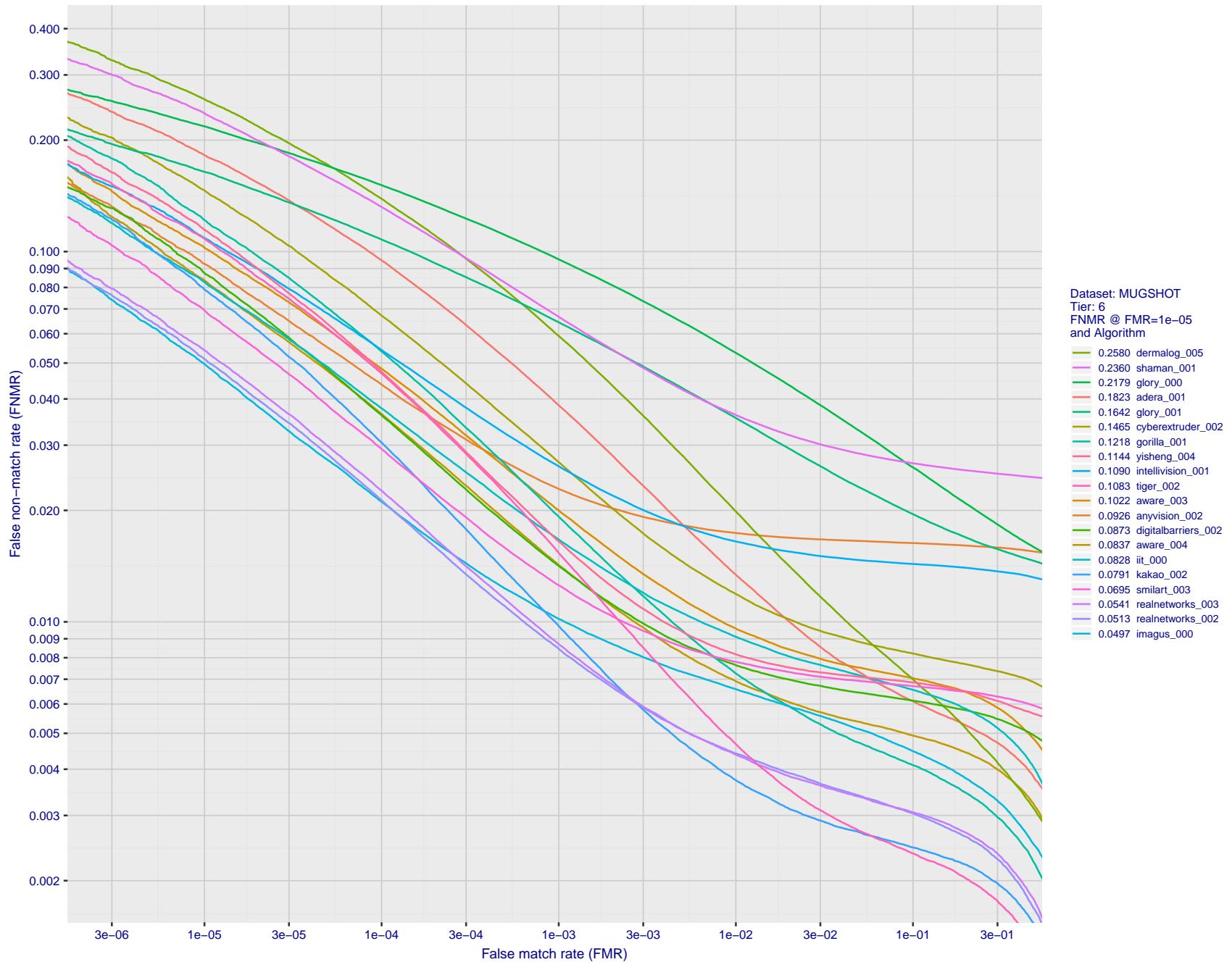


Figure 29: For the mugshot images, detection error tradeoff (DET) characteristics showing false non-match rate vs. false match rate plotted parametrically on threshold,  $T$ . The scales are logarithmic in order to show decades of FMR.

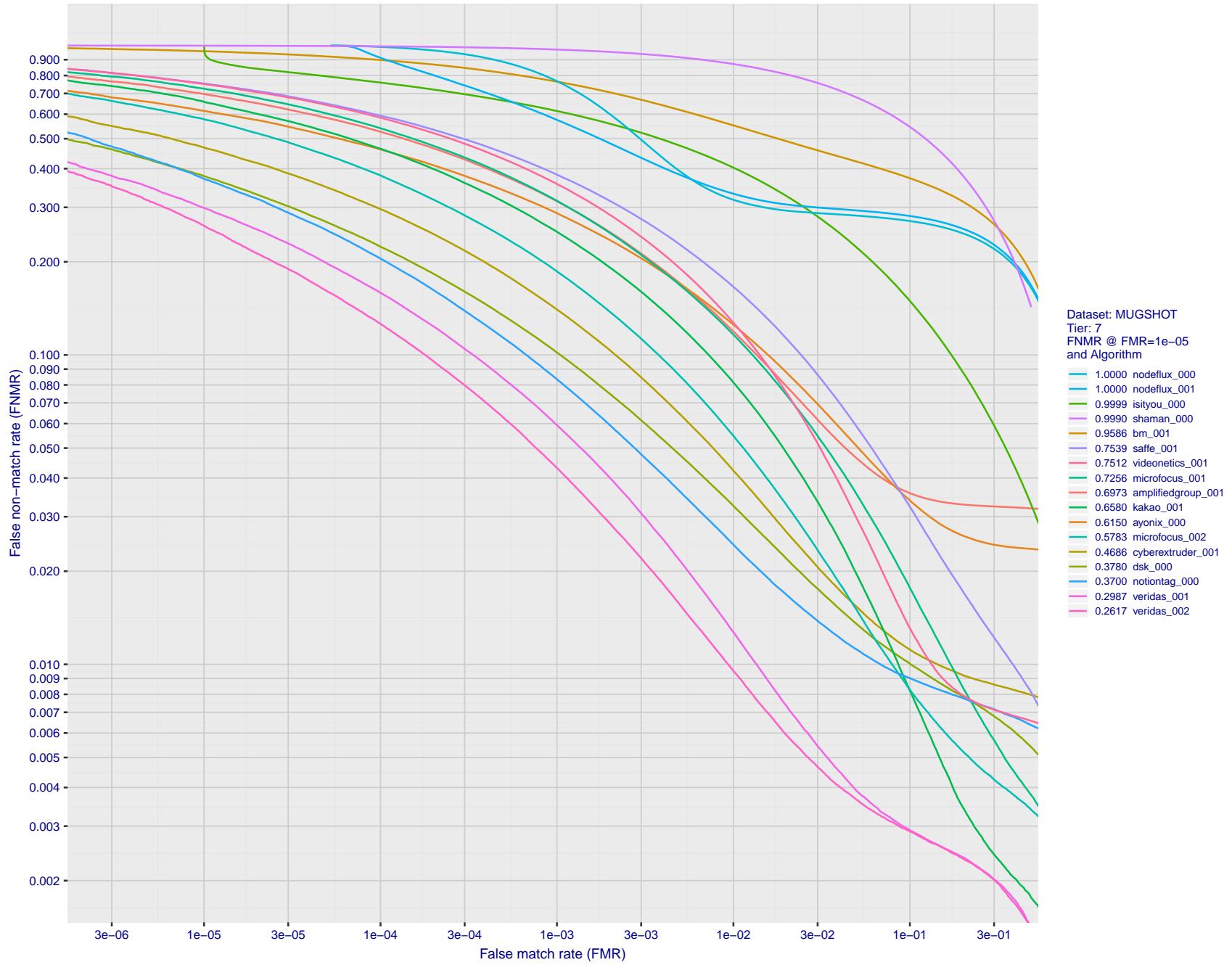


Figure 30: For the mugshot images, detection error tradeoff (DET) characteristics showing false non-match rate vs. false match rate plotted parametrically on threshold,  $T$ . The scales are logarithmic in order to show decades of FMR.

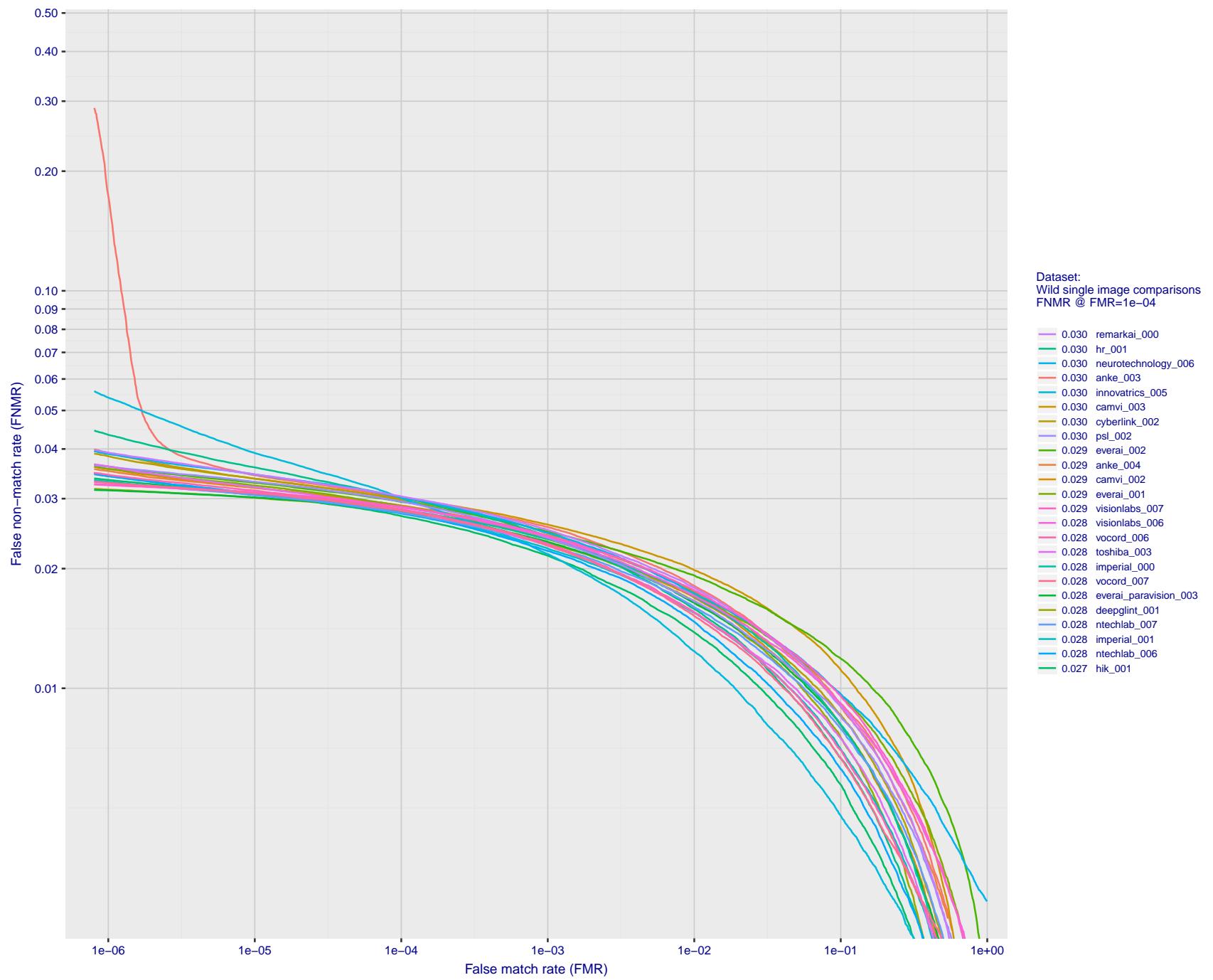


Figure 31: For the 2018 wild image comparisons, detection error tradeoff (DET) characteristics showing false non-match rate vs. false match rate plotted parametrically on threshold,  $T$ . The scales are logarithmic in order to show several decades of FMR.

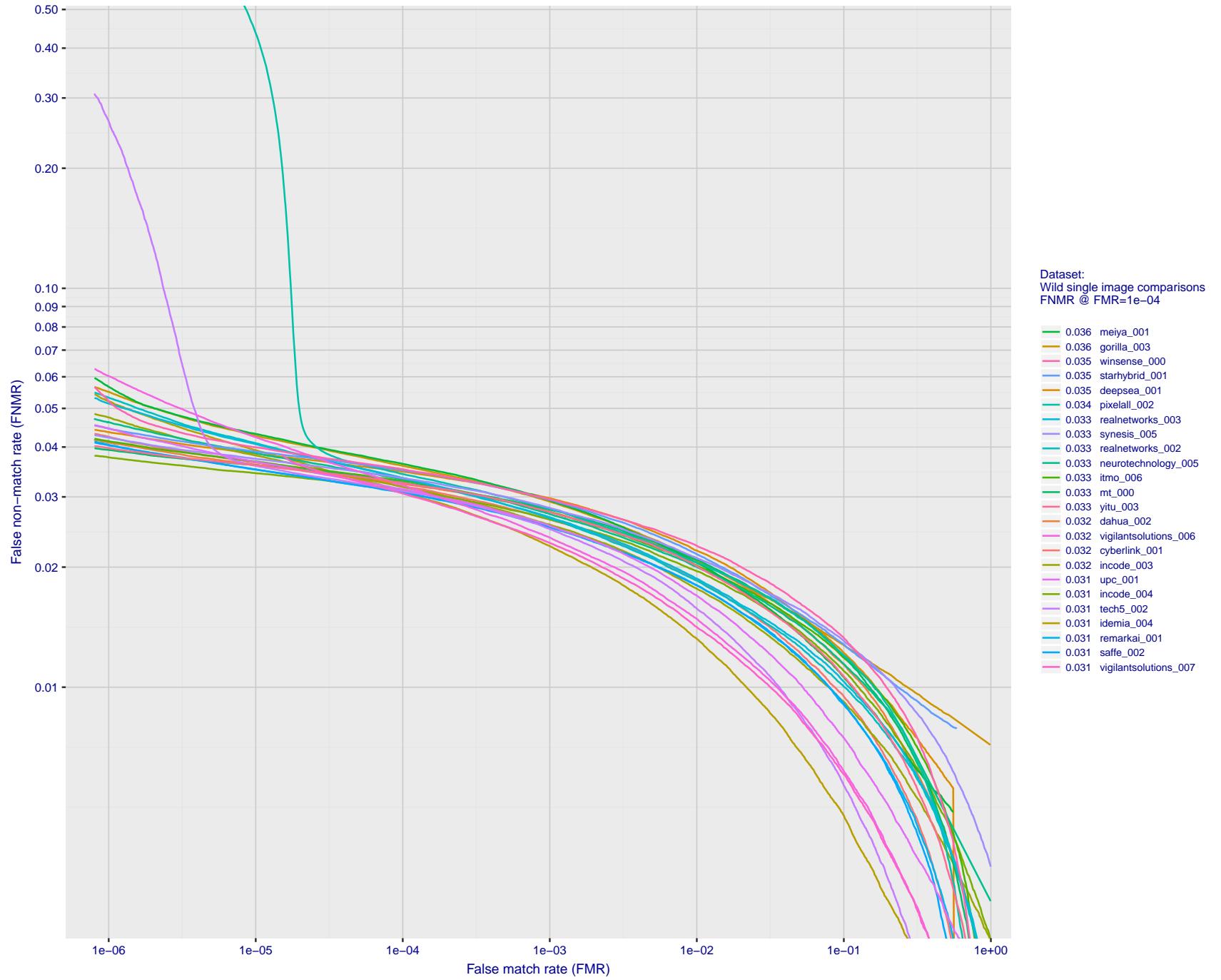


Figure 32: For the 2018 wild image comparisons, detection error tradeoff (DET) characteristics showing false non-match rate vs. false match rate plotted parametrically on threshold,  $T$ . The scales are logarithmic in order to show several decades of FMR.

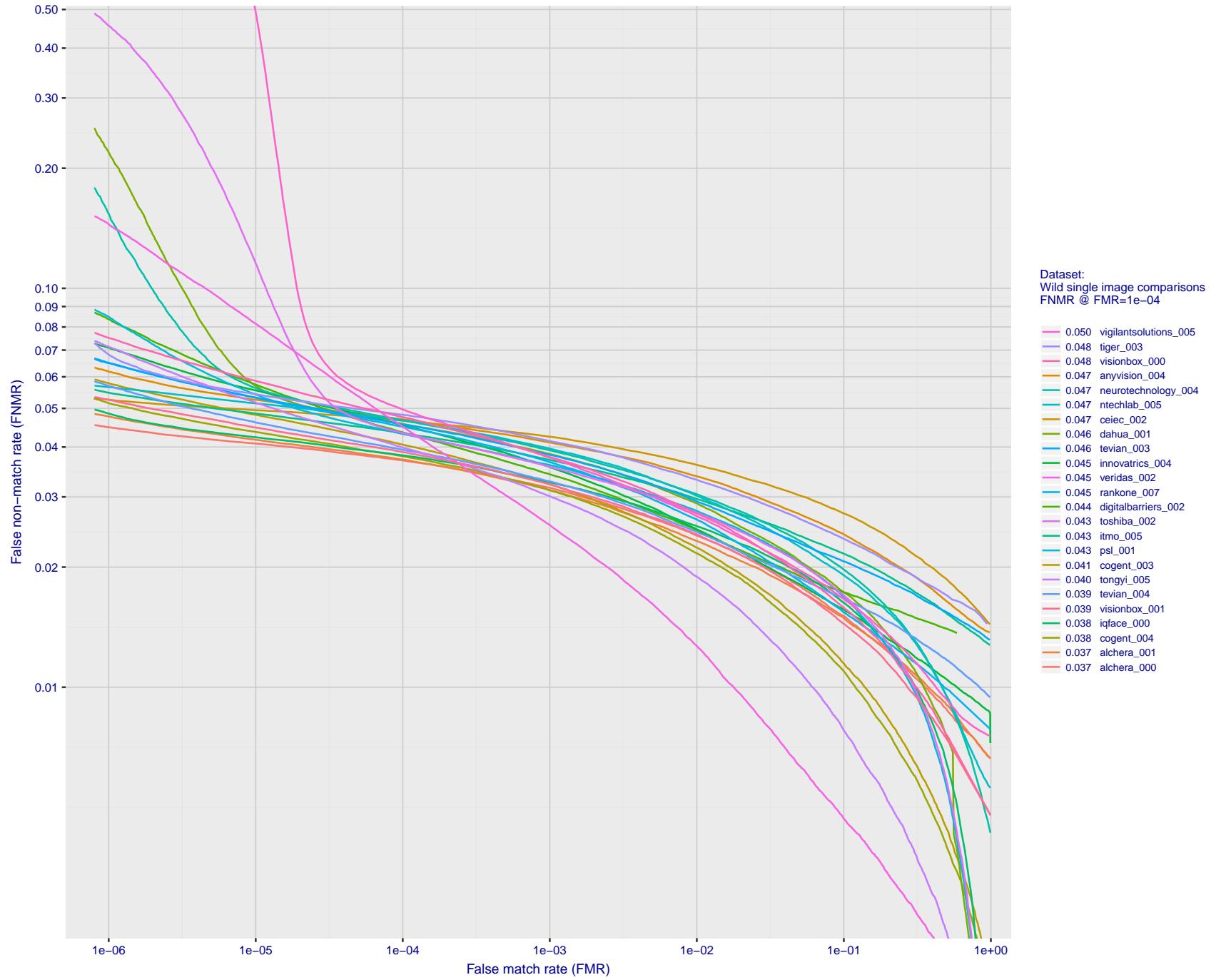


Figure 33: For the 2018 wild image comparisons, detection error tradeoff (DET) characteristics showing false non-match rate vs. false match rate plotted parametrically on threshold, T. The scales are logarithmic in order to show several decades of FMR.

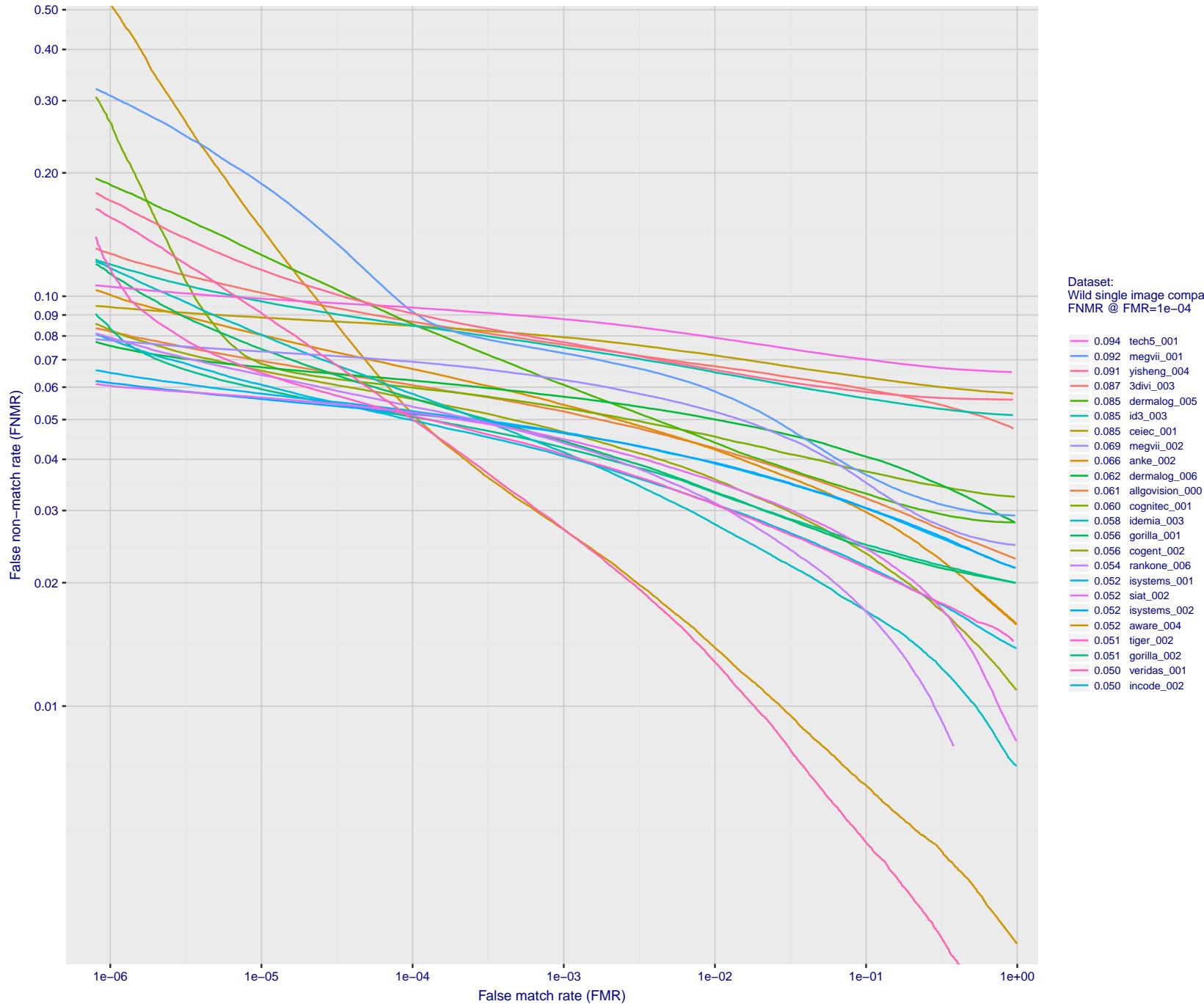


Figure 34: For the 2018 wild image comparisons, detection error tradeoff (DET) characteristics showing false non-match rate vs. false match rate plotted parametrically on threshold,  $T$ . The scales are logarithmic in order to show several decades of FMR.

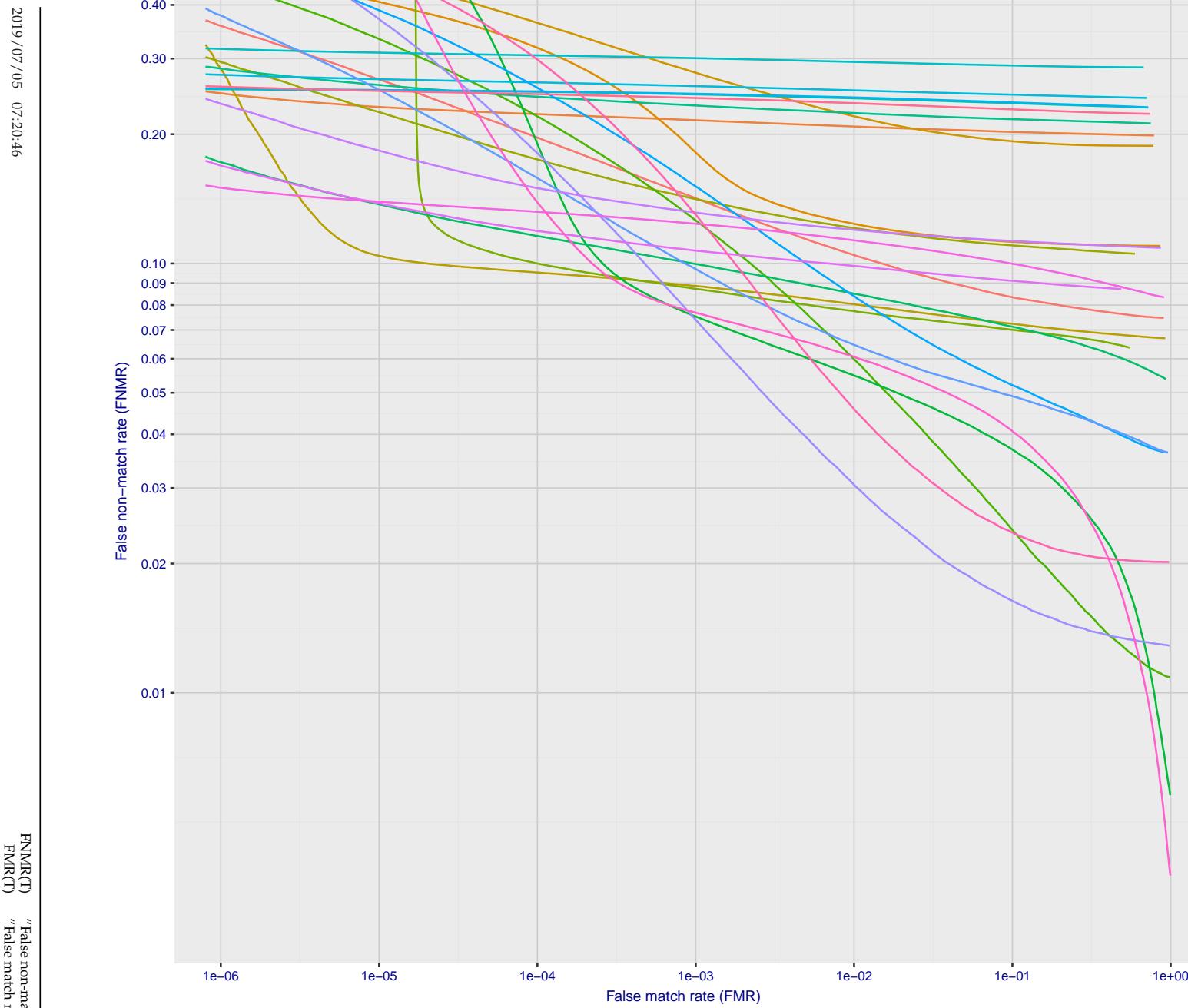


Figure 35: For the 2018 wild image comparisons, detection error tradeoff (DET) characteristics showing false non-match rate vs. false match rate plotted parametrically on threshold,  $T$ . The scales are logarithmic in order to show several decades of FMR.

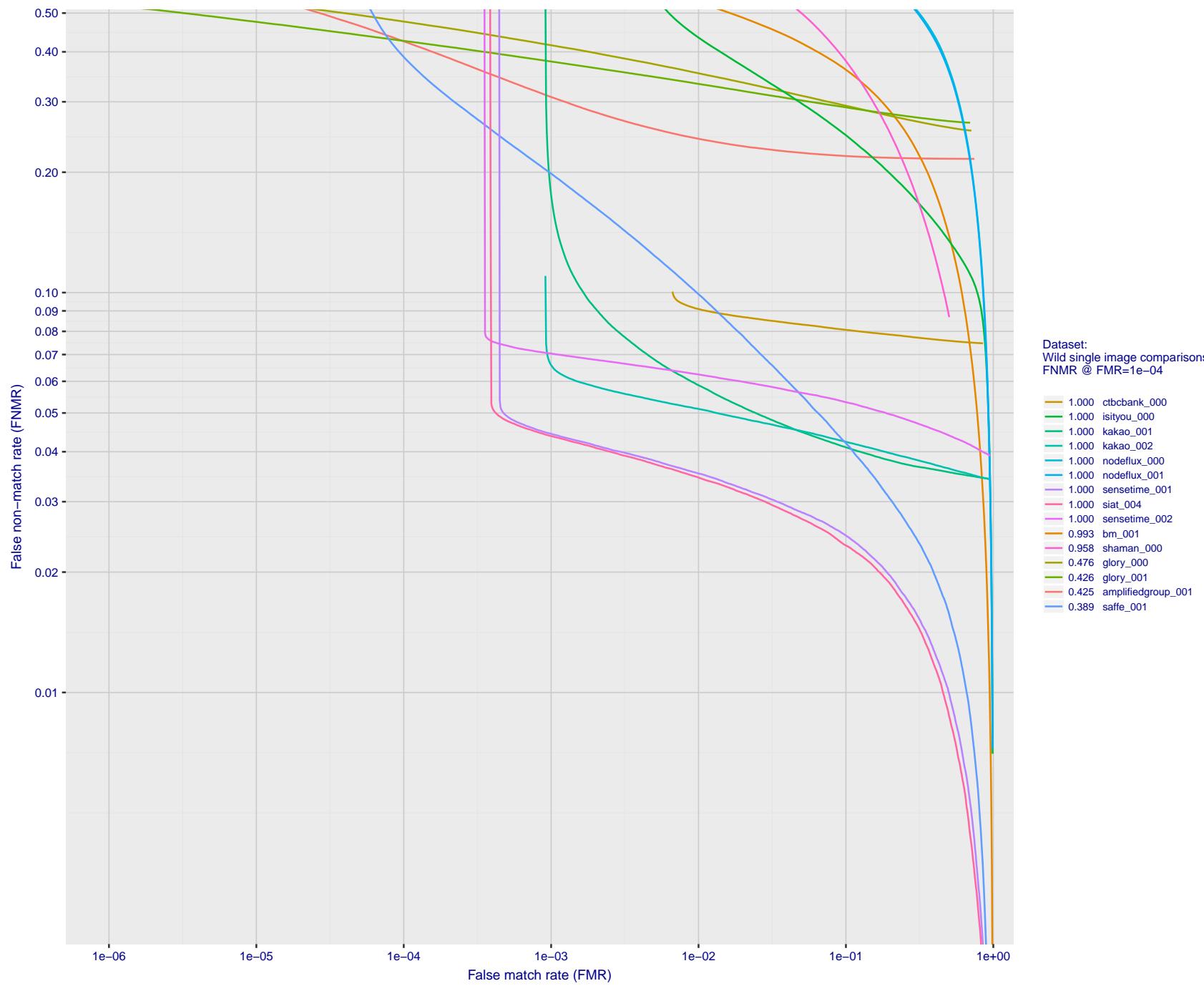


Figure 36: For the 2018 wild image comparisons, detection error tradeoff (DET) characteristics showing false non-match rate vs. false match rate plotted parametrically on threshold,  $T$ . The scales are logarithmic in order to show several decades of FMR.

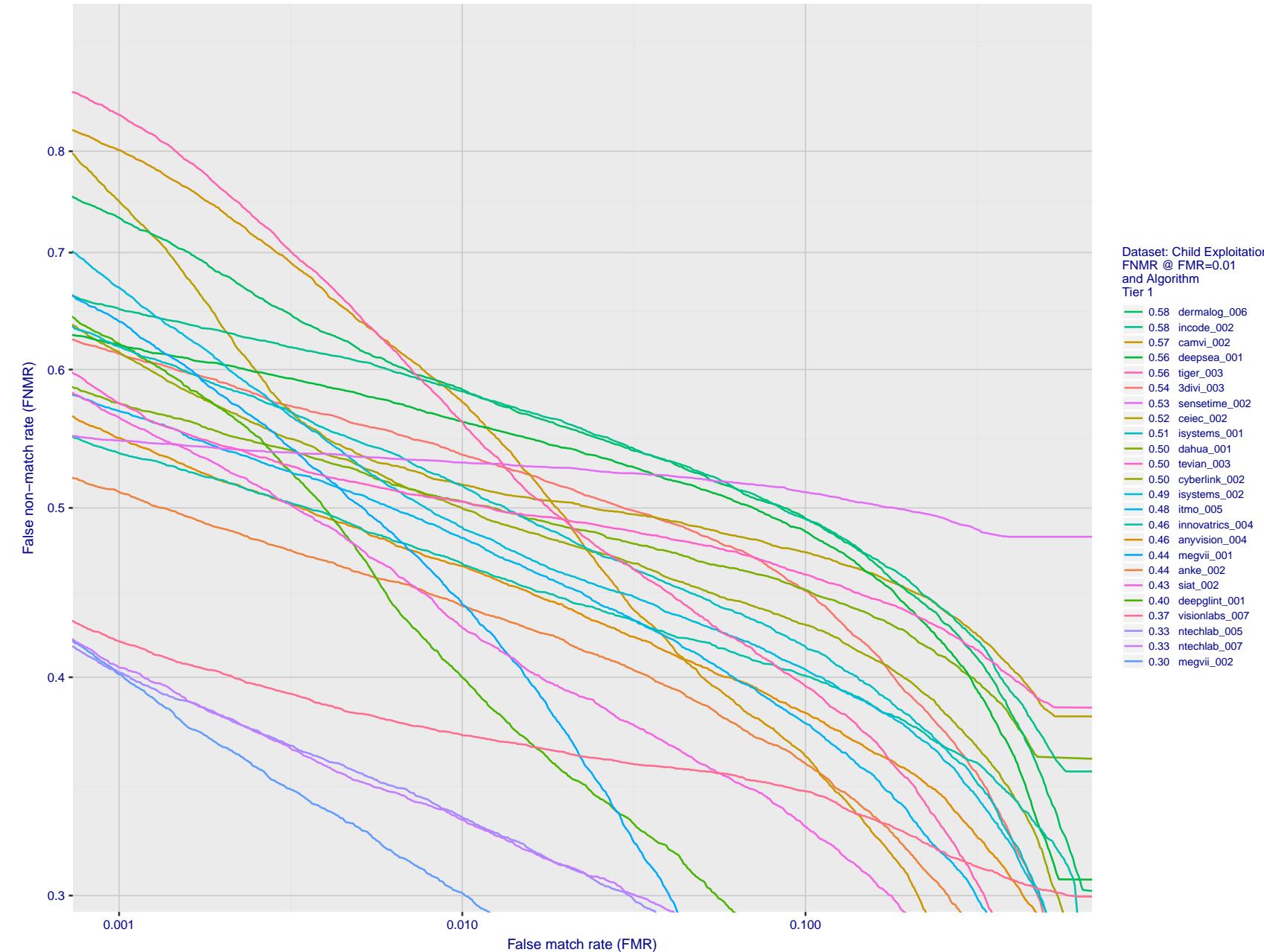


Figure 37: For child exploitation images, detection error tradeoff (DET) characteristics showing false non-match rate vs. false match rate plotted parametrically on threshold,  $T$ . The scales are logarithmic in order to show many decades of FMR. Accuracy is poor because many images have adverse quality characteristics, and because detection and enrollment fails.

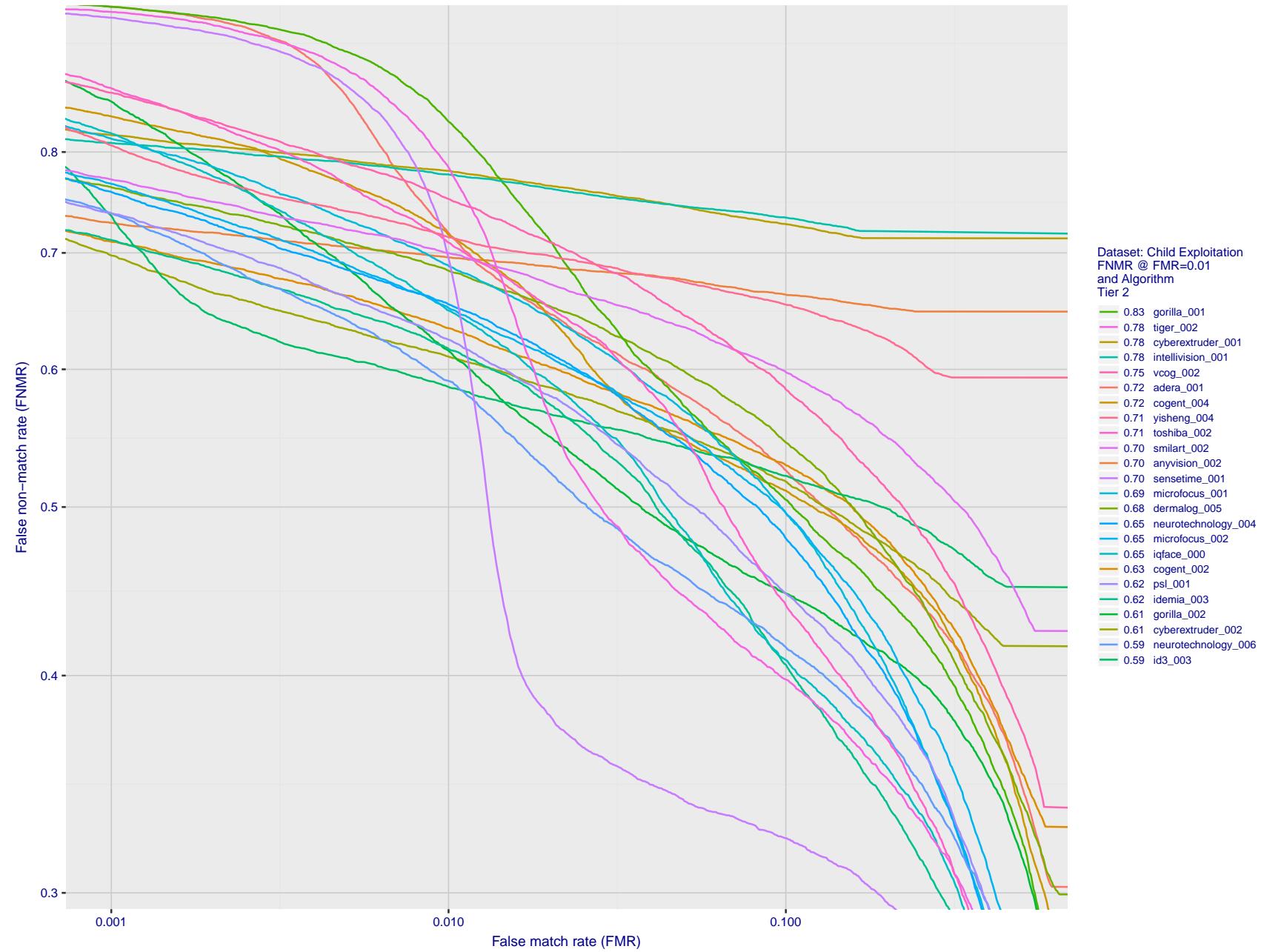


Figure 38: For child exploitation images, detection error tradeoff (DET) characteristics showing false non-match rate vs. false match rate plotted parametrically on threshold, T. The scales are logarithmic in order to show many decades of FMR. Accuracy is poor because many images have adverse quality characteristics, and because detection and enrollment fails.

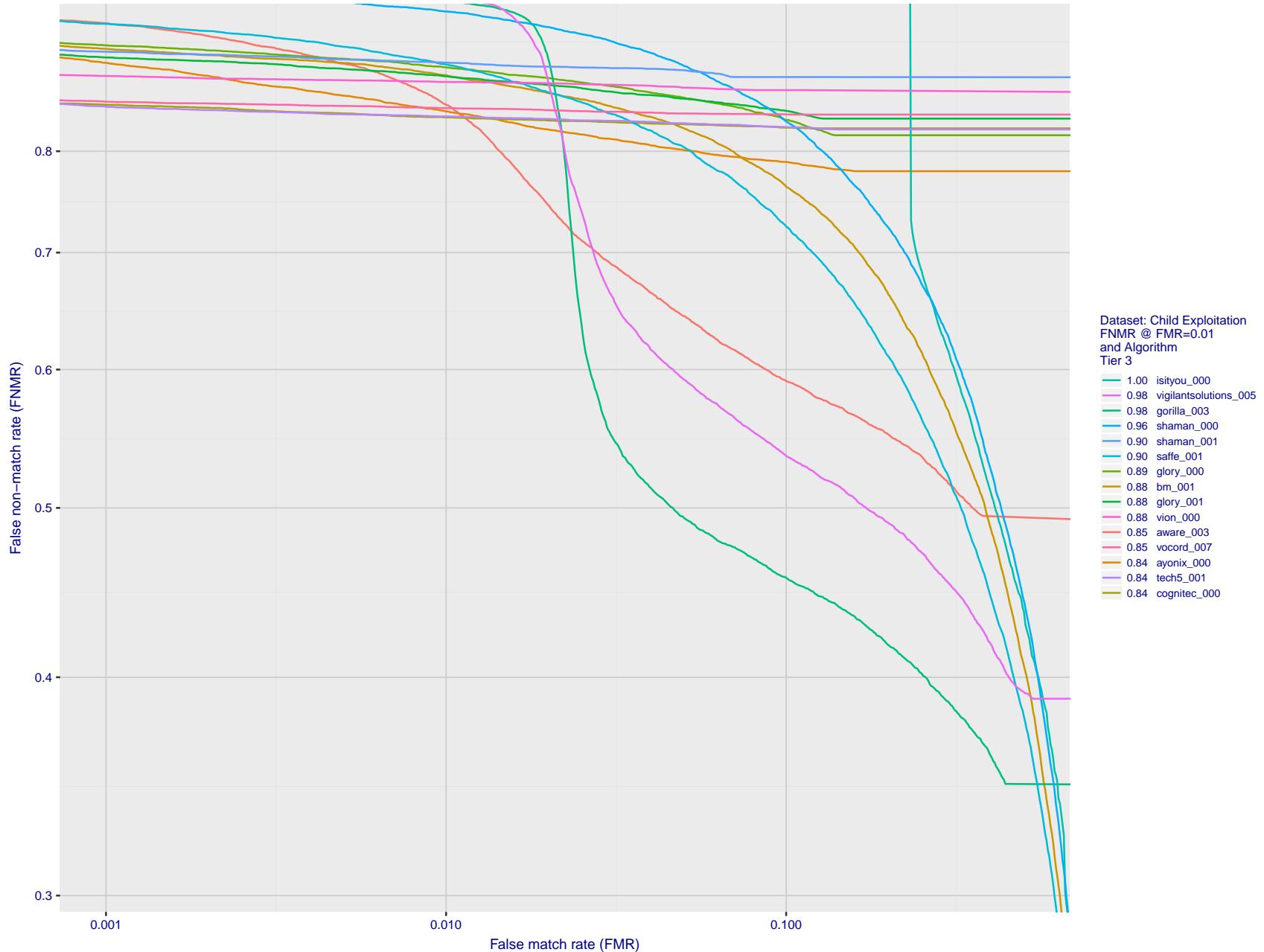


Figure 39: For child exploitation images, detection error tradeoff (DET) characteristics showing false non-match rate vs. false match rate plotted parametrically on threshold, T. The scales are logarithmic in order to show many decades of FMR. Accuracy is poor because many images have adverse quality characteristics, and because detection and enrollment fails.

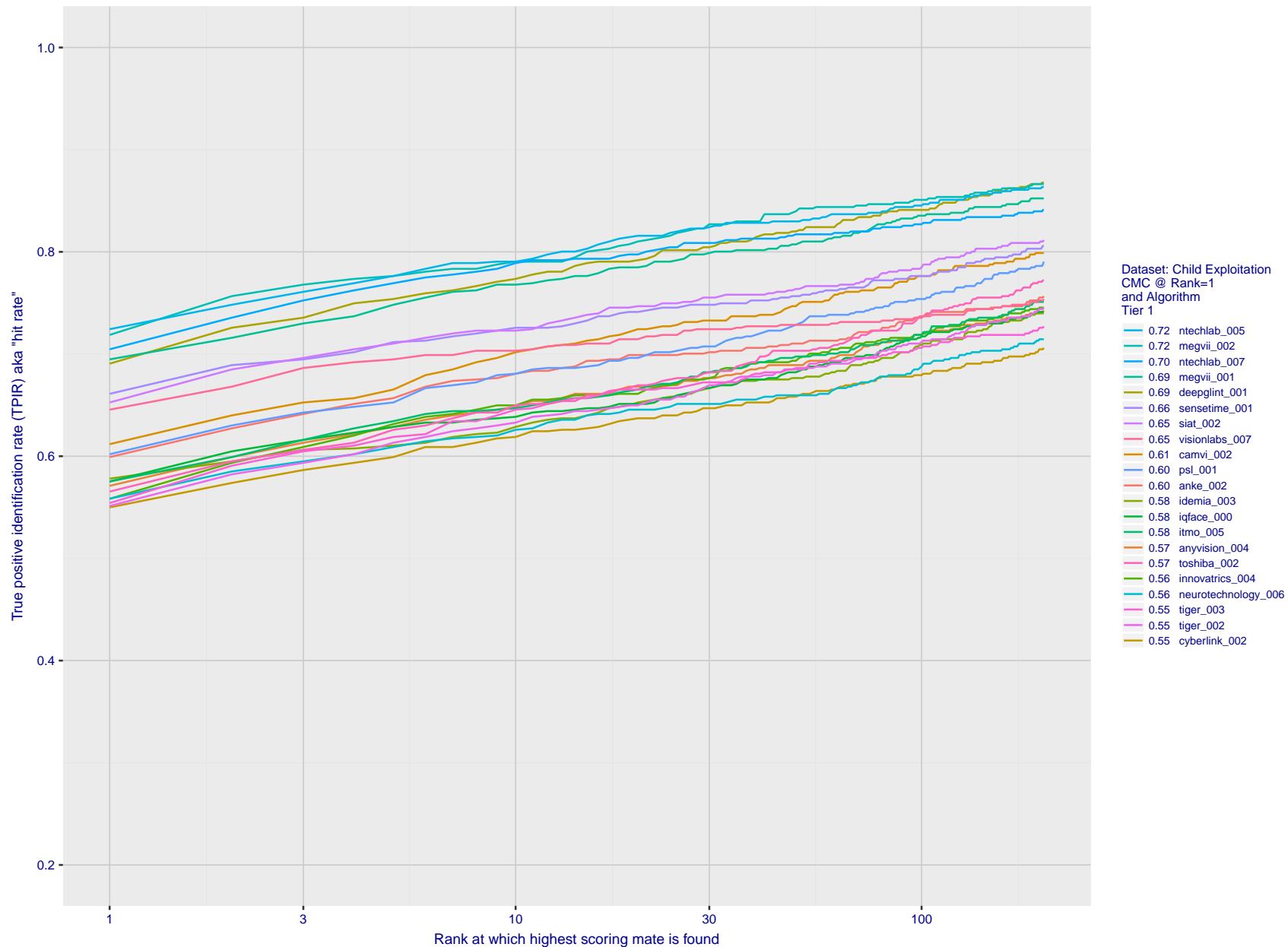


Figure 40: For child exploitation images, cumulative match characteristics (CMC) showing true positive identification rate vs. rank. This is simulation of a one-to-many search experiment - see discussion in section 3.2. The scales are logarithmic in order to show the effect of long candidate lists. Accuracy is poor but much improved relative to the 1:1 DETs of Fig. 39 because a search can succeed if any of a subject's several enrolled images matches the search image with a high score.

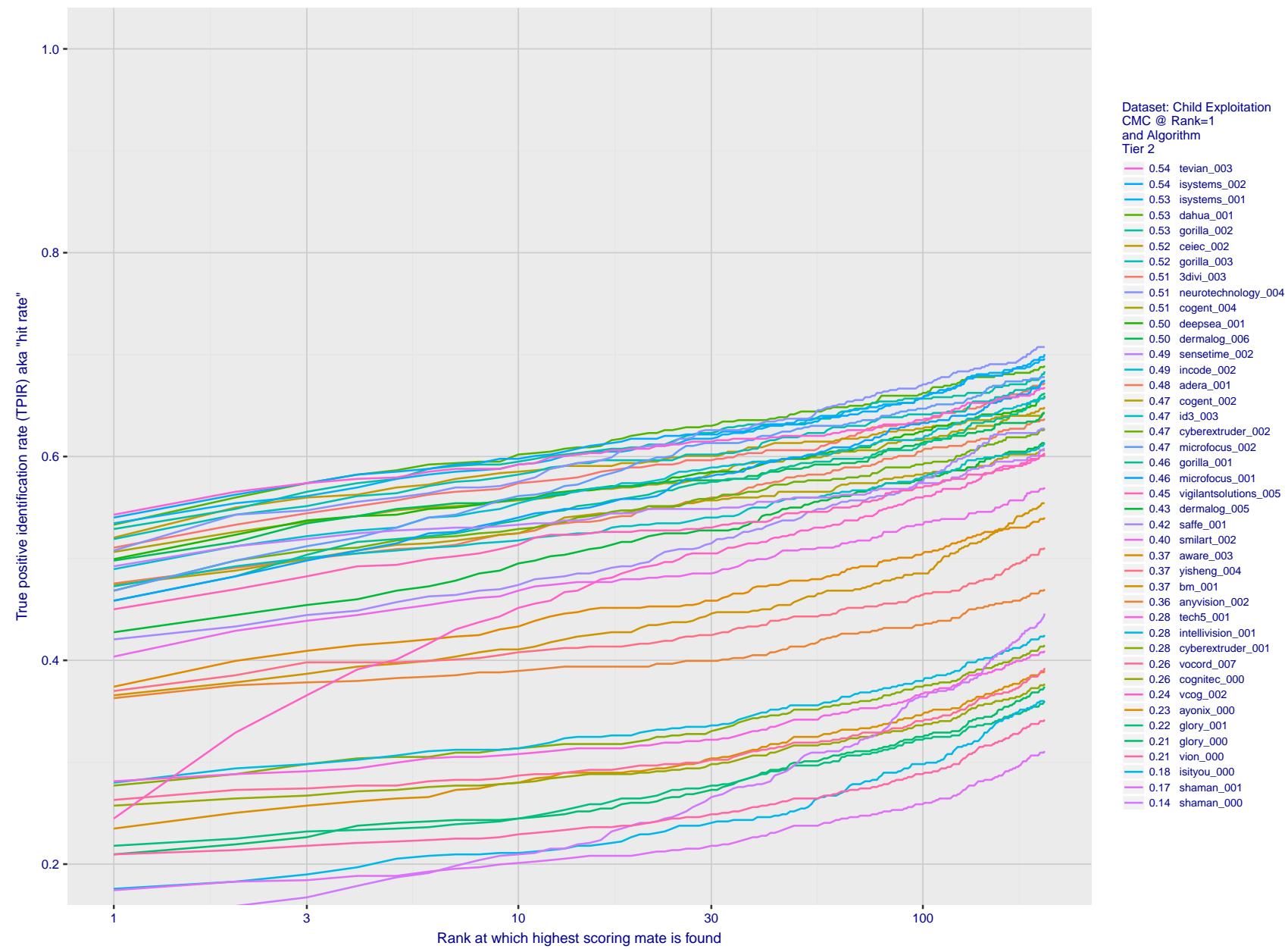


Figure 41: For child exploitation images, cumulative match characteristics (CMC) showing true positive identification rate vs. rank. This is simulation of a one-to-many search experiment - see discussion in section 3.2. The scales are logarithmic in order to show the effect of long candidate lists. Accuracy is poor but much improved relative to the 1:1 DETs of Fig. 39 because a search can succeed if any of a subject's several enrolled images matches the search image with a high score.

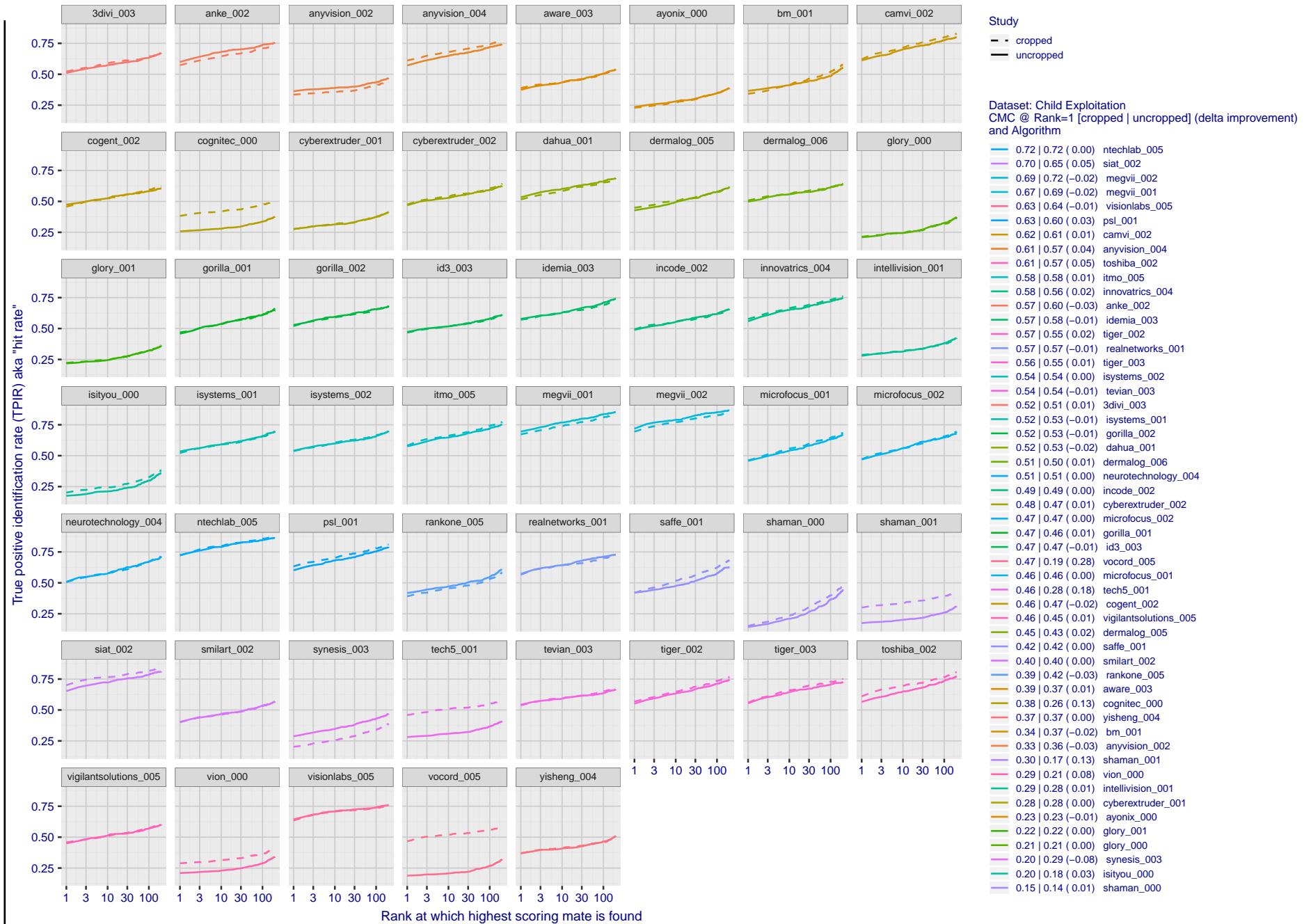


Figure 42: For child exploitation images, cumulative match characteristics (CMC) showing true positive identification rate vs. rank for two cases: 1. Whole image provided to the algorithm; 2. Human annotated rectangular region, cropped and provided to the algorithm. The difference between the traces is associated with detection of difficult faces, and fine localization.

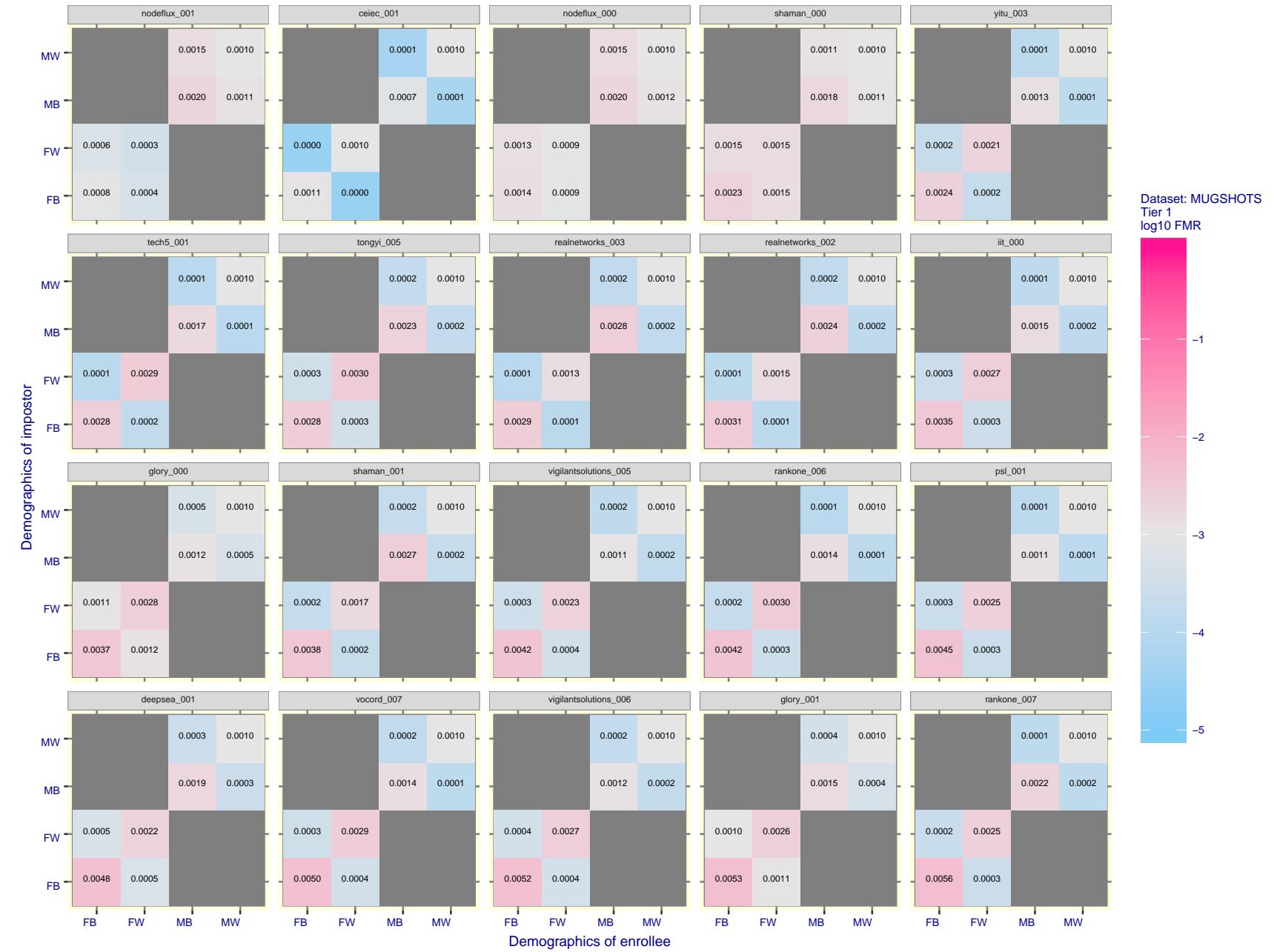


Figure 43: For the mugshot images, FMR for same-sex impostor pairs of images annotated with codes for black female, black male, white female, white male. The threshold is set for each algorithm to give  $\text{FMR} = 0.001$  for white males which is the demographic that usually gives the lowest FMR. This means the top right box is the same color in all panels. The panels are sorted over multiple pages in order of FMR on black females, which is the demographic that usually gives the highest FMR.

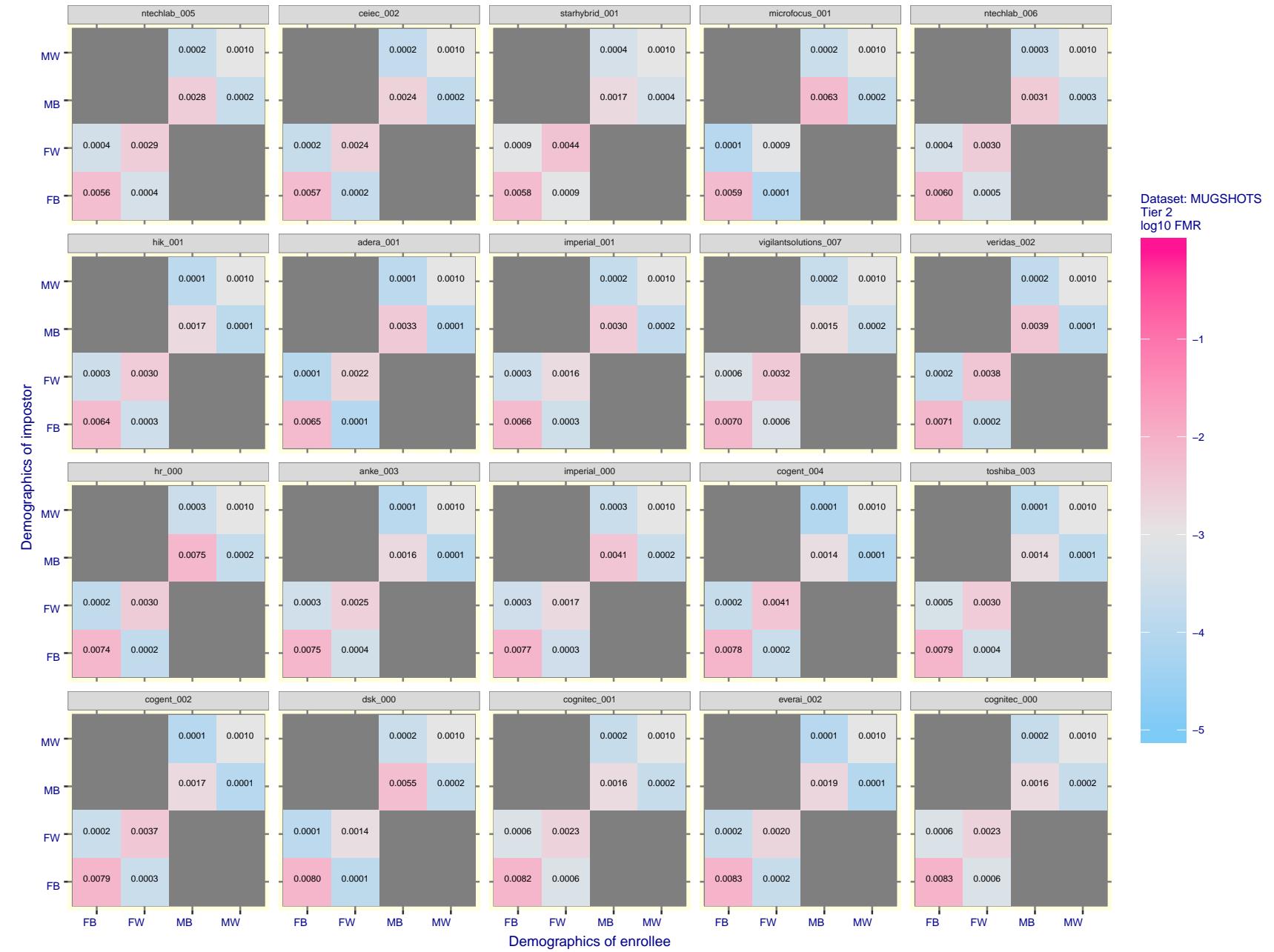


Figure 44: For the mugshot images, FMR for same-sex impostor pairs of images annotated with codes for black female, black male, white female, white male. The threshold is set for each algorithm to give  $\text{FMR} = 0.001$  for white males which is the demographic that usually gives the lowest FMR. This means the top right box is the same color in all panels. The panels are sorted over multiple pages in order of FMR on black females, which is the demographic that usually gives the highest FMR.

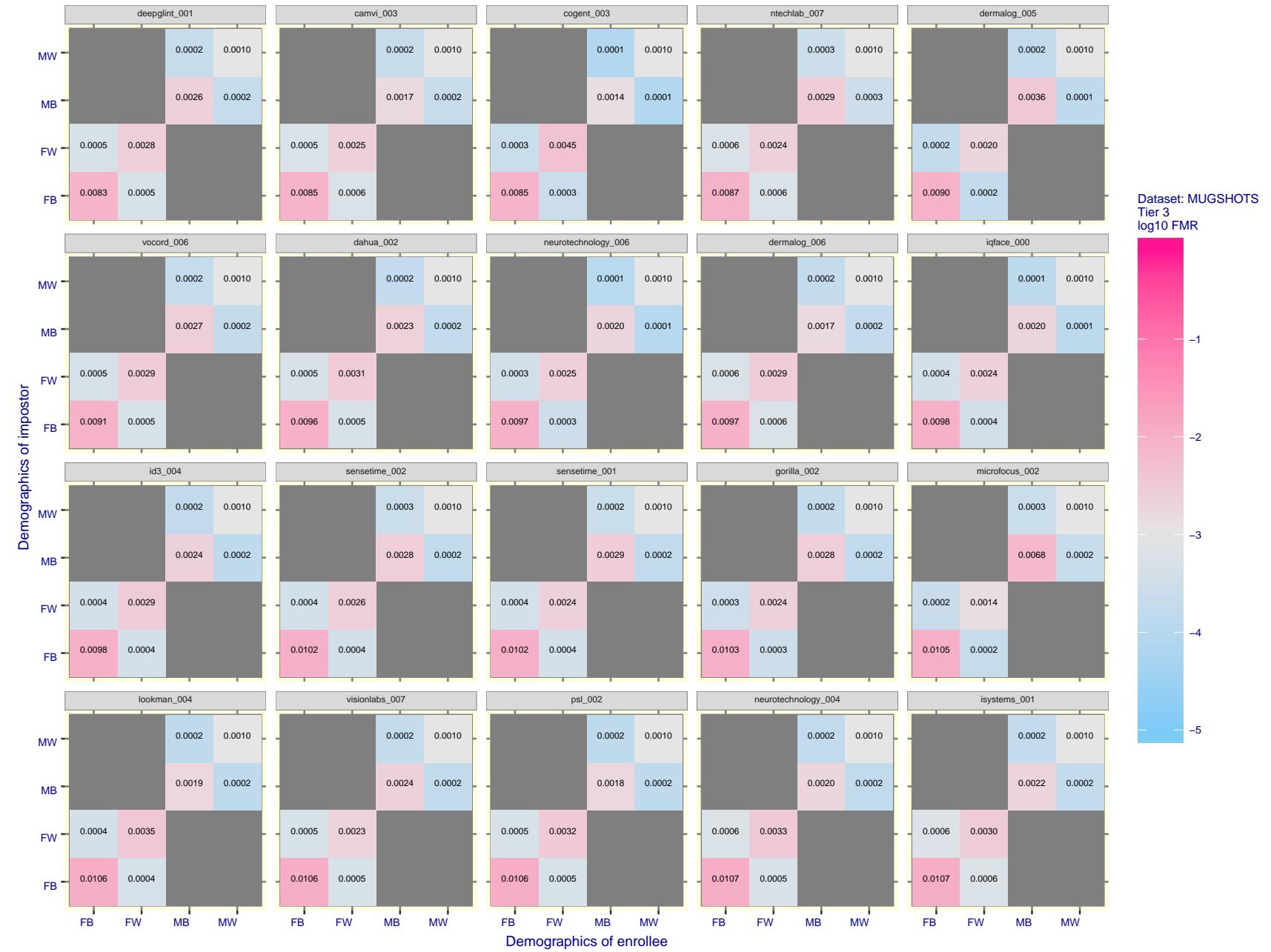


Figure 45: For the mugshot images, FMR for same-sex impostor pairs of images annotated with codes for black female, black male, white female, white male. The threshold is set for each algorithm to give  $FMR = 0.001$  for white males which is the demographic that usually gives the lowest FMR. This means the top right box is the same color in all panels. The panels are sorted over multiple pages in order of FMR on black females, which is the demographic that usually gives the highest FMR.

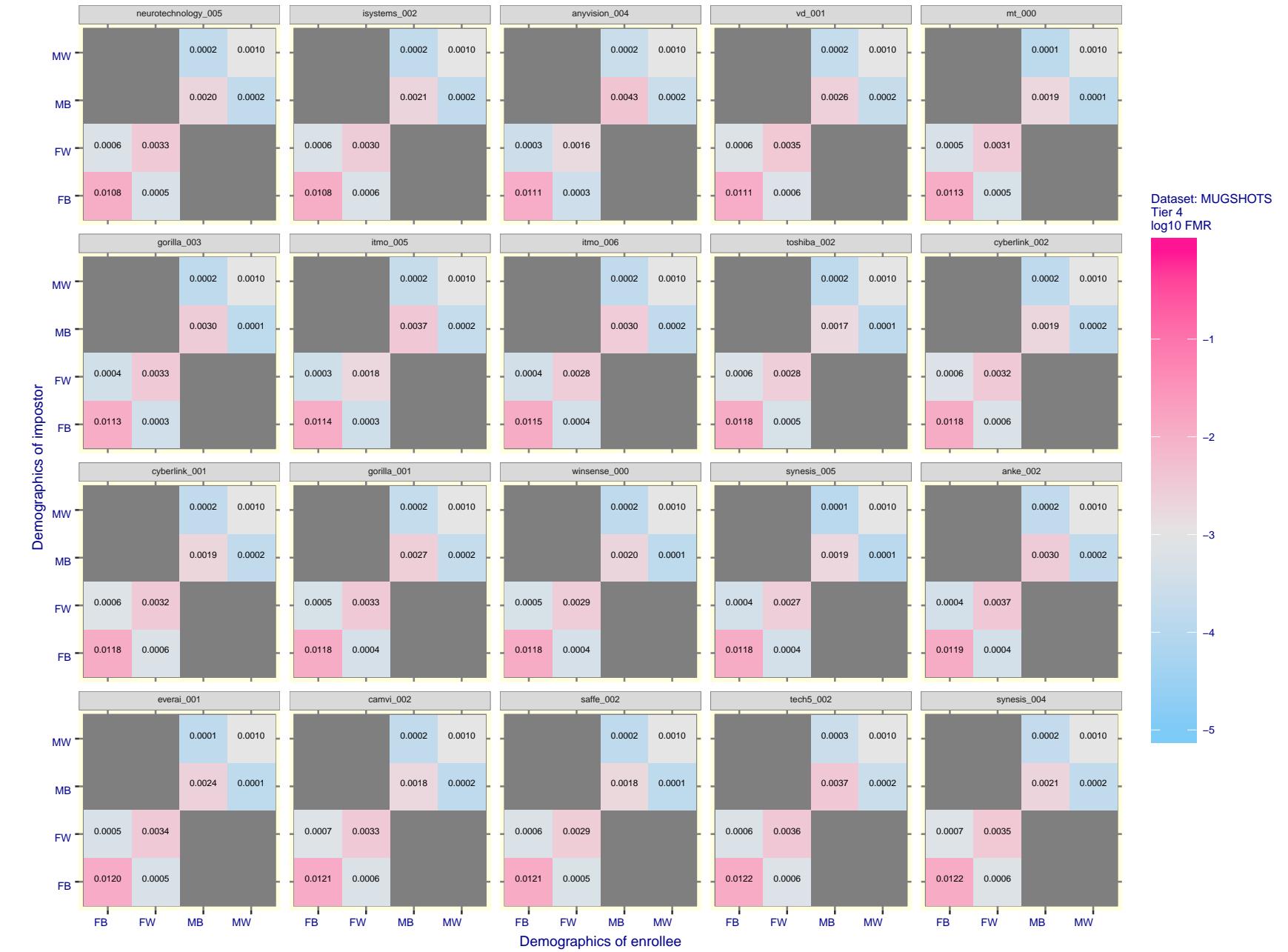


Figure 46: For the mugshot images, FMR for same-sex impostor pairs of images annotated with codes for black female, black male, white female, white male. The threshold is set for each algorithm to give  $\text{FMR} = 0.001$  for white males which is the demographic that usually gives the lowest FMR. This means the top right box is the same color in all panels. The panels are sorted over multiple pages in order of FMR on black females, which is the demographic that usually gives the highest FMR.

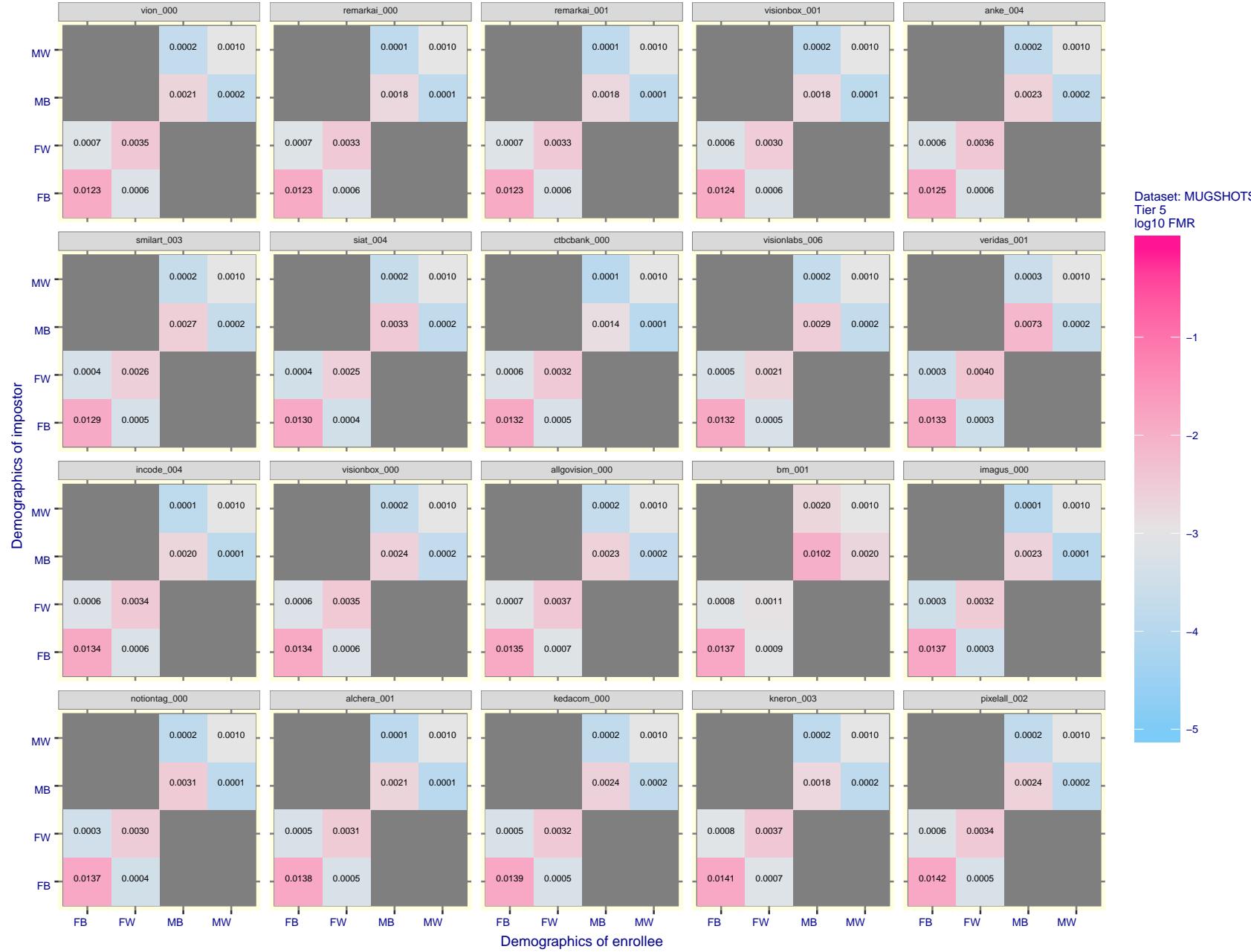


Figure 47: For the mugshot images, FMR for same-sex impostor pairs of images annotated with codes for black female, black male, white female, white male. The threshold is set for each algorithm to give  $FMR = 0.001$  for white males which is the demographic that usually gives the lowest FMR. This means the top right box is the same color in all panels. The panels are sorted over multiple pages in order of FMR on black females, which is the demographic that usually gives the highest FMR.

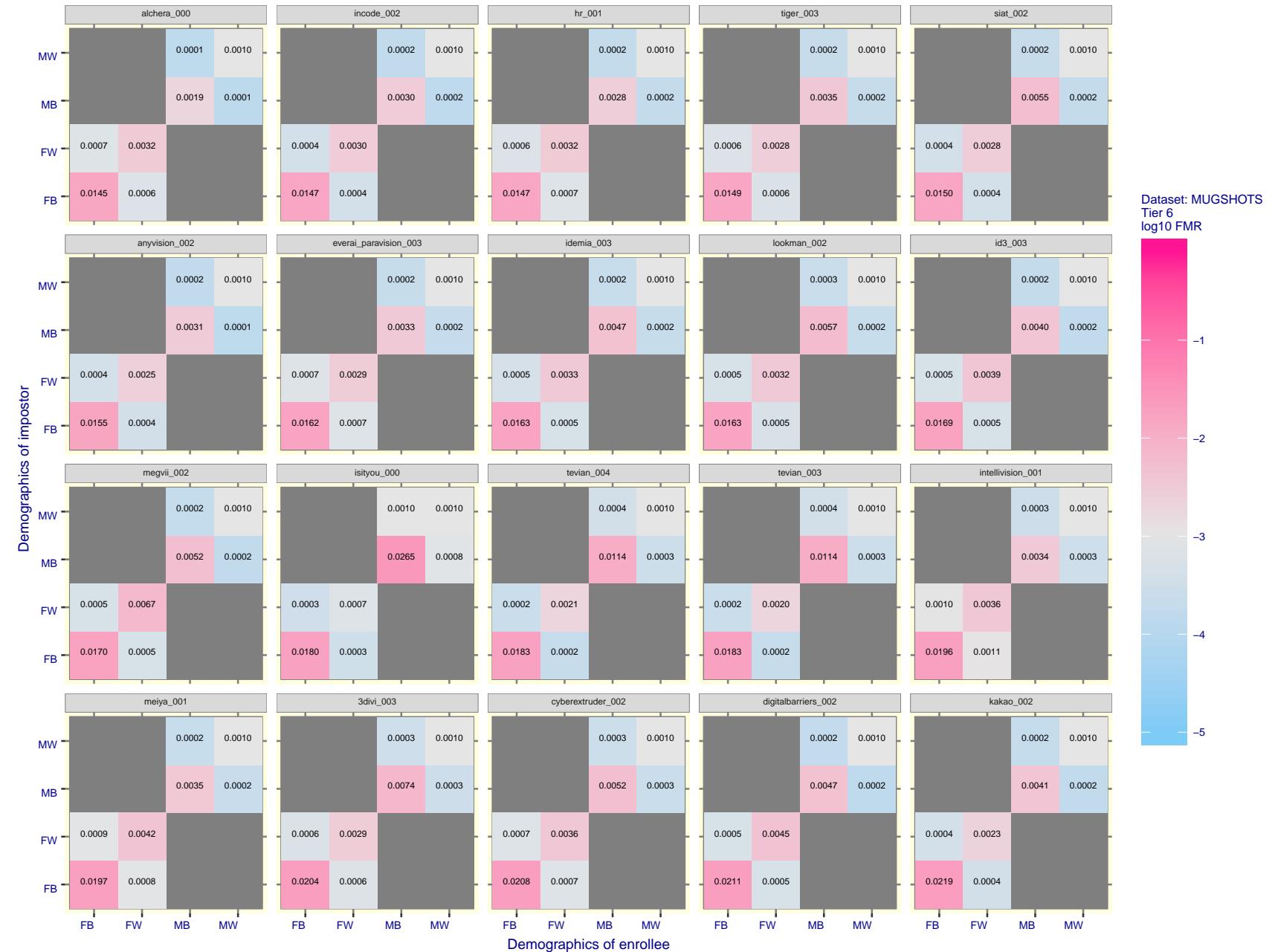


Figure 48: For the mugshot images, FMR for same-sex impostor pairs of images annotated with codes for black female, black male, white female, white male. The threshold is set for each algorithm to give  $\text{FMR} = 0.001$  for white males which is the demographic that usually gives the lowest FMR. This means the top right box is the same color in all panels. The panels are sorted over multiple pages in order of FMR on black females, which is the demographic that usually gives the highest FMR.

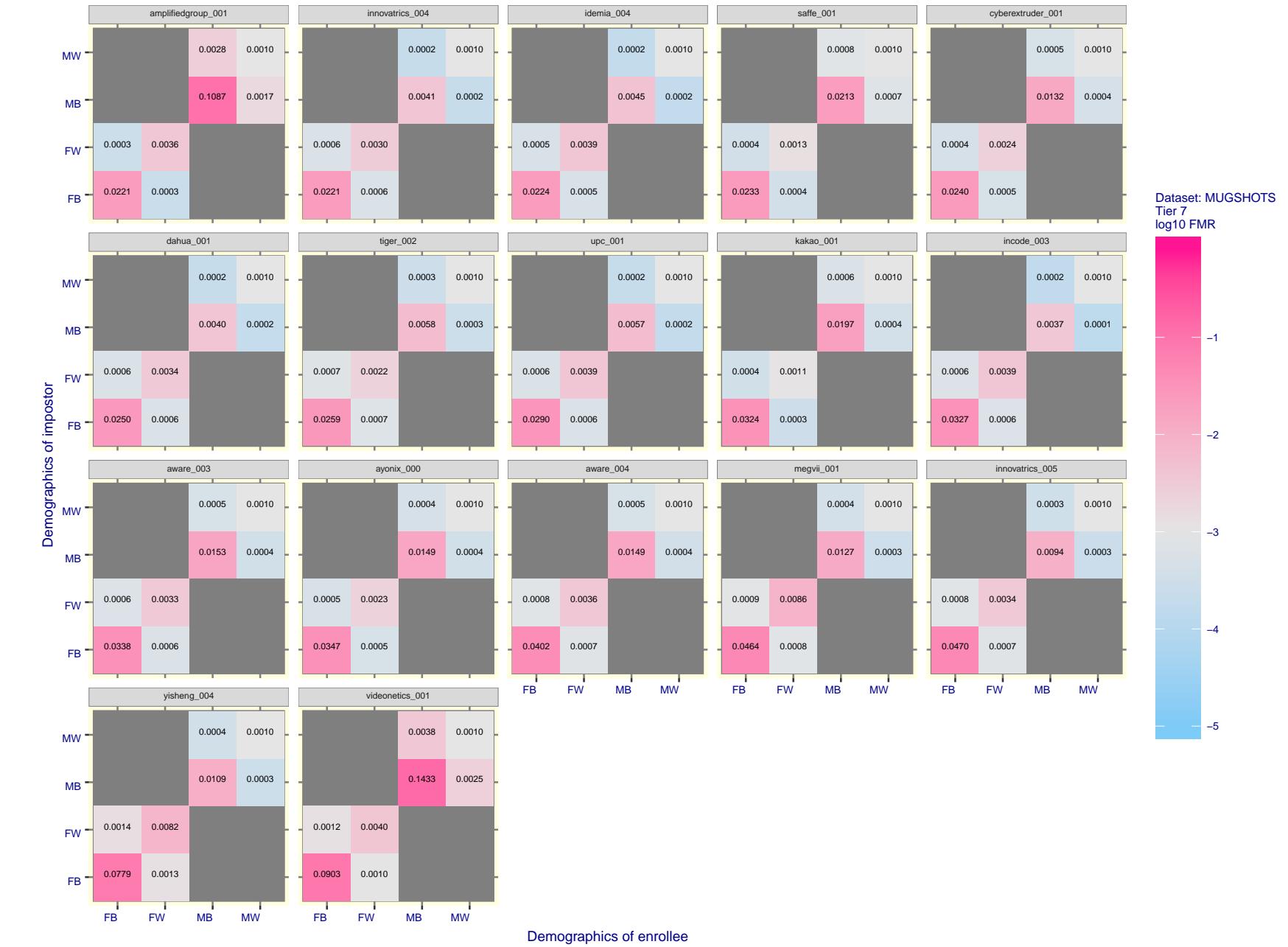


Figure 49: For the mugshot images, FMR for same-sex impostor pairs of images annotated with codes for black female, black male, white female, white male. The threshold is set for each algorithm to give  $FMR = 0.001$  for white males which is the demographic that usually gives the lowest FMR. This means the top right box is the same color in all panels. The panels are sorted over multiple pages in order of FMR on black females, which is the demographic that usually gives the highest FMR.

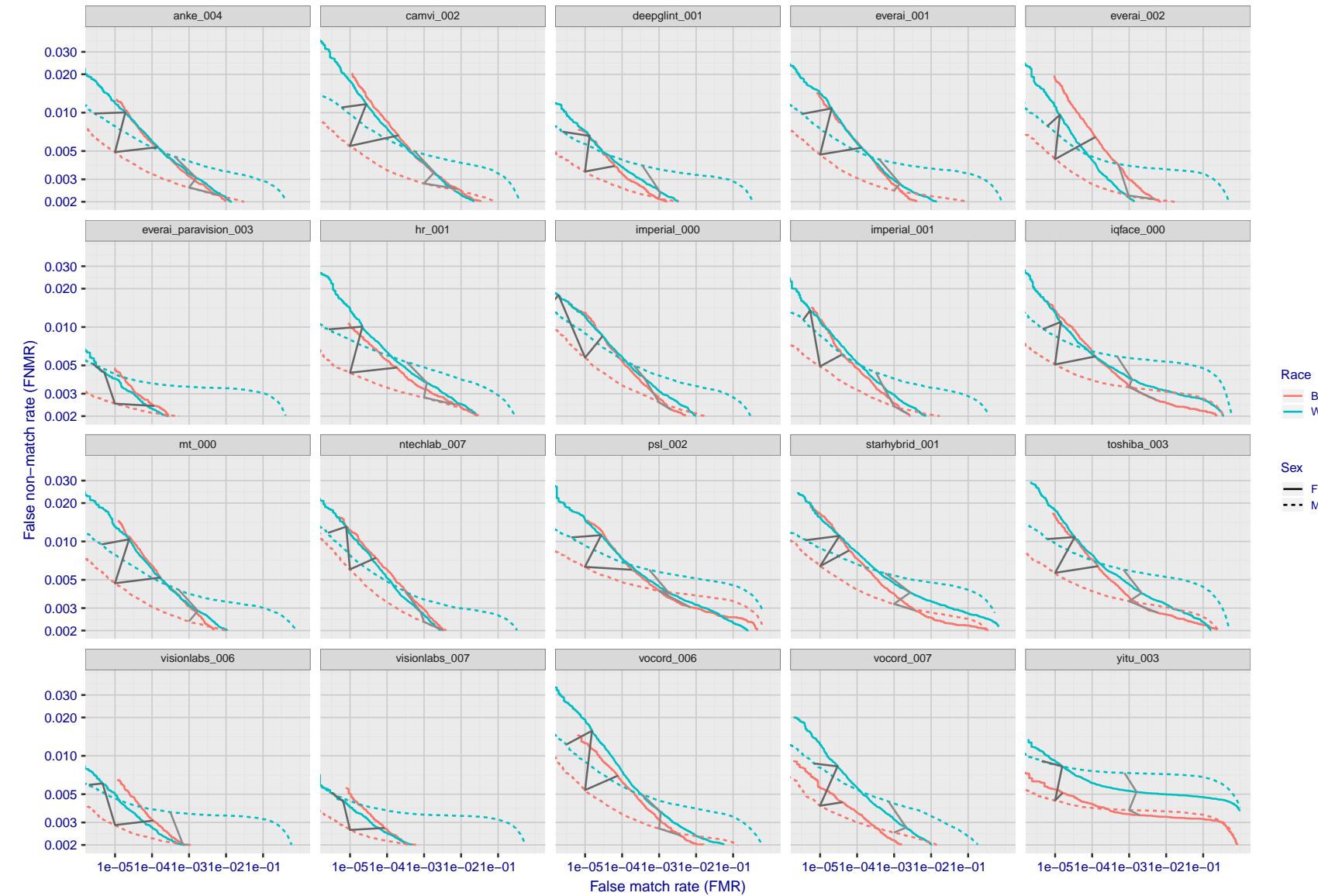


Figure 50: For the mugshot images, error tradeoff characteristics for white females, black females, black males and white males. The Z-shaped grey lines correspond to fixed thresholds, showing both FNMR and FMR vary at one  $T$  value. Note: Many of the plots will naively be read as saying women gives worse error rates than men because the solid traces lie above the dotted ones. However, this is misleading and incomplete: The grey lines show the traces reveal horizontal shifts. Thus for the cogent-003 algorithm FNMR for men is higher than for women at a fixed threshold but, at the same time, FMR is higher for women - see Figure 75. As access control systems almost always operate at a fixed threshold, the naive interpretation is incorrect.

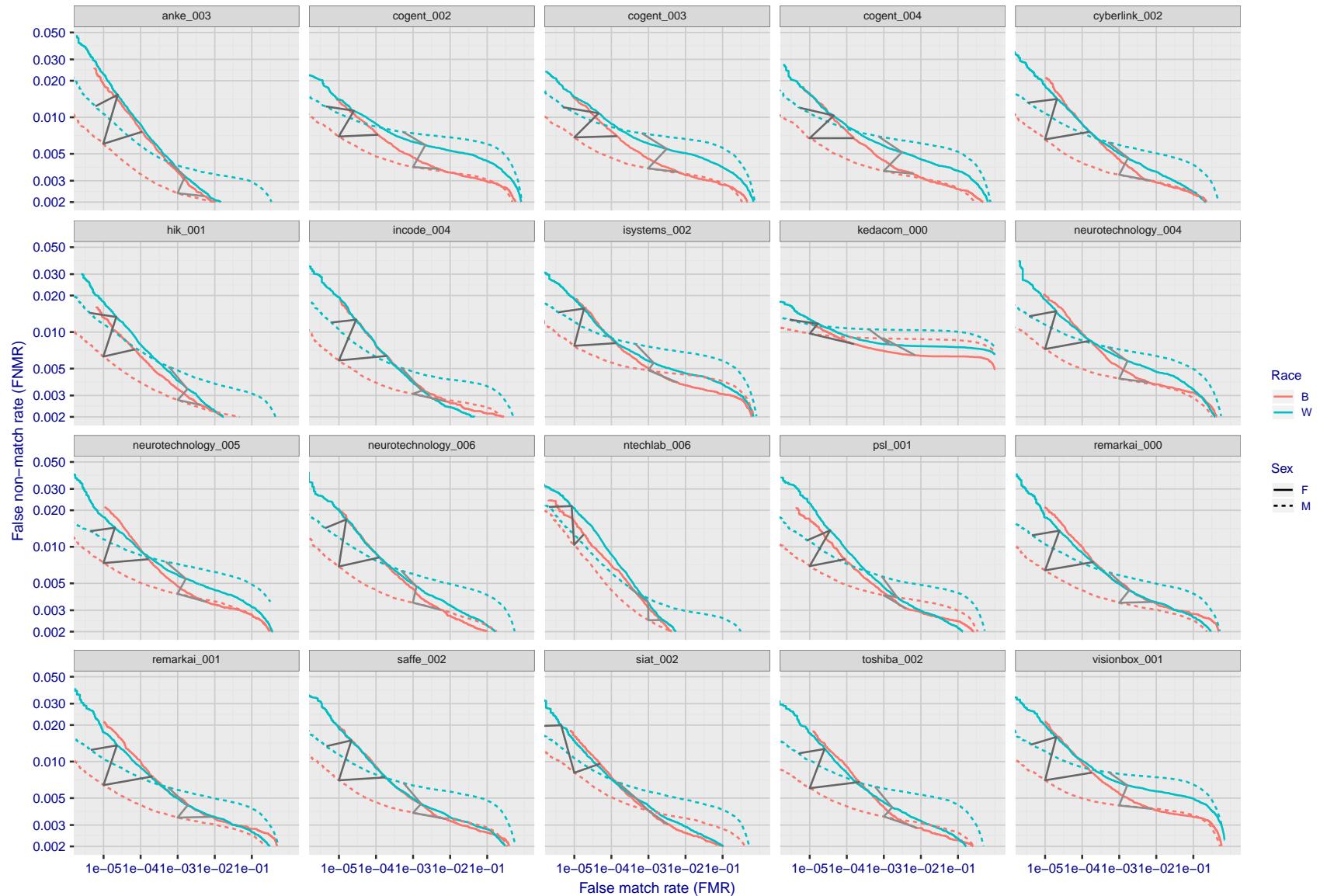


Figure 51: For the mugshot images, error tradeoff characteristics for white females, black females, black males and white males. The Z-shaped grey lines correspond to fixed thresholds, showing both FNMR and FMR vary at one T value. Note: Many of the plots will naively be read as saying women gives worse error rates than men because the solid traces lie above the dotted ones. However, this is misleading and incomplete: The grey lines show the traces reveal horizontal shifts. Thus for the cogent-003 algorithm FNMR for men is higher than for women at a fixed threshold but, at the same time, FMR is higher for women - see Figure 75. As access control systems almost always operate at a fixed threshold, the naive interpretation is incorrect.

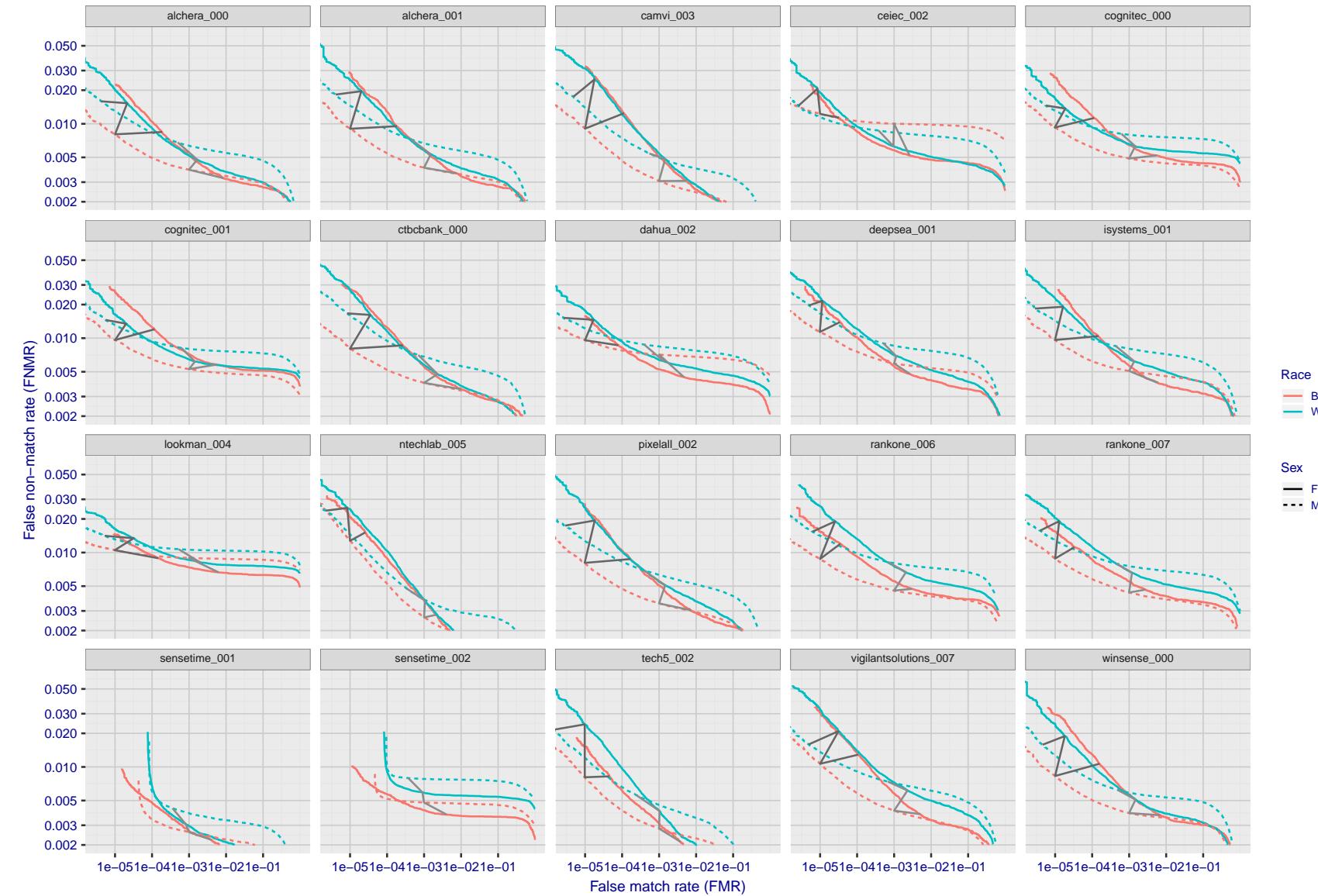


Figure 52: For the mugshot images, error tradeoff characteristics for white females, black females, black males and white males. The Z-shaped grey lines correspond to fixed thresholds, showing both FNMR and FMR vary at one T value. Note: Many of the plots will naively be read as saying women gives worse error rates than men because the solid traces lie above the dotted ones. However, this is misleading and incomplete: The grey lines show the traces reveal horizontal shifts. Thus for the cogent-003 algorithm FNMR for men is higher than for women at a fixed threshold but, at the same time, FMR is higher for women - see Figure 75. As access control systems almost always operate at a fixed threshold, the naive interpretation is incorrect.

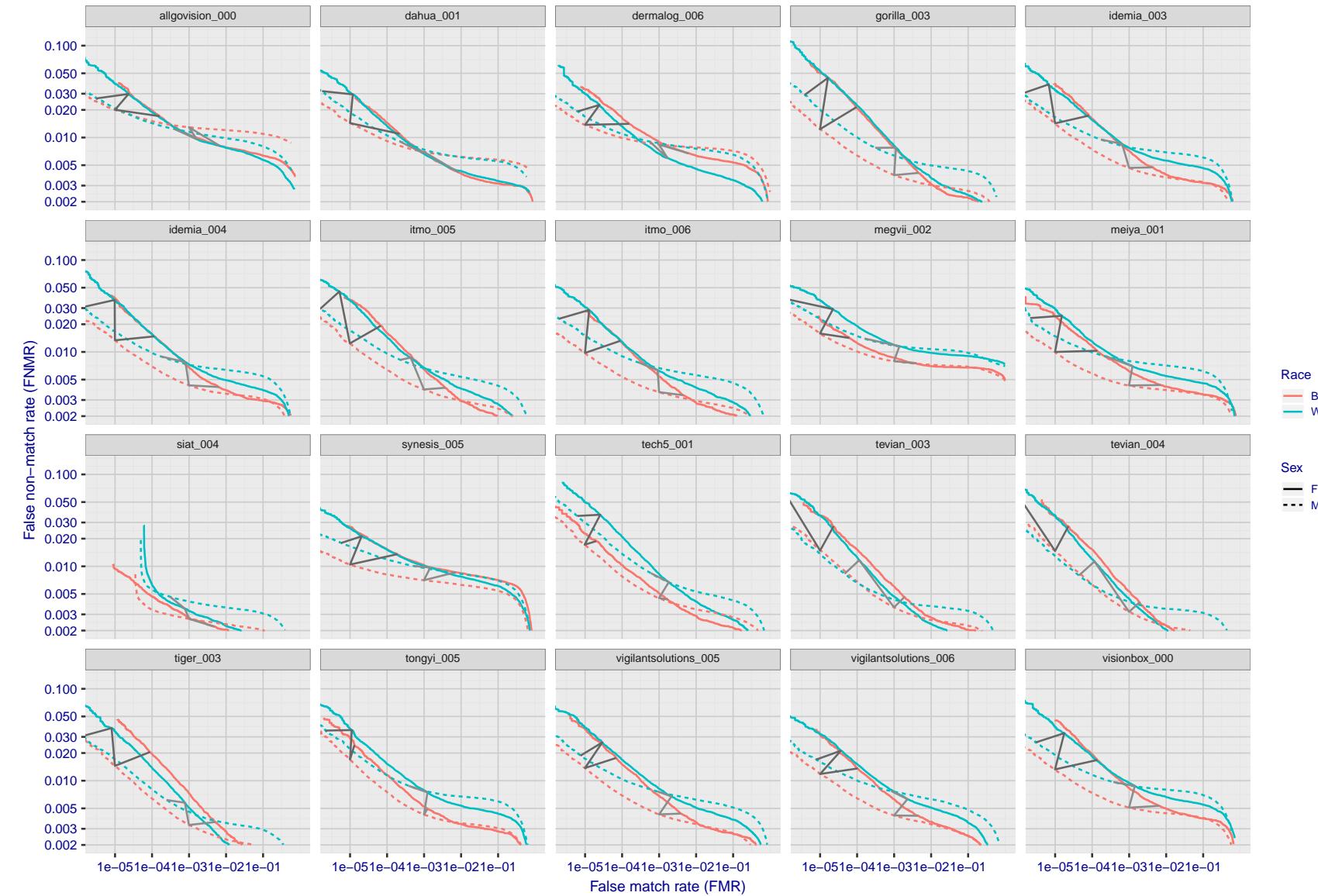


Figure 53: For the mugshot images, error tradeoff characteristics for white females, black females, black males and white males. The Z-shaped grey lines correspond to fixed thresholds, showing both FNMR and FMR vary at one T value. Note: Many of the plots will naively be read as saying women gives worse error rates than men because the solid traces lie above the dotted ones. However, this is misleading and incomplete: The grey lines show the traces reveal horizontal shifts. Thus for the cogent-003 algorithm FNMR for men is higher than for women at a fixed threshold but, at the same time, FMR is higher for women - see Figure 75. As access control systems almost always operate at a fixed threshold, the naive interpretation is incorrect.

2019/07/05 07:20:46

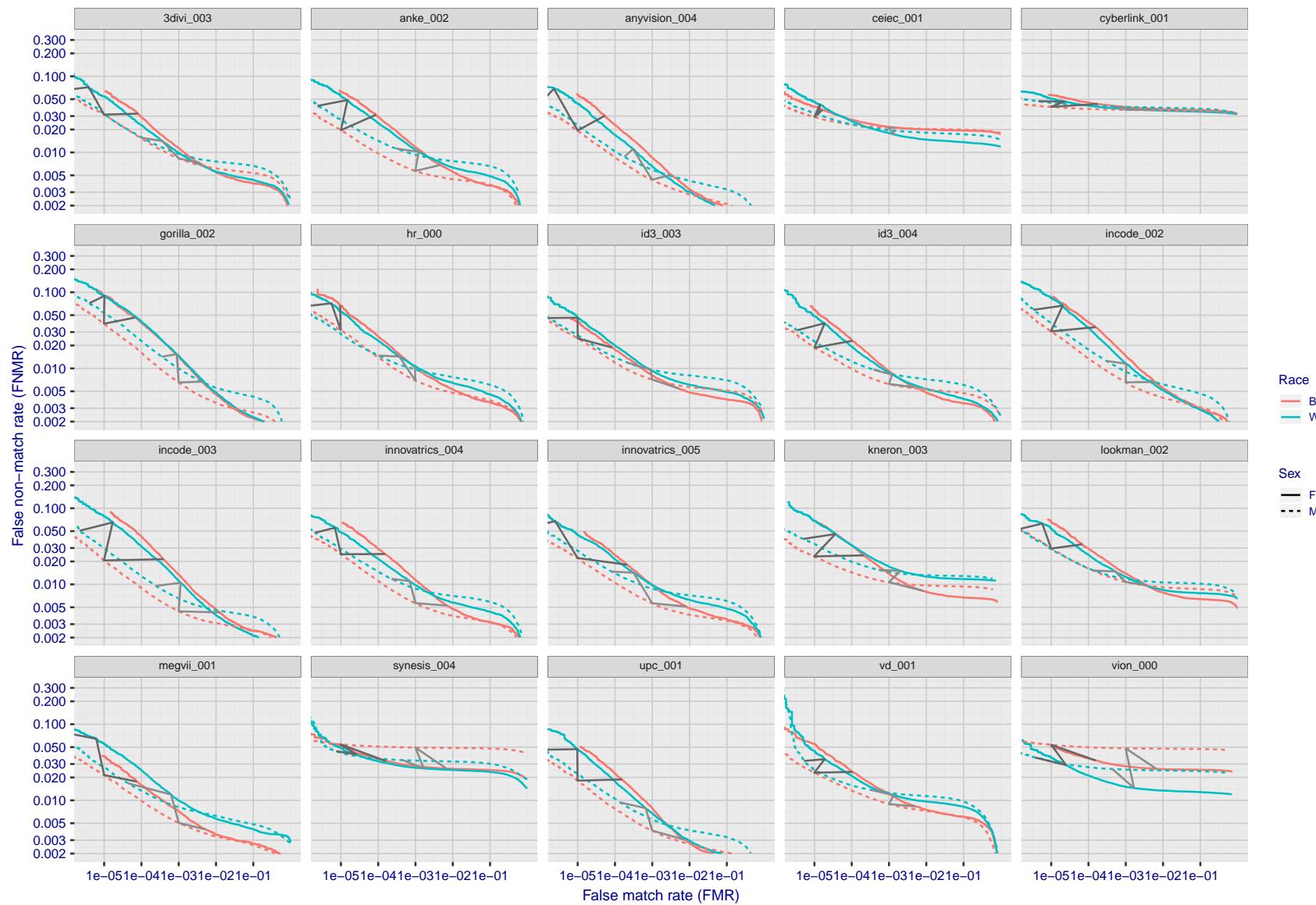


Figure 54: For the mugshot images, error tradeoff characteristics for white females, black females, black males and white males. The Z-shaped grey lines correspond to fixed thresholds, showing both FNMR and FMR vary at one T value. Note: Many of the plots will naively be read as saying women gives worse error rates than men because the solid traces lie above the dotted ones. However, this is misleading and incomplete: The grey lines show the traces reveal horizontal shifts. Thus for the cogent-003 algorithm FNMR for men is higher than for women at a fixed threshold but, at the same time, FMR is higher for women - see Figure 75. As access control systems almost always operate at a fixed threshold, the naive interpretation is incorrect.

FNMR( $T$ )  
FMR( $T$ )  
"False non-match rate"  
"False match rate"

2019/07/05 07:20:46

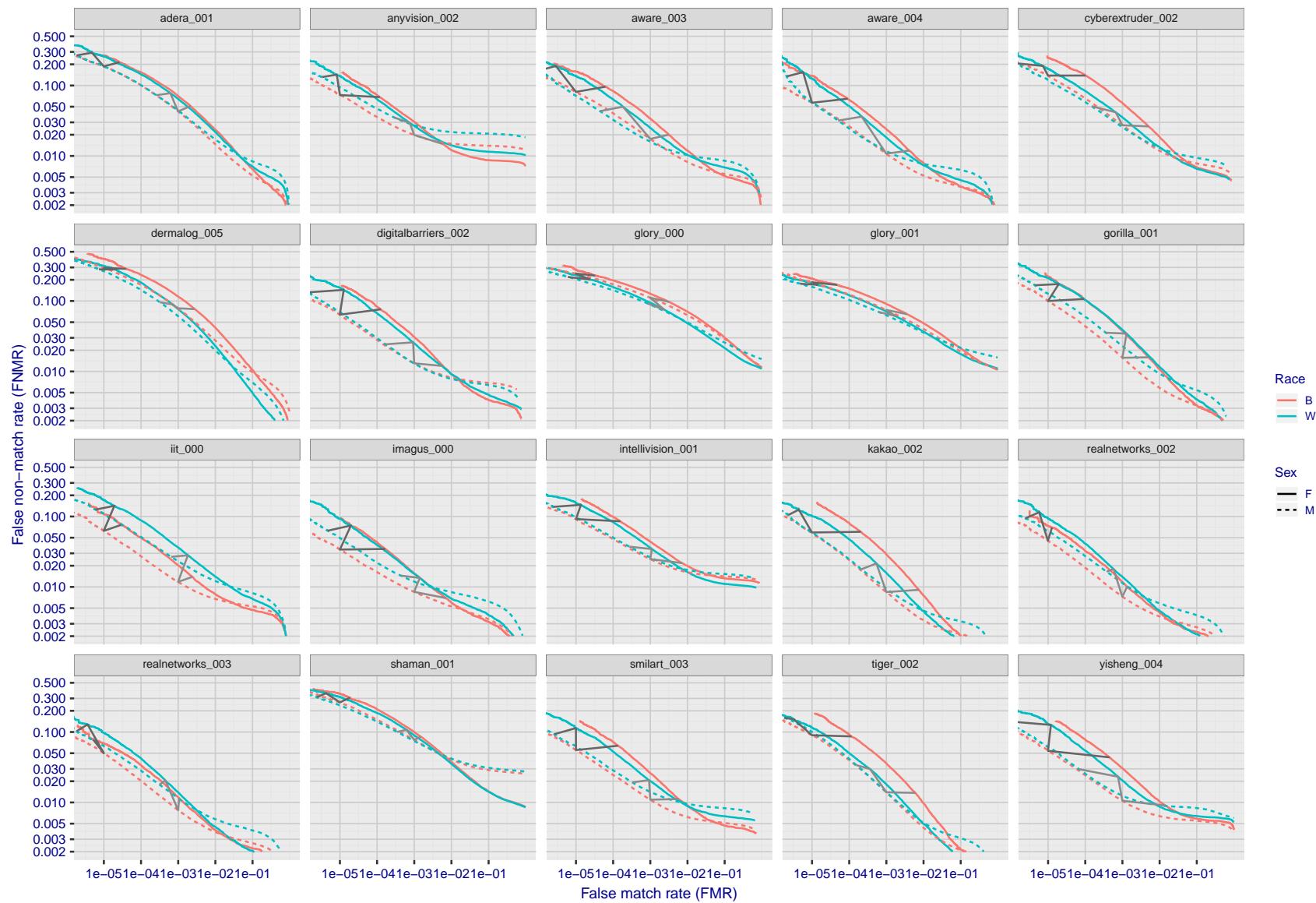


Figure 55: For the mugshot images, error tradeoff characteristics for white females, black females, black males and white males. The Z-shaped grey lines correspond to fixed thresholds, showing both FNMR and FMR vary at one T value. Note: Many of the plots will naively be read as saying women gives worse error rates than men because the solid traces lie above the dotted ones. However, this is misleading and incomplete: The grey lines show the traces reveal horizontal shifts. Thus for the cogent-003 algorithm FNMR for men is higher than for women at a fixed threshold but, at the same time, FMR is higher for women - see Figure 75. As access control systems almost always operate at a fixed threshold, the naive interpretation is incorrect.

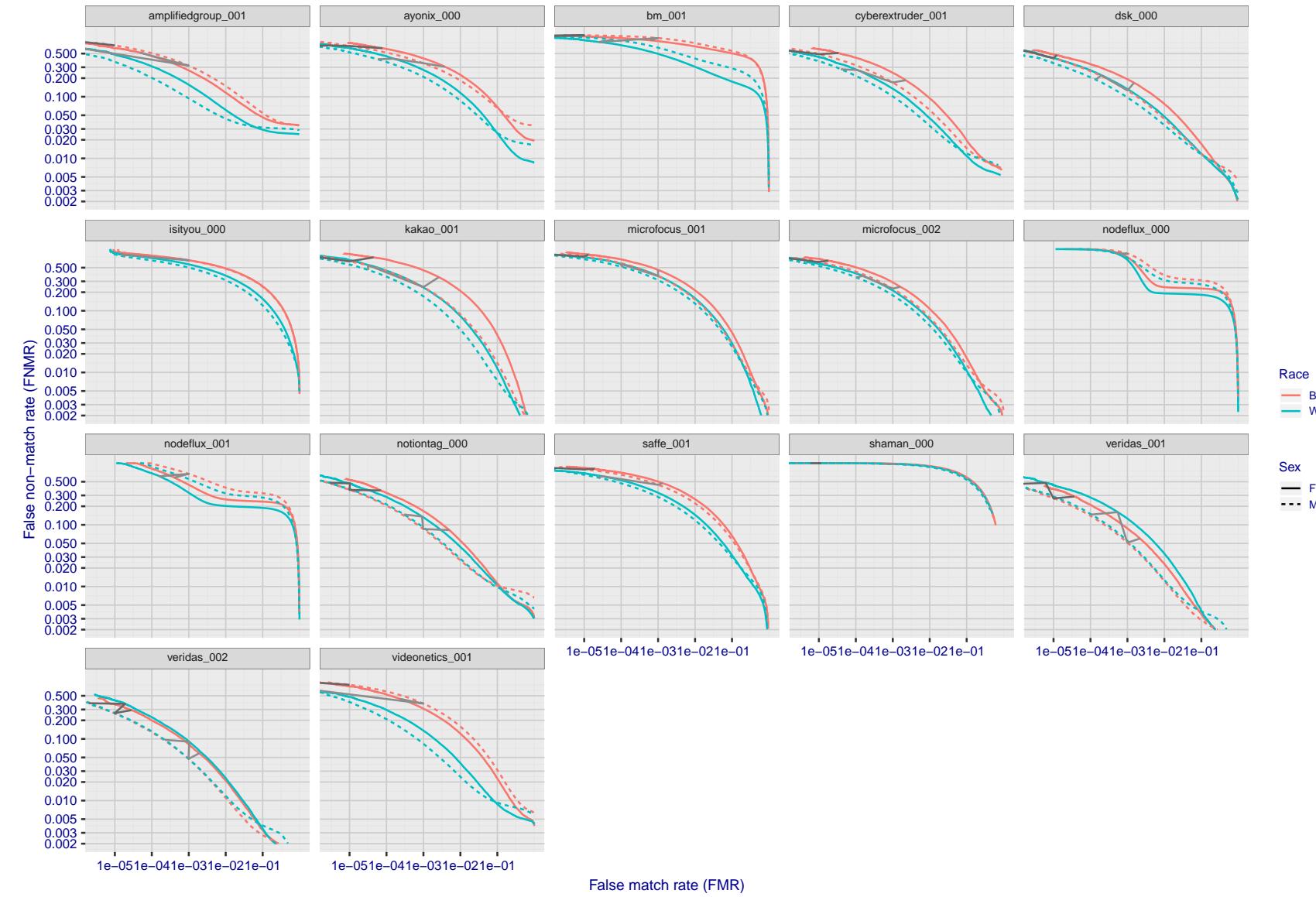


Figure 56: For the mugshot images, error tradeoff characteristics for white females, black females, black males and white males. The Z-shaped grey lines correspond to fixed thresholds, showing both FNMR and FMR vary at one T value. Note: Many of the plots will naively be read as saying women gives worse error rates than men because the solid traces lie above the dotted ones. However, this is misleading and incomplete: The grey lines show the traces reveal horizontal shifts. Thus for the cogent-003 algorithm FNMR for men is higher than for women at a fixed threshold but, at the same time, FMR is higher for women - see Figure 75. As access control systems almost always operate at a fixed threshold, the naive interpretation is incorrect.

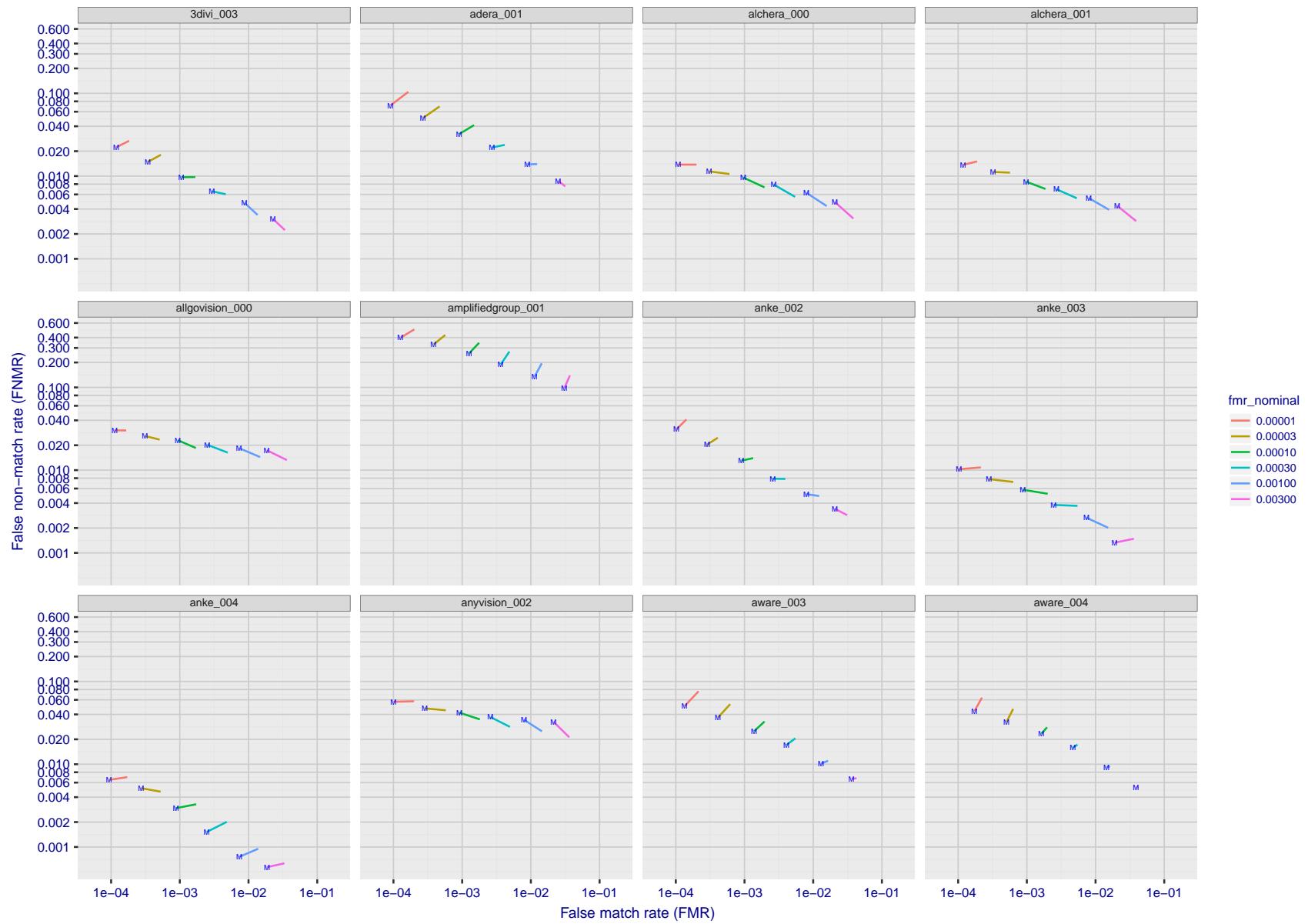


Figure 57: For the visa images, FNMR and FMR at six operating points along the DET characteristic. At each point a line is drawn between  $(FMR, FNMR)_{MALE}$  and  $(FMR, FNMR)_{FEMALE}$  showing how which sex has lower FMR and/or FNMR. The "M" label denotes male, the other end of the line corresponds to female. The six operating thresholds are selected to give the nominal false match rates given in the legend, and are computed over all impostor pairs regardless of age, sex, and place of birth. The plotted FMR values are broadly an order of magnitude larger than the nominal rates because FMR is computed over demographically-matched impostor pairs i.e individuals of the same sex, from the same geographic region (see section 3.6.1), and the same age group (see section 3.6.2).

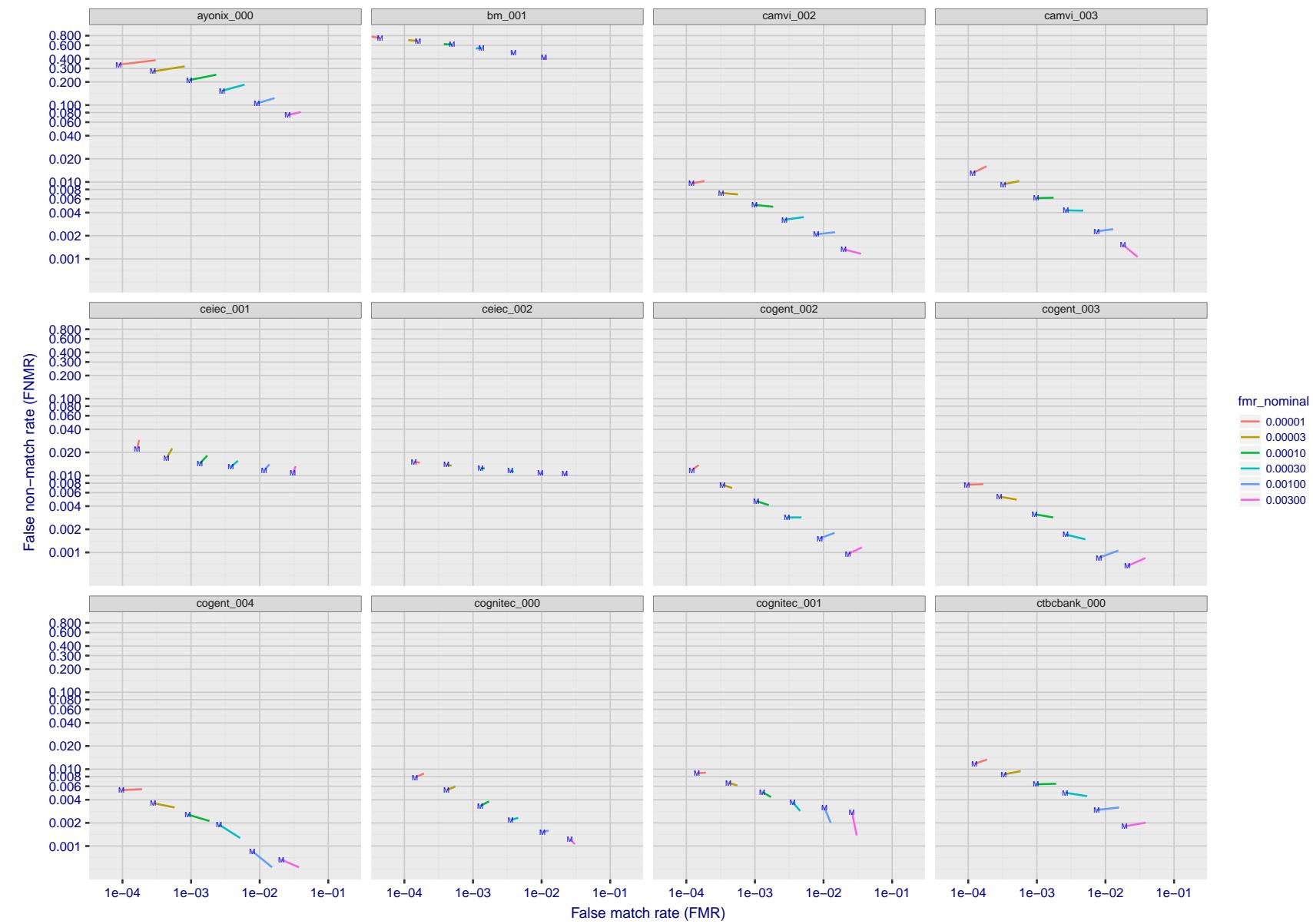


Figure 58: For the visa images, FNMR and FMR at six operating points along the DET characteristic. At each point a line is drawn between  $(FMR, FNMR)_{MALE}$  and  $(FMR, FNMR)_{FEMALE}$  showing how which sex has lower FMR and/or FNMR. The "M" label denotes male, the other end of the line corresponds to female. The six operating thresholds are selected to give the nominal false match rates given in the legend, and are computed over all impostor pairs regardless of age, sex, and place of birth. The plotted FMR values are broadly an order of magnitude larger than the nominal rates because FMR is computed over demographically-matched impostor pairs i.e individuals of the same sex, from the same geographic region (see section 3.6.1), and the same age group (see section 3.6.2).

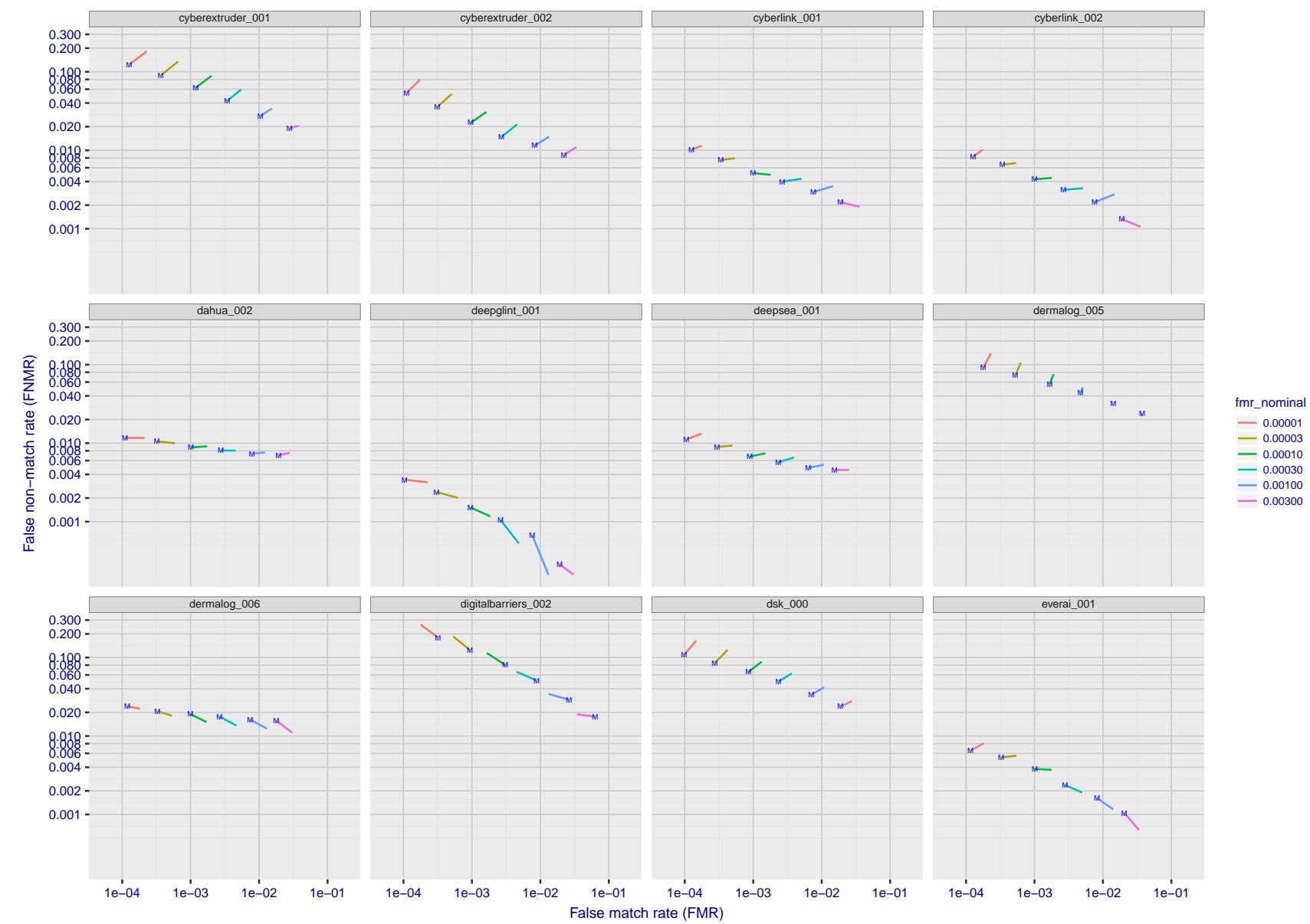


Figure 59: For the visa images, FNMR and FMR at six operating points along the DET characteristic. At each point a line is drawn between  $(FMR, FNMR)_{MALE}$  and  $(FMR, FNMR)_{FEMALE}$  showing how which sex has lower FMR and/or FNMR. The "M" label denotes male, the other end of the line corresponds to female. The six operating thresholds are selected to give the nominal false match rates given in the legend, and are computed over all impostor pairs regardless of age, sex, and place of birth. The plotted FMR values are broadly an order of magnitude larger than the nominal rates because FMR is computed over demographically-matched impostor pairs i.e individuals of the same sex, from the same geographic region (see section 3.6.1), and the same age group (see section 3.6.2).

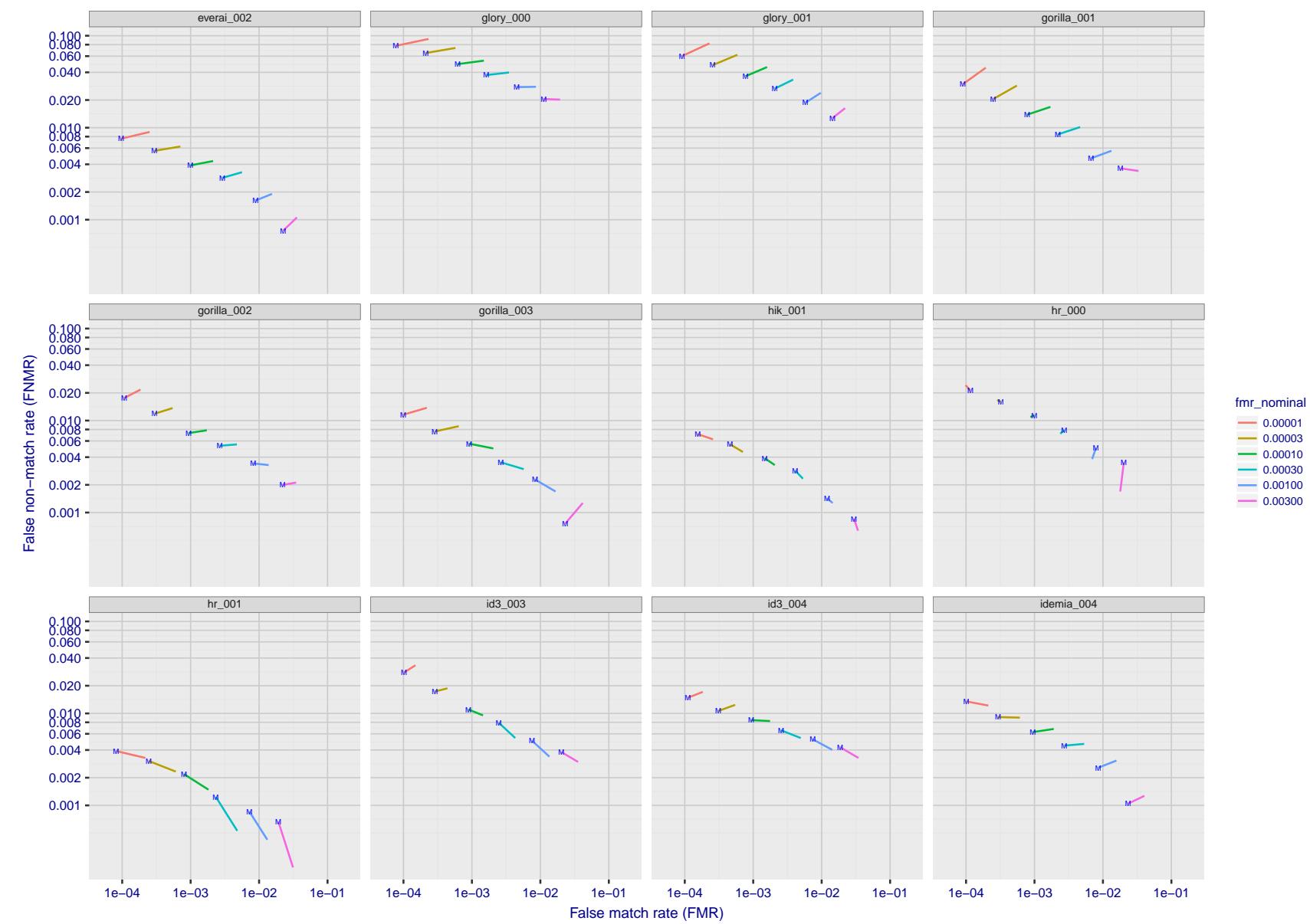


Figure 60: For the visa images, FNMR and FMR at six operating points along the DET characteristic. At each point a line is drawn between  $(FMR, FNMR)_{MALE}$  and  $(FMR, FNMR)_{FEMALE}$  showing how which sex has lower FMR and/or FNMR. The "M" label denotes male, the other end of the line corresponds to female. The six operating thresholds are selected to give the nominal false match rates given in the legend, and are computed over all impostor pairs regardless of age, sex, and place of birth. The plotted FMR values are broadly an order of magnitude larger than the nominal rates because FMR is computed over demographically-matched impostor pairs i.e individuals of the same sex, from the same geographic region (see section 3.6.1), and the same age group (see section 3.6.2).

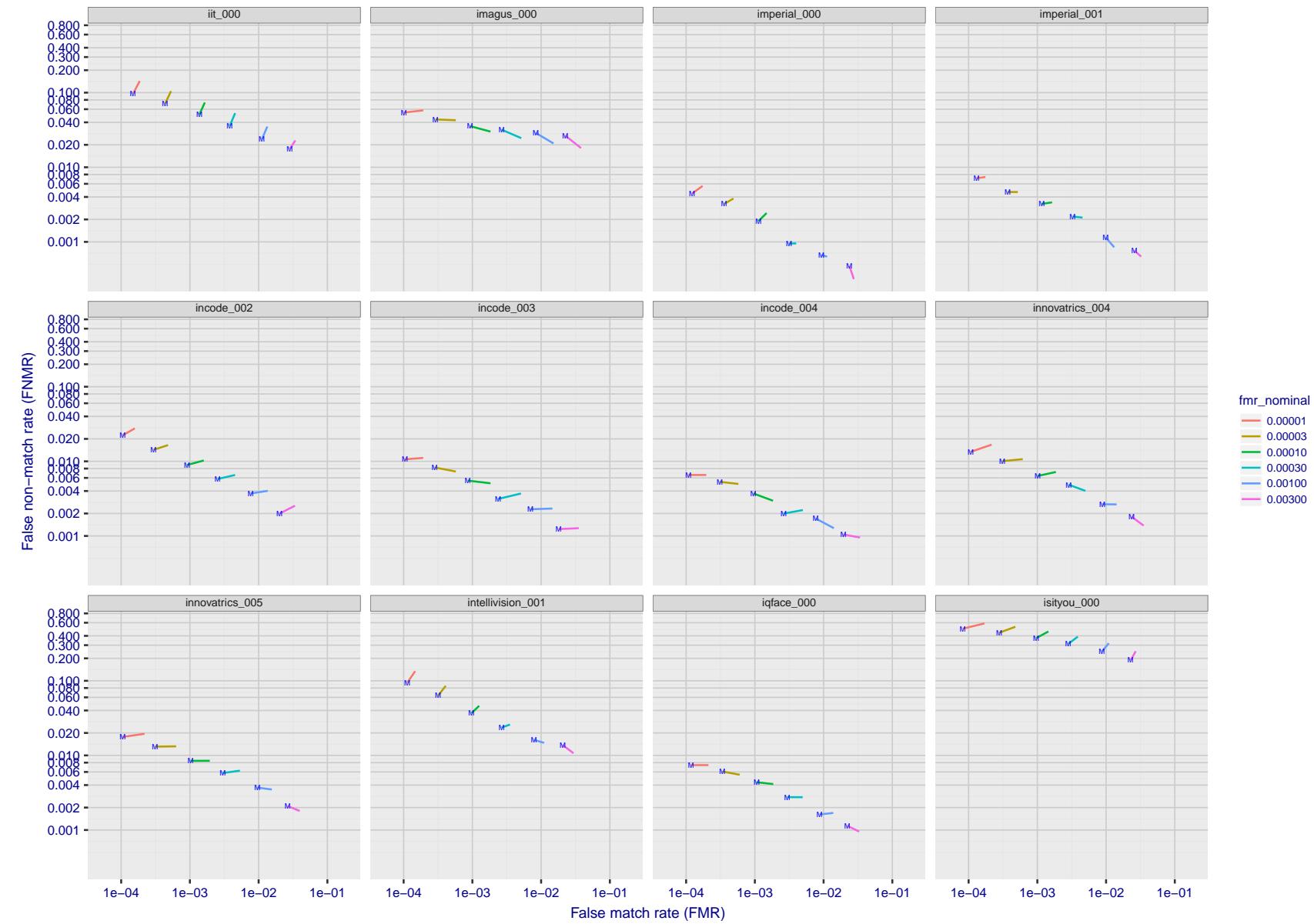


Figure 61: For the visa images, FNMR and FMR at six operating points along the DET characteristic. At each point a line is drawn between  $(FMR, FNMR)_{MALE}$  and  $(FMR, FNMR)_{FEMALE}$  showing how which sex has lower FMR and/or FNMR. The "M" label denotes male, the other end of the line corresponds to female. The six operating thresholds are selected to give the nominal false match rates given in the legend, and are computed over all impostor pairs regardless of age, sex, and place of birth. The plotted FMR values are broadly an order of magnitude larger than the nominal rates because FMR is computed over demographically-matched impostor pairs i.e individuals of the same sex, from the same geographic region (see section 3.6.1), and the same age group (see section 3.6.2).

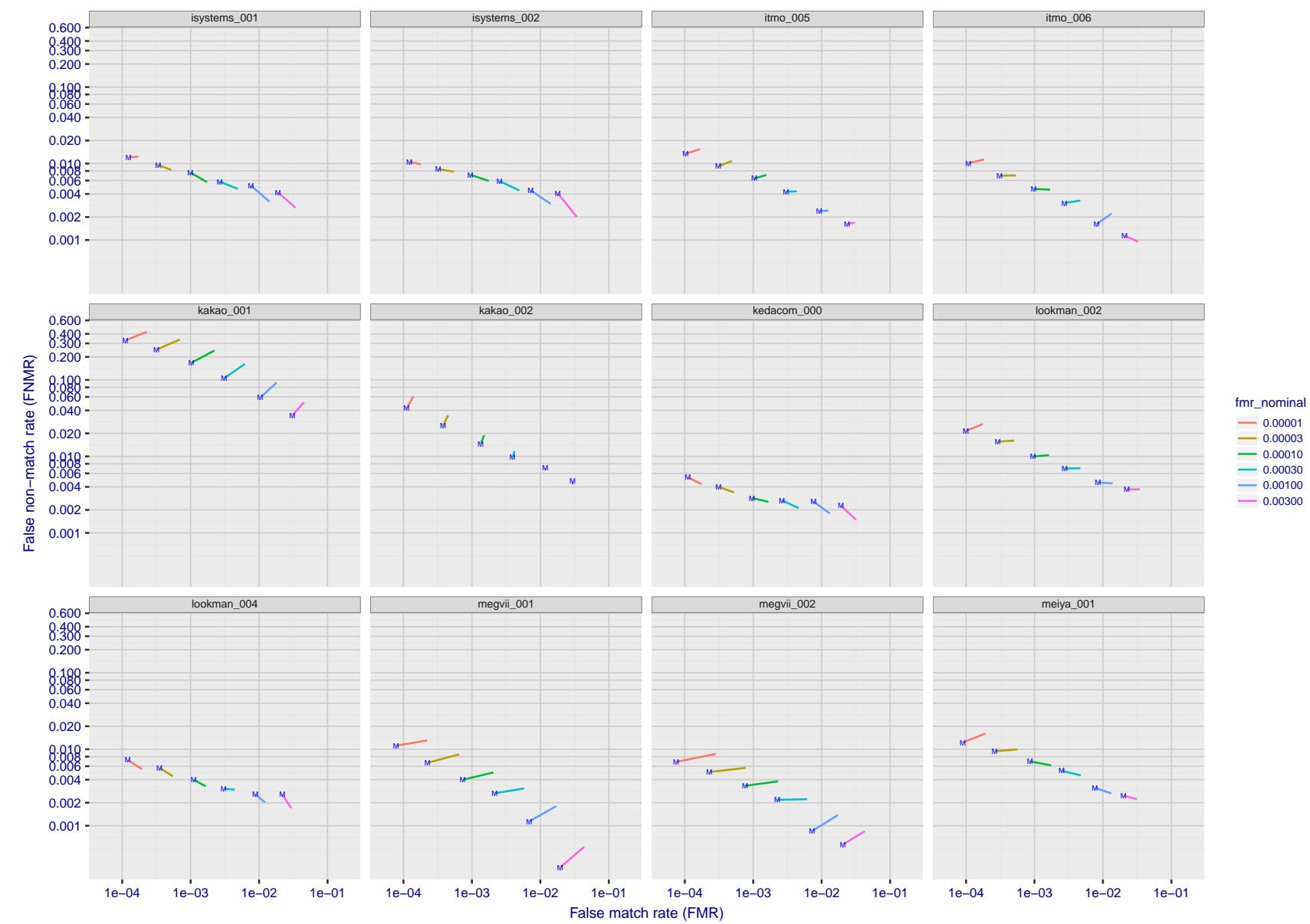


Figure 62: For the visa images, FNMR and FMR at six operating points along the DET characteristic. At each point a line is drawn between  $(FMR, FNMR)_{MALE}$  and  $(FMR, FNMR)_{FEMALE}$  showing how which sex has lower FMR and/or FNMR. The "M" label denotes male, the other end of the line corresponds to female. The six operating thresholds are selected to give the nominal false match rates given in the legend, and are computed over all impostor pairs regardless of age, sex, and place of birth. The plotted FMR values are broadly an order of magnitude larger than the nominal rates because FMR is computed over demographically-matched impostor pairs i.e individuals of the same sex, from the same geographic region (see section 3.6.1), and the same age group (see section 3.6.2).

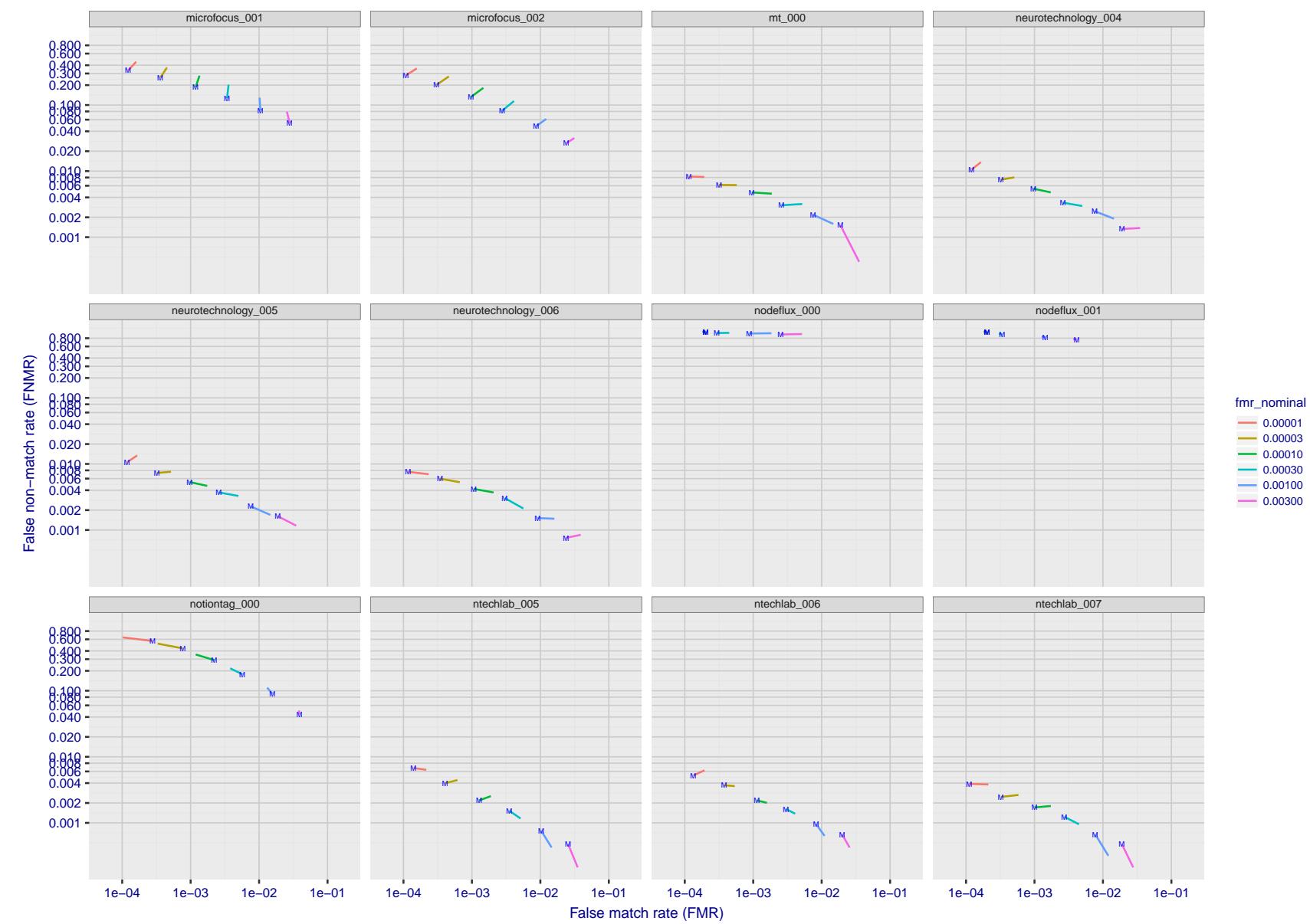


Figure 63: For the visa images, FNMR and FMR at six operating points along the DET characteristic. At each point a line is drawn between  $(FMR, FNMR)_{MALE}$  and  $(FMR, FNMR)_{FEMALE}$  showing how which sex has lower FMR and/or FNMR. The "M" label denotes male, the other end of the line corresponds to female. The six operating thresholds are selected to give the nominal false match rates given in the legend, and are computed over all impostor pairs regardless of age, sex, and place of birth. The plotted FMR values are broadly an order of magnitude larger than the nominal rates because FMR is computed over demographically-matched impostor pairs i.e individuals of the same sex, from the same geographic region (see section 3.6.1), and the same age group (see section 3.6.2).

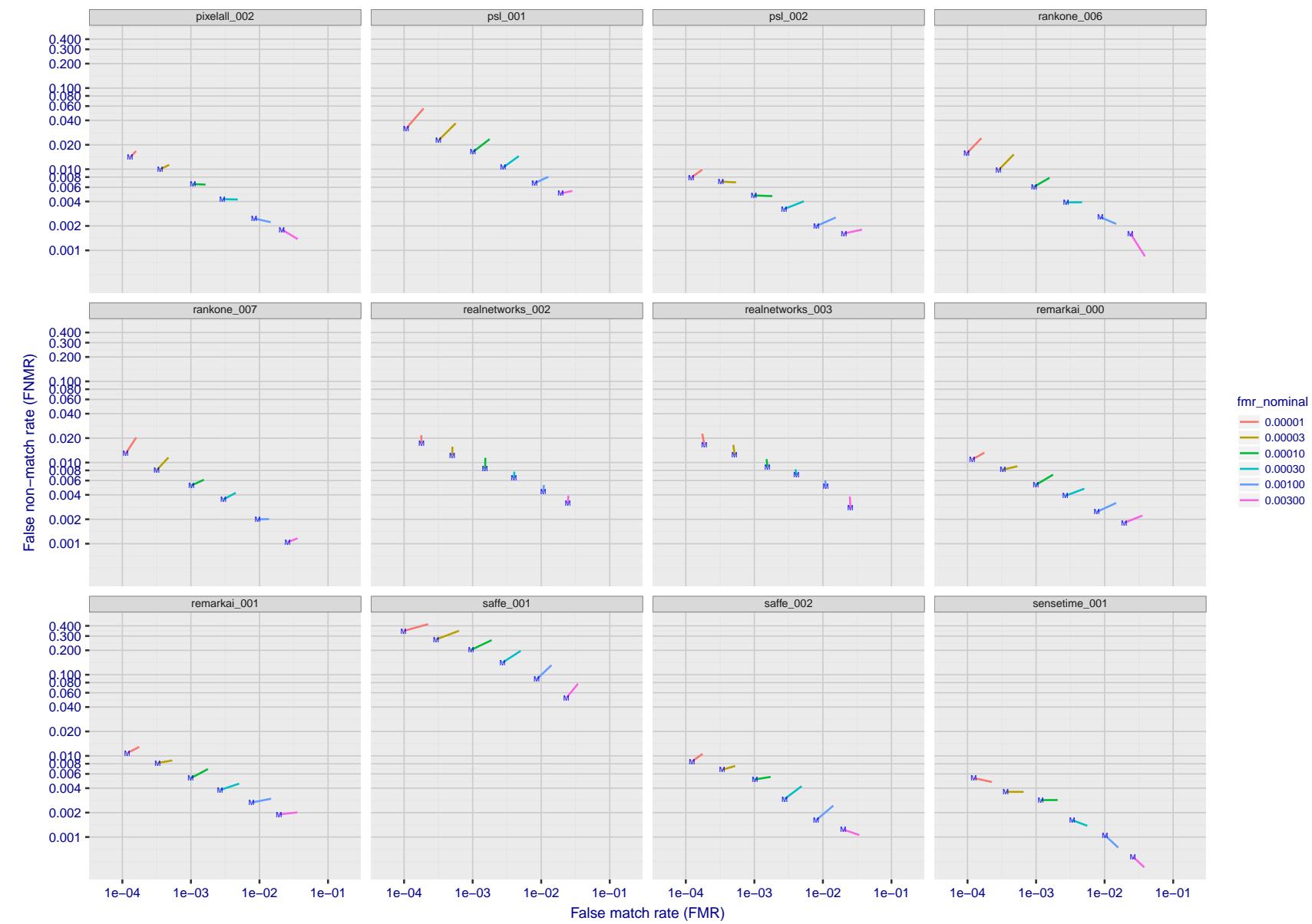


Figure 64: For the visa images, FNMR and FMR at six operating points along the DET characteristic. At each point a line is drawn between  $(FMR, FNMR)_{MALE}$  and  $(FMR, FNMR)_{FEMALE}$  showing how which sex has lower FMR and/or FNMR. The "M" label denotes male, the other end of the line corresponds to female. The six operating thresholds are selected to give the nominal false match rates given in the legend, and are computed over all impostor pairs regardless of age, sex, and place of birth. The plotted FMR values are broadly an order of magnitude larger than the nominal rates because FMR is computed over demographically-matched impostor pairs i.e individuals of the same sex, from the same geographic region (see section 3.6.1), and the same age group (see section 3.6.2).

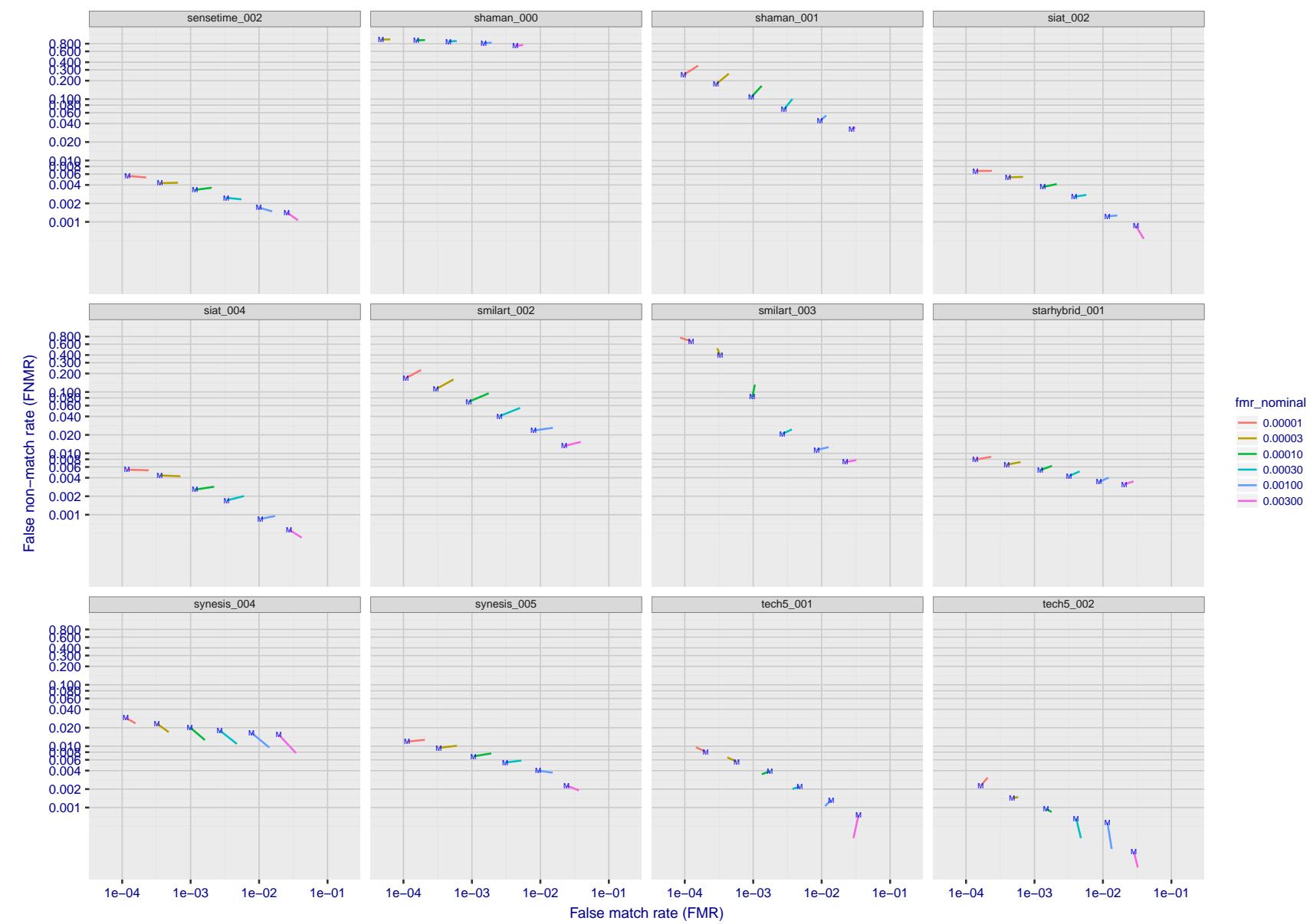


Figure 65: For the visa images, FNMR and FMR at six operating points along the DET characteristic. At each point a line is drawn between  $(FMR, FNMR)_{MALE}$  and  $(FMR, FNMR)_{FEMALE}$  showing how which sex has lower FMR and/or FNMR. The "M" label denotes male, the other end of the line corresponds to female. The six operating thresholds are selected to give the nominal false match rates given in the legend, and are computed over all impostor pairs regardless of age, sex, and place of birth. The plotted FMR values are broadly an order of magnitude larger than the nominal rates because FMR is computed over demographically-matched impostor pairs i.e individuals of the same sex, from the same geographic region (see section 3.6.1), and the same age group (see section 3.6.2).

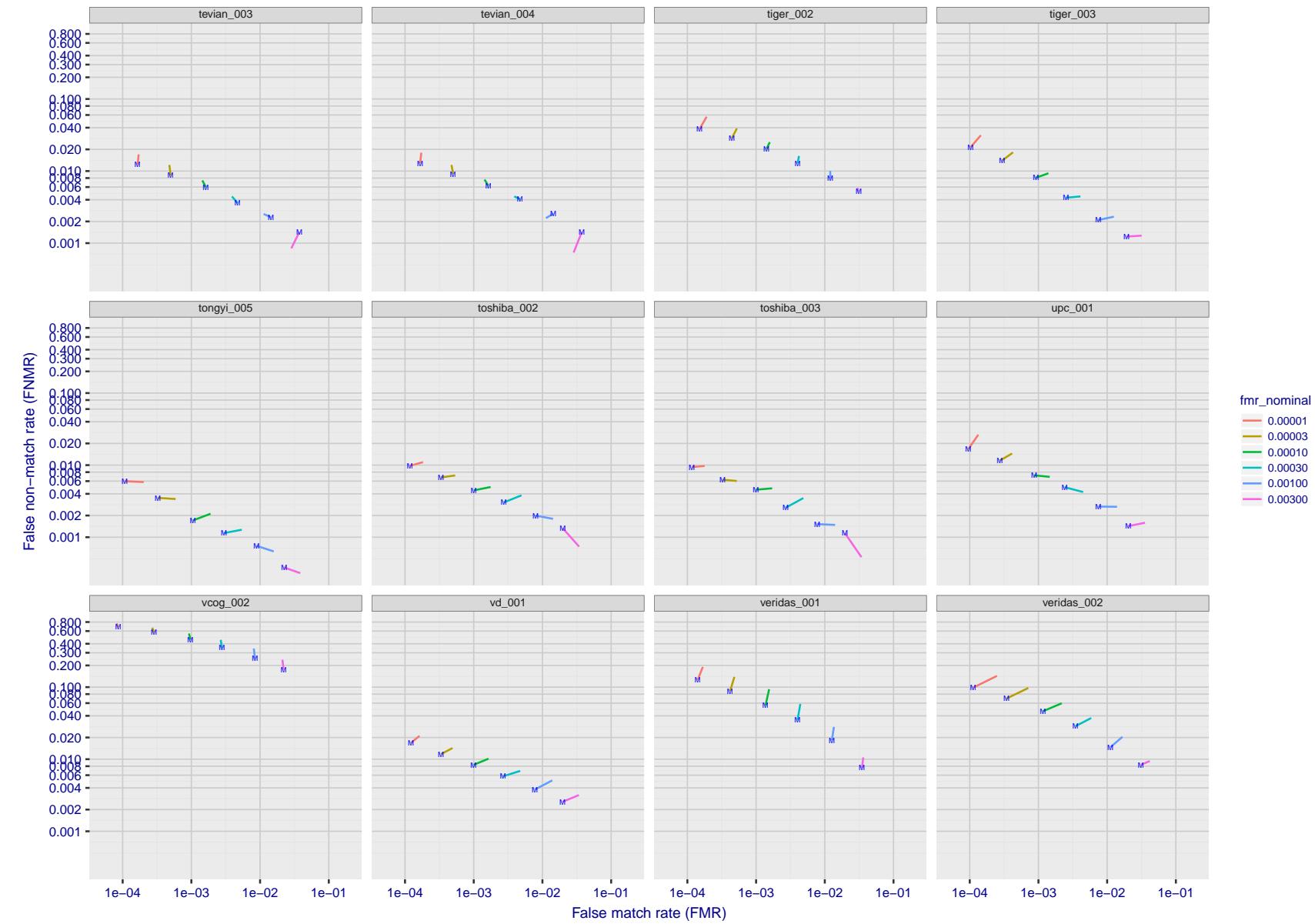


Figure 66: For the visa images, FNMR and FMR at six operating points along the DET characteristic. At each point a line is drawn between  $(FMR, FNMR)_{MALE}$  and  $(FMR, FNMR)_{FEMALE}$  showing how which sex has lower FMR and/or FNMR. The "M" label denotes male, the other end of the line corresponds to female. The six operating thresholds are selected to give the nominal false match rates given in the legend, and are computed over all impostor pairs regardless of age, sex, and place of birth. The plotted FMR values are broadly an order of magnitude larger than the nominal rates because FMR is computed over demographically-matched impostor pairs i.e individuals of the same sex, from the same geographic region (see section 3.6.1), and the same age group (see section 3.6.2).

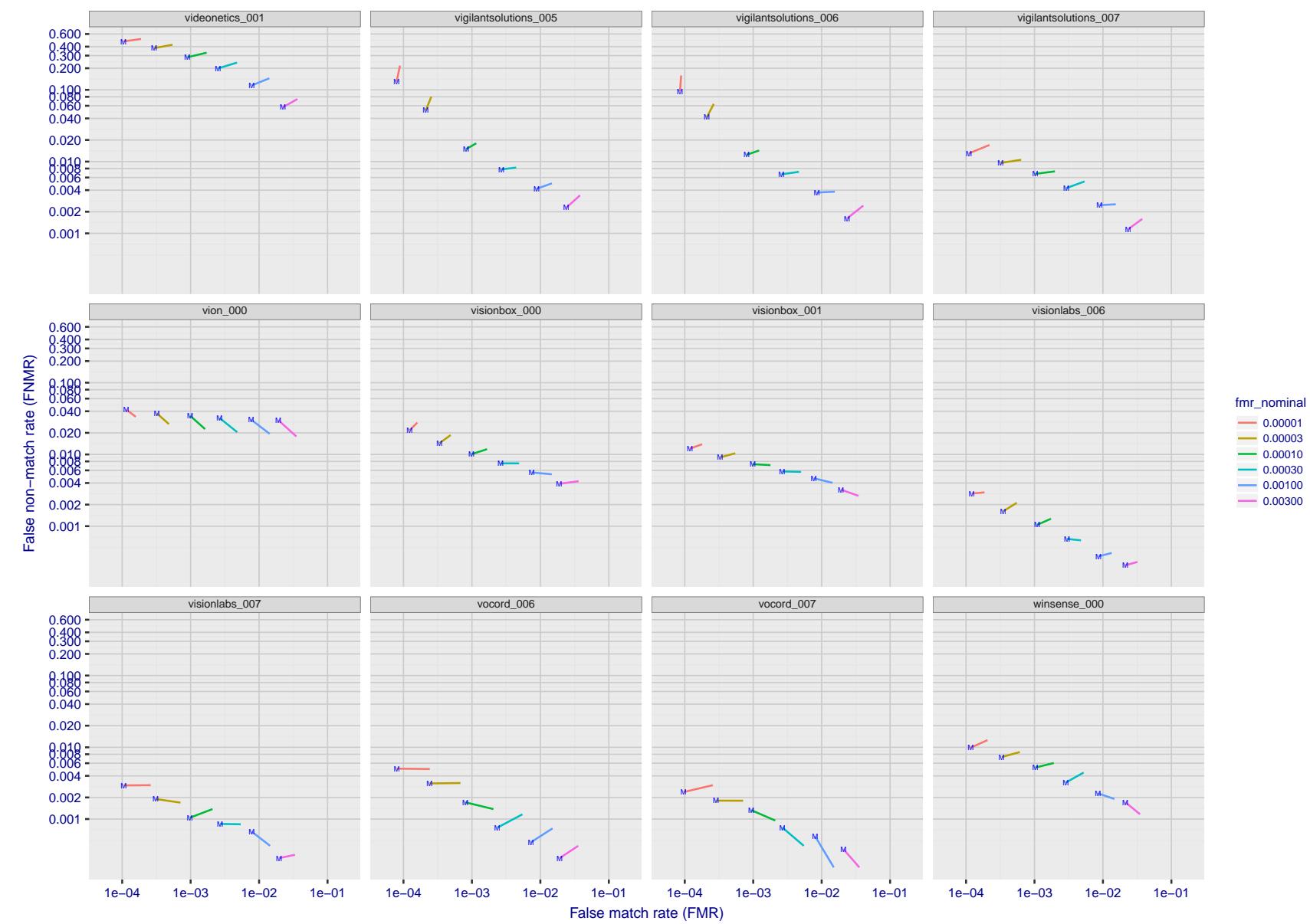


Figure 67: For the visa images, FNMR and FMR at six operating points along the DET characteristic. At each point a line is drawn between  $(FMR, FNMR)_{MALE}$  and  $(FMR, FNMR)_{FEMALE}$  showing how which sex has lower FMR and/or FNMR. The "M" label denotes male, the other end of the line corresponds to female. The six operating thresholds are selected to give the nominal false match rates given in the legend, and are computed over all impostor pairs regardless of age, sex, and place of birth. The plotted FMR values are broadly an order of magnitude larger than the nominal rates because FMR is computed over demographically-matched impostor pairs i.e individuals of the same sex, from the same geographic region (see section 3.6.1), and the same age group (see section 3.6.2).

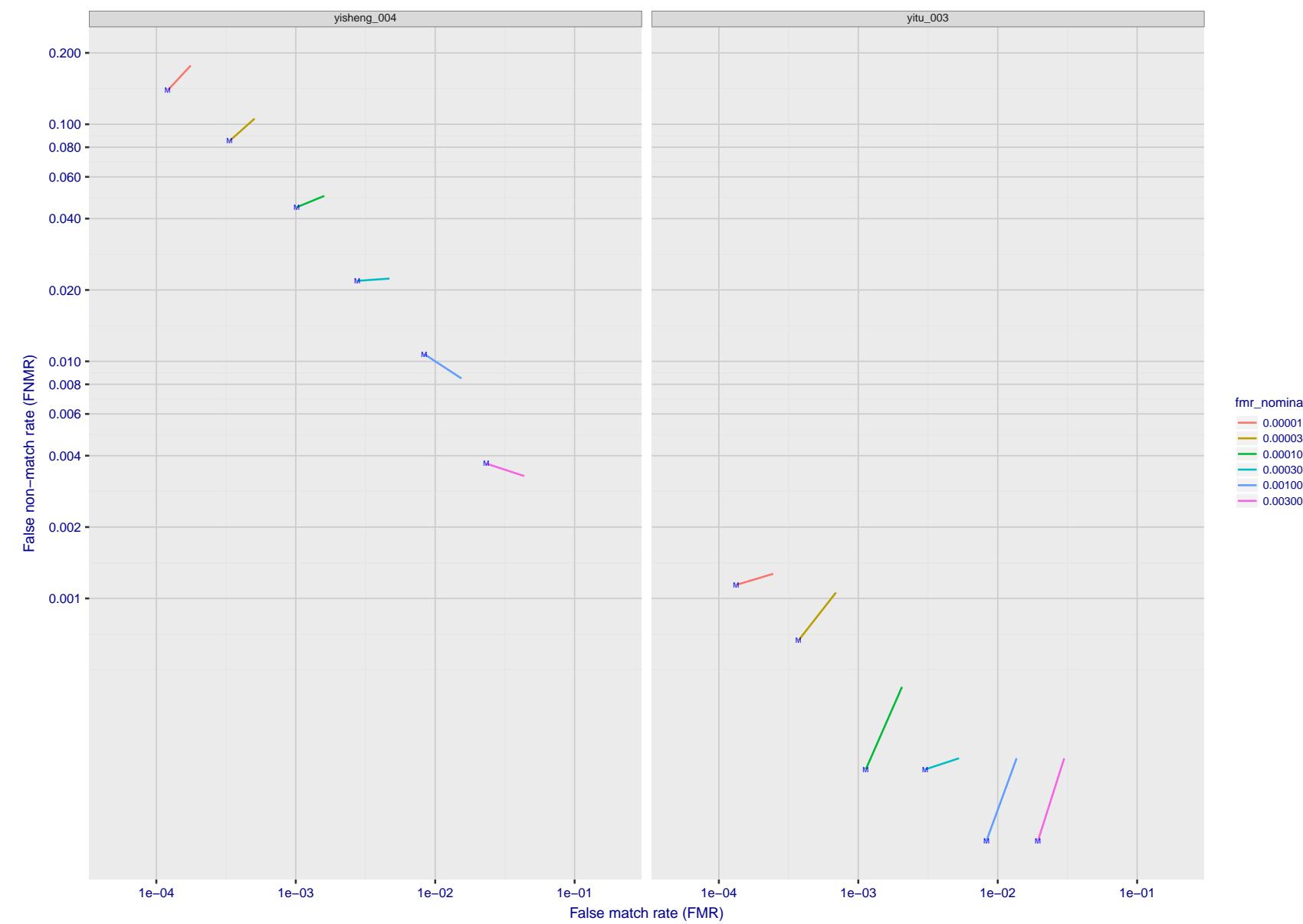


Figure 68: For the visa images, FNMR and FMR at six operating points along the DET characteristic. At each point a line is drawn between  $(FMR, FNMR)_{MALE}$  and  $(FMR, FNMR)_{FEMALE}$  showing how which sex has lower FMR and/or FNMR. The "M" label denotes male, the other end of the line corresponds to female. The six operating thresholds are selected to give the nominal false match rates given in the legend, and are computed over all impostor pairs regardless of age, sex, and place of birth. The plotted FMR values are broadly an order of magnitude larger than the nominal rates because FMR is computed over demographically-matched impostor pairs i.e individuals of the same sex, from the same geographic region (see section 3.6.1), and the same age group (see section 3.6.2).

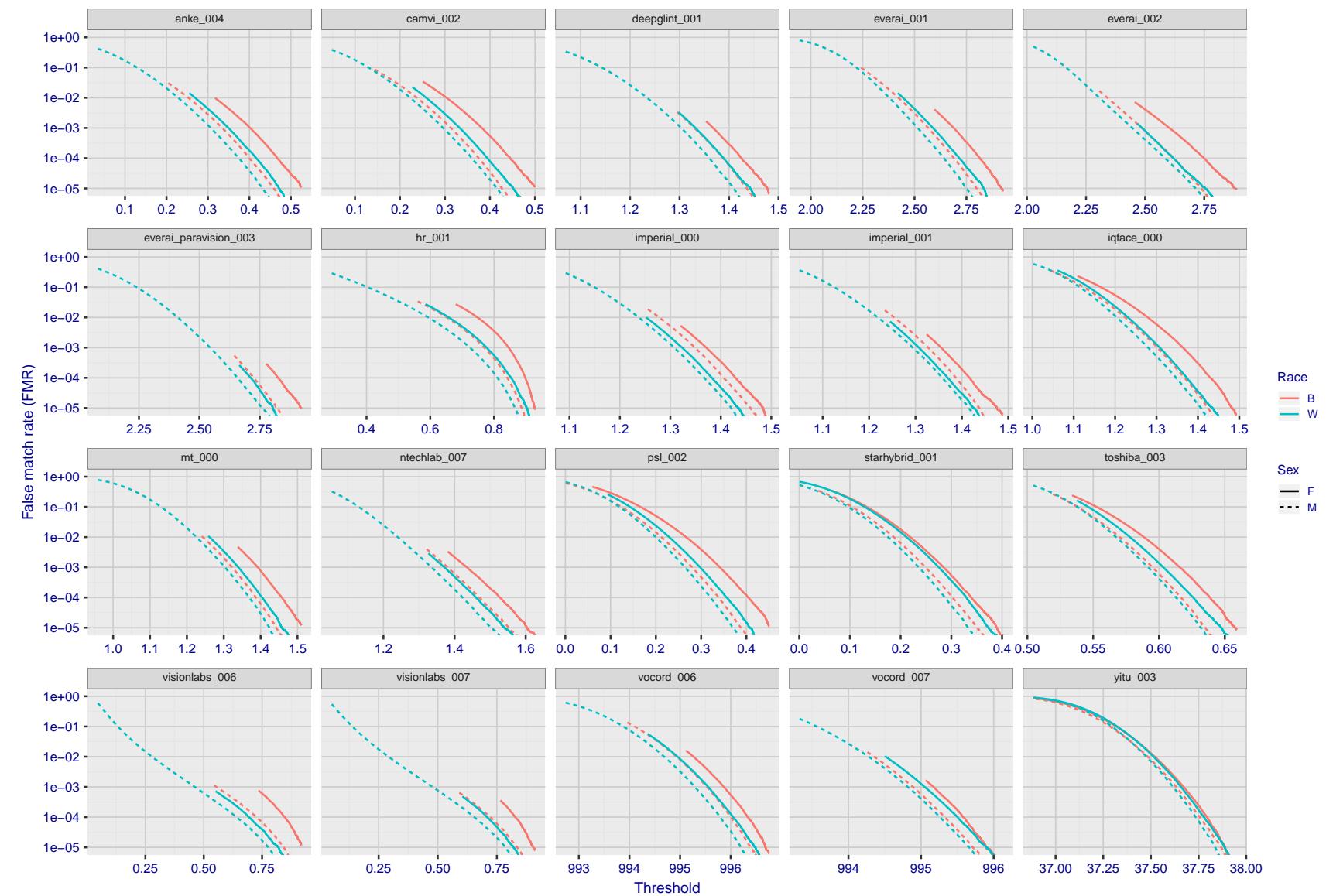


Figure 69: For the mugshot images, the false match calibration curves show false match rate vs. threshold. Separate curves appear for white females, black females, black males and white males.

2019/07/05 07:20:46

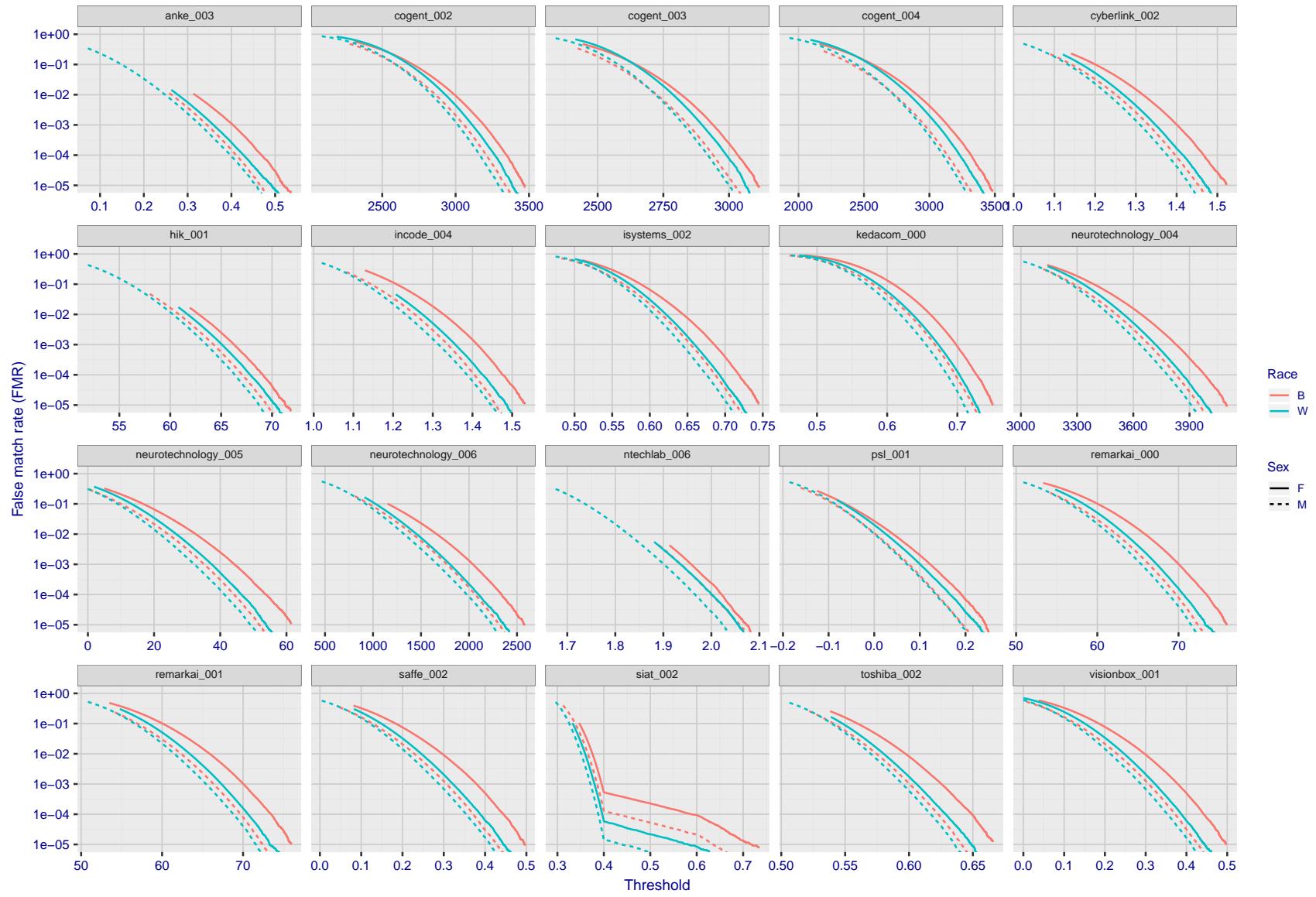


Figure 70: For the mugshot images, the false match calibration curves show false match rate vs. threshold. Separate curves appear for white females, black females, black males and white males.

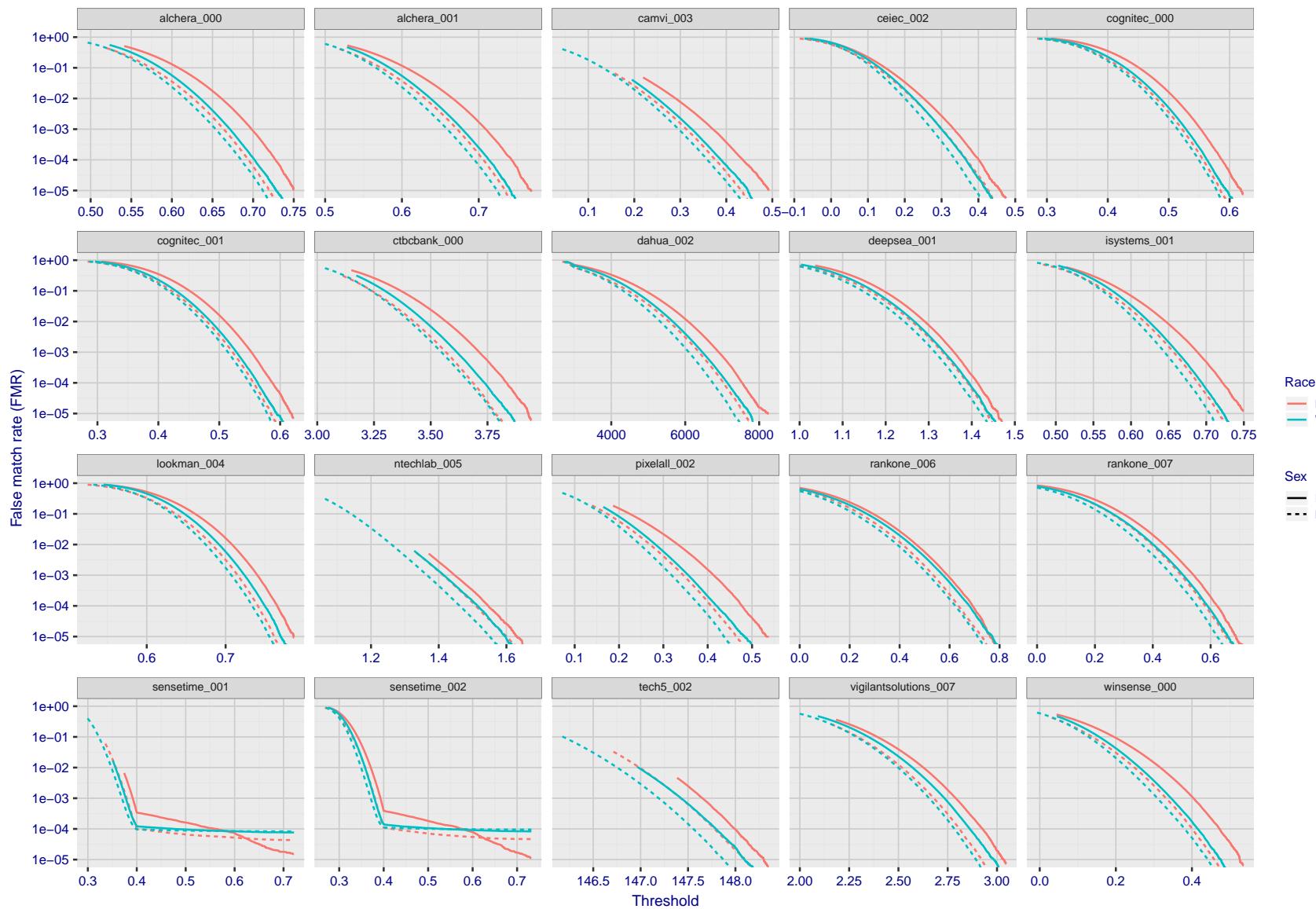
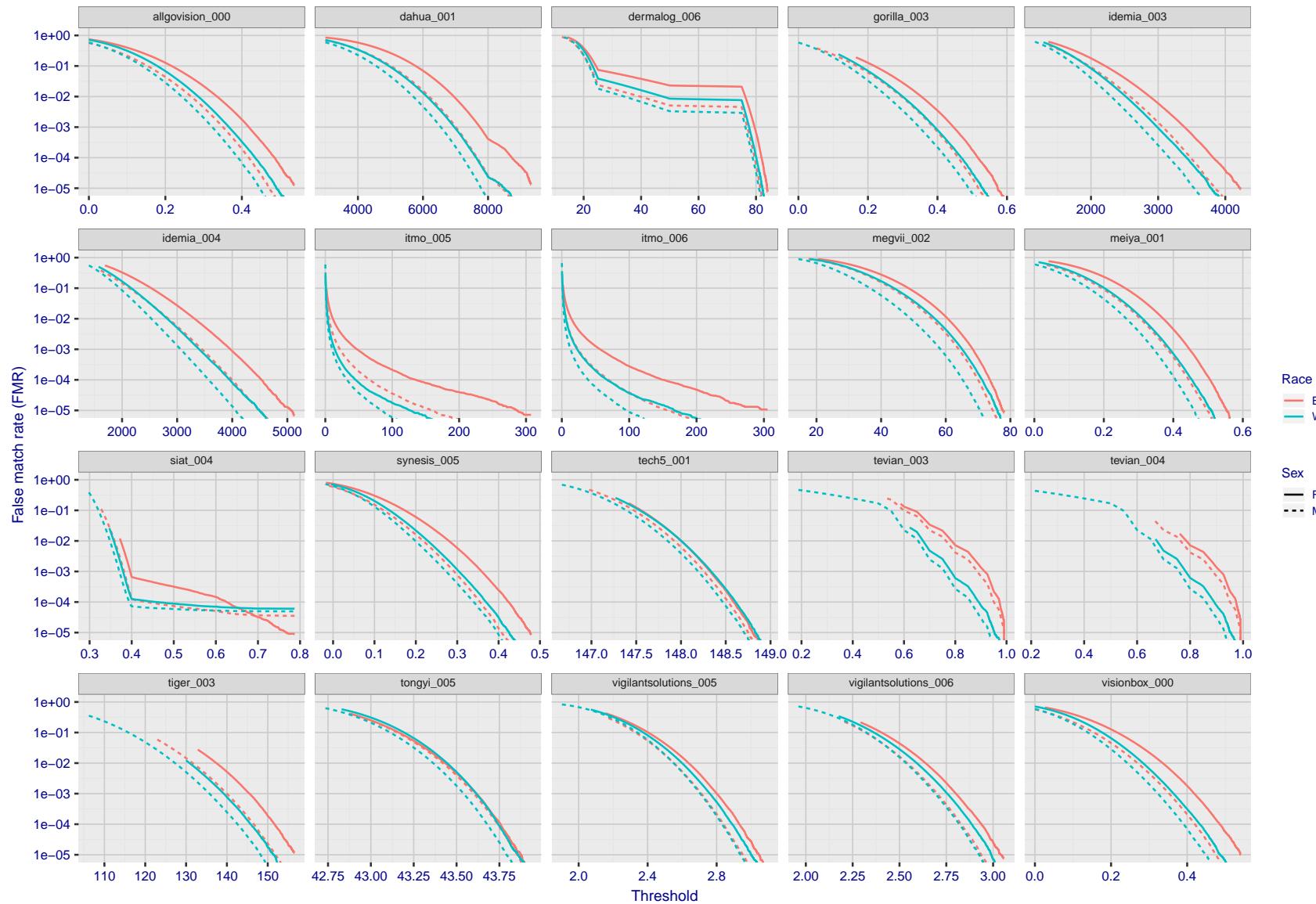


Figure 71: For the mugshot images, the false match calibration curves show false match rate vs. threshold. Separate curves appear for white females, black females, black males and white males.

2019/07/05 07:20:46



FNMR(T)  
"False non-match rate"  
"False match rate"

Figure 72: For the mugshot images, the false match calibration curves show false match rate vs. threshold. Separate curves appear for white females, black females, black males and white males.

2019/07/05 07:20:46

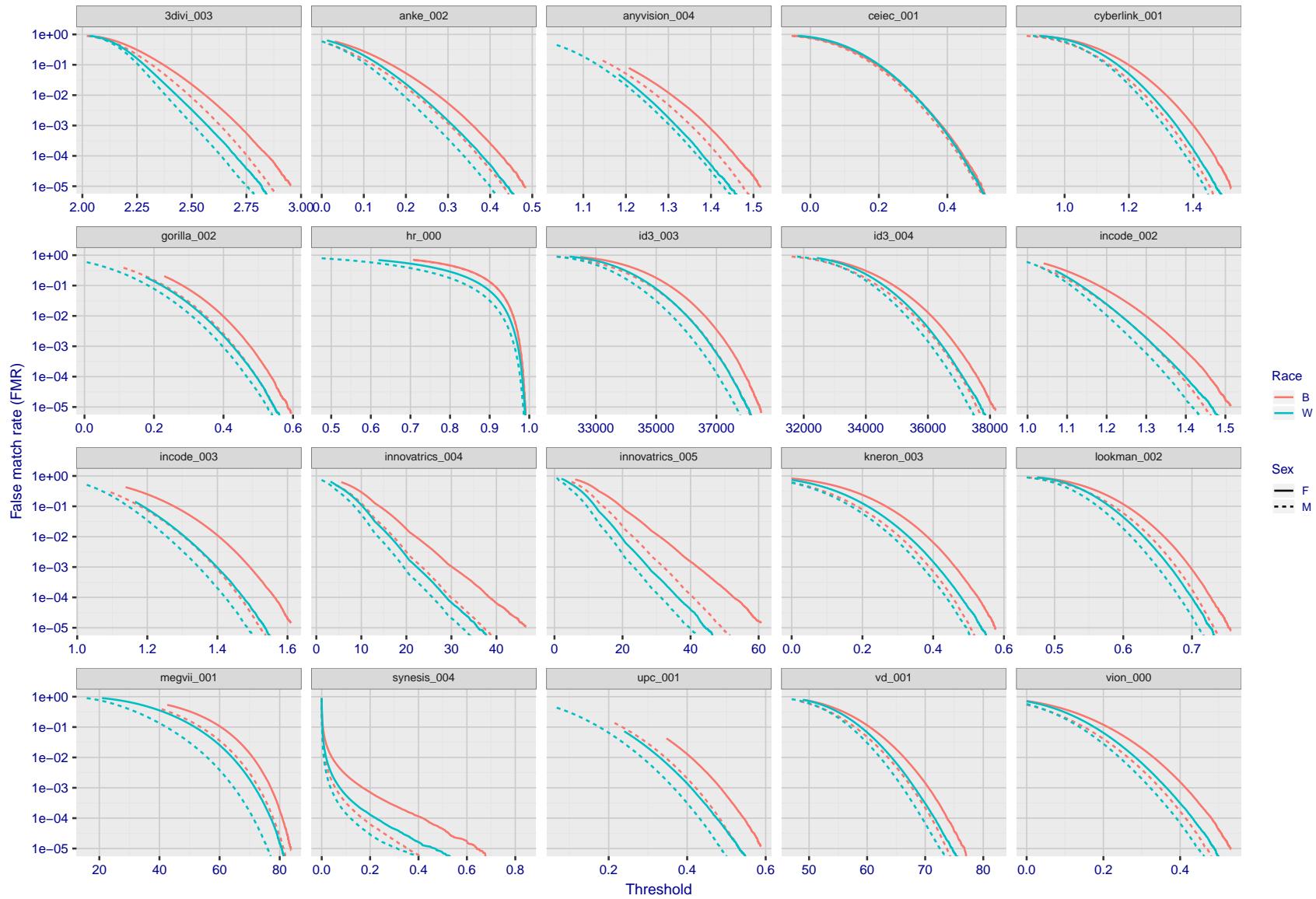


Figure 73: For the mugshot images, the false match calibration curves show false match rate vs. threshold. Separate curves appear for white females, black females, black males and white males.

FNMR(T)

"False non-match rate"

"False match rate"

2019/07/05 07:20:46

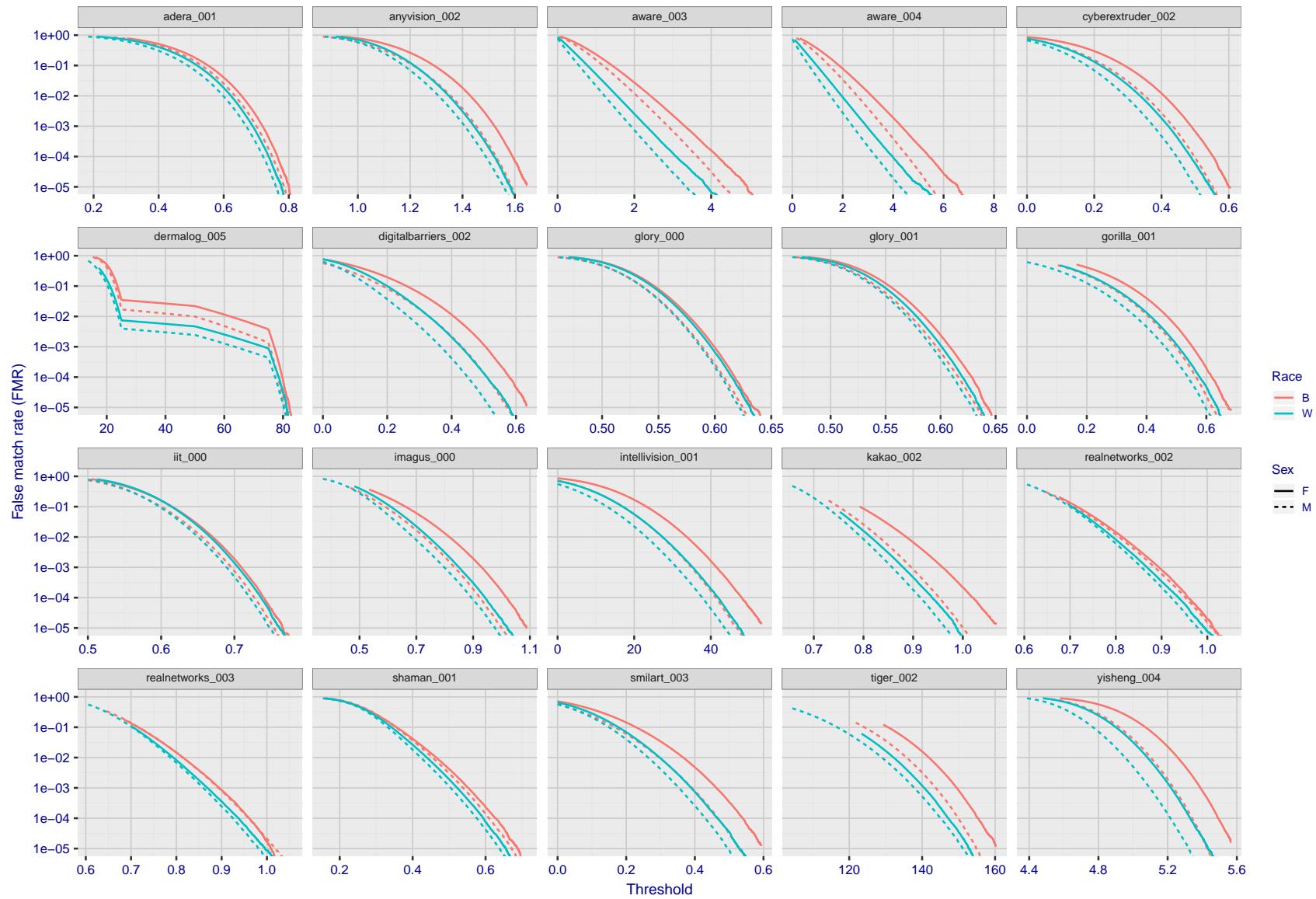


Figure 74: For the mugshot images, the false match calibration curves show false match rate vs. threshold. Separate curves appear for white females, black females, black males and white males.

2019/07/05 07:20:46

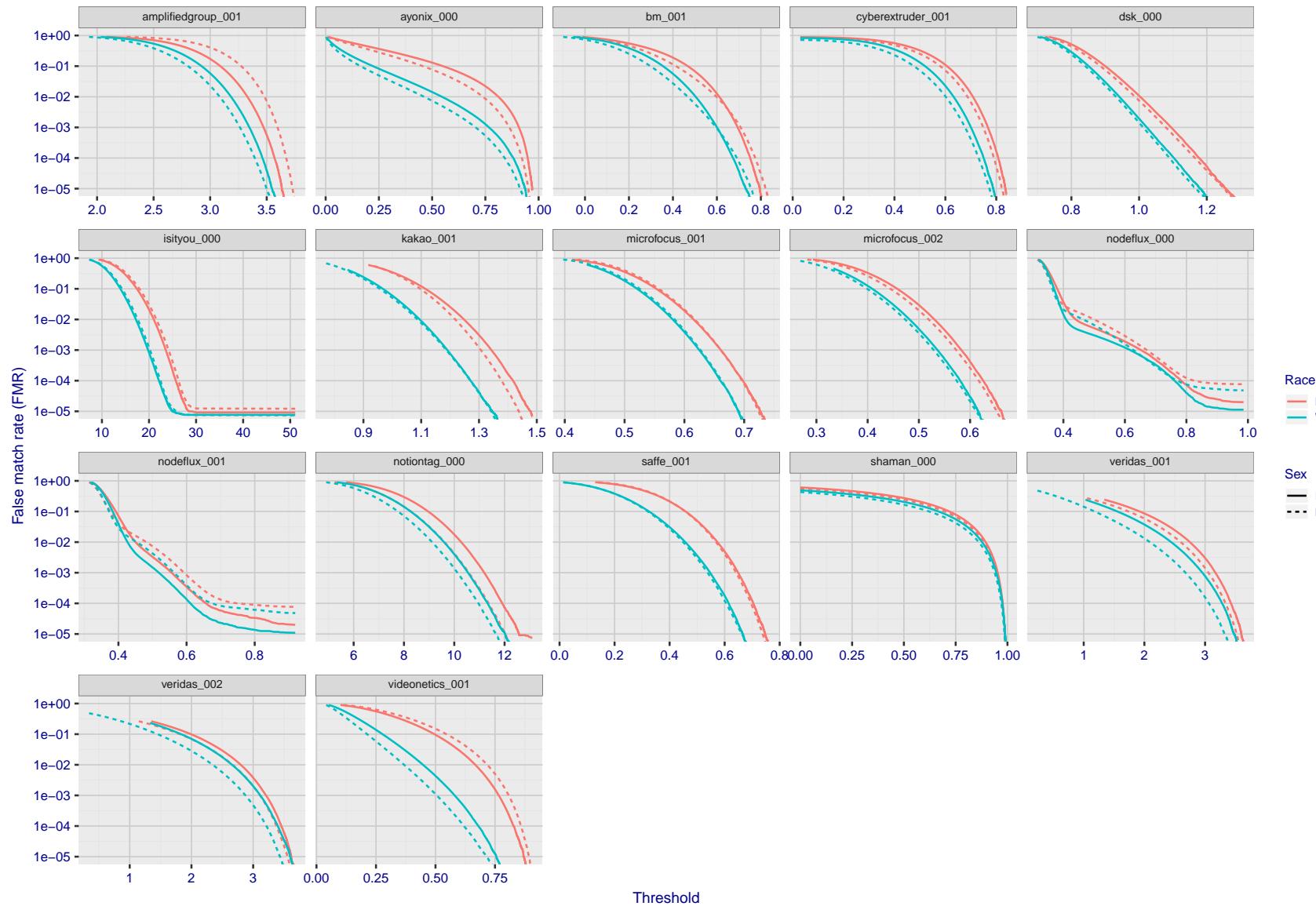


Figure 75: For the mugshot images, the false match calibration curves show false match rate vs. threshold. Separate curves appear for white females, black females, black males and white males.

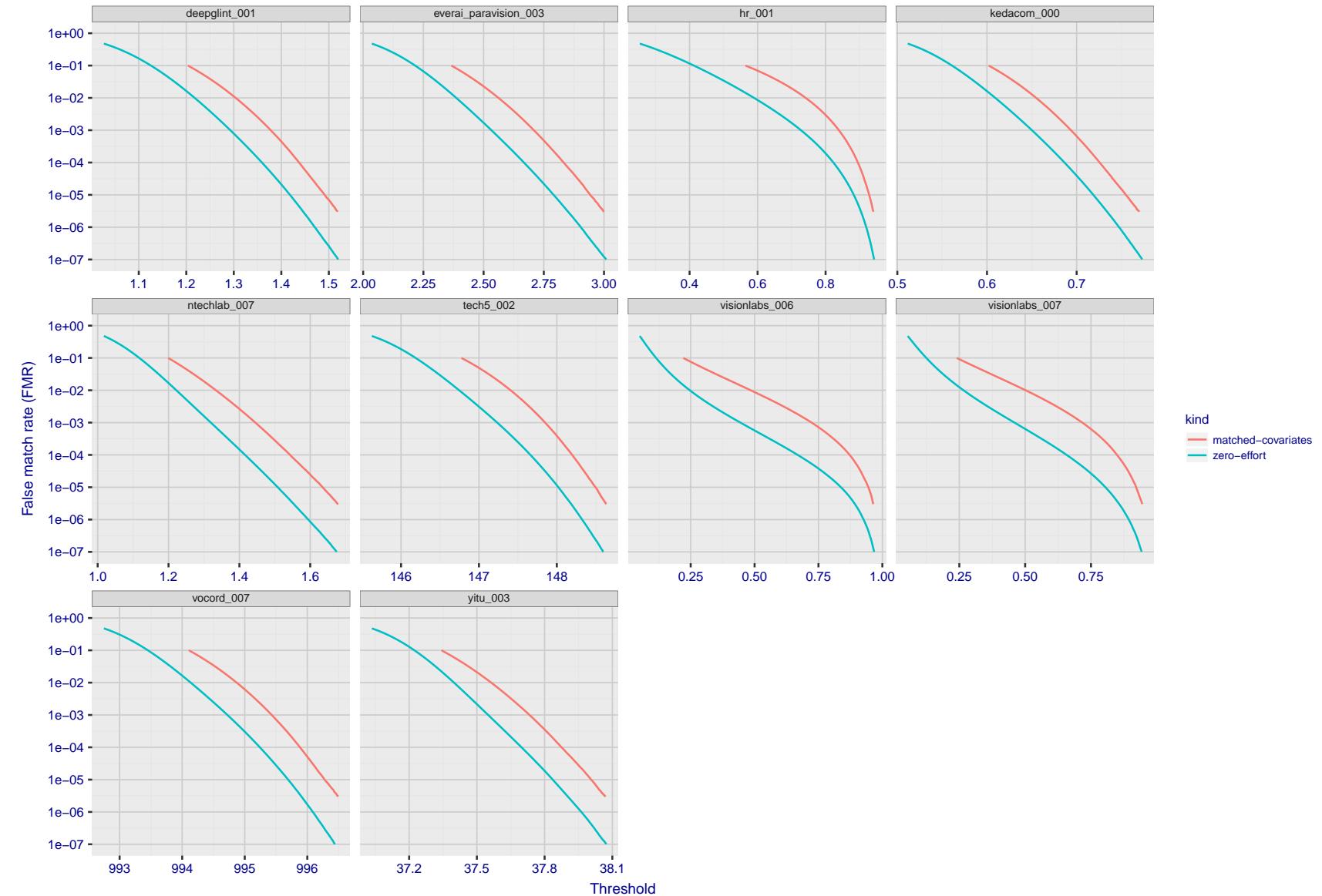


Figure 76: For the visa images, the false match calibration curves show FMR vs. threshold,  $T$ . The blue (lower) curves are for zero-effort impostors (i.e. comparing all images against all). The red (upper) curves are for persons of the same-sex, same-age, and same national-origin. This shows that FMR is underestimated (by a factor of 10 or more) by using a zero-effort impostor calculation to calibrate  $T$ . As shown later (sec. 3.6), FMR is higher for demographic-matched impostors.

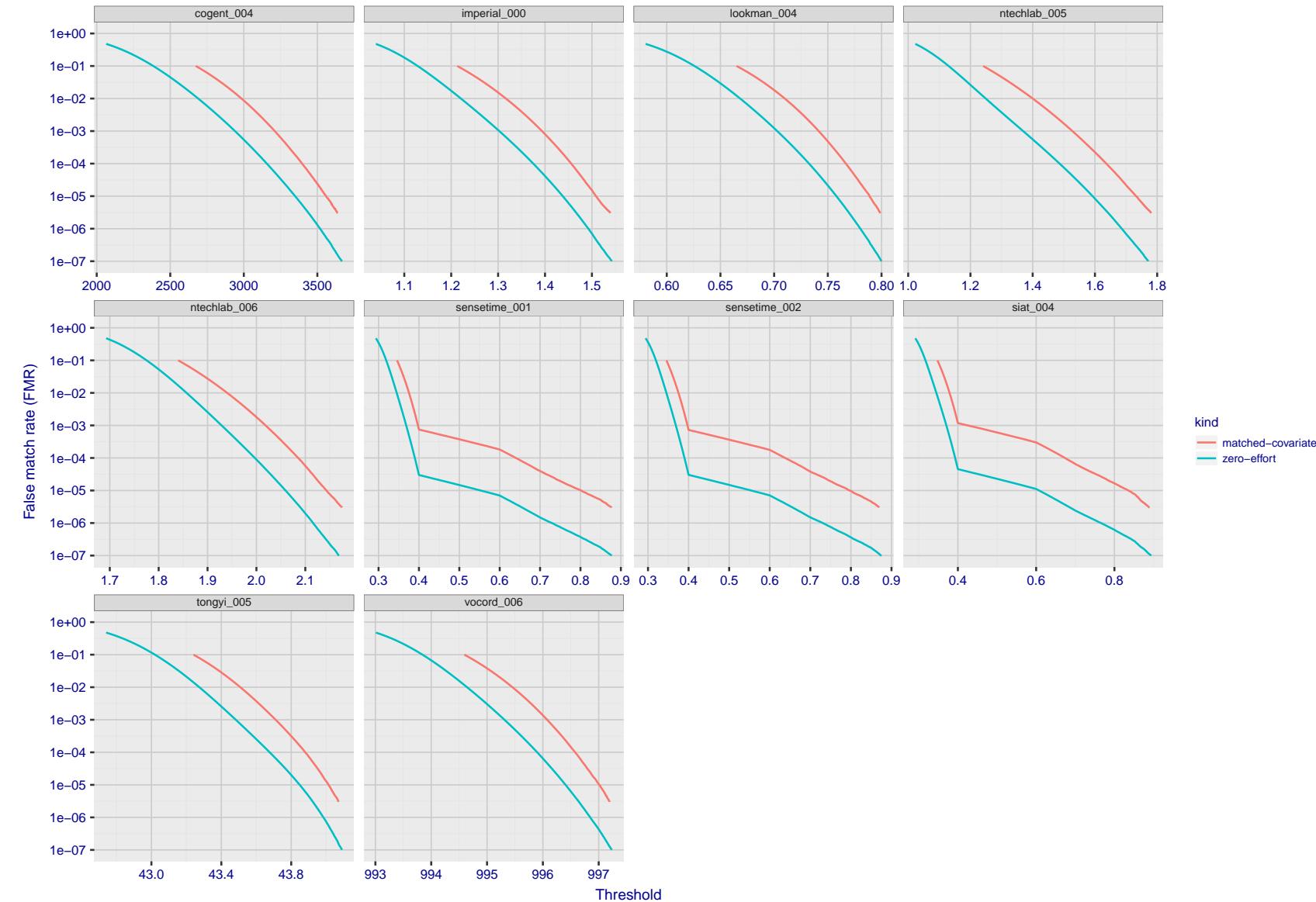


Figure 77: For the visa images, the false match calibration curves show FMR vs. threshold,  $T$ . The blue (lower) curves are for zero-effort impostors (i.e. comparing all images against all). The red (upper) curves are for persons of the same-sex, same-age, and same national-origin. This shows that FMR is underestimated (by a factor of 10 or more) by using a zero-effort impostor calculation to calibrate  $T$ . As shown later (sec. 3.6), FMR is higher for demographic-matched impostors.

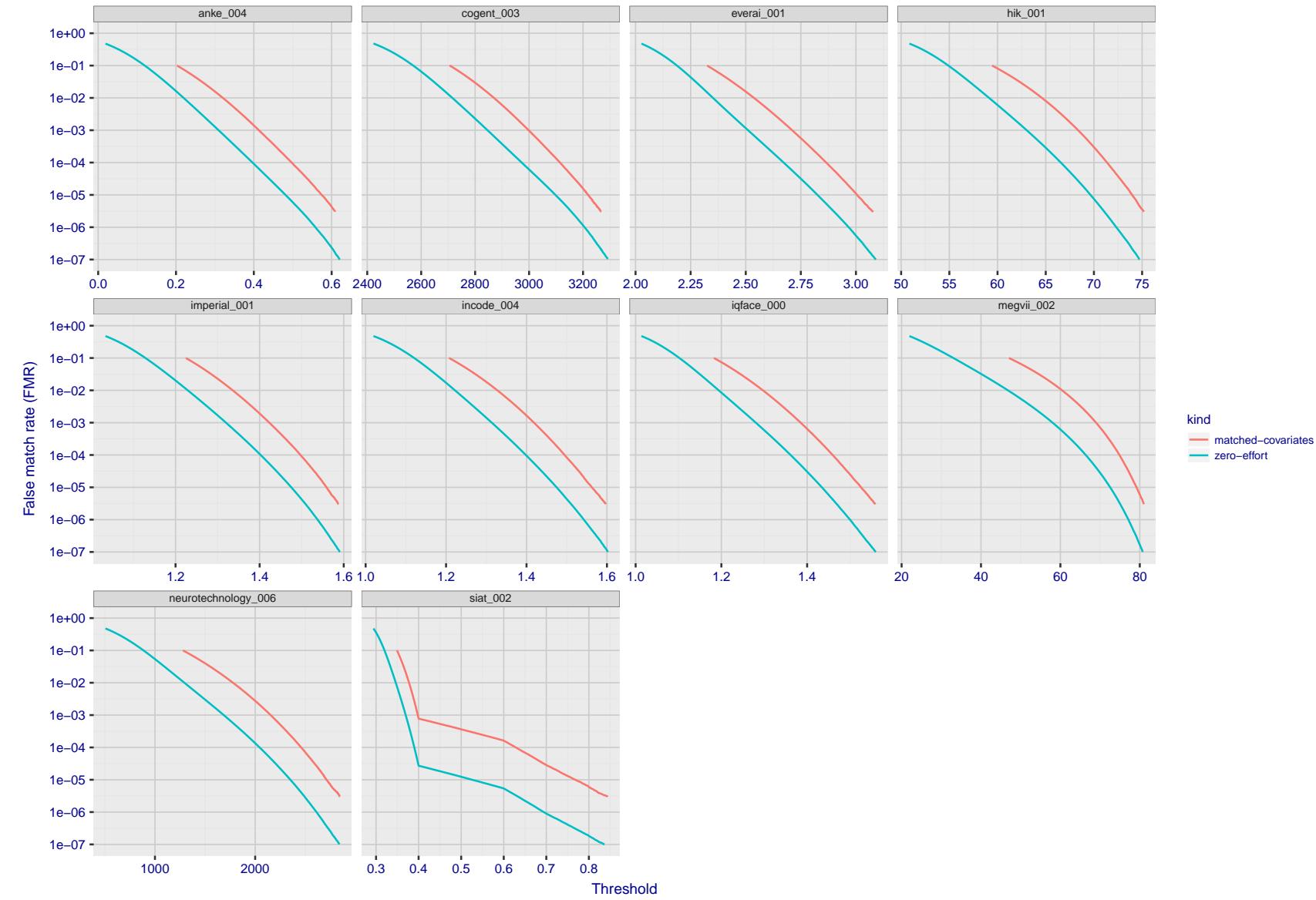


Figure 78: For the visa images, the false match calibration curves show FMR vs. threshold,  $T$ . The blue (lower) curves are for zero-effort impostors (i.e. comparing all images against all). The red (upper) curves are for persons of the same-sex, same-age, and same national-origin. This shows that FMR is underestimated (by a factor of 10 or more) by using a zero-effort impostor calculation to calibrate  $T$ . As shown later (sec. 3.6), FMR is higher for demographic-matched impostors.

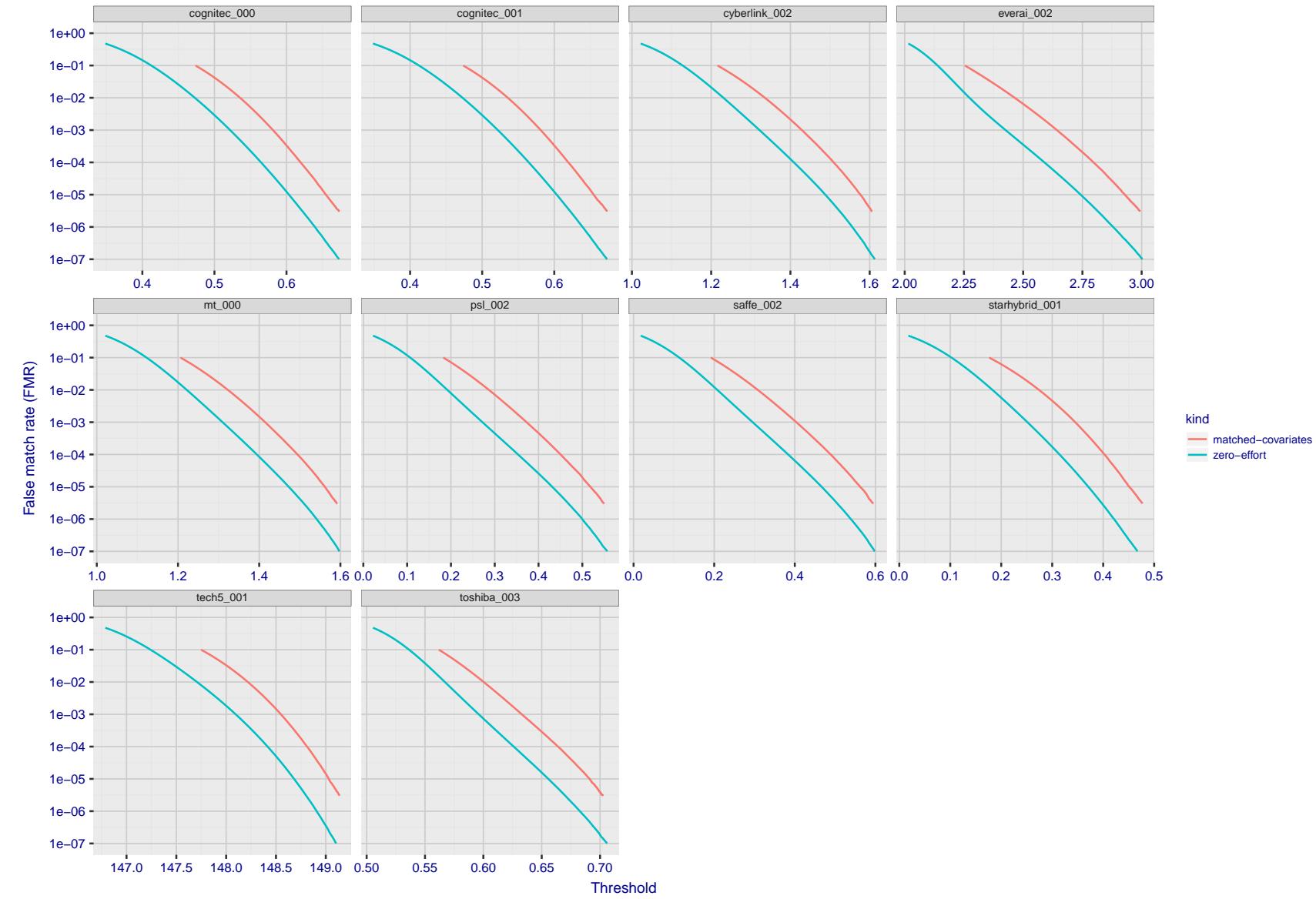


Figure 79: For the visa images, the false match calibration curves show FMR vs. threshold,  $T$ . The blue (lower) curves are for zero-effort impostors (i.e. comparing all images against all). The red (upper) curves are for persons of the same-sex, same-age, and same national-origin. This shows that FMR is underestimated (by a factor of 10 or more) by using a zero-effort impostor calculation to calibrate  $T$ . As shown later (sec. 3.6), FMR is higher for demographic-matched impostors.

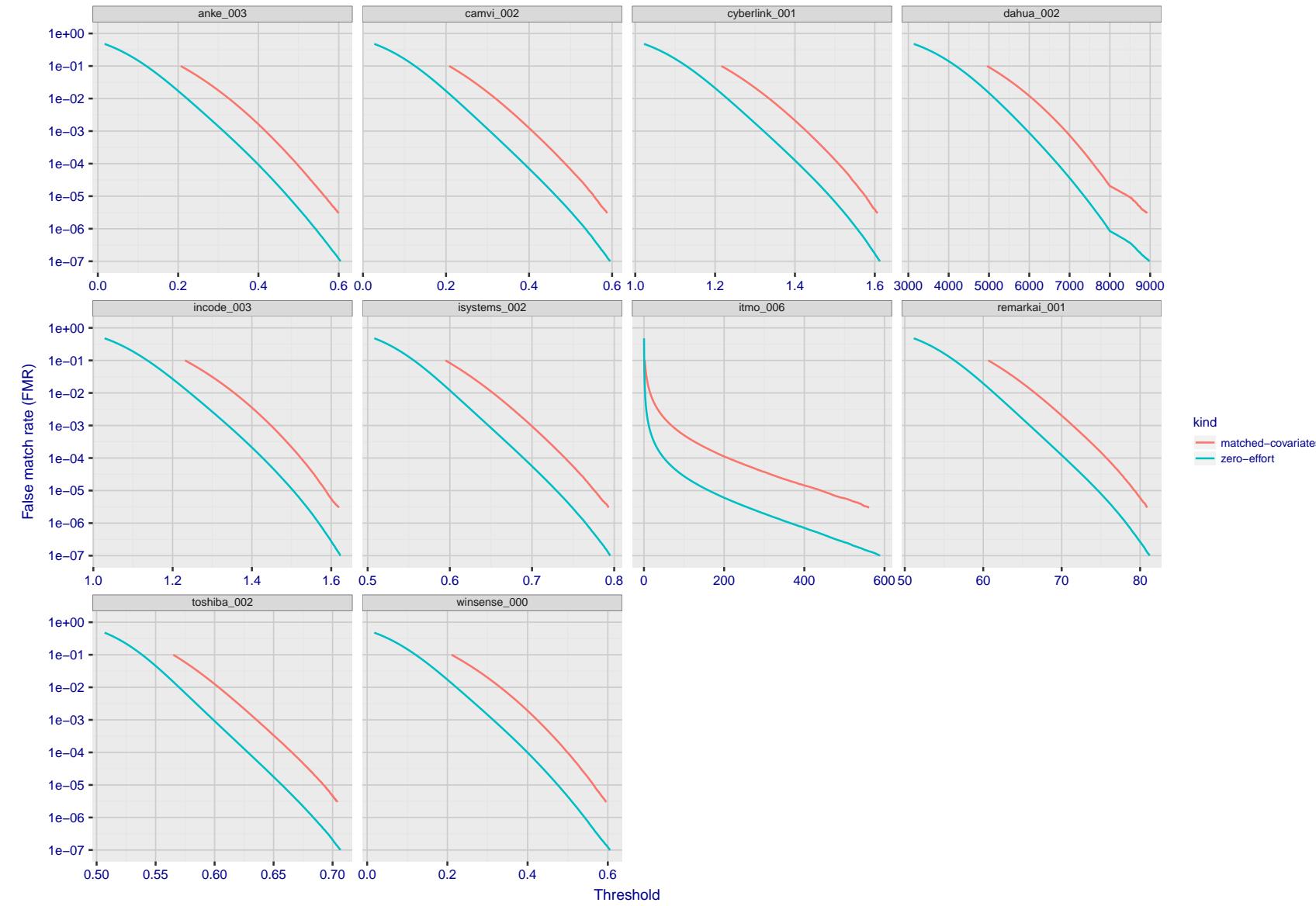


Figure 80: For the visa images, the false match calibration curves show FMR vs. threshold,  $T$ . The blue (lower) curves are for zero-effort impostors (i.e. comparing all images against all). The red (upper) curves are for persons of the same-sex, same-age, and same national-origin. This shows that FMR is underestimated (by a factor of 10 or more) by using a zero-effort impostor calculation to calibrate  $T$ . As shown later (sec. 3.6), FMR is higher for demographic-matched impostors.

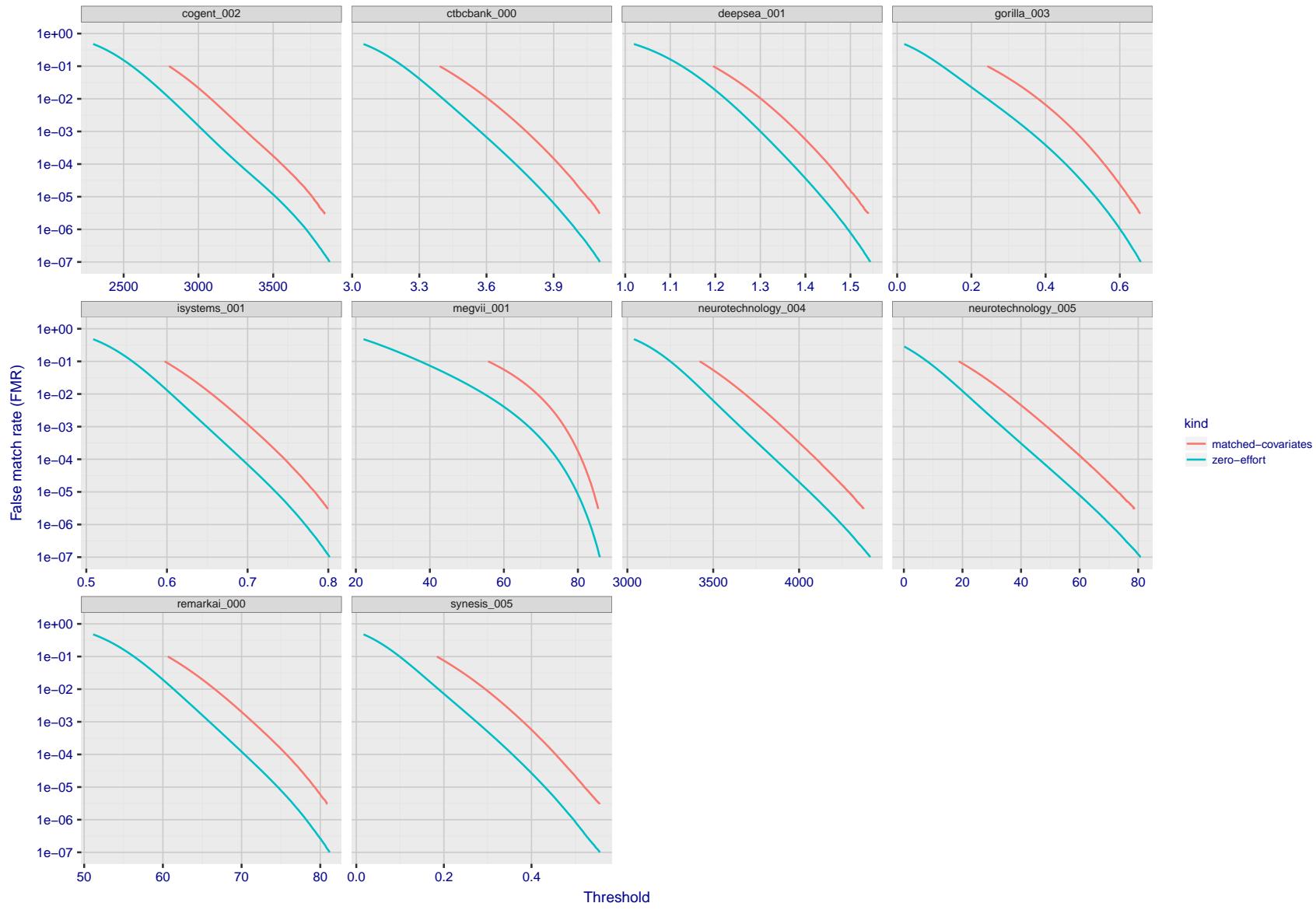


Figure 81: For the visa images, the false match calibration curves show FMR vs. threshold,  $T$ . The blue (lower) curves are for zero-effort impostors (i.e. comparing all images against all). The red (upper) curves are for persons of the same-sex, same-age, and same national-origin. This shows that FMR is underestimated (by a factor of 10 or more) by using a zero-effort impostor calculation to calibrate  $T$ . As shown later (sec. 3.6), FMR is higher for demographic-matched impostors.

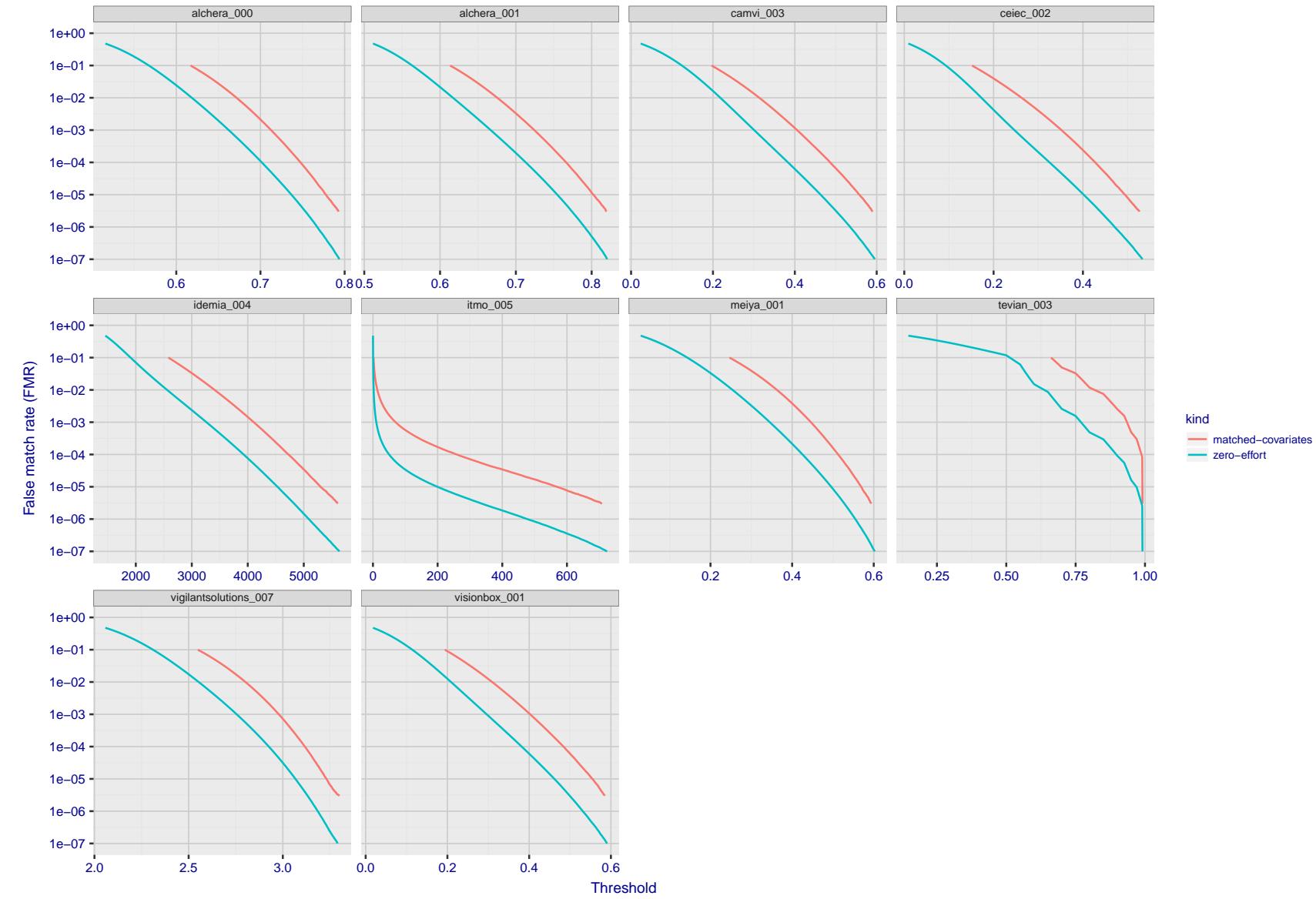


Figure 82: For the visa images, the false match calibration curves show FMR vs. threshold,  $T$ . The blue (lower) curves are for zero-effort impostors (i.e. comparing all images against all). The red (upper) curves are for persons of the same-sex, same-age, and same national-origin. This shows that FMR is underestimated (by a factor of 10 or more) by using a zero-effort impostor calculation to calibrate  $T$ . As shown later (sec. 3.6), FMR is higher for demographic-matched impostors.

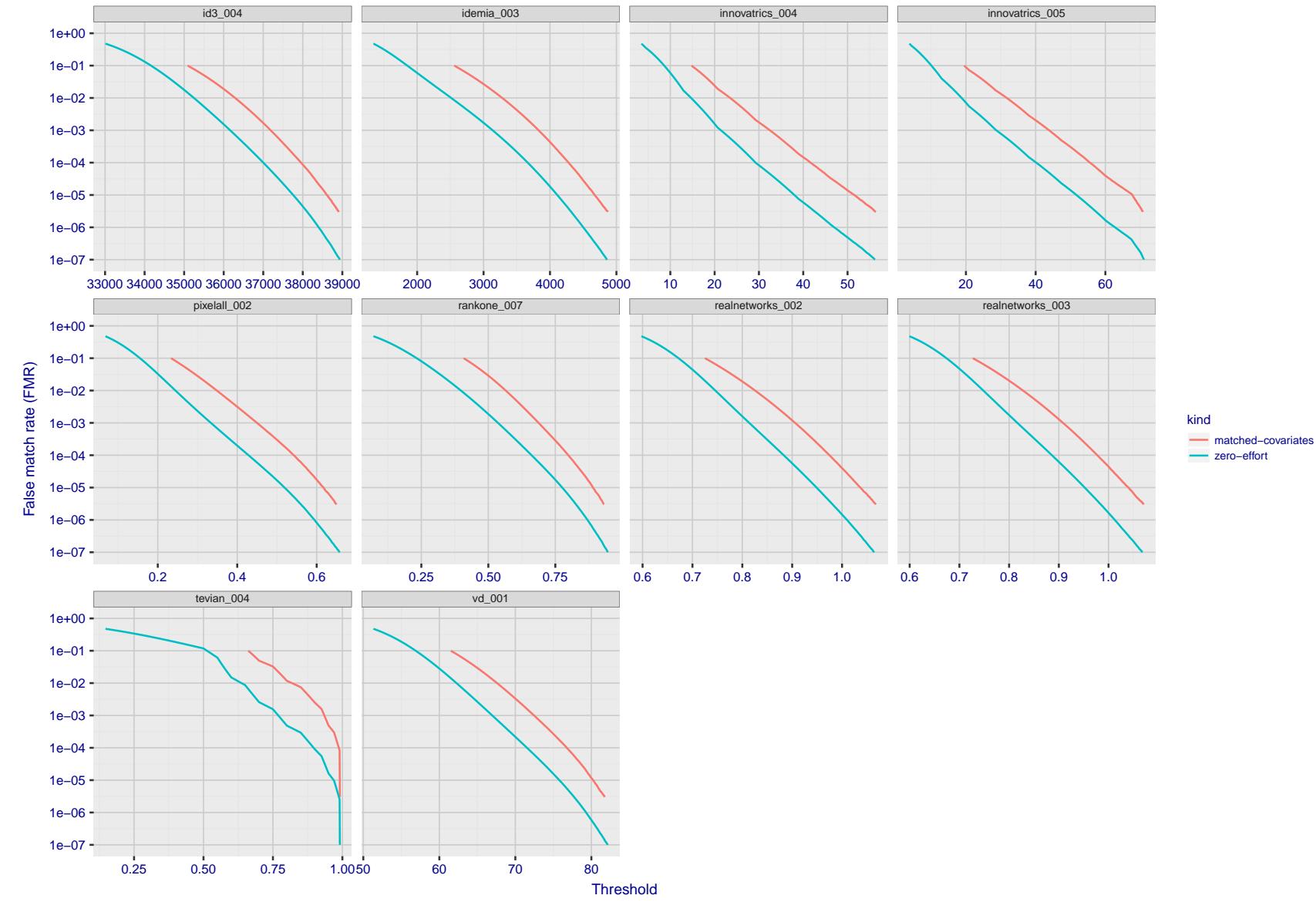


Figure 83: For the visa images, the false match calibration curves show FMR vs. threshold,  $T$ . The blue (lower) curves are for zero-effort impostors (i.e. comparing all images against all). The red (upper) curves are for persons of the same-sex, same-age, and same national-origin. This shows that FMR is underestimated (by a factor of 10 or more) by using a zero-effort impostor calculation to calibrate  $T$ . As shown later (sec. 3.6), FMR is higher for demographic-matched impostors.

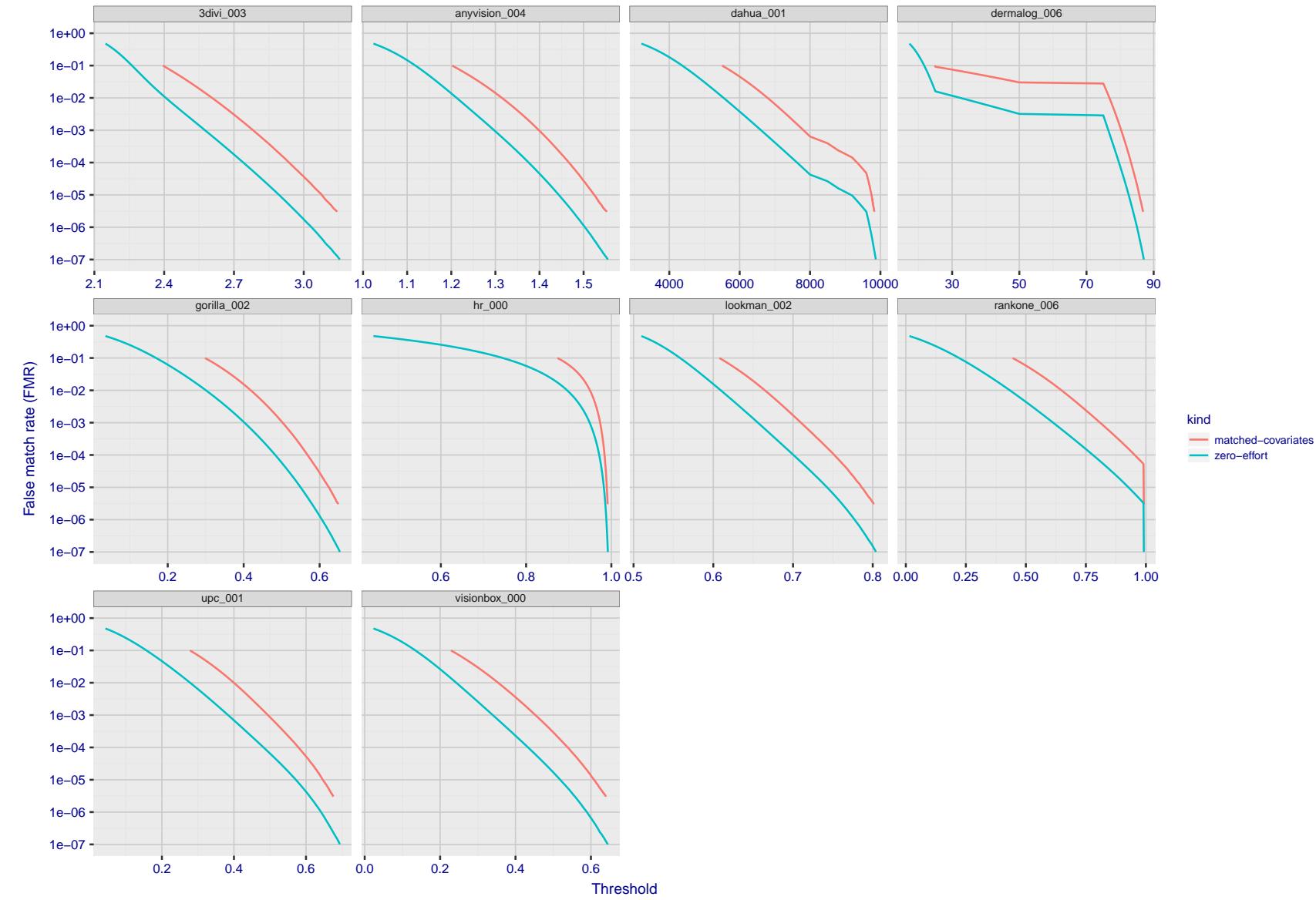


Figure 84: For the visa images, the false match calibration curves show FMR vs. threshold,  $T$ . The blue (lower) curves are for zero-effort impostors (i.e. comparing all images against all). The red (upper) curves are for persons of the same-sex, same-age, and same national-origin. This shows that FMR is underestimated (by a factor of 10 or more) by using a zero-effort impostor calculation to calibrate  $T$ . As shown later (sec. 3.6), FMR is higher for demographic-matched impostors.

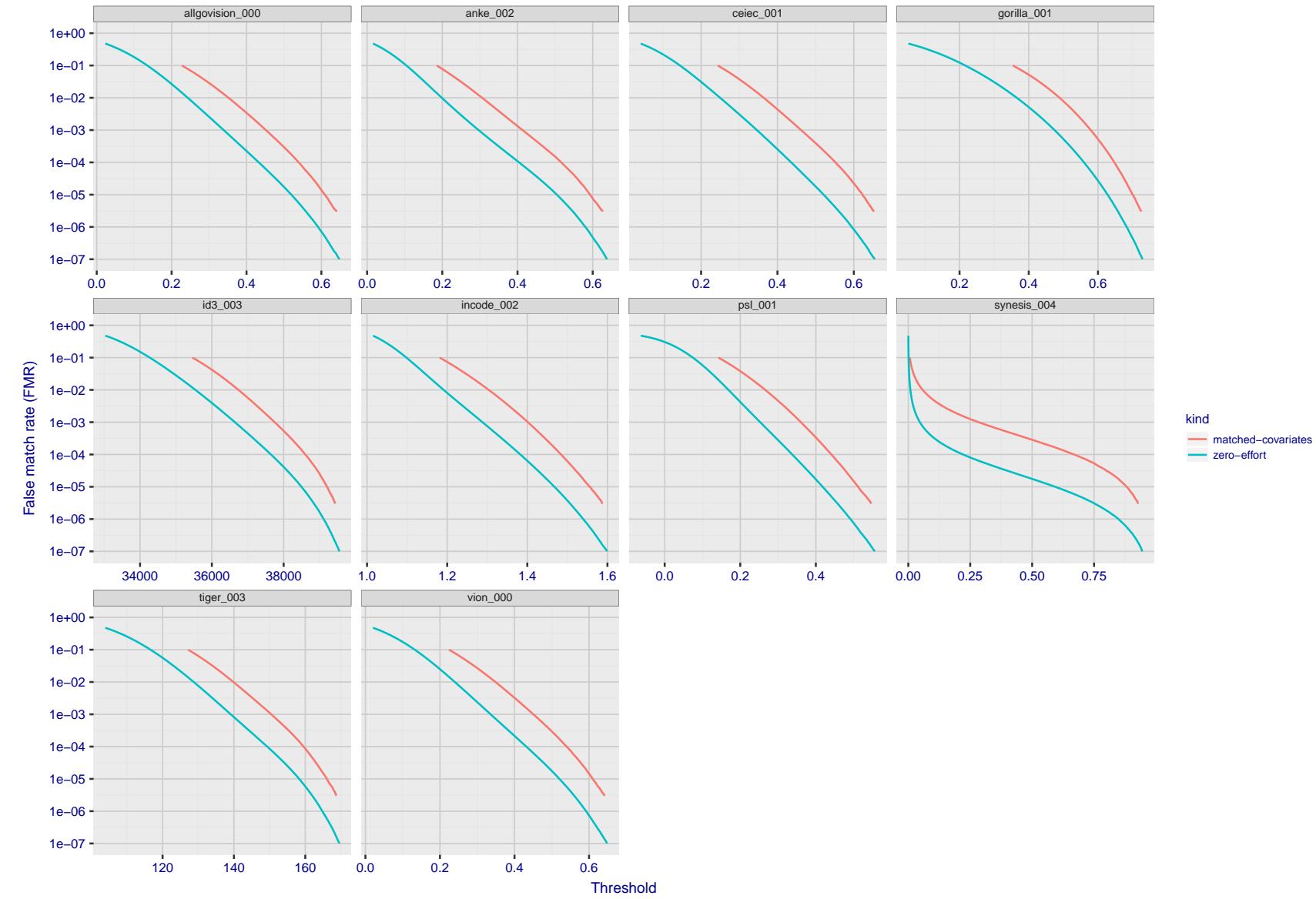


Figure 85: For the visa images, the false match calibration curves show FMR vs. threshold,  $T$ . The blue (lower) curves are for zero-effort impostors (i.e. comparing all images against all). The red (upper) curves are for persons of the same-sex, same-age, and same national-origin. This shows that FMR is underestimated (by a factor of 10 or more) by using a zero-effort impostor calculation to calibrate  $T$ . As shown later (sec. 3.6), FMR is higher for demographic-matched impostors.

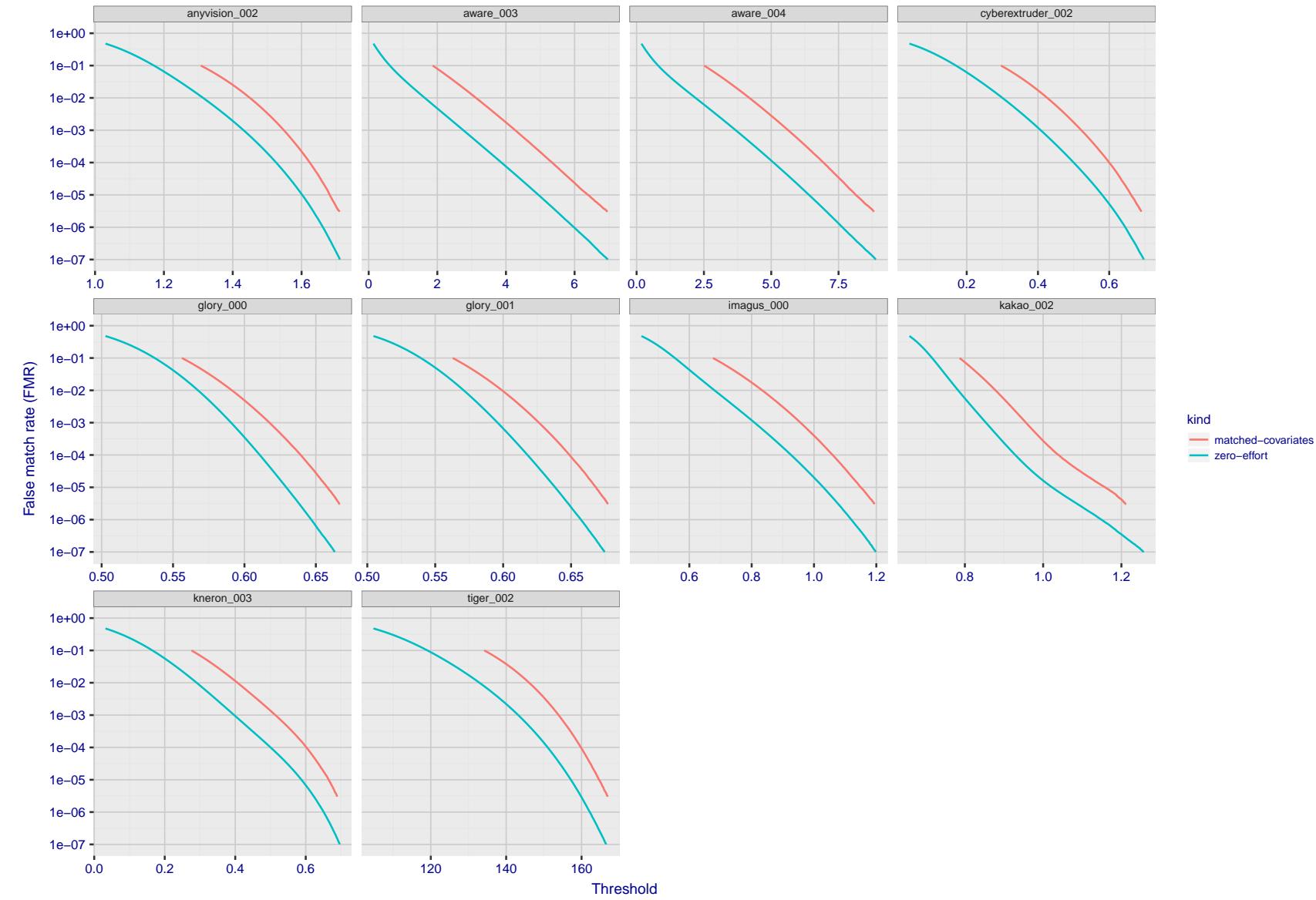


Figure 86: For the visa images, the false match calibration curves show FMR vs. threshold,  $T$ . The blue (lower) curves are for zero-effort impostors (i.e. comparing all images against all). The red (upper) curves are for persons of the same-sex, same-age, and same national-origin. This shows that FMR is underestimated (by a factor of 10 or more) by using a zero-effort impostor calculation to calibrate  $T$ . As shown later (sec. 3.6), FMR is higher for demographic-matched impostors.

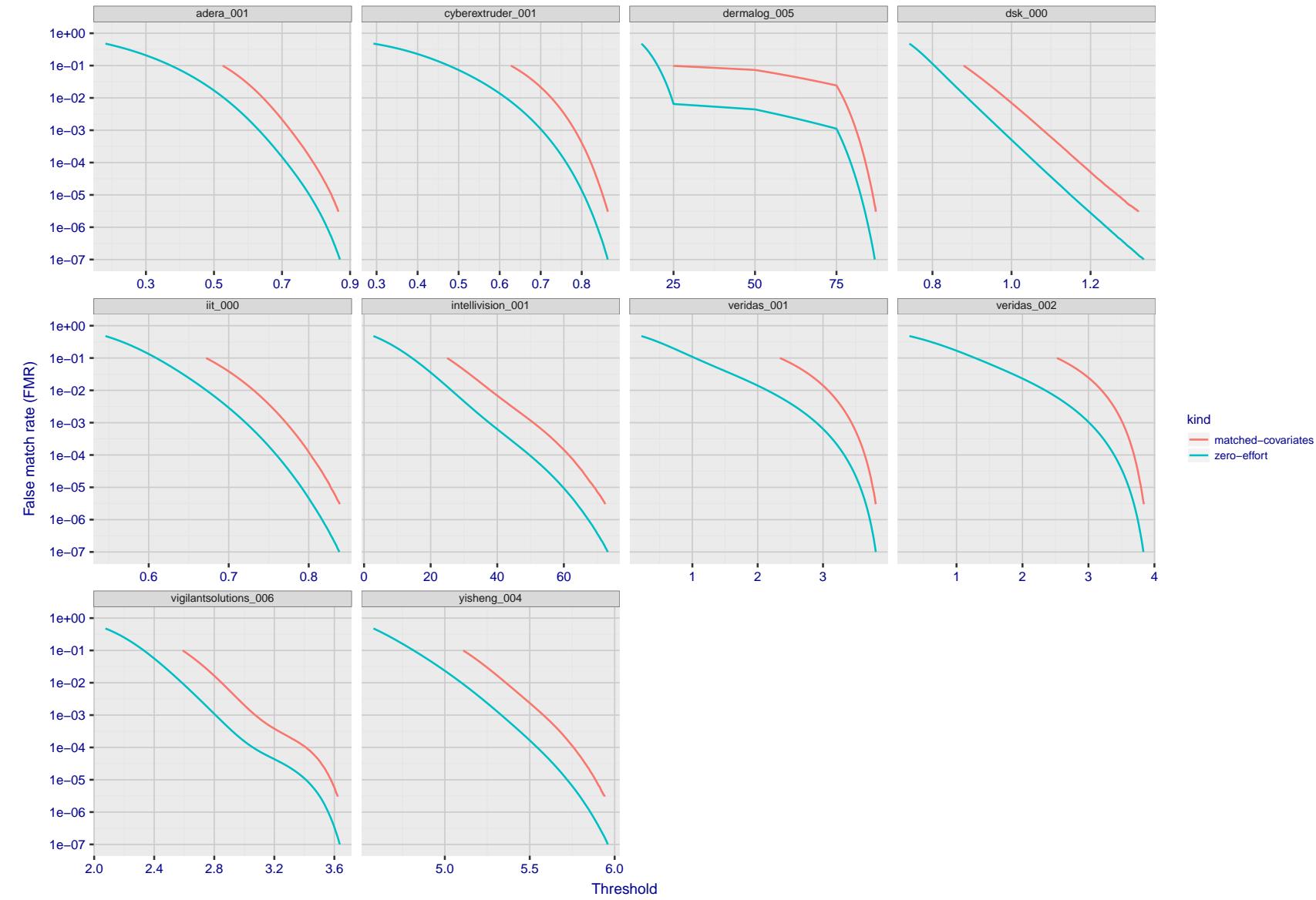


Figure 87: For the visa images, the false match calibration curves show FMR vs. threshold,  $T$ . The blue (lower) curves are for zero-effort impostors (i.e. comparing all images against all). The red (upper) curves are for persons of the same-sex, same-age, and same national-origin. This shows that FMR is underestimated (by a factor of 10 or more) by using a zero-effort impostor calculation to calibrate  $T$ . As shown later (sec. 3.6), FMR is higher for demographic-matched impostors.

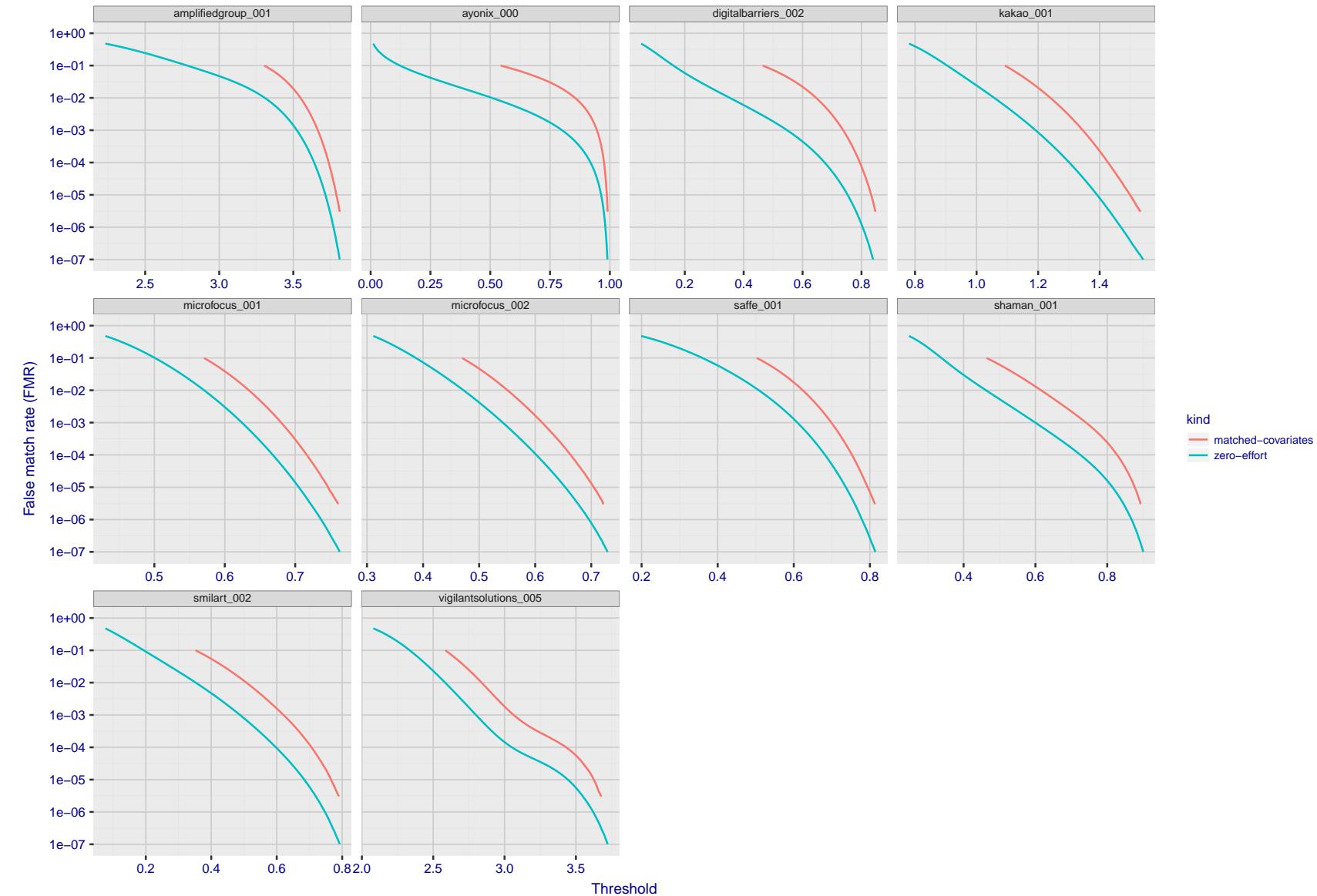


Figure 88: For the visa images, the false match calibration curves show FMR vs. threshold,  $T$ . The blue (lower) curves are for zero-effort impostors (i.e. comparing all images against all). The red (upper) curves are for persons of the same-sex, same-age, and same national-origin. This shows that FMR is underestimated (by a factor of 10 or more) by using a zero-effort impostor calculation to calibrate  $T$ . As shown later (sec. 3.6), FMR is higher for demographic-matched impostors.

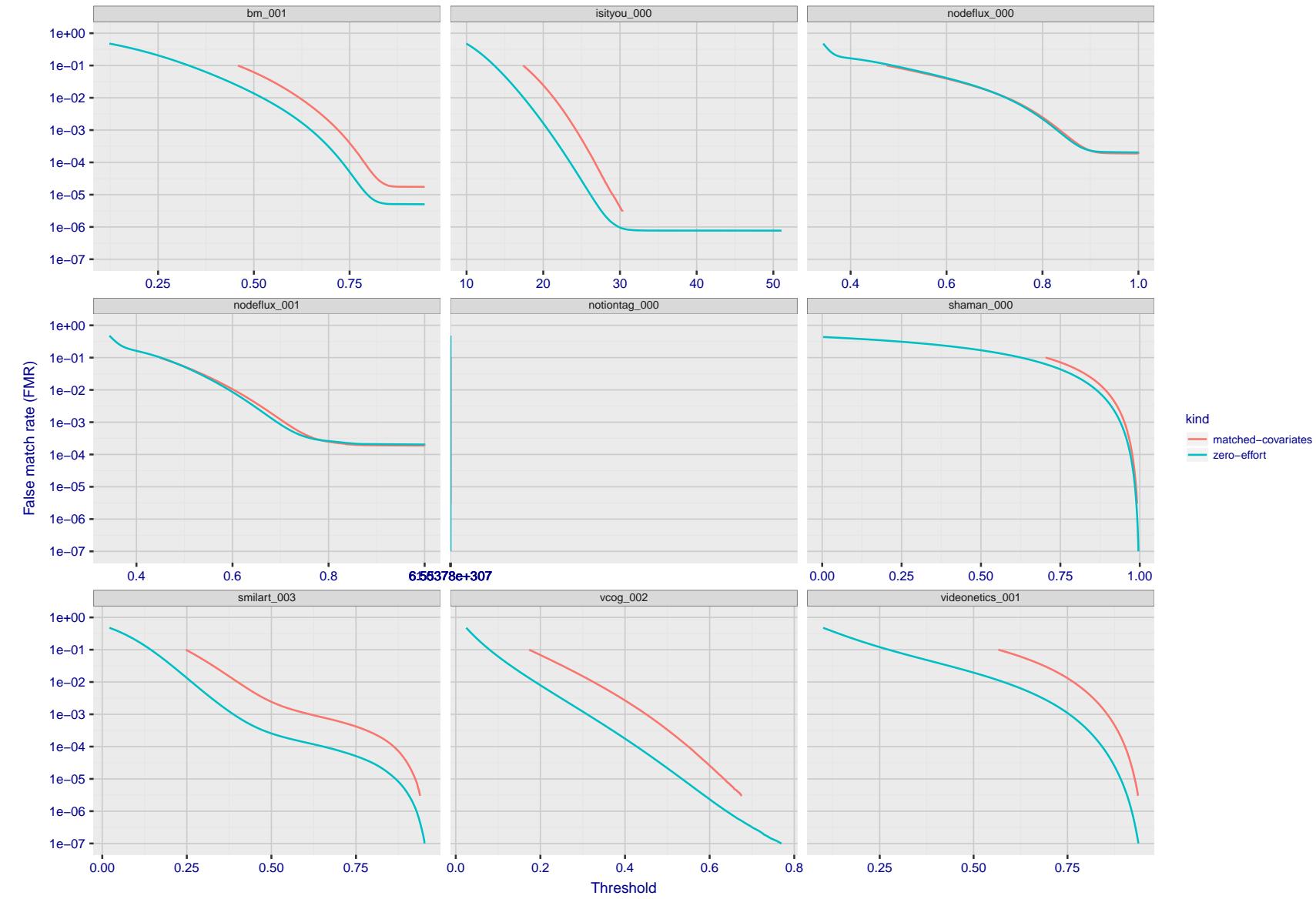


Figure 89: For the visa images, the false match calibration curves show FMR vs. threshold,  $T$ . The blue (lower) curves are for zero-effort impostors (i.e. comparing all images against all). The red (upper) curves are for persons of the same-sex, same-age, and same national-origin. This shows that FMR is underestimated (by a factor of 10 or more) by using a zero-effort impostor calculation to calibrate  $T$ . As shown later (sec. 3.6), FMR is higher for demographic-matched impostors.

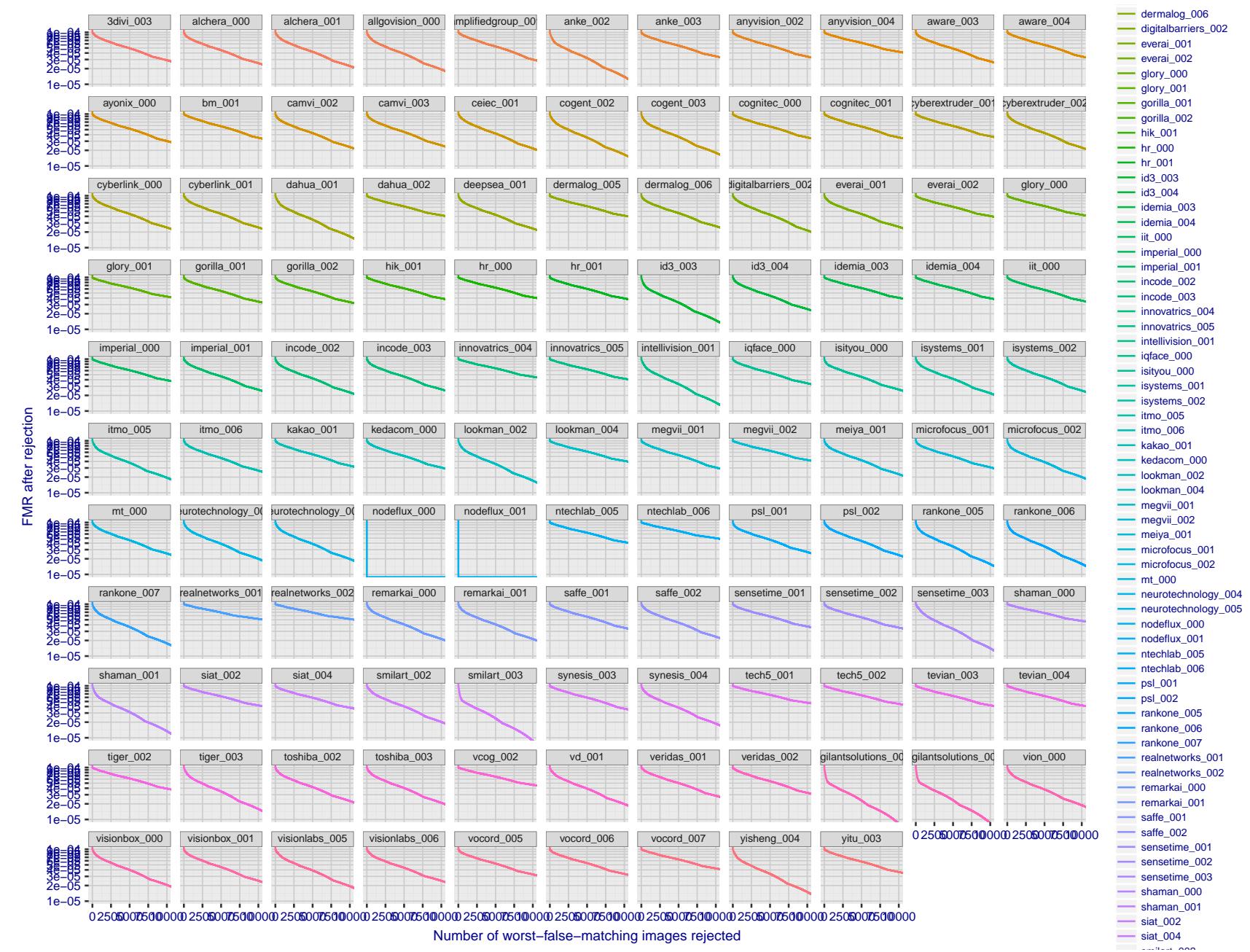


Figure 90: For the visa images, the curves show how false matches are concentrated in certain images. Specifically each line plots  $FMR(k)$  with  $k$  the number of images rejected in decreasing order of how many false matches that image was involved in.  $FMR(0) = 10^{-4}$ . In terms of the biometric zoo, the most “wolf-ish” images are rejected first i.e. those enrollment or verification images most often involved in false matches. A flatter response is considered superior. A steeply descending response indicates that certain kinds of images false match against others, e.g. if hypothetically images of men with particular mustaches would falsely match others.

## 3.5 Genuine distribution stability

### 3.5.1 Effect of birth place on the genuine distribution

**Background:** Both skin tone and bone structure vary geographically. Prior studies have reported variations in FNMR and FMR.

**Goal:** To measure false non-match rate (FNMR) variation with country of birth.

**Methods:** Thresholds are determined that give  $FMR = \{0.001, 0.0001\}$  over the entire impostor set. Then FNMR is measured over 1000 bootstrap replications of the genuine scores. Only those countries with at least 140 individuals are included in the analysis.

**Results:** Figure 101 shows FNMR by country of birth for the two thresholds.

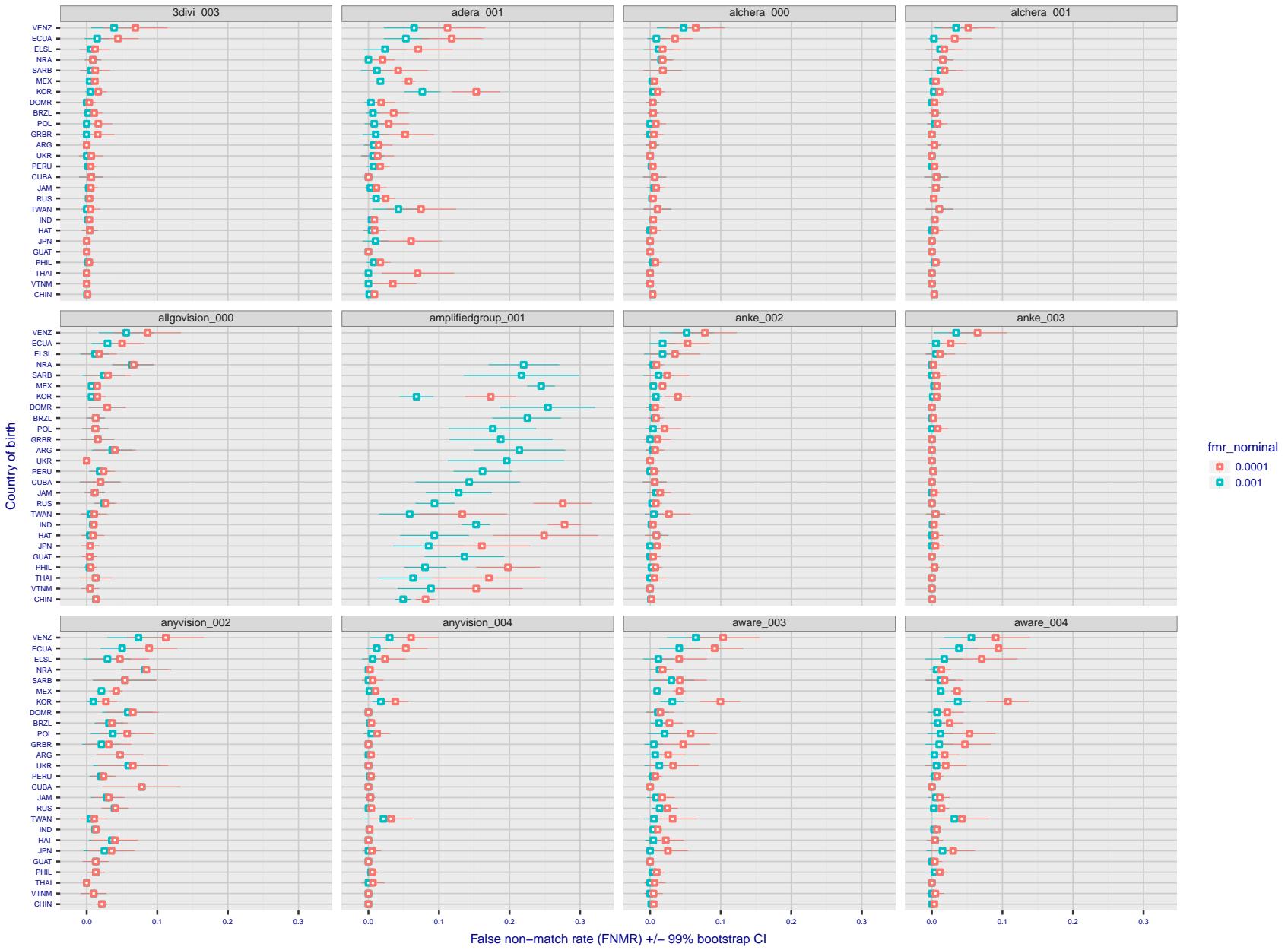


Figure 91: For the visa images, the dots show FNMR by country of birth for two globally set operating thresholds corresponding to  $FMR = \{0.001, 0.0001\}$  computed over all on the order of  $10^{10}$  impostor scores. The FMR in each bin will vary also - see subsequent impostor heatmaps in sec. 3.6.1. The figures shows an order of magnitude variation in FNMR across country of birth; these effects are likely due quality variations, then demographics like age and race. The error rates in some cases are zero, and in others the DET is flat so the error rates at the two thresholds are identical. The lines span 1% and 99% of bootstrap replicated FNMR estimates.

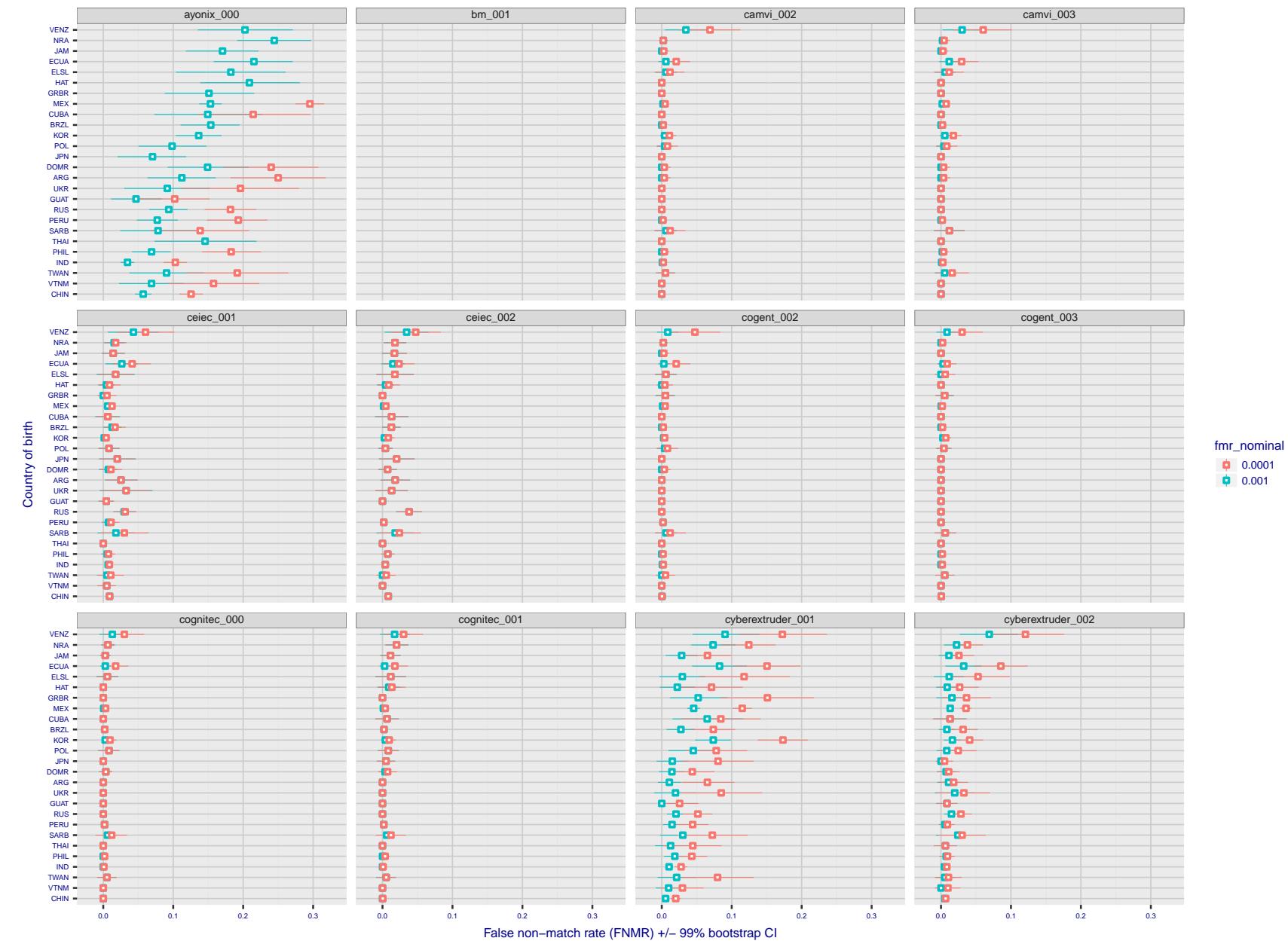


Figure 92: For the visa images, the dots show FNMR by country of birth for two globally set operating thresholds corresponding to  $FMR = \{0.001, 0.0001\}$  computed over all on the order of  $10^{10}$  impostor scores. The FMR in each bin will vary also - see subsequent impostor heatmaps in sec. 3.6.1. The figures shows an order of magnitude variation in FNMR across country of birth; these effects are likely due quality variations, then demographics like age and race. The error rates in some cases are zero, and in others the DET is flat so the error rates at the two thresholds are identical. The lines span 1% and 99% of bootstrap replicated FNMR estimates.

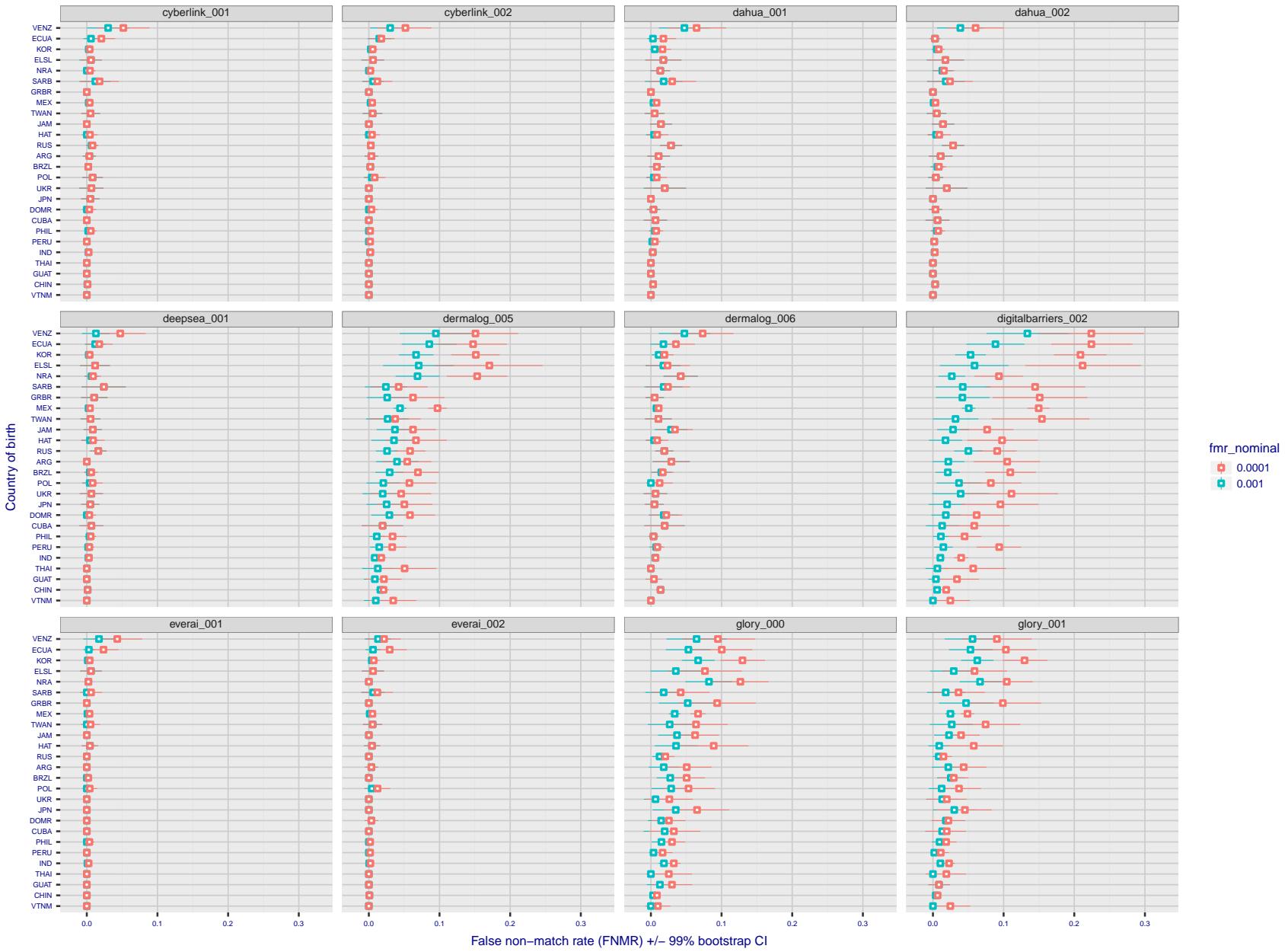


Figure 93: For the visa images, the dots show FNMR by country of birth for two globally set operating thresholds corresponding to  $FMR = \{0.001, 0.0001\}$  computed over all on the order of  $10^{10}$  impostor scores. The FMR in each bin will vary also - see subsequent impostor heatmaps in sec. 3.6.1. The figures shows an order of magnitude variation in FNMR across country of birth; these effects are likely due quality variations, then demographics like age and race. The error rates in some cases are zero, and in others the DET is flat so the error rates at the two thresholds are identical. The lines span 1% and 99% of bootstrap replicated FNMR estimates.

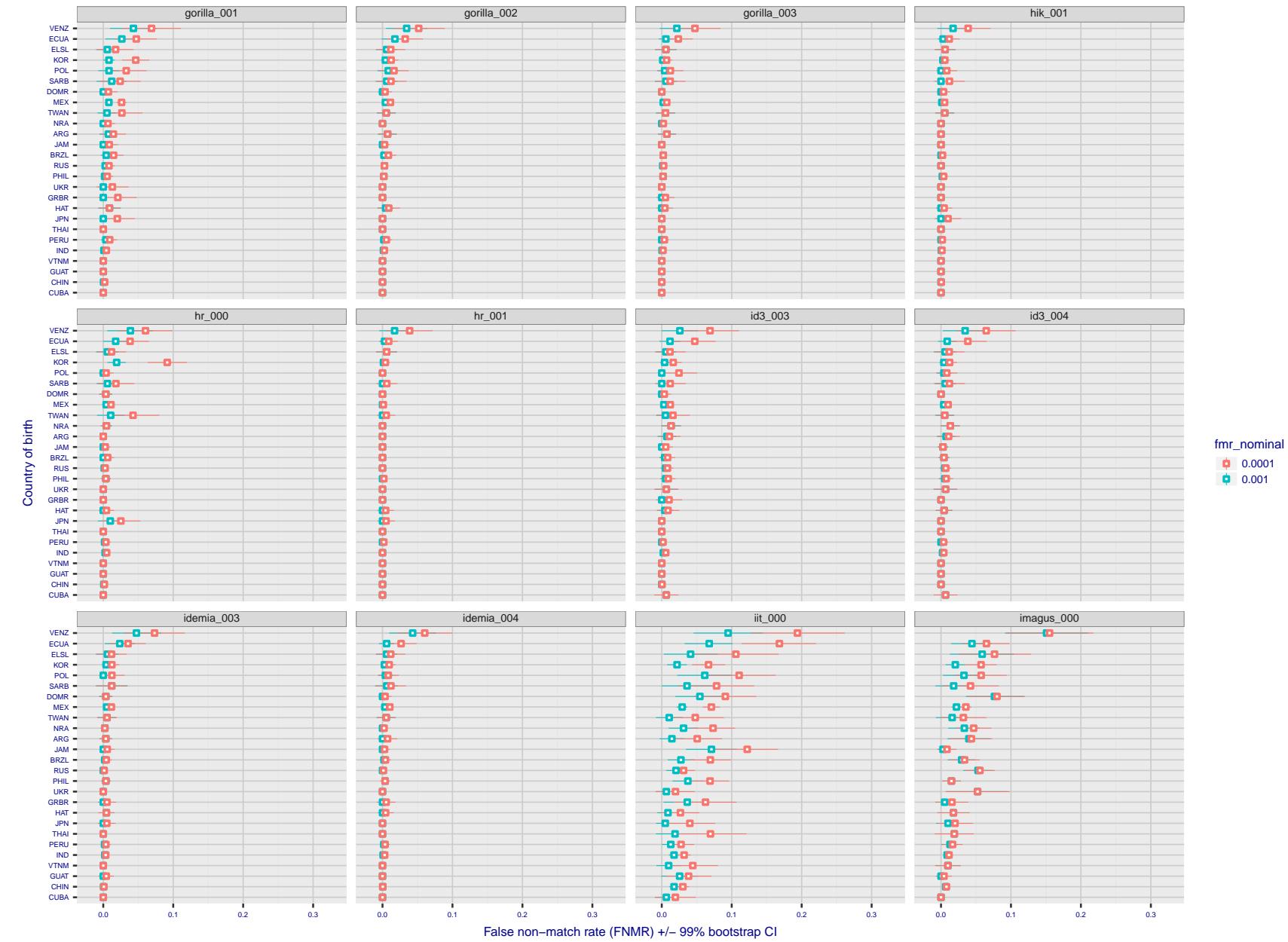


Figure 94: For the visa images, the dots show FNMR by country of birth for two globally set operating thresholds corresponding to  $FMR = \{0.001, 0.0001\}$  computed over all on the order of  $10^{10}$  impostor scores. The FMR in each bin will vary also - see subsequent impostor heatmaps in sec. 3.6.1. The figures shows an order of magnitude variation in FNMR across country of birth; these effects are likely due quality variations, then demographics like age and race. The error rates in some cases are zero, and in others the DET is flat so the error rates at the two thresholds are identical. The lines span 1% and 99% of bootstrap replicated FNMR estimates.

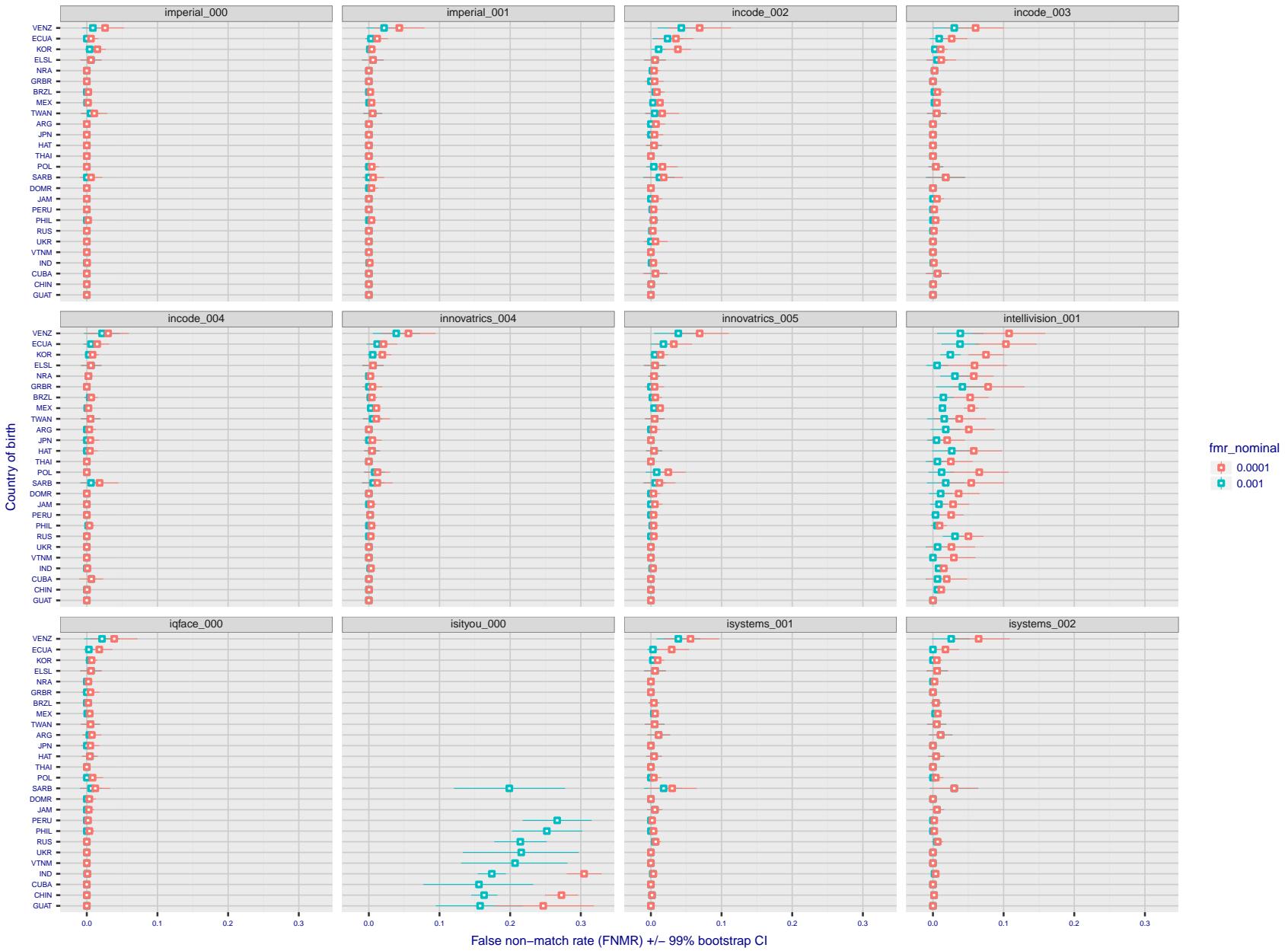


Figure 95: For the visa images, the dots show FNMR by country of birth for two globally set operating thresholds corresponding to  $FMR = \{0.001, 0.0001\}$  computed over all on the order of  $10^{10}$  impostor scores. The FMR in each bin will vary also - see subsequent impostor heatmaps in sec. 3.6.1. The figures shows an order of magnitude variation in FNMR across country of birth; these effects are likely due quality variations, then demographics like age and race. The error rates in some cases are zero, and in others the DET is flat so the error rates at the two thresholds are identical. The lines span 1% and 99% of bootstrap replicated FNMR estimates.

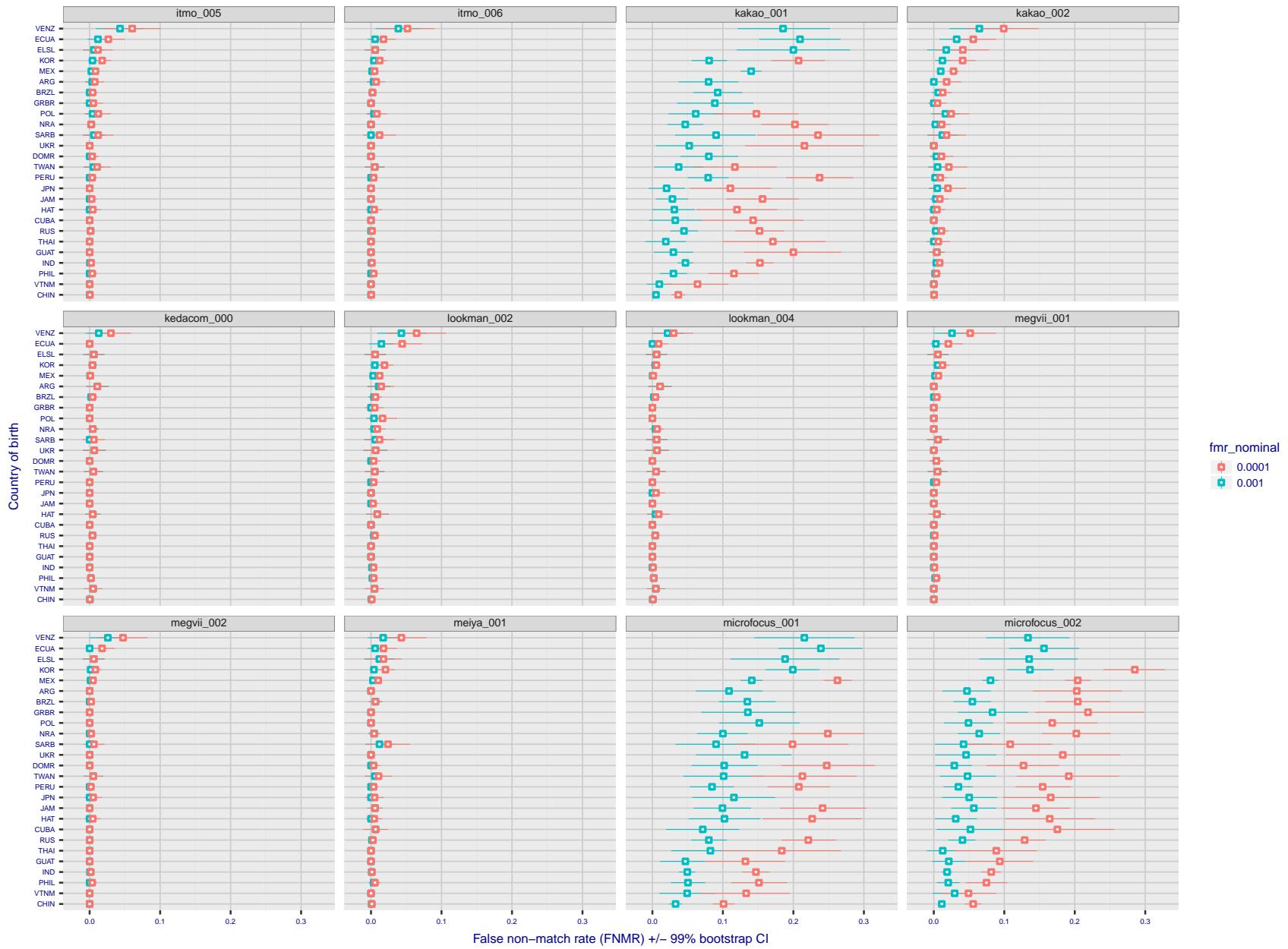


Figure 96: For the visa images, the dots show FNMR by country of birth for two globally set operating thresholds corresponding to  $FMR = \{0.001, 0.0001\}$  computed over all on the order of  $10^{10}$  impostor scores. The FMR in each bin will vary also - see subsequent impostor heatmaps in sec. 3.6.1. The figures shows an order of magnitude variation in FNMR across country of birth; these effects are likely due quality variations, then demographics like age and race. The error rates in some cases are zero, and in others the DET is flat so the error rates at the two thresholds are identical. The lines span 1% and 99% of bootstrap replicated FNMR estimates.

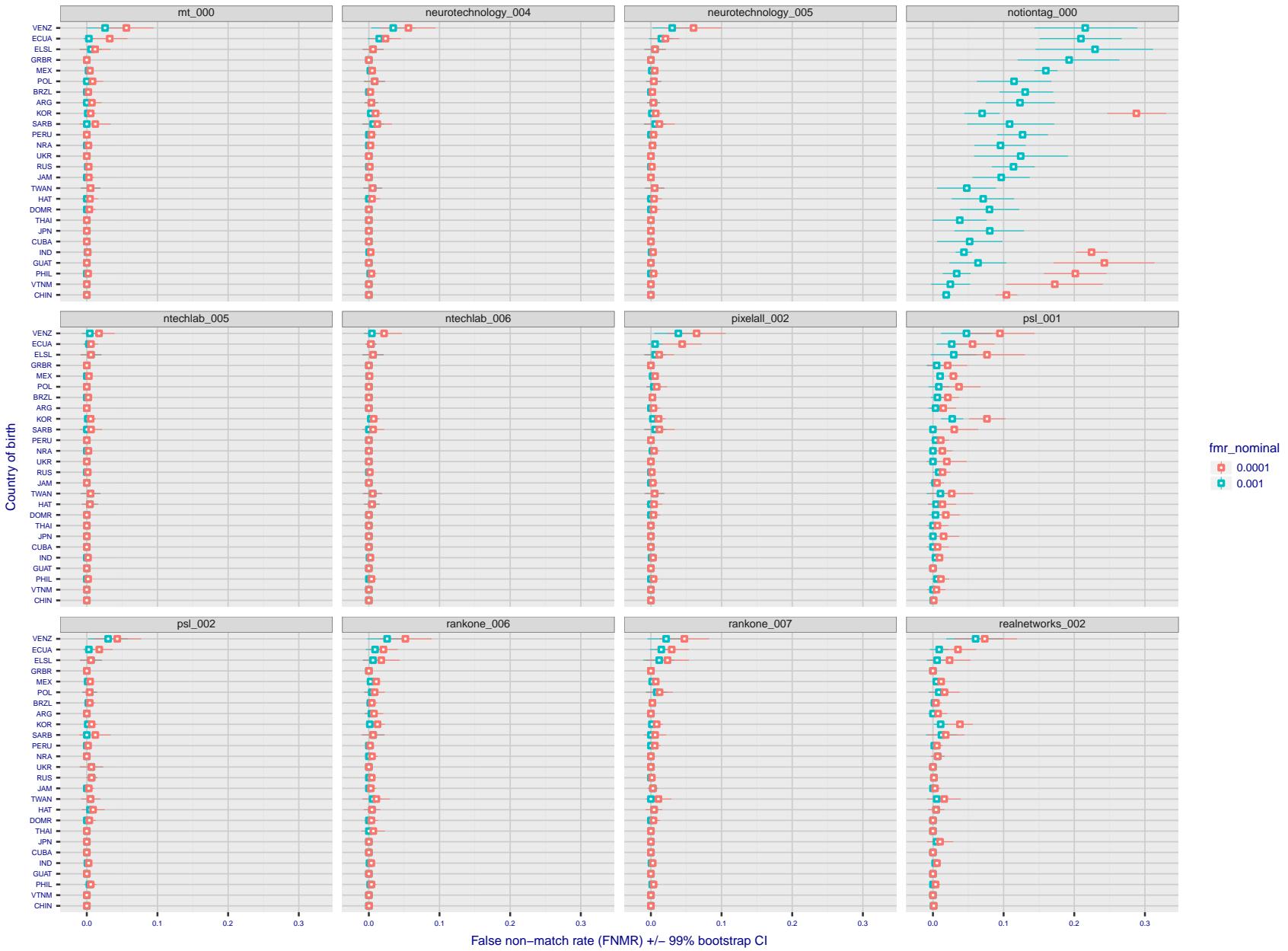


Figure 97: For the visa images, the dots show FNMR by country of birth for two globally set operating thresholds corresponding to  $FMR = \{0.001, 0.0001\}$  computed over all on the order of  $10^{10}$  impostor scores. The FMR in each bin will vary also - see subsequent impostor heatmaps in sec. 3.6.1. The figures shows an order of magnitude variation in FNMR across country of birth; these effects are likely due quality variations, then demographics like age and race. The error rates in some cases are zero, and in others the DET is flat so the error rates at the two thresholds are identical. The lines span 1% and 99% of bootstrap replicated FNMR estimates.

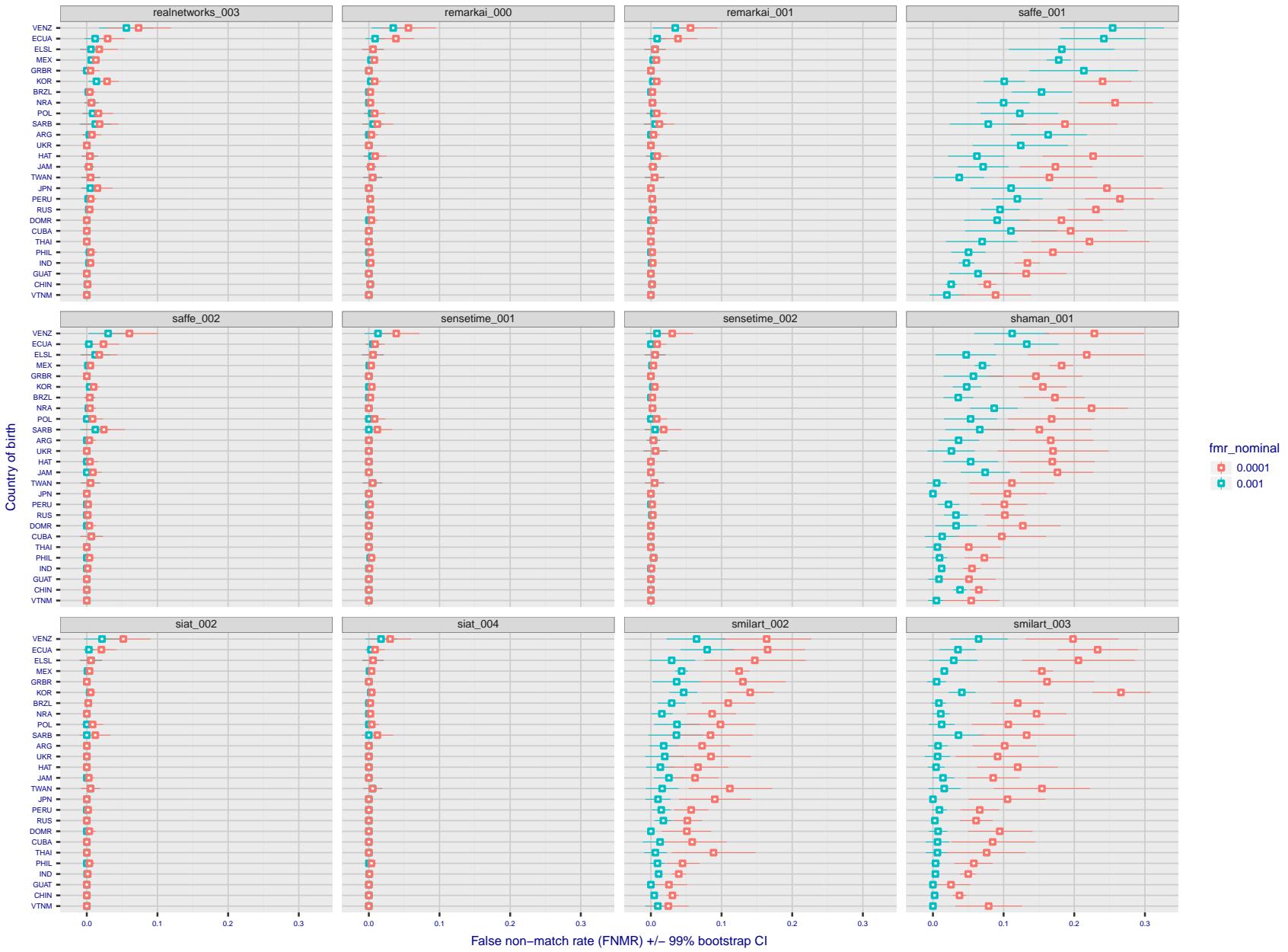


Figure 98: For the visa images, the dots show FNMR by country of birth for two globally set operating thresholds corresponding to  $FMR = \{0.001, 0.0001\}$  computed over all on the order of  $10^{10}$  impostor scores. The FMR in each bin will vary also - see subsequent impostor heatmaps in sec. 3.6.1. The figures shows an order of magnitude variation in FNMR across country of birth; these effects are likely due quality variations, then demographics like age and race. The error rates in some cases are zero, and in others the DET is flat so the error rates at the two thresholds are identical. The lines span 1% and 99% of bootstrap replicated FNMR estimates.

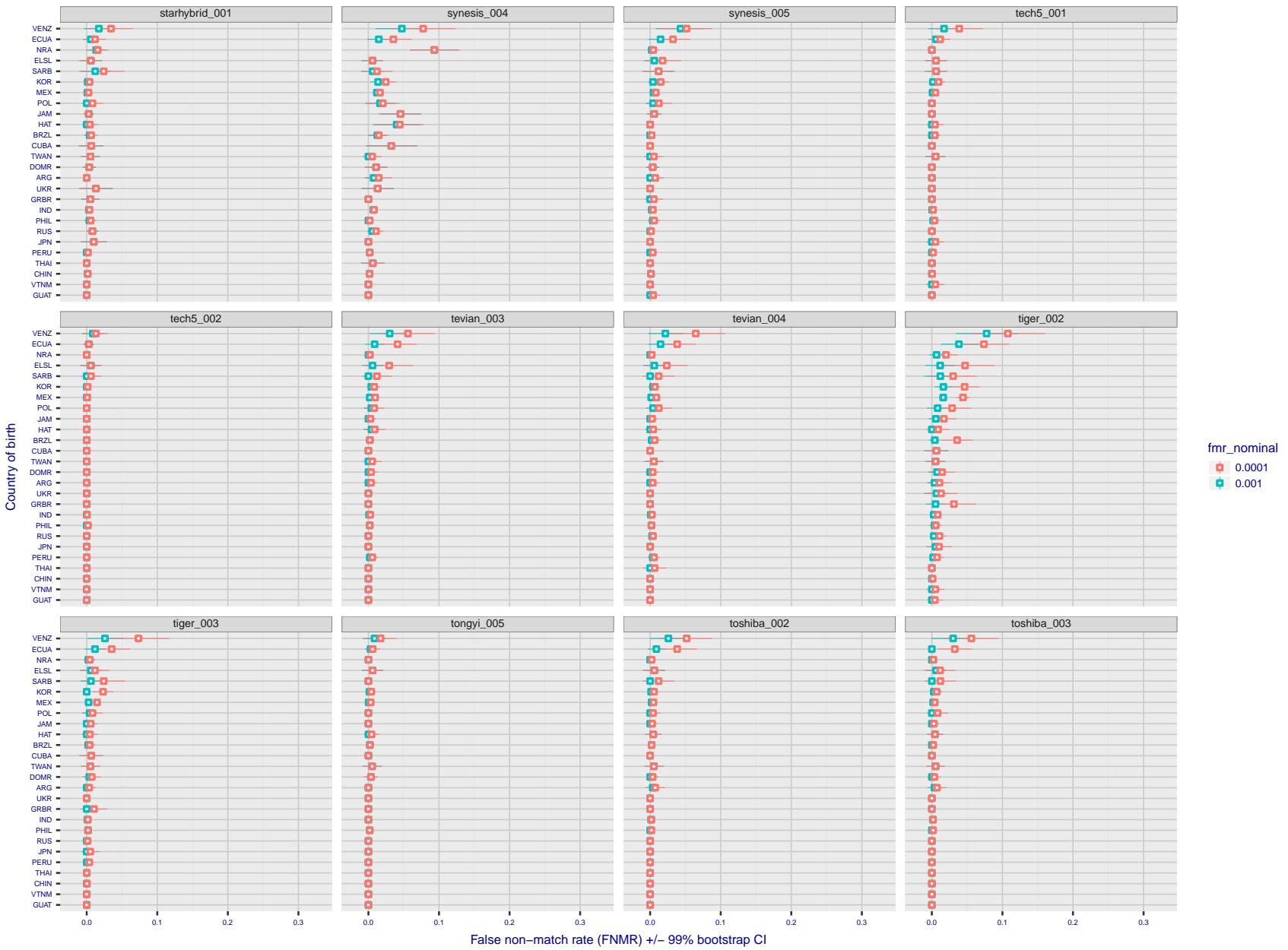


Figure 99: For the visa images, the dots show FNMR by country of birth for two globally set operating thresholds corresponding to  $FMR = \{0.001, 0.0001\}$  computed over all on the order of  $10^{10}$  impostor scores. The FMR in each bin will vary also - see subsequent impostor heatmaps in sec. 3.6.1. The figures shows an order of magnitude variation in FNMR across country of birth; these effects are likely due quality variations, then demographics like age and race. The error rates in some cases are zero, and in others the DET is flat so the error rates at the two thresholds are identical. The lines span 1% and 99% of bootstrap replicated FNMR estimates.

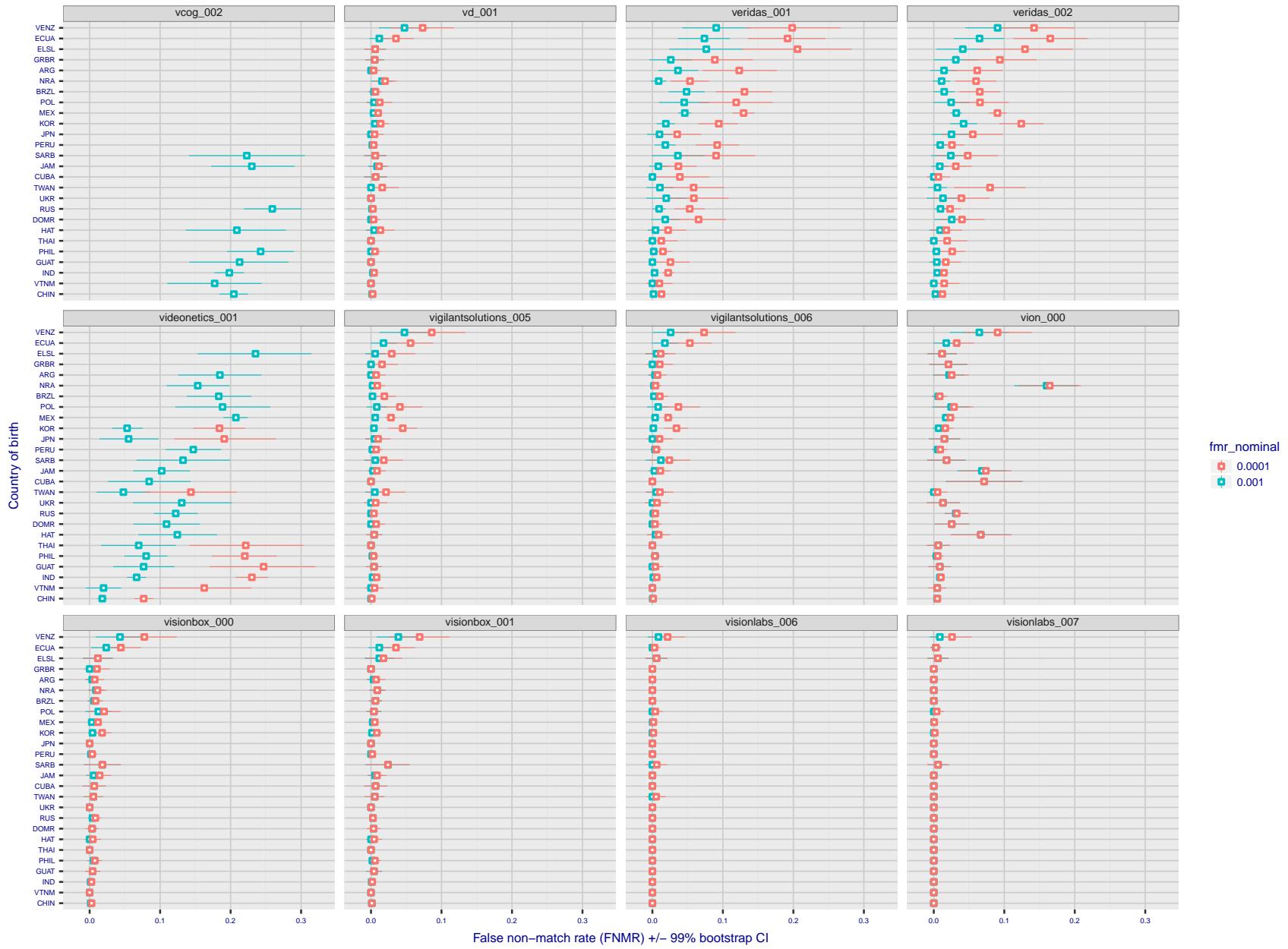


Figure 100: For the visa images, the dots show FNMR by country of birth for two globally set operating thresholds corresponding to  $FMR = \{0.001, 0.0001\}$  computed over all on the order of  $10^{10}$  impostor scores. The FMR in each bin will vary also - see subsequent impostor heatmaps in sec. 3.6.1. The figures shows an order of magnitude variation in FNMR across country of birth; these effects are likely due quality variations, then demographics like age and race. The error rates in some cases are zero, and in others the DET is flat so the error rates at the two thresholds are identical. The lines span 1% and 99% of bootstrap replicated FNMR estimates.

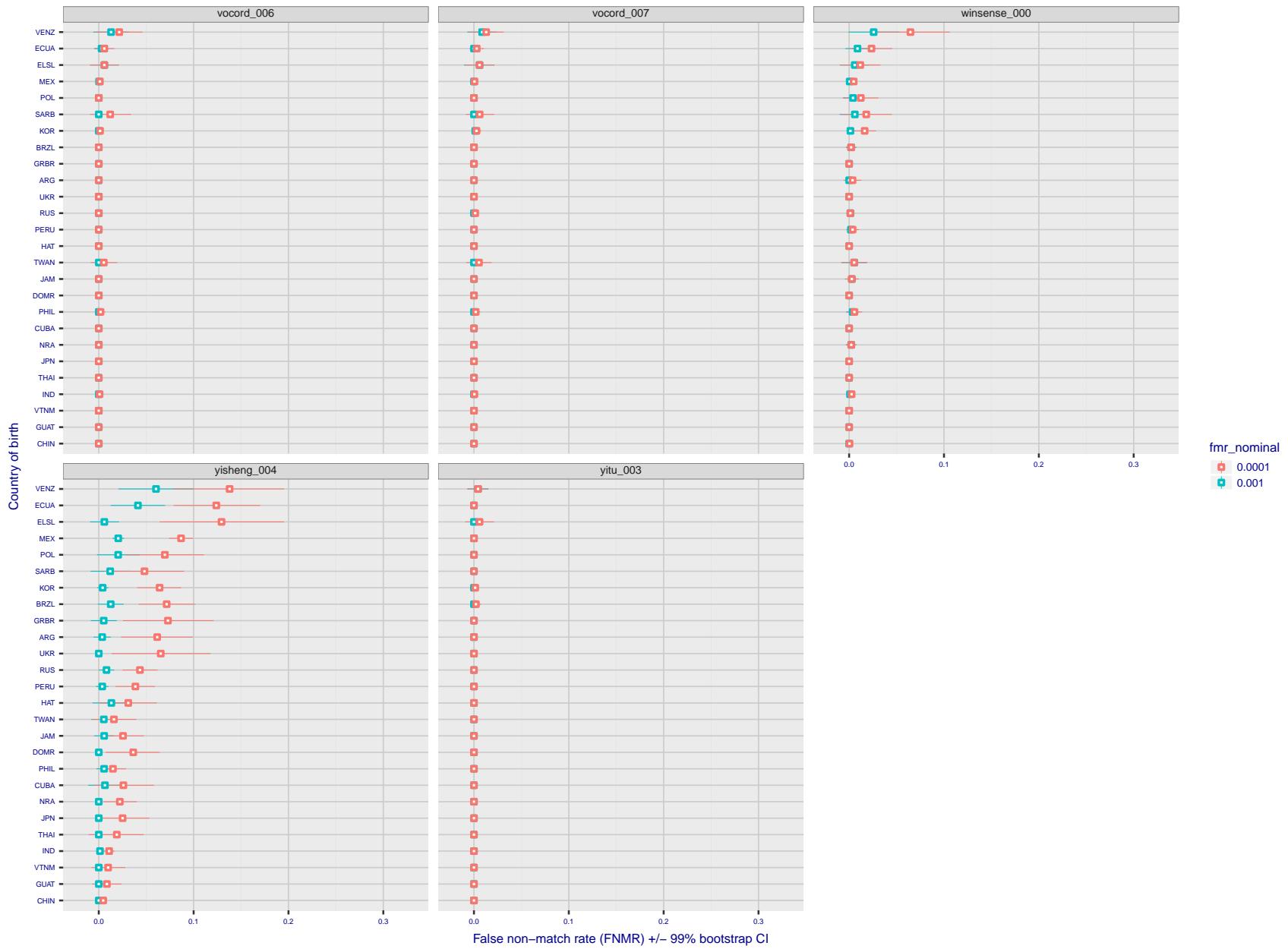


Figure 101: For the visa images, the dots show FNMR by country of birth for two globally set operating thresholds corresponding to  $FMR = \{0.001, 0.0001\}$  computed over all on the order of  $10^{10}$  impostor scores. The FMR in each bin will vary also - see subsequent impostor heatmaps in sec. 3.6.1. The figures shows an order of magnitude variation in FNMR across country of birth; these effects are likely due quality variations, then demographics like age and race. The error rates in some cases are zero, and in others the DET is flat so the error rates at the two thresholds are identical. The lines span 1% and 99% of bootstrap replicated FNMR estimates.

**Caveats:** The results may not relate to subject-specific properties. Instead they could reflect image-specific quality differences, which could occur due to collection protocol or software processing variations.

### 3.5.2 Effect of ageing

**Background:** Faces change appearance throughout life. This change gradually reduces similarity of a new image to an earlier image. Face recognition algorithms give reduced similarity scores and more frequent false rejections.

**Goal:** To quantify false non-match rates (FNMR) as a function of elapsed time in an adult population.

**Methods:** Using the mugshot images, a threshold is set to give FMR = 0.00001 over the entire impostor set. Then FNMR is measured over 1000 bootstrap replications of the genuine scores.

**Results:** For the visa images, Figure 110 shows how false non-match rates for genuine users, as a function of age group.

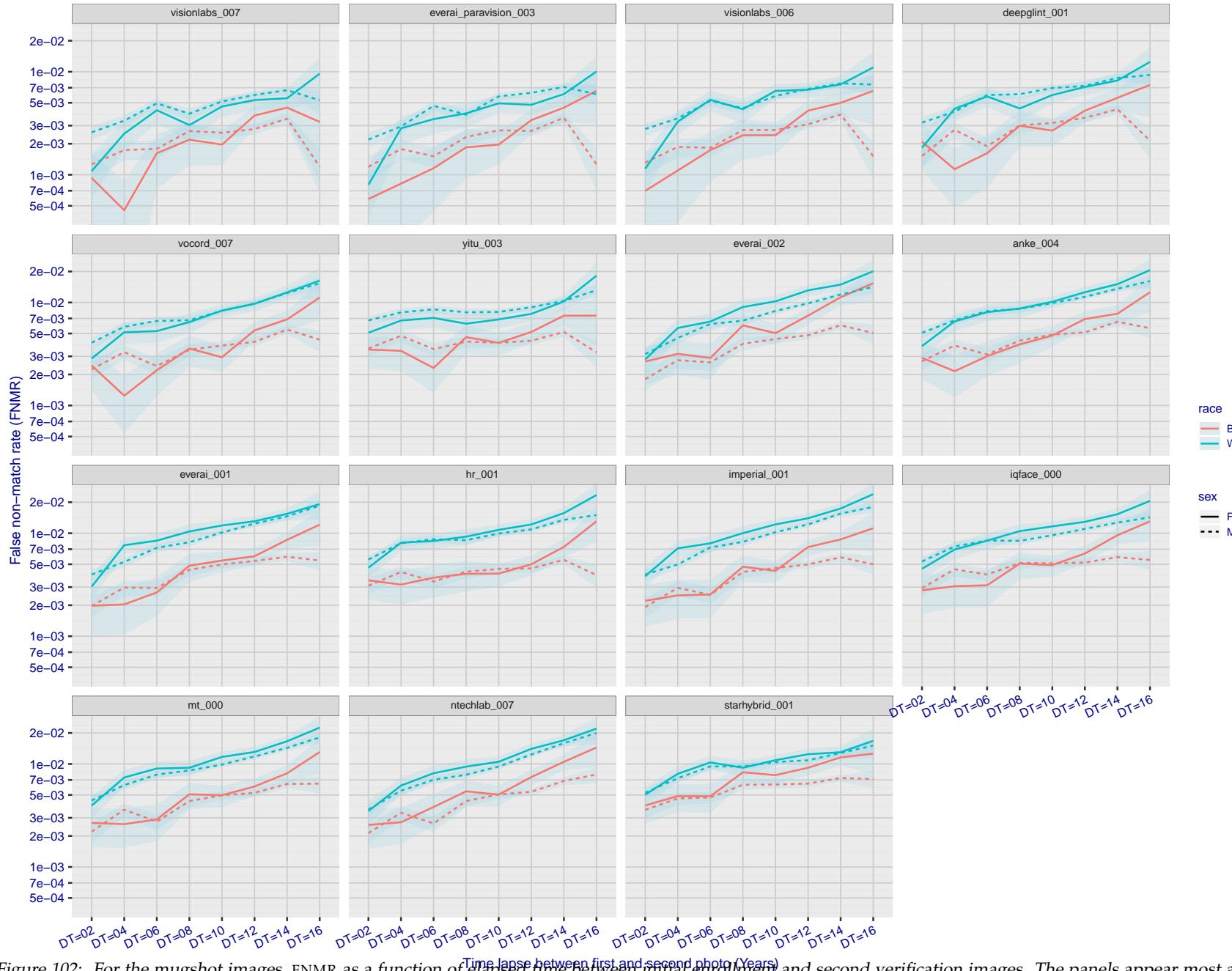


Figure 102: For the mugshot images, FNMR as a function of elapsed time between initial enrollment and second verification images. The panels appear most accurate first, and vertical scale changes on each page. The four traces correspond to images annotated with codes for black female, black male, white female, white male. The threshold is fixed for each algorithm to give FMR = 0.00001 over all ( $10^8$ ) impostor comparisons. For short time-lapses, the most accurate algorithms give very few errors (FNMR < 0.001) so that the uncertainty estimates are high.

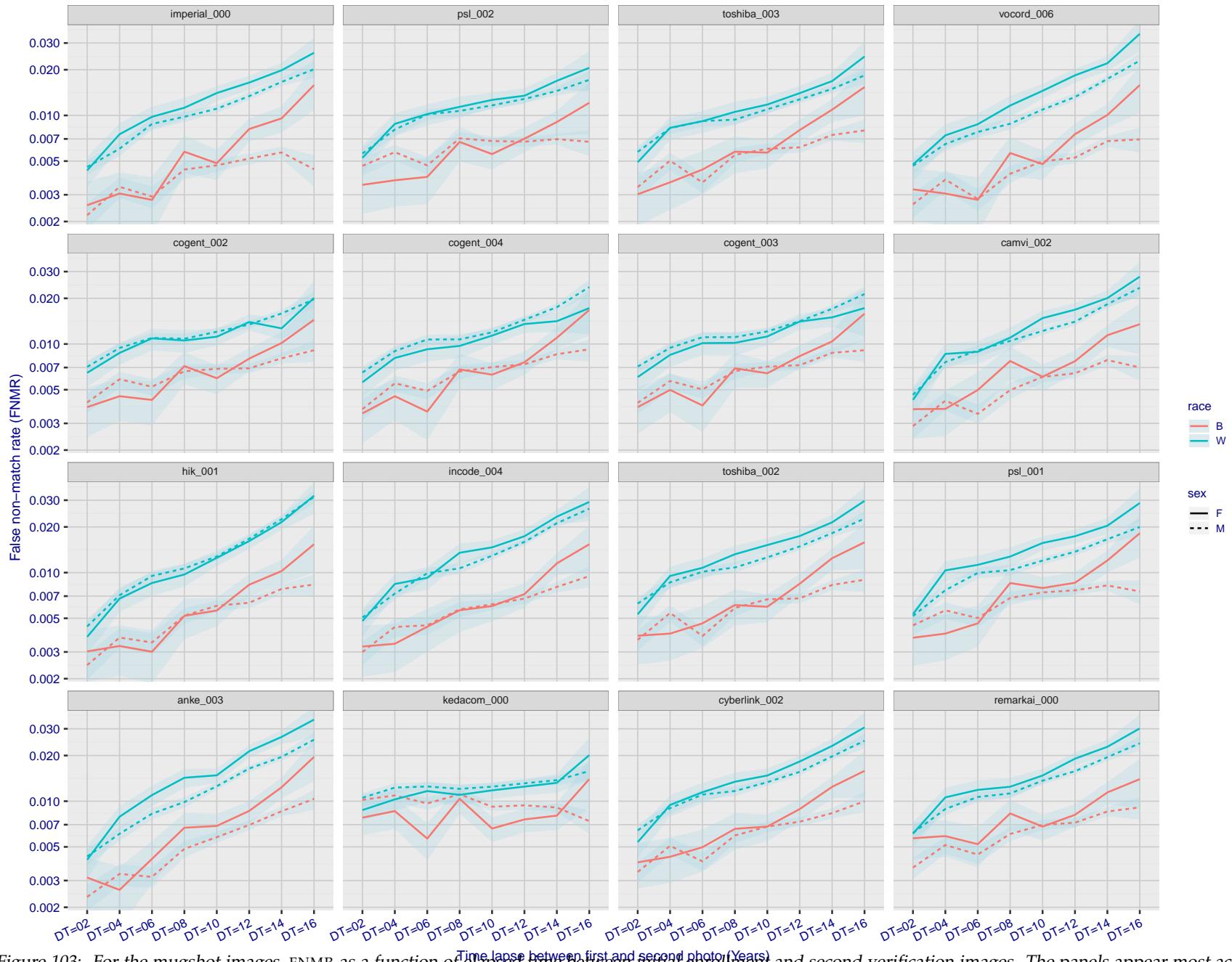


Figure 103: For the mugshot images, FNMR as a function of elapsed time between initial enrollment and second verification images. The panels appear most accurate first, and vertical scale changes on each page. The four traces correspond to images annotated with codes for black female, black male, white female, white male. The threshold is fixed for each algorithm to give FMR = 0.00001 over all ( $10^8$ ) impostor comparisons. For short time-lapses, the most accurate algorithms give very few errors (FNMR < 0.001) so that the uncertainty estimates are high.

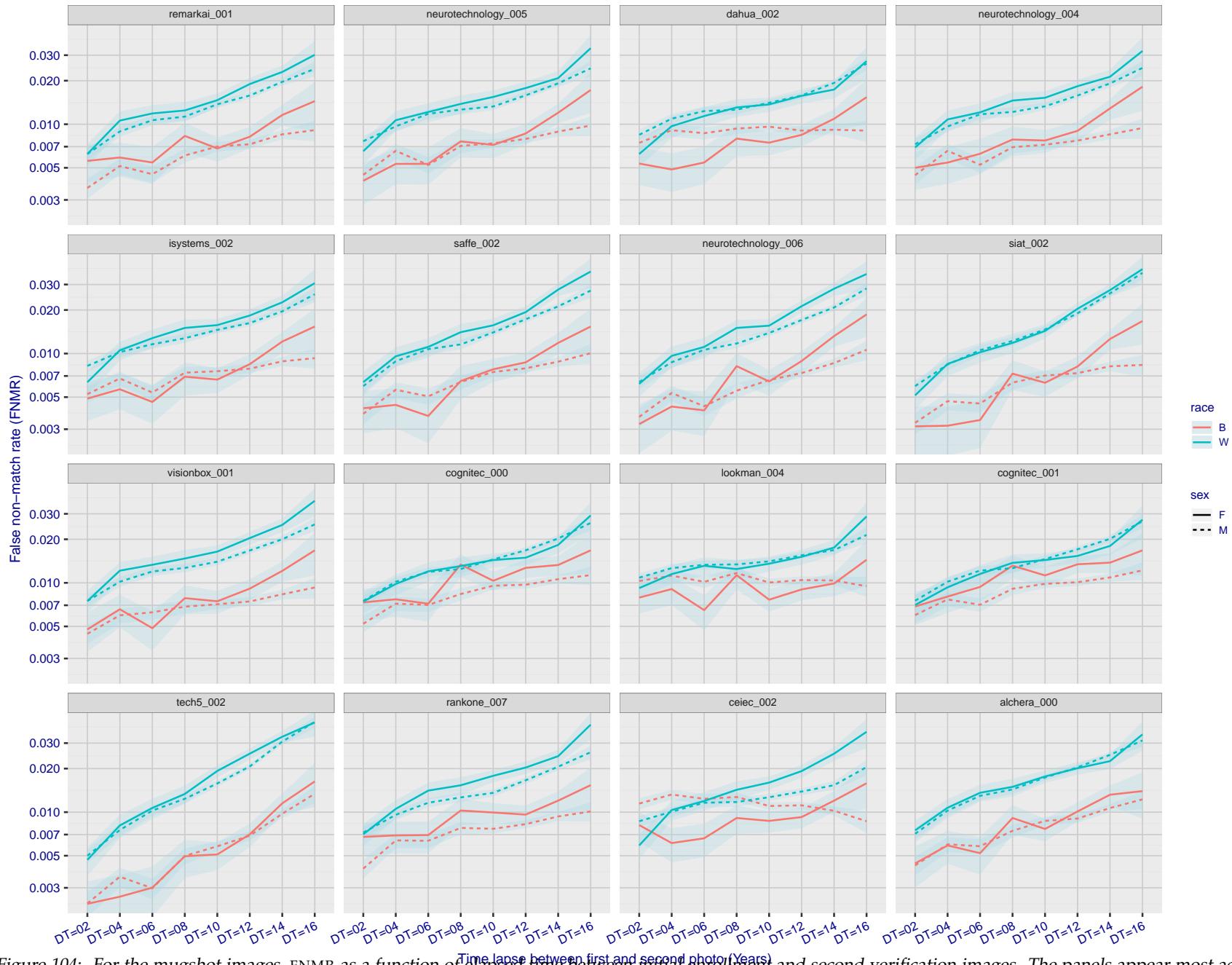


Figure 104: For the mugshot images, FNMR as a function of elapsed time between initial enrollment and second verification images. The panels appear most accurate first, and vertical scale changes on each page. The four traces correspond to images annotated with codes for black female, black male, white female, white male. The threshold is fixed for each algorithm to give FMR = 0.00001 over all ( $10^8$ ) impostor comparisons. For short time-lapses, the most accurate algorithms give very few errors (FNMR < 0.001) so that the uncertainty estimates are high.

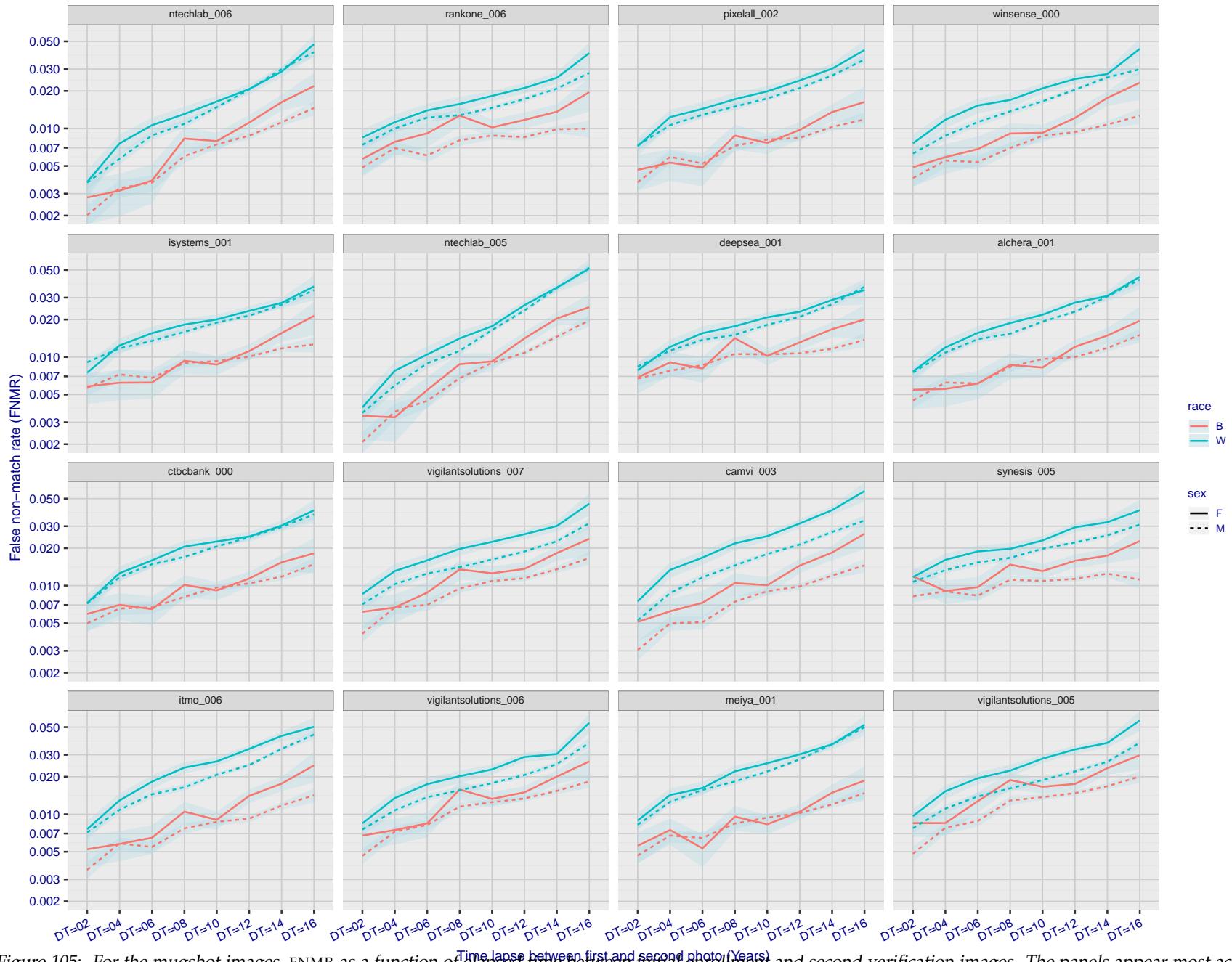


Figure 105: For the mugshot images, FNMR as a function of elapsed time between initial enrollment and second verification images. The panels appear most accurate first, and vertical scale changes on each page. The four traces correspond to images annotated with codes for black female, black male, white female, white male. The threshold is fixed for each algorithm to give  $FMR = 0.00001$  over all ( $10^8$ ) impostor comparisons. For short time-lapses, the most accurate algorithms give very few errors ( $FNMR < 0.001$ ) so that the uncertainty estimates are high.

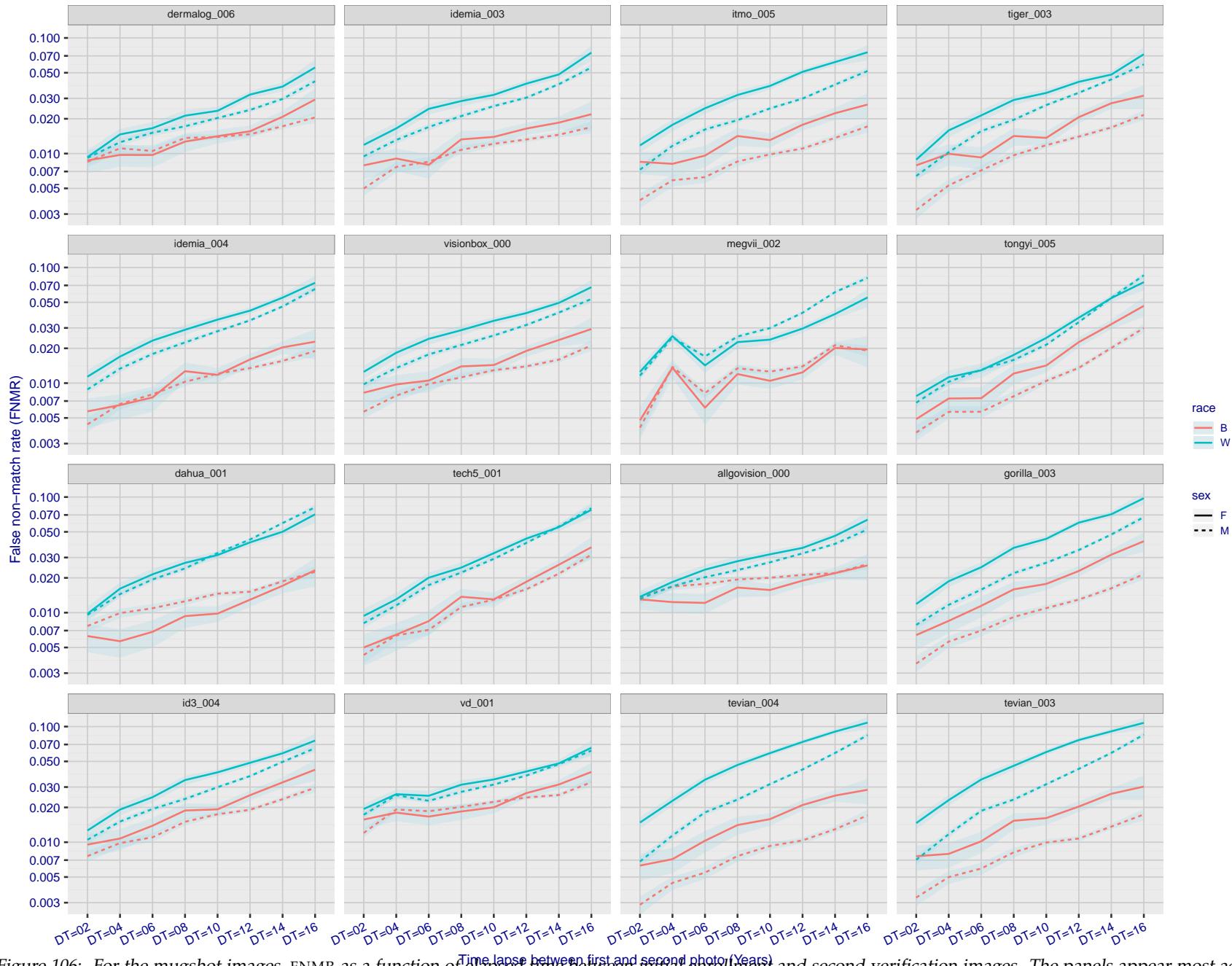


Figure 106: For the mugshot images, FNMR as a function of elapsed time between initial enrollment and second verification images. The panels appear most accurate first, and vertical scale changes on each page. The four traces correspond to images annotated with codes for black female, black male, white female, white male. The threshold is fixed for each algorithm to give  $FMR = 0.00001$  over all ( $10^8$ ) impostor comparisons. For short time-lapses, the most accurate algorithms give very few errors ( $FNMR < 0.001$ ) so that the uncertainty estimates are high.

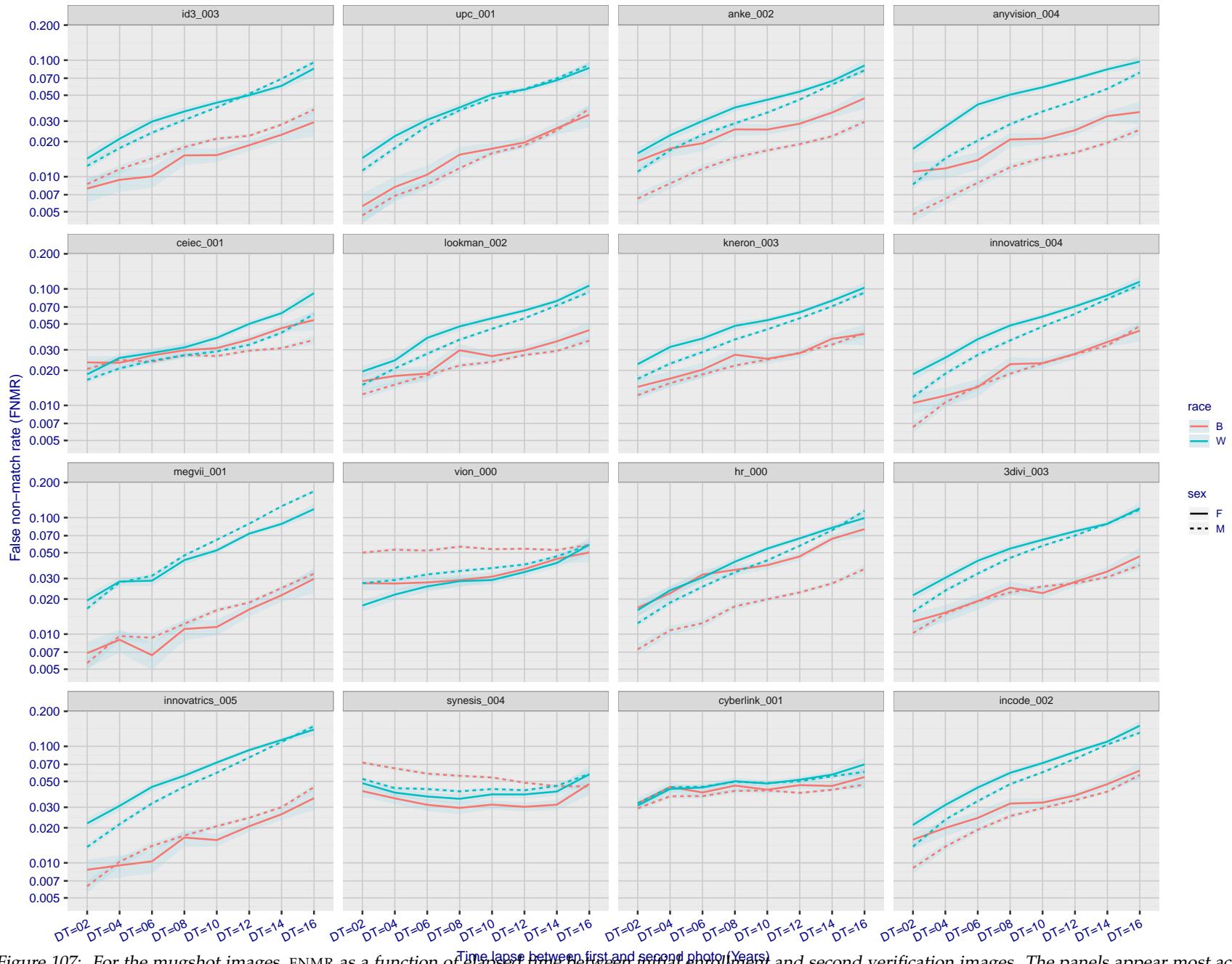


Figure 107: For the mugshot images, FNMR as a function of elapsed time between initial enrollment and second verification images. The panels appear most accurate first, and vertical scale changes on each page. The four traces correspond to images annotated with codes for black female, black male, white female, white male. The threshold is fixed for each algorithm to give FMR = 0.00001 over all ( $10^8$ ) impostor comparisons. For short time-lapses, the most accurate algorithms give very few errors (FNMR < 0.001) so that the uncertainty estimates are high.

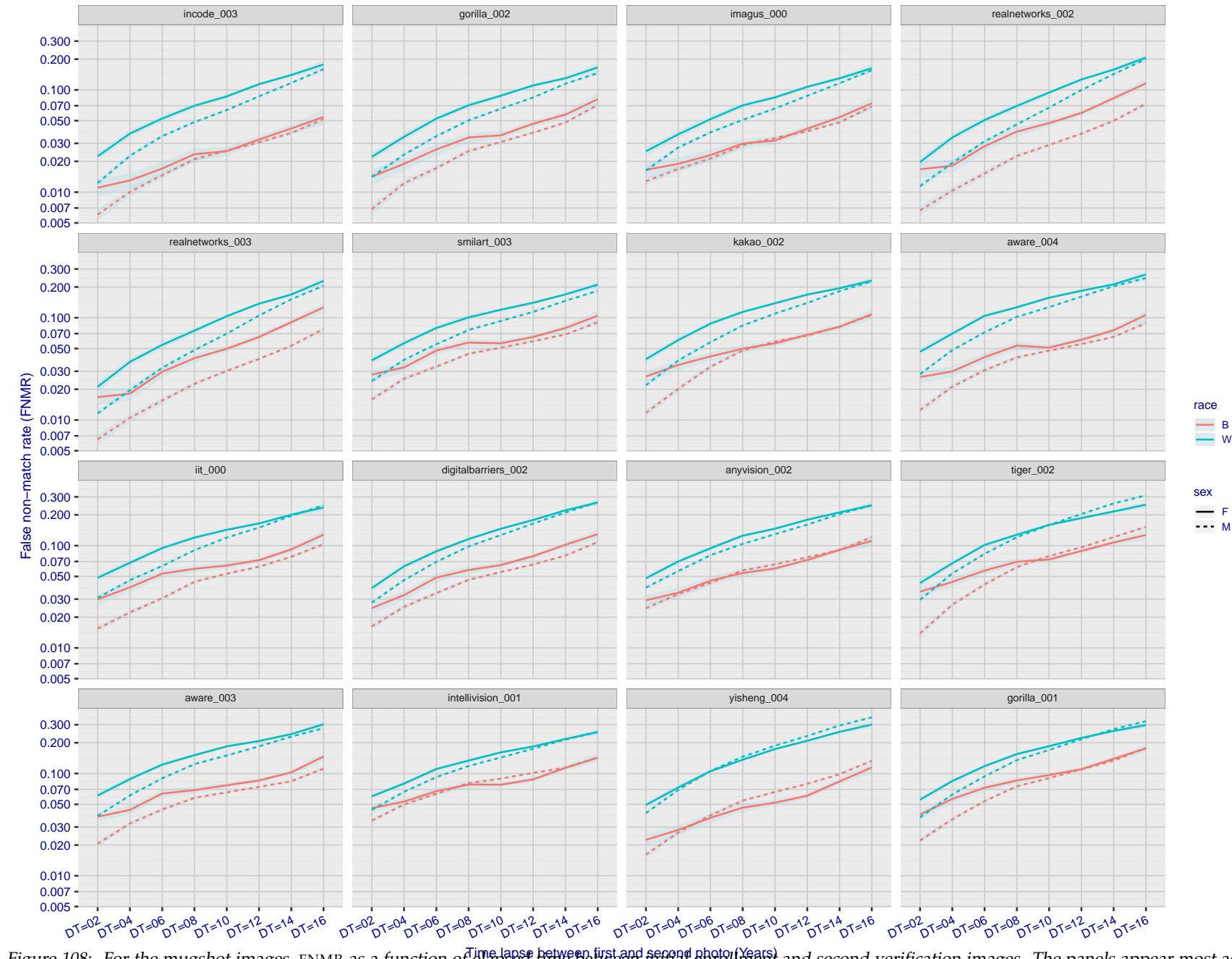


Figure 108: For the mugshot images, FNMR as a function of elapsed time between initial enrollment and second verification images. The panels appear most accurate first, and vertical scale changes on each page. The four traces correspond to images annotated with codes for black female, black male, white female, white male. The threshold is fixed for each algorithm to give FMR = 0.00001 over all ( $10^8$ ) impostor comparisons. For short time-lapses, the most accurate algorithms give very few errors (FNMR < 0.001) so that the uncertainty estimates are high.

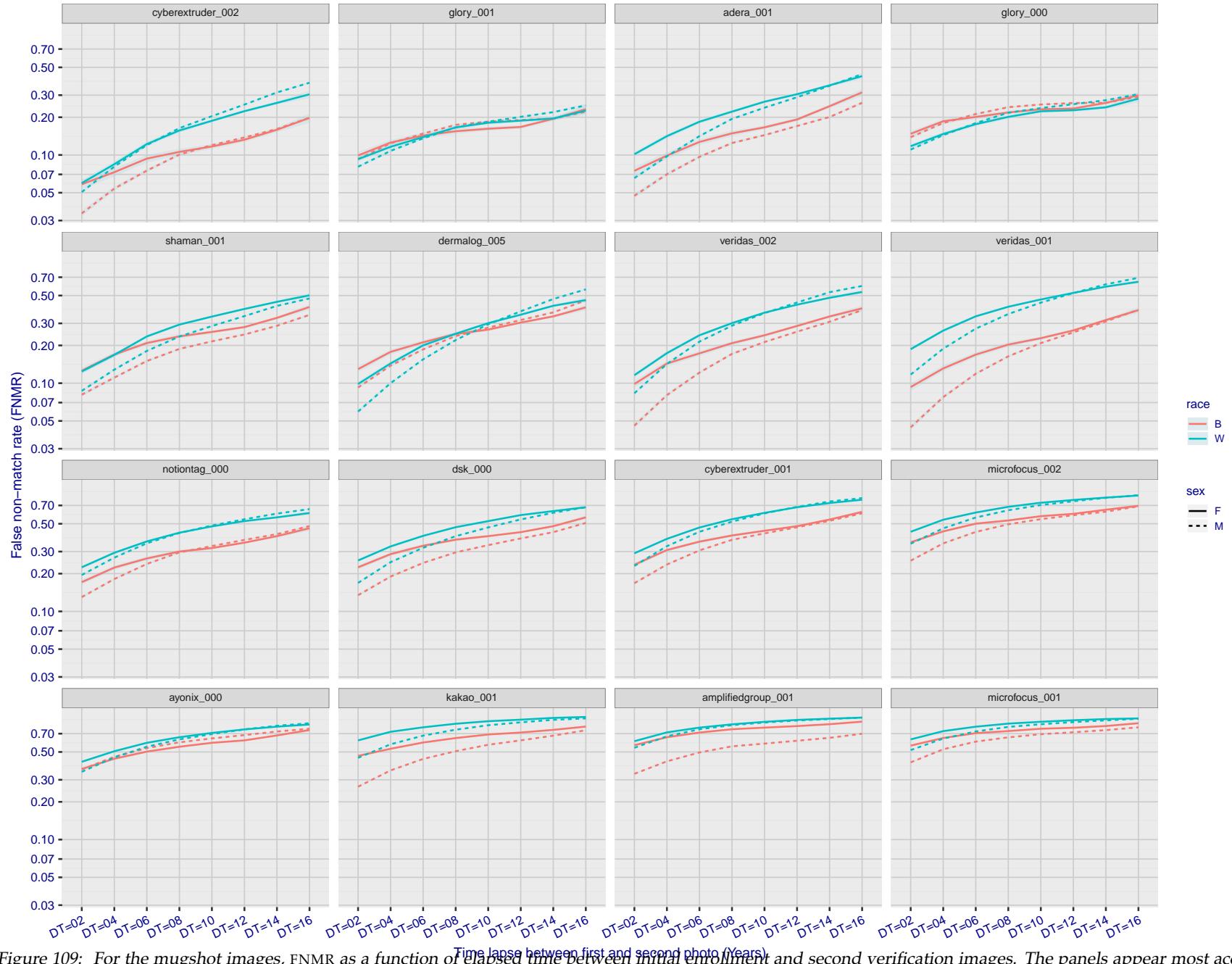


Figure 109: For the mugshot images, FNMR as a function of elapsed time between initial enrollment and second verification images. The panels appear most accurate first, and vertical scale changes on each page. The four traces correspond to images annotated with codes for black female, black male, white female, white male. The threshold is fixed for each algorithm to give FMR = 0.00001 over all ( $10^8$ ) impostor comparisons. For short time-lapses, the most accurate algorithms give very few errors (FNMR < 0.001) so that the uncertainty estimates are high.

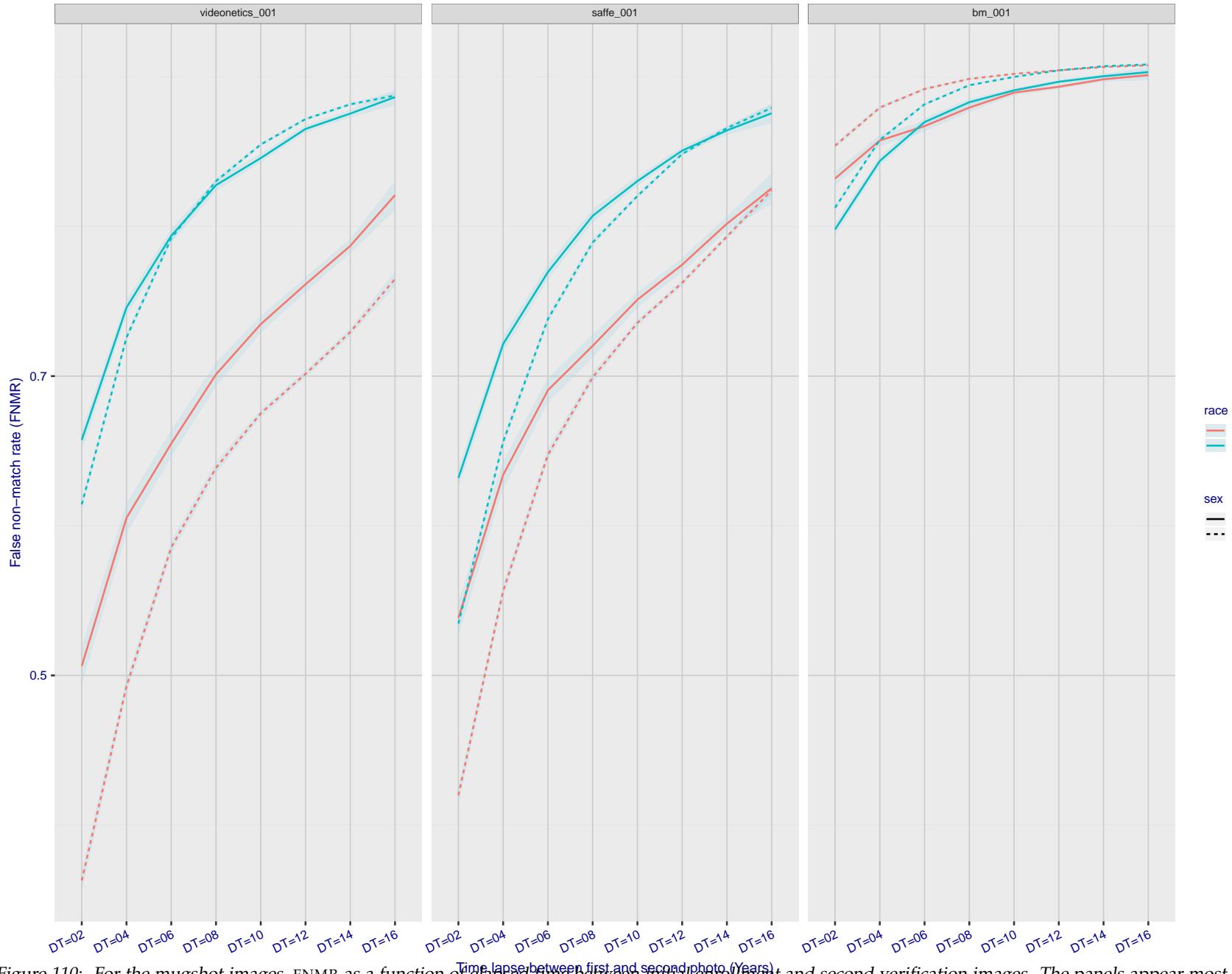


Figure 110: For the mugshot images, FNMR as a function of elapsed time between initial enrollment and second verification images. The panels appear most accurate first, and vertical scale changes on each page. The four traces correspond to images annotated with codes for black female, black male, white female, white male. The threshold is fixed for each algorithm to give FMR = 0.00001 over all ( $10^8$ ) impostor comparisons. For short time-lapses, the most accurate algorithms give very few errors (FNMR < 0.001) so that the uncertainty estimates are high.

### 3.5.3 Effect of age on genuine subjects

**Background:** Faces change appearance throughout life. Face recognition algorithms have previously been reported to give better accuracy on older individuals (See NIST IR 8009).

**Goal:** To quantify false non-match rates (FNMR) as a function of age, without an ageing component.

**Methods:** Using the visa images, which span fewer than five years, thresholds are determined that give FMR = 0.001 and 0.0001 over the entire impostor set. Then FNMR is measured over 1000 bootstrap replications of the genuine scores.

**Results:** For the visa images, Figure 122 shows how false non-match rates for genuine users, as a function of age group.

The notable aspects are:

- ▷ Younger subjects give considerably higher FNMR. This is likely due to rapid growth and change in facial appearance.
- ▷ FNMR trends down throughout life. The last bin, AGE > 72, contains fewer than 140 mated pairs, and may be affected by small sample size.

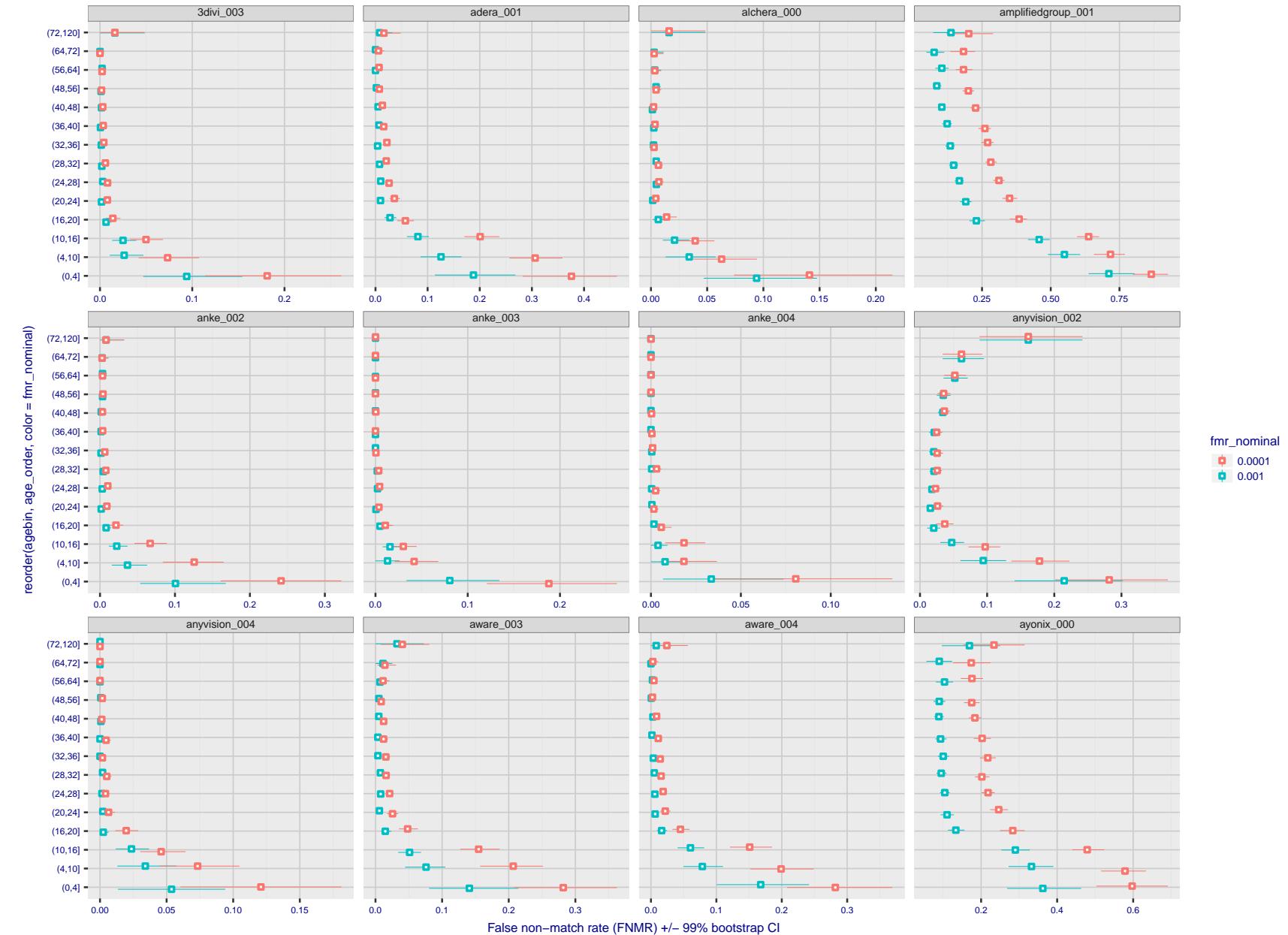


Figure 111: For the visa images, the dots show FNMR by age group for two operating thresholds corresponding to  $FMR = \{0.001, 0.0001\}$  computed over all on the order of  $10^{10}$  impostor scores. The FMR in each bin will vary also - see subsequent impostor heatmaps in sec. 3.6.2. Given a pair of face images taken at different times, we assign the comparison to the bin that is the arithmetic average of the subject's ages. This plot shows only the effect of age, not ageing. The number of comparisons in each bin is generally in the thousands, however the first and last bins are computed over 149 and 124 respectively. The error rates in some (adult) cases are zero, and in others the DET is flat so the error rates at the two thresholds are identical. The lines span 1% and 99% of bootstrap replicated FNMR estimates.

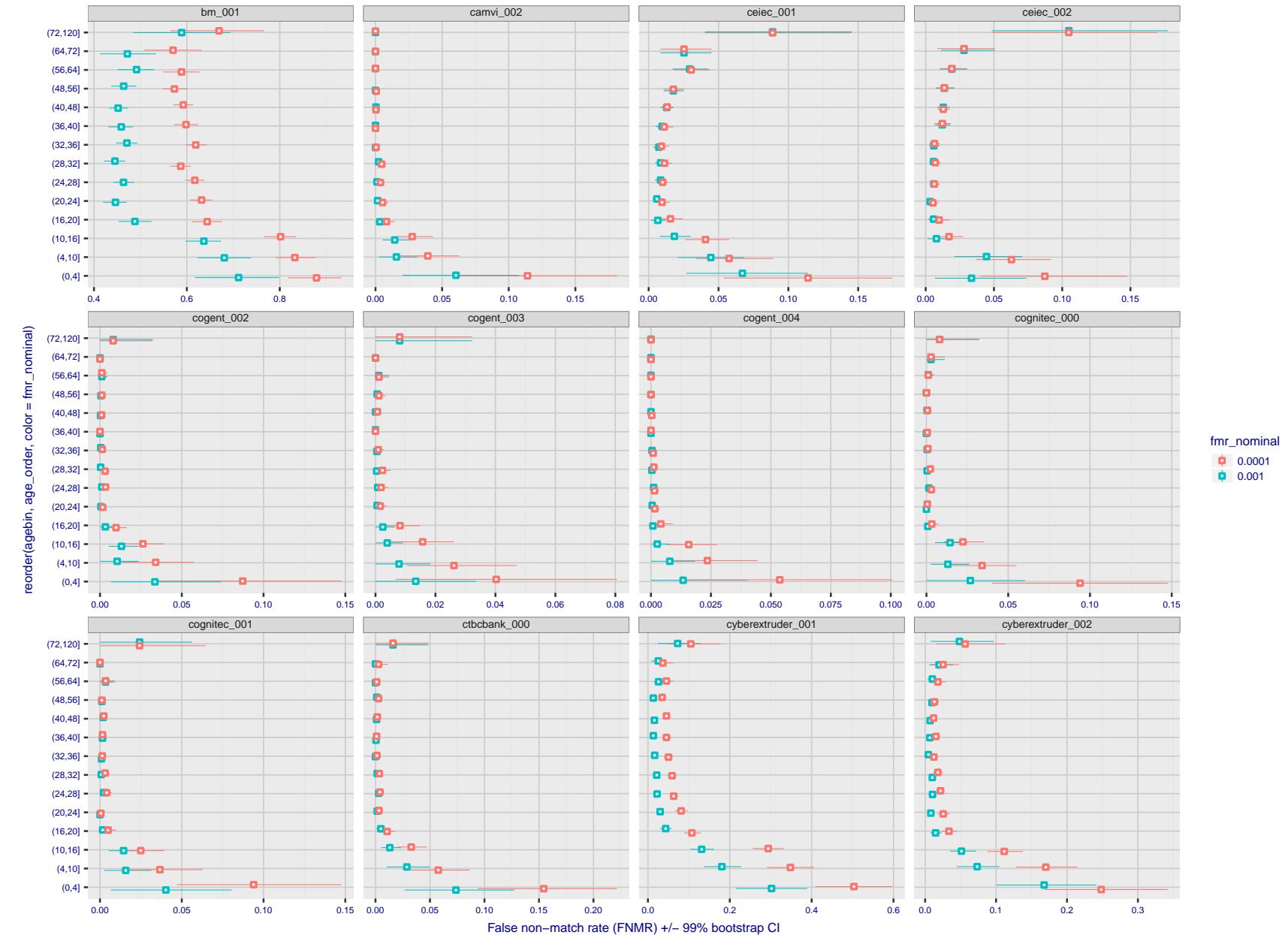


Figure 112: For the visa images, the dots show FNMR by age group for two operating thresholds corresponding to  $FMR = \{0.001, 0.0001\}$  computed over all on the order of  $10^{10}$  impostor scores. The FMR in each bin will vary also - see subsequent impostor heatmaps in sec. 3.6.2. Given a pair of face images taken at different times, we assign the comparison to the bin that is the arithmetic average of the subject's ages. This plot shows only the effect of age, not ageing. The number of comparisons in each bin is generally in the thousands, however the first and last bins are computed over 149 and 124 respectively. The error rates in some (adult) cases are zero, and in others the DET is flat so the error rates at the two thresholds are identical. The lines span 1% and 99% of bootstrap replicated FNMR estimates.

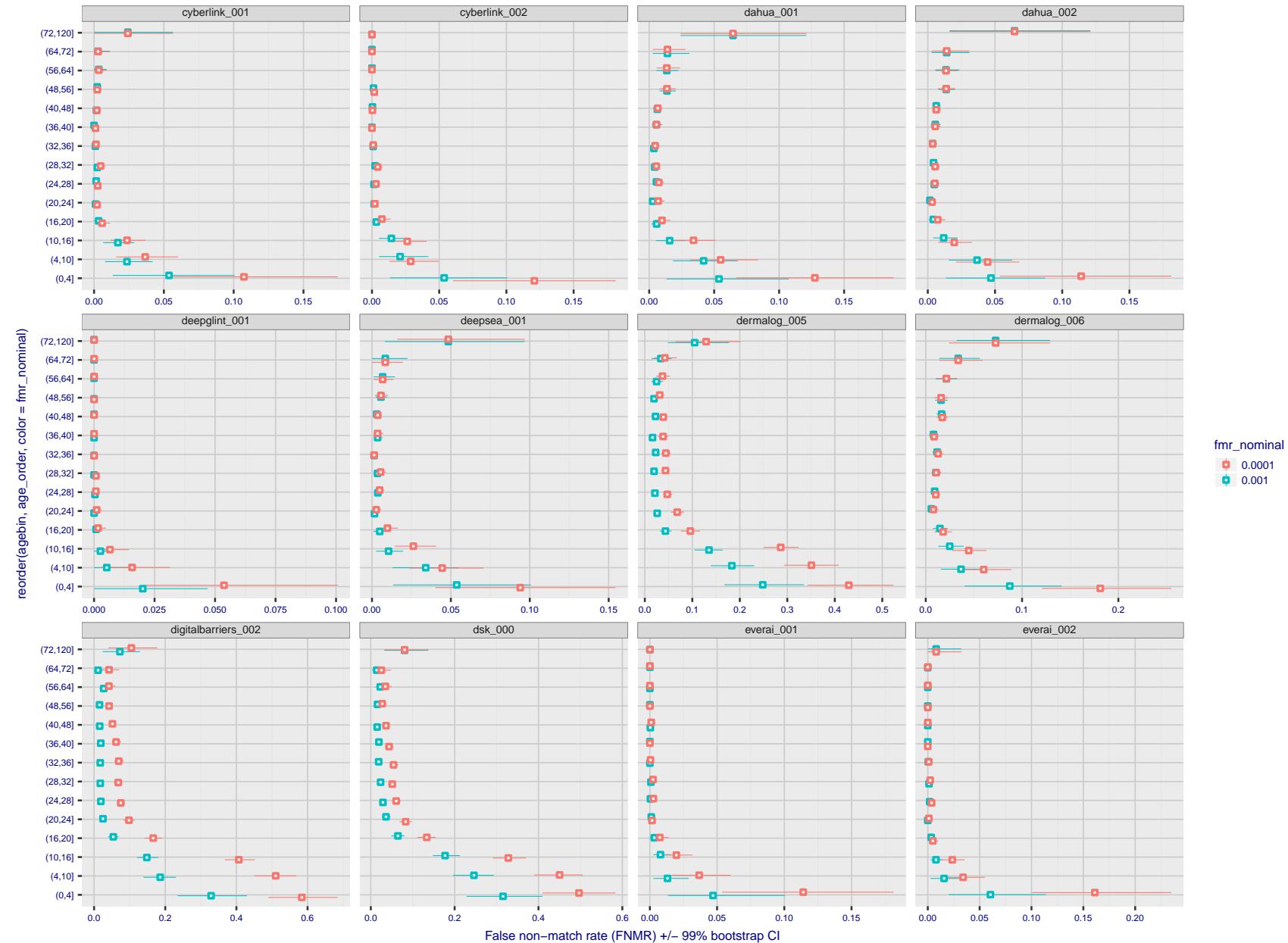


Figure 113: For the visa images, the dots show FNMR by age group for two operating thresholds corresponding to  $FMR = \{0.001, 0.0001\}$  computed over all on the order of  $10^{10}$  impostor scores. The FMR in each bin will vary also - see subsequent impostor heatmaps in sec. 3.6.2. Given a pair of face images taken at different times, we assign the comparison to the bin that is the arithmetic average of the subject's ages. This plot shows only the effect of age, not ageing. The number of comparisons in each bin is generally in the thousands, however the first and last bins are computed over 149 and 124 respectively. The error rates in some (adult) cases are zero, and in others the DET is flat so the error rates at the two thresholds are identical. The lines span 1% and 99% of bootstrap replicated FNMR estimates.

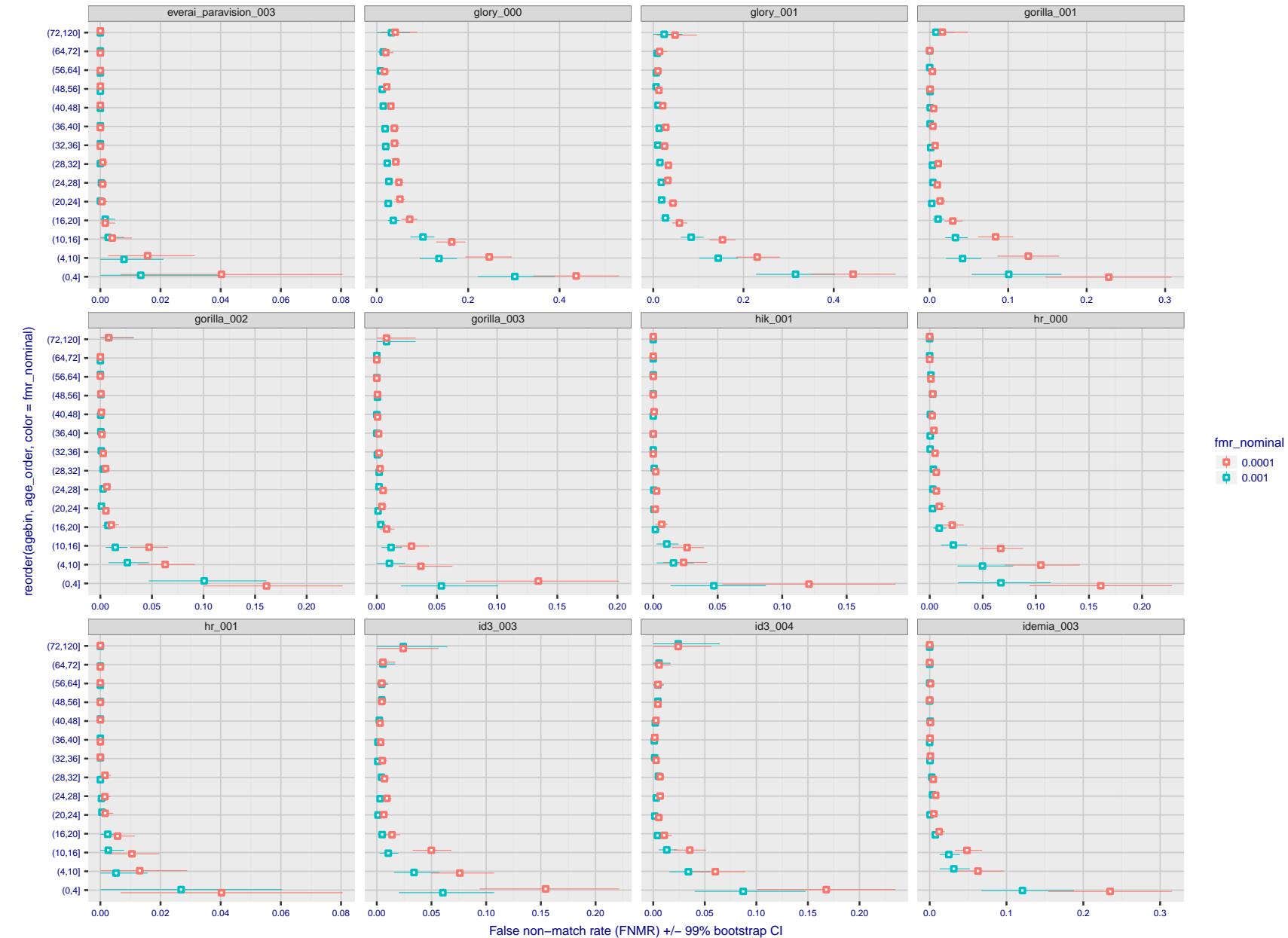


Figure 114: For the visa images, the dots show FNMR by age group for two operating thresholds corresponding to  $FMR = \{0.001, 0.0001\}$  computed over all on the order of  $10^{10}$  impostor scores. The FMR in each bin will vary also - see subsequent impostor heatmaps in sec. 3.6.2. Given a pair of face images taken at different times, we assign the comparison to the bin that is the arithmetic average of the subject's ages. This plot shows only the effect of age, not ageing. The number of comparisons in each bin is generally in the thousands, however the first and last bins are computed over 149 and 124 respectively. The error rates in some (adult) cases are zero, and in others the DET is flat so the error rates at the two thresholds are identical. The lines span 1% and 99% of bootstrap replicated FNMR estimates.

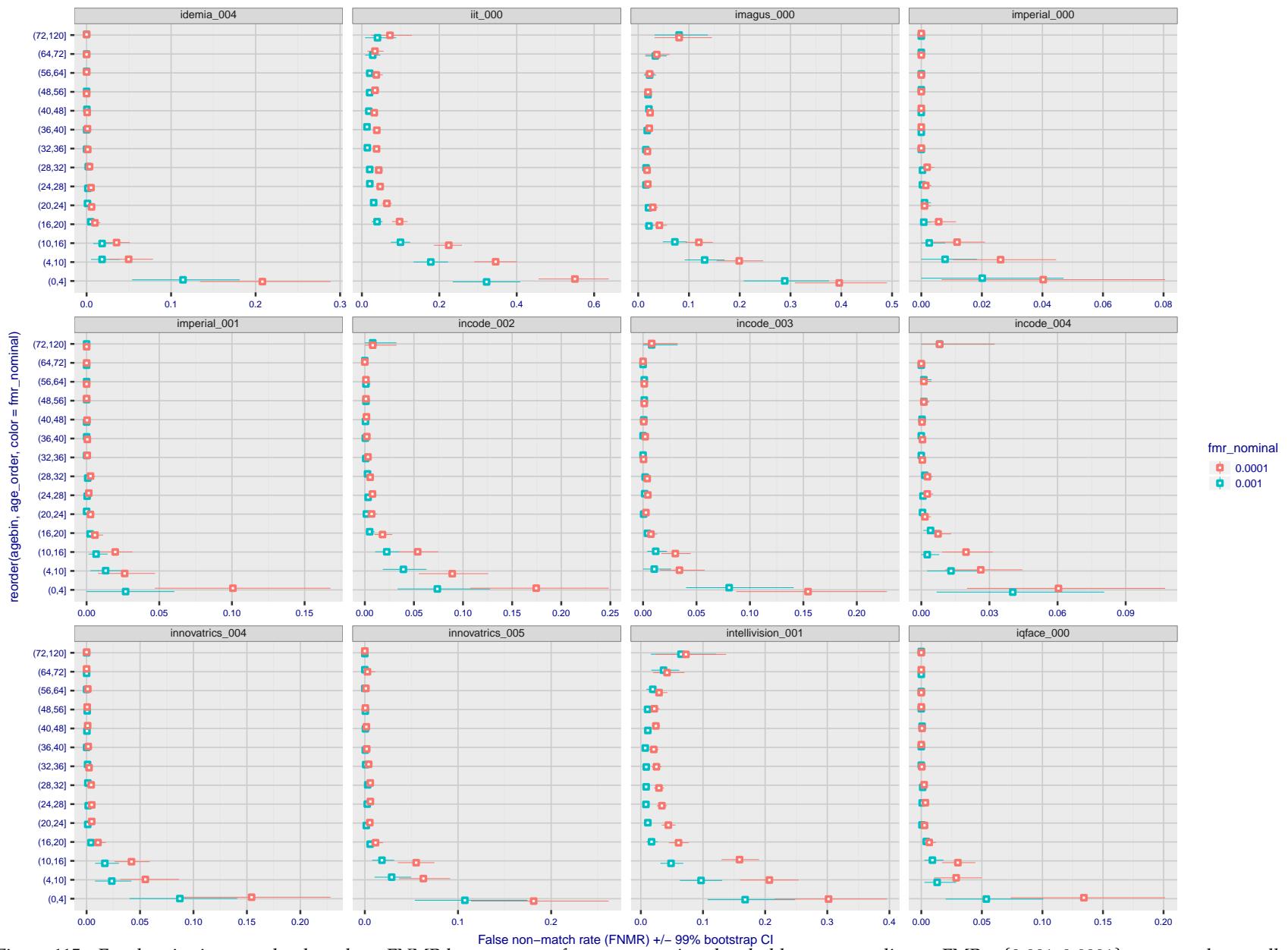


Figure 115: For the visa images, the dots show FNMR by age group for two operating thresholds corresponding to  $FMR = \{0.001, 0.0001\}$  computed over all on the order of  $10^{10}$  impostor scores. The FMR in each bin will vary also - see subsequent impostor heatmaps in sec. 3.6.2. Given a pair of face images taken at different times, we assign the comparison to the bin that is the arithmetic average of the subject's ages. This plot shows only the effect of age, not ageing. The number of comparisons in each bin is generally in the thousands, however the first and last bins are computed over 149 and 124 respectively. The error rates in some (adult) cases are zero, and in others the DET is flat so the error rates at the two thresholds are identical. The lines span 1% and 99% of bootstrap replicated FNMR estimates.

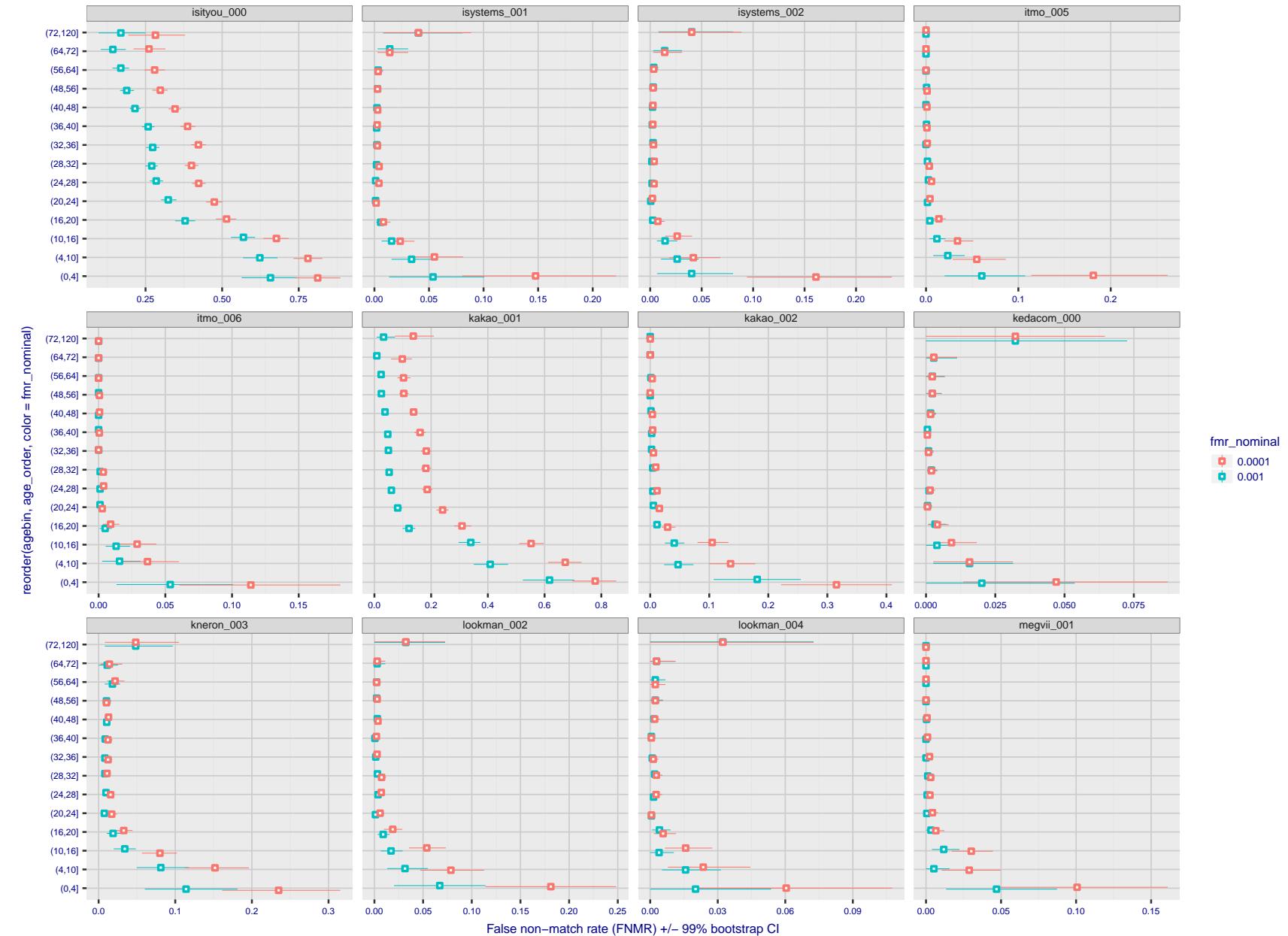


Figure 116: For the visa images, the dots show FNMR by age group for two operating thresholds corresponding to  $FMR = \{0.001, 0.0001\}$  computed over all on the order of  $10^{10}$  impostor scores. The FMR in each bin will vary also - see subsequent impostor heatmaps in sec. 3.6.2. Given a pair of face images taken at different times, we assign the comparison to the bin that is the arithmetic average of the subject's ages. This plot shows only the effect of age, not ageing. The number of comparisons in each bin is generally in the thousands, however the first and last bins are computed over 149 and 124 respectively. The error rates in some (adult) cases are zero, and in others the DET is flat so the error rates at the two thresholds are identical. The lines span 1% and 99% of bootstrap replicated FNMR estimates.

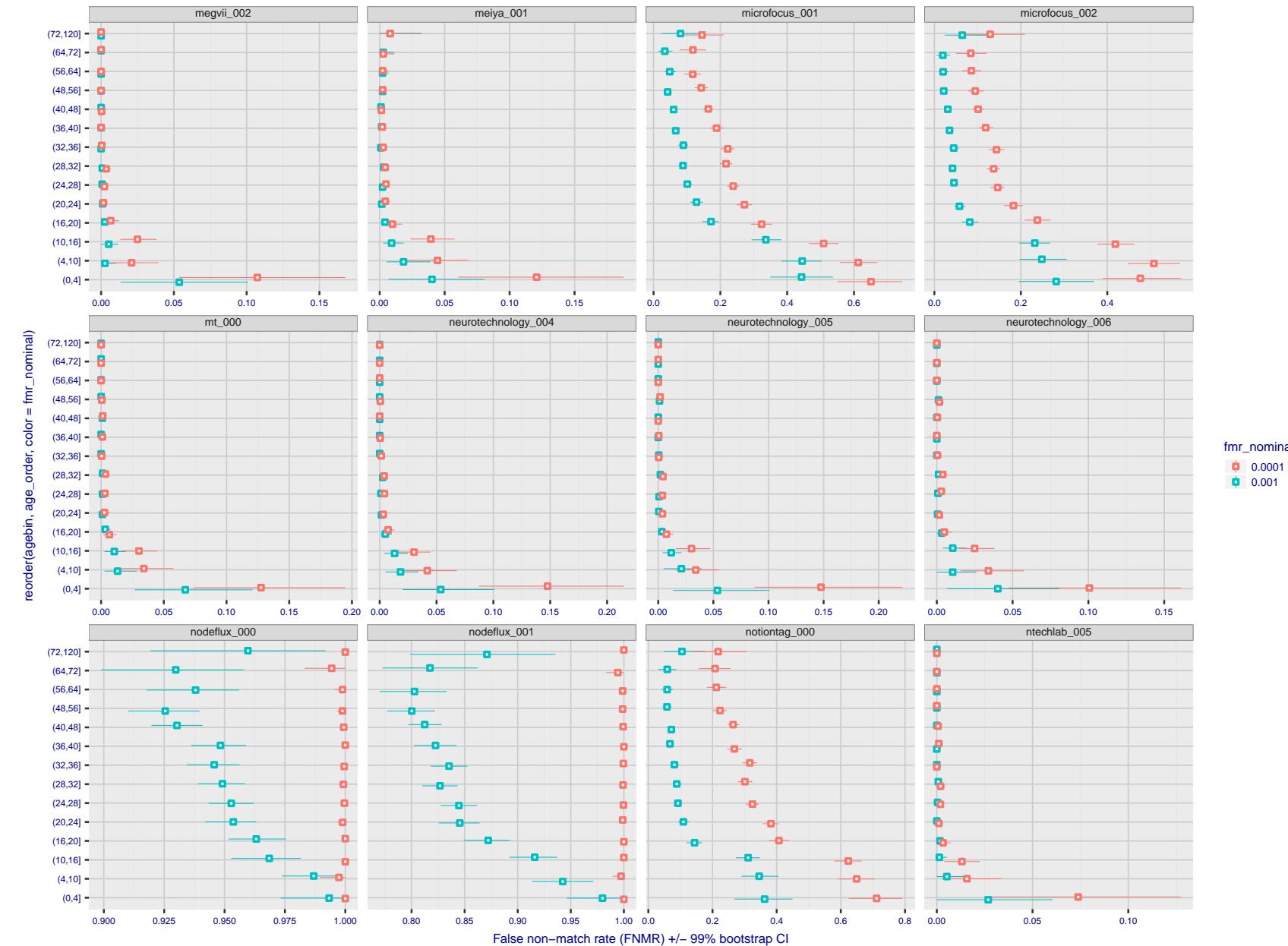


Figure 117: For the visa images, the dots show FNMR by age group for two operating thresholds corresponding to  $FMR = \{0.001, 0.0001\}$  computed over all on the order of  $10^{10}$  impostor scores. The FMR in each bin will vary also - see subsequent impostor heatmaps in sec. 3.6.2. Given a pair of face images taken at different times, we assign the comparison to the bin that is the arithmetic average of the subject's ages. This plot shows only the effect of age, not ageing. The number of comparisons in each bin is generally in the thousands, however the first and last bins are computed over 149 and 124 respectively. The error rates in some (adult) cases are zero, and in others the DET is flat so the error rates at the two thresholds are identical. The lines span 1% and 99% of bootstrap replicated FNMR estimates.

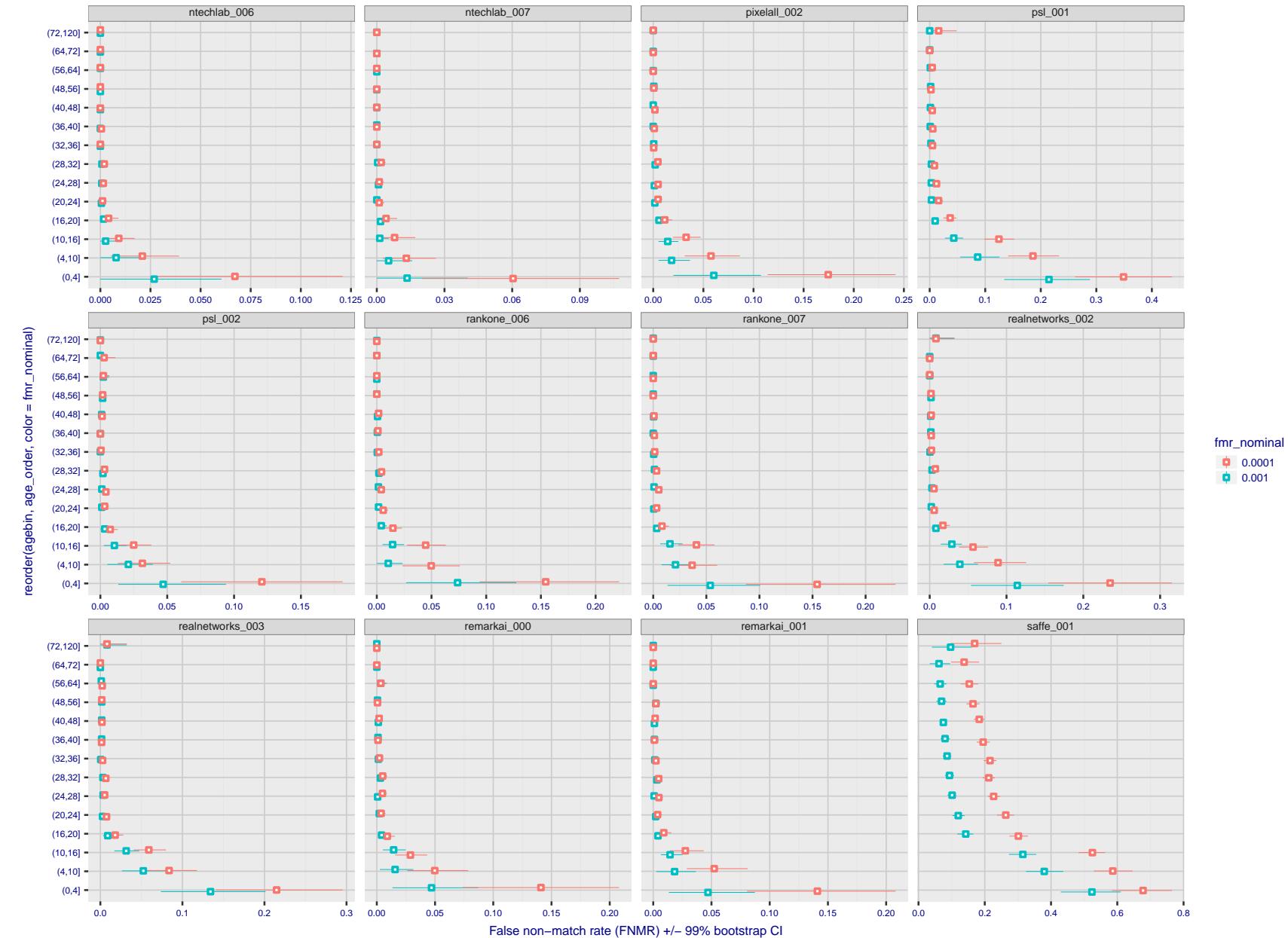


Figure 118: For the visa images, the dots show FNMR by age group for two operating thresholds corresponding to  $FMR = \{0.001, 0.0001\}$  computed over all on the order of  $10^{10}$  impostor scores. The FMR in each bin will vary also - see subsequent impostor heatmaps in sec. 3.6.2. Given a pair of face images taken at different times, we assign the comparison to the bin that is the arithmetic average of the subject's ages. This plot shows only the effect of age, not ageing. The number of comparisons in each bin is generally in the thousands, however the first and last bins are computed over 149 and 124 respectively. The error rates in some (adult) cases are zero, and in others the DET is flat so the error rates at the two thresholds are identical. The lines span 1% and 99% of bootstrap replicated FNMR estimates.

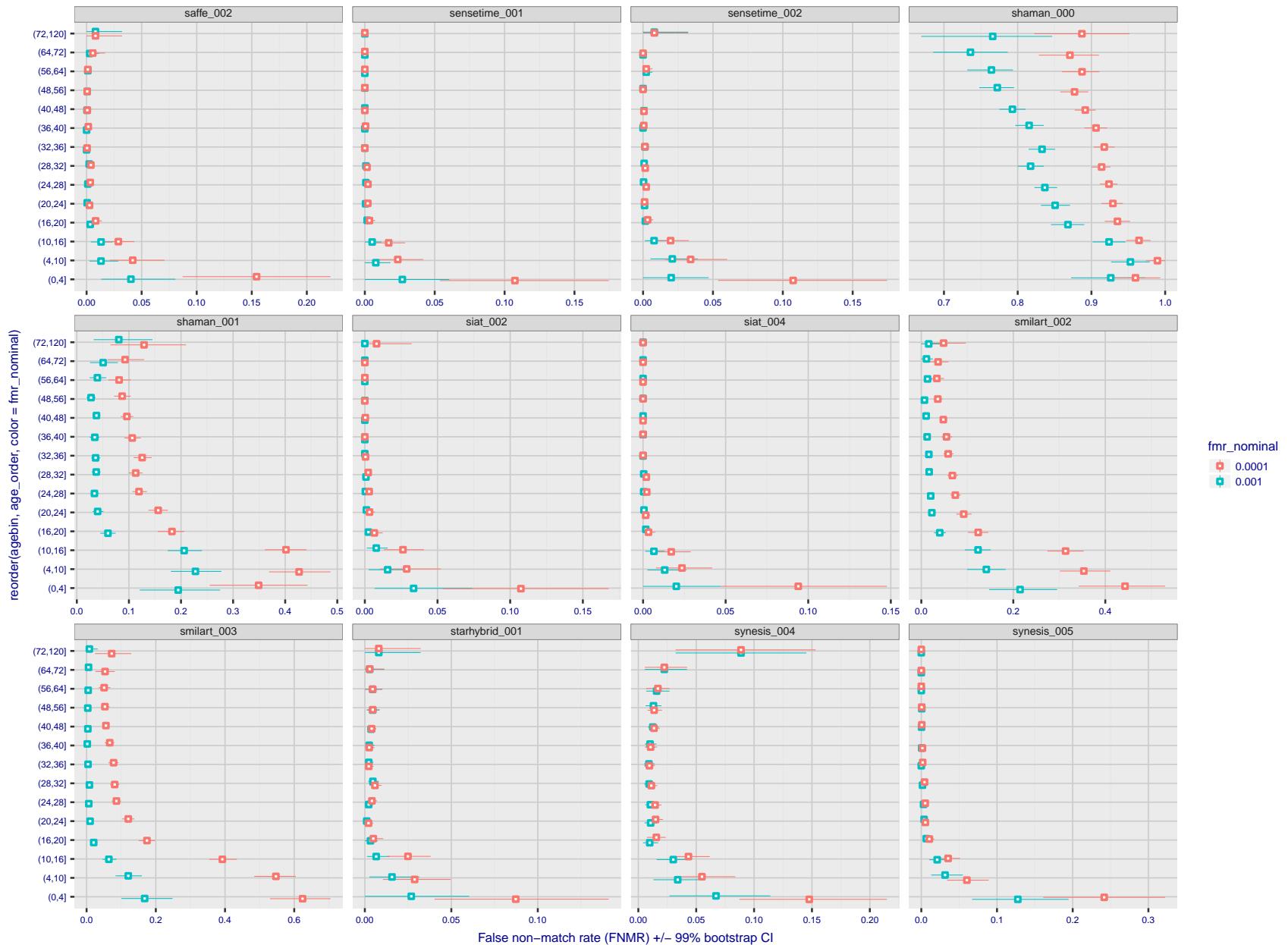


Figure 119: For the visa images, the dots show FNMR by age group for two operating thresholds corresponding to  $FMR = \{0.001, 0.0001\}$  computed over all on the order of  $10^{10}$  impostor scores. The FMR in each bin will vary also - see subsequent impostor heatmaps in sec. 3.6.2. Given a pair of face images taken at different times, we assign the comparison to the bin that is the arithmetic average of the subject's ages. This plot shows only the effect of age, not ageing. The number of comparisons in each bin is generally in the thousands, however the first and last bins are computed over 149 and 124 respectively. The error rates in some (adult) cases are zero, and in others the DET is flat so the error rates at the two thresholds are identical. The lines span 1% and 99% of bootstrap replicated FNMR estimates.

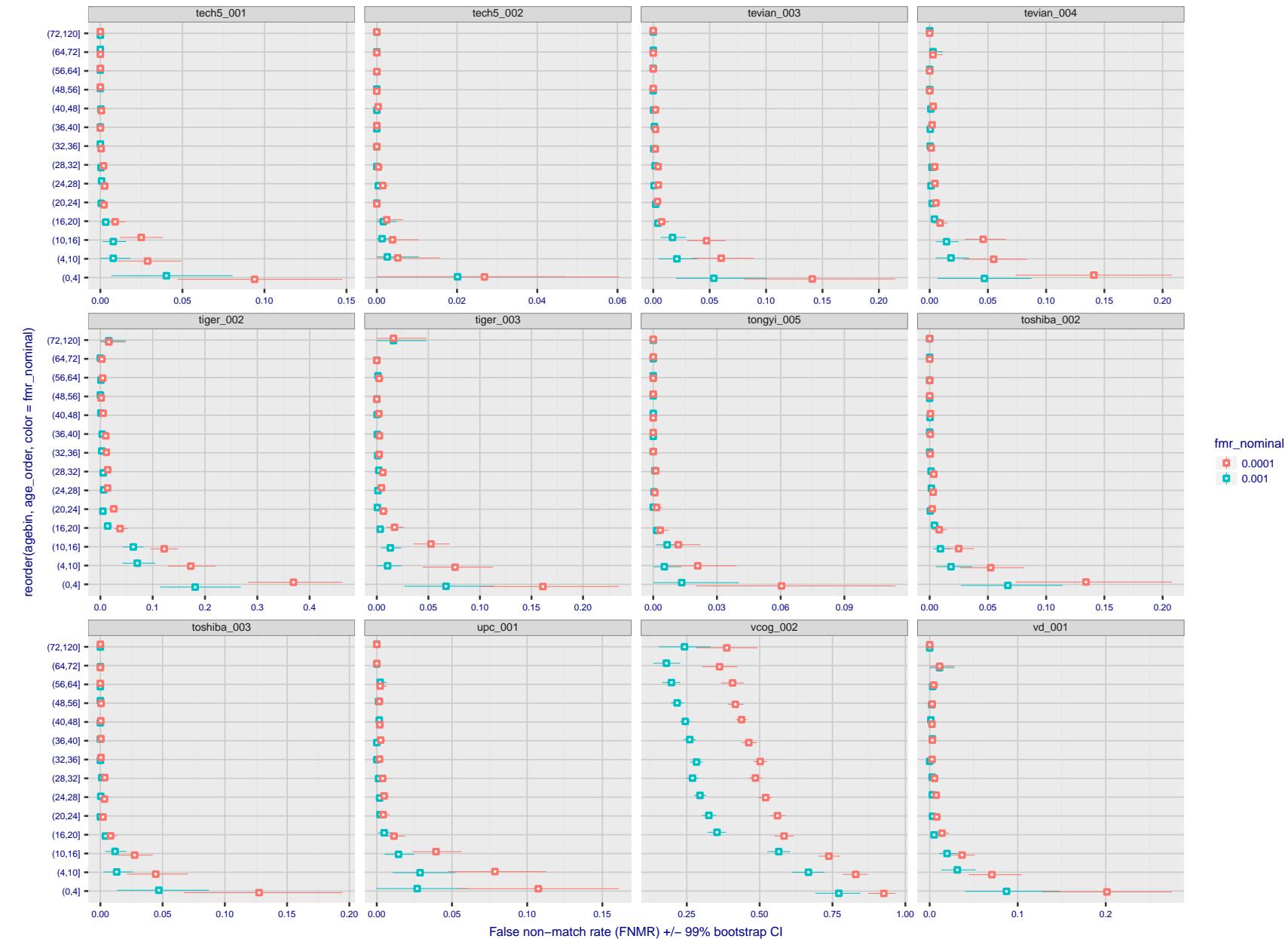


Figure 120: For the visa images, the dots show FNMR by age group for two operating thresholds corresponding to  $FMR = \{0.001, 0.0001\}$  computed over all on the order of  $10^{10}$  impostor scores. The FMR in each bin will vary also - see subsequent impostor heatmaps in sec. 3.6.2. Given a pair of face images taken at different times, we assign the comparison to the bin that is the arithmetic average of the subject's ages. This plot shows only the effect of age, not ageing. The number of comparisons in each bin is generally in the thousands, however the first and last bins are computed over 149 and 124 respectively. The error rates in some (adult) cases are zero, and in others the DET is flat so the error rates at the two thresholds are identical. The lines span 1% and 99% of bootstrap replicated FNMR estimates.

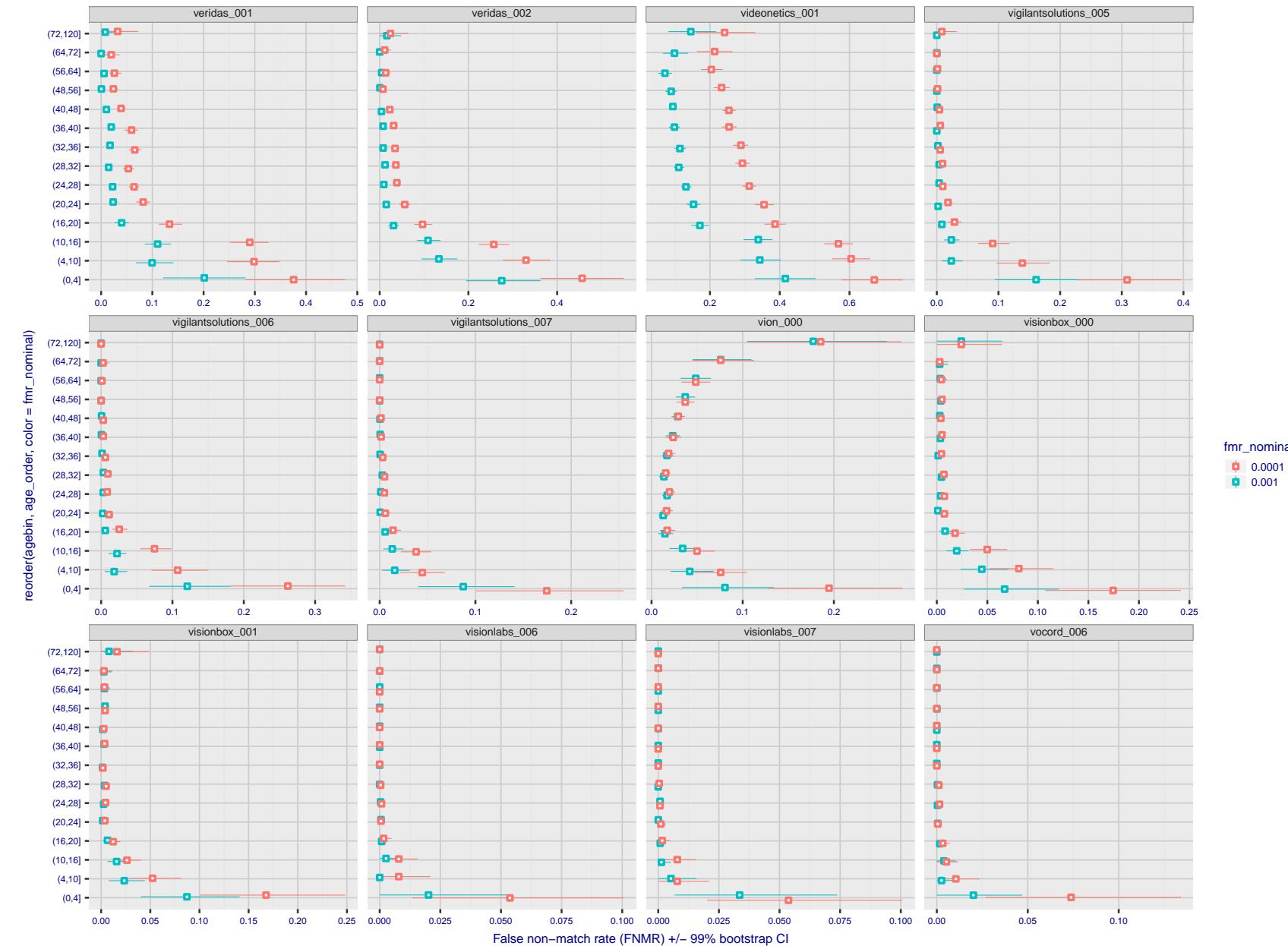


Figure 121: For the visa images, the dots show FNMR by age group for two operating thresholds corresponding to  $FMR = \{0.001, 0.0001\}$  computed over all on the order of  $10^{10}$  impostor scores. The FMR in each bin will vary also - see subsequent impostor heatmaps in sec. 3.6.2. Given a pair of face images taken at different times, we assign the comparison to the bin that is the arithmetic average of the subject's ages. This plot shows only the effect of age, not ageing. The number of comparisons in each bin is generally in the thousands, however the first and last bins are computed over 149 and 124 respectively. The error rates in some (adult) cases are zero, and in others the DET is flat so the error rates at the two thresholds are identical. The lines span 1% and 99% of bootstrap replicated FNMR estimates.

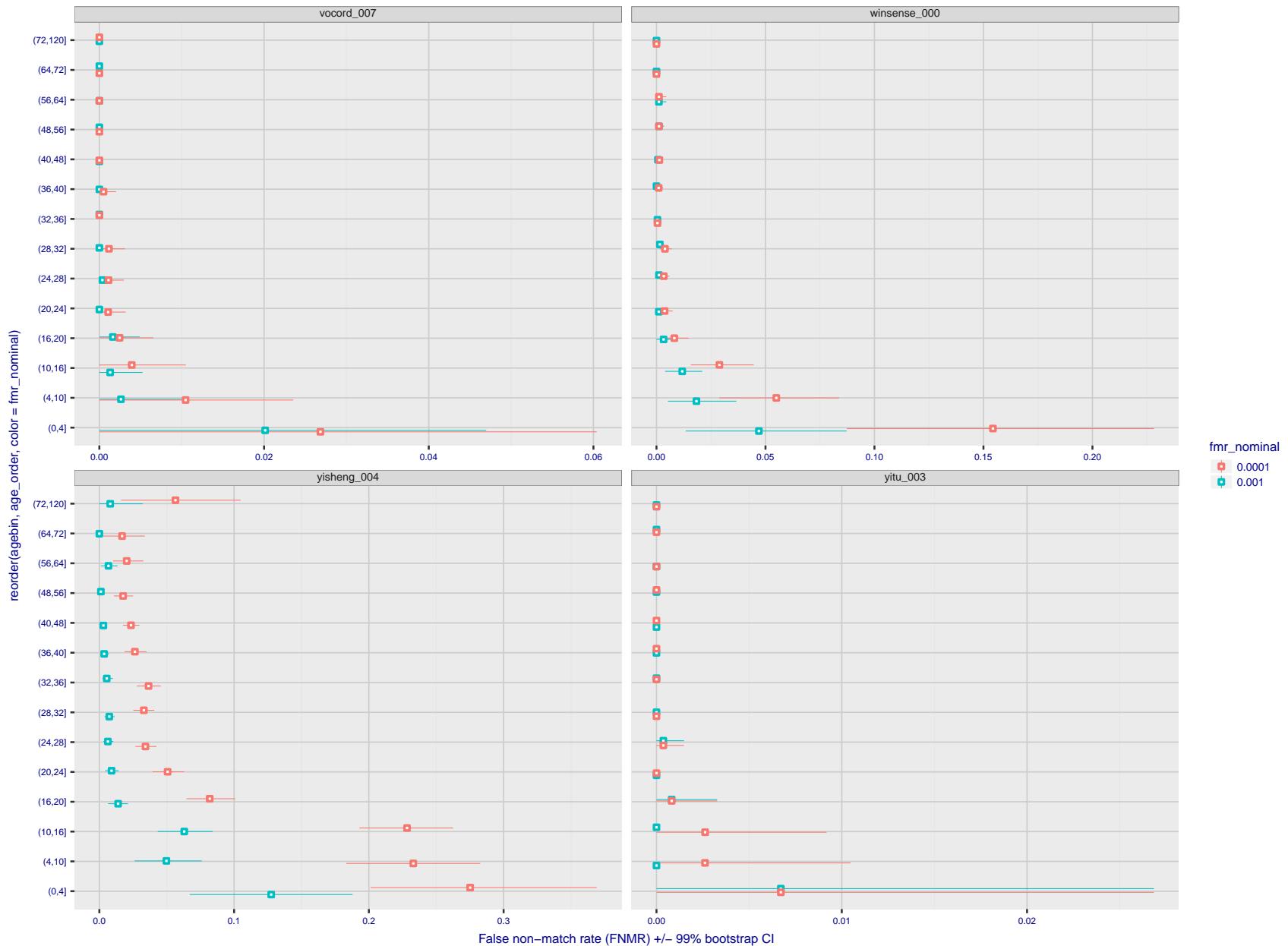


Figure 122: For the visa images, the dots show FNMR by age group for two operating thresholds corresponding to  $FMR = \{0.001, 0.0001\}$  computed over all on the order of  $10^{10}$  impostor scores. The FMR in each bin will vary also - see subsequent impostor heatmaps in sec. 3.6.2. Given a pair of face images taken at different times, we assign the comparison to the bin that is the arithmetic average of the subject's ages. This plot shows only the effect of age, not ageing. The number of comparisons in each bin is generally in the thousands, however the first and last bins are computed over 149 and 124 respectively. The error rates in some (adult) cases are zero, and in others the DET is flat so the error rates at the two thresholds are identical. The lines span 1% and 99% of bootstrap replicated FNMR estimates.

**Caveats:** None.

## 3.6 Impostor distribution stability

### 3.6.1 Effect of birth place on the impostor distribution

**Background:** Facial appearance varies geographically, both in terms of skin tone, cranio-facial structure and size. This section addresses whether false match rates vary intra- and inter-regionally.

**Goals:**

- ▷ To show the effect of birth region of the impostor and enrollee on false match rates.
- ▷ To determine whether some algorithms give better impostor distribution stability.

**Methods:**

- ▷ For the visa images, NIST defined 10 regions: Sub-Saharan Africa, South Asia, Polynesia, North Africa, Middle East, Europe, East Asia, Central and South America, Central Asia, and the Caribbean.
- ▷ For the visa images, NIST mapped each country of birth to a region. There is some arbitrariness to this. For example, Egypt could reasonably be assigned to the Middle East instead of North Africa. An alternative methodology could, for example, assign the Philippines to *both* Polynesia and East Asia.
- ▷ FMR is computed for cases where all face images of impostors born in region  $r_2$  are compared with enrolled face images of persons born in region  $r_1$ .

$$\text{FMR}(r_1, r_2, T) = \frac{\sum_{i=1}^{N_{r_1, r_2}} H(s_i - T)}{N_{r_1, r_2}} \quad (5)$$

where the same threshold,  $T$ , is used in all cells, and  $H$  is the unit step function. The threshold is set to give  $\text{FMR}(T) = 0.001$  over the entire set of visa image impostor comparisons.

- ▷ This analysis is then repeated by country-pair, but only for those country pairs where both have at least 1000 images available. The countries<sup>1</sup> appear in the axes of graphs that follow.
- ▷ The mean number of impostor scores in any cross-region bin is 33 million. The smallest number of impostor scores in any bin is 135000, for Central Asia - North Africa. While these counts are large enough to support reasonable significance, the number of individual faces is much smaller, on the order of  $N^{0.5}$ .
- ▷ The numbers of impostor scores in any cross-country bin is shown in Figure 350.

**Results:** Subsequent figures show heatmaps that use color to represent the base-10 logarithm of the false match rate. Red colors indicate high (bad) false match rates. Dark colors indicate benign false match rates. There are two series of graphs corresponding to aggregated geographical regions, and to countries. The notable observations are:

- ▷ The on-diagonal elements correspond to within-region impostors. FMR is generally above the nominal value of  $\text{FMR} = 0.001$ . Particularly there is usually higher FMR in, Sub-Saharan Africa, South Asia, and the Caribbean. Europe and Central Asia, on the other hand, usually give FMR closer to the nominal value.
- ▷ The off-diagonal elements correspond to across-region impostors. The highest FMR is produced between the Caribbean and Sub-Saharan Africa.
- ▷ Algorithms vary.

<sup>1</sup>These are Argentina, Australia, Brazil, Chile, China, Costa Rica, Cuba, Czech Republic, Dominican Republic, Ecuador, Egypt, El Salvador, Germany, Ghana, Great Britain, Greece, Guatemala, Haiti, Hong Kong, Honduras, Indonesia, India, Israel, Jamaica, Japan, Kenya, Korea, Lebanon, Mexico, Malaysia, Nepal, Nigeria, Peru, Philippines, Pakistan, Poland, Romania, Russia, South Africa, Saudi Arabia, Thailand, Trinidad, Turkey, Taiwan, Ukraine, Venezuela, and Vietnam.

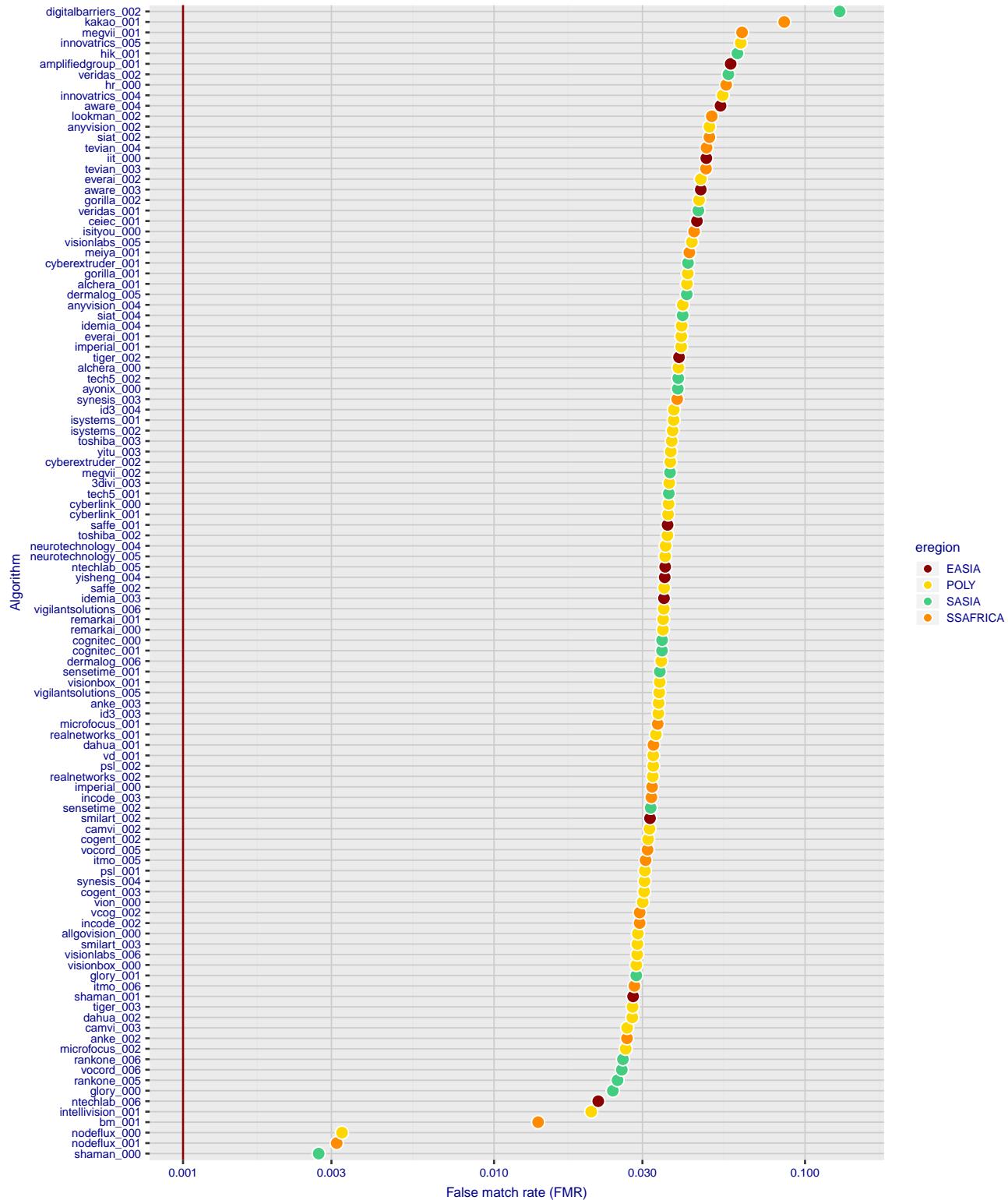


Figure 123: For the visa images, the dots show FMR for impostor comparisons of individuals of the same sex and same age group for the region of the world that gives the worst (highest) FMR when the threshold is set to give  $FMR = 0.001$  (red vertical line) over all on the order of  $10^{10}$  impostor scores i.e. zero-effort. The shift of the dots to right shows massive increases in FMR when impostors have the same sex, age, and region of birth. The color code indicates which region gives the worst case FMR. If the observed variation is due to the prevalence of one kind of images in the training imagery, then algorithms developed on one kind of data might be expected to give higher FMR on other kinds.

- ▷ We computed the same quantities for a global FMR = 0.0001. The effects are similar.

**Caveats:**

- ▷ The effects of variable impostor rates on one-to-many identification systems may well differ from what's implied by these one-to-one verification results. Two reasons for this are a) the enrollment galleries are usually imbalanced across countries of birth, age and sex; b) one-to-many identification algorithms often implement techniques aimed at stabilizing the impostor distribution. Further research is necessary.
- ▷ In principle, the effects seen in this subsection could be due to differences in the image capture process. We consider this unlikely since the effects are maintained across geography - e.g. Caribbean vs. Africa, or Japan vs. China.

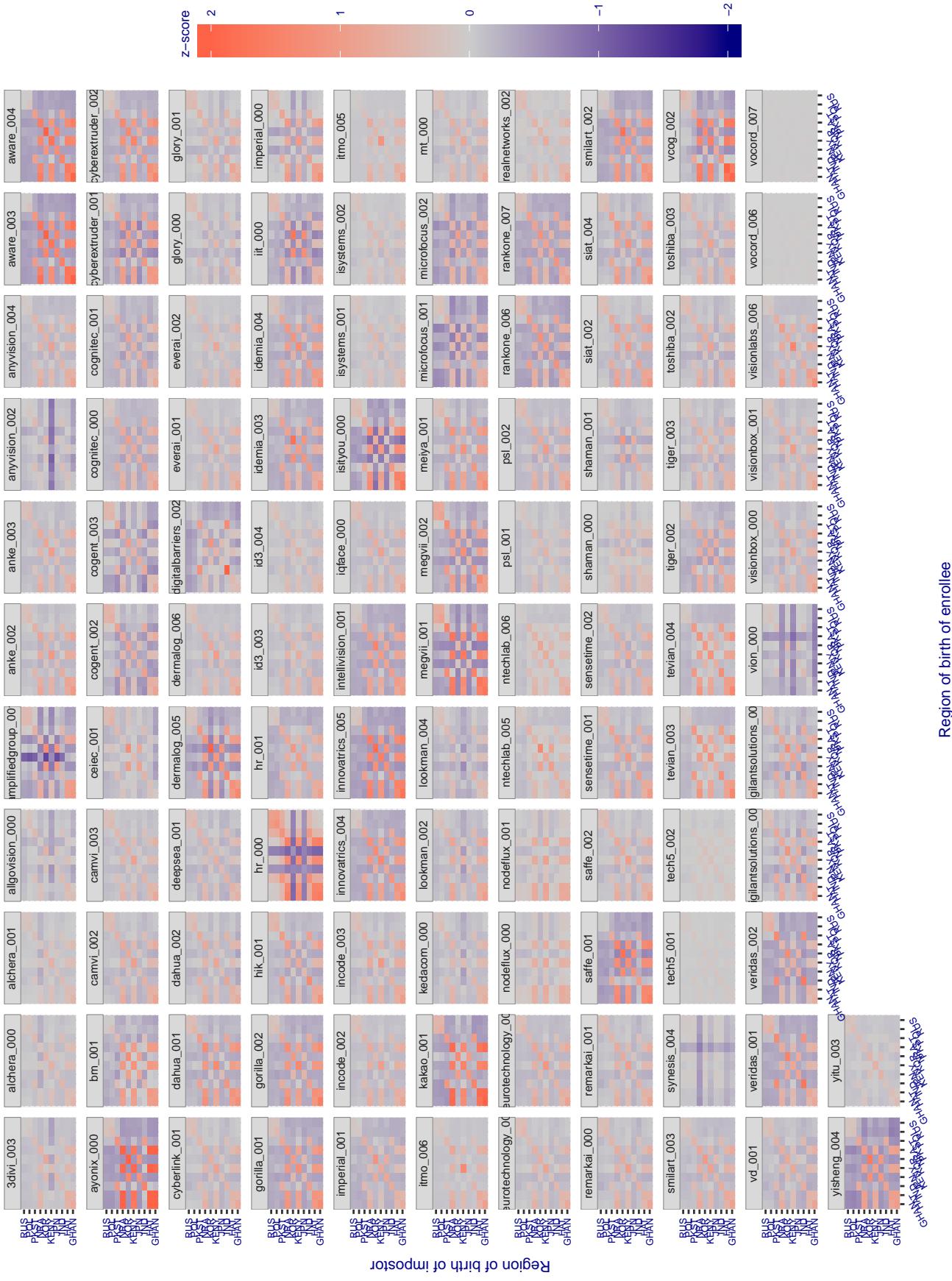


Figure 124: For visa images, the heatmap shows how the mean of the impostor distribution for the country pair (a,b) is shifted relative to the mean of the global impostor distribution, expressed as a number of standard deviations of the global impostor distribution. This statistic is designed to show shifts in the entire impostor distribution, not just tail effects that manifest as the anomalously high (or low) false match rates that appear in the subsequent figures. The countries are chosen to show that skin tone alone does not explain impostor distribution shifts. The reduced shift in Asian populations with the Yitu and Tong YiTrans algorithms, is accompanied by positive shifts in the European populations. This reversal relative to most other algorithms, may derive from use of nationally weighted training sets. The Visionlabs algorithm appears most insensitive to country effects. The figure is computed from same-sex and same-age impostor pairs.

### Cross region FMR at threshold T = 2.740 for algorithm 3divi\_003, giving FMR(T) = 0.0001 globally.

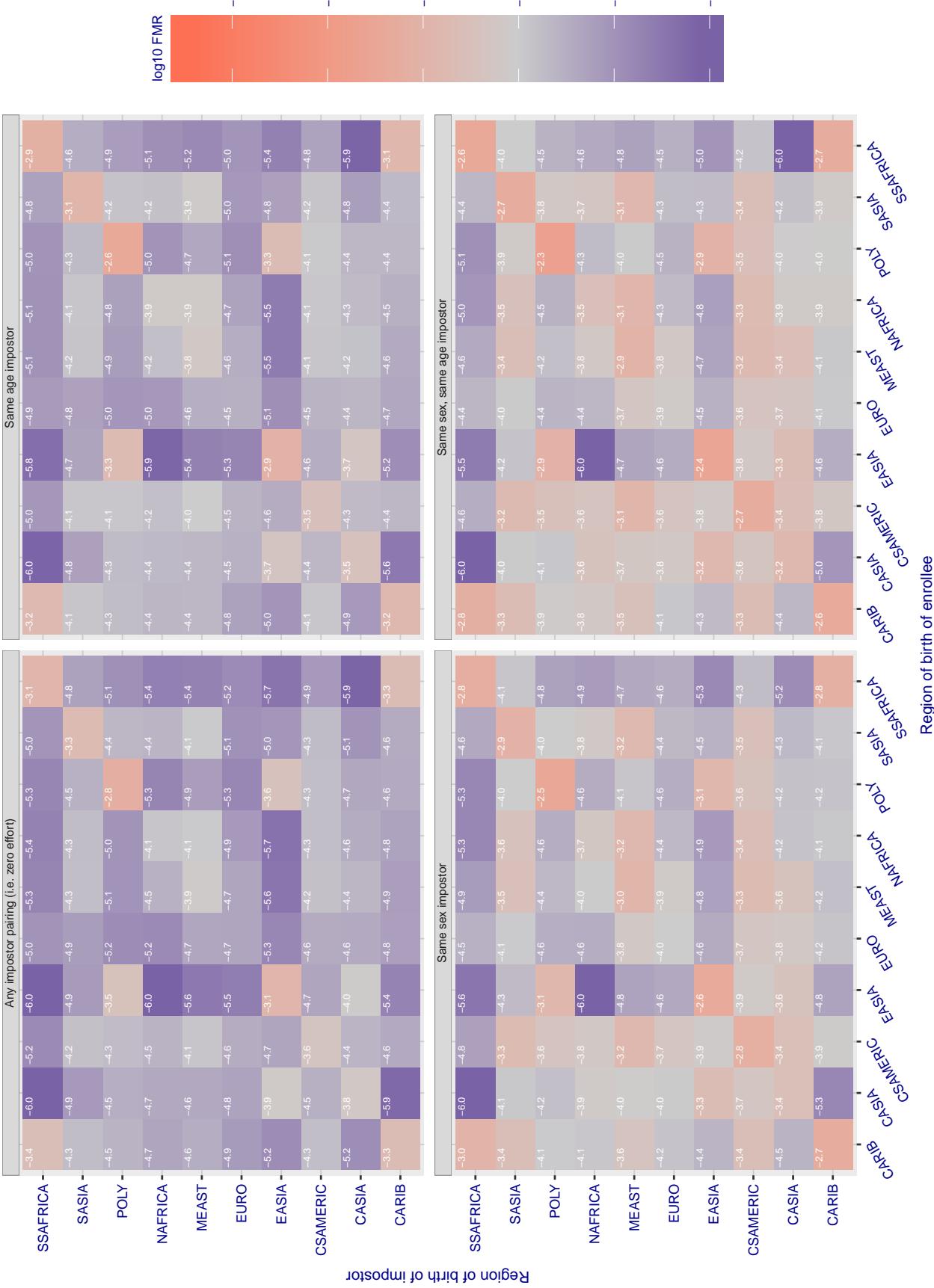


Figure 125: For algorithm 3divi-003 operating on visa images, the heatmap shows false match rates observed over impostor comparisons of faces from different individuals who were born in the given region pair. False matches are counted against a recognition threshold fixed globally to give the target FMR in the plot title, computed over all on the order of  $10^{10}$  impostor comparisons. If text appears in each box it give the same quantity as that coded by the color. Grey indicates FMR is at the intended FMR target level. Light red colors present a security vulnerability to, for example, a passport gate. Each +1 increase in  $\log_{10}$  FMR corresponds to a factor of 10 increase in FMR. The matrix is not quite symmetric because images in the enrollment and verification sets are different.

### Cross region FMR at threshold T = 0.713 for algorithm adera\_001, giving FMR(T) = 0.0001 globally.

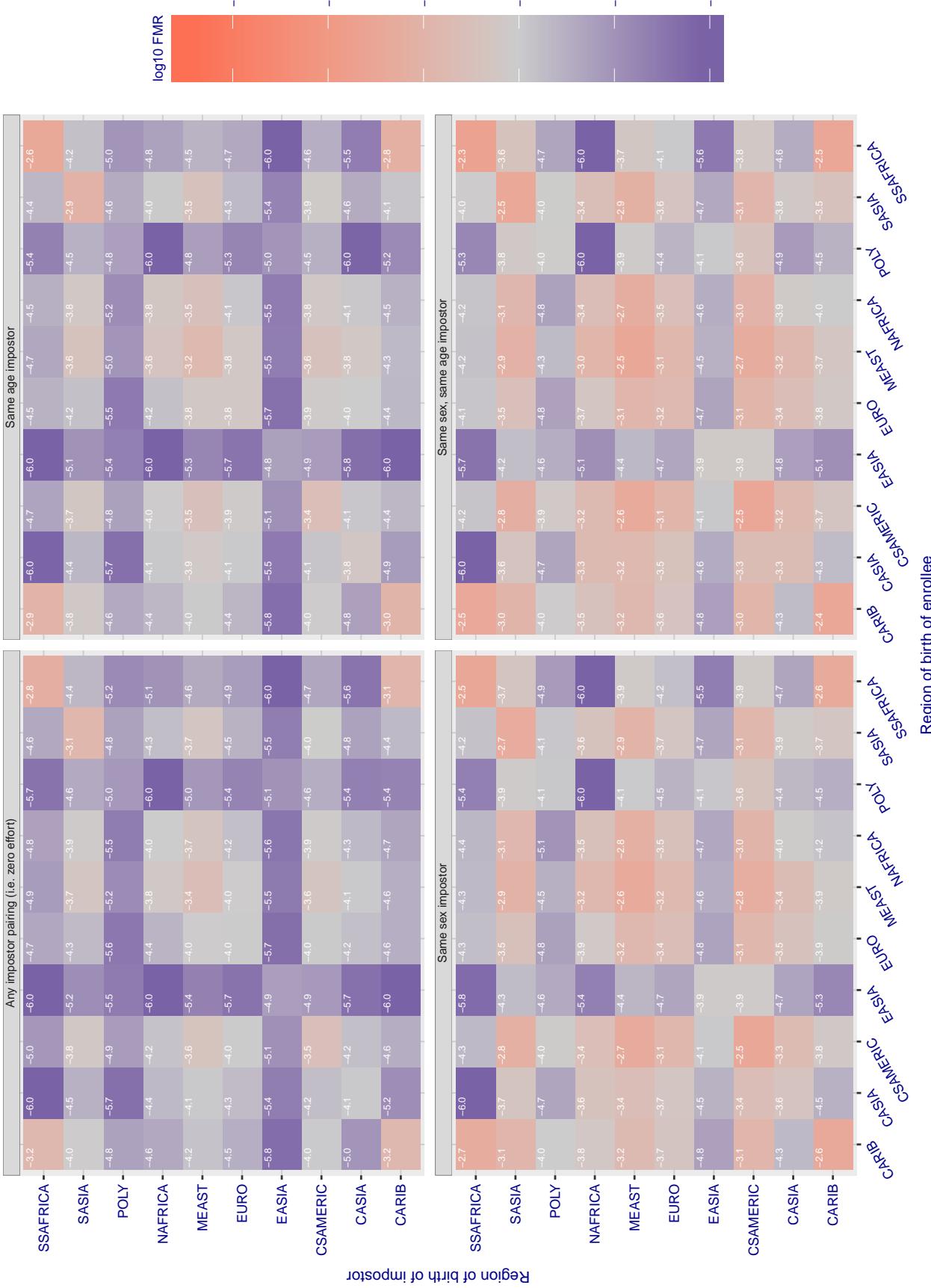


Figure 126: For algorithm adera-001 operating on visa images, the heatmap shows false match rates observed over impostor comparisons of faces from different individuals who were born in the given region pair. False matches are counted against a recognition threshold fixed globally to give the target FMR in the plot title, computed over all on the order of  $10^{10}$  impostor comparisons. If text appears in each box it give the same quantity as that coded by the color. Grey indicates FMR is at the intended FMR target level. Light red colors present a security vulnerability to, for example, a passport gate. Each +1 increase in  $\log_{10} \text{FMR}$  corresponds to a factor of 10 increase in FMR. The matrix is not quite symmetric because images in the enrollment and verification sets are different.

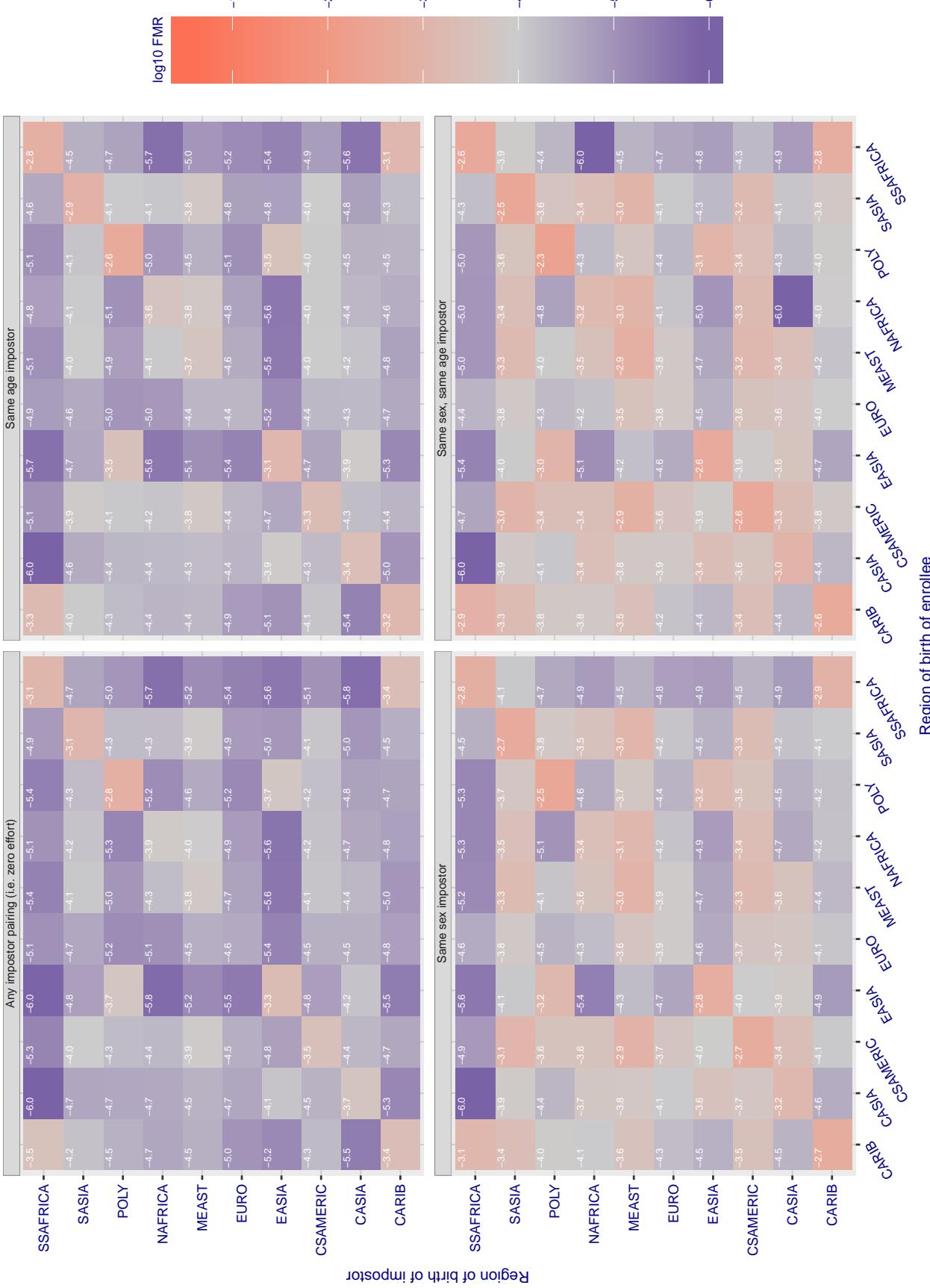
**Cross region FMR at threshold T = 0.702 for algorithm alchera\_000, giving FMR(T) = 0.0001 globally.**

Figure 127: For algorithm alchera-000 operating on visa images, the heatmap shows false match rates observed over impostor comparisons of faces from different individuals who were born in the given region pair. False matches are counted against a recognition threshold fixed globally to give the target FMR in the plot title, computed over all on the order of  $10^{10}$  impostor comparisons. If text appears in each box it give the same quantity as that coded by the color. Grey indicates FMR is at the intended FMR target level. Light red colors present a security vulnerability to, for example, a passport gate. Each +1 increase in  $\log_{10} \text{FMR}$  corresponds to a factor of 10 increase in FMR. The matrix is not quite symmetric because images in the enrollment and verification sets are different.

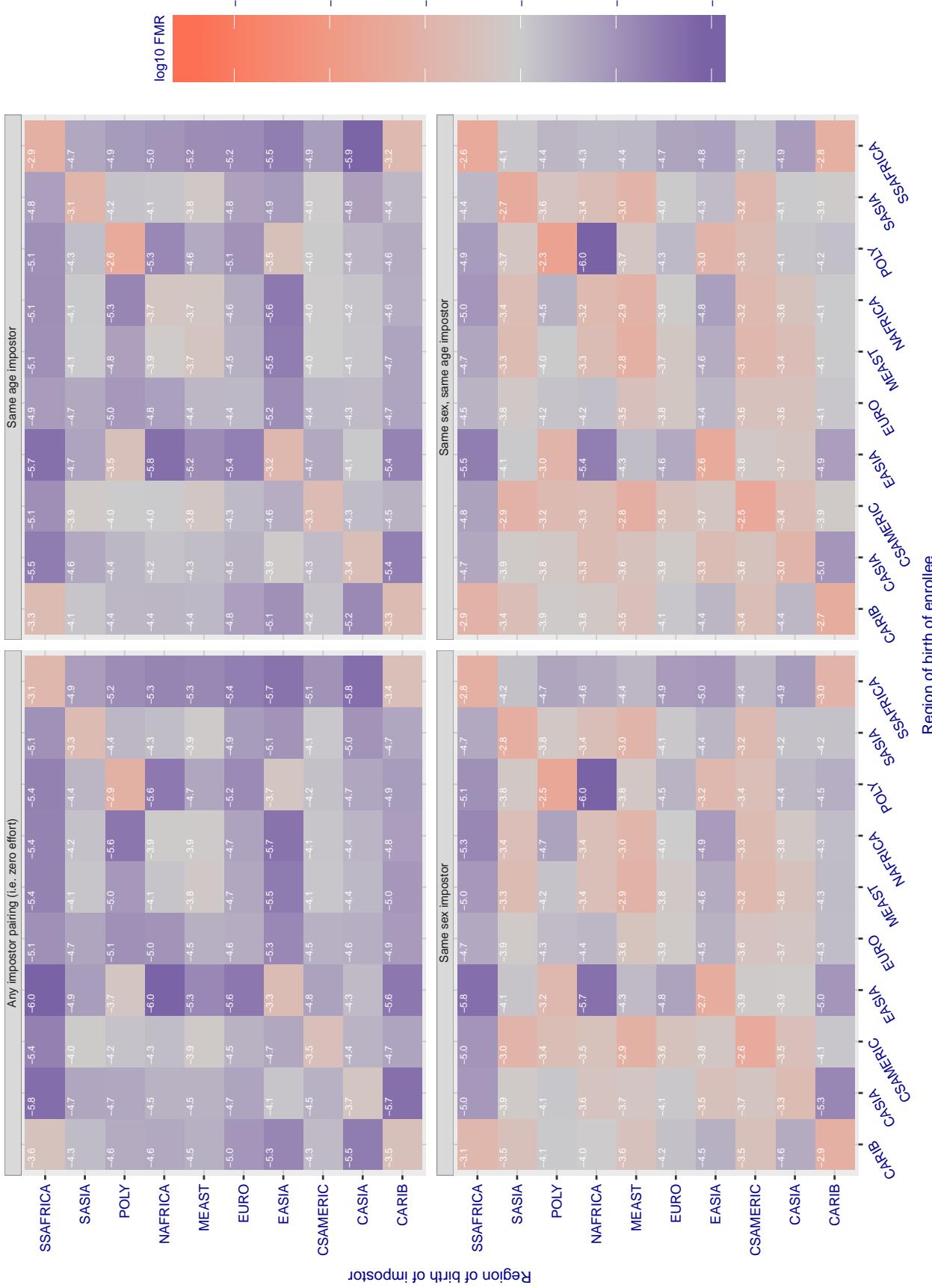
**Cross region FMR at threshold T = 0.713 for algorithm alchera\_001, giving FMR(T) = 0.0001 globally.**

Figure 128: For algorithm alchera-001 operating on visa images, the heatmap shows false match rates observed over impostor comparisons of faces from different individuals who were born in the given region pair. False matches are counted against a recognition threshold fixed globally to give the target FMR in the plot title, computed over all on the order of  $10^{10}$  impostor comparisons. If text appears in each box it give the same quantity as that coded by the color. Grey indicates FMR is at the intended FMR target level. Light red colors present a security vulnerability to, for example, a passport gate. Each +1 increase in  $\log_{10} FMR$  corresponds to a factor of 10 increase in FMR. The matrix is not quite symmetric because images in the enrollment and verification sets are different.

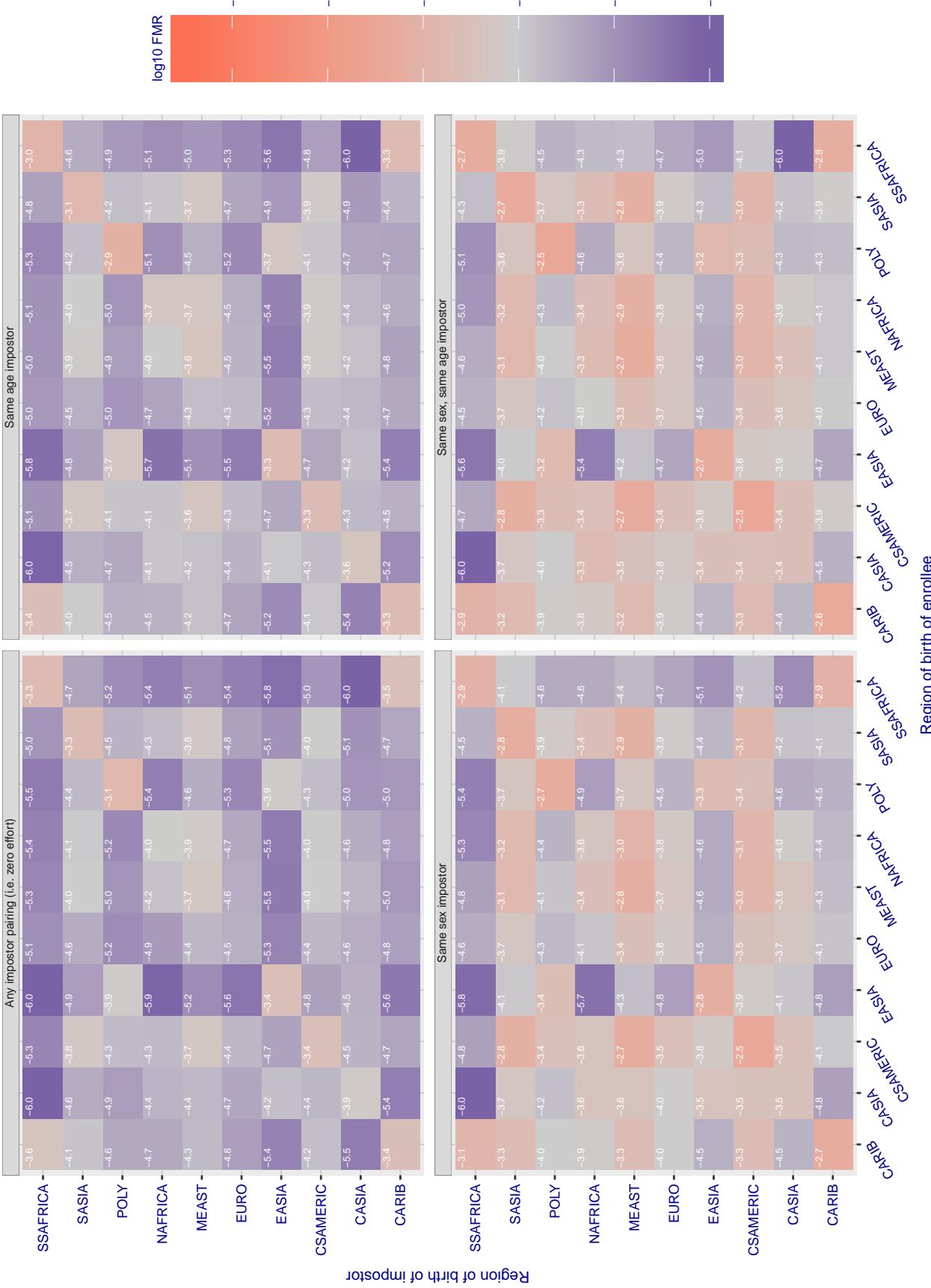
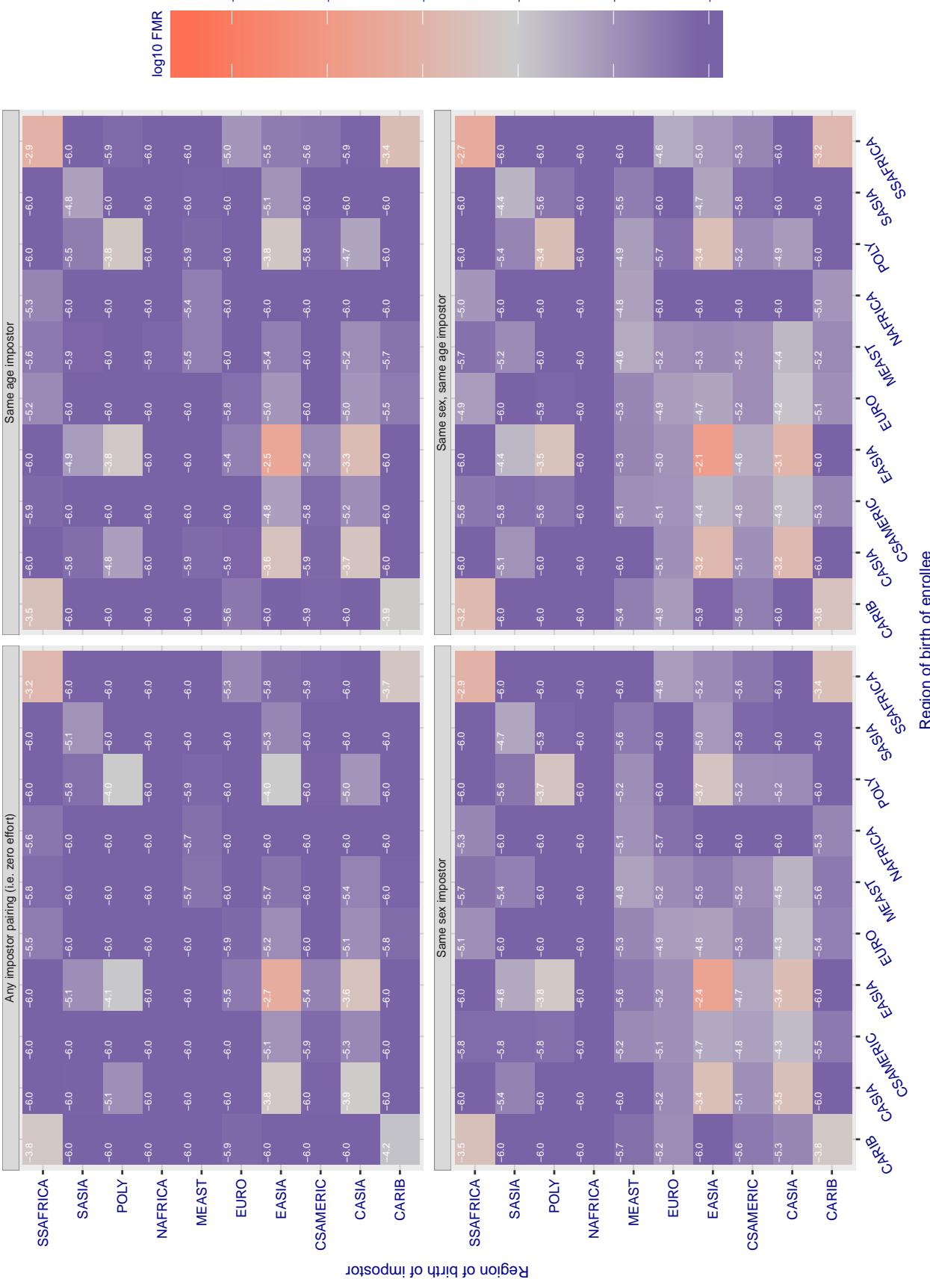
**Cross region FMR at threshold T = 0.433 for algorithm allgovision\_000, giving FMR(T) = 0.0001 globally.**

Figure 129: For algorithm allgovision-000 operating on visa images, the heatmap shows false match rates observed over impostor comparisons of faces from different individuals who were born in the given region pair. False matches are counted against a recognition threshold fixed globally to give the target FMR in the plot title, computed over all on the order of  $10^{10}$  impostor comparisons. If text appears in each box it give the same quantity as that coded by the color. Grey indicates FMR is at the intended FMR target level. Light red colors present a security vulnerability to, for example, a passport gate. Each +1 increase in  $\log_{10} FMR$  corresponds to a factor of 10 increase in FMR. The matrix is not quite symmetric because images in the enrollment and verification sets are different.

### Cross region FMR at threshold T = 3.640 for algorithm amplifiedgroup\_001, giving FMR(T) = 0.0001 globally.



FNMR(T)  
FMR(T) "False non-match rate"  
"False match rate"

Figure 130: For algorithm amplifiedgroup-001 operating on visa images, the heatmap shows false match rates observed over impostor comparisons of faces from different individuals who were born in the given region pair. False matches are counted against a recognition threshold fixed globally to give the target FMR in the plot title, computed over all on the order of  $10^{10}$  impostor comparisons. If text appears in each box it give the same quantity as that coded by the color. Grey indicates FMR is at the intended FMR target level. Light red colors present a security vulnerability to, for example, a passport gate. Each +1 increase in  $\log_{10}$  FMR corresponds to a factor of 10 increase in FMR. The matrix is not quite symmetric because images in the enrollment and verification sets are different.

### Cross region FMR at threshold T = 0.397 for algorithm anke\_003, giving FMR(T) = 0.0001 globally.

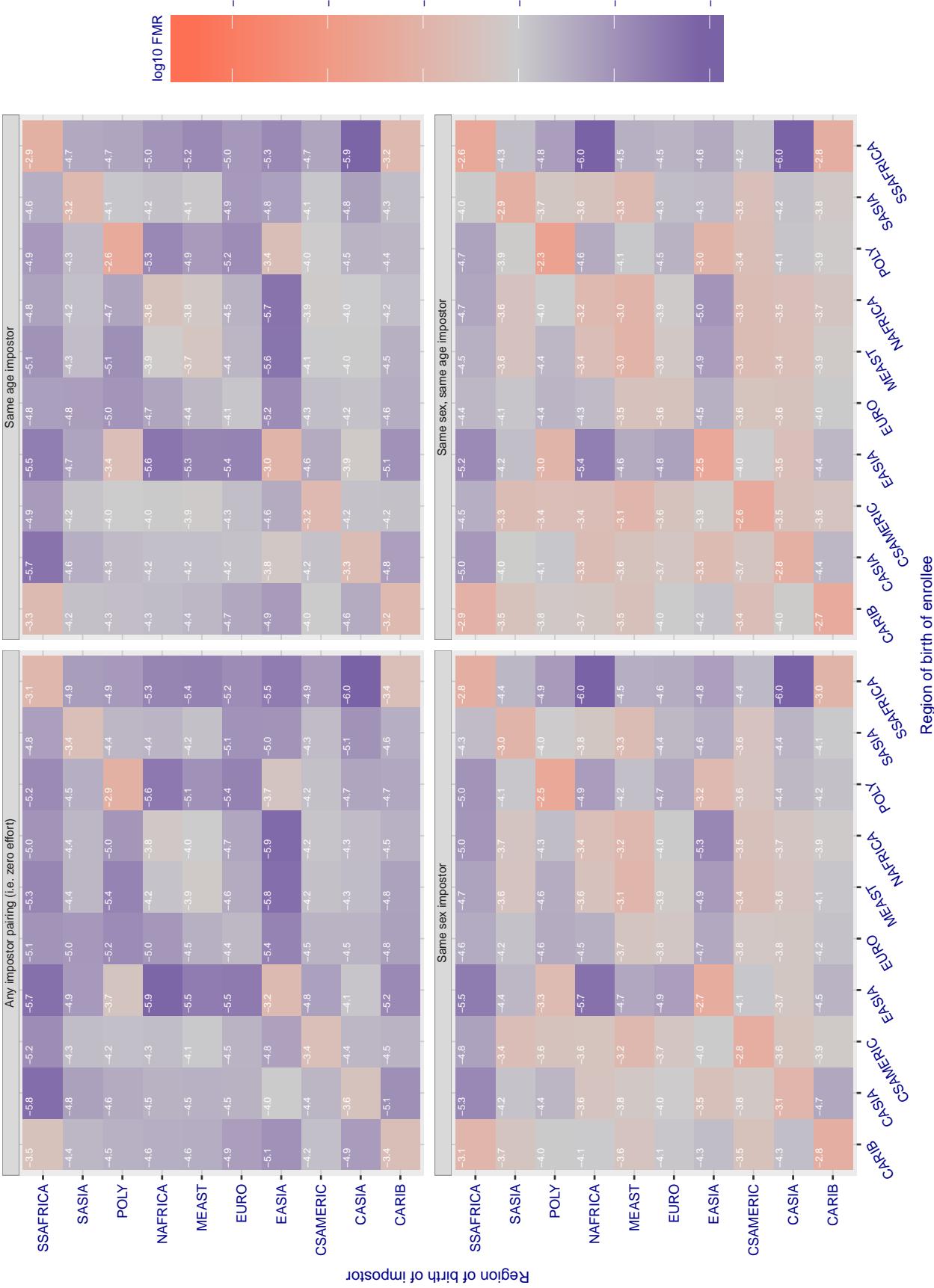


Figure 131: For algorithm anke-003 operating on visa images, the heatmap shows false match rates observed over impostor comparisons of faces from different individuals who were born in the given region pair. False matches are counted against a recognition threshold fixed globally to give the target FMR in the plot title, computed over all on the order of  $10^{10}$  impostor comparisons. If text appears in each box it give the same quantity as that coded by the color. Grey indicates FMR is at the intended FMR target level. Light red colors present a security vulnerability to, for example, a passport gate. Each +1 increase in  $\log 10$  FMR corresponds to a factor of 10 increase in FMR. The matrix is not quite symmetric because images in the enrollment and verification sets are different.

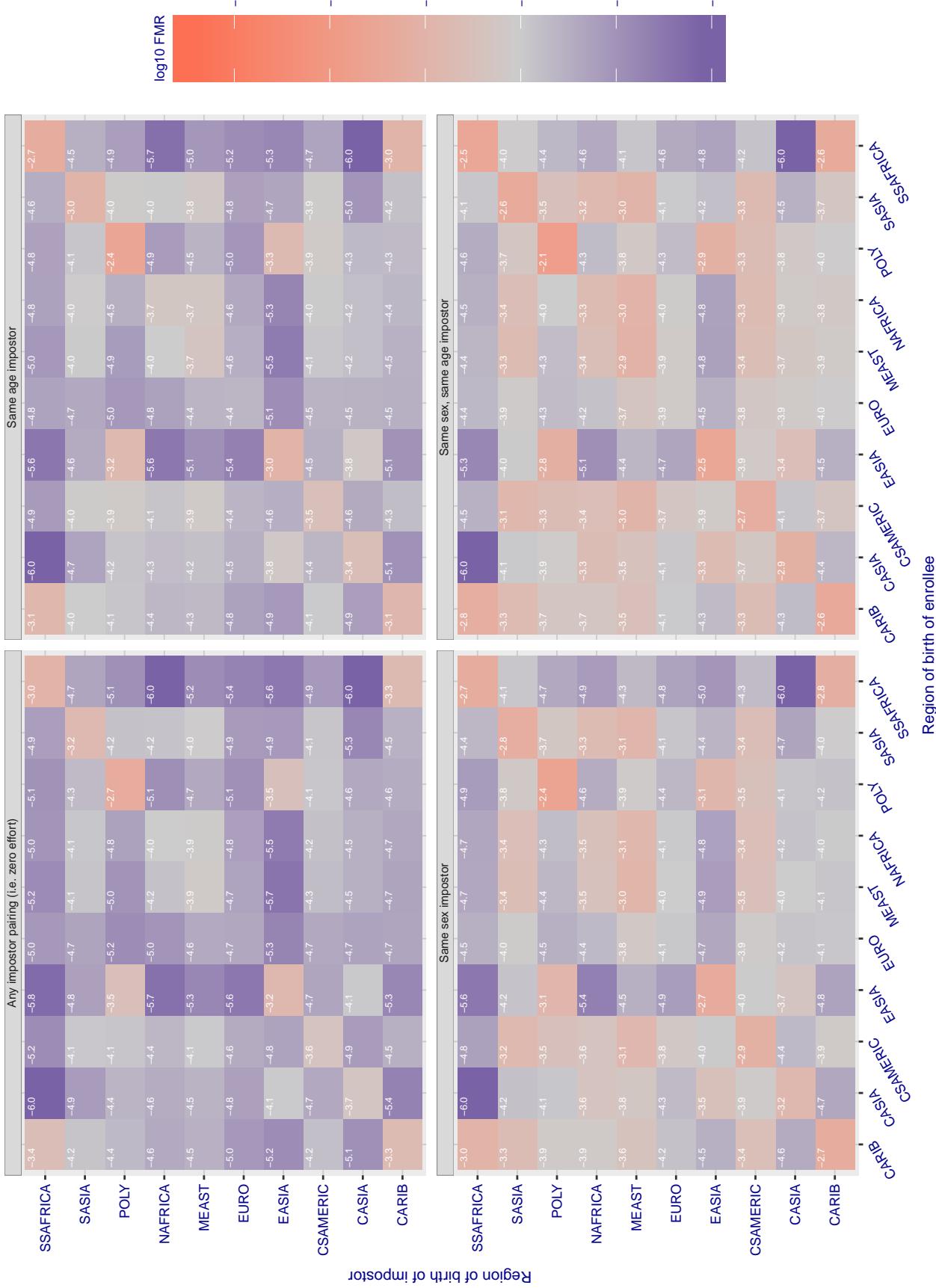
**Cross region FMR at threshold T = 1.526 for algorithm anyvision\_002, giving FMR(T) = 0.0001 globally.**

Figure 132: For algorithm anyvision-002 operating on visa images, the heatmap shows false match rates observed over impostor comparisons of faces from different individuals who were born in the given region pair. False matches are counted against a recognition threshold fixed globally to give the target FMR in the plot title, computed over all on the order of  $10^{10}$  impostor comparisons. If text appears in each box it give the same quantity as that coded by the color. Grey indicates FMR is at the intended FMR target level. Light red colors present a security vulnerability to, for example, a passport gate. Each +1 increase in  $\log_{10} \text{FMR}$  corresponds to a factor of 10 increase in FMR. The matrix is not quite symmetric because images in the enrollment and verification sets are different.

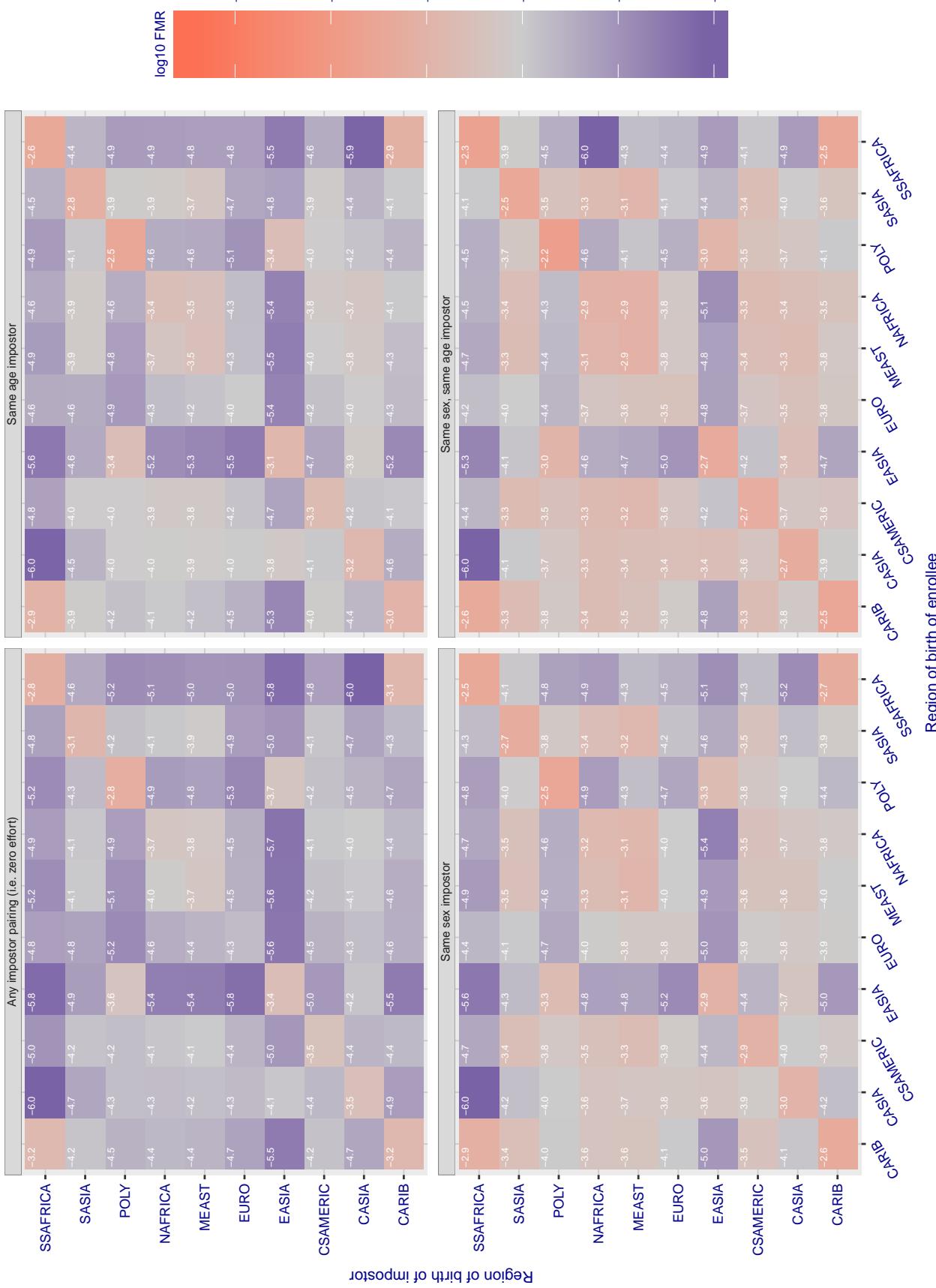
**Cross region FMR at threshold T = 1.375 for algorithm anyvision\_004, giving FMR(T) = 0.0001 globally.**

Figure 133: For algorithm anyvision-004 operating on visa images, the heatmap shows false match rates observed over impostor comparisons of faces from different individuals who were born in the given region pair. False matches are counted against a recognition threshold fixed globally to give the target FMR in the plot title, computed over all on the order of  $10^{10}$  impostor comparisons. If text appears in each box it give the same quantity as that coded by the color. Grey indicates FMR is at the intended FMR target level. Light red colors present a security vulnerability to, for example, a passport gate. Each +1 increase in  $\log_{10} \text{FMR}$  corresponds to a factor of 10 increase in FMR. The matrix is not quite symmetric because images in the enrollment and verification sets are different.

### Cross region FMR at threshold T = 3.868 for algorithm aware\_003, giving FMR(T) = 0.0001 globally.

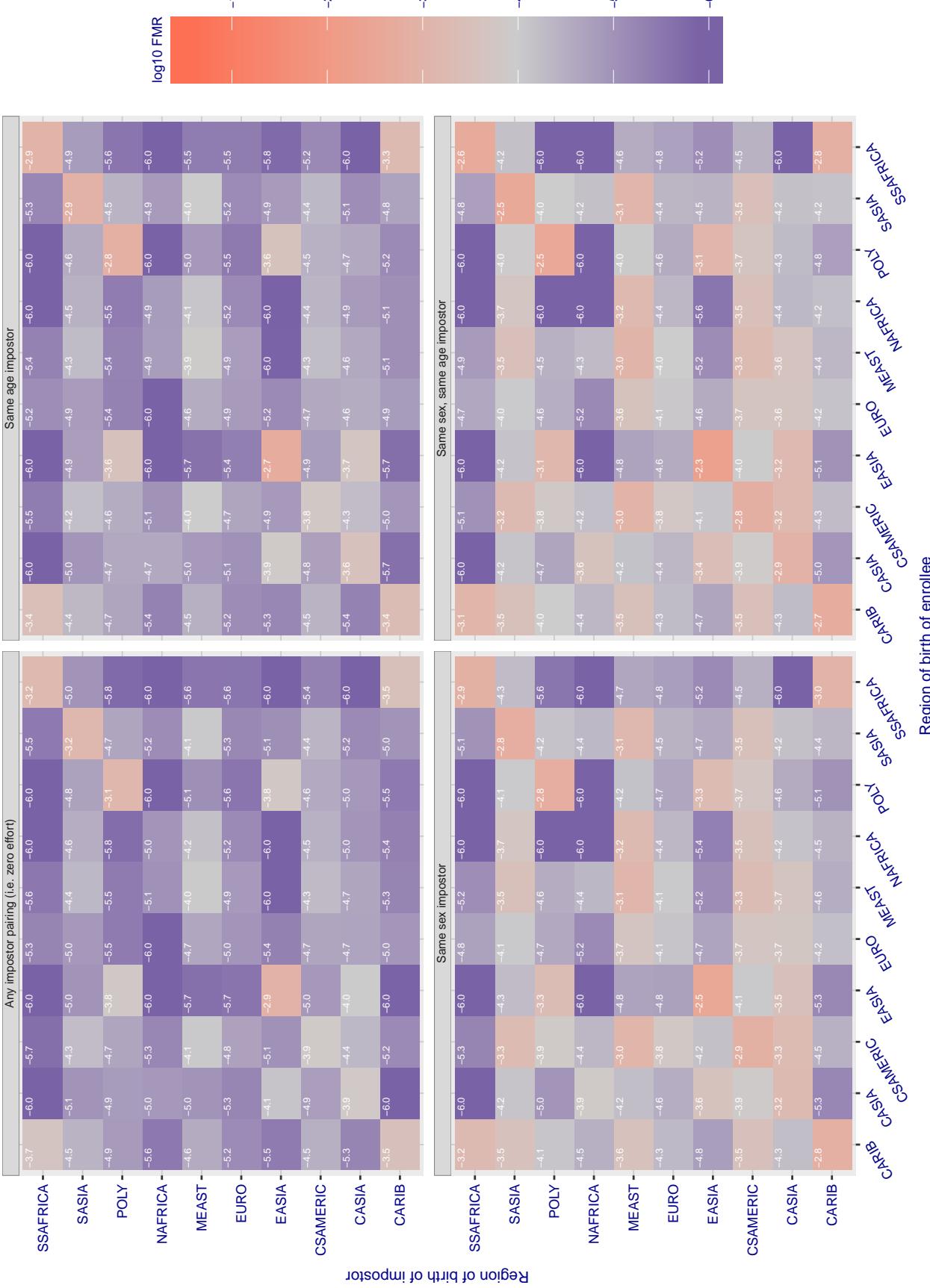


Figure 134: For algorithm aware-003 operating on visa images, the heatmap shows false match rates observed over impostor comparisons of faces from different individuals who were born in the given region pair. False matches are counted against a recognition threshold fixed globally to give the target FMR in the plot title, computed over all on the order of  $10^{10}$  impostor comparisons. If text appears in each box it give the same quantity as that coded by the color. Grey indicates FMR is at the intended FMR target level. Light red colors present a security vulnerability to, for example, a passport gate. Each +1 increase in  $\log_{10} FMR$  corresponds to a factor of 10 increase in FMR. The matrix is not quite symmetric because images in the enrollment and verification sets are different.

### Cross region FMR at threshold T = 5.084 for algorithm aware\_004, giving FMR(T) = 0.0001 globally.

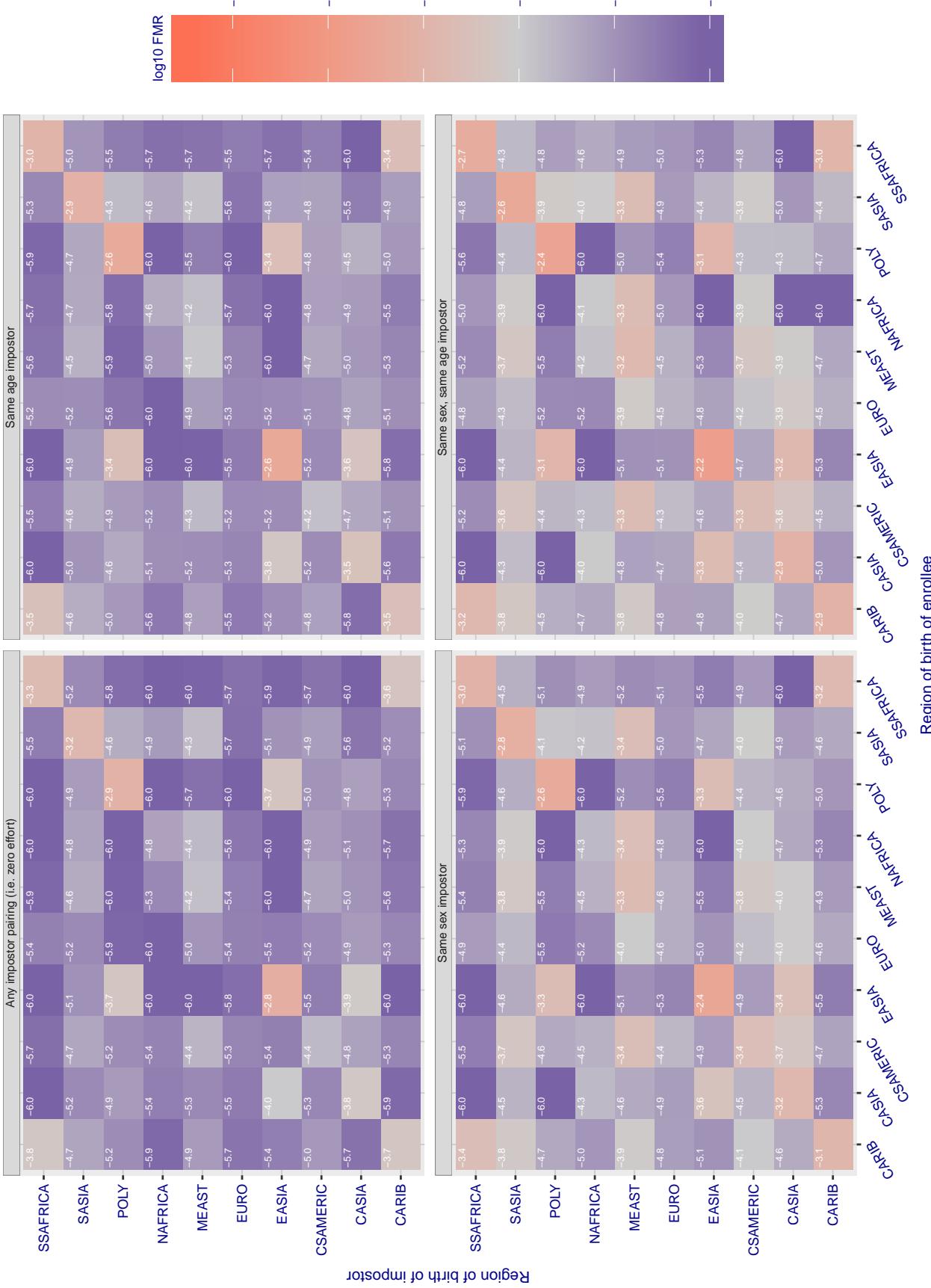


Figure 135: For algorithm aware-004 operating on visa images, the heatmap shows false match rates observed over impostor comparisons of faces from different individuals who were born in the given region pair. False matches are counted against a recognition threshold fixed globally to give the target FMR in the plot title, computed over all on the order of  $10^{10}$  impostor comparisons. If text appears in each box it give the same quantity as that coded by the color. Grey indicates FMR is at the intended FMR target level. Light red colors present a security vulnerability to, for example, a passport gate. Each +1 increase in  $\log_{10} \text{FMR}$  corresponds to a factor of 10 increase in FMR. The matrix is not quite symmetric because images in the enrollment and verification sets are different.

### Cross region FMR at threshold T = 0.919 for algorithm ayonix\_000, giving FMR(T) = 0.0001 globally.

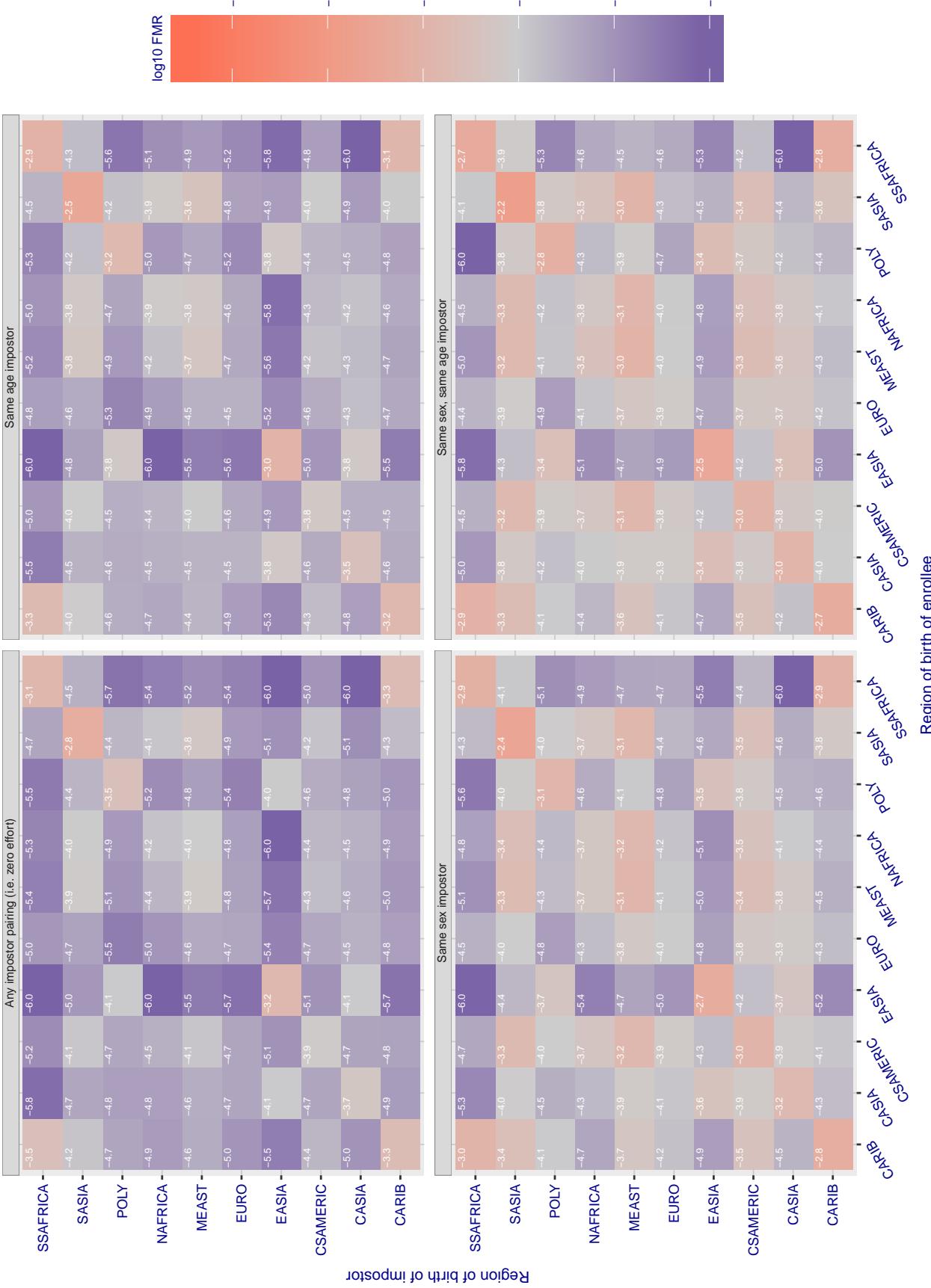


Figure 136: For algorithm ayonix-000 operating on visa images, the heatmap shows false match rates observed over impostor comparisons of faces from different individuals who were born in the given region pair. False matches are counted against a recognition threshold fixed globally to give the target FMR in the plot title, computed over all on the order of  $10^{10}$  impostor comparisons. If text appears in each box it give the same quantity as that coded by the color. Grey indicates FMR is at the intended FMR target level. Light red colors present a security vulnerability to, for example, a passport gate. Each +1 increase in  $\log_{10} FMR$  corresponds to a factor of 10 increase in FMR. The matrix is not quite symmetric because images in the enrollment and verification sets are different.

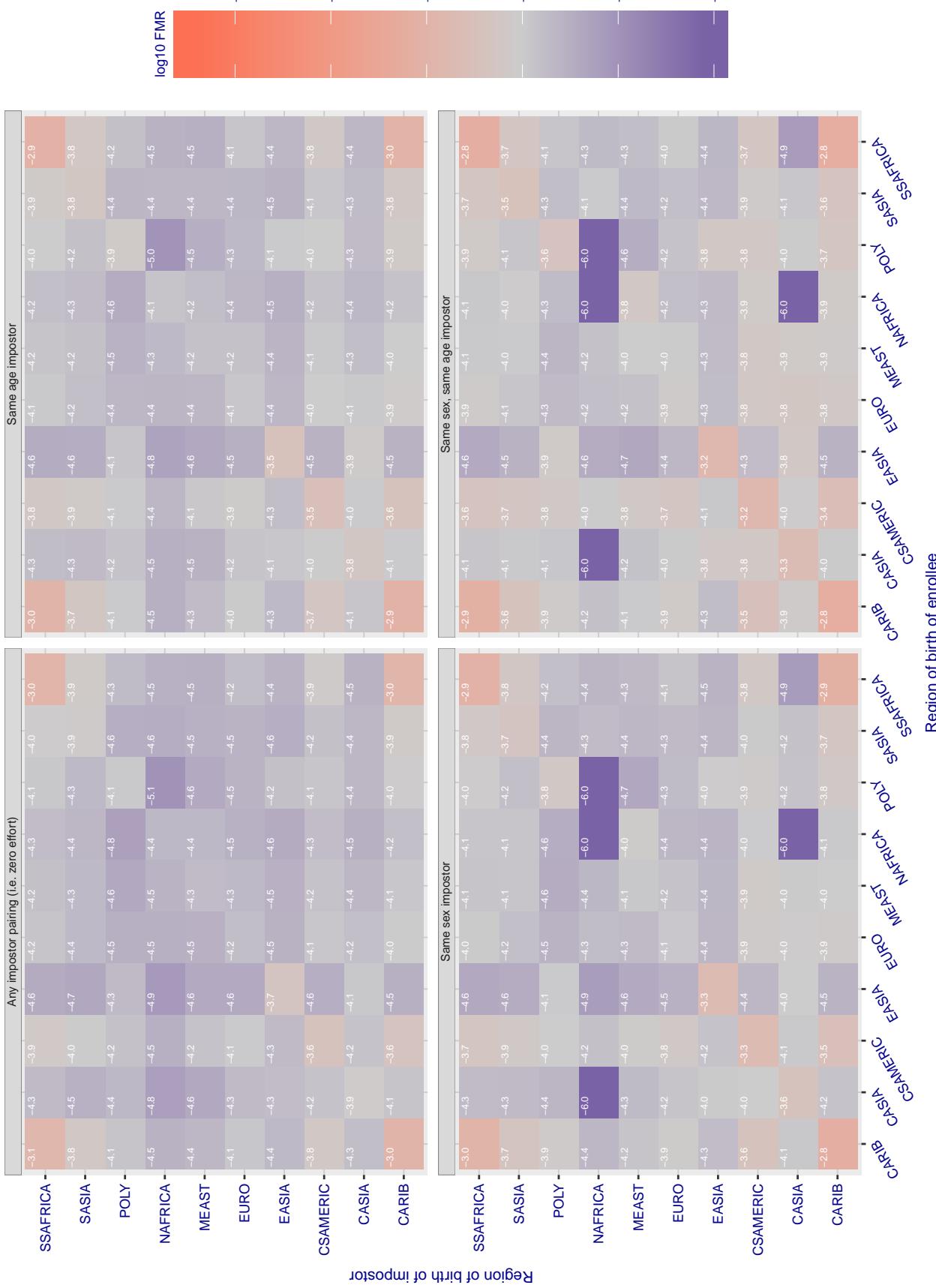


Figure 137: For algorithm *bm-001* operating on visa images, the heatmap shows false match rates observed over impostor comparisons of faces from different individuals who were born in the given region pair. False matches are counted against a recognition threshold fixed globally to give the target *FMR* in the plot title, computed over all on the order of  $10^{10}$  impostor comparisons. If text appears in each box it give the same quantity as that coded by the color. Grey indicates *FMR* is at the intended *FMR* target level. Light red colors present a security vulnerability to, for example, a passport gate. Each +1 increase in  $\log_{10} FMR$  corresponds to a factor of 10 increase in *FMR*. The matrix is not quite symmetric because images in the enrollment and verification sets are different.

### Cross region FMR at threshold T = 0.388 for algorithm camvi\_002, giving FMR(T) = 0.0001 globally.

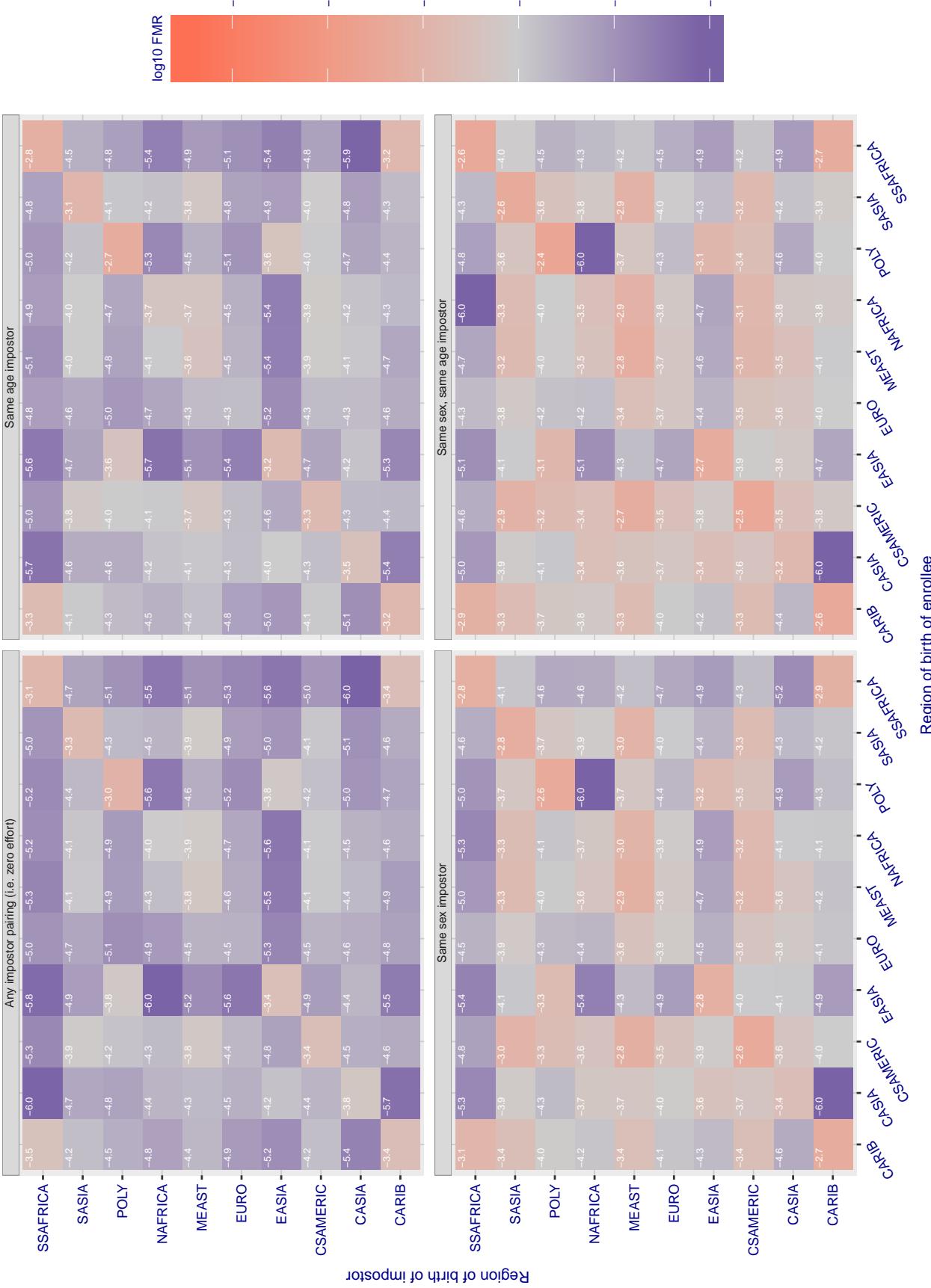


Figure 138: For algorithm camvi-002 operating on visa images, the heatmap shows false match rates observed over impostor comparisons of faces from different individuals who were born in the given region pair. False matches are counted against a recognition threshold fixed globally to give the target FMR in the plot title, computed over all on the order of  $10^{10}$  impostor comparisons. If text appears in each box it give the same quantity as that coded by the color. Grey indicates FMR is at the intended FMR target level. Light red colors present a security vulnerability to, for example, a passport gate. Each +1 increase in  $\log_{10} \text{FMR}$  corresponds to a factor of 10 increase in FMR. The matrix is not quite symmetric because images in the enrollment and verification sets are different.

### Cross region FMR at threshold T = 0.383 for algorithm camvi\_003, giving FMR(T) = 0.0001 globally.

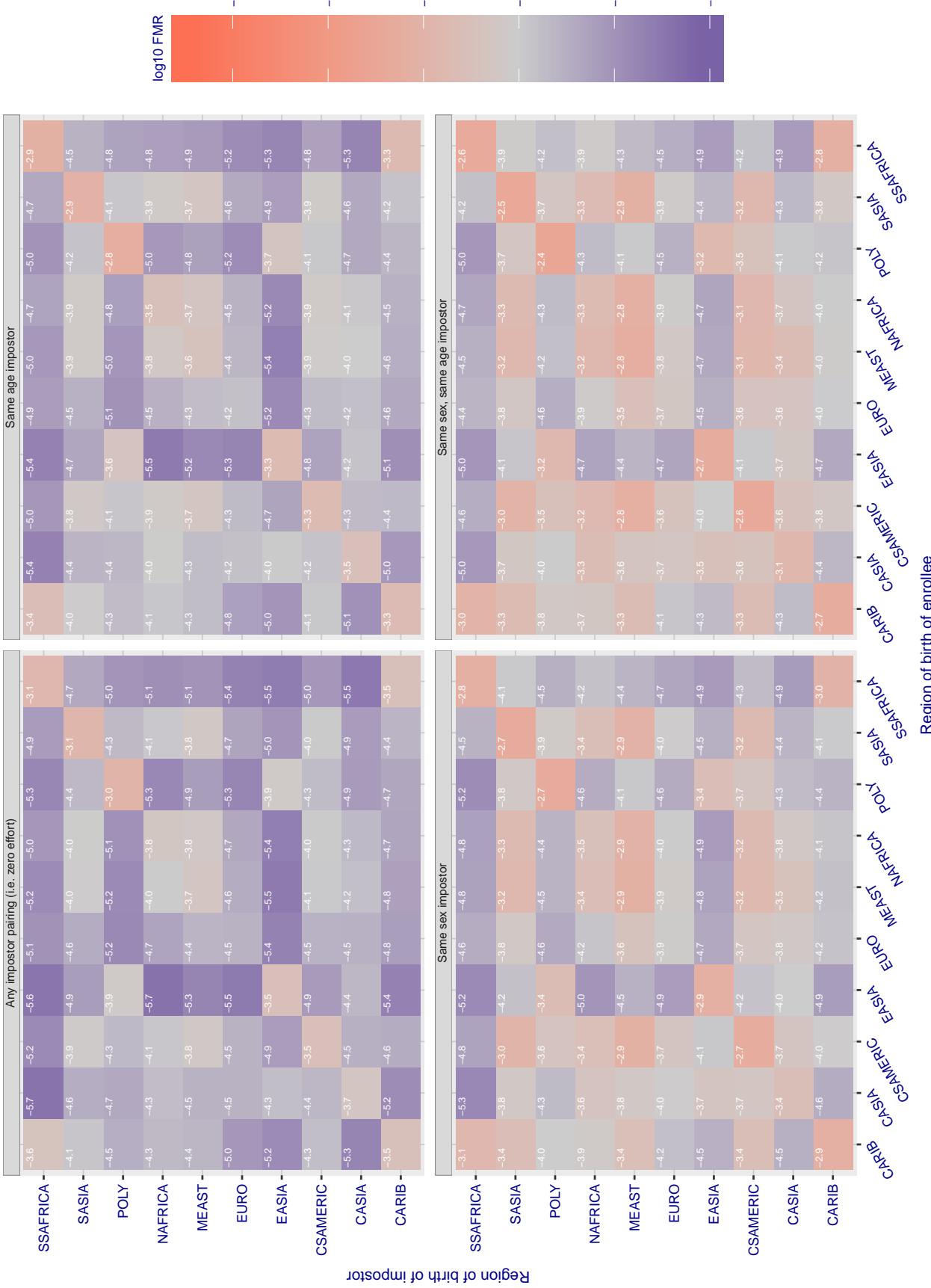


Figure 139: For algorithm camvi-003 operating on visa images, the heatmap shows false match rates observed over impostor comparisons of faces from different individuals who were born in the given region pair. False matches are counted against a recognition threshold fixed globally to give the target FMR in the plot title, computed over all on the order of  $10^{10}$  impostor comparisons. If text appears in each box it give the same quantity as that coded by the color. Grey indicates FMR is at the intended FMR target level. Light red colors present a security vulnerability to, for example, a passport gate. Each +1 increase in  $\log_{10} FMR$  corresponds to a factor of 10 increase in FMR. The matrix is not quite symmetric because images in the enrollment and verification sets are different.

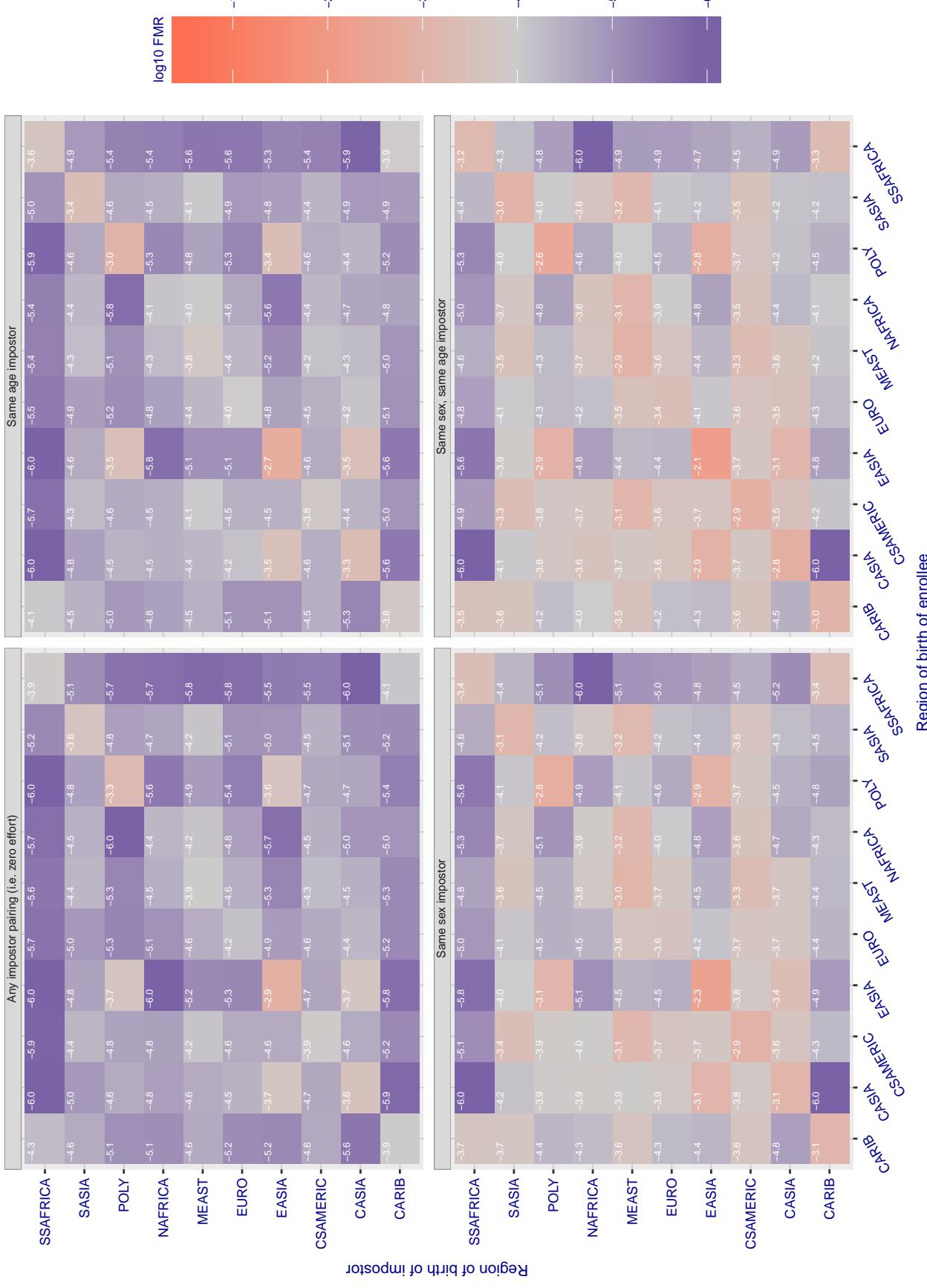
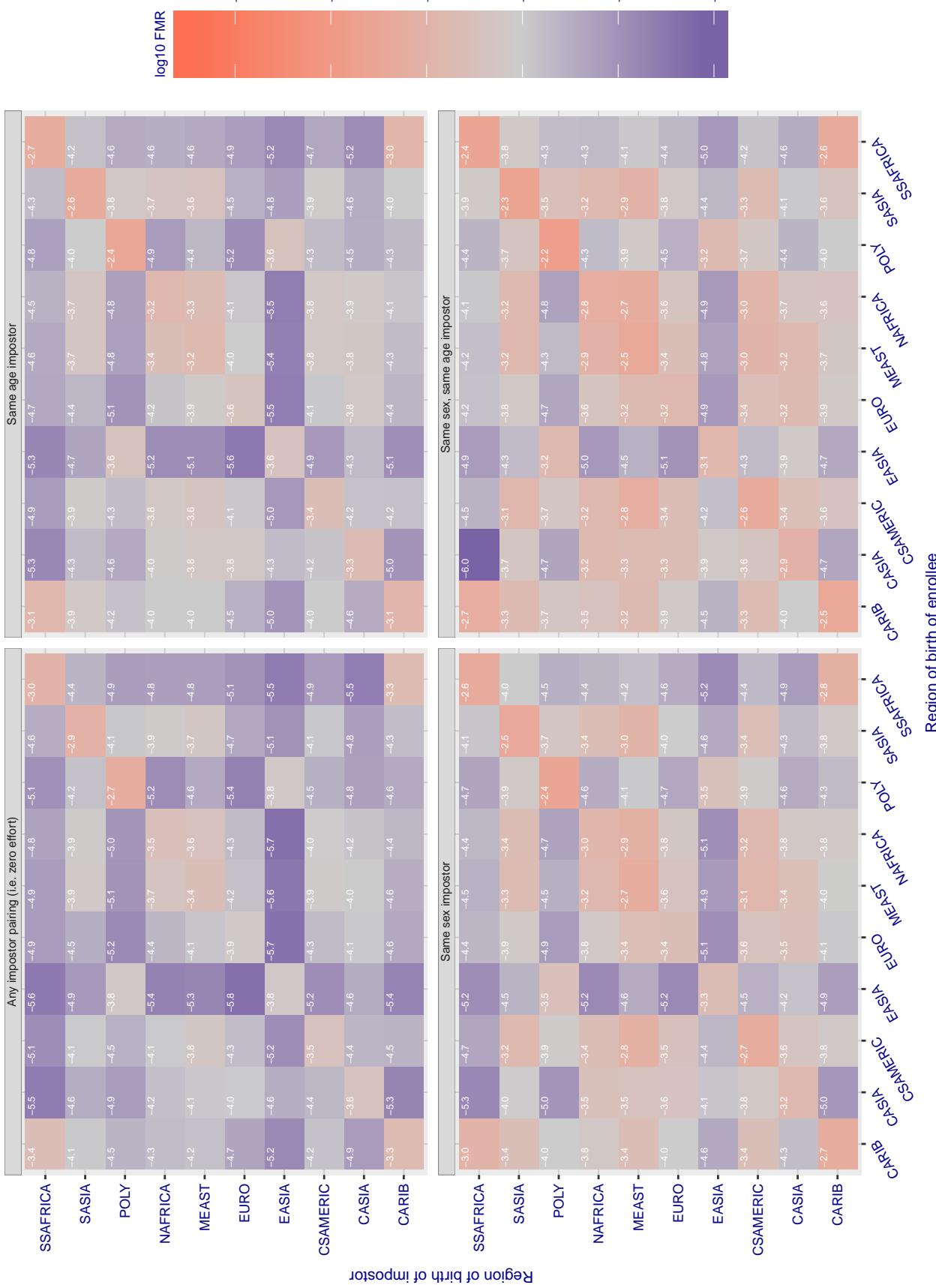
**Cross region FMR at threshold T = 0.436 for algorithm ceiec\_001, giving FMR(T) = 0.0001 globally.**

Figure 140: For algorithm ceiec\_001 operating on visa images, the heatmap shows false match rates observed over impostor comparisons of faces from different individuals who were born in the given region pair. False matches are counted against a recognition threshold fixed globally to give the target FMR in the plot title, computed over all on the order of  $10^{10}$  impostor comparisons. If text appears in each box it give the same quantity as that coded by the color. Grey indicates FMR is at the intended FMR target level. Light red colors present a security vulnerability to, for example, a passport gate. Each +1 increase in  $\log 10 \text{ FMR}$  corresponds to a factor of 10 increase in FMR. The matrix is not quite symmetric because images in the enrollment and verification sets are different.

**Cross region FMR at threshold T = 0.325 for algorithm ceiec\_002, giving FMR(T) = 0.0001 globally.**

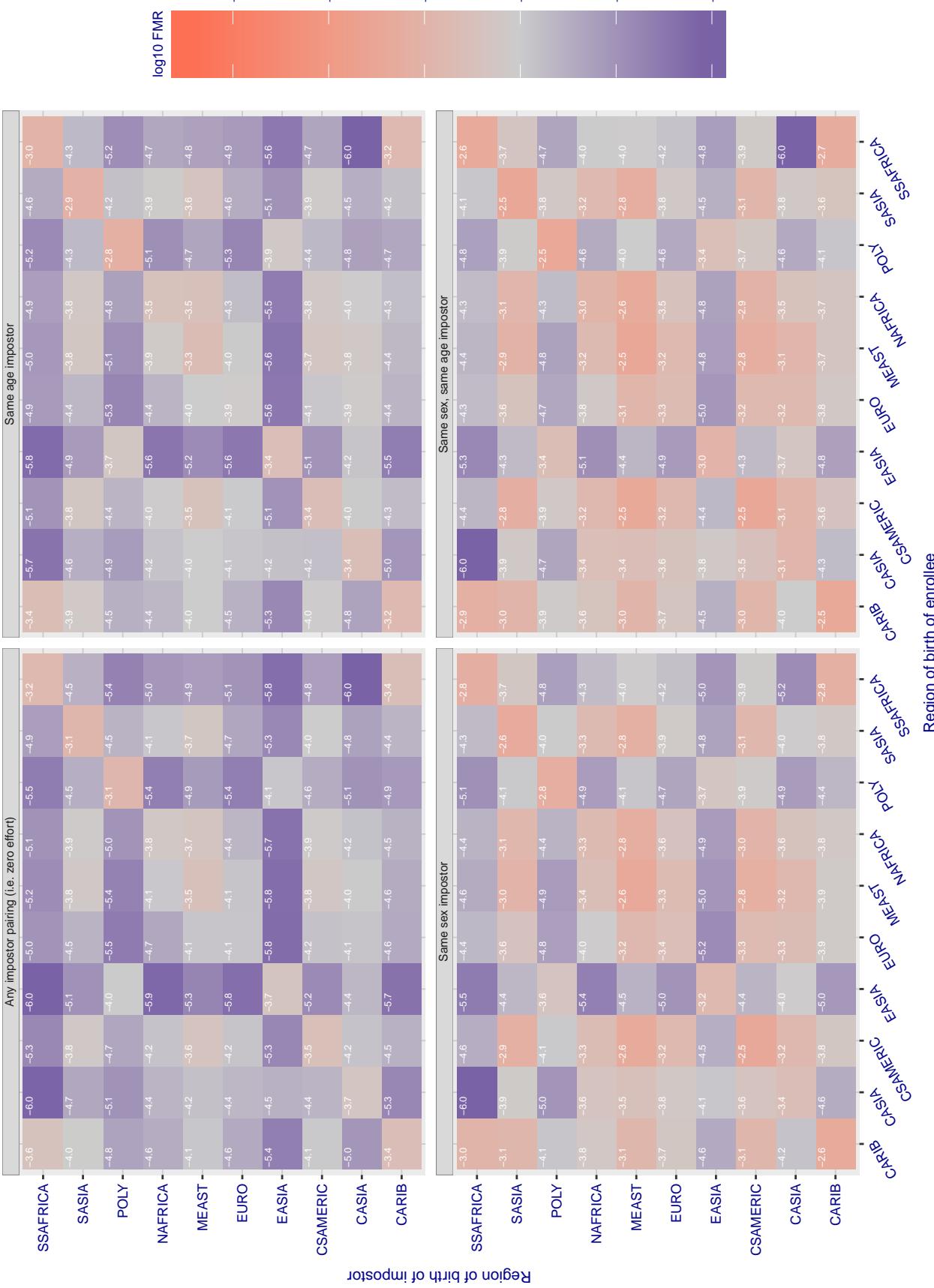
**Cross region FMR at threshold T = 2972.000 for algorithm cogent\_003, giving FMR(T) = 0.0001 globally.**

Figure 142: For algorithm cogent-003 operating on visa images, the heatmap shows false match rates observed over impostor comparisons of faces from different individuals who were born in the given region pair. False matches are counted against a recognition threshold fixed globally to give the target FMR in the plot title, computed over all on the order of  $10^{10}$  impostor comparisons. If text appears in each box it give the same quantity as that coded by the color. Grey indicates FMR is at the intended FMR target level. Light red colors present a security vulnerability to, for example, a passport gate. Each +1 increase in  $\log_{10} FMR$  corresponds to a factor of 10 increase in FMR. The matrix is not quite symmetric because images in the enrollment and verification sets are different.

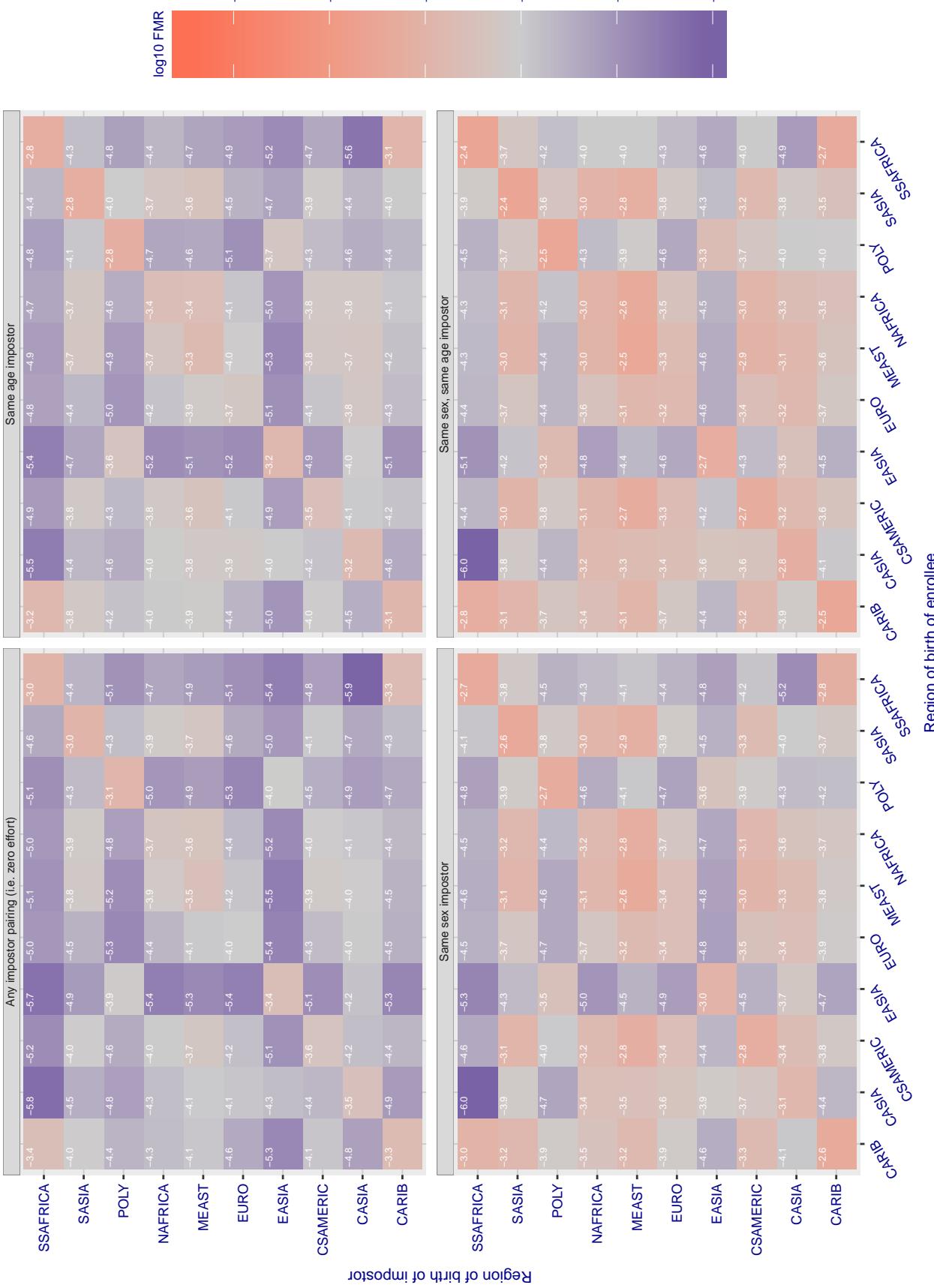
**Cross region FMR at threshold T = 3156.000 for algorithm cogent\_004, giving FMR(T) = 0.0001 globally.**

Figure 143: For algorithm cogent-004 operating on visa images, the heatmap shows false match rates observed over impostor comparisons of faces from different individuals who were born in the given region pair. False matches are counted against a recognition threshold fixed globally to give the target FMR in the plot title, computed over all on the order of  $10^{10}$  impostor comparisons. If text appears in each box it give the same quantity as that coded by the color. Grey indicates FMR is at the intended FMR target level. Light red colors present a security vulnerability to, for example, a passport gate. Each +1 increase in  $\log_{10} FMR$  corresponds to a factor of 10 increase in FMR. The matrix is not quite symmetric because images in the enrollment and verification sets are different.

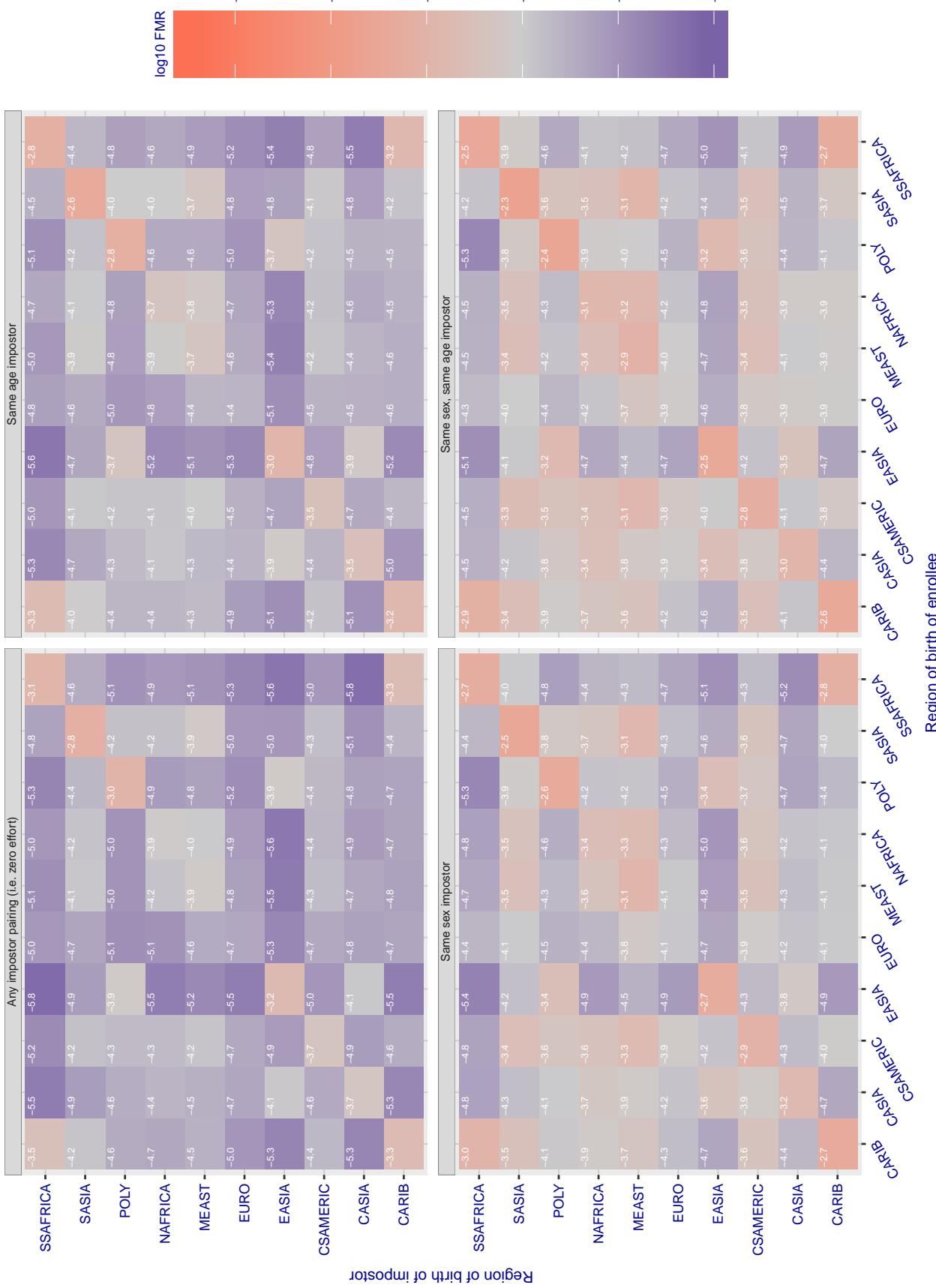
**Cross region FMR at threshold T = 0.565 for algorithm cognitec\_000, giving FMR(T) = 0.0001 globally.**

Figure 144: For algorithm cognitec-000 operating on visa images, the heatmap shows false match rates observed over impostor comparisons of faces from different individuals who were born in the given region pair. False matches are counted against a recognition threshold fixed globally to give the target FMR in the plot title, computed over all on the order of  $10^{10}$  impostor comparisons. If text appears in each box it give the same quantity as that coded by the color. Grey indicates FMR is at the intended FMR target level. Light red colors present a security vulnerability to, for example, a passport gate. Each +1 increase in  $\log_{10} \text{FMR}$  corresponds to a factor of 10 increase in FMR. The matrix is not quite symmetric because images in the enrollment and verification sets are different.

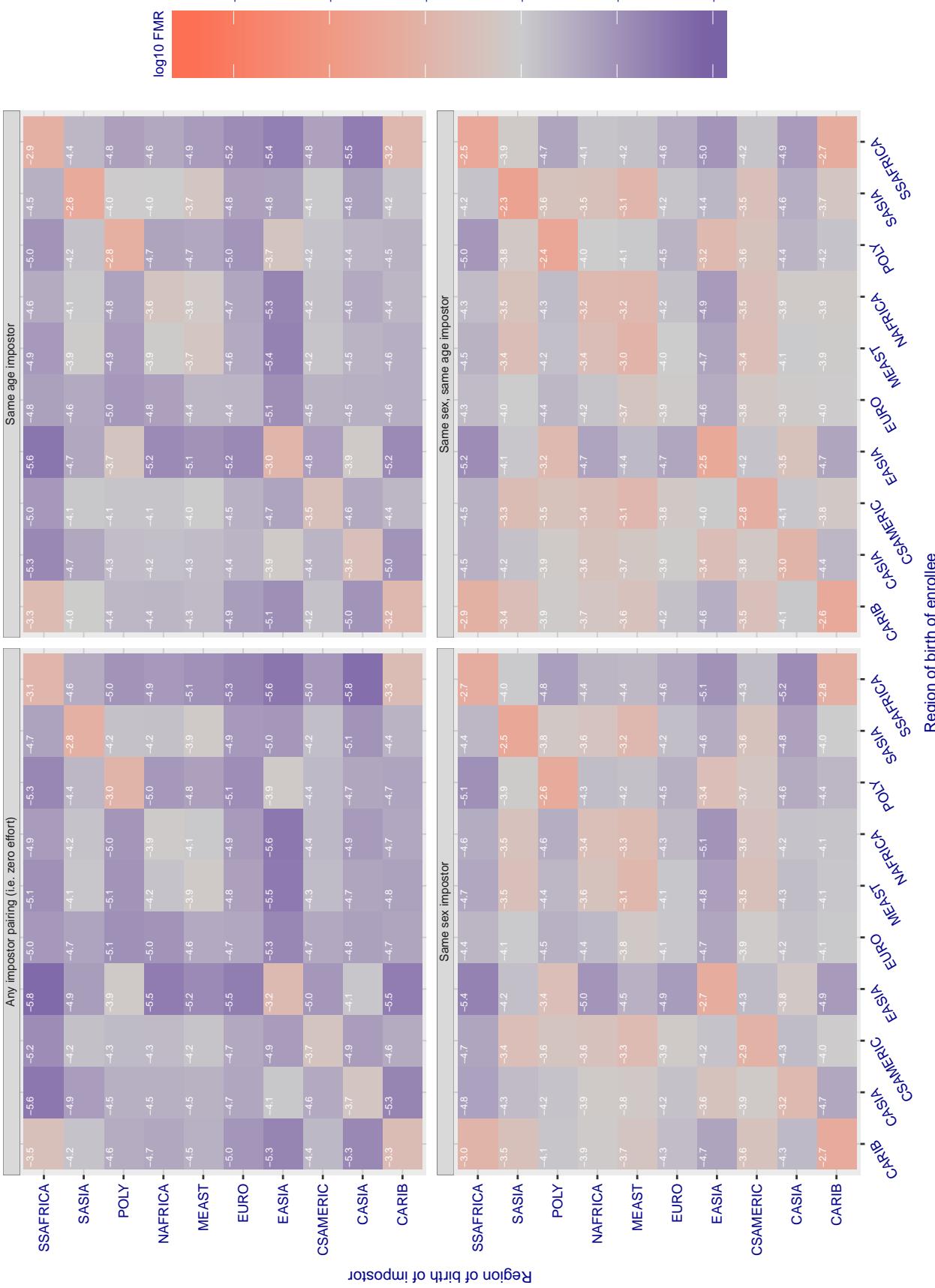
**Cross region FMR at threshold T = 0.565 for algorithm cognitec\_001, giving FMR(T) = 0.0001 globally.**

Figure 145: For algorithm cognitec-001 operating on visa images, the heatmap shows false match rates observed over impostor comparisons of faces from different individuals who were born in the given region pair. False matches are counted against a recognition threshold fixed globally to give the target FMR in the plot title, computed over all on the order of  $10^{10}$  impostor comparisons. If text appears in each box it give the same quantity as that coded by the color. Grey indicates FMR is at the intended FMR target level. Light red colors present a security vulnerability to, for example, a passport gate. Each +1 increase in  $\log_{10} FMR$  corresponds to a factor of 10 increase in FMR. The matrix is not quite symmetric because images in the enrollment and verification sets are different.

### Cross region FMR at threshold T = 0.762 for algorithm cyberextruder\_001, giving FMR(T) = 0.0001 globally.

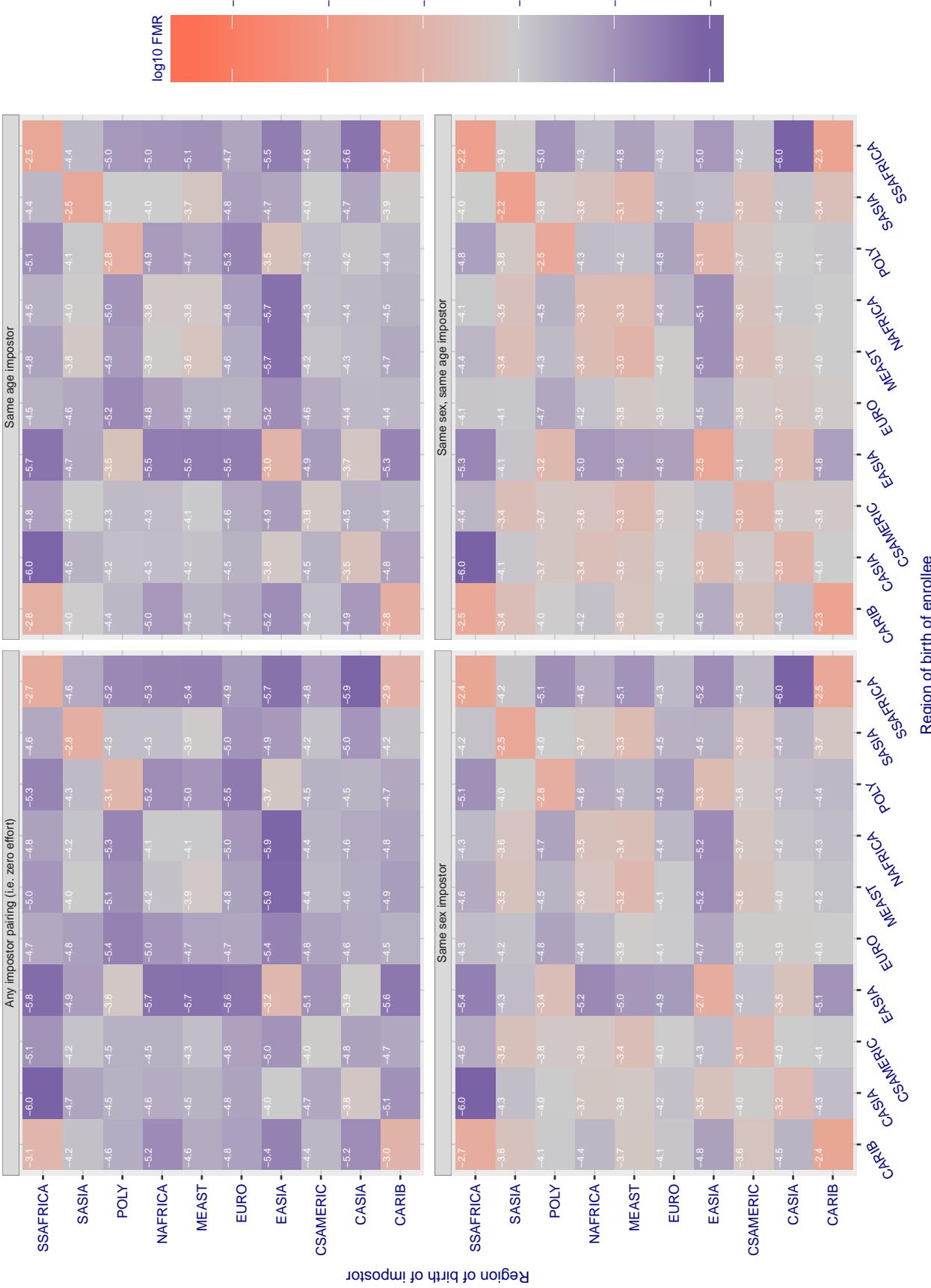


Figure 146: For algorithm cyberextruder-001 operating on visa images, the heatmap shows false match rates observed over impostor comparisons of faces from different individuals who were born in the given region pair. False matches are counted against a recognition threshold fixed globally to give the target FMR in the plot title, computed over all on the order of  $10^{10}$  impostor comparisons. If text appears in each box it give the same quantity as that coded by the color. Grey indicates FMR is at the intended FMR target level. Light red colors present a security vulnerability to, for example, a passport gate. Each +1 increase in  $\log_{10} FMR$  corresponds to a factor of 10 increase in FMR. The matrix is not quite symmetric because images in the enrollment and verification sets are different.

### Cross region FMR at threshold T = 0.500 for algorithm cyberextruder\_002, giving FMR(T) = 0.0001 globally.

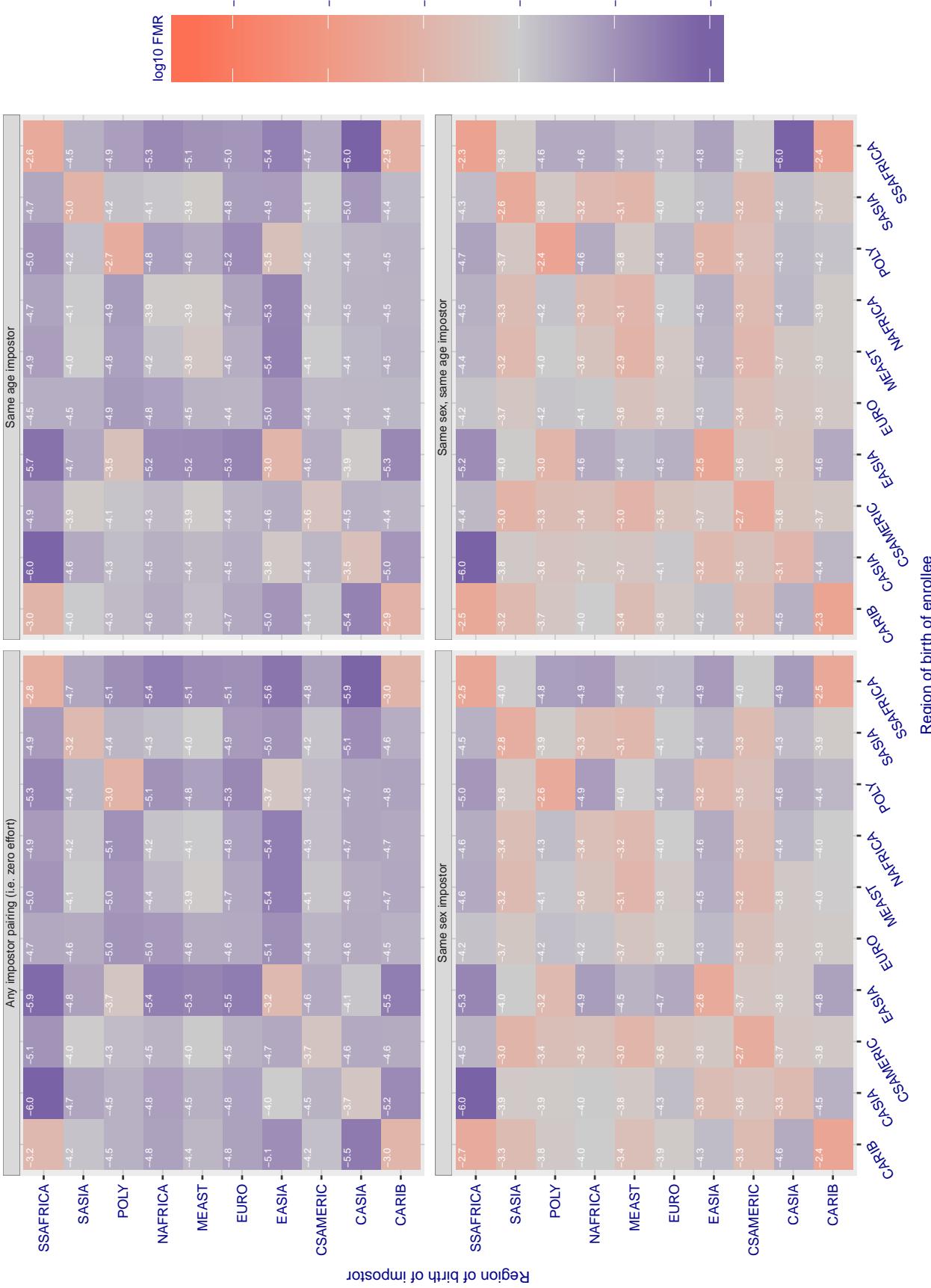


Figure 147: For algorithm cyberextruder-002 operating on visa images, the heatmap shows false match rates observed over impostor comparisons of faces from different individuals who were born in the given region pair. False matches are counted against a recognition threshold fixed globally to give the target FMR in the plot title, computed over all on the order of  $10^{10}$  impostor comparisons. If text appears in each box it give the same quantity as that coded by the color. Grey indicates FMR is at the intended FMR target level. Light red colors present a security vulnerability to, for example, a passport gate. Each +1 increase in  $\log_{10} \text{FMR}$  corresponds to a factor of 10 increase in FMR. The matrix is not quite symmetric because images in the enrollment and verification sets are different.

### Cross region FMR at threshold T = 1.408 for algorithm cyberlink\_001, giving FMR(T) = 0.00001 globally.

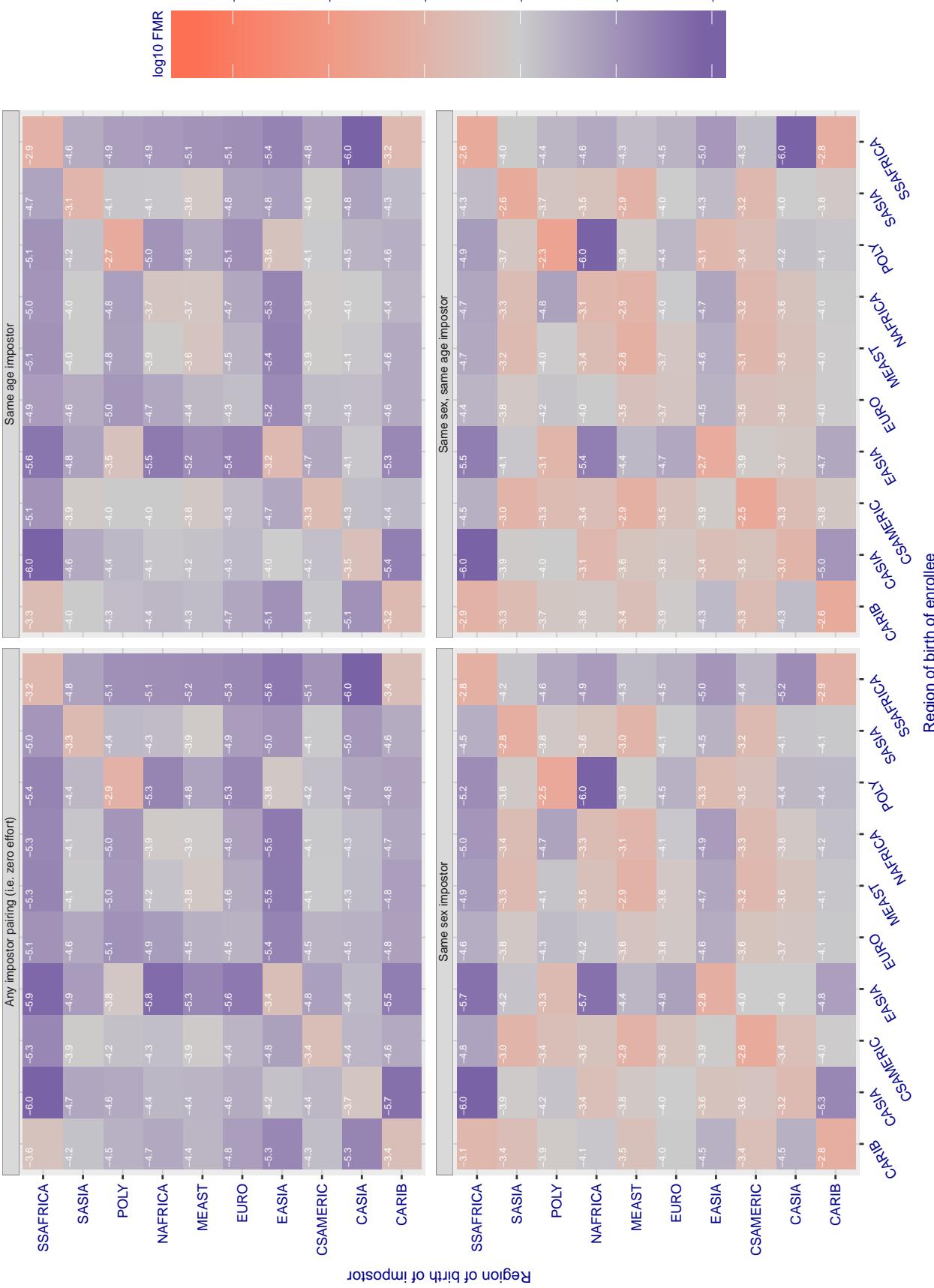


Figure 148: For algorithm cyberlink-001 operating on visa images, the heatmap shows false match rates observed over impostor comparisons of faces from different individuals who were born in the given region pair. False matches are counted against a recognition threshold fixed globally to give the target FMR in the plot title, computed over all on the order of  $10^{10}$  impostor comparisons. If text appears in each box it give the same quantity as that coded by the color. Grey indicates FMR is at the intended FMR target level. Light red colors present a security vulnerability to, for example, a passport gate. Each +1 increase in  $\log_{10} FMR$  corresponds to a factor of 10 increase in FMR. The matrix is not quite symmetric because images in the enrollment and verification sets are different.

### Cross region FMR at threshold T = 1.409 for algorithm cyberlink\_002, giving FMR(T) = 0.00001 globally.

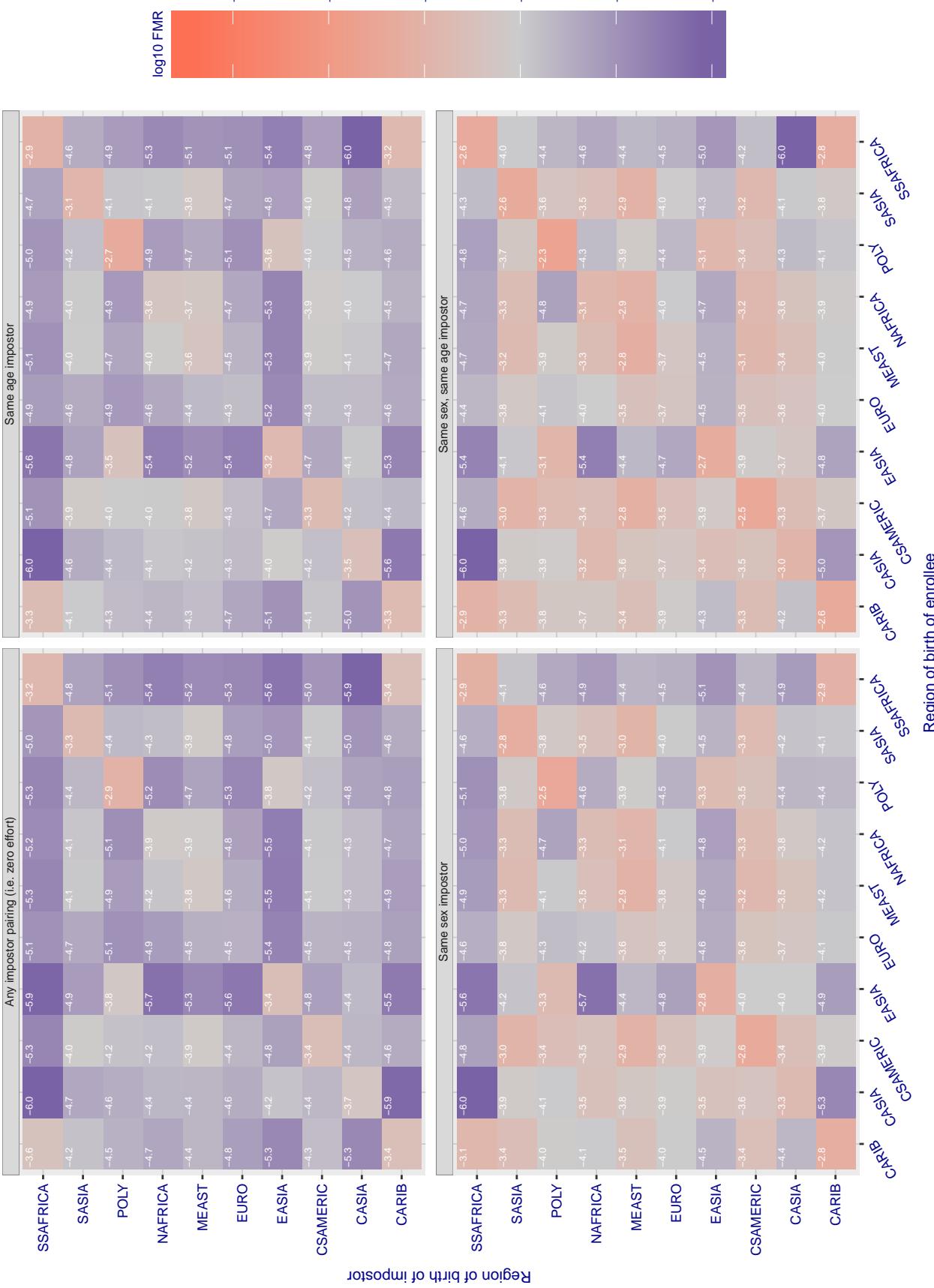


Figure 149: For algorithm cyberlink-002 operating on visa images, the heatmap shows false match rates observed over impostor comparisons of faces from different individuals who were born in the given region pair. False matches are counted against a recognition threshold fixed globally to give the target FMR in the plot title, computed over all on the order of  $10^{10}$  impostor comparisons. If text appears in each box it give the same quantity as that coded by the color. Grey indicates FMR is at the intended FMR target level. Light red colors present a security vulnerability to, for example, a passport gate. Each +1 increase in  $\log_{10} FMR$  corresponds to a factor of 10 increase in FMR. The matrix is not quite symmetric because images in the enrollment and verification sets are different.

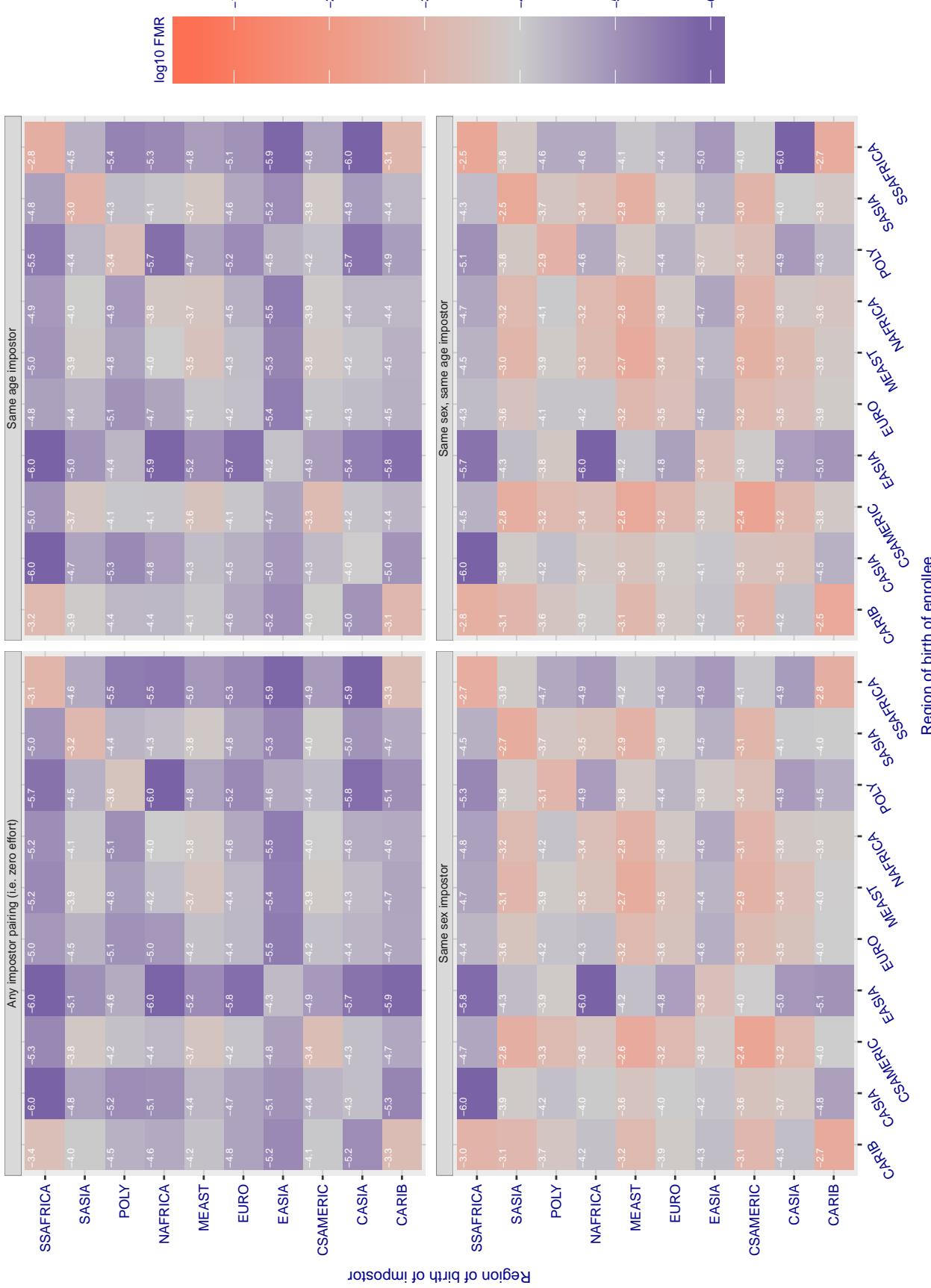
**Cross region FMR at threshold T = 7630.000 for algorithm dahua\_001, giving FMR(T) = 0.0001 globally.**

Figure 150: For algorithm dahua-001 operating on visa images, the heatmap shows false match rates observed over impostor comparisons of faces from different individuals who were born in the given region pair. False matches are counted against a recognition threshold fixed globally to give the target FMR in the plot title, computed over all on the order of  $10^{10}$  impostor comparisons. If text appears in each box it give the same quantity as that coded by the color. Grey indicates FMR is at the intended FMR target level. Light red colors present a security vulnerability to, for example, a passport gate. Each +1 increase in  $\log_{10} \text{FMR}$  corresponds to a factor of 10 increase in FMR. The matrix is not quite symmetric because images in the enrollment and verification sets are different.

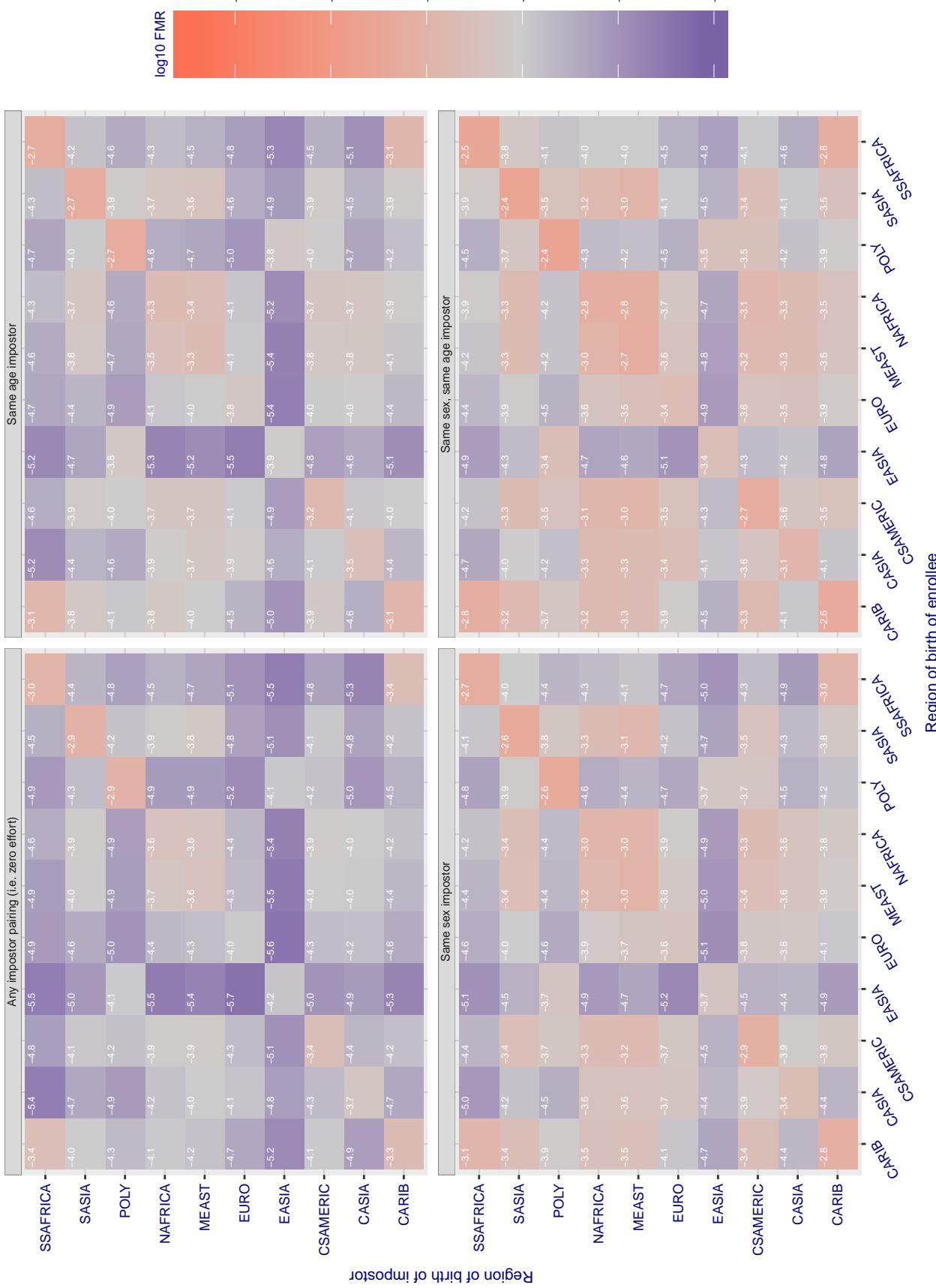
**Cross region FMR at threshold T = 6696.000 for algorithm dahua\_002, giving FMR(T) = 0.0001 globally.**

Figure 151: For algorithm dahua-002 operating on visa images, the heatmap shows false match rates observed over impostor comparisons of faces from different individuals who were born in the given region pair. False matches are counted against a recognition threshold fixed globally to give the target FMR in the plot title, computed over all on the order of  $10^{10}$  impostor comparisons. If text appears in each box it give the same quantity as that coded by the color. Grey indicates FMR is at the intended FMR target level. Light red colors present a security vulnerability to, for example, a passport gate. Each +1 increase in  $\log_{10} \text{FMR}$  corresponds to a factor of 10 increase in FMR. The matrix is not quite symmetric because images in the enrollment and verification sets are different.

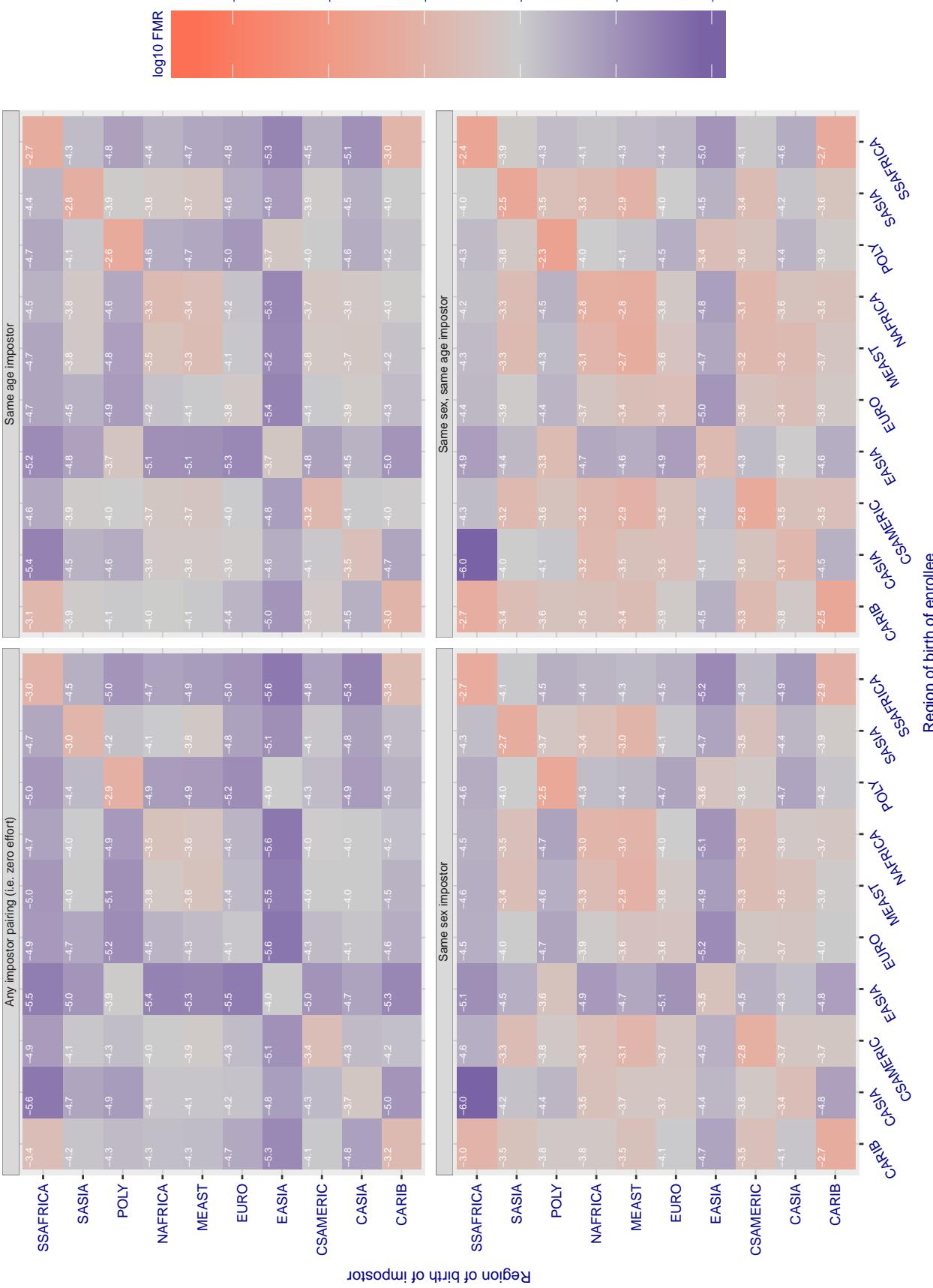
**Cross region FMR at threshold T = 1.359 for algorithm deepglint\_001, giving FMR(T) = 0.0001 globally.**

Figure 152: For algorithm deepglint-001 operating on visa images, the heatmap shows false match rates observed over impostor comparisons of faces from different individuals who were born in the given region pair. False matches are counted against a recognition threshold fixed globally to give the target FMR in the plot title, computed over all on the order of  $10^{10}$  impostor comparisons. If text appears in each box it give the same quantity as that coded by the color. Grey indicates FMR is at the intended FMR target level. Light red colors present a security vulnerability to, for example, a passport gate. Each +1 increase in  $\log_{10} \text{FMR}$  corresponds to a factor of 10 increase in FMR. The matrix is not quite symmetric because images in the enrollment and verification sets are different.

### Cross region FMR at threshold T = 1.371 for algorithm deepsea\_001, giving FMR(T) = 0.0001 globally.

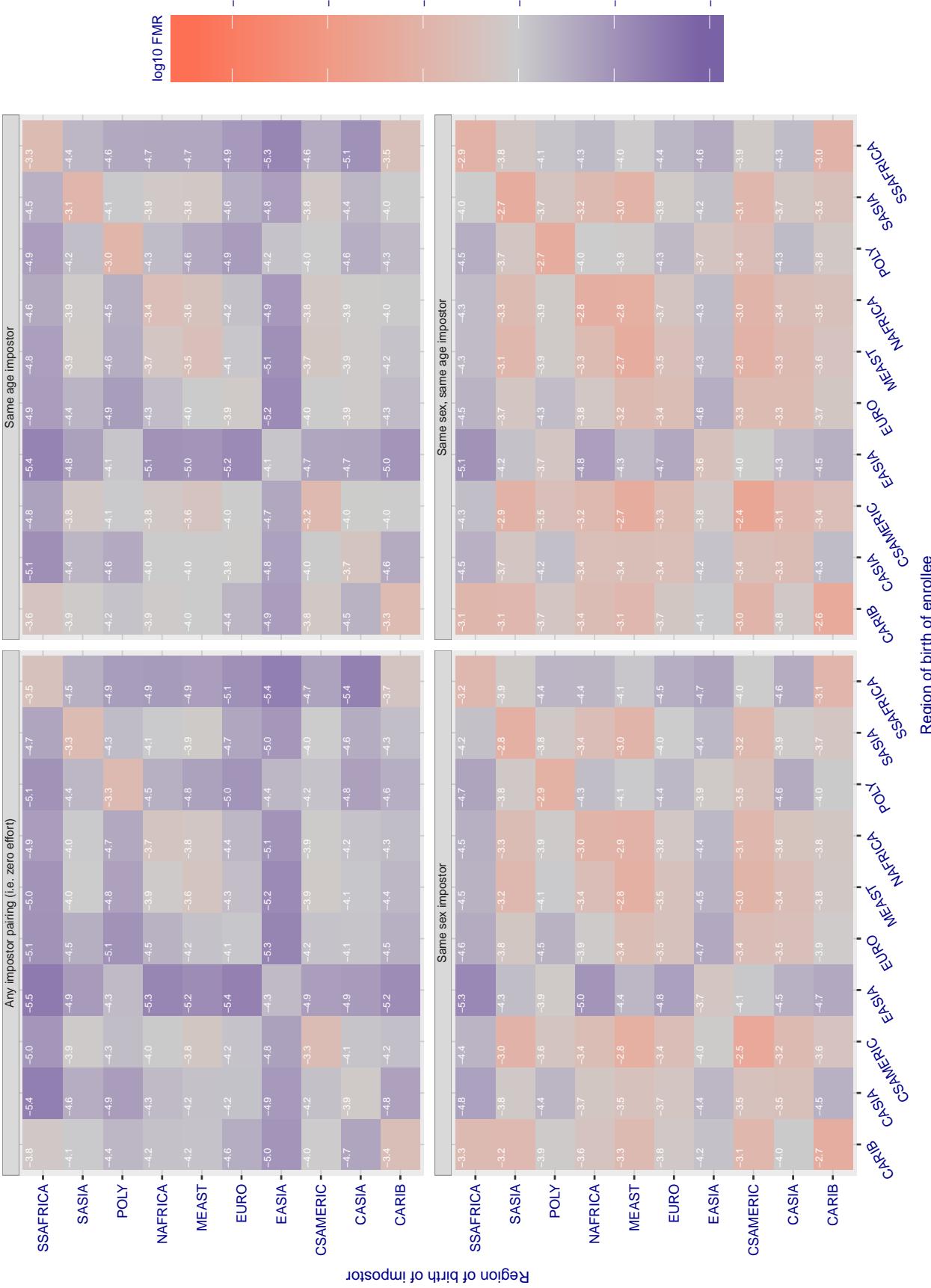


Figure 153: For algorithm deepsea-001 operating on visa images, the heatmap shows false match rates observed over impostor comparisons of faces from different individuals who were born in the given region pair. False matches are counted against a recognition threshold fixed globally to give the target FMR in the plot title, computed over all on the order of  $10^{10}$  impostor comparisons. If text appears in each box it give the same quantity as that coded by the color. Grey indicates FMR is at the intended FMR target level. Light red colors present a security vulnerability to, for example, a passport gate. Each +1 increase in  $\log_{10} FMR$  corresponds to a factor of 10 increase in FMR. The matrix is not quite symmetric because images in the enrollment and verification sets are different.

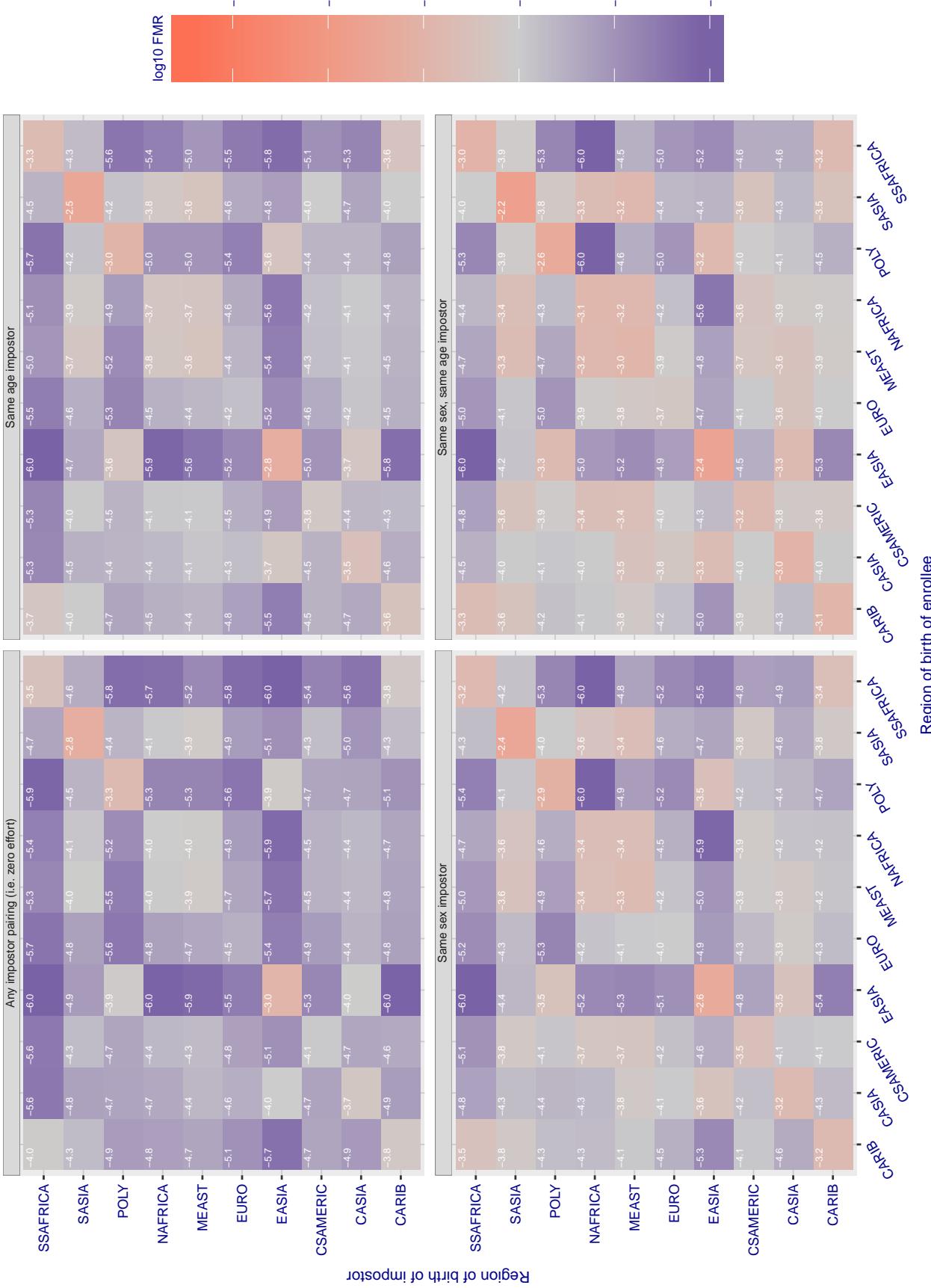
**Cross region FMR at threshold T = 79.344 for algorithm dermalog\_005, giving FMR(T) = 0.0001 globally.**

Figure 154: For algorithm dermalog-005 operating on visa images, the heatmap shows false match rates observed over impostor comparisons of faces from different individuals who were born in the given region pair. False matches are counted against a recognition threshold fixed globally to give the target FMR in the plot title, computed over all on the order of  $10^{10}$  impostor comparisons. If text appears in each box it give the same quantity as that coded by the color. Grey indicates FMR is at the intended FMR target level. Light red colors present a security vulnerability to, for example, a passport gate. Each +1 increase in  $\log_{10} \text{FMR}$  corresponds to a factor of 10 increase in FMR. The matrix is not quite symmetric because images in the enrollment and verification sets are different.

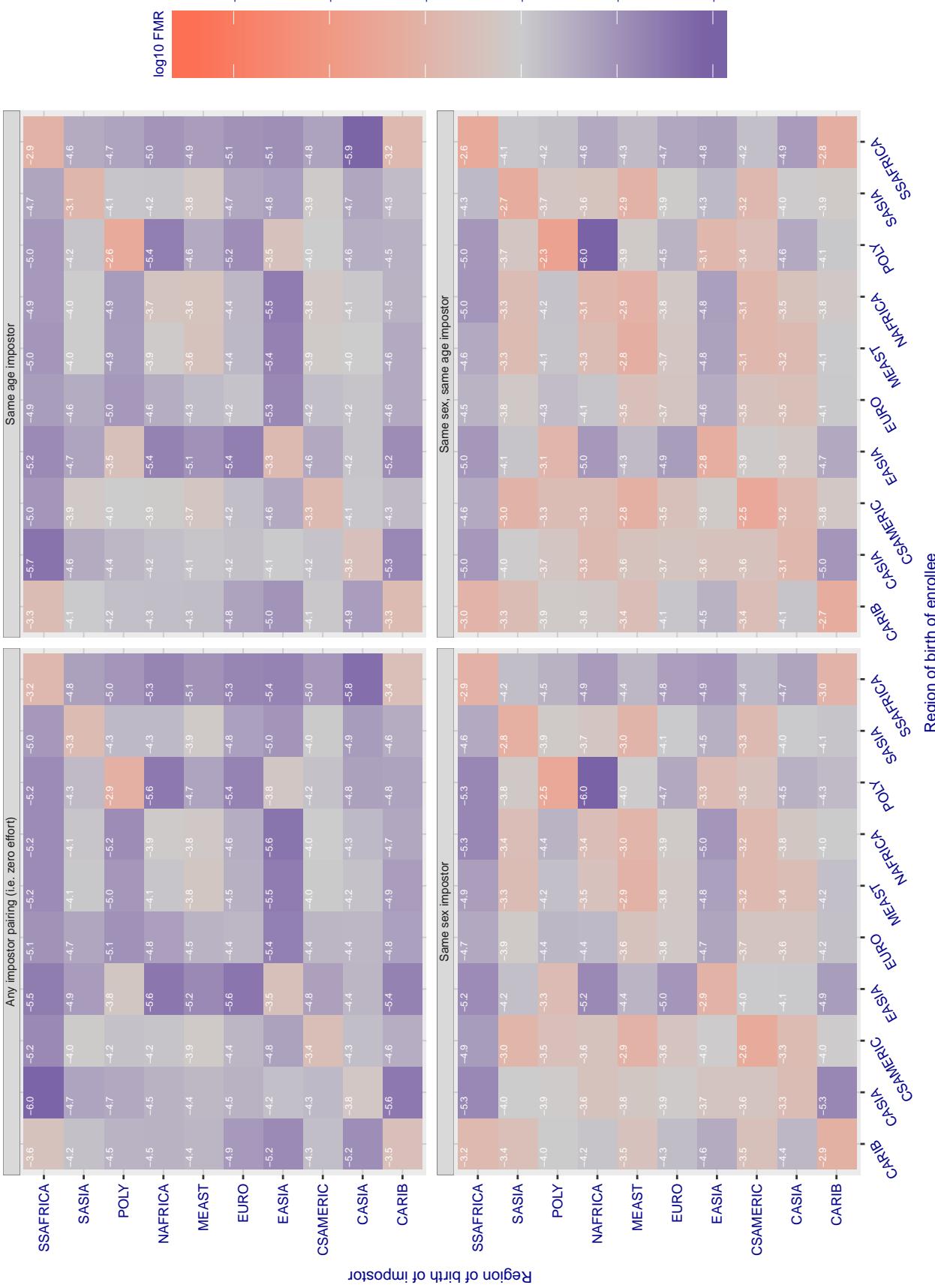
**Cross region FMR at threshold T = 79.670 for algorithm dermalog\_006, giving FMR(T) = 0.0001 globally.**

Figure 155: For algorithm dermalog-006 operating on visa images, the heatmap shows false match rates observed over impostor comparisons of faces from different individuals who were born in the given region pair. False matches are counted against a recognition threshold fixed globally to give the target FMR in the plot title, computed over all on the order of  $10^{10}$  impostor comparisons. If text appears in each box it give the same quantity as that coded by the color. Grey indicates FMR is at the intended FMR target level. Light red colors present a security vulnerability to, for example, a passport gate. Each +1 increase in  $\log_{10} FMR$  corresponds to a factor of 10 increase in FMR. The matrix is not quite symmetric because images in the enrollment and verification sets are different.

### Cross region FMR at threshold T = 0.675 for algorithm digitalbarriers\_002, giving FMR(T) = 0.0001 globally.

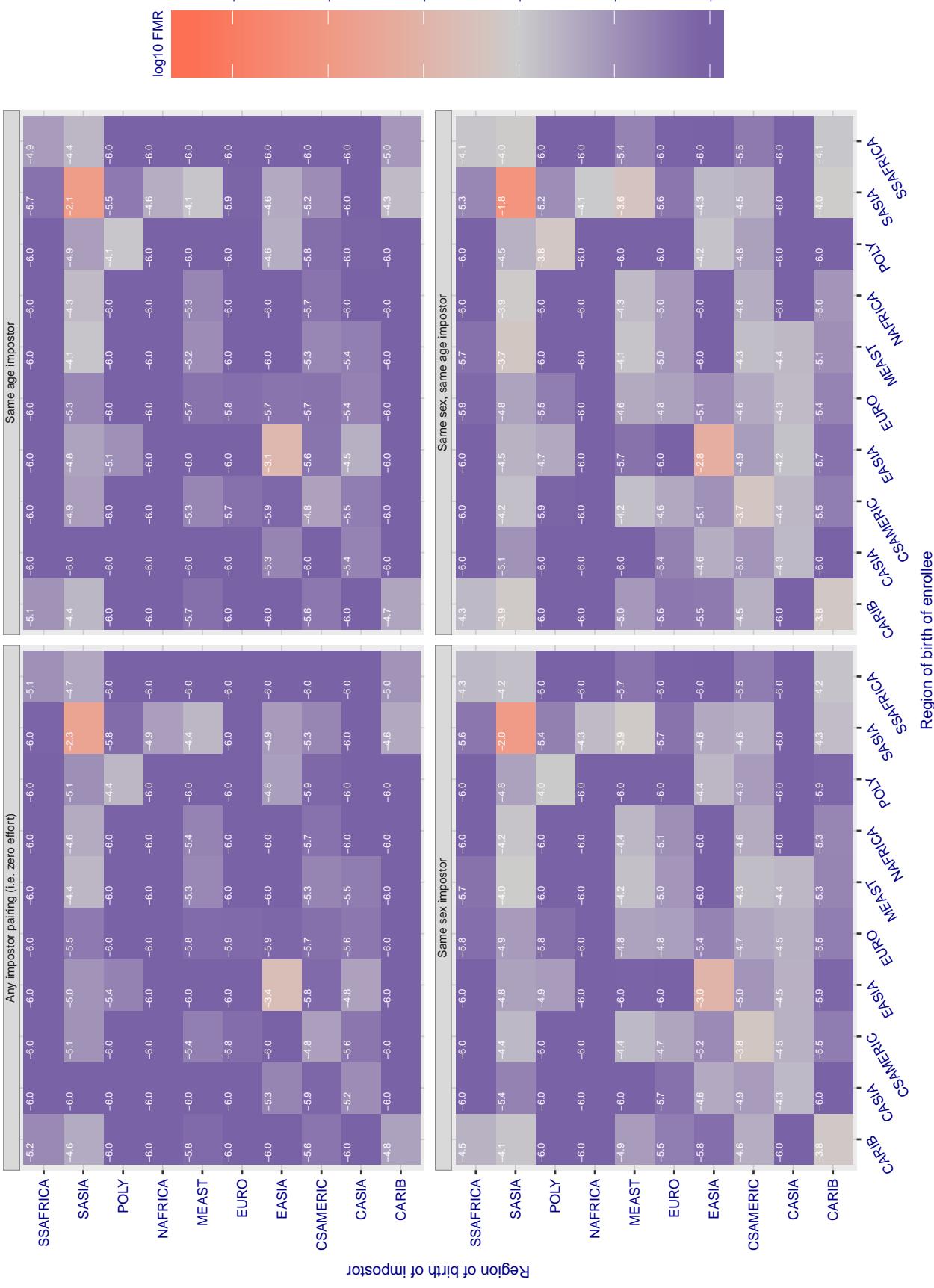


Figure 156: For algorithm digitalbarriers-002 operating on visa images, the heatmap shows false match rates observed over impostor comparisons of faces from different individuals who were born in the given region pair. False matches are counted against a recognition threshold fixed globally to give the target FMR in the plot title, computed over all on the order of  $10^{10}$  impostor comparisons. If text appears in each box it give the same quantity as that coded by the color. Grey indicates FMR is at the intended FMR target level. Light red colors present a security vulnerability to, for example, a passport gate. Each +1 increase in  $\log_{10} FMR$  corresponds to a factor of 10 increase in FMR. The matrix is not quite symmetric because images in the enrollment and verification sets are different.

### Cross region FMR at threshold T = 2.589 for algorithm everai\_002, giving FMR(T) = 0.0001 globally.

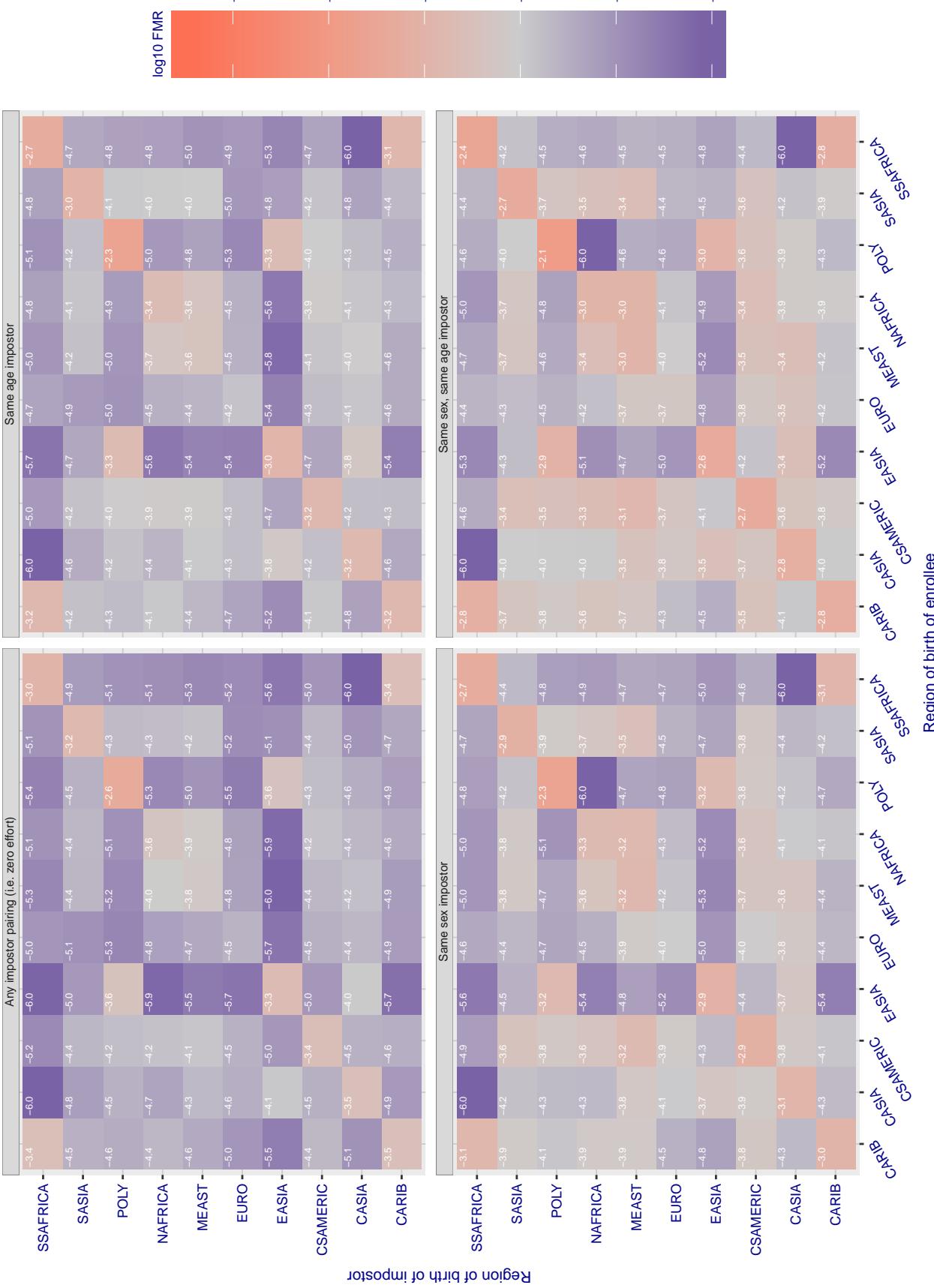


Figure 157: For algorithm everai-002 operating on visa images, the heatmap shows false match rates observed over impostor comparisons of faces from different individuals who were born in the given region pair. False matches are counted against a recognition threshold fixed globally to give the target FMR in the plot title, computed over all on the order of  $10^{10}$  impostor comparisons. If text appears in each box it give the same quantity as that coded by the color. Grey indicates FMR is at the intended FMR target level. Light red colors present a security vulnerability to, for example, a passport gate. Each +1 increase in  $\log_{10} FMR$  corresponds to a factor of 10 increase in FMR. The matrix is not quite symmetric because images in the enrollment and verification sets are different.

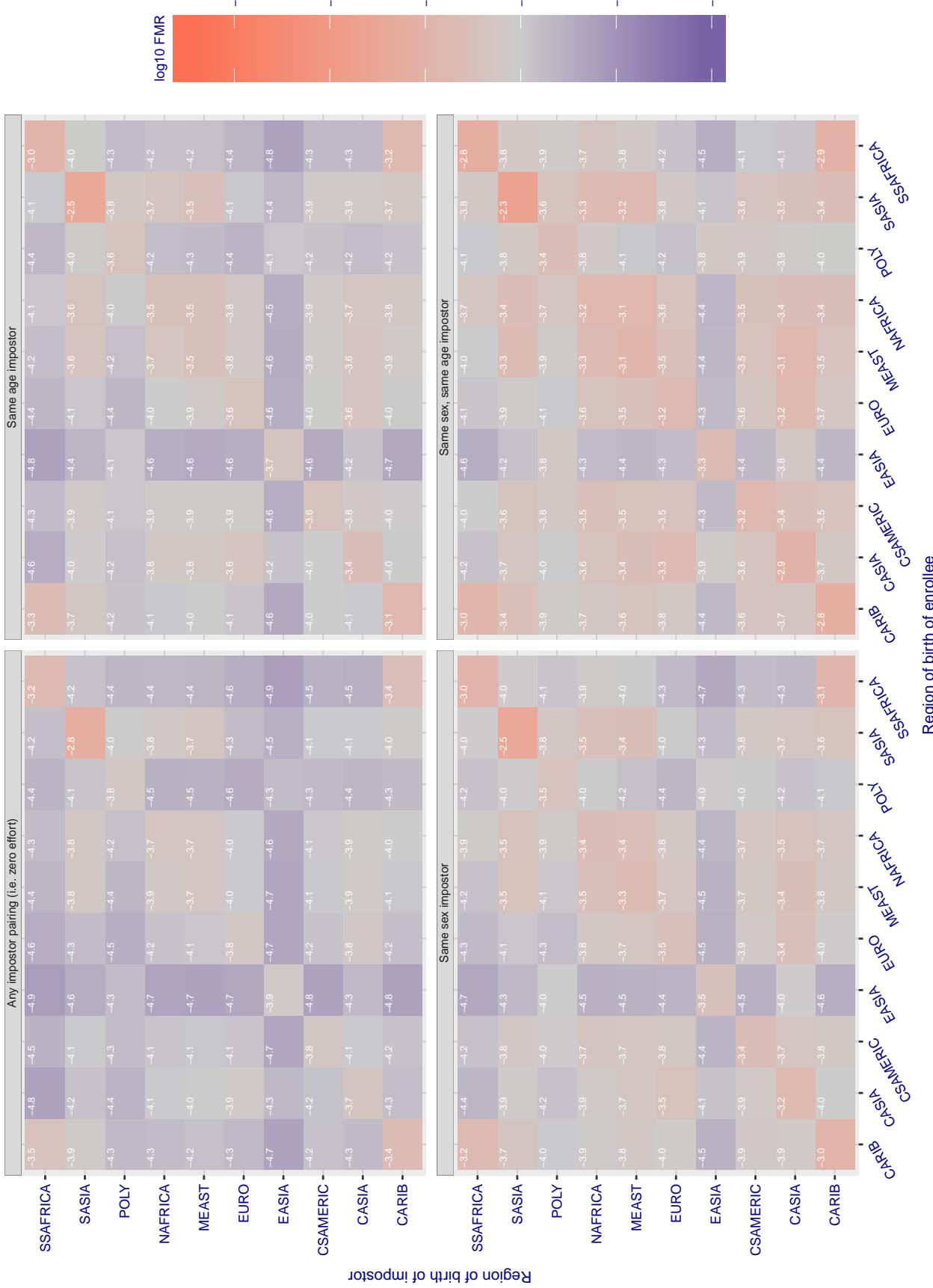
**Cross region FMR at threshold T = 0.611 for algorithm glory\_000, giving FMR(T) = 0.0001 globally.**

Figure 158: For algorithm glory-000 operating on visa images, the heatmap shows false match rates observed over impostor comparisons of faces from different individuals who were born in the given region pair. False matches are counted against a recognition threshold fixed globally to give the target FMR in the plot title, computed over all on the order of  $10^{10}$  impostor comparisons. If text appears in each box it give the same quantity as that coded by the color. Grey indicates FMR is at the intended FMR target level. Light red colors present a security vulnerability to, for example, a passport gate. Each +1 increase in  $\log_{10} \text{FMR}$  corresponds to a factor of 10 increase in FMR. The matrix is not quite symmetric because images in the enrollment and verification sets are different.

### Cross region FMR at threshold T = 0.618 for algorithm glory\_001, giving FMR(T) = 0.0001 globally.

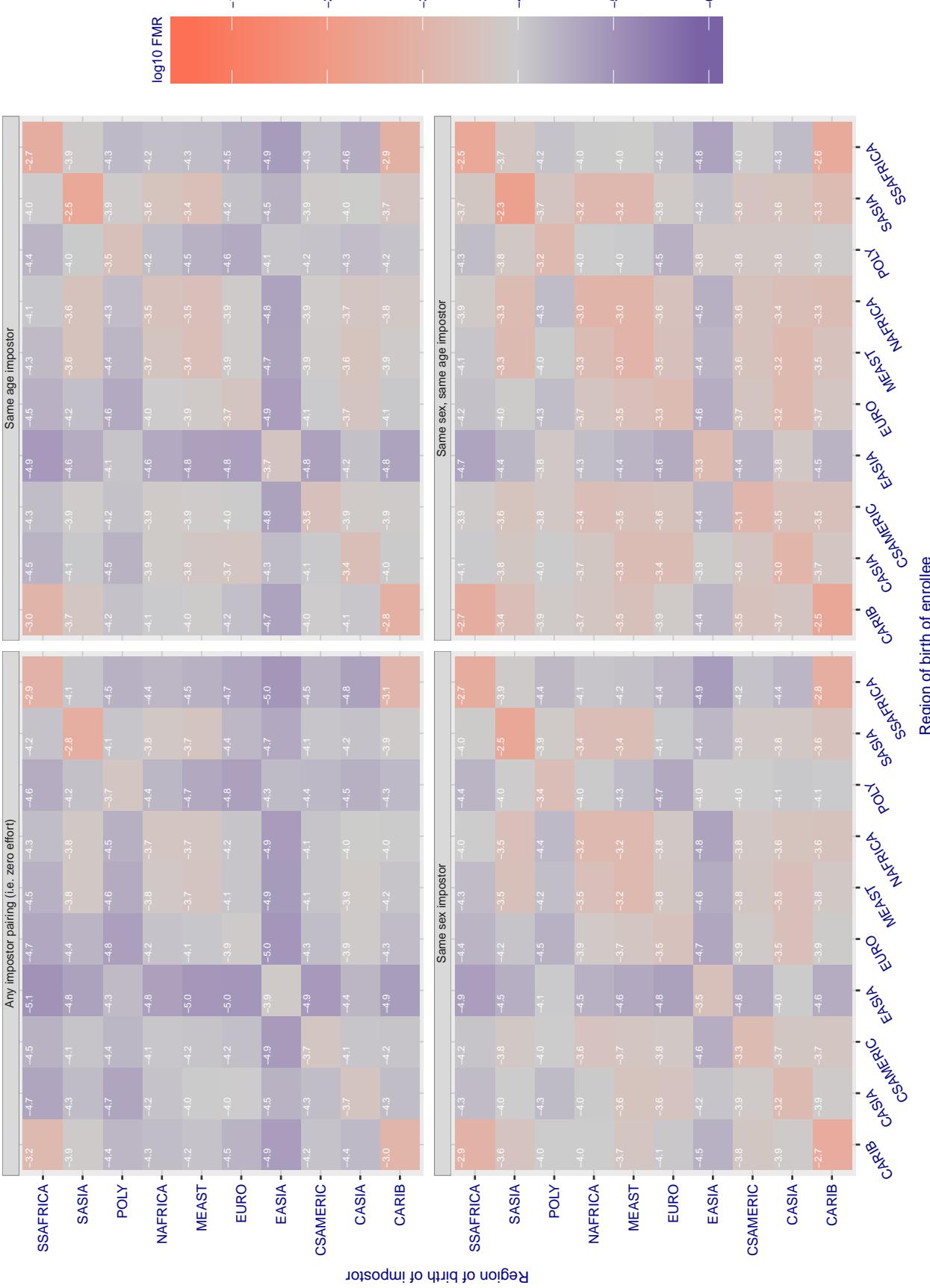


Figure 159: For algorithm *glory-001* operating on visa images, the heatmap shows false match rates observed over impostor comparisons of faces from different individuals who were born in the given region pair. False matches are counted against a recognition threshold fixed globally to give the target FMR in the plot title, computed over all on the order of  $10^{10}$  impostor comparisons. If text appears in each box it give the same quantity as that coded by the color. Grey indicates FMR is at the intended FMR target level. Light red colors present a security vulnerability to, for example, a passport gate. Each +1 increase in  $\log_{10} \text{FMR}$  corresponds to a factor of 10 increase in FMR. The matrix is not quite symmetric because images in the enrollment and verification sets are different.

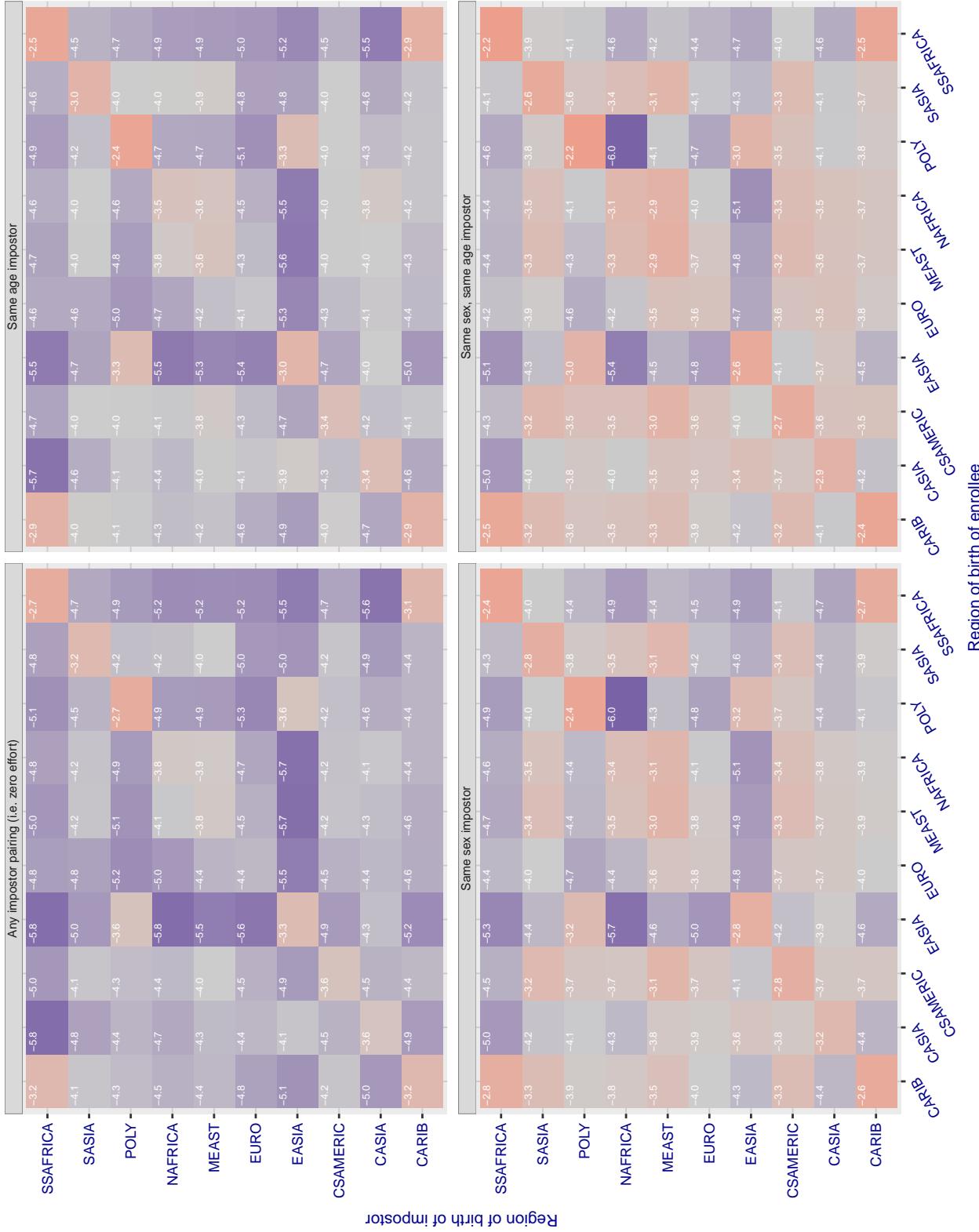


Figure 160: For algorithm gorilla-002 operating on visa images, the heatmap shows false match rates observed over impostor comparisons of faces from different individuals who were born in the given region pair. False matches are counted against a recognition threshold fixed globally to give the target FMR in the plot title, computed over all on the order of  $10^{10}$  impostor comparisons. If text appears in each box it give the same quantity as that coded by the color. Grey indicates FMR is at the intended FMR target level. Light red colors present a security vulnerability to, for example, a passport gate. Each +1 increase in  $\log_{10}$  FMR corresponds to a factor of 10 increase in FMR. The matrix is not quite symmetric because images in the enrollment and verification sets are different.

### Cross region FMR at threshold T = 0.454 for algorithm gorilla\_003, giving FMR(T) = 0.0001 globally.

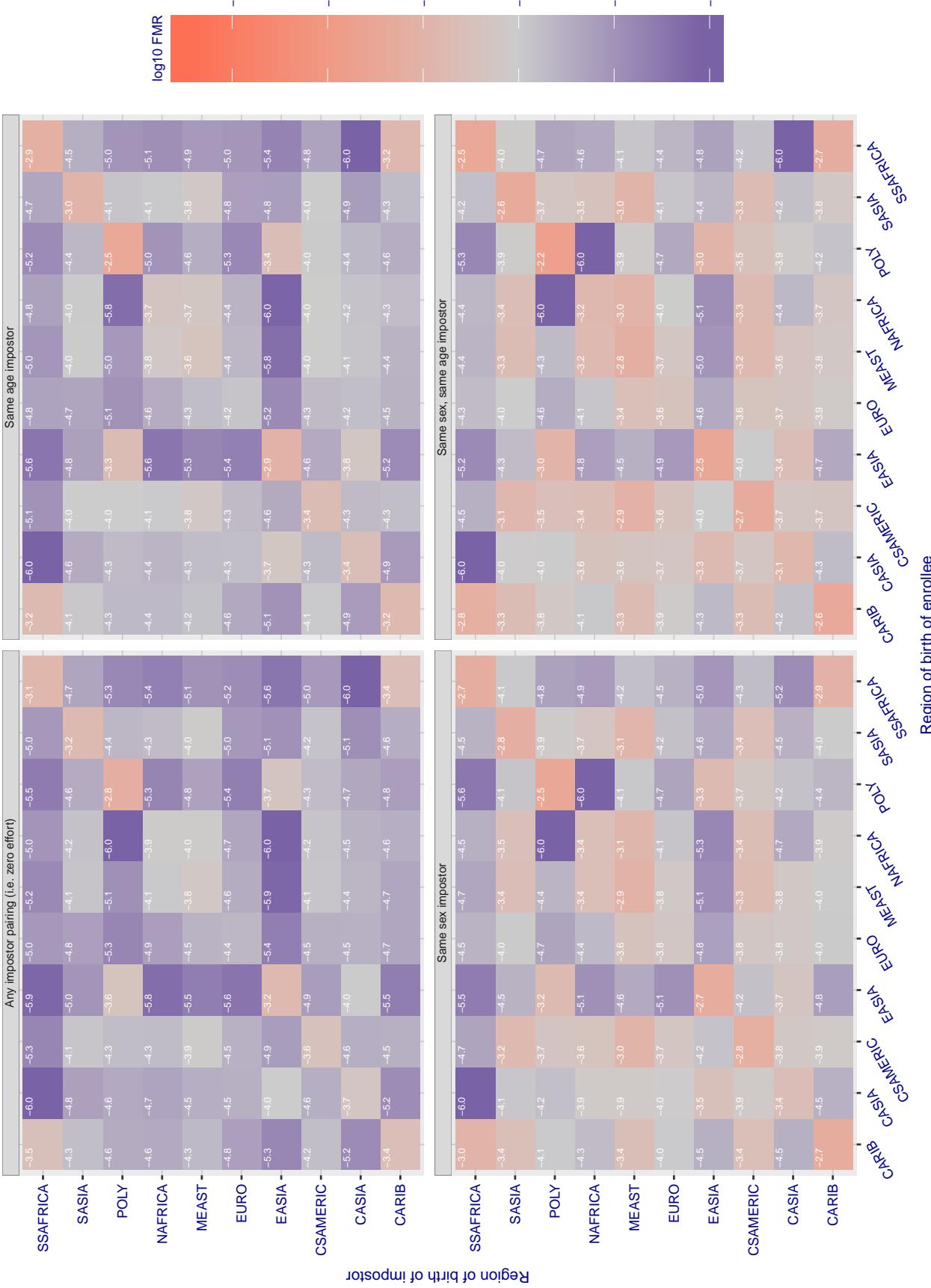


Figure 161: For algorithm gorilla-003 operating on visa images, the heatmap shows false match rates observed over impostor comparisons of faces from different individuals who were born in the given region pair. False matches are counted against a recognition threshold fixed globally to give the target FMR in the plot title, computed over all on the order of  $10^{10}$  impostor comparisons. If text appears in each box it give the same quantity as that coded by the color. Grey indicates FMR is at the intended FMR target level. Light red colors present a security vulnerability to, for example, a passport gate. Each +1 increase in  $\log_{10} FMR$  corresponds to a factor of 10 increase in FMR. The matrix is not quite symmetric because images in the enrollment and verification sets are different.

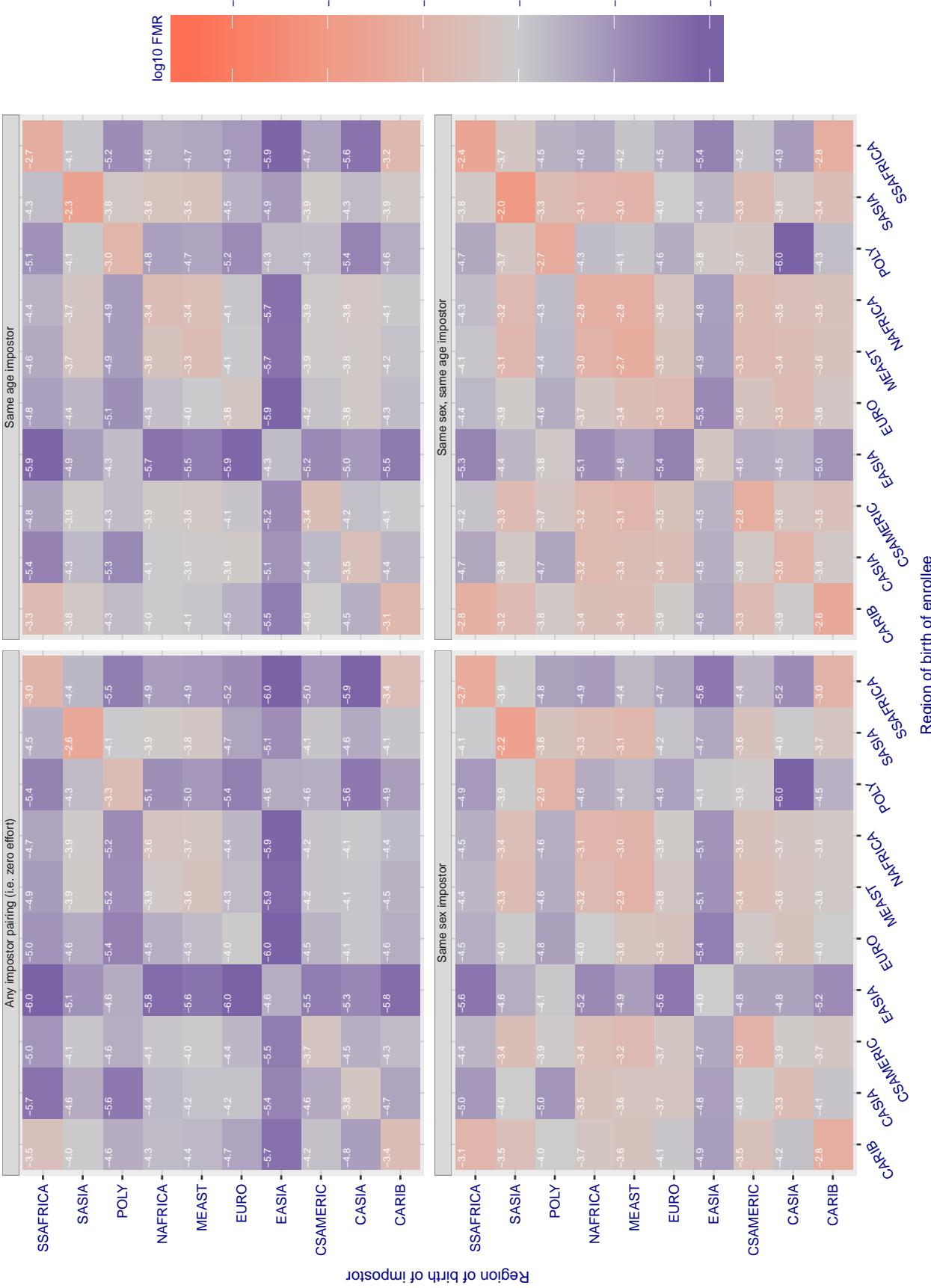
**Cross region FMR at threshold T = 66.565 for algorithm hik\_001, giving FMR(T) = 0.0001 globally.**

Figure 162: For algorithm hik-001 operating on visa images, the heatmap shows false match rates observed over impostor comparisons of faces from different individuals who were born in the given region pair. False matches are counted against a recognition threshold fixed globally to give the target FMR in the plot title, computed over all on the order of  $10^{10}$  impostor comparisons. If text appears in each box it give the same quantity as that coded by the color. Grey indicates FMR is at the intended FMR target level. Light red colors present a security vulnerability to, for example, a passport gate. Each +1 increase in  $\log_{10} \text{FMR}$  corresponds to a factor of 10 increase in FMR. The matrix is not quite symmetric because images in the enrollment and verification sets are different.

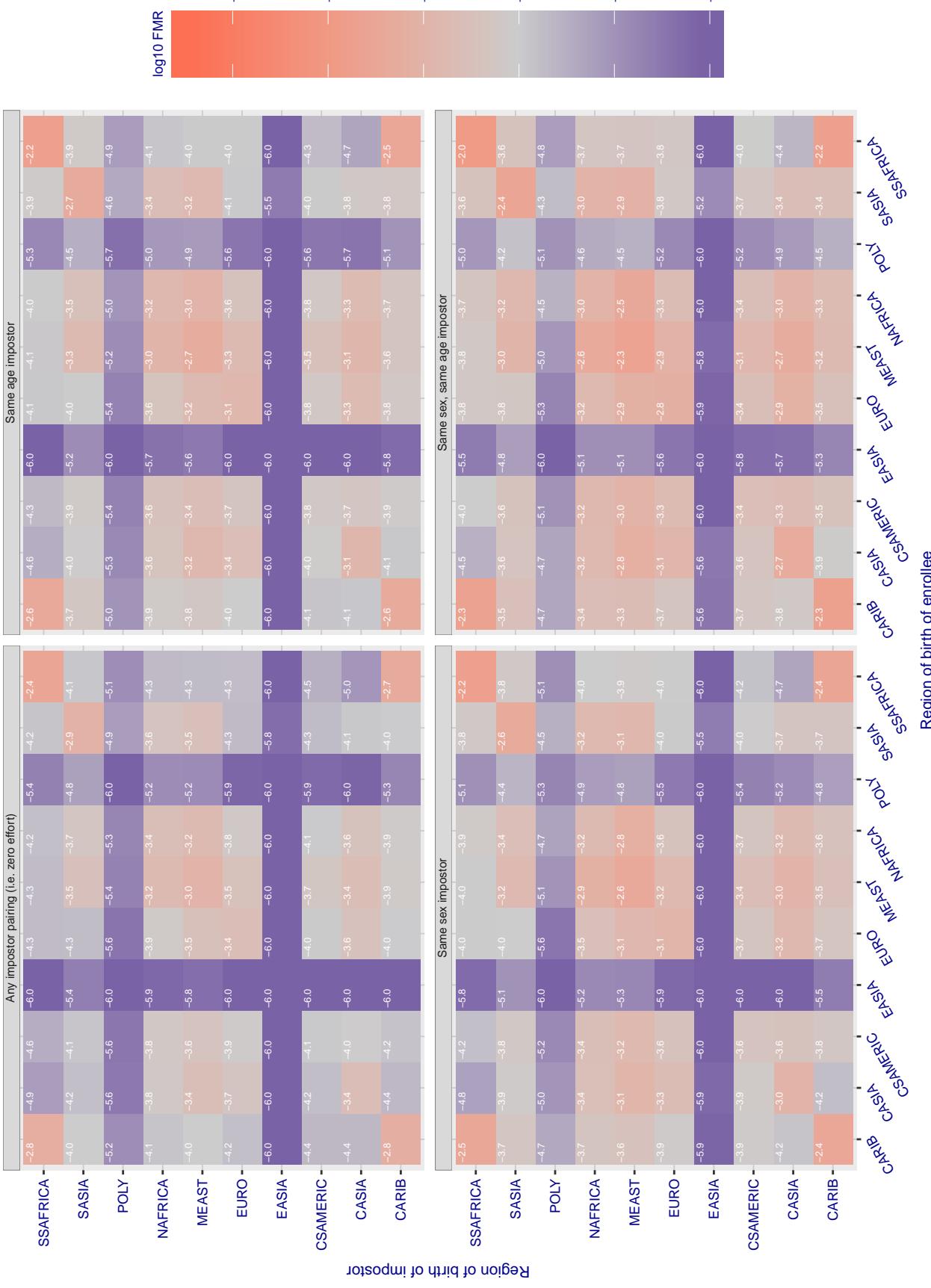
**Cross region FMR at threshold T = 0.971 for algorithm hr\_000, giving FMR(T) = 0.0001 globally.**

Figure 163: For algorithm hr-000 operating on visa images, the heatmap shows false match rates observed over impostor comparisons of faces from different individuals who were born in the given region pair. False matches are counted against a recognition threshold fixed globally to give the target FMR in the plot title, computed over all on the order of  $10^{10}$  impostor comparisons. If text appears in each box it give the same quantity as that coded by the color. Grey indicates FMR is at the intended FMR target level. Light red colors present a security vulnerability to, for example, a passport gate. Each +1 increase in  $\log_{10}$  FMR corresponds to a factor of 10 increase in FMR. The matrix is not quite symmetric because images in the enrollment and verification sets are different.

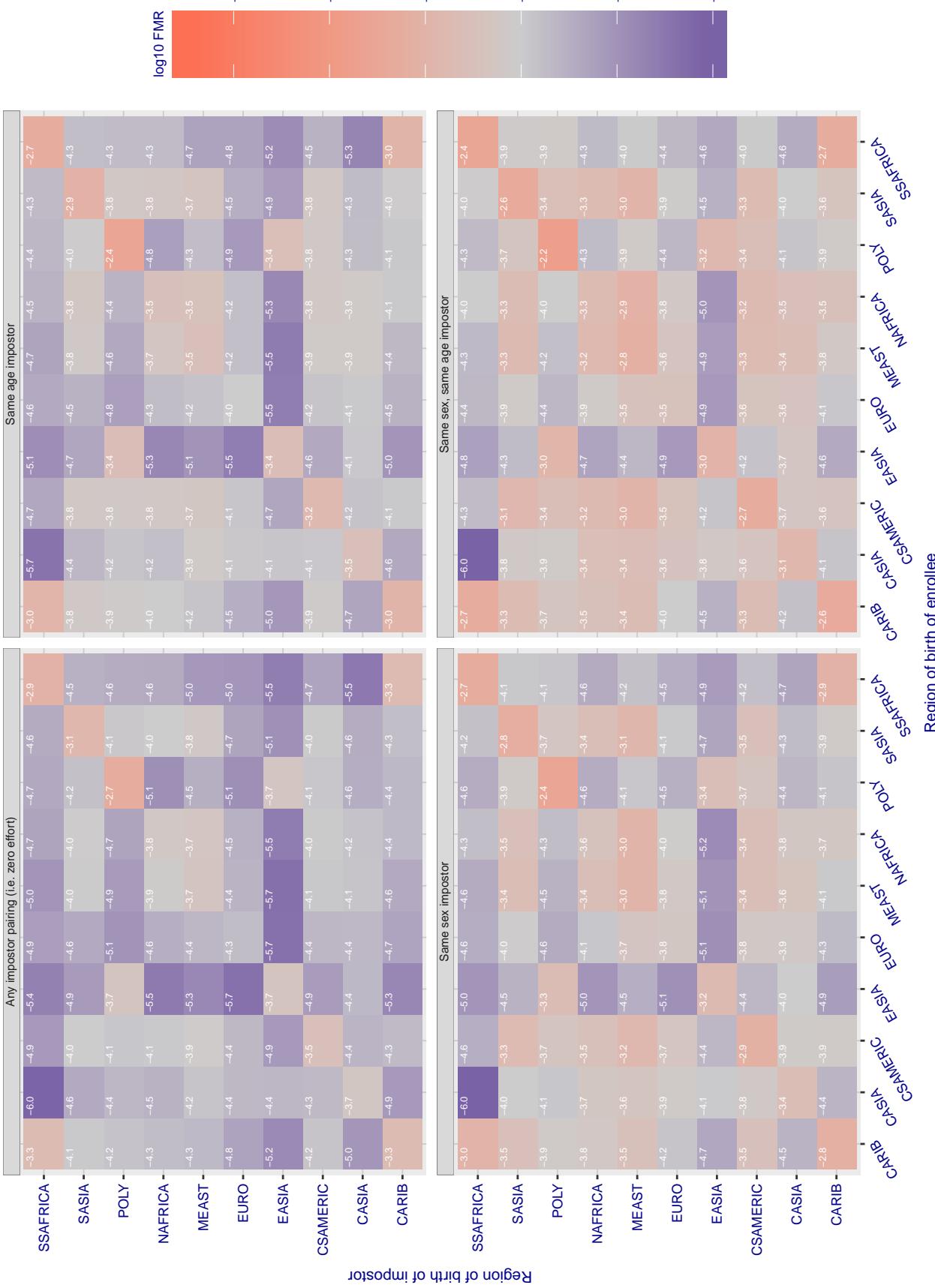
**Cross region FMR at threshold T = 0.823 for algorithm hr\_001, giving FMR(T) = 0.00001 globally.**

Figure 164: For algorithm hr-001 operating on visa images, the heatmap shows false match rates observed over impostor comparisons of faces from different individuals who were born in the given region pair. False matches are counted against a recognition threshold fixed globally to give the target FMR in the plot title, computed over all on the order of  $10^{10}$  impostor comparisons. If text appears in each box it give the same quantity as that coded by the color. Grey indicates FMR is at the intended FMR target level. Light red colors present a security vulnerability to, for example, a passport gate. Each +1 increase in  $\log_{10}$  FMR corresponds to a factor of 10 increase in FMR. The matrix is not quite symmetric because images in the enrollment and verification sets are different.

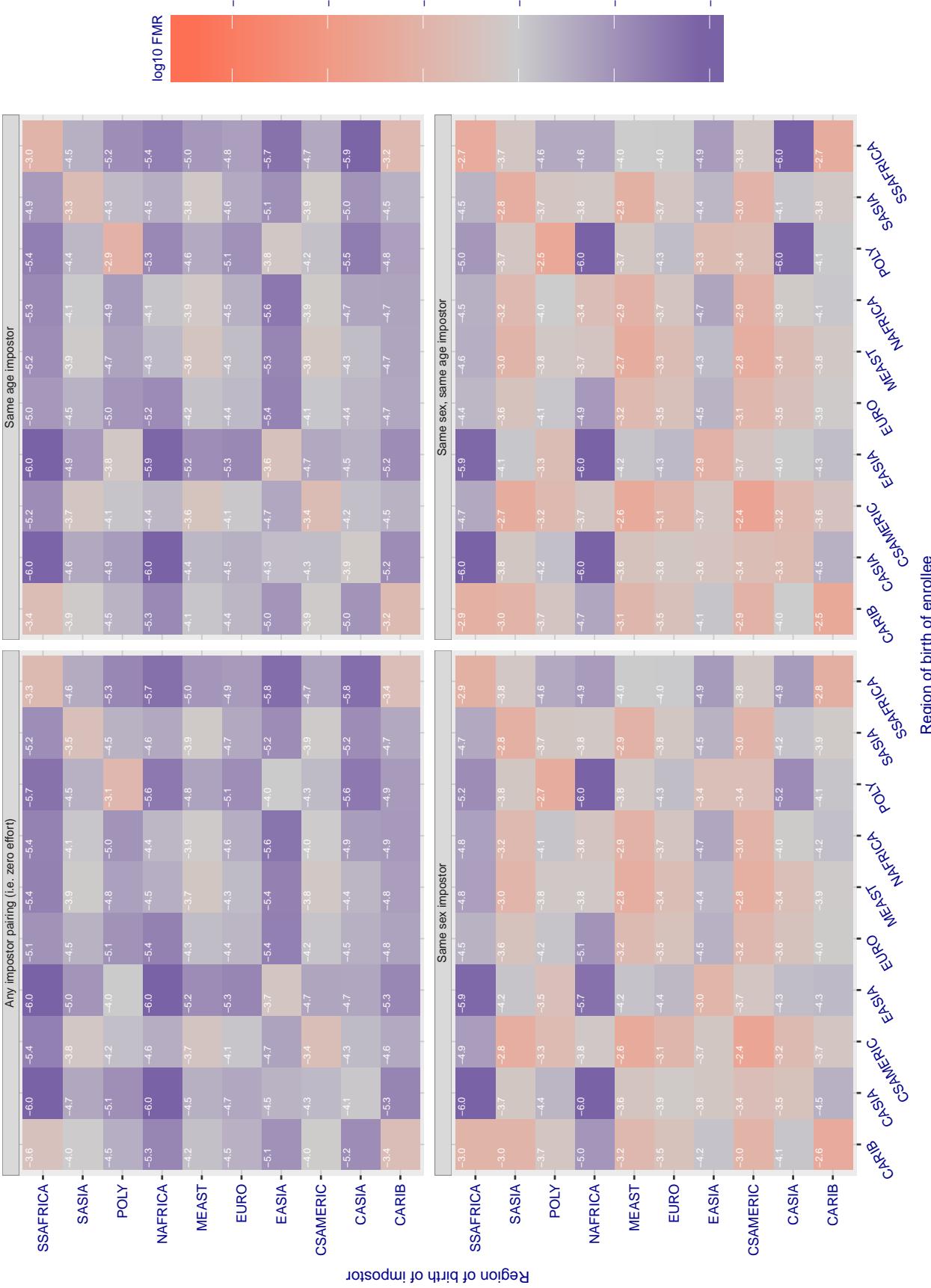
**Cross region FMR at threshold T = 37645.000 for algorithm id3\_003, giving FMR(T) = 0.0001 globally.**

Figure 165: For algorithm id3\_003 operating on visa images, the heatmap shows false match rates observed over impostor comparisons of faces from different individuals who were born in the given region pair. False matches are counted against a recognition threshold fixed globally to give the target FMR in the plot title, computed over all on the order of  $10^{10}$  impostor comparisons. If text appears in each box it give the same quantity as that coded by the color. Grey indicates FMR is at the intended FMR target level. Light red colors present a security vulnerability to, for example, a passport gate. Each +1 increase in  $\log_{10}$  FMR corresponds to a factor of 10 increase in FMR. The matrix is not quite symmetric because images in the enrollment and verification sets are different.

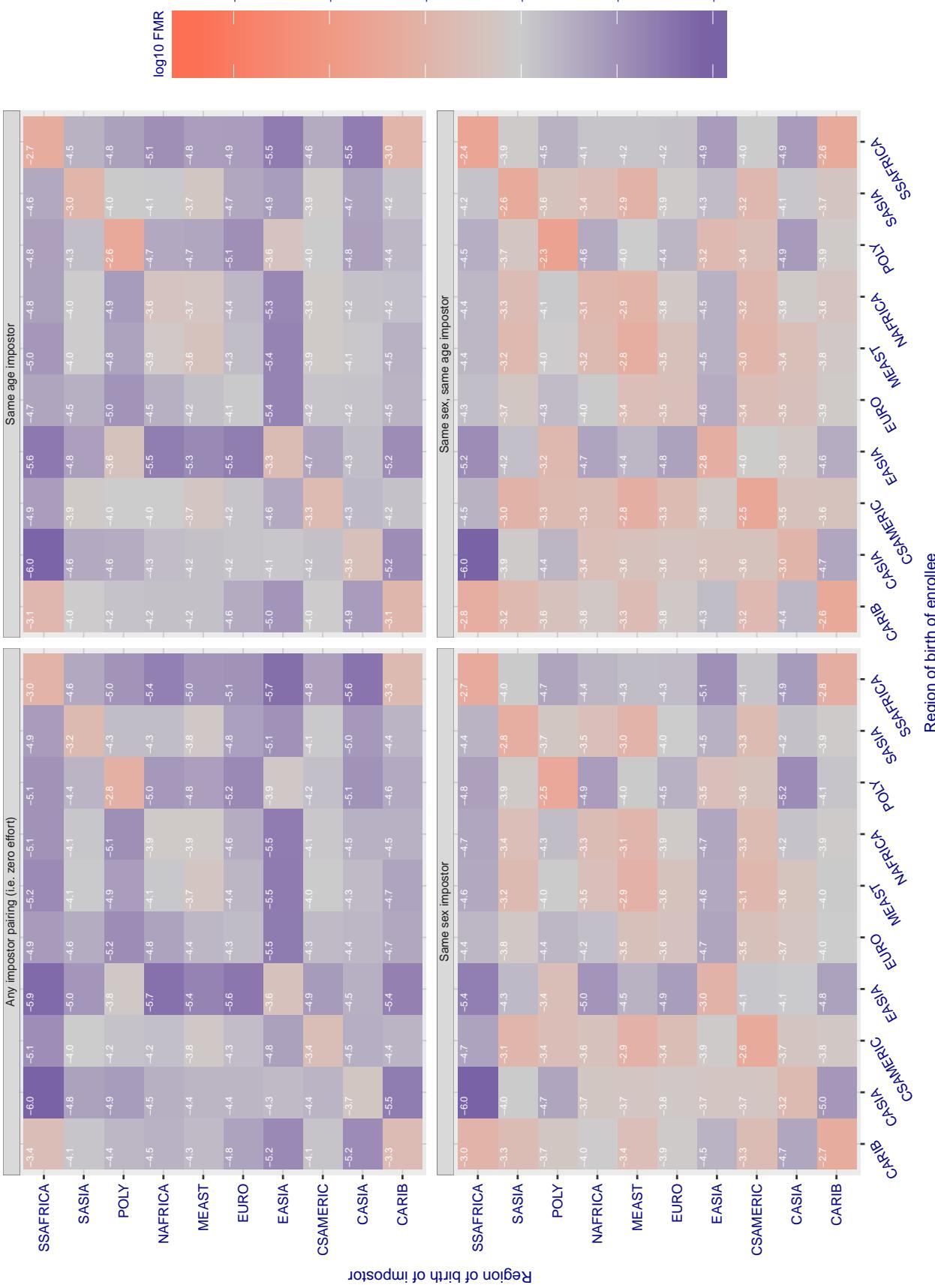
**Cross region FMR at threshold T = 37001.000 for algorithm id3\_004, giving FMR(T) = 0.0001 globally.**

Figure 166: For algorithm id3\_004 operating on visa images, the heatmap shows false match rates observed over impostor comparisons of faces from different individuals who were born in the given region pair. False matches are counted against a recognition threshold fixed globally to give the target FMR in the plot title, computed over all on the order of  $10^{10}$  impostor comparisons. If text appears in each box it give the same quantity as that coded by the color. Grey indicates FMR is at the intended FMR target level. Light red colors present a security vulnerability to, for example, a passport gate. Each +1 increase in  $\log_{10} \text{FMR}$  corresponds to a factor of 10 increase in FMR. The matrix is not quite symmetric because images in the enrollment and verification sets are different.

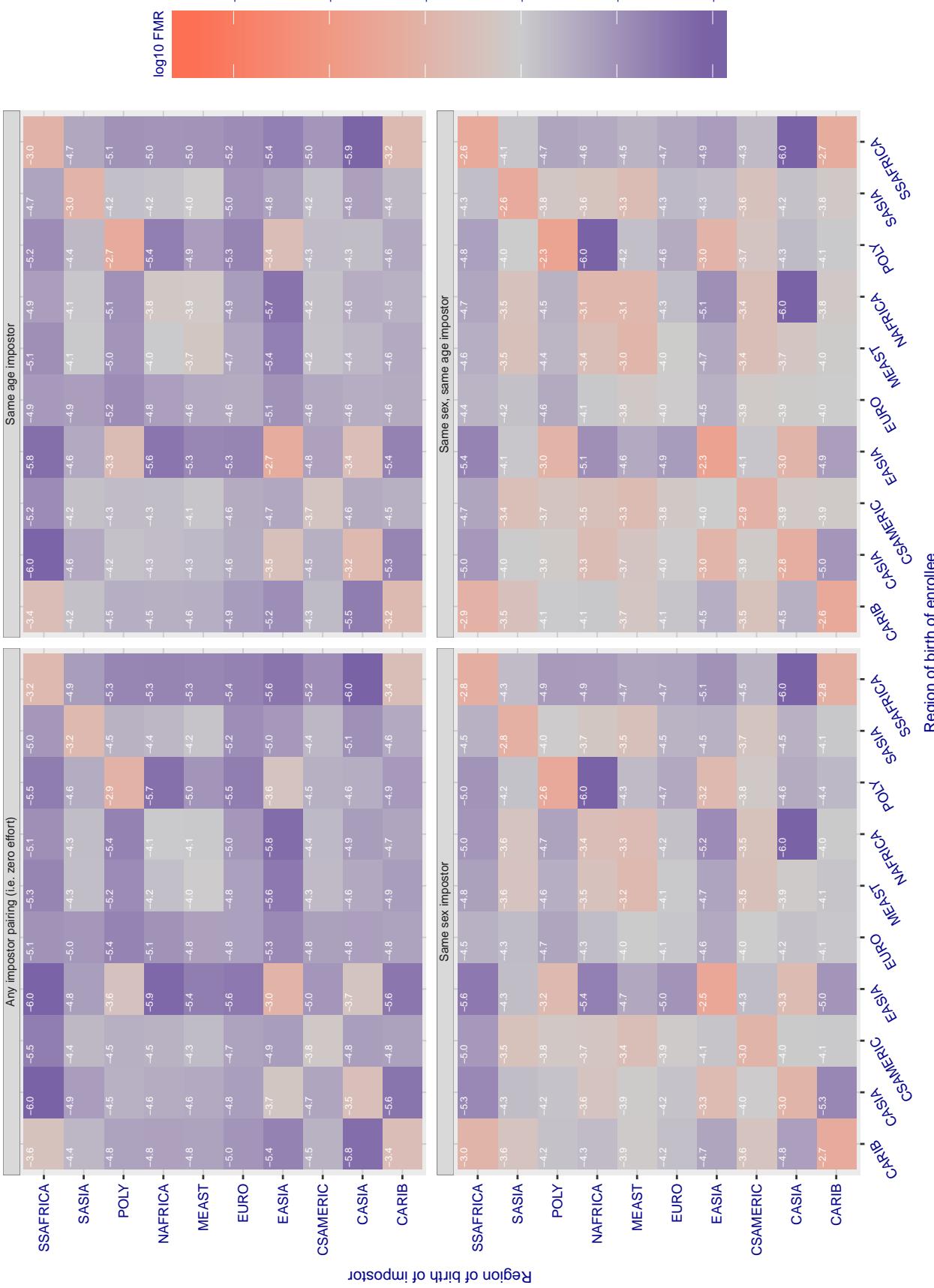
**Cross region FMR at threshold T = 3664.380 for algorithm idemia\_003, giving FMR(T) = 0.0001 globally.**

Figure 167: For algorithm idemia-003 operating on visa images, the heatmap shows false match rates observed over impostor comparisons of faces from different individuals who were born in the given region pair. False matches are counted against a recognition threshold fixed globally to give the target FMR in the plot title, computed over all on the order of  $10^{10}$  impostor comparisons. If text appears in each box it give the same quantity as that coded by the color. Grey indicates FMR is at the intended FMR target level. Light red colors present a security vulnerability to, for example, a passport gate. Each +1 increase in  $\log_{10} FMR$  corresponds to a factor of 10 increase in FMR. The matrix is not quite symmetric because images in the enrollment and verification sets are different.

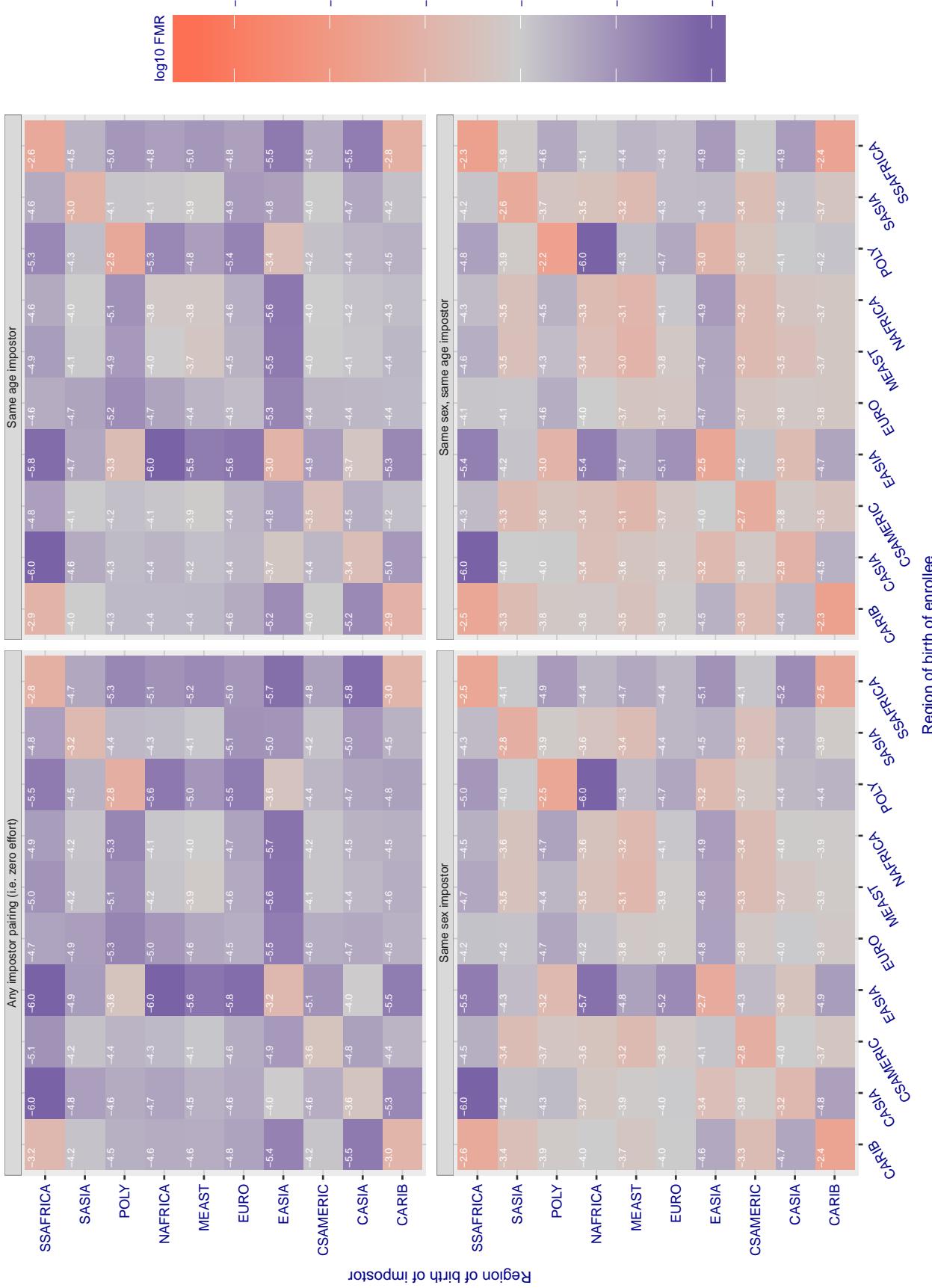
**Cross region FMR at threshold T = 3925.463 for algorithm idemia\_004, giving FMR(T) = 0.0001 globally.**

Figure 168: For algorithm idemia-004 operating on visa images, the heatmap shows false match rates observed over impostor comparisons of faces from different individuals who were born in the given region pair. False matches are counted against a recognition threshold fixed globally to give the target FMR in the plot title, computed over all on the order of  $10^{10}$  impostor comparisons. If text appears in each box it give the same quantity as that coded by the color. Grey indicates FMR is at the intended FMR target level. Light red colors present a security vulnerability to, for example, a passport gate. Each +1 increase in  $\log_{10} \text{FMR}$  corresponds to a factor of 10 increase in FMR. The matrix is not quite symmetric because images in the enrollment and verification sets are different.

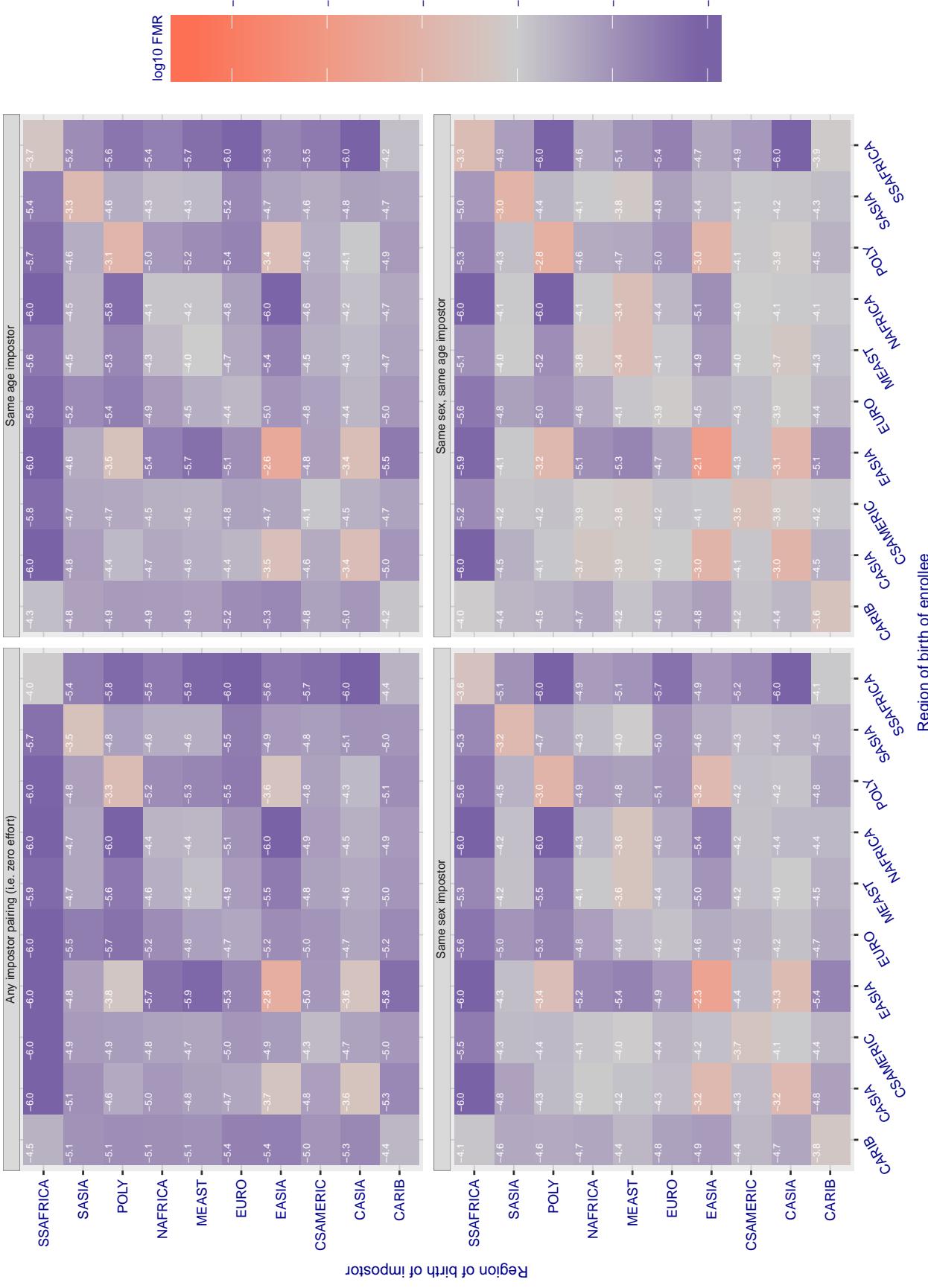
**Cross region FMR at threshold T = 0.760 for algorithm iit\_000, giving FMR(T) = 0.0001 globally.**

Figure 169: For algorithm iit-000 operating on visa images, the heatmap shows false match rates observed over impostor comparisons of faces from different individuals who were born in the given region pair. False matches are counted against a recognition threshold fixed globally to give the target FMR in the plot title, computed over all on the order of  $10^{10}$  impostor comparisons. If text appears in each box it give the same quantity as that coded by the color. Grey indicates FMR is at the intended FMR target level. Light red colors present a security vulnerability to, for example, a passport gate. Each +1 increase in  $\log_{10} \text{FMR}$  corresponds to a factor of 10 increase in FMR. The matrix is not quite symmetric because images in the enrollment and verification sets are different.

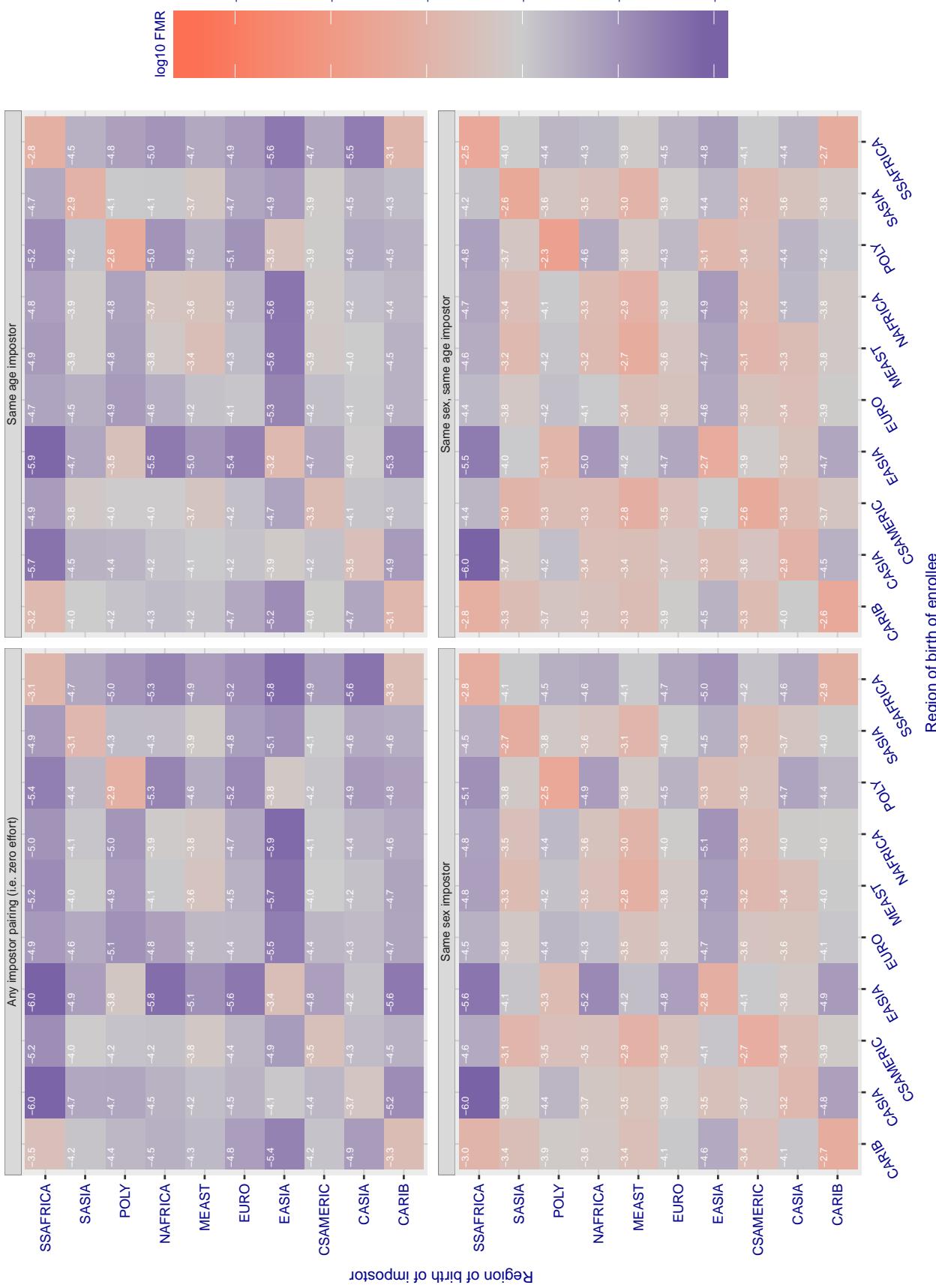
**Cross region FMR at threshold T = 0.926 for algorithm imagus\_000, giving FMR(T) = 0.0001 globally.**

Figure 170: For algorithm imagus-000 operating on visa images, the heatmap shows false match rates observed over impostor comparisons of faces from different individuals who were born in the given region pair. False matches are counted against a recognition threshold fixed globally to give the target FMR in the plot title, computed over all on the order of  $10^{10}$  impostor comparisons. If text appears in each box it give the same quantity as that coded by the color. Grey indicates FMR is at the intended FMR target level. Light red colors present a security vulnerability to, for example, a passport gate. Each +1 increase in  $\log_{10} FMR$  corresponds to a factor of 10 increase in FMR. The matrix is not quite symmetric because images in the enrollment and verification sets are different.

### Cross region FMR at threshold T = 1.375 for algorithm imperial\_000, giving FMR(T) = 0.0001 globally.

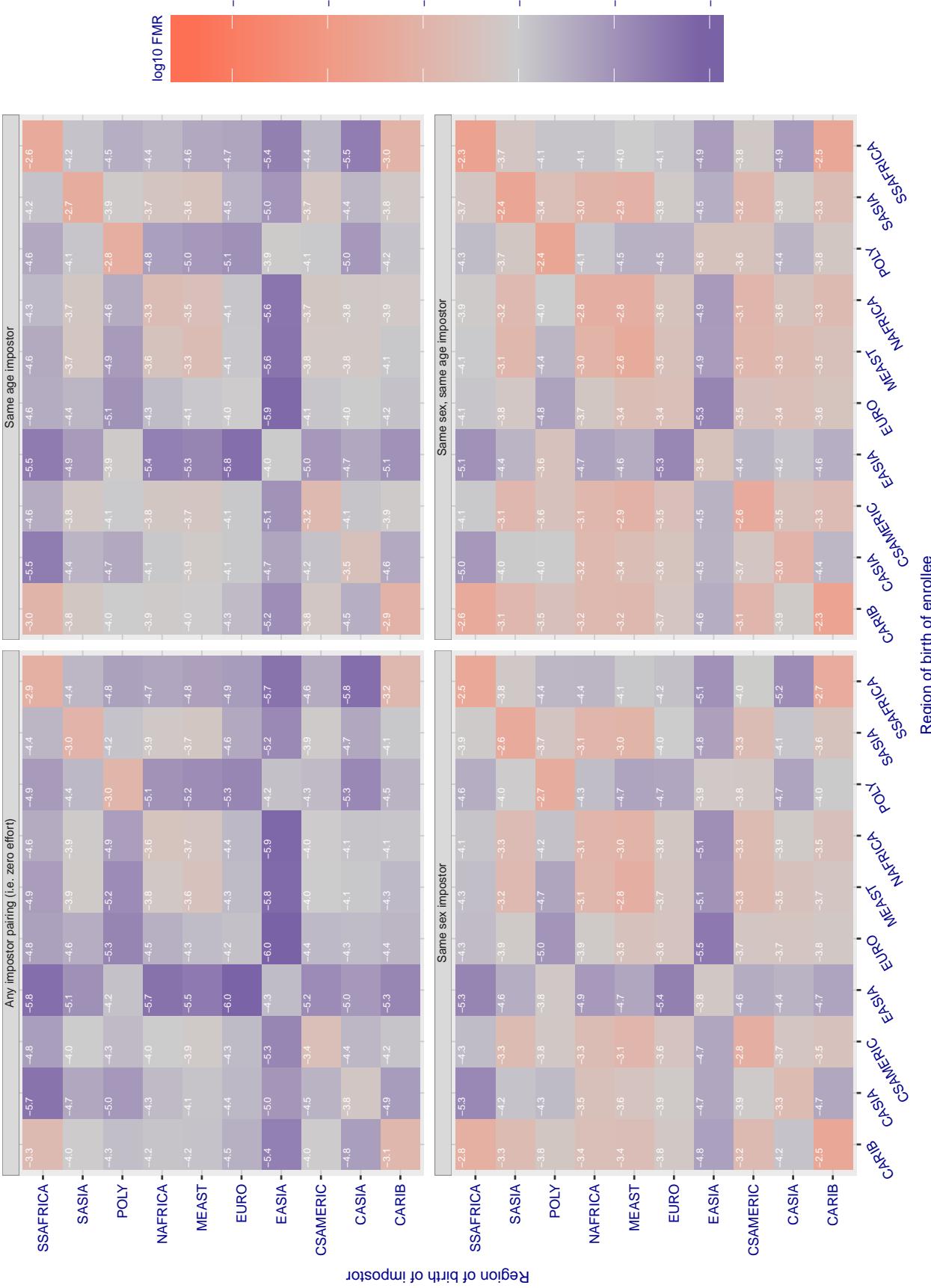


Figure 171: For algorithm imperial-000 operating on visa images, the heatmap shows false match rates observed over impostor comparisons of faces from different individuals who were born in the given region pair. False matches are counted against a recognition threshold fixed globally to give the target FMR in the plot title, computed over all on the order of  $10^{10}$  impostor comparisons. If text appears in each box it give the same quantity as that coded by the color. Grey indicates FMR is at the intended FMR target level. Light red colors present a security vulnerability to, for example, a passport gate. Each +1 increase in  $\log_{10} FMR$  corresponds to a factor of 10 increase in FMR. The matrix is not quite symmetric because images in the enrollment and verification sets are different.

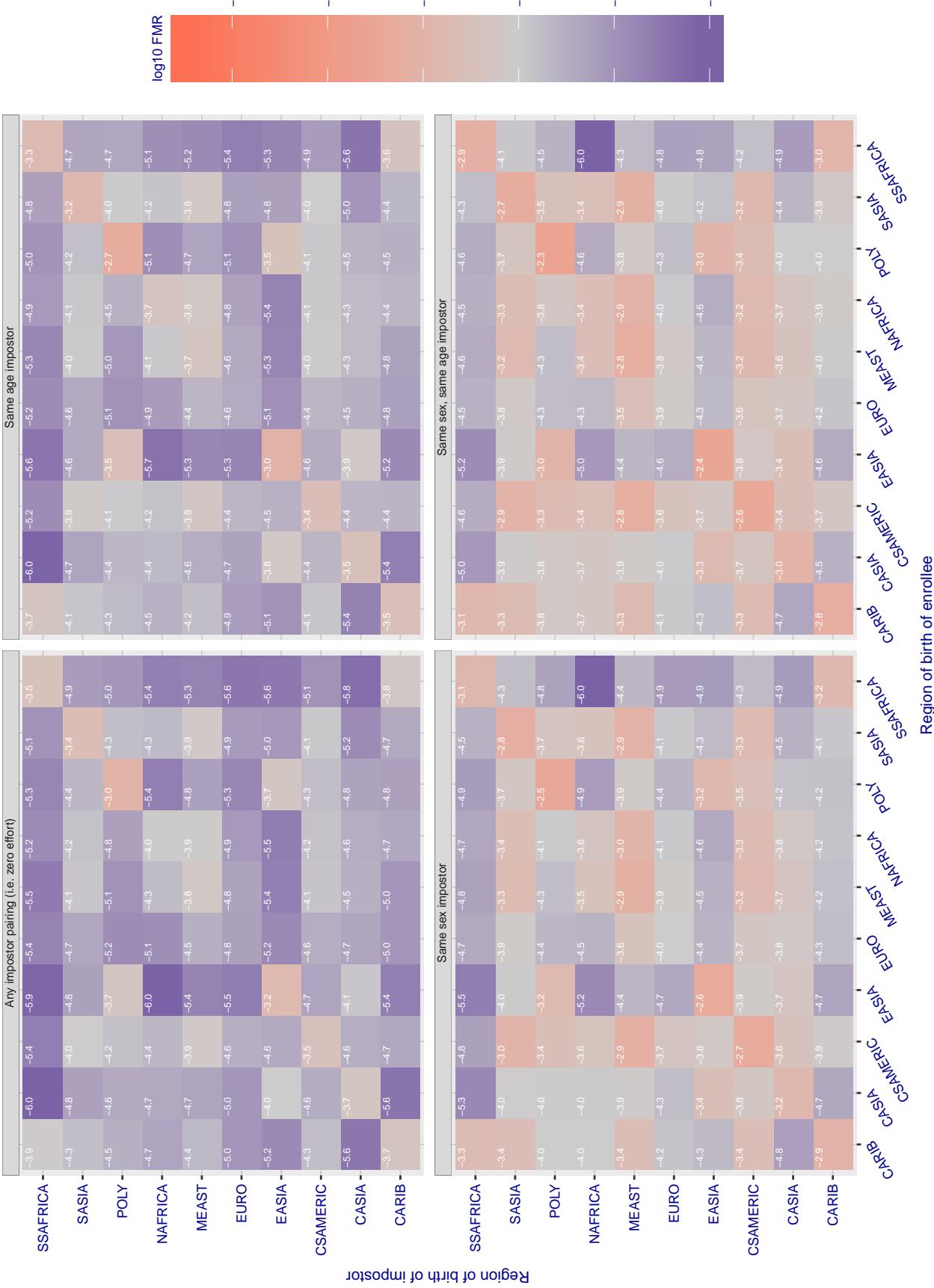
**Cross region FMR at threshold T = 1.402 for algorithm imperial\_001, giving FMR(T) = 0.0001 globally.**

Figure 172: For algorithm imperial-001 operating on visa images, the heatmap shows false match rates observed over impostor comparisons of faces from different individuals who were born in the given region pair. False matches are counted against a recognition threshold fixed globally to give the target FMR in the plot title, computed over all on the order of  $10^{10}$  impostor comparisons. If text appears in each box it give the same quantity as that coded by the color. Grey indicates FMR is at the intended FMR target level. Light red colors present a security vulnerability to, for example, a passport gate. Each +1 increase in  $\log_{10} FMR$  corresponds to a factor of 10 increase in FMR. The matrix is not quite symmetric because images in the enrollment and verification sets are different.

### Cross region FMR at threshold T = 1.427 for algorithm incode\_003, giving FMR(T) = 0.0001 globally.

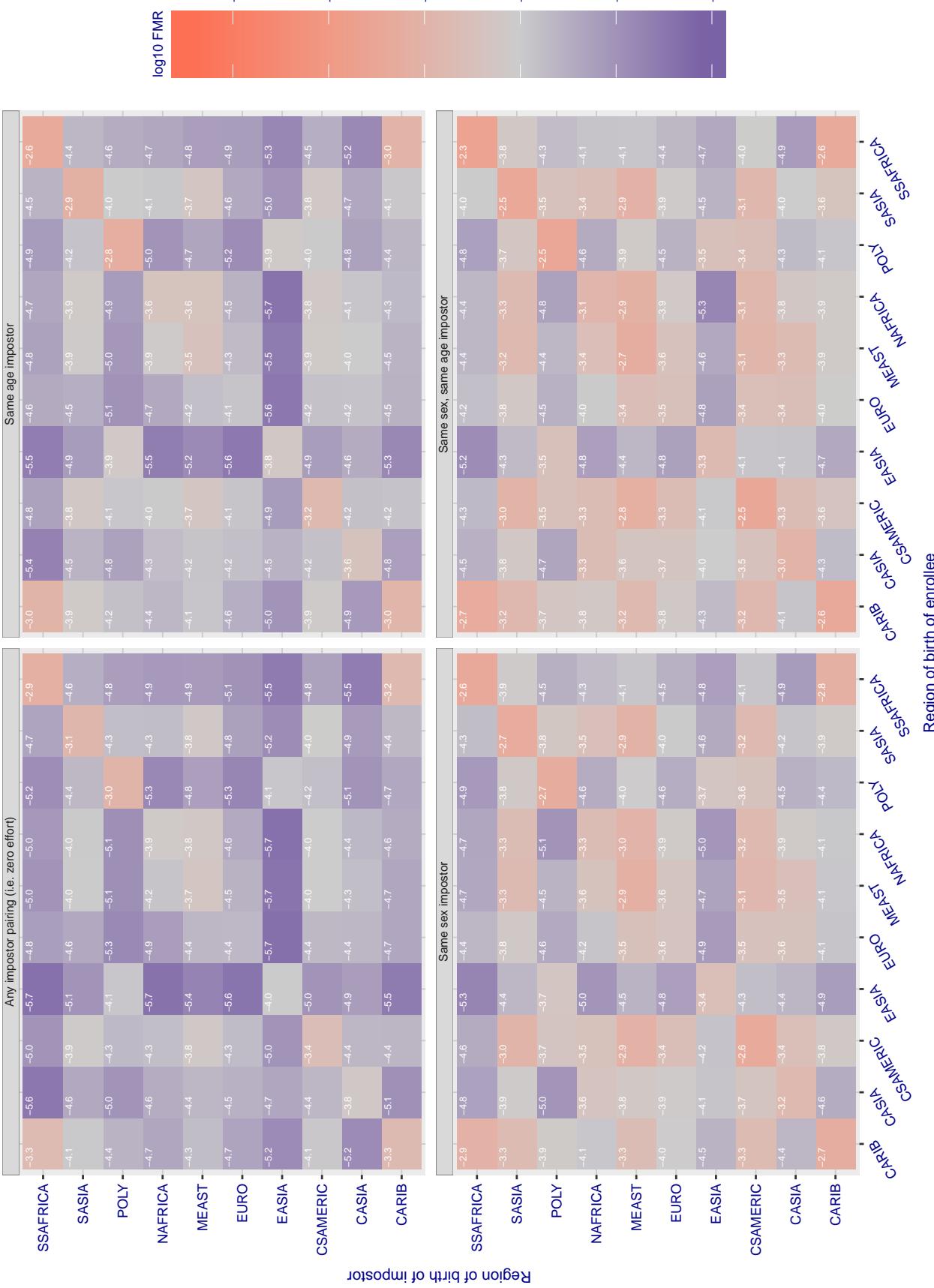


Figure 173: For algorithm incode-003 operating on visa images, the heatmap shows false match rates observed over impostor comparisons of faces from different individuals who were born in the given region pair. False matches are counted against a recognition threshold fixed globally to give the target FMR in the plot title, computed over all on the order of  $10^{10}$  impostor comparisons. If text appears in each box it give the same quantity as that coded by the color. Grey indicates FMR is at the intended FMR target level. Light red colors present a security vulnerability to, for example, a passport gate. Each +1 increase in  $\log_{10} FMR$  corresponds to a factor of 10 increase in FMR. The matrix is not quite symmetric because images in the enrollment and verification sets are different.

### Cross region FMR at threshold T = 1.398 for algorithm incode\_004, giving FMR(T) = 0.0001 globally.

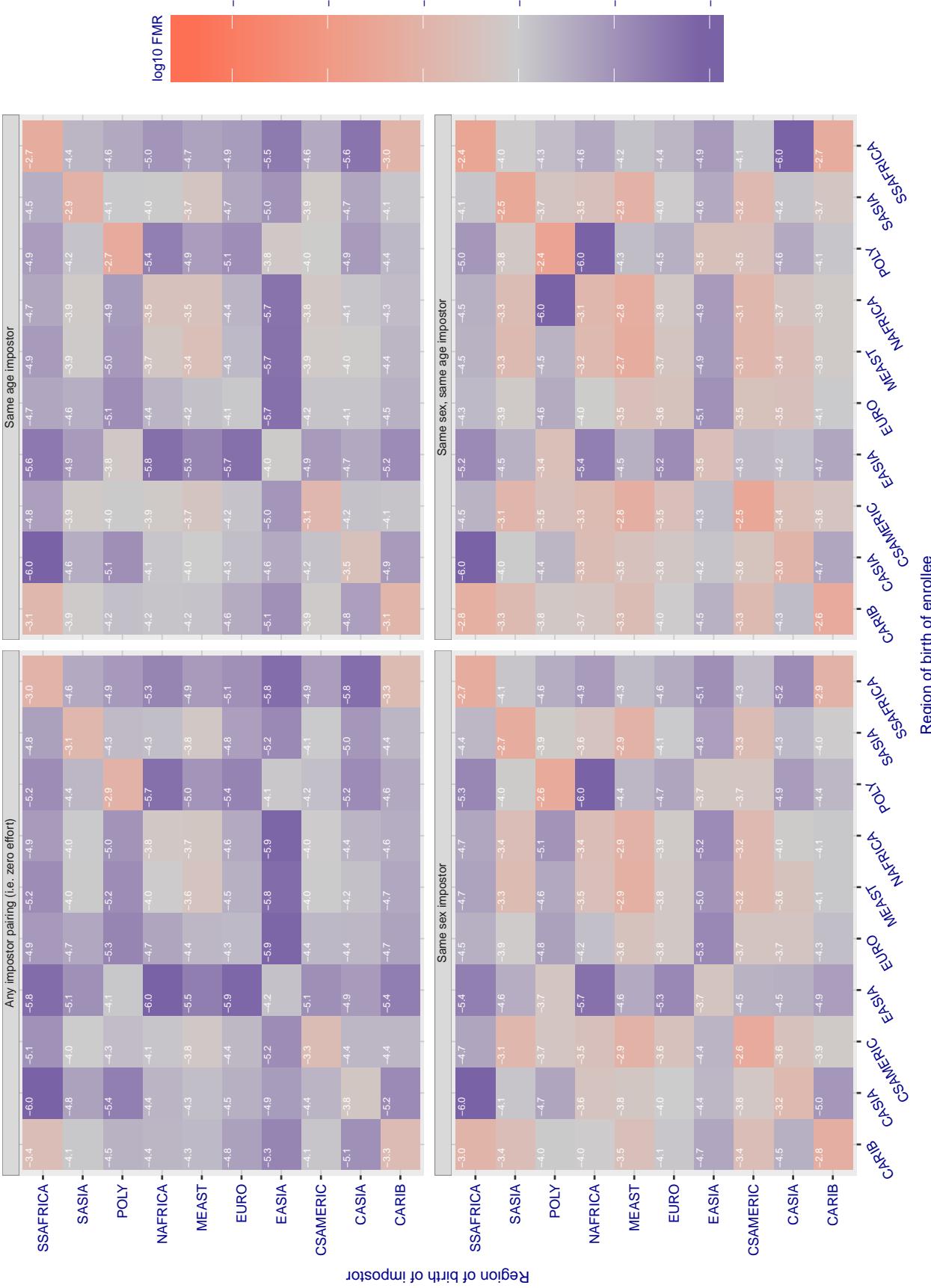


Figure 174: For algorithm incode-004 operating on visa images, the heatmap shows false match rates observed over impostor comparisons of faces from different individuals who were born in the given region pair. False matches are counted against a recognition threshold fixed globally to give the target FMR in the plot title, computed over all on the order of  $10^{10}$  impostor comparisons. If text appears in each box it give the same quantity as that coded by the color. Grey indicates FMR is at the intended FMR target level. Light red colors present a security vulnerability to, for example, a passport gate. Each +1 increase in  $\log_{10} \text{FMR}$  corresponds to a factor of 10 increase in FMR. The matrix is not quite symmetric because images in the enrollment and verification sets are different.

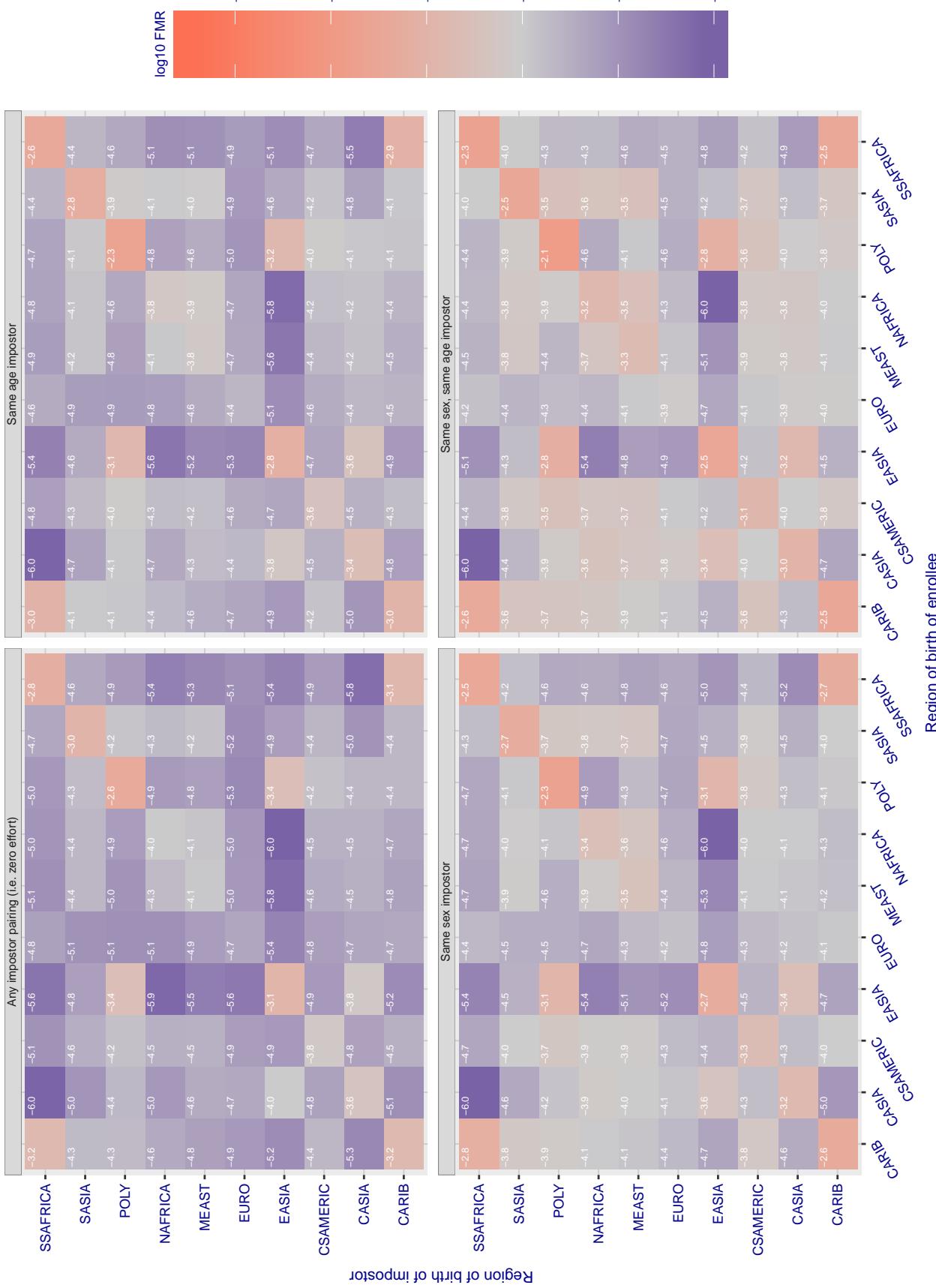
**Cross region FMR at threshold T = 29.232 for algorithm innovatrics\_004, giving FMR(T) = 0.0001 globally.**

Figure 175: For algorithm innovatrics-004 operating on visa images, the heatmap shows false match rates observed over impostor comparisons of faces from different individuals who were born in the given region pair. False matches are counted against a recognition threshold fixed globally to give the target FMR in the plot title, computed over all on the order of  $10^{10}$  impostor comparisons. If text appears in each box it give the same quantity as that coded by the color. Grey indicates FMR is at the intended FMR target level. Light red colors present a security vulnerability to, for example, a passport gate. Each +1 increase in  $\log_{10} FMR$  corresponds to a factor of 10 increase in FMR. The matrix is not quite symmetric because images in the enrollment and verification sets are different.

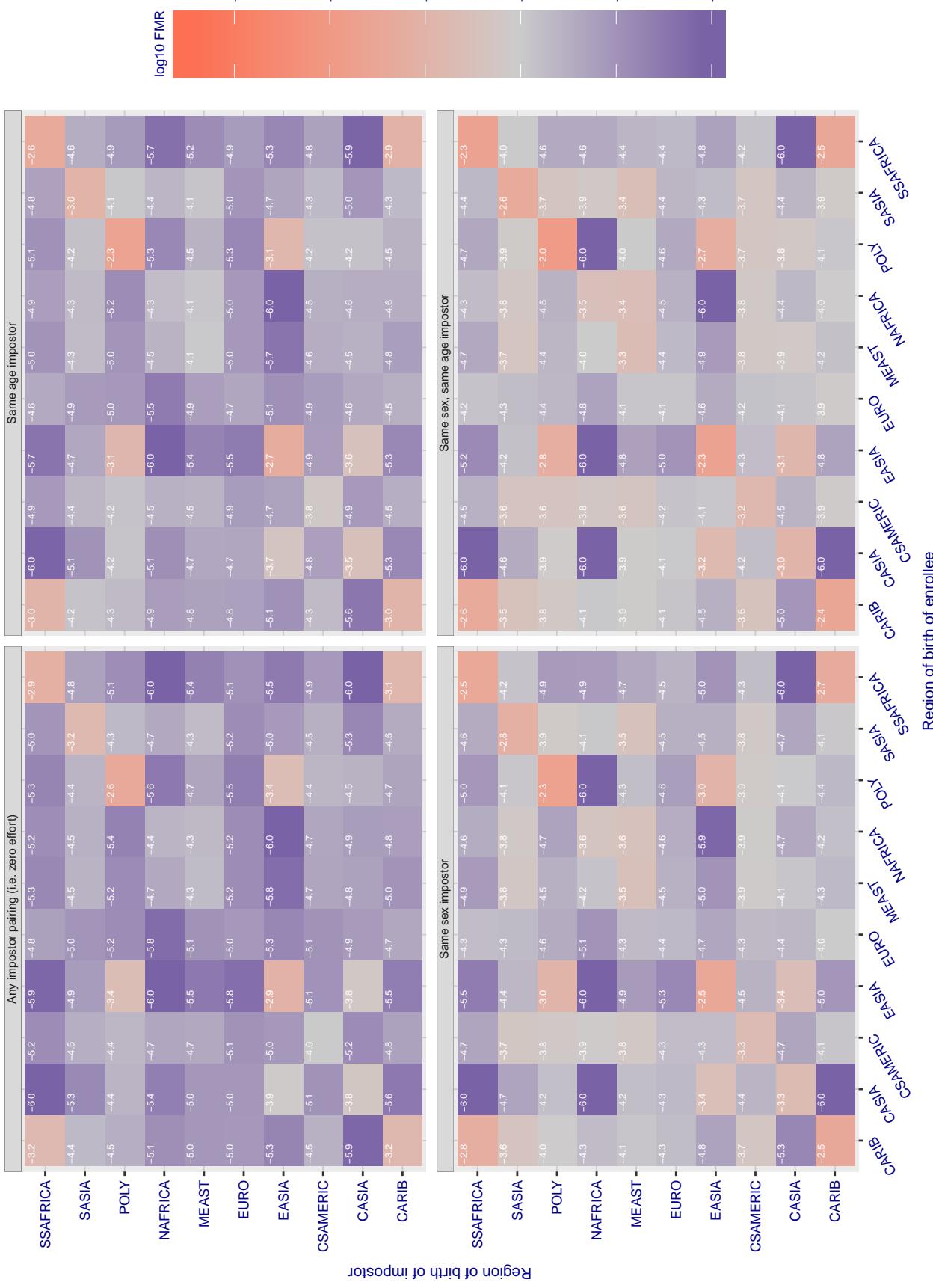
**Cross region FMR at threshold T = 40.157 for algorithm innovatrics\_005, giving FMR(T) = 0.0001 globally.**

Figure 176: For algorithm innovatrics-005 operating on visa images, the heatmap shows false match rates observed over impostor comparisons of faces from different individuals who were born in the given region pair. False matches are counted against a recognition threshold fixed globally to give the target FMR in the plot title, computed over all on the order of  $10^{10}$  impostor comparisons. If text appears in each box it give the same quantity as that coded by the color. Grey indicates FMR is at the intended FMR target level. Light red colors present a security vulnerability to, for example, a passport gate. Each +1 increase in  $\log_{10} FMR$  corresponds to a factor of 10 increase in FMR. The matrix is not quite symmetric because images in the enrollment and verification sets are different.

### Cross region FMR at threshold T = 49.664 for algorithm intellivision\_001, giving FMR(T) = 0.0001 globally.

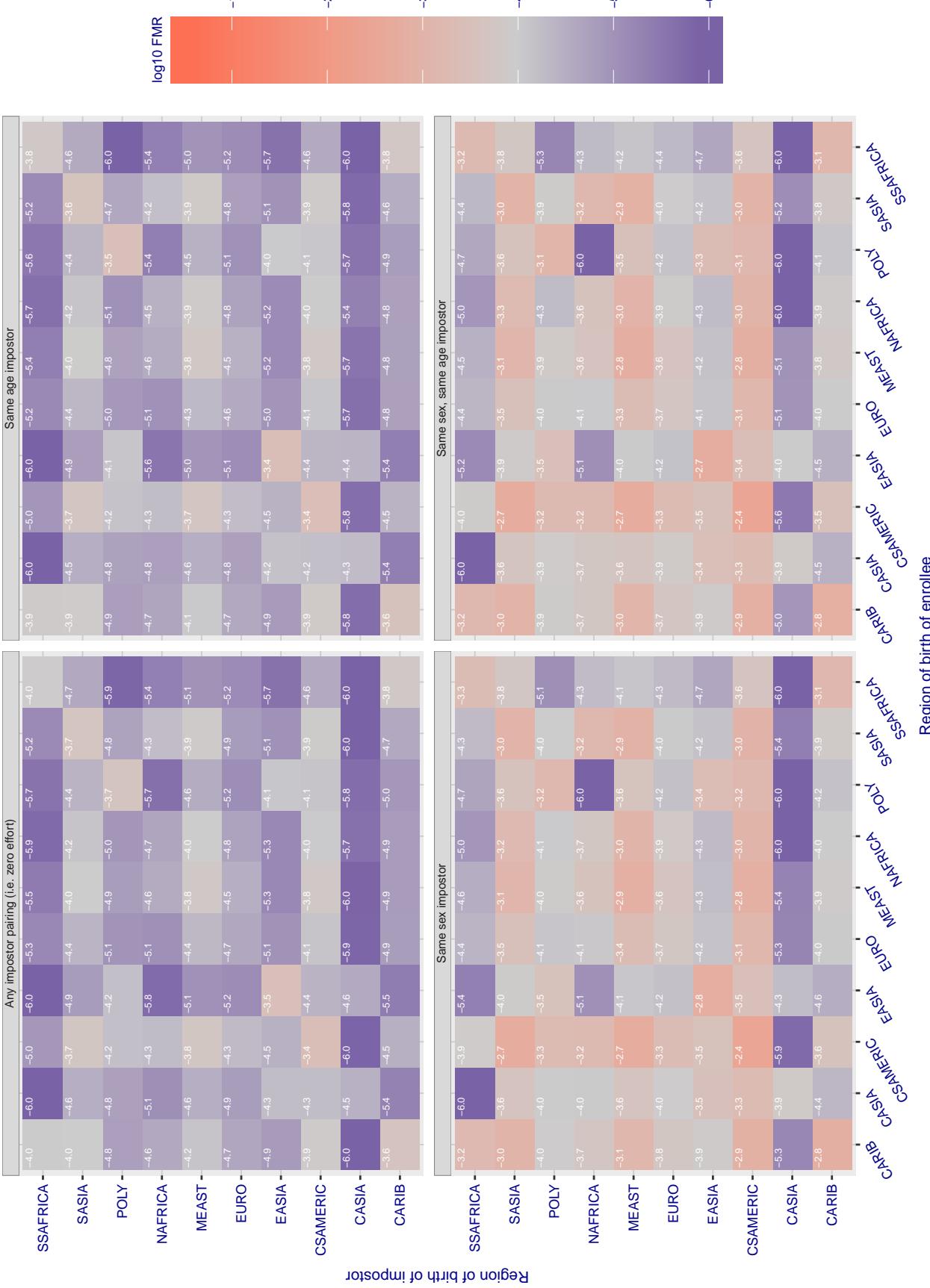


Figure 177: For algorithm intellivision-001 operating on visa images, the heatmap shows false match rates observed over impostor comparisons of faces from different individuals who were born in the given region pair. False matches are counted against a recognition threshold fixed globally to give the target FMR in the plot title, computed over all on the order of  $10^{10}$  impostor comparisons. If text appears in each box it give the same quantity as that coded by the color. Grey indicates FMR is at the intended FMR target level. Light red colors present a security vulnerability to, for example, a passport gate. Each +1 increase in  $\log_{10} FMR$  corresponds to a factor of 10 increase in FMR. The matrix is not quite symmetric because images in the enrollment and verification sets are different.

### Cross region FMR at threshold T = 1.361 for algorithm iiface\_000, giving FMR(T) = 0.0001 globally.

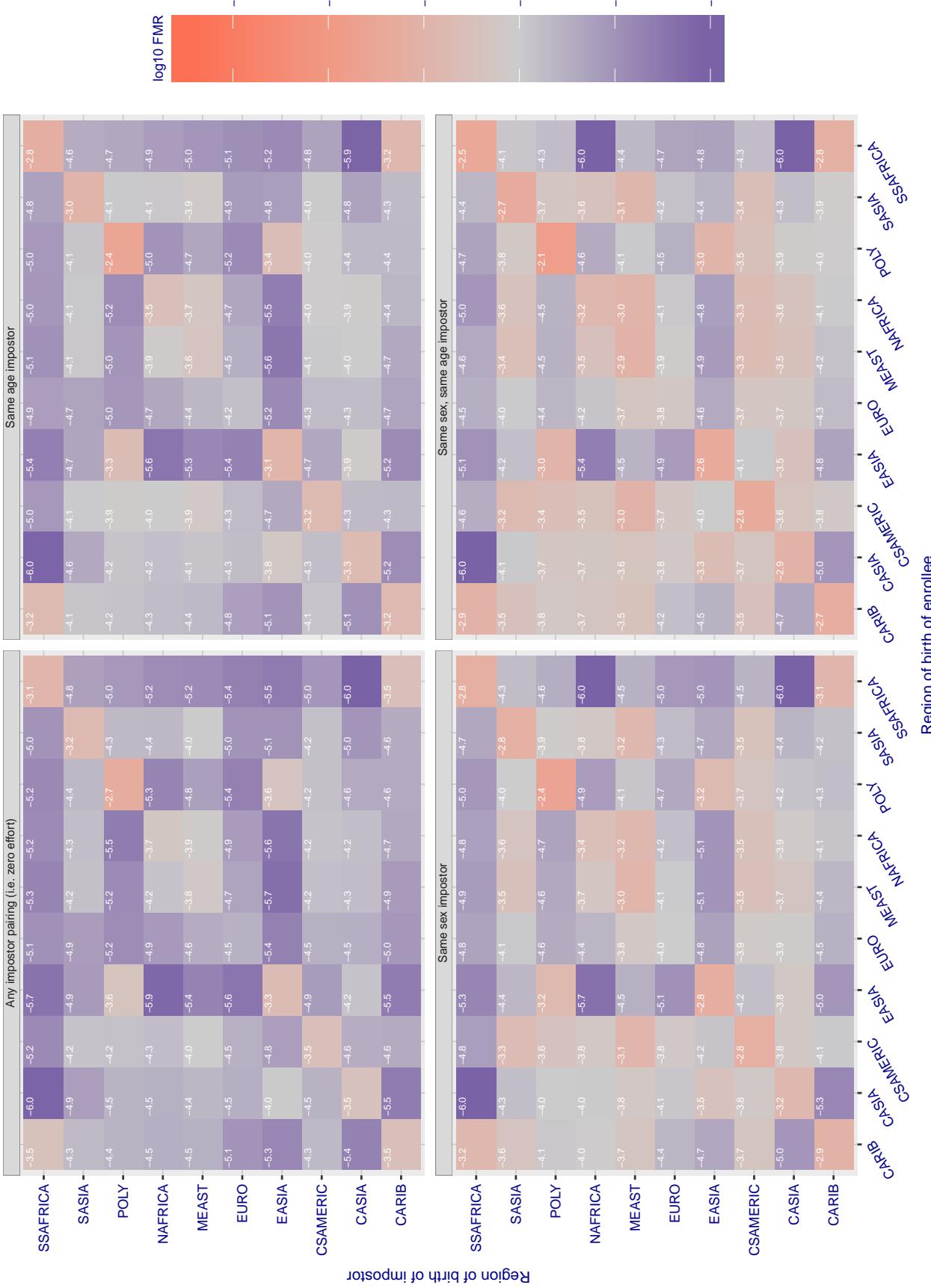


Figure 178: For algorithm iiface-000 operating on visa images, the heatmap shows false match rates observed over impostor comparisons of faces from different individuals who were born in the given region pair. False matches are counted against a recognition threshold fixed globally to give the target FMR in the plot title, computed over all on the order of  $10^{10}$  impostor comparisons. If text appears in each box it give the same quantity as that coded by the color. Grey indicates FMR is at the intended FMR target level. Light red colors present a security vulnerability to, for example, a passport gate. Each +1 increase in  $\log_{10} FMR$  corresponds to a factor of 10 increase in FMR. The matrix is not quite symmetric because images in the enrollment and verification sets are different.

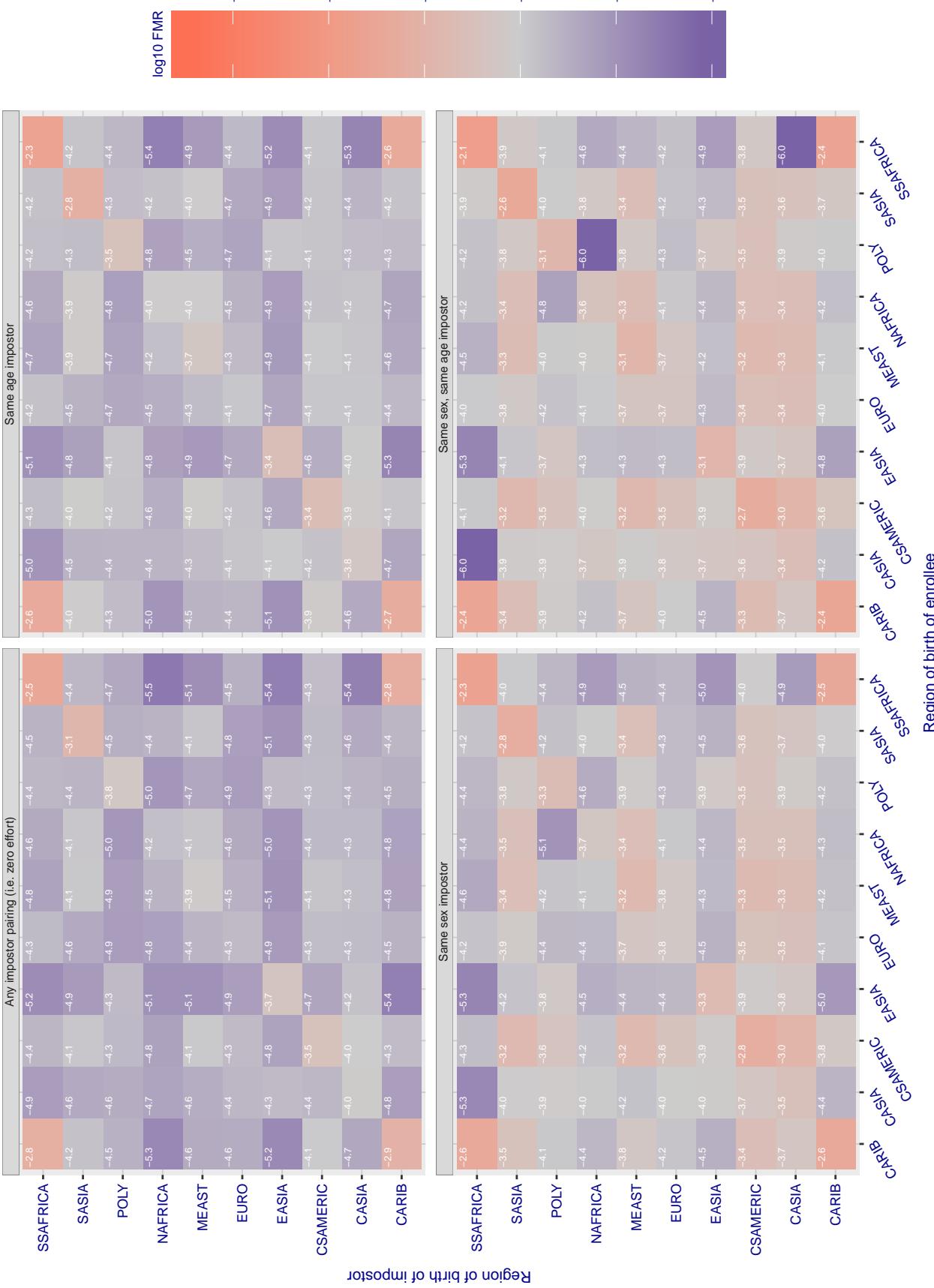
**Cross region FMR at threshold T = 23.498 for algorithm isityou\_000, giving FMR(T) = 0.0001 globally.**

Figure 179: For algorithm isityou-000 operating on visa images, the heatmap shows false match rates observed over impostor comparisons of faces from different individuals who were born in the given region pair. False matches are counted against a recognition threshold fixed globally to give the target FMR in the plot title, computed over all on the order of  $10^{10}$  impostor comparisons. If text appears in each box it give the same quantity as that coded by the color. Grey indicates FMR is at the intended FMR target level. Light red colors present a security vulnerability to, for example, a passport gate. Each +1 increase in  $\log_{10} FMR$  corresponds to a factor of 10 increase in FMR. The matrix is not quite symmetric because images in the enrollment and verification sets are different.

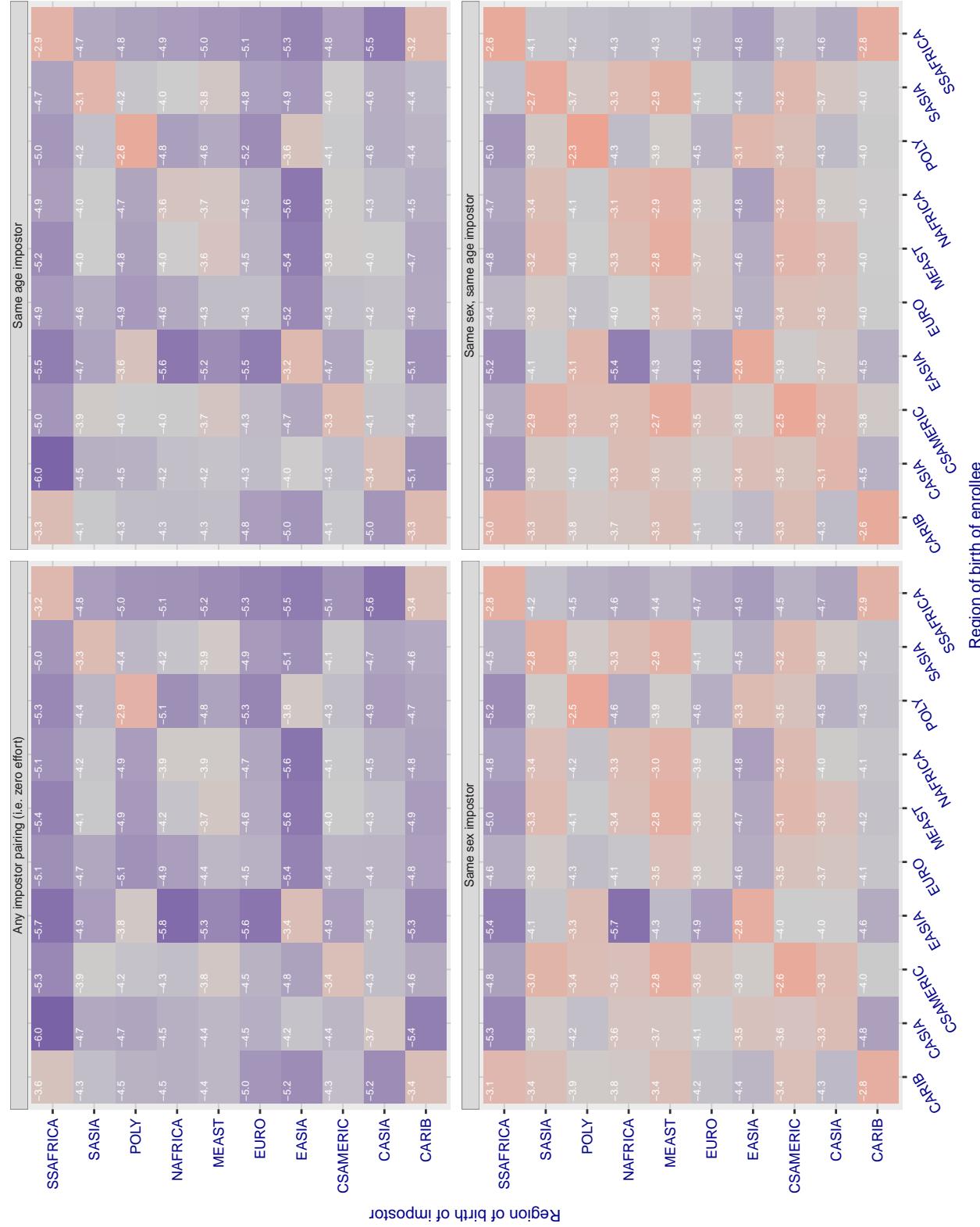


Figure 180: For algorithm isystems-001 operating on visa images, the heatmap shows false match rates observed over impostor comparisons of faces from different individuals who were born in the given region pair. False matches are counted against a recognition threshold fixed globally to give the target FMR in the plot title, computed over all on the order of  $10^{10}$  impostor comparisons. If text appears in each box it give the same quantity as that coded by the color. Grey indicates FMR is at the intended FMR target level. Light red colors present a security vulnerability to, for example, a passport gate. Each +1 increase in  $\log_{10}$  FMR corresponds to a factor of 10 increase in FMR. The matrix is not quite symmetric because images in the enrollment and verification sets are different.

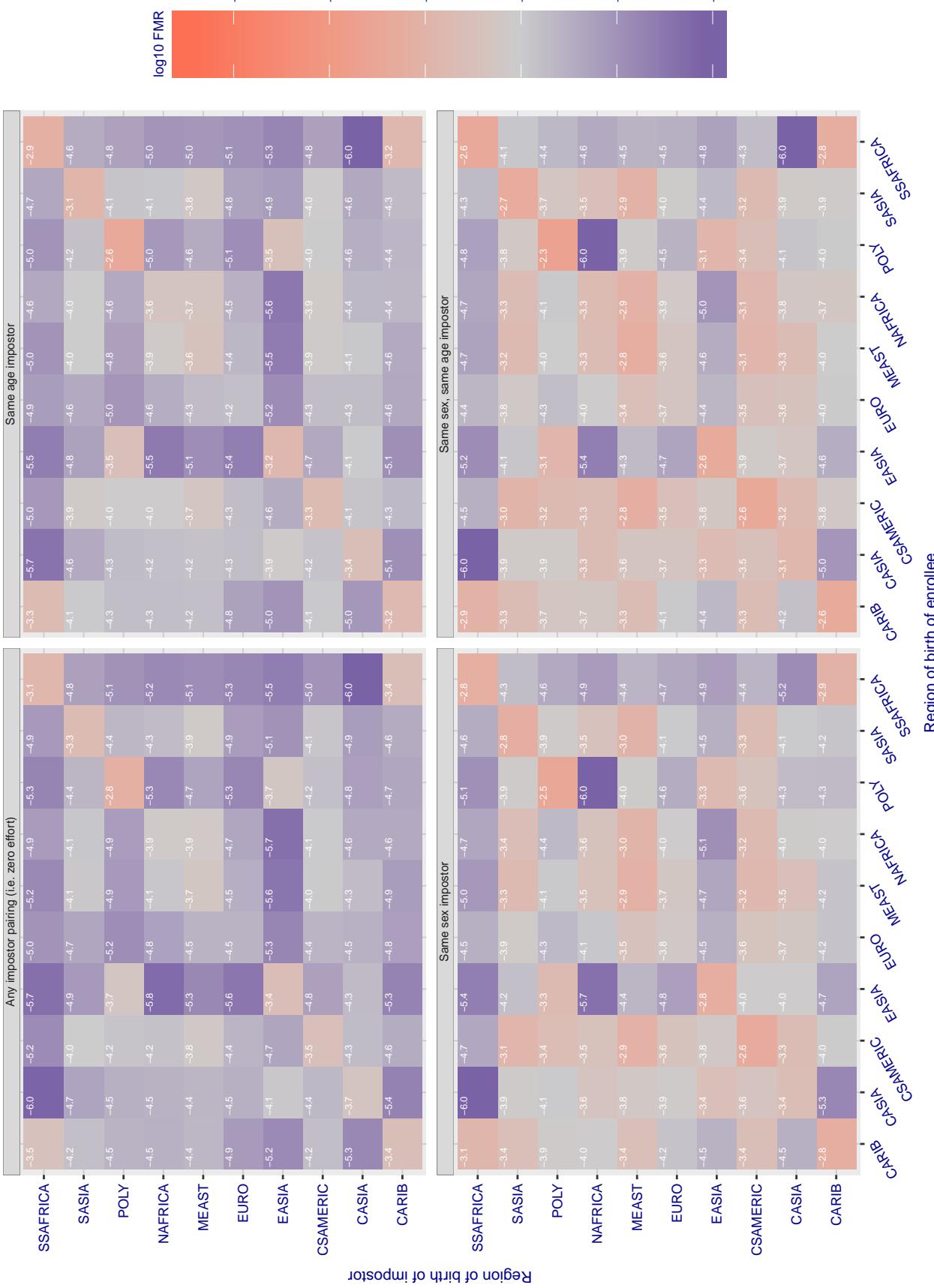
**Cross region FMR at threshold T = 0.690 for algorithm systems\_002, giving FMR(T) = 0.00001 globally.**

Figure 181: For algorithm systems-002 operating on visa images, the heatmap shows false match rates observed over impostor comparisons of faces from different individuals who were born in the given region pair. False matches are counted against a recognition threshold fixed globally to give the target FMR in the plot title, computed over all on the order of  $10^{10}$  impostor comparisons. If text appears in each box it give the same quantity as that coded by the color. Grey indicates FMR is at the intended FMR target level. Light red colors present a security vulnerability to, for example, a passport gate. Each +1 increase in  $\log_{10} FMR$  corresponds to a factor of 10 increase in FMR. The matrix is not quite symmetric because images in the enrollment and verification sets are different.

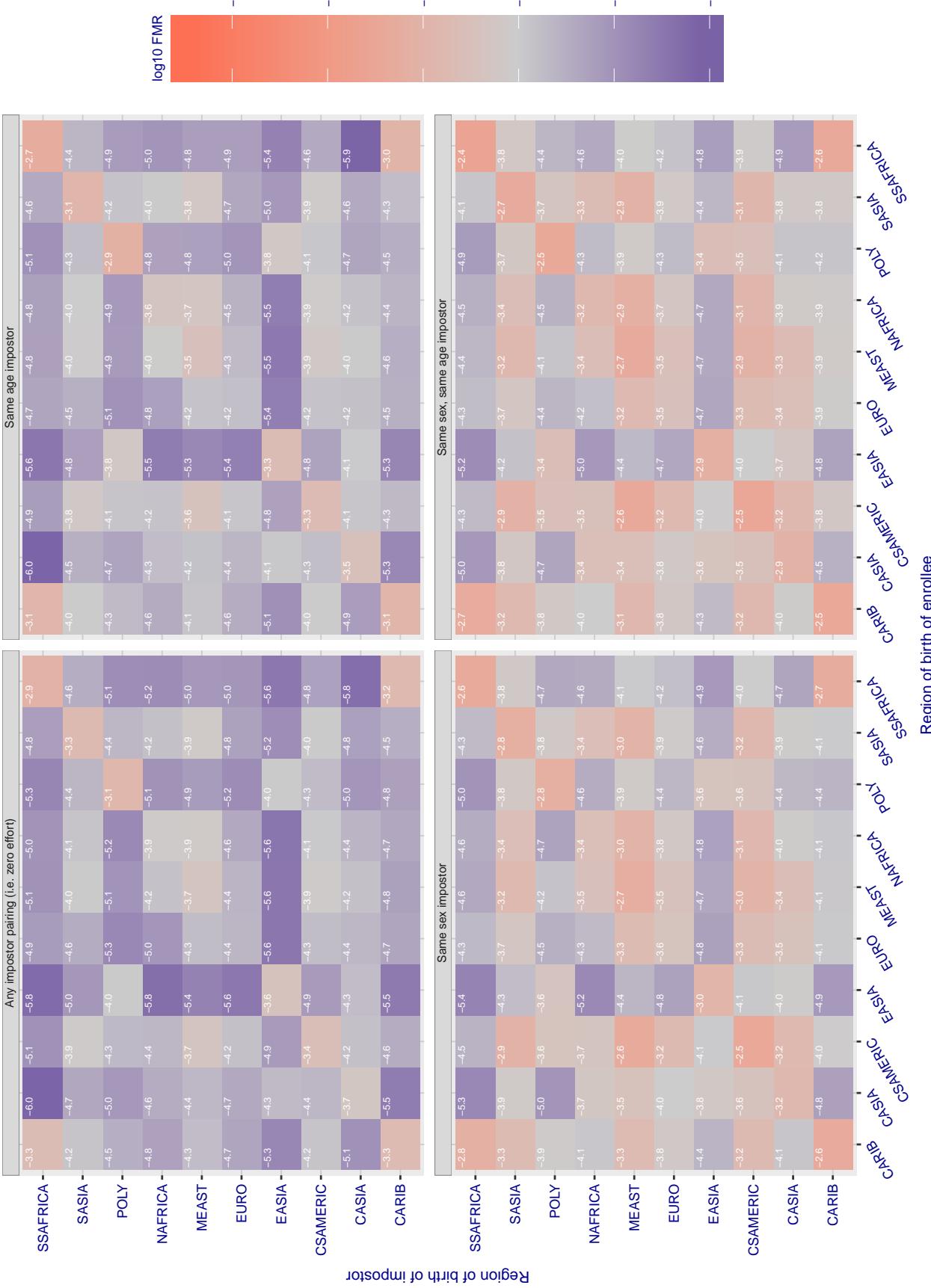
**Cross region FMR at threshold T = 49.879 for algorithm itmo\_005, giving FMR(T) = 0.0001 globally.**

Figure 182: For algorithm itmo-005 operating on visa images, the heatmap shows false match rates observed over impostor comparisons of faces from different individuals who were born in the given region pair. False matches are counted against a recognition threshold fixed globally to give the target FMR in the plot title, computed over all on the order of  $10^{10}$  impostor comparisons. If text appears in each box it give the same quantity as that coded by the color. Grey indicates FMR is at the intended FMR target level. Light red colors present a security vulnerability to, for example, a passport gate. Each +1 increase in  $\log 10$  FMR corresponds to a factor of 10 increase in FMR. The matrix is not quite symmetric because images in the enrollment and verification sets are different.

### Cross region FMR at threshold T = 49.789 for algorithm itmo\_006, giving FMR(T) = 0.0001 globally.

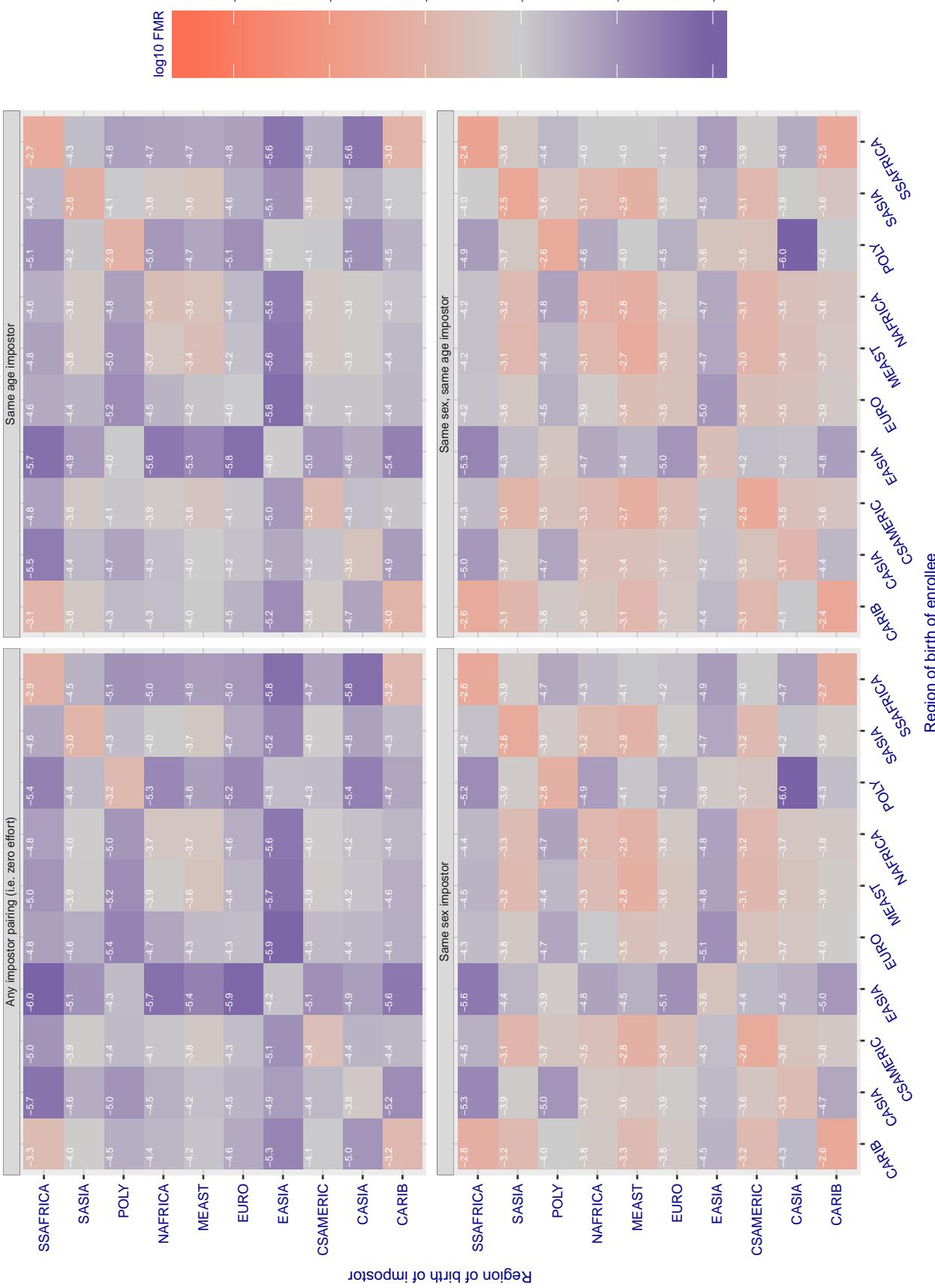


Figure 183: For algorithm itmo\_006 operating on visa images, the heatmap shows false match rates observed over impostor comparisons of faces from different individuals who were born in the given region pair. False matches are counted against a recognition threshold fixed globally to give the target FMR in the plot title, computed over all on the order of  $10^{10}$  impostor comparisons. If text appears in each box it give the same quantity as that coded by the color. Grey indicates FMR is at the intended FMR target level. Light red colors present a security vulnerability to, for example, a passport gate. Each +1 increase in  $\log_{10}$  FMR corresponds to a factor of 10 increase in FMR. The matrix is not quite symmetric because images in the enrollment and verification sets are different.

## Cross region FMR at threshold T = 1.301 for algorithm kakao\_001, giving FMR(T) = 0.0001 globally.

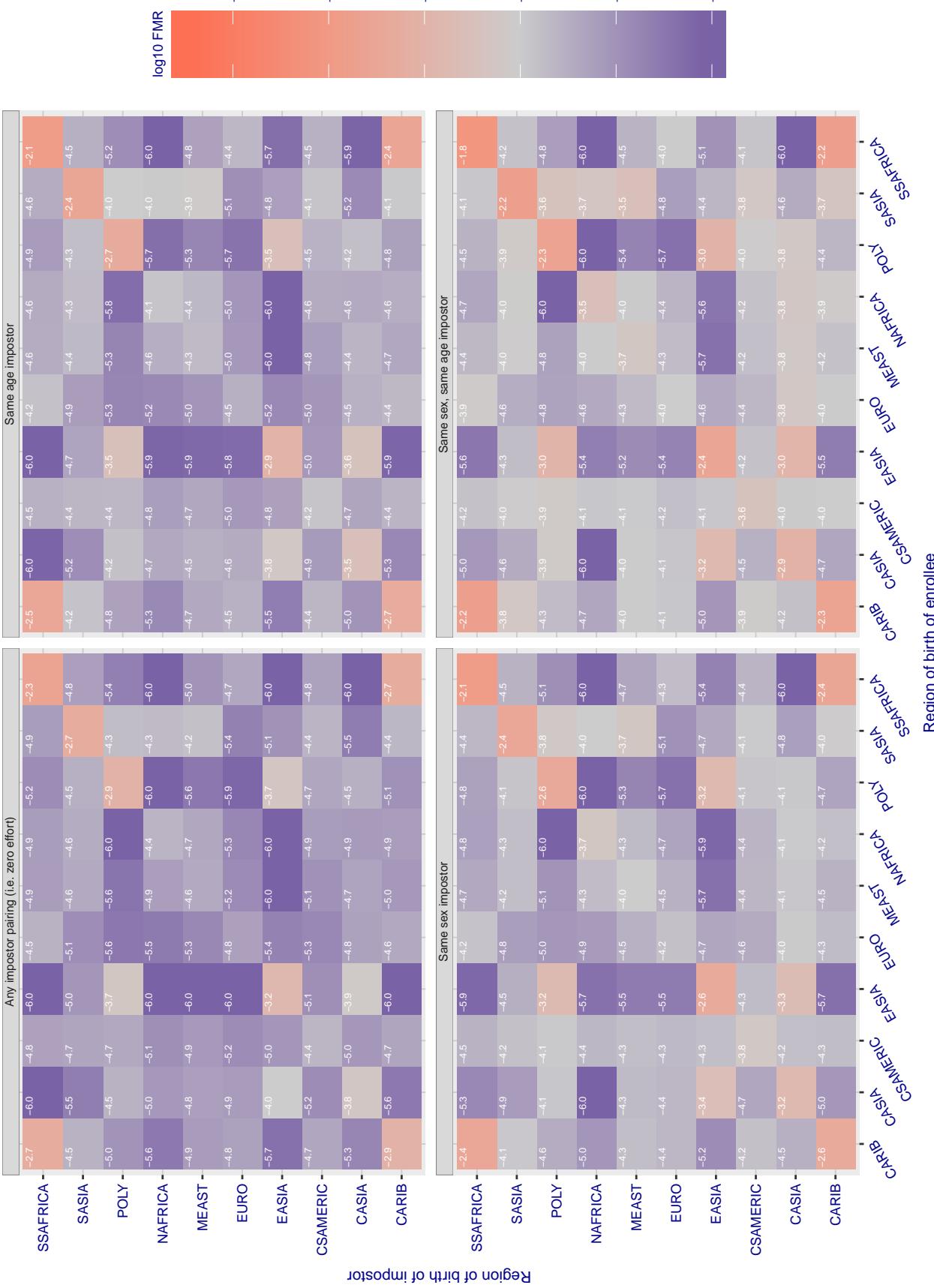


Figure 184: For algorithm kakao-001 operating on visa images, the heatmap shows false match rates observed over impostor comparisons of faces from different individuals who were born in the given region pair. False matches are counted against a recognition threshold fixed globally to give the target FMR in the plot title, computed over all on the order of  $10^{10}$  impostor comparisons. If text appears in each box it give the same quantity as that coded by the color. Grey indicates FMR is at the intended FMR target level. Light red colors present a security vulnerability to, for example, a passport gate. Each +1 increase in  $\log_{10} FMR$  corresponds to a factor of 10 increase in FMR. The matrix is not quite symmetric because images in the enrollment and verification sets are different.

### Cross region FMR at threshold T = 0.929 for algorithm kakao\_002, giving FMR(T) = 0.0001 globally.

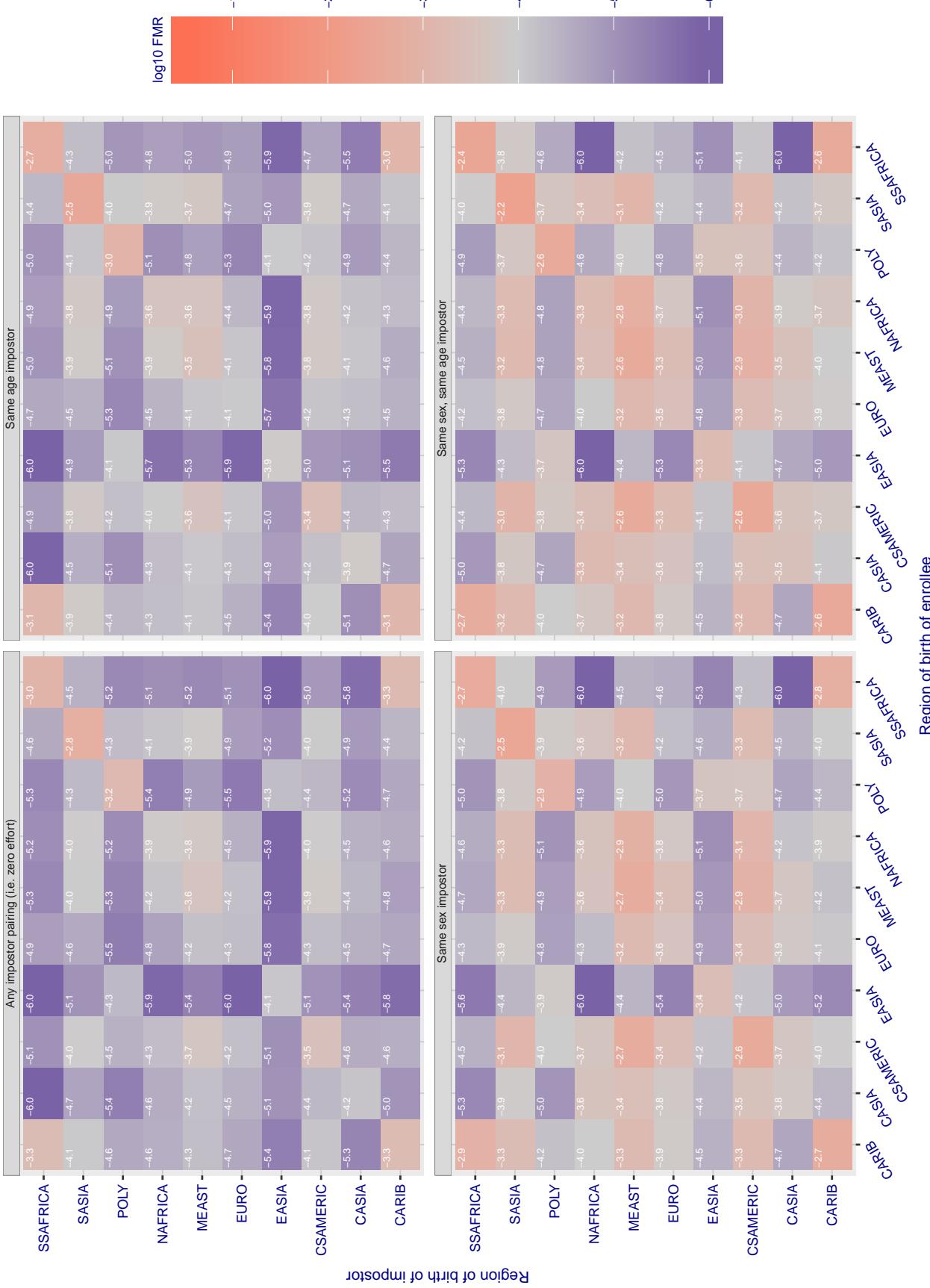


Figure 185: For algorithm kakao-002 operating on visa images, the heatmap shows false match rates observed over impostor comparisons of faces from different individuals who were born in the given region pair. False matches are counted against a recognition threshold fixed globally to give the target FMR in the plot title, computed over all on the order of  $10^{10}$  impostor comparisons. If text appears in each box it give the same quantity as that coded by the color. Grey indicates FMR is at the intended FMR target level. Light red colors present a security vulnerability to, for example, a passport gate. Each +1 increase in  $\log_{10} \text{FMR}$  corresponds to a factor of 10 increase in FMR. The matrix is not quite symmetric because images in the enrollment and verification sets are different.

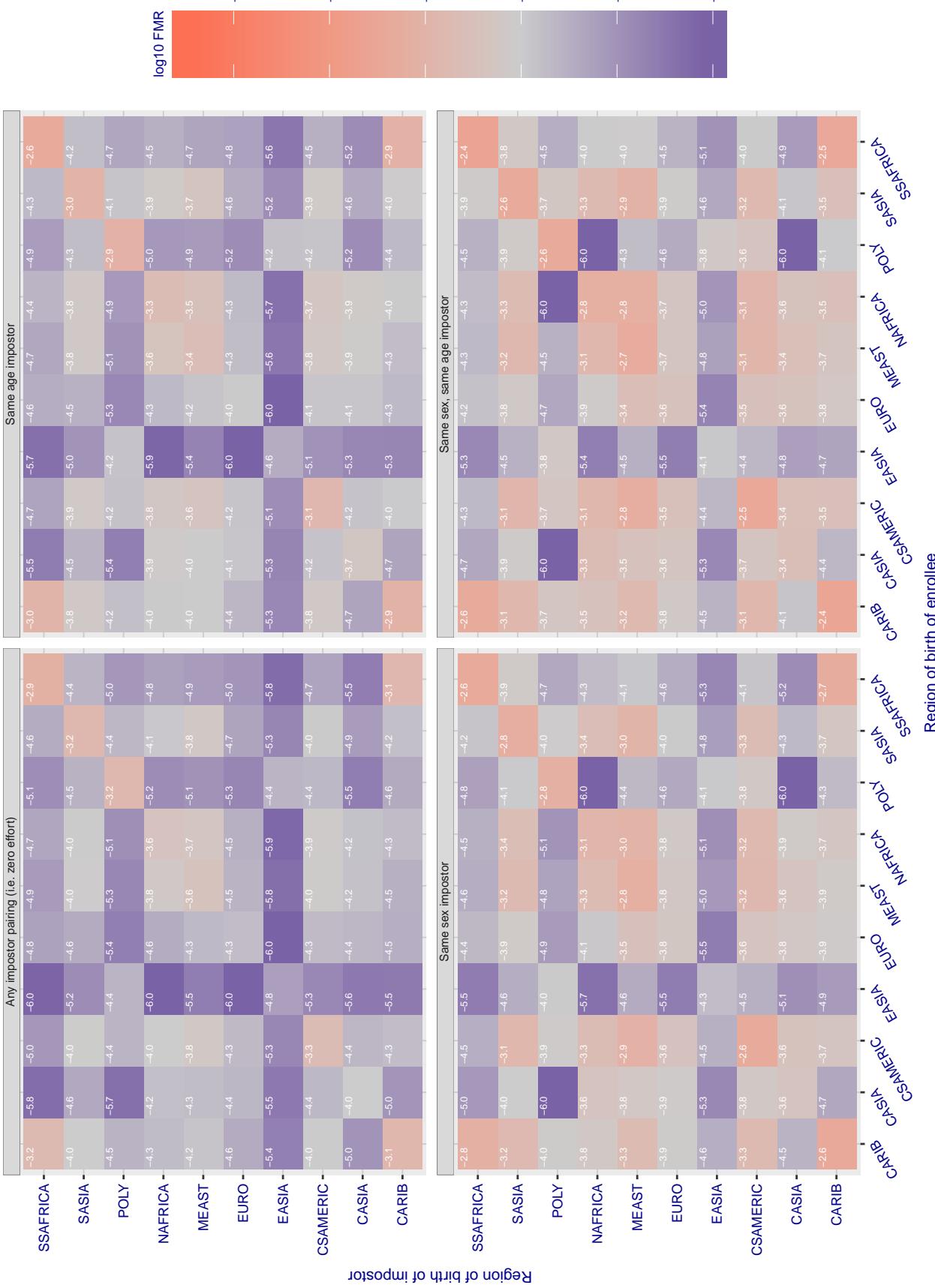
**Cross region FMR at threshold T = 0.686 for algorithm kedacom\_000, giving FMR(T) = 0.00001 globally.**

Figure 186: For algorithm kedacom-000 operating on visa images, the heatmap shows false match rates observed over impostor comparisons of faces from different individuals who were born in the given region pair. False matches are counted against a recognition threshold fixed globally to give the target FMR in the plot title, computed over all on the order of  $10^{10}$  impostor comparisons. If text appears in each box it give the same quantity as that coded by the color. Grey indicates FMR is at the intended FMR target level. Light red colors present a security vulnerability to, for example, a passport gate. Each +1 increase in  $\log_{10} FMR$  corresponds to a factor of 10 increase in FMR. The matrix is not quite symmetric because images in the enrollment and verification sets are different.

### Cross region FMR at threshold T = 0.701 for algorithm lookman\_002, giving FMR(T) = 0.0001 globally.

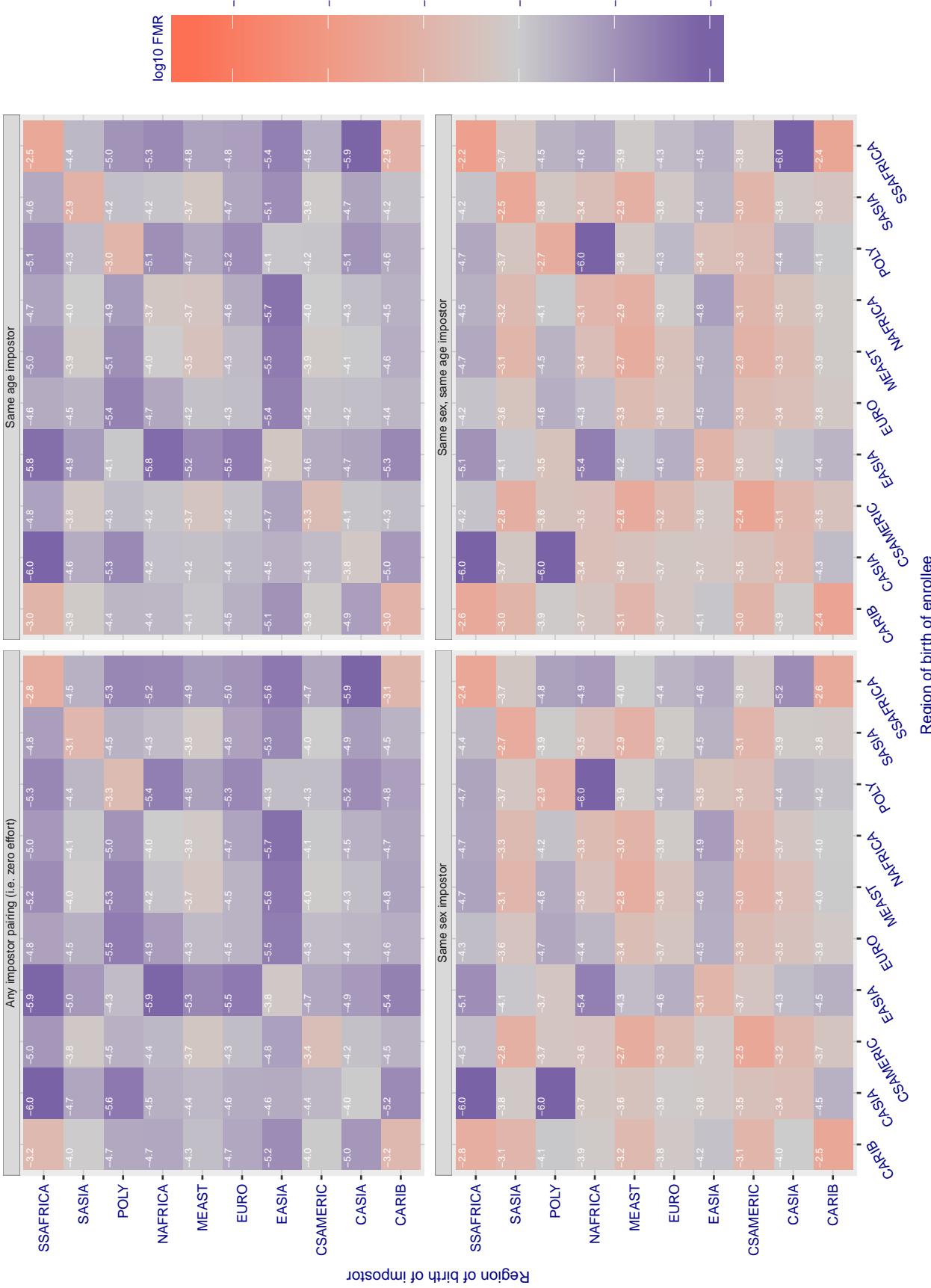


Figure 187: For algorithm lookman-002 operating on visa images, the heatmap shows false match rates observed over impostor comparisons of faces from different individuals who were born in the given region pair. False matches are counted against a recognition threshold fixed globally to give the target FMR in the plot title, computed over all on the order of  $10^{10}$  impostor comparisons. If text appears in each box it give the same quantity as that coded by the color. Grey indicates FMR is at the intended FMR target level. Light red colors present a security vulnerability to, for example, a passport gate. Each +1 increase in  $\log_{10} FMR$  corresponds to a factor of 10 increase in FMR. The matrix is not quite symmetric because images in the enrollment and verification sets are different.

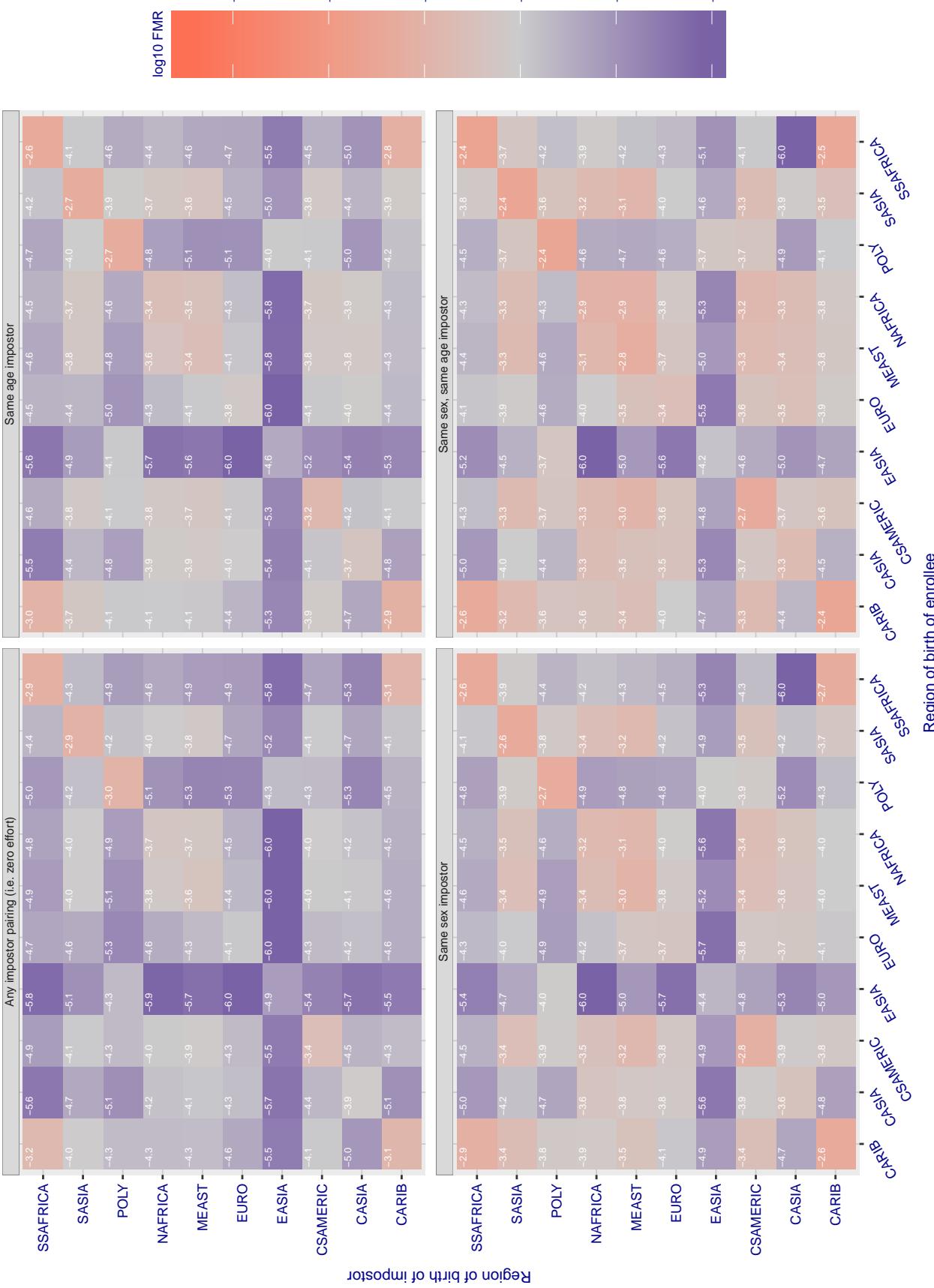
**Cross region FMR at threshold T = 0.733 for algorithm lookman\_004, giving FMR(T) = 0.0001 globally.**

Figure 188: For algorithm lookman-004 operating on visa images, the heatmap shows false match rates observed over impostor comparisons of faces from different individuals who were born in the given region pair. False matches are counted against a recognition threshold fixed globally to give the target FMR in the plot title, computed over all on the order of  $10^{10}$  impostor comparisons. If text appears in each box it give the same quantity as that coded by the color. Grey indicates FMR is at the intended FMR target level. Light red colors present a security vulnerability to, for example, a passport gate. Each +1 increase in  $\log_{10} FMR$  corresponds to a factor of 10 increase in FMR. The matrix is not quite symmetric because images in the enrollment and verification sets are different.

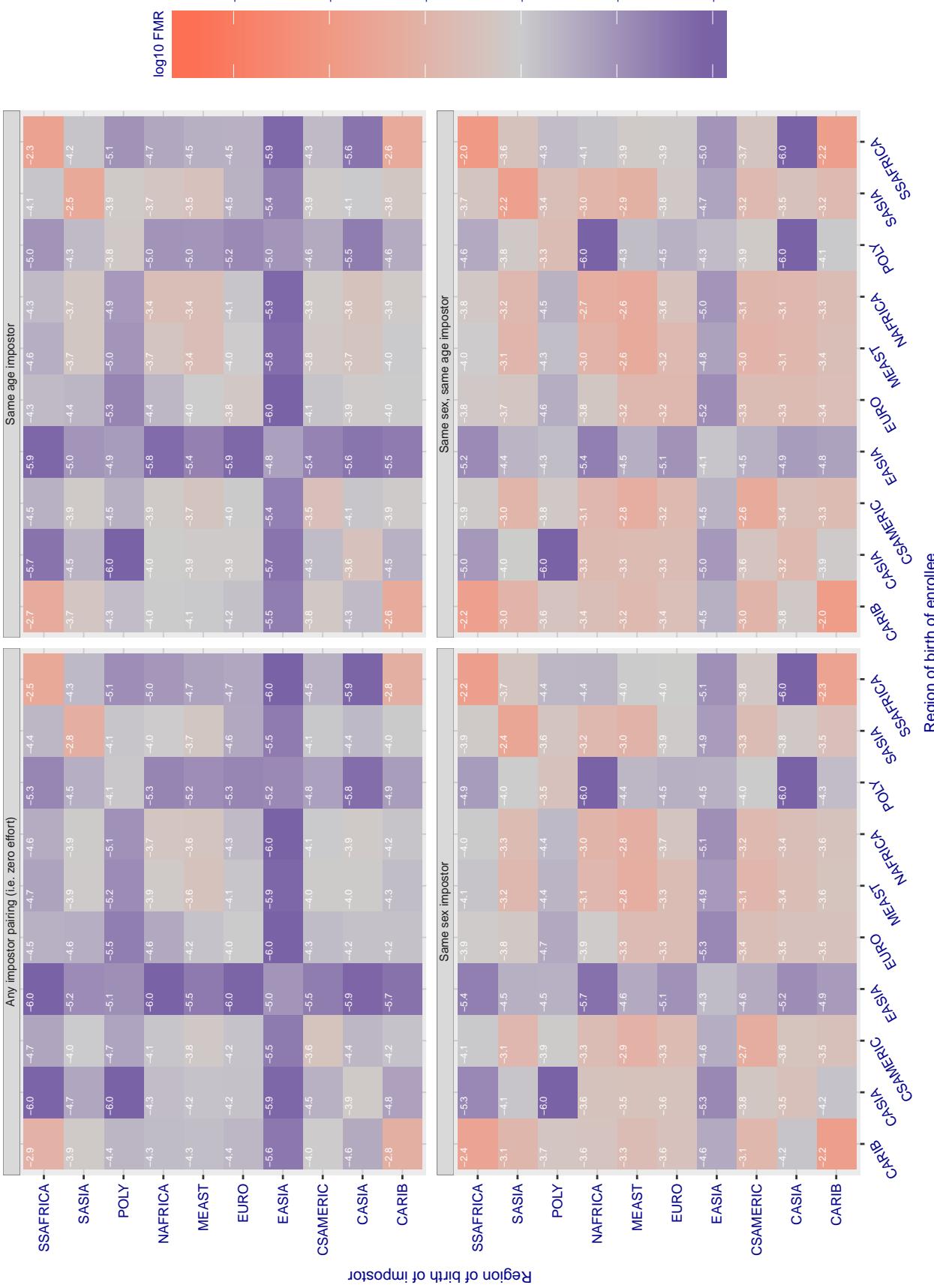
**Cross region FMR at threshold T = 74.511 for algorithm megvii\_001, giving FMR(T) = 0.0001 globally.**

Figure 189: For algorithm megvii-001 operating on visa images, the heatmap shows false match rates observed over impostor comparisons of faces from different individuals who were born in the given region pair. False matches are counted against a recognition threshold fixed globally to give the target FMR in the plot title, computed over all on the order of  $10^{10}$  impostor comparisons. If text appears in each box it give the same quantity as that coded by the color. Grey indicates FMR is at the intended FMR target level. Light red colors present a security vulnerability to, for example, a passport gate. Each +1 increase in  $\log_{10} FMR$  corresponds to a factor of 10 increase in FMR. The matrix is not quite symmetric because images in the enrollment and verification sets are different.

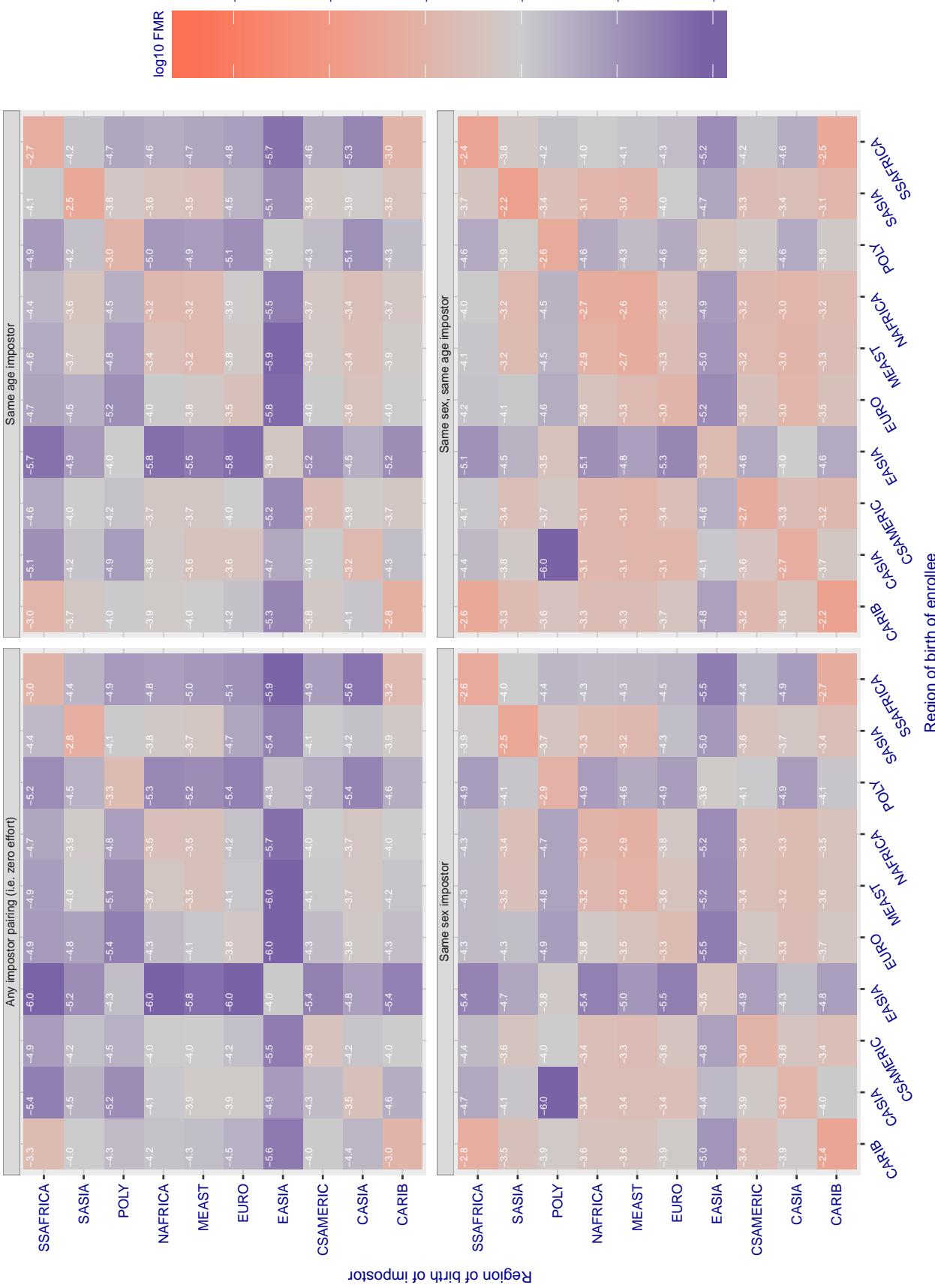
**Cross region FMR at threshold T = 66.384 for algorithm megvii\_002, giving FMR(T) = 0.0001 globally.**

Figure 190: For algorithm megvii-002 operating on visa images, the heatmap shows false match rates observed over impostor comparisons of faces from different individuals who were born in the given region pair. False matches are counted against a recognition threshold fixed globally to give the target FMR in the plot title, computed over all on the order of  $10^{10}$  impostor comparisons. If text appears in each box it give the same quantity as that coded by the color. Grey indicates FMR is at the intended FMR target level. Light red colors present a security vulnerability to, for example, a passport gate. Each +1 increase in  $\log_{10} FMR$  corresponds to a factor of 10 increase in FMR. The matrix is not quite symmetric because images in the enrollment and verification sets are different.

### Cross region FMR at threshold T = 0.425 for algorithm meiya\_001, giving FMR(T) = 0.0001 globally.

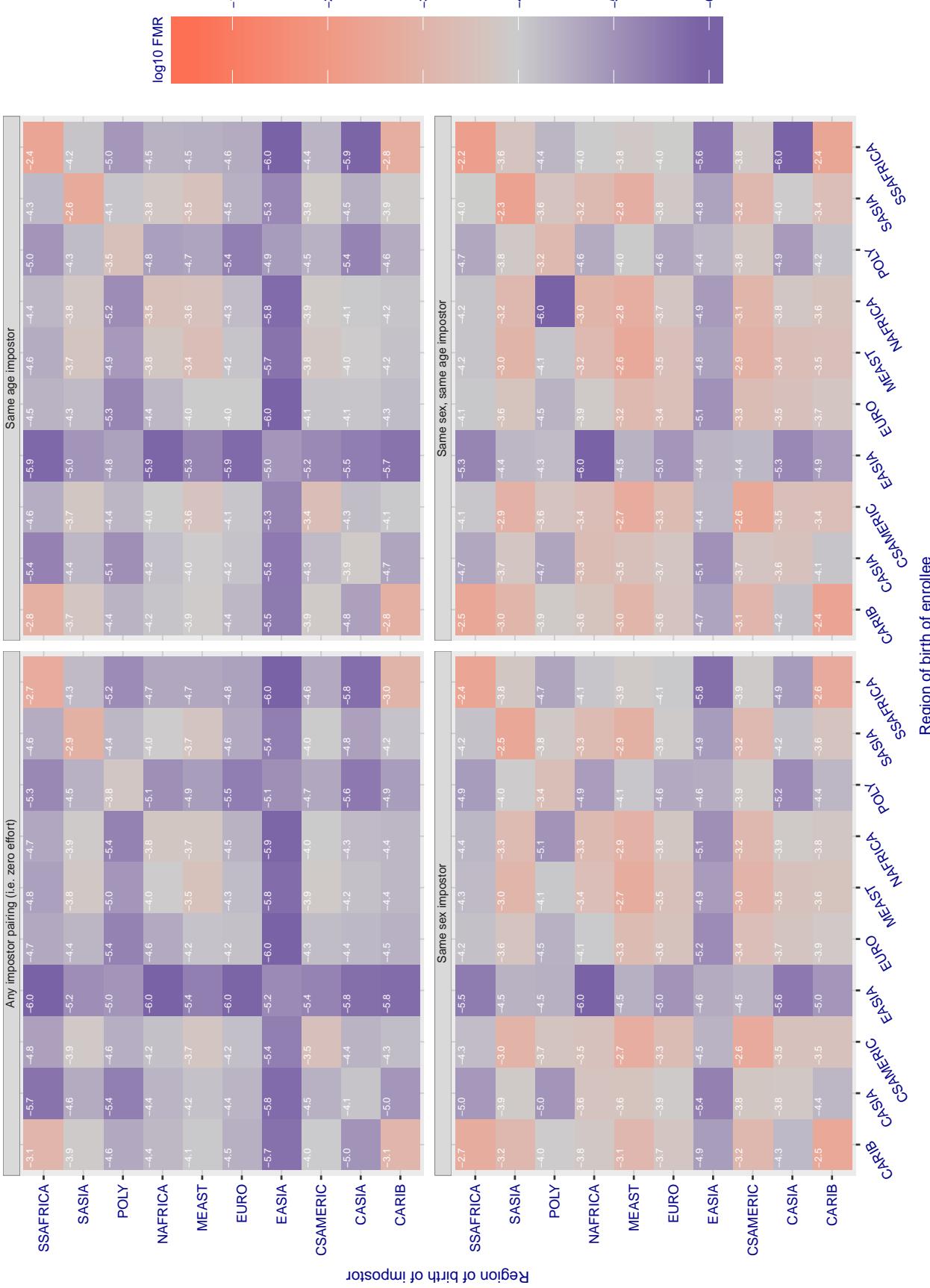


Figure 191: For algorithm meiya-001 operating on visa images, the heatmap shows false match rates observed over impostor comparisons of faces from different individuals who were born in the given region pair. False matches are counted against a recognition threshold fixed globally to give the target FMR in the plot title, computed over all on the order of  $10^{10}$  impostor comparisons. If text appears in each box it give the same quantity as that coded by the color. Grey indicates FMR is at the intended FMR target level. Light red colors present a security vulnerability to, for example, a passport gate. Each +1 increase in  $\log_{10} FMR$  corresponds to a factor of 10 increase in FMR. The matrix is not quite symmetric because images in the enrollment and verification sets are different.

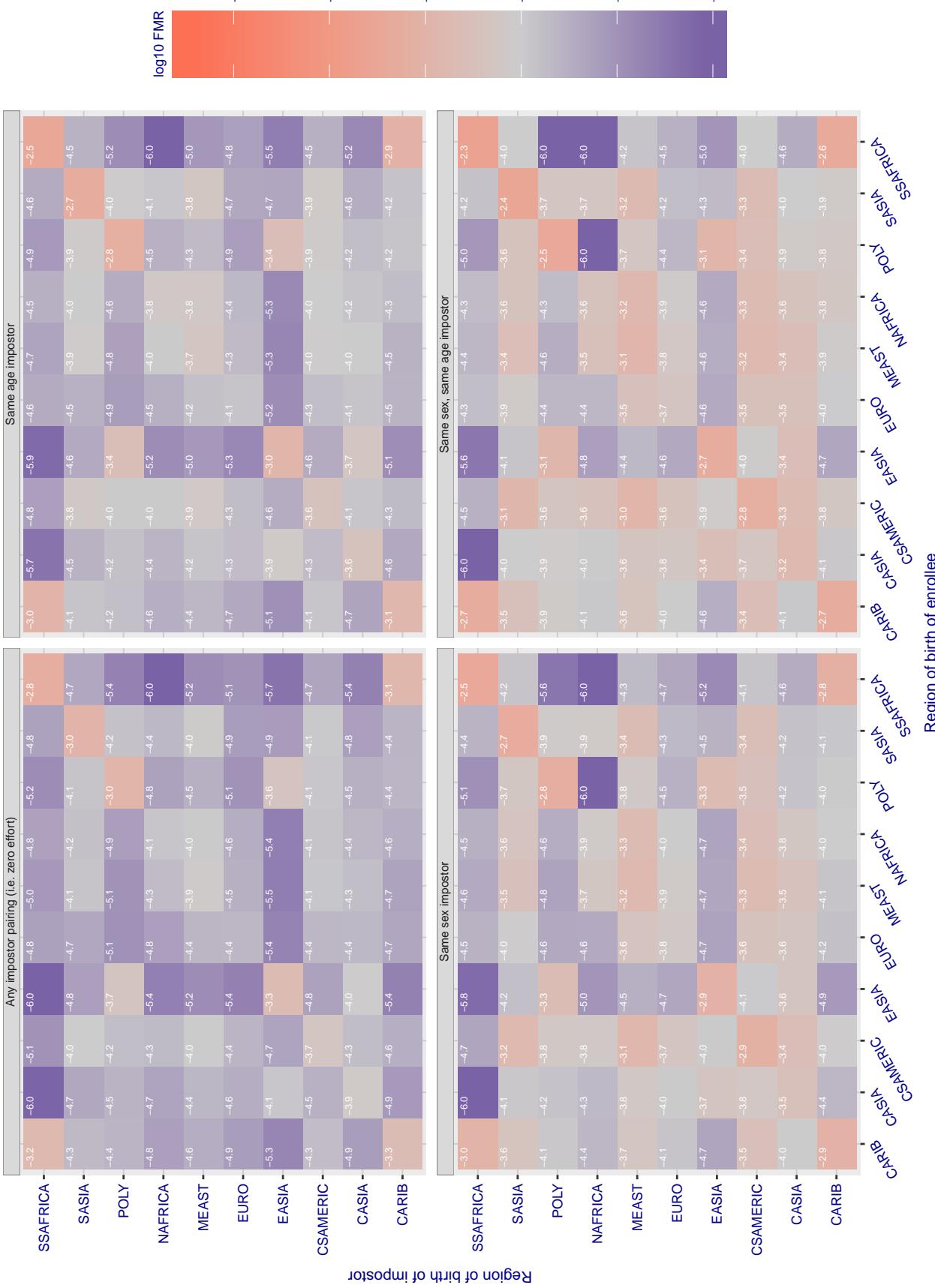
**Cross region FMR at threshold T = 0.668 for algorithm microfocus\_001, giving FMR(T) = 0.00001 globally.**

Figure 192: For algorithm microfocus-001 operating on visa images, the heatmap shows false match rates observed over impostor comparisons of faces from different individuals who were born in the given region pair. False matches are counted against a recognition threshold fixed globally to give the target FMR in the plot title, computed over all on the order of  $10^{10}$  impostor comparisons. If text appears in each box it give the same quantity as that coded by the color. Grey indicates FMR is at the intended FMR target level. Light red colors present a security vulnerability to, for example, a passport gate. Each +1 increase in  $\log_{10} FMR$  corresponds to a factor of 10 increase in FMR. The matrix is not quite symmetric because images in the enrollment and verification sets are different.

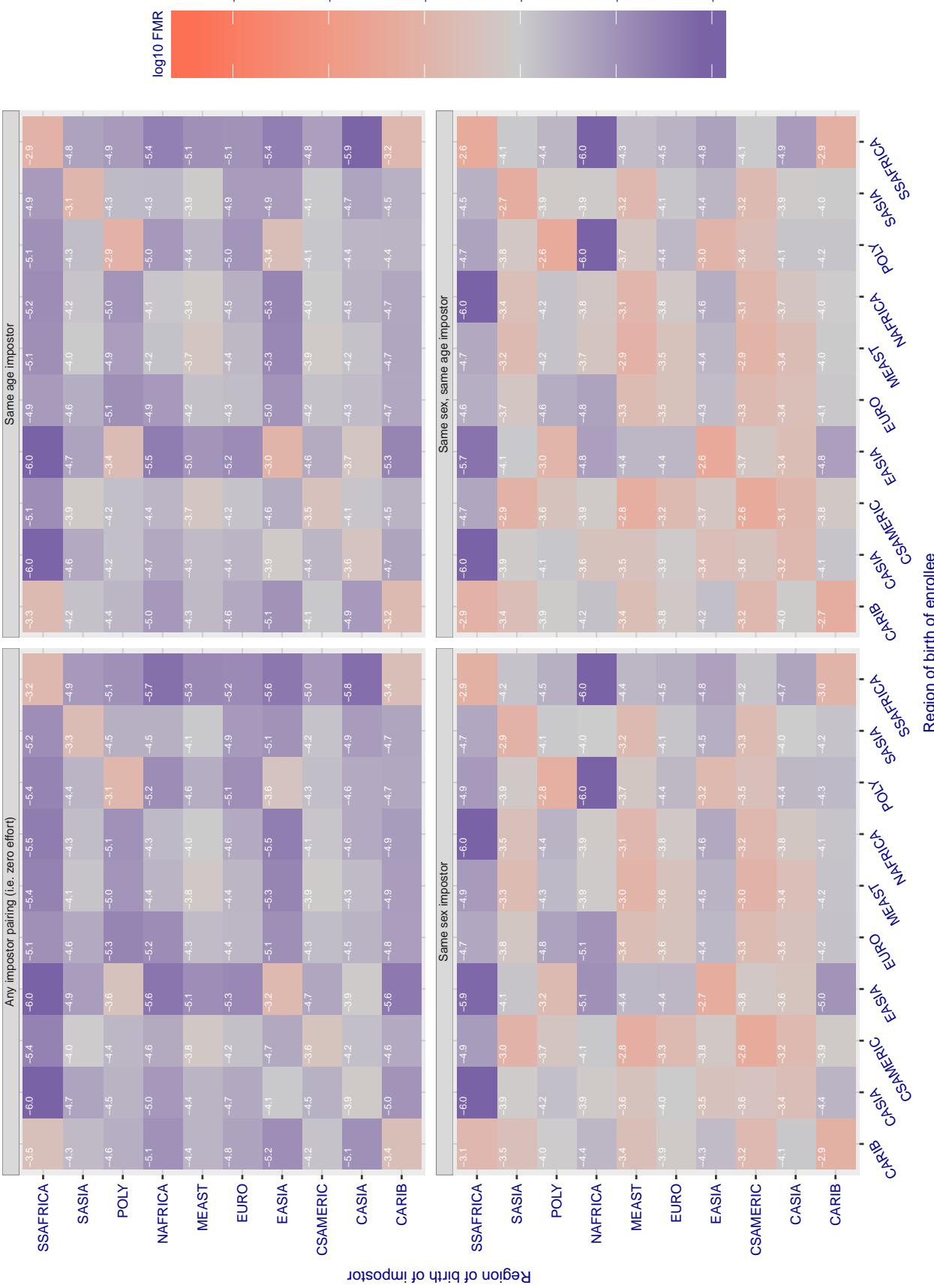
**Cross region FMR at threshold T = 0.602 for algorithm microfocus\_002, giving FMR(T) = 0.00001 globally.**

Figure 193: For algorithm microfocus-002 operating on visa images, the heatmap shows false match rates observed over impostor comparisons of faces from different individuals who were born in the given region pair. False matches are counted against a recognition threshold fixed globally to give the target FMR in the plot title, computed over all on the order of  $10^{10}$  impostor comparisons. If text appears in each box it give the same quantity as that coded by the color. Grey indicates FMR is at the intended FMR target level. Light red colors present a security vulnerability to, for example, a passport gate. Each +1 increase in  $\log_{10} FMR$  corresponds to a factor of 10 increase in FMR. The matrix is not quite symmetric because images in the enrollment and verification sets are different.

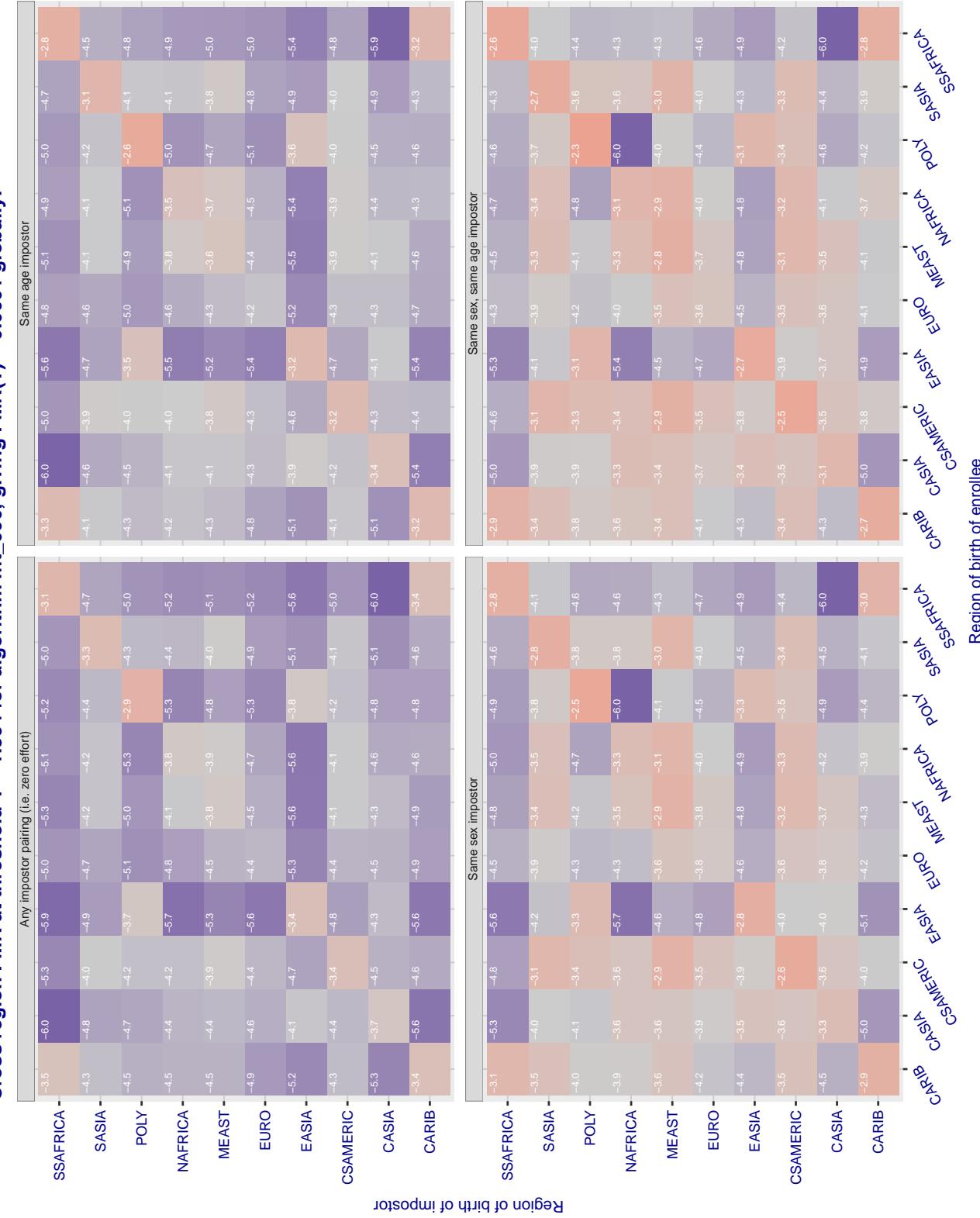


Figure 194: For algorithm *mt-000* operating on visa images, the heatmap shows false match rates observed over impostor comparisons of faces from different individuals who were born in the given region pair. False matches are counted against a recognition threshold fixed globally to give the target *FMR* in the plot title, computed over all on the order of  $10^{10}$  impostor comparisons. If text appears in each box it give the same quantity as that coded by the color. Grey indicates *FMR* is at the intended *FMR* target level. Light red colors present a security vulnerability to, for example, a passport gate. Each +1 increase in  $\log_{10} FMR$  corresponds to a factor of 10 increase in *FMR*. The matrix is not quite symmetric because images in the enrollment and verification sets are different.

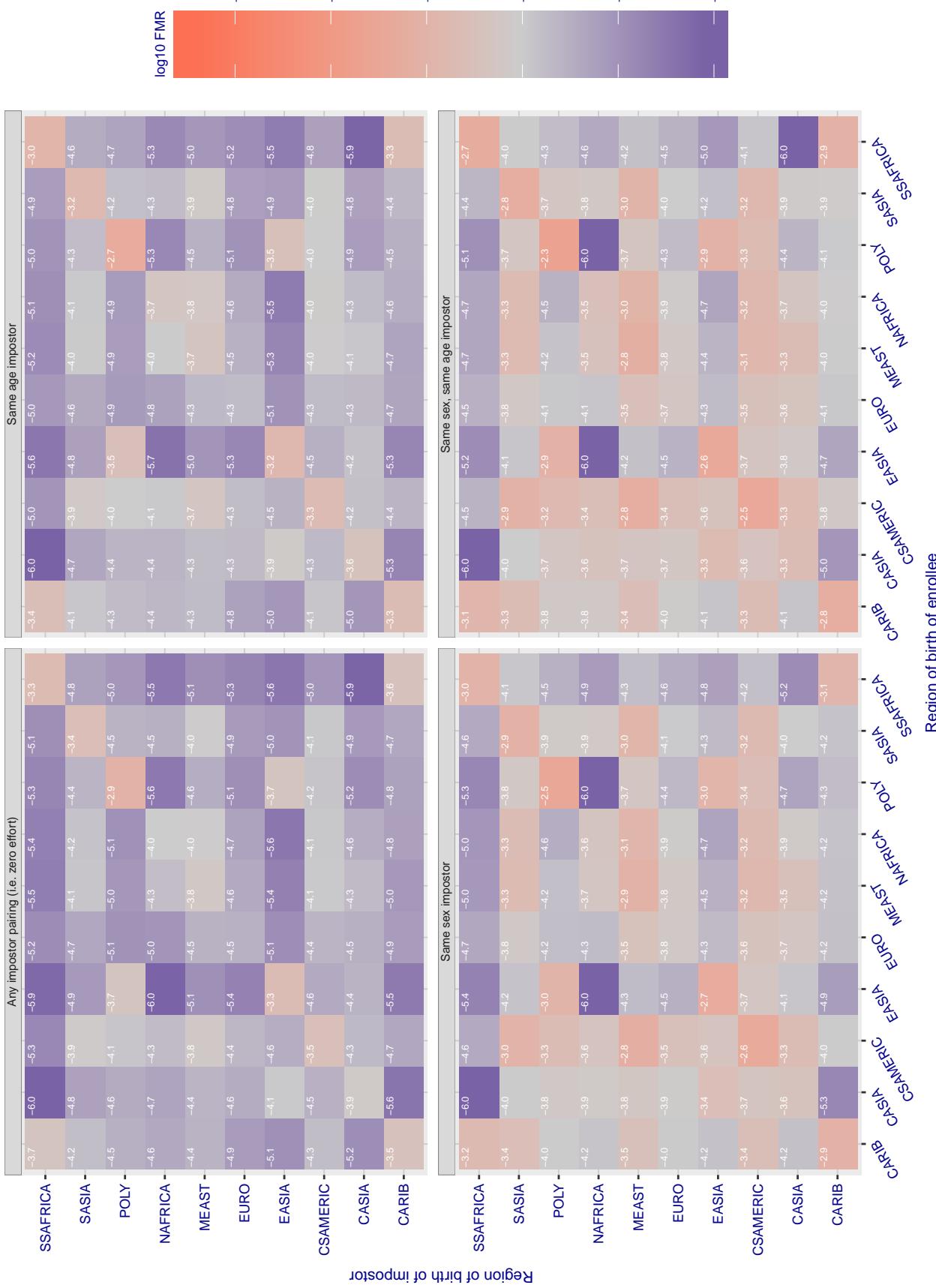
**Cross region FMR at threshold T = 46.101 for algorithm neurotechnology\_005, giving FMR(T) = 0.00001 globally.**

Figure 195: For algorithm neurotechnology-005 operating on visa images, the heatmap shows false match rates observed over impostor comparisons of faces from different individuals who were born in the given region pair. False matches are counted against a recognition threshold fixed globally to give the target FMR in the plot title, computed over all on the order of  $10^{10}$  impostor comparisons. If text appears in each box it give the same quantity as that coded by the color. Grey indicates FMR is at the intended FMR target level. Light red colors present a security vulnerability to, for example, a passport gate. Each +1 increase in  $\log_{10} FMR$  corresponds to a factor of 10 increase in FMR. The matrix is not quite symmetric because images in the enrollment and verification sets are different.

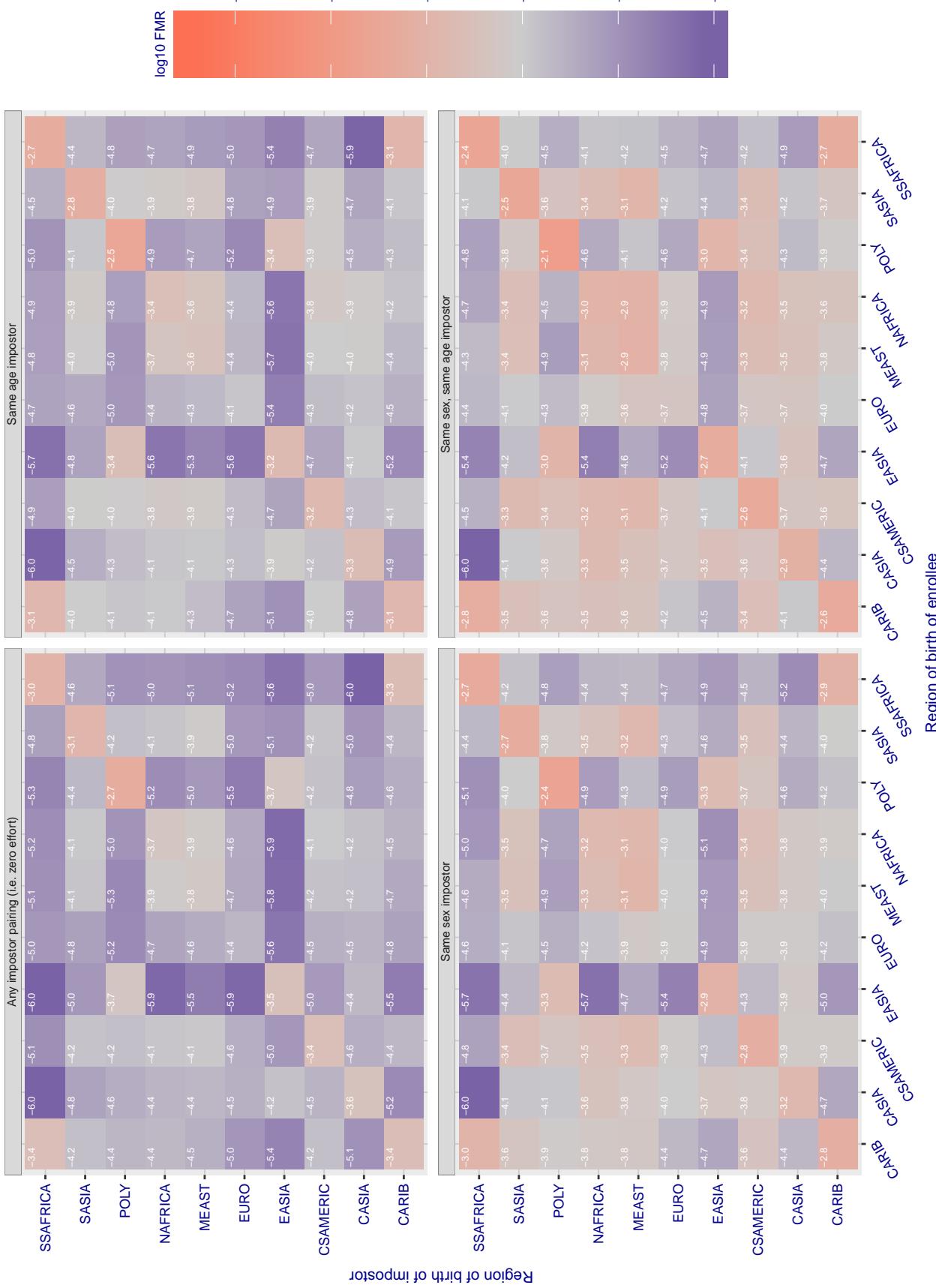
**Cross region FMR at threshold T = 2044.000 for algorithm neurotechnology\_006, giving FMR(T) = 0.00001 globally.**

Figure 196: For algorithm neurotechnology-006 operating on visa images, the heatmap shows false match rates observed over impostor comparisons of faces from different individuals who were born in the given region pair. False matches are counted against a recognition threshold fixed globally to give the target FMR in the plot title, computed over all on the order of  $10^{10}$  impostor comparisons. If text appears in each box it give the same quantity as that coded by the color. Grey indicates FMR is at the intended FMR target level. Light red colors present a security vulnerability to, for example, a passport gate. Each +1 increase in  $\log_{10} \text{FMR}$  corresponds to a factor of 10 increase in FMR. The matrix is not quite symmetric because images in the enrollment and verification sets are different.

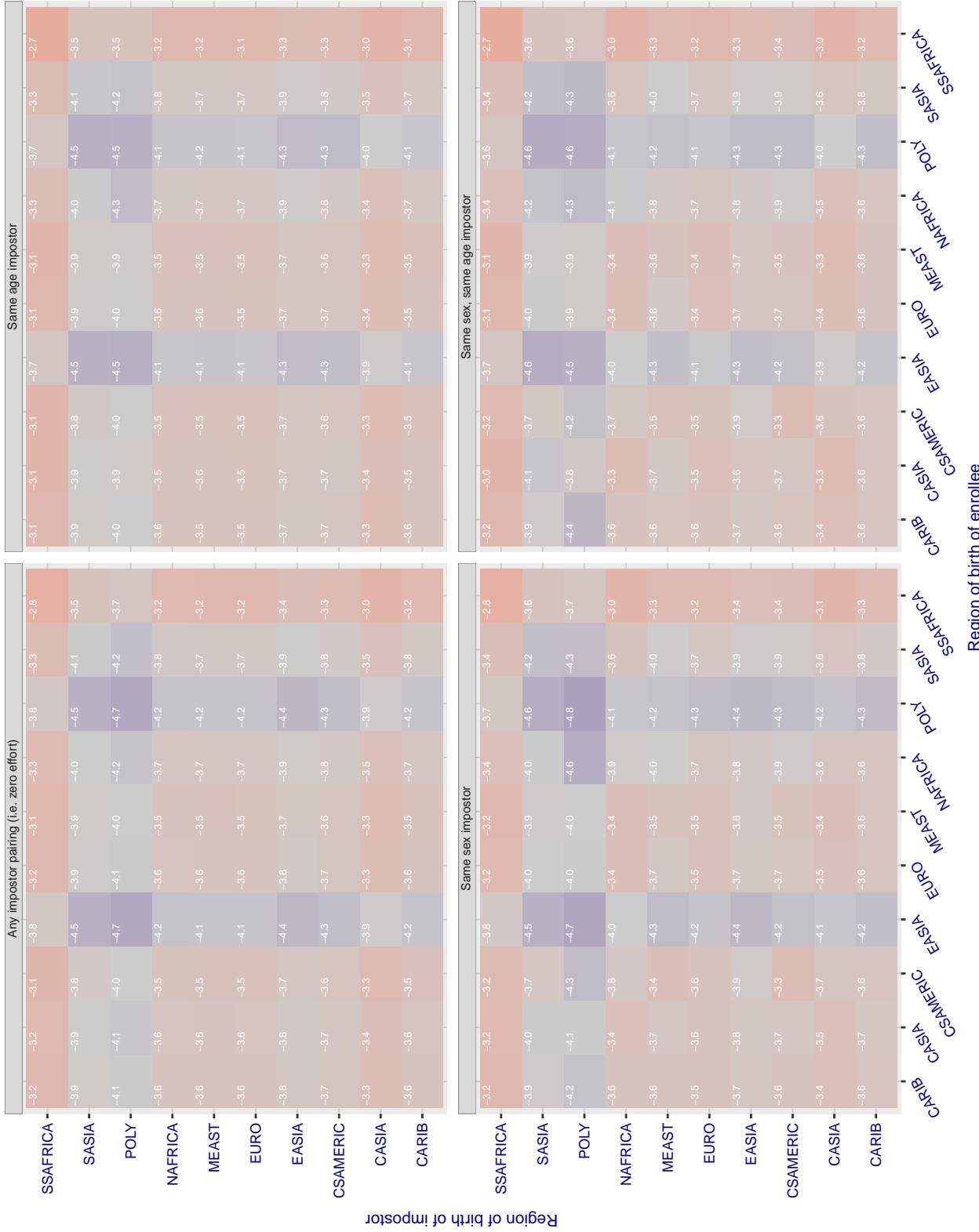


Figure 197: For algorithm nodeflux-000 operating on visa images, the heatmap shows false match rates observed over impostor comparisons of faces from different individuals who were born in the given region pair. False matches are counted against a recognition threshold fixed globally to give the target FMR in the plot title, computed over all on the order of  $10^{10}$  impostor comparisons. If text appears in each box it give the same quantity as that coded by the color. Grey indicates FMR is at the intended FMR target level. Light red colors present a security vulnerability to, for example, a passport gate. Each +1 increase in  $\log_{10}$  FMR corresponds to a factor of 10 increase in FMR. The matrix is not quite symmetric because images in the enrollment and verification sets are different.

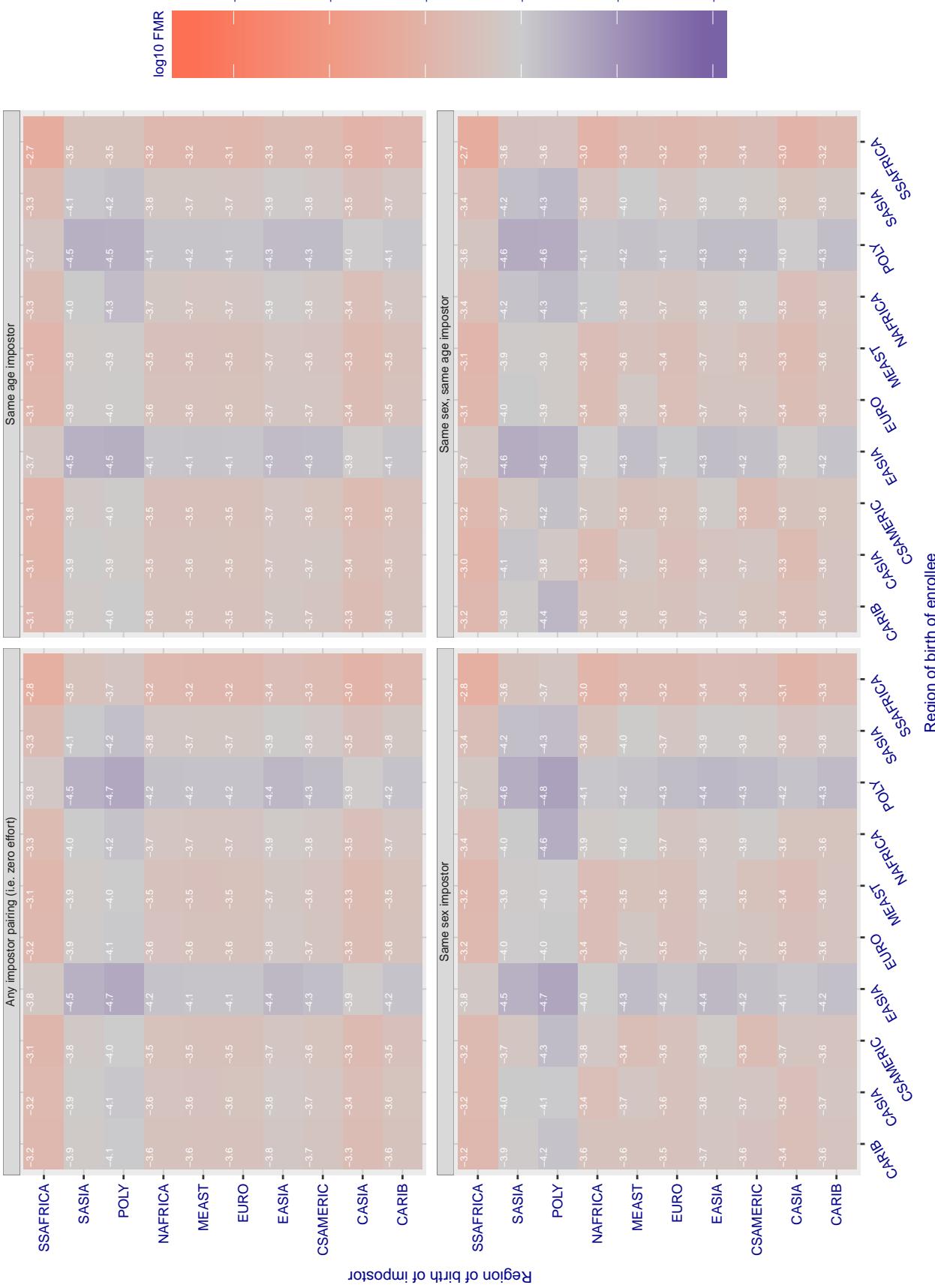
**Cross region FMR at threshold T = 1.000 for algorithm nodeflux\_001, giving FMR(T) = 0.0001 globally.**

Figure 198: For algorithm nodeflux-001 operating on visa images, the heatmap shows false match rates observed over impostor comparisons of faces from different individuals who were born in the given region pair. False matches are counted against a recognition threshold fixed globally to give the target FMR in the plot title, computed over all on the order of  $10^{10}$  impostor comparisons. If text appears in each box it give the same quantity as that coded by the color. Grey indicates FMR is at the intended FMR target level. Light red colors present a security vulnerability to, for example, a passport gate. Each +1 increase in  $\log_{10} FMR$  corresponds to a factor of 10 increase in FMR. The matrix is not quite symmetric because images in the enrollment and verification sets are different.

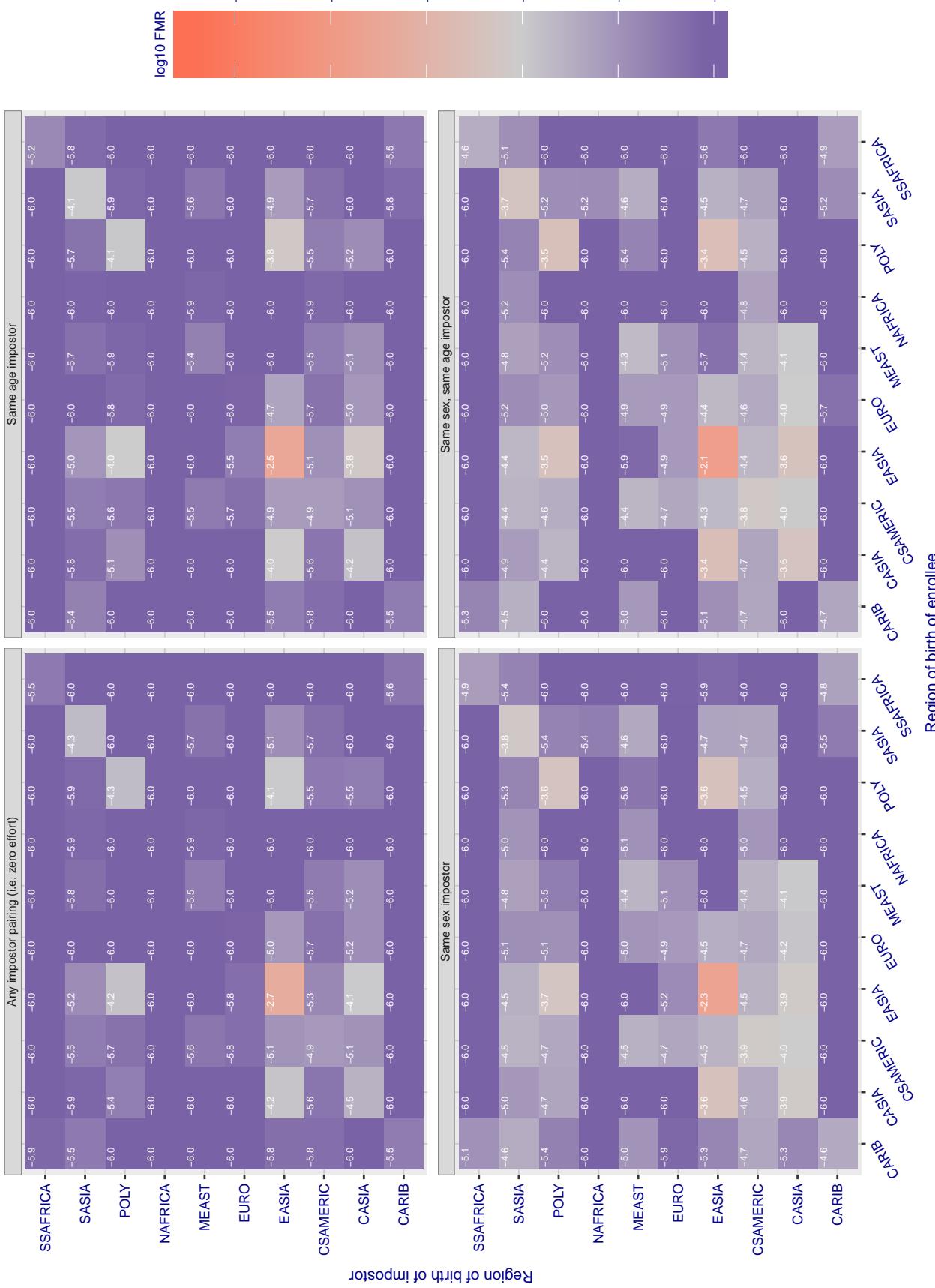
**Cross region FMR at threshold T = 1684638382164870077977436979131033446238075281200095429962596511771518105060865483**

Figure 199: For algorithm notiontag-000 operating on visa images, the heatmap shows false match rates observed over impostor comparisons of faces from different individuals who were born in the given region pair. False matches are counted against a recognition threshold fixed globally to give the target FMR in the plot title, computed over all on the order of  $10^{10}$  impostor comparisons. If text appears in each box it give the same quantity as that coded by the color. Grey indicates FMR is at the intended FMR target level. Light red colors present a security vulnerability to, for example, a passport gate. Each +1 increase in  $\log_{10} \text{FMR}$  corresponds to a factor of 10 increase in FMR. The matrix is not quite symmetric because images in the enrollment and verification sets are different.

### Cross region FMR at threshold T = 1.997 for algorithm ntechlab\_006, giving $\text{FMR}(\text{T}) = 0.0001$ globally.

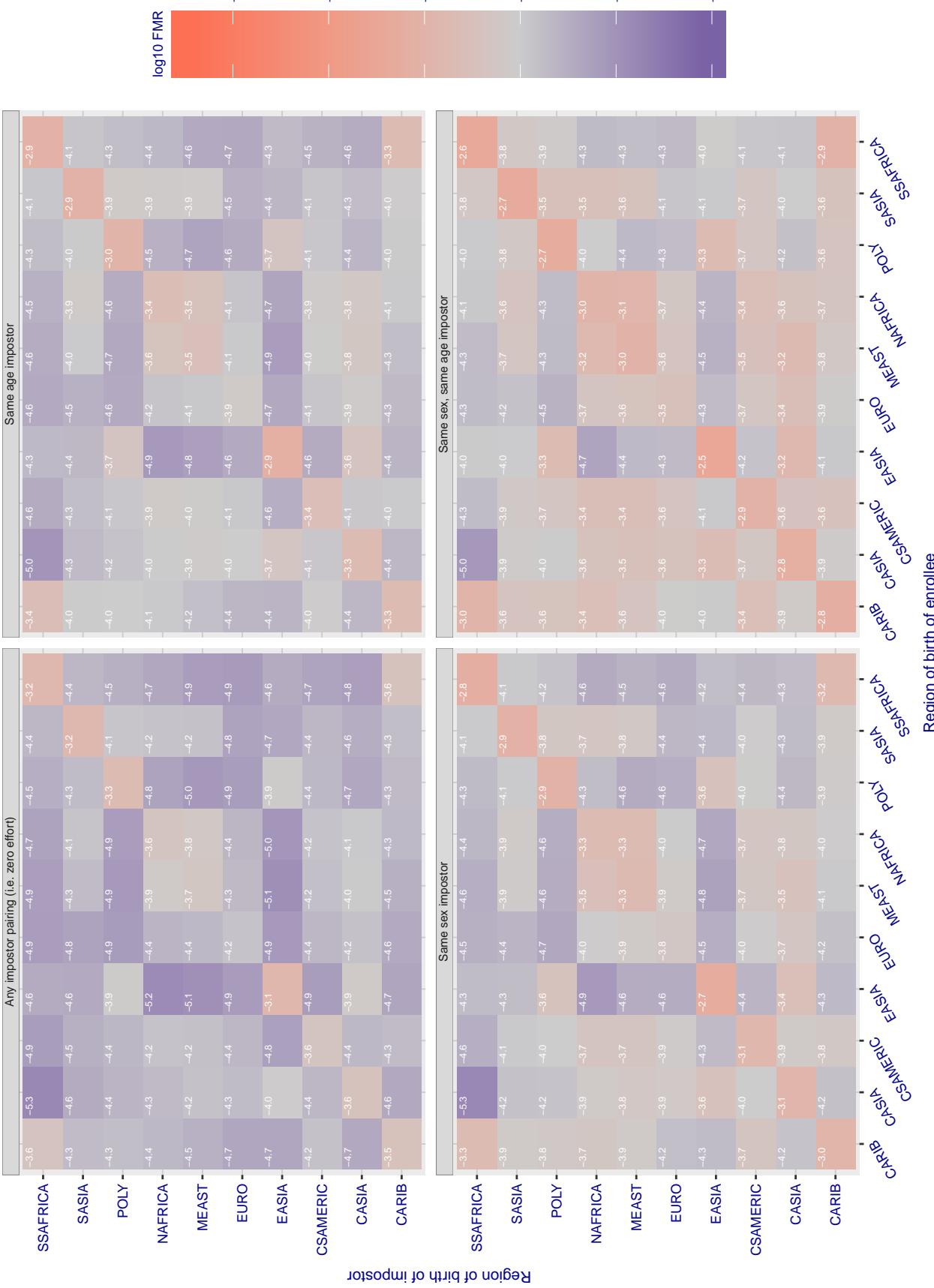


Figure 200: For algorithm ntechlab-006 operating on visa images, the heatmap shows false match rates observed over impostor comparisons of faces from different individuals who were born in the given region pair. False matches are counted against a recognition threshold fixed globally to give the target FMR in the plot title, computed over all on the order of  $10^{10}$  impostor comparisons. If text appears in each box it give the same quantity as that coded by the color. Grey indicates FMR is at the intended FMR target level. Light red colors present a security vulnerability to, for example, a passport gate. Each +1 increase in  $\log_{10} \text{FMR}$  corresponds to a factor of 10 increase in FMR. The matrix is not quite symmetric because images in the enrollment and verification sets are different.

### Cross region FMR at threshold T = 1.416 for algorithm ntechlab\_007, giving FMR(T) = 0.0001 globally.

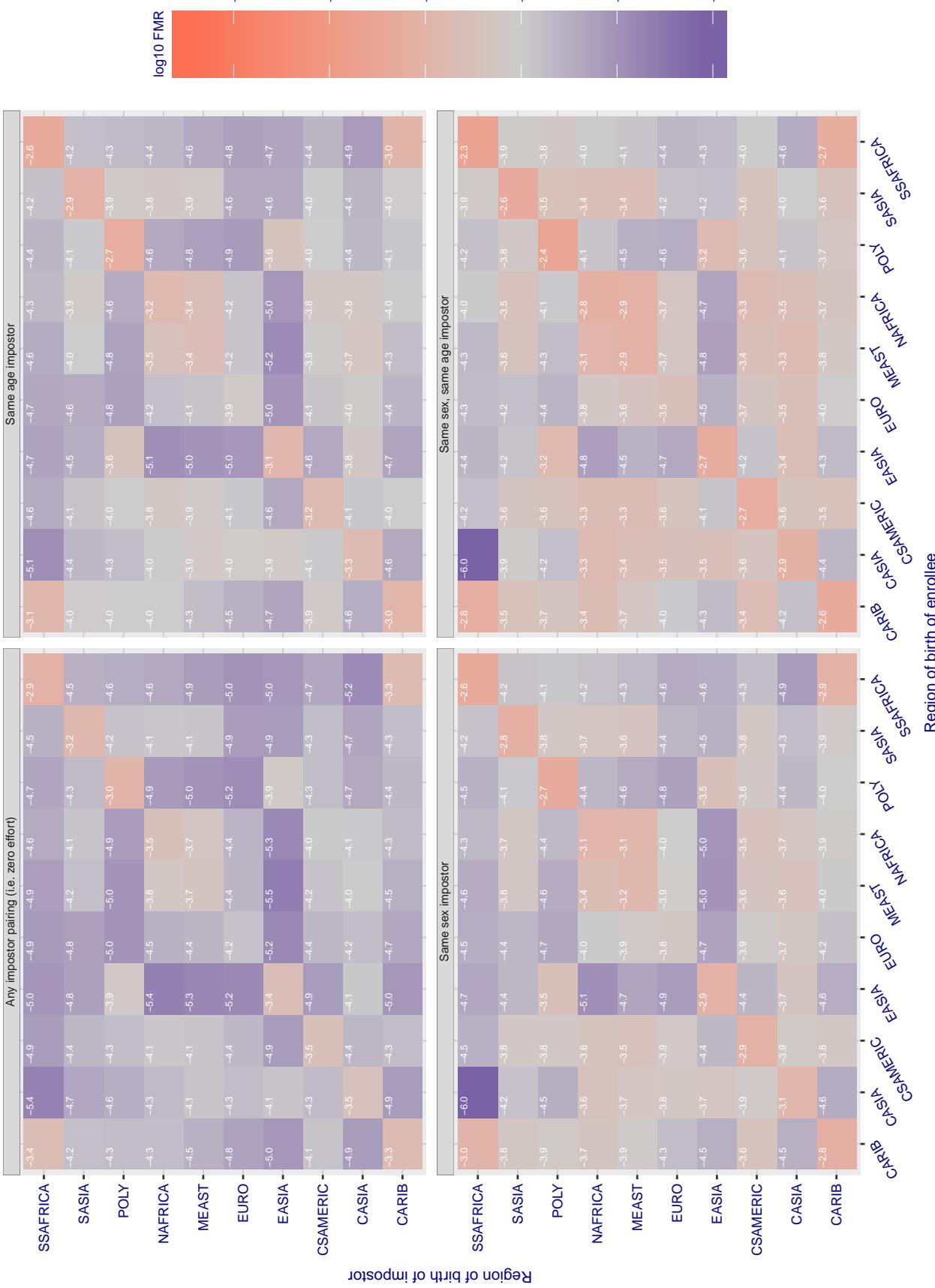


Figure 201: For algorithm ntechlab-007 operating on visa images, the heatmap shows false match rates observed over impostor comparisons of faces from different individuals who were born in the given region pair. False matches are counted against a recognition threshold fixed globally to give the target FMR in the plot title, computed over all on the order of  $10^{10}$  impostor comparisons. If text appears in each box it give the same quantity as that coded by the color. Grey indicates FMR is at the intended FMR target level. Light red colors present a security vulnerability to, for example, a passport gate. Each +1 increase in  $\log_{10} FMR$  corresponds to a factor of 10 increase in FMR. The matrix is not quite symmetric because images in the enrollment and verification sets are different.

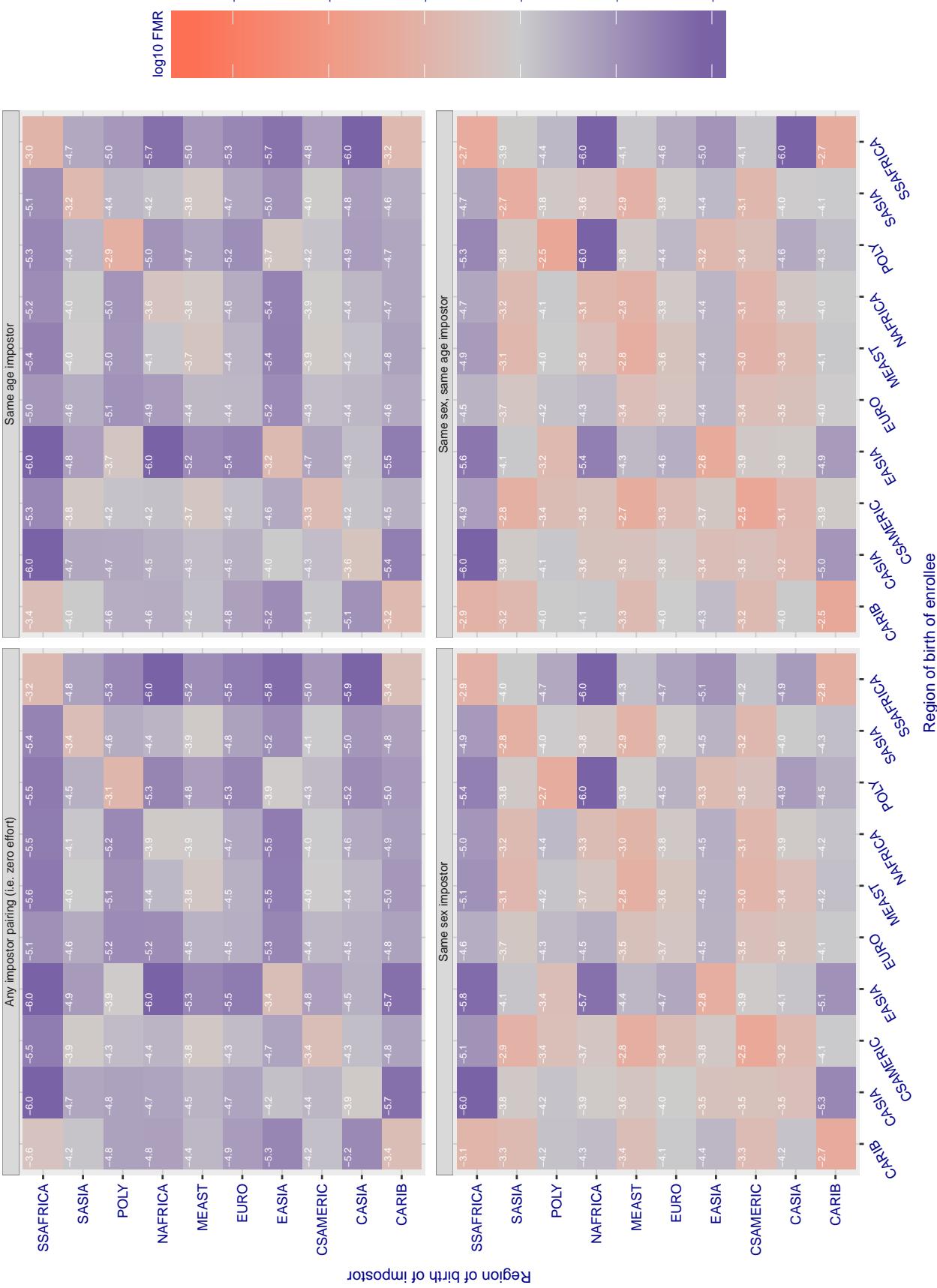
**Cross region FMR at threshold T = 0.428 for algorithm pixelall\_002, giving FMR(T) = 0.0001 globally.**

Figure 202: For algorithm pixelall-002 operating on visa images, the heatmap shows false match rates observed over impostor comparisons of faces from different individuals who were born in the given region pair. False matches are counted against a recognition threshold fixed globally to give the target FMR in the plot title, computed over all on the order of  $10^{10}$  impostor comparisons. If text appears in each box it give the same quantity as that coded by the color. Grey indicates FMR is at the intended FMR target level. Light red colors present a security vulnerability to, for example, a passport gate. Each +1 increase in  $\log_{10} FMR$  corresponds to a factor of 10 increase in FMR. The matrix is not quite symmetric because images in the enrollment and verification sets are different.

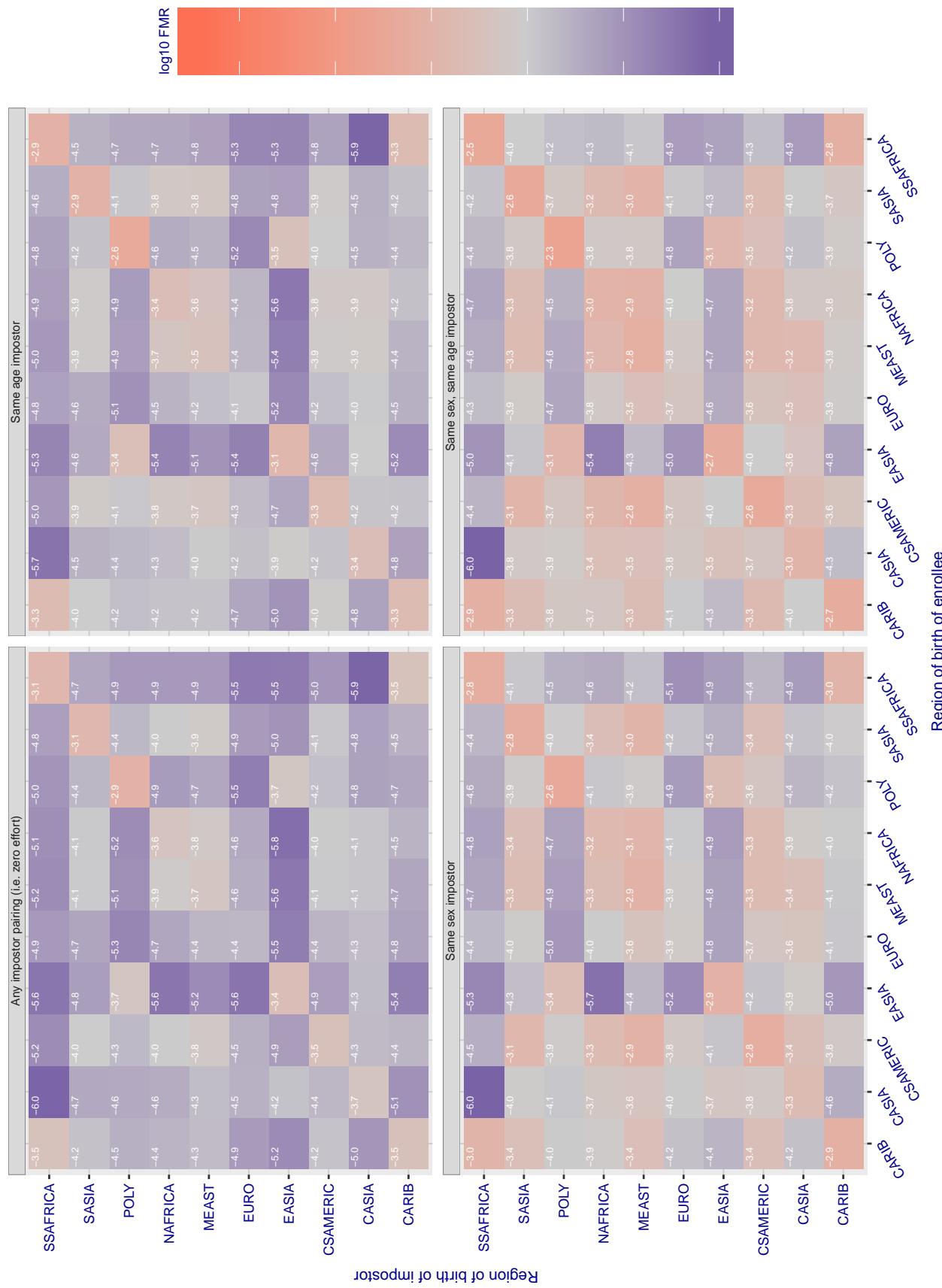
**Cross region FMR at threshold T = 0.337 for algorithm psl\_001, giving FMR(T) = 0.0001 globally.**

Figure 203: For algorithm psl-001 operating on visa images, the heatmap shows false match rates observed over impostor comparisons of faces from different individuals who were born in the given region pair. False matches are counted against a recognition threshold fixed globally to give the target FMR in the plot title, computed over all on the order of  $10^{10}$  impostor comparisons. If text appears in each box it give the same quantity as that coded by the color. Grey indicates FMR is at the intended FMR target level. Light red colors present a security vulnerability to, for example, a passport gate. Each +1 increase in  $\log_{10}$  FMR corresponds to a factor of 10 increase in FMR. The matrix is not quite symmetric because images in the enrollment and verification sets are different.

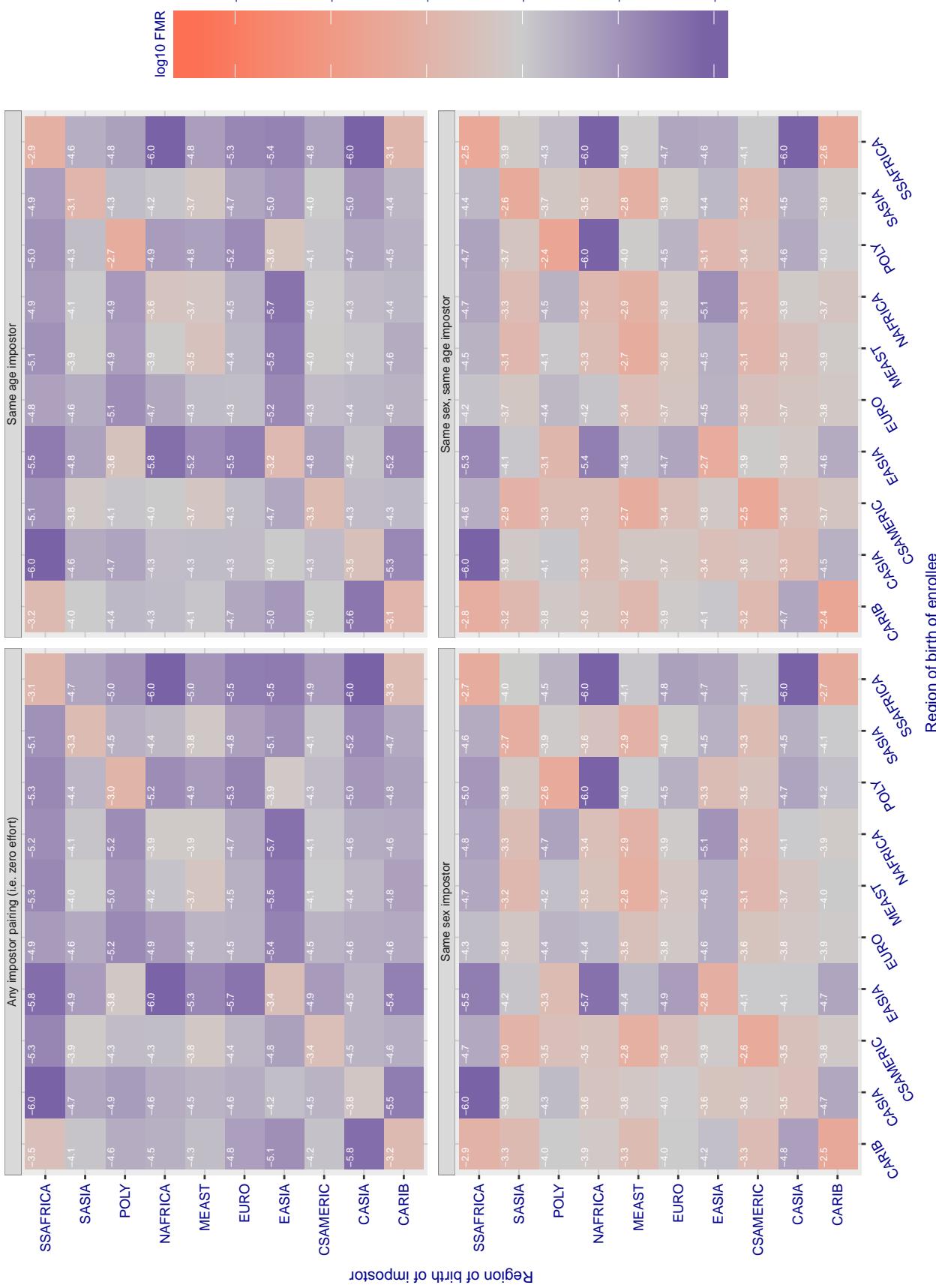
**Cross region FMR at threshold T = 0.353 for algorithm psl\_002, giving FMR(T) = 0.0001 globally.**

Figure 204: For algorithm psl-002 operating on visa images, the heatmap shows false match rates observed over impostor comparisons of faces from different individuals who were born in the given region pair. False matches are counted against a recognition threshold fixed globally to give the target FMR in the plot title, computed over all on the order of  $10^{10}$  impostor comparisons. If text appears in each box it give the same quantity as that coded by the color. Grey indicates FMR is at the intended FMR target level. Light red colors present a security vulnerability to, for example, a passport gate. Each +1 increase in  $\log_{10}$  FMR corresponds to a factor of 10 increase in FMR. The matrix is not quite symmetric because images in the enrollment and verification sets are different.

### Cross region FMR at threshold T = 0.779 for algorithm rankone\_006, giving FMR(T) = 0.0001 globally.

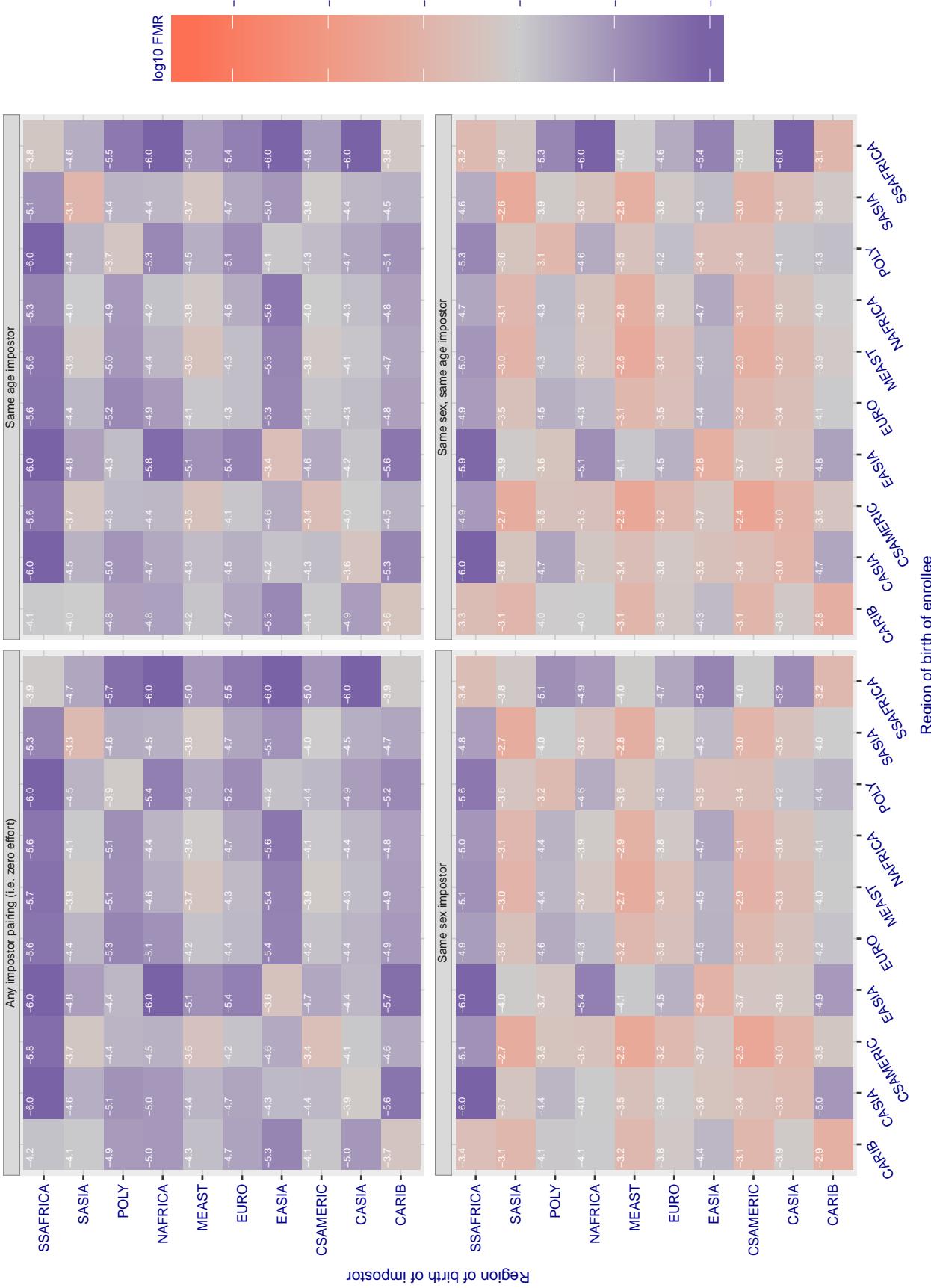


Figure 205: For algorithm rankone-006 operating on visa images, the heatmap shows false match rates observed over impostor comparisons of faces from different individuals who were born in the given region pair. False matches are counted against a recognition threshold fixed globally to give the target FMR in the plot title, computed over all on the order of  $10^{10}$  impostor comparisons. If text appears in each box it give the same quantity as that coded by the color. Grey indicates FMR is at the intended FMR target level. Light red colors present a security vulnerability to, for example, a passport gate. Each +1 increase in  $\log_{10} FMR$  corresponds to a factor of 10 increase in FMR. The matrix is not quite symmetric because images in the enrollment and verification sets are different.

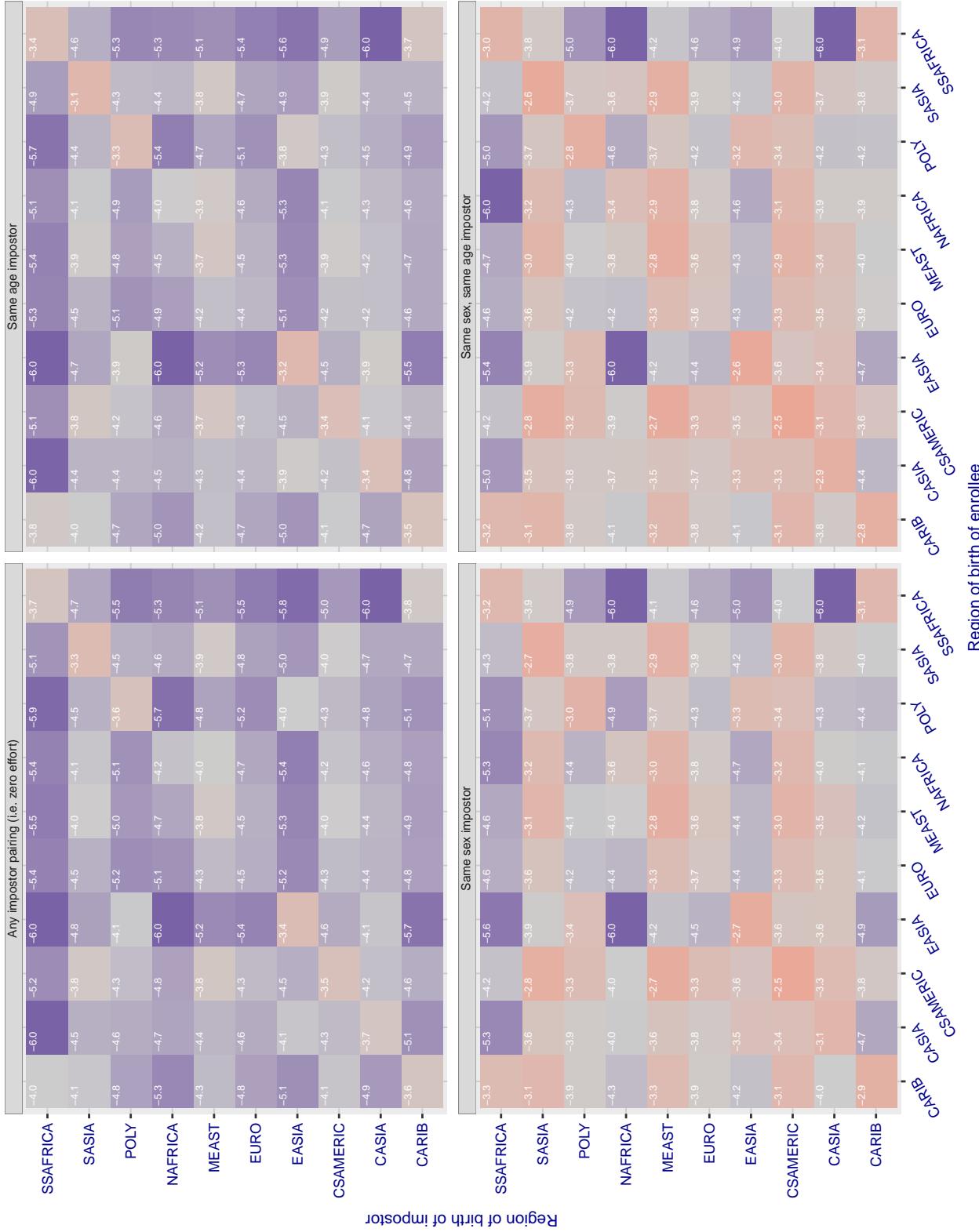


Figure 206: For algorithm rankone-007 operating on visa images, the heatmap shows false match rates observed over impostor comparisons of faces from different individuals who were born in the given region pair. False matches are counted against a recognition threshold fixed globally to give the target *FMR* in the plot title, computed over all on the order of  $10^{10}$  impostor comparisons. If text appears in each box it give the same quantity as that coded by the color. Grey indicates *FMR* is at the intended *FMR* target level. Light red colors present a security vulnerability to, for example, a passport gate. Each +1 increase in  $\log_{10} \text{FMR}$  corresponds to a factor of 10 increase in *FMR*. The matrix is not quite symmetric because images in the enrollment and verification sets are different.

### Cross region FMR at threshold T = 0.883 for algorithm realnetworks\_002, giving FMR(T) = 0.0001 globally.

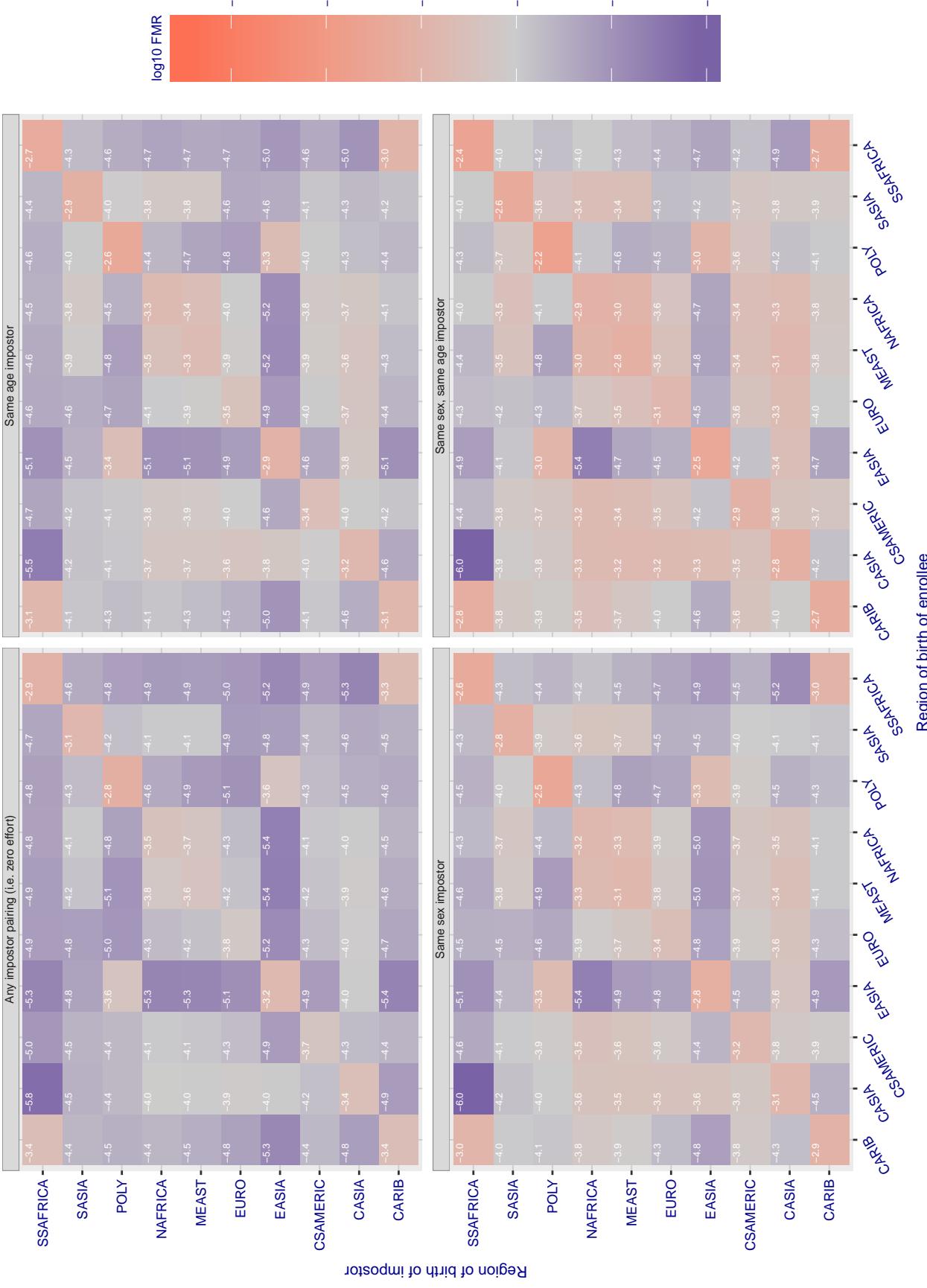


Figure 207: For algorithm realnetworks-002 operating on visa images, the heatmap shows false match rates observed over impostor comparisons of faces from different individuals who were born in the given region pair. False matches are counted against a recognition threshold fixed globally to give the target FMR in the plot title, computed over all on the order of  $10^{10}$  impostor comparisons. If text appears in each box it give the same quantity as that coded by the color. Grey indicates FMR is at the intended FMR target level. Light red colors present a security vulnerability to, for example, a passport gate. Each +1 increase in  $\log_{10} FMR$  corresponds to a factor of 10 increase in FMR. The matrix is not quite symmetric because images in the enrollment and verification sets are different.

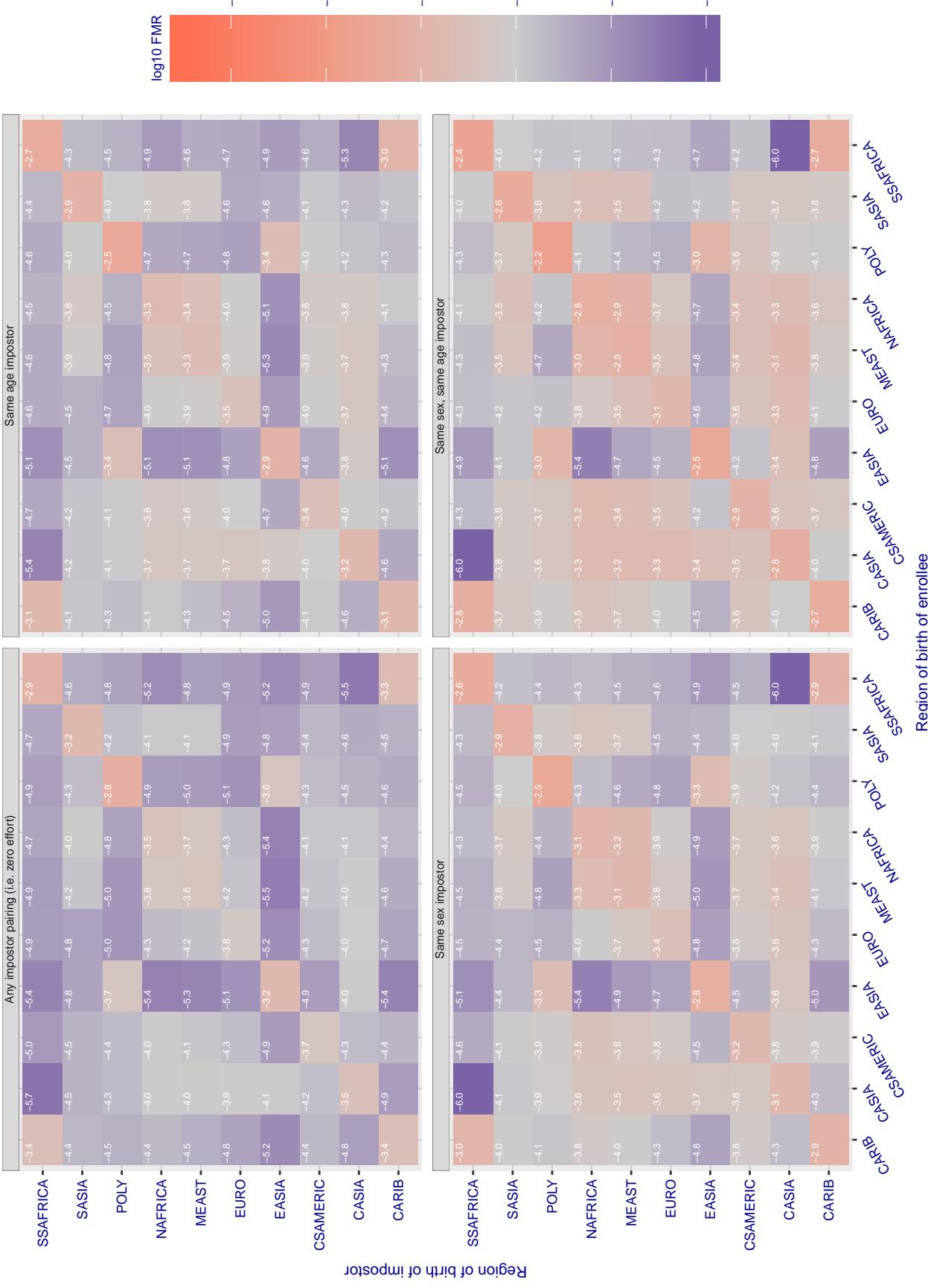
**Cross region FMR at threshold T = 0.886 for algorithm realnetworks\_003, giving FMR(T) = 0.0001 globally.**

Figure 208: For algorithm realnetworks-003 operating on visa images, the heatmap shows false match rates observed over impostor comparisons of faces from different individuals who were born in the given region pair. False matches are counted against a recognition threshold fixed globally to give the target FMR in the plot title, computed over all on the order of  $10^{10}$  impostor comparisons. If text appears in each box it give the same quantity as that coded by the color. Grey indicates FMR is at the intended FMR target level. Light red colors present a security vulnerability to, for example, a passport gate. Each +1 increase in  $\log_{10} FMR$  corresponds to a factor of 10 increase in FMR. The matrix is not quite symmetric because images in the enrollment and verification sets are different.

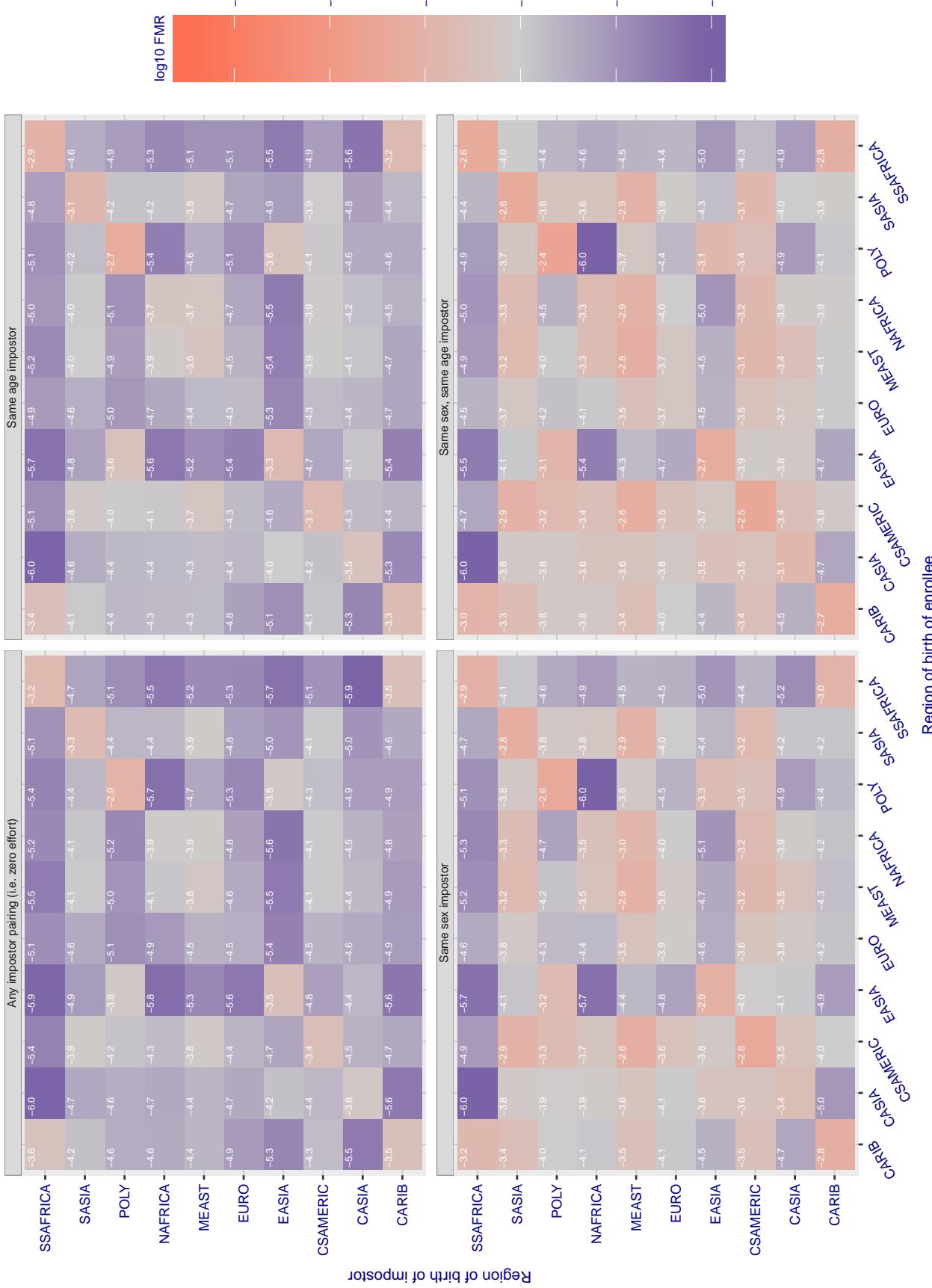
**Cross region FMR at threshold T = 70.373 for algorithm remarkai\_000, giving FMR(T) = 0.0001 globally.**

Figure 209: For algorithm remarkai-000 operating on visa images, the heatmap shows false match rates observed over impostor comparisons of faces from different individuals who were born in the given region pair. False matches are counted against a recognition threshold fixed globally to give the target FMR in the plot title, computed over all on the order of  $10^{10}$  impostor comparisons. If text appears in each box it give the same quantity as that coded by the color. Grey indicates FMR is at the intended FMR target level. Light red colors present a security vulnerability to, for example, a passport gate. Each +1 increase in  $\log_{10} FMR$  corresponds to a factor of 10 increase in FMR. The matrix is not quite symmetric because images in the enrollment and verification sets are different.

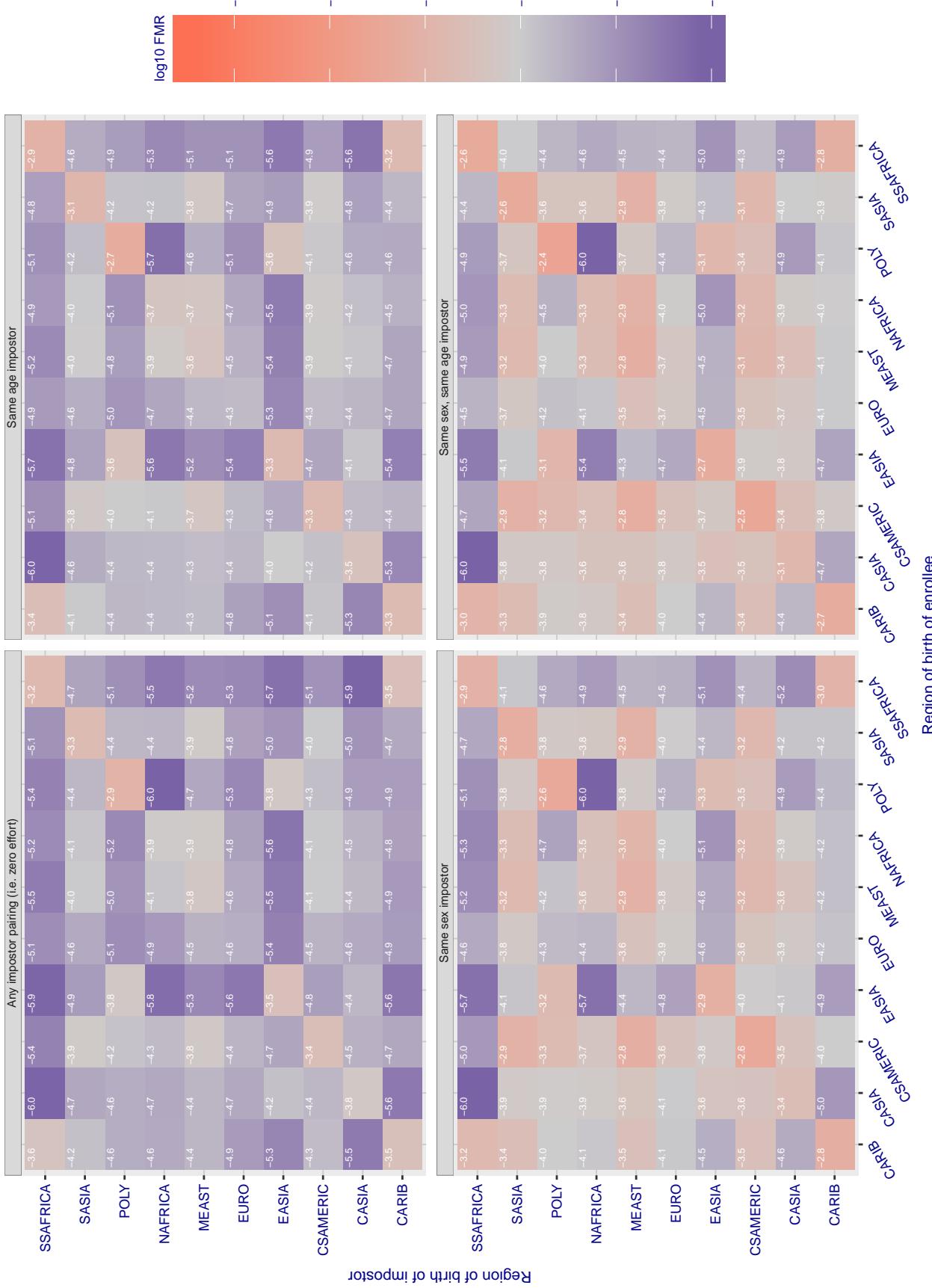
**Cross region FMR at threshold T = 70.384 for algorithm remarkai\_001, giving FMR(T) = 0.0001 globally.**

Figure 210: For algorithm remarkai-001 operating on visa images, the heatmap shows false match rates observed over impostor comparisons of faces from different individuals who were born in the given region pair. False matches are counted against a recognition threshold fixed globally to give the target FMR in the plot title, computed over all on the order of  $10^{10}$  impostor comparisons. If text appears in each box it give the same quantity as that coded by the color. Grey indicates FMR is at the intended FMR target level. Light red colors present a security vulnerability to, for example, a passport gate. Each +1 increase in  $\log_{10} FMR$  corresponds to a factor of 10 increase in FMR. The matrix is not quite symmetric because images in the enrollment and verification sets are different.

### Cross region FMR at threshold T = 0.682 for algorithm saffe\_001, giving FMR(T) = 0.0001 globally.

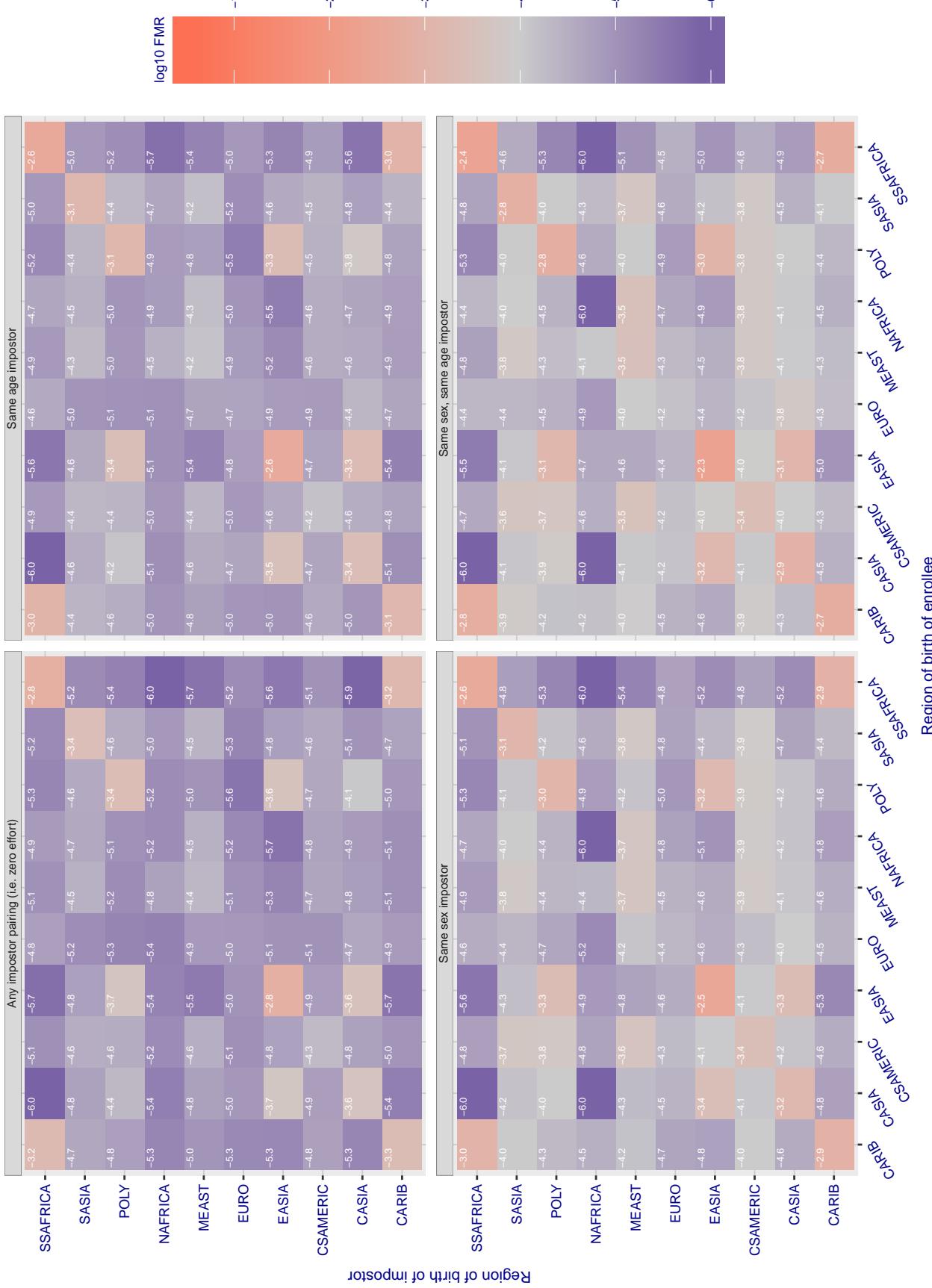


Figure 211: For algorithm saffe-001 operating on visa images, the heatmap shows false match rates observed over impostor comparisons of faces from different individuals who were born in the given region pair. False matches are counted against a recognition threshold fixed globally to give the target FMR in the plot title, computed over all on the order of  $10^{10}$  impostor comparisons. If text appears in each box it give the same quantity as that coded by the color. Grey indicates FMR is at the intended FMR target level. Light red colors present a security vulnerability to, for example, a passport gate. Each +1 increase in  $\log_{10} \text{FMR}$  corresponds to a factor of 10 increase in FMR. The matrix is not quite symmetric because images in the enrollment and verification sets are different.

### Cross region FMR at threshold T = 0.383 for algorithm saffe\_002, giving FMR(T) = 0.0001 globally.

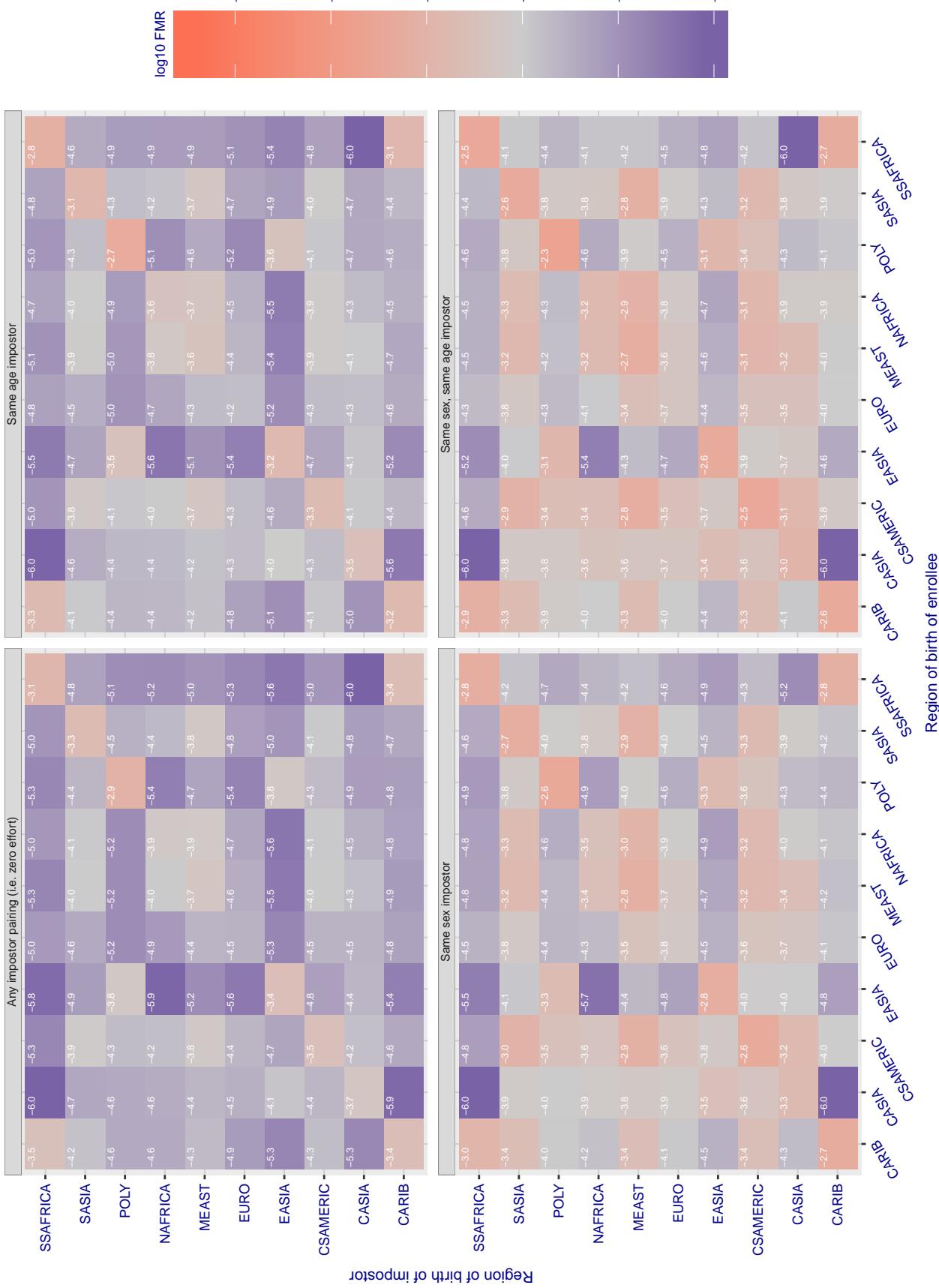


Figure 212: For algorithm saffe-002 operating on visa images, the heatmap shows false match rates observed over impostor comparisons of faces from different individuals who were born in the given region pair. False matches are counted against a recognition threshold fixed globally to give the target FMR in the plot title, computed over all on the order of  $10^{10}$  impostor comparisons. If text appears in each box it give the same quantity as that coded by the color. Grey indicates FMR is at the intended FMR target level. Light red colors present a security vulnerability to, for example, a passport gate. Each +1 increase in  $\log_{10} \text{FMR}$  corresponds to a factor of 10 increase in FMR. The matrix is not quite symmetric because images in the enrollment and verification sets are different.

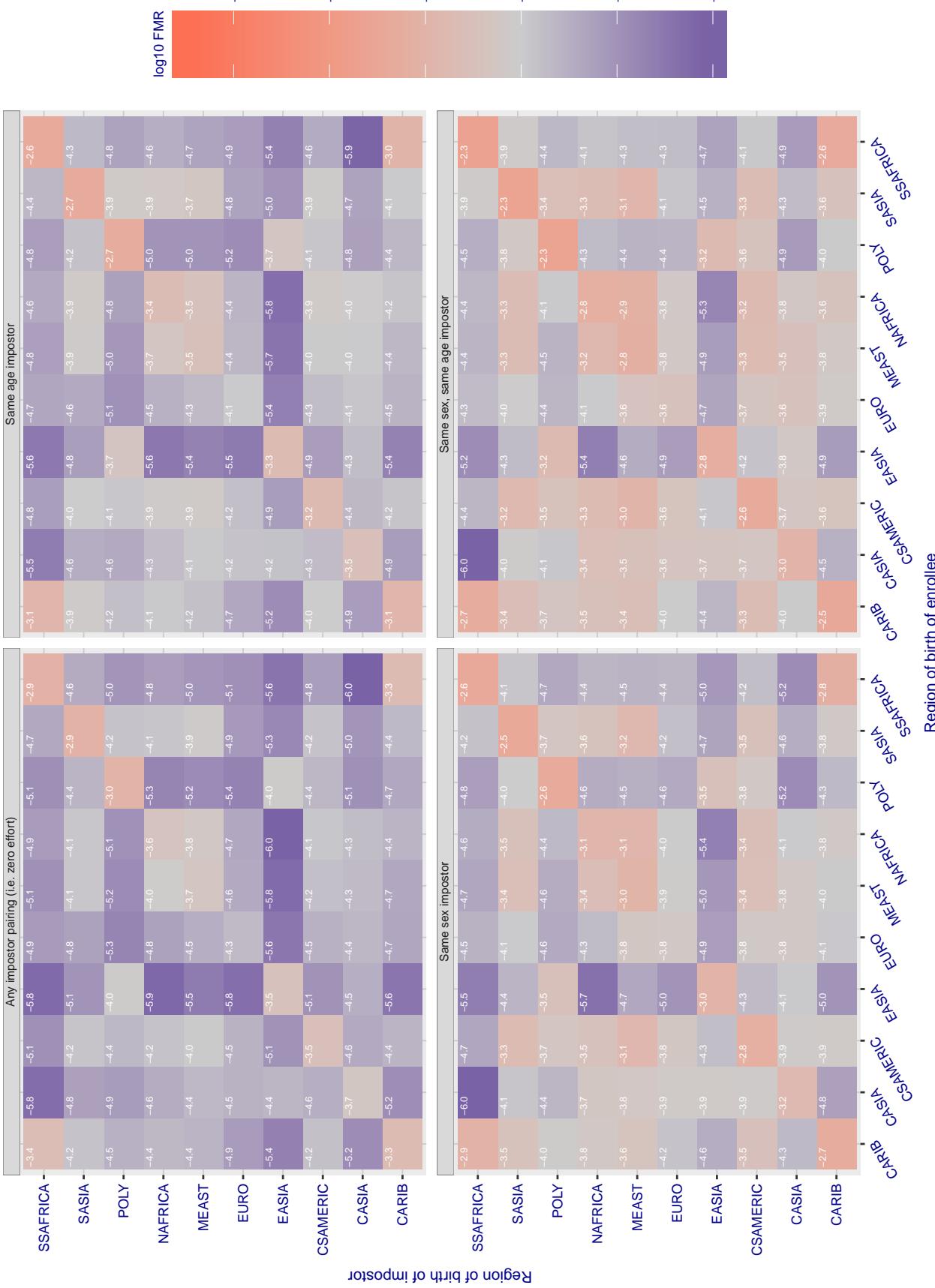
**Cross region FMR at threshold T = 0.390 for algorithm sensetime\_001, giving FMR(T) = 0.0001 globally.**

Figure 213: For algorithm sensetime-001 operating on visa images, the heatmap shows false match rates observed over impostor comparisons of faces from different individuals who were born in the given region pair. False matches are counted against a recognition threshold fixed globally to give the target FMR in the plot title, computed over all on the order of  $10^{10}$  impostor comparisons. If text appears in each box it give the same quantity as that coded by the color. Grey indicates FMR is at the intended FMR target level. Light red colors present a security vulnerability to, for example, a passport gate. Each +1 increase in  $\log_{10} FMR$  corresponds to a factor of 10 increase in FMR. The matrix is not quite symmetric because images in the enrollment and verification sets are different.

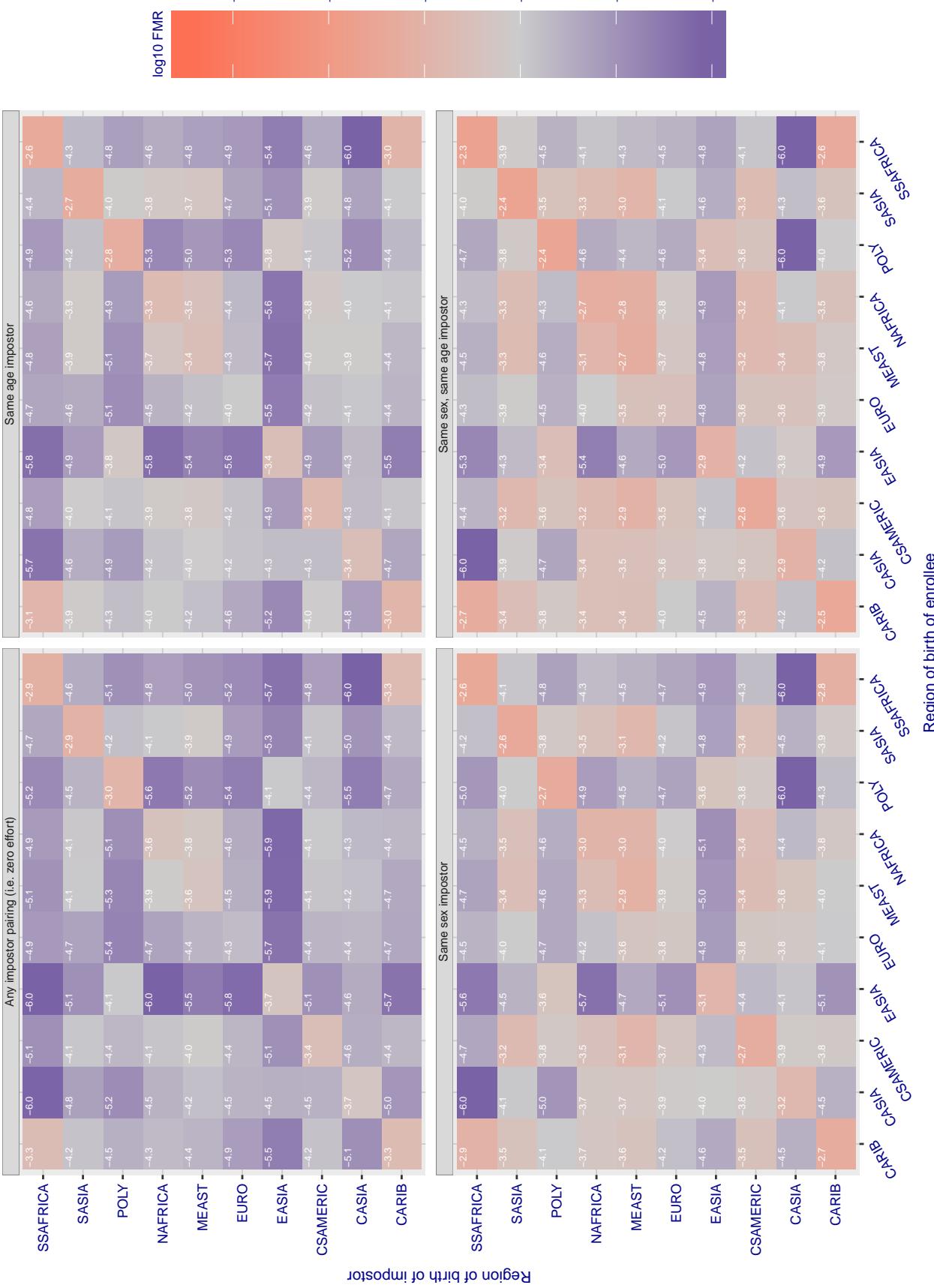
**Cross region FMR at threshold T = 0.390 for algorithm sensetime\_002, giving FMR(T) = 0.0001 globally.**

Figure 214: For algorithm sensetime-002 operating on visa images, the heatmap shows false match rates observed over impostor comparisons of faces from different individuals who were born in the given region pair. False matches are counted against a recognition threshold fixed globally to give the target FMR in the plot title, computed over all on the order of  $10^{10}$  impostor comparisons. If text appears in each box it give the same quantity as that coded by the color. Grey indicates FMR is at the intended FMR target level. Light red colors present a security vulnerability to, for example, a passport gate. Each +1 increase in  $\log_{10} FMR$  corresponds to a factor of 10 increase in FMR. The matrix is not quite symmetric because images in the enrollment and verification sets are different.

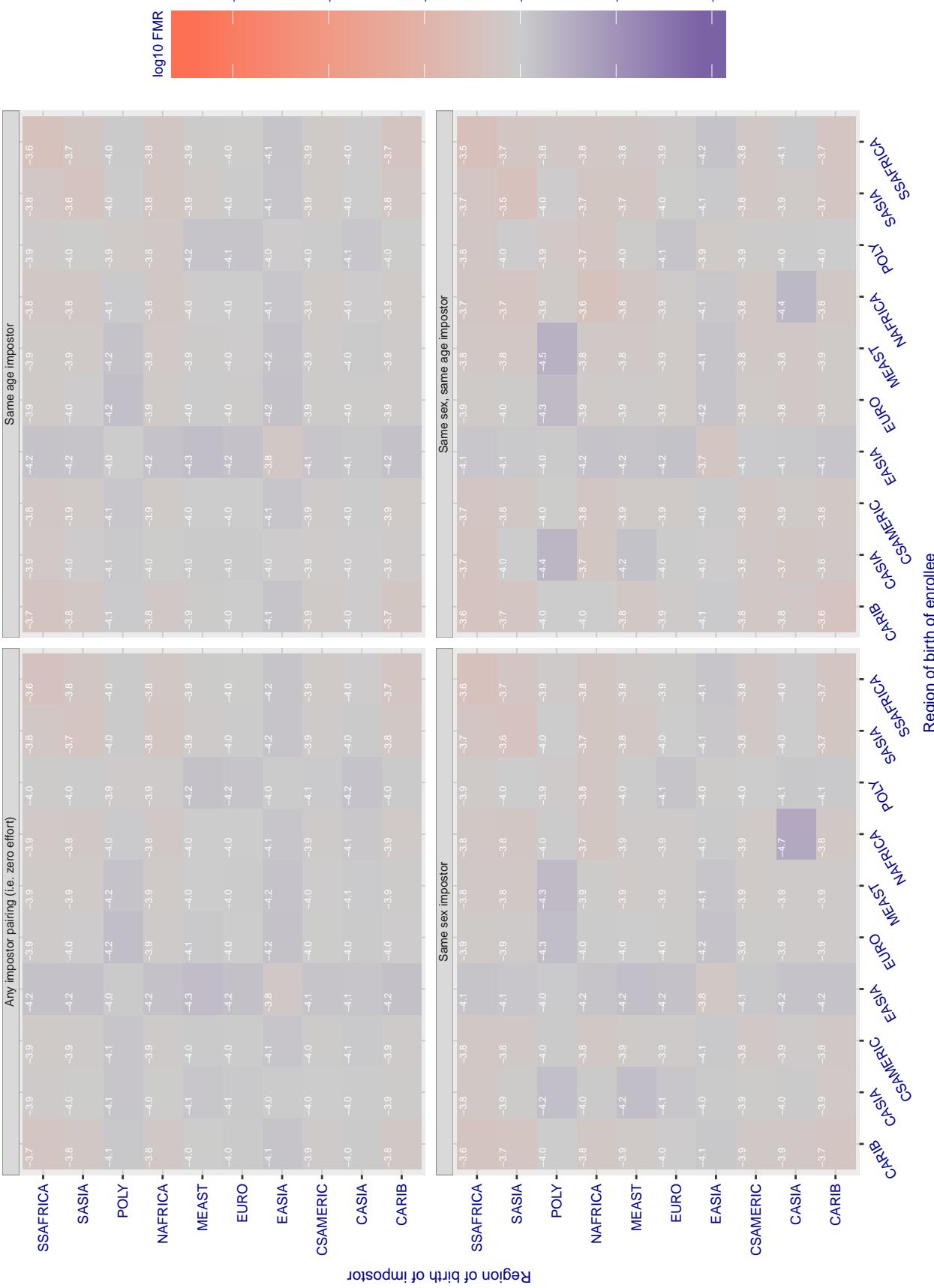
**Cross region FMR at threshold T = 0.970 for algorithm shaman\_000, giving FMR(T) = 0.0001 globally.**

Figure 215: For algorithm shaman-000 operating on visa images, the heatmap shows false match rates observed over impostor comparisons of faces from different individuals who were born in the given region pair. False matches are counted against a recognition threshold fixed globally to give the target FMR in the plot title, computed over all on the order of  $10^{10}$  impostor comparisons. If text appears in each box it give the same quantity as that coded by the color. Grey indicates FMR is at the intended FMR target level. Light red colors present a security vulnerability to, for example, a passport gate. Each +1 increase in  $\log_{10} FMR$  corresponds to a factor of 10 increase in FMR. The matrix is not quite symmetric because images in the enrollment and verification sets are different.

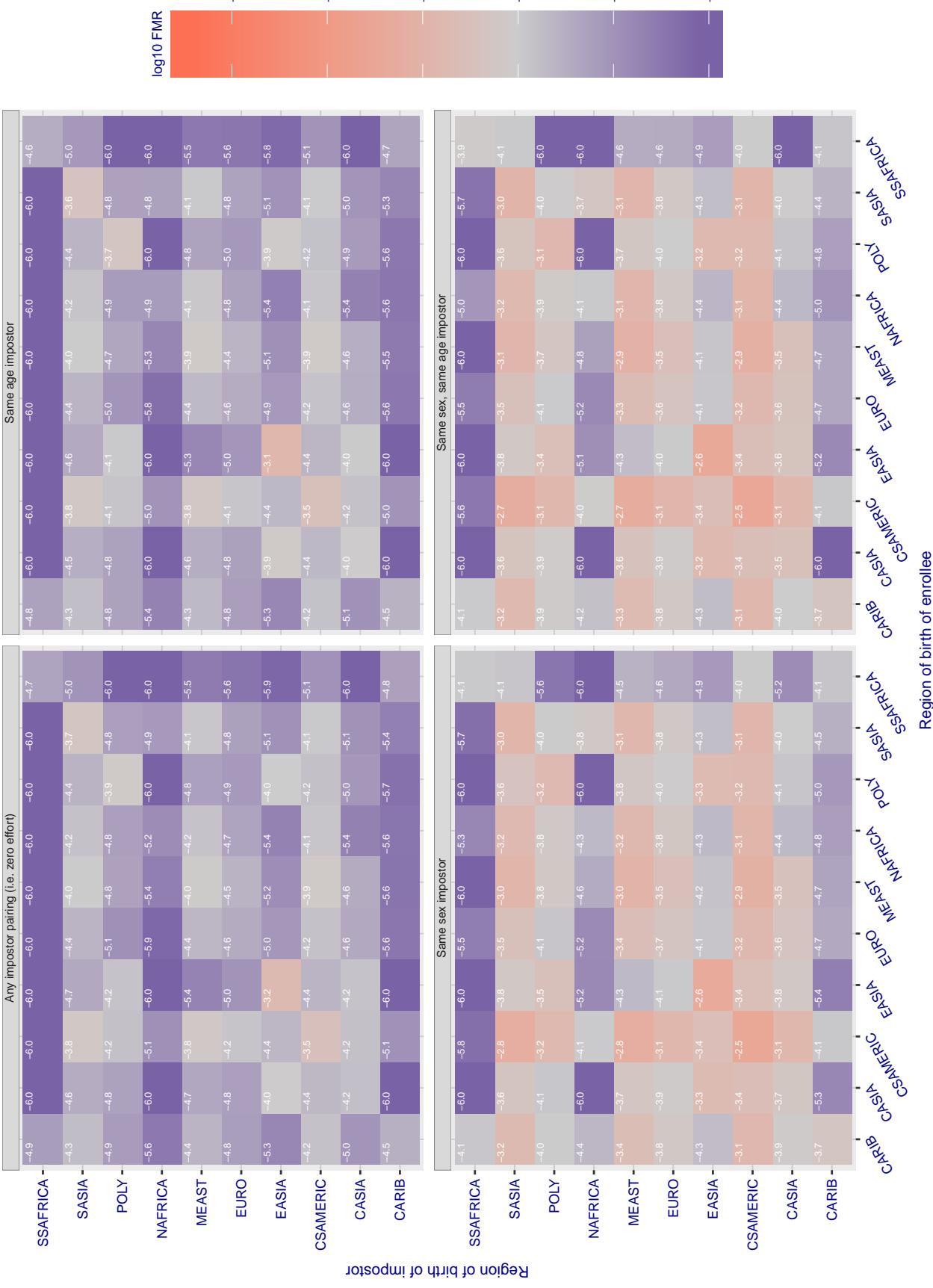
**Cross region FMR at threshold T = 0.725 for algorithm shaman\_001, giving FMR(T) = 0.0001 globally.**

Figure 216: For algorithm shaman-001 operating on visa images, the heatmap shows false match rates observed over impostor comparisons of faces from different individuals who were born in the given region pair. False matches are counted against a recognition threshold fixed globally to give the target FMR in the plot title, computed over all on the order of  $10^{10}$  impostor comparisons. If text appears in each box it give the same quantity as that coded by the color. Grey indicates FMR is at the intended FMR target level. Light red colors present a security vulnerability to, for example, a passport gate. Each +1 increase in  $\log_{10} FMR$  corresponds to a factor of 10 increase in FMR. The matrix is not quite symmetric because images in the enrollment and verification sets are different.

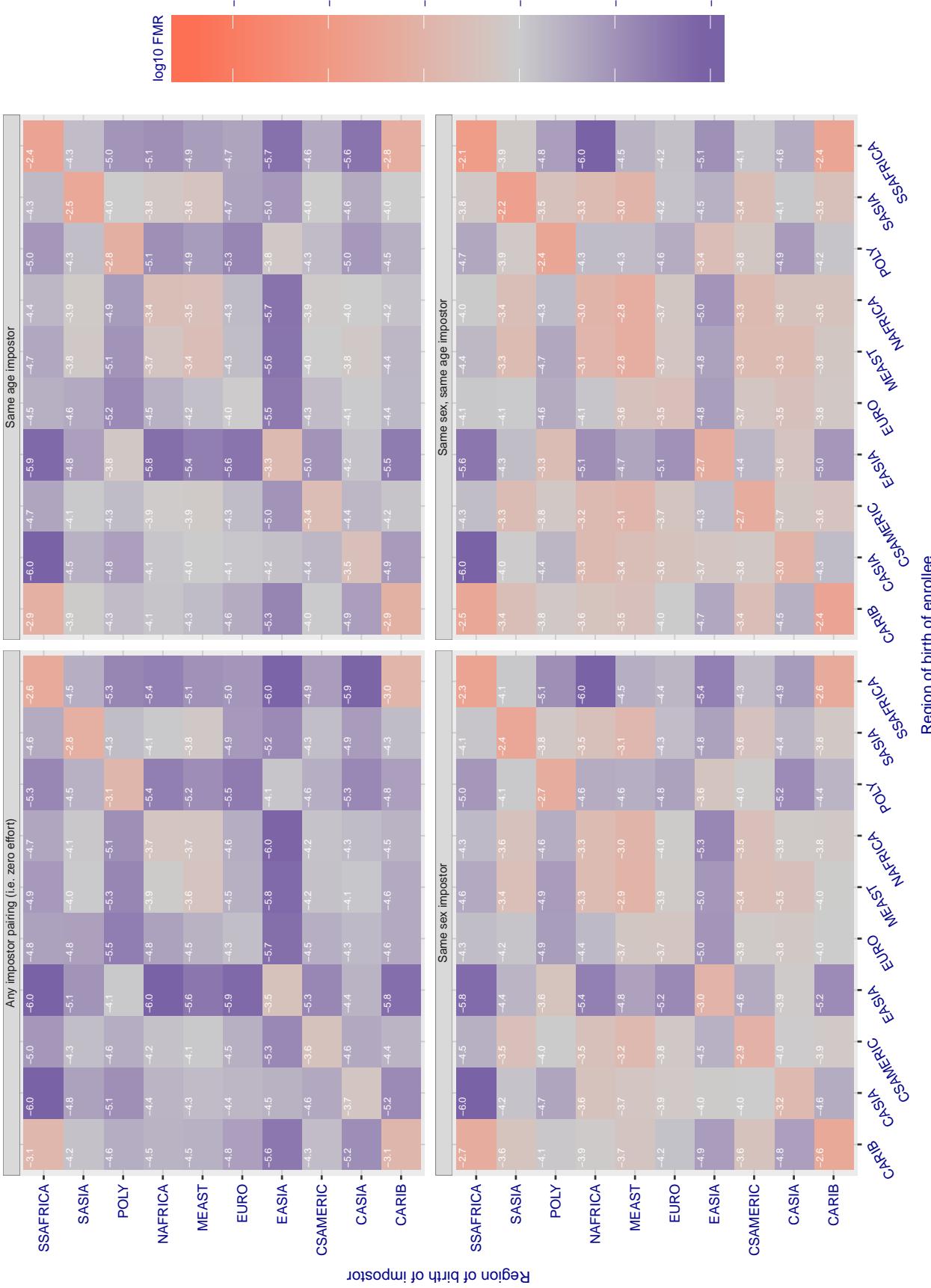
**Cross region FMR at threshold T = 0.390 for algorithm siat\_002, giving FMR(T) = 0.0001 globally.**

Figure 217: For algorithm siat-002 operating on visa images, the heatmap shows false match rates observed over impostor comparisons of faces from different individuals who were born in the given region pair. False matches are counted against a recognition threshold fixed globally to give the target FMR in the plot title, computed over all on the order of  $10^{10}$  impostor comparisons. If text appears in each box it give the same quantity as that coded by the color. Grey indicates FMR is at the intended FMR target level. Light red colors present a security vulnerability to, for example, a passport gate. Each +1 increase in  $\log 10$  FMR corresponds to a factor of 10 increase in FMR. The matrix is not quite symmetric because images in the enrollment and verification sets are different.

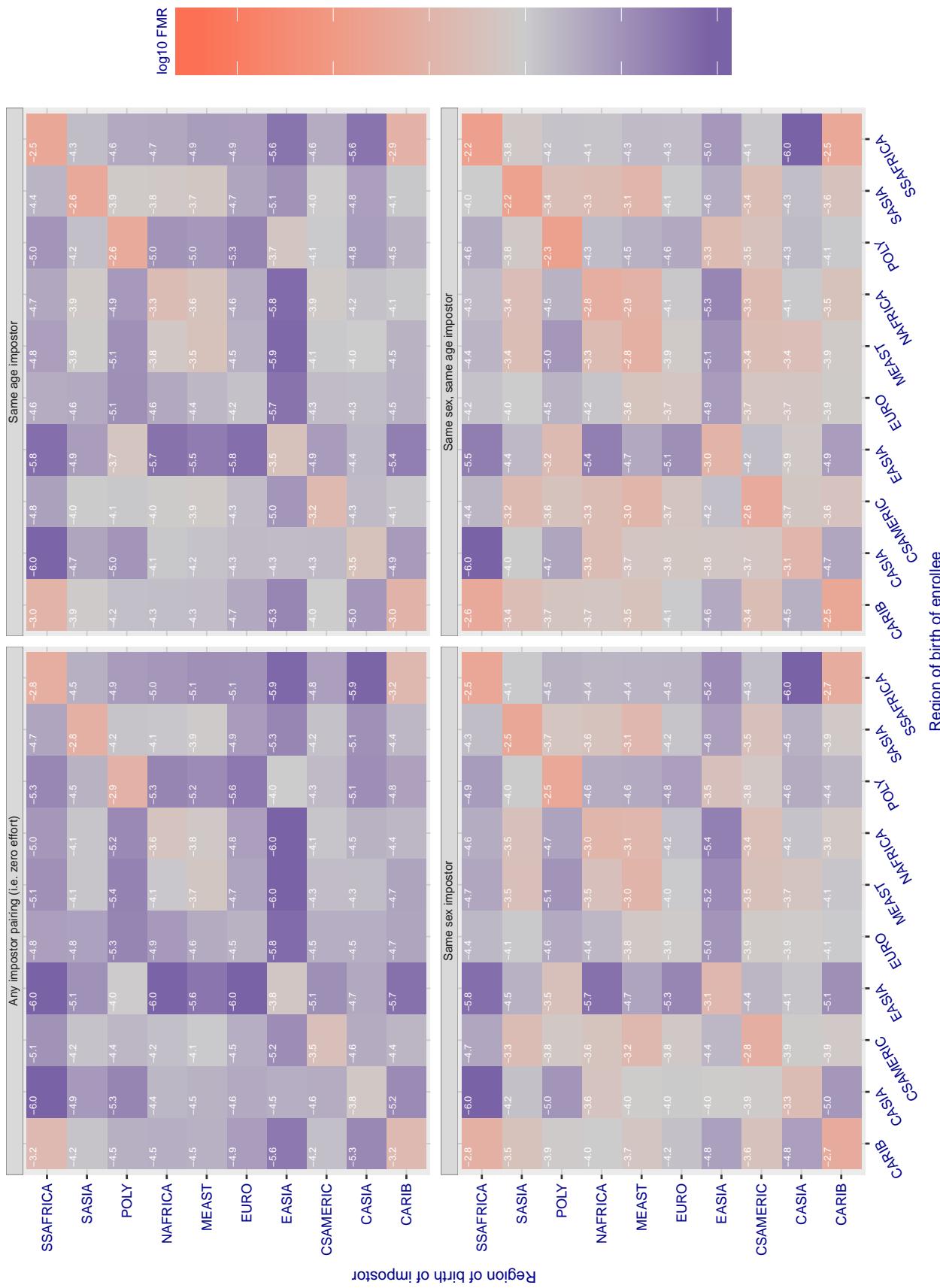
**Cross region FMR at threshold T = 0.393 for algorithm sat\_004, giving FMR(T) = 0.0001 globally.**

Figure 218: For algorithm sat-004 operating on visa images, the heatmap shows false match rates observed over impostor comparisons of faces from different individuals who were born in the given region pair. False matches are counted against a recognition threshold fixed globally to give the target FMR in the plot title, computed over all on the order of  $10^{10}$  impostor comparisons. If text appears in each box it give the same quantity as that coded by the color. Grey indicates FMR is at the intended FMR target level. Light red colors present a security vulnerability to, for example, a passport gate. Each +1 increase in  $\log_{10}$  FMR corresponds to a factor of 10 increase in FMR. The matrix is not quite symmetric because images in the enrollment and verification sets are different.

### Cross region FMR at threshold T = 0.598 for algorithm smilart\_002, giving FMR(T) = 0.0001 globally.

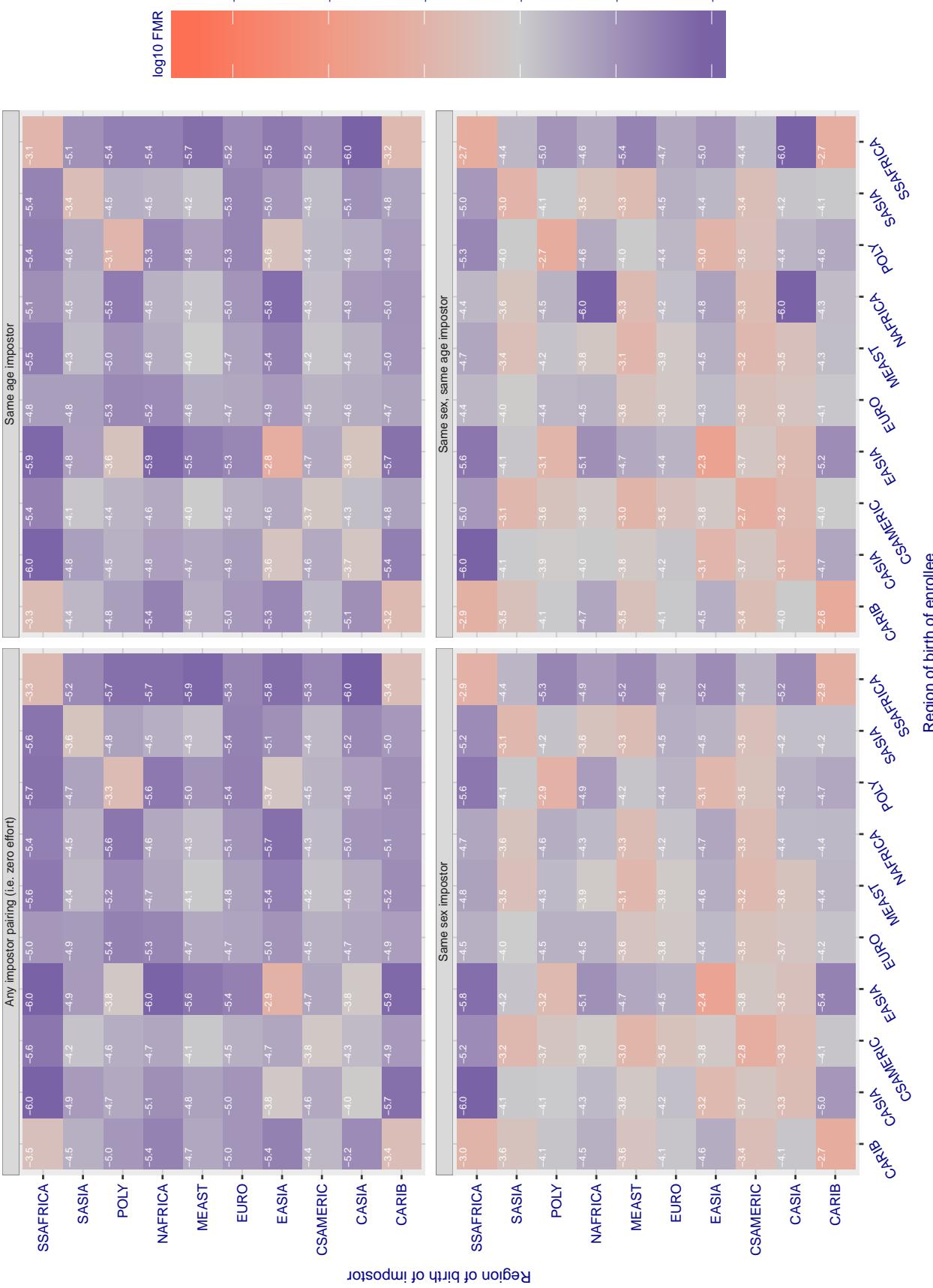


Figure 219: For algorithm smilart-002 operating on visa images, the heatmap shows false match rates observed over impostor comparisons of faces from different individuals who were born in the given region pair. False matches are counted against a recognition threshold fixed globally to give the target FMR in the plot title, computed over all on the order of  $10^{10}$  impostor comparisons. If text appears in each box it give the same quantity as that coded by the color. Grey indicates FMR is at the intended FMR target level. Light red colors present a security vulnerability to, for example, a passport gate. Each +1 increase in  $\log_{10} FMR$  corresponds to a factor of 10 increase in FMR. The matrix is not quite symmetric because images in the enrollment and verification sets are different.

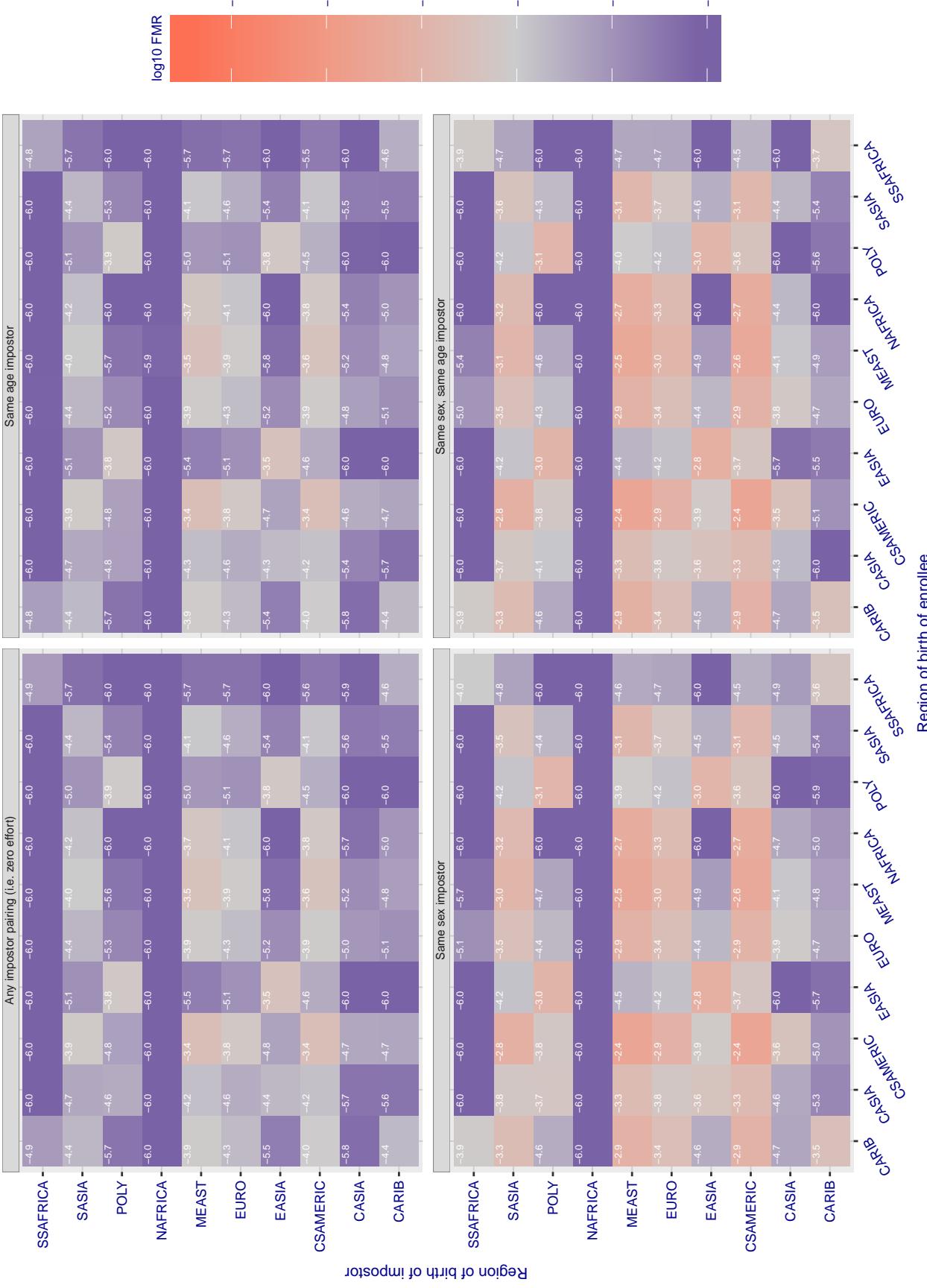
**Cross region FMR at threshold T = 0.654 for algorithm smilart\_003, giving FMR(T) = 0.0001 globally.**

Figure 220: For algorithm smilart-003 operating on visa images, the heatmap shows false match rates observed over impostor comparisons of faces from different individuals who were born in the given region pair. False matches are counted against a recognition threshold fixed globally to give the target FMR in the plot title, computed over all on the order of  $10^{10}$  impostor comparisons. If text appears in each box it give the same quantity as that coded by the color. Grey indicates FMR is at the intended FMR target level. Light red colors present a security vulnerability to, for example, a passport gate. Each +1 increase in  $\log_{10} FMR$  corresponds to a factor of 10 increase in FMR. The matrix is not quite symmetric because images in the enrollment and verification sets are different.

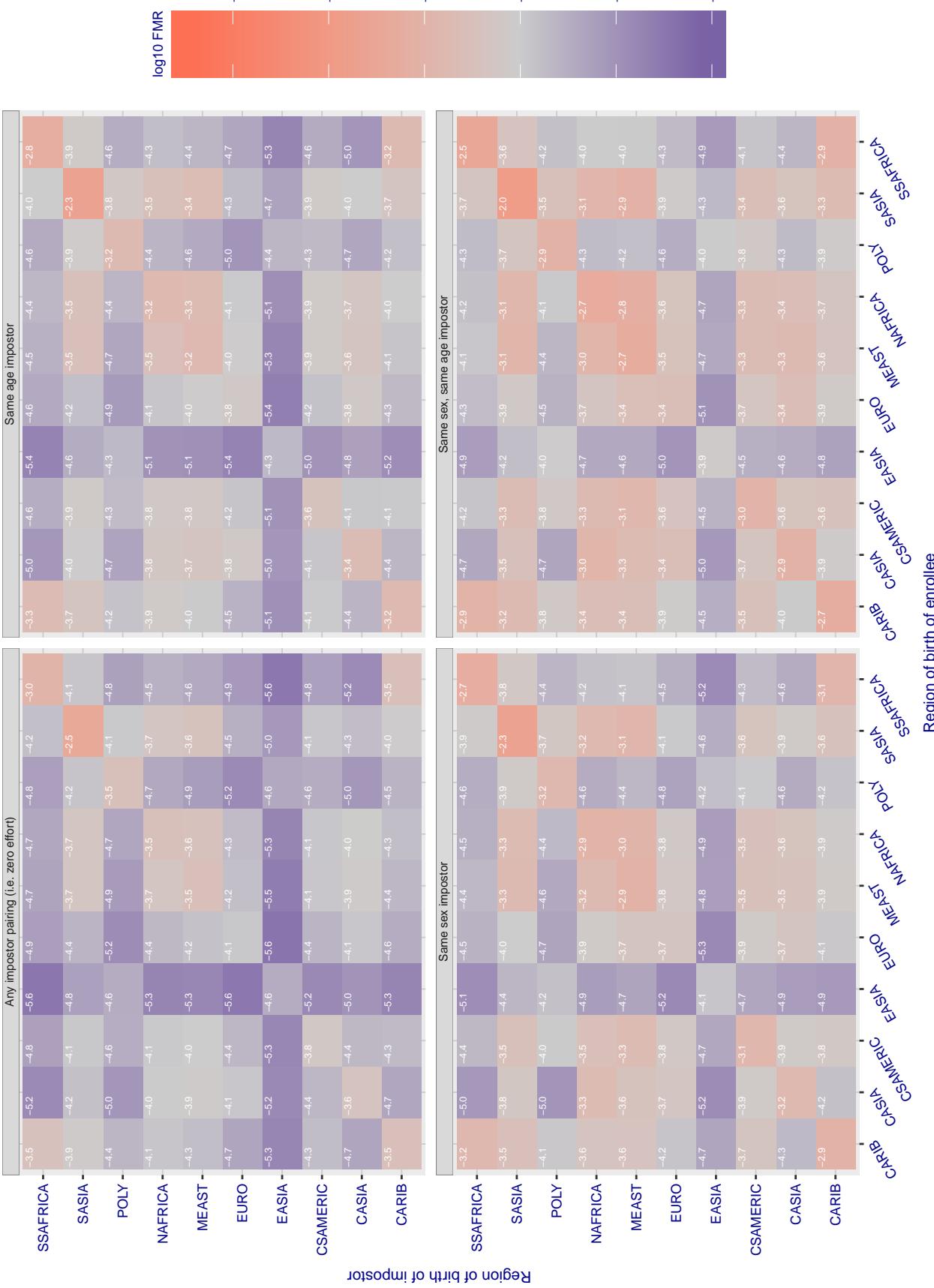
**Cross region FMR at threshold T = 0.314 for algorithm starhybrid\_001, giving FMR(T) = 0.0001 globally.**

Figure 221: For algorithm starhybrid-001 operating on visa images, the heatmap shows false match rates observed over impostor comparisons of faces from different individuals who were born in the given region pair. False matches are counted against a recognition threshold fixed globally to give the target FMR in the plot title, computed over all on the order of  $10^{10}$  impostor comparisons. If text appears in each box it give the same quantity as that coded by the color. Grey indicates FMR is at the intended FMR target level. Light red colors present a security vulnerability to, for example, a passport gate. Each +1 increase in  $\log_{10} FMR$  corresponds to a factor of 10 increase in FMR. The matrix is not quite symmetric because images in the enrollment and verification sets are different.

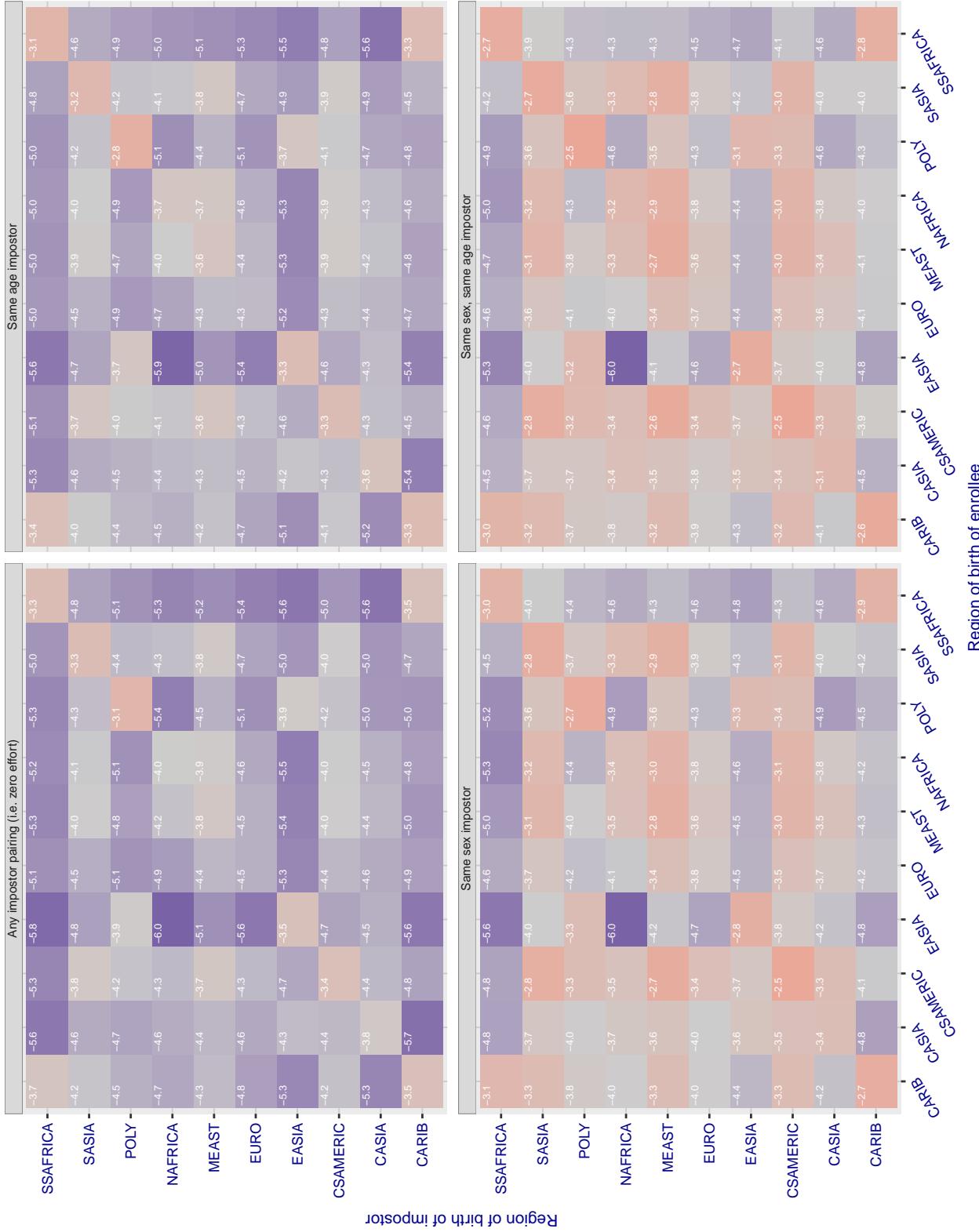


Figure 222: For algorithm *synesis-004* operating on visa images, the heatmap shows false match rates observed over impostor comparisons of faces from different individuals who were born in the given region pair. False matches are counted against a recognition threshold fixed globally to give the target *FMR* in the plot title, computed over all on the order of  $10^{10}$  impostor comparisons. If text appears in each box it give the same quantity as that coded by the color. Grey indicates *FMR* is at the intended *FMR* target level. Light red colors present a security vulnerability to, for example, a passport gate. Each +1 increase in  $\log_{10} \text{FMR}$  corresponds to a factor of 10 increase in *FMR*. The matrix is not quite symmetric because images in the enrollment and verification sets are different.

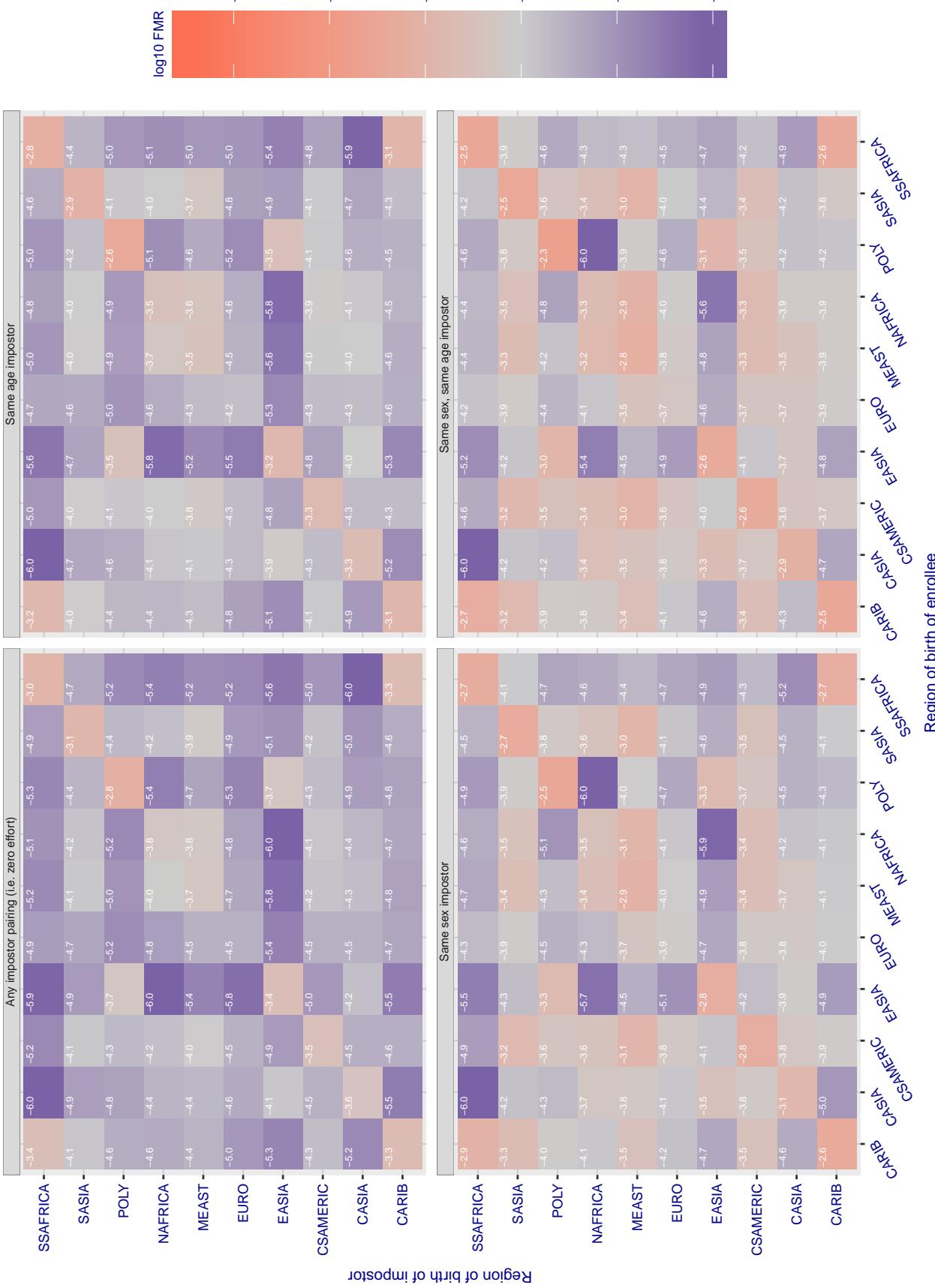
**Cross region FMR at threshold T = 0.356 for algorithm synthesis\_005, giving FMR(T) = 0.0001 globally.**

Figure 223: For algorithm synthesis-005 operating on visa images, the heatmap shows false match rates observed over impostor comparisons of faces from different individuals who were born in the given region pair. False matches are counted against a recognition threshold fixed globally to give the target FMR in the plot title, computed over all on the order of  $10^{10}$  impostor comparisons. If text appears in each box it give the same quantity as that coded by the color. Grey indicates FMR is at the intended FMR target level. Light red colors present a security vulnerability to, for example, a passport gate. Each +1 increase in  $\log_{10} FMR$  corresponds to a factor of 10 increase in FMR. The matrix is not quite symmetric because images in the enrollment and verification sets are different.

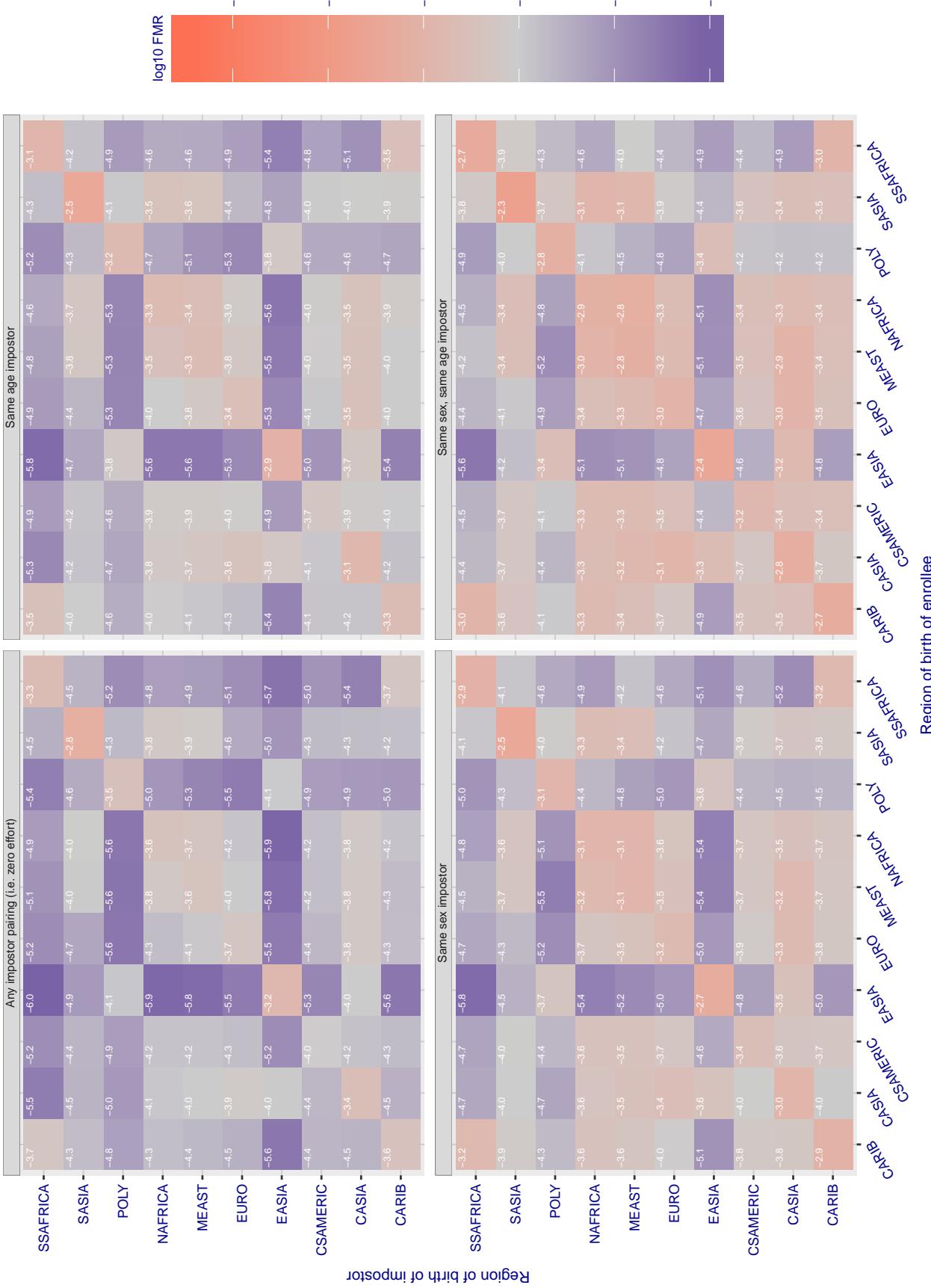
**Cross region FMR at threshold T = 148.416 for algorithm tech5\_001, giving FMR(T) = 0.0001 globally.**

Figure 224: For algorithm tech5-001 operating on visa images, the heatmap shows false match rates observed over impostor comparisons of faces from different individuals who were born in the given region pair. False matches are counted against a recognition threshold fixed globally to give the target FMR in the plot title, computed over all on the order of  $10^{10}$  impostor comparisons. If text appears in each box it give the same quantity as that coded by the color. Grey indicates FMR is at the intended FMR target level. Light red colors present a security vulnerability to, for example, a passport gate. Each +1 increase in  $\log_{10} \text{FMR}$  corresponds to a factor of 10 increase in FMR. The matrix is not quite symmetric because images in the enrollment and verification sets are different.

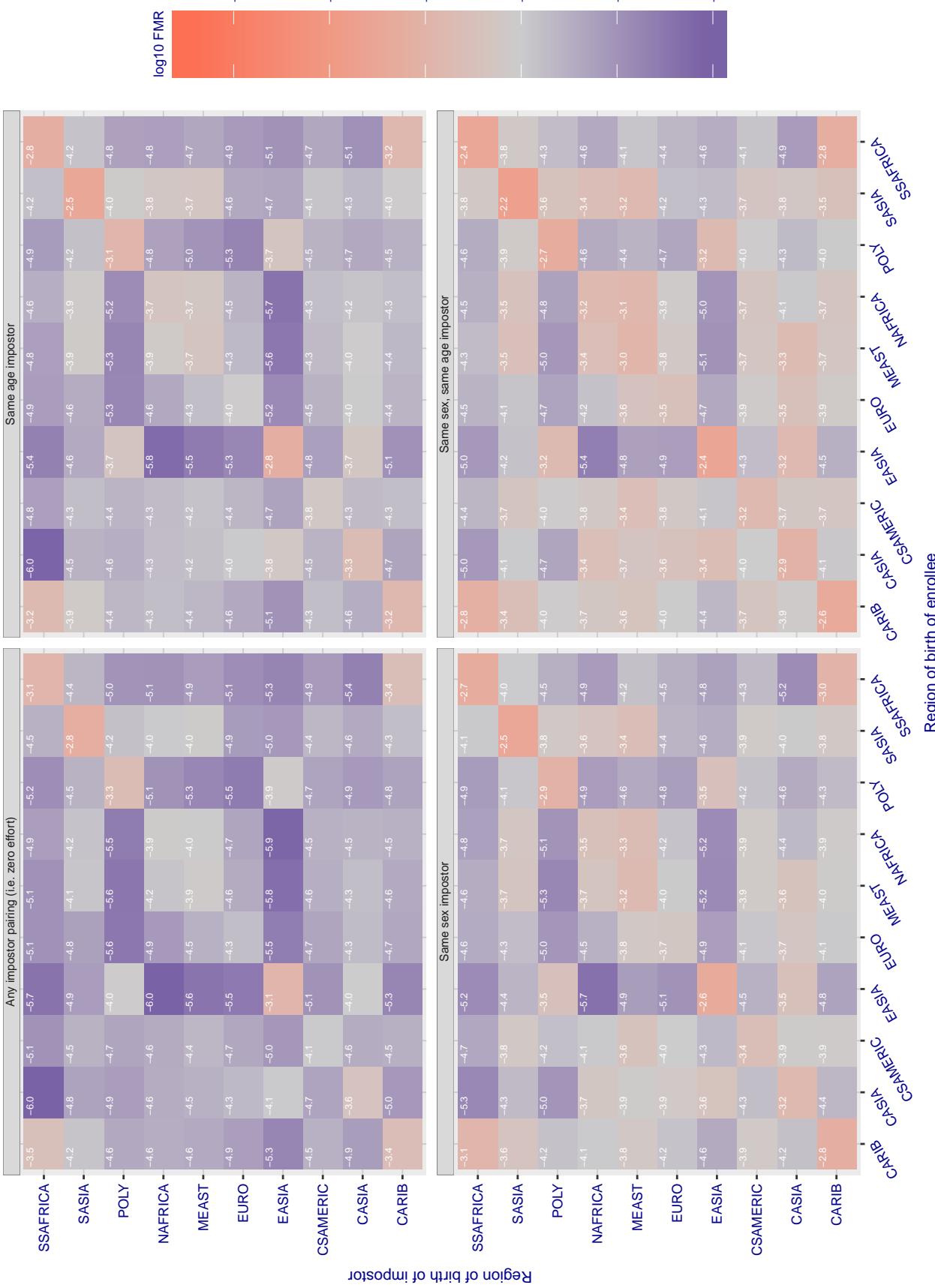
**Cross region FMR at threshold T = 147.661 for algorithm tech5\_002, giving FMR(T) = 0.0001 globally.**

Figure 225: For algorithm tech5-002 operating on visa images, the heatmap shows false match rates observed over impostor comparisons of faces from different individuals who were born in the given region pair. False matches are counted against a recognition threshold fixed globally to give the target FMR in the plot title, computed over all on the order of  $10^{10}$  impostor comparisons. If text appears in each box it give the same quantity as that coded by the color. Grey indicates FMR is at the intended FMR target level. Light red colors present a security vulnerability to, for example, a passport gate. Each +1 increase in  $\log_{10} FMR$  corresponds to a factor of 10 increase in FMR. The matrix is not quite symmetric because images in the enrollment and verification sets are different.

### Cross region FMR at threshold T = 0.896 for algorithm tevian\_003, giving FMR(T) = 0.0001 globally.

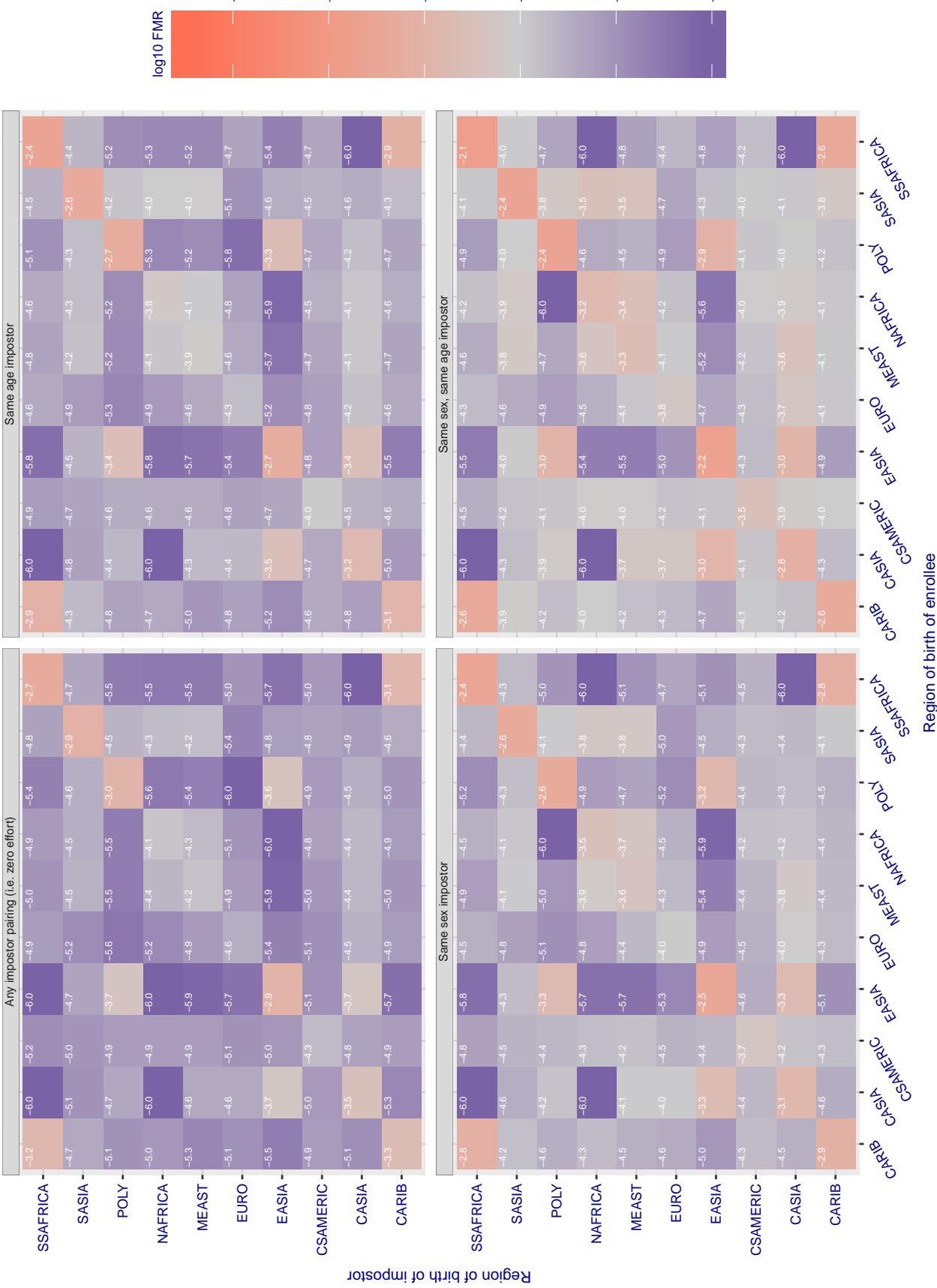


Figure 226: For algorithm tevian-003 operating on visa images, the heatmap shows false match rates observed over impostor comparisons of faces from different individuals who were born in the given region pair. False matches are counted against a recognition threshold fixed globally to give the target FMR in the plot title, computed over all on the order of  $10^{10}$  impostor comparisons. If text appears in each box it give the same quantity as that coded by the color. Grey indicates FMR is at the intended FMR target level. Light red colors present a security vulnerability to, for example, a passport gate. Each +1 increase in  $\log_{10} \text{FMR}$  corresponds to a factor of 10 increase in FMR. The matrix is not quite symmetric because images in the enrollment and verification sets are different.

Cross region FMR at threshold  $T = 0.896$  for algorithm tevian\_004, giving  $FMR(T) = 0.0001$  globally.

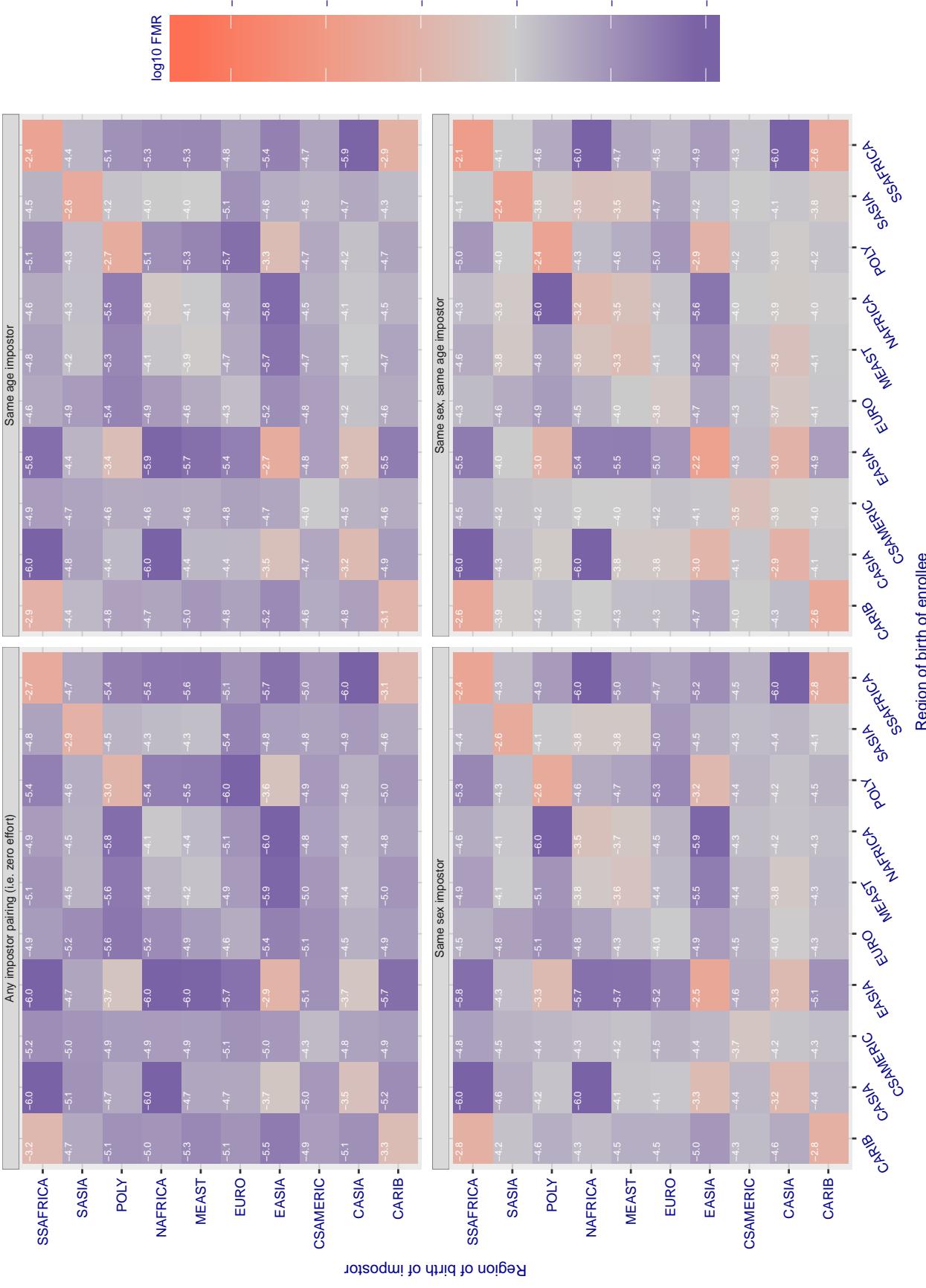


Figure 227: For algorithm tevian-004 operating on visa images, the heatmap shows false match rates observed over impostor comparisons of faces from different individuals who were born in the given region pair. False matches are counted against a recognition threshold fixed globally to give the target FMR in the plot title, computed over all on the order of  $10^{10}$  impostor comparisons. If text appears in each box it give the same quantity as that coded by the color. Grey indicates FMR is at the intended FMR target level. Light red colors present a security vulnerability to, for example, a passport gate. Each +1 increase in  $\log_{10}$  FMR corresponds to a factor of 10 increase in FMR. The matrix is not quite symmetric because images in the enrollment and verification sets are different.

### Cross region FMR at threshold T = 151.011 for algorithm tiger\_002, giving FMR(T) = 0.0001 globally.

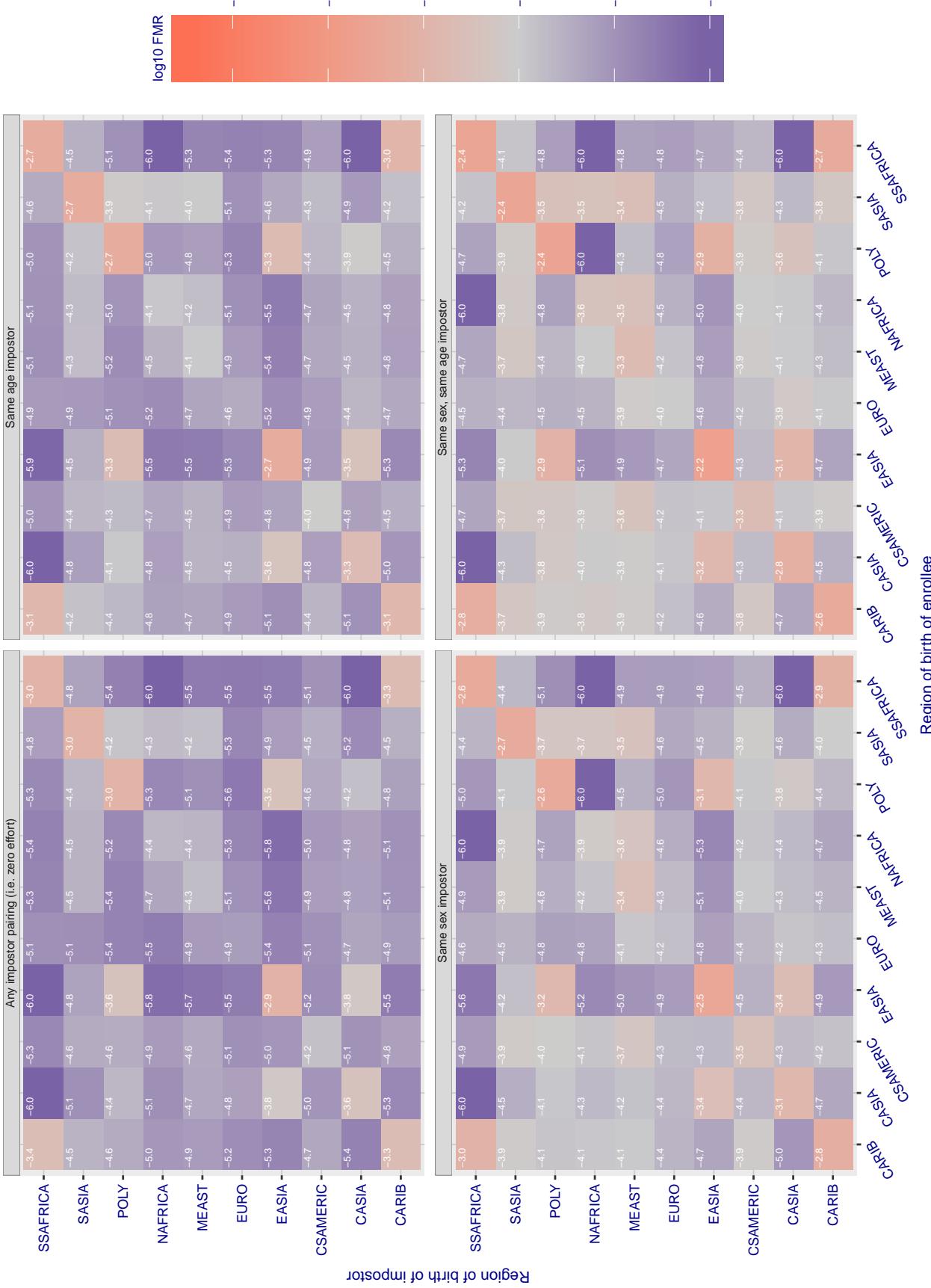


Figure 228: For algorithm tiger-002 operating on visa images, the heatmap shows false match rates observed over impostor comparisons of faces from different individuals who were born in the given region pair. False matches are counted against a recognition threshold fixed globally to give the target FMR in the plot title, computed over all on the order of  $10^{10}$  impostor comparisons. If text appears in each box it give the same quantity as that coded by the color. Grey indicates FMR is at the intended FMR target level. Light red colors present a security vulnerability to, for example, a passport gate. Each +1 increase in  $\log 10$  FMR corresponds to a factor of 10 increase in FMR. The matrix is not quite symmetric because images in the enrollment and verification sets are different.

### Cross region FMR at threshold T = 149.313 for algorithm tiger\_003, giving FMR(T) = 0.0001 globally.

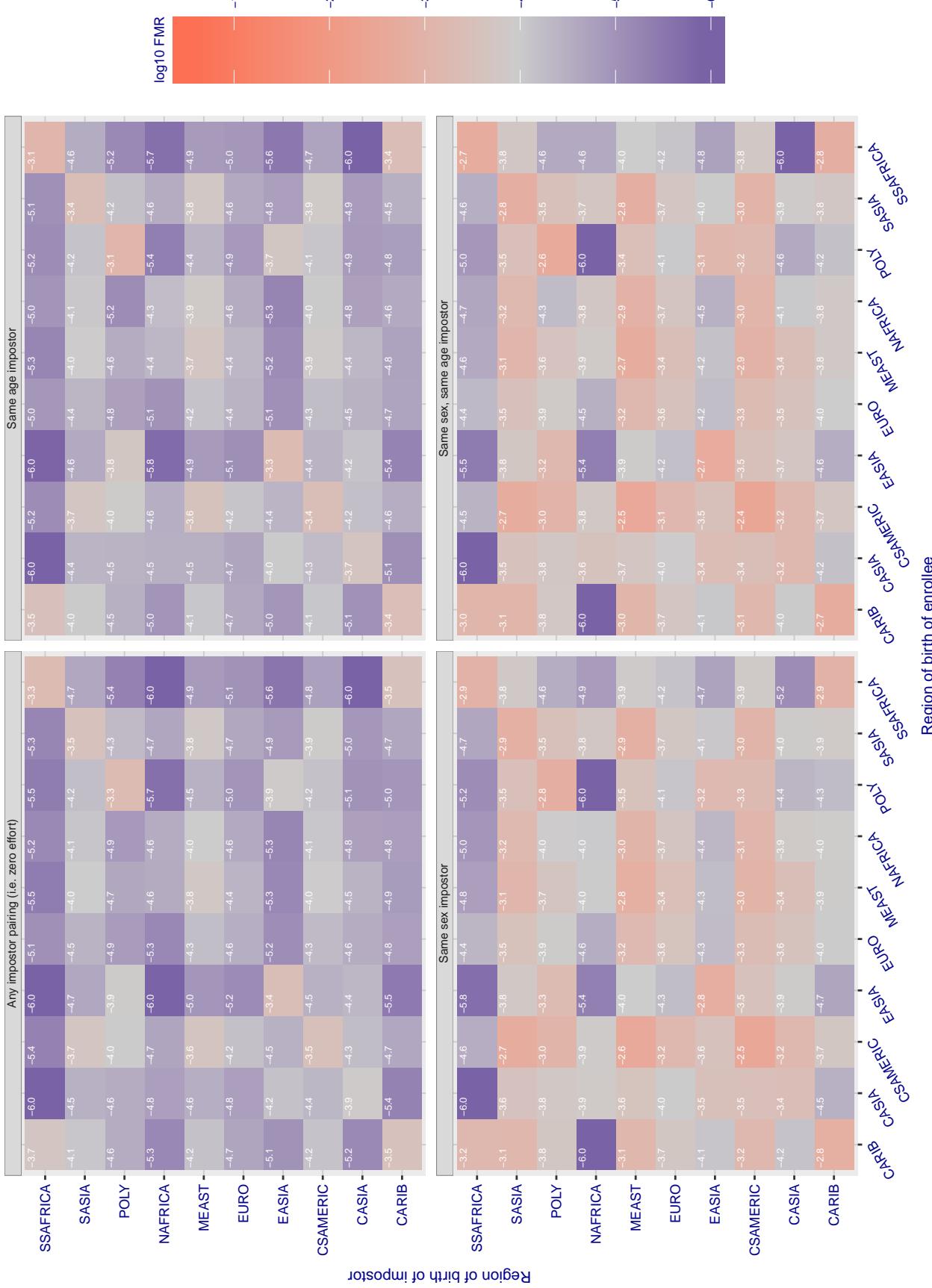


Figure 229: For algorithm tiger-003 operating on visa images, the heatmap shows false match rates observed over impostor comparisons of faces from different individuals who were born in the given region pair. False matches are counted against a recognition threshold fixed globally to give the target FMR in the plot title, computed over all on the order of  $10^{10}$  impostor comparisons. If text appears in each box it give the same quantity as that coded by the color. Grey indicates FMR is at the intended FMR target level. Light red colors present a security vulnerability to, for example, a passport gate. Each +1 increase in  $\log_{10} \text{FMR}$  corresponds to a factor of 10 increase in FMR. The matrix is not quite symmetric because images in the enrollment and verification sets are different.

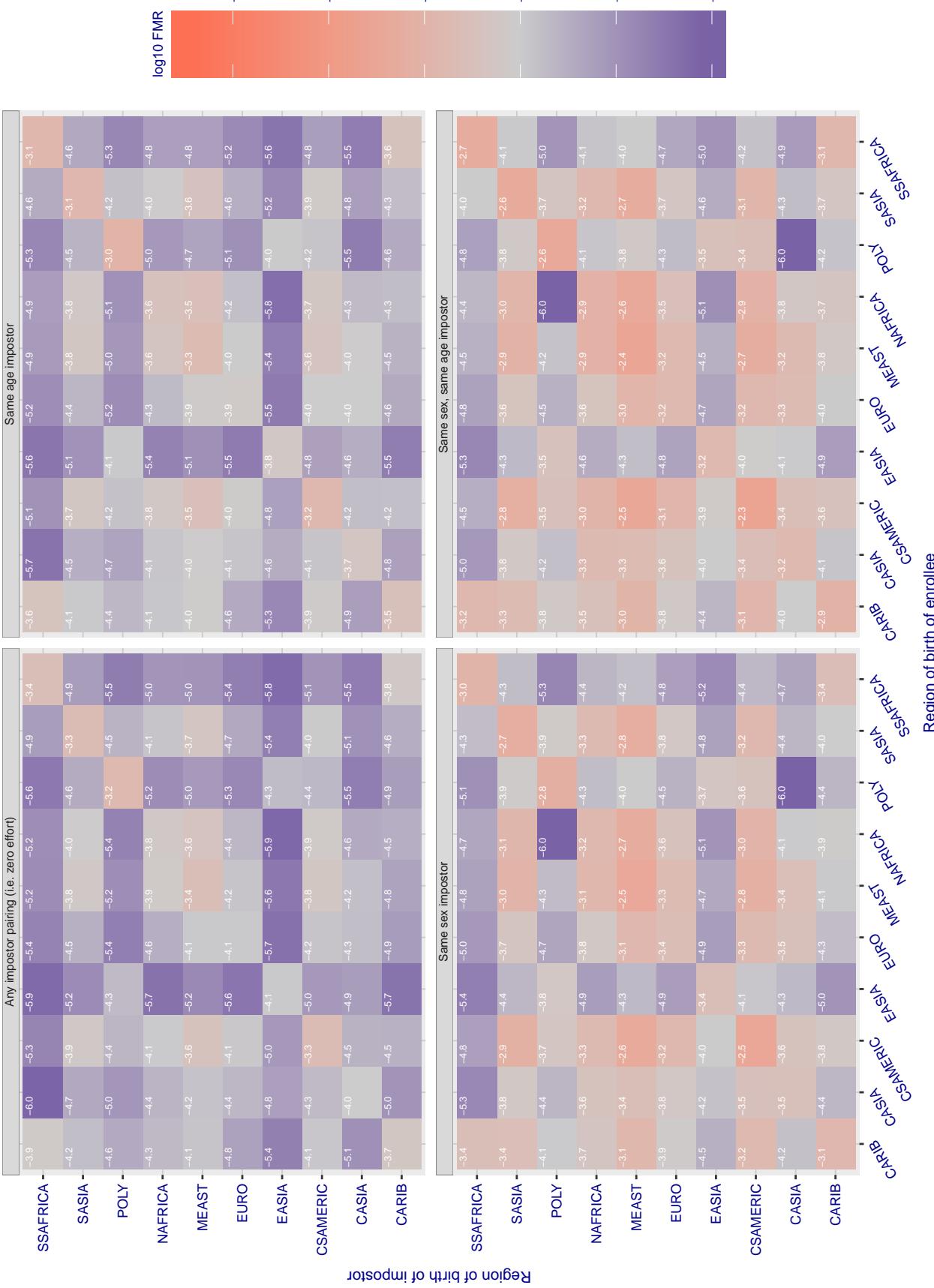
**Cross region FMR at threshold T = 43.677 for algorithm tongyi\_005, giving FMR(T) = 0.0001 globally.**

Figure 230: For algorithm tongyi-005 operating on visa images, the heatmap shows false match rates observed over impostor comparisons of faces from different individuals who were born in the given region pair. False matches are counted against a recognition threshold fixed globally to give the target FMR in the plot title, computed over all on the order of  $10^{10}$  impostor comparisons. If text appears in each box it give the same quantity as that coded by the color. Grey indicates FMR is at the intended FMR target level. Light red colors present a security vulnerability to, for example, a passport gate. Each +1 increase in  $\log_{10} \text{FMR}$  corresponds to a factor of 10 increase in FMR. The matrix is not quite symmetric because images in the enrollment and verification sets are different.

### Cross region FMR at threshold T = 0.628 for algorithm toshiba\_002, giving FMR(T) = 0.0001 globally.

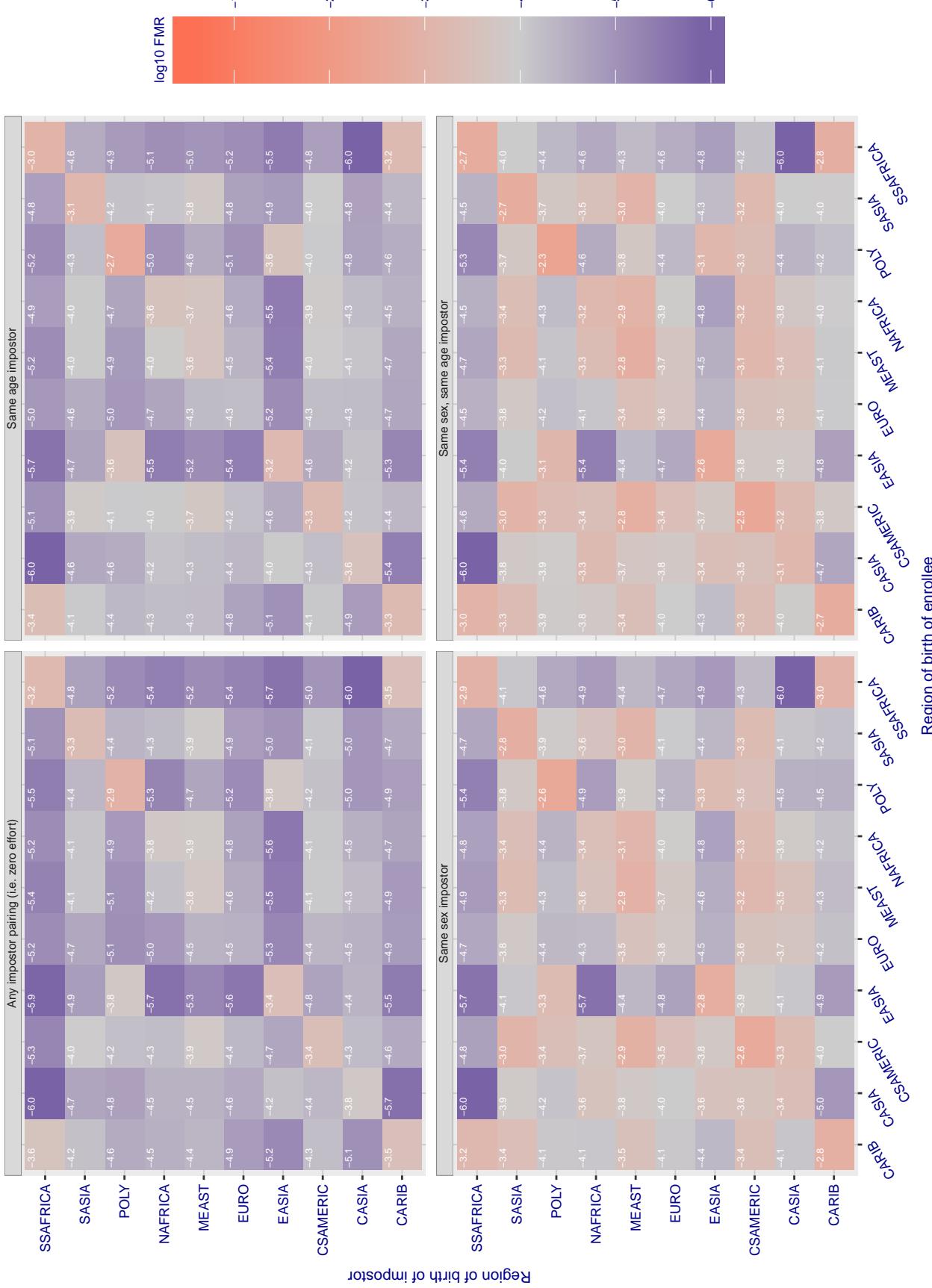


Figure 231: For algorithm toshiba-002 operating on visa images, the heatmap shows false match rates observed over impostor comparisons of faces from different individuals who were born in the given region pair. False matches are counted against a recognition threshold fixed globally to give the target FMR in the plot title, computed over all on the order of  $10^{10}$  impostor comparisons. If text appears in each box it give the same quantity as that coded by the color. Grey indicates FMR is at the intended FMR target level. Light red colors present a security vulnerability to, for example, a passport gate. Each +1 increase in  $\log_{10} FMR$  corresponds to a factor of 10 increase in FMR. The matrix is not quite symmetric because images in the enrollment and verification sets are different.

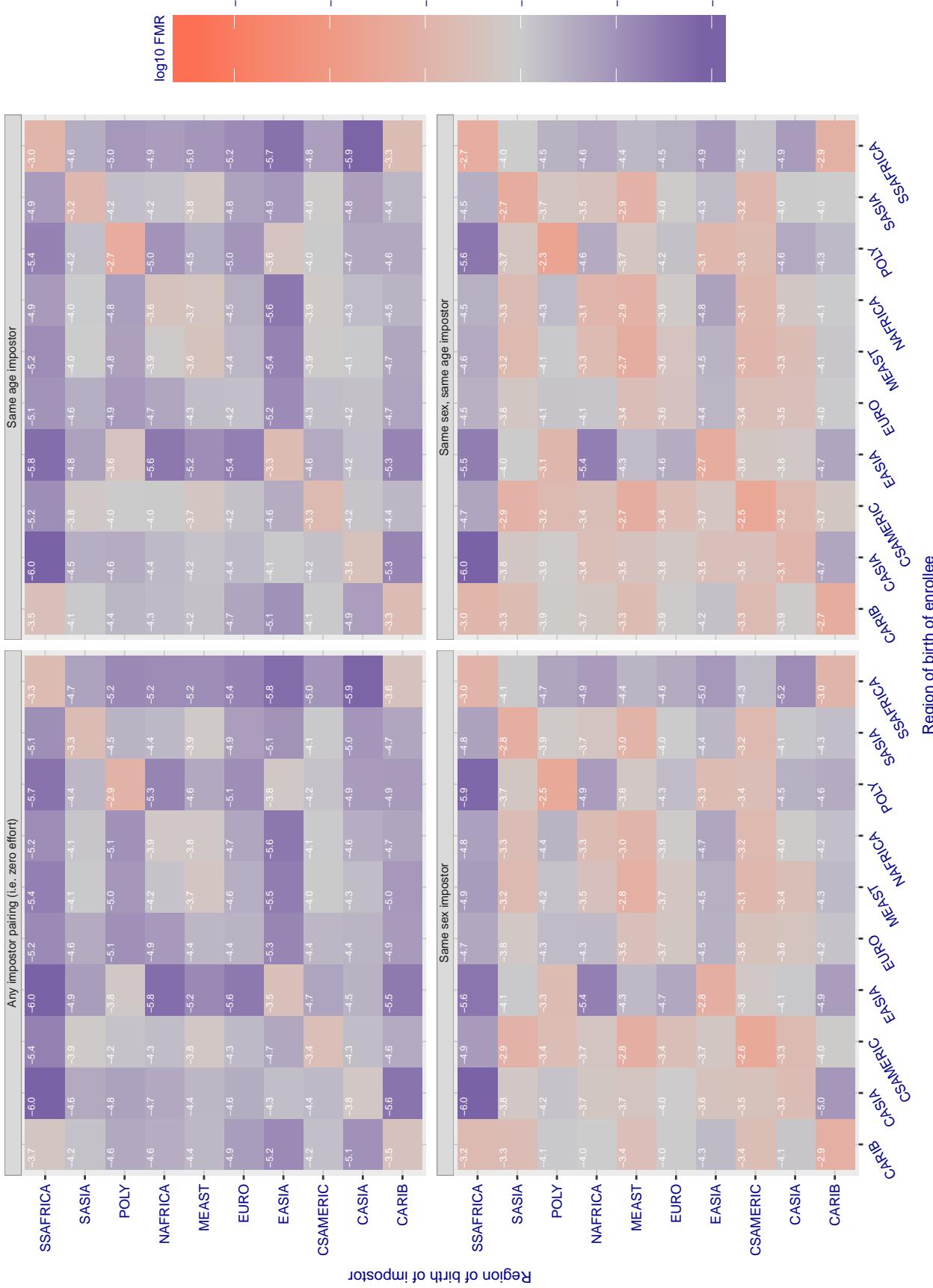
**Cross region FMR at threshold T = 0.626 for algorithm toshiba\_003, giving FMR(T) = 0.0001 globally.**

Figure 232: For algorithm toshiba-003 operating on visa images, the heatmap shows false match rates observed over impostor comparisons of faces from different individuals who were born in the given region pair. False matches are counted against a recognition threshold fixed globally to give the target FMR in the plot title, computed over all on the order of  $10^{10}$  impostor comparisons. If text appears in each box it give the same quantity as that coded by the color. Grey indicates FMR is at the intended FMR target level. Light red colors present a security vulnerability to, for example, a passport gate. Each +1 increase in  $\log_{10} FMR$  corresponds to a factor of 10 increase in FMR. The matrix is not quite symmetric because images in the enrollment and verification sets are different.

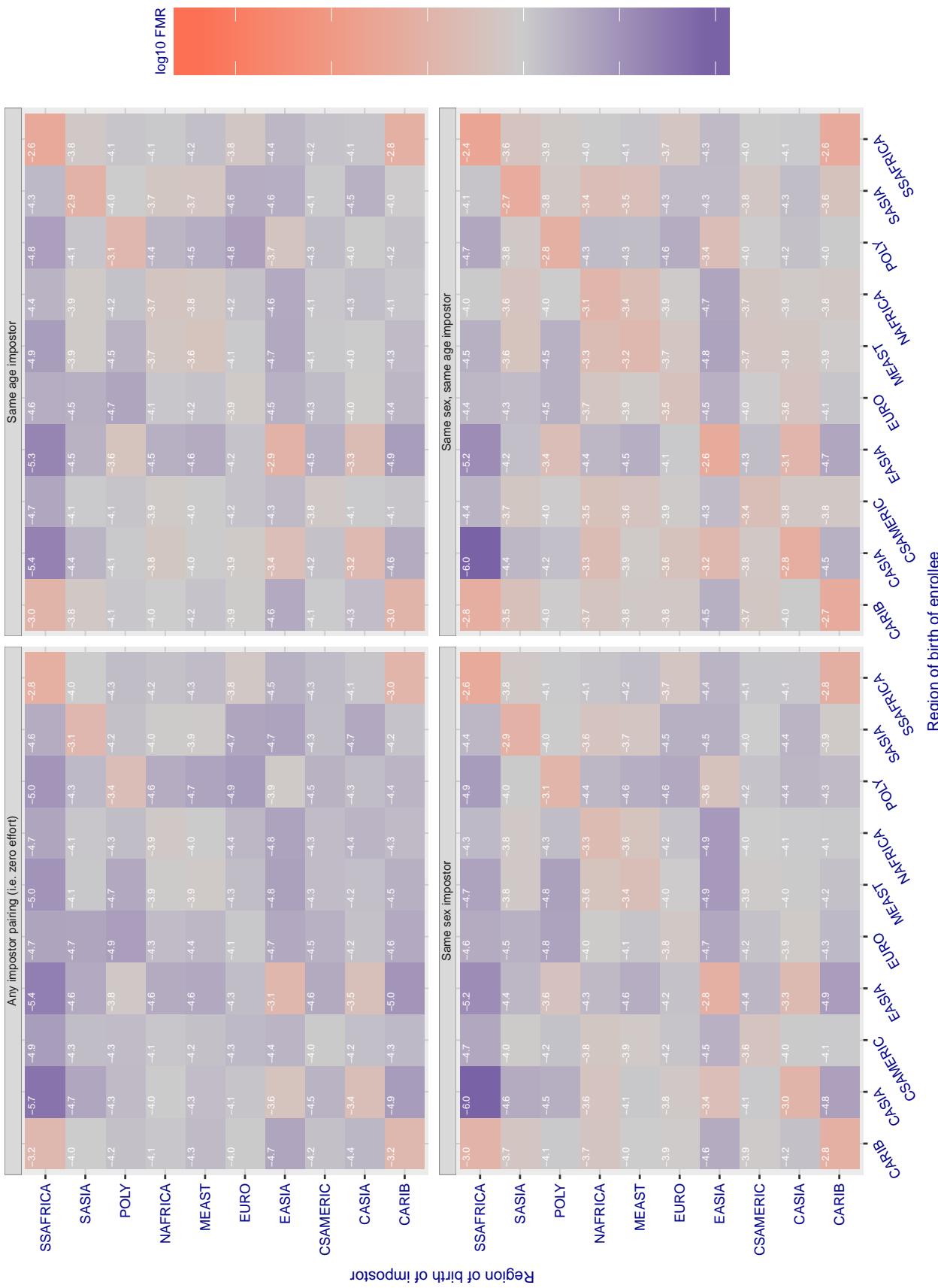


Figure 233: For algorithm vcog-002 operating on visa images, the heatmap shows false match rates observed over impostor comparisons of faces from different individuals who were born in the given region pair. False matches are counted against a recognition threshold fixed globally to give the target FMR in the plot title, computed over all on the order of  $10^{10}$  impostor comparisons. If text appears in each box it give the same quantity as that coded by the color. Grey indicates FMR is at the intended FMR target level. Light red colors present a security vulnerability to, for example, a passport gate. Each +1 increase in  $\log_{10} \text{FMR}$  corresponds to a factor of 10 increase in FMR. The matrix is not quite symmetric because images in the enrollment and verification sets are different.

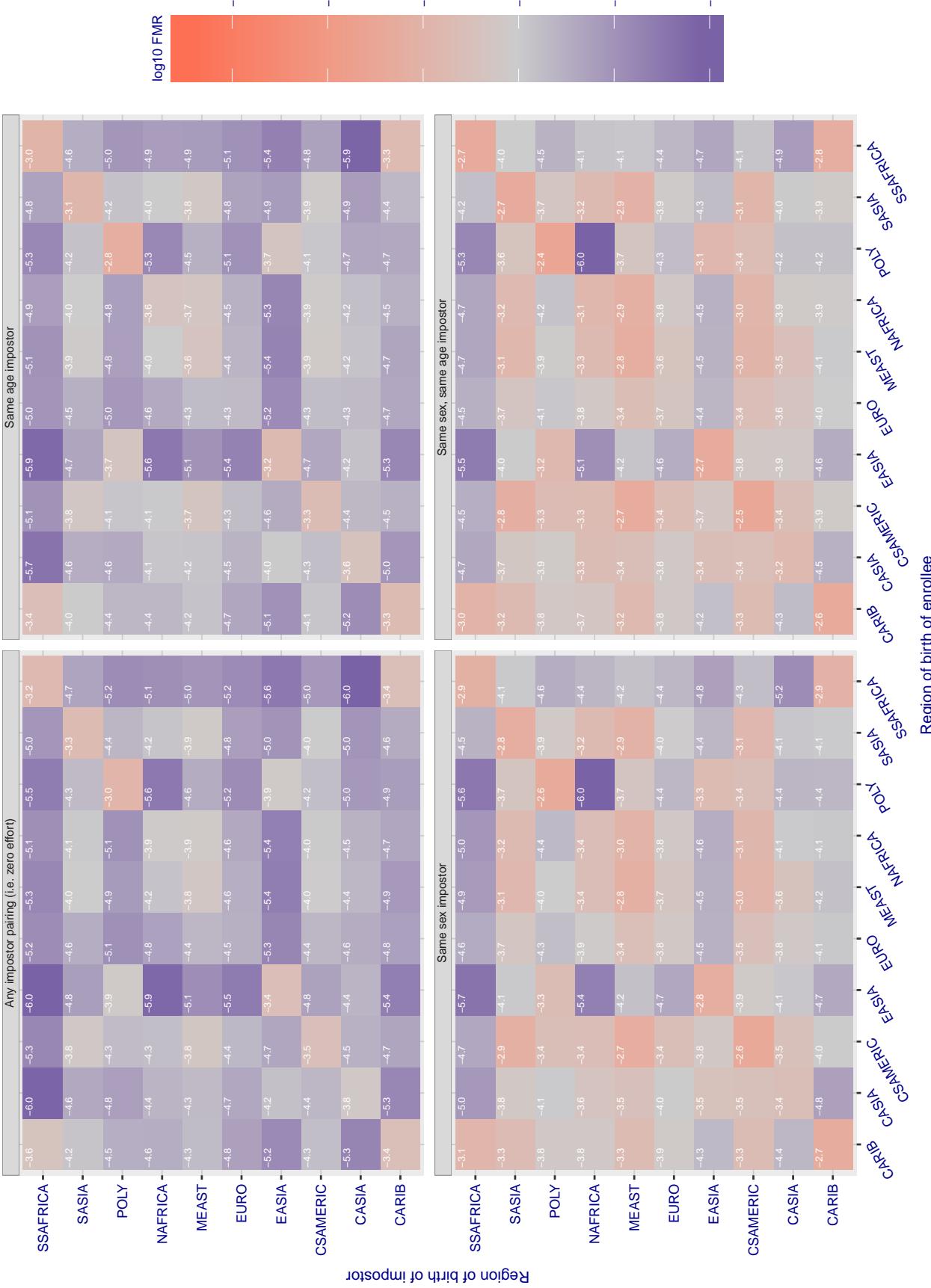
**Cross region FMR at threshold T = 71.529 for algorithm vd\_001, giving FMR(T) = 0.0001 globally.**

Figure 234: For algorithm vd\_001 operating on visa images, the heatmap shows false match rates observed over impostor comparisons of faces from different individuals who were born in the given region pair. False matches are counted against a recognition threshold fixed globally to give the target FMR in the plot title, computed over all on the order of  $10^{10}$  impostor comparisons. If text appears in each box it give the same quantity as that coded by the color. Grey indicates FMR is at the intended FMR target level. Light red colors present a security vulnerability to, for example, a passport gate. Each +1 increase in  $\log_{10} \text{FMR}$  corresponds to a factor of 10 increase in FMR. The matrix is not quite symmetric because images in the enrollment and verification sets are different.

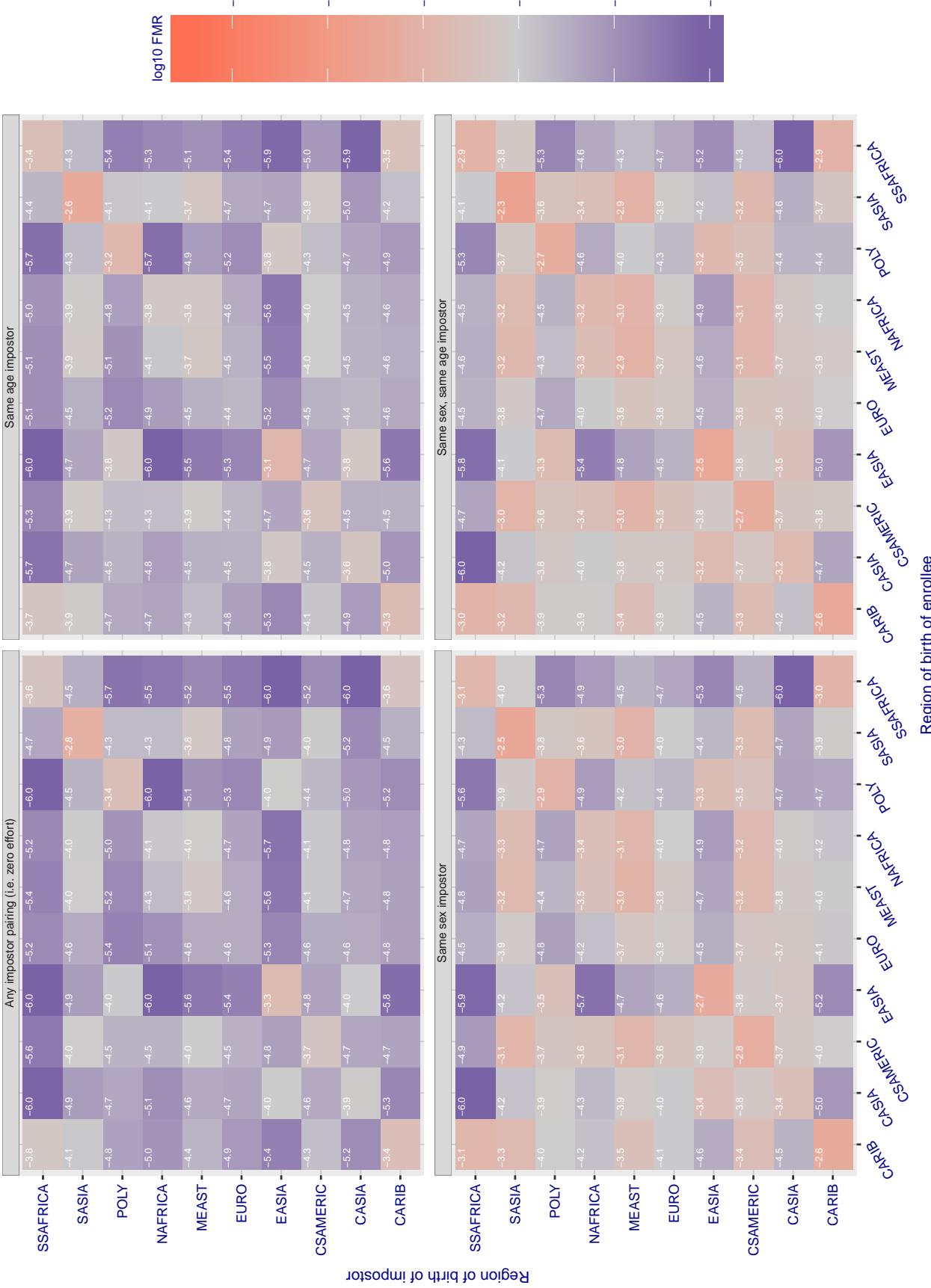
**Cross region FMR at threshold T = 3.325 for algorithm veridas\_001, giving FMR(T) = 0.0001 globally.**

Figure 235: For algorithm veridas-001 operating on visa images, the heatmap shows false match rates observed over impostor comparisons of faces from different individuals who were born in the given region pair. False matches are counted against a recognition threshold fixed globally to give the target FMR in the plot title, computed over all on the order of  $10^{10}$  impostor comparisons. If text appears in each box it give the same quantity as that coded by the color. Grey indicates FMR is at the intended FMR target level. Light red colors present a security vulnerability to, for example, a passport gate. Each +1 increase in  $\log_{10} FMR$  corresponds to a factor of 10 increase in FMR. The matrix is not quite symmetric because images in the enrollment and verification sets are different.

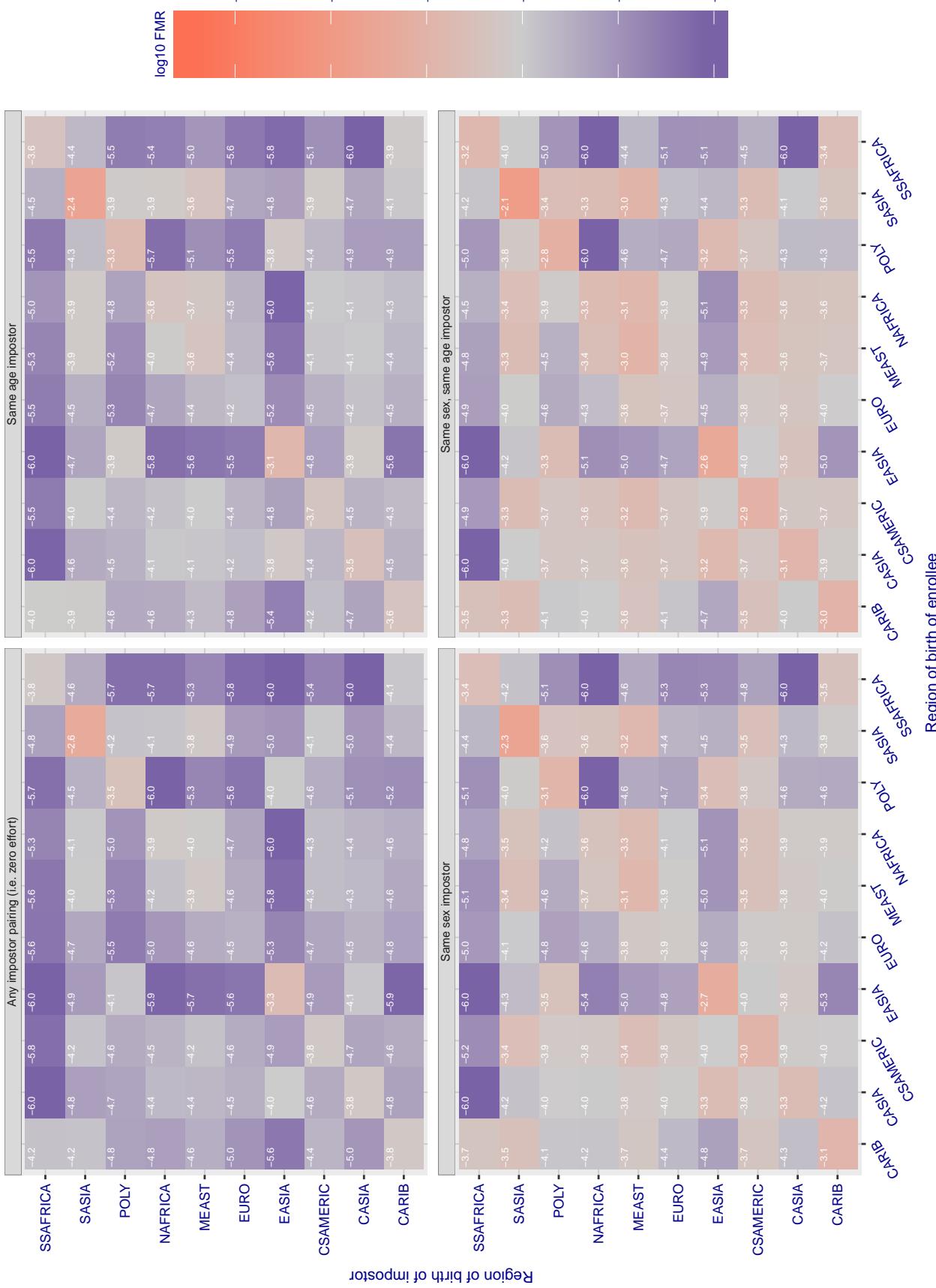
**Cross region FMR at threshold T = 3.389 for algorithm veridas\_002, giving FMR(T) = 0.0001 globally.**

Figure 236: For algorithm veridas-002 operating on visa images, the heatmap shows false match rates observed over impostor comparisons of faces from different individuals who were born in the given region pair. False matches are counted against a recognition threshold fixed globally to give the target FMR in the plot title, computed over all on the order of  $10^{10}$  impostor comparisons. If text appears in each box it give the same quantity as that coded by the color. Grey indicates FMR is at the intended FMR target level. Light red colors present a security vulnerability to, for example, a passport gate. Each +1 increase in  $\log_{10} FMR$  corresponds to a factor of 10 increase in FMR. The matrix is not quite symmetric because images in the enrollment and verification sets are different.

### Cross region FMR at threshold T = 0.842 for algorithm videonetics\_001, giving FMR(T) = 0.0001 globally.

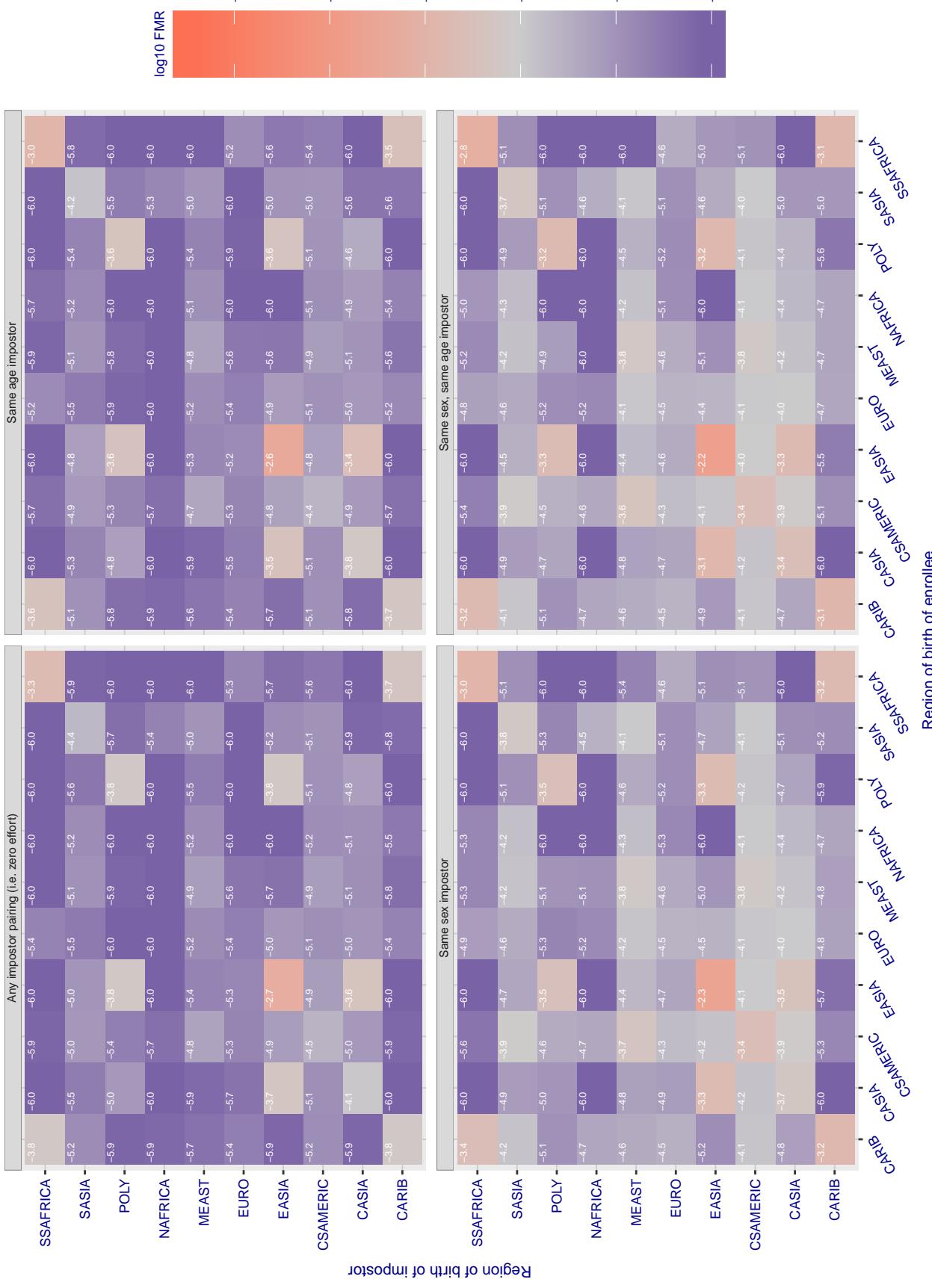


Figure 237: For algorithm videonetics-001 operating on visa images, the heatmap shows false match rates observed over impostor comparisons of faces from different individuals who were born in the given region pair. False matches are counted against a recognition threshold fixed globally to give the target FMR in the plot title, computed over all on the order of  $10^{10}$  impostor comparisons. If text appears in each box it give the same quantity as that coded by the color. Grey indicates FMR is at the intended FMR target level. Light red colors present a security vulnerability to, for example, a passport gate. Each +1 increase in  $\log_{10} FMR$  corresponds to a factor of 10 increase in FMR. The matrix is not quite symmetric because images in the enrollment and verification sets are different.

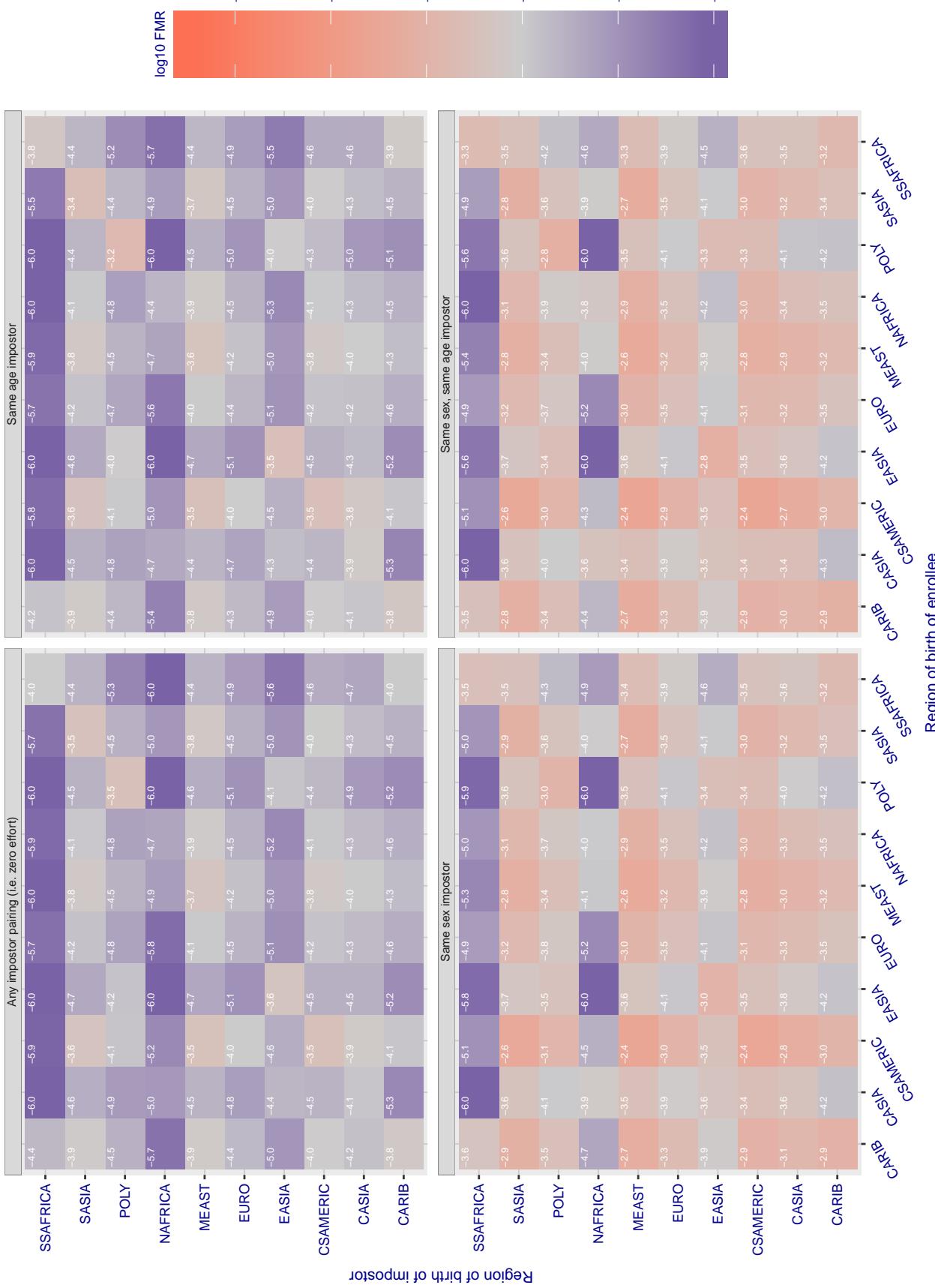
**Cross region FMR at threshold T = 3.057 for algorithm vigilantsolutions\_006, giving FMR(T) = 0.0001 globally.**

Figure 238: For algorithm vigilantsolutions-006 operating on visa images, the heatmap shows false match rates observed over impostor comparisons of faces from different individuals who were born in the given region pair. False matches are counted against a recognition threshold fixed globally to give the target FMR in the plot title, computed over all on the order of  $10^{10}$  impostor comparisons. If text appears in each box it give the same quantity as that coded by the color. Grey indicates FMR is at the intended FMR target level. Light red colors present a security vulnerability to, for example, a passport gate. Each +1 increase in  $\log_{10} FMR$  corresponds to a factor of 10 increase in FMR. The matrix is not quite symmetric because images in the enrollment and verification sets are different.

### Cross region FMR at threshold T = 0.432 for algorithm vion\_000, giving FMR(T) = 0.0001 globally.

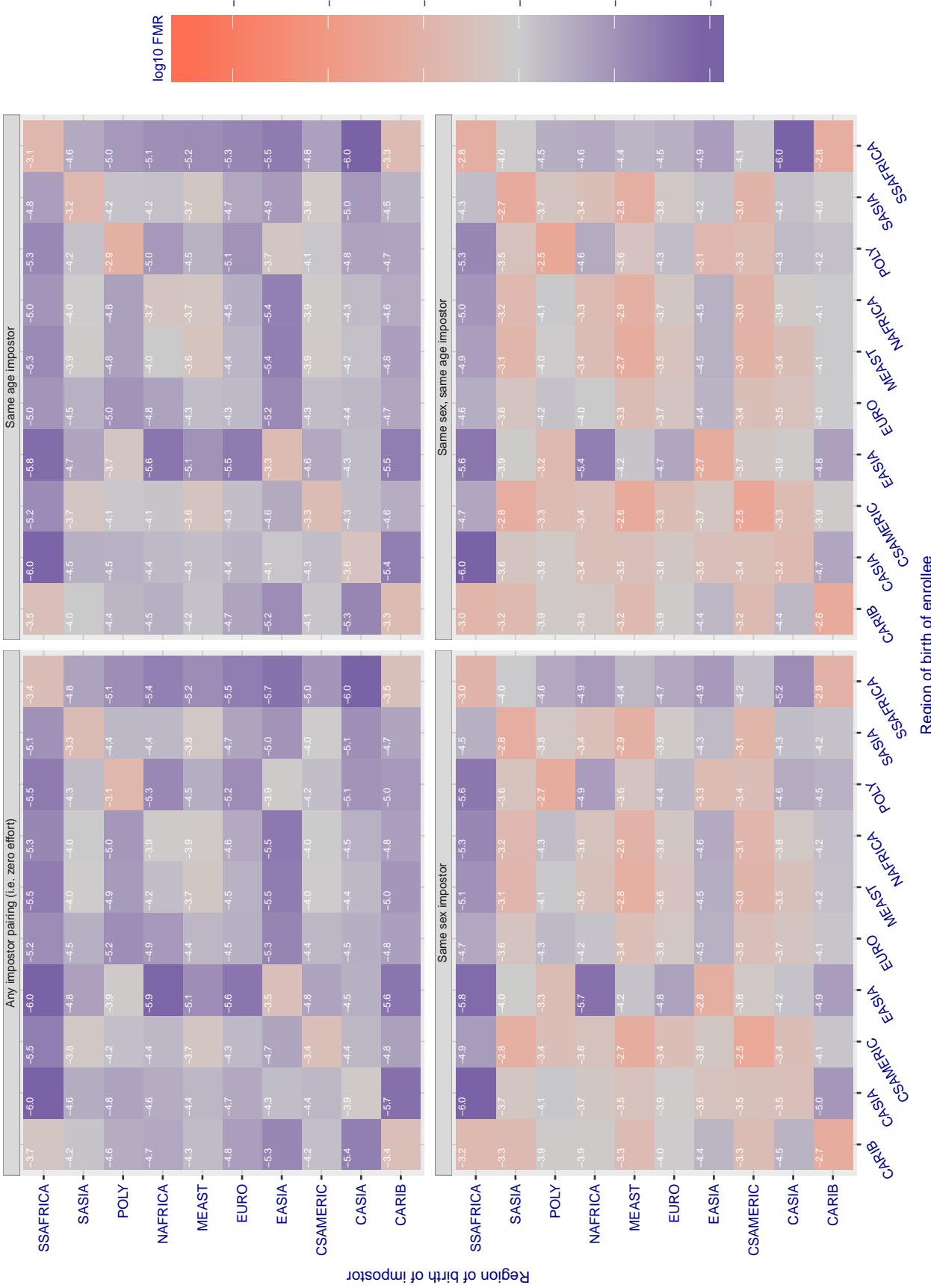


Figure 239: For algorithm vion-000 operating on visa images, the heatmap shows false match rates observed over impostor comparisons of faces from different individuals who were born in the given region pair. False matches are counted against a recognition threshold fixed globally to give the target FMR in the plot title, computed over all on the order of  $10^{10}$  impostor comparisons. If text appears in each box it give the same quantity as that coded by the color. Grey indicates FMR is at the intended FMR target level. Light red colors present a security vulnerability to, for example, a passport gate. Each +1 increase in  $\log 10$  FMR corresponds to a factor of 10 increase in FMR. The matrix is not quite symmetric because images in the enrollment and verification sets are different.

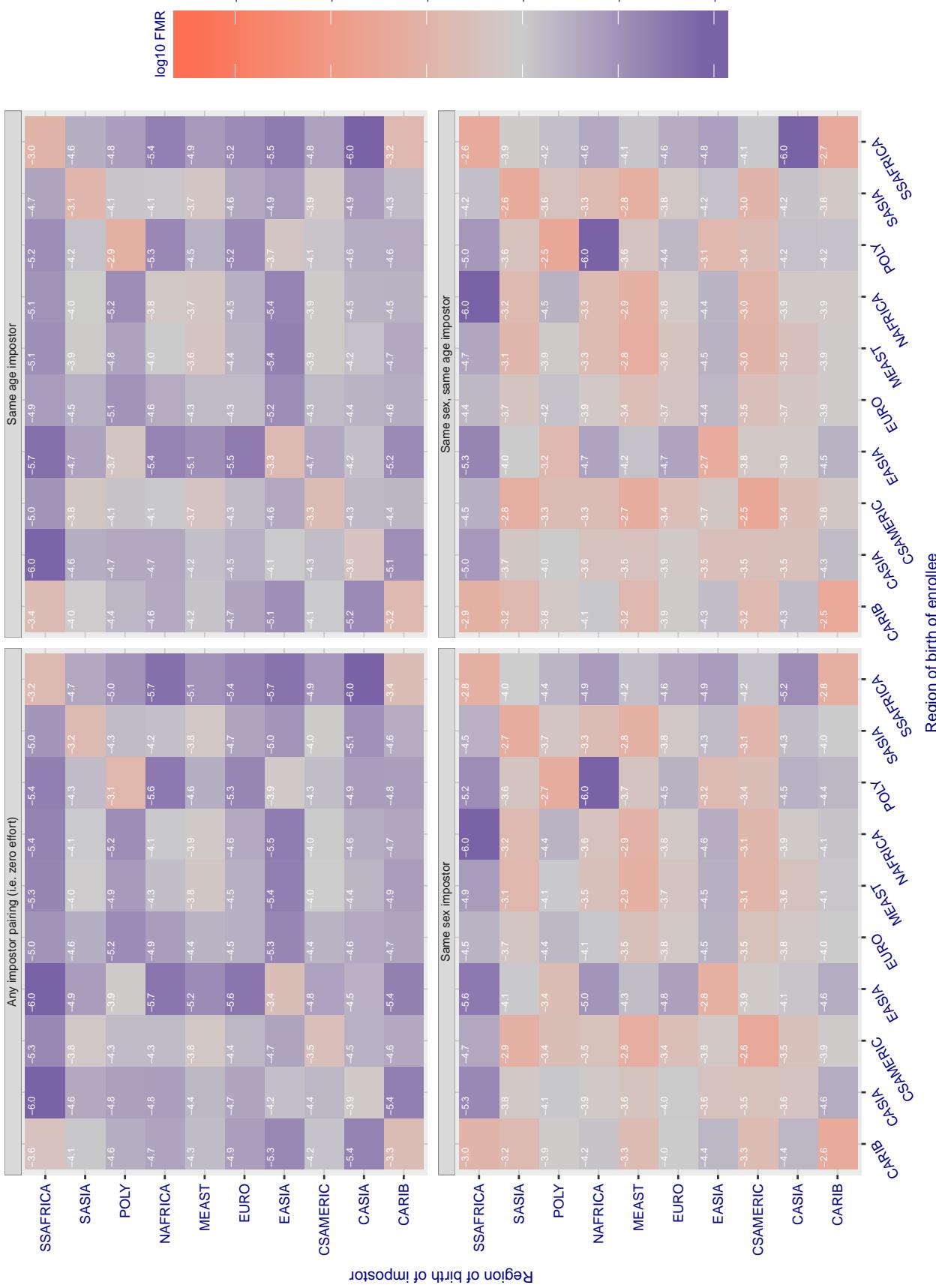
**Cross region FMR at threshold T = 0.433 for algorithm visionbox\_000, giving FMR(T) = 0.0001 globally.**

Figure 240: For algorithm visionbox-000 operating on visa images, the heatmap shows false match rates observed over impostor comparisons of faces from different individuals who were born in the given region pair. False matches are counted against a recognition threshold fixed globally to give the target FMR in the plot title, computed over all on the order of  $10^{10}$  impostor comparisons. If text appears in each box it give the same quantity as that coded by the color. Grey indicates FMR is at the intended FMR target level. Light red colors present a security vulnerability to, for example, a passport gate. Each +1 increase in  $\log_{10} FMR$  corresponds to a factor of 10 increase in FMR. The matrix is not quite symmetric because images in the enrollment and verification sets are different.

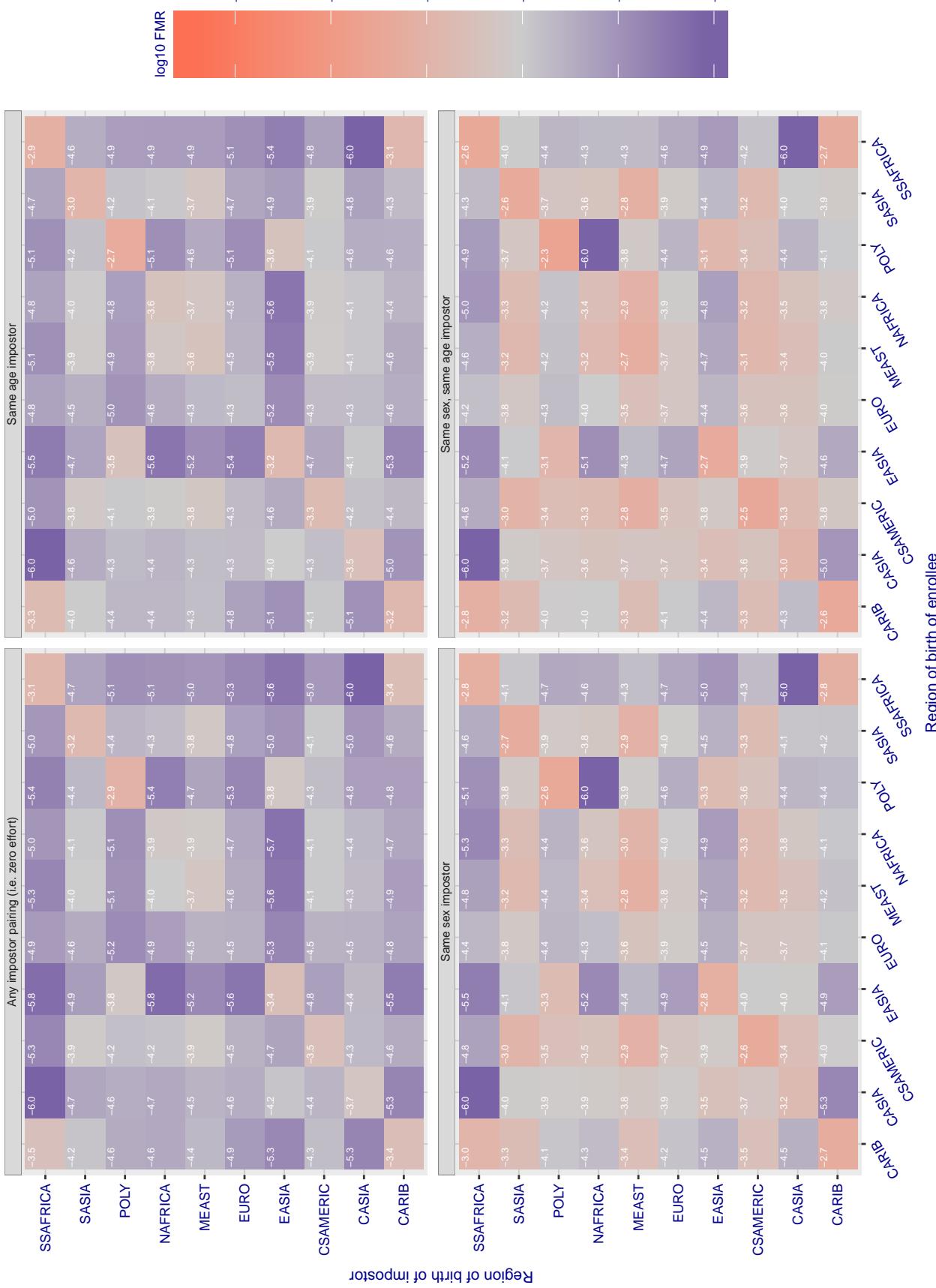
**Cross region FMR at threshold T = 0.382 for algorithm visionbox\_001, giving FMR(T) = 0.0001 globally.**

Figure 241: For algorithm visionbox-001 operating on visa images, the heatmap shows false match rates observed over impostor comparisons of faces from different individuals who were born in the given region pair. False matches are counted against a recognition threshold fixed globally to give the target FMR in the plot title, computed over all on the order of  $10^{10}$  impostor comparisons. If text appears in each box it give the same quantity as that coded by the color. Grey indicates FMR is at the intended FMR target level. Light red colors present a security vulnerability to, for example, a passport gate. Each +1 increase in  $\log_{10} FMR$  corresponds to a factor of 10 increase in FMR. The matrix is not quite symmetric because images in the enrollment and verification sets are different.

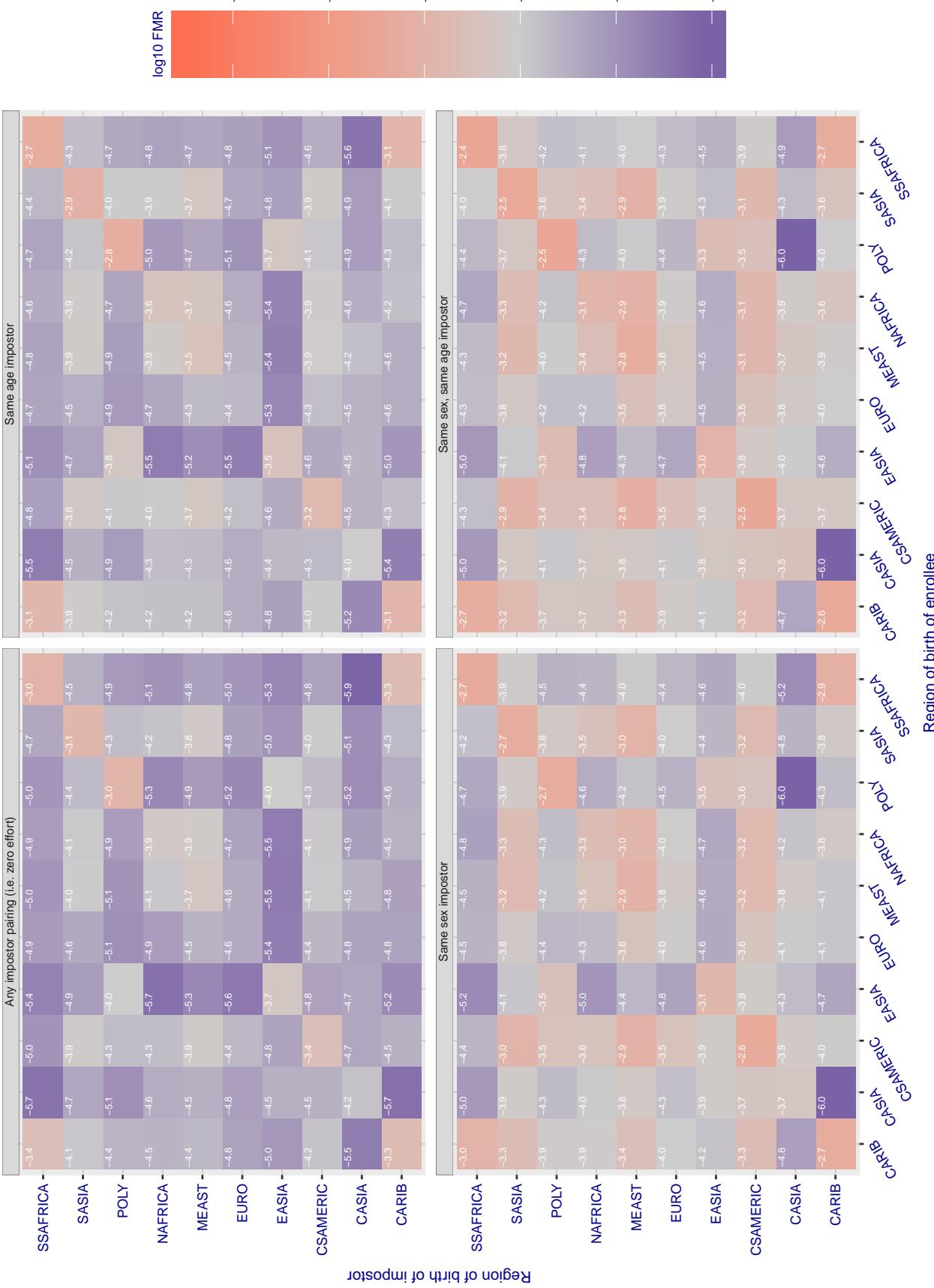
**Cross region FMR at threshold T = 0.669 for algorithm visionlabs\_006, giving FMR(T) = 0.0001 globally.**

Figure 242: For algorithm visionlabs-006 operating on visa images, the heatmap shows false match rates observed over impostor comparisons of faces from different individuals who were born in the given region pair. False matches are counted against a recognition threshold fixed globally to give the target FMR in the plot title, computed over all on the order of  $10^{10}$  impostor comparisons. If text appears in each box it give the same quantity as that coded by the color. Grey indicates FMR is at the intended FMR target level. Light red colors present a security vulnerability to, for example, a passport gate. Each +1 increase in  $\log_{10} FMR$  corresponds to a factor of 10 increase in FMR. The matrix is not quite symmetric because images in the enrollment and verification sets are different.

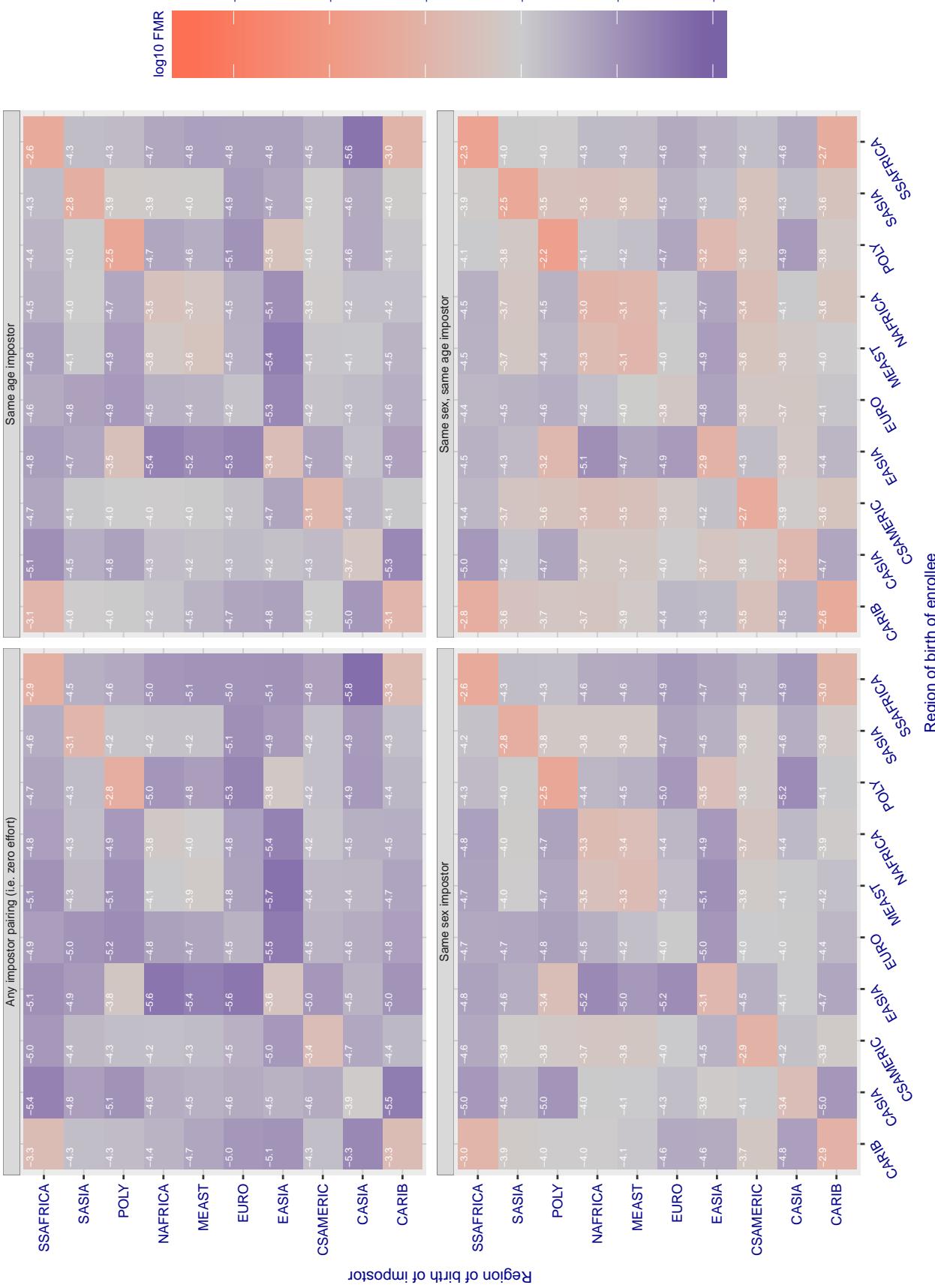
**Cross region FMR at threshold T = 0.657 for algorithm visionlabs\_007, giving FMR(T) = 0.0001 globally.**

Figure 243: For algorithm visionlabs-007 operating on visa images, the heatmap shows false match rates observed over impostor comparisons of faces from different individuals who were born in the given region pair. False matches are counted against a recognition threshold fixed globally to give the target FMR in the plot title, computed over all on the order of  $10^{10}$  impostor comparisons. If text appears in each box it give the same quantity as that coded by the color. Grey indicates FMR is at the intended FMR target level. Light red colors present a security vulnerability to, for example, a passport gate. Each +1 increase in  $\log_{10} \text{FMR}$  corresponds to a factor of 10 increase in FMR. The matrix is not quite symmetric because images in the enrollment and verification sets are different.

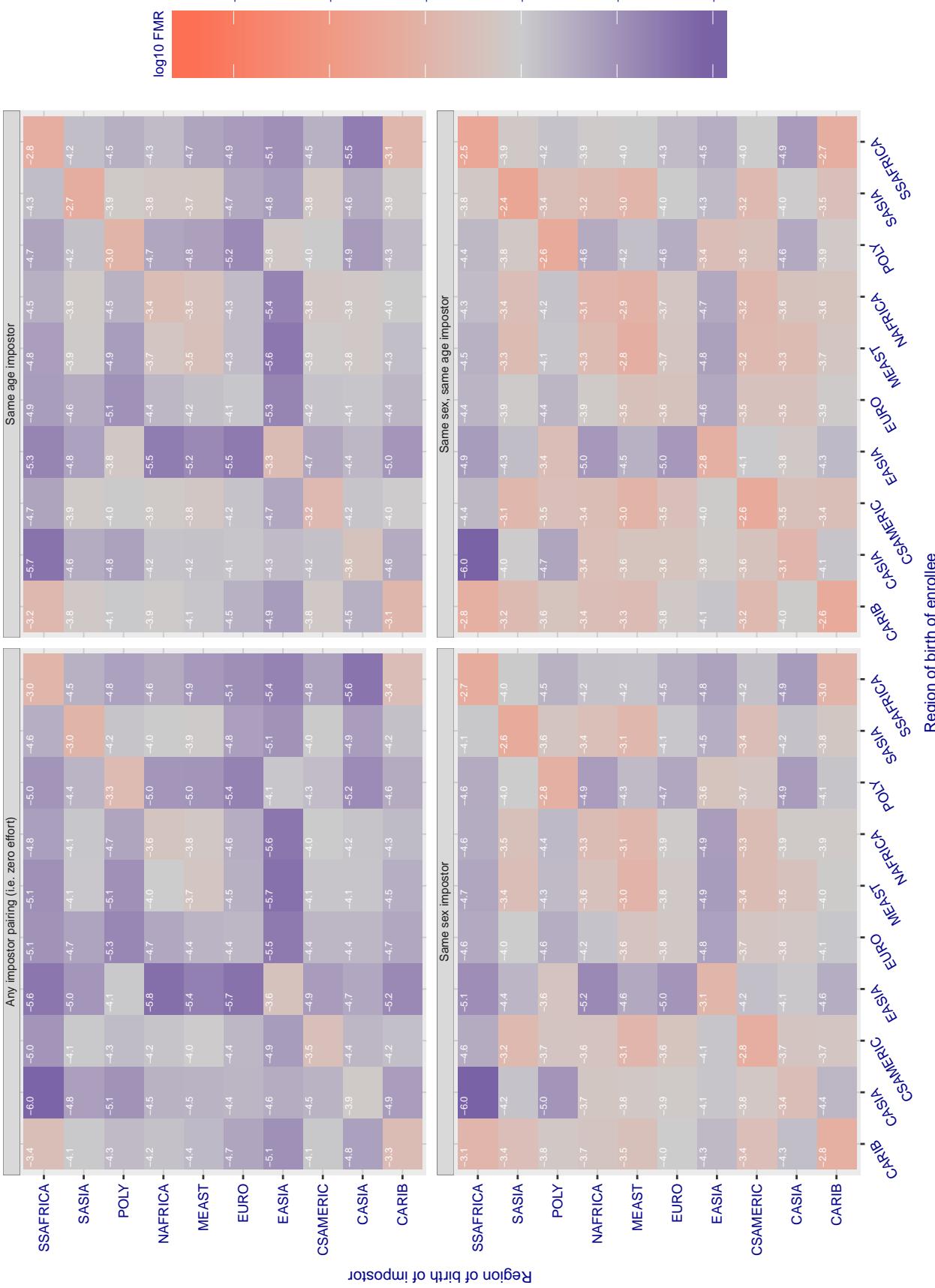
**Cross region FMR at threshold T = 995.898 for algorithm vocord\_006, giving FMR(T) = 0.0001 globally.**

Figure 244: For algorithm vocord-006 operating on visa images, the heatmap shows false match rates observed over impostor comparisons of faces from different individuals who were born in the given region pair. False matches are counted against a recognition threshold fixed globally to give the target FMR in the plot title, computed over all on the order of  $10^{10}$  impostor comparisons. If text appears in each box it give the same quantity as that coded by the color. Grey indicates FMR is at the intended FMR target level. Light red colors present a security vulnerability to, for example, a passport gate. Each +1 increase in  $\log_{10} FMR$  corresponds to a factor of 10 increase in FMR. The matrix is not quite symmetric because images in the enrollment and verification sets are different.

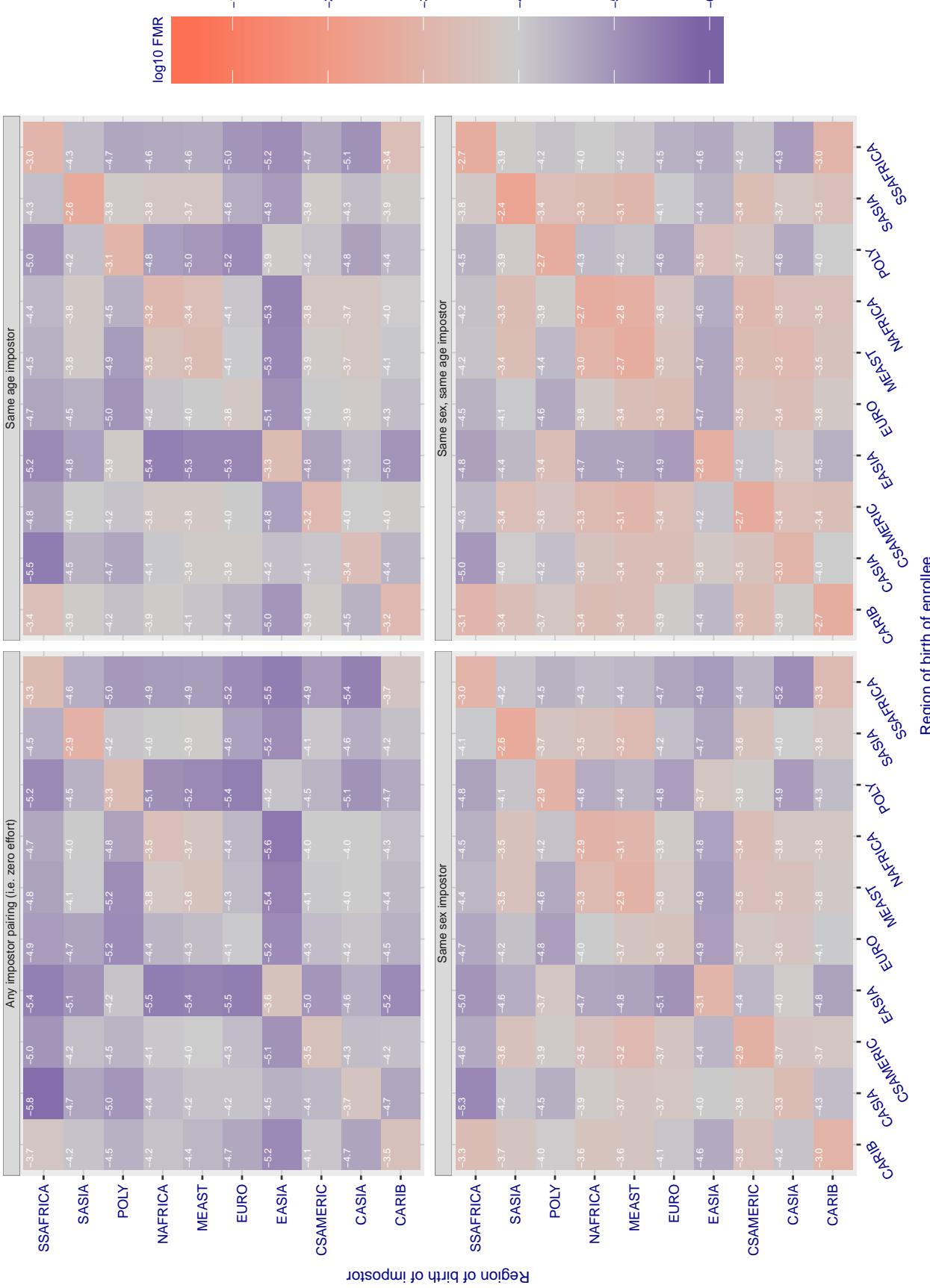
**Cross region FMR at threshold T = 995.241 for algorithm vocord\_007, giving FMR(T) = 0.0001 globally.**

Figure 245: For algorithm vocord-007 operating on visa images, the heatmap shows false match rates observed over impostor comparisons of faces from different individuals who were born in the given region pair. False matches are counted against a recognition threshold fixed globally to give the target FMR in the plot title, computed over all on the order of  $10^{10}$  impostor comparisons. If text appears in each box it give the same quantity as that coded by the color. Grey indicates FMR is at the intended FMR target level. Light red colors present a security vulnerability to, for example, a passport gate. Each +1 increase in  $\log_{10} FMR$  corresponds to a factor of 10 increase in FMR. The matrix is not quite symmetric because images in the enrollment and verification sets are different.

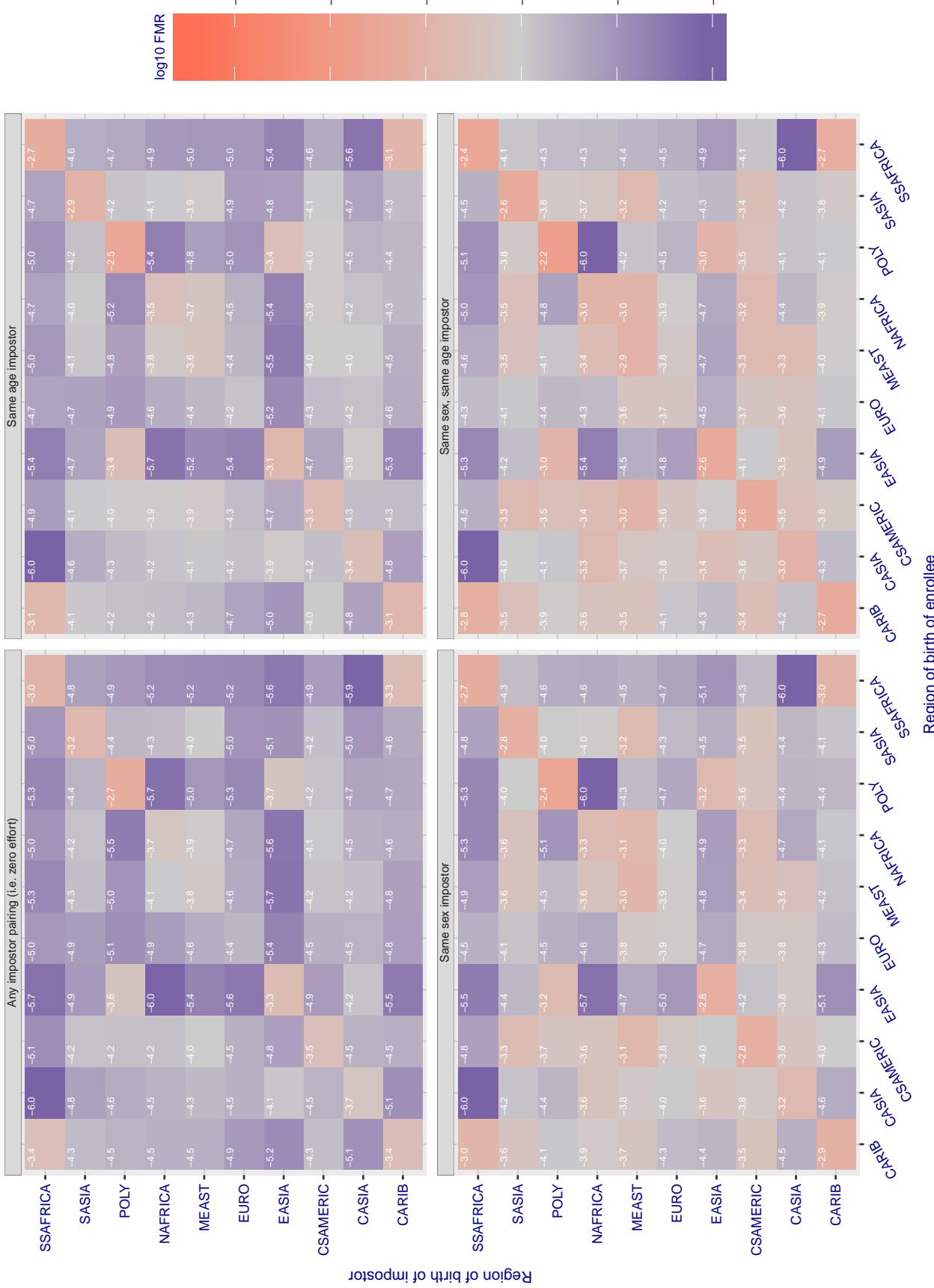
**Cross region FMR at threshold T = 0.400 for algorithm winsense\_000, giving FMR(T) = 0.0001 globally.**

Figure 246: For algorithm winsense-000 operating on visa images, the heatmap shows false match rates observed over impostor comparisons of faces from different individuals who were born in the given region pair. False matches are counted against a recognition threshold fixed globally to give the target FMR in the plot title, computed over all on the order of  $10^{10}$  impostor comparisons. If text appears in each box it give the same quantity as that coded by the color. Grey indicates FMR is at the intended FMR target level. Light red colors present a security vulnerability to, for example, a passport gate. Each +1 increase in  $\log_{10} FMR$  corresponds to a factor of 10 increase in FMR. The matrix is not quite symmetric because images in the enrollment and verification sets are different.

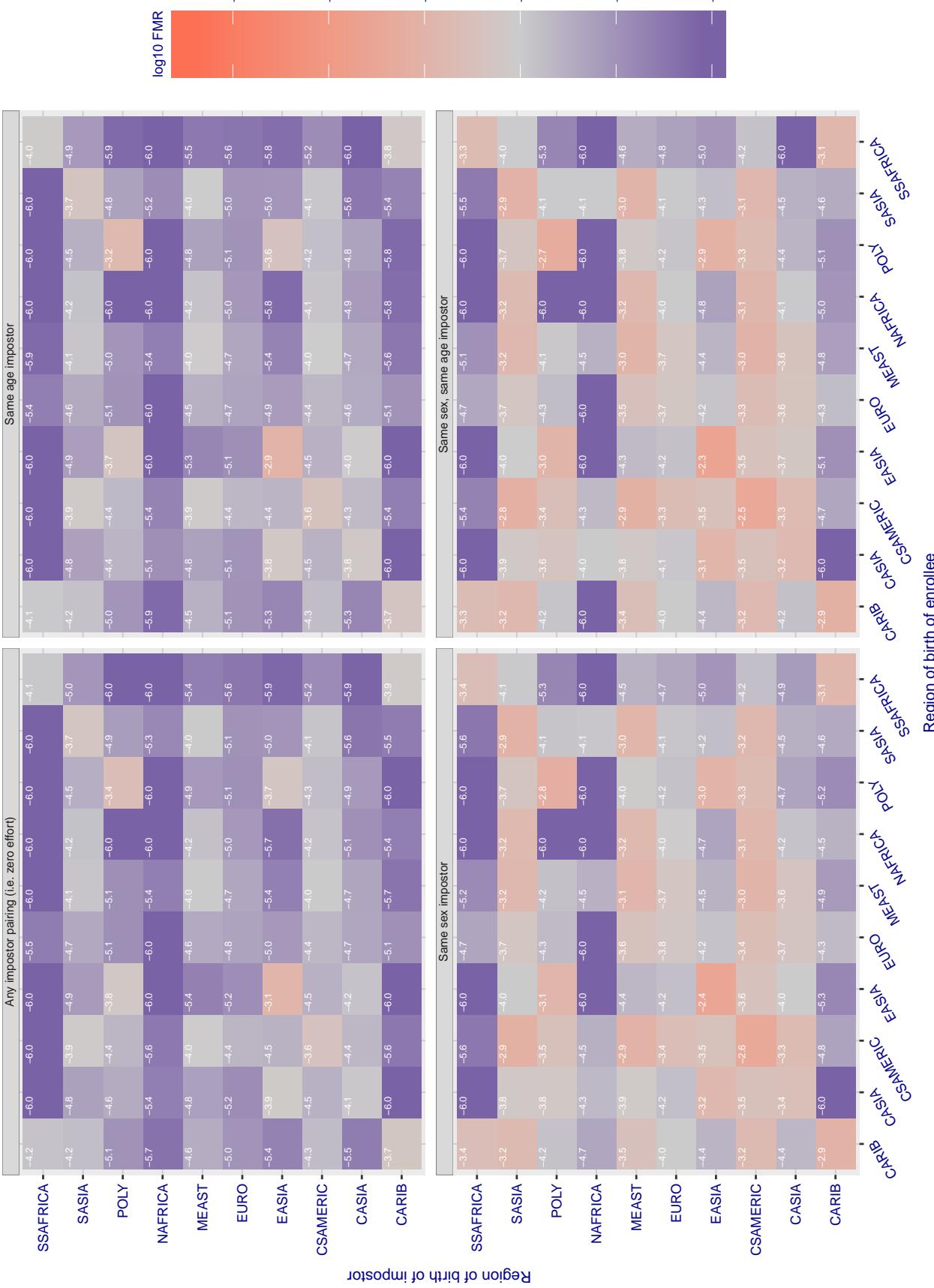
**Cross region FMR at threshold T = 5.544 for algorithm yisheng\_004, giving FMR(T) = 0.0001 globally.**

Figure 247: For algorithm yisheng-004 operating on visa images, the heatmap shows false match rates observed over impostor comparisons of faces from different individuals who were born in the given region pair. False matches are counted against a recognition threshold fixed globally to give the target FMR in the plot title, computed over all on the order of  $10^{10}$  impostor comparisons. If text appears in each box it give the same quantity as that coded by the color. Grey indicates FMR is at the intended FMR target level. Light red colors present a security vulnerability to, for example, a passport gate. Each +1 increase in  $\log_{10} FMR$  corresponds to a factor of 10 increase in FMR. The matrix is not quite symmetric because images in the enrollment and verification sets are different.

### Cross region FMR at threshold T = 37.698 for algorithm yitu\_003, giving FMR(T) = 0.0001 globally.

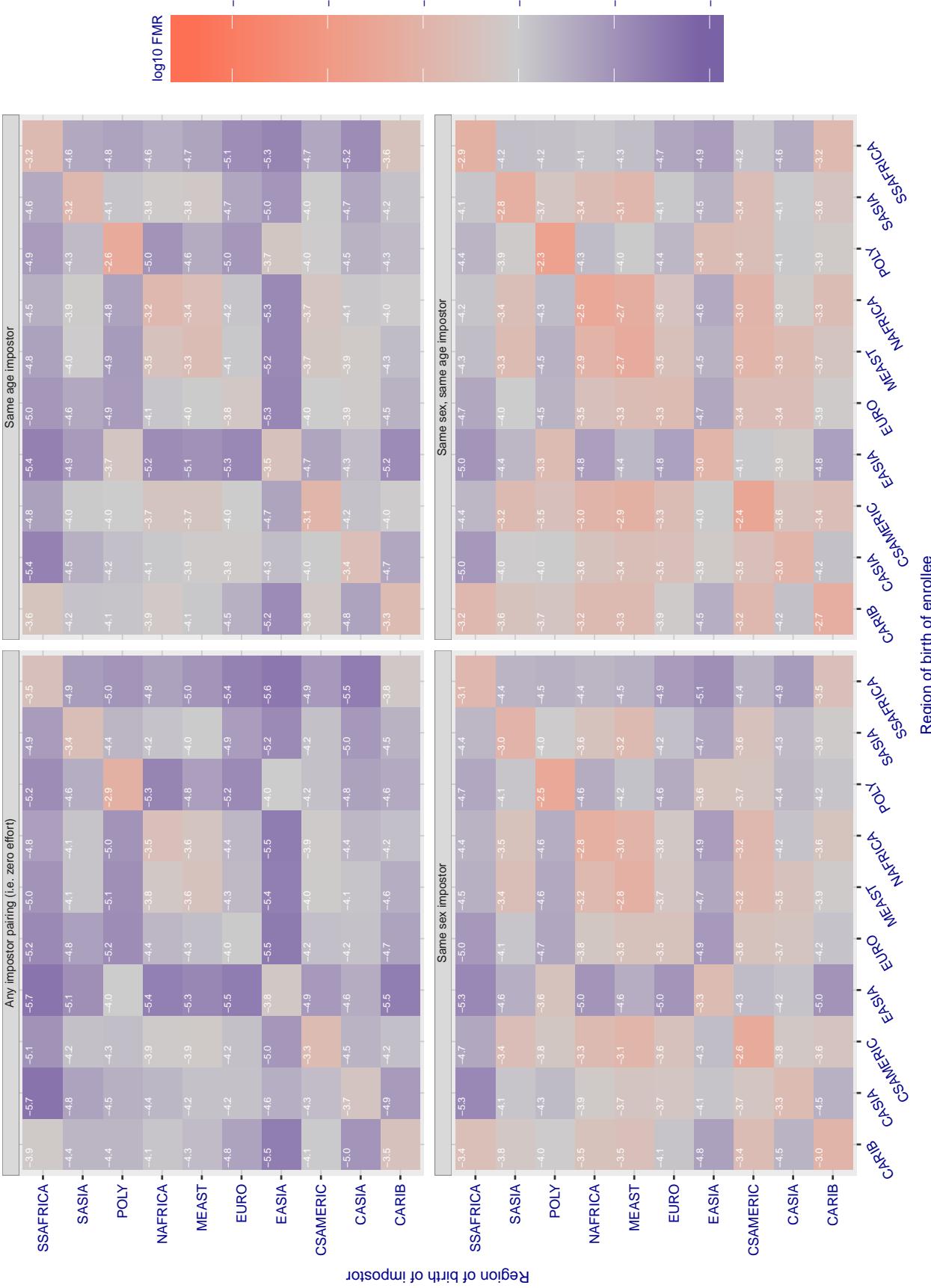


Figure 248: For algorithm yitu-003 operating on visa images, the heatmap shows false match rates observed over impostor comparisons of faces from different individuals who were born in the given region pair. False matches are counted against a recognition threshold fixed globally to give the target FMR in the plot title, computed over all on the order of  $10^{10}$  impostor comparisons. If text appears in each box it give the same quantity as that coded by the color. Grey indicates FMR is at the intended FMR target level. Light red colors present a security vulnerability to, for example, a passport gate. Each +1 increase in  $\log_{10}$  FMR corresponds to a factor of 10 increase in FMR. The matrix is not quite symmetric because images in the enrollment and verification sets are different.

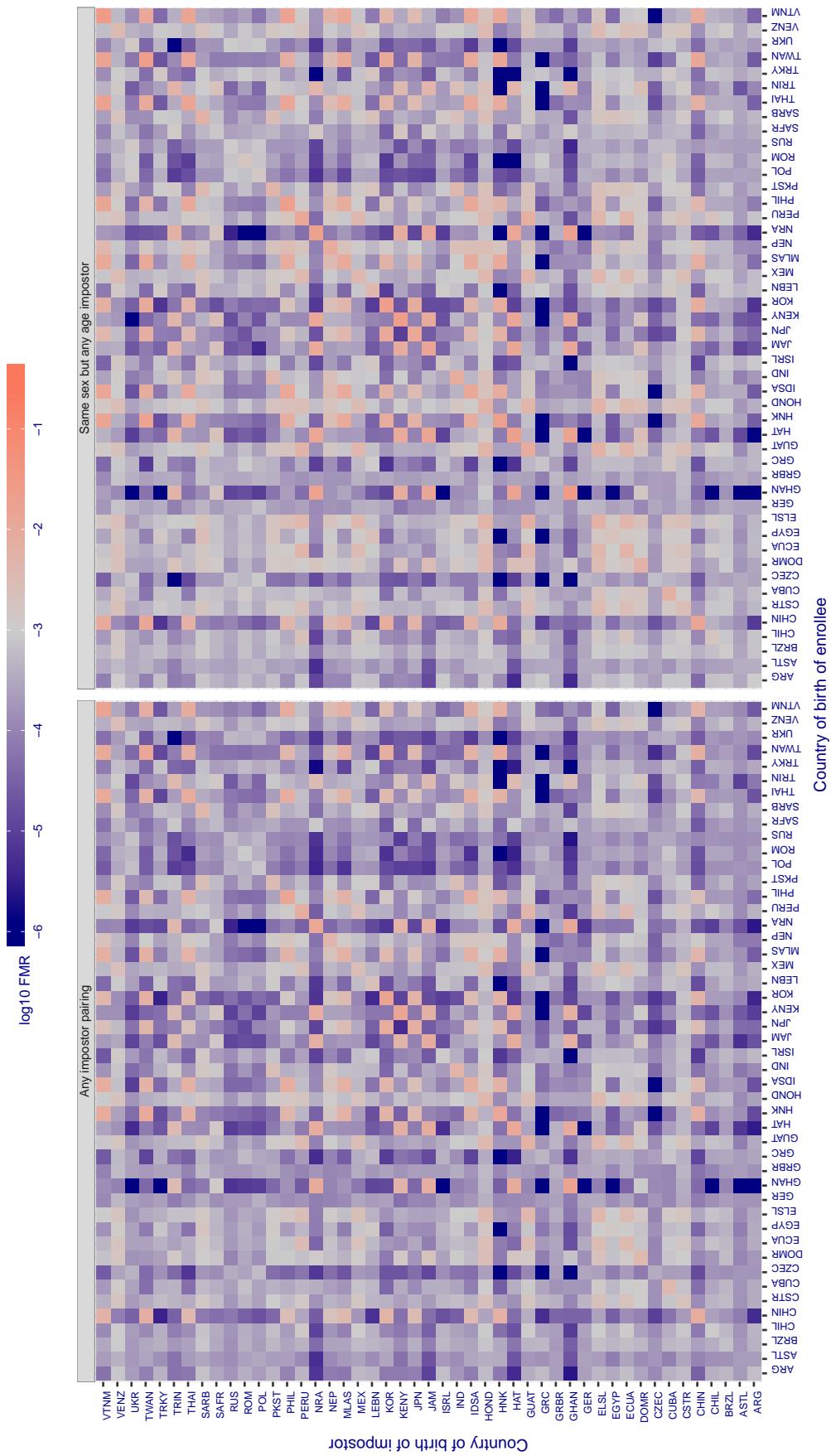
**Cross country FMR at threshold T = 2.575 for algorithm 3divi\_003, giving FMR(T) = 0.001 globally.**

Figure 249: For algorithm 3divi-003 operating on visa images, the heatmap shows false match rates observed over impostor comparisons of faces from different individuals who were born in the given country pair. False matches are counted against a recognition threshold fixed globally to give the target FMR in the plot title, computed over all on the order of  $10^{10}$  impostor comparisons. If text appears in each box it give the same quantity as that coded by the color. Grey indicates FMR is at the intended FMR target level. Light red colors present a security vulnerability to, for example, a passport gate. Each +1 increase in  $\log_{10} \text{FMR}$  corresponds to a factor of 10 increase in FMR. The matrix is not quite symmetric because images in the enrollment and verification sets are different.

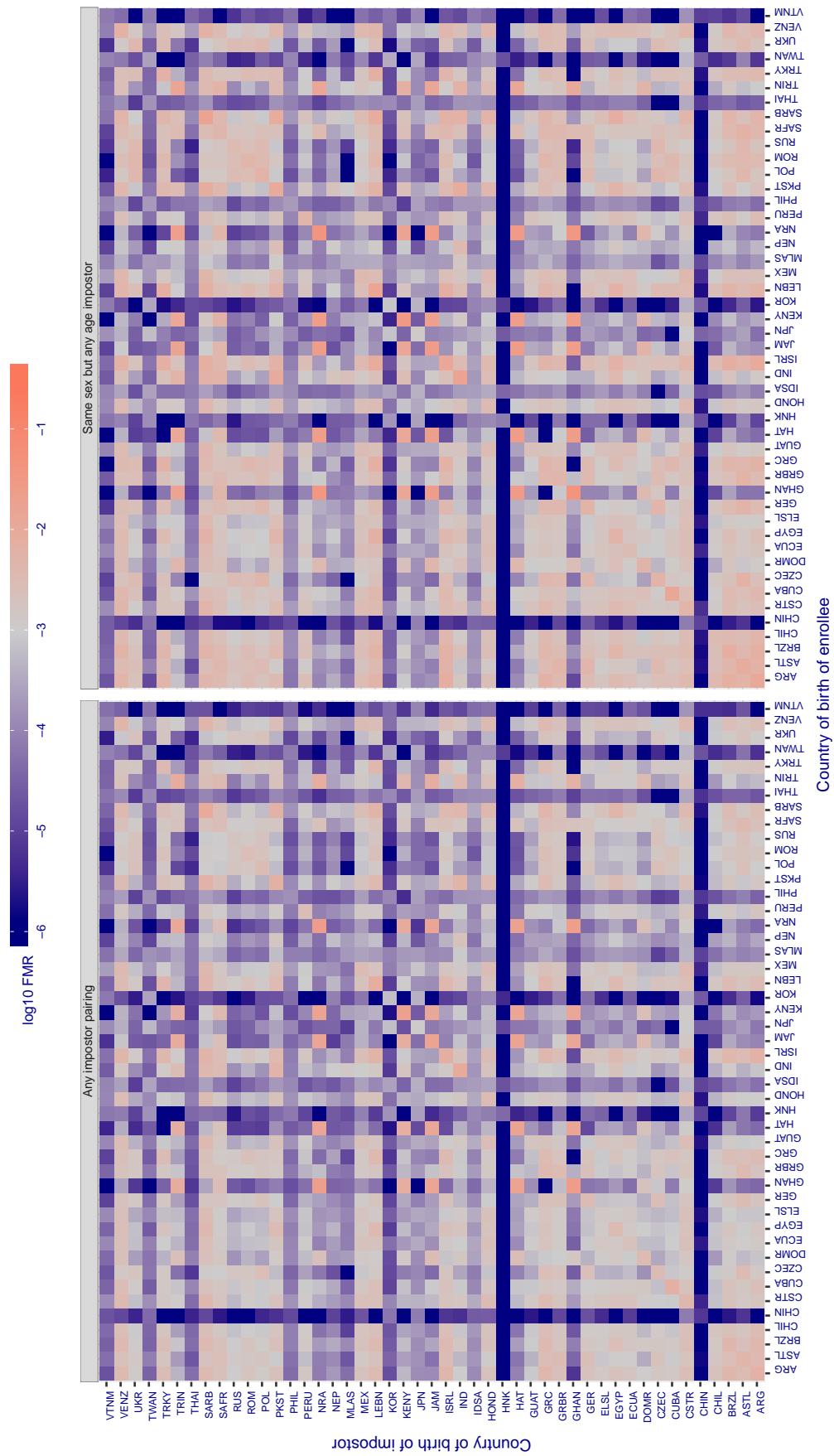
**Cross country FMR at threshold T = 0.632 for algorithm adera\_001, giving FMR(T) = 0.001 globally.**

Figure 250: For algorithm adera-001 operating on visa images, the heatmap shows false match rates observed over impostor comparisons of faces from different individuals who were born in the given country pair. False matches are counted against a recognition threshold fixed globally to give the target FMR in the plot title, computed over all on the order of  $10^{10}$  impostor comparisons. If text appears in each box it give the same quantity as that coded by the color. Grey indicates FMR is at the intended FMR target level. Light red colors present a security vulnerability to, for example, a passport gate. Each +1 increase in  $\log_{10} FMR$  corresponds to a factor of 10 increase in FMR. The matrix is not quite symmetric because images in the enrollment and verification sets are different.

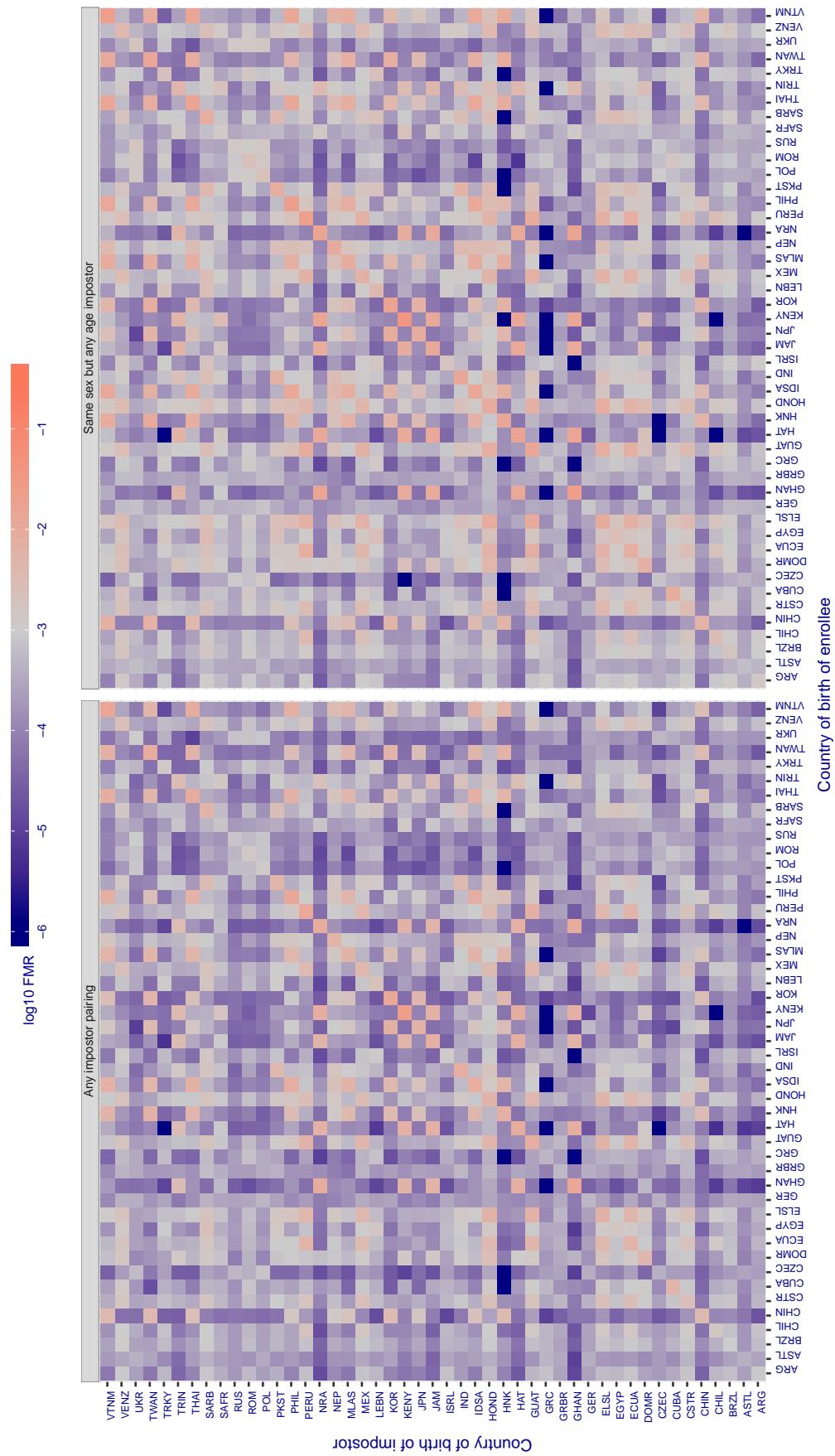
**Cross country FMR at threshold T = 0.662 for algorithm alchera\_000, giving FMR(T) = 0.001 globally.**

Figure 251: For algorithm alchera-000 operating on visa images, the heatmap shows false match rates observed over impostor comparisons of faces from different individuals who were born in the given country pair. False matches are counted against a recognition threshold fixed globally to give the target FMR in the plot title, computed over all on the order of  $10^{10}$  impostor comparisons. If text appears in each box it give the same quantity as that coded by the color. Grey indicates FMR is at the intended FMR target level. Light red colors present a security vulnerability to, for example, a passport gate. Each +1 increase in  $\log_{10} FMR$  corresponds to a factor of 10 increase in FMR. The matrix is not quite symmetric because images in the enrollment and verification sets are different.

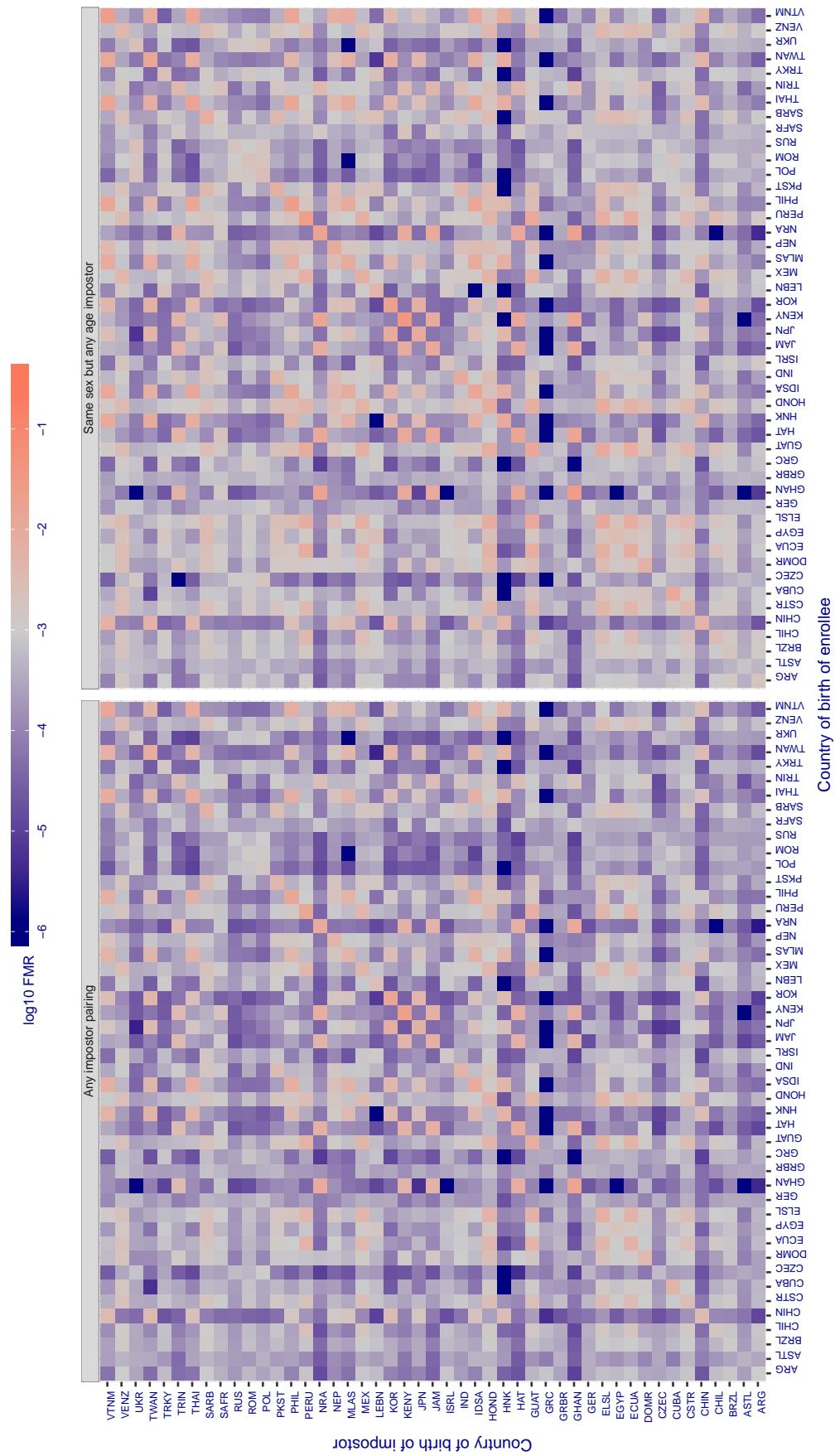
**Cross country FMR at threshold T = 0.667 for algorithm alchera\_001, giving FMR(T) = 0.001 globally.**

Figure 252: For algorithm alchera-001 operating on visa images, the heatmap shows false match rates observed over impostor comparisons of faces from different individuals who were born in the given country pair. False matches are counted against a recognition threshold fixed globally to give the target FMR in the plot title, computed over all on the order of  $10^{10}$  impostor comparisons. If text appears in each box it give the same quantity as that coded by the color. Grey indicates FMR is at the intended FMR target level. Light red colors present a security vulnerability to, for example, a passport gate. Each +1 increase in  $\log_{10} FMR$  corresponds to a factor of 10 increase in FMR. The matrix is not quite symmetric because images in the enrollment and verification sets are different.

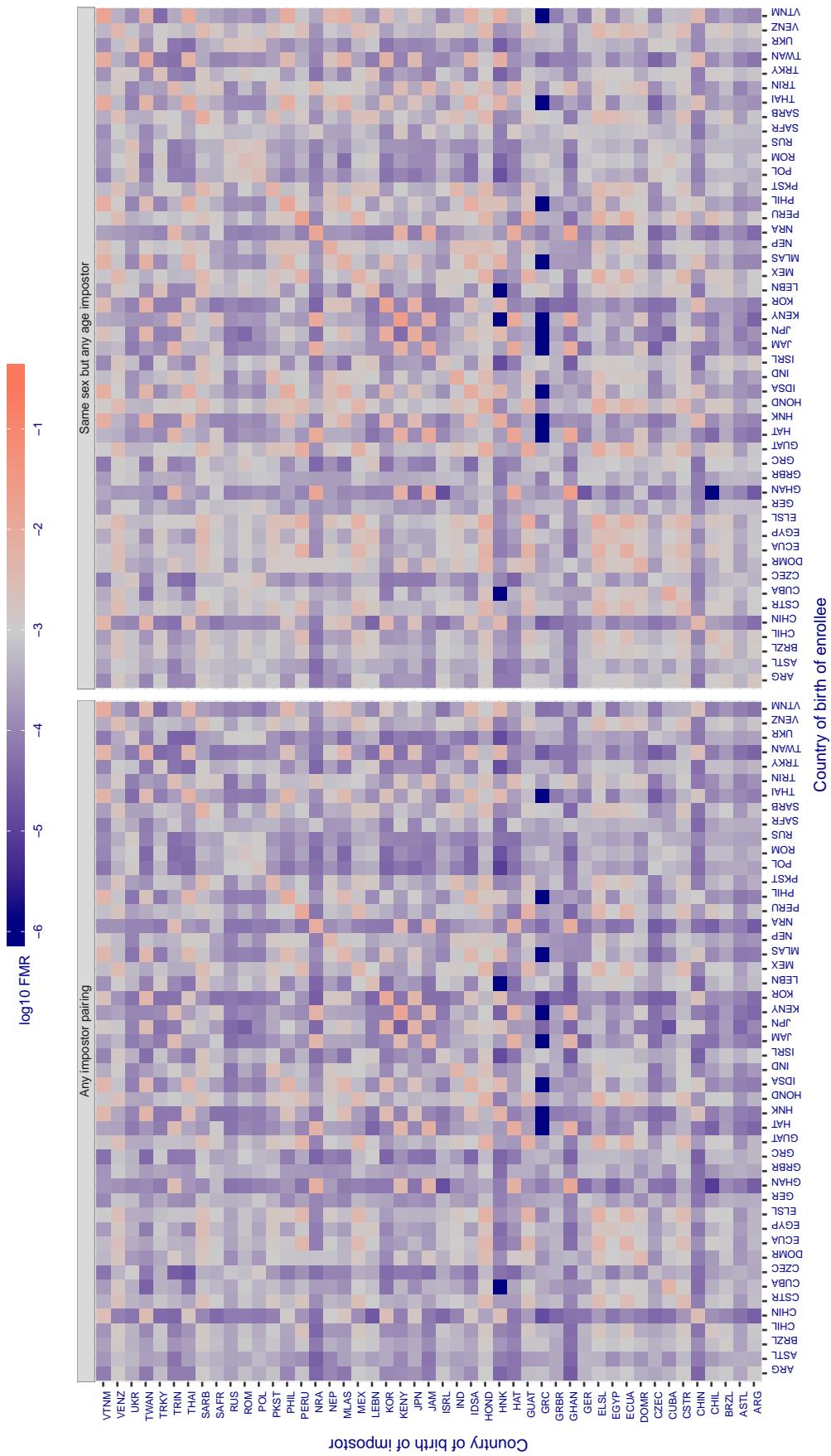
**Cross country FMR at threshold T = 0.339 for algorithm allgvision\_000, giving FMR(T) = 0.001 globally.**

Figure 253: For algorithm allgvision-000 operating on visa images, the heatmap shows false match rates observed over impostor comparisons of faces from different individuals who were born in the given country pair. False matches are counted against a recognition threshold fixed globally to give the target FMR in the plot title, computed over all on the order of  $10^{10}$  impostor comparisons. If text appears in each box it give the same quantity as that coded by the color. Grey indicates FMR is at the intended FMR target level. Light red colors present a security vulnerability to, for example, a passport gate. Each +1 increase in  $\log_{10} FMR$  corresponds to a factor of 10 increase in FMR. The matrix is not quite symmetric because images in the enrollment and verification sets are different.

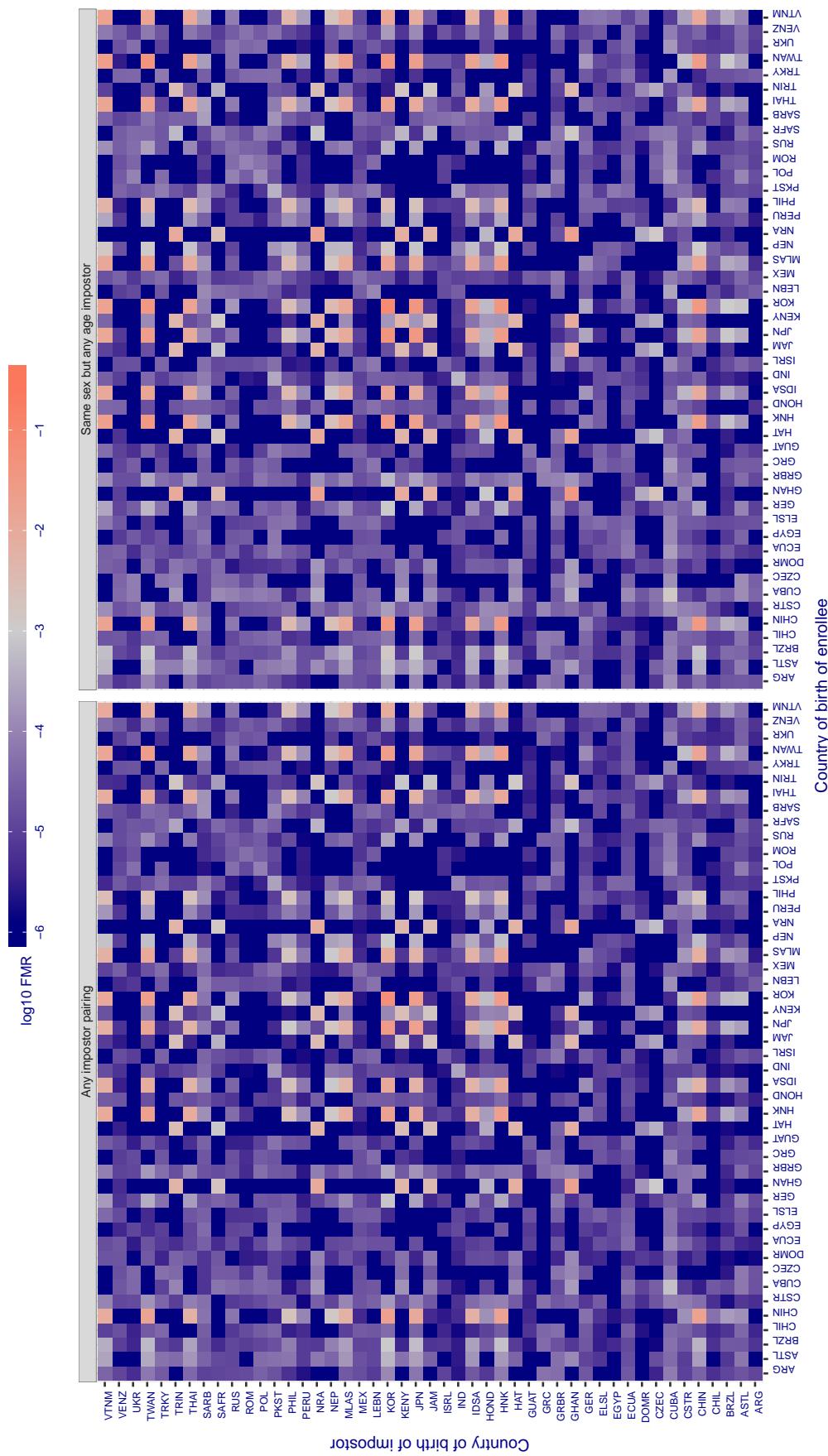
**Cross country FMR at threshold T = 3.524 for algorithm amplifiedgroup\_001, giving FMR(T) = 0.001 globally.**

Figure 254: For algorithm amplifiedgroup-001 operating on visa images, the heatmap shows false match rates observed over impostor comparisons of faces from different individuals who were born in the given country pair. False matches are counted against a recognition threshold fixed globally to give the target FMR in the plot title, computed over all on the order of  $10^{10}$  impostor comparisons. If text appears in each box it give the same quantity as that coded by the color. Grey indicates FMR is at the intended FMR target level. Light red colors present a security vulnerability to, for example, a passport gate. Each +1 increase in  $\log_{10} FMR$  corresponds to a factor of 10 increase in FMR. The matrix is not quite symmetric because images in the enrollment and verification sets are different.

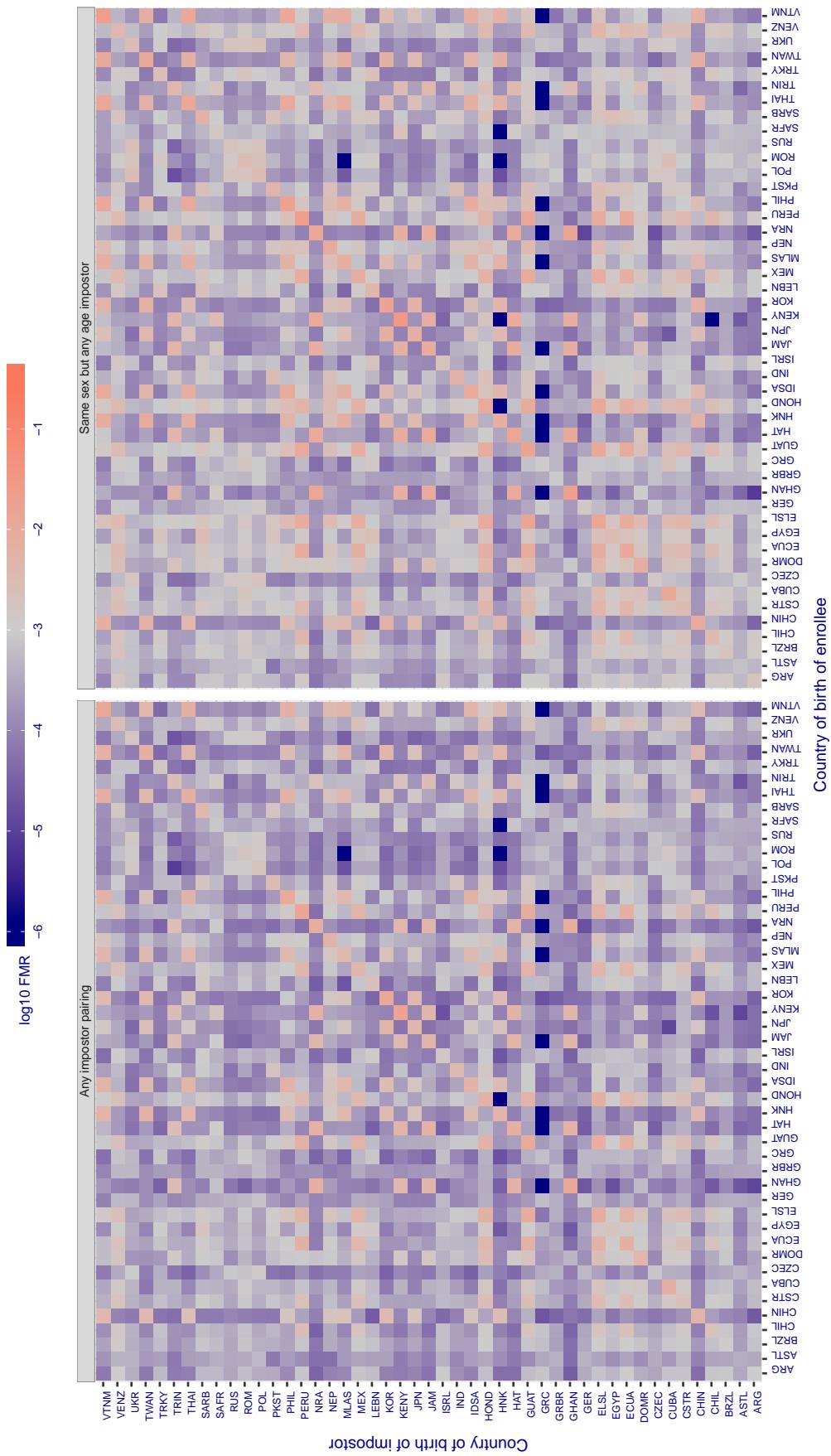
**Cross country FMR at threshold T = 0.313 for algorithm anke\_003, giving FMR(T) = 0.001 globally.**

Figure 255: For algorithm anke-003 operating on visa images, the heatmap shows false match rates observed over impostor comparisons of faces from different individuals who were born in the given country pair. False matches are counted against a recognition threshold fixed globally to give the target FMR in the plot title, computed over all on the order of  $10^{10}$  impostor comparisons. If text appears in each box it give the same quantity as that coded by the color. Grey indicates FMR is at the intended FMR target level. Light red colors present a security vulnerability to, for example, a passport gate. Each +1 increase in  $\log_{10}$  FMR corresponds to a factor of 10 increase in FMR. The matrix is not quite symmetric because images in the enrollment and verification sets are different.

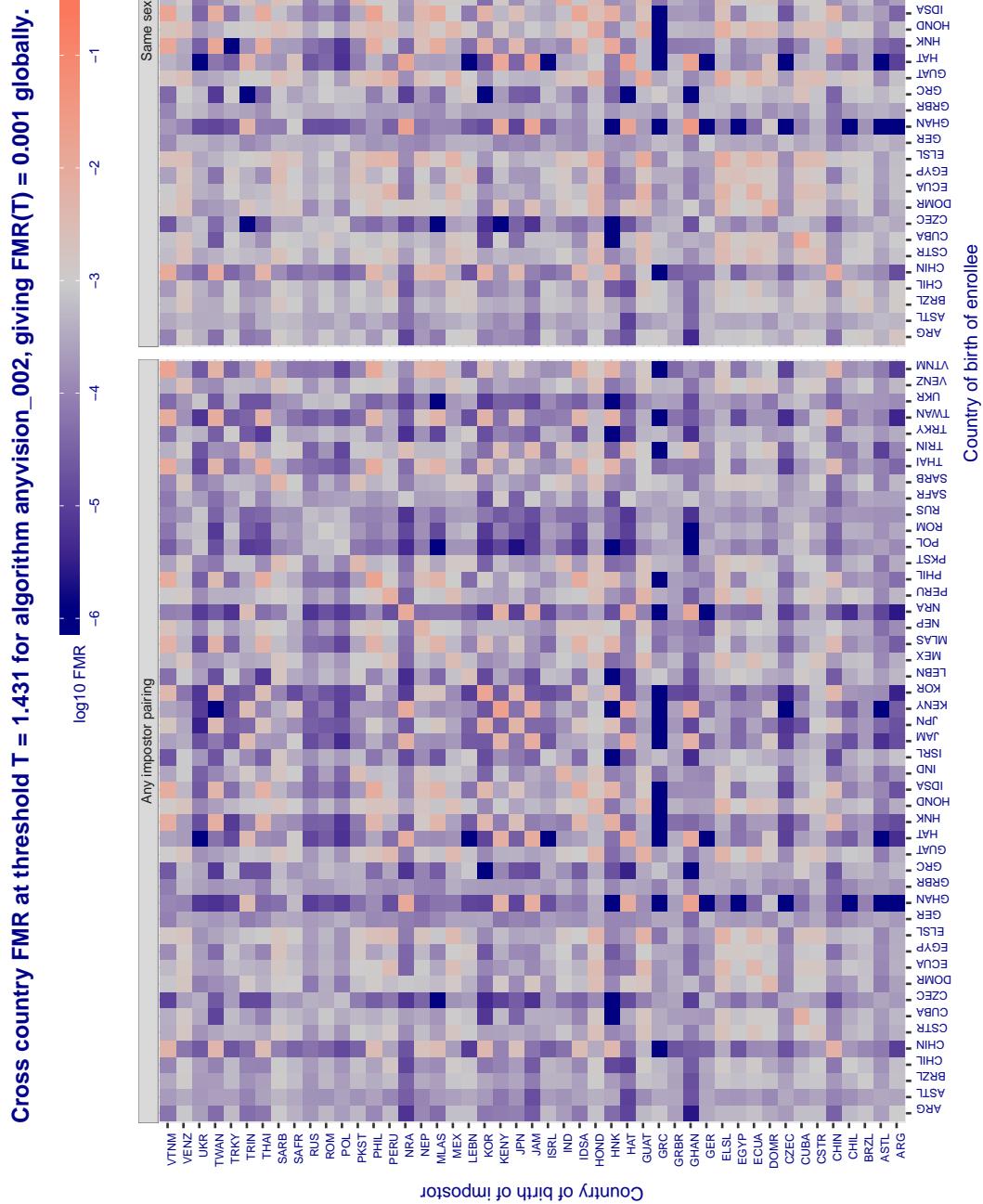


Figure 256: For algorithm anyvision-002 operating on visa images, the heatmap shows false match rates observed over impostor comparisons of faces from different individuals who were born in the given country pair. False matches are counted against a recognition threshold fixed globally to give the target FMR in the plot title, computed over all on the order of  $10^{10}$  impostor comparisons. If text appears in each box it give the same quantity as that coded by the color. Grey indicates FMR is at the intended FMR target level. Light red colors present a security vulnerability to, for example, a passport gate. Each +1 increase in  $\log_{10}$  FMR corresponds to a factor of 10 increase in FMR. The matrix is not quite symmetric because images in the enrollment and verification sets are different.

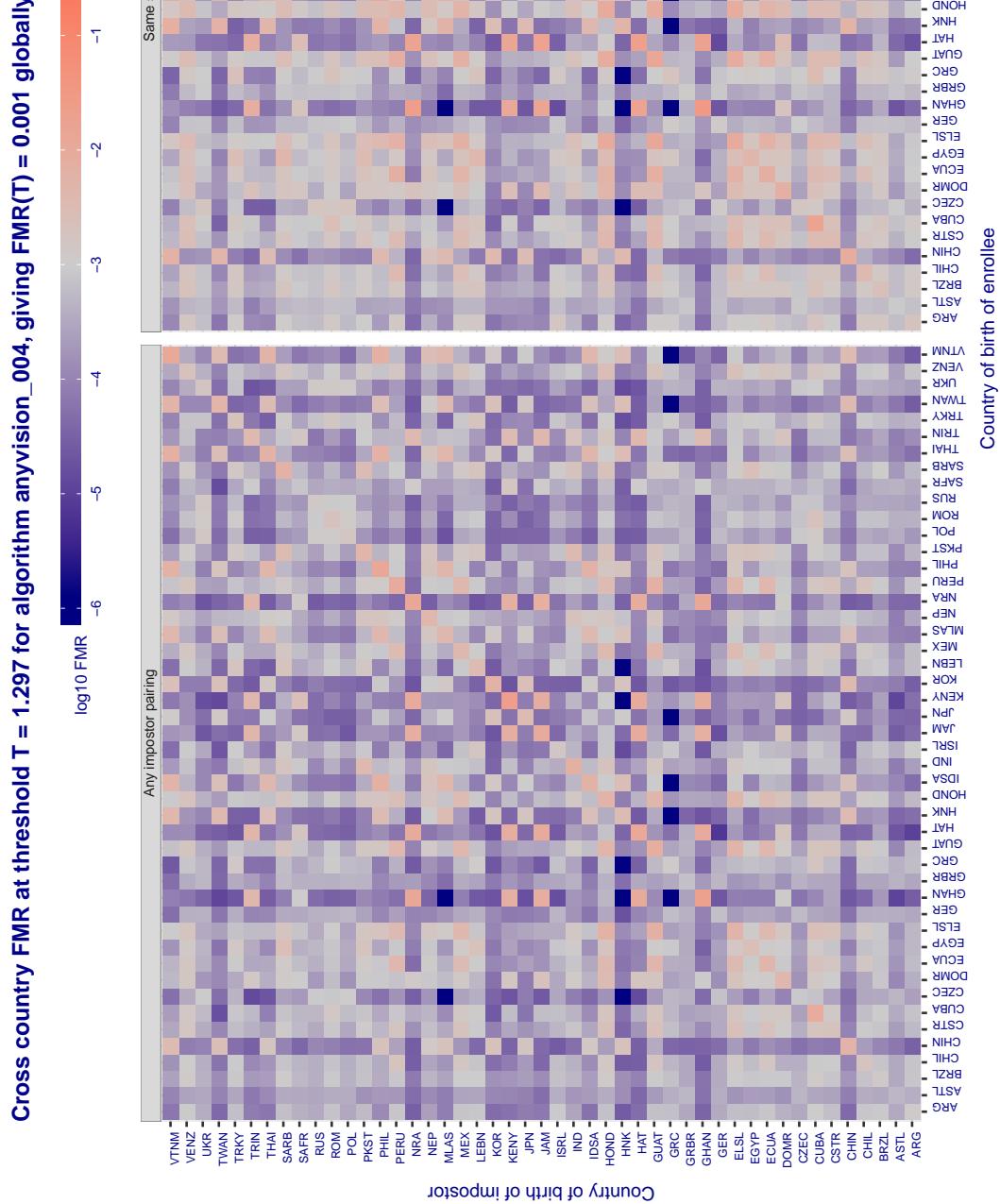


Figure 257: For algorithm anyvision-004 operating on visa images, the heatmap shows false match rates observed over impostor comparisons of faces from different individuals who were born in the given country pair. False matches are counted against a recognition threshold fixed globally to give the target FMR in the plot title, computed over all on the order of  $10^{10}$  impostor comparisons. If text appears in each box it give the same quantity as that coded by the color. Grey indicates FMR is at the intended FMR target level. Light red colors present a security vulnerability to, for example, a passport gate. Each +1 increase in  $\log_{10}$  FMR corresponds to a factor of 10 increase in FMR. The matrix is not quite symmetric because images in the enrollment and verification sets are different.

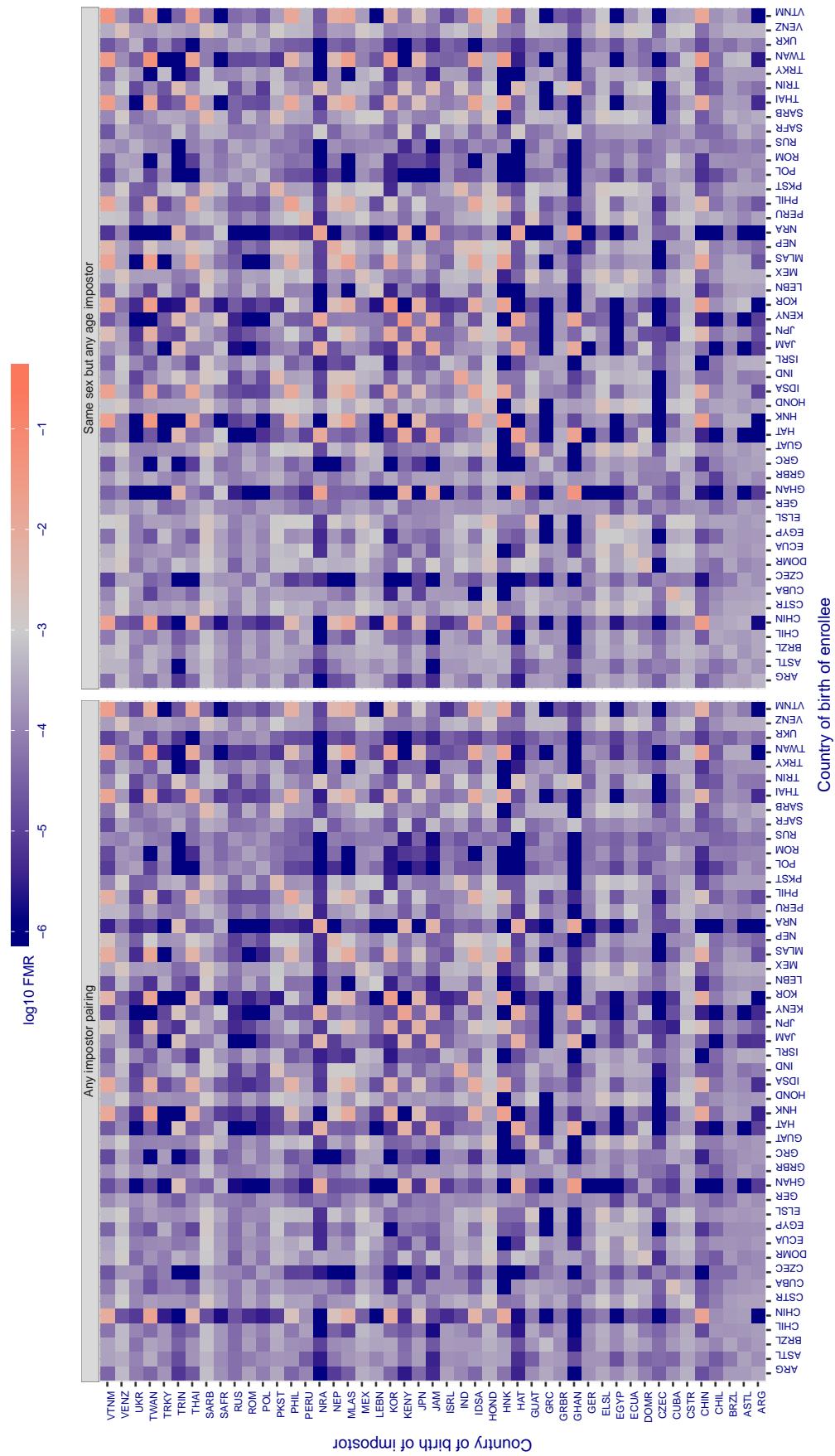
**Cross country FMR at threshold T = 2.758 for algorithm aware\_003, giving FMR(T) = 0.001 globally.**

Figure 258: For algorithm aware-003 operating on visa images, the heatmap shows false match rates observed over impostor comparisons of faces from different individuals who were born in the given country pair. False matches are counted against a recognition threshold fixed globally to give the target FMR in the plot title, computed over all on the order of  $10^{10}$  impostor comparisons. If text appears in each box it give the same quantity as that coded by the color. Grey indicates FMR is at the intended FMR target level. Light red colors present a security vulnerability to, for example, a passport gate. Each +1 increase in  $\log_{10} FMR$  corresponds to a factor of 10 increase in FMR. The matrix is not quite symmetric because images in the enrollment and verification sets are different.

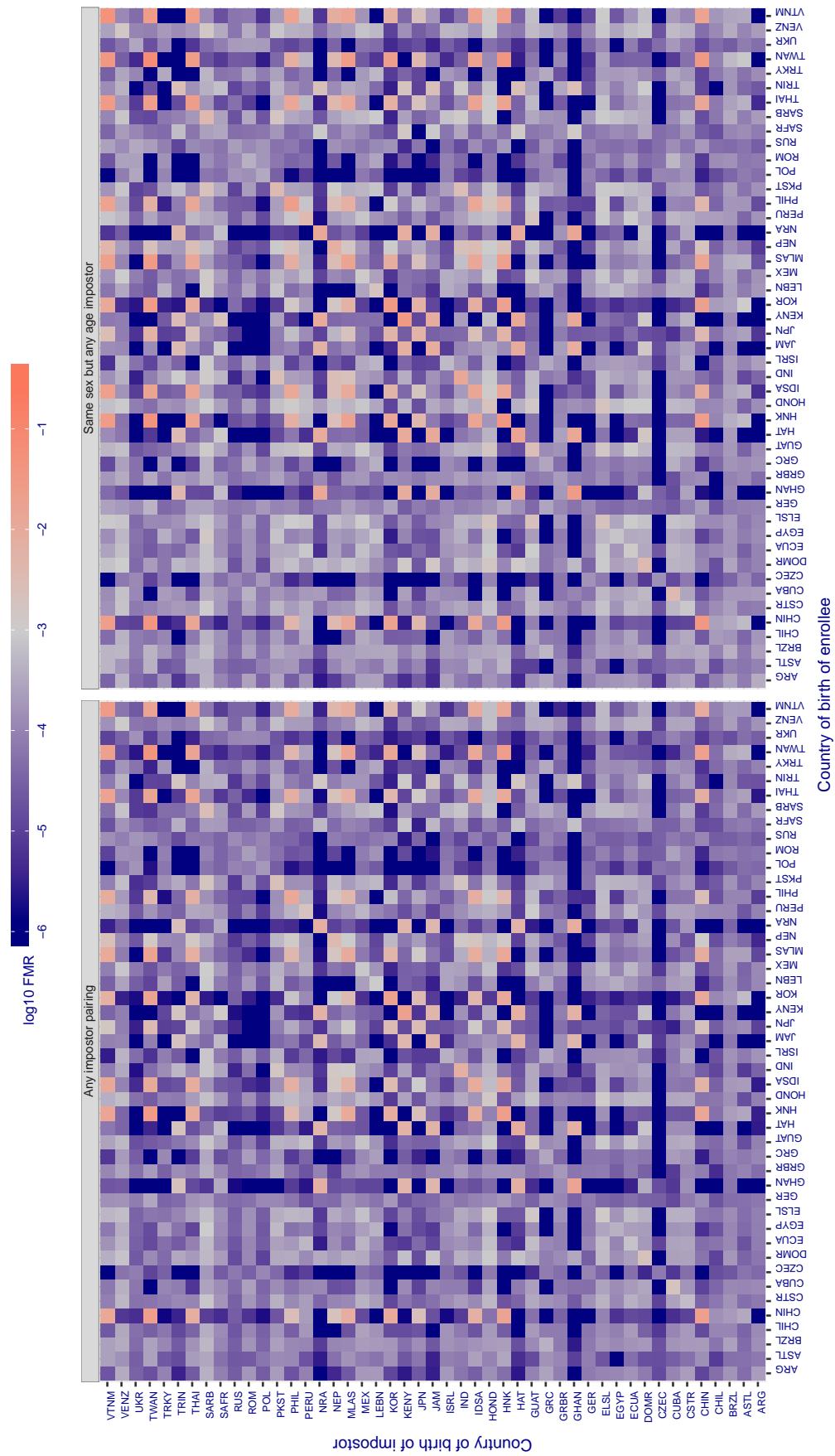
**Cross country FMR at threshold T = 3.681 for algorithm aware\_004, giving FMR(T) = 0.001 globally.**

Figure 259: For algorithm aware-004 operating on visa images, the heatmap shows false match rates observed over impostor comparisons of faces from different individuals who were born in the given country pair. False matches are counted against a recognition threshold fixed globally to give the target FMR in the plot title, computed over all on the order of  $10^{10}$  impostor comparisons. If text appears in each box it give the same quantity as that coded by the color. Grey indicates FMR is at the intended FMR target level. Light red colors present a security vulnerability to, for example, a passport gate. Each +1 increase in  $\log_{10} \text{FMR}$  corresponds to a factor of 10 increase in FMR. The matrix is not quite symmetric because images in the enrollment and verification sets are different.

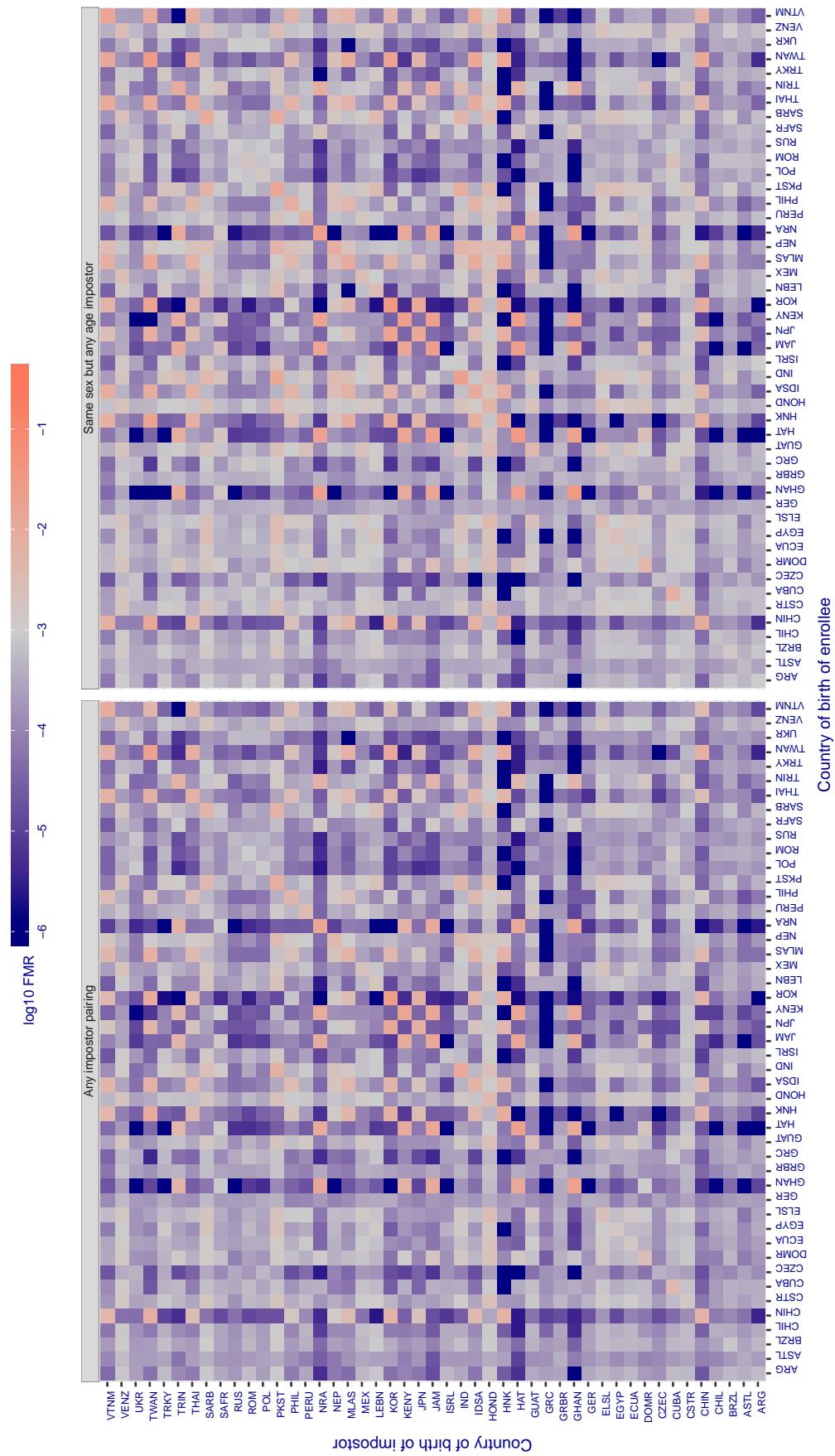
**Cross country FMR at threshold T = 0.800 for algorithm ayonix\_000, giving FMR(T) = 0.001 globally.**

Figure 260: For algorithm ayonix-000 operating on visa images, the heatmap shows false match rates observed over impostor comparisons of faces from different individuals who were born in the given country pair. False matches are counted against a recognition threshold fixed globally to give the target FMR in the plot title, computed over all on the order of  $10^{10}$  impostor comparisons. If text appears in each box it give the same quantity as that coded by the color. Grey indicates FMR is at the intended FMR target level. Light red colors present a security vulnerability to, for example, a passport gate. Each +1 increase in  $\log_{10} FMR$  corresponds to a factor of 10 increase in FMR. The matrix is not quite symmetric because images in the enrollment and verification sets are different.

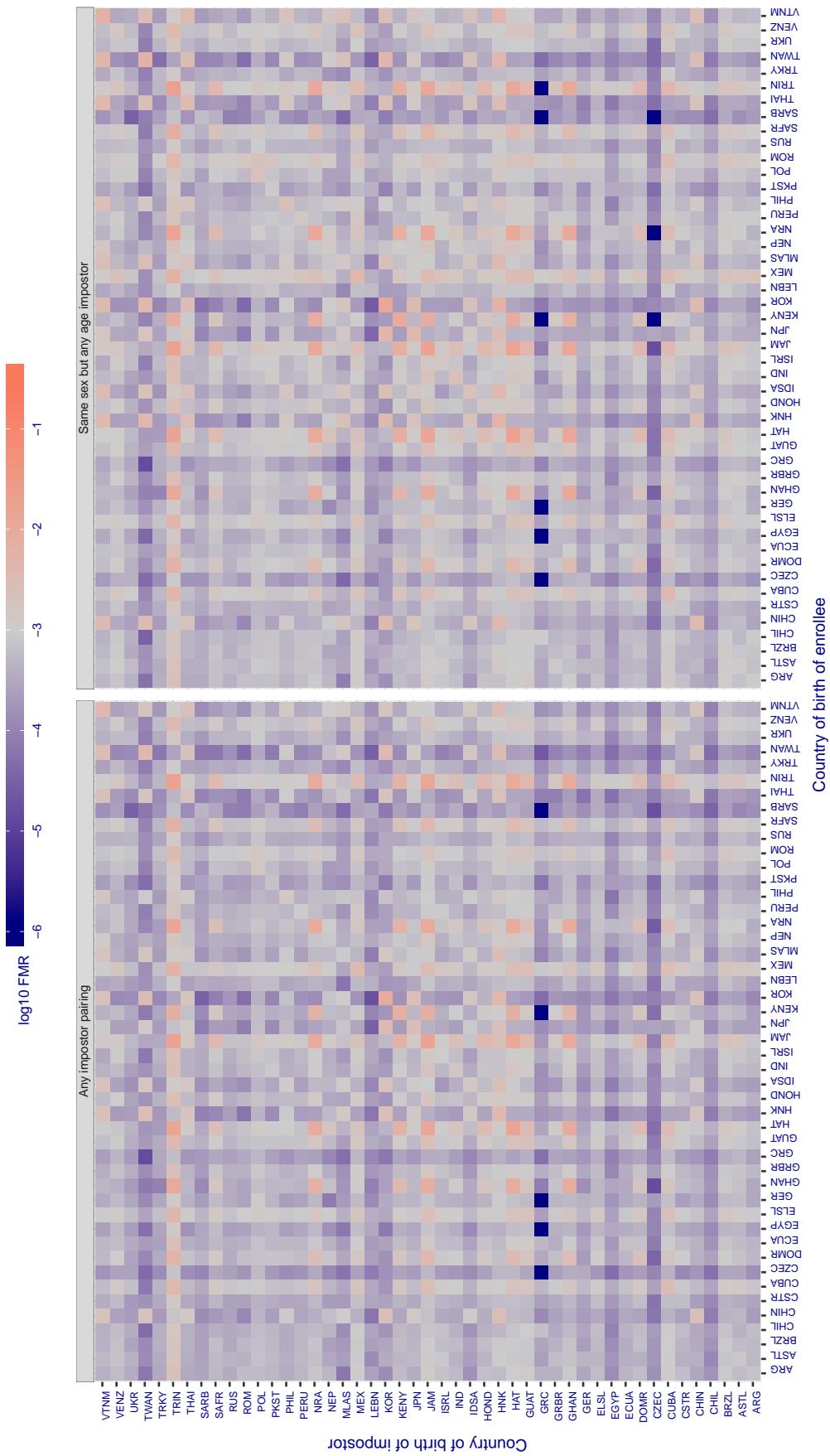
**Cross country FMR at threshold T = 0.649 for algorithm bm\_001, giving FMR(T) = 0.001 globally.**

Figure 261: For algorithm *bm-001* operating on visa images, the heatmap shows false match rates observed over impostor comparisons of faces from different individuals who were born in the given country pair. False matches are counted against a recognition threshold fixed globally to give the target FMR in the plot title, computed over all on the order of  $10^{10}$  impostor comparisons. If text appears in each box it give the same quantity as that coded by the color. Grey indicates FMR is at the intended FMR target level. Light red colors present a security vulnerability to, for example, a passport gate. Each +1 increase in  $\log_{10} \text{FMR}$  corresponds to a factor of 10 increase in FMR. The matrix is not quite symmetric because images in the enrollment and verification sets are different.

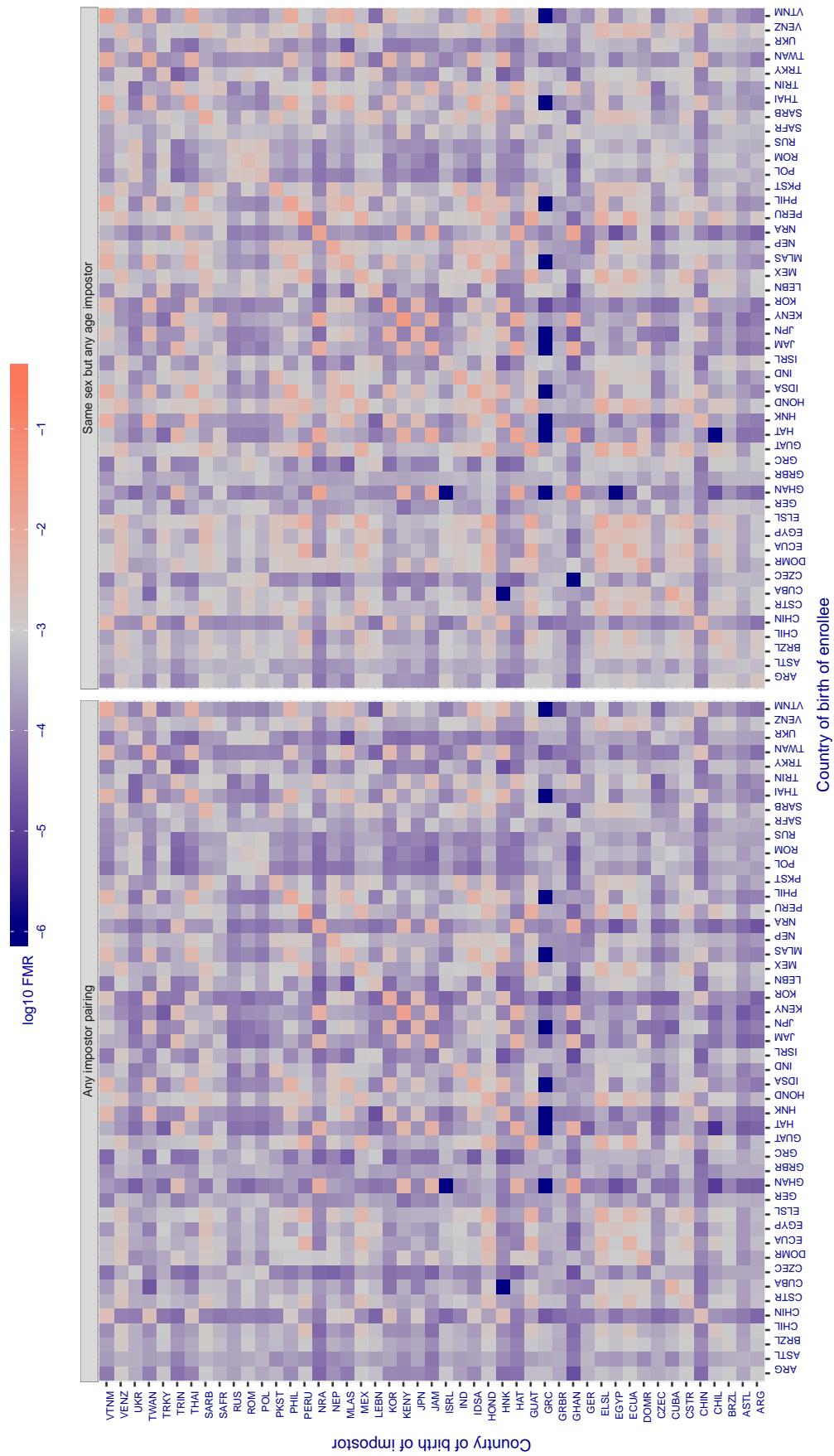
**Cross country FMR at threshold T = 0.306 for algorithm camvi\_002, giving FMR(T) = 0.001 globally.**

Figure 262: For algorithm camvi-002 operating on visa images, the heatmap shows false match rates observed over impostor comparisons of faces from different individuals who were born in the given country pair. False matches are counted against a recognition threshold fixed globally to give the target FMR in the plot title, computed over all on the order of  $10^{10}$  impostor comparisons. If text appears in each box it give the same quantity as that coded by the color. Grey indicates FMR is at the intended FMR target level. Light red colors present a security vulnerability to, for example, a passport gate. Each +1 increase in  $\log_{10} \text{FMR}$  corresponds to a factor of 10 increase in FMR. The matrix is not quite symmetric because images in the enrollment and verification sets are different.

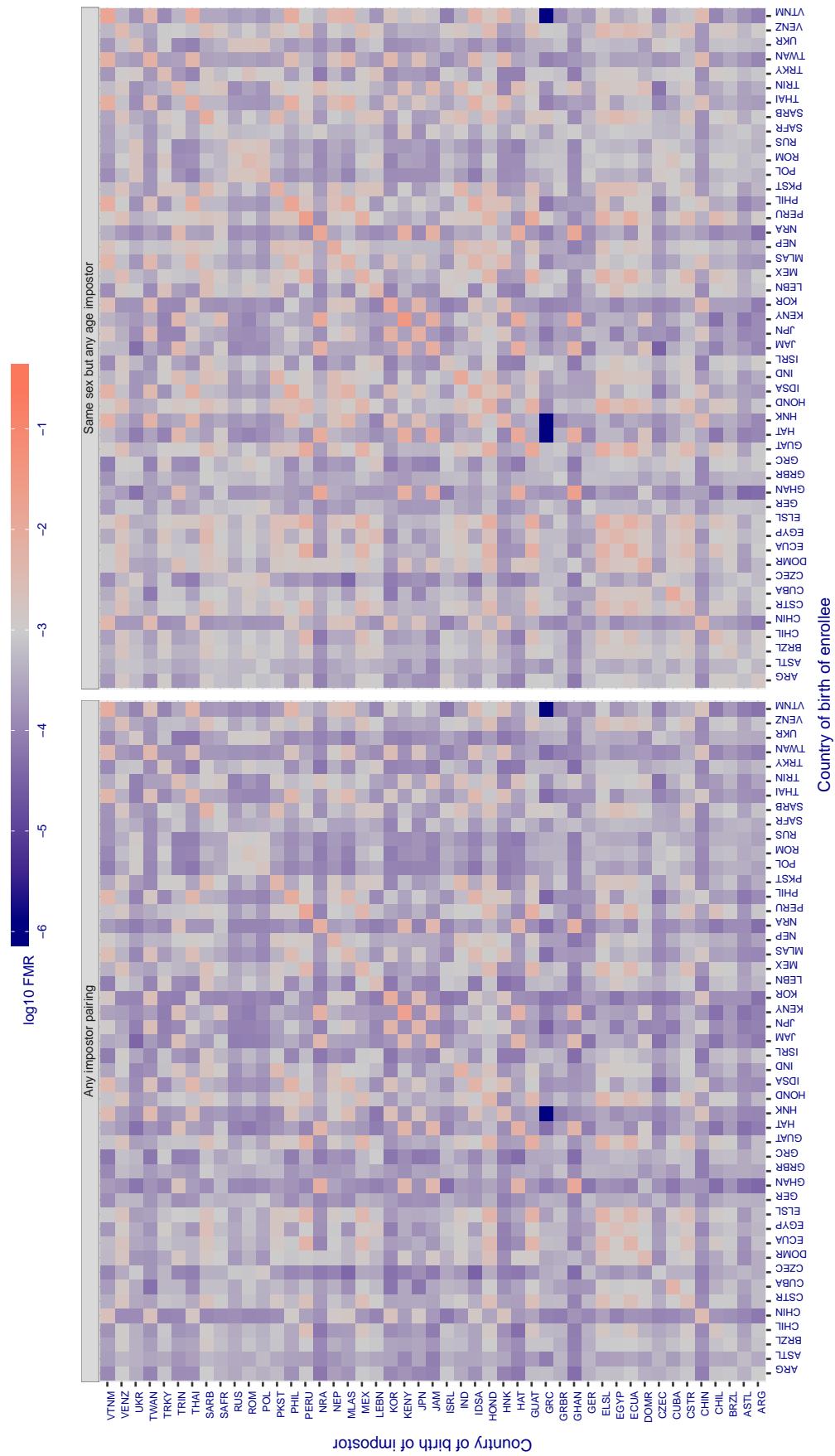
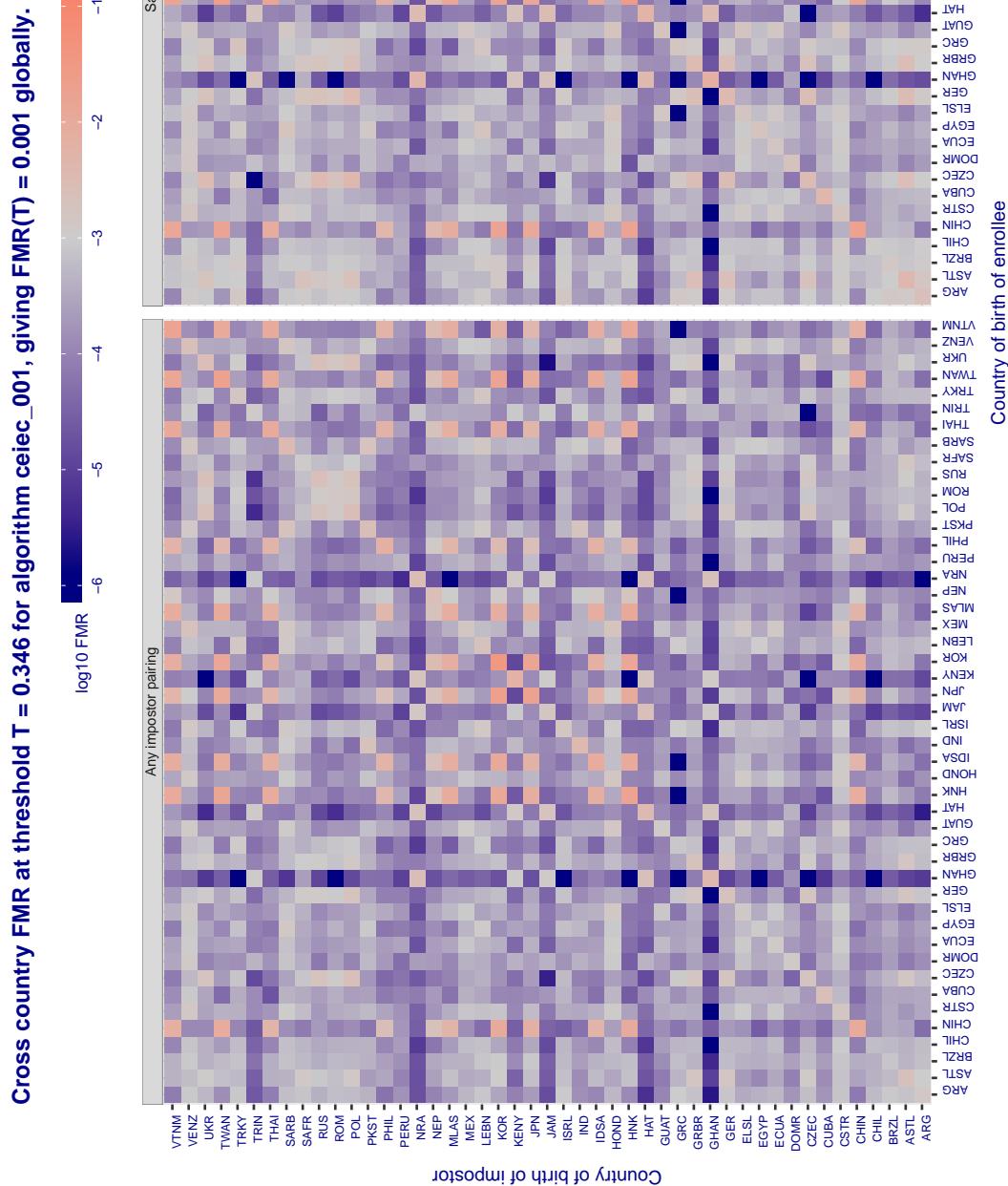
**Cross country FMR at threshold T = 0.301 for algorithm camvi\_003, giving FMR(T) = 0.001 globally.**

Figure 263: For algorithm camvi-003 operating on visa images, the heatmap shows false match rates observed over impostor comparisons of faces from different individuals who were born in the given country pair. False matches are counted against a recognition threshold fixed globally to give the target FMR in the plot title, computed over all on the order of  $10^{10}$  impostor comparisons. If text appears in each box it give the same quantity as that coded by the color. Grey indicates FMR is at the intended FMR target level. Light red colors present a security vulnerability to, for example, a passport gate. Each +1 increase in  $\log_{10} \text{FMR}$  corresponds to a factor of 10 increase in FMR. The matrix is not quite symmetric because images in the enrollment and verification sets are different.



*Figure 264: For algorithm ceiec-001 operating on visa images, the heatmap shows false match rates observed over impostor comparisons of faces from different individuals who were born in the given country pair. False matches are counted against a recognition threshold fixed globally to give the target FMR in the plot title, computed over all on the order of  $10^{10}$  impostor comparisons. If text appears in each box it give the same quantity as that coded by the color. Grey indicates FMR is at the intended FMR target level. Light red colors present a security vulnerability to, for example, a passport gate. Each +1 increase in  $\log_{10} FMR$  corresponds to a factor of 10 increase in FMR. The matrix is not quite symmetric because images in the enrollment and verification sets are different.*

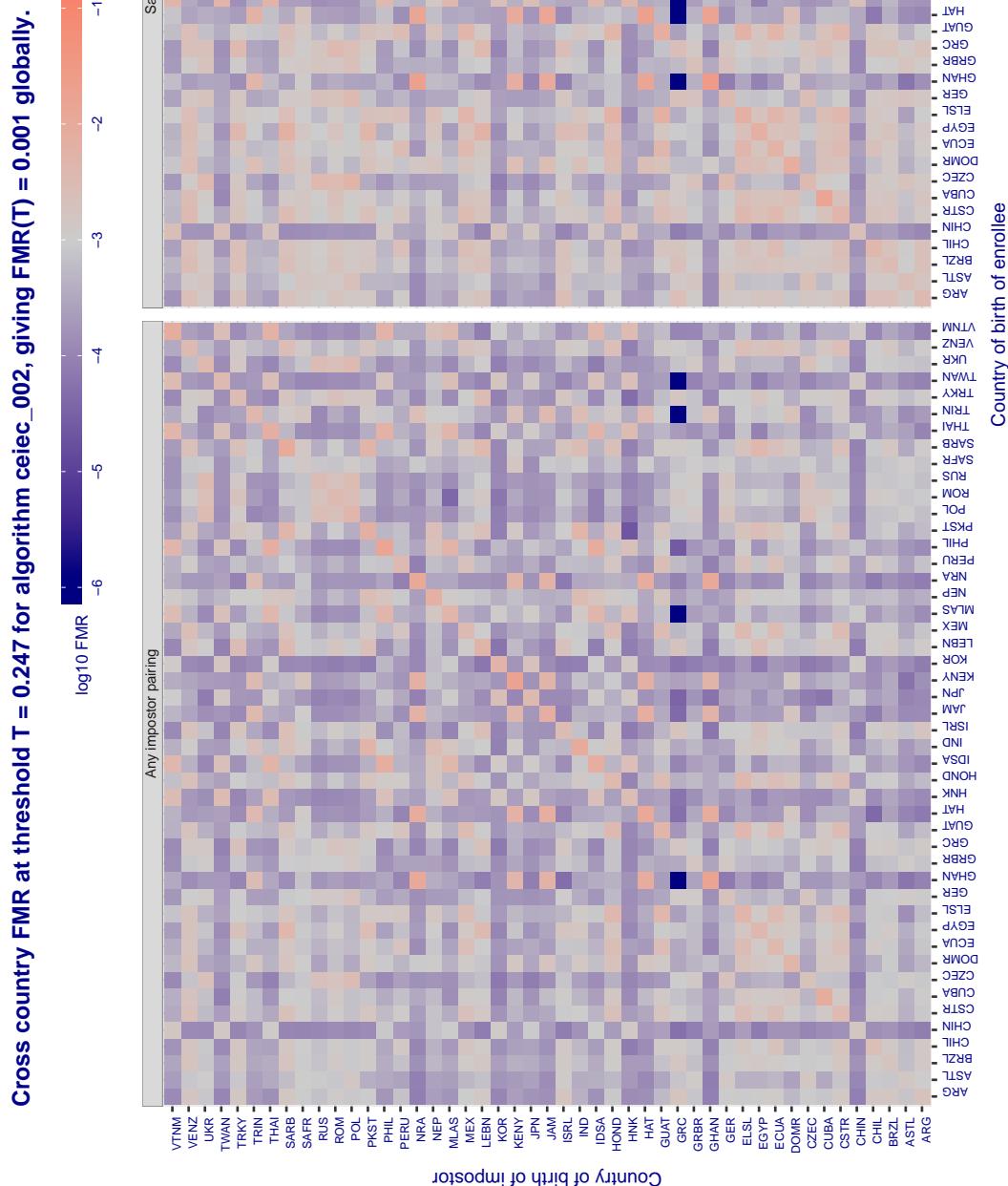


Figure 265: For algorithm ceiec-002 operating on visa images, the heatmap shows false match rates observed over impostor comparisons of faces from different individuals who were born in the given country pair. False matches are counted against a recognition threshold fixed globally to give the target FMR in the plot title, computed over all on the order of  $10^{10}$  impostor comparisons. If text appears in each box it give the same quantity as that coded by the color. Grey indicates FMR is at the intended FMR target level. Light red colors present a security vulnerability to, for example, a passport gate. Each +1 increase in  $\log_{10} \text{FMR}$  corresponds to a factor of 10 increase in FMR. The matrix is not quite symmetric because images in the enrollment and verification sets are different.

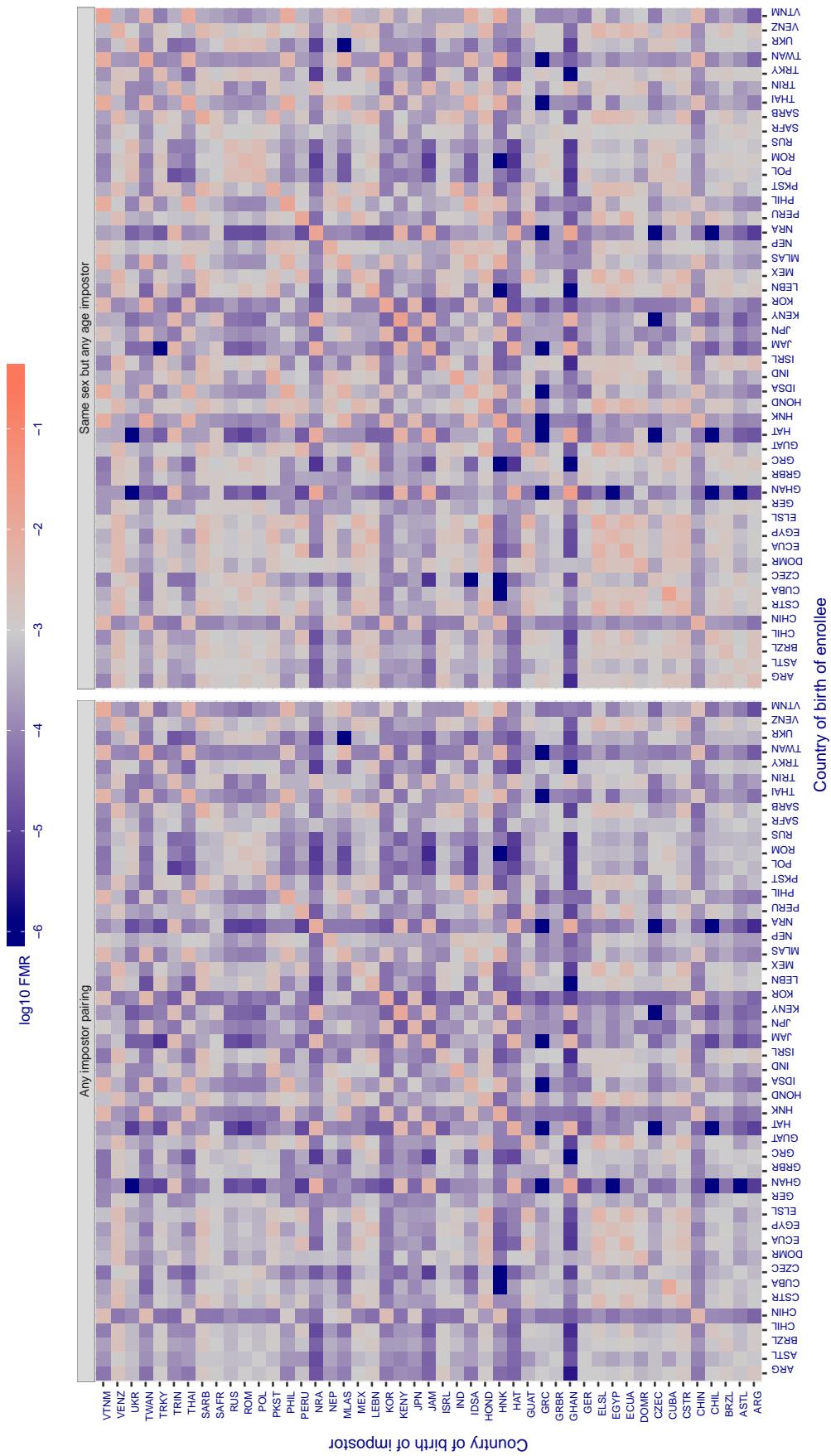
**Cross country FMR at threshold T = 2845.000 for algorithm cogent\_003, giving FMR(T) = 0.001 globally.**

Figure 266: For algorithm cogent-003 operating on visa images, the heatmap shows false match rates observed over impostor comparisons of faces from different individuals who were born in the given country pair. False matches are counted against a recognition threshold fixed globally to give the target FMR in the plot title, computed over all on the order of  $10^{10}$  impostor comparisons. If text appears in each box it give the same quantity as that coded by the color. Grey indicates FMR is at the intended FMR target level. Light red colors present a security vulnerability to, for example, a passport gate. Each +1 increase in  $\log_{10} FMR$  corresponds to a factor of 10 increase in FMR. The matrix is not quite symmetric because images in the enrollment and verification sets are different.

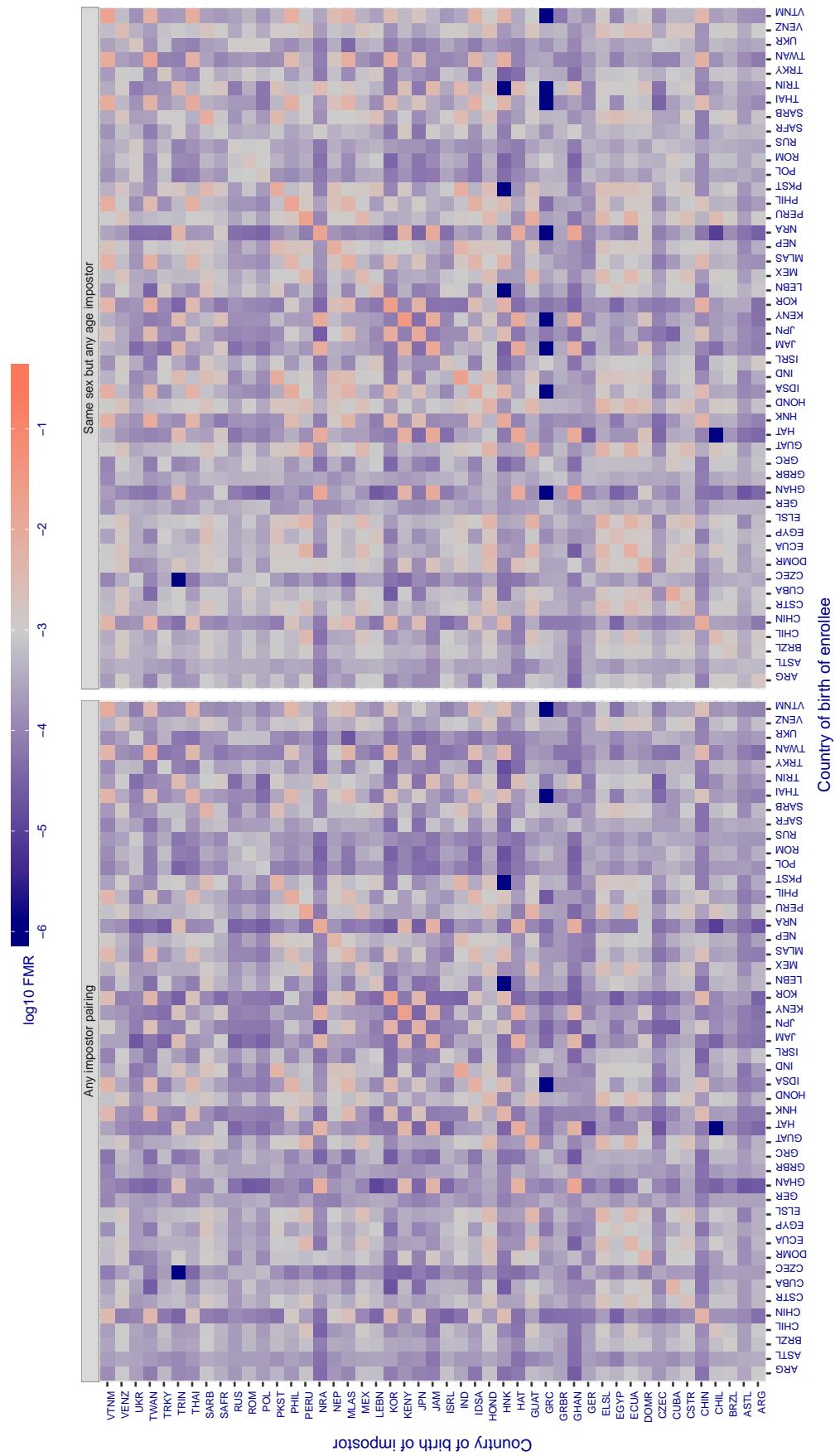
**Cross country FMR at threshold T = 0.522 for algorithm cognitec\_000, giving  $\text{FMR}(T) = 0.001$  globally.**

Figure 267: For algorithm cognitec-000 operating on visa images, the heatmap shows false match rates observed over impostor comparisons of faces from different individuals who were born in the given country pair. False matches are counted against a recognition threshold fixed globally to give the target  $\text{FMR}$  in the plot title, computed over all on the order of  $10^{10}$  impostor comparisons. If text appears in each box it give the same quantity as that coded by the color. Grey indicates  $\text{FMR}$  is at the intended  $\text{FMR}$  target level. Light red colors present a security vulnerability to, for example, a passport gate. Each +1 increase in  $\log_{10} \text{FMR}$  corresponds to a factor of 10 increase in  $\text{FMR}$ . The matrix is not quite symmetric because images in the enrollment and verification sets are different.

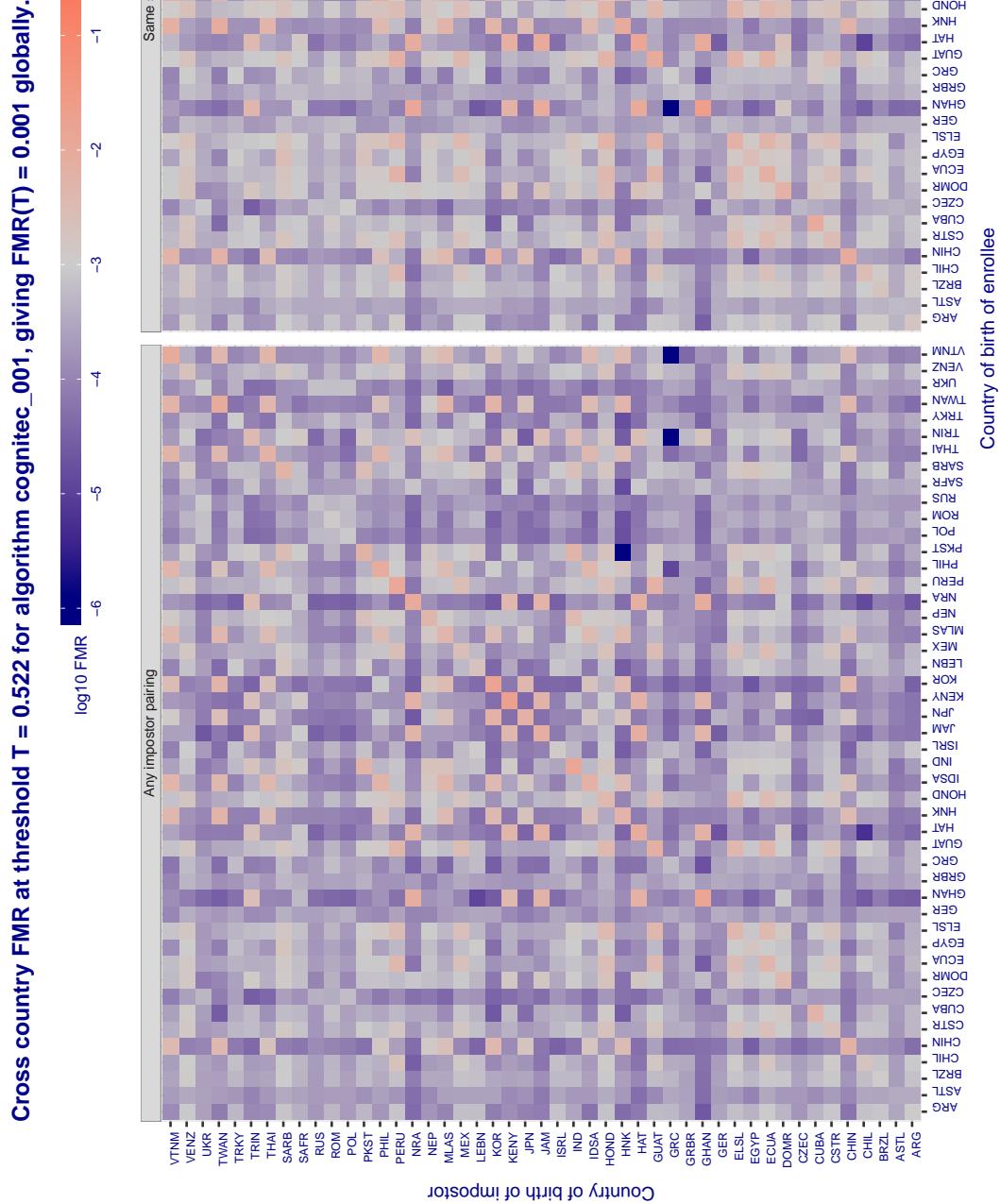


Figure 268: For algorithm cognitec-001 operating on visa images, the heatmap shows false match rates observed over impostor comparisons of faces from different individuals who were born in the given country pair. False matches are counted against a recognition threshold fixed globally to give the target FMR in the plot title, computed over all on the order of  $10^{10}$  impostor comparisons. If text appears in each box it give the same quantity as that coded by the color. Grey indicates FMR is at the intended FMR target level. Light red colors present a security vulnerability to, for example, a passport gate. Each +1 increase in  $\log_{10}$  FMR corresponds to a factor of 10 increase in FMR. The matrix is not quite symmetric because images in the enrollment and verification sets are different.

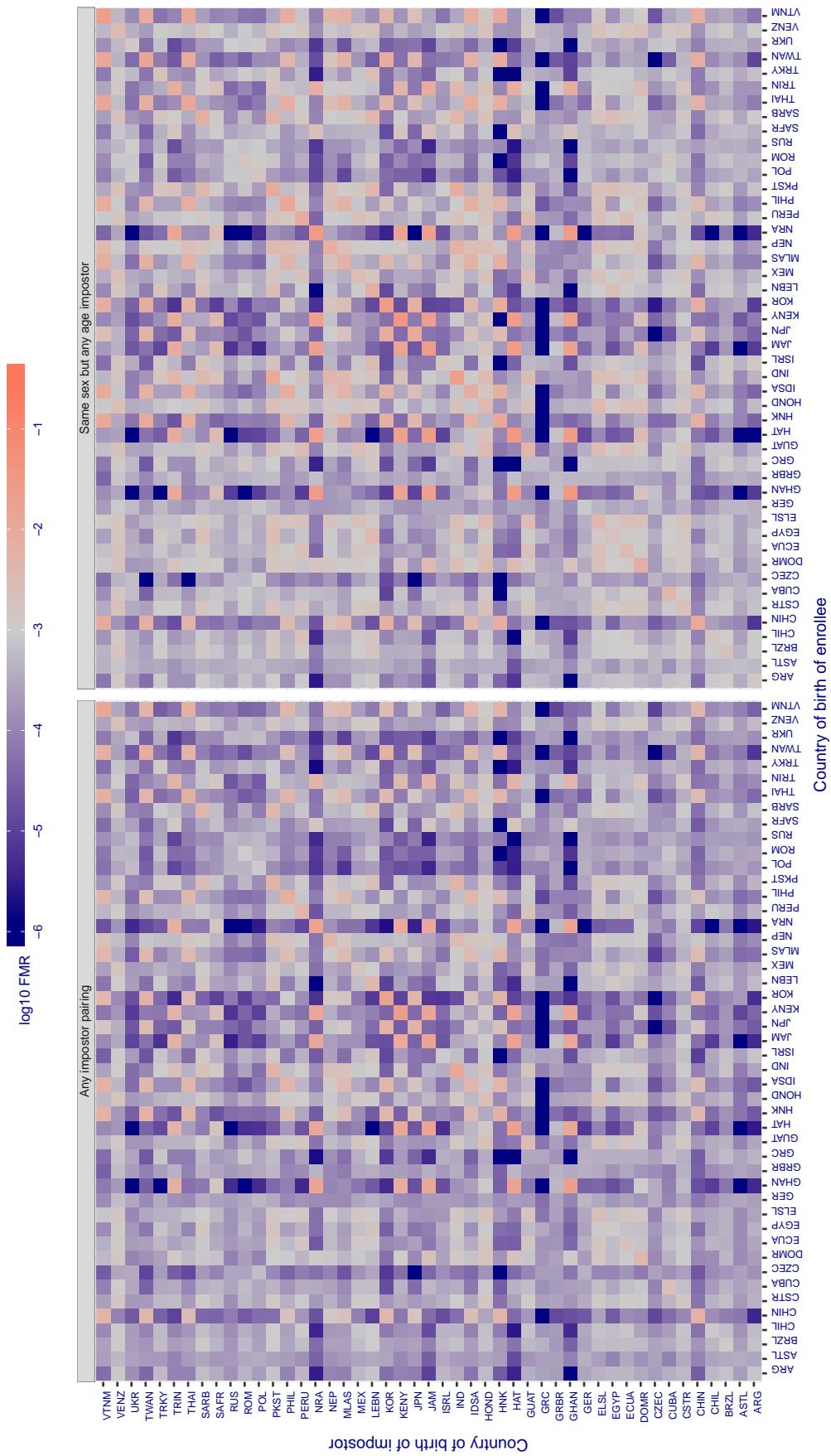
**Cross country FMR at threshold T = 0.702 for algorithm cyberextruder\_001, giving FMR(T) = 0.001 globally.**

Figure 269: For algorithm cyberextruder-001 operating on visa images, the heatmap shows false match rates observed over impostor comparisons of faces from different individuals who were born in the given country pair. False matches are counted against a recognition threshold fixed globally to give the target FMR in the plot title, computed over all on the order of  $10^{10}$  impostor comparisons. If text appears in each box it give the same quantity as that coded by the color. Grey indicates FMR is at the intended FMR target level. Light red colors present a security vulnerability to, for example, a passport gate. Each +1 increase in  $\log_{10} FMR$  corresponds to a factor of 10 increase in FMR. The matrix is not quite symmetric because images in the enrollment and verification sets are different.

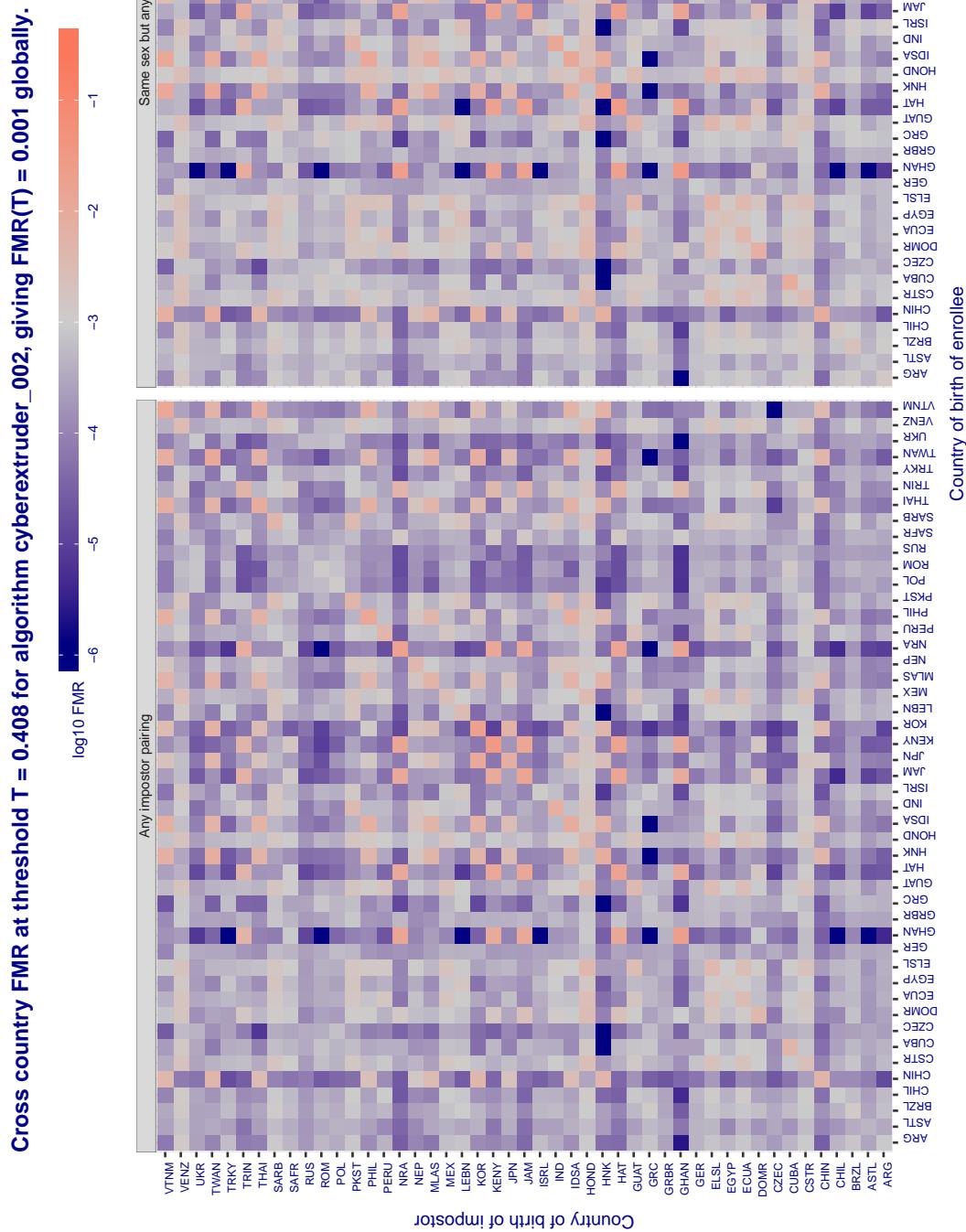


Figure 270: For algorithm cyberextruder-002 operating on visa images, the heatmap shows false match rates observed over impostor comparisons of faces from different individuals who were born in the given country pair. False matches are counted against a recognition threshold fixed globally to give the target FMR in the plot title, computed over all on the order of  $10^{10}$  impostor comparisons. If text appears in each box it give the same quantity as that coded by the color. Grey indicates FMR is at the intended FMR target level. Light red colors present a security vulnerability to, for example, a passport gate. Each +1 increase in  $\log_{10}$  FMR corresponds to a factor of 10 increase in FMR. The matrix is not quite symmetric because images in the enrollment and verification sets are different.

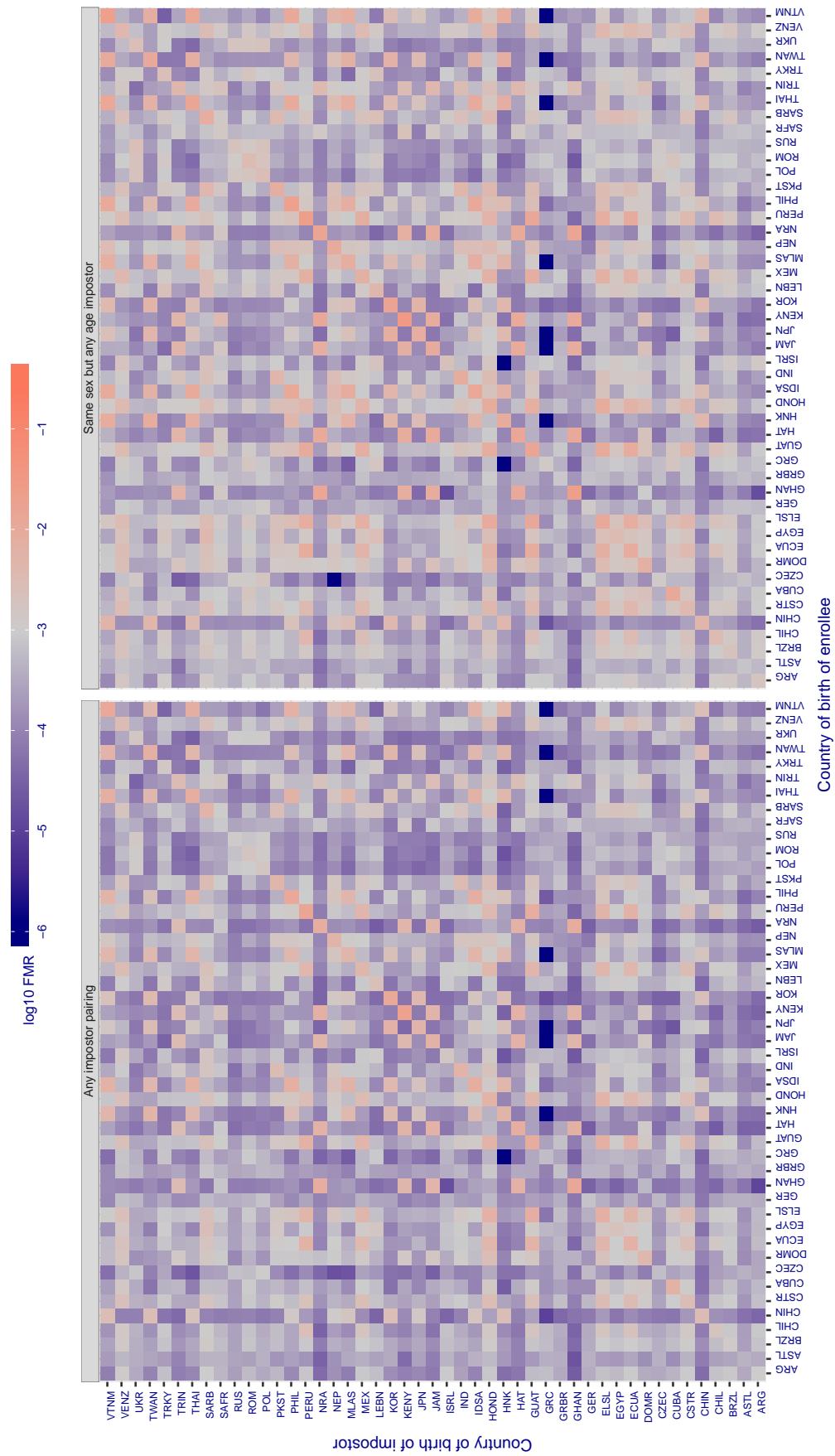
**Cross country FMR at threshold T = 1.322 for algorithm cyberlink\_001, giving FMR(T) = 0.001 globally.**

Figure 271: For algorithm cyberlink-001 operating on visa images, the heatmap shows false match rates observed over impostor comparisons of faces from different individuals who were born in the given country pair. False matches are counted against a recognition threshold fixed globally to give the target FMR in the plot title, computed over all on the order of  $10^{10}$  impostor comparisons. If text appears in each box it give the same quantity as that coded by the color. Grey indicates FMR is at the intended FMR target level. Light red colors present a security vulnerability to, for example, a passport gate. Each +1 increase in  $\log_{10} FMR$  corresponds to a factor of 10 increase in FMR. The matrix is not quite symmetric because images in the enrollment and verification sets are different.

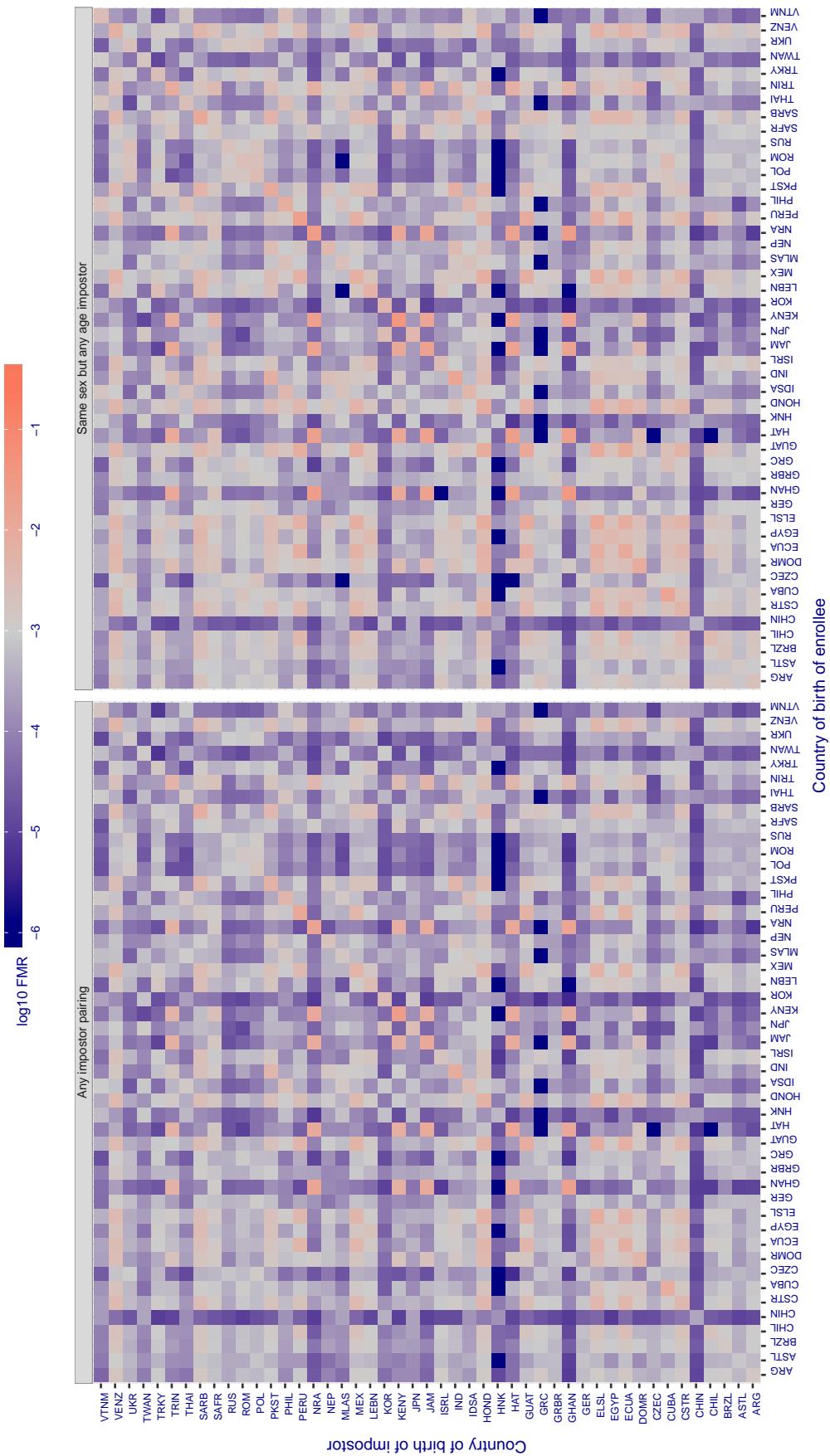
**Cross country FMR at threshold T = 6606.000 for algorithm dahua\_001, giving FMR(T) = 0.001 globally.**

Figure 272: For algorithm dahua-001 operating on visa images, the heatmap shows false match rates observed over impostor comparisons of faces from different individuals who were born in the given country pair. False matches are counted against a recognition threshold fixed globally to give the target FMR in the plot title, computed over all on the order of  $10^{10}$  impostor comparisons. If text appears in each box it give the same quantity as that coded by the color. Grey indicates FMR is at the intended FMR target level. Light red colors present a security vulnerability to, for example, a passport gate. Each +1 increase in  $\log_{10} FMR$  corresponds to a factor of 10 increase in FMR. The matrix is not quite symmetric because images in the enrollment and verification sets are different.

**Cross country FMR at threshold  $T = 5958.000$  for algorithm dahua\_002, giving  $FMR(T) = 0.001$  globally.**

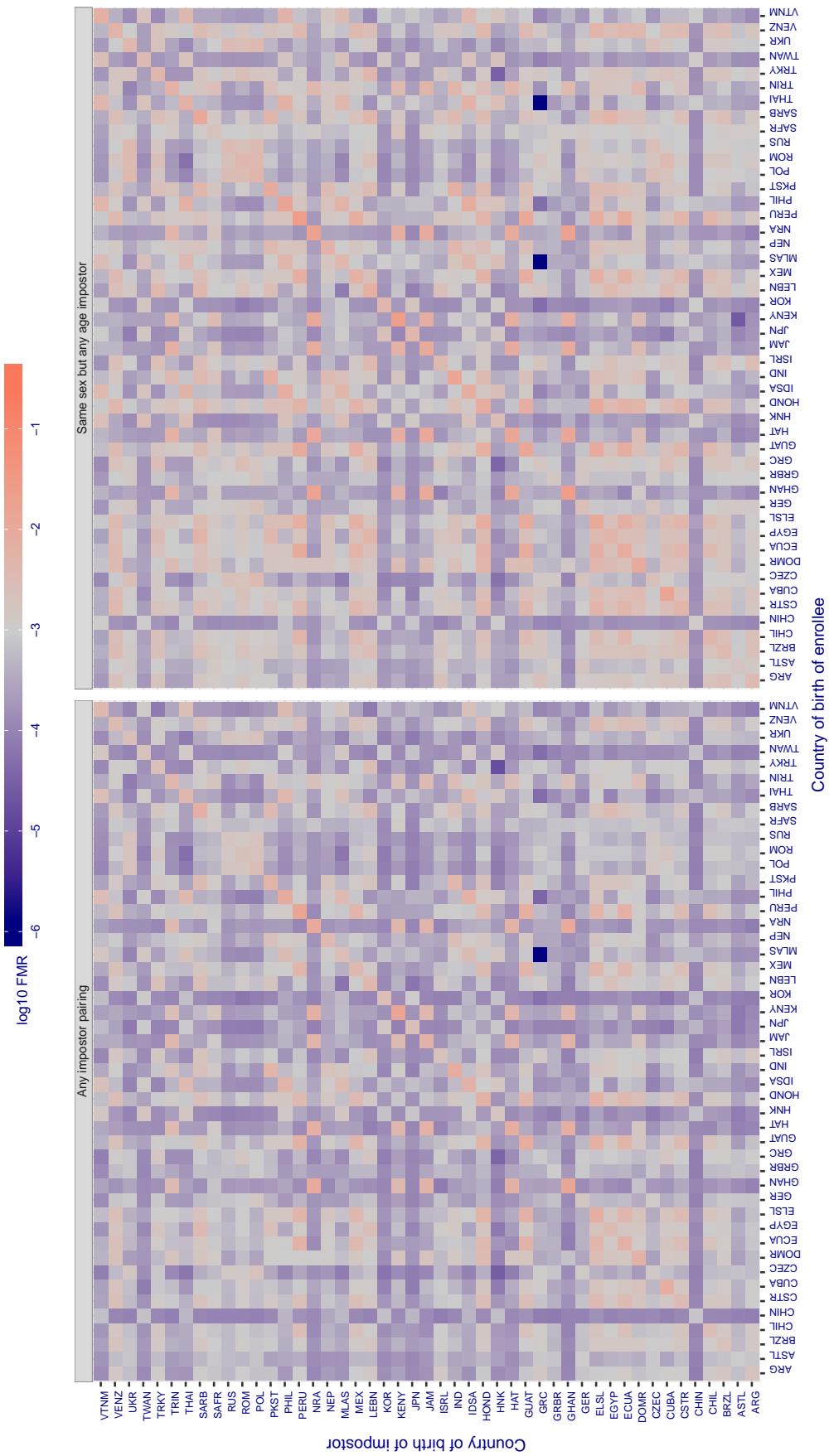


Figure 273: For algorithm dahua-002 operating on visa images, the heatmap shows false match rates observed over impostor comparisons of faces from different individuals who were born in the given country pair. False matches are counted against a recognition threshold fixed globally to give the target FMR in the plot title, computed over all on the order of  $10^{10}$  impostor comparisons. If text appears in each box it give the same quantity as that coded by the color. Grey indicates FMR is at the intended FMR target level. Light red colors present a security vulnerability to, for example, a passport gate. Each +1 increase in  $\log_{10} FMR$  corresponds to a factor of 10 increase in FMR. The matrix is not quite symmetric because images in the enrollment and verification sets are different.

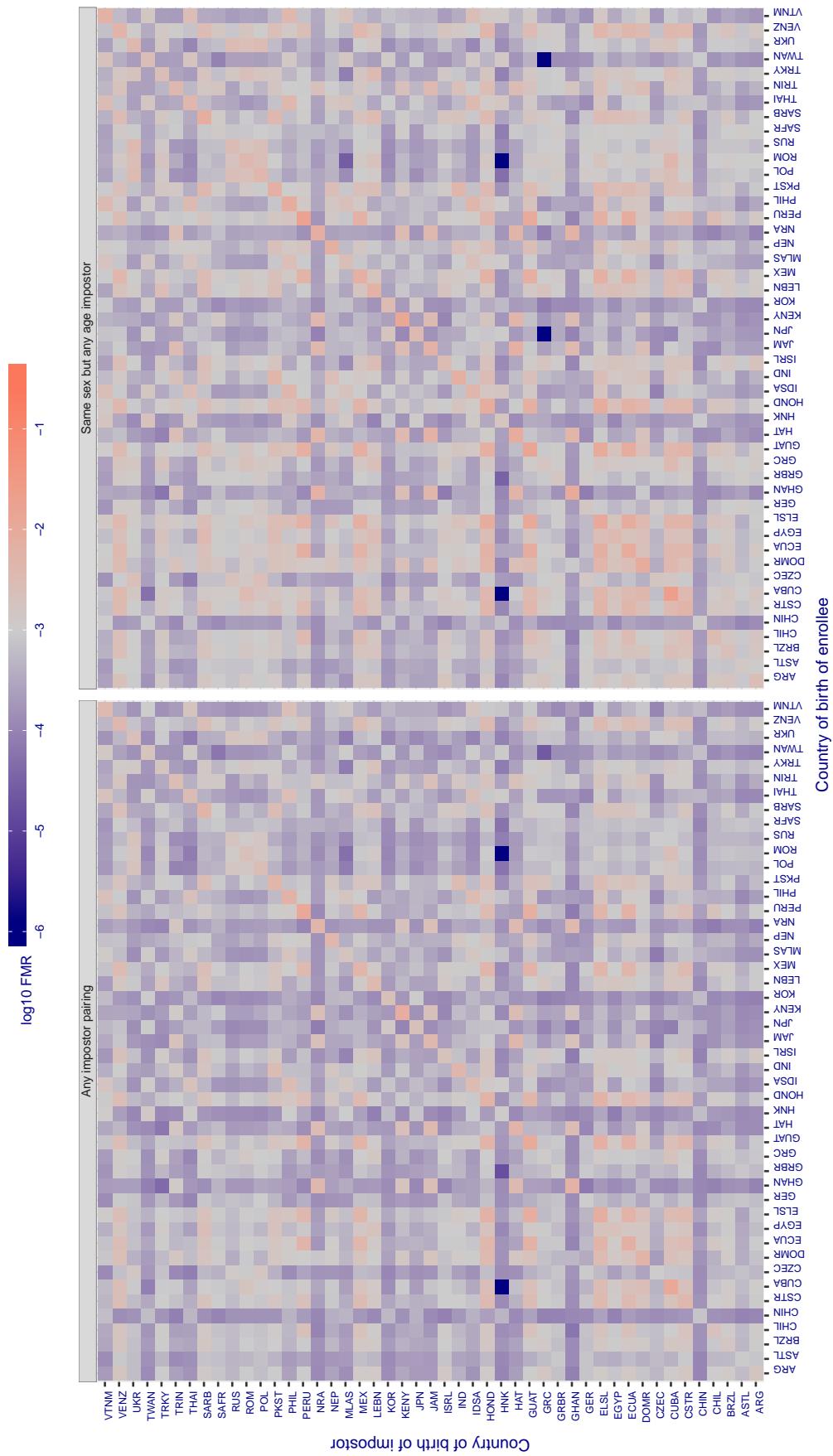
**Cross country FMR at threshold T = 1.300 for algorithm deepsea\_001, giving FMR(T) = 0.001 globally.**

Figure 274: For algorithm deepsea-001 operating on visa images, the heatmap shows false match rates observed over impostor comparisons of faces from different individuals who were born in the given country pair. False matches are counted against a recognition threshold fixed globally to give the target FMR in the plot title, computed over all on the order of  $10^{10}$  impostor comparisons. If text appears in each box it give the same quantity as that coded by the color. Grey indicates FMR is at the intended FMR target level. Light red colors present a security vulnerability to, for example, a passport gate. Each +1 increase in  $\log_{10} \text{FMR}$  corresponds to a factor of 10 increase in FMR. The matrix is not quite symmetric because images in the enrollment and verification sets are different.

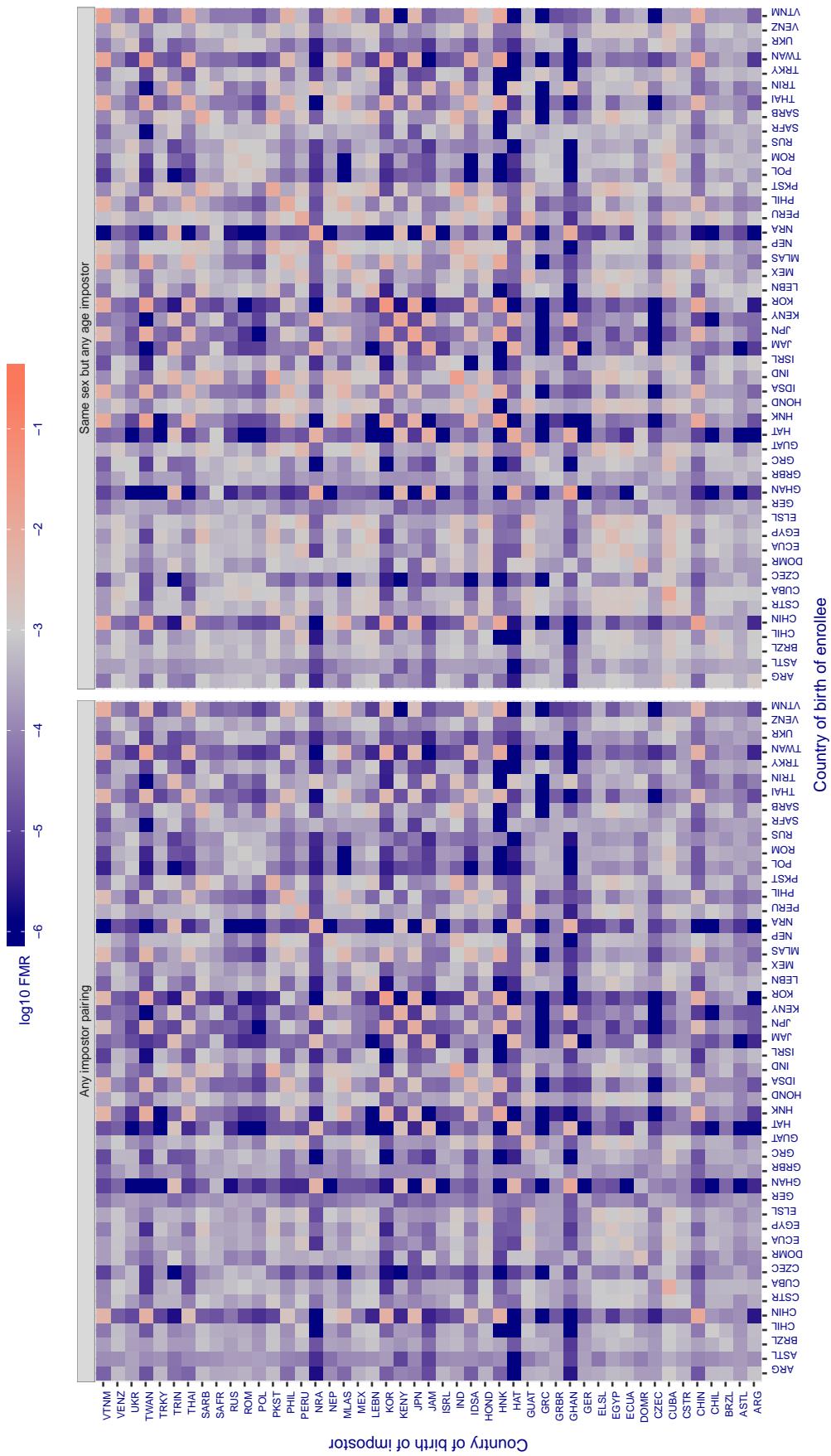
**Cross country FMR at threshold T = 75.231 for algorithm dermalog\_005, giving FMR(T) = 0.001 globally.**

Figure 275: For algorithm dermalog-005 operating on visa images, the heatmap shows false match rates observed over impostor comparisons of faces from different individuals who were born in the given country pair. False matches are counted against a recognition threshold fixed globally to give the target FMR in the plot title, computed over all on the order of  $10^{10}$  impostor comparisons. If text appears in each box it give the same quantity as that coded by the color. Grey indicates FMR is at the intended FMR target level. Light red colors present a security vulnerability to, for example, a passport gate. Each +1 increase in  $\log_{10}$  FMR corresponds to a factor of 10 increase in FMR. The matrix is not quite symmetric because images in the enrollment and verification sets are different.

**Cross country FMR at threshold T = 76.496 for algorithm dermalog\_006, giving FMR(T) = 0.001 globally.**

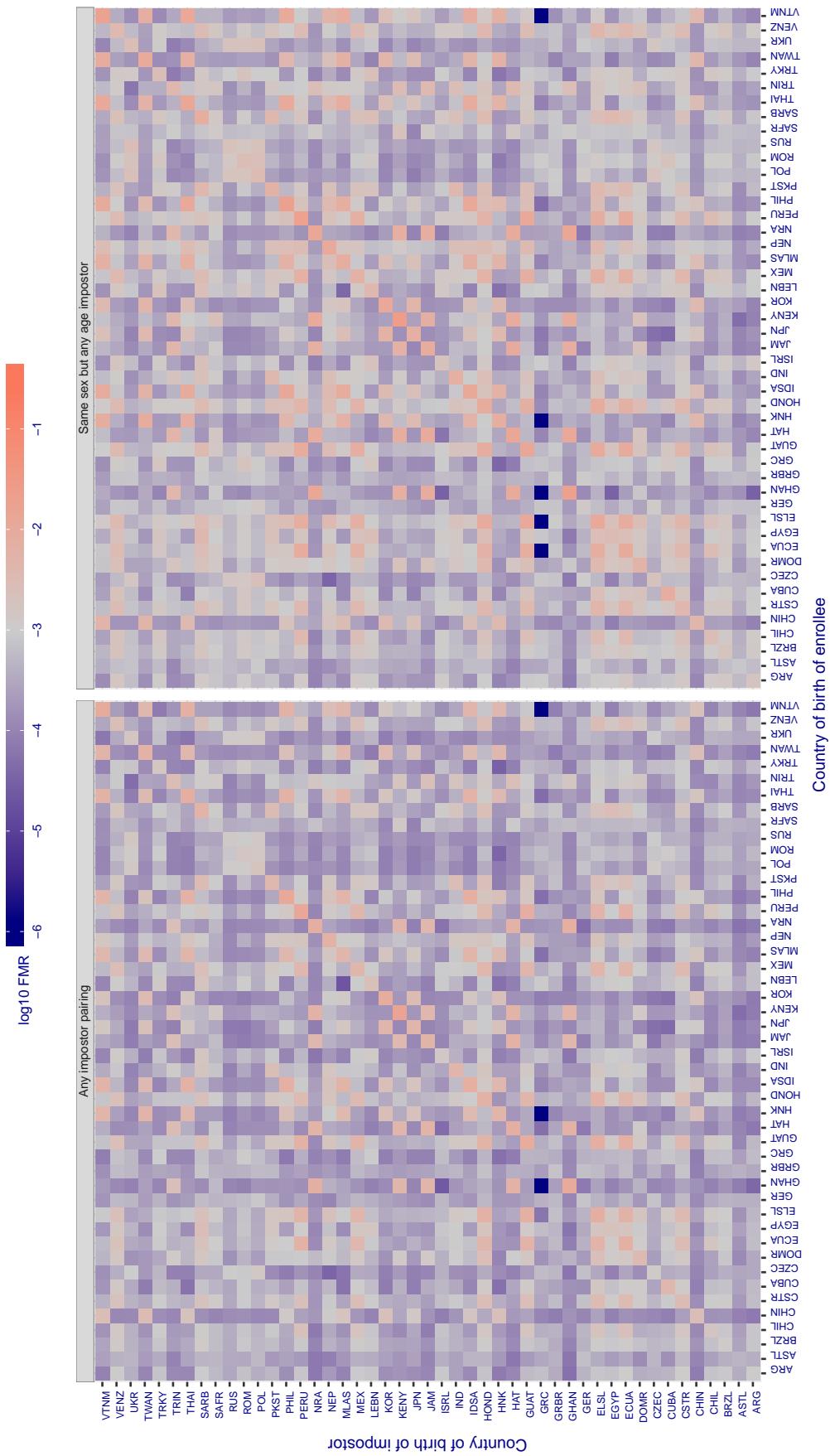


Figure 276: For algorithm dermalog-006 operating on visa images, the heatmap shows false match rates observed over impostor comparisons of faces from different individuals who were born in the given country pair. False matches are counted against a recognition threshold fixed globally to give the target FMR in the plot title, computed over all on the order of  $10^{10}$  impostor comparisons. If text appears in each box it give the same quantity as that coded by the color. Grey indicates FMR is at the intended FMR target level. Light red colors present a security vulnerability to, for example, a passport gate. Each +1 increase in  $\log_{10} \text{FMR}$  corresponds to a factor of 10 increase in FMR. The matrix is not quite symmetric because images in the enrollment and verification sets are different.

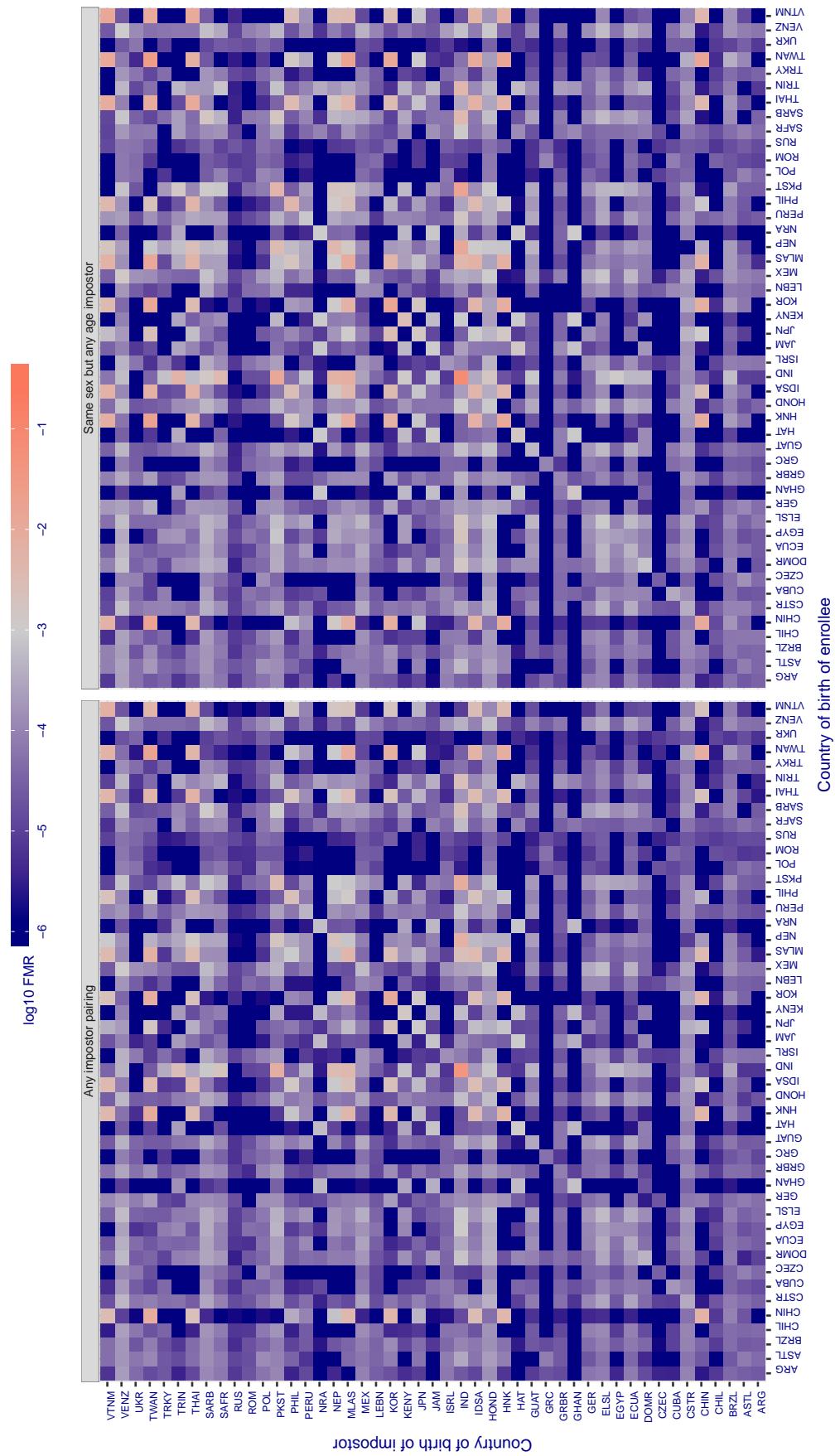
**Cross country FMR at threshold T = 0.547 for algorithm digitalbarriers\_002, giving FMR(T) = 0.001 globally.**

Figure 277: For algorithm digitalbarriers-002 operating on visa images, the heatmap shows false match rates observed over impostor comparisons of faces from different individuals who were born in the given country pair. False matches are counted against a recognition threshold fixed globally to give the target FMR in the plot title, computed over all on the order of  $10^{10}$  impostor comparisons. If text appears in each box it give the same quantity as that coded by the color. Grey indicates FMR is at the intended FMR target level. Light red colors present a security vulnerability to, for example, a passport gate. Each +1 increase in  $\log_{10} FMR$  corresponds to a factor of 10 increase in FMR. The matrix is not quite symmetric because images in the enrollment and verification sets are different.

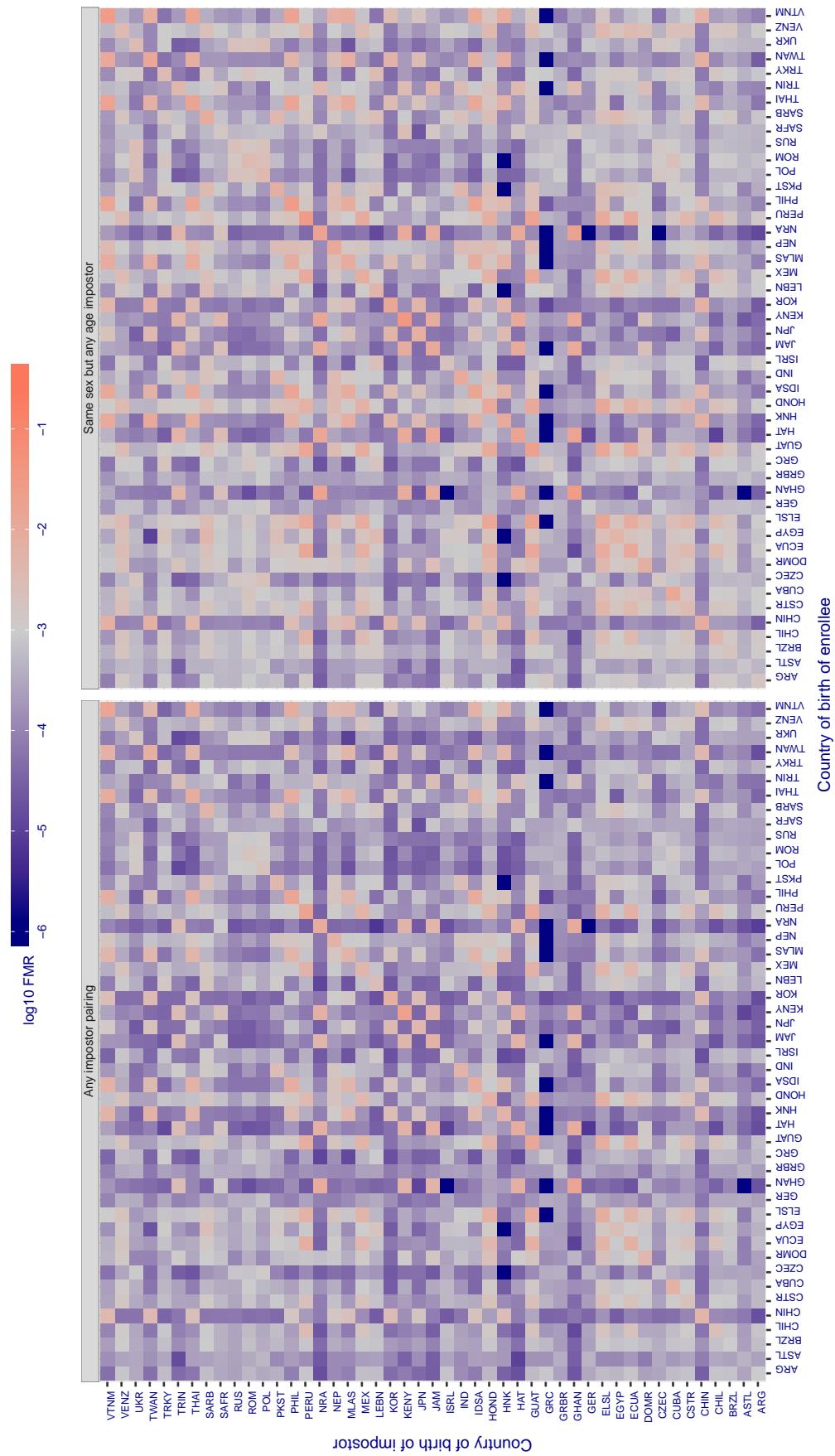
**Cross country FMR at threshold T = 2.426 for algorithm everai\_002, giving FMR(T) = 0.001 globally.**

Figure 278: For algorithm everai-002 operating on visa images, the heatmap shows false match rates observed over impostor comparisons of faces from different individuals who were born in the given country pair. False matches are counted against a recognition threshold fixed globally to give the target FMR in the plot title, computed over all on the order of  $10^{10}$  impostor comparisons. If text appears in each box it give the same quantity as that coded by the color. Grey indicates FMR is at the intended FMR target level. Light red colors present a security vulnerability to, for example, a passport gate. Each +1 increase in  $\log_{10} FMR$  corresponds to a factor of 10 increase in FMR. The matrix is not quite symmetric because images in the enrollment and verification sets are different.

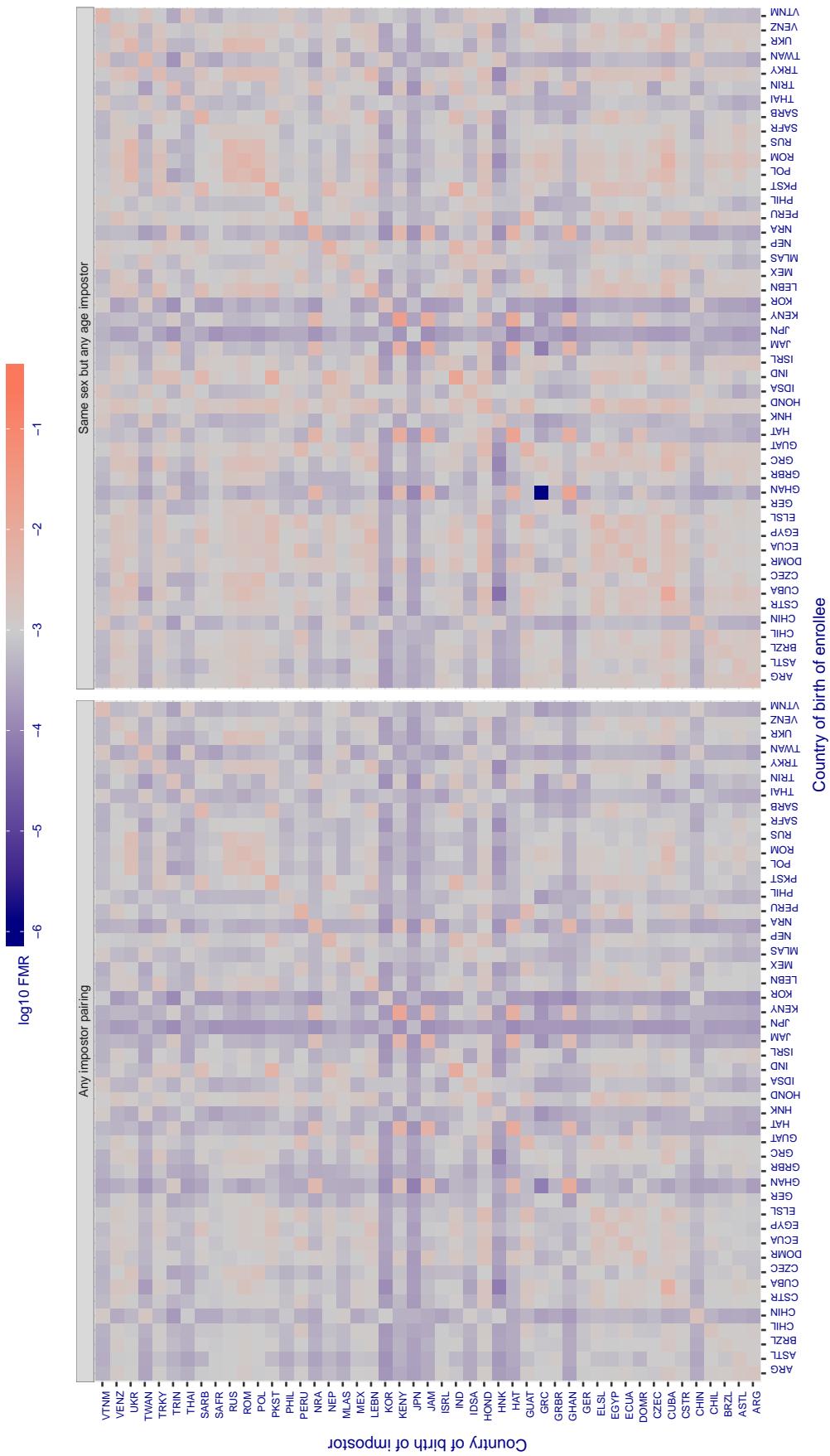
**Cross country FMR at threshold T = 0.591 for algorithm glory\_000, giving FMR(T) = 0.001 globally.**

Figure 279: For algorithm *glory-000* operating on visa images, the heatmap shows false match rates observed over impostor comparisons of faces from different individuals who were born in the given country pair. False matches are counted against a recognition threshold fixed globally to give the target FMR in the plot title, computed over all on the order of  $10^{10}$  impostor comparisons. If text appears in each box it give the same quantity as that coded by the color. Grey indicates FMR is at the intended FMR target level. Light red colors present a security vulnerability to, for example, a passport gate. Each +1 increase in  $\log_{10} FMR$  corresponds to a factor of 10 increase in FMR. The matrix is not quite symmetric because images in the enrollment and verification sets are different.

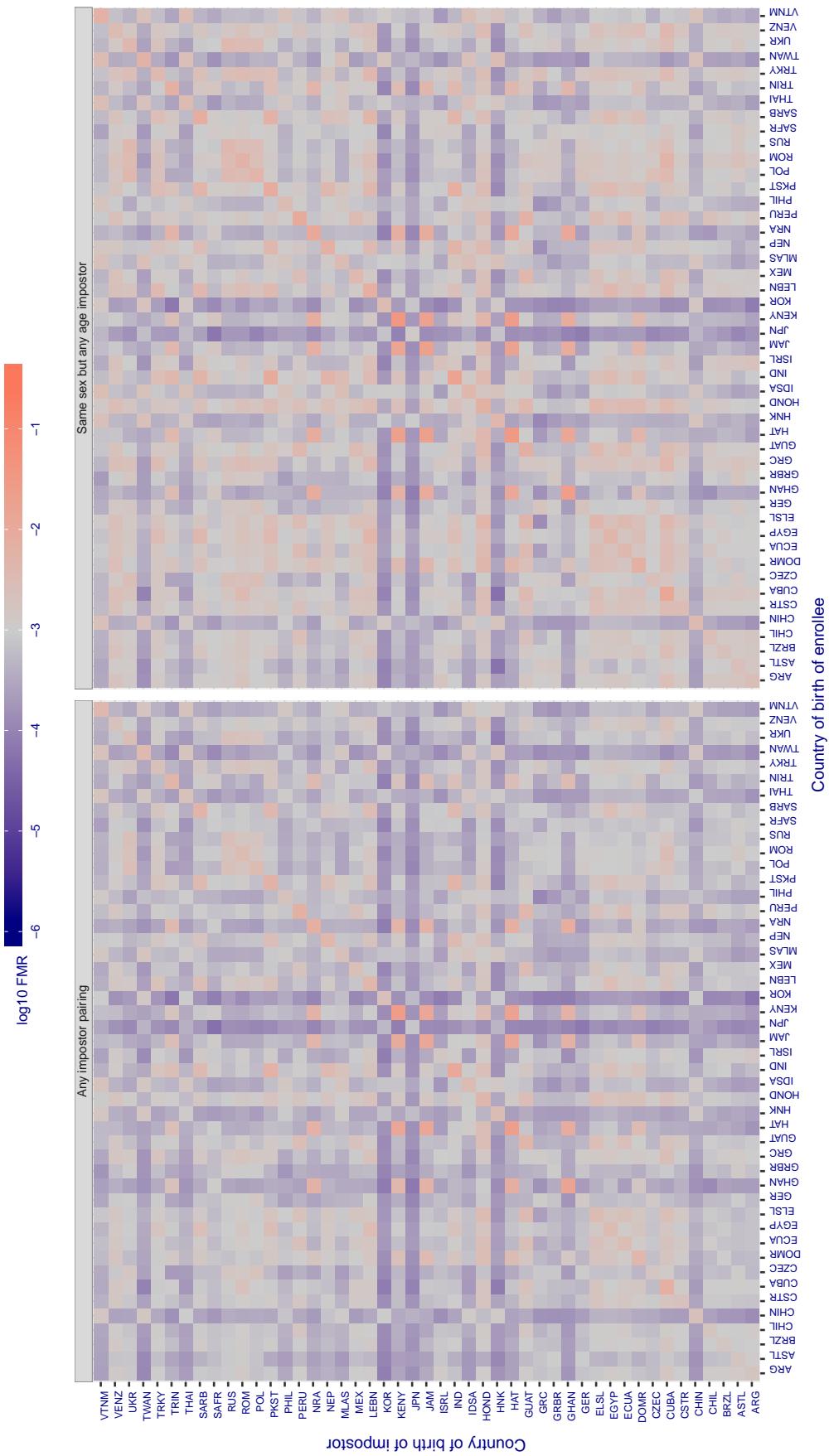
**Cross country FMR at threshold T = 0.596 for algorithm glory\_001, giving FMR(T) = 0.001 globally.**

Figure 280: For algorithm *glory-001* operating on visa images, the heatmap shows false match rates observed over impostor comparisons of faces from different individuals who were born in the given country pair. False matches are counted against a recognition threshold fixed globally to give the target FMR in the plot title, computed over all on the order of  $10^{10}$  impostor comparisons. If text appears in each box it give the same quantity as that coded by the color. Grey indicates FMR is at the intended FMR target level. Light red colors present a security vulnerability to, for example, a passport gate. Each +1 increase in  $\log_{10} FMR$  corresponds to a factor of 10 increase in FMR. The matrix is not quite symmetric because images in the enrollment and verification sets are different.

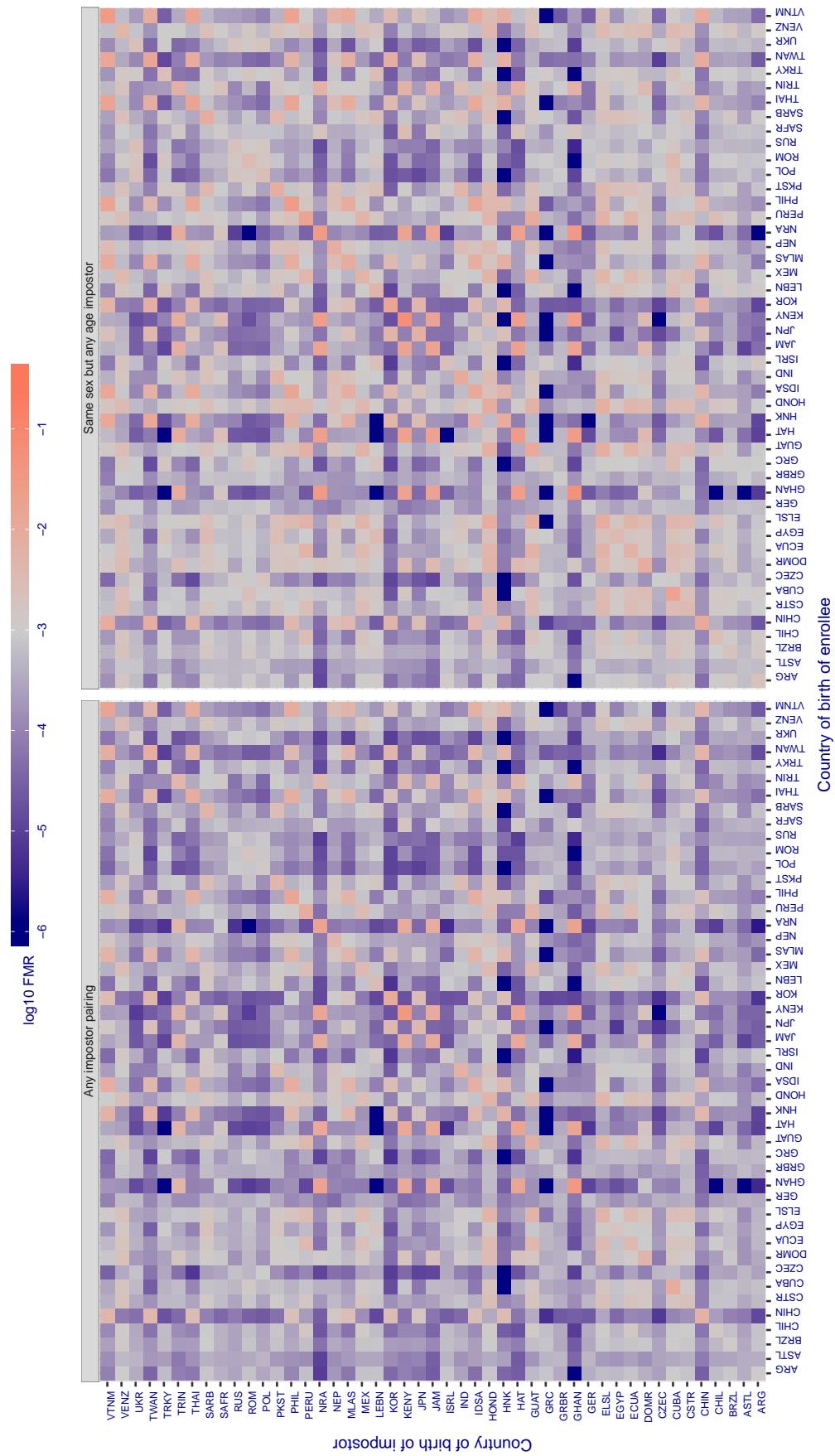
**Cross country FMR at threshold T = 0.402 for algorithm gorilla\_002, giving FMR(T) = 0.001 globally.**

Figure 281: For algorithm gorilla-002 operating on visa images, the heatmap shows false match rates observed over impostor comparisons of faces from different individuals who were born in the given country pair. False matches are counted against a recognition threshold fixed globally to give the target FMR in the plot title, computed over all on the order of  $10^{10}$  impostor comparisons. If text appears in each box it give the same quantity as that coded by the color. Grey indicates FMR is at the intended FMR target level. Light red colors present a security vulnerability to, for example, a passport gate. Each +1 increase in  $\log_{10} FMR$  corresponds to a factor of 10 increase in FMR. The matrix is not quite symmetric because images in the enrollment and verification sets are different.

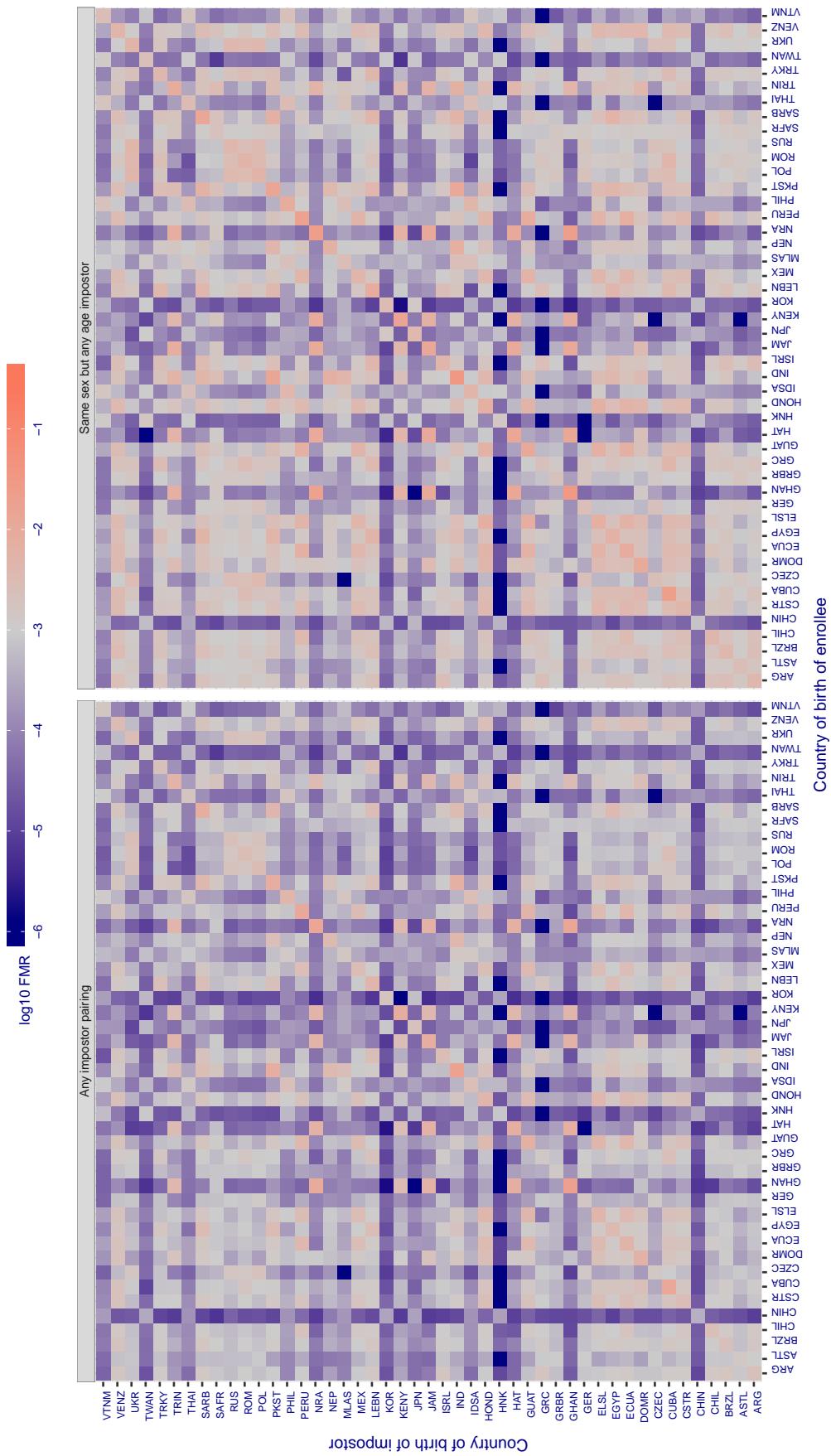
**Cross country FMR at threshold T = 63.025 for algorithm hik\_001, giving FMR(T) = 0.001 globally.**

Figure 282: For algorithm hik-001 operating on visa images, the heatmap shows false match rates observed over impostor comparisons of faces from different individuals who were born in the given country pair. False matches are counted against a recognition threshold fixed globally to give the target FMR in the plot title, computed over all on the order of  $10^{10}$  impostor comparisons. If text appears in each box it give the same quantity as that coded by the color. Grey indicates FMR is at the intended FMR target level. Light red colors present a security vulnerability to, for example, a passport gate. Each +1 increase in  $\log_{10} \text{FMR}$  corresponds to a factor of 10 increase in FMR. The matrix is not quite symmetric because images in the enrollment and verification sets are different.

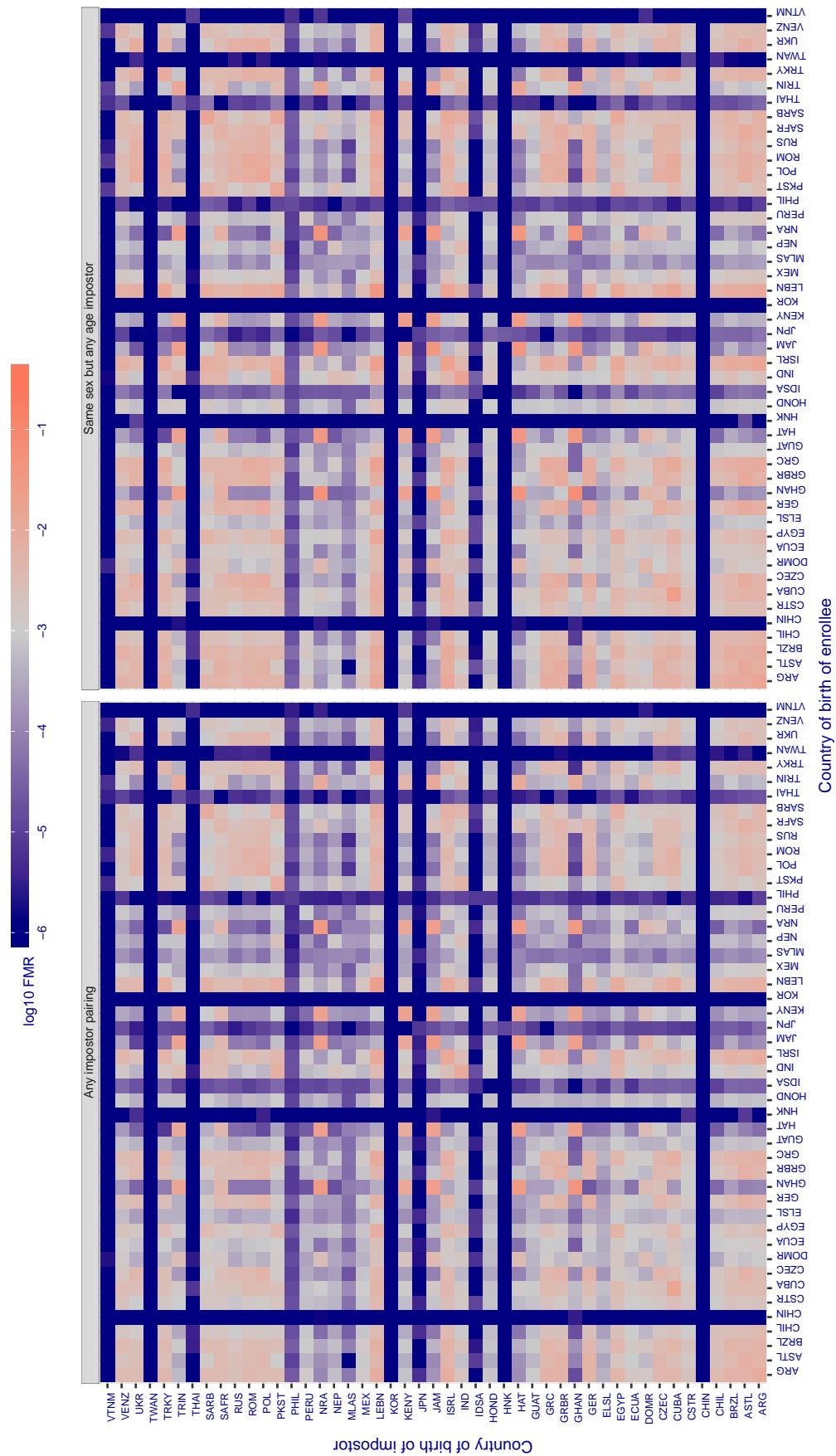
**Cross country FMR at threshold T = 0.949 for algorithm hr\_000, giving FMR(T) = 0.001 globally.**

Figure 283: For algorithm hr-000 operating on visa images, the heatmap shows false match rates observed over impostor comparisons of faces from different individuals who were born in the given country pair. False matches are counted against a recognition threshold fixed globally to give the target FMR in the plot title, computed over all on the order of  $10^{10}$  impostor comparisons. If text appears in each box it give the same quantity as that coded by the color. Grey indicates FMR is at the intended FMR target level. Light red colors present a security vulnerability to, for example, a passport gate. Each +1 increase in  $\log_{10}$  FMR corresponds to a factor of 10 increase in FMR. The matrix is not quite symmetric because images in the enrollment and verification sets are different.

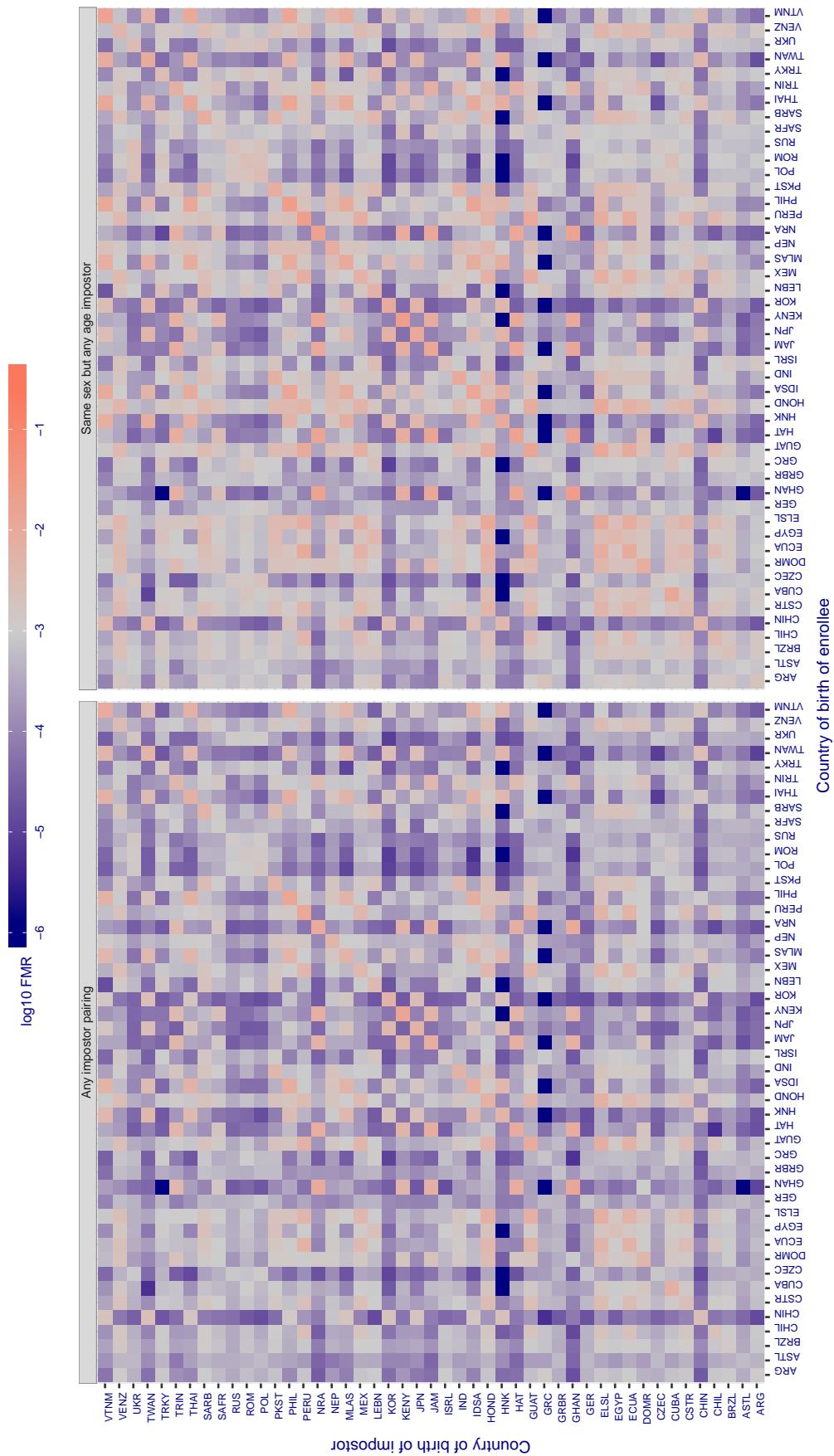
**Cross country FMR at threshold T = 0.727 for algorithm hr\_001, giving FMR(T) = 0.001 globally.**

Figure 284: For algorithm hr-001 operating on visa images, the heatmap shows false match rates observed over impostor comparisons of faces from different individuals who were born in the given country pair. False matches are counted against a recognition threshold fixed globally to give the target FMR in the plot title, computed over all on the order of  $10^{10}$  impostor comparisons. If text appears in each box it give the same quantity as that coded by the color. Grey indicates FMR is at the intended FMR target level. Light red colors present a security vulnerability to, for example, a passport gate. Each +1 increase in  $\log_{10} \text{FMR}$  corresponds to a factor of 10 increase in FMR. The matrix is not quite symmetric because images in the enrollment and verification sets are different.

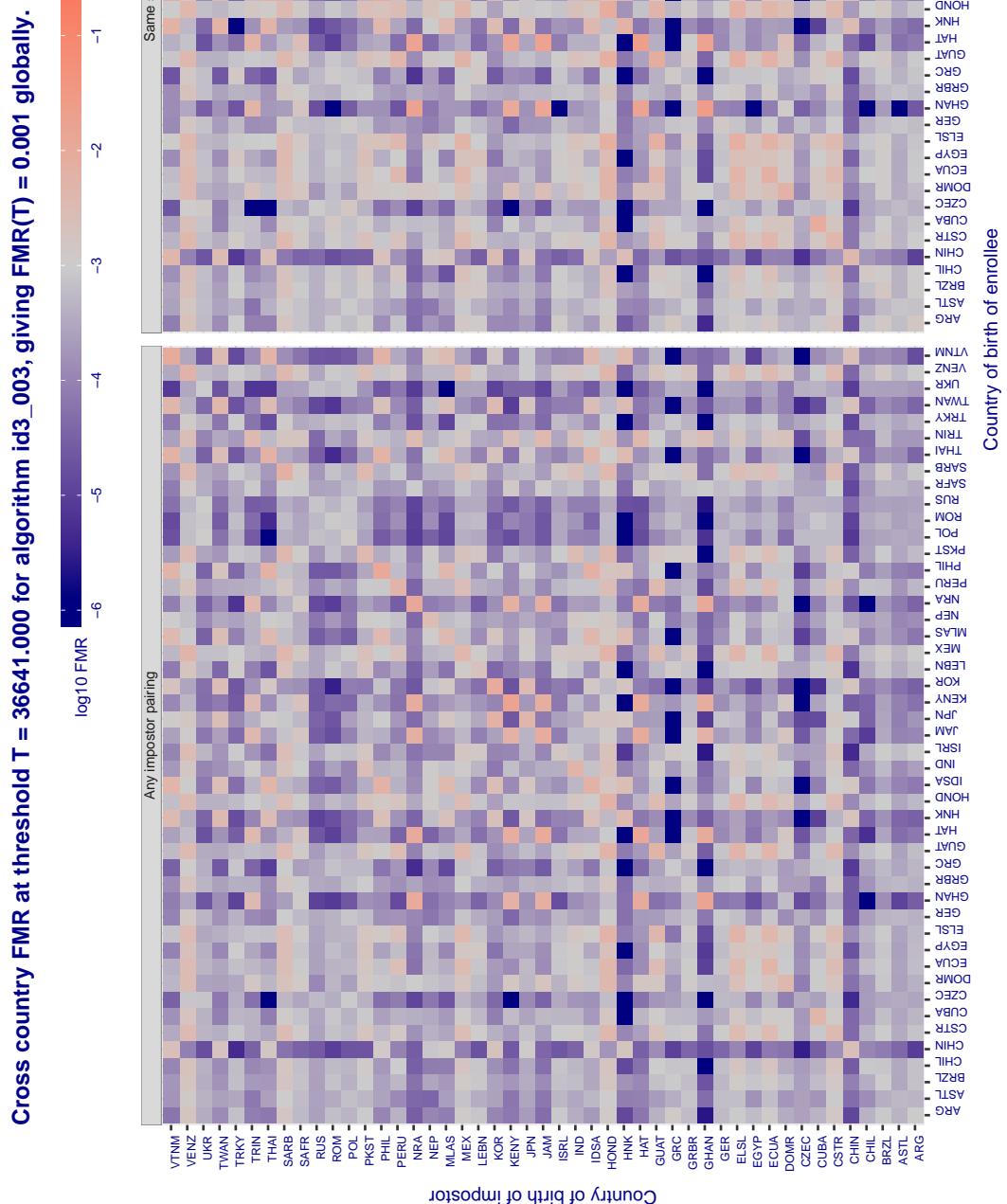


Figure 285: For algorithm id3-003 operating on visa images, the heatmap shows false match rates observed over impostor comparisons of faces from different individuals who were born in the given country pair. False matches are counted against a recognition threshold fixed globally to give the target FMR in the plot title, computed over all on the order of  $10^{10}$  impostor comparisons. If text appears in each box it give the same quantity as that coded by the color. Grey indicates FMR is at the intended FMR target level. Light red colors present a security vulnerability to, for example, a passport gate. Each +1 increase in  $\log_{10} \text{FMR}$  corresponds to a factor of 10 increase in FMR. The matrix is not quite symmetric because images in the enrollment and verification sets are different.

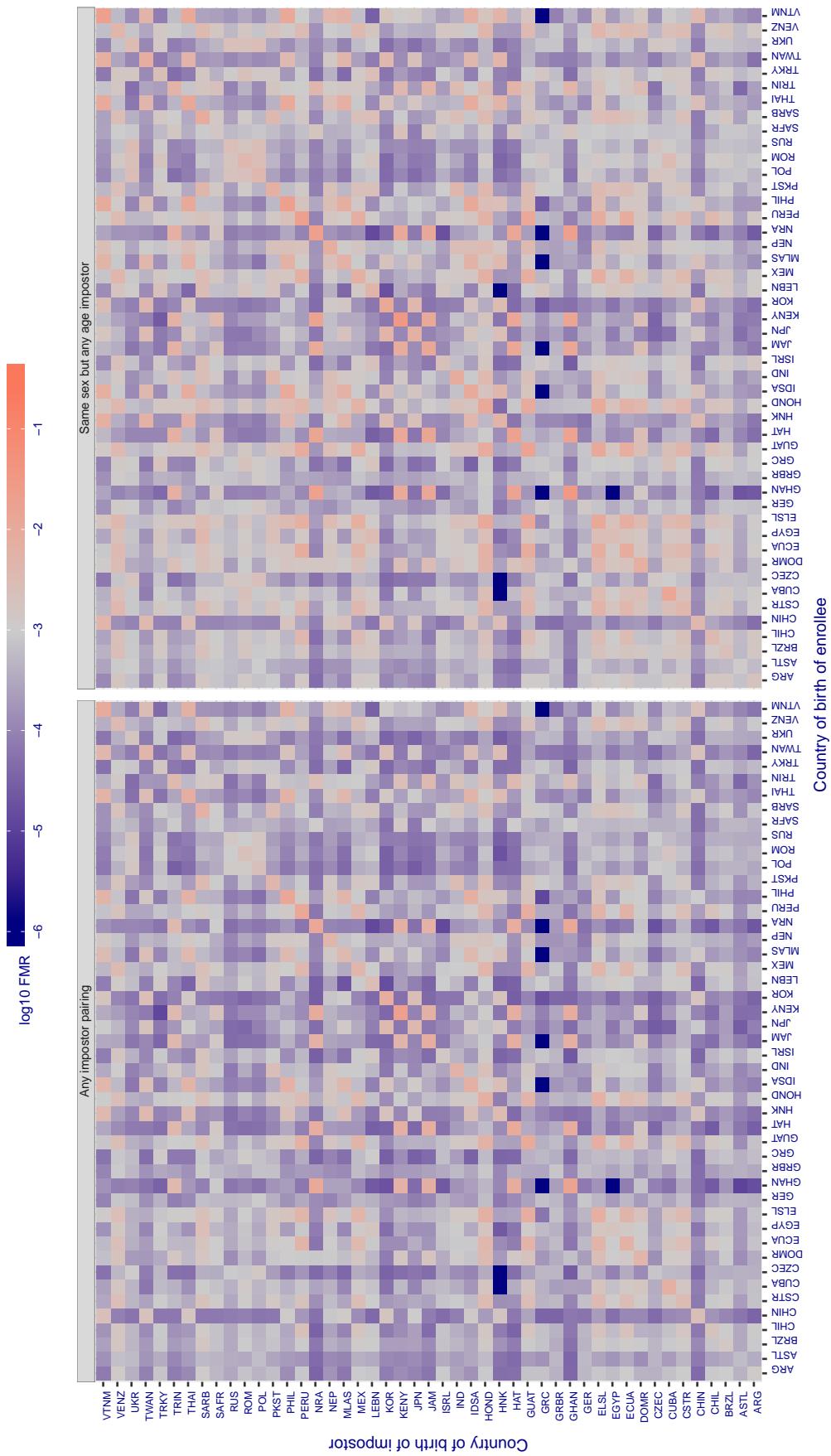
**Cross country FMR at threshold T = 36163.000 for algorithm id3\_004, giving FMR(T) = 0.001 globally.**

Figure 286: For algorithm id3\_004 operating on visa images, the heatmap shows false match rates observed over impostor comparisons of faces from different individuals who were born in the given country pair. False matches are counted against a recognition threshold fixed globally to give the target FMR in the plot title, computed over all on the order of  $10^{10}$  impostor comparisons. If text appears in each box it give the same quantity as that coded by the color. Grey indicates FMR is at the intended FMR target level. Light red colors present a security vulnerability to, for example, a passport gate. Each +1 increase in  $\log_{10} \text{FMR}$  corresponds to a factor of 10 increase in FMR. The matrix is not quite symmetric because images in the enrollment and verification sets are different.

**Cross country FMR at threshold T = 3136.629 for algorithm idemia\_003, giving  $\text{FMR}(T) = 0.001$  globally.**

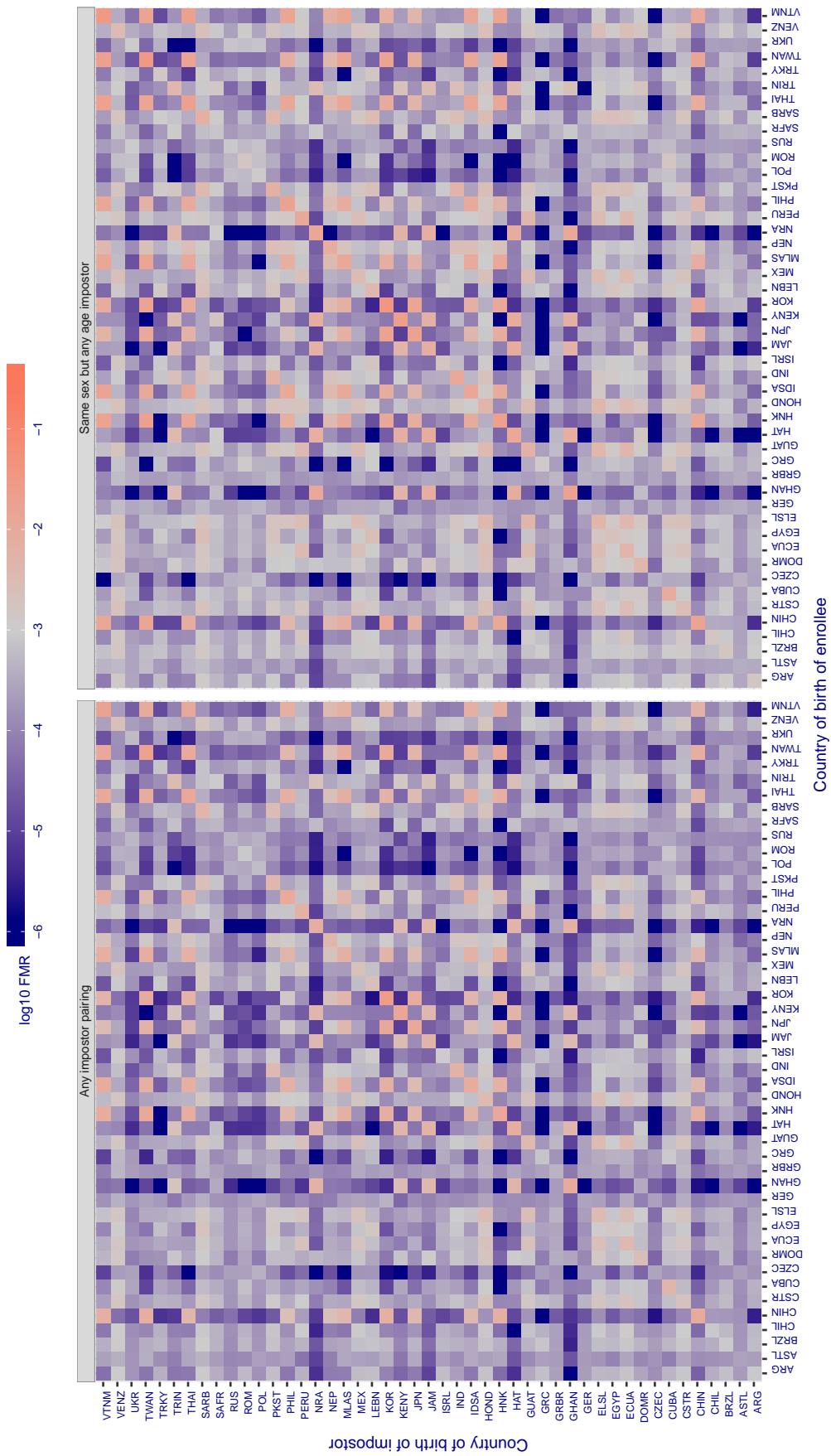


Figure 287: For algorithm idemia-003 operating on visa images, the heatmap shows false match rates observed over impostor comparisons of faces from different individuals who were born in the given country pair. False matches are counted against a recognition threshold fixed globally to give the target  $\text{FMR}$  in the plot title, computed over all on the order of  $10^{10}$  impostor comparisons. If text appears in each box it give the same quantity as that coded by the color. Grey indicates  $\text{FMR}$  is at the intended  $\text{FMR}$  target level. Light red colors present a security vulnerability to, for example, a passport gate. Each +1 increase in  $\log_{10} \text{FMR}$  corresponds to a factor of 10 increase in  $\text{FMR}$ . The matrix is not quite symmetric because images in the enrollment and verification sets are different.

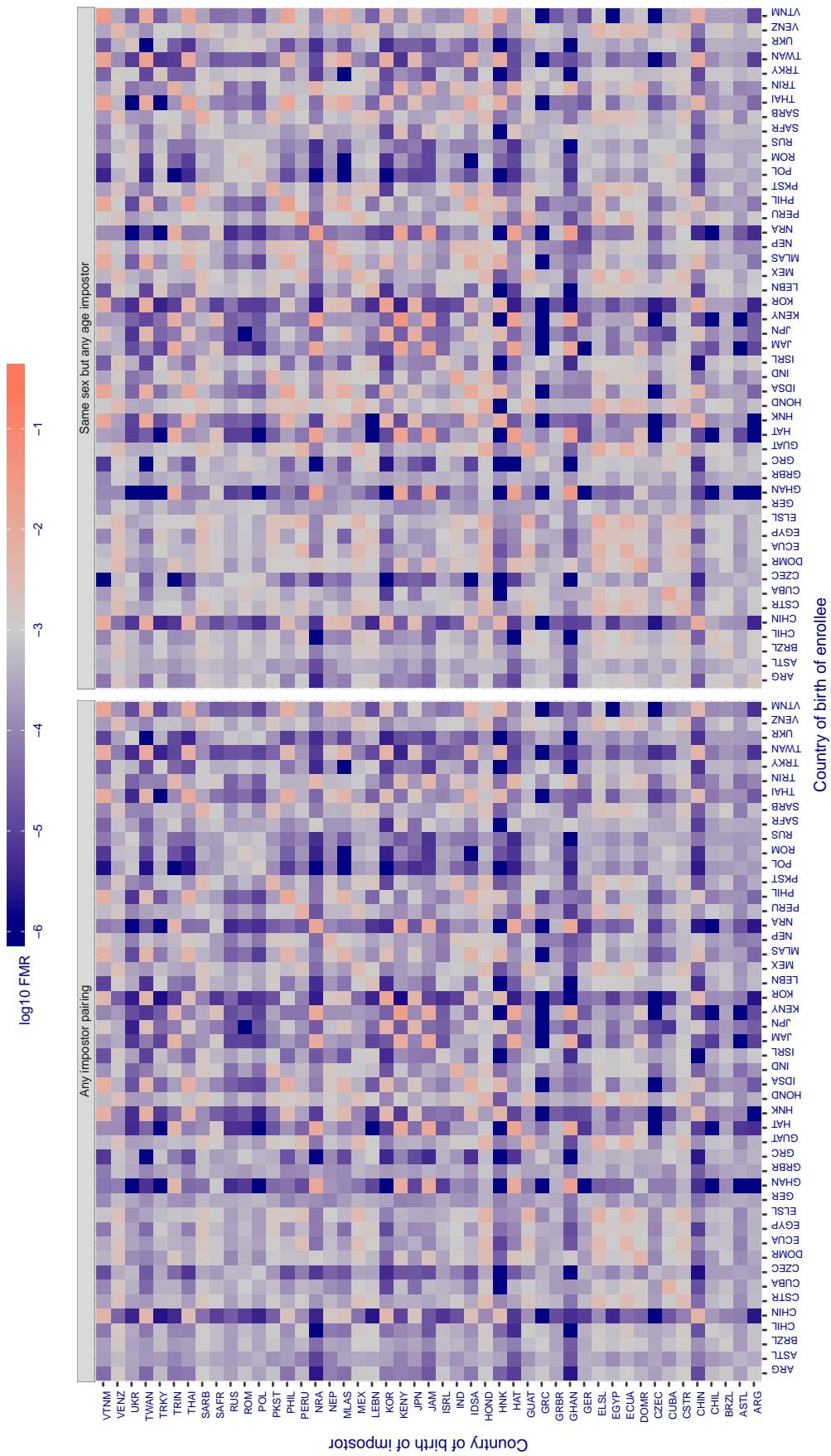
**Cross country FMR at threshold T = 3261.090 for algorithm idemia\_004, giving  $\text{FMR}(T) = 0.001$  globally.**

Figure 288: For algorithm idemia-004 operating on visa images, the heatmap shows false match rates observed over impostor comparisons of faces from different individuals who were born in the given country pair. False matches are counted against a recognition threshold fixed globally to give the target  $\text{FMR}$  in the plot title, computed over all on the order of  $10^{10}$  impostor comparisons. If text appears in each box it give the same quantity as that coded by the color. Grey indicates  $\text{FMR}$  is at the intended  $\text{FMR}$  target level. Light red colors present a security vulnerability to, for example, a passport gate. Each +1 increase in  $\log_{10} \text{FMR}$  corresponds to a factor of 10 increase in  $\text{FMR}$ . The matrix is not quite symmetric because images in the enrollment and verification sets are different.

**Cross country FMR at threshold T = 0.721 for algorithm iit\_000, giving FMR(T) = 0.001 globally.**

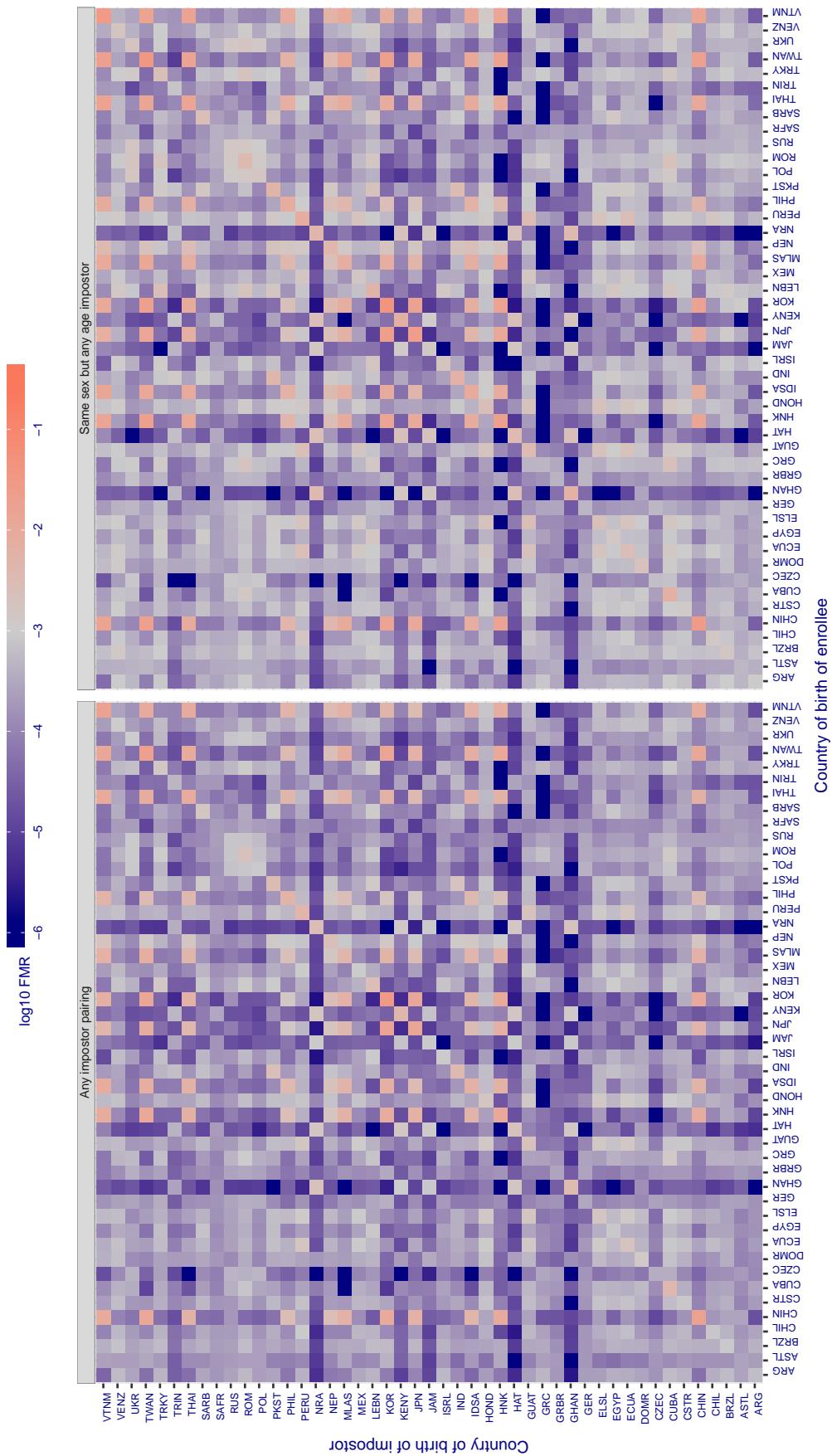


Figure 289: For algorithm iit-000 operating on visa images, the heatmap shows false match rates observed over impostor comparisons of faces from different individuals who were born in the given country pair. False matches are counted against a recognition threshold fixed globally to give the target FMR in the plot title, computed over all on the order of  $10^{10}$  impostor comparisons. If text appears in each box it give the same quantity as that coded by the color. Grey indicates FMR is at the intended FMR target level. Light red colors present a security vulnerability to, for example, a passport gate. Each +1 increase in  $\log_{10} \text{FMR}$  corresponds to a factor of 10 increase in FMR. The matrix is not quite symmetric because images in the enrollment and verification sets are different.

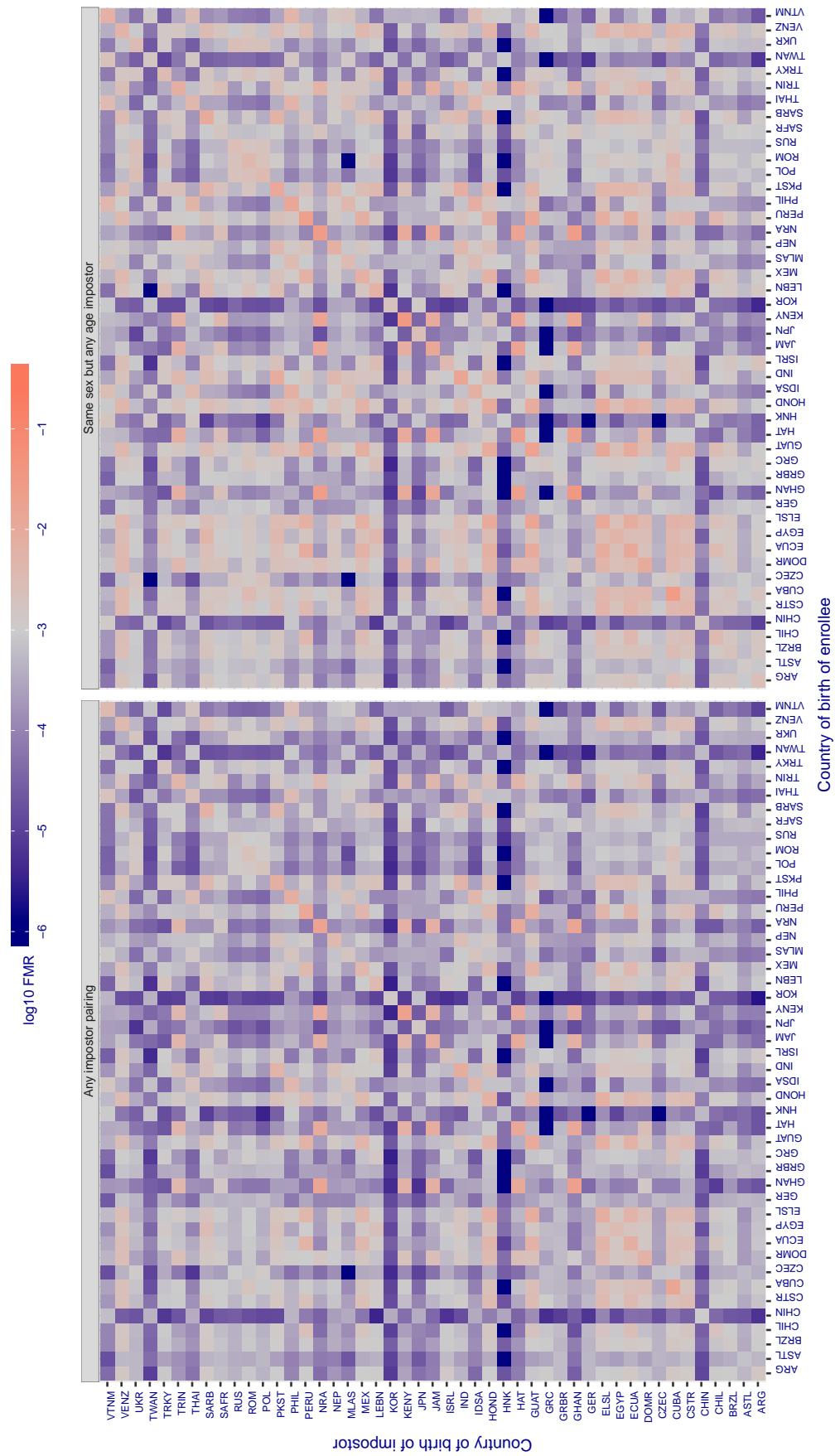
**Cross country FMR at threshold T = 1.302 for algorithm imperial\_000, giving FMR(T) = 0.001 globally.**

Figure 290: For algorithm imperial-000 operating on visa images, the heatmap shows false match rates observed over impostor comparisons of faces from different individuals who were born in the given country pair. False matches are counted against a recognition threshold fixed globally to give the target FMR in the plot title, computed over all on the order of  $10^{10}$  impostor comparisons. If text appears in each box it give the same quantity as that coded by the color. Grey indicates FMR is at the intended FMR target level. Light red colors present a security vulnerability to, for example, a passport gate. Each +1 increase in  $\log_{10}$  FMR corresponds to a factor of 10 increase in FMR. The matrix is not quite symmetric because images in the enrollment and verification sets are different.

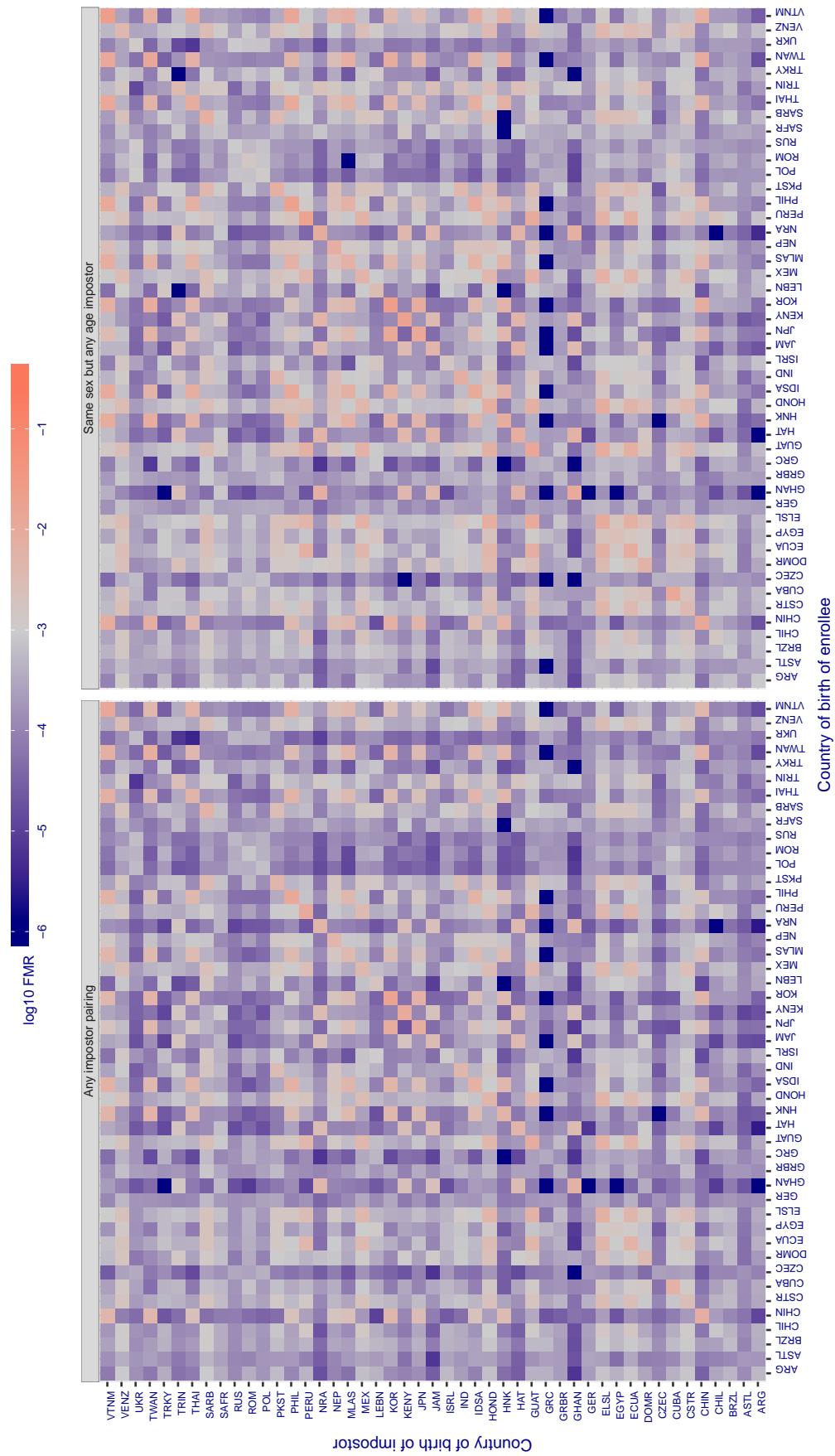
**Cross country FMR at threshold T = 1.320 for algorithm imperial\_001, giving FMR(T) = 0.001 globally.**

Figure 291: For algorithm imperial-001 operating on visa images, the heatmap shows false match rates observed over impostor comparisons of faces from different individuals who were born in the given country pair. False matches are counted against a recognition threshold fixed globally to give the target FMR in the plot title, computed over all on the order of  $10^{10}$  impostor comparisons. If text appears in each box it give the same quantity as that coded by the color. Grey indicates FMR is at the intended FMR target level. Light red colors present a security vulnerability to, for example, a passport gate. Each +1 increase in  $\log_{10} \text{FMR}$  corresponds to a factor of 10 increase in FMR. The matrix is not quite symmetric because images in the enrollment and verification sets are different.

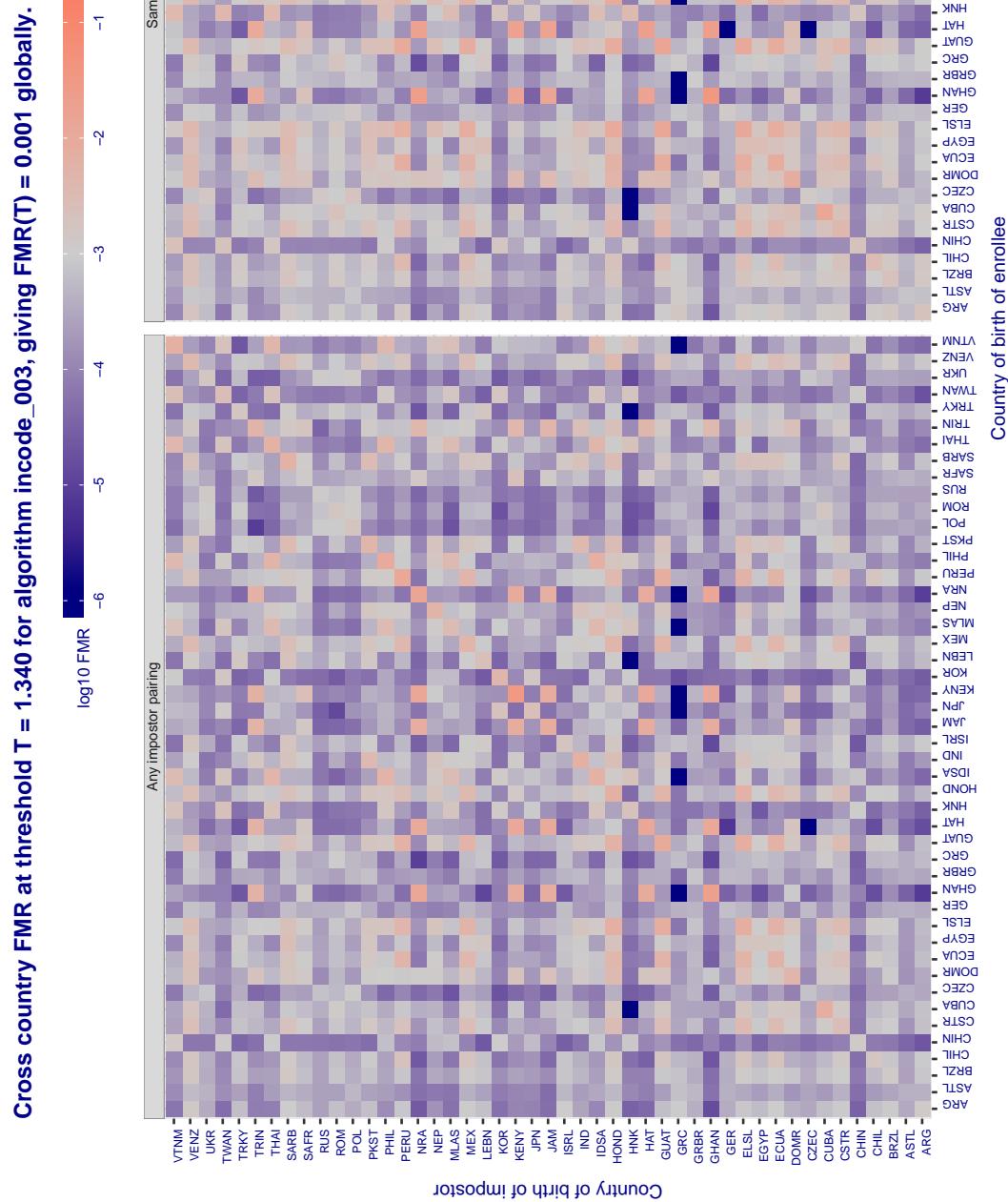


Figure 292: For algorithm incode-003 operating on visa images, the heatmap shows false match rates observed over impostor comparisons of faces from different individuals who were born in the given country pair. False matches are counted against a recognition threshold fixed globally to give the target FMR in the plot title, computed over all on the order of  $10^{10}$  impostor comparisons. If text appears in each box it give the same quantity as that coded by the color. Grey indicates FMR is at the intended FMR target level. Light red colors present a security vulnerability to, for example, a passport gate. Each +1 increase in  $\log_{10}$  FMR corresponds to a factor of 10 increase in FMR. The matrix is not quite symmetric because images in the enrollment and verification sets are different.

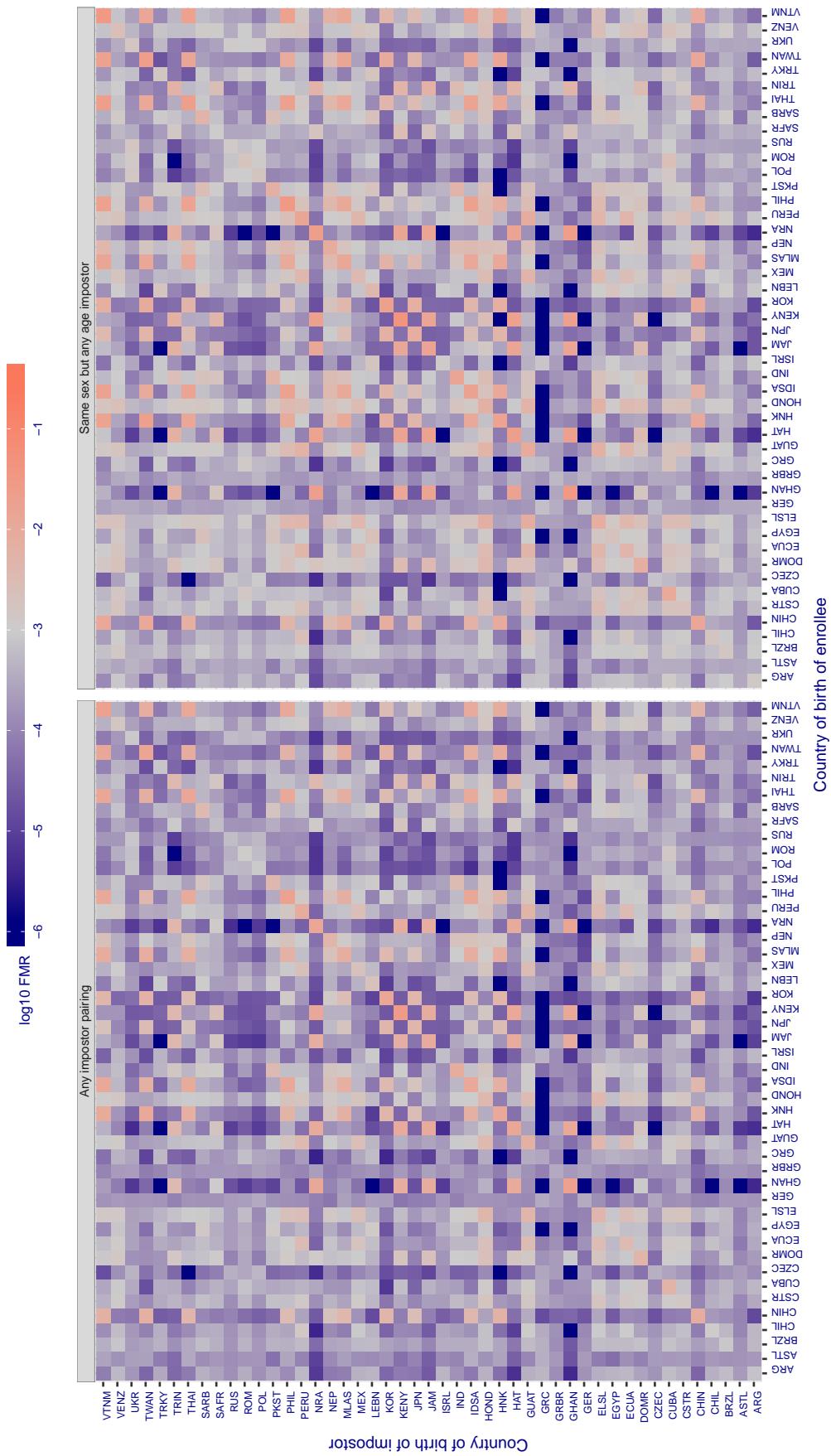
**Cross country FMR at threshold T = 21.422 for algorithm innovatrics\_004, giving FMR(T) = 0.001 globally.**

Figure 293: For algorithm innovatrics-004 operating on visa images, the heatmap shows false match rates observed over impostor comparisons of faces from different individuals who were born in the given country pair. False matches are counted against a recognition threshold fixed globally to give the target FMR in the plot title, computed over all on the order of  $10^{10}$  impostor comparisons. If text appears in each box it give the same quantity as that coded by the color. Grey indicates FMR is at the intended FMR target level. Light red colors present a security vulnerability to, for example, a passport gate. Each +1 increase in  $\log_{10} FMR$  corresponds to a factor of 10 increase in FMR. The matrix is not quite symmetric because images in the enrollment and verification sets are different.

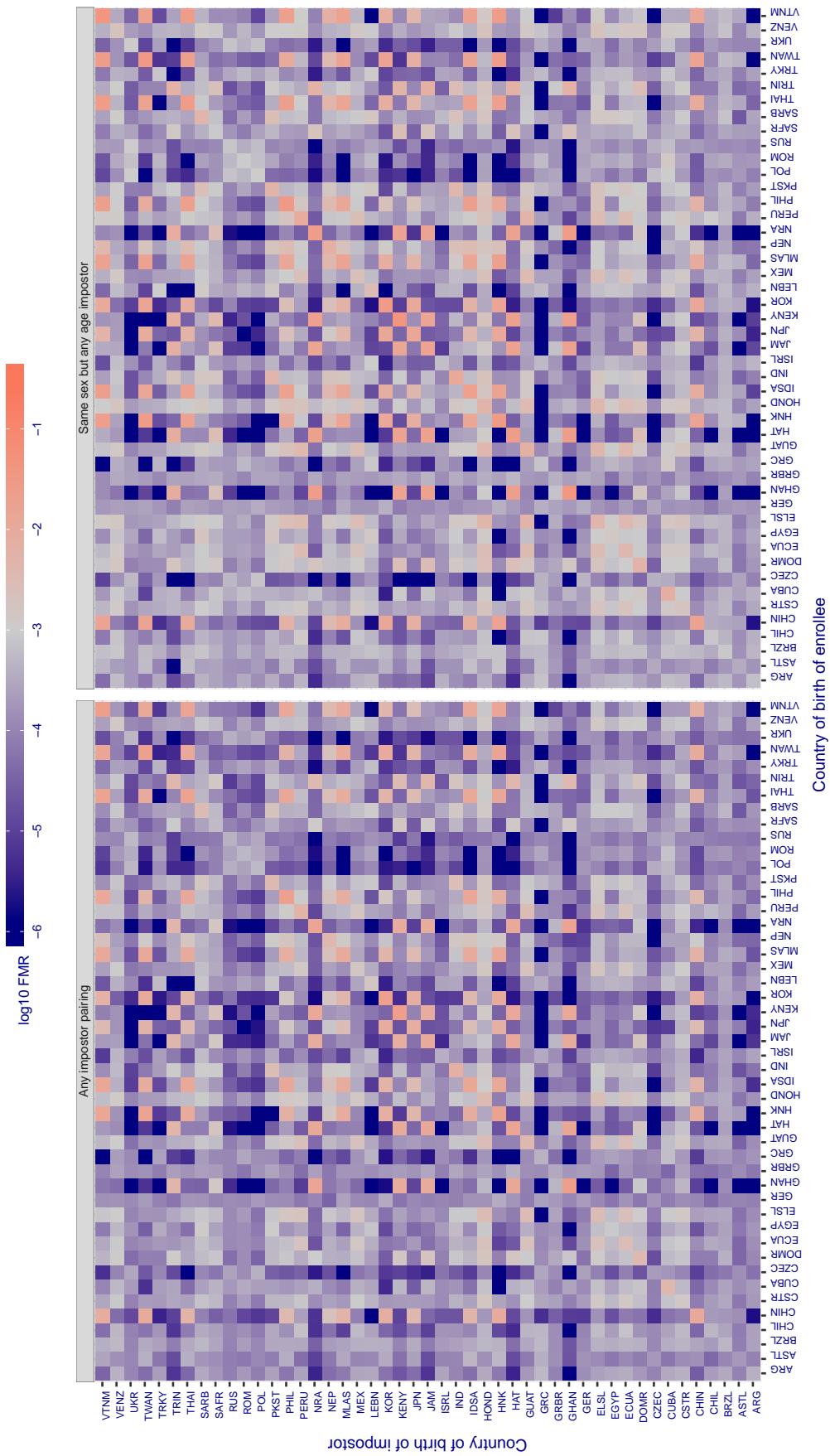
**Cross country FMR at threshold T = 28.706 for algorithm innovatrics\_005, giving FMR(T) = 0.001 globally.**

Figure 294: For algorithm innovatrics-005 operating on visa images, the heatmap shows false match rates observed over impostor comparisons of faces from different individuals who were born in the given country pair. False matches are counted against a recognition threshold fixed globally to give the target FMR in the plot title, computed over all on the order of  $10^{10}$  impostor comparisons. If text appears in each box it give the same quantity as that coded by the color. Grey indicates FMR is at the intended FMR target level. Light red colors present a security vulnerability to, for example, a passport gate. Each +1 increase in  $\log_{10} \text{FMR}$  corresponds to a factor of 10 increase in FMR. The matrix is not quite symmetric because images in the enrollment and verification sets are different.

**Cross country FMR at threshold T = 37.554 for algorithm intellivision\_001, giving  $FMR(T) = 0.001$  globally.**

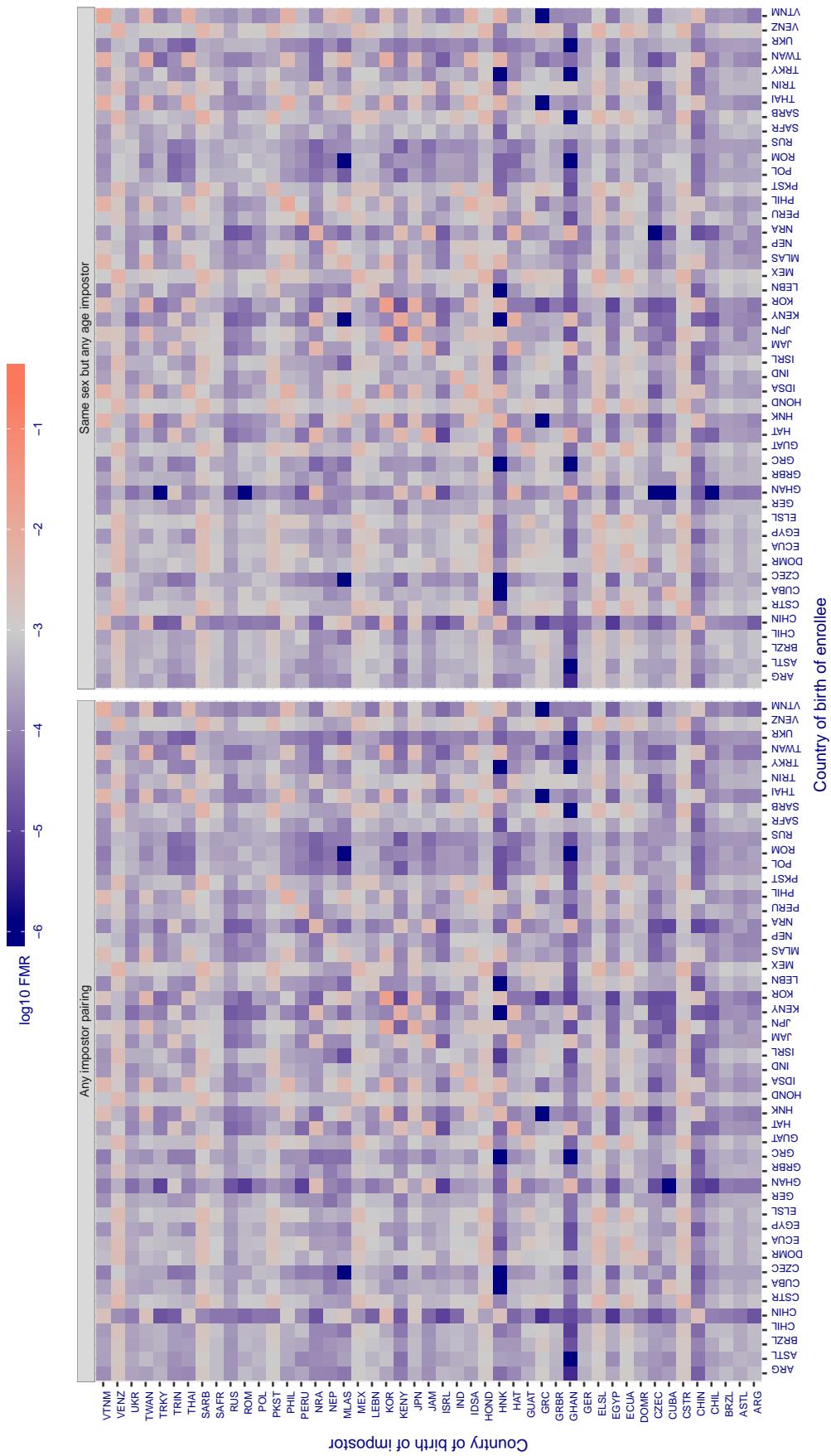


Figure 295: For algorithm intellivision-001 operating on visa images, the heatmap shows false match rates observed over impostor comparisons of faces from different individuals who were born in the given country pair. False matches are counted against a recognition threshold fixed globally to give the target  $FMR$  in the plot title, computed over all on the order of  $10^{10}$  impostor comparisons. If text appears in each box it give the same quantity as that coded by the color. Grey indicates  $FMR$  is at the intended  $FMR$  target level. Light red colors present a security vulnerability to, for example, a passport gate. Each +1 increase in  $\log_{10} FMR$  corresponds to a factor of 10 increase in  $FMR$ . The matrix is not quite symmetric because images in the enrollment and verification sets are different.

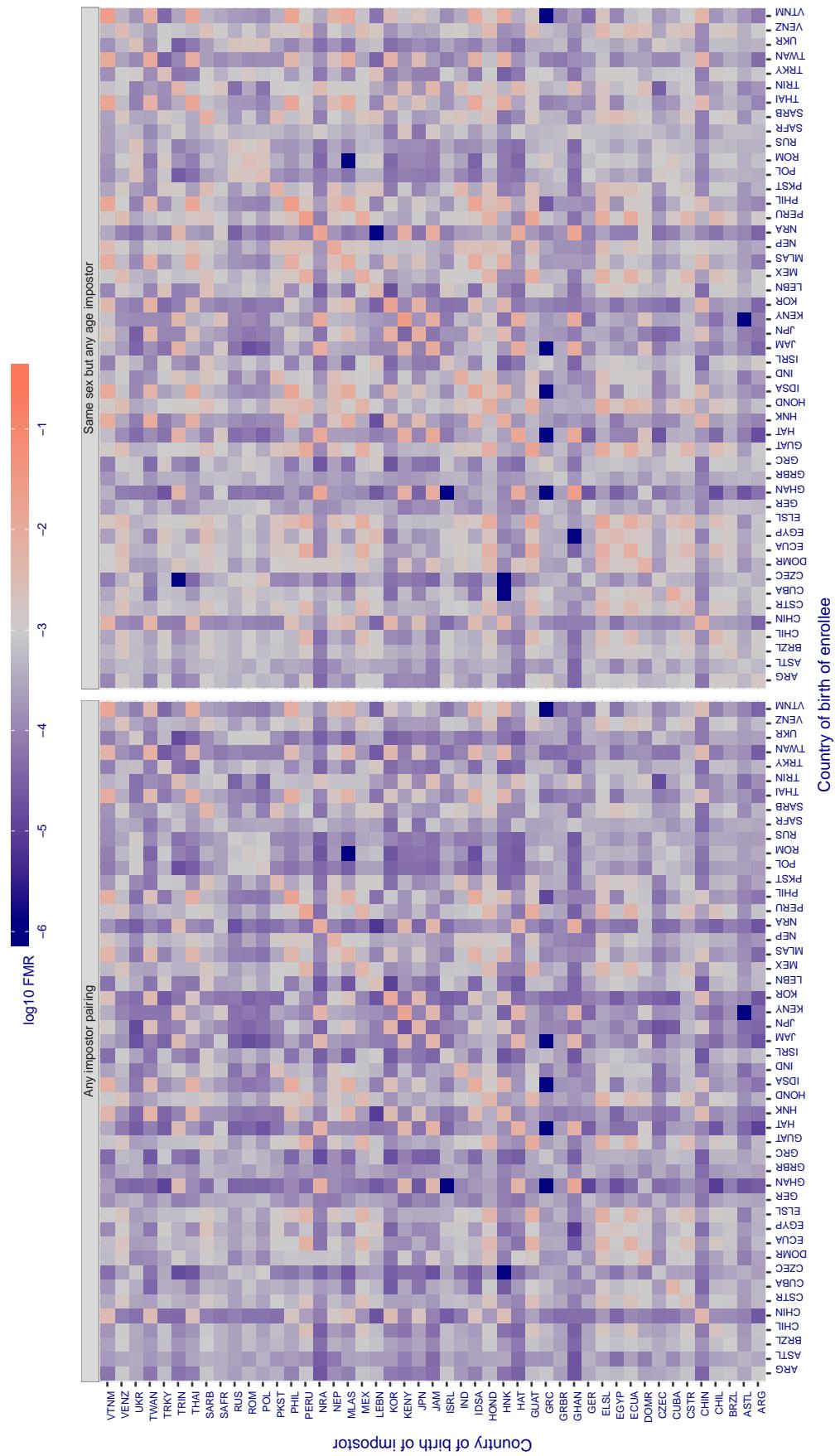
**Cross country FMR at threshold T = 1.280 for algorithm iqface\_000, giving FMR(T) = 0.001 globally.**

Figure 296: For algorithm iqface-000 operating on visa images, the heatmap shows false match rates observed over impostor comparisons of faces from different individuals who were born in the given country pair. False matches are counted against a recognition threshold fixed globally to give the target FMR in the plot title, computed over all on the order of  $10^{10}$  impostor comparisons. If text appears in each box it give the same quantity as that coded by the color. Grey indicates FMR is at the intended FMR target level. Light red colors present a security vulnerability to, for example, a passport gate. Each +1 increase in  $\log_{10} FMR$  corresponds to a factor of 10 increase in FMR. The matrix is not quite symmetric because images in the enrollment and verification sets are different.

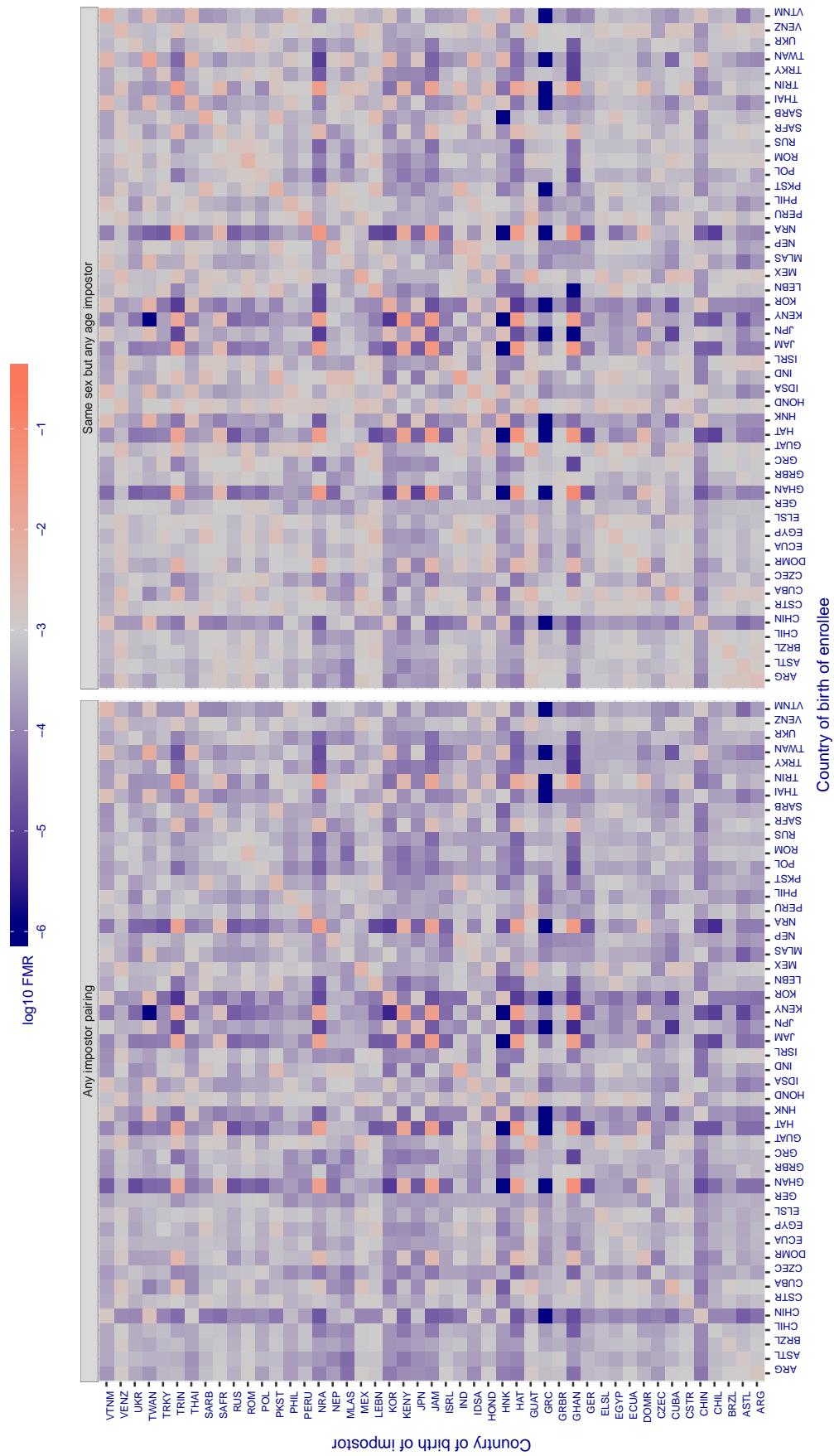
**Cross country FMR at threshold T = 20.648 for algorithm isityou\_000, giving FMR(T) = 0.001 globally.**

Figure 297: For algorithm isityou-000 operating on visa images, the heatmap shows false match rates observed over impostor comparisons of faces from different individuals who were born in the given country pair. False matches are counted against a recognition threshold fixed globally to give the target FMR in the plot title, computed over all on the order of  $10^{10}$  impostor comparisons. If text appears in each box it give the same quantity as that coded by the color. Grey indicates FMR is at the intended FMR target level. Light red colors present a security vulnerability to, for example, a passport gate. Each +1 increase in  $\log_{10} FMR$  corresponds to a factor of 10 increase in FMR. The matrix is not quite symmetric because images in the enrollment and verification sets are different.

**Cross country FMR at threshold T = 0.649 for algorithm isystems\_001, giving FNMR(T) = 0.001 globally.**

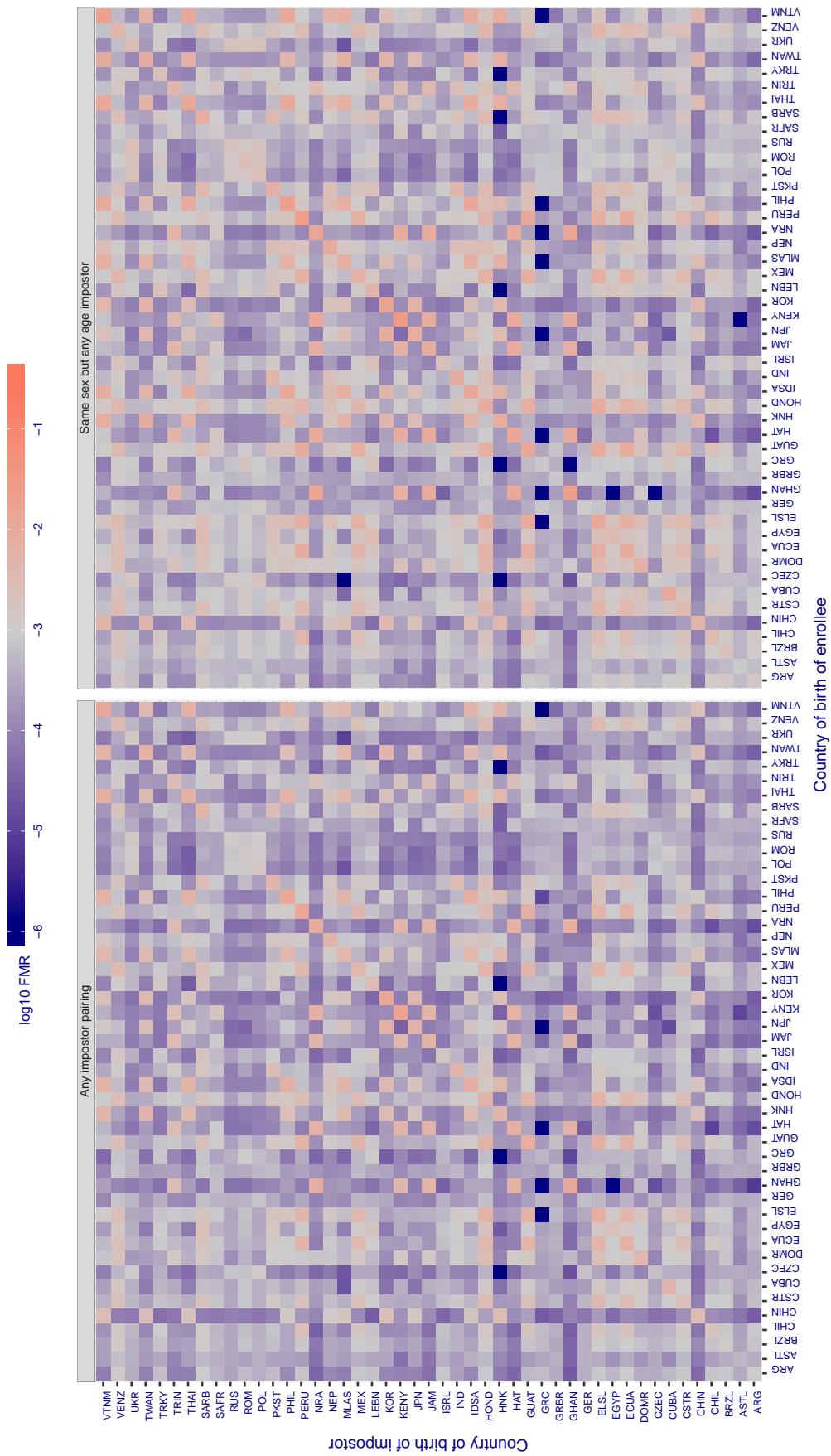


Figure 298: For algorithm isystems-001 operating on visa images, the heatmap shows false match rates observed over impostor comparisons of faces from different individuals who were born in the given country pair. False matches are counted against a recognition threshold fixed globally to give the target FMR in the plot title, computed over all on the order of  $10^{10}$  impostor comparisons. If text appears in each box it give the same quantity as that coded by the color. Grey indicates FMR is at the intended FMR target level. Light red colors present a security vulnerability to, for example, a passport gate. Each +1 increase in  $\log_{10} \text{FMR}$  corresponds to a factor of 10 increase in FMR. The matrix is not quite symmetric because images in the enrollment and verification sets are different.

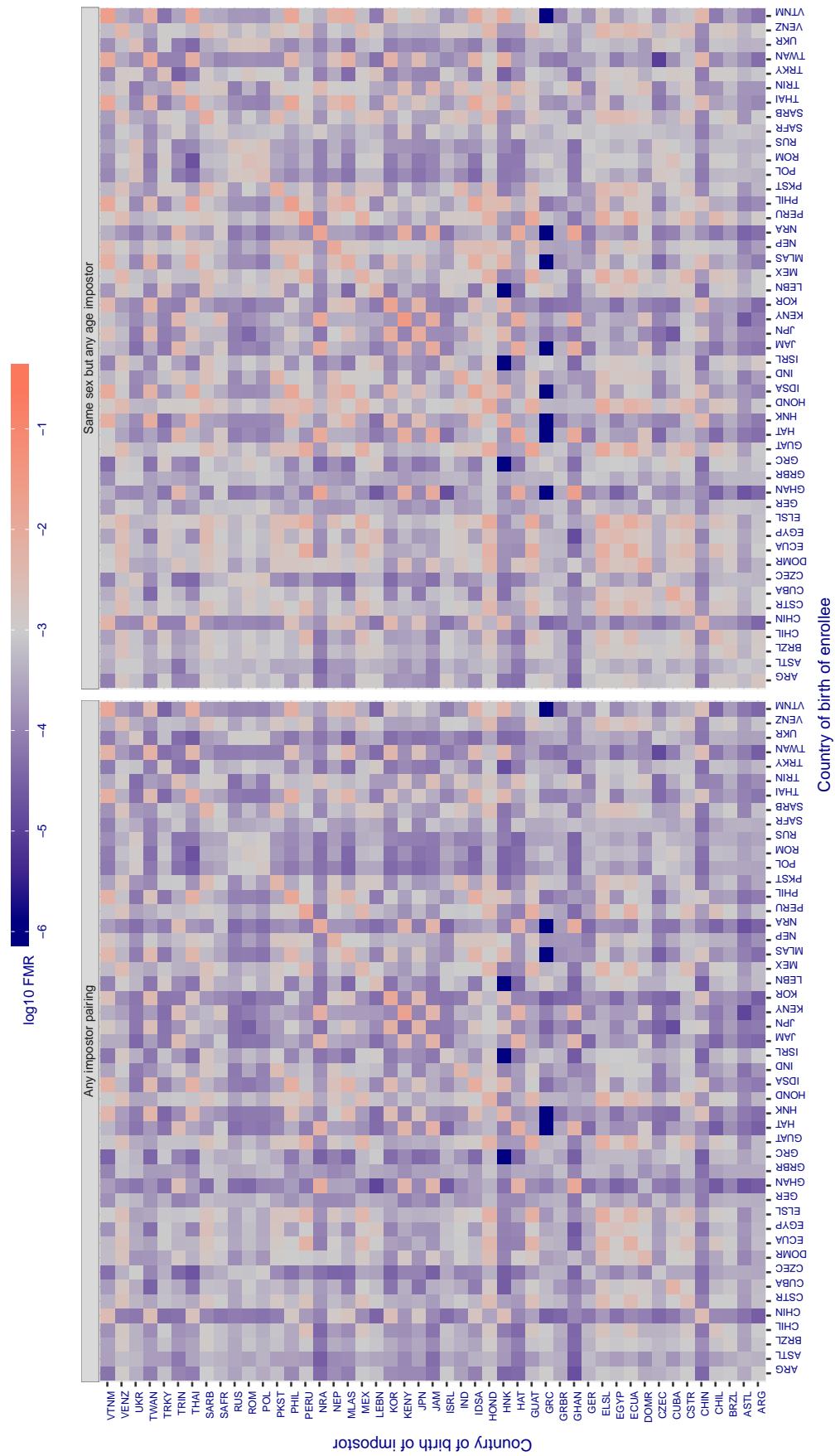
**Cross country FMR at threshold T = 0.647 for algorithm isystems\_002, giving  $\text{FMR}(T) = 0.001$  globally.**

Figure 299: For algorithm isystems-002 operating on visa images, the heatmap shows false match rates observed over impostor comparisons of faces from different individuals who were born in the given country pair. False matches are counted against a recognition threshold fixed globally to give the target FMR in the plot title, computed over all on the order of  $10^{10}$  impostor comparisons. If text appears in each box it give the same quantity as that coded by the color. Grey indicates FMR is at the intended FMR target level. Light red colors present a security vulnerability to, for example, a passport gate. Each +1 increase in  $\log_{10} \text{FMR}$  corresponds to a factor of 10 increase in FMR. The matrix is not quite symmetric because images in the enrollment and verification sets are different.

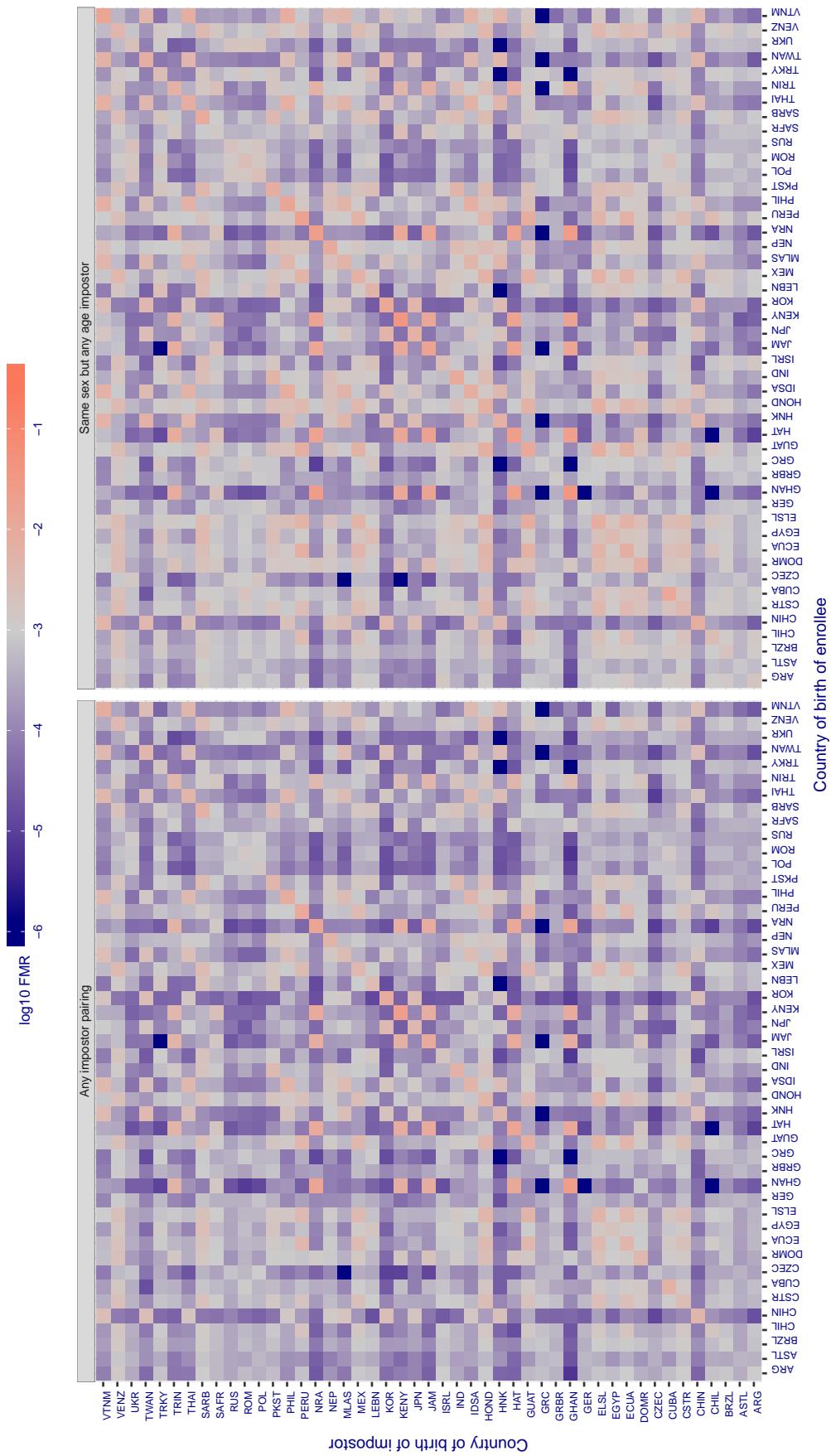
**Cross country FMR at threshold T = 10.316 for algorithm itmo\_005, giving FMR(T) = 0.001 globally.**

Figure 30: For algorithm itmo-005 operating on visa images, the heatmap shows false match rates observed over impostor comparisons of faces from different individuals who were born in the given country pair. False matches are counted against a recognition threshold fixed globally to give the target FMR in the plot title, computed over all on the order of  $10^{10}$  impostor comparisons. If text appears in each box it give the same quantity as that coded by the color. Grey indicates FMR is at the intended FMR target level. Light red colors present a security vulnerability to, for example, a passport gate. Each +1 increase in  $\log_{10} \text{FMR}$  corresponds to a factor of 10 increase in FMR. The matrix is not quite symmetric because images in the enrollment and verification sets are different.

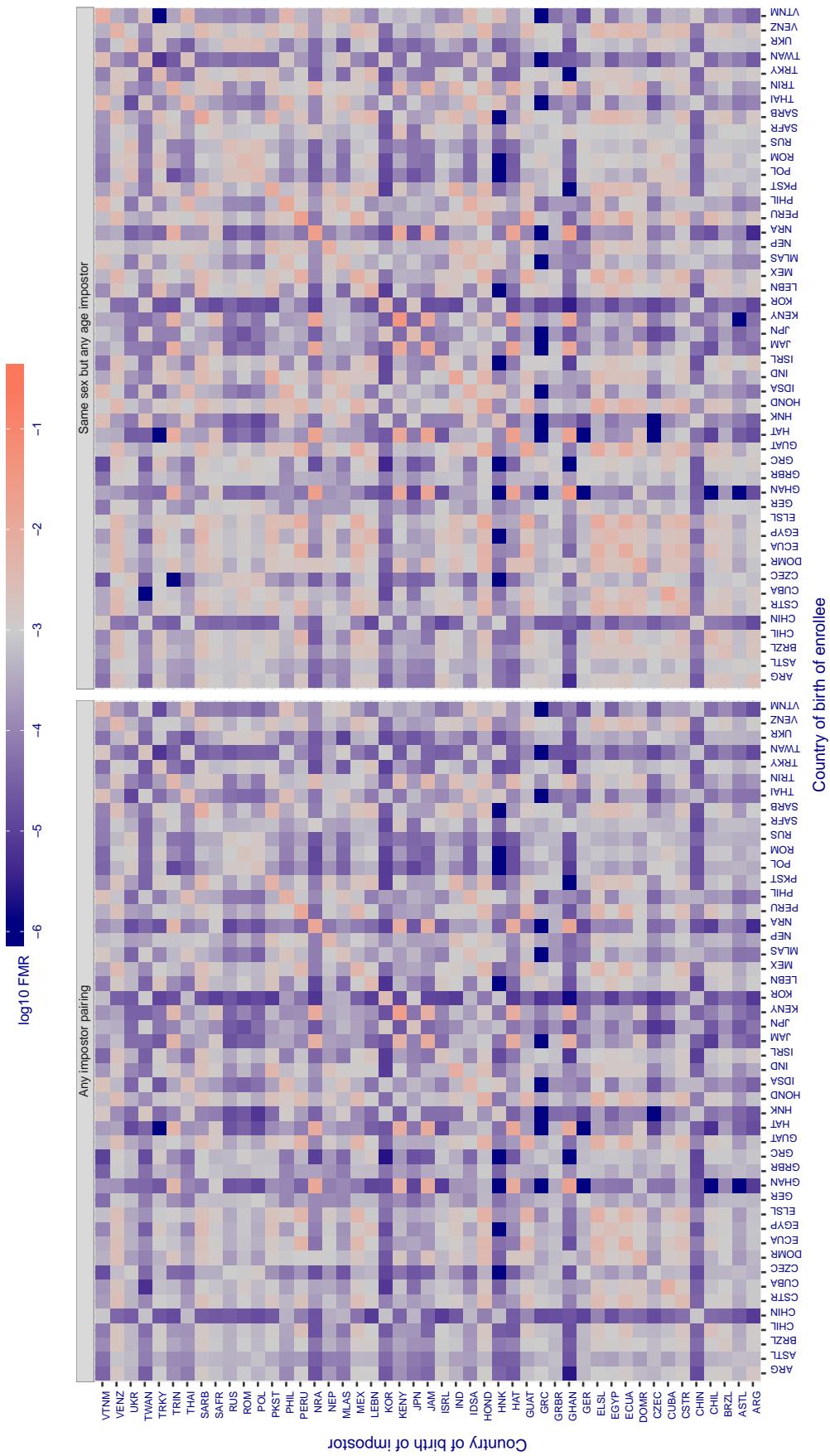
**Cross country FMR at threshold T = 12.030 for algorithm itmo\_006, giving FMR(T) = 0.001 globally.**

Figure 301: For algorithm itmo-006 operating on visa images, the heatmap shows false match rates observed over impostor comparisons of faces from different individuals who were born in the given country pair. False matches are counted against a recognition threshold fixed globally to give the target FMR in the plot title, computed over all on the order of  $10^{10}$  impostor comparisons. If text appears in each box it give the same quantity as that coded by the color. Grey indicates FMR is at the intended FMR target level. Light red colors present a security vulnerability to, for example, a passport gate. Each +1 increase in  $\log_{10} \text{FMR}$  corresponds to a factor of 10 increase in FMR. The matrix is not quite symmetric because images in the enrollment and verification sets are different.

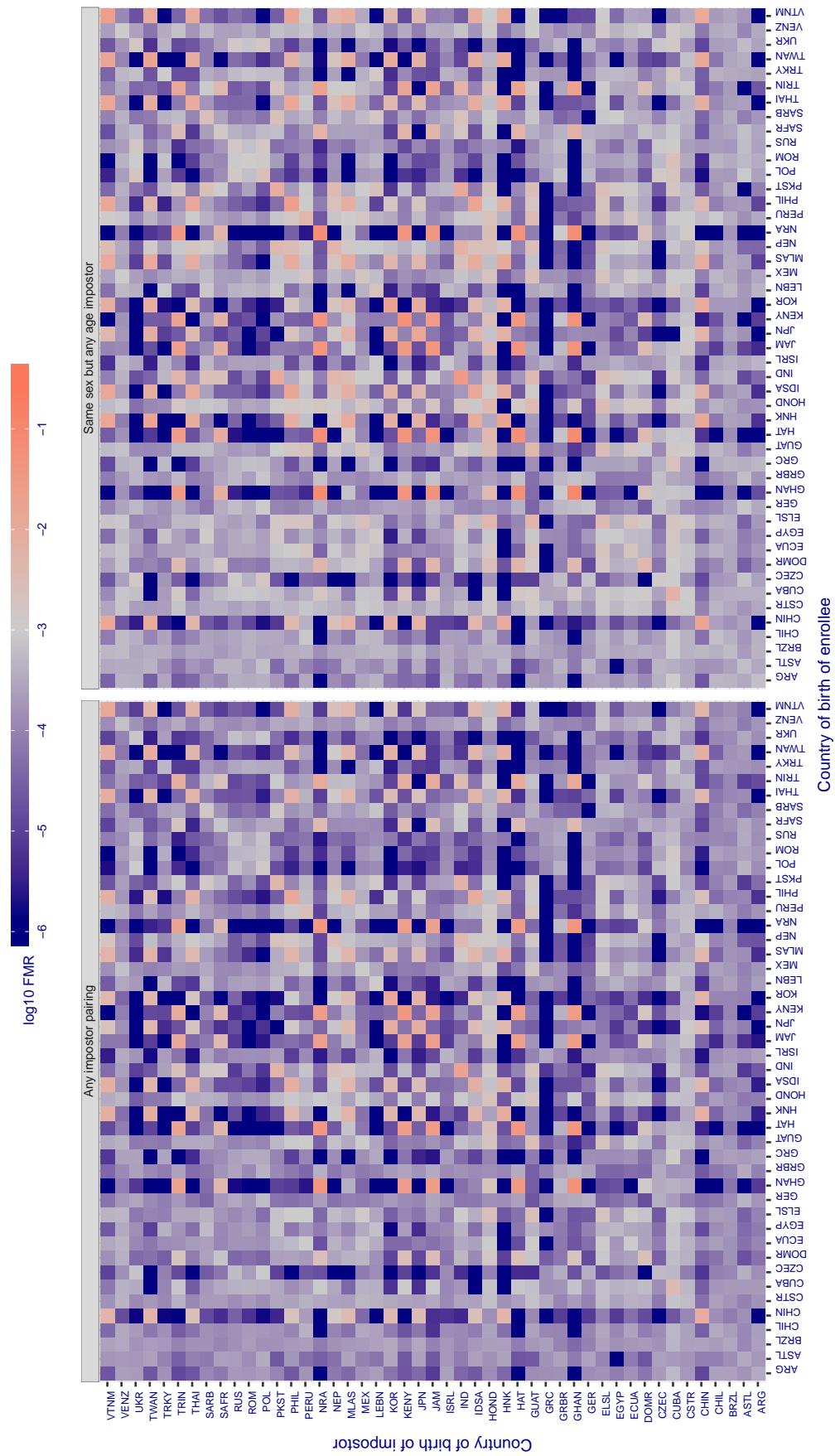
**Cross country FMR at threshold T = 1.192 for algorithm kakao\_001, giving FMR(T) = 0.001 globally.**

Figure 302: For algorithm kakao-001 operating on visa images, the heatmap shows false match rates observed over impostor comparisons of faces from different individuals who were born in the given country pair. False matches are counted against a recognition threshold fixed globally to give the target FMR in the plot title, computed over all on the order of  $10^{10}$  impostor comparisons. If text appears in each box it give the same quantity as that coded by the color. Grey indicates FMR is at the intended FMR target level. Light red colors present a security vulnerability to, for example, a passport gate. Each +1 increase in  $\log_{10} FMR$  corresponds to a factor of 10 increase in FMR. The matrix is not quite symmetric because images in the enrollment and verification sets are different.

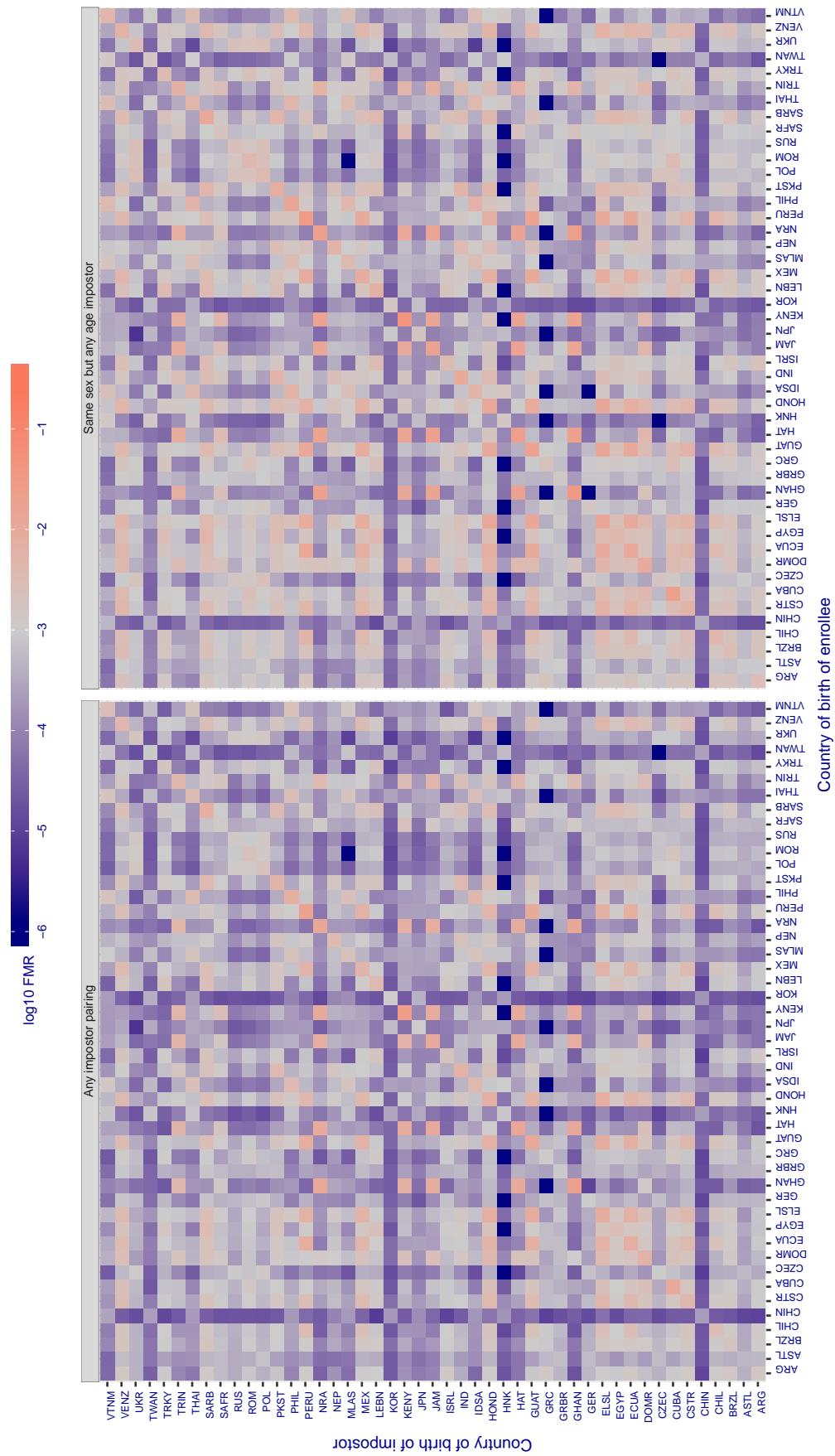
**Cross country FMR at threshold T = 0.650 for algorithm kedacom\_000, giving FMR(T) = 0.001 globally.**

Figure 303: For algorithm kedacom-000 operating on visa images, the heatmap shows false match rates observed over impostor comparisons of faces from different individuals who were born in the given country pair. False matches are counted against a recognition threshold fixed globally to give the target FMR in the plot title, computed over all on the order of  $10^{10}$  impostor comparisons. If text appears in each box it give the same quantity as that coded by the color. Grey indicates FMR is at the intended FMR target level. Light red colors present a security vulnerability to, for example, a passport gate. Each +1 increase in  $\log_{10} \text{FMR}$  corresponds to a factor of 10 increase in FMR. The matrix is not quite symmetric because images in the enrollment and verification sets are different.

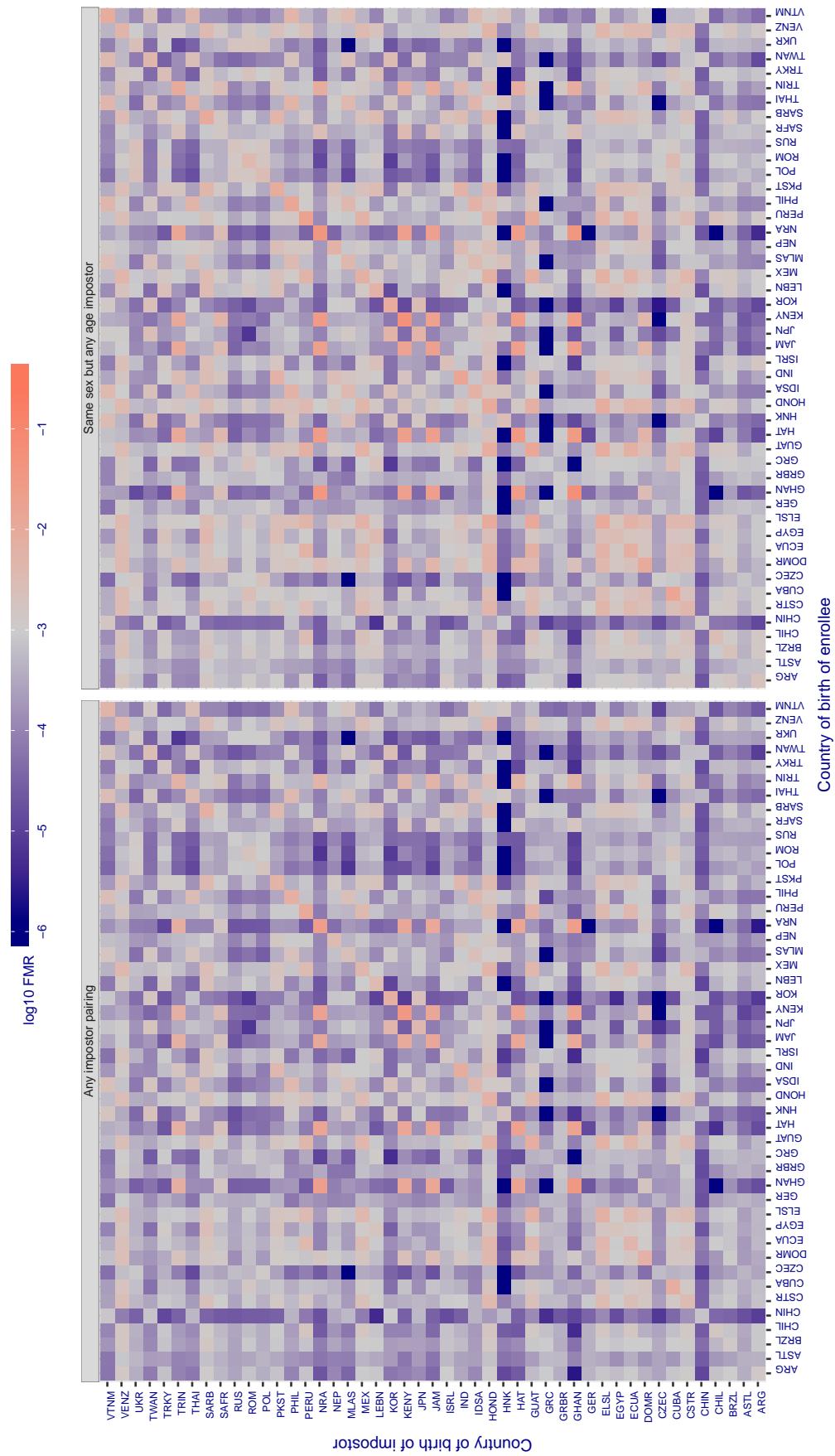
**Cross country FMR at threshold T = 0.656 for algorithm lookman\_002, giving  $\text{FMR}(T) = 0.001$  globally.**

Figure 304: For algorithm lookman-002 operating on visa images, the heatmap shows false match rates observed over impostor comparisons of faces from different individuals who were born in the given country pair. False matches are counted against a recognition threshold fixed globally to give the target FMR in the plot title, computed over all on the order of  $10^{10}$  impostor comparisons. If text appears in each box it give the same quantity as that coded by the color. Grey indicates FMR is at the intended FMR target level. Light red colors present a security vulnerability to, for example, a passport gate. Each +1 increase in  $\log_{10} \text{FMR}$  corresponds to a factor of 10 increase in FMR. The matrix is not quite symmetric because images in the enrollment and verification sets are different.

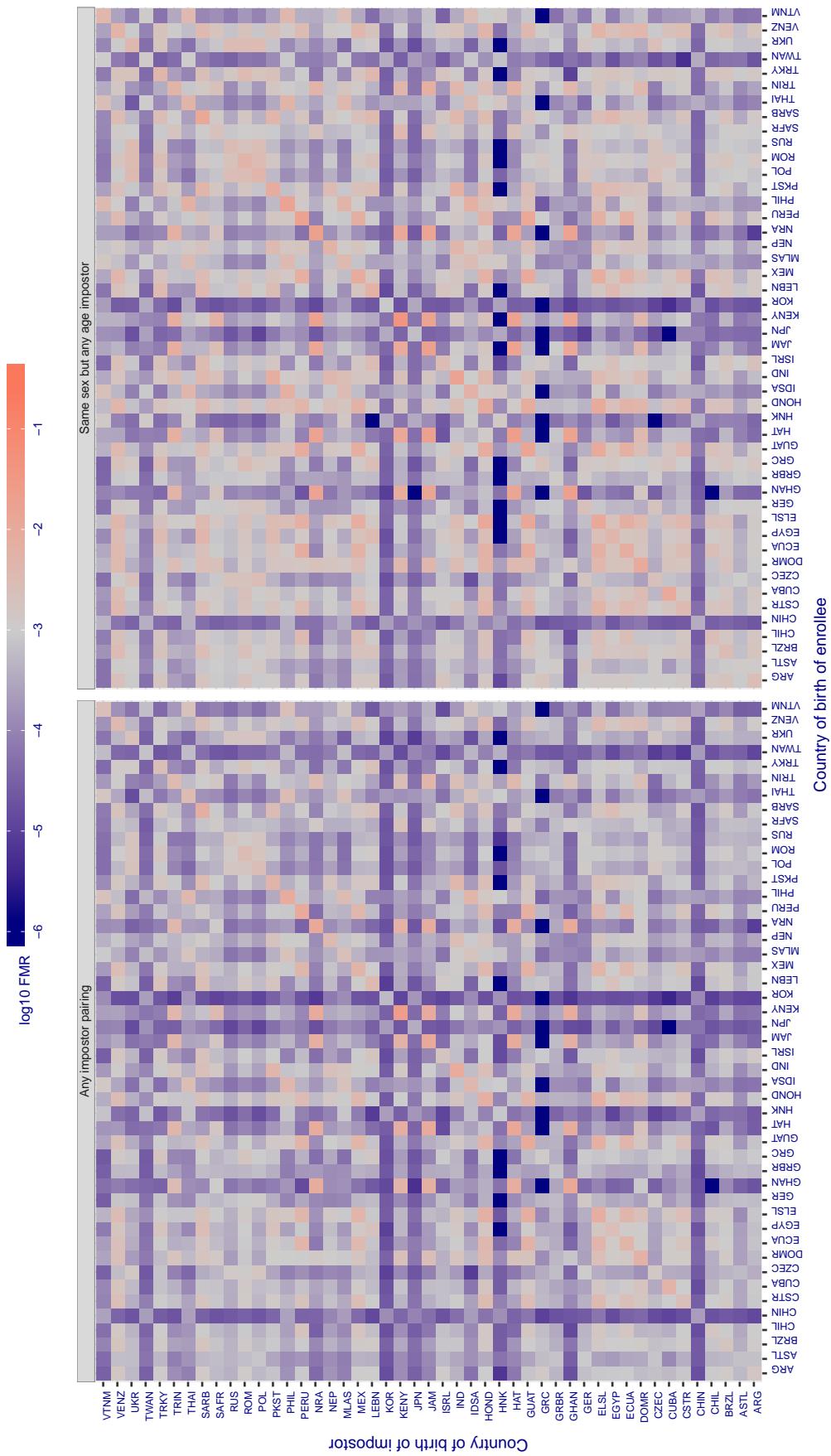


Figure 305. For algorithm lookman-004 operating on visa images, the heatmap shows false match rates observed over impostor comparisons of faces from different individuals who were born in the given country pair. False matches are counted against a recognition threshold fixed globally to give the target FMR in the plot title, computed over all on the order of  $10^{10}$  impostor comparisons. If text appears in each box it give the same quantity as that coded by the color. Grey indicates FMR is at the intended FMR target level. Light red colors present a security vulnerability to, for example, a passport gate. Each +1 increase in  $\log_{10}$  FMR corresponds to a factor of 10 increase in FMR. The matrix is not quite symmetric because images in the enrollment and verification sets are different.

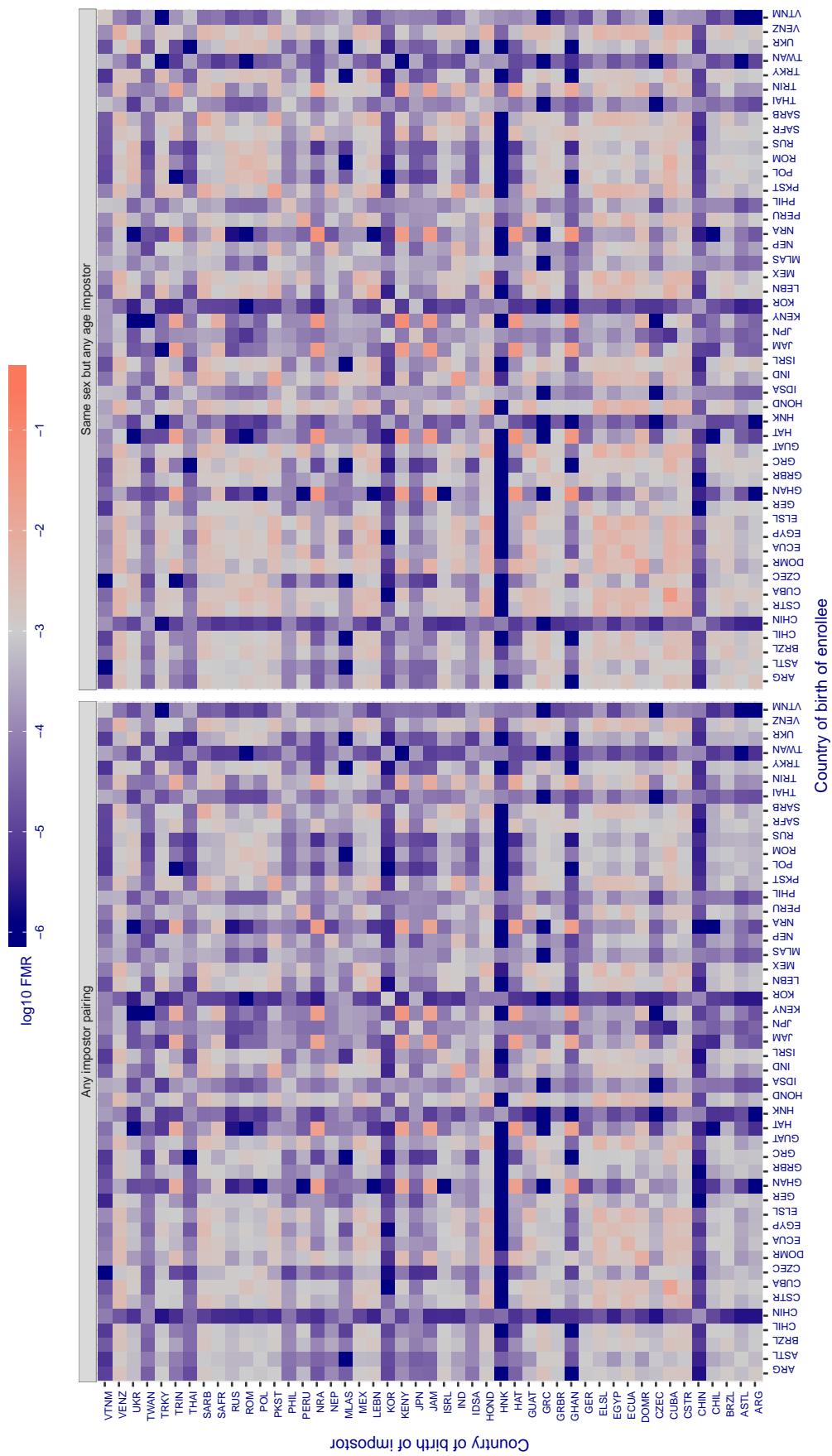
**Cross country FMR at threshold T = 66.706 for algorithm megvii\_001, giving  $FMR(T) = 0.001$  globally.**

Figure 306: For algorithm megvii-001 operating on visa images, the heatmap shows false match rates observed over impostor comparisons of faces from different individuals who were born in the given country pair. False matches are counted against a recognition threshold fixed globally to give the target  $FMR$  in the plot title, computed over all on the order of  $10^{10}$  impostor comparisons. If text appears in each box it give the same quantity as that coded by the color. Grey indicates  $FMR$  is at the intended  $FMR$  target level. Light red colors present a security vulnerability to, for example, a passport gate. Each +1 increase in  $\log_{10} FMR$  corresponds to a factor of 10 increase in  $FMR$ . The matrix is not quite symmetric because images in the enrollment and verification sets are different.

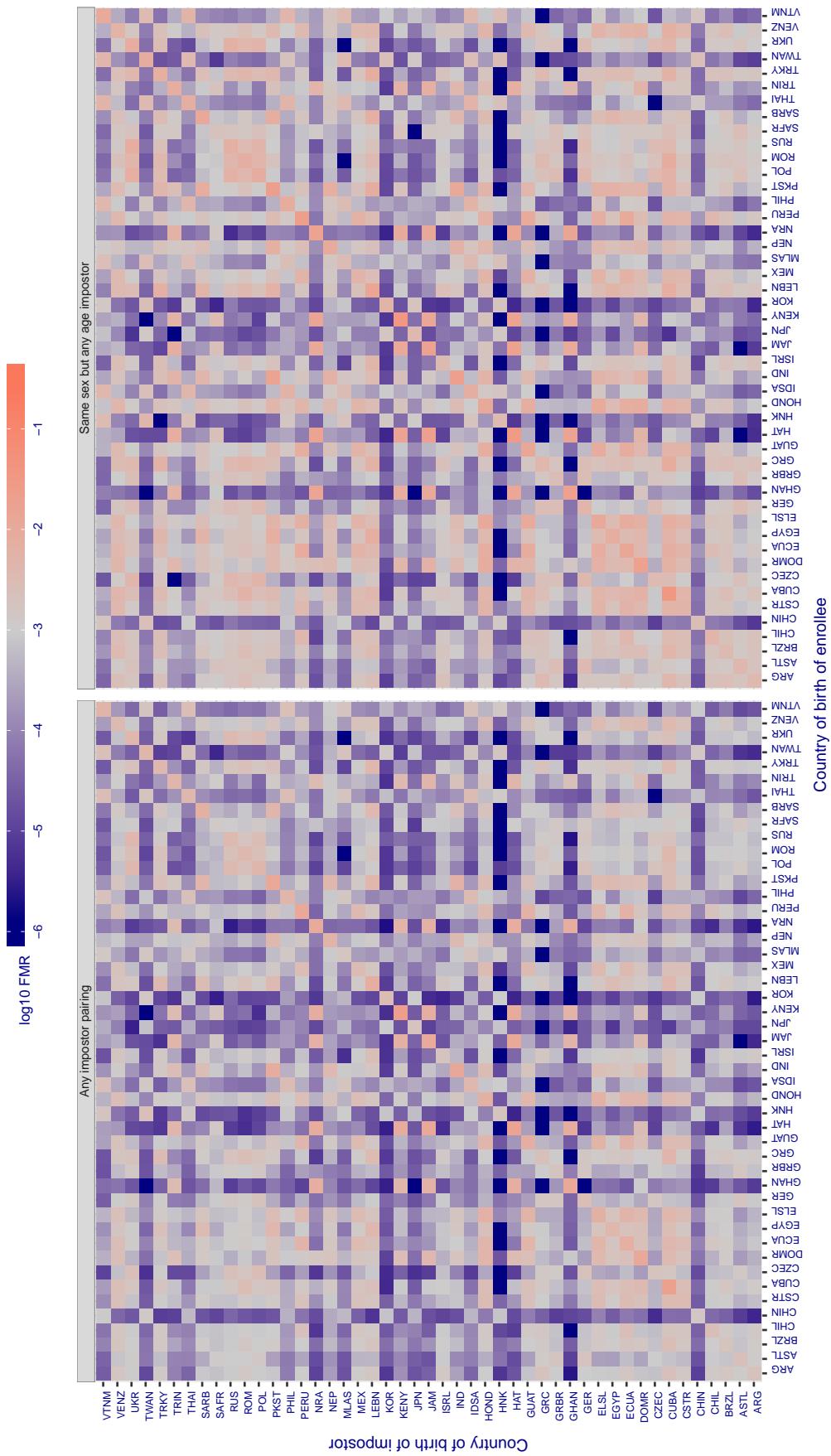
**Cross country FMR at threshold T = 58.026 for algorithm megvii\_002, giving FMR(T) = 0.001 globally.**

Figure 307: For algorithm megvii-002 operating on visa images, the heatmap shows false match rates observed over impostor comparisons of faces from different individuals who were born in the given country pair. False matches are counted against a recognition threshold fixed globally to give the target FMR in the plot title, computed over all on the order of  $10^{10}$  impostor comparisons. If text appears in each box it give the same quantity as that coded by the color. Grey indicates FMR is at the intended FMR target level. Light red colors present a security vulnerability to, for example, a passport gate. Each +1 increase in  $\log_{10} FMR$  corresponds to a factor of 10 increase in FMR. The matrix is not quite symmetric because images in the enrollment and verification sets are different.

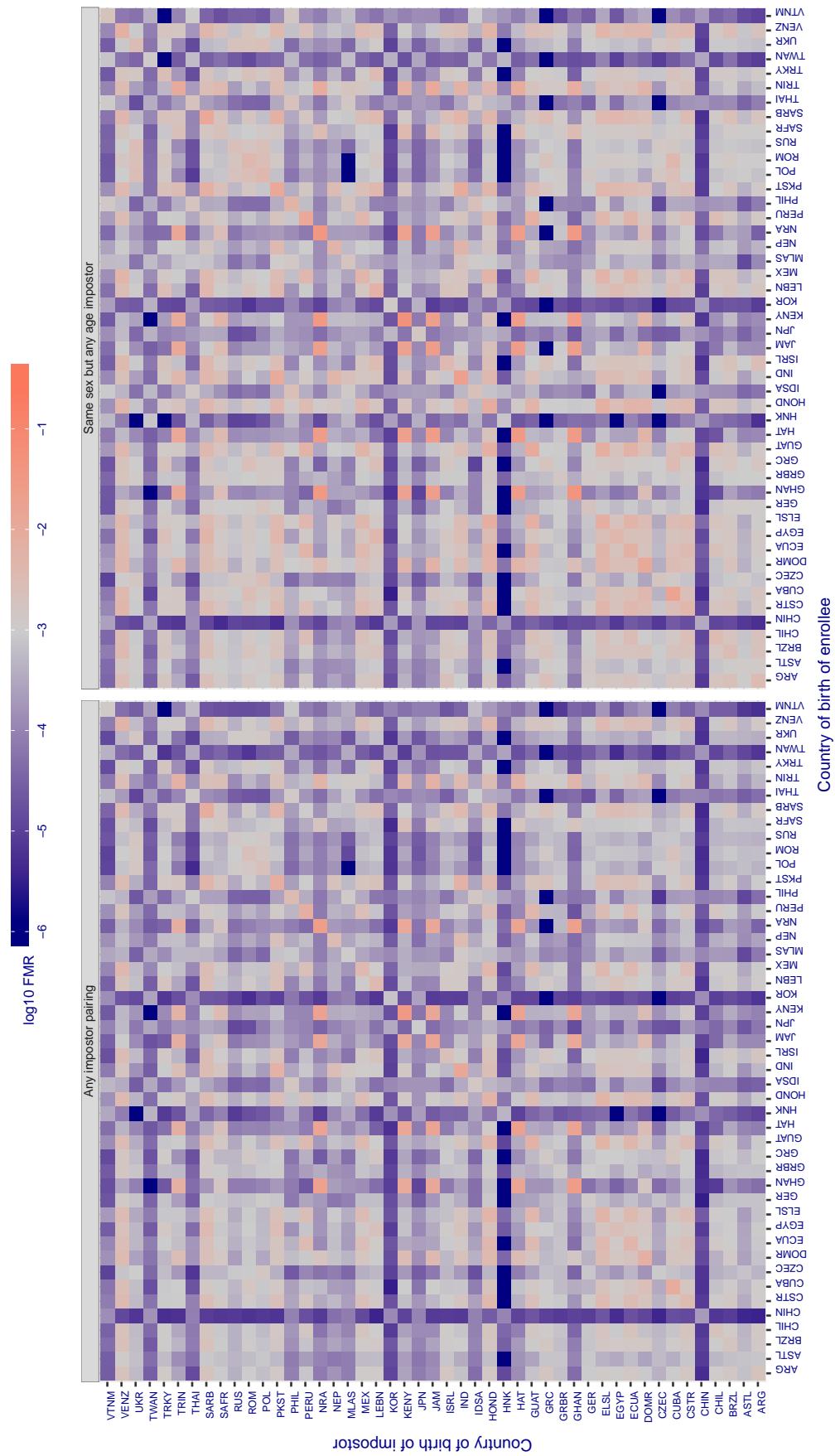
**Cross country FMR at threshold T = 0.345 for algorithm meiya\_001, giving FMR(T) = 0.001 globally.**

Figure 308: For algorithm meiya-001 operating on visa images, the heatmap shows false match rates observed over impostor comparisons of faces from different individuals who were born in the given country pair. False matches are counted against a recognition threshold fixed globally to give the target FMR in the plot title, computed over all on the order of  $10^{10}$  impostor comparisons. If text appears in each box it give the same quantity as that coded by the color. Grey indicates FMR is at the intended FMR target level. Light red colors present a security vulnerability to, for example, a passport gate. Each +1 increase in  $\log_{10} FMR$  corresponds to a factor of 10 increase in FMR. The matrix is not quite symmetric because images in the enrollment and verification sets are different.

**Cross country FMR at threshold T = 0.624 for algorithm microfocus\_001, giving FMR(T) = 0.001 globally.**

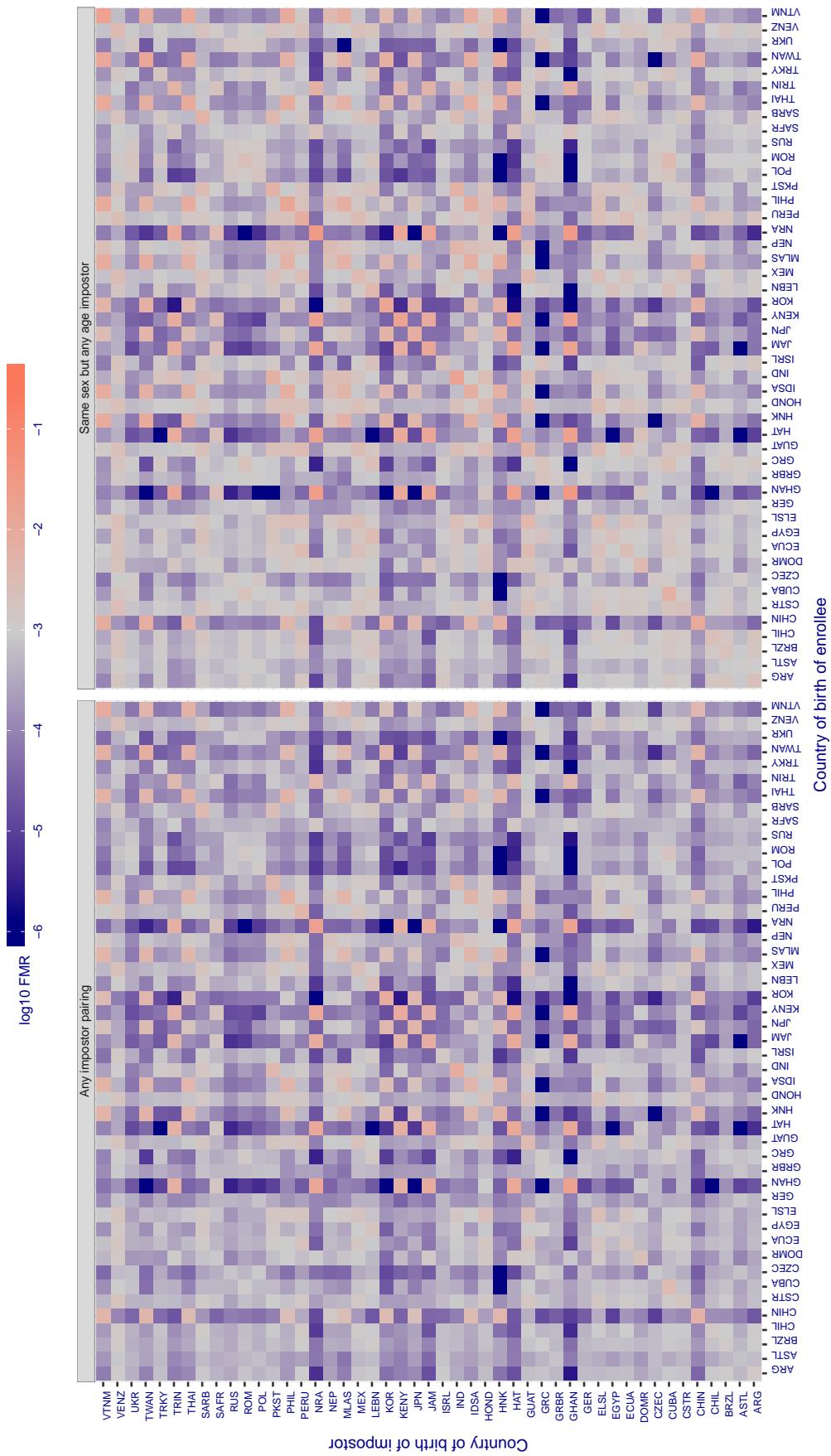


Figure 309: For algorithm microfocus-001 operating on visa images, the heatmap shows false match rates observed over impostor comparisons of faces from different individuals who were born in the given country pair. False matches are counted against a recognition threshold fixed globally to give the target FMR in the plot title, computed over all on the order of  $10^{10}$  impostor comparisons. If text appears in each box it give the same quantity as that coded by the color. Grey indicates FMR is at the intended FMR target level. Light red colors present a security vulnerability to, for example, a passport gate. Each +1 increase in  $\log_{10} FMR$  corresponds to a factor of 10 increase in FMR. The matrix is not quite symmetric because images in the enrollment and verification sets are different.

**Cross country FMR at threshold T = 0.542 for algorithm microfocus\_002, giving FMR(T) = 0.001 globally.**

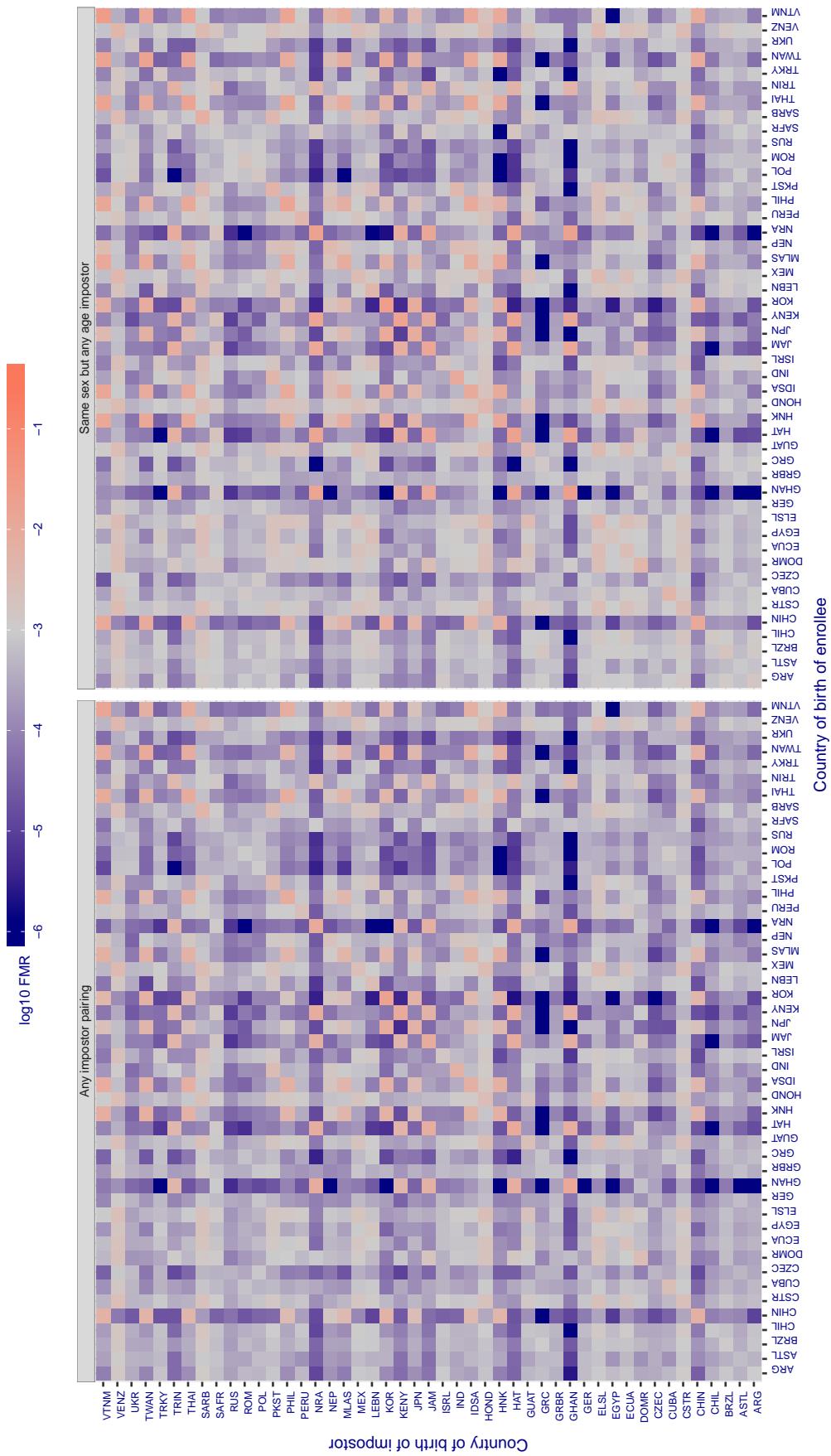


Figure 310: For algorithm microfocus-002 operating on visa images, the heatmap shows false match rates observed over impostor comparisons of faces from different individuals who were born in the given country pair. False matches are counted against a recognition threshold fixed globally to give the target FMR in the plot title, computed over all on the order of  $10^{10}$  impostor comparisons. If text appears in each box it give the same quantity as that coded by the color. Grey indicates FMR is at the intended FMR target level. Light red colors present a security vulnerability to, for example, a passport gate. Each +1 increase in  $\log_{10} FMR$  corresponds to a factor of 10 increase in FMR. The matrix is not quite symmetric because images in the enrollment and verification sets are different.

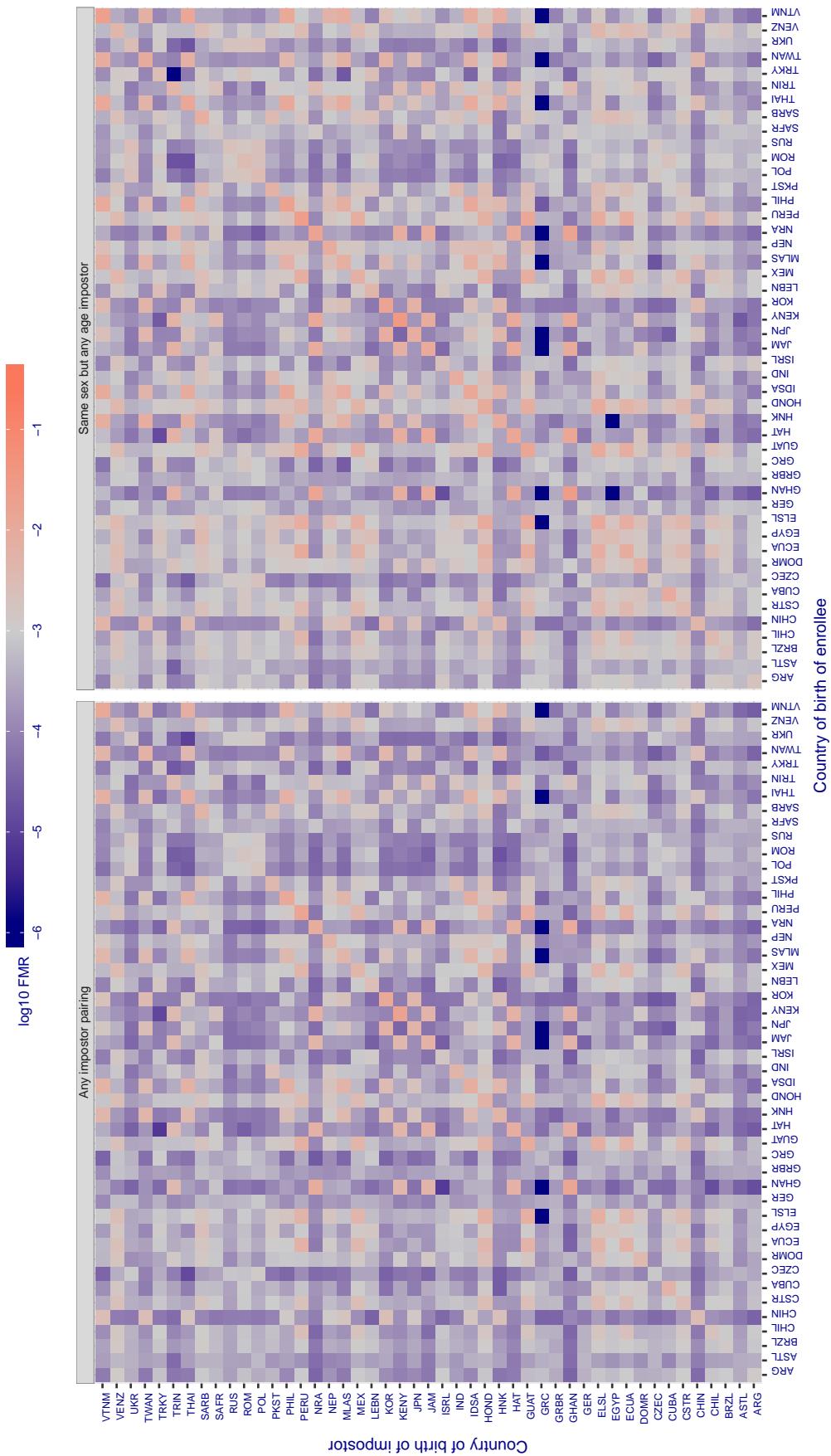


Figure 311. For algorithm mt-000 operating on visa images, the heatmap shows false match rates observed over impostor comparisons of faces from different individuals who were born in the given country pair. False matches are counted against a recognition threshold fixed globally to give the target  $FMR$  in the plot title, computed over all on the order of  $10^{10}$  impostor comparisons. If text appears in each box it give the same quantity as that coded by the color. Grey indicates  $FMR$  is at the intended  $FMR$  target level. Light red colors present a security vulnerability to, for example, a passport gate. Each +1 increase in  $\log_{10} FMR$  corresponds to a factor of 10 increase in  $FMR$ . The matrix is not quite symmetric because images in the enrollment and verification sets are different.

**Cross country FMR at threshold T = 33.449 for algorithm neurotechnology\_005, giving FMR(T) = 0.001 globally.**

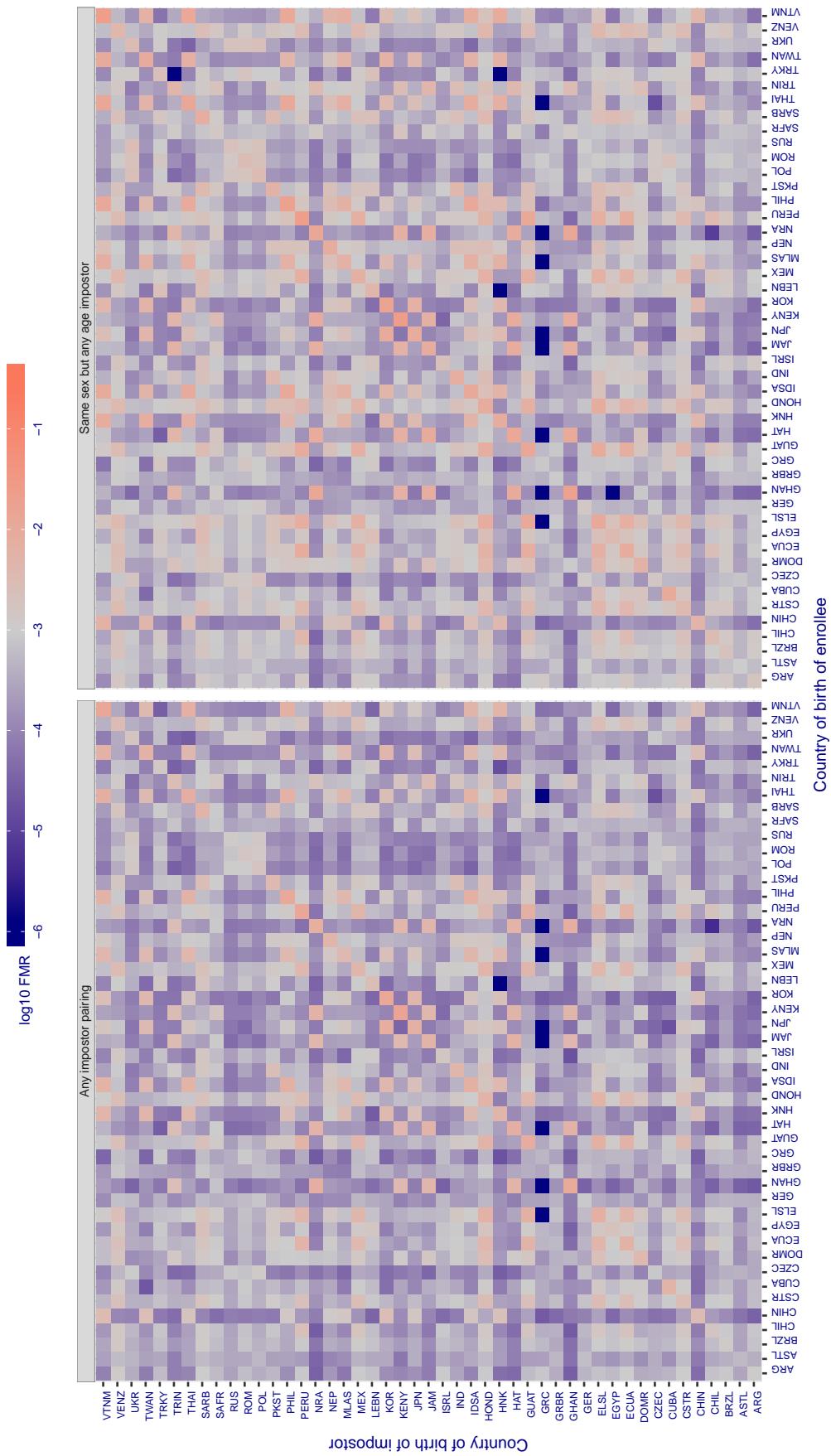


Figure 312: For algorithm neurotechnology-005 operating on visa images, the heatmap shows false match rates observed over impostor comparisons of faces from different individuals who were born in the given country pair. False matches are counted against a recognition threshold fixed globally to give the target FMR in the plot title, computed over all on the order of  $10^{10}$  impostor comparisons. If text appears in each box it give the same quantity as that coded by the color. Grey indicates FMR is at the intended FMR target level. Light red colors present a security vulnerability to, for example, a passport gate. Each +1 increase in  $\log_{10}$  FMR corresponds to a factor of 10 increase in FMR. The matrix is not quite symmetric because images in the enrollment and verification sets are different.

**Cross country FMR at threshold T = 0.693 for algorithm nodeflux\_001, giving  $\text{FMR}(T) = 0.001$  globally.**

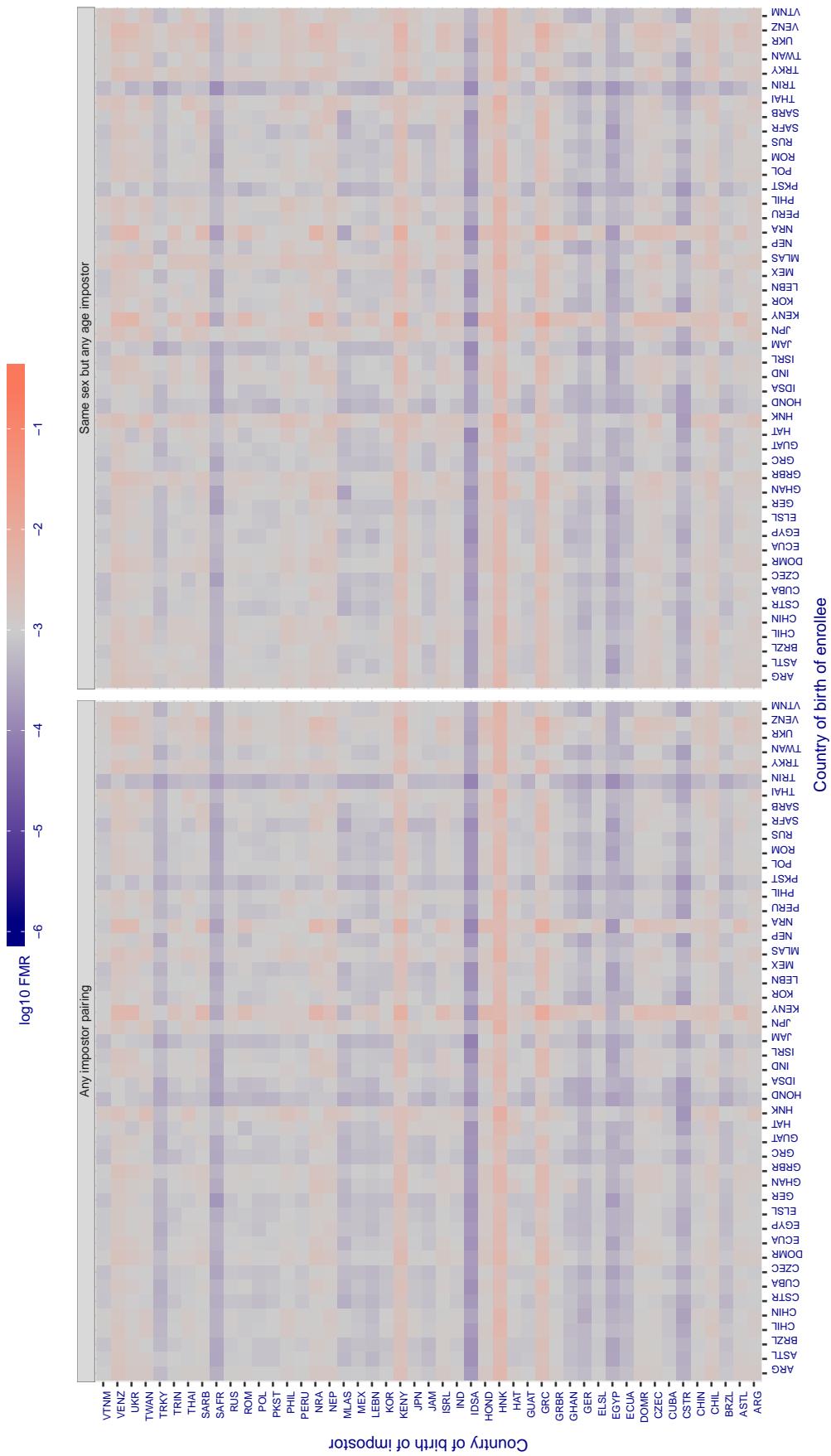


Figure 313: For algorithm nodeflux-001 operating on visa images, the heatmap shows false match rates observed over impostor comparisons of faces from different individuals who were born in the given country pair. False matches are counted against a recognition threshold fixed globally to give the target FMR in the plot title, computed over all on the order of  $10^{10}$  impostor comparisons. If text appears in each box it give the same quantity as that coded by the color. Grey indicates FMR is at the intended FMR target level. Light red colors present a security vulnerability to, for example, a passport gate. Each +1 increase in  $\log_{10} \text{FMR}$  corresponds to a factor of 10 increase in FMR. The matrix is not quite symmetric because images in the enrollment and verification sets are different.

**Cross country FMR at threshold T = 1.929 for algorithm ntchlab\_006, giving  $\text{FMR}(T) = 0.001$  globally.**

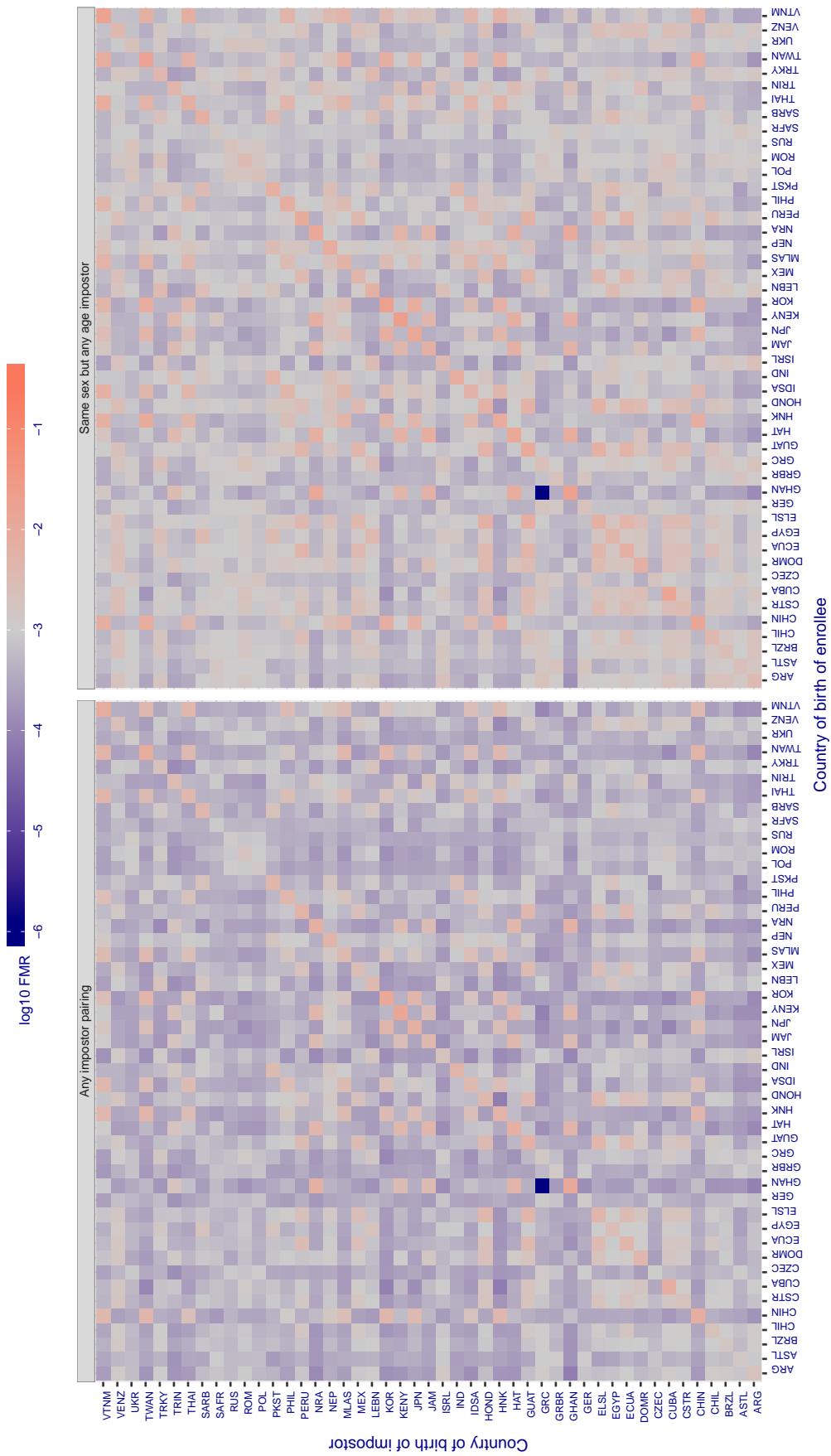


Figure 314: For algorithm ntchlab-006 operating on visa images, the heatmap shows false match rates observed over impostor comparisons of faces from different individuals who were born in the given country pair. False matches are counted against a recognition threshold fixed globally to give the target FMR in the plot title, computed over all on the order of  $10^{10}$  impostor comparisons. If text appears in each box it give the same quantity as that coded by the color. Grey indicates FMR is at the intended FMR target level. Light red colors present a security vulnerability to, for example, a passport gate. Each +1 increase in  $\log_{10} \text{FMR}$  corresponds to a factor of 10 increase in FMR. The matrix is not quite symmetric because images in the enrollment and verification sets are different.

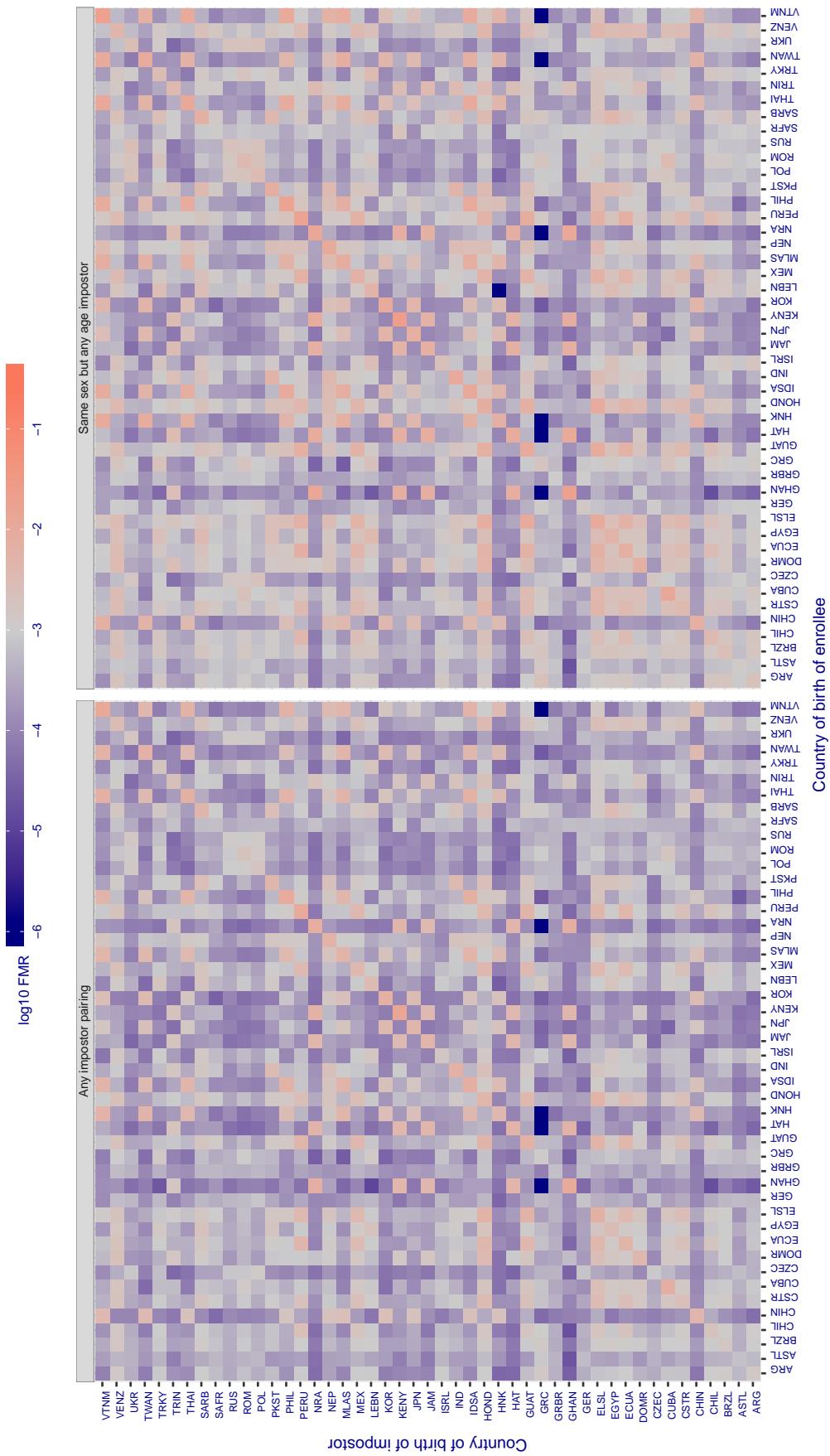
**Cross country FMR at threshold T = 0.253 for algorithm ps1\_001, giving FMR(T) = 0.001 globally.**

Figure 315: For algorithm ps1-001 operating on visa images, the heatmap shows false match rates observed over impostor comparisons of faces from different individuals who were born in the given country pair. False matches are counted against a recognition threshold fixed globally to give the target FMR in the plot title, computed over all on the order of  $10^{10}$  impostor comparisons. If text appears in each box it give the same quantity as that coded by the color. Grey indicates FMR is at the intended FMR target level. Light red colors present a security vulnerability to, for example, a passport gate. Each +1 increase in  $\log_{10} \text{FMR}$  corresponds to a factor of 10 increase in FMR. The matrix is not quite symmetric because images in the enrollment and verification sets are different.

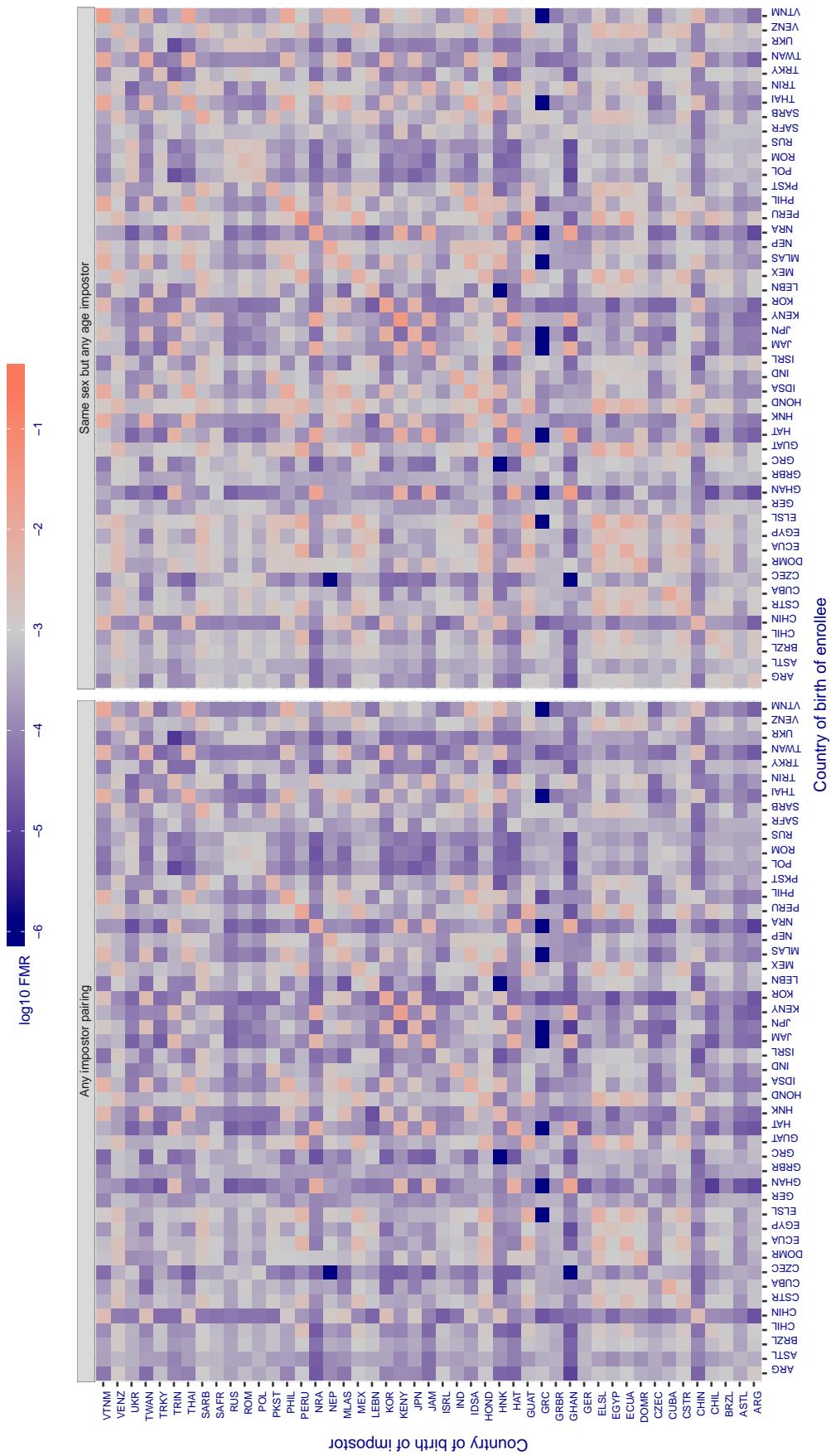
**Cross country FMR at threshold T = 0.272 for algorithm ps1\_002, giving  $\text{FMR}(T) = 0.001$  globally.**

Figure 316: For algorithm ps1\_002 operating on visa images, the heatmap shows false match rates observed over impostor comparisons of faces from different individuals who were born in the given country pair. False matches are counted against a recognition threshold fixed globally to give the target FMR in the plot title, computed over all on the order of  $10^{10}$  impostor comparisons. If text appears in each box it give the same quantity as that coded by the color. Grey indicates FMR is at the intended FMR target level. Light red colors present a security vulnerability to, for example, a passport gate. Each +1 increase in  $\log_{10} \text{FMR}$  corresponds to a factor of 10 increase in FMR. The matrix is not quite symmetric because images in the enrollment and verification sets are different.

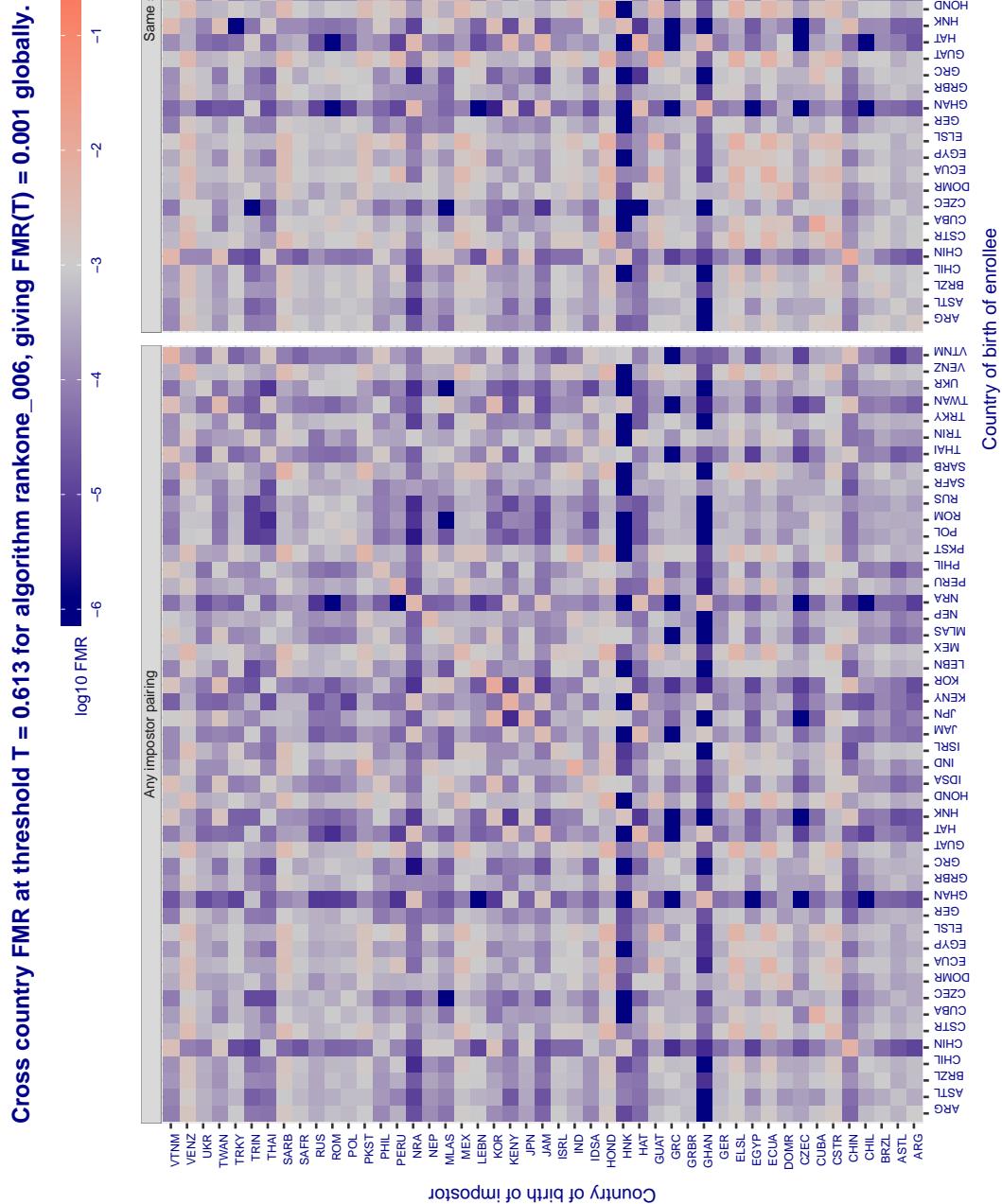


Figure 317: For algorithm rankone-006 operating on visa images, the heatmap shows false match rates observed over impostor comparisons of faces from different individuals who were born in the given country pair. False matches are counted against a recognition threshold fixed globally to give the target FMR in the plot title, computed over all on the order of  $10^{10}$  impostor comparisons. If text appears in each box it give the same quantity as that coded by the color. Grey indicates FMR is at the intended FMR target level. Light red colors present a security vulnerability to, for example, a passport gate. Each +1 increase in  $\log_{10}$  FMR corresponds to a factor of 10 increase in FMR. The matrix is not quite symmetric because images in the enrollment and verification sets are different.

**Cross country FMR at threshold T = 0.814 for algorithm realnetworks\_002, giving  $\text{FMR}(T) = 0.001$  globally.**

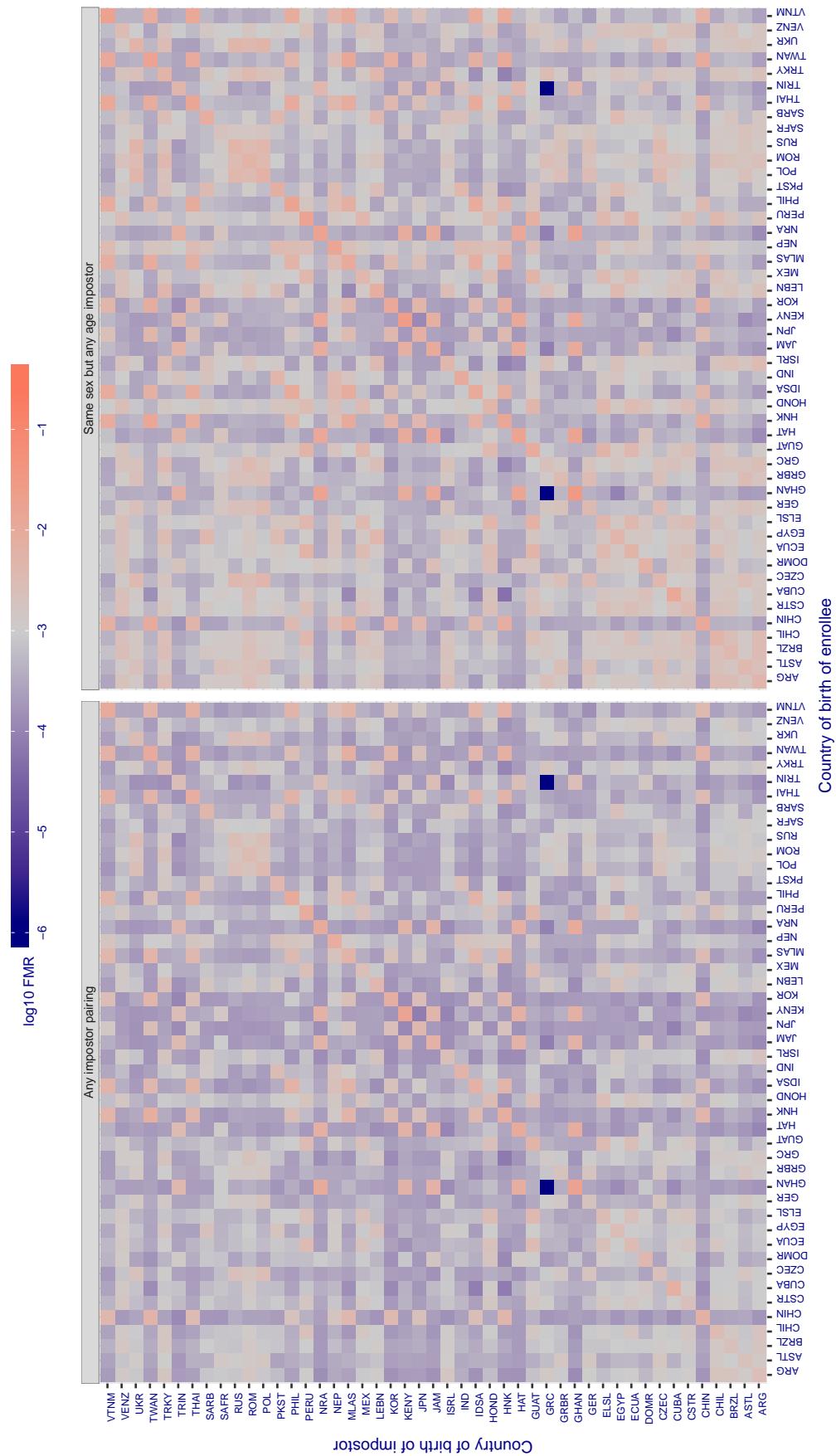


Figure 318: For algorithm realnetworks-002 operating on visa images, the heatmap shows false match rates observed over impostor comparisons of faces from different individuals who were born in the given country pair. False matches are counted against a recognition threshold fixed globally to give the target  $\text{FMR}$  in the plot title, computed over all on the order of  $10^{10}$  impostor comparisons. If text appears in each box it give the same quantity as that coded by the color. Grey indicates  $\text{FMR}$  is at the intended  $\text{FMR}$  target level. Light red colors present a security vulnerability to, for example, a passport gate. Each +1 increase in  $\log_{10} \text{FMR}$  corresponds to a factor of 10 increase in  $\text{FMR}$ . The matrix is not quite symmetric because images in the enrollment and verification sets are different.

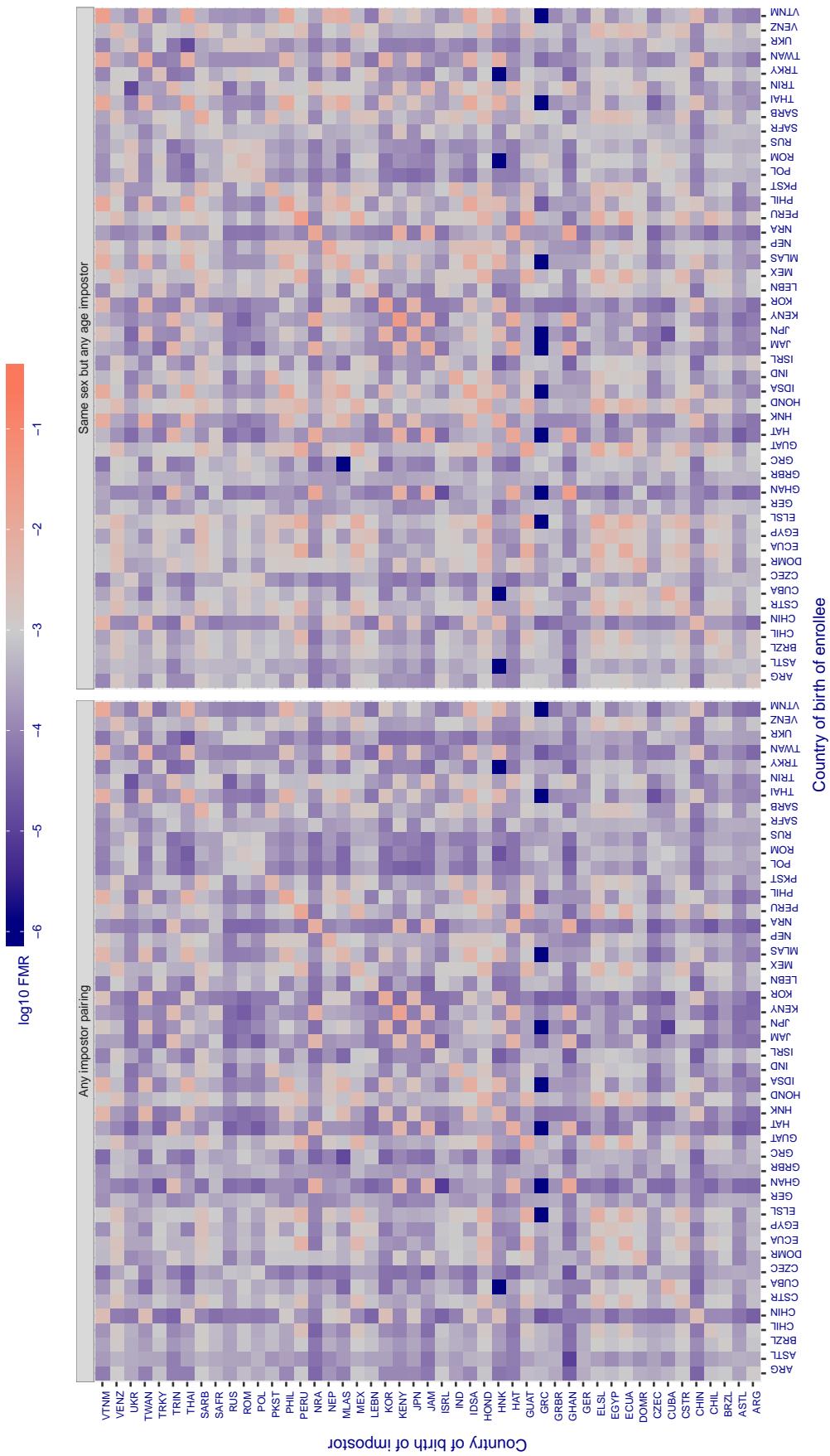
**Cross country FMR at threshold T = 65.920 for algorithm remarkai\_000, giving FMR(T) = 0.001 globally.**

Figure 319: For algorithm remarkai-000 operating on visa images, the heatmap shows false match rates observed over impostor comparisons of faces from different individuals who were born in the given country pair. False matches are counted against a recognition threshold fixed globally to give the target FMR in the plot title, computed over all on the order of  $10^{10}$  impostor comparisons. If text appears in each box it give the same quantity as that coded by the color. Grey indicates FMR is at the intended FMR target level. Light red colors present a security vulnerability to, for example, a passport gate. Each +1 increase in  $\log_{10} \text{FMR}$  corresponds to a factor of 10 increase in FMR. The matrix is not quite symmetric because images in the enrollment and verification sets are different.

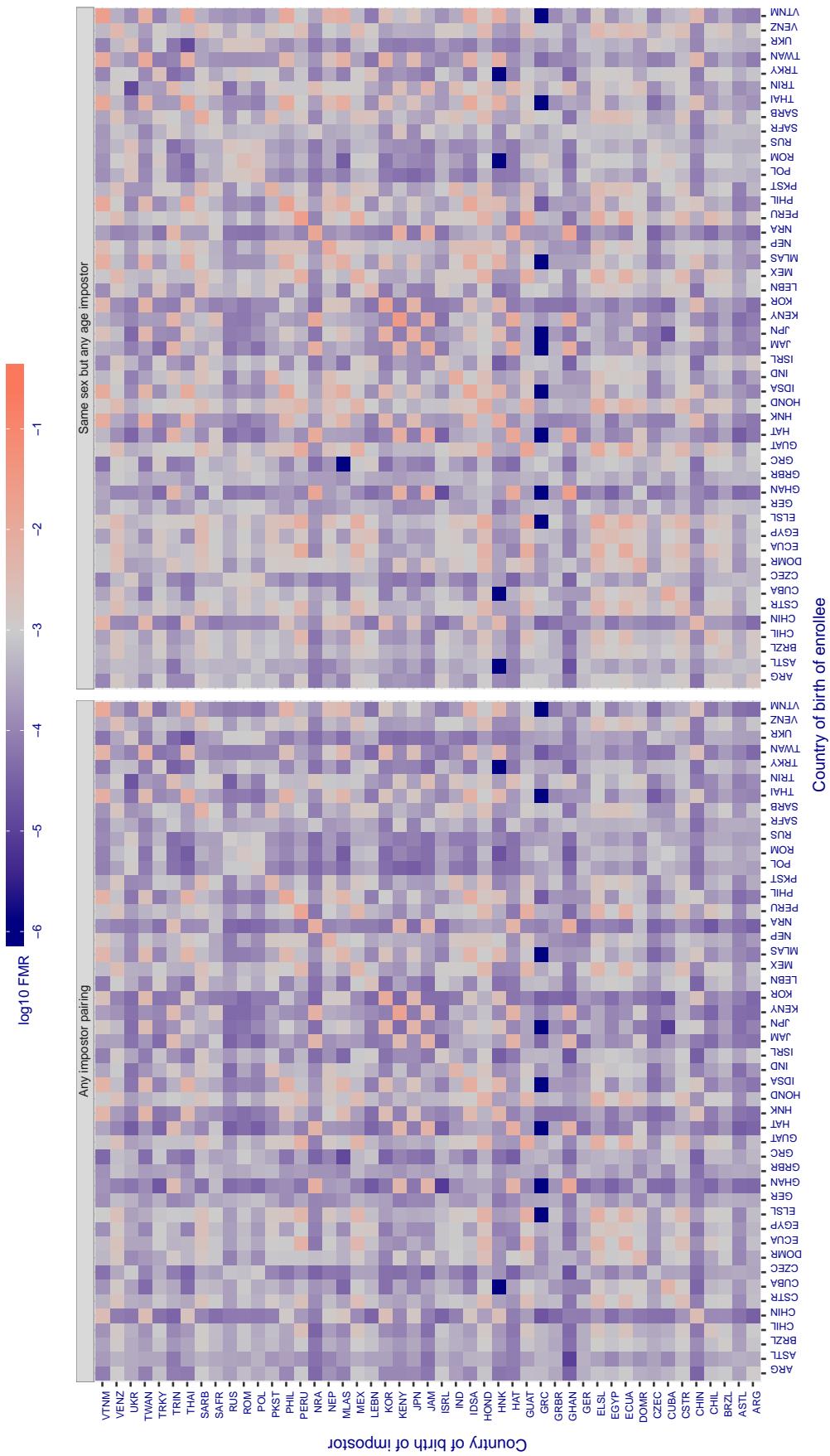
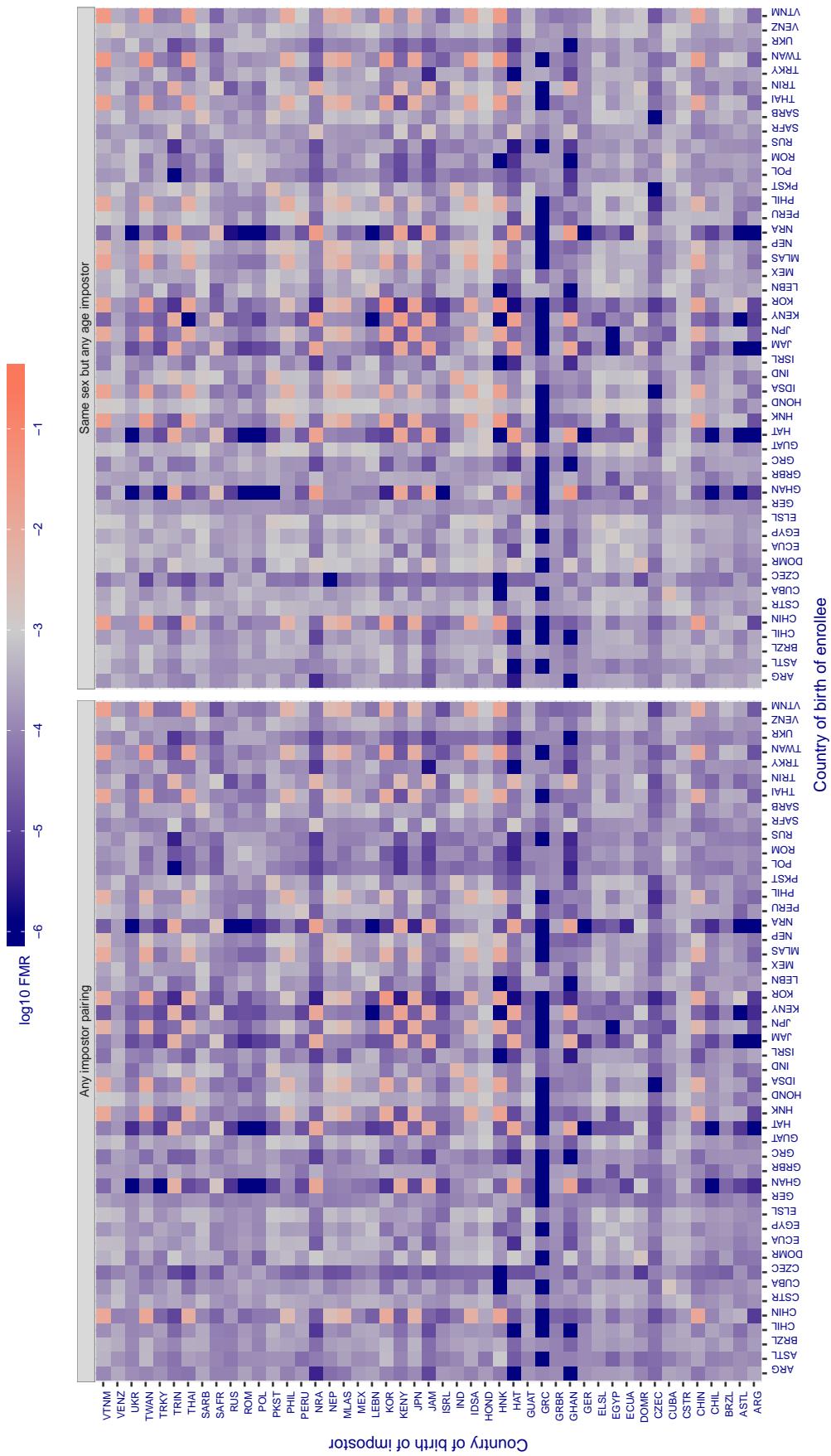
**Cross country FMR at threshold T = 65.928 for algorithm remarkai\_001, giving FMR(T) = 0.001 globally.**

Figure 320: For algorithm remarkai-001 operating on visa images, the heatmap shows false match rates observed over impostor comparisons of faces from different individuals who were born in the given country pair. False matches are counted against a recognition threshold fixed globally to give the target FMR in the plot title, computed over all on the order of  $10^{10}$  impostor comparisons. If text appears in each box it give the same quantity as that coded by the color. Grey indicates FMR is at the intended FMR target level. Light red colors present a security vulnerability to, for example, a passport gate. Each +1 increase in  $\log_{10} \text{FMR}$  corresponds to a factor of 10 increase in FMR. The matrix is not quite symmetric because images in the enrollment and verification sets are different.



**Figure 321:** For algorithm *saffe-001* operating on visa images, the heatmap shows false match rates observed over impostor comparisons of faces from different individuals who were born in the given country pair. False matches are counted against a recognition threshold fixed globally to give the target FMR in the plot title, computed over all on the order of  $10^{10}$  impostor comparisons. If text appears in each box it give the same quantity as that coded by the color. Grey indicates FMR is at the intended FMR target level. Light red colors present a security vulnerability to, for example, a passport gate. Each +1 increase in  $\log_{10} \text{FMR}$  corresponds to a factor of 10 increase in FMR. The matrix is not quite symmetric because images in the enrollment and verification sets are different.

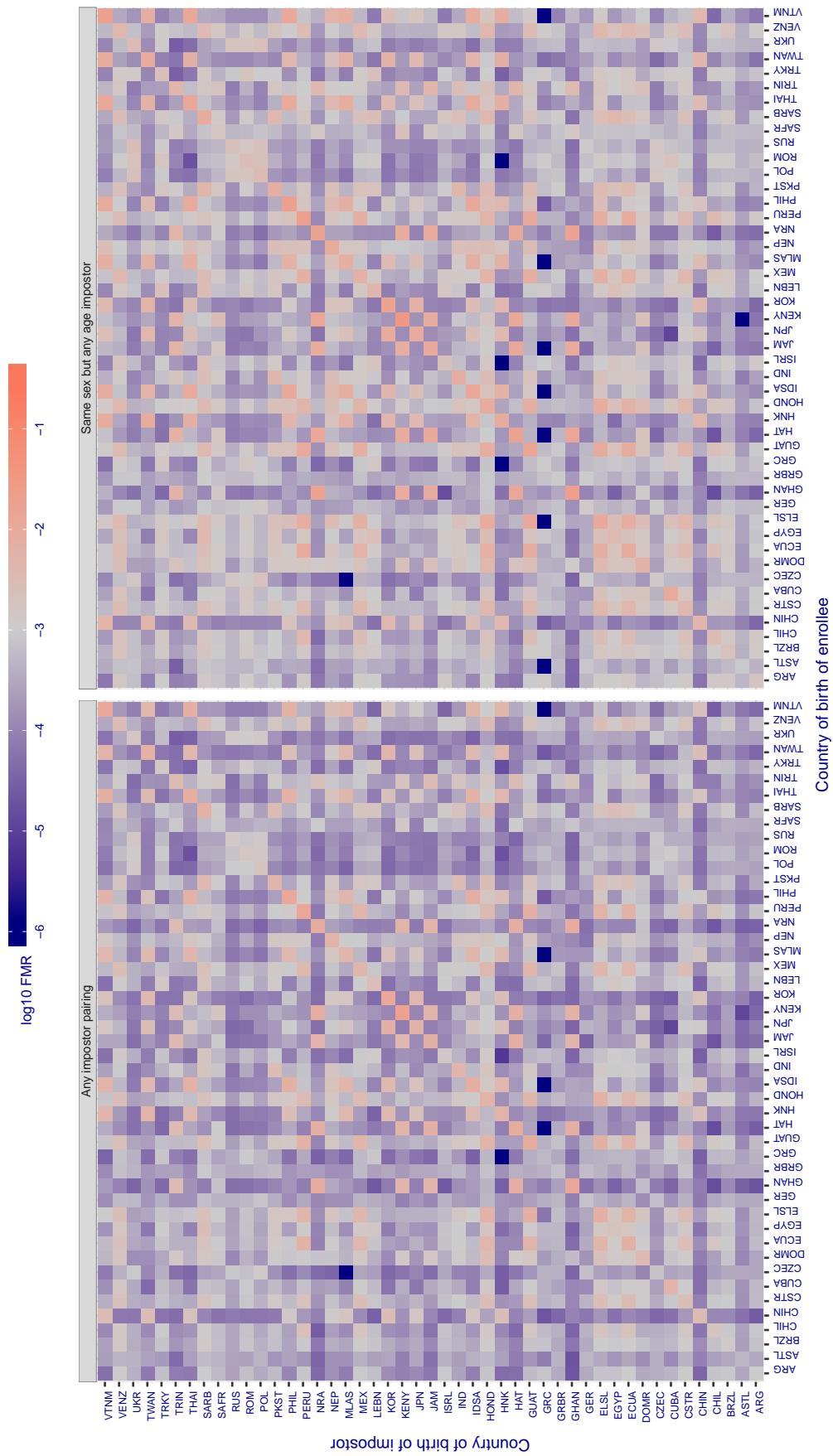
**Cross country FMR at threshold T = 0.295 for algorithm saffe\_002, giving FMR(T) = 0.001 globally.**

Figure 322: For algorithm saffe-002 operating on visa images, the heatmap shows false match rates observed over impostor comparisons of faces from different individuals who were born in the given country pair. False matches are counted against a recognition threshold fixed globally to give the target FMR in the plot title, computed over all on the order of  $10^{10}$  impostor comparisons. If text appears in each box it give the same quantity as that coded by the color. Grey indicates FMR is at the intended FMR target level. Light red colors present a security vulnerability to, for example, a passport gate. Each +1 increase in  $\log_{10} \text{FMR}$  corresponds to a factor of 10 increase in FMR. The matrix is not quite symmetric because images in the enrollment and verification sets are different.

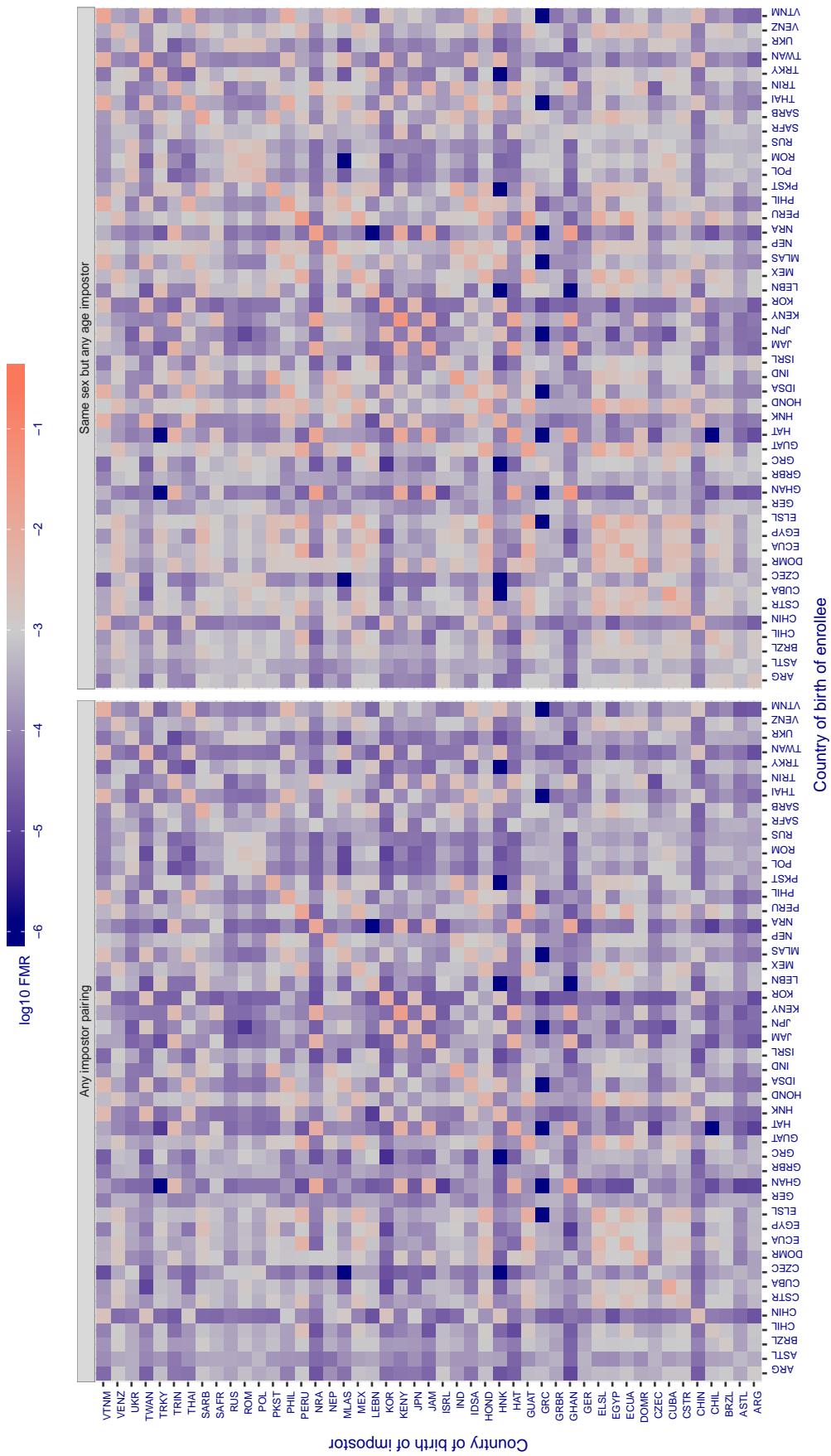
**Cross country FMR at threshold T = 0.368 for algorithm sensetime\_001, giving FMR(T) = 0.001 globally.**

Figure 323: For algorithm sensetime-001 operating on visa images, the heatmap shows false match rates observed over impostor comparisons of faces from different individuals who were born in the given country pair. False matches are counted against a recognition threshold fixed globally to give the target FMR in the plot title, computed over all on the order of  $10^{10}$  impostor comparisons. If text appears in each box it give the same quantity as that coded by the color. Grey indicates FMR is at the intended FMR target level. Light red colors present a security vulnerability to, for example, a passport gate. Each +1 increase in  $\log_{10} \text{FMR}$  corresponds to a factor of 10 increase in FMR. The matrix is not quite symmetric because images in the enrollment and verification sets are different.

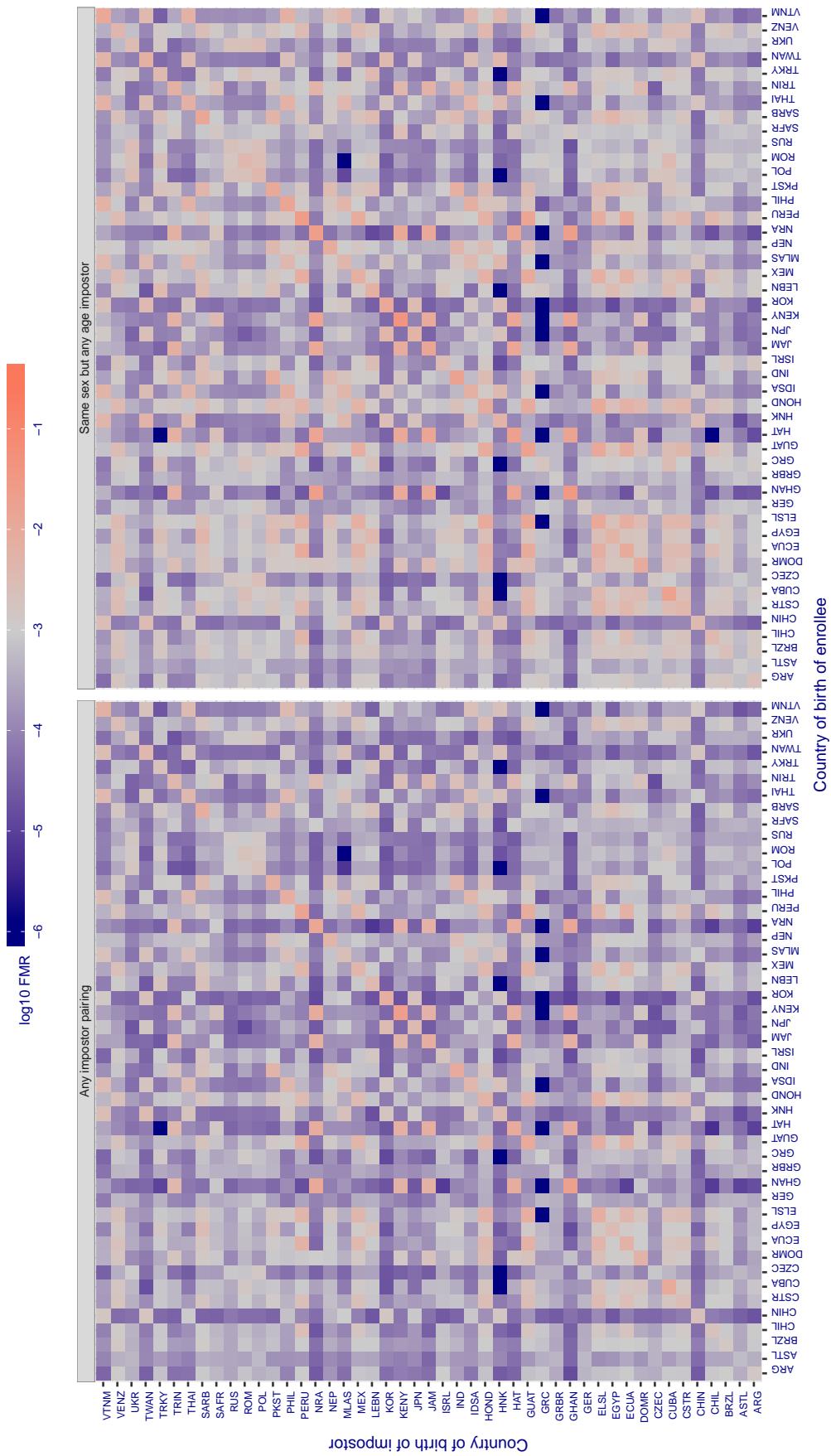
**Cross country FMR at threshold T = 0.369 for algorithm sensetime\_002, giving FMR(T) = 0.001 globally.**

Figure 324: For algorithm sensetime-002 operating on visa images, the heatmap shows false match rates observed over impostor comparisons of faces from different individuals who were born in the given country pair. False matches are counted against a recognition threshold fixed globally to give the target FMR in the plot title, computed over all on the order of  $10^{10}$  impostor comparisons. If text appears in each box it give the same quantity as that coded by the color. Grey indicates FMR is at the intended FMR target level. Light red colors present a security vulnerability to, for example, a passport gate. Each +1 increase in  $\log_{10} FMR$  corresponds to a factor of 10 increase in FMR. The matrix is not quite symmetric because images in the enrollment and verification sets are different.

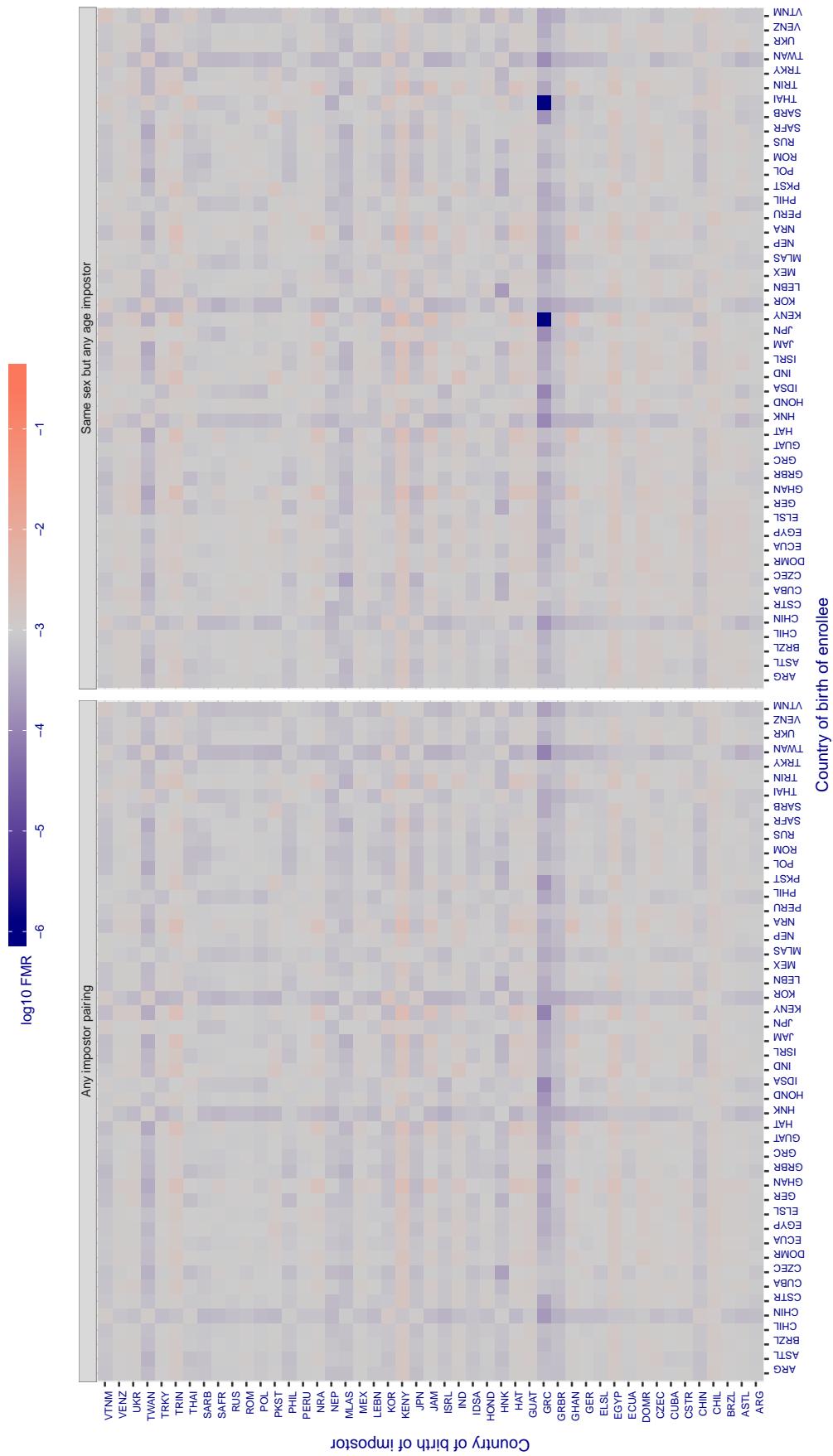
**Cross country FMR at threshold T = 0.939 for algorithm shaman\_000, giving FMR(T) = 0.001 globally.**

Figure 325: For algorithm shaman-000 operating on visa images, the heatmap shows false match rates observed over impostor comparisons of faces from different individuals who were born in the given country pair. False matches are counted against a recognition threshold fixed globally to give the target FMR in the plot title, computed over all on the order of  $10^{10}$  impostor comparisons. If text appears in each box it give the same quantity as that coded by the color. Grey indicates FMR is at the intended FMR target level. Light red colors present a security vulnerability to, for example, a passport gate. Each +1 increase in  $\log_{10} \text{FMR}$  corresponds to a factor of 10 increase in FMR. The matrix is not quite symmetric because images in the enrollment and verification sets are different.

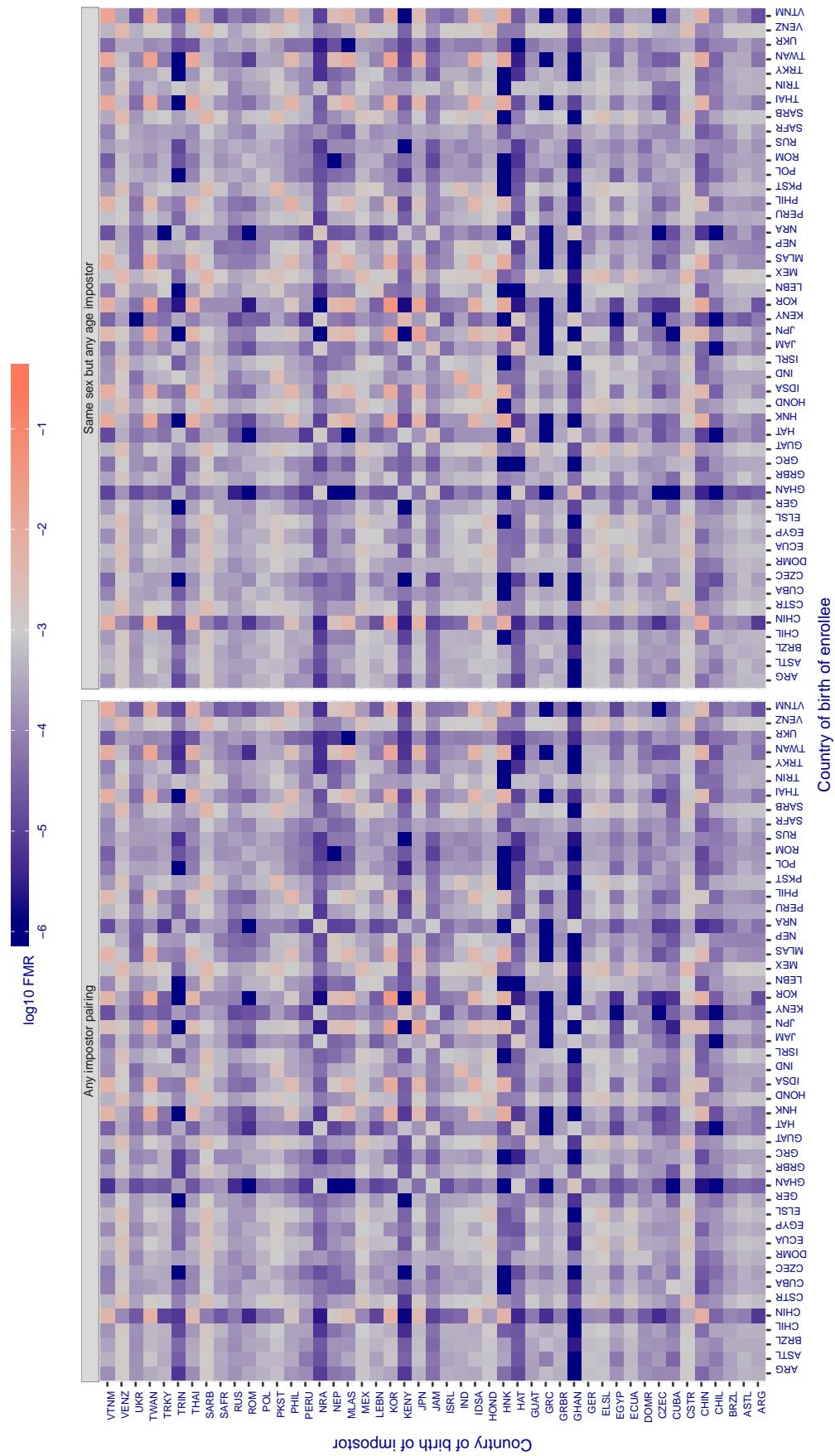
**Cross country FMR at threshold T = 0.599 for algorithm shaman\_001, giving FMR(T) = 0.001 globally.**

Figure 326: For algorithm shaman-001 operating on visa images, the heatmap shows false match rates observed over impostor comparisons of faces from different individuals who were born in the given country pair. False matches are counted against a recognition threshold fixed globally to give the target FMR in the plot title, computed over all on the order of  $10^{10}$  impostor comparisons. If text appears in each box it give the same quantity as that coded by the color. Grey indicates FMR is at the intended FMR target level. Light red colors present a security vulnerability to, for example, a passport gate. Each +1 increase in  $\log_{10} FMR$  corresponds to a factor of 10 increase in FMR. The matrix is not quite symmetric because images in the enrollment and verification sets are different.

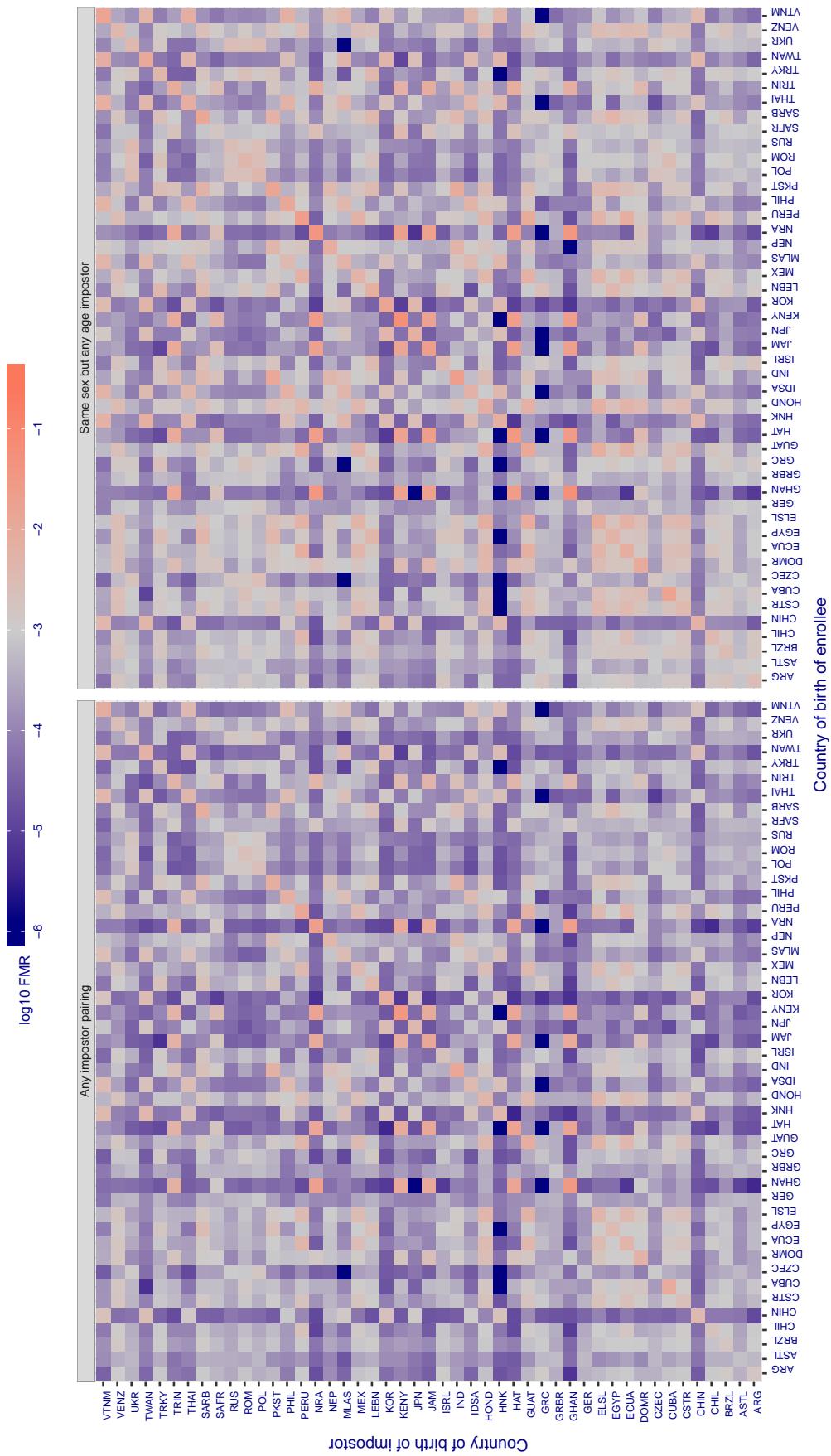
**Cross country FMR at threshold T = 0.370 for algorithm siat\_002, giving FMR(T) = 0.001 globally.**

Figure 327: For algorithm siat-002 operating on visa images, the heatmap shows false match rates observed over impostor comparisons of faces from different individuals who were born in the given country pair. False matches are counted against a recognition threshold fixed globally to give the target FMR in the plot title, computed over all on the order of  $10^{10}$  impostor comparisons. If text appears in each box it give the same quantity as that coded by the color. Grey indicates FMR is at the intended FMR target level. Light red colors present a security vulnerability to, for example, a passport gate. Each +1 increase in  $\log_{10} \text{FMR}$  corresponds to a factor of 10 increase in FMR. The matrix is not quite symmetric because images in the enrollment and verification sets are different.

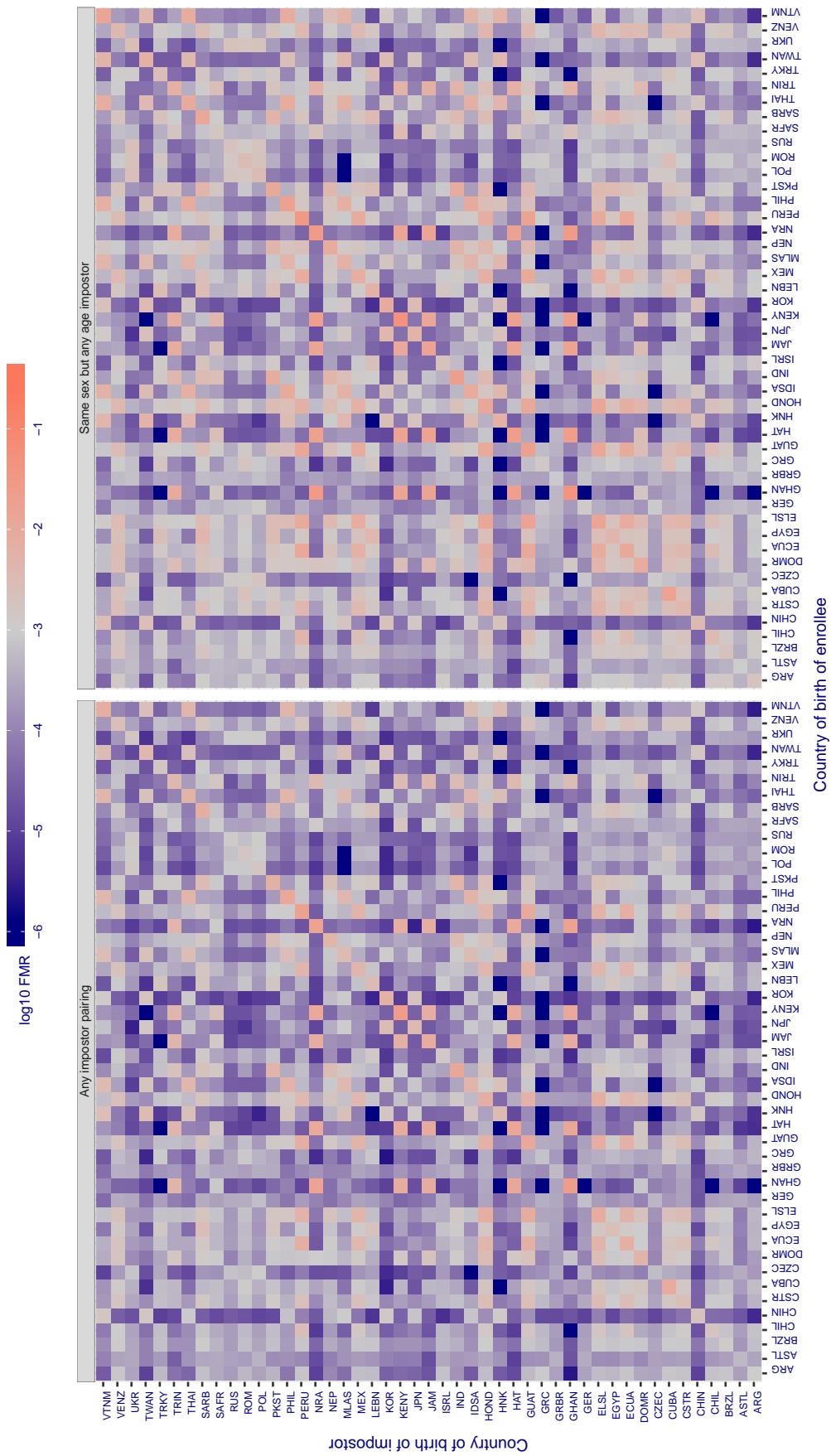
**Cross country FMR at threshold T = 0.371 for algorithm siat\_004, giving FMR(T) = 0.001 globally.**

Figure 328: For algorithm siat-004 operating on visa images, the heatmap shows false match rates observed over impostor comparisons of faces from different individuals who were born in the given country pair. False matches are counted against a recognition threshold fixed globally to give the target FMR in the plot title, computed over all on the order of  $10^{10}$  impostor comparisons. If text appears in each box it give the same quantity as that coded by the color. Grey indicates FMR is at the intended FMR target level. Light red colors present a security vulnerability to, for example, a passport gate. Each +1 increase in  $\log_{10} \text{FMR}$  corresponds to a factor of 10 increase in FMR. The matrix is not quite symmetric because images in the enrollment and verification sets are different.

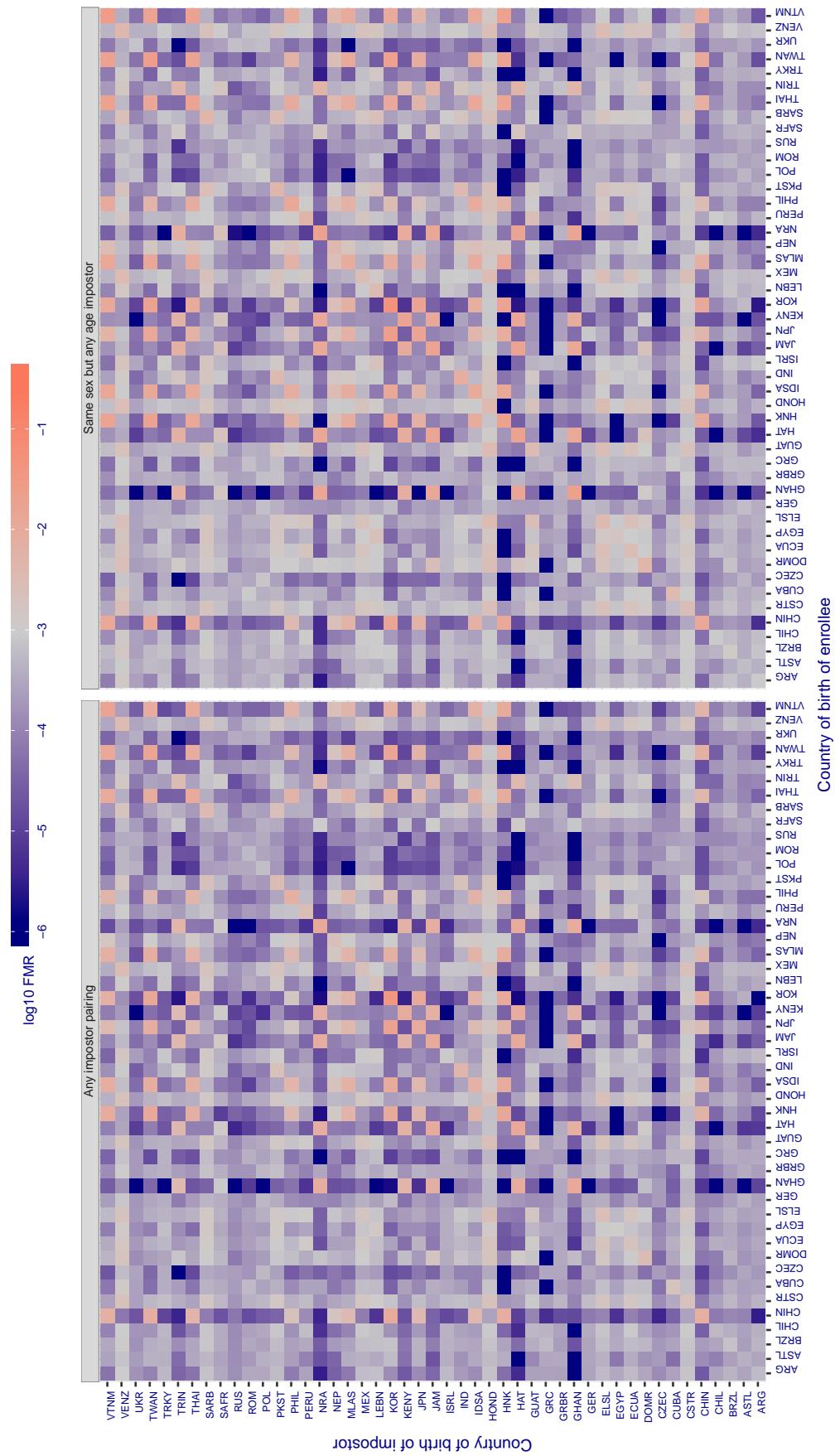
**Cross country FMR at threshold T = 0.488 for algorithm smilart\_002, giving FMR(T) = 0.001 globally.**

Figure 329: For algorithm smilart-002 operating on visa images, the heatmap shows false match rates observed over impostor comparisons of faces from different individuals who were born in the given country pair. False matches are counted against a recognition threshold fixed globally to give the target FMR in the plot title, computed over all on the order of  $10^{10}$  impostor comparisons. If text appears in each box it give the same quantity as that coded by the color. Grey indicates FMR is at the intended FMR target level. Light red colors present a security vulnerability to, for example, a passport gate. Each +1 increase in  $\log_{10}$  FMR corresponds to a factor of 10 increase in FMR. The matrix is not quite symmetric because images in the enrollment and verification sets are different.

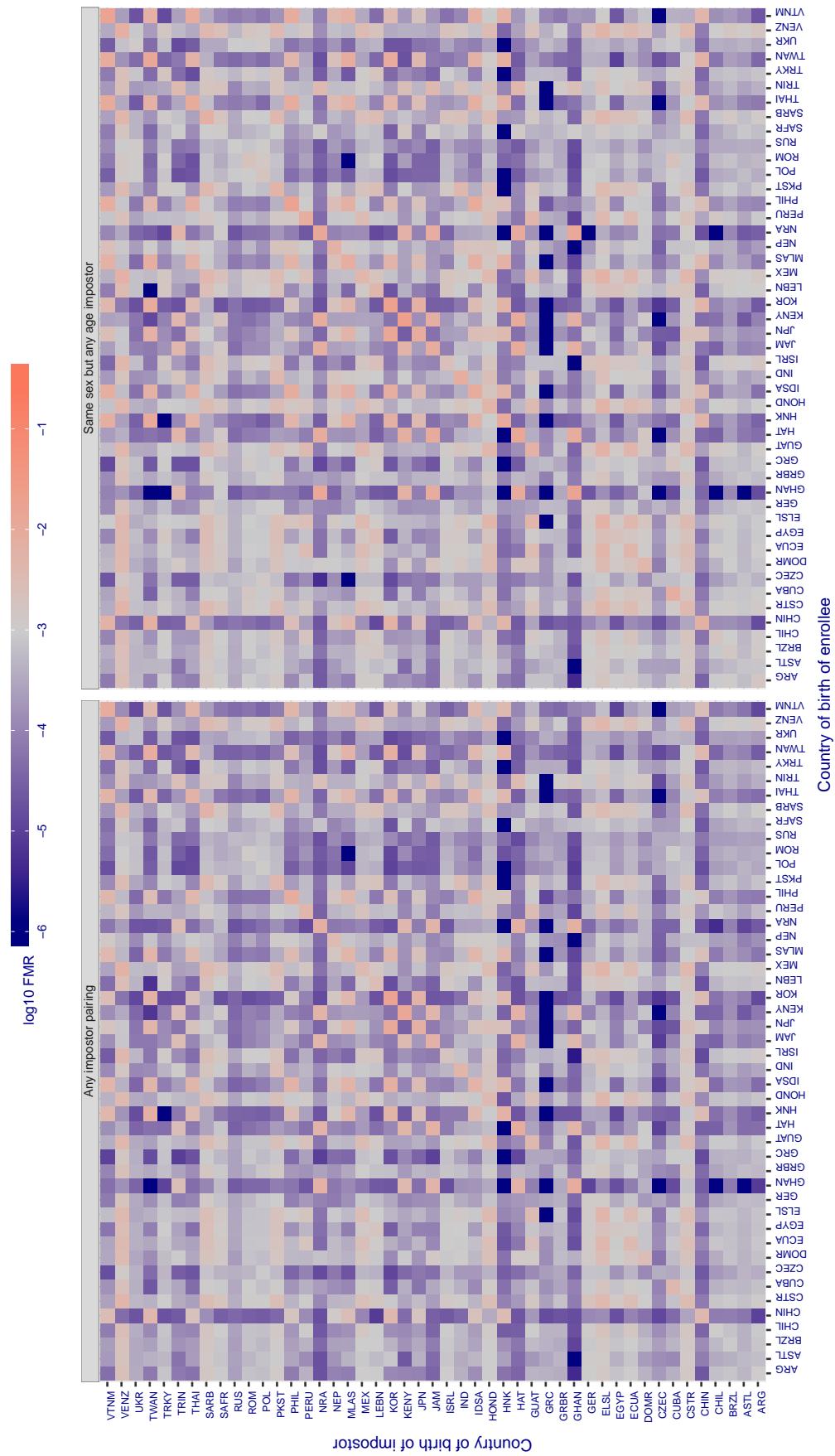
**Cross country FMR at threshold T = 0.388 for algorithm smilart\_003, giving FMR(T) = 0.001 globally.**

Figure 330: For algorithm smilart-003 operating on visa images, the heatmap shows false match rates observed over impostor comparisons of faces from different individuals who were born in the given country pair. False matches are counted against a recognition threshold fixed globally to give the target FMR in the plot title, computed over all on the order of  $10^{10}$  impostor comparisons. If text appears in each box it give the same quantity as that coded by the color. Grey indicates FMR is at the intended FMR target level. Light red colors present a security vulnerability to, for example, a passport gate. Each +1 increase in  $\log_{10} FMR$  corresponds to a factor of 10 increase in FMR. The matrix is not quite symmetric because images in the enrollment and verification sets are different.

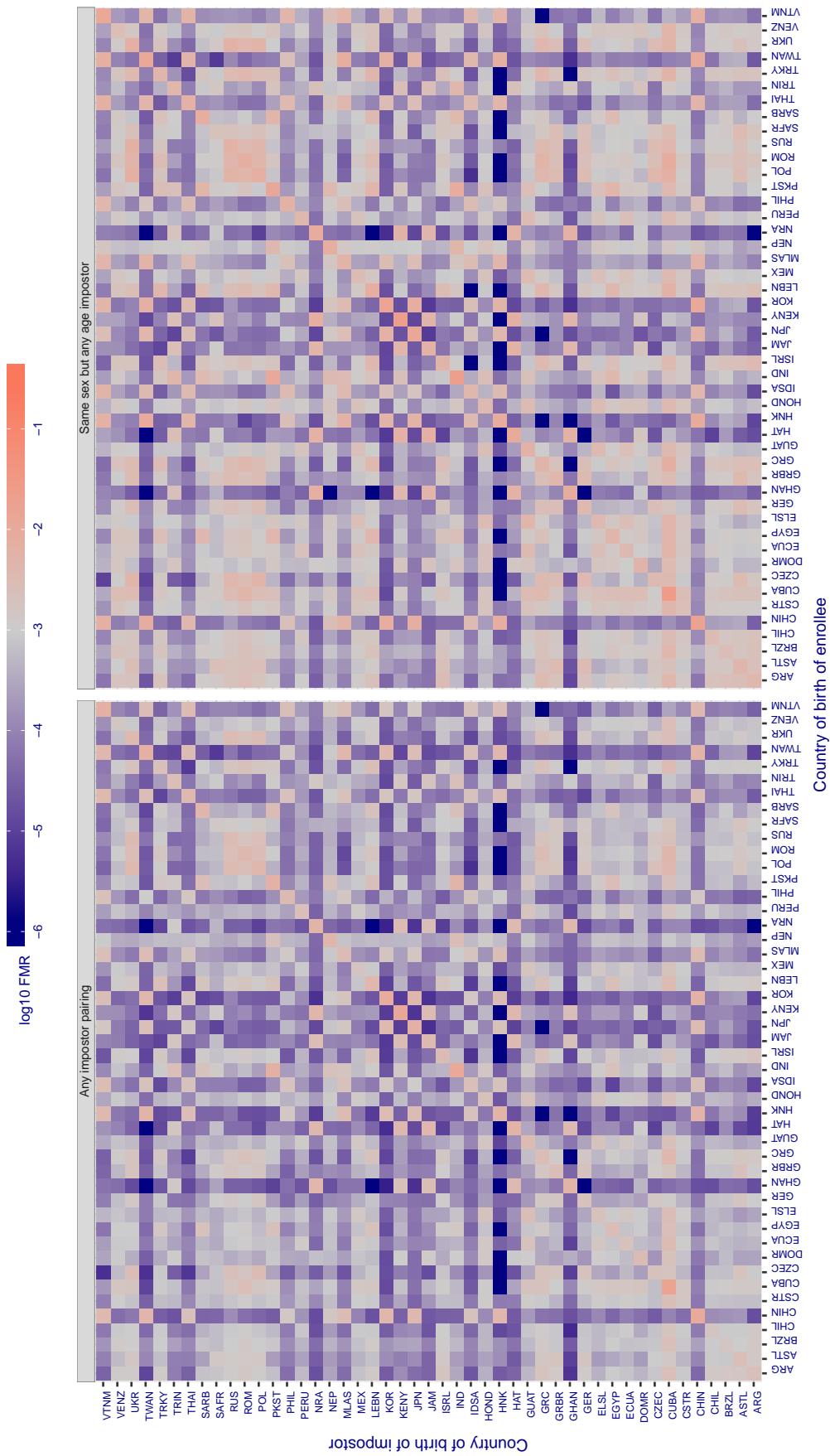
**Cross country FMR at threshold T = 148.095 for algorithm tech5\_001, giving  $FMR(T) = 0.001$  globally.**

Figure 331: For algorithm tech5-001 operating on visa images, the heatmap shows false match rates observed over impostor comparisons of faces from different individuals who were born in the given country pair. False matches are counted against a recognition threshold fixed globally to give the target FMR in the plot title, computed over all on the order of  $10^{10}$  impostor comparisons. If text appears in each box it give the same quantity as that coded by the color. Grey indicates FMR is at the intended FMR target level. Light red colors present a security vulnerability to, for example, a passport gate. Each +1 increase in  $\log_{10} FMR$  corresponds to a factor of 10 increase in FMR. The matrix is not quite symmetric because images in the enrollment and verification sets are different.

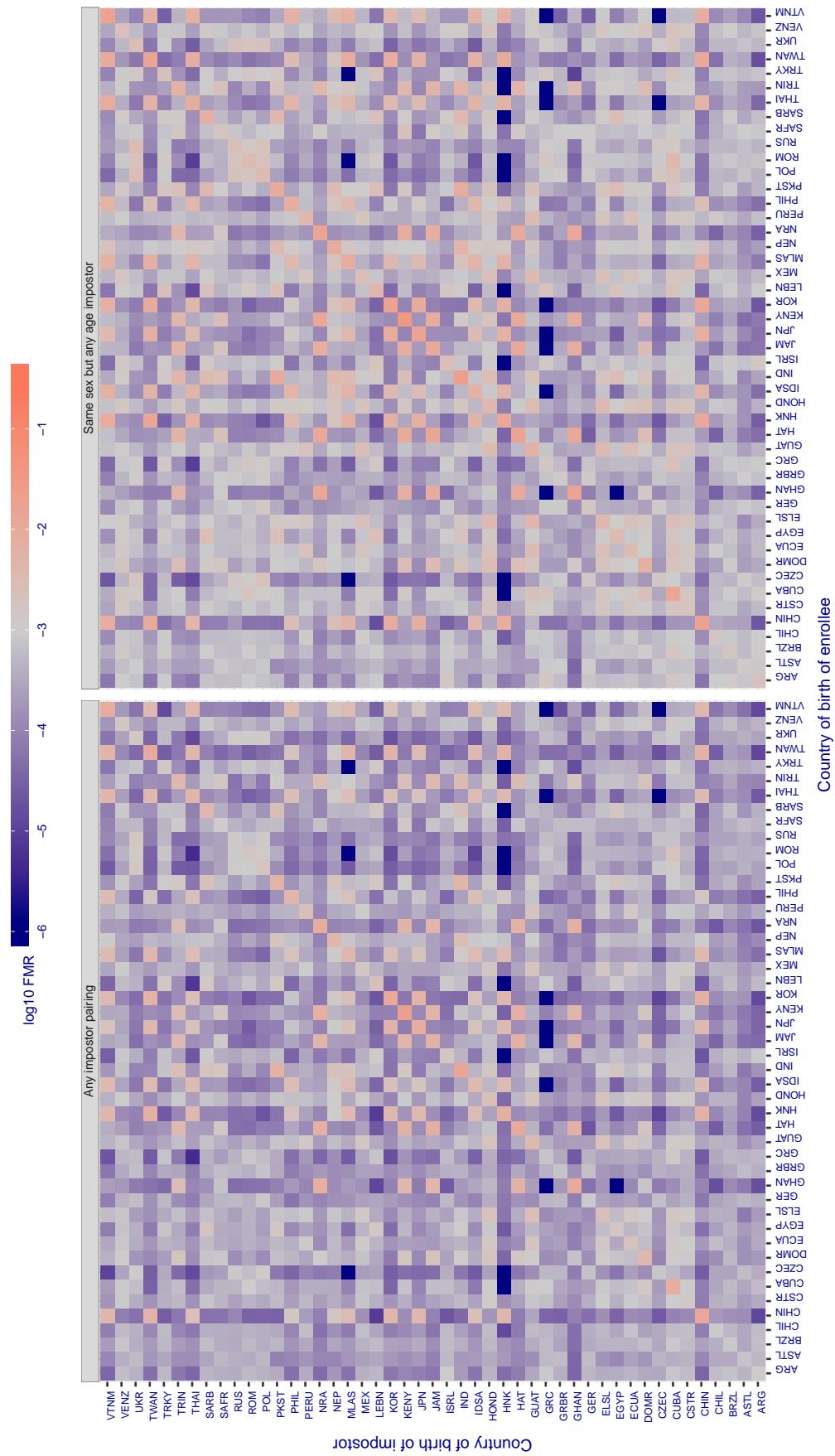
**Cross country FMR at threshold T = 147.234 for algorithm tech5\_002, giving  $FMR(T) = 0.001$  globally.**

Figure 332: For algorithm tech5-002 operating on visa images, the heatmap shows false match rates observed over impostor comparisons of faces from different individuals who were born in the given country pair. False matches are counted against a recognition threshold fixed globally to give the target FMR in the plot title, computed over all on the order of  $10^{10}$  impostor comparisons. If text appears in each box it give the same quantity as that coded by the color. Grey indicates FMR is at the intended FMR target level. Light red colors present a security vulnerability to, for example, a passport gate. Each +1 increase in  $\log_{10} FMR$  corresponds to a factor of 10 increase in FMR. The matrix is not quite symmetric because images in the enrollment and verification sets are different.

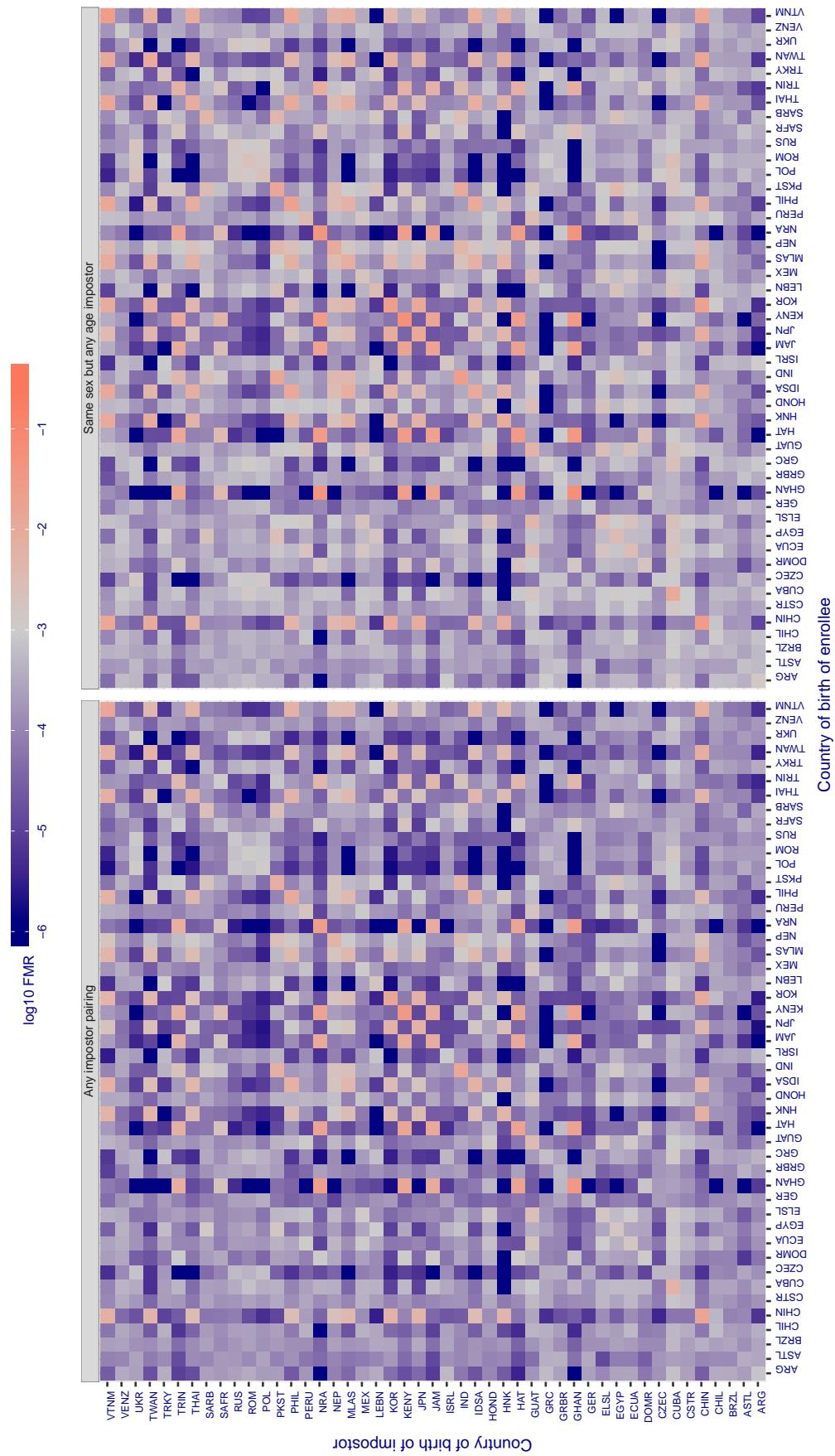
**Cross country FMR at threshold T = 0.769 for algorithm tevian\_003, giving FMR(T) = 0.001 globally.**

Figure 333: For algorithm tevian-003 operating on visa images, the heatmap shows false match rates observed over impostor comparisons of faces from different individuals who were born in the given country pair. False matches are counted against a recognition threshold fixed globally to give the target FMR in the plot title, computed over all on the order of  $10^{10}$  impostor comparisons. If text appears in each box it give the same quantity as that coded by the color. Grey indicates FMR is at the intended FMR target level. Light red colors present a security vulnerability to, for example, a passport gate. Each +1 increase in  $\log_{10} FMR$  corresponds to a factor of 10 increase in FMR. The matrix is not quite symmetric because images in the enrollment and verification sets are different.

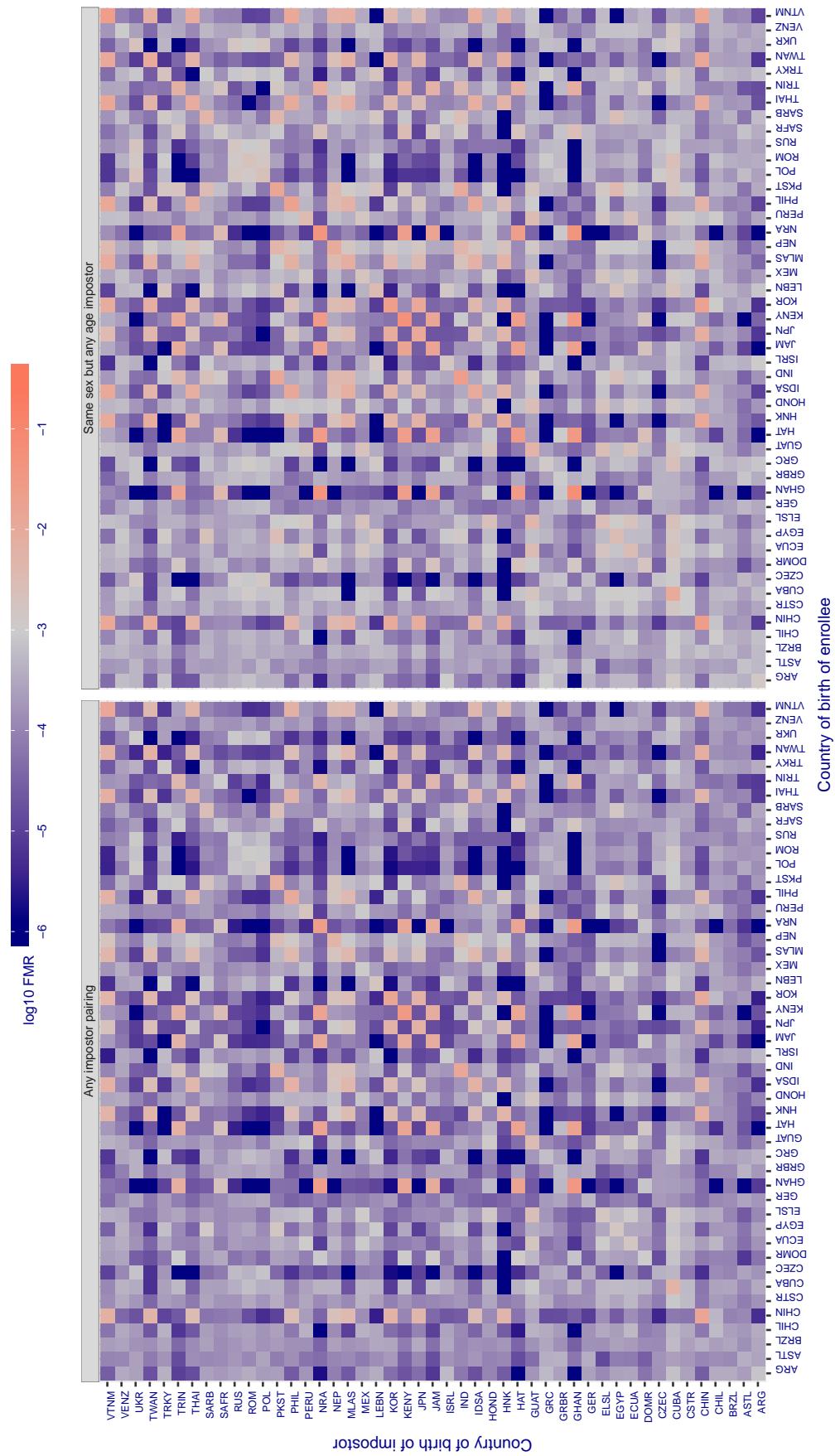
**Cross country FMR at threshold T = 0.769 for algorithm tevian\_004, giving FMR(T) = 0.001 globally.**

Figure 334: For algorithm tevian-004 operating on visa images, the heatmap shows false match rates observed over impostor comparisons of faces from different individuals who were born in the given country pair. False matches are counted against a recognition threshold fixed globally to give the target FMR in the plot title, computed over all on the order of  $10^{10}$  impostor comparisons. If text appears in each box it give the same quantity as that coded by the color. Grey indicates FMR is at the intended FMR target level. Light red colors present a security vulnerability to, for example, a passport gate. Each +1 increase in  $\log_{10} FMR$  corresponds to a factor of 10 increase in FMR. The matrix is not quite symmetric because images in the enrollment and verification sets are different.

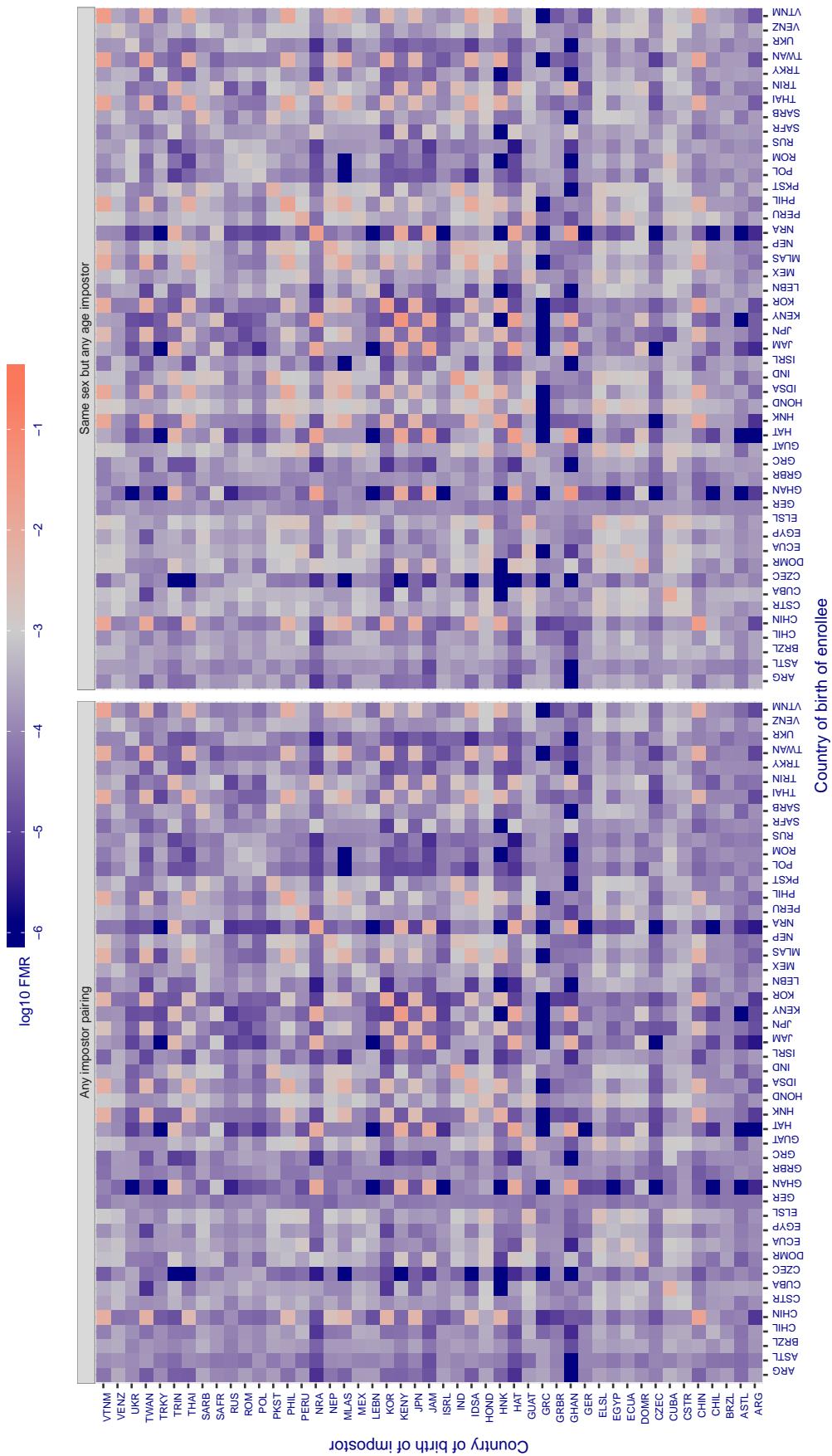


Figure 335: For algorithm tiger-002 operating on visa images, the heatmap shows false match rates observed over impostor comparisons of faces from different individuals who were born in the given country pair. False matches are counted against a recognition threshold fixed globally to give the target FMR in the plot title, computed over all on the order of  $10^{10}$  impostor comparisons. If text appears in each box it give the same quantity as that coded by the color. Grey indicates FMR is at the intended FMR target level. Light red colors present a security vulnerability to, for example, a passport gate. Each +1 increase in  $\log_{10} \text{FMR}$  corresponds to a factor of 10 increase in FMR. The matrix is not quite symmetric because images in the enrollment and verification sets are different.

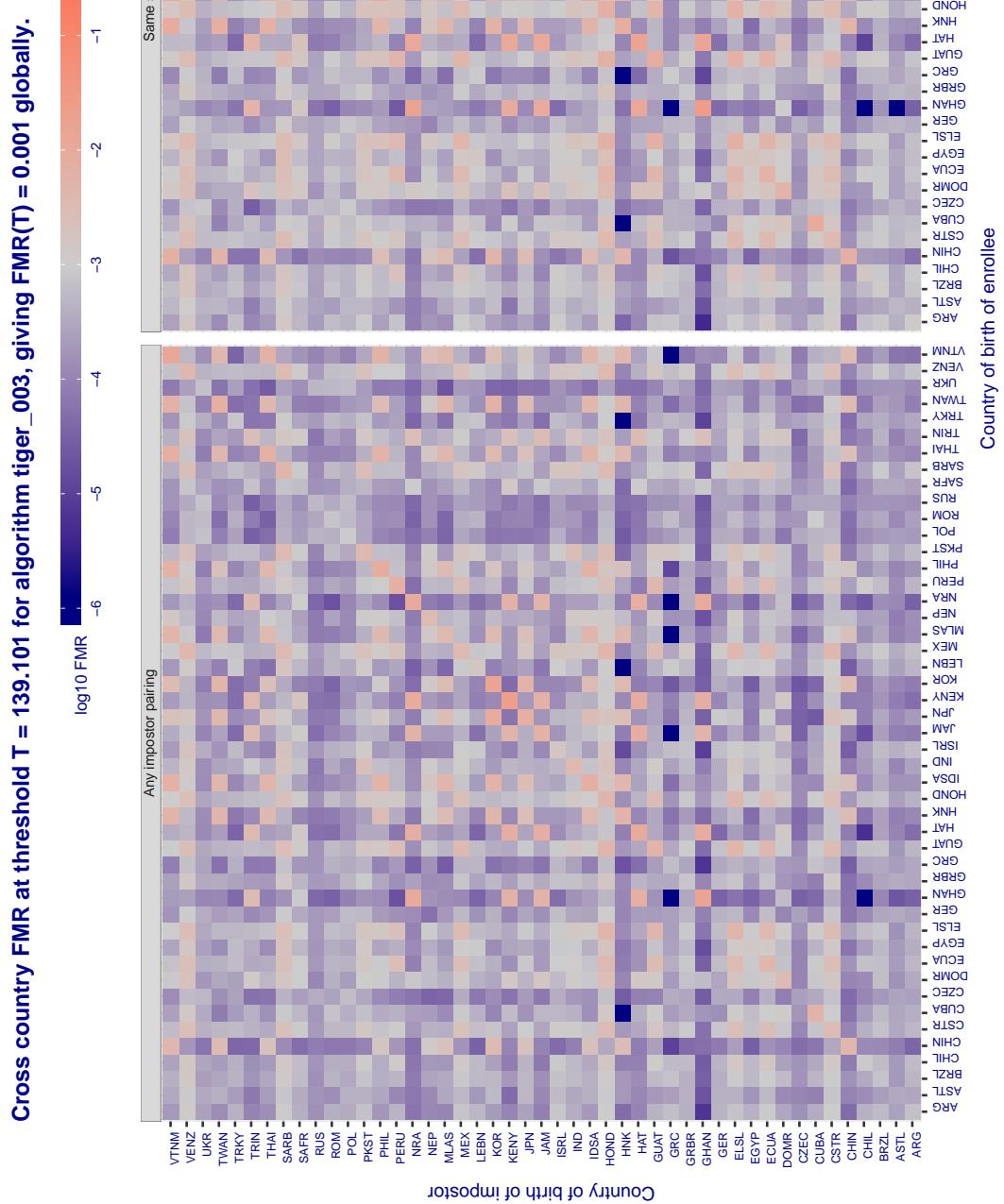


Figure 336: For algorithm tiger-003 operating on visa images, the heatmap shows false match rates observed over impostor comparisons of faces from different individuals who were born in the given country pair. False matches are counted against a recognition threshold fixed globally to give the target FMR in the plot title, computed over all on the order of  $10^{10}$  impostor comparisons. If text appears in each box it give the same quantity as that coded by the color. Grey indicates FMR is at the intended FMR target level. Light red colors present a security vulnerability to, for example, a passport gate. Each +1 increase in  $\log_{10} \text{FMR}$  corresponds to a factor of 10 increase in FMR. The matrix is not quite symmetric because images in the enrollment and verification sets are different.

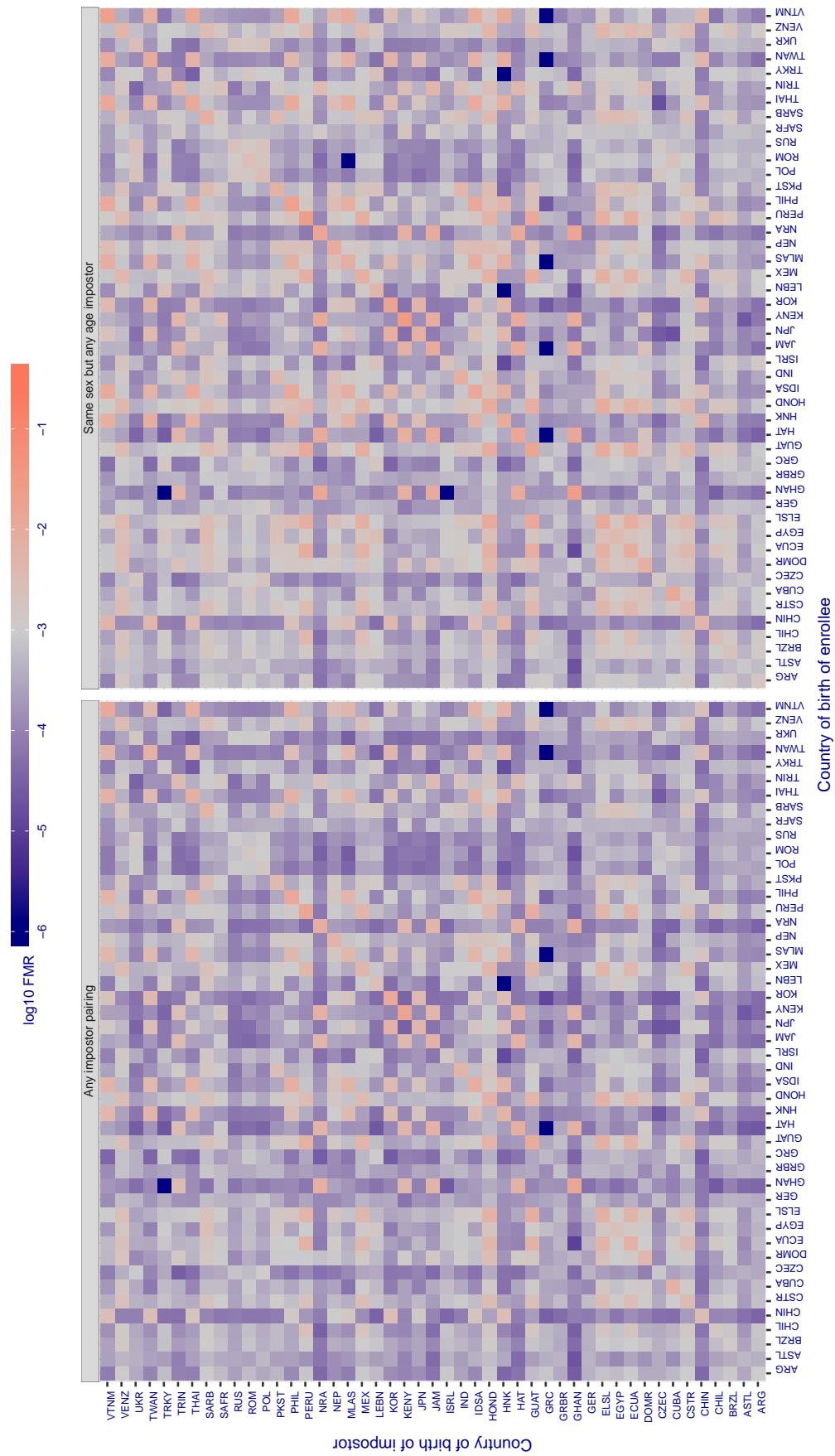
**Cross country FMR at threshold T = 0.599 for algorithm toshiba\_002, giving  $\text{FMR}(T) = 0.001$  globally.**

Figure 337: For algorithm toshiba-002 operating on visa images, the heatmap shows false match rates observed over impostor comparisons of faces from different individuals who were born in the given country pair. False matches are counted against a recognition threshold fixed globally to give the target  $\text{FMR}$  in the plot title, computed over all on the order of  $10^{10}$  impostor comparisons. If text appears in each box it give the same quantity as that coded by the color. Grey indicates  $\text{FMR}$  is at the intended  $\text{FMR}$  target level. Light red colors present a security vulnerability to, for example, a passport gate. Each +1 increase in  $\log_{10} \text{FMR}$  corresponds to a factor of 10 increase in  $\text{FMR}$ . The matrix is not quite symmetric because images in the enrollment and verification sets are different.

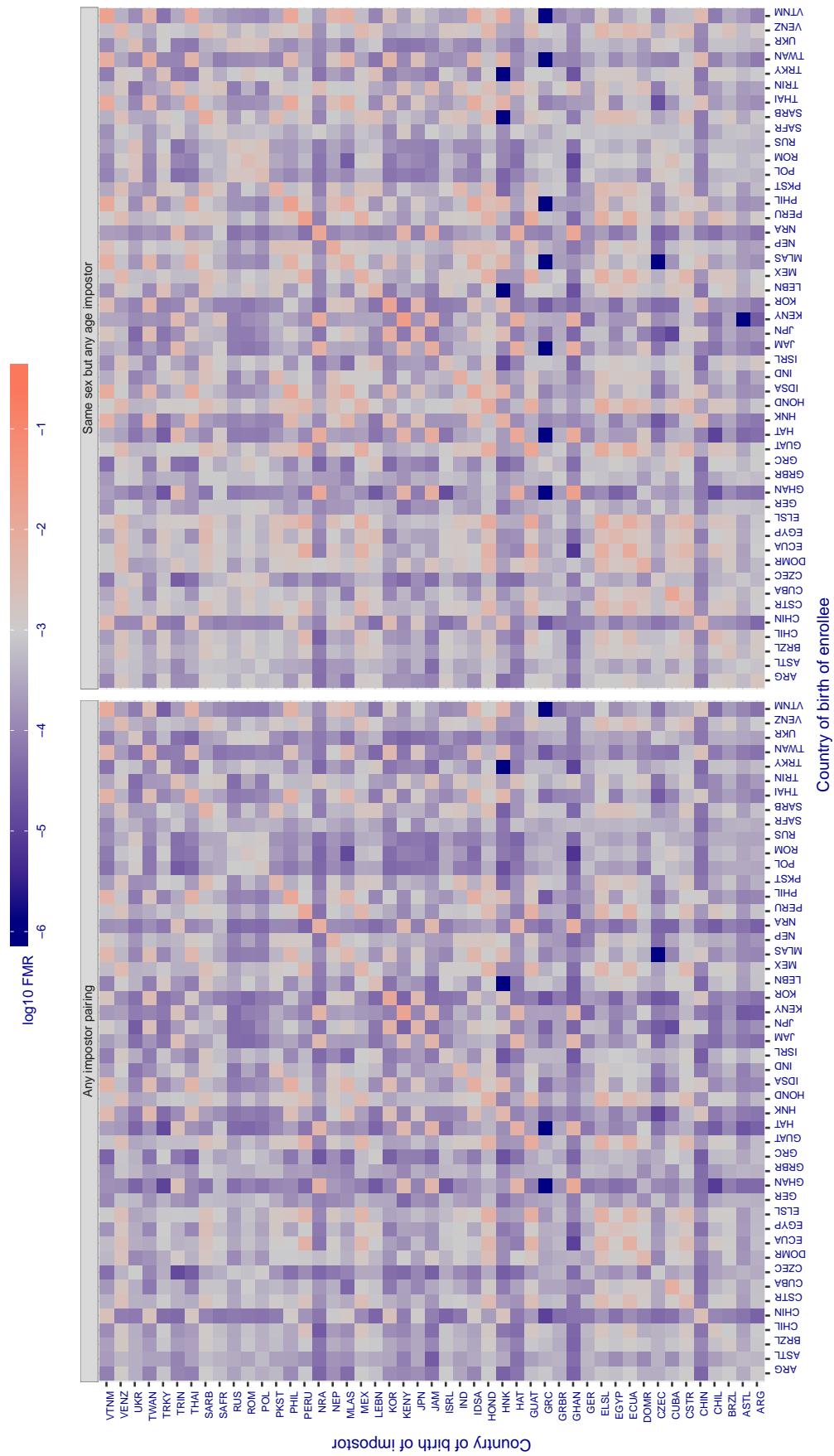
**Cross country FMR at threshold T = 0.596 for algorithm toshiba\_003, giving FMR(T) = 0.001 globally.**

Figure 338: For algorithm toshiba-003 operating on visa images, the heatmap shows false match rates observed over impostor comparisons of faces from different individuals who were born in the given country pair. False matches are counted against a recognition threshold fixed globally to give the target FMR in the plot title, computed over all on the order of  $10^{10}$  impostor comparisons. If text appears in each box it give the same quantity as that coded by the color. Grey indicates FMR is at the intended FMR target level. Light red colors present a security vulnerability to, for example, a passport gate. Each +1 increase in  $\log_{10} FMR$  corresponds to a factor of 10 increase in FMR. The matrix is not quite symmetric because images in the enrollment and verification sets are different.

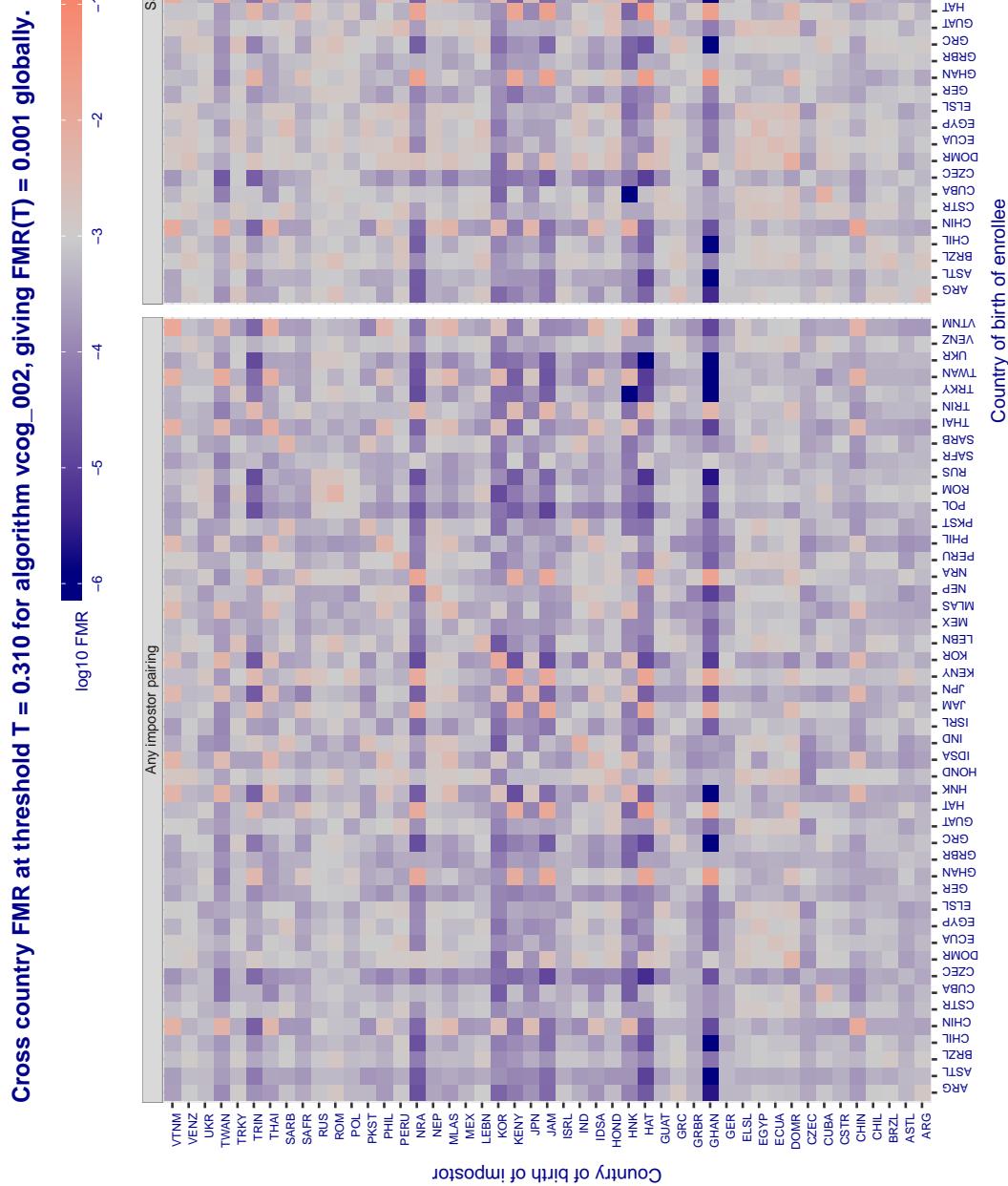


Figure 339: For algorithm vcog-002 operating on visa images, the heatmap shows false match rates observed over impostor comparisons of faces from different individuals who were born in the given country pair. False matches are counted against a recognition threshold fixed globally to give the target FMR in the plot title, computed over all on the order of  $10^{10}$  impostor comparisons. If text appears in each box it give the same quantity as that coded by the color. Grey indicates FMR is at the intended FMR target level. Light red colors present a security vulnerability to, for example, a passport gate. Each +1 increase in  $\log_{10} \text{FMR}$  corresponds to a factor of 10 increase in FMR. The matrix is not quite symmetric because images in the enrollment and verification sets are different.

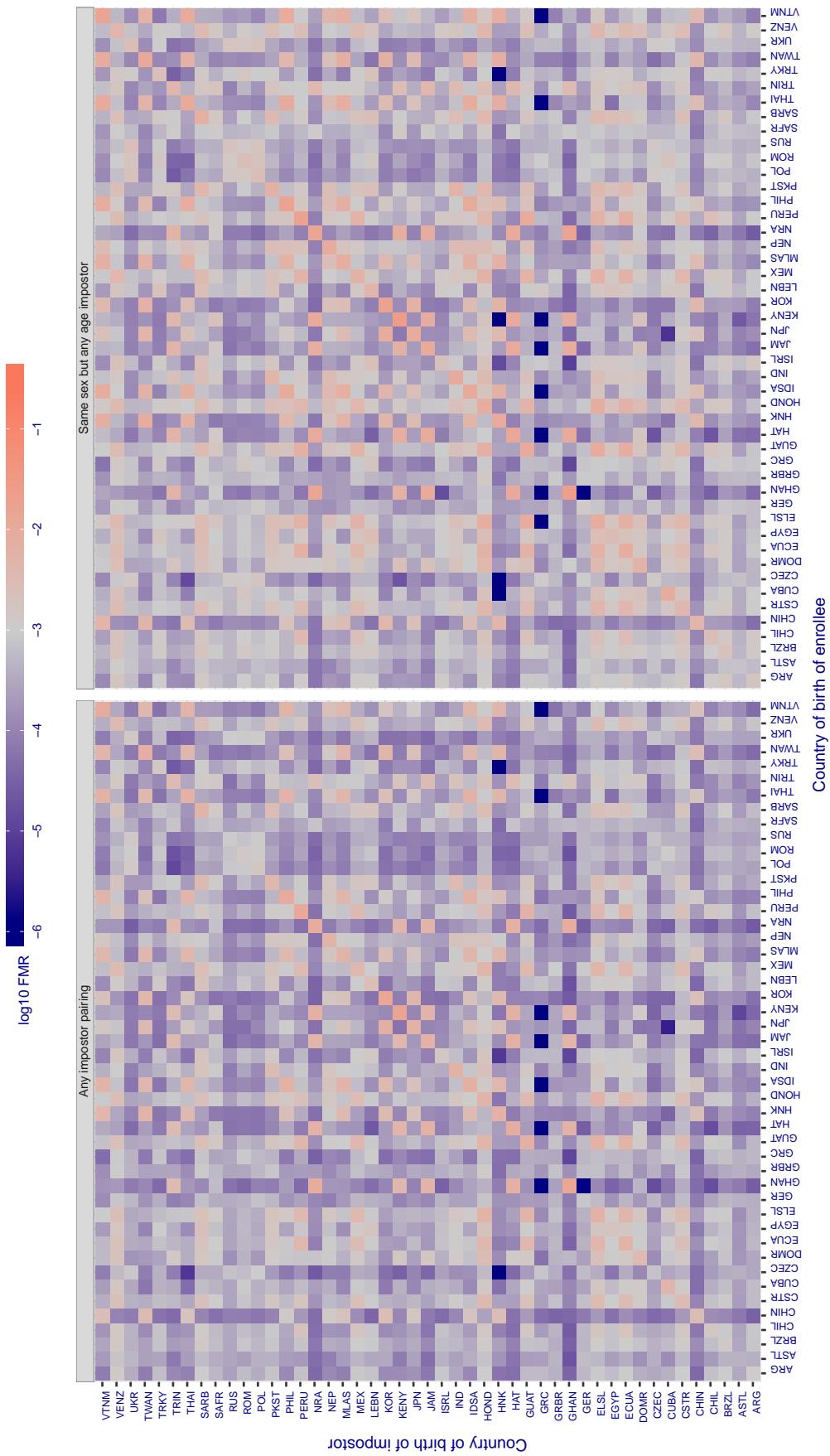
**Cross country FMR at threshold T = 66.962 for algorithm vd\_001, giving FMR(T) = 0.001 globally.**

Figure 340: For algorithm vd\_001 operating on visa images, the heatmap shows false match rates observed over impostor comparisons of faces from different individuals who were born in the given country pair. False matches are counted against a recognition threshold fixed globally to give the target FMR in the plot title, computed over all on the order of  $10^{10}$  impostor comparisons. If text appears in each box it give the same quantity as that coded by the color. Grey indicates FMR is at the intended FMR target level. Light red colors present a security vulnerability to, for example, a passport gate. Each +1 increase in  $\log_{10} \text{FMR}$  corresponds to a factor of 10 increase in FMR. The matrix is not quite symmetric because images in the enrollment and verification sets are different.

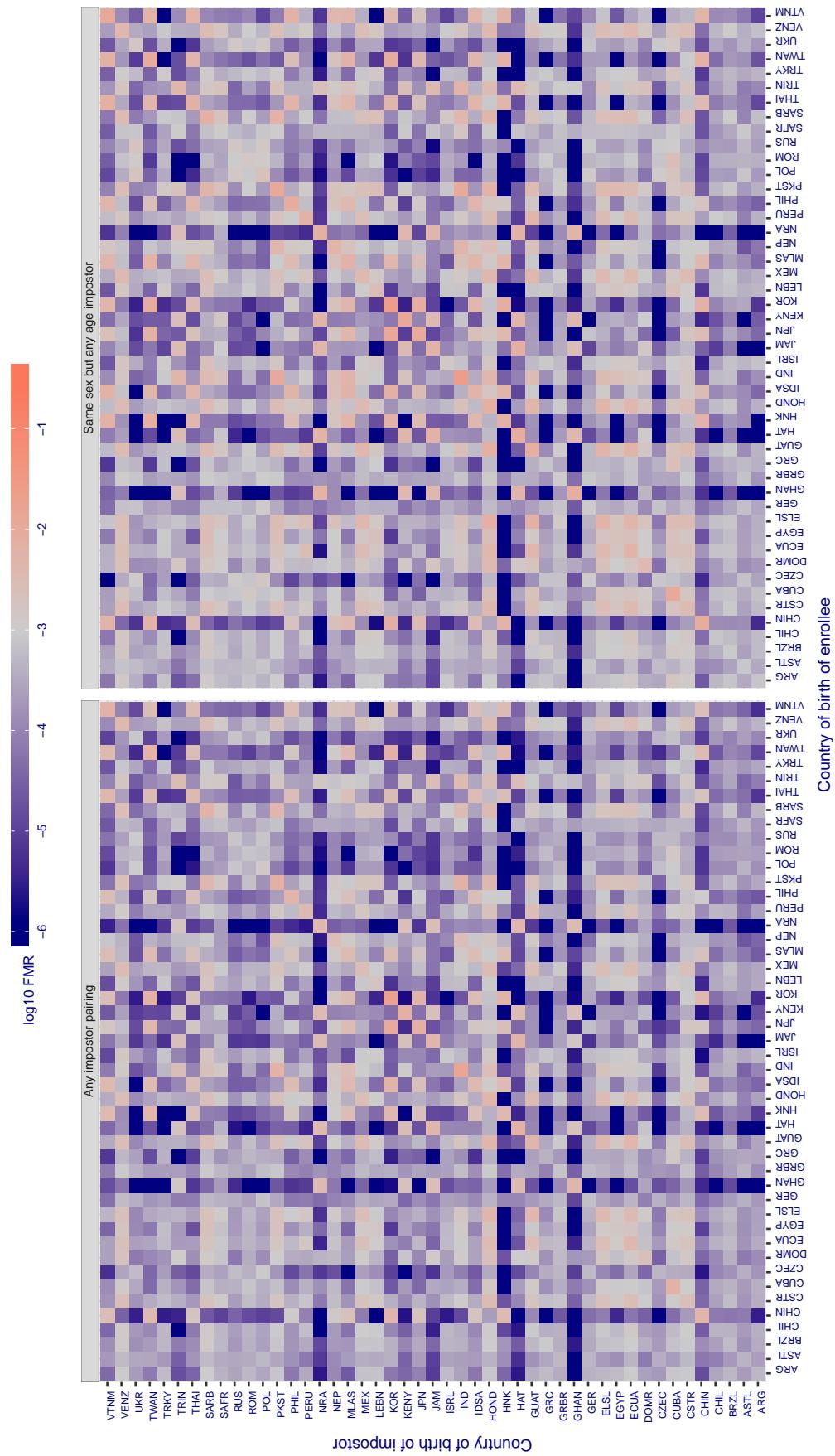
**Cross country FMR at threshold T = 2.897 for algorithm veridas\_001, giving FMR(T) = 0.001 globally.**

Figure 341: For algorithm veridas-001 operating on visa images, the heatmap shows false match rates observed over impostor comparisons of faces from different individuals who were born in the given country pair. False matches are counted against a recognition threshold fixed globally to give the target FMR in the plot title, computed over all on the order of  $10^{10}$  impostor comparisons. If text appears in each box it give the same quantity as that coded by the color. Grey indicates FMR is at the intended FMR target level. Light red colors present a security vulnerability to, for example, a passport gate. Each +1 increase in  $\log_{10} \text{FMR}$  corresponds to a factor of 10 increase in FMR. The matrix is not quite symmetric because images in the enrollment and verification sets are different.

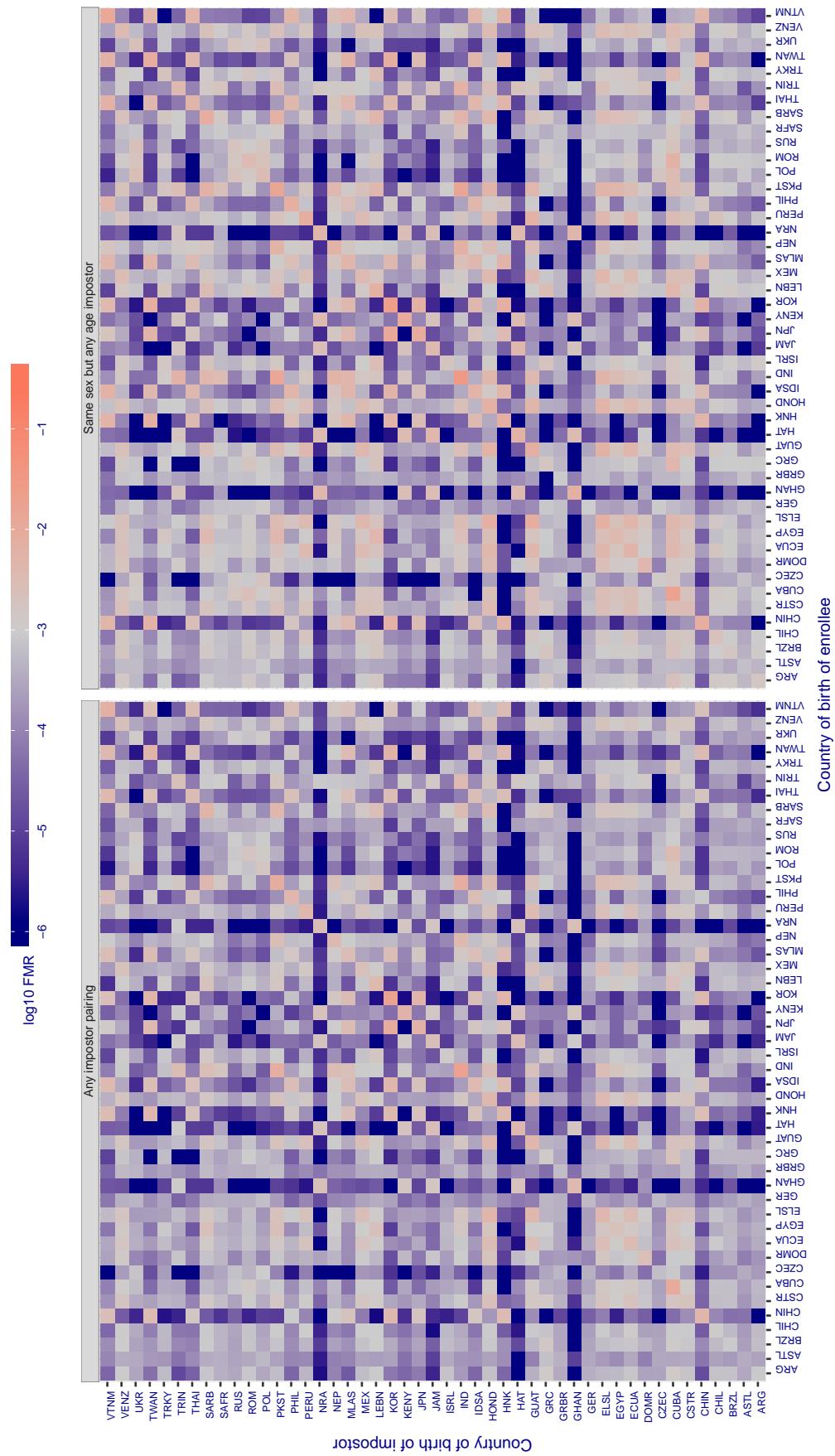
**Cross country FMR at threshold T = 3.010 for algorithm veridas\_002, giving FMR(T) = 0.001 globally.**

Figure 342: For algorithm veridas-002 operating on visa images, the heatmap shows false match rates observed over impostor comparisons of faces from different individuals who were born in the given country pair. False matches are counted against a recognition threshold fixed globally to give the target FMR in the plot title, computed over all on the order of  $10^{10}$  impostor comparisons. If text appears in each box it give the same quantity as that coded by the color. Grey indicates FMR is at the intended FMR target level. Light red colors present a security vulnerability to, for example, a passport gate. Each +1 increase in  $\log_{10}$  FMR corresponds to a factor of 10 increase in FMR. The matrix is not quite symmetric because images in the enrollment and verification sets are different.

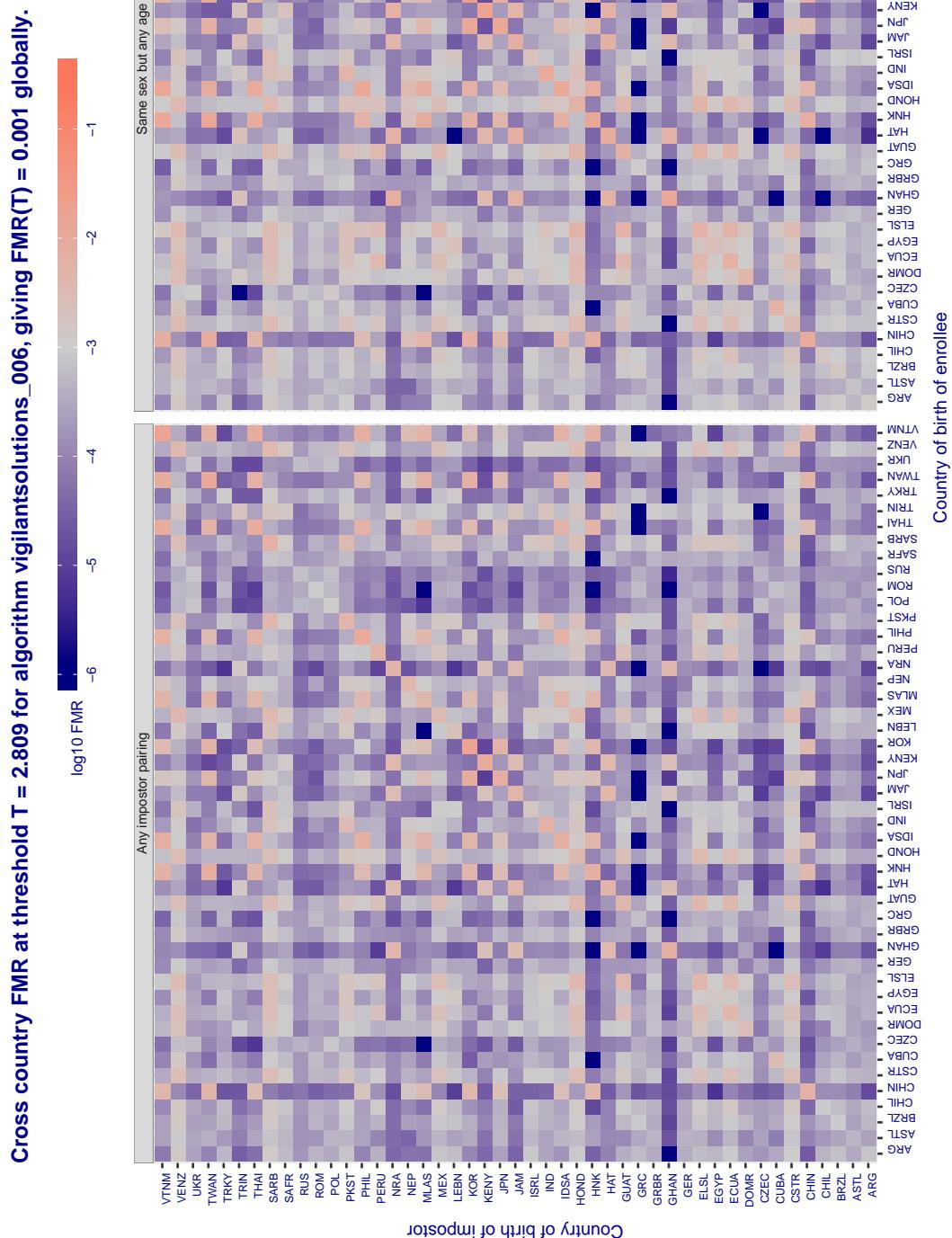


Figure 343: For algorithm *vigilantsolutions-006* operating on visa images, the heatmap shows false match rates observed over impostor comparisons of faces from different individuals who were born in the given country pair. False matches are counted against a recognition threshold fixed globally to give the target *FMR* in the plot title, computed over all on the order of  $10^{10}$  impostor comparisons. If text appears in each box it give the same quantity as that coded by the color. Grey indicates *FMR* is at the intended *FMR* target level. Light red colors present a security vulnerability to, for example, a passport gate. Each +1 increase in  $\log_{10} \text{FMR}$  corresponds to a factor of 10 increase in *FMR*. The matrix is not quite symmetric because images in the enrollment and verification sets are different.

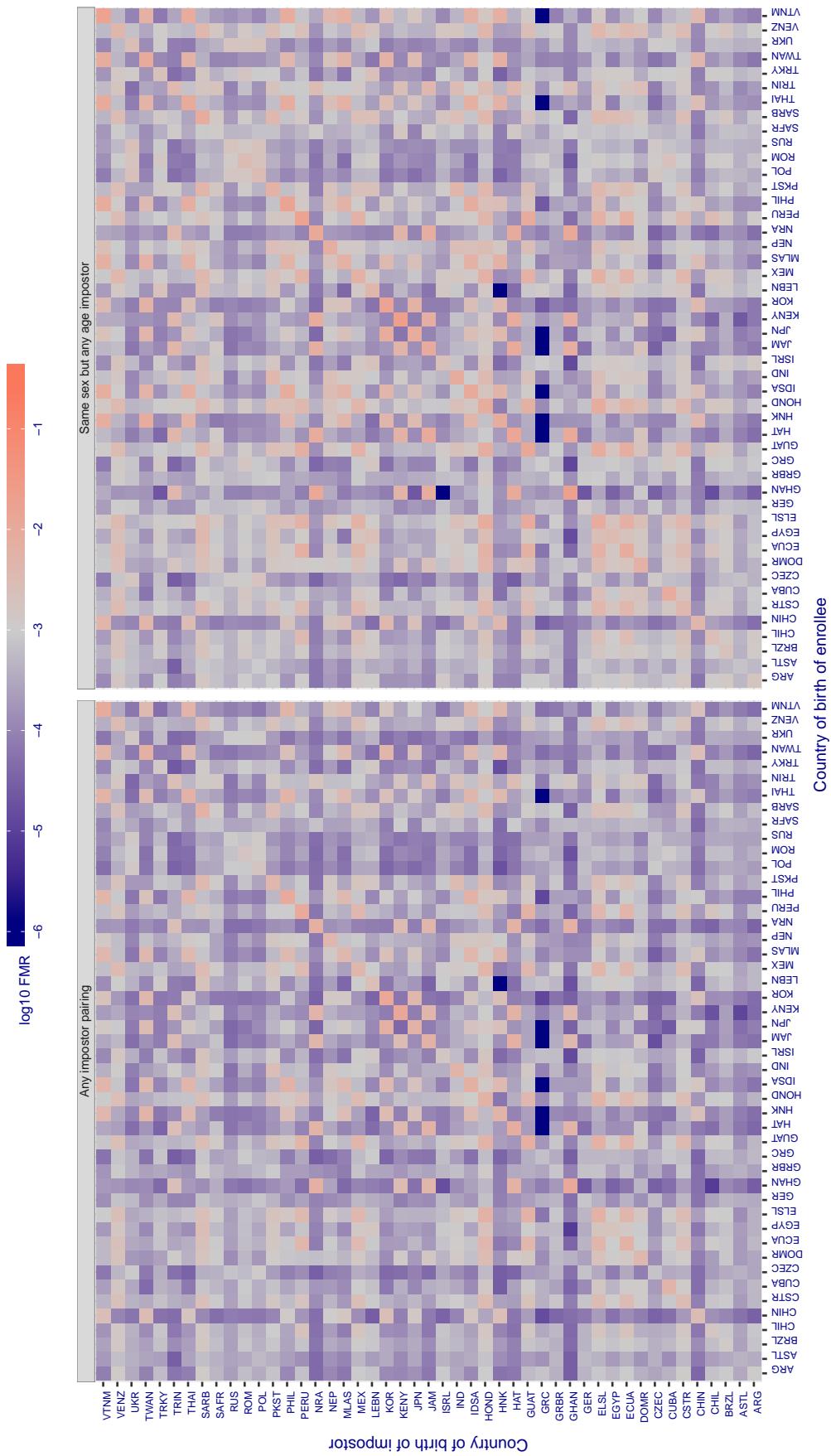
**Cross country FMR at threshold T = 0.336 for algorithm vion\_000, giving FMR(T) = 0.001 globally.**

Figure 344: For algorithm vion-000 operating on visa images, the heatmap shows false match rates observed over impostor comparisons of faces from different individuals who were born in the given country pair. False matches are counted against a recognition threshold fixed globally to give the target FMR in the plot title, computed over all on the order of  $10^{10}$  impostor comparisons. If text appears in each box it give the same quantity as that coded by the color. Grey indicates FMR is at the intended FMR target level. Light red colors present a security vulnerability to, for example, a passport gate. Each +1 increase in  $\log_{10} \text{FMR}$  corresponds to a factor of 10 increase in FMR. The matrix is not quite symmetric because images in the enrollment and verification sets are different.

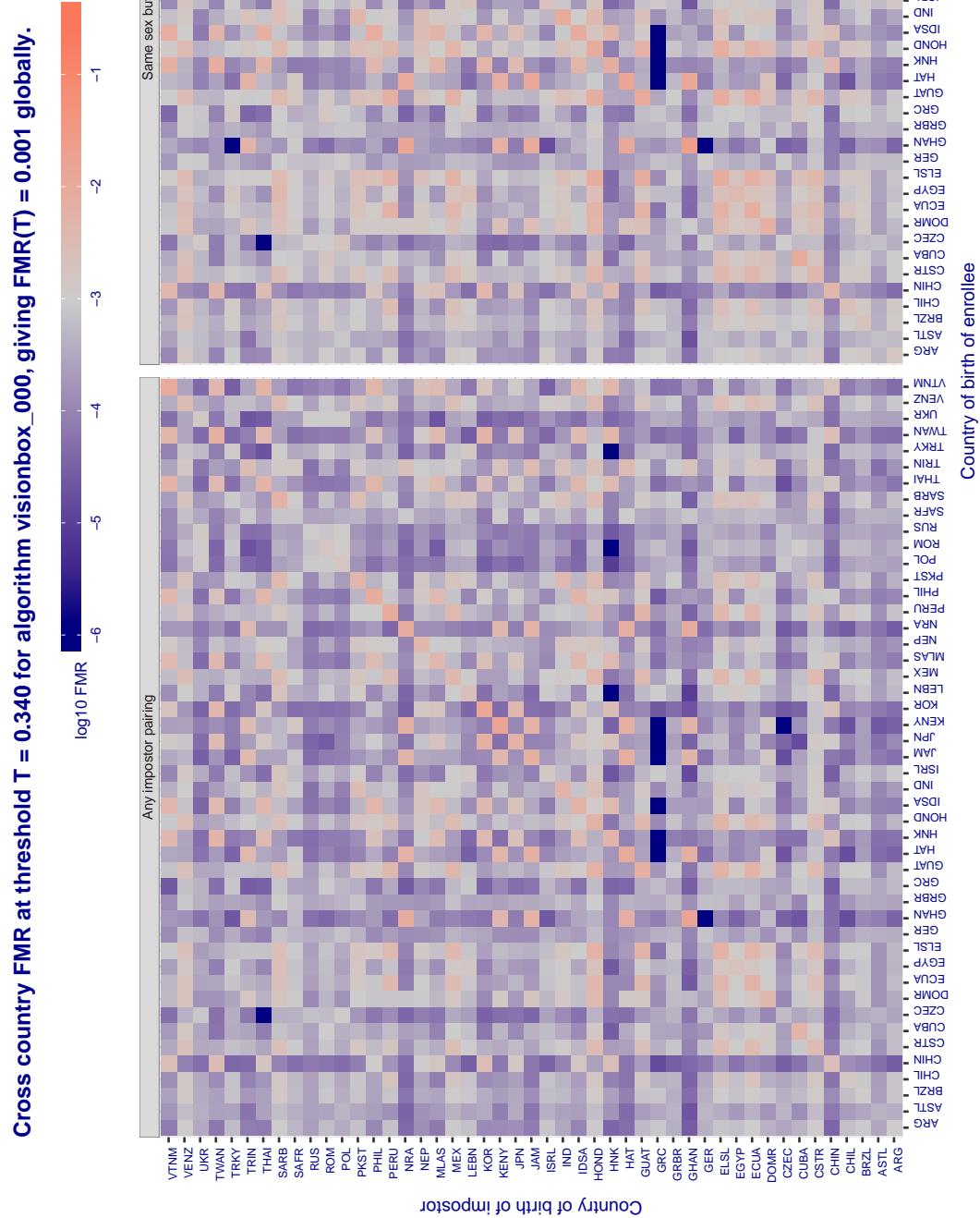


Figure 345: For algorithm visionbox-000 operating on visa images, the heatmap shows false match rates observed over impostor comparisons of faces from different individuals who were born in the given country pair. False matches are counted against a recognition threshold fixed globally to give the target FMR in the plot title, computed over all on the order of  $10^{10}$  impostor comparisons. If text appears in each box it give the same quantity as that coded by the color. Grey indicates FMR is at the intended FMR target level. Light red colors present a security vulnerability to, for example, a passport gate. Each +1 increase in  $\log_{10}$  FMR corresponds to a factor of 10 increase in FMR. The matrix is not quite symmetric because images in the enrollment and verification sets are different.

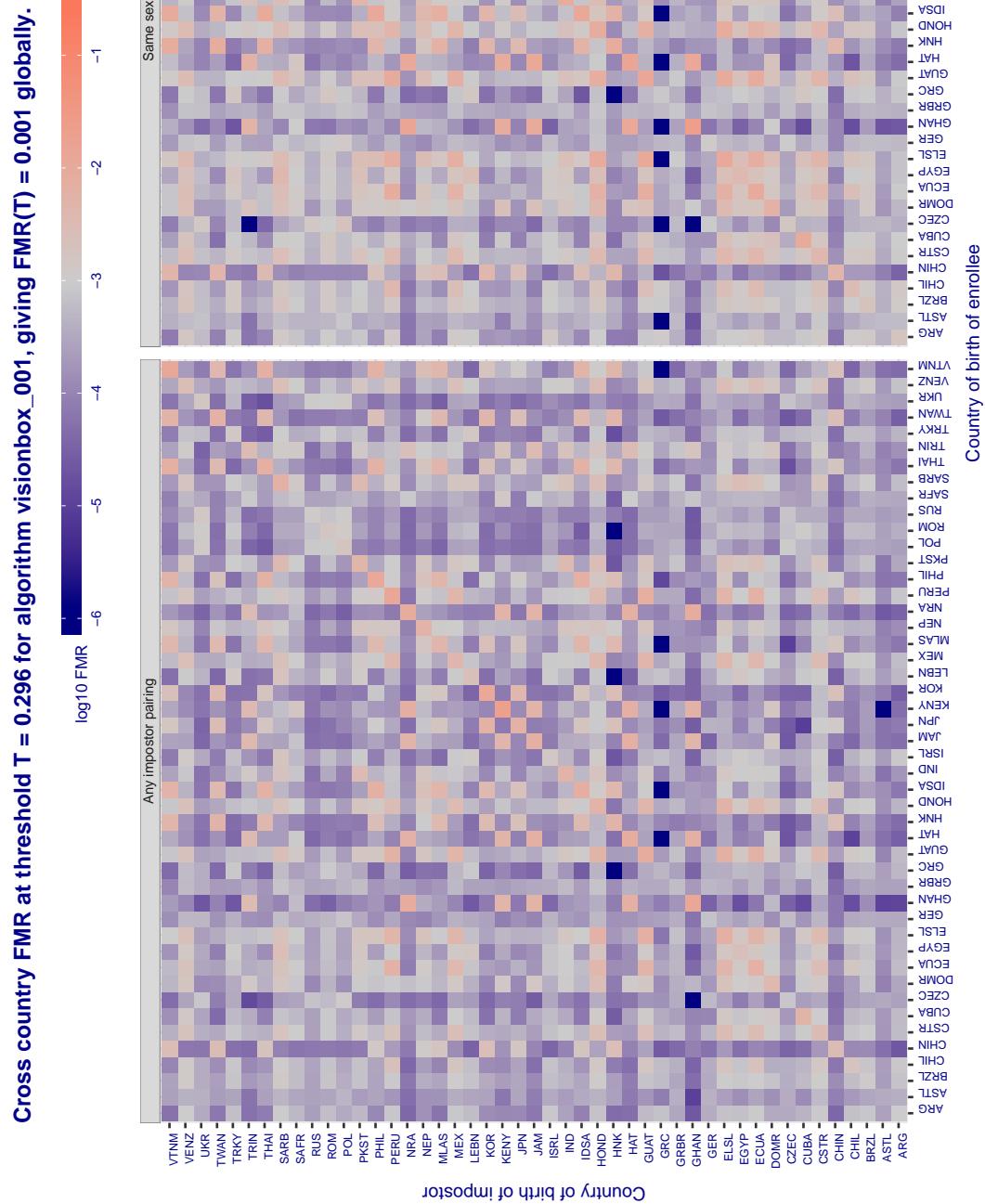


Figure 346: For algorithm visionbox-001 operating on visa images, the heatmap shows false match rates observed over impostor comparisons of faces from different individuals who were born in the given country pair. False matches are counted against a recognition threshold fixed globally to give the target FMR in the plot title, computed over all on the order of  $10^{10}$  impostor comparisons. If text appears in each box it give the same quantity as that coded by the color. Grey indicates FMR is at the intended FMR target level. Light red colors present a security vulnerability to, for example, a passport gate. Each +1 increase in  $\log_{10}$  FMR corresponds to a factor of 10 increase in FMR. The matrix is not quite symmetric because images in the enrollment and verification sets are different.

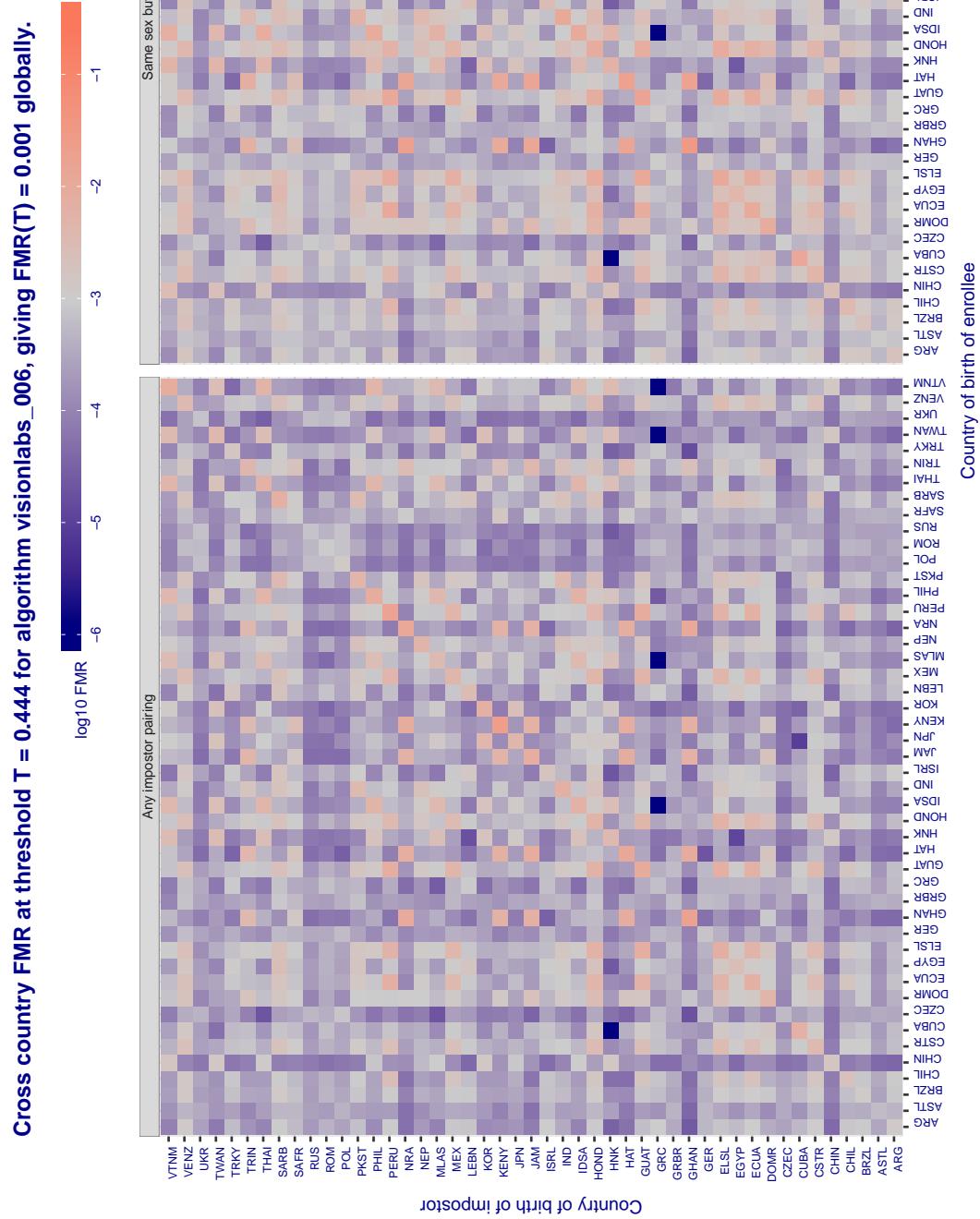


Figure 347: For algorithm visionlabs-006 operating on visa images, the heatmap shows false match rates observed over impostor comparisons of faces from different individuals who were born in the given country pair. False matches are counted against a recognition threshold fixed globally to give the target FMR in the plot title, computed over all on the order of  $10^{10}$  impostor comparisons. If text appears in each box it give the same quantity as that coded by the color. Grey indicates FMR is at the intended FMR target level. Light red colors present a security vulnerability to, for example, a passport gate. Each +1 increase in  $\log_{10}$  FMR corresponds to a factor of 10 increase in FMR. The matrix is not quite symmetric because images in the enrollment and verification sets are different.

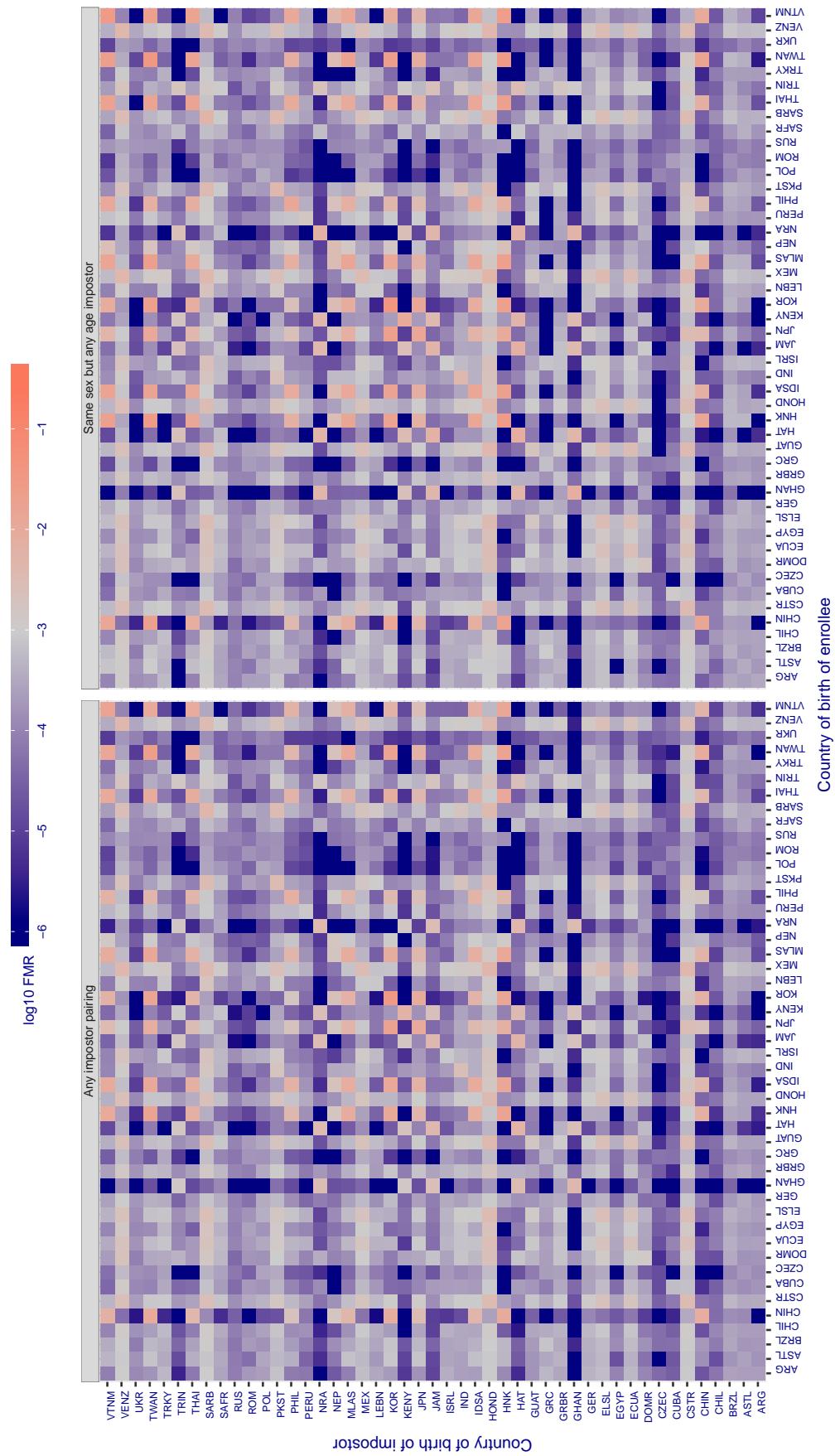
**Cross country FMR at threshold T = 5.333 for algorithm yisheng\_004, giving FMR(T) = 0.001 globally.**

Figure 348: For algorithm *yisheng-004* operating on visa images, the heatmap shows false match rates observed over impostor comparisons of faces from different individuals who were born in the given country pair. False matches are counted against a recognition threshold fixed globally to give the target FMR in the plot title, computed over all on the order of  $10^{10}$  impostor comparisons. If text appears in each box it give the same quantity as that coded by the color. Grey indicates FMR is at the intended FMR target level. Light red colors present a security vulnerability to, for example, a passport gate. Each +1 increase in  $\log_{10} FMR$  corresponds to a factor of 10 increase in FMR. The matrix is not quite symmetric because images in the enrollment and verification sets are different.

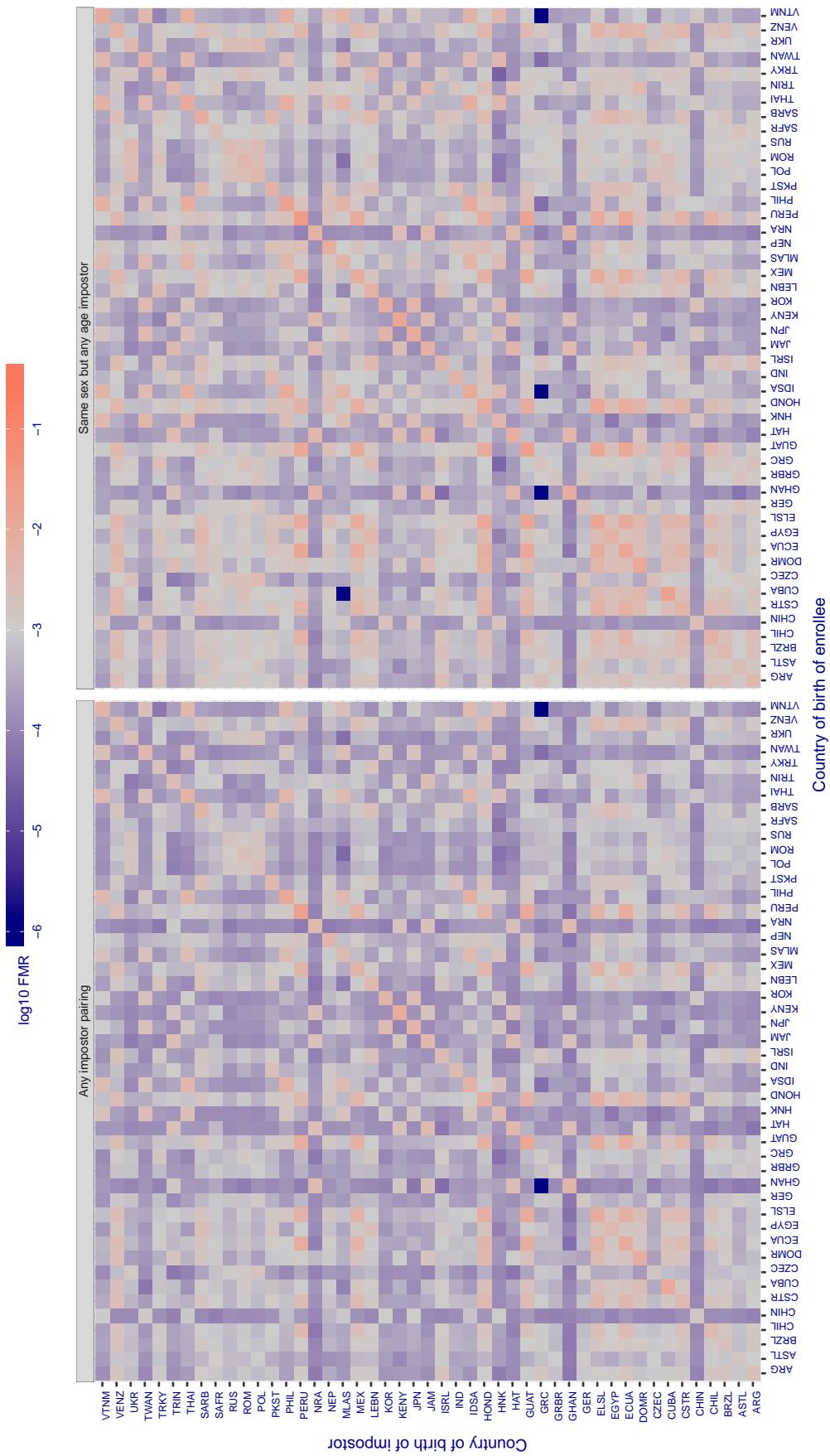
**Cross country FMR at threshold T = 37.550 for algorithm yitu\_003, giving FMR(T) = 0.001 globally.**

Figure 349: For algorithm yitu-003 operating on visa images, the heatmap shows false match rates observed over impostor comparisons of faces from different individuals who were born in the given country pair. False matches are counted against a recognition threshold fixed globally to give the target FMR in the plot title, computed over all on the order of  $10^{10}$  impostor comparisons. If text appears in each box it give the same quantity as that coded by the color. Grey indicates FMR is at the intended FMR target level. Light red colors present a security vulnerability to, for example, a passport gate. Each +1 increase in  $\log_{10} \text{FMR}$  corresponds to a factor of 10 increase in FMR. The matrix is not quite symmetric because images in the enrollment and verification sets are different.

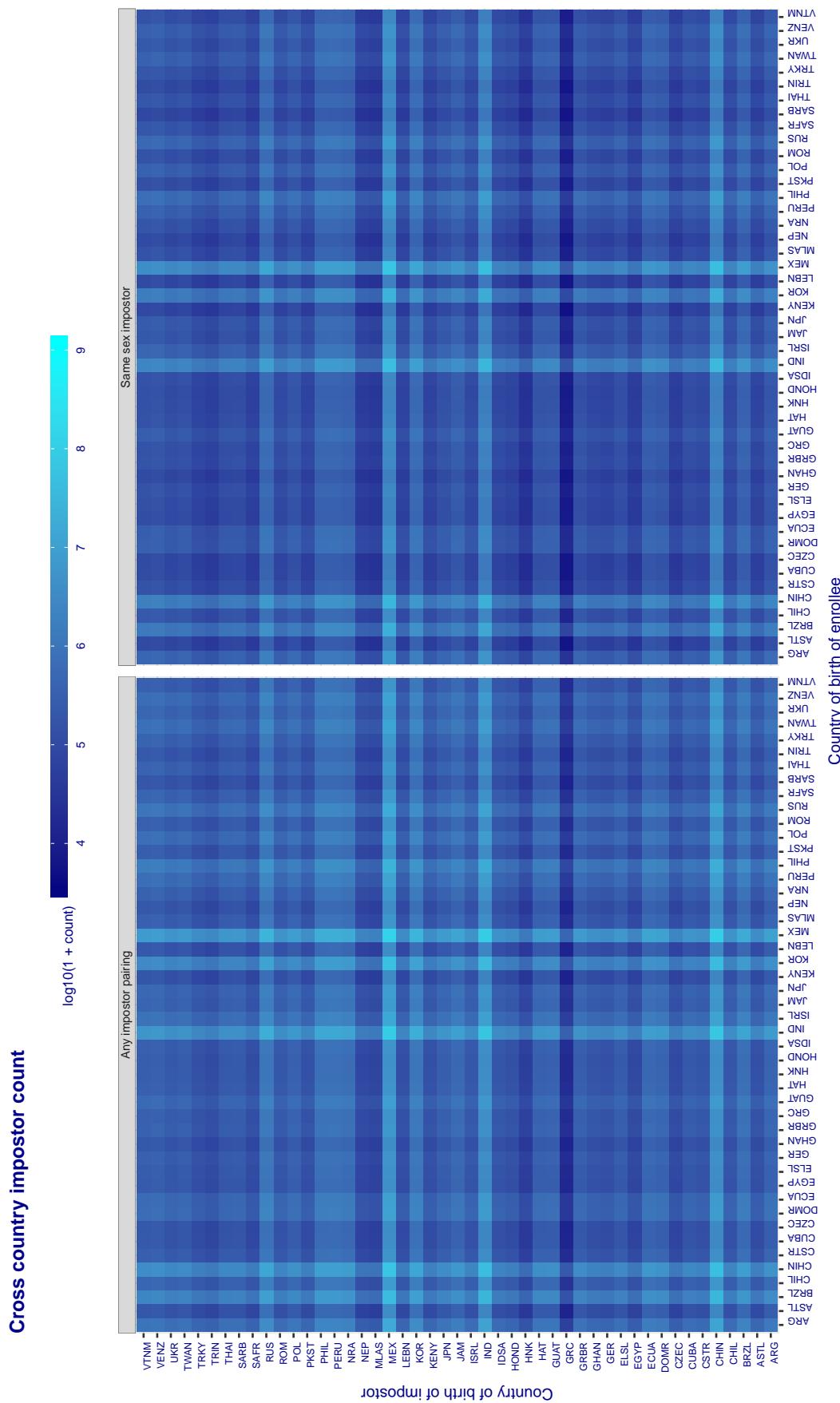


Figure 350: For visa images, the heatmap shows the count of impostor comparisons of faces from different individuals who were born in the given country pair.

### 3.6.2 Effect of age on impostors

**Background:** This section shows the effect of age on the impostor distribution. The ideal behaviour is that the age of the enrollee and the impostor would not affect impostor scores. This would support FMR stability over sub-populations.

**Goals:**

- ▷ To show the effect of relative ages of the impostor and enrollee on false match rates.
- ▷ To determine whether some algorithms have better impostor distribution stability.

**Methods:**

- ▷ Define 14 age group bins, spanning 0 to over 100 years old.
- ▷ Compute FMR over all impostor comparisons for which the subjects in the enrollee and impostor images have ages in two bins.
- ▷ Compute FMR over all impostor comparisons for which the subjects are additionally of the same sex, and born in the same geographic region.

**Results:**

The notable aspects are:

- ▷ Diagonal dominance: Impostors are more likely to be matched against their same age group.
- ▷ Same sex and same region impostors are more successful. On the diagonal, an impostor is more likely to succeed by posing as someone of the same sex. If  $\Delta \log_{10} \text{FMR} = 0.2$ , then same-sex same-region FMR exceeds the all-pairs FMR by factor of  $10^{0.2} = 1.6$ .
- ▷ Young children impostors give elevated FMR against young children. Older adult impostor give elevated FMR against older adults. These effects are quite large, for example if  $\Delta \log_{10} \text{FMR} = 1.0$  larger than a 32 year old, then these groups have higher FMR by a factor of  $10^1 = 10$ . This would imply an FMR above 0.01 for a nominal (global) FMR = 0.001.
- ▷ Algorithms vary.
- ▷ We computed the same quantities for a global FMR = 0.0001. The effects are similar.

Note the calculations in this section include impostors paired across all countries of birth.

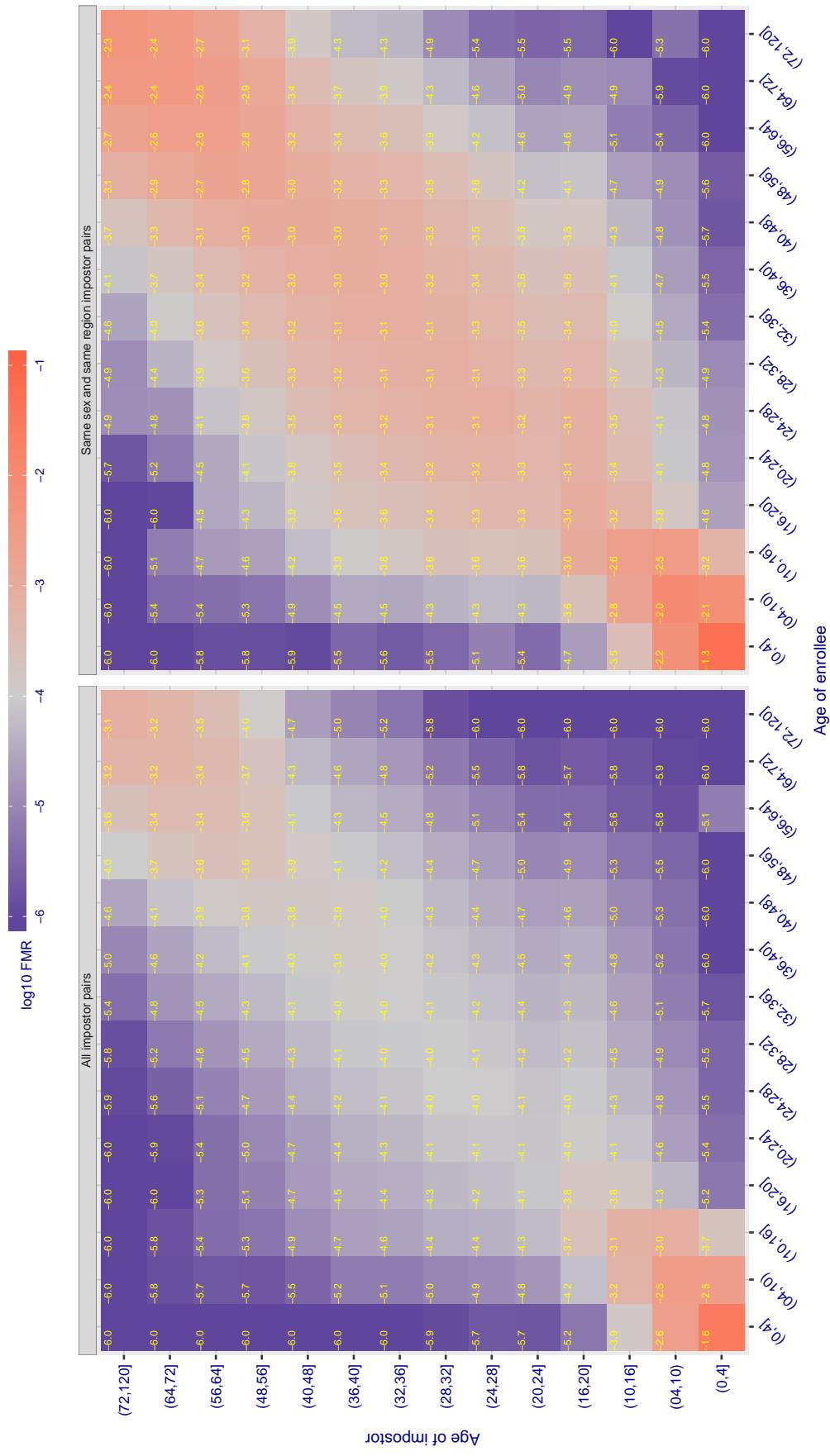
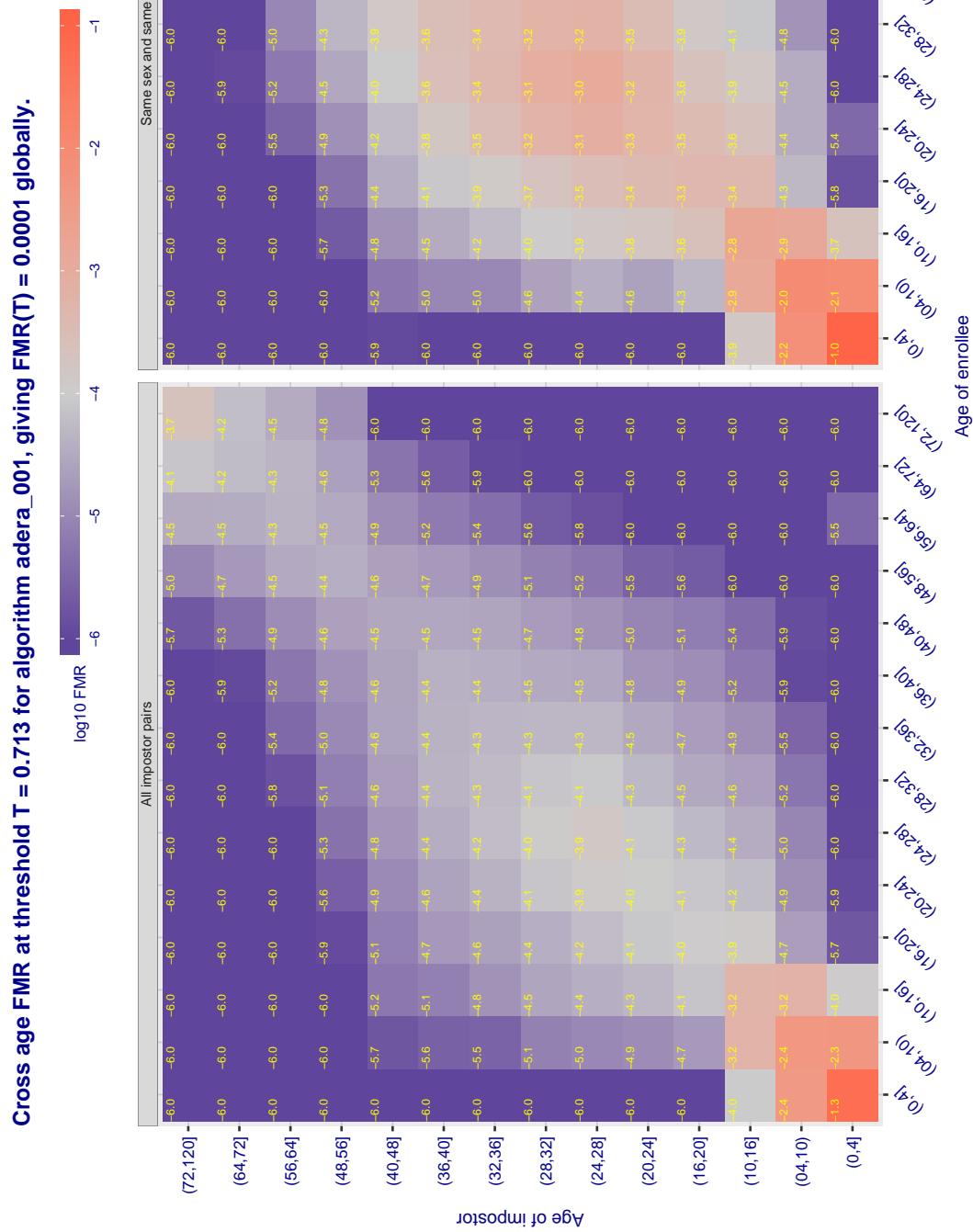
Cross age FMR at threshold T = 2.740 for algorithm 3divi\_003, giving  $FMR(T) = 0.0001$  globally.

Figure 351: For algorithm 3divi-003 operating on visa images, the heatmap shows false match observed over impostor comparisons of faces from different individuals who have the given age pair. False matches are counted against a recognition threshold fixed globally to give  $FMR = 0.001$  over all on the order of  $10^{10}$  impostor comparisons. The text in each box gives the same quantity as that coded by the color. Light colors present a security vulnerability to, for example, a passport gate.



**Figure 352:** For algorithm adera-001 operating on visa images, the heatmap shows false match observed over impostor comparisons of faces from different individuals who have the given age pair. False matches are counted against a recognition threshold fixed globally to give  $FMR = 0.001$  over all on the order of  $10^{10}$  impostor comparisons. The text in each box gives the same quantity as that coded by the color. Light colors present a security vulnerability to, for example, a passport gate.

Cross age FMR at threshold T = 0.702 for algorithm alchera\_000, giving FMR(T) = 0.0001 globally.

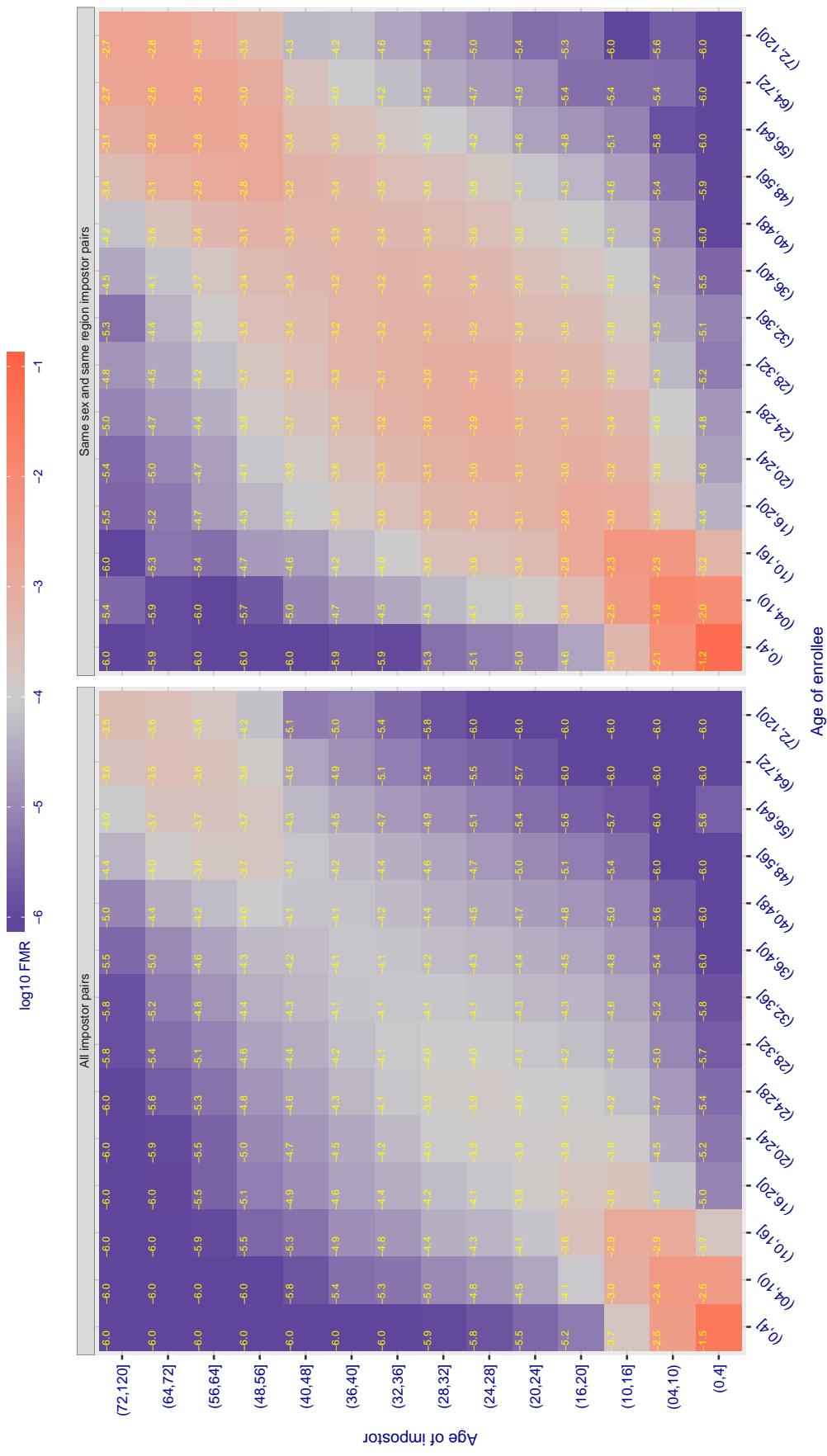


Figure 353: For algorithm alchera-000 operating on visa images, the heatmap shows false match observed over impostor comparisons of faces from different individuals who have the given age pair. False matches are counted against a recognition threshold fixed globally to give  $FMR = 0.001$  over all on the order of  $10^{10}$  impostor comparisons. The text in each box gives the same quantity as that coded by the color. Light colors present a security vulnerability to, for example, a passport gate.

Cross age FMR at threshold T = 0.713 for algorithm alchera\_001, giving FMR(T) = 0.0001 globally.

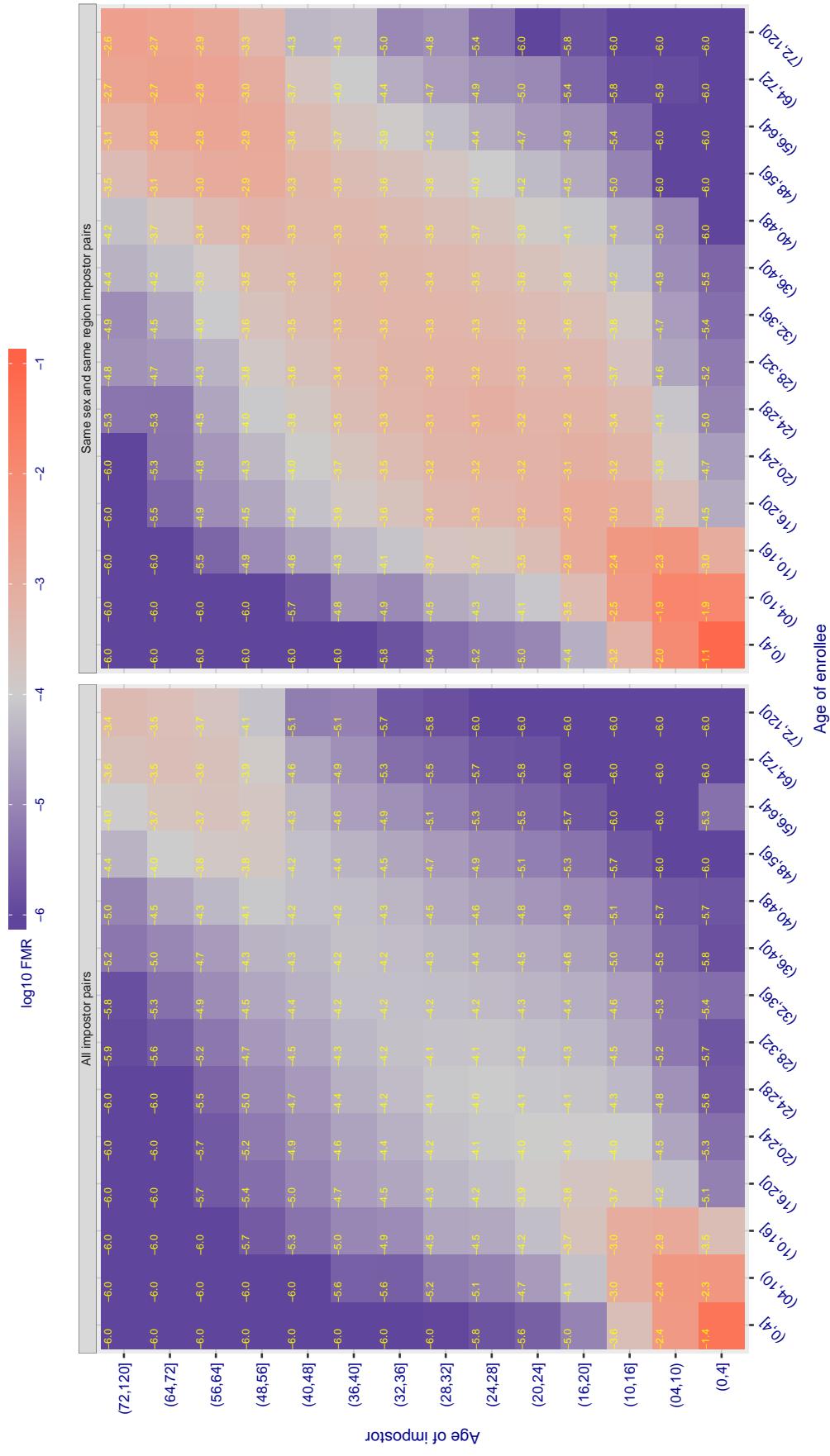


Figure 354: For algorithm alchera-001 operating on visa images, the heatmap shows false match observed over impostor comparisons of faces from different individuals who have the given age pair. False matches are counted against a recognition threshold fixed globally to give FMR = 0.001 over all on the order of  $10^{10}$  impostor comparisons. The text in each box gives the same quantity as that coded by the color. Light colors present a security vulnerability to, for example, a passport gate.

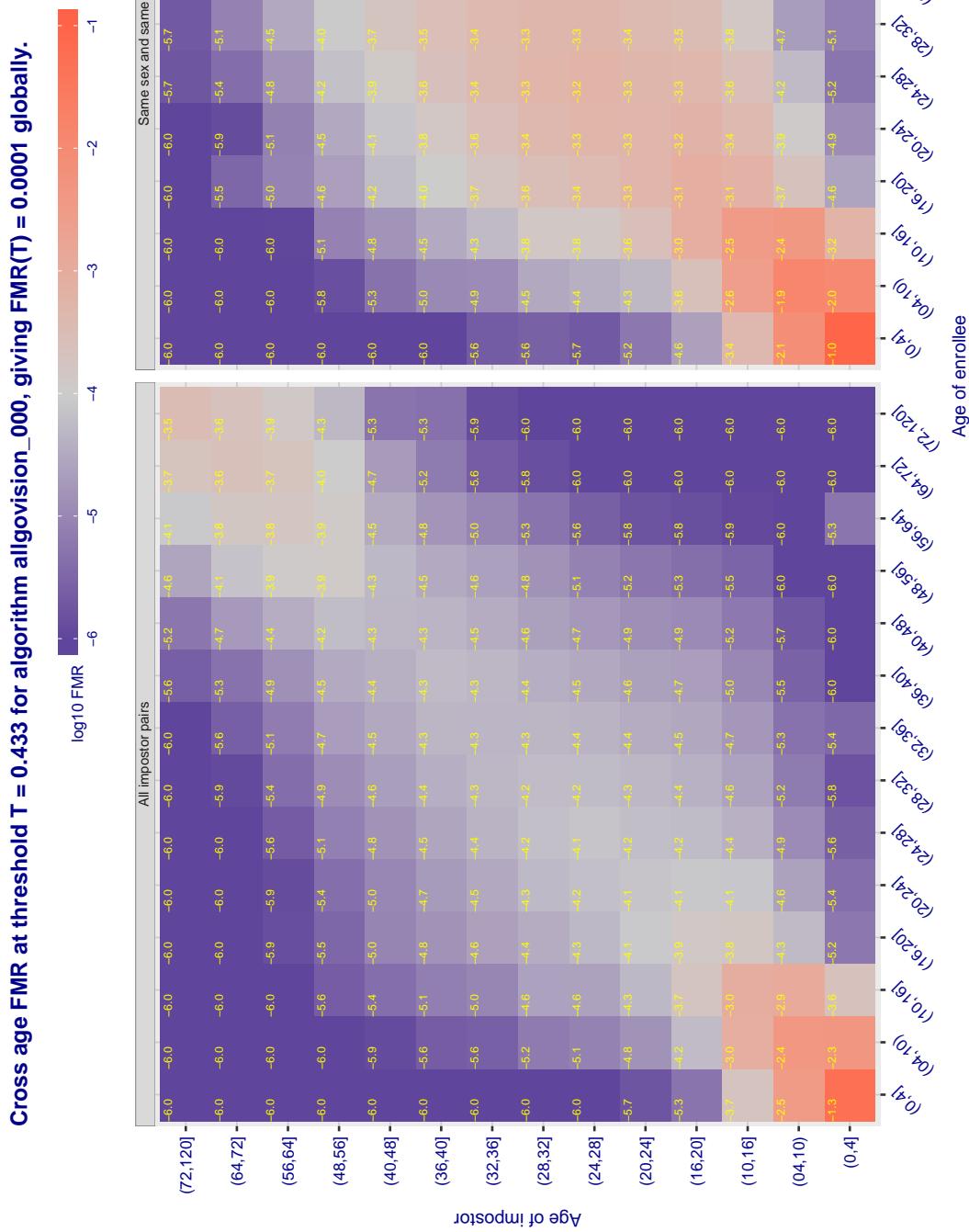


Figure 355: For algorithm allgovidision-000 operating on visa images, the heatmap shows false match observed over impostor comparisons of faces from different individuals who have the given age pair. False matches are counted against a recognition threshold fixed globally to give  $FMR = 0.001$  over all on the order of  $10^{10}$  impostor comparisons. The text in each box gives the same quantity as that coded by the color. Light colors present a security vulnerability to, for example, a passport gate.

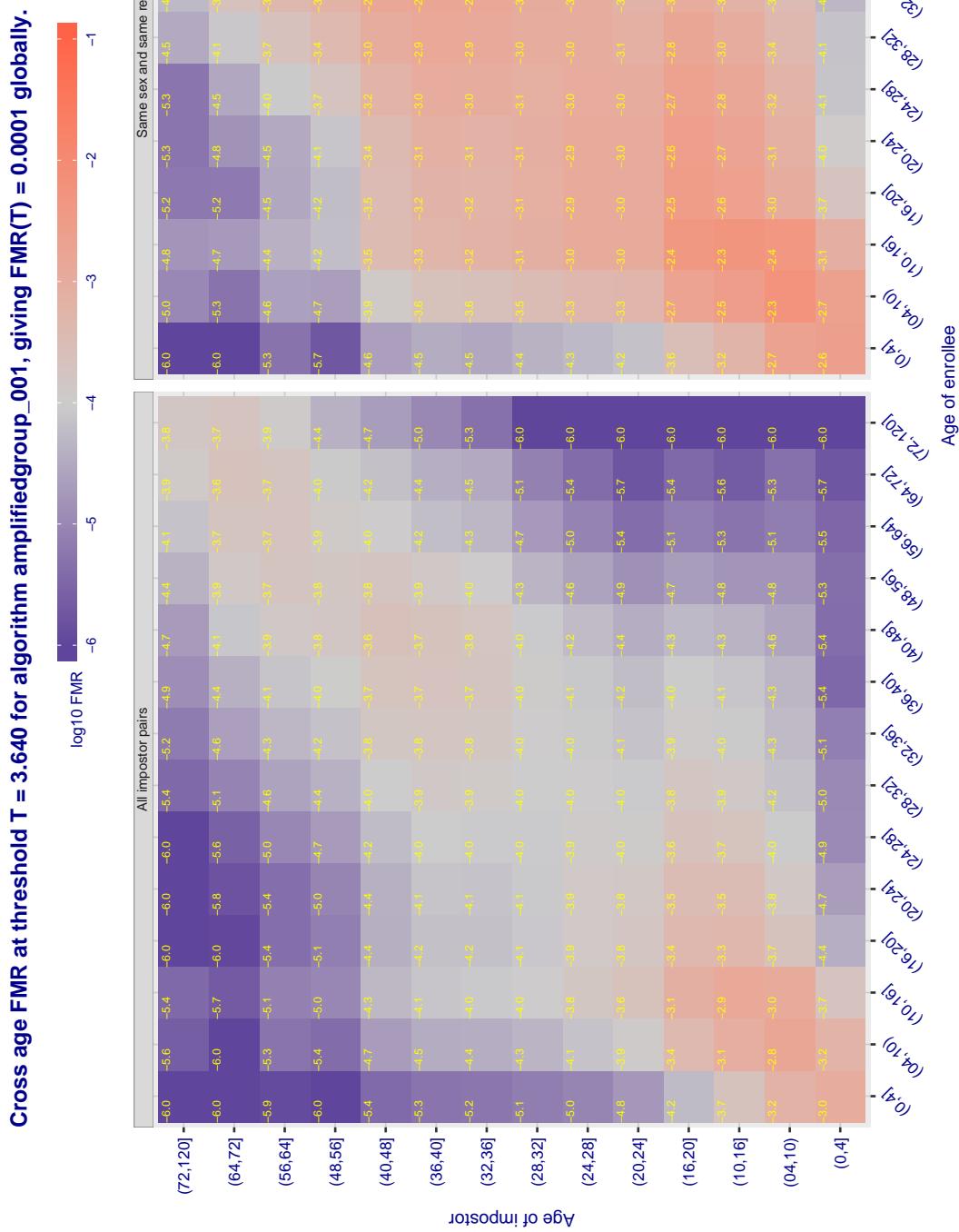
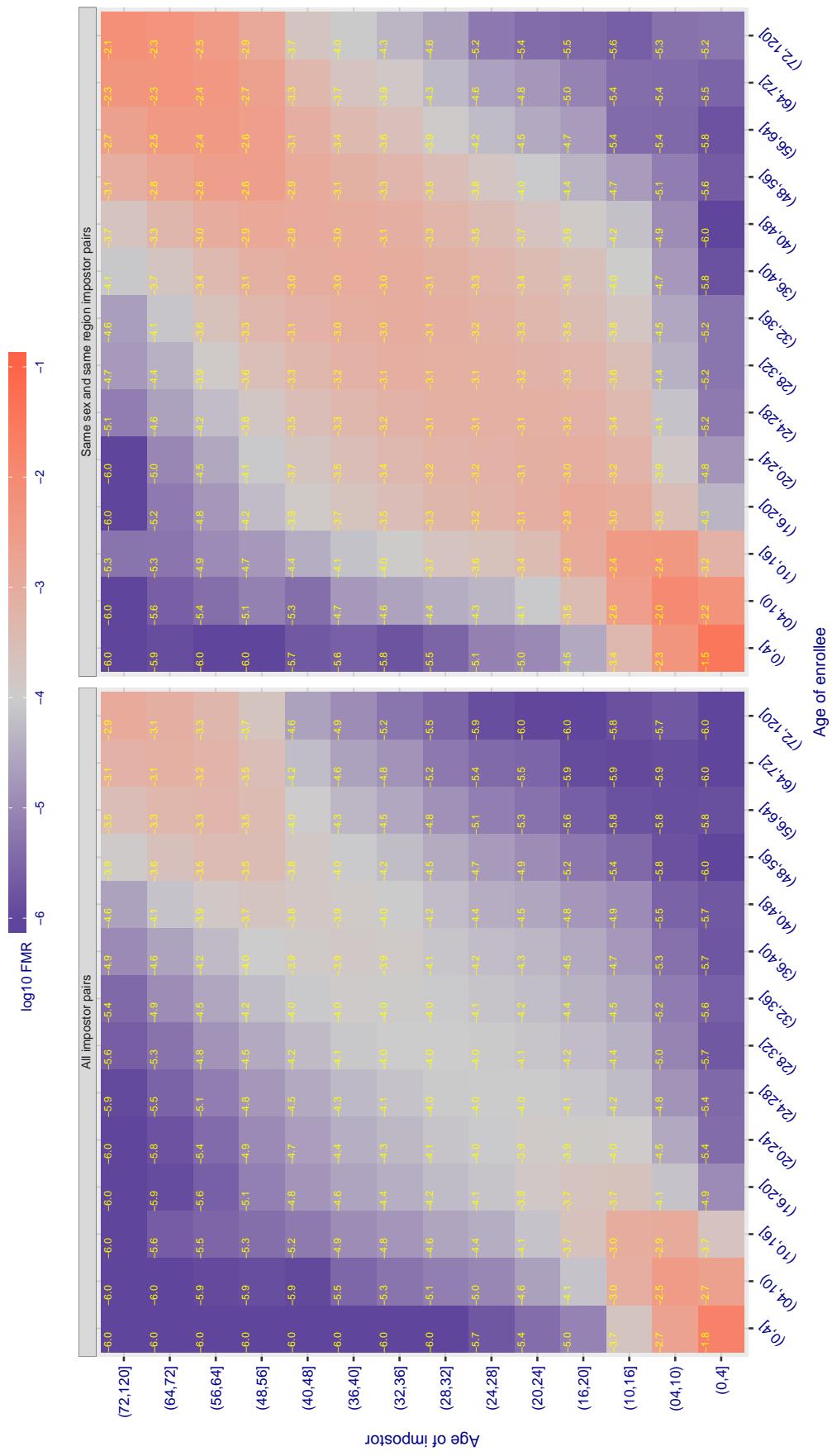
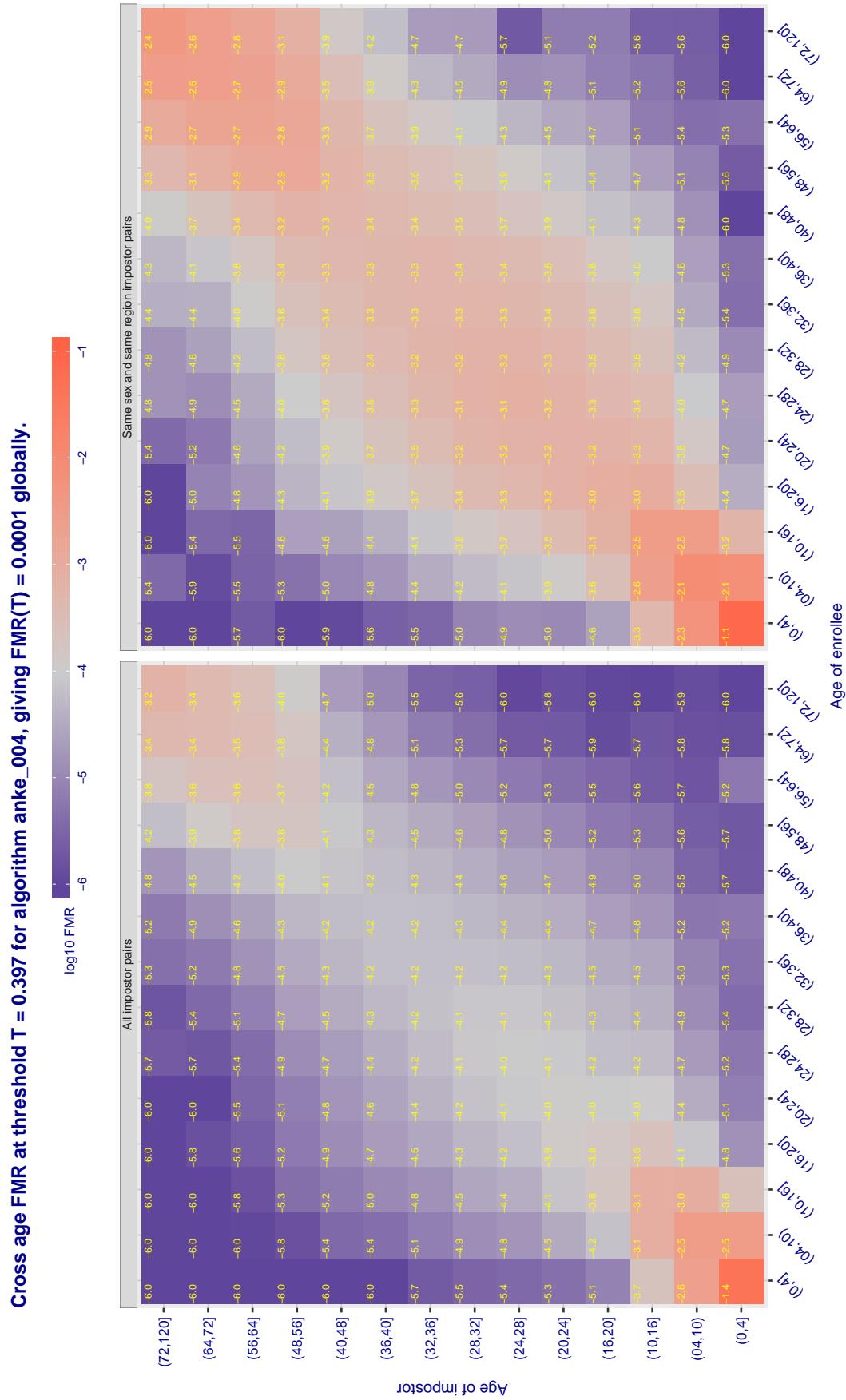
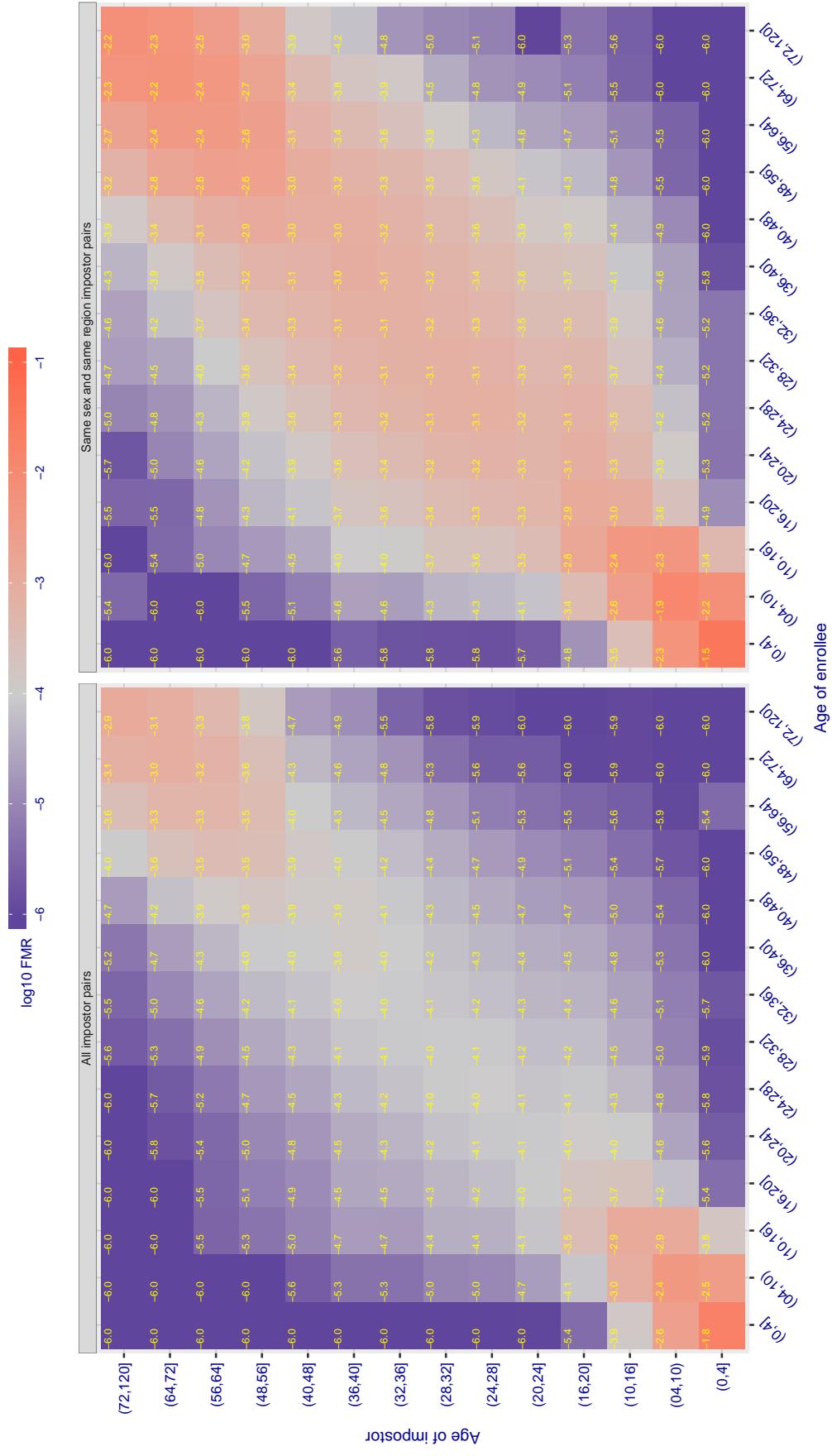


Figure 356: For algorithm amplifiedgroup-001 operating on visa images, the heatmap shows false match observed over impostor comparisons of faces from different individuals who have the given age pair. False matches are counted against a recognition threshold fixed globally to give  $FMR = 0.001$  over all on the order of  $10^{10}$  impostor comparisons. The text in each box gives the same quantity as that coded by the color. Light colors present a security vulnerability to, for example, a passport gate.

Cross age FMR at threshold T = 0.397 for algorithm anke\_003, giving  $FMR(T) = 0.0001$  globally.



**Figure 358:** For algorithm anke-004 operating on visa images, the heatmap shows false match observed over impostor comparisons of faces from different individuals who have the given age pair. False matches are counted against a recognition threshold fixed globally to give  $FMR = 0.001$  over all on the order of  $10^{10}$  impostor comparisons. The text in each box gives the same quantity as that coded by the color. Light colors present a security vulnerability to, for example, a passport gate.

Cross age FMR at threshold T = 1.526 for algorithm anyvision\_002, giving  $\text{FMR}(\text{T}) = 0.0001$  globally.

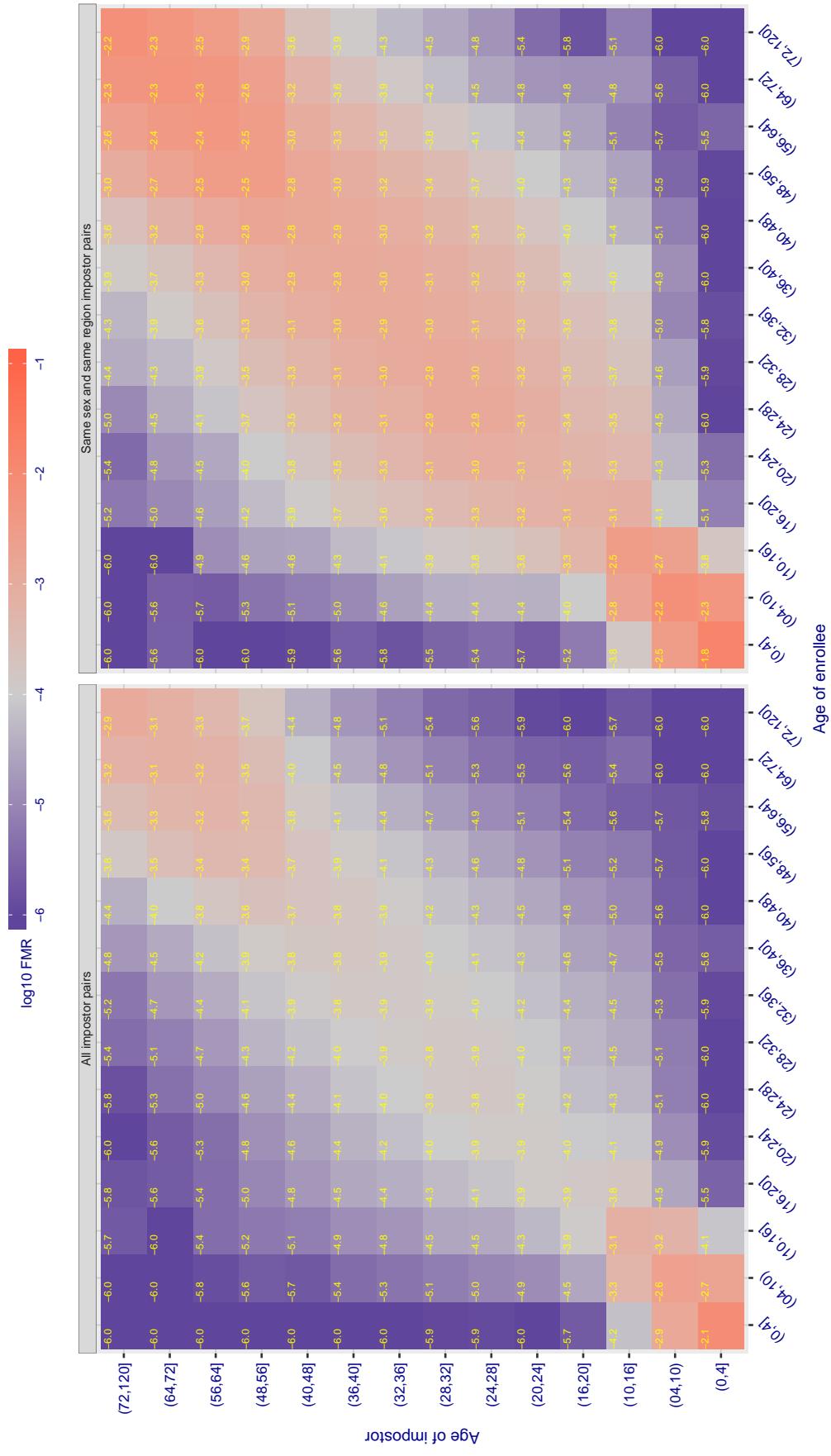
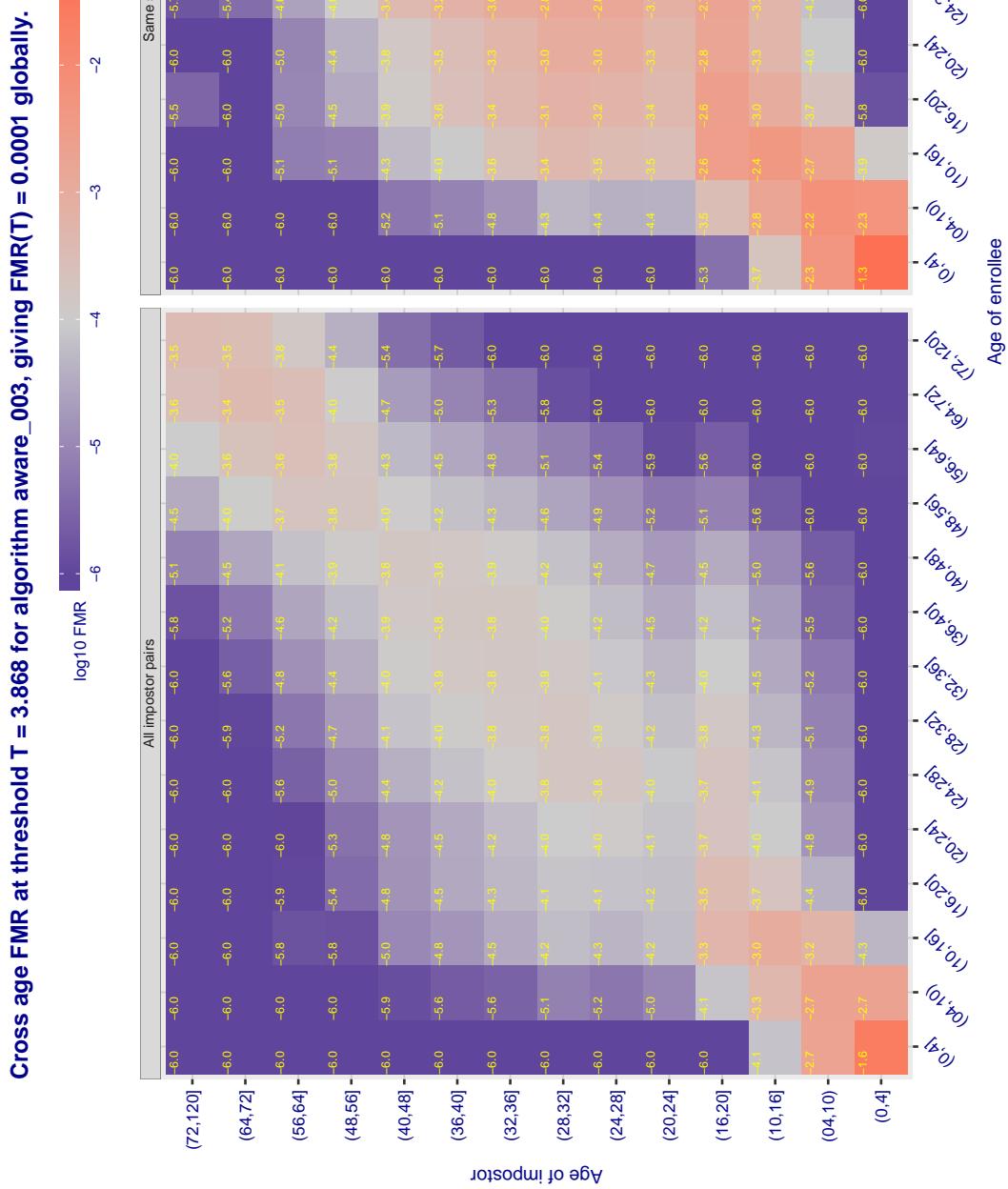
Cross age FMR at threshold T = 1.375 for algorithm anyvision\_004, giving  $FMR(T) = 0.0001$  globally.

Figure 360: For algorithm anyvision-004 operating on visa images, the heatmap shows false match observed over impostor comparisons of faces from different individuals who have the given age pair. False matches are counted against a recognition threshold fixed globally to give  $FMR = 0.001$  over all on the order of  $10^{10}$  impostor comparisons. The text in each box gives the same quantity as that coded by the color. Light colors present a security vulnerability to, for example, a passport gate.



**Figure 361:** For algorithm aware-003 operating on visa images, the heatmap shows false match observed over impostor comparisons of faces from different individuals who have the given age pair. False matches are counted against a recognition threshold fixed globally to give  $FMR = 0.001$  over all on the order of  $10^{10}$  impostor comparisons. The text in each box gives the same quantity as that coded by the color. Light colors present a security vulnerability to, for example, a passport gate.

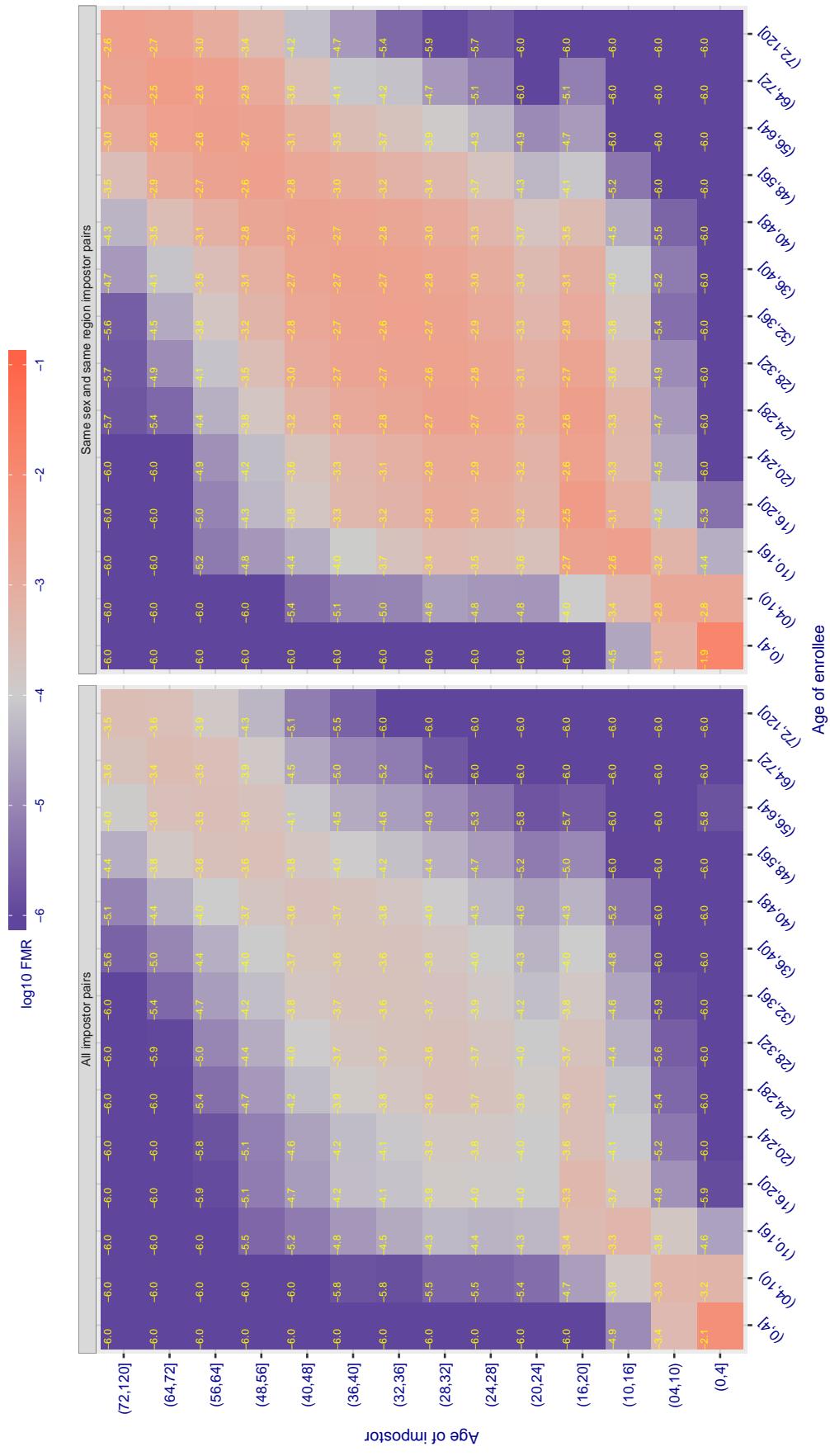
Cross age FMR at threshold T = 5.084 for algorithm aware\_004, giving  $\text{FMR}(\text{T}) = 0.0001$  globally.

Figure 362: For algorithm aware-004 operating on visa images, the heatmap shows false match observed over impostor comparisons of faces from different individuals who have the given age pair. False matches are counted against a recognition threshold fixed globally to give  $\text{FMR} = 0.001$  over all on the order of  $10^{10}$  impostor comparisons. The text in each box gives the same quantity as that coded by the color. Light colors present a security vulnerability to, for example, a passport gate.

Cross age FMR at threshold T = 0.919 for algorithm ayonix\_000, giving FMR(T) = 0.0001 globally.

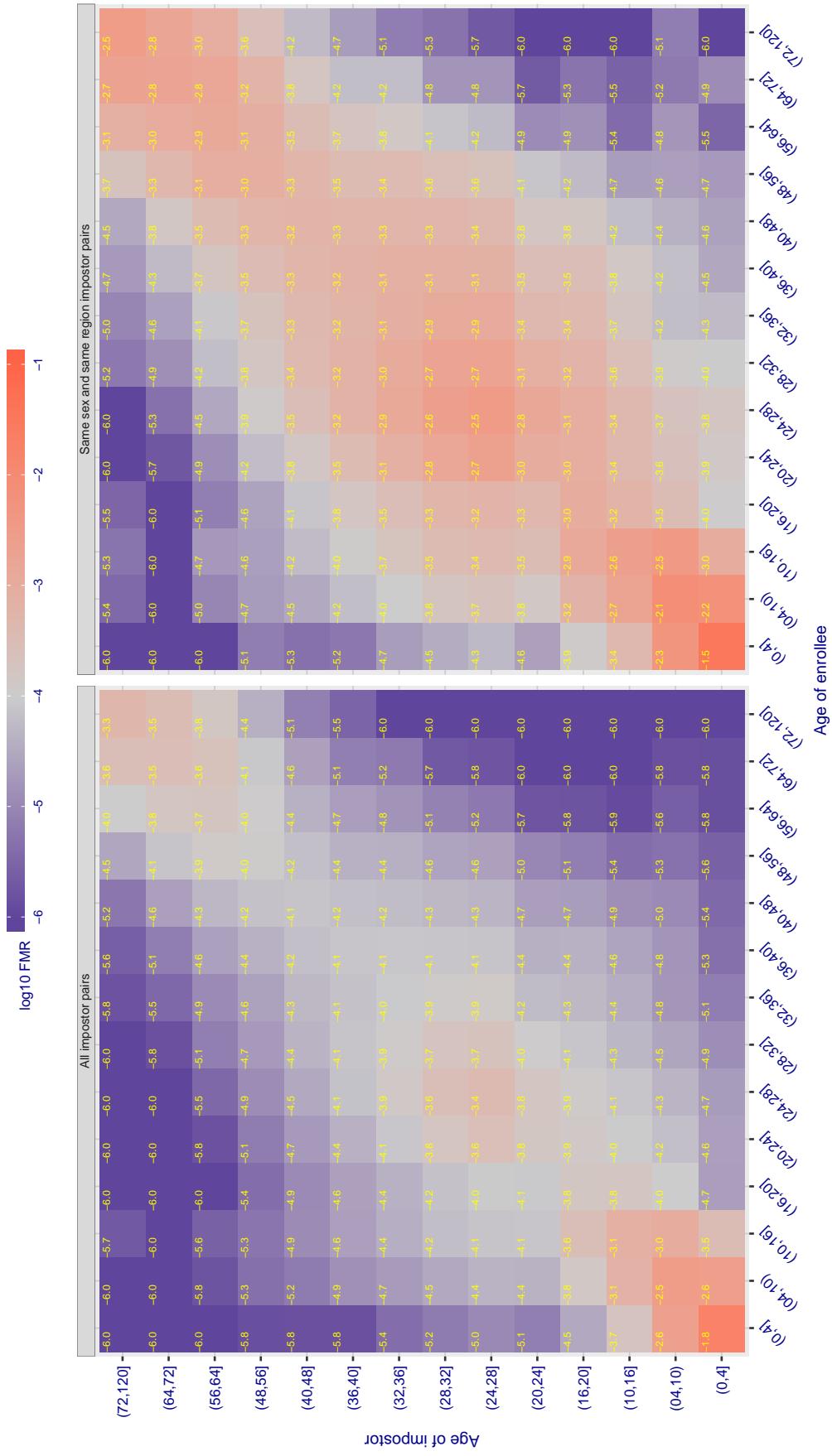


Figure 363: For algorithm ayonix-000 operating on visa images, the heatmap shows false match observed over impostor comparisons of faces from different individuals who have the given age pair. False matches are counted against a recognition threshold fixed globally to give FMR = 0.001 over all on the order of  $10^{10}$  impostor comparisons. The text in each box gives the same quantity as that coded by the color. Light colors present a security vulnerability to, for example, a passport gate.

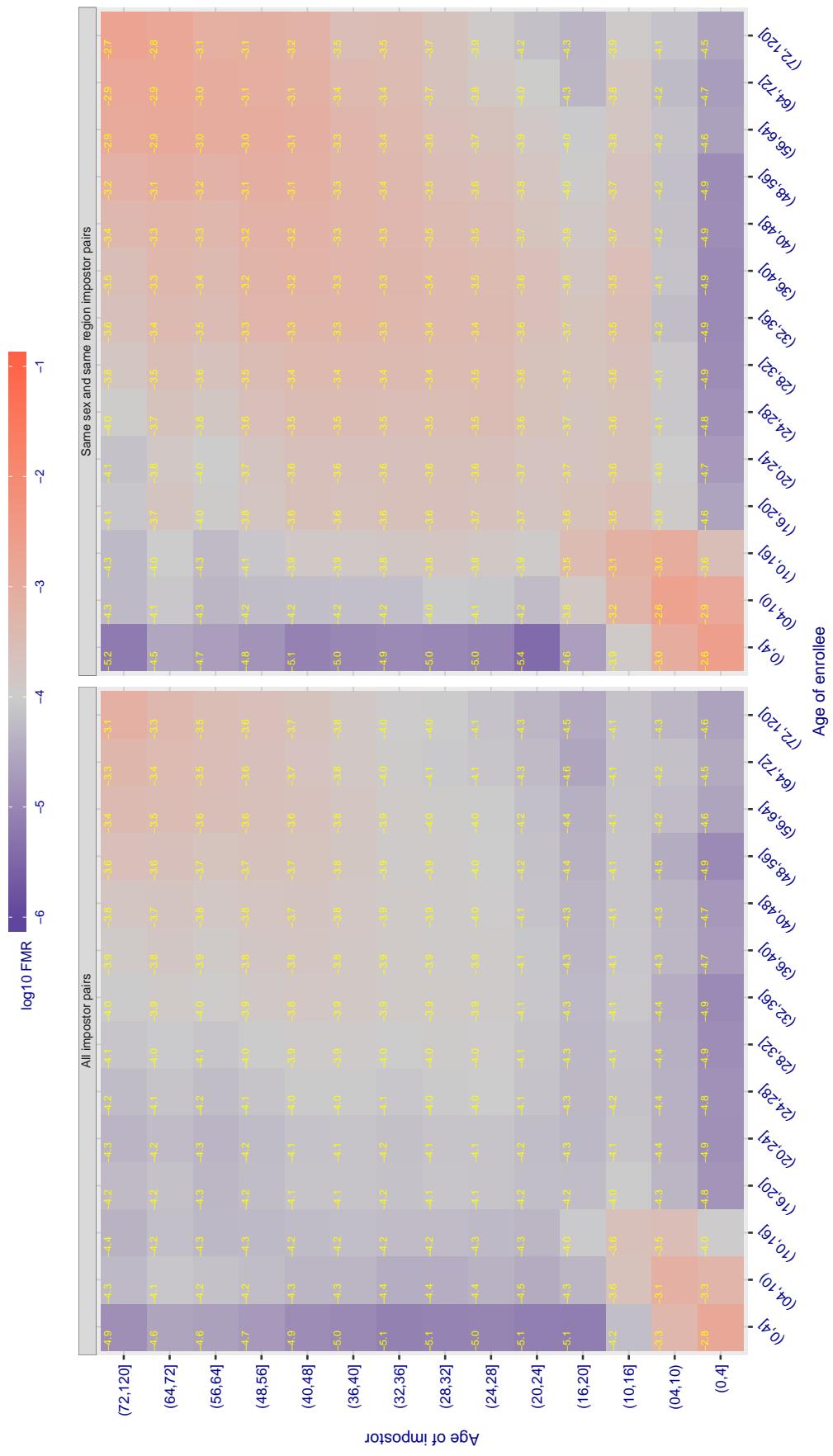
Cross age FMR at threshold T = 0.731 for algorithm bm\_001, giving  $FMR(T) = 0.0001$  globally.

Figure 364: For algorithm bm\_001 operating on visa images, the heatmap shows false match observed over impostor comparisons of faces from different individuals who have the given age pair. False matches are counted against a recognition threshold fixed globally to give  $FMR = 0.001$  over all on the order of  $10^{10}$  impostor comparisons. The text in each box gives the same quantity as that coded by the color. Light colors present a security vulnerability to, for example, a passport gate.

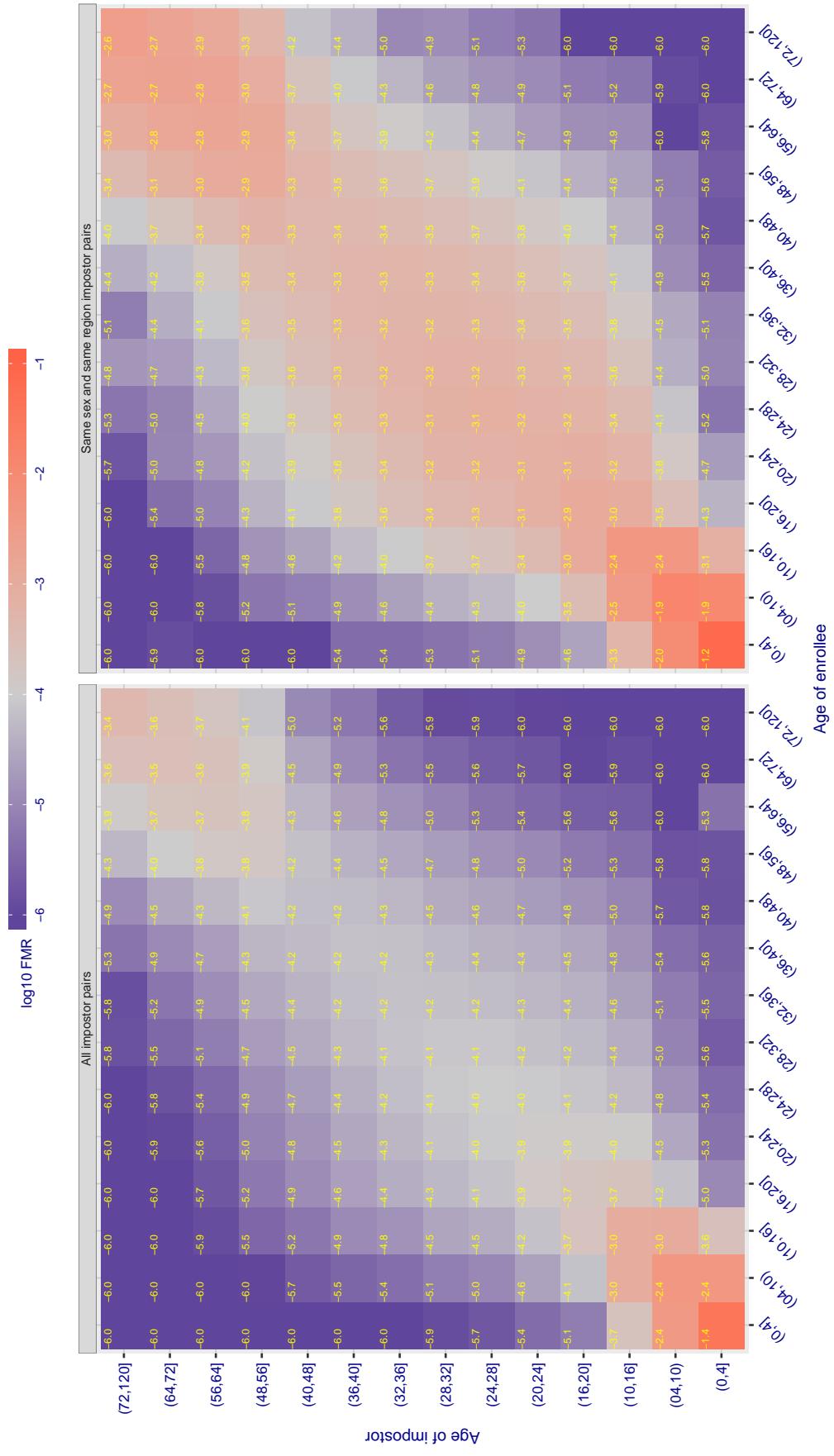
Cross age FMR at threshold T = 0.388 for algorithm camvi\_002, giving  $\text{FMR}(\text{T}) = 0.0001$  globally.

Figure 365: For algorithm camvi-002 operating on visa images, the heatmap shows false match observed over impostor comparisons of faces from different individuals who have the given age pair. False matches are counted against a recognition threshold fixed globally to give  $\text{FMR} = 0.001$  over all on the order of  $10^{10}$  impostor comparisons. The text in each box gives the same quantity as that coded by the color. Light colors present a security vulnerability to, for example, a passport gate.

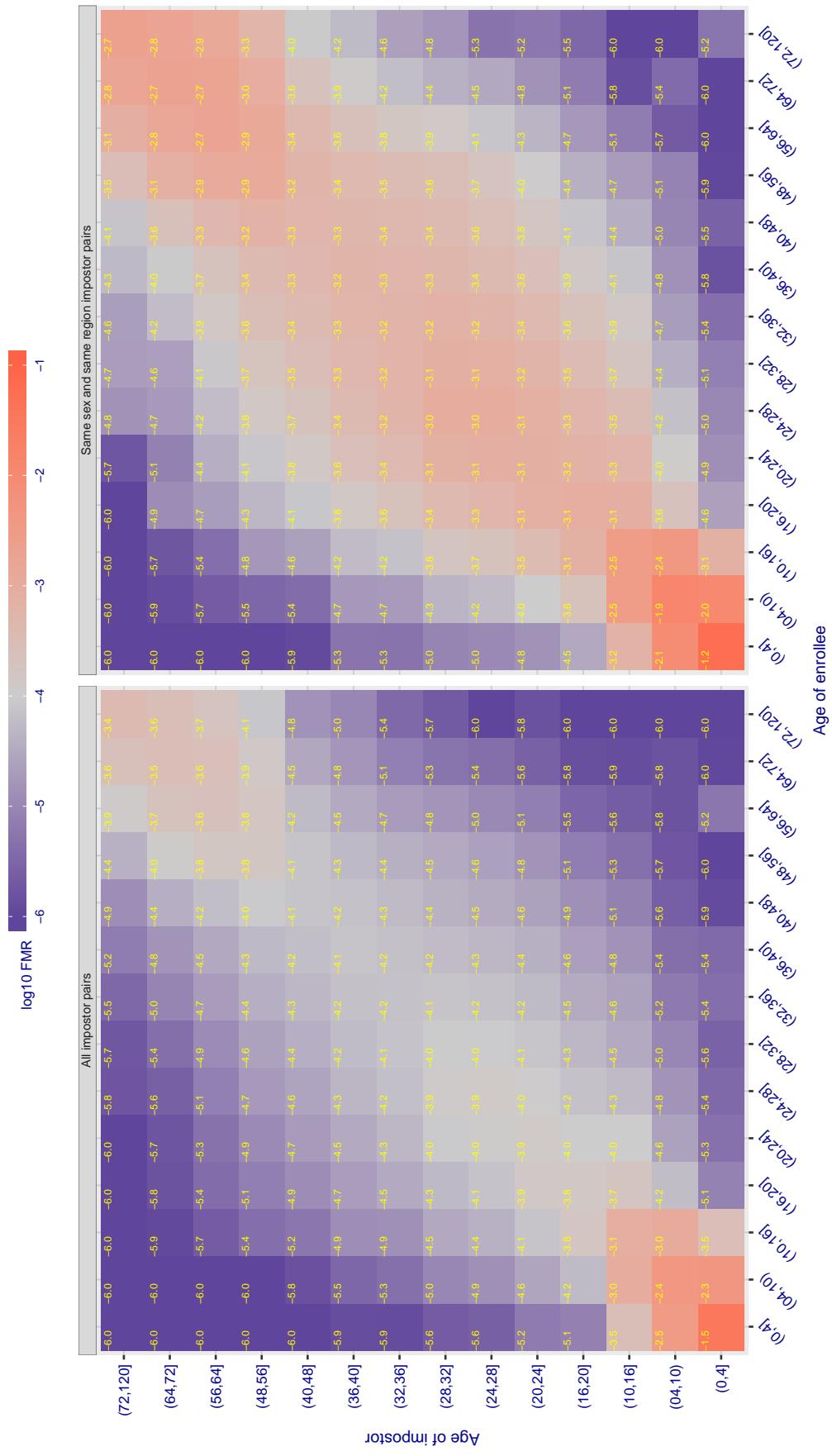
Cross age FMR at threshold T = 0.383 for algorithm camvi\_003, giving  $\text{FMR}(\text{T}) = 0.0001$  globally.

Figure 366: For algorithm camvi-003 operating on visa images, the heatmap shows false match observed over impostor comparisons of faces from different individuals who have the given age pair. False matches are counted against a recognition threshold fixed globally to give  $\text{FMR} = 0.001$  over all on the order of  $10^{10}$  impostor comparisons. The text in each box gives the same quantity as that coded by the color. Light colors present a security vulnerability to, for example, a passport gate.

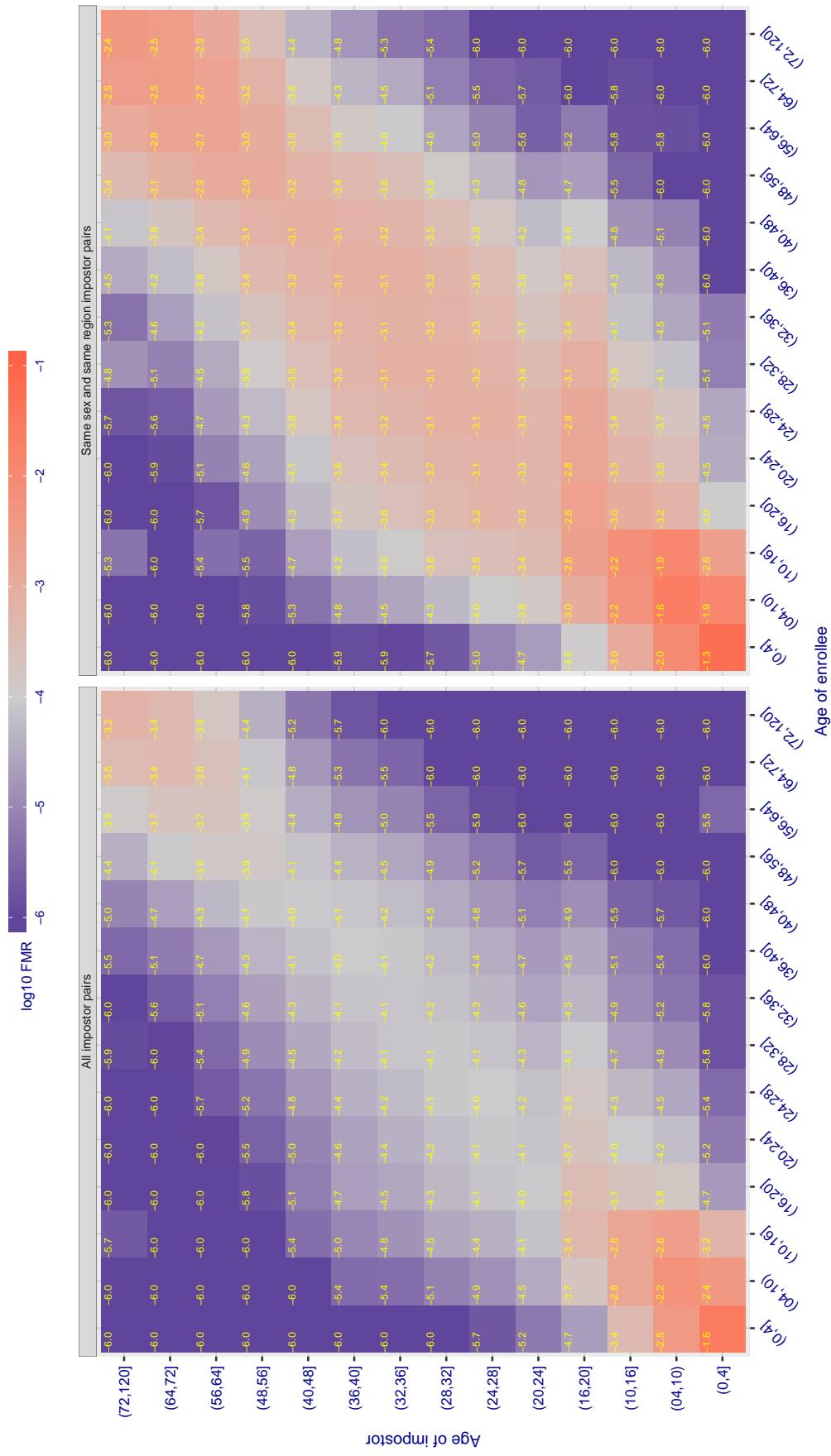
Cross age FMR at threshold T = 0.436 for algorithm ceiec\_001, giving  $FMR(T) = 0.0001$  globally.

Figure 367: For algorithm ceiec-001 operating on visa images, the heatmap shows false match observed over impostor comparisons of faces from different individuals who have the given age pair. False matches are counted against a recognition threshold fixed globally to give  $FMR = 0.001$  over all on the order of  $10^{10}$  impostor comparisons. The text in each box gives the same quantity as that coded by the color. Light colors present a security vulnerability to, for example, a passport gate.

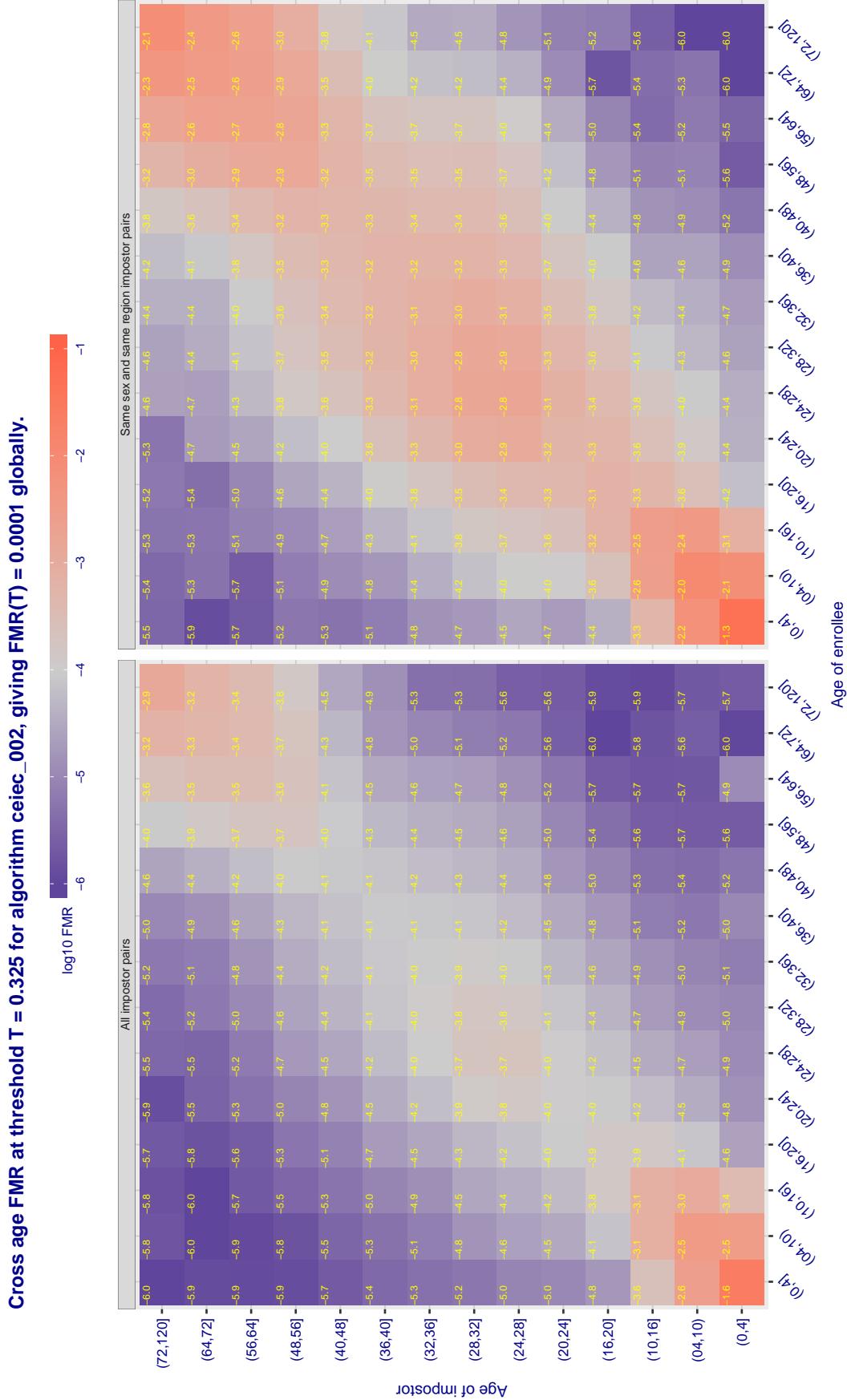
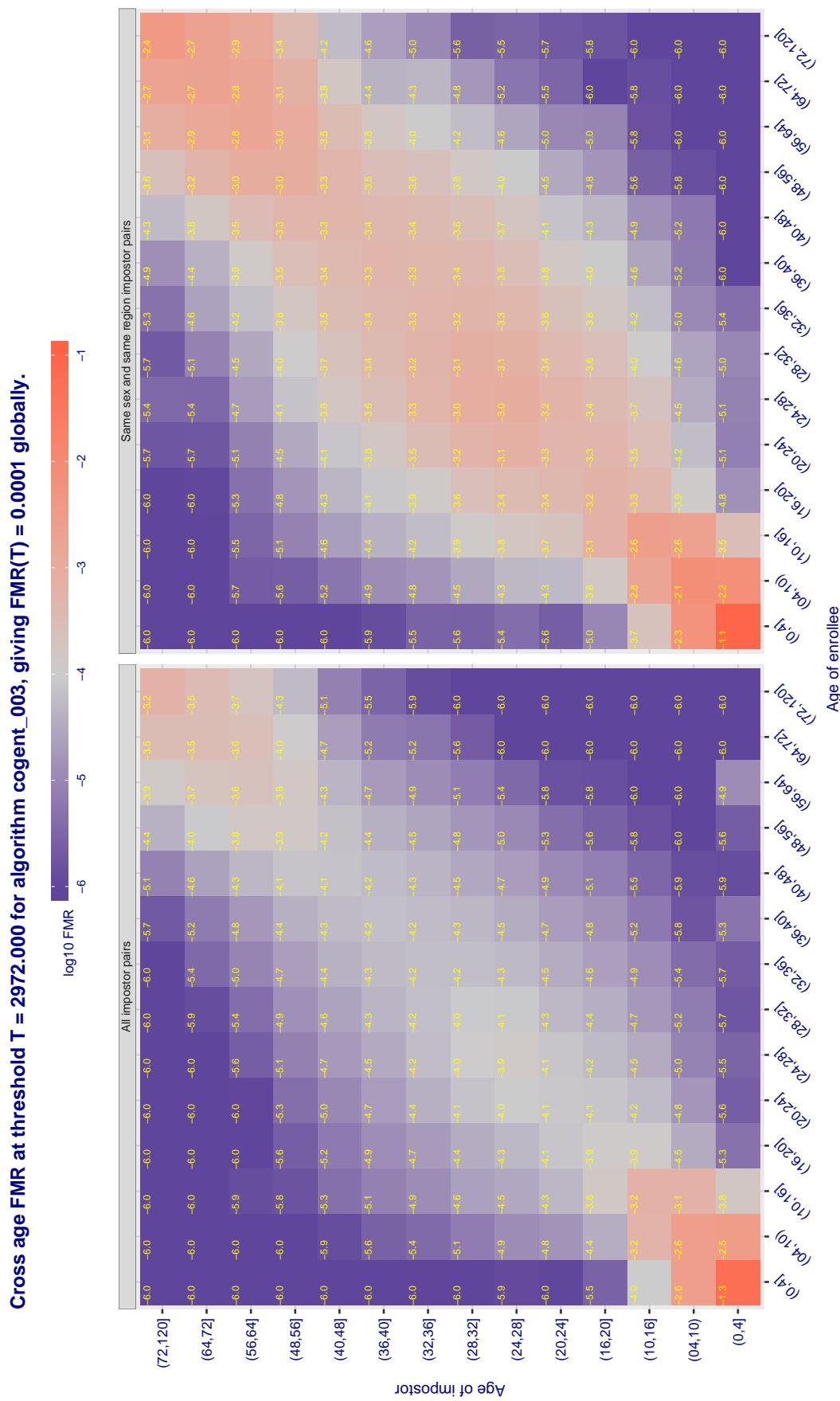
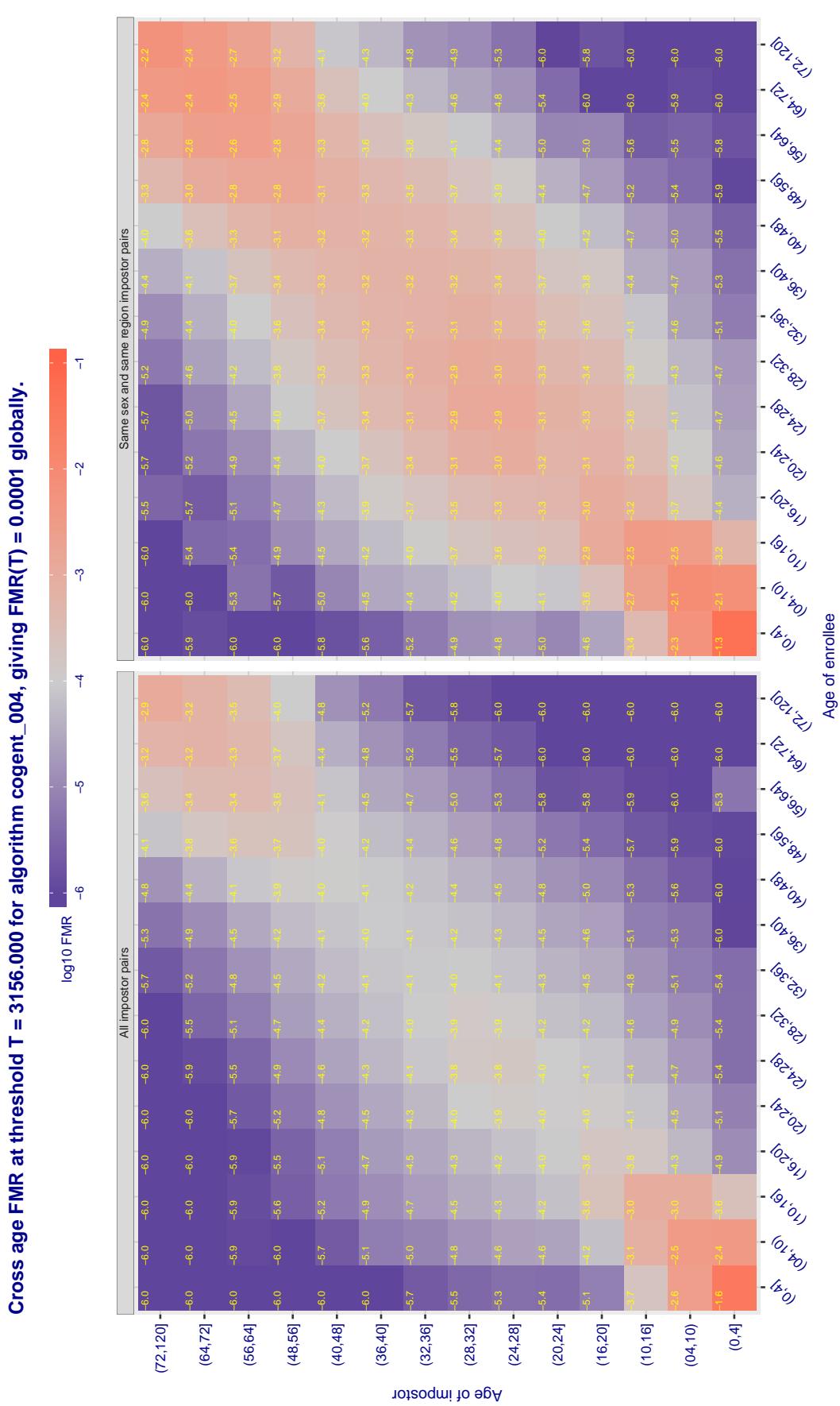


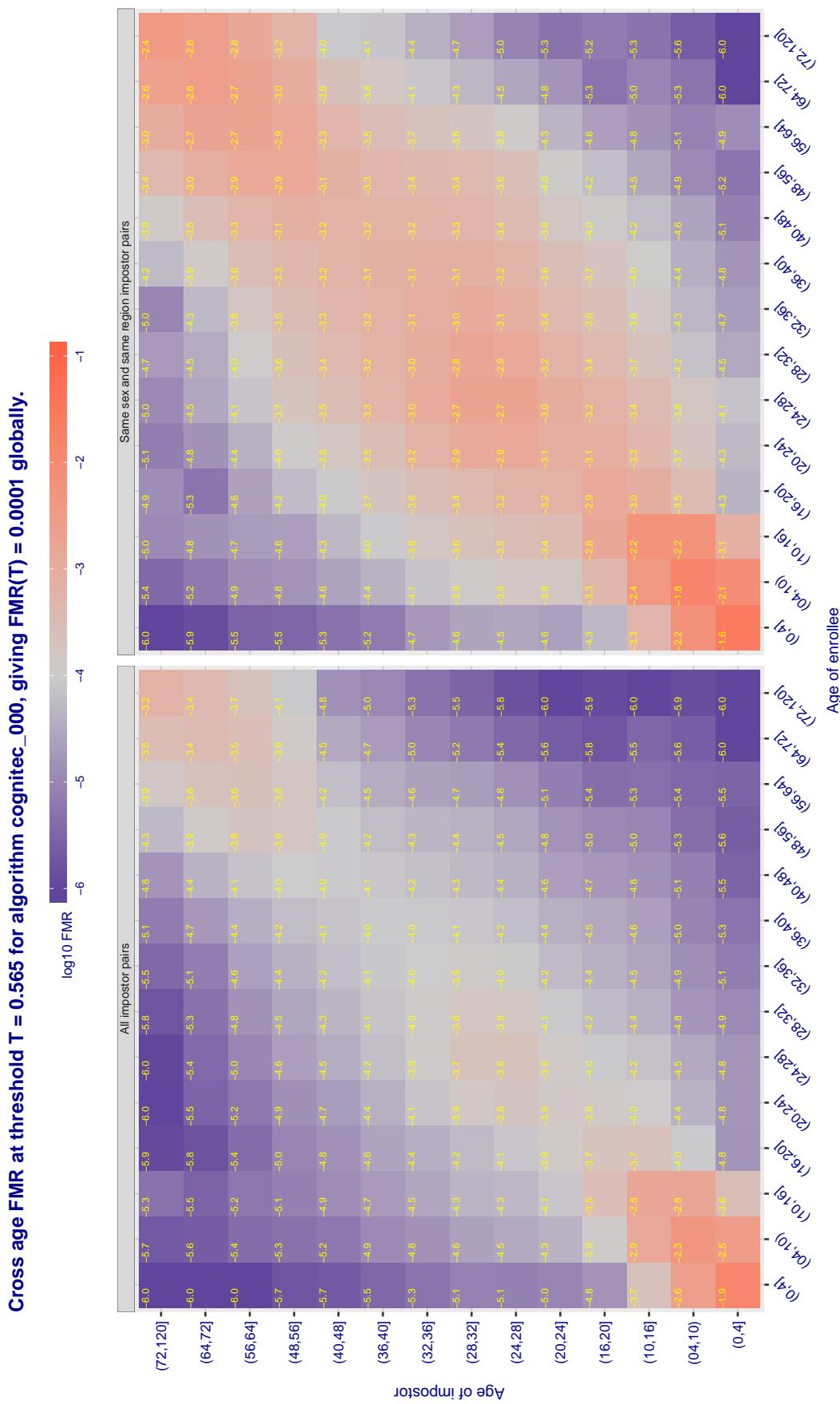
Figure 368: For algorithm ceiec-002 operating on visa images, the heatmap shows false match observed over impostor comparisons of faces from different individuals who have the given age pair. False matches are counted against a recognition threshold fixed globally to give  $FMR = 0.001$  over all on the order of  $10^{10}$  impostor comparisons. The text in each box gives the same quantity as that coded by the color. Light colors present a security vulnerability to, for example, a passport gate.



**Figure 369:** For algorithm cogent-003 operating on visa images, the heatmap shows false match observed over impostor comparisons of faces from different individuals who have the given age pair. False matches are counted against a recognition threshold fixed globally to give  $FMR = 0.001$  over all on the order of  $10^{10}$  impostor comparisons. The text in each box gives the same quantity as that coded by the color. Light colors present a security vulnerability to, for example, a passport gate.

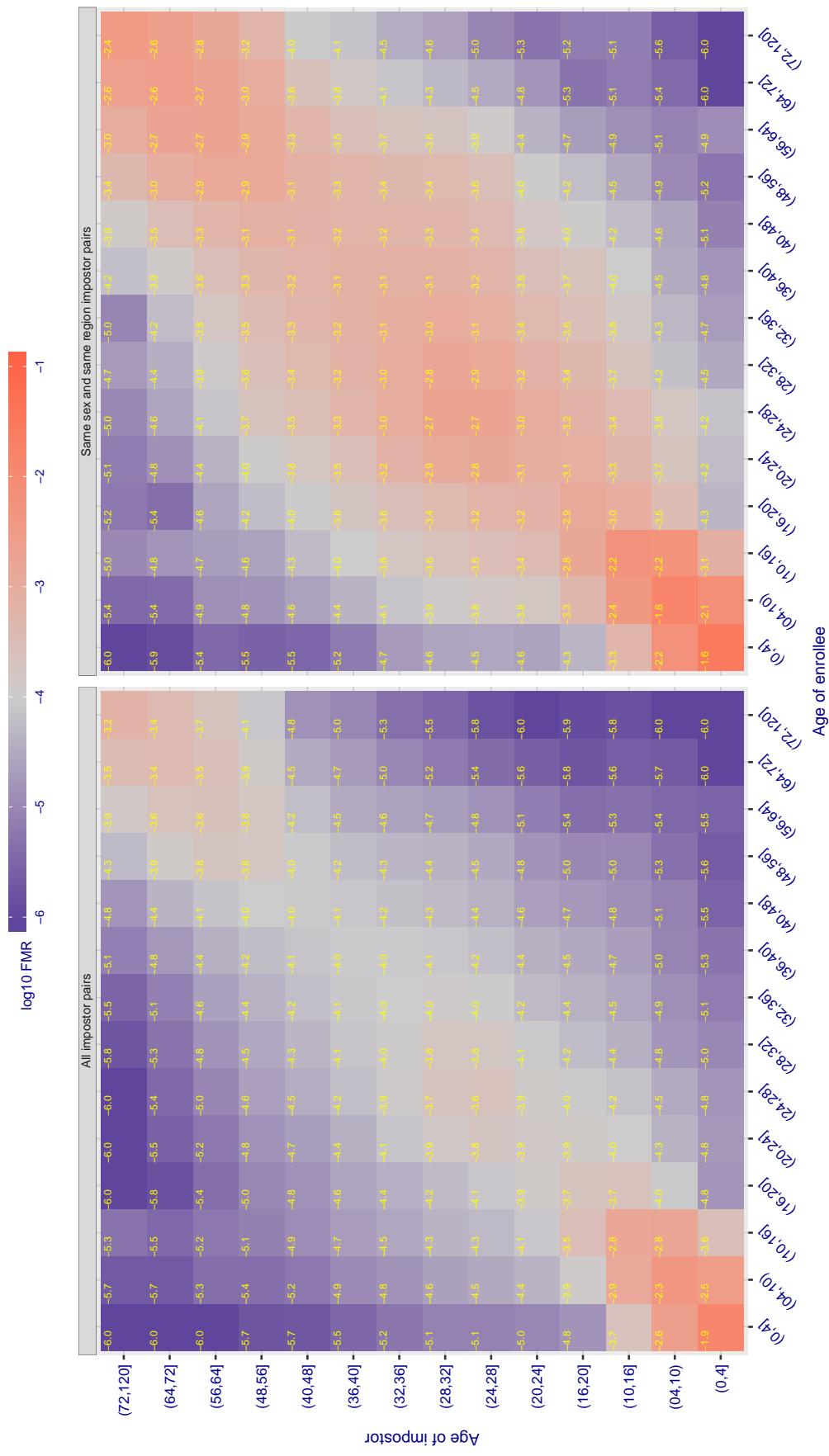


**Figure 370:** For algorithm cogent-004 operating on visa images, the heatmap shows false match observed over impostor comparisons of faces from different individuals who have the given age pair. False matches are counted against a recognition threshold fixed globally to give  $FMR = 0.001$  over all on the order of  $10^{10}$  impostor comparisons. The text in each box gives the same quantity as that coded by the color. Light colors present a security vulnerability to, for example, a passport gate.



**Figure 371:** For algorithm cognitec-000 operating on visa images, the heatmap shows false match observed over impostor comparisons of faces from different individuals who have the given age pair. False matches are counted against a recognition threshold fixed globally to give  $FMR = 0.001$  over all on the order of  $10^{10}$  impostor comparisons. The text in each box gives the same quantity as that coded by the color. Light colors present a security vulnerability to, for example, a passport gate.

Cross age FMR at threshold T = 0.565 for algorithm cognitec\_001, giving FMR(T) = 0.0001 globally.

Figure 372: For algorithm cognitec-001 operating on visa images, the heatmap shows false match observed over impostor comparisons of faces from different individuals who have the given age pair. False matches are counted against a recognition threshold fixed globally to give FMR = 0.001 over all on the order of  $10^{10}$  impostor comparisons. The text in each box gives the same quantity as that coded by the color. Light colors present a security vulnerability to, for example, a passport gate.

Cross age FMR at threshold T = 3.730 for algorithm ctbcbank\_000, giving FMR(T) = 0.0001 globally.

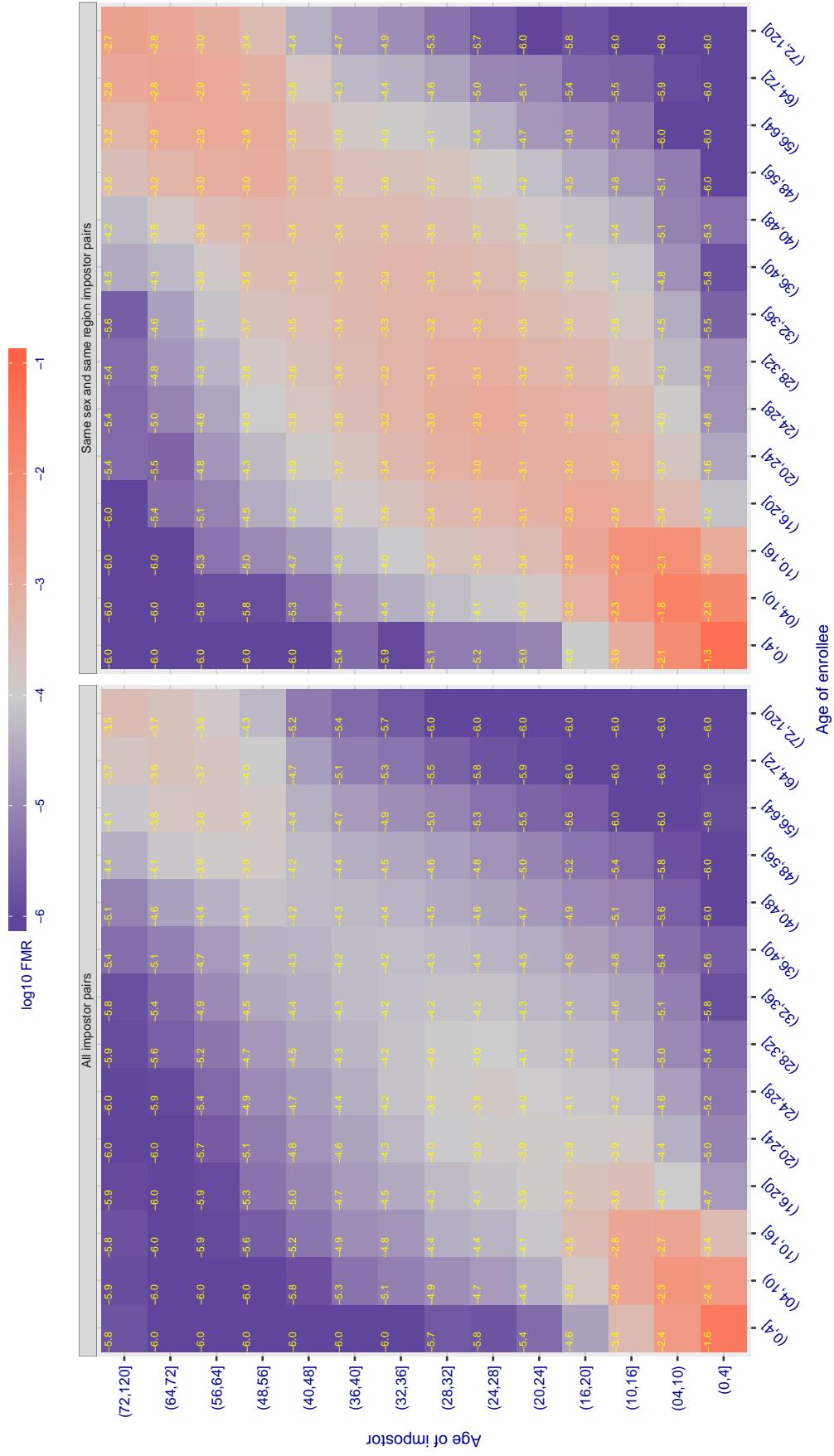
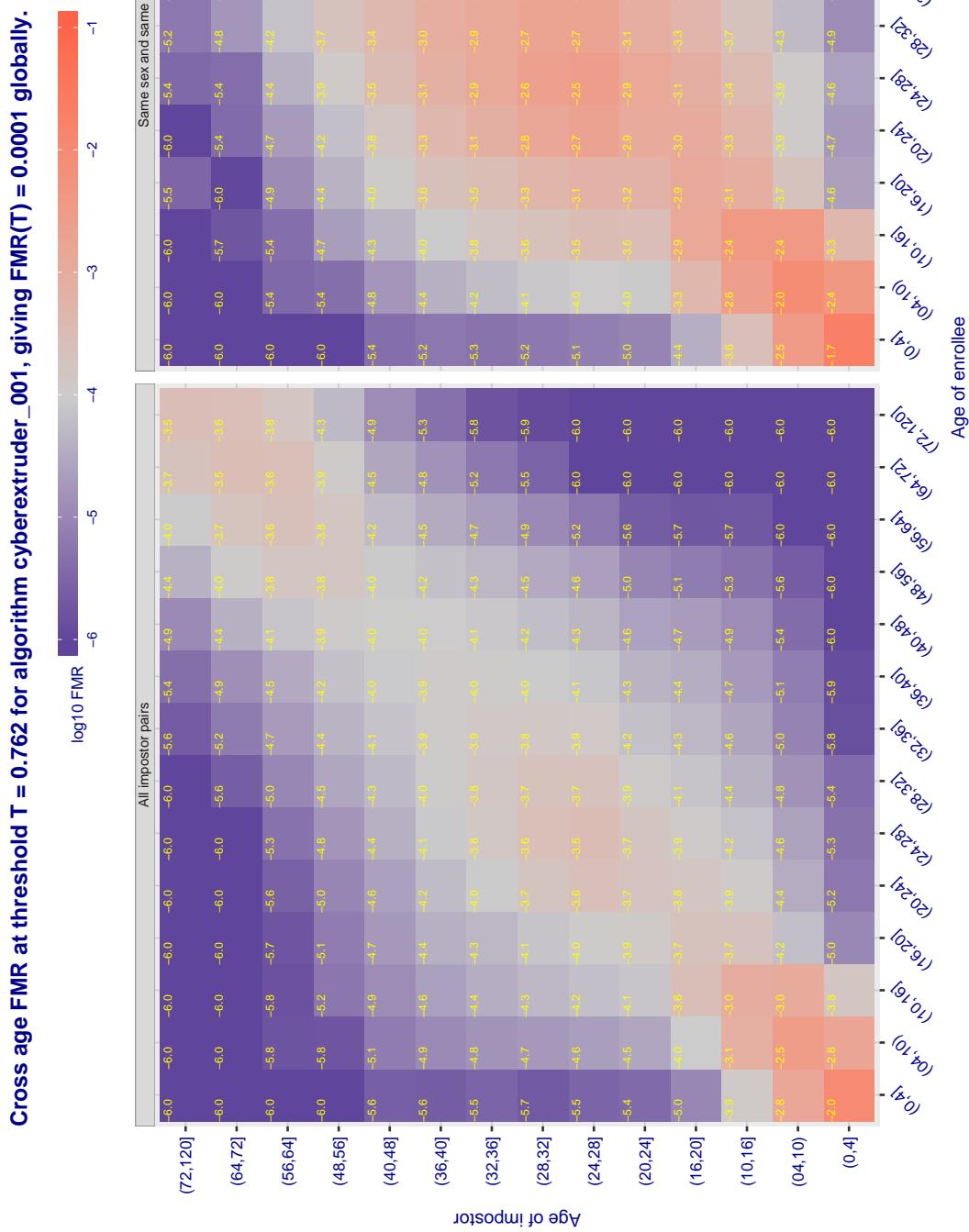


Figure 373: For algorithm ctbcbank-000 operating on visa images, the heatmap shows false match observed over impostor comparisons of faces from different individuals who have the given age pair. False matches are counted against a recognition threshold fixed globally to give FMR = 0.001 over all on the order of  $10^{10}$  impostor comparisons. The text in each box gives the same quantity as that coded by the color. Light colors present a security vulnerability to, for example, a passport gate.



**Figure 374:** For algorithm `cyberextruder-001` operating on visa images, the heatmap shows false match observed over impostor comparisons of faces from different individuals who have the given age pair. False matches are counted against a recognition threshold fixed globally to give  $FMR = 0.001$  over all on the order of  $10^{10}$  impostor comparisons. The text in each box gives the same quantity as that coded by the color. Light colors present a security vulnerability to, for example, a passport gate.

**Cross age FMR at threshold T = 0.500 for algorithm cyberextruder\_002, giving FMR(T) = 0.0001 globally.**

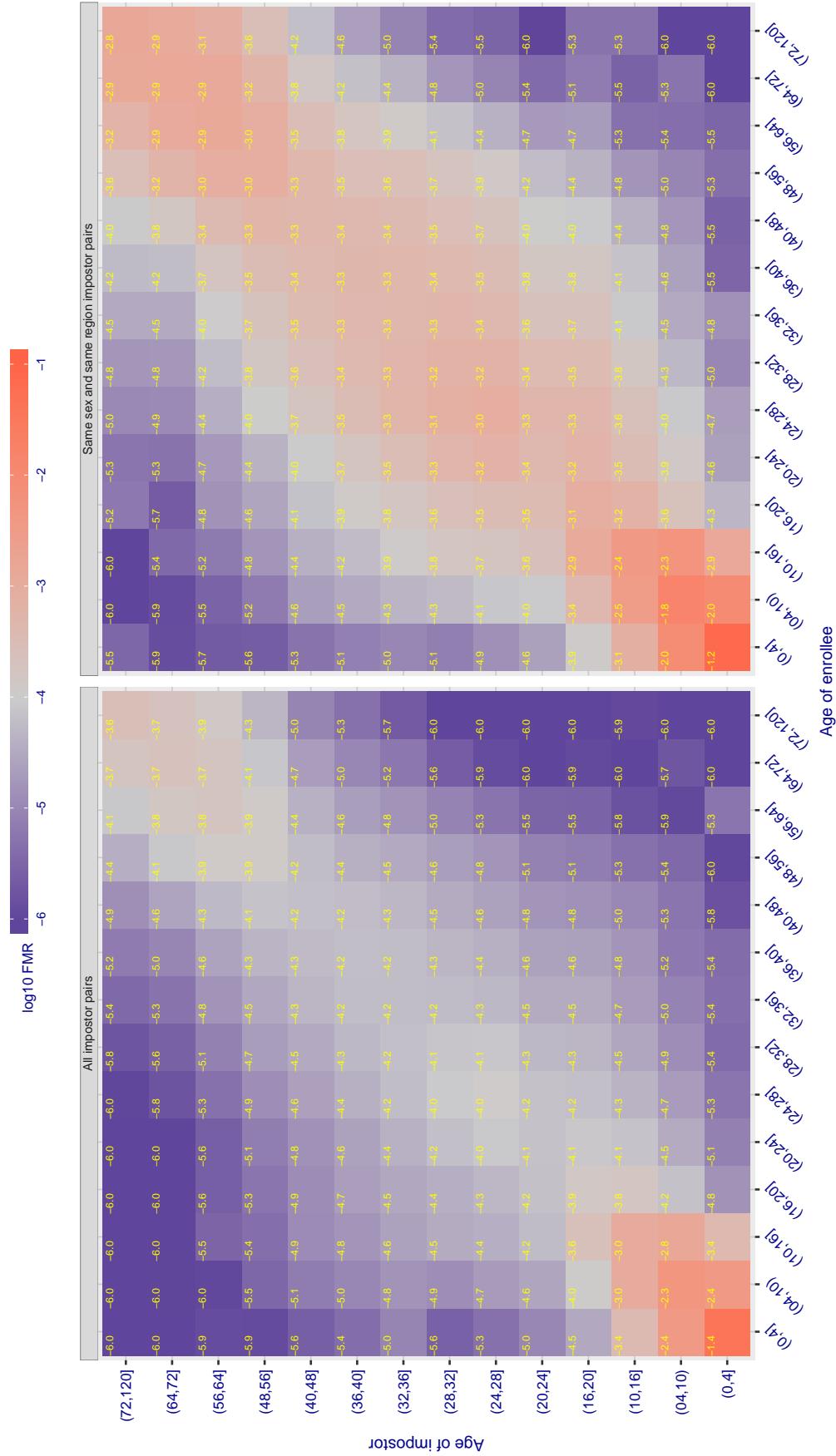


Figure 375: For algorithm cyberextruder-002 operating on visa images, the heatmap shows false match observed over impostor comparisons of faces from different individuals who have the given age pair. False matches are counted against a recognition threshold fixed globally to give  $FMR = 0.001$  over all on the order of  $10^{10}$  impostor comparisons. The text in each box gives the same quantity as that coded by the color. Light colors present a security vulnerability to, for example, a passport gate.

Cross age FMR at threshold T = 1.403 for algorithm cyberlink\_001, giving FMR(T) = 0.0001 globally.

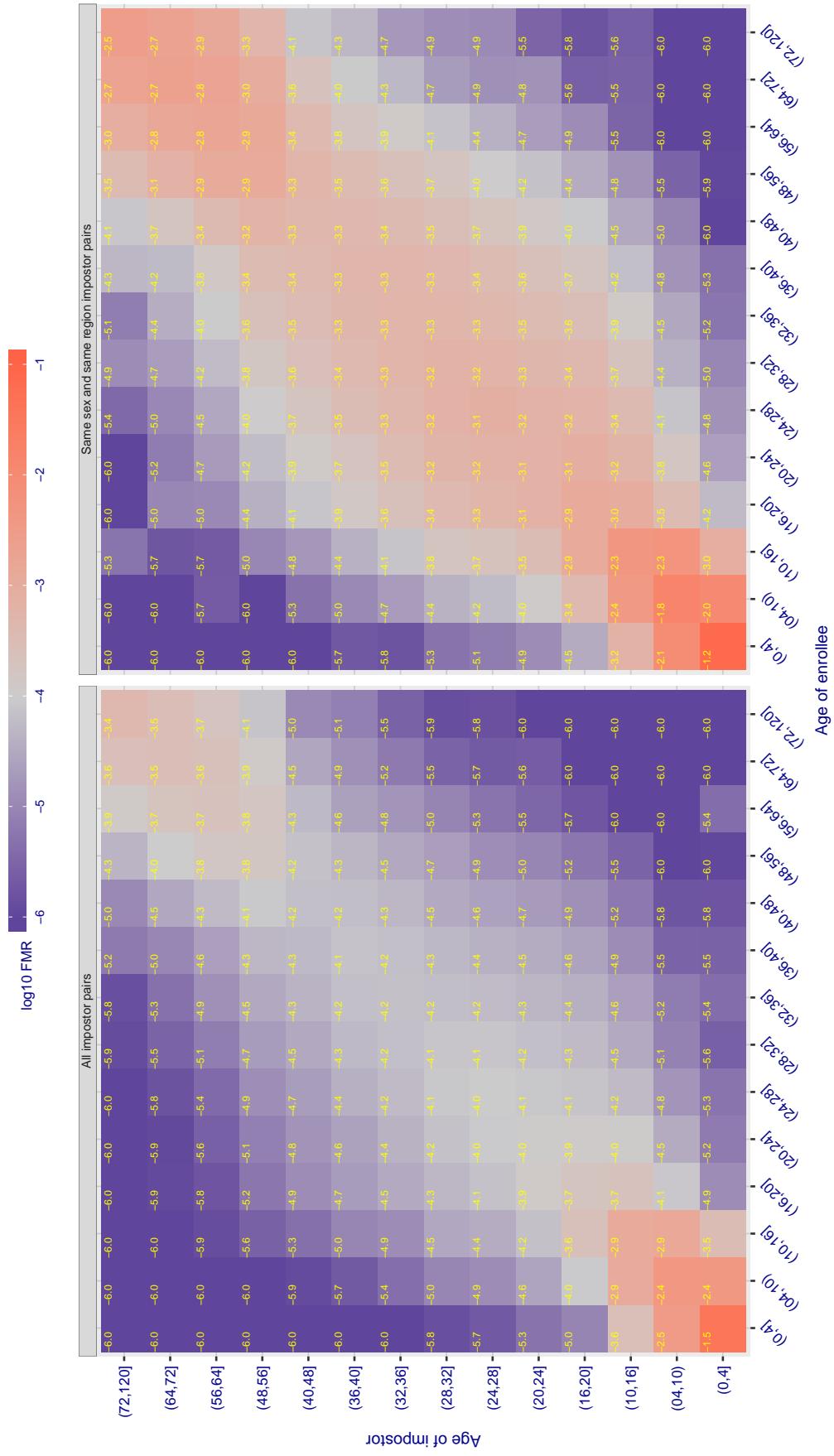
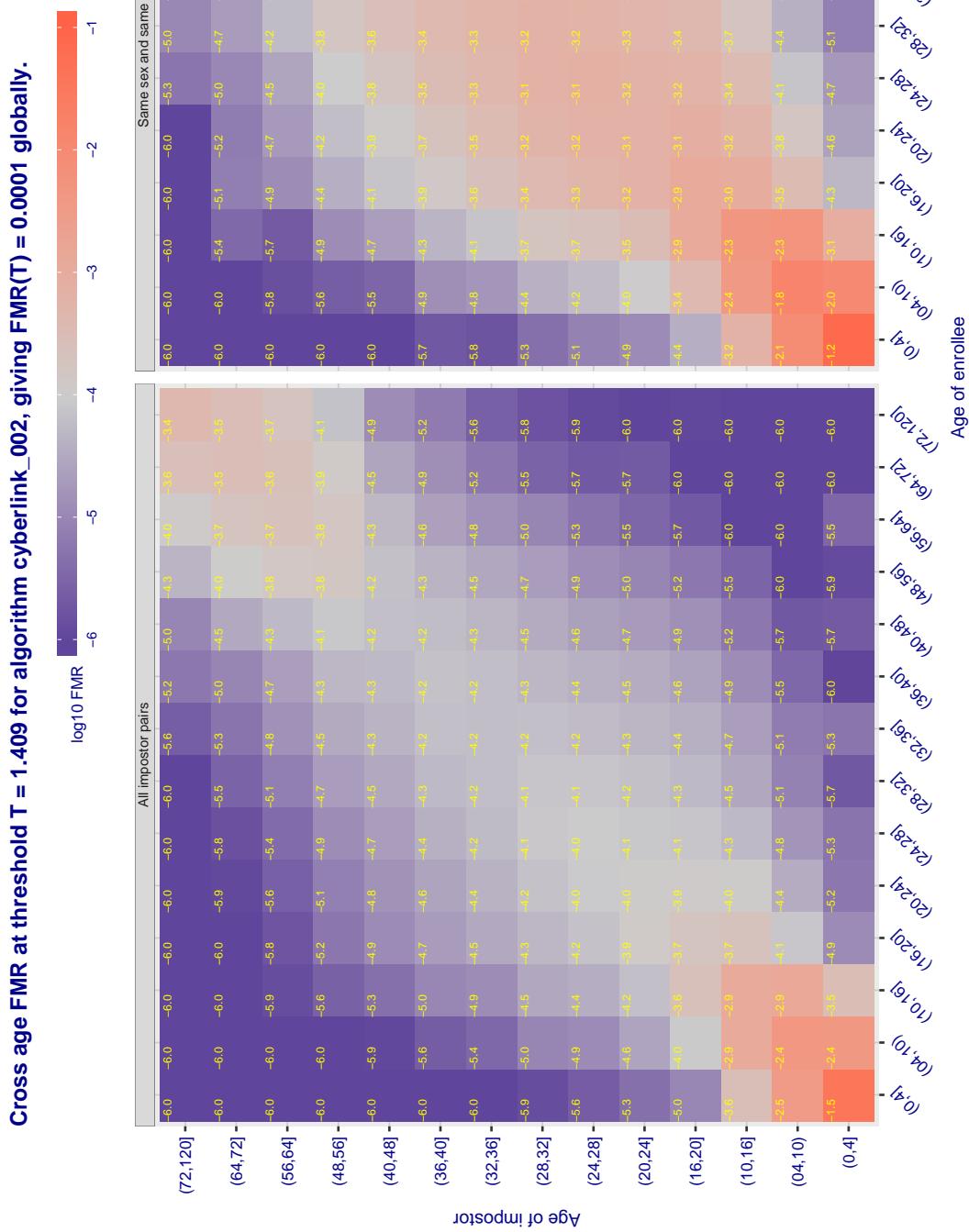
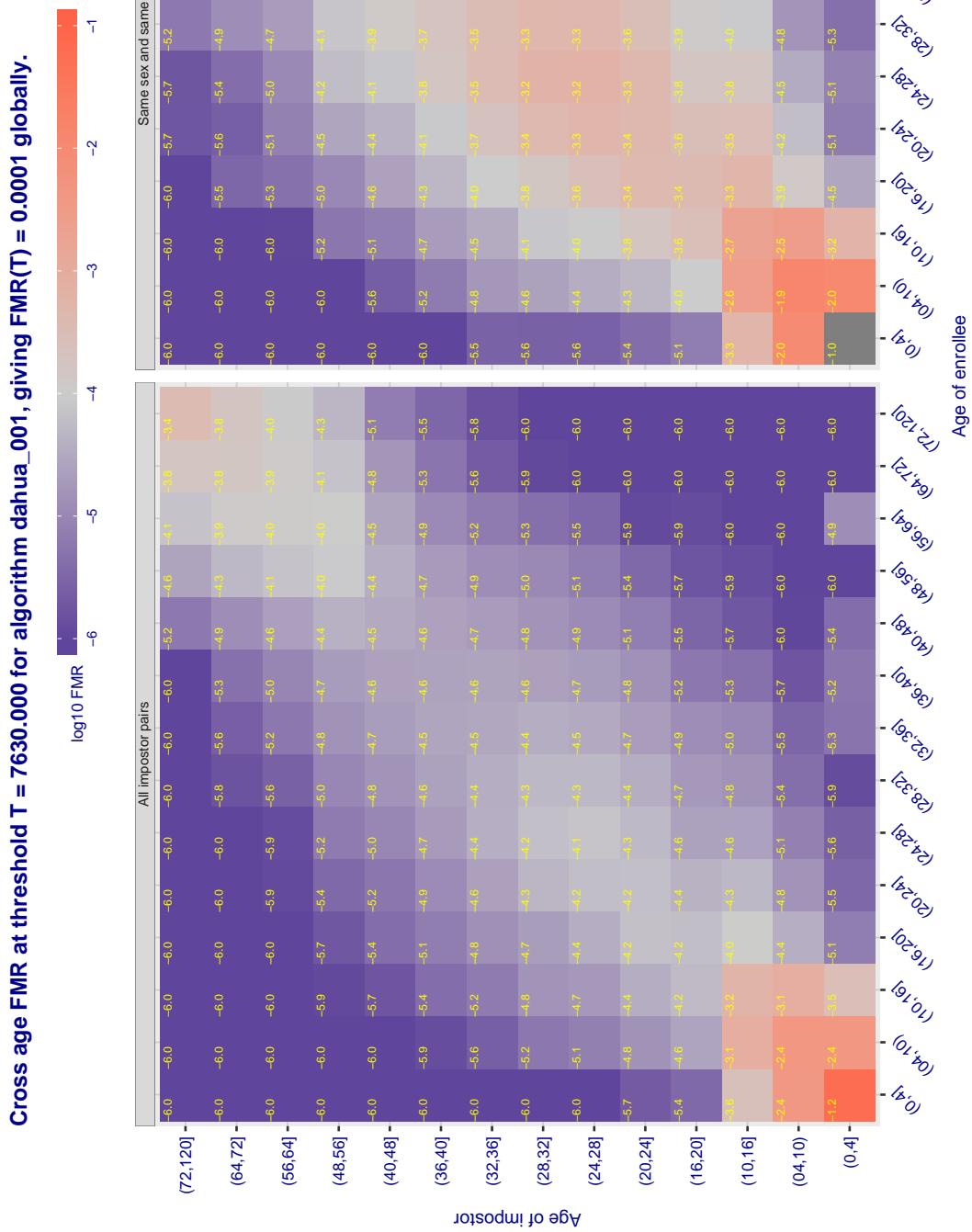


Figure 376: For algorithm cyberlink-001 operating on visa images, the heatmap shows false match observed over impostor comparisons of faces from different individuals who have the given age pair. False matches are counted against a recognition threshold fixed globally to give FMR = 0.001 over all on the order of  $10^{10}$  impostor comparisons. The text in each box gives the same quantity as that coded by the color. Light colors present a security vulnerability to, for example, a passport gate.



**Figure 377:** For algorithm cyberlink-002 operating on visa images, the heatmap shows false match observed over impostor comparisons of faces from different individuals who have the given age pair. False matches are counted against a recognition threshold fixed globally to give  $FMR = 0.001$  over all on the order of  $10^{10}$  impostor comparisons. The text in each box gives the same quantity as that coded by the color. Light colors present a security vulnerability to, for example, a passport gate.



**Figure 378:** For algorithm *dahua-001* operating on visa images, the heatmap shows false match observed over impostor comparisons of faces from different individuals who have the given age pair. False matches are counted against a recognition threshold fixed globally to give  $FMR = 0.001$  over all on the order of  $10^{10}$  impostor comparisons. The text in each box gives the same quantity as that coded by the color. Light colors present a security vulnerability to, for example, a passport gate.

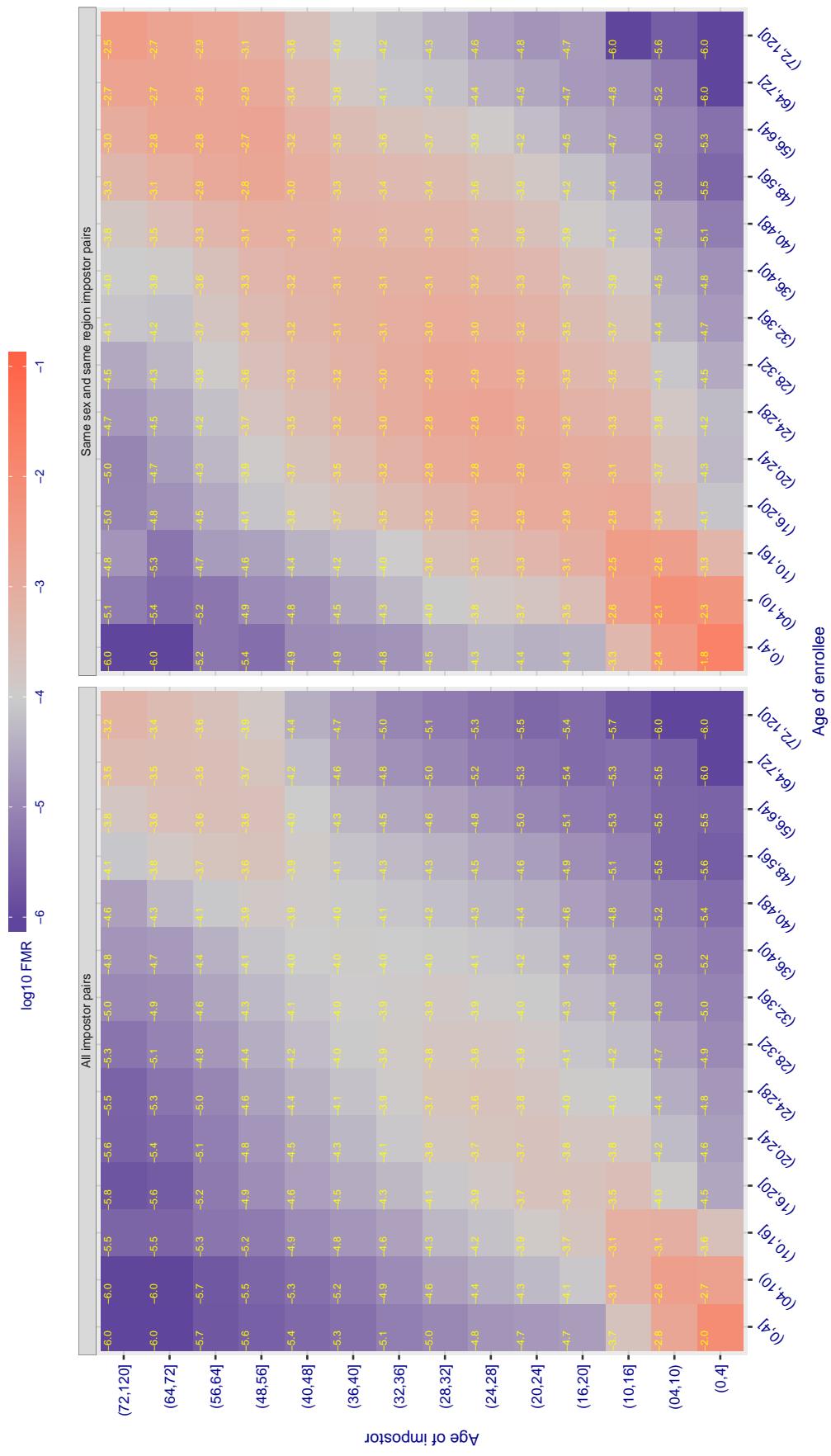
Cross age FMR at threshold T = 6696.000 for algorithm dahua\_002, giving  $FMR(T) = 0.00001$  globally.

Figure 379: For algorithm dahua-002 operating on visa images, the heatmap shows false match observed over impostor comparisons of faces from different individuals who have the given age pair. False matches are counted against a recognition threshold fixed globally to give  $FMR = 0.001$  over all on the order of  $10^{10}$  impostor comparisons. The text in each box gives the same quantity as that coded by the color. Light colors present a security vulnerability to, for example, a passport gate.

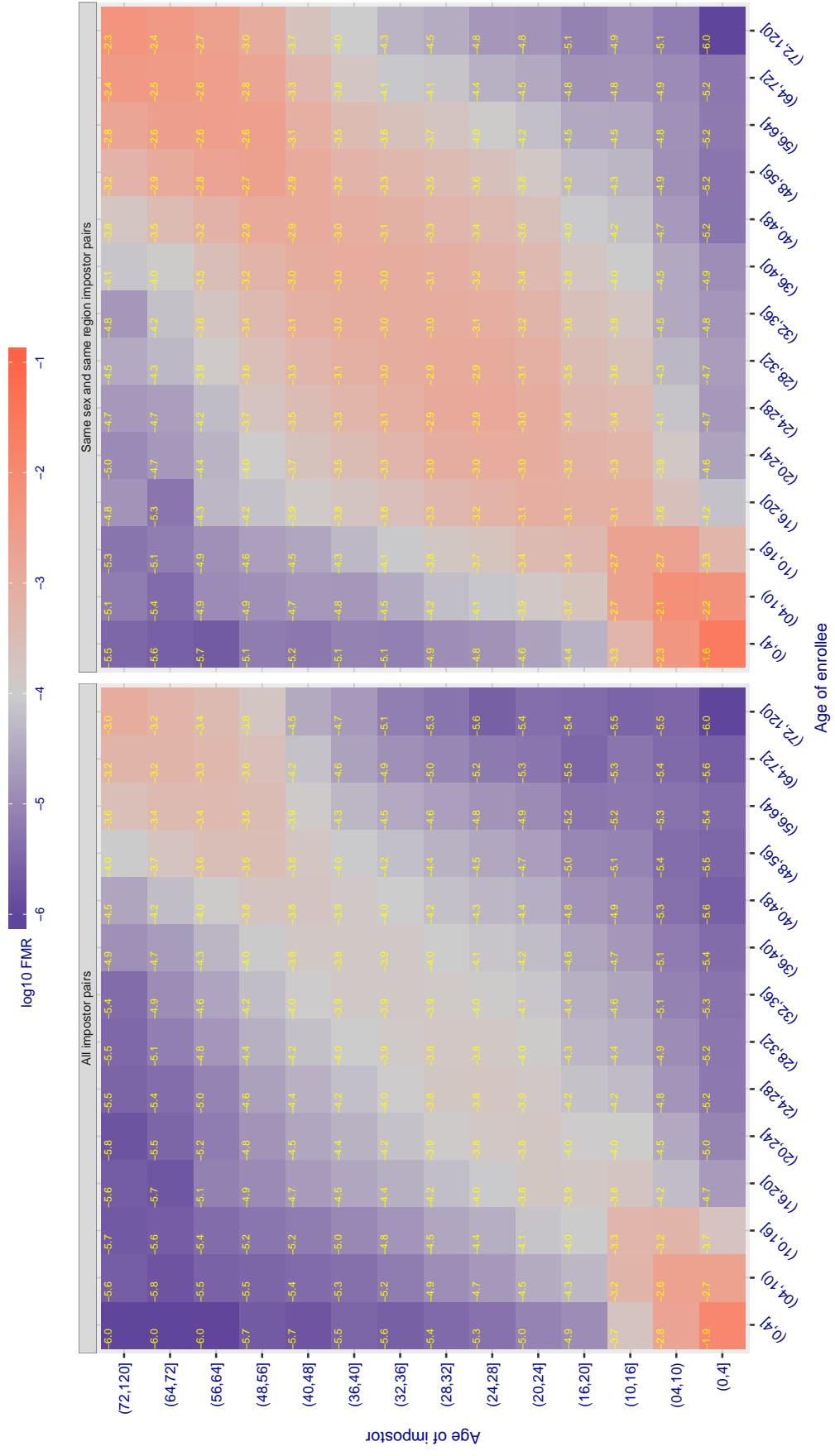
Cross age FMR at threshold T = 1.359 for algorithm `deepglint_001`, giving  $\text{FMR}(\text{T}) = 0.0001$  globally.

Figure 380: For algorithm `deepglint-001` operating on visa images, the heatmap shows false match observed over impostor comparisons of faces from different individuals who have the given age pair. False matches are counted against a recognition threshold fixed globally to give  $\text{FMR} = 0.001$  over all on the order of  $10^{10}$  impostor comparisons. The text in each box gives the same quantity as that coded by the color. Light colors present a security vulnerability to, for example, a passport gate.

Cross age FMR at threshold T = 1.371 for algorithm deepsea\_001, giving FMR(T) = 0.0001 globally.

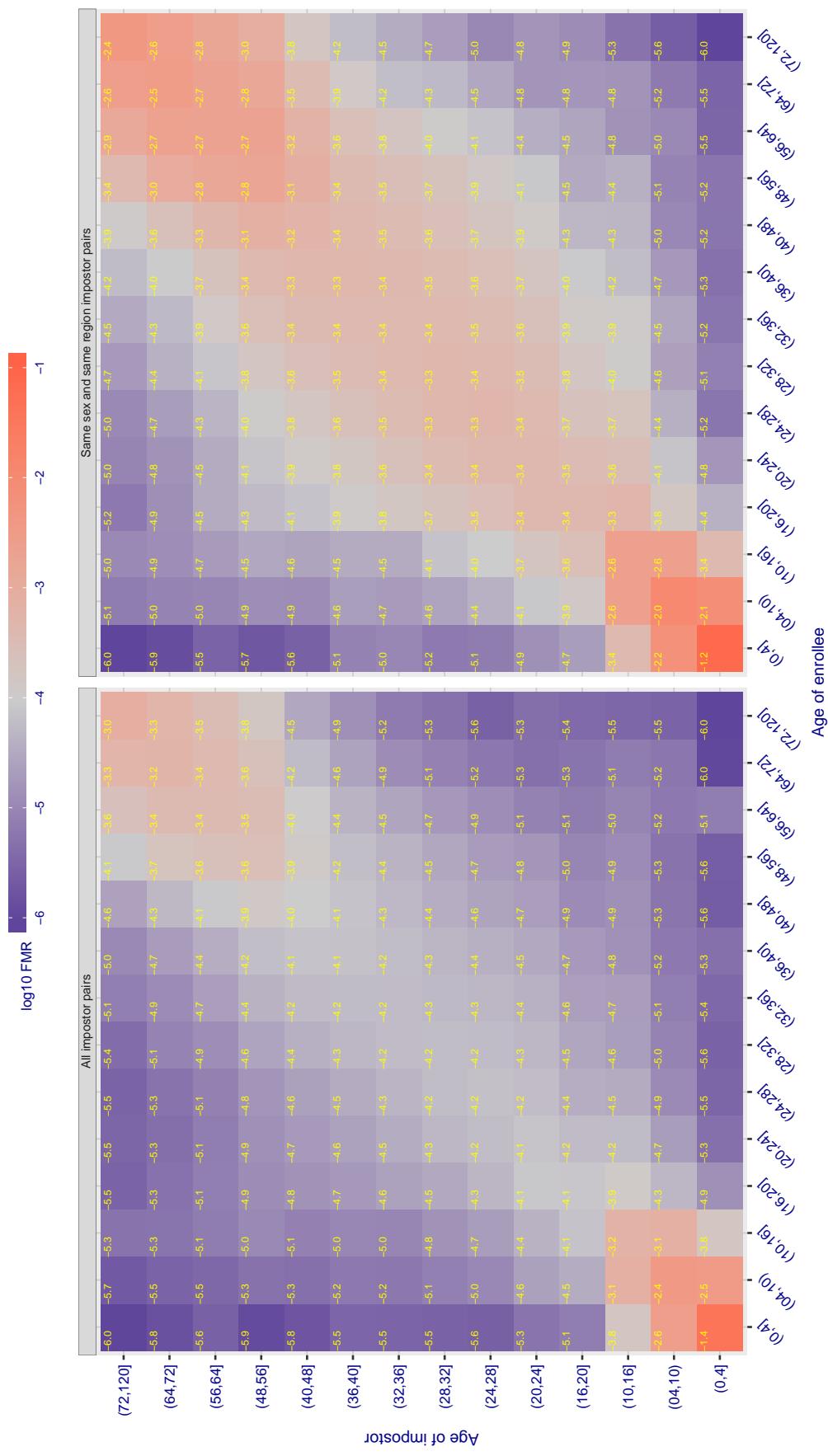
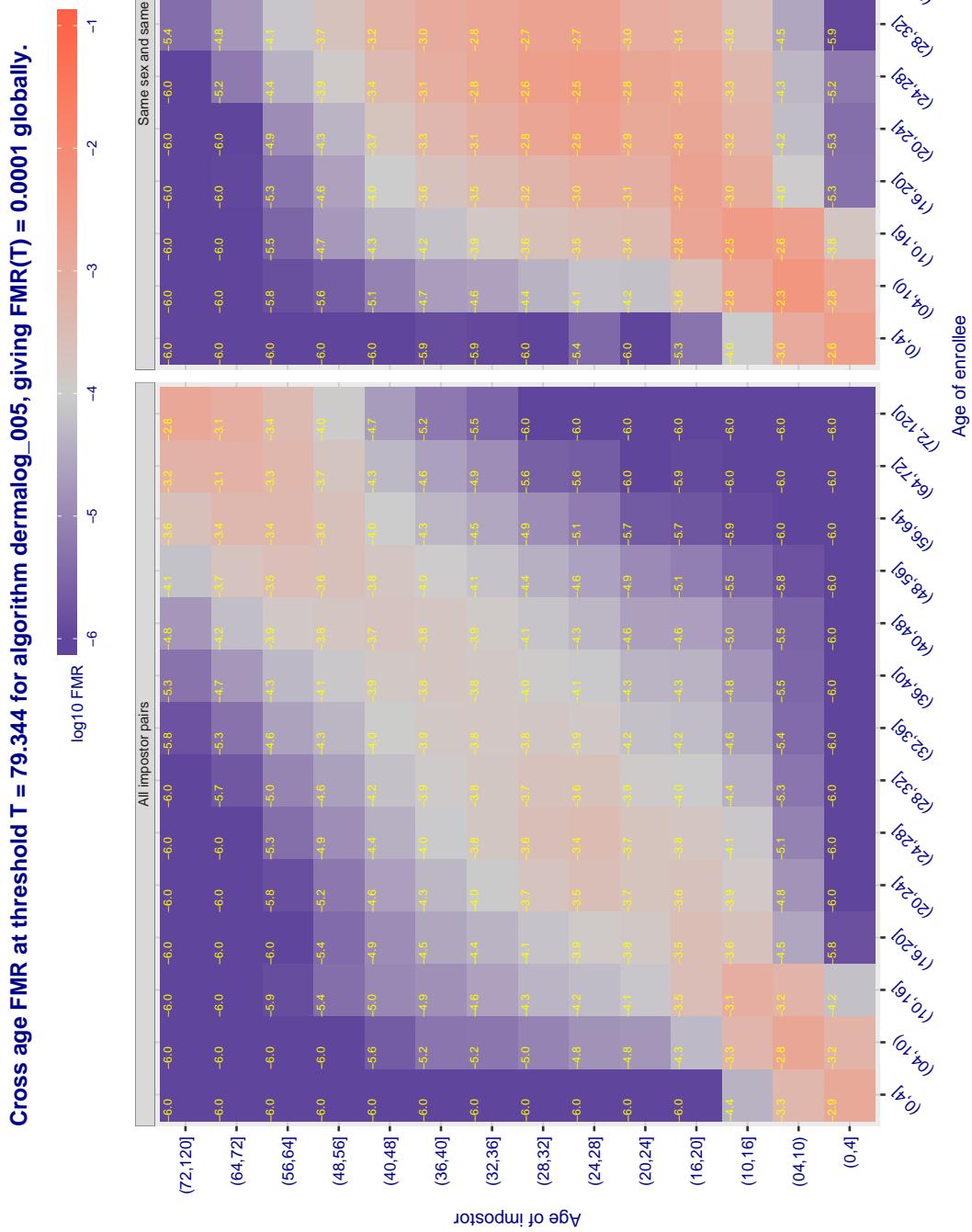


Figure 381: For algorithm deepsea-001 operating on visa images, the heatmap shows false match observed over impostor comparisons of faces from different individuals who have the given age pair. False matches are counted against a recognition threshold fixed globally to give FMR = 0.001 over all on the order of  $10^{10}$  impostor comparisons. The text in each box gives the same quantity as that coded by the color. Light colors present a security vulnerability to, for example, a passport gate.



**Figure 382:** For algorithm dermalog-005 operating on visa images, the heatmap shows false match observed over impostor comparisons of faces from different individuals who have the given age pair. False matches are counted against a recognition threshold fixed globally to give  $FMR = 0.001$  over all on the order of  $10^{10}$  impostor comparisons. The text in each box gives the same quantity as that coded by the color. Light colors present a security vulnerability to, for example, a passport gate.

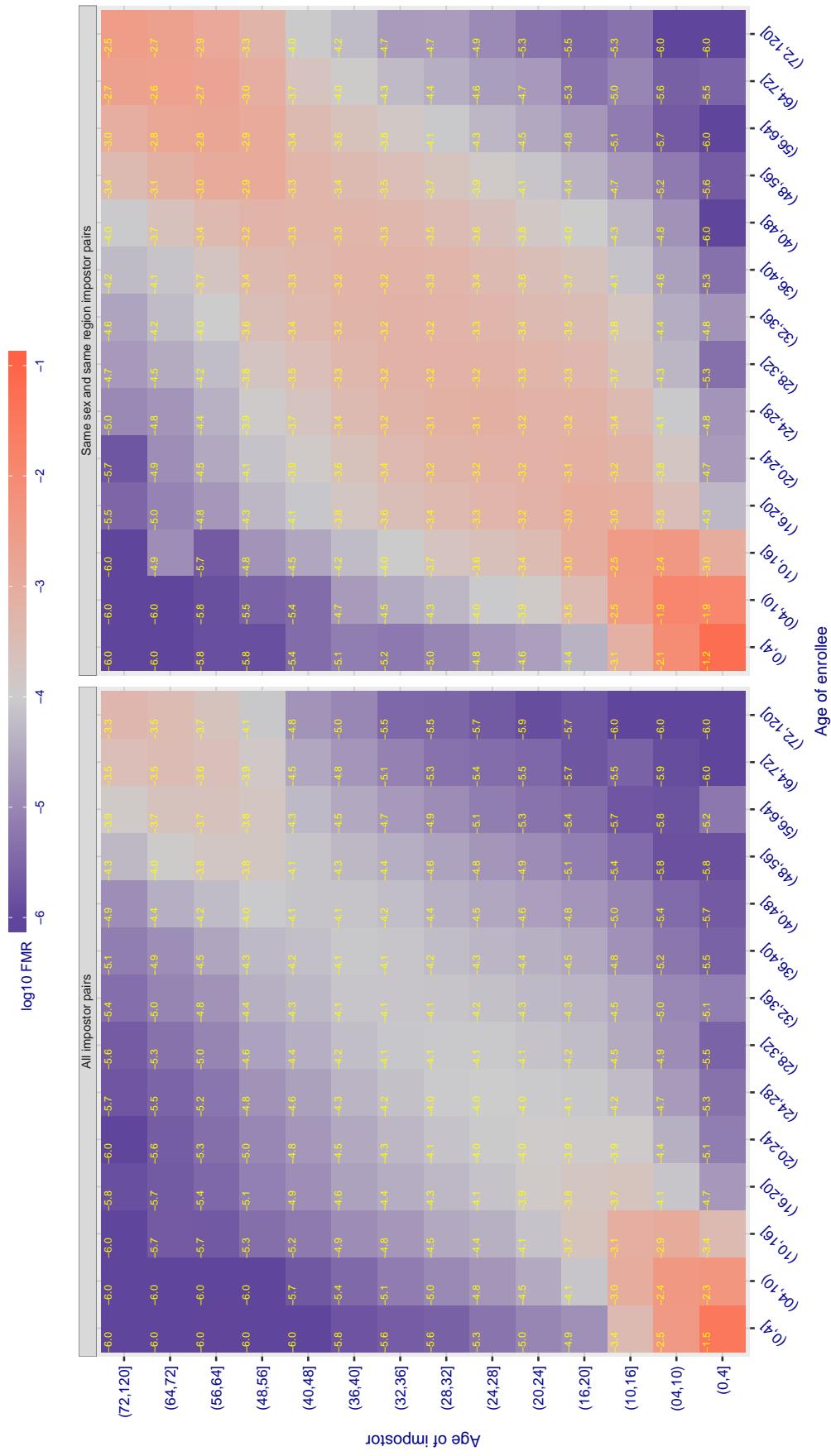
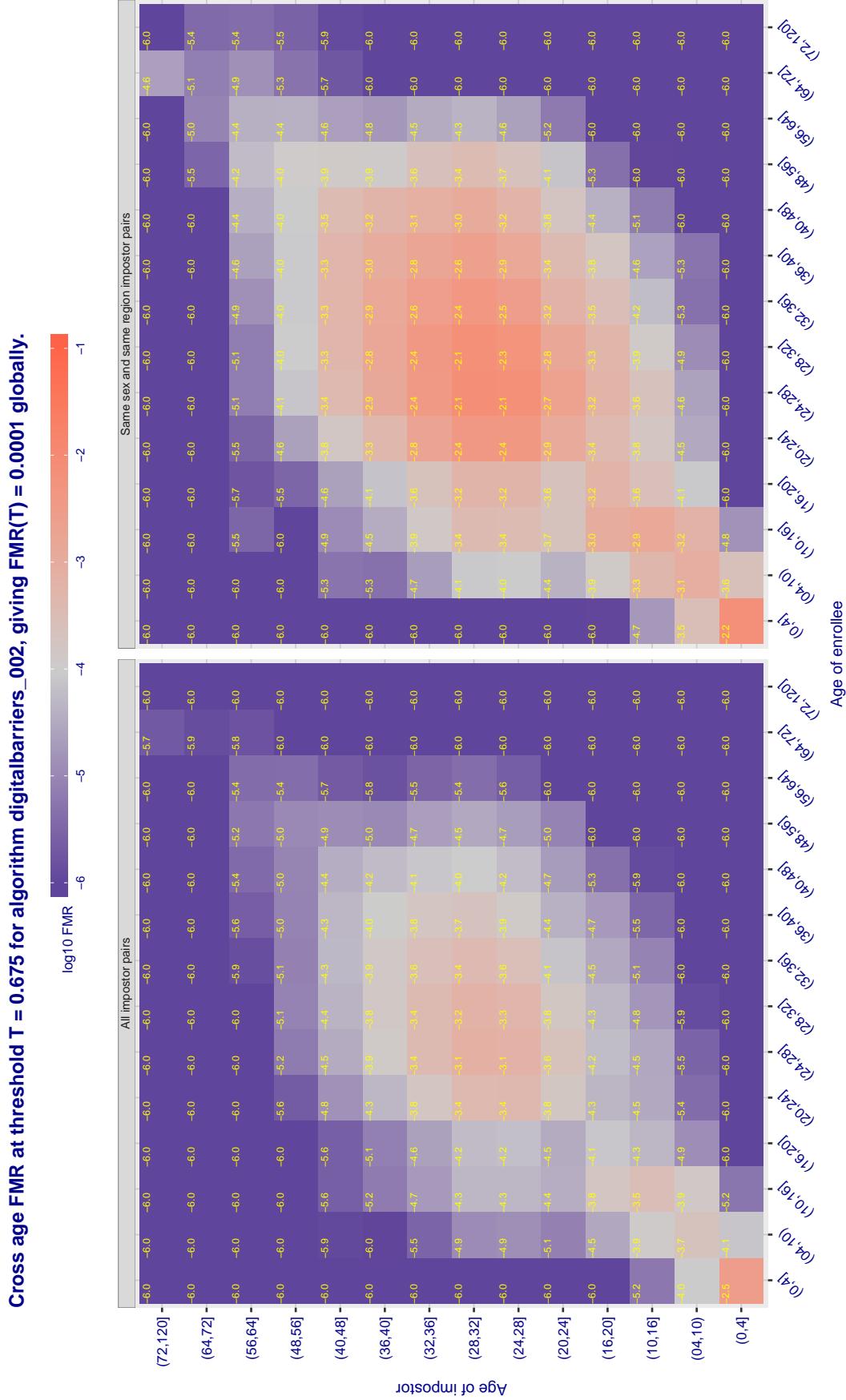
Cross age FMR at threshold T = 79.670 for algorithm dermalog\_006, giving  $FMR(T) = 0.0001$  globally.

Figure 383: For algorithm dermalog-006 operating on visa images, the heatmap shows false match observed over impostor comparisons of faces from different individuals who have the given age pair. False matches are counted against a recognition threshold fixed globally to give  $FMR = 0.001$  over all on the order of  $10^{10}$  impostor comparisons. The text in each box gives the same quantity as that coded by the color. Light colors present a security vulnerability to, for example, a passport gate.



**Figure 384:** For algorithm digitalbarriers-002 operating on visa images, the heatmap shows false match observed over impostor comparisons of faces from different individuals who have the given age pair. False matches are counted against a recognition threshold fixed globally to give  $FMR = 0.001$  over all on the order of  $10^{10}$  impostor comparisons. The text in each box gives the same quantity as that coded by the color. Light colors present a security vulnerability to, for example, a passport gate.

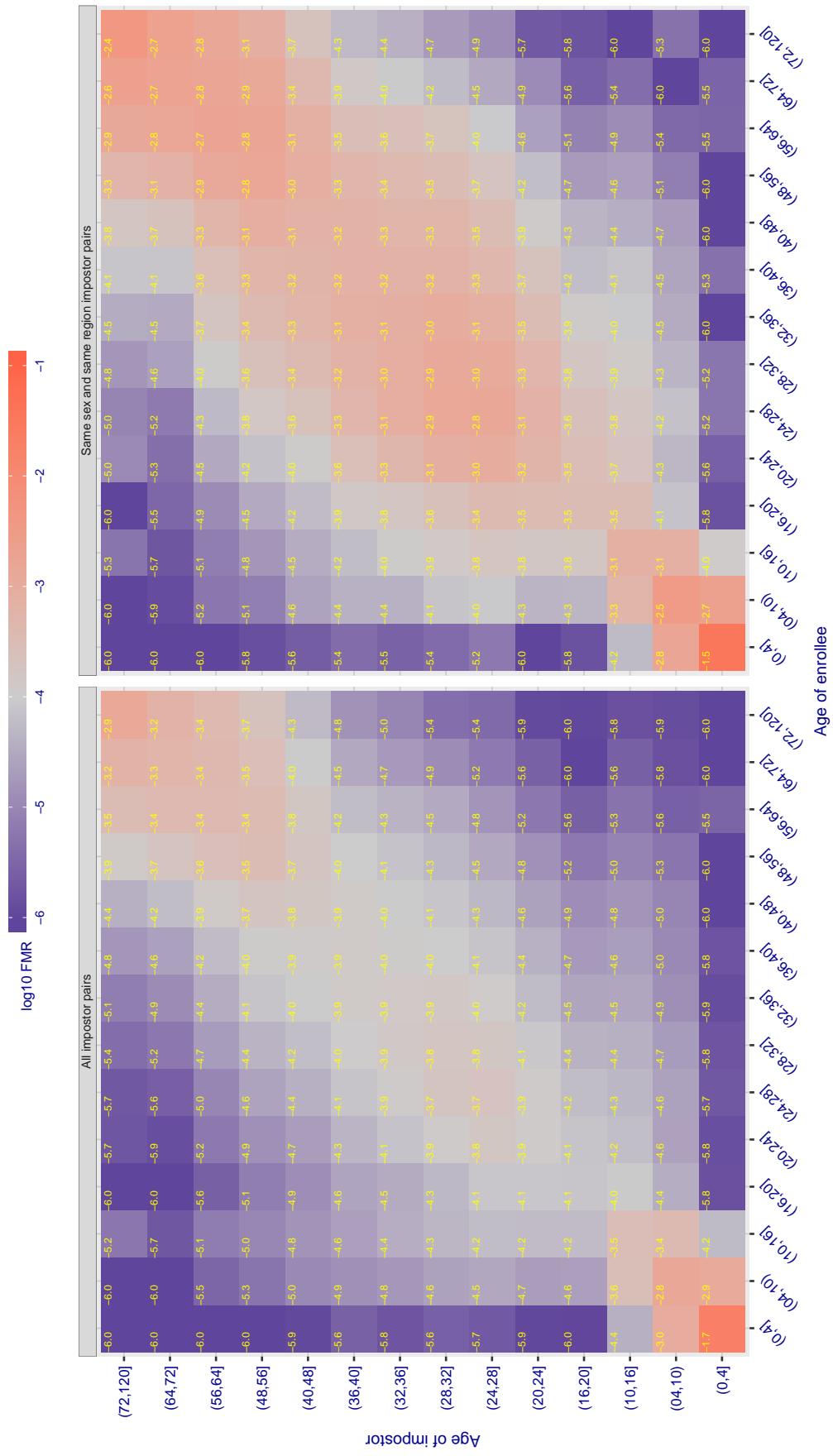
Cross age FMR at threshold T = 1.061 for algorithm dsk\_000, giving  $\text{FMR}(\text{T}) = 0.0001$  globally.

Figure 385: For algorithm dsk-000 operating on visa images, the heatmap shows false match observed over impostor comparisons of faces from different individuals who have the given age pair. False matches are counted against a recognition threshold fixed globally to give  $\text{FMR} = 0.001$  over all on the order of  $10^{10}$  impostor comparisons. The text in each box gives the same quantity as that coded by the color. Light colors present a security vulnerability to, for example, a passport gate.

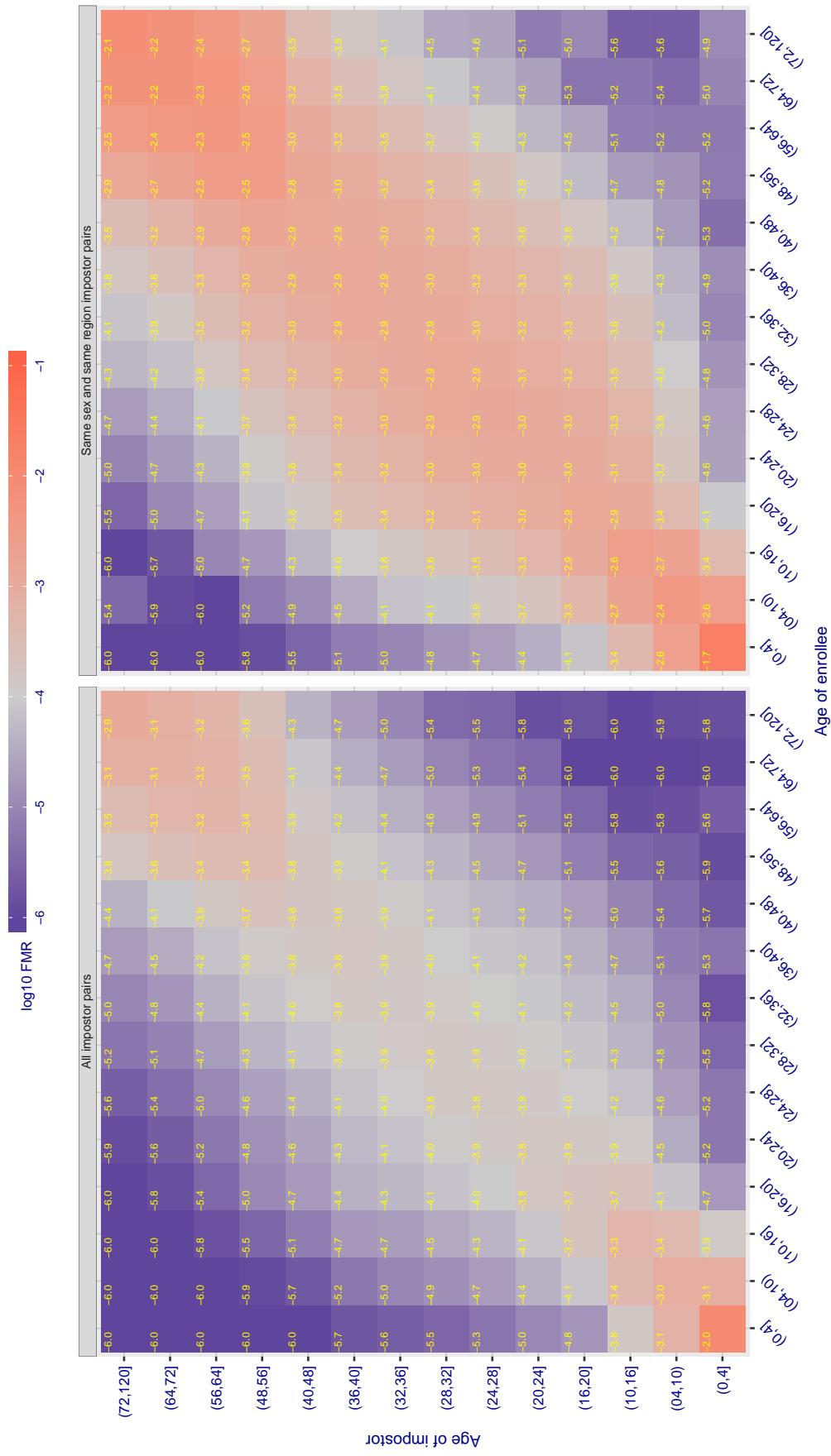
Cross age FMR at threshold T = 2.589 for algorithm everai\_002, giving  $\text{FMR}(\text{T}) = 0.0001$  globally.

Figure 386: For algorithm everai-002 operating on visa images, the heatmap shows false match observed over impostor comparisons of faces from different individuals who have the given age pair. False matches are counted against a recognition threshold fixed globally to give  $\text{FMR} = 0.001$  over all on the order of  $10^{10}$  impostor comparisons. The text in each box gives the same quantity as that coded by the color. Light colors present a security vulnerability to, for example, a passport gate.

Cross age FMR at threshold T = 0.613 for algorithm glory\_001, giving FMR(T) = 0.0001 globally.

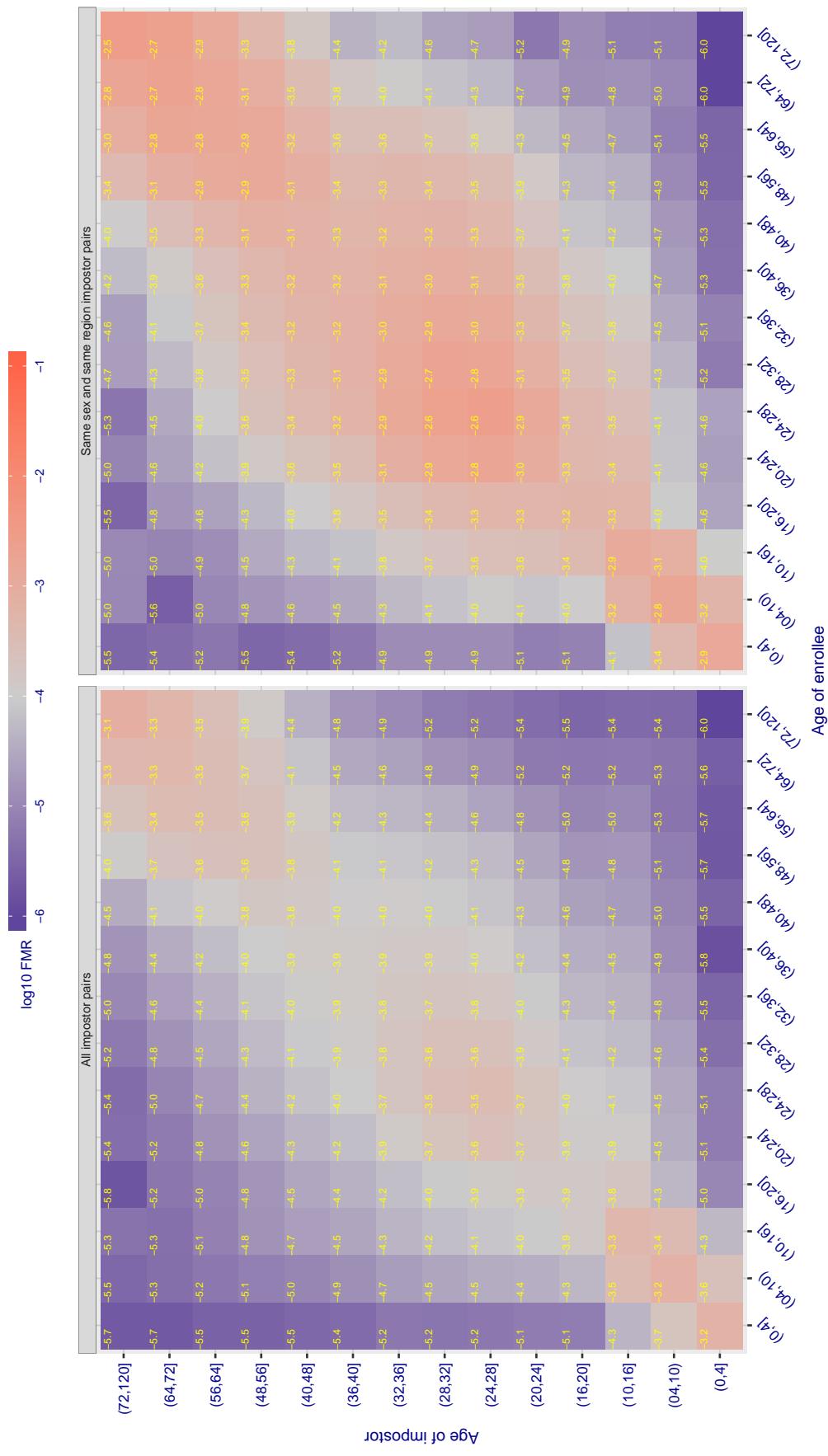


Figure 387: For algorithm glory-001 operating on visa images, the heatmap shows false match observed over impostor comparisons of faces from different individuals who have the given age pair. False matches are counted against a recognition threshold fixed globally to give  $FMR = 0.001$  over all on the order of  $10^{10}$  impostor comparisons. The text in each box gives the same quantity as that coded by the color. Light colors present a security vulnerability to, for example, a passport gate.

Cross age FMR at threshold T = 0.483 for algorithm gorilla\_002, giving FMR(T) = 0.0001 globally.

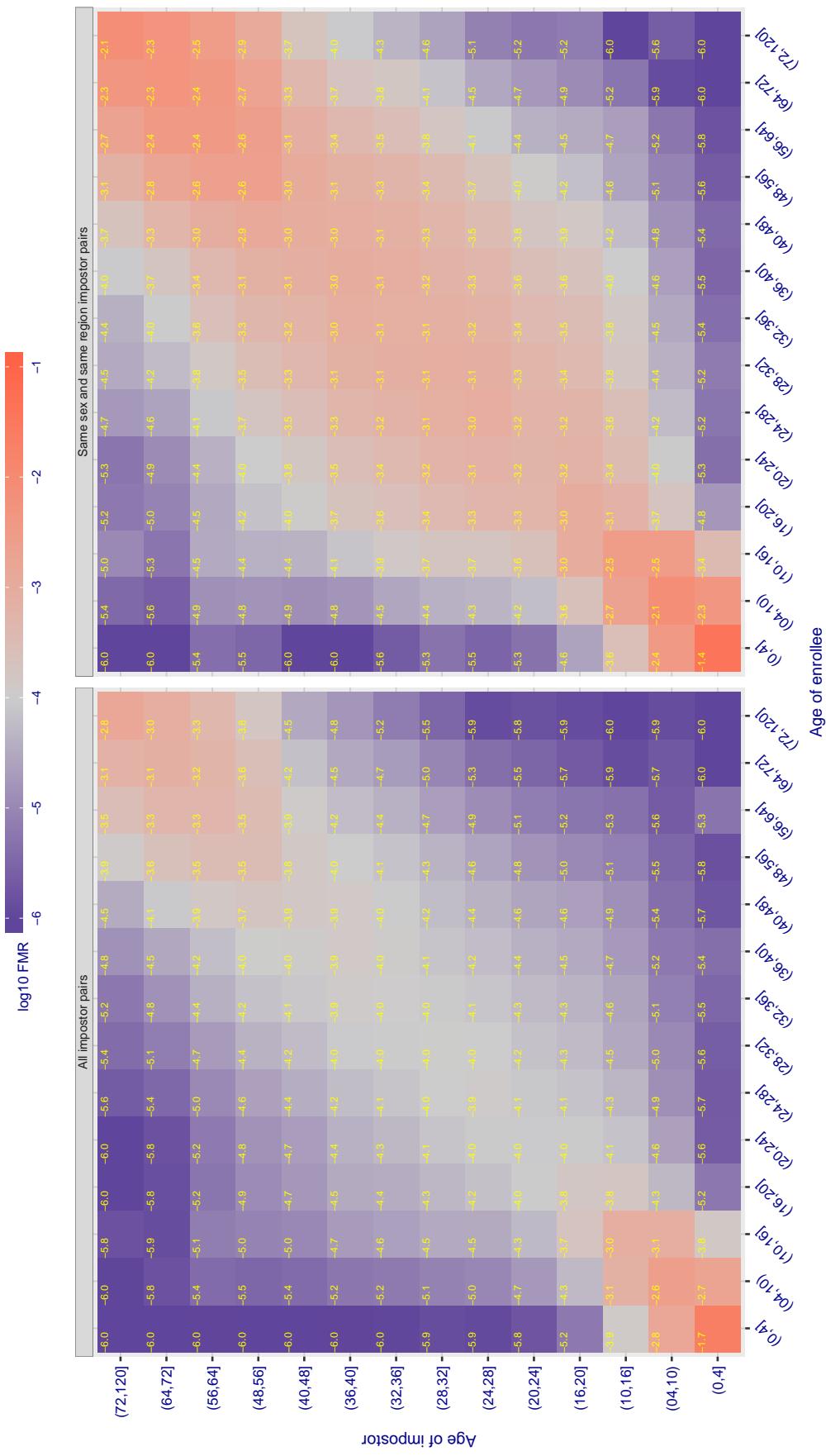


Figure 388: For algorithm gorilla-002 operating on visa images, the heatmap shows false match observed over impostor comparisons of faces from different individuals who have the given age pair. False matches are counted against a recognition threshold fixed globally to give FMR = 0.001 over all on the order of  $10^{10}$  impostor comparisons. The text in each box gives the same quantity as that coded by the color. Light colors present a security vulnerability to, for example, a passport gate.

Cross age FMR at threshold T = 0.454 for algorithm gorilla\_003, giving FMR(T) = 0.0001 globally.

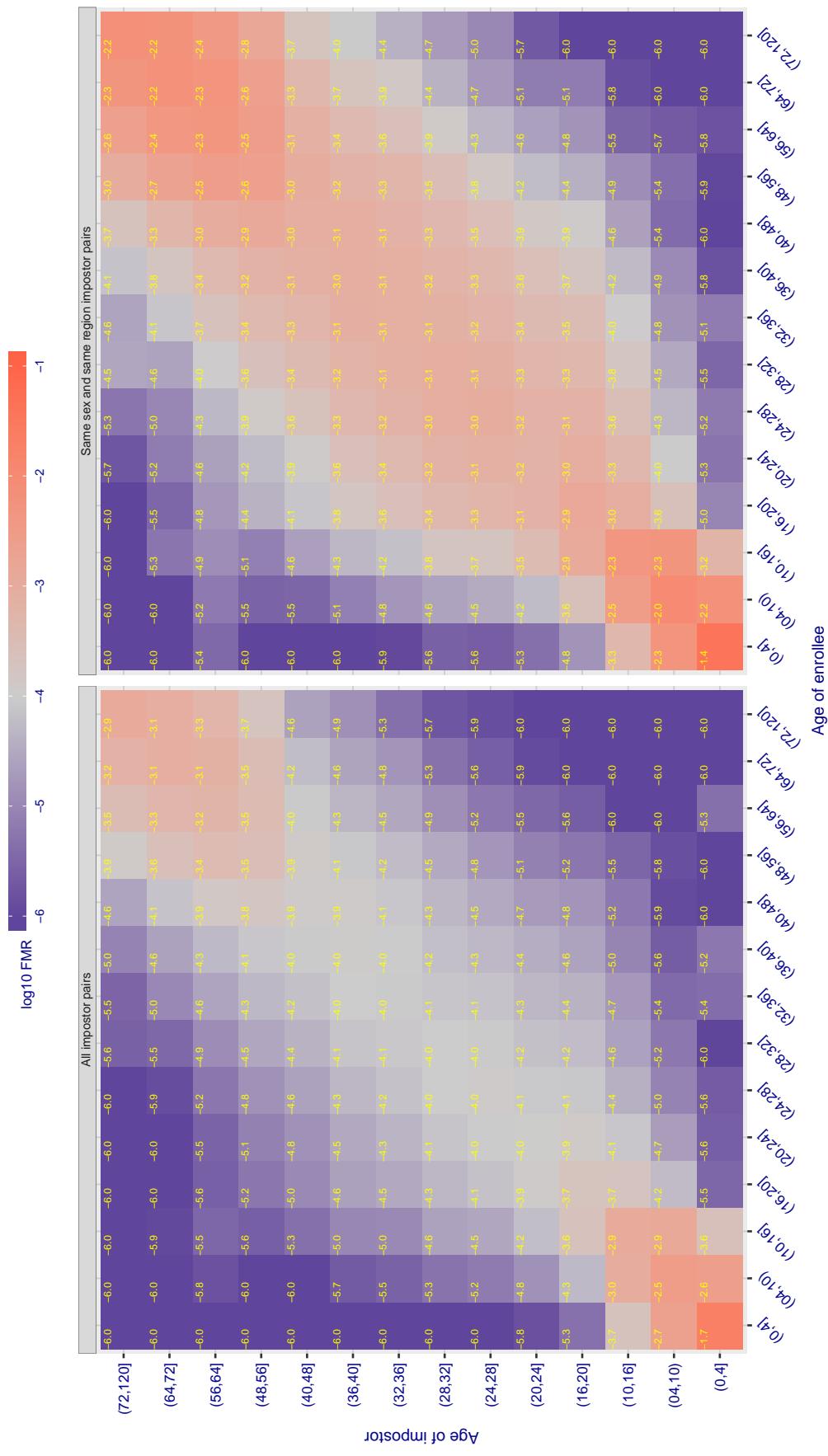


Figure 389: For algorithm gorilla-003 operating on visa images, the heatmap shows false match observed over impostor comparisons of faces from different individuals who have the given age pair. False matches are counted against a recognition threshold fixed globally to give  $FMR = 0.001$  over all on the order of  $10^{10}$  impostor comparisons. The text in each box gives the same quantity as that coded by the color. Light colors present a security vulnerability to, for example, a passport gate.

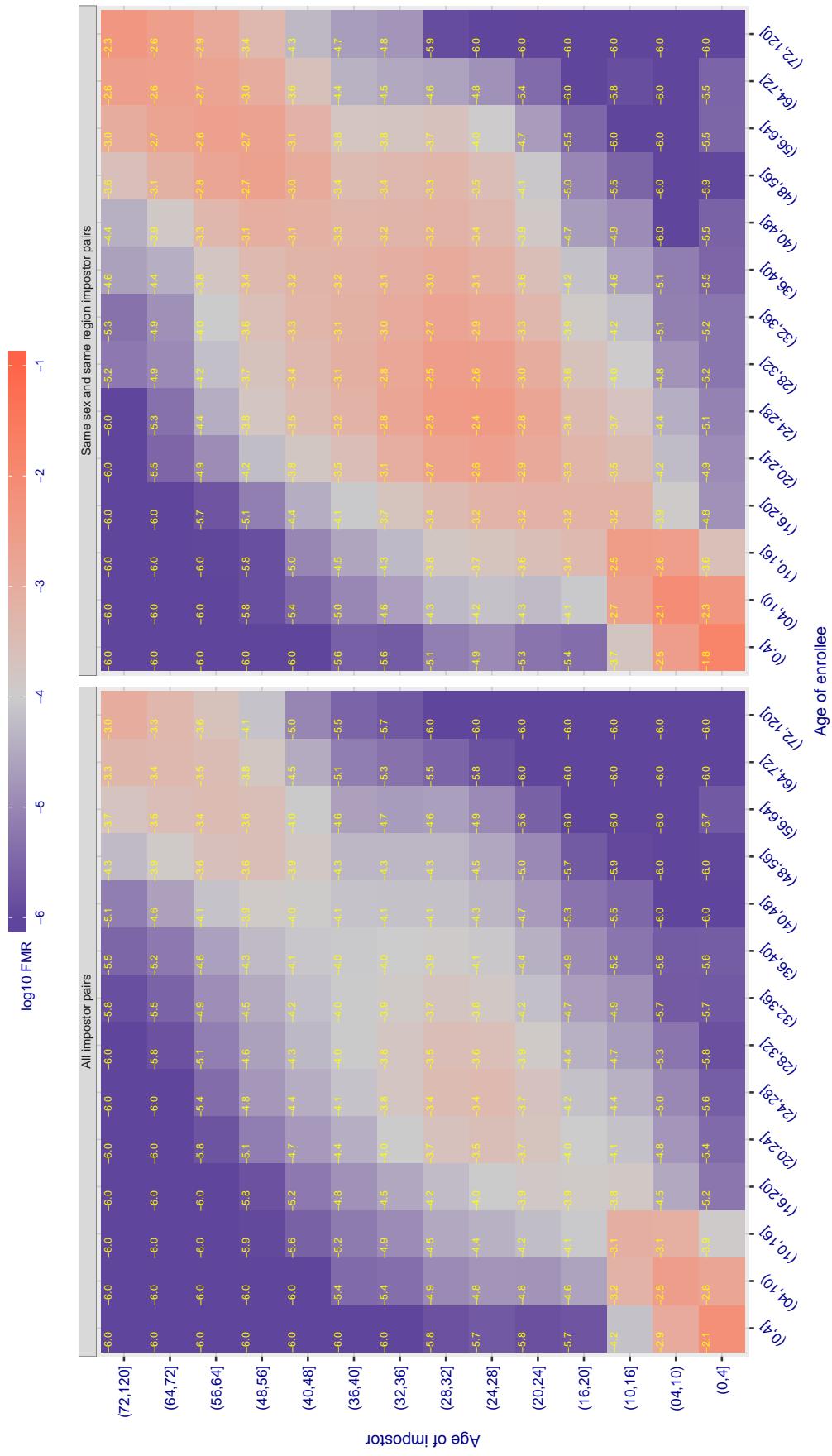
Cross age FMR at threshold T = 66.565 for algorithm hik\_001, giving  $FMR(T) = 0.0001$  globally.

Figure 390: For algorithm hik-001 operating on visa images, the heatmap shows false match observed over impostor comparisons of faces from different individuals who have the given age pair. False matches are counted against a recognition threshold fixed globally to give  $FMR = 0.001$  over all on the order of  $10^{10}$  impostor comparisons. The text in each box gives the same quantity as that coded by the color. Light colors present a security vulnerability to, for example, a passport gate.

Cross age FMR at threshold T = 0.971 for algorithm hr\_000, giving  $\text{FMR}(\text{T}) = 0.0001$  globally.

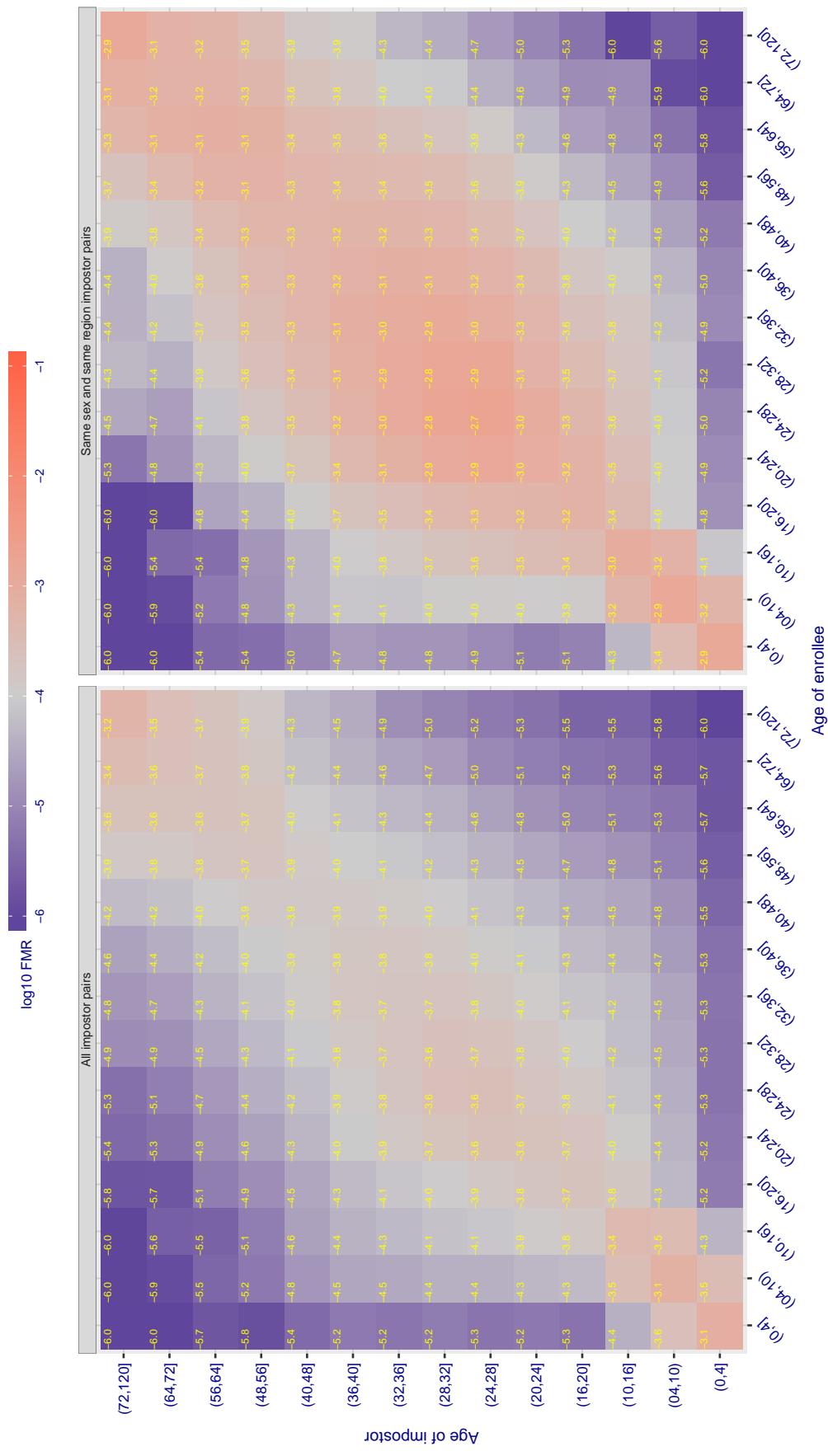


Figure 391: For algorithm hr-000 operating on visa images, the heatmap shows false match observed over impostor comparisons of faces from different individuals who have the given age pair. False matches are counted against a recognition threshold fixed globally to give  $\text{FMR} = 0.001$  over all on the order of  $10^{10}$  impostor comparisons. The text in each box gives the same quantity as that coded by the color. Light colors present a security vulnerability to, for example, a passport gate.

Cross age FMR at threshold T = 0.823 for algorithm hr\_001, giving  $\text{FMR}(\text{T}) = 0.0001$  globally.

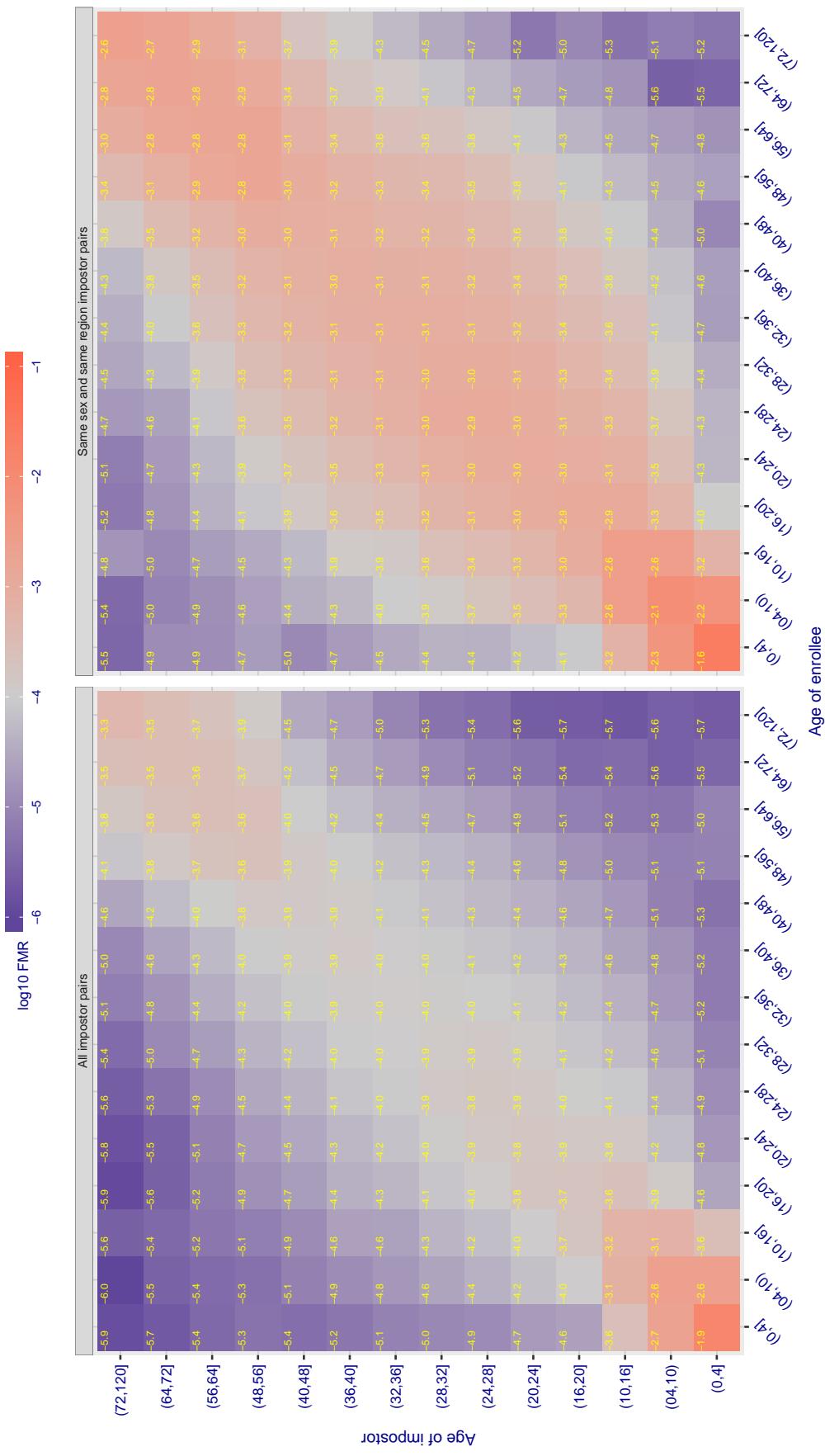
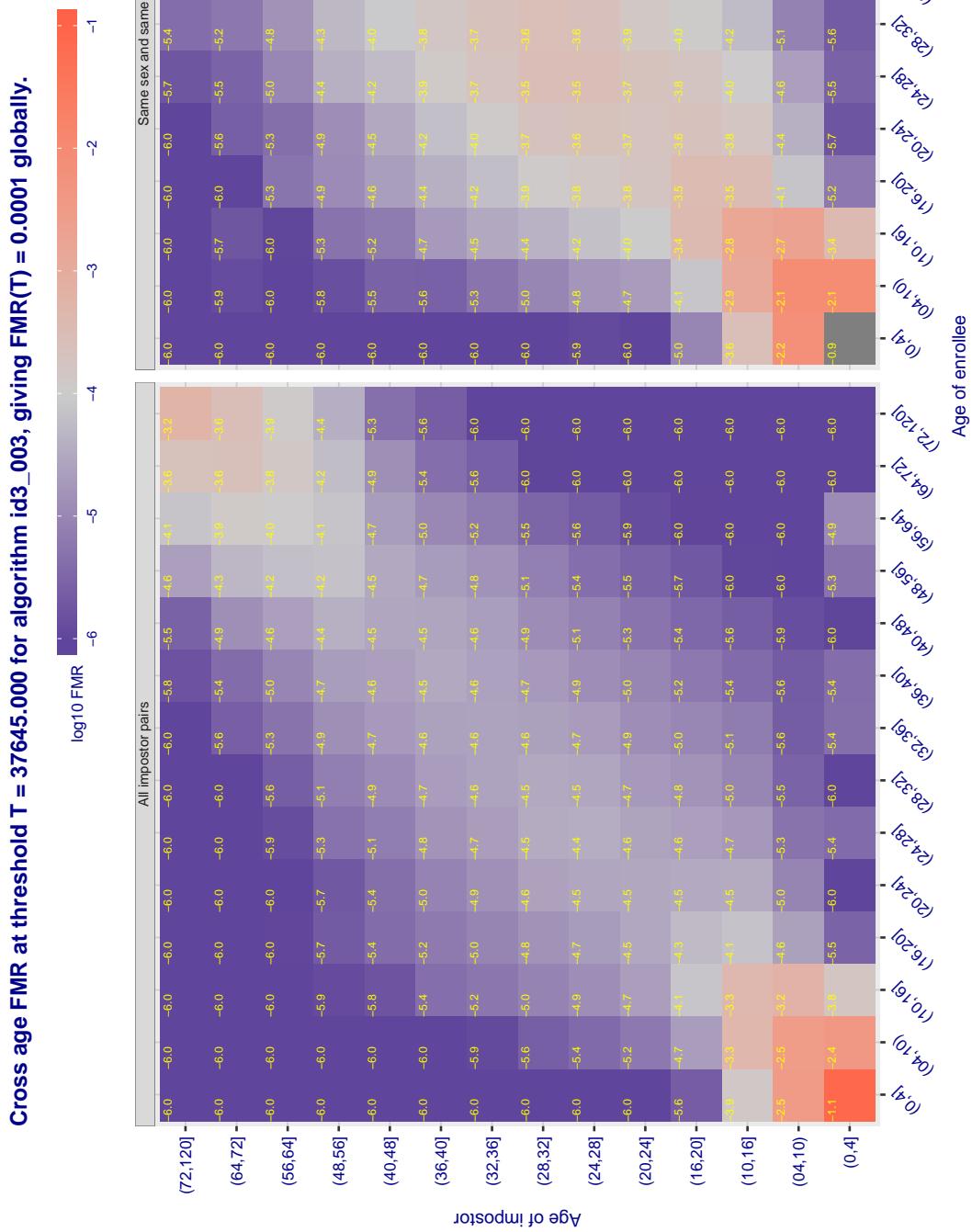


Figure 392: For algorithm hr-001 operating on visa images, the heatmap shows false match observed over impostor comparisons of faces from different individuals who have the given age pair. False matches are counted against a recognition threshold fixed globally to give  $\text{FMR} = 0.001$  over all on the order of  $10^{10}$  impostor comparisons. The text in each box gives the same quantity as that coded by the color. Light colors present a security vulnerability to, for example, a passport gate.



**Figure 393:** For algorithm id3-003 operating on visa images, the heatmap shows false match observed over impostor comparisons of faces from different individuals who have the given age pair. False matches are counted against a recognition threshold fixed globally to give FMR = 0.001 over all on the order of  $10^{10}$  impostor comparisons. The text in each box gives the same quantity as that coded by the color. Light colors present a security vulnerability to, for example, a passport gate.

Cross age FMR at threshold T = 37001.000 for algorithm id3\_004, giving FMR(T) = 0.0001 globally.

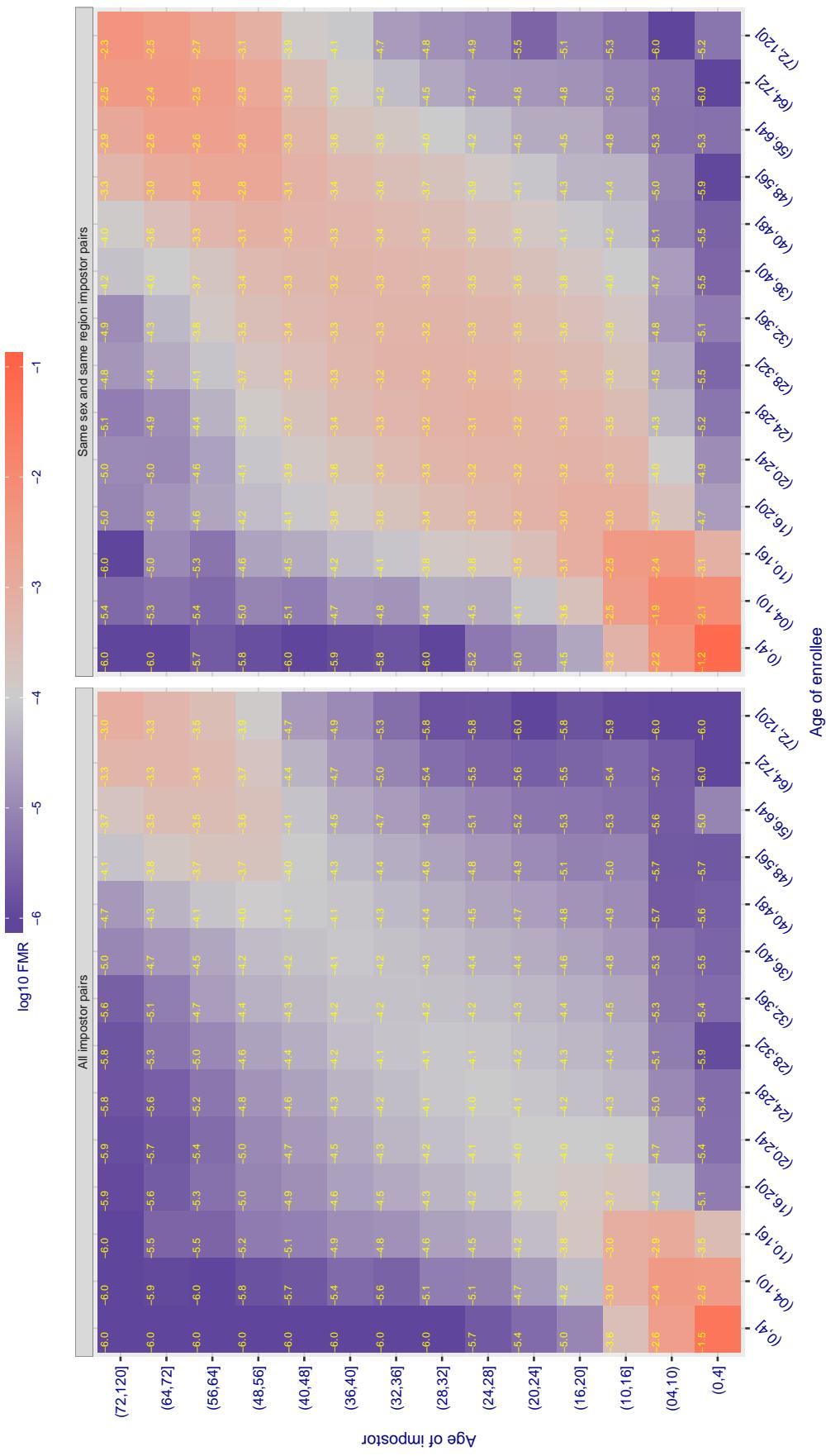
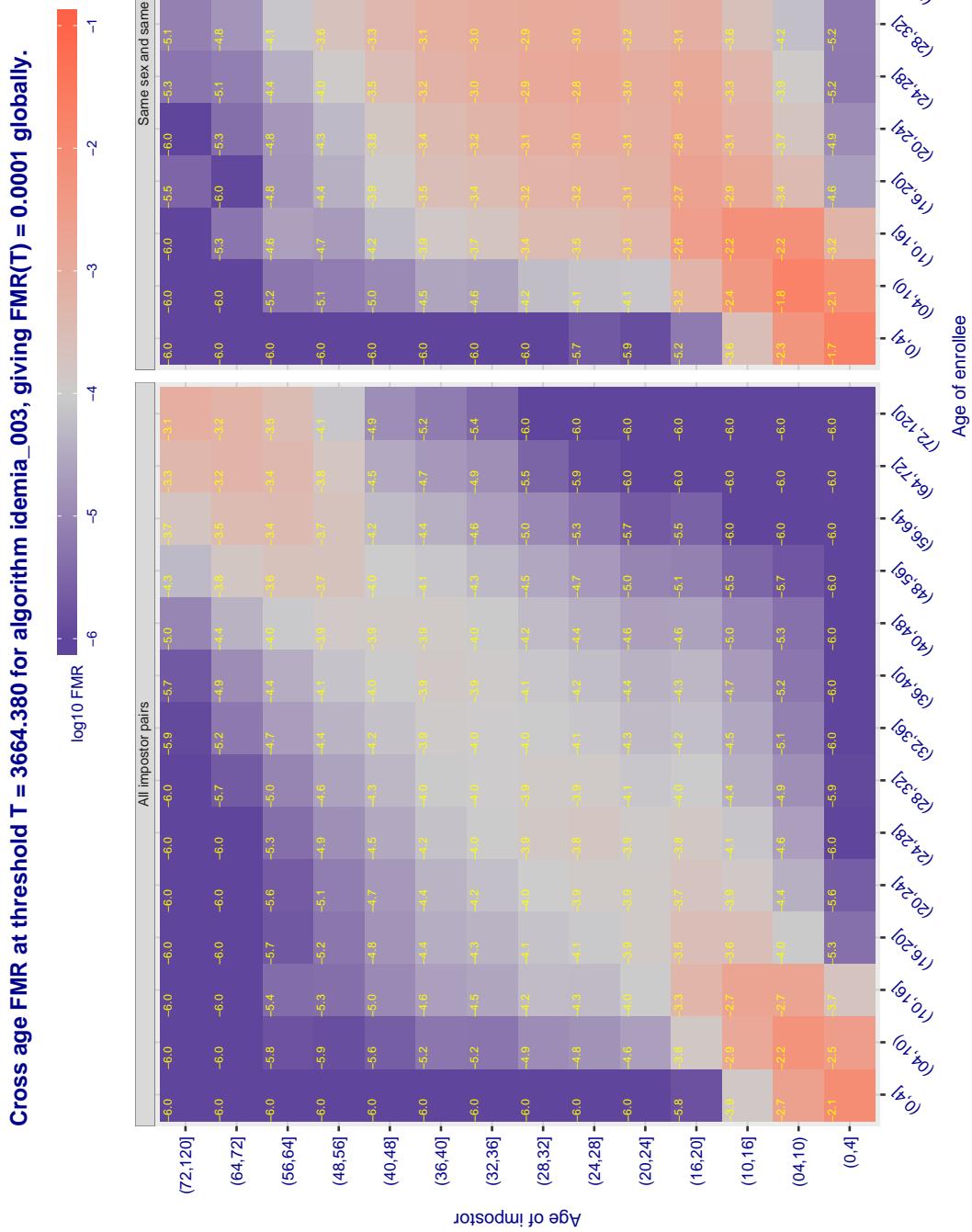


Figure 394: For algorithm id3-004 operating on visa images, the heatmap shows false match observed over impostor comparisons of faces from different individuals who have the given age pair. False matches are counted against a recognition threshold fixed globally to give FMR = 0.001 over all on the order of  $10^{10}$  impostor comparisons. The text in each box gives the same quantity as that coded by the color. Light colors present a security vulnerability to, for example, a passport gate.



**Figure 395:** For algorithm idemia-003 operating on visa images, the heatmap shows false match observed over impostor comparisons of faces from different individuals who have the given age pair. False matches are counted against a recognition threshold fixed globally to give  $FMR = 0.001$  over all on the order of  $10^{10}$  impostor comparisons. The text in each box gives the same quantity as that coded by the color. Light colors present a security vulnerability to, for example, a passport gate.

Cross age FMR at threshold T = 3925.463 for algorithm idemia\_004, giving FMR(T) = 0.0001 globally.

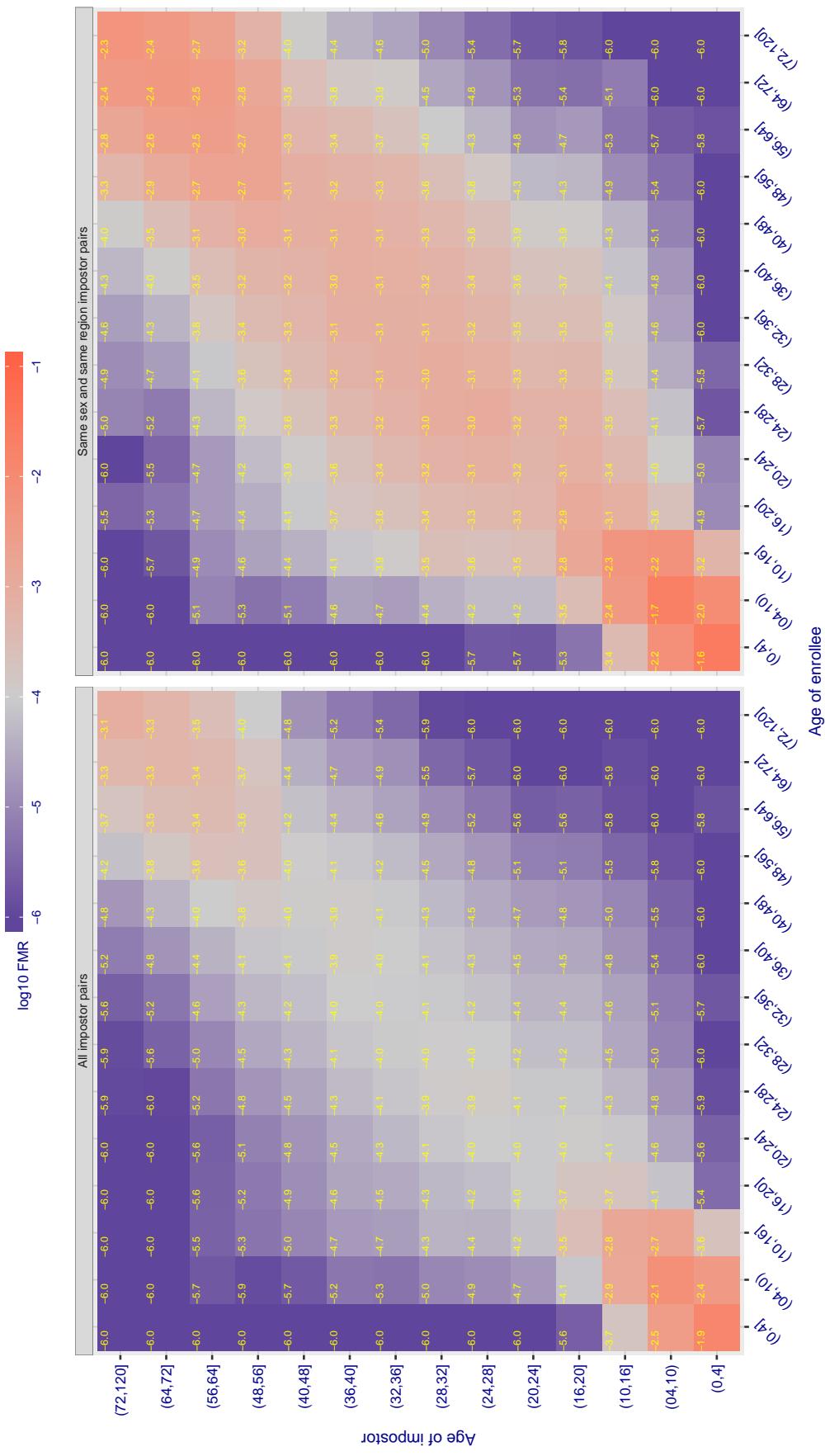
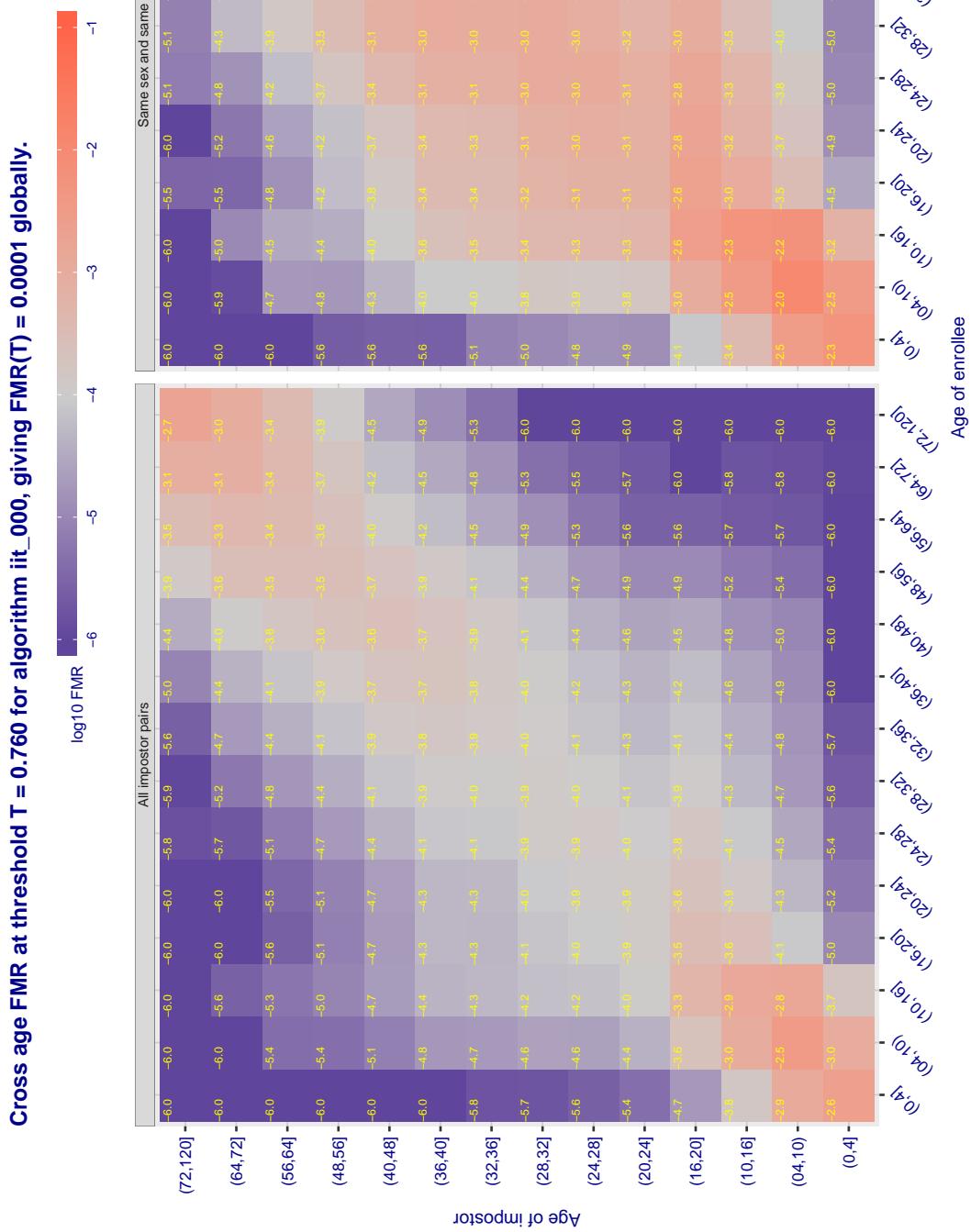


Figure 396: For algorithm idemia-004 operating on visa images, the heatmap shows false match observed over impostor comparisons of faces from different individuals who have the given age pair. False matches are counted against a recognition threshold fixed globally to give FMR = 0.001 over all on the order of  $10^{10}$  impostor comparisons. The text in each box gives the same quantity as that coded by the color. Light colors present a security vulnerability to, for example, a passport gate.



**Figure 397:** For algorithm *iit-000* operating on visa images, the heatmap shows false match observed over impostor comparisons of faces from different individuals who have the given age pair. False matches are counted against a recognition threshold fixed globally to give  $FMR = 0.001$  over all on the order of  $10^{10}$  impostor comparisons. The text in each box gives the same quantity as that coded by the color. Light colors present a security vulnerability to, for example, a passport gate.

Cross age FMR at threshold T = 0.926 for algorithm imagus\_000, giving FMR(T) = 0.0001 globally.

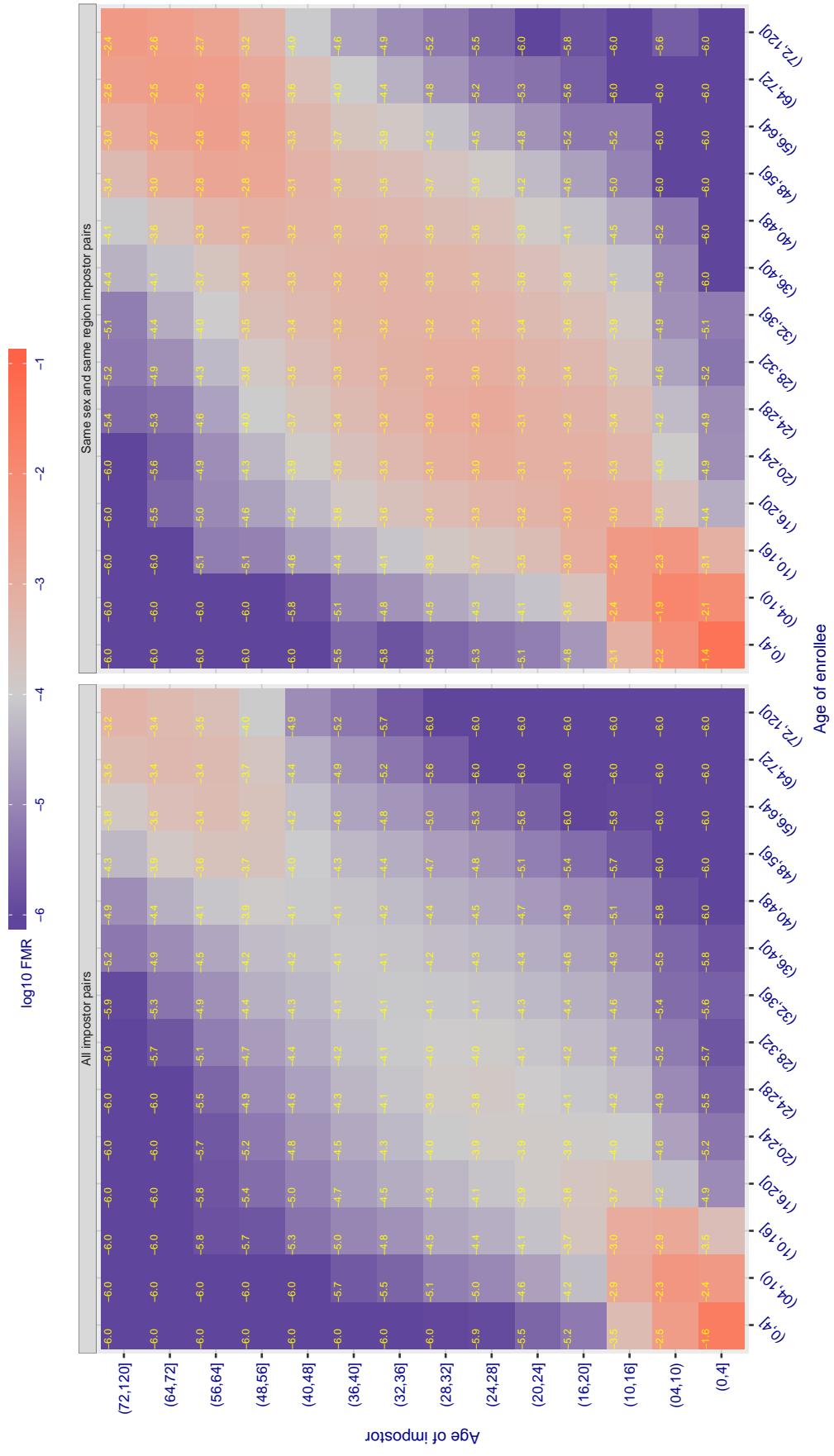


Figure 398: For algorithm imagus-000 operating on visa images, the heatmap shows false match observed over impostor comparisons of faces from different individuals who have the given age pair. False matches are counted against a recognition threshold fixed globally to give FMR = 0.001 over all on the order of  $10^{10}$  impostor comparisons. The text in each box gives the same quantity as that coded by the color. Light colors present a security vulnerability to, for example, a passport gate.

Cross age FMR at threshold T = 1.375 for algorithm imperial\_000, giving FMR(T) = 0.0001 globally.

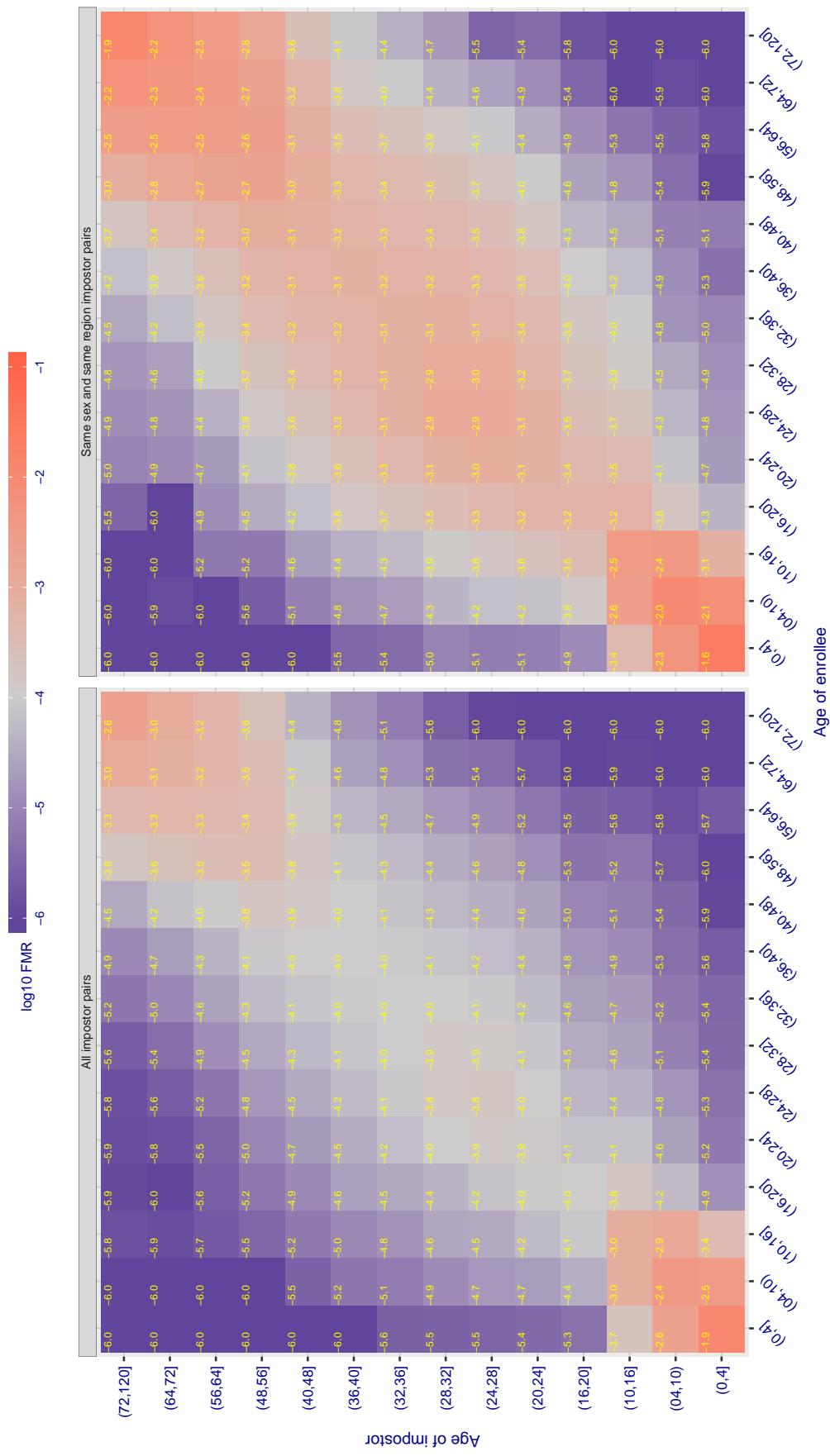
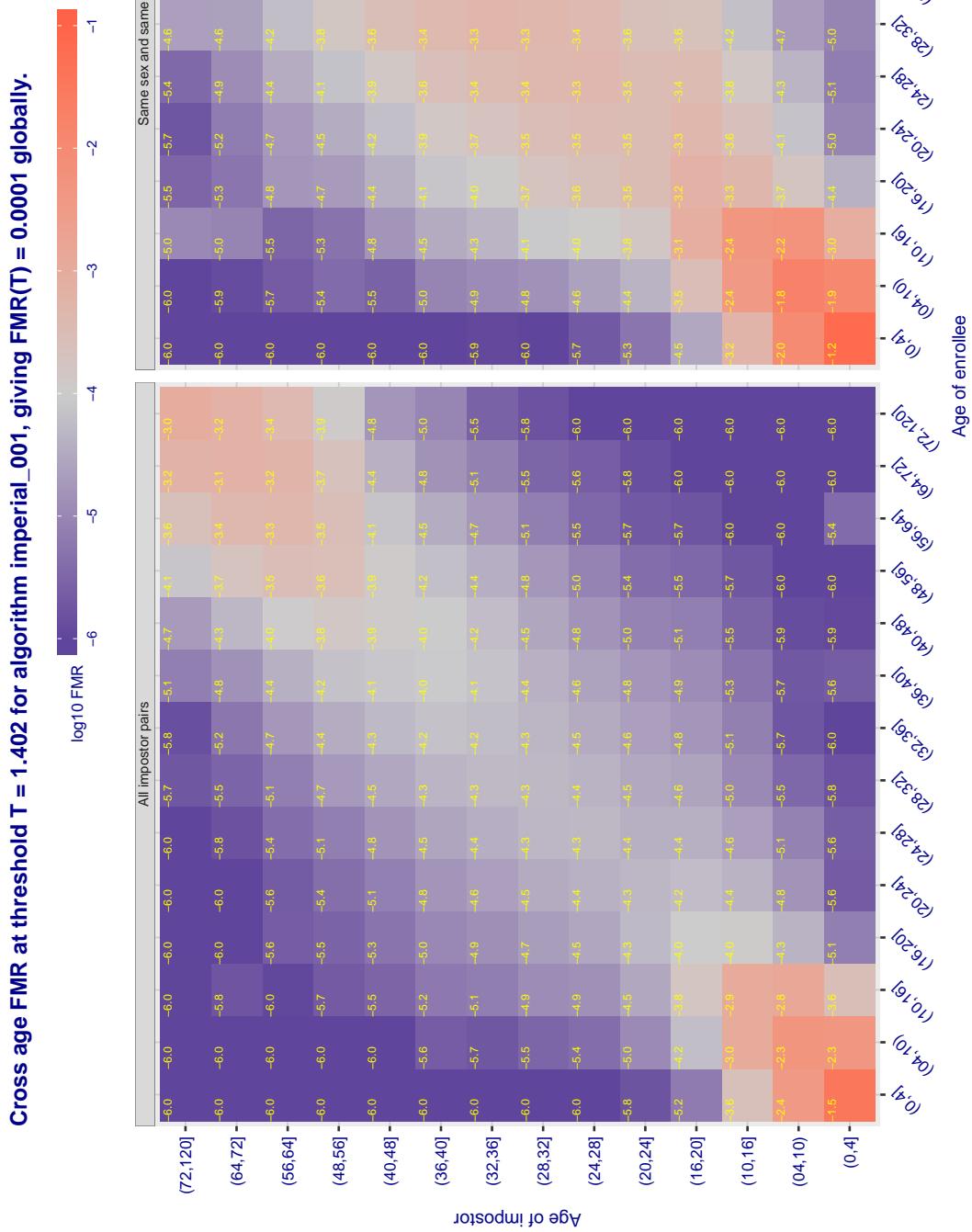
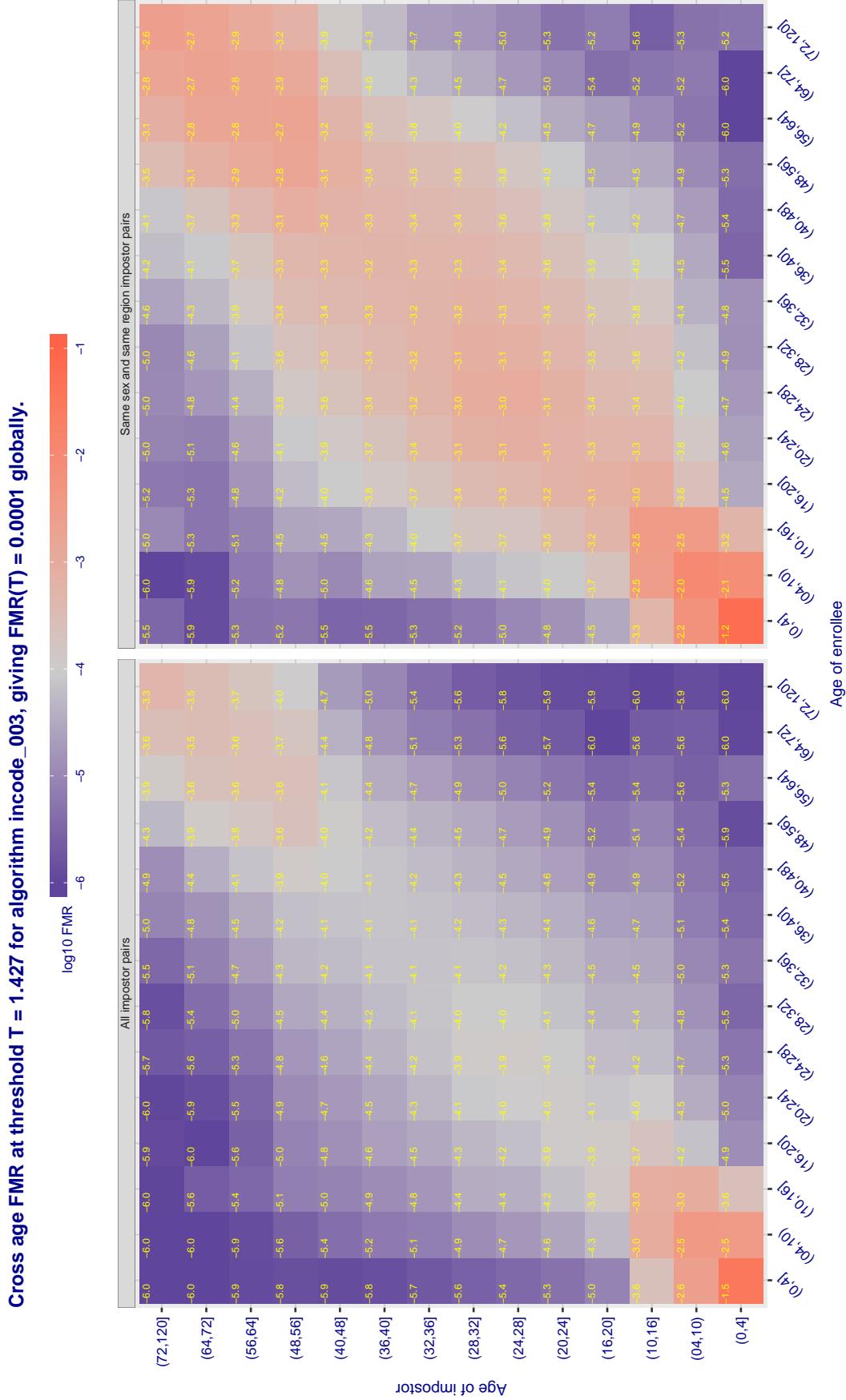


Figure 399: For algorithm imperial-000 operating on visa images, the heatmap shows false match observed over impostor comparisons of faces from different individuals who have the given age pair. False matches are counted against a recognition threshold fixed globally to give FMR = 0.001 over all on the order of  $10^{10}$  impostor comparisons. The text in each box gives the same quantity as that coded by the color. Light colors present a security vulnerability to, for example, a passport gate.



**Figure 400:** For algorithm imperial-001 operating on visa images, the heatmap shows false match observed over impostor comparisons of faces from different individuals who have the given age pair. False matches are counted against a recognition threshold fixed globally to give  $FMR = 0.001$  over all on the order of  $10^{10}$  impostor comparisons. The text in each box gives the same quantity as that coded by the color. Light colors present a security vulnerability to, for example, a passport gate.



**Figure 401:** For algorithm incode-003 operating on visa images, the heatmap shows false match observed over impostor comparisons of faces from different individuals who have the given age pair. False matches are counted against a recognition threshold fixed globally to give  $FMR = 0.001$  over all on the order of  $10^{10}$  impostor comparisons. The text in each box gives the same quantity as that coded by the color. Light colors present a security vulnerability to, for example, a passport gate.

Cross age FMR at threshold T = 1.398 for algorithm incode\_004, giving FMR(T) = 0.0001 globally.

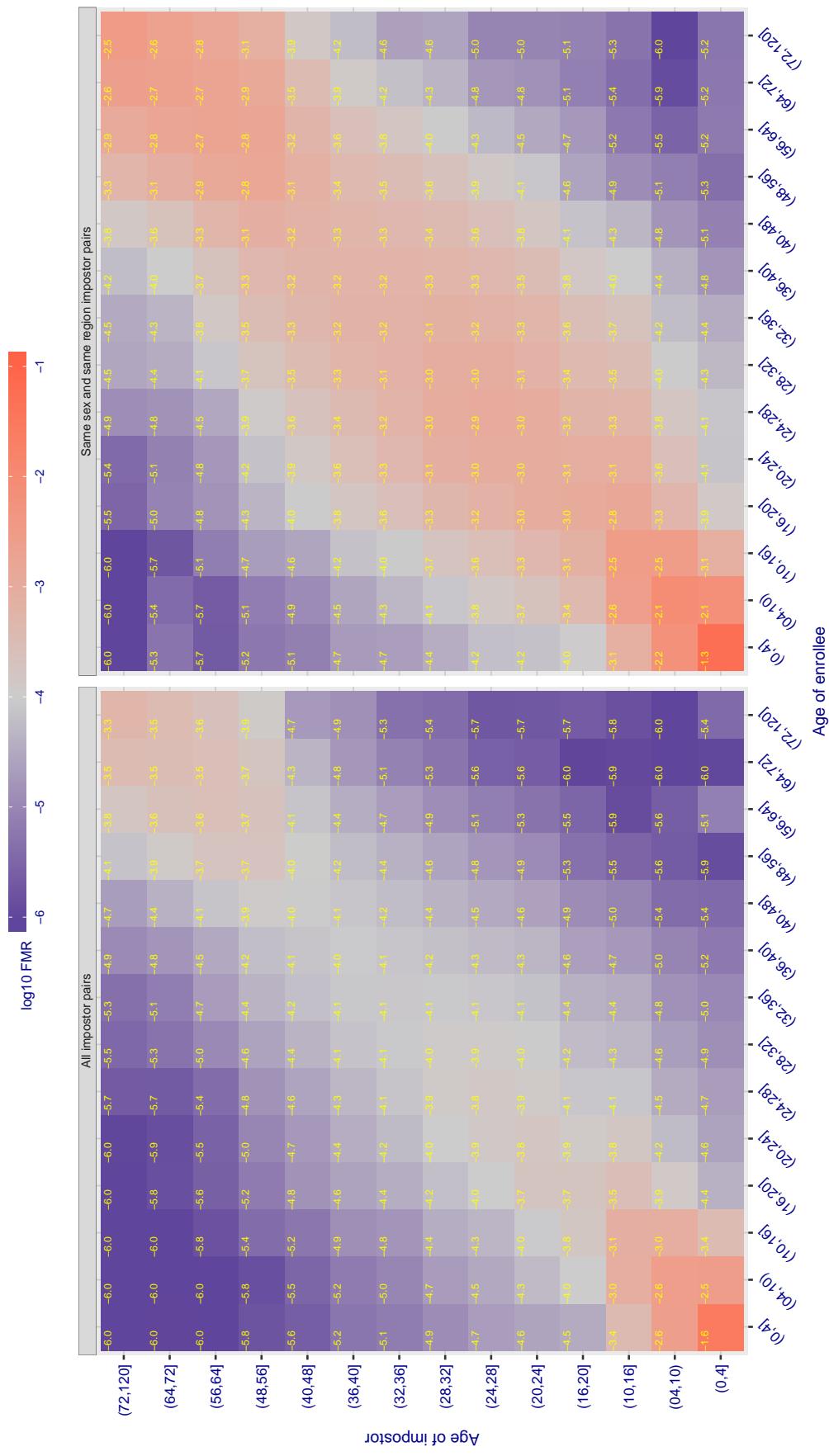


Figure 402: For algorithm incode-004 operating on visa images, the heatmap shows false match observed over impostor comparisons of faces from different individuals who have the given age pair. False matches are counted against a recognition threshold fixed globally to give  $FMR = 0.001$  over all on the order of  $10^{10}$  impostor comparisons. The text in each box gives the same quantity as that coded by the color. Light colors present a security vulnerability to, for example, a passport gate.

Cross age FMR at threshold T = 29.232 for algorithm innovatrics\_004, giving  $FMR(T) = 0.0001$  globally.

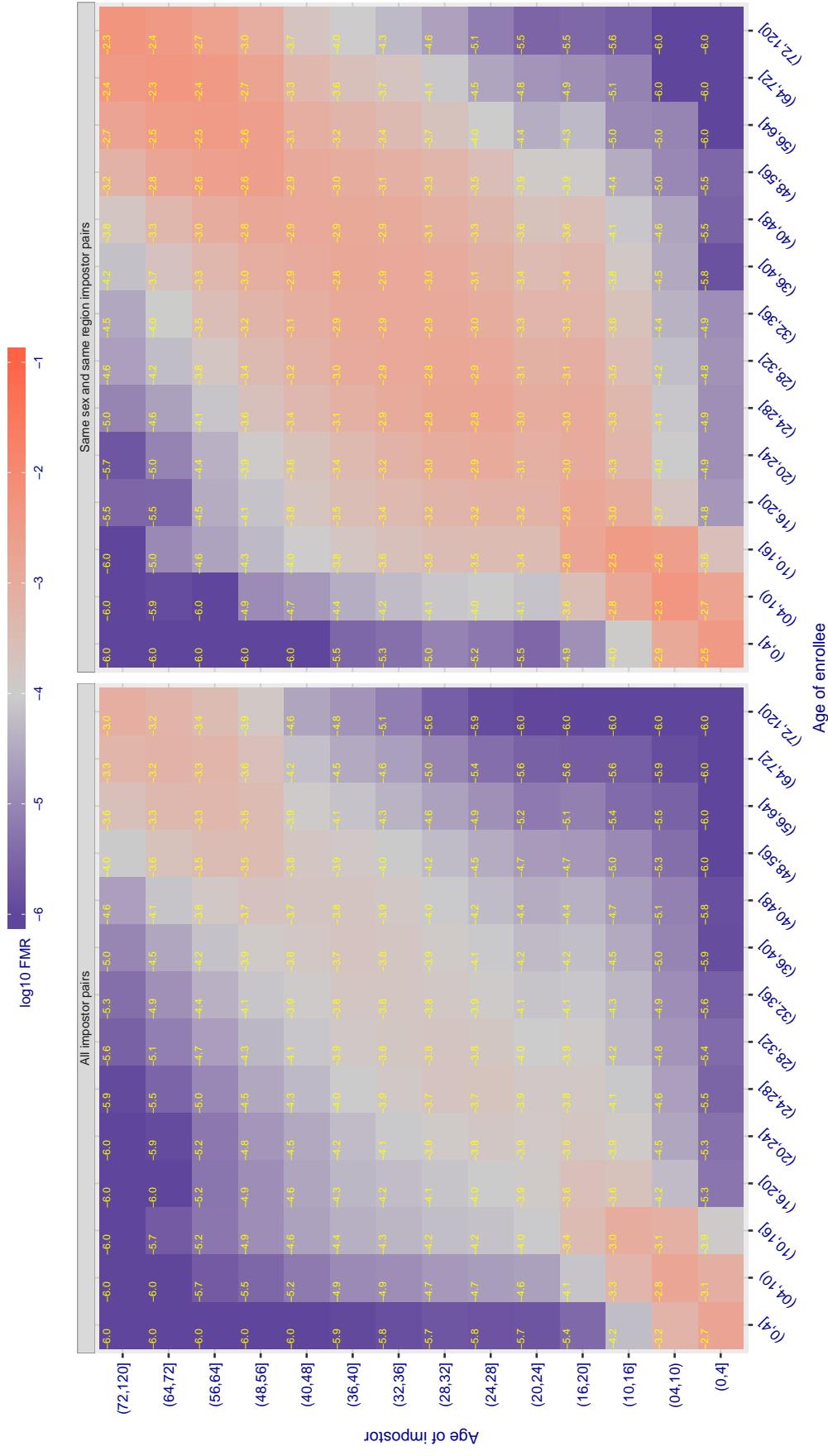
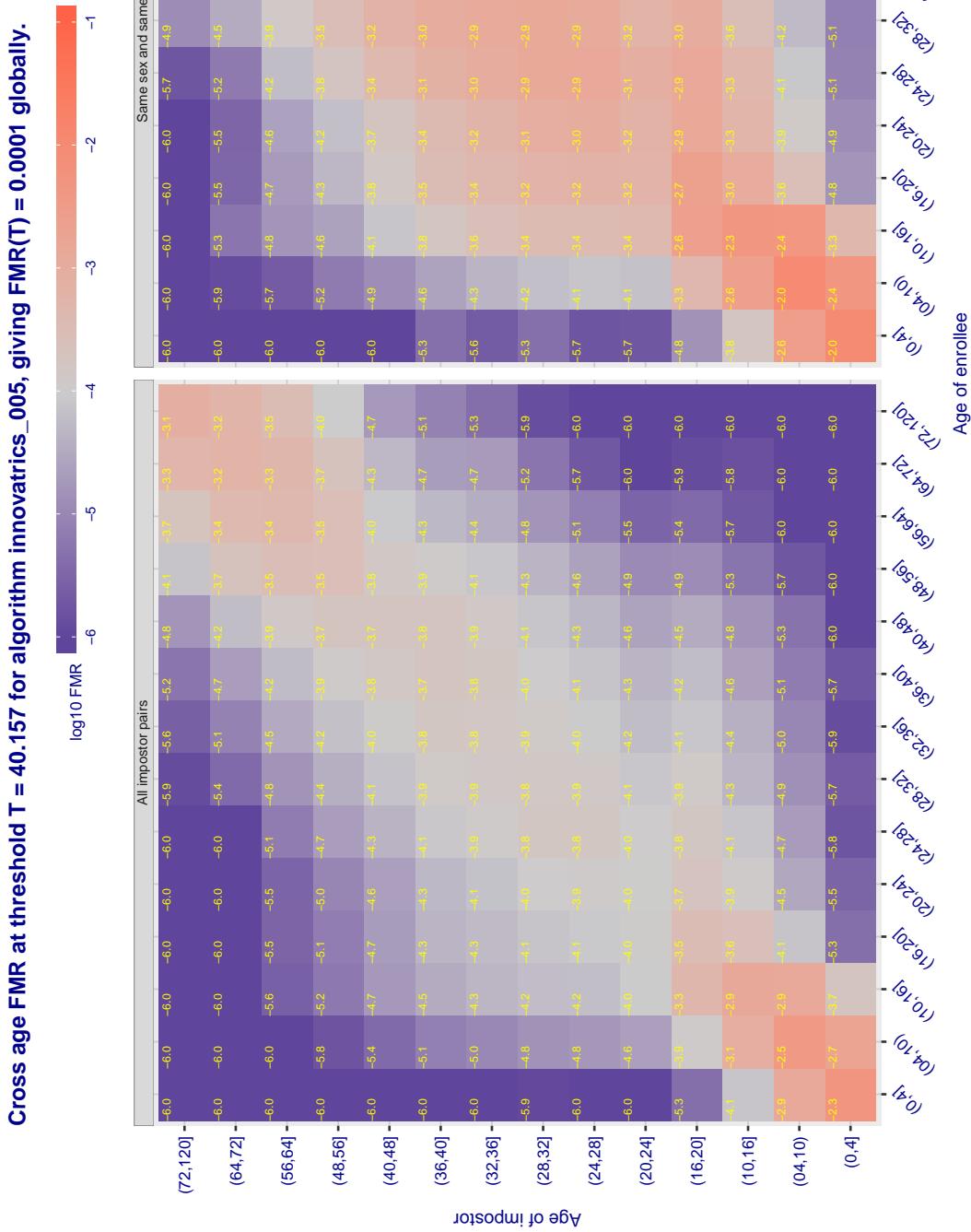


Figure 403: For algorithm innovatrics-004 operating on visa images, the heatmap shows false match observed over imposter comparisons of faces from different individuals who have the given age pair. False matches are counted against a recognition threshold fixed globally to give  $FMR = 0.001$  over all on the order of  $10^{10}$  imposter comparisons. The text in each box gives the same quantity as that coded by the color. Light colors present a security vulnerability to, for example, a passport gate.



**Figure 404:** For algorithm innovatrics-005 operating on visa images, the heatmap shows false match observed over impostor comparisons of faces from different individuals who have the given age pair. False matches are counted against a recognition threshold fixed globally to give  $FMR = 0.001$  over all on the order of  $10^{10}$  impostor comparisons. The text in each box gives the same quantity as that coded by the color. Light colors present a security vulnerability to, for example, a passport gate.

Cross age FMR at threshold T = 49.664 for algorithm intellivision\_001, giving  $FMR(T) = 0.0001$  globally.

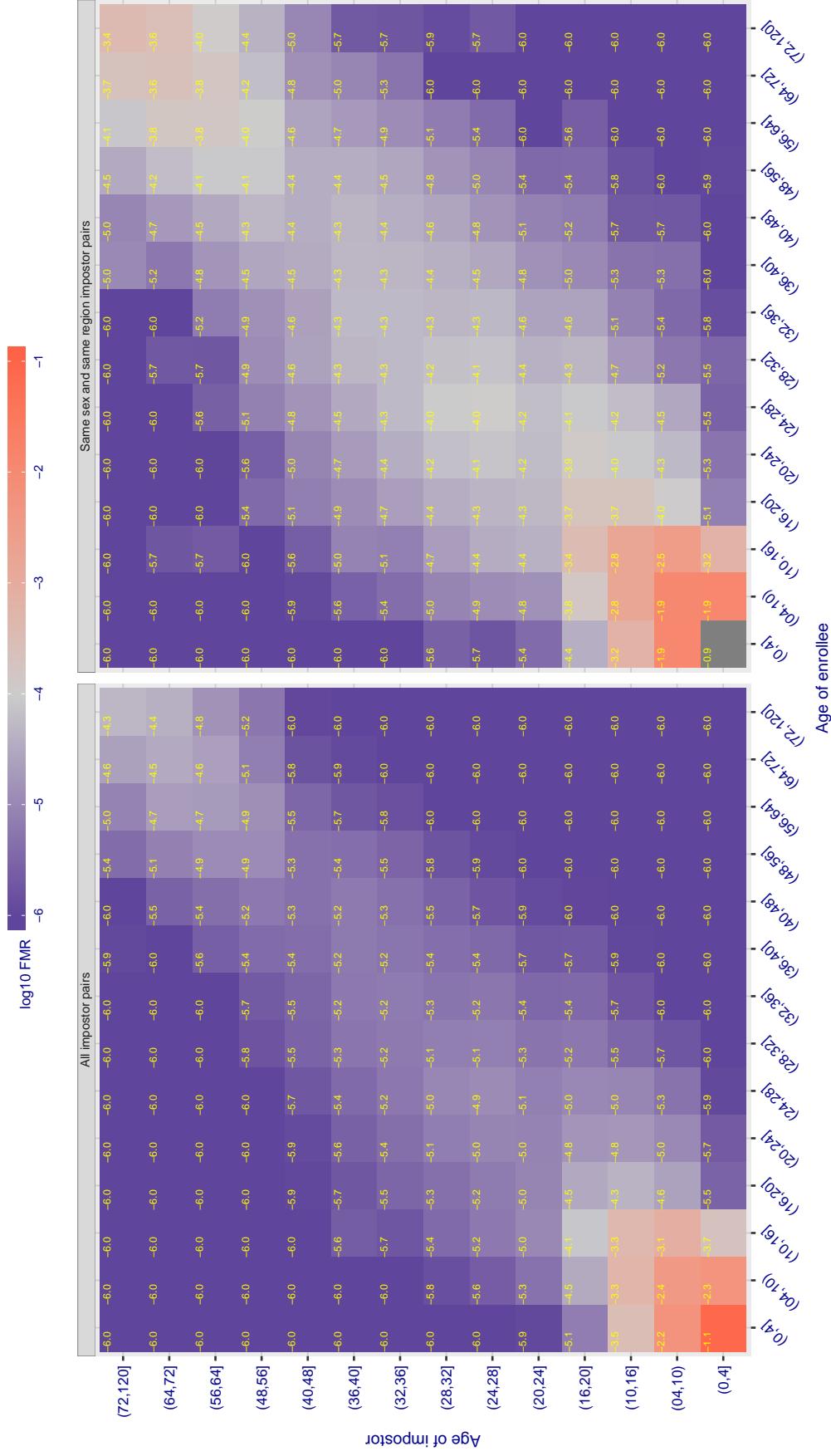


Figure 405: For algorithm intellivision\_001 operating on visa images, the heatmap shows false match observed over impostor comparisons of faces from different individuals who have the given age pair. False matches are counted against a recognition threshold fixed globally to give  $FMR = 0.001$  over all on the order of  $10^{10}$  impostor comparisons. The text in each box gives the same quantity as that coded by the color. Light colors present a security vulnerability to, for example, a passport gate.

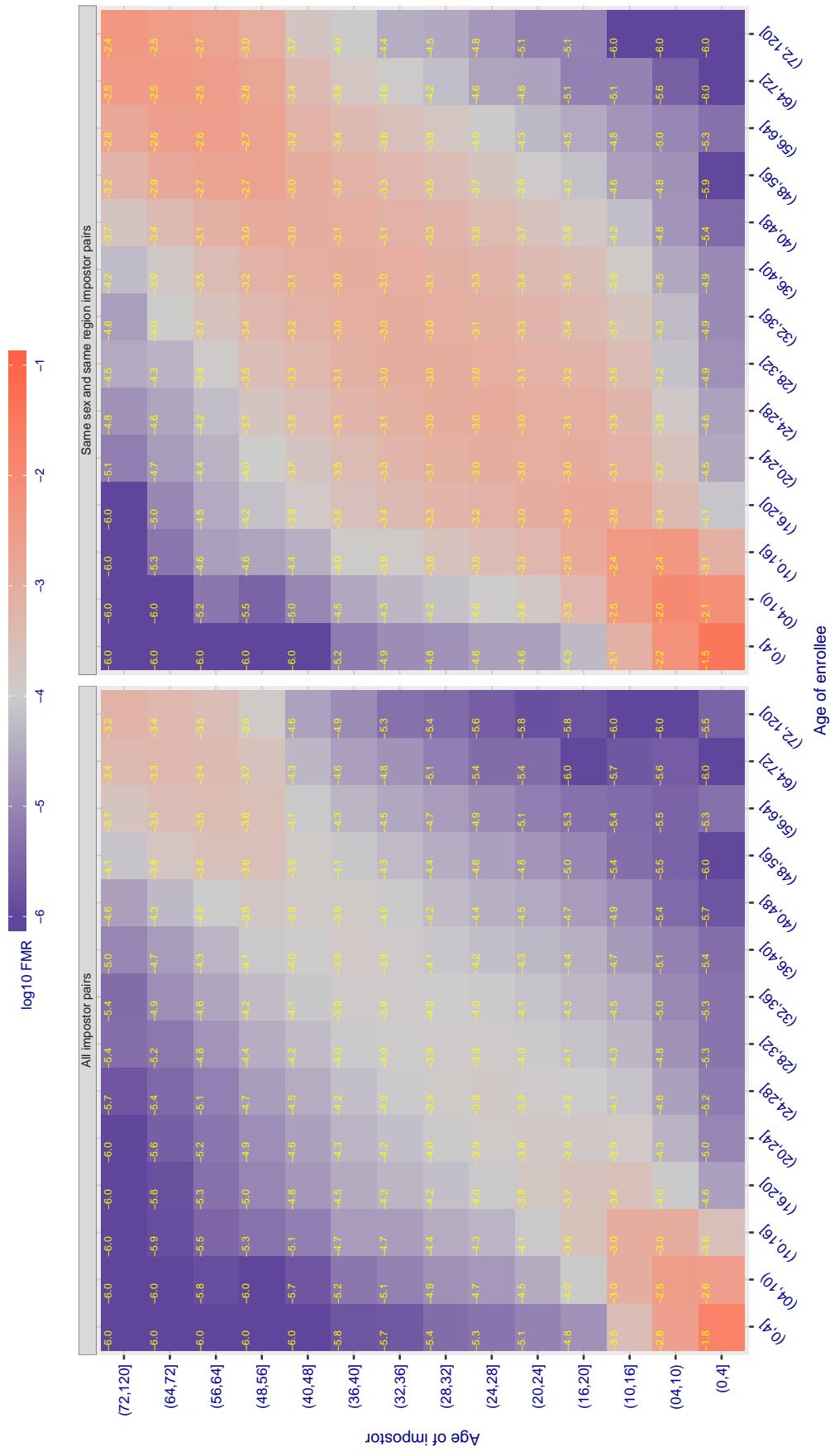
Cross age FMR at threshold T = 1.361 for algorithm iqface\_000, giving  $\text{FMR}(\text{T}) = 0.0001$  globally.

Figure 406: For algorithm iqface-000 operating on visa images, the heatmap shows false match observed over impostor comparisons of faces from different individuals who have the given age pair. False matches are counted against a recognition threshold fixed globally to give  $\text{FMR} = 0.001$  over all on the order of  $10^{10}$  impostor comparisons. The text in each box gives the same quantity as that coded by the color. Light colors present a security vulnerability to, for example, a passport gate.

Cross age FMR at threshold T = 23.498 for algorithm isityou\_000, giving FMR(T) = 0.0001 globally.

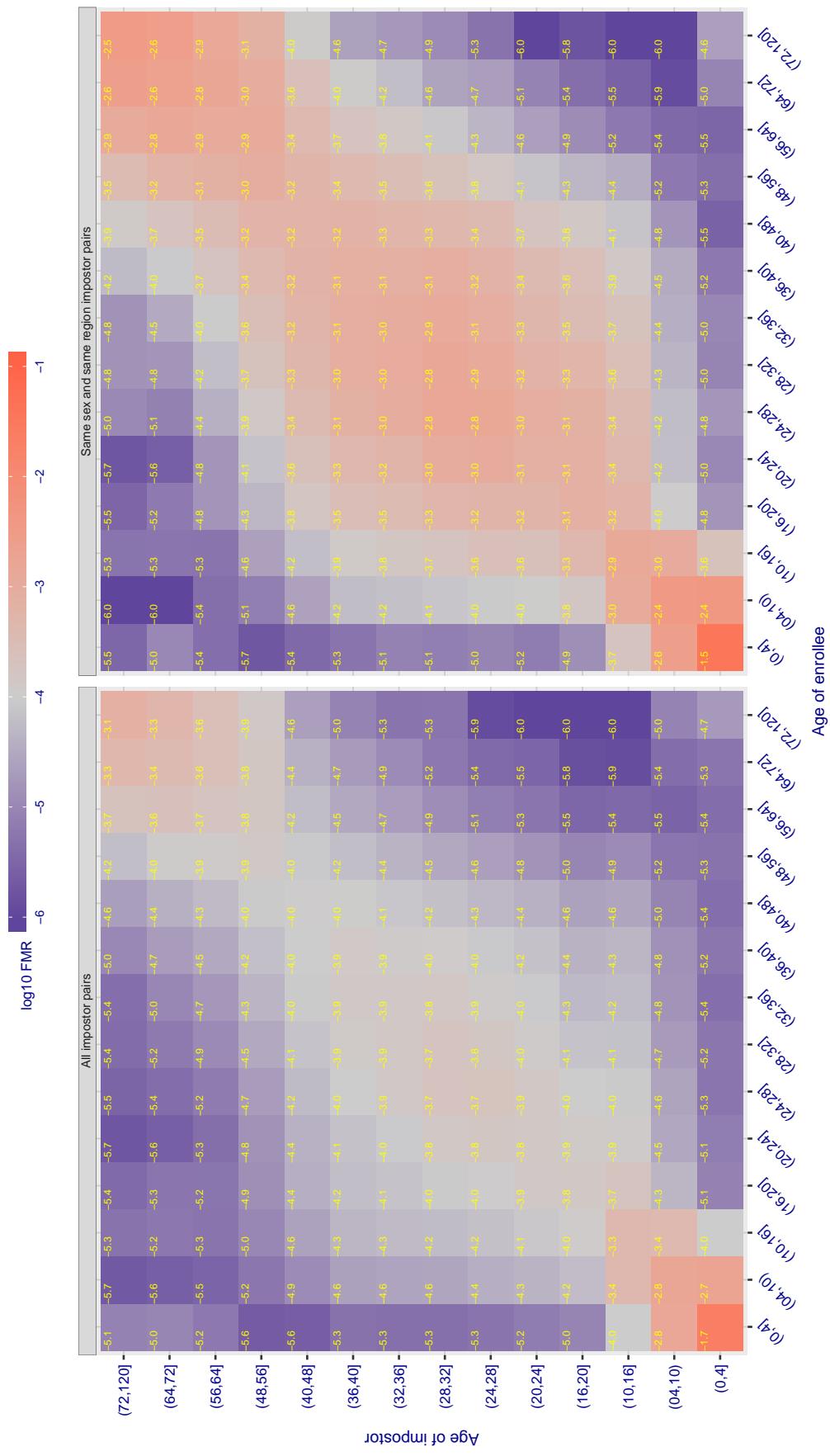


Figure 407: For algorithm isityou-000 operating on visa images, the heatmap shows false match observed over impostor comparisons of faces from different individuals who have the given age pair. False matches are counted against a recognition threshold fixed globally to give  $FMR = 0.00$  over all on the order of  $10^{10}$  impostor comparisons. The text in each box gives the same quantity as that coded by the color. Light colors present a security vulnerability to, for example, a passport gate.

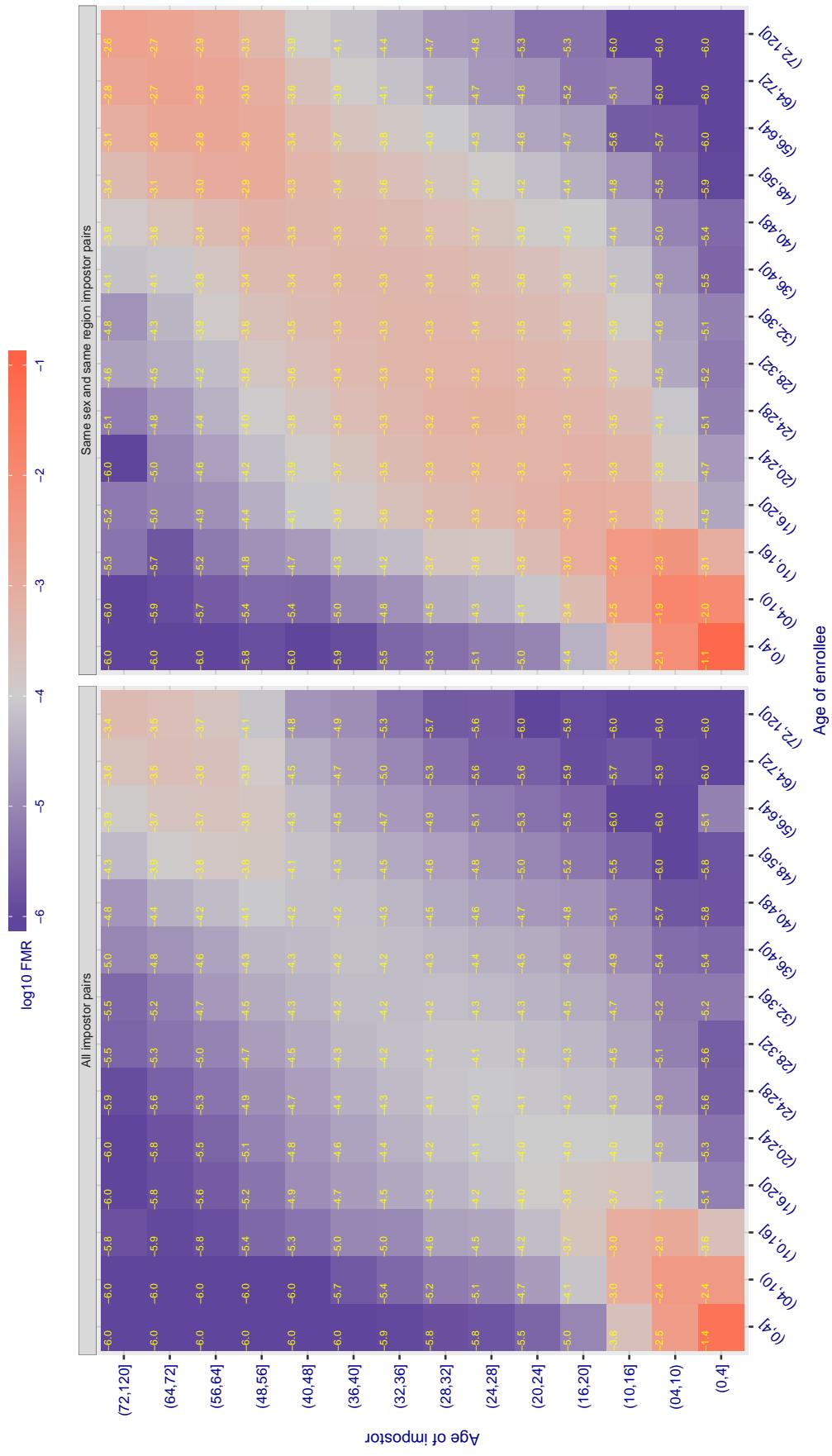
Cross age FMR at threshold T = 0.693 for algorithm **systems\_001**, giving  $\text{FMR}(\text{T}) = 0.0001$  globally.

Figure 408: For algorithm **systems-001** operating on visa images, the heatmap shows false match observed over impostor comparisons of faces from different individuals who have the given age pair. False matches are counted against a recognition threshold fixed globally to give  $\text{FMR} = 0.001$  over all on the order of  $10^{10}$  impostor comparisons. The text in each box gives the same quantity as that coded by the color. Light colors present a security vulnerability to, for example, a passport gate.

Cross age FMR at threshold T = 0.690 for algorithm systems\_002, giving FMR(T) = 0.0001 globally.

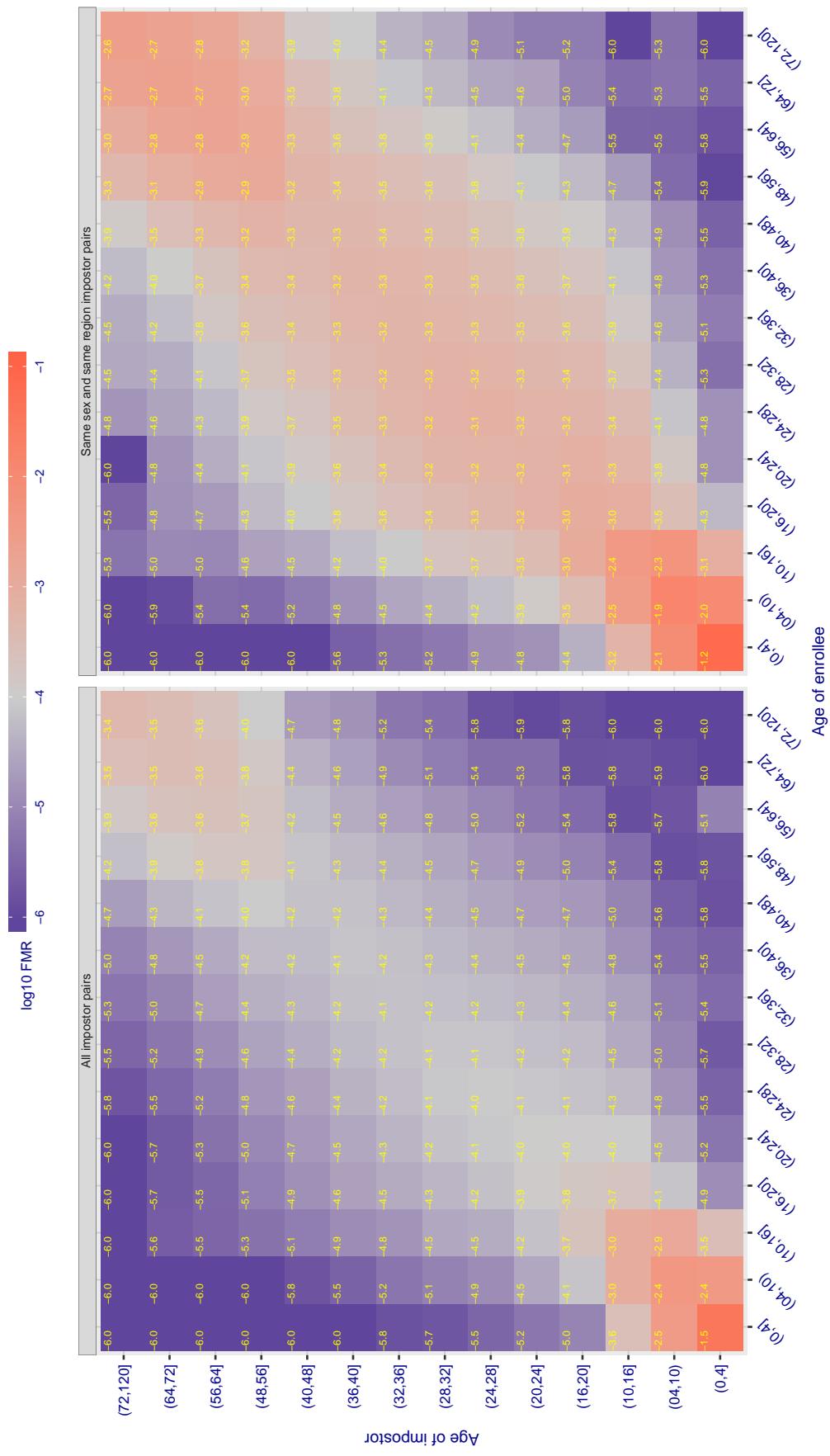


Figure 409: For algorithm systems-002 operating on visa images, the heatmap shows false match observed over impostor comparisons of faces from different individuals who have the given age pair. False matches are counted against a recognition threshold fixed globally to give FMR = 0.001 over all on the order of  $10^{10}$  impostor comparisons. The text in each box gives the same quantity as that coded by the color. Light colors present a security vulnerability to, for example, a passport gate.

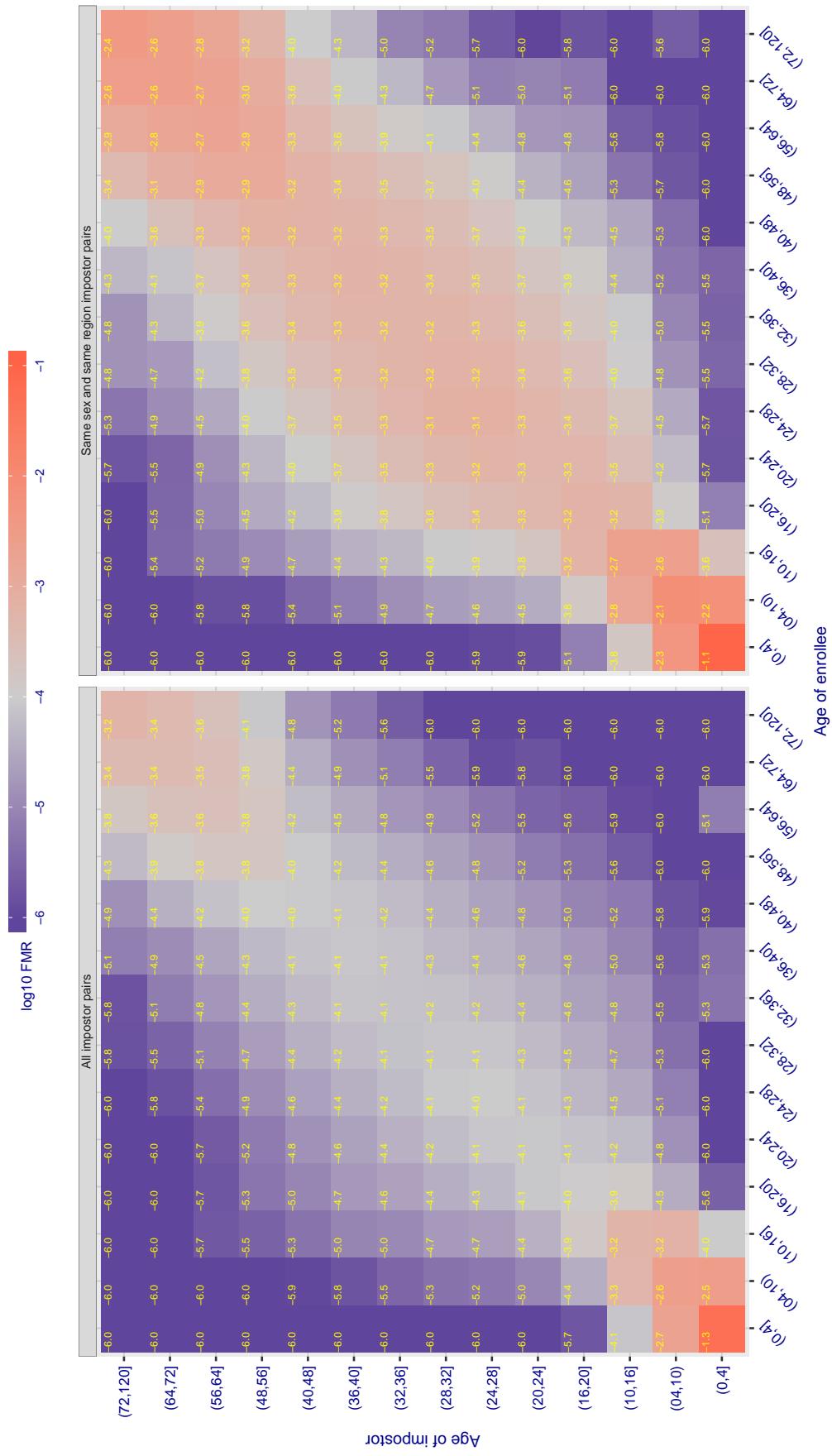
Cross age FMR at threshold T = 49.879 for algorithm itmo\_005, giving  $FMR(T) = 0.0001$  globally.

Figure 410: For algorithm itmo\_005 operating on visa images, the heatmap shows false match observed over impostor comparisons of faces from different individuals who have the given age pair. False matches are counted against a recognition threshold fixed globally to give  $FMR = 0.001$  over all on the order of  $10^{10}$  impostor comparisons. The text in each box gives the same quantity as that coded by the color. Light colors present a security vulnerability to, for example, a passport gate.

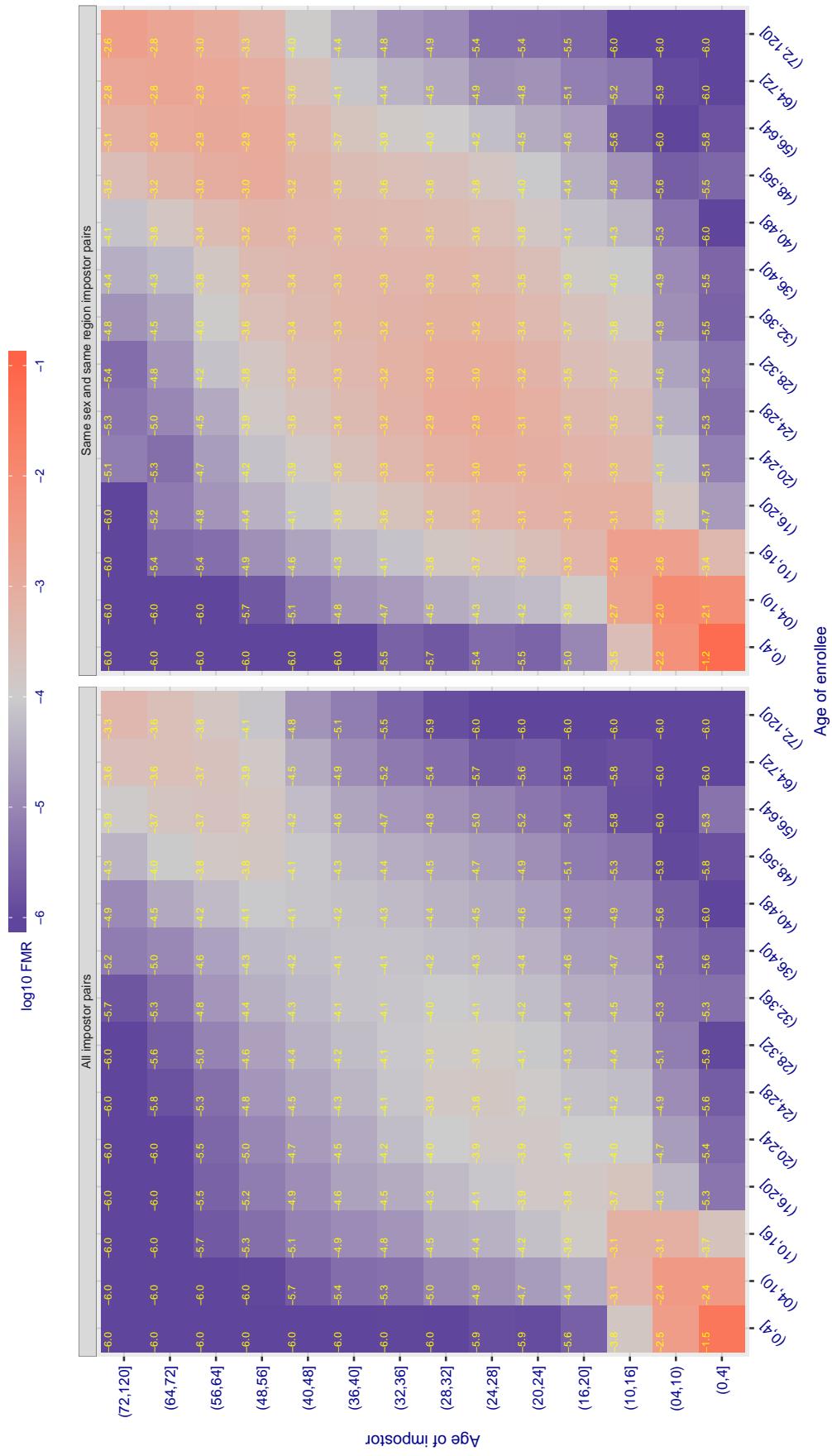
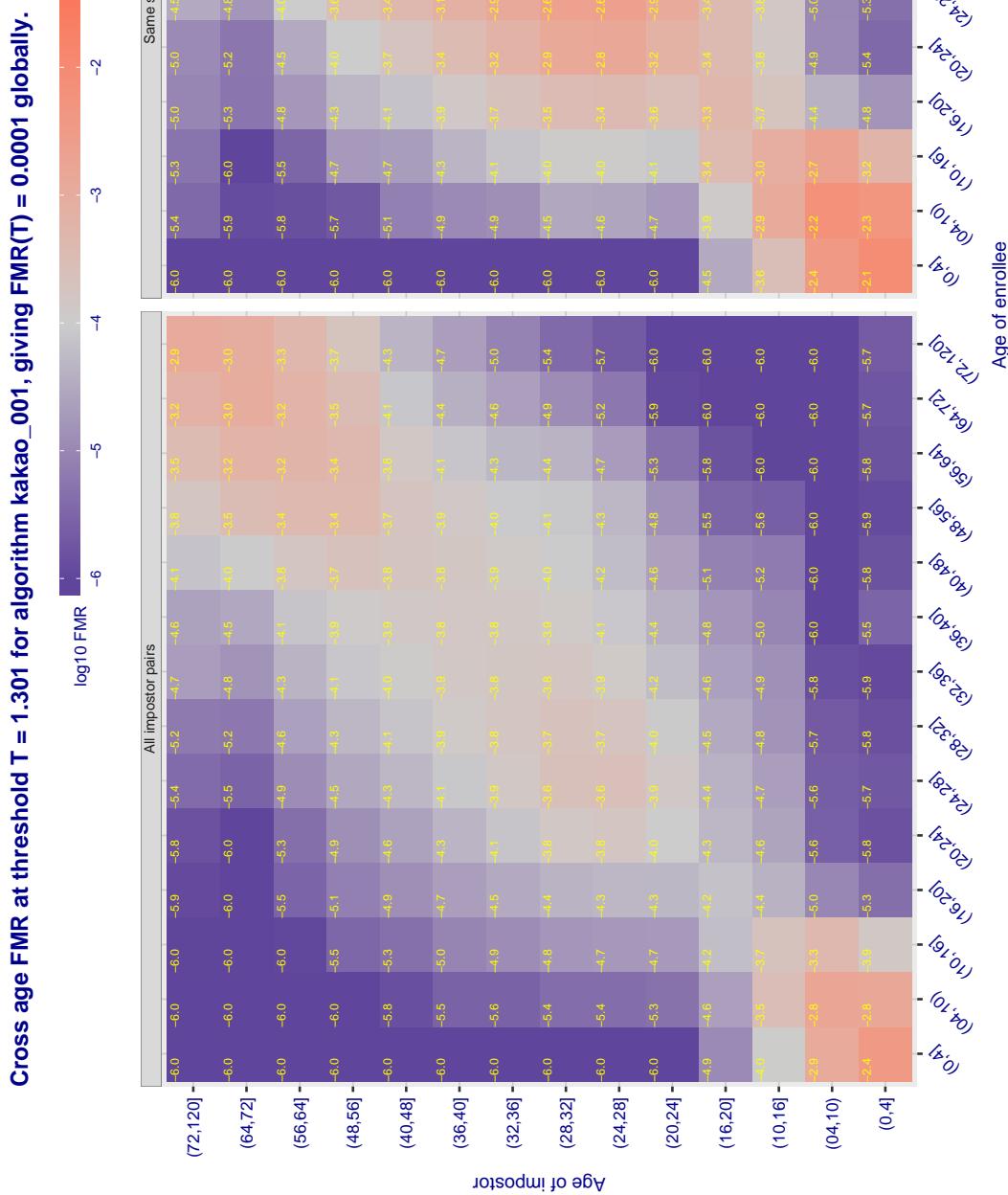
Cross age FMR at threshold T = 49.739 for algorithm itmo\_006, giving  $FMR(T) = 0.0001$  globally.

Figure 411: For algorithm itmo-006 operating on visa images, the heatmap shows false match observed over impostor comparisons of faces from different individuals who have the given age pair. False matches are counted against a recognition threshold fixed globally to give  $FMR = 0.001$  over all on the order of  $10^{10}$  impostor comparisons. The text in each box gives the same quantity as that coded by the color. Light colors present a security vulnerability to, for example, a passport gate.



**Figure 412:** For algorithm kakao-001 operating on visa images, the heatmap shows false match observed over impostor comparisons of faces from different individuals who have the given age pair. False matches are counted against a recognition threshold fixed globally to give  $FMR = 0.001$  over all on the order of  $10^{10}$  impostor comparisons. The text in each box gives the same quantity as that coded by the color. Light colors present a security vulnerability to, for example, a passport gate.

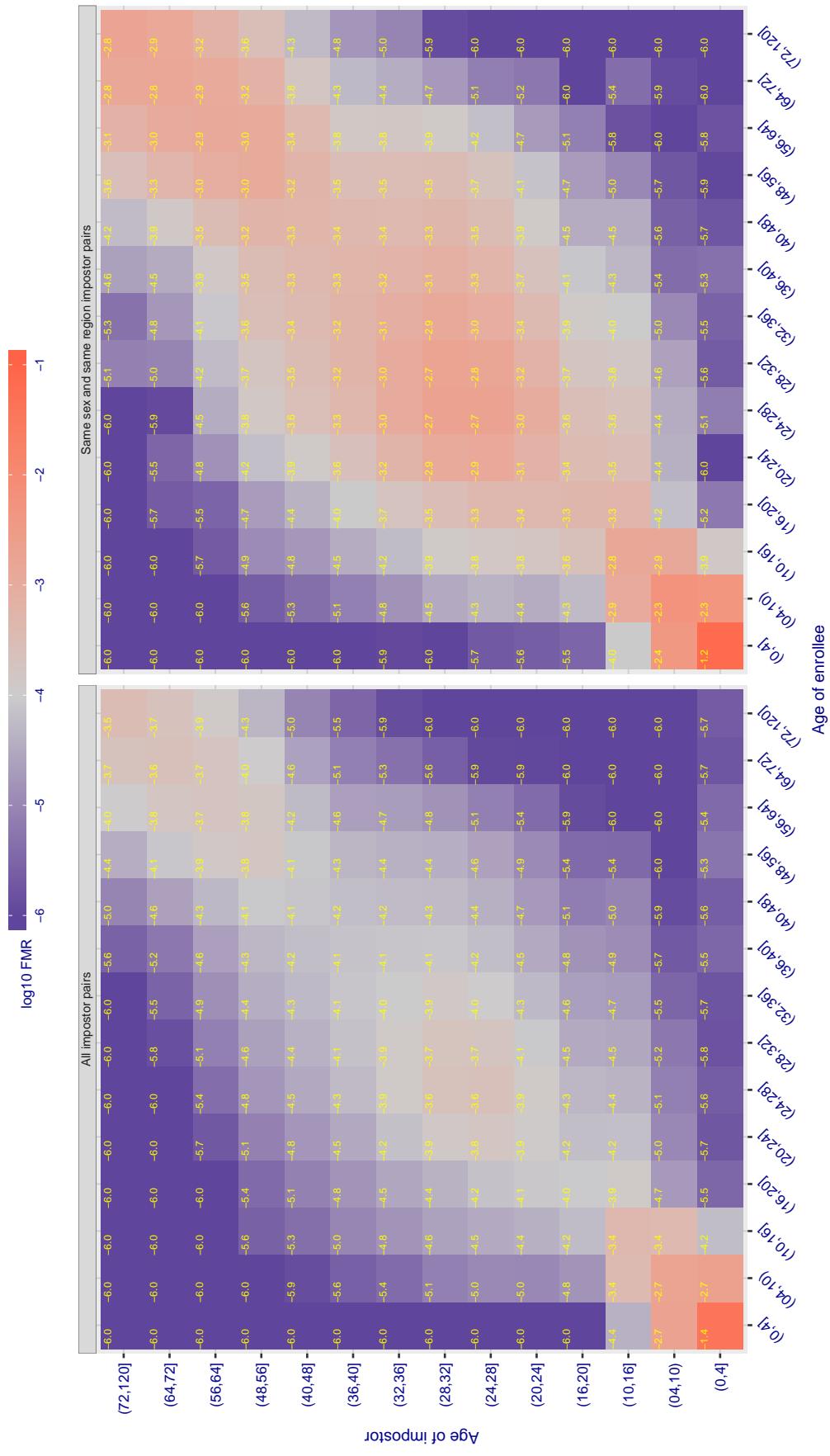
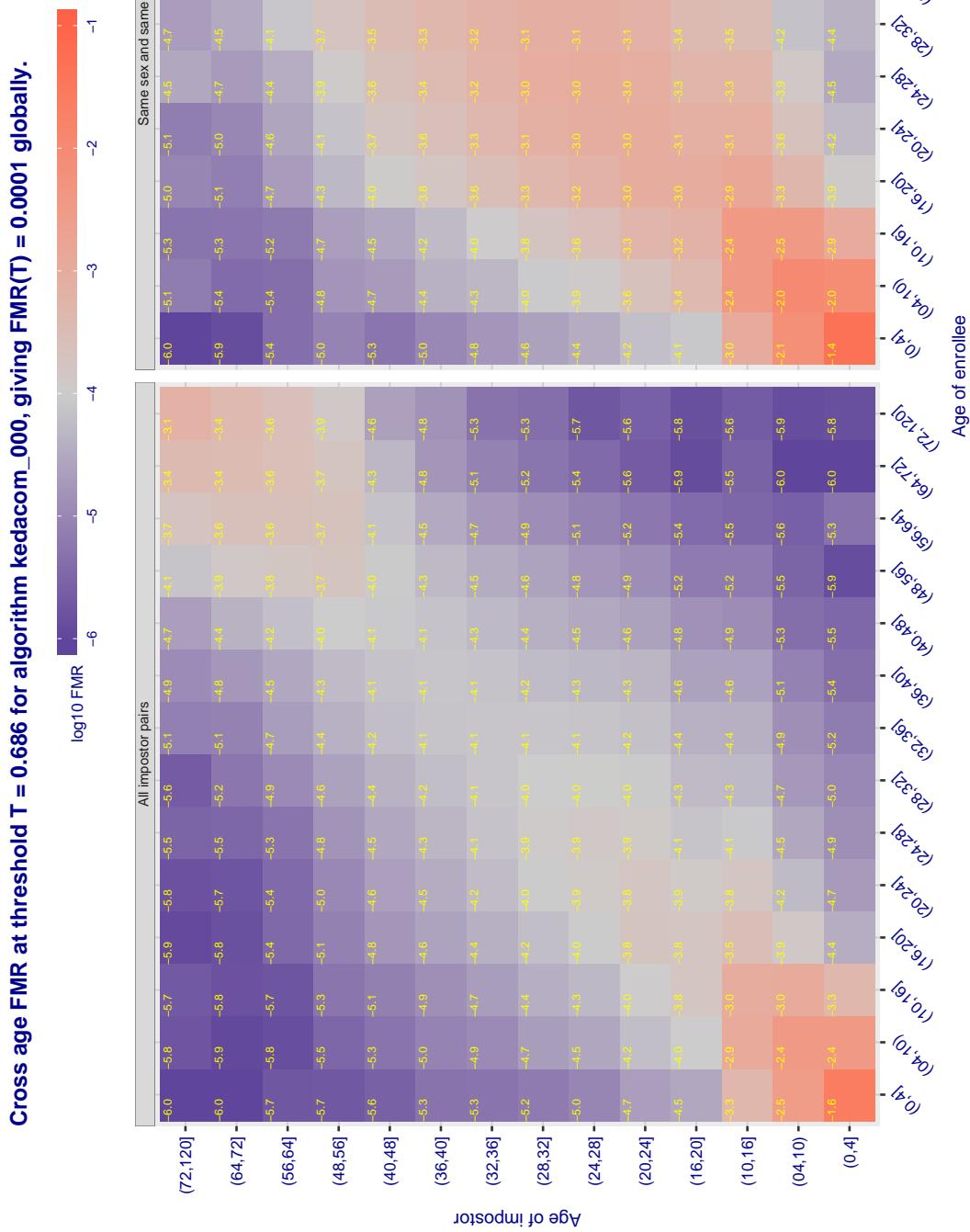
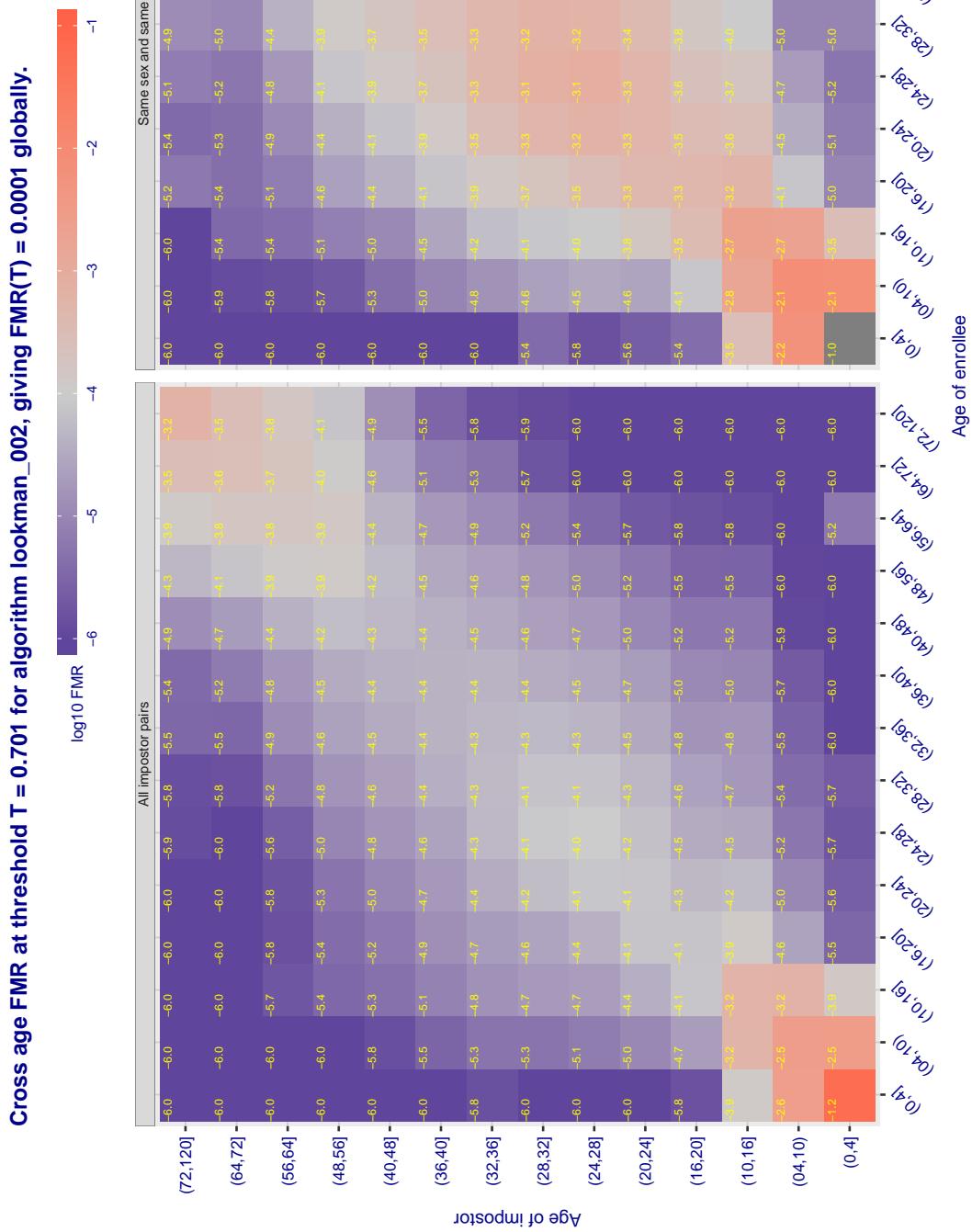
Cross age FMR at threshold T = 0.929 for algorithm kakao\_002, giving  $\text{FMRT} = 0.0001$  globally.

Figure 413: For algorithm kakao-002 operating on visa images, the heatmap shows false match observed over impostor comparisons of faces from different individuals who have the given age pair. False matches are counted against a recognition threshold fixed globally to give  $\text{FMR} = 0.001$  over all on the order of  $10^{10}$  impostor comparisons. The text in each box gives the same quantity as that coded by the color. Light colors present a security vulnerability to, for example, a passport gate.



**Figure 44:** For algorithm kedacom-000 operating on visa images, the heatmap shows false match observed over impostor comparisons of faces from different individuals who have the given age pair. False matches are counted against a recognition threshold fixed globally to give  $FMR = 0.001$  over all on the order of  $10^{10}$  impostor comparisons. The text in each box gives the same quantity as that coded by the color. Light colors present a security vulnerability to, for example, a passport gate.



**Figure 415:** For algorithm lookman-002 operating on visa images, the heatmap shows false match observed over impostor comparisons of faces from different individuals who have the given age pair. False matches are counted against a recognition threshold fixed globally to give  $FMR = 0.001$  over all on the order of  $10^{10}$  impostor comparisons. The text in each box gives the same quantity as that coded by the color. Light colors present a security vulnerability to, for example, a passport gate.

Cross age FMR at threshold T = 0.733 for algorithm lookman\_004, giving FMR(T) = 0.0001 globally.

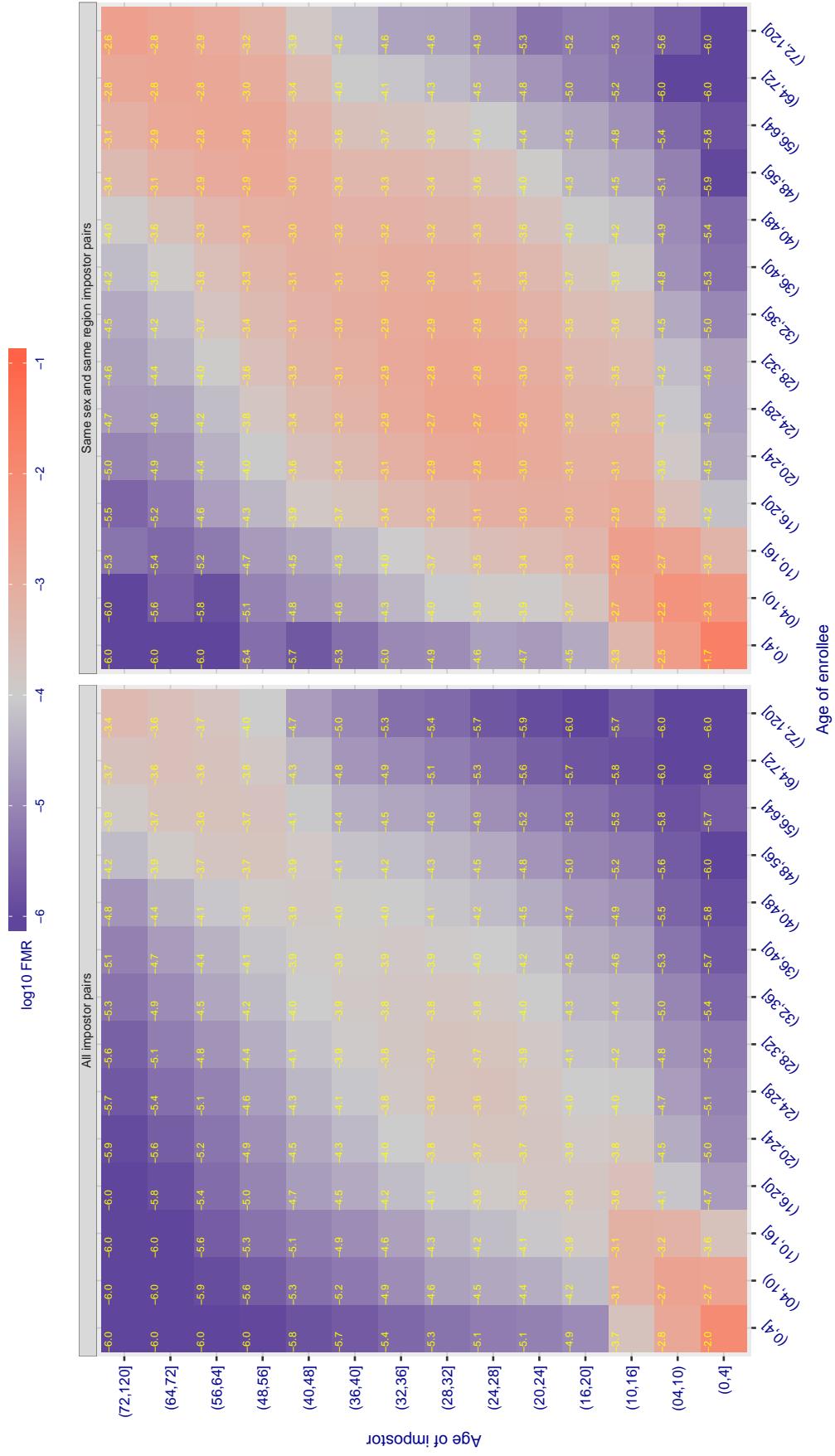


Figure 416: For algorithm lookman-004 operating on visa images, the heatmap shows false match observed over impostor comparisons of faces from different individuals who have the given age pair. False matches are counted against a recognition threshold fixed globally to give FMR = 0.001 over all on the order of  $10^{10}$  impostor comparisons. The text in each box gives the same quantity as that coded by the color. Light colors present a security vulnerability to, for example, a passport gate.

Cross age FMR at threshold T = 74.511 for algorithm megvii\_001, giving FMR(T) = 0.0001 globally.

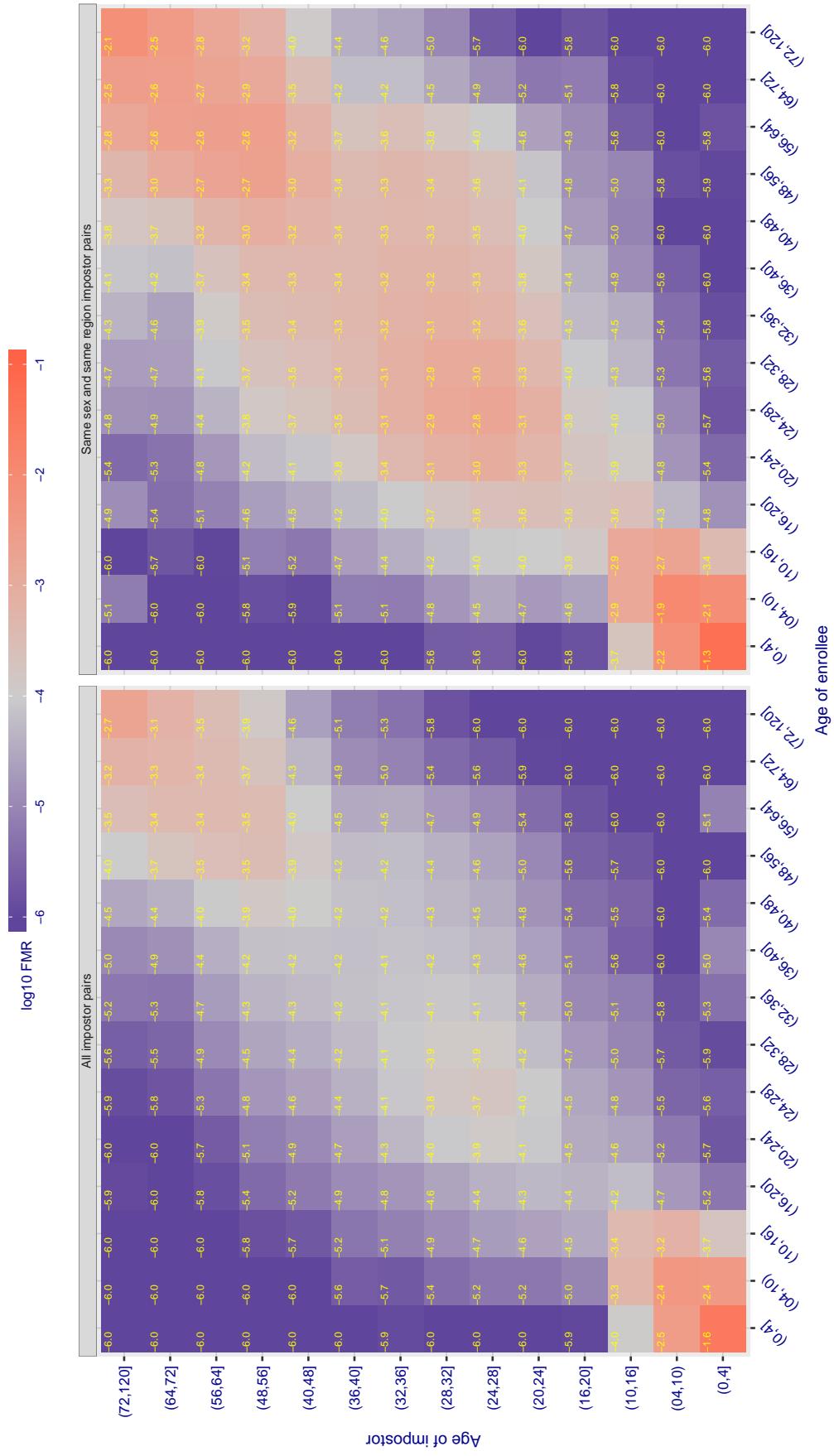


Figure 417: For algorithm megvii-001 operating on visa images, the heatmap shows false match observed over impostor comparisons of faces from different individuals who have the given age pair. False matches are counted against a recognition threshold fixed globally to give FMR = 0.00 over all on the order of  $10^{10}$  impostor comparisons. The text in each box gives the same quantity as that coded by the color. Light colors present a security vulnerability to, for example, a passport gate.

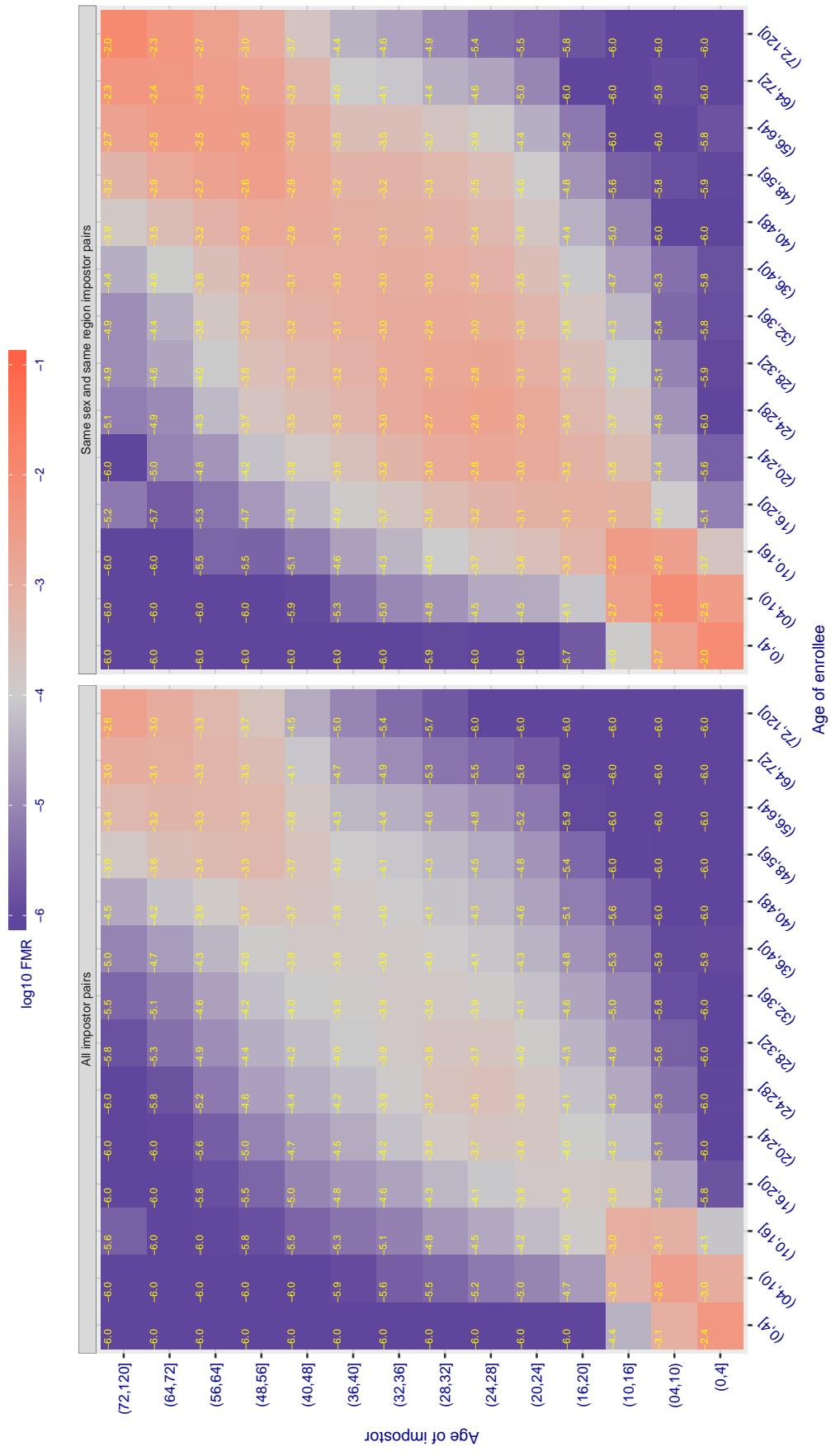
Cross age FMR at threshold T = 66.384 for algorithm megvii\_002, giving  $FMR(T) = 0.0001$  globally.

Figure 418: For algorithm megvii-002 operating on visa images, the heatmap shows false match observed over impostor comparisons of faces from different individuals who have the given age pair. False matches are counted against a recognition threshold fixed globally to give  $FMR = 0.00$  over all on the order of  $10^{10}$  impostor comparisons. The text in each box gives the same quantity as that coded by the color. Light colors present a security vulnerability to, for example, a passport gate.

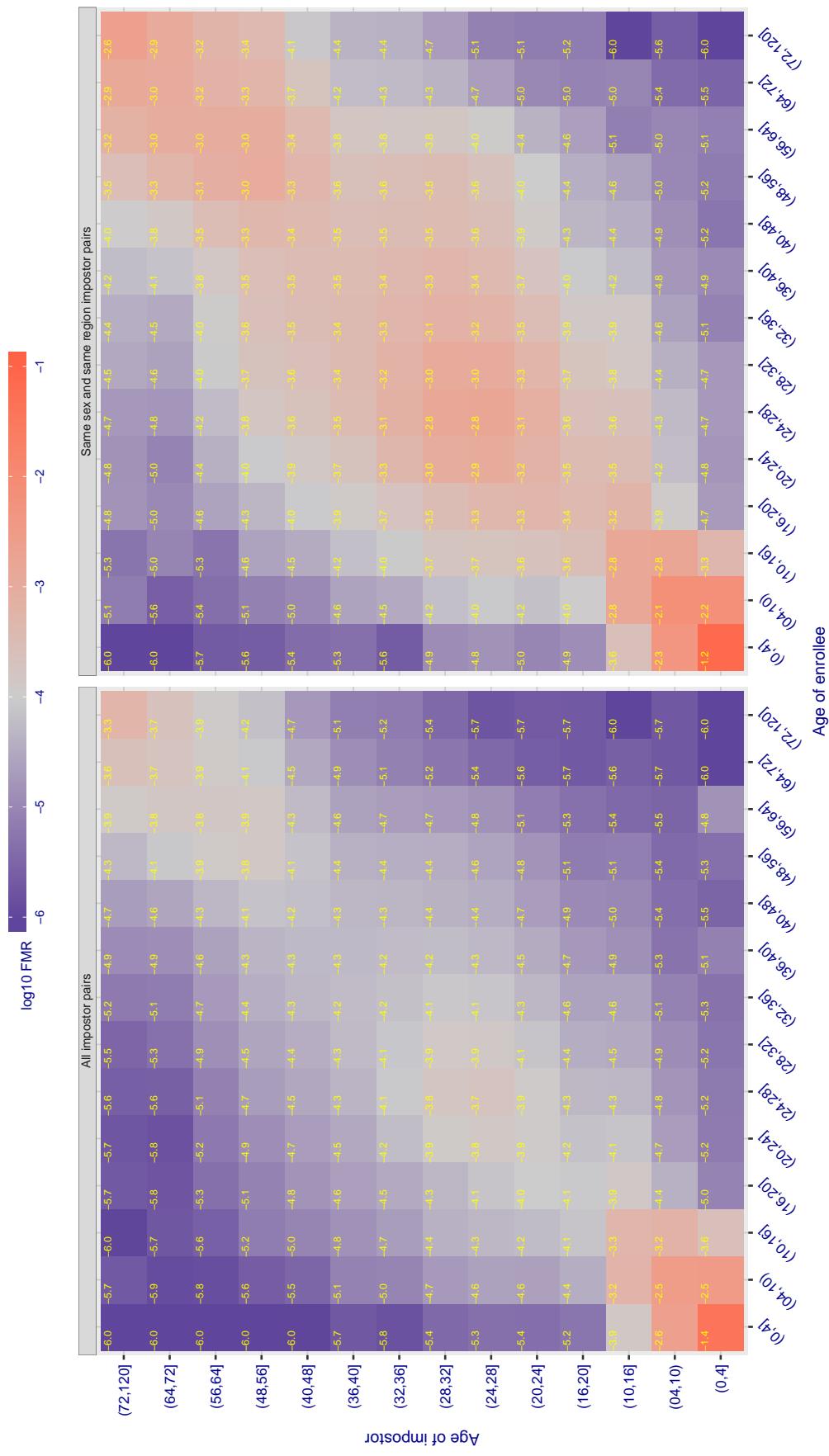
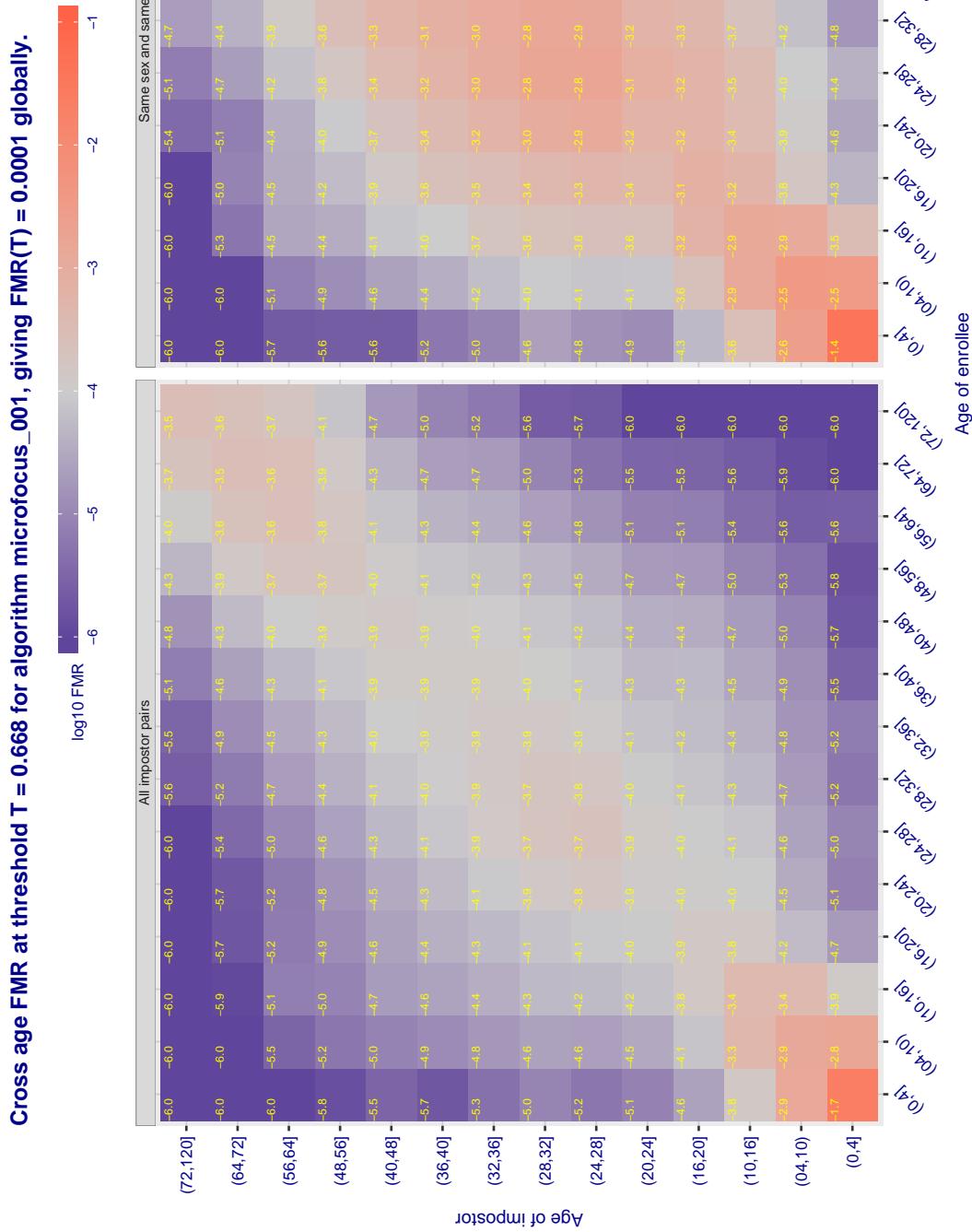
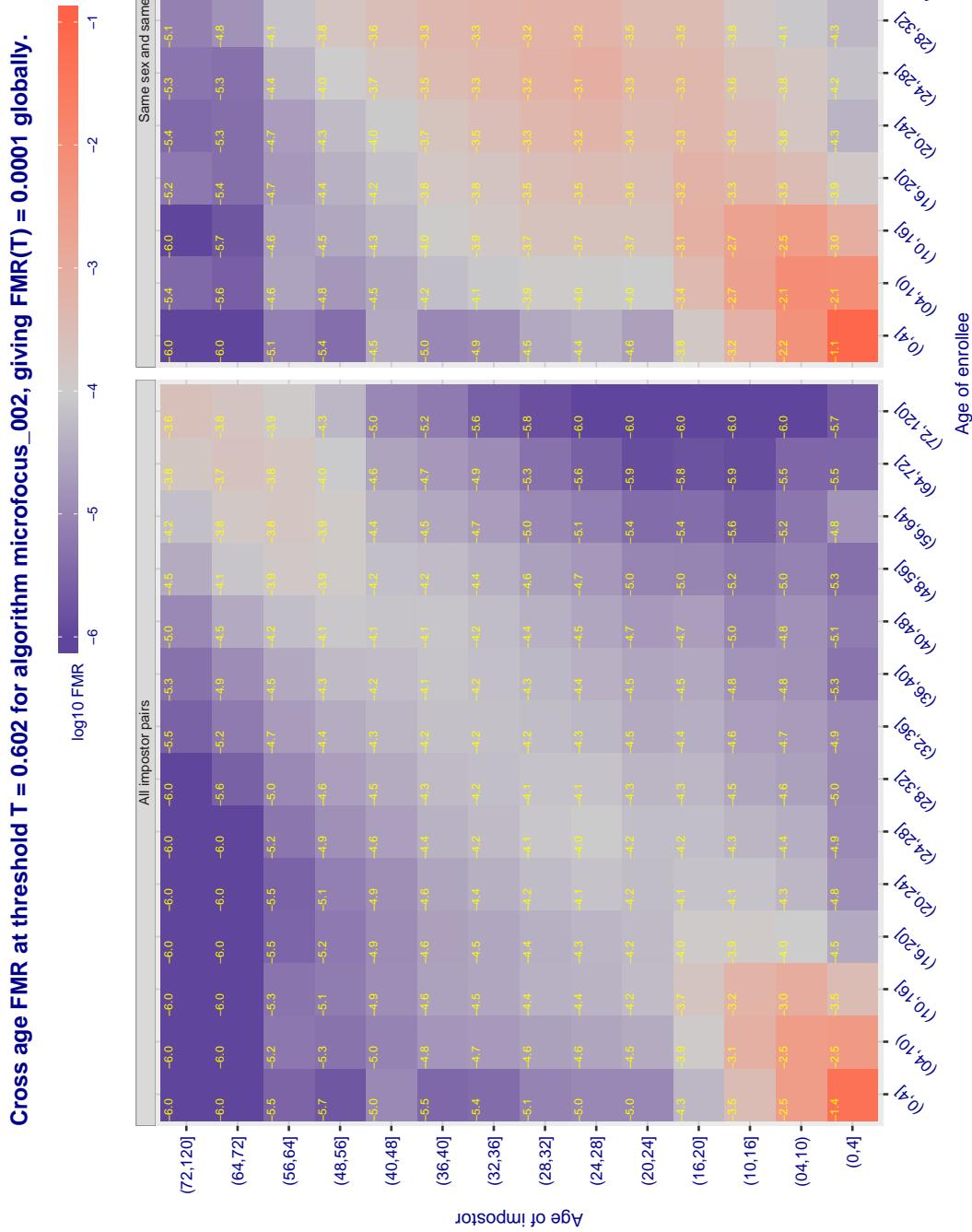
Cross age FMR at threshold T = 0.425 for algorithm meiya\_001, giving  $\text{FMR}(\text{T}) = 0.0001$  globally.

Figure 419: For algorithm meiya-001 operating on visa images, the heatmap shows false match observed over impostor comparisons of faces from different individuals who have the given age pair. False matches are counted against a recognition threshold fixed globally to give  $\text{FMR} = 0.001$  over all on the order of  $10^{10}$  impostor comparisons. The text in each box gives the same quantity as that coded by the color. Light colors present a security vulnerability to, for example, a passport gate.



**Figure 420:** For algorithm microfocus-001 operating on visa images, the heatmap shows false match observed over impostor comparisons of faces from different individuals who have the given age pair. False matches are counted against a recognition threshold fixed globally to give  $FMR = 0.001$  over all on the order of  $10^{10}$  impostor comparisons. The text in each box gives the same quantity as that coded by the color. Light colors present a security vulnerability to, for example, a passport gate.



**Figure 421:** For algorithm microfocus-002 operating on visa images, the heatmap shows false match observed over impostor comparisons of faces from different individuals who have the given age pair. False matches are counted against a recognition threshold fixed globally to give  $FMR = 0.001$  over all on the order of  $10^{10}$  impostor comparisons. The text in each box gives the same quantity as that coded by the color. Light colors present a security vulnerability to, for example, a passport gate.

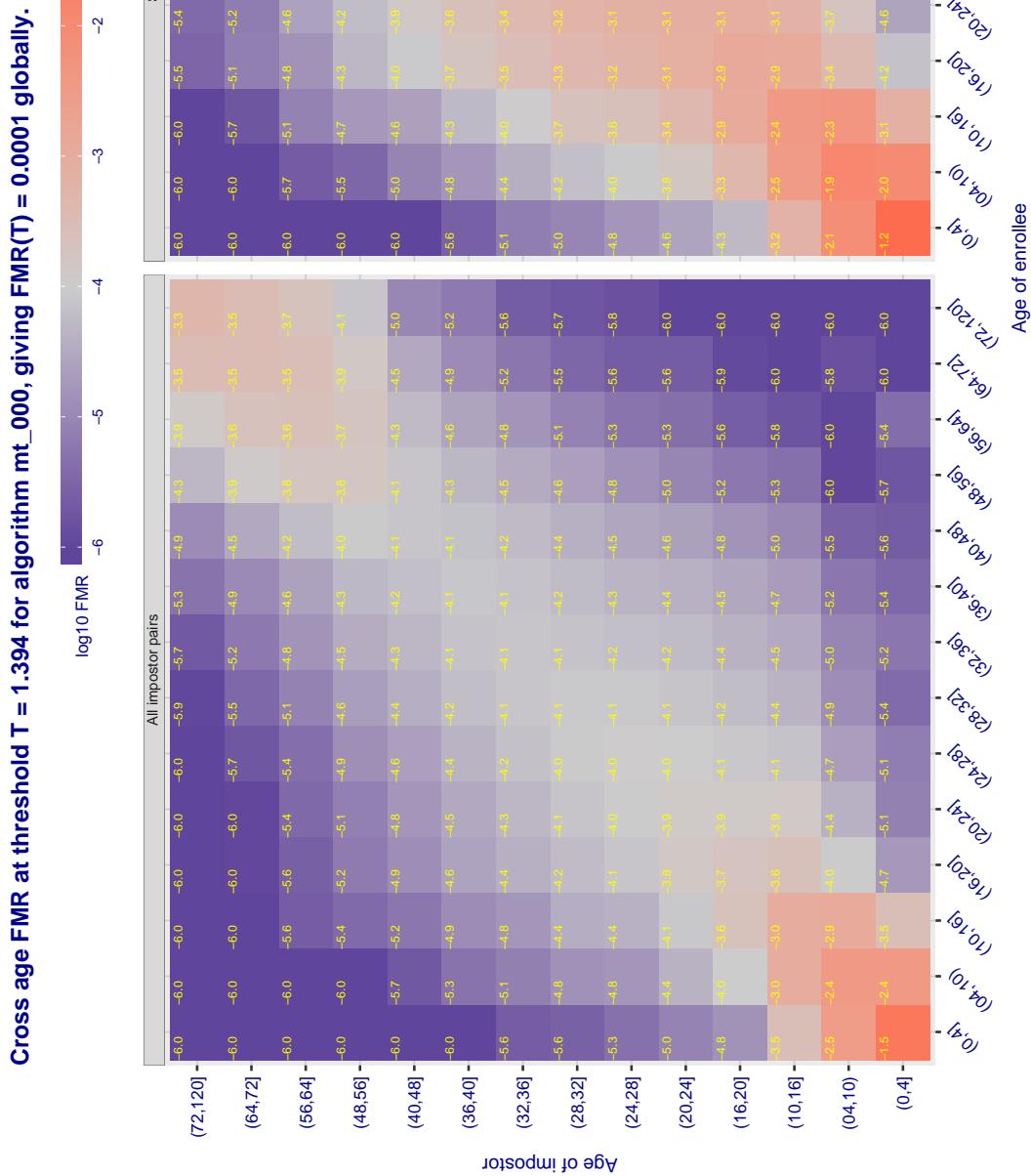


**Figure 422:** For algorithm mt-000 operating on visa images, the heatmap shows false match comparisons of faces from different individuals who have the given age pair. False matches are counted against a recognition threshold fixed globally to give  $FMR = 0.001$  over all on the order of  $10^{10}$  impostor comparisons. The text in each box gives the same quantity as that coded by the color. Light colors present a security vulnerability to, for example, a passport gate.

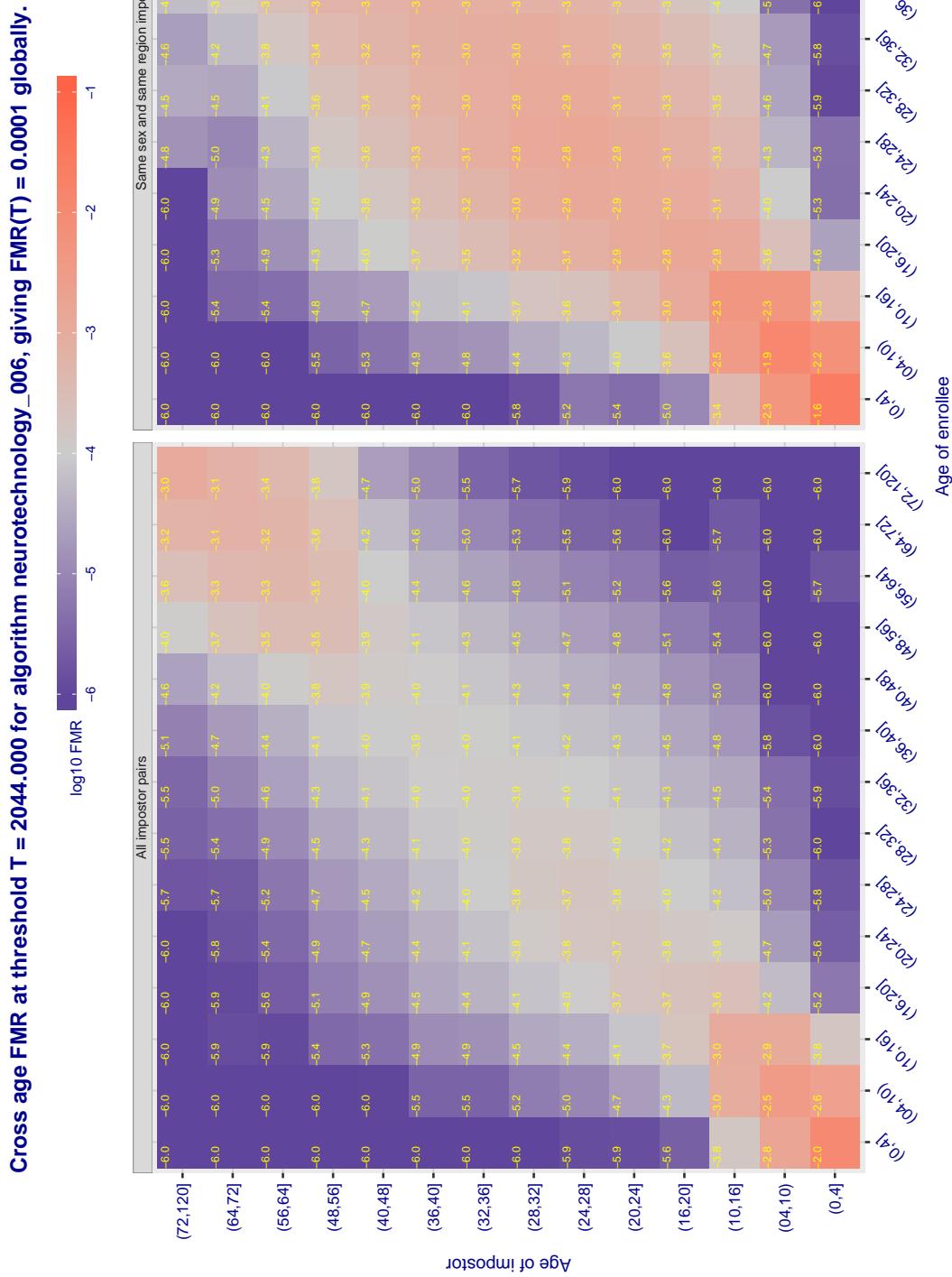


Figure 423: For algorithm neurotechnology-006 operating on visa images, the heatmap shows false match observed over impostor comparisons of faces from different individuals who have the given age pair. False matches are counted against a recognition threshold fixed globally to give  $FMR = 0.001$  over all on the order of  $10^{10}$  impostor comparisons. The text in each box gives the same quantity as that coded by the color. Light colors present a security vulnerability to, for example, a passport gate.

Cross age FMR at threshold T = 1.000 for algorithm nodeflux\_001, giving FMR(T) = 0.0001 globally.

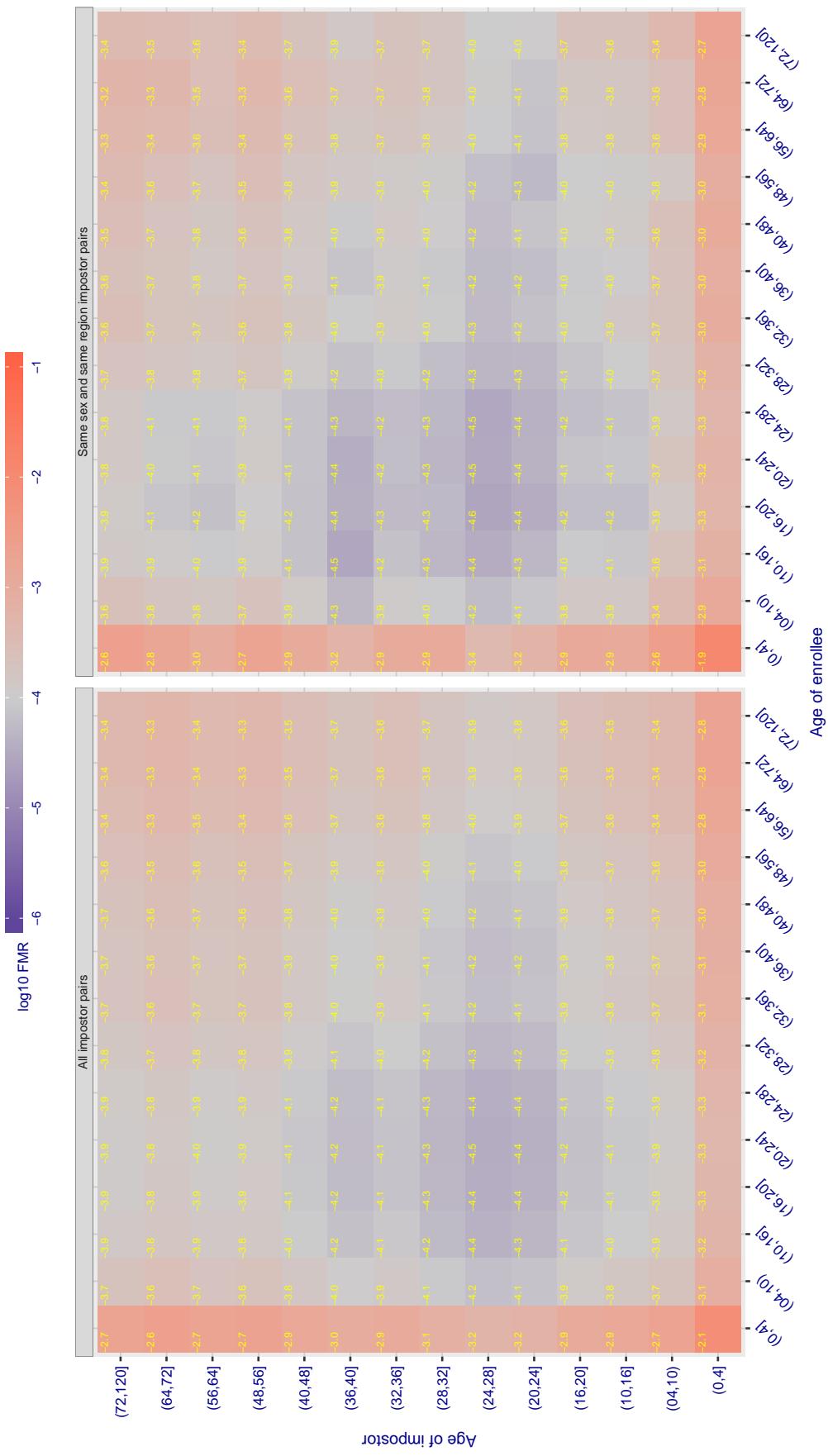
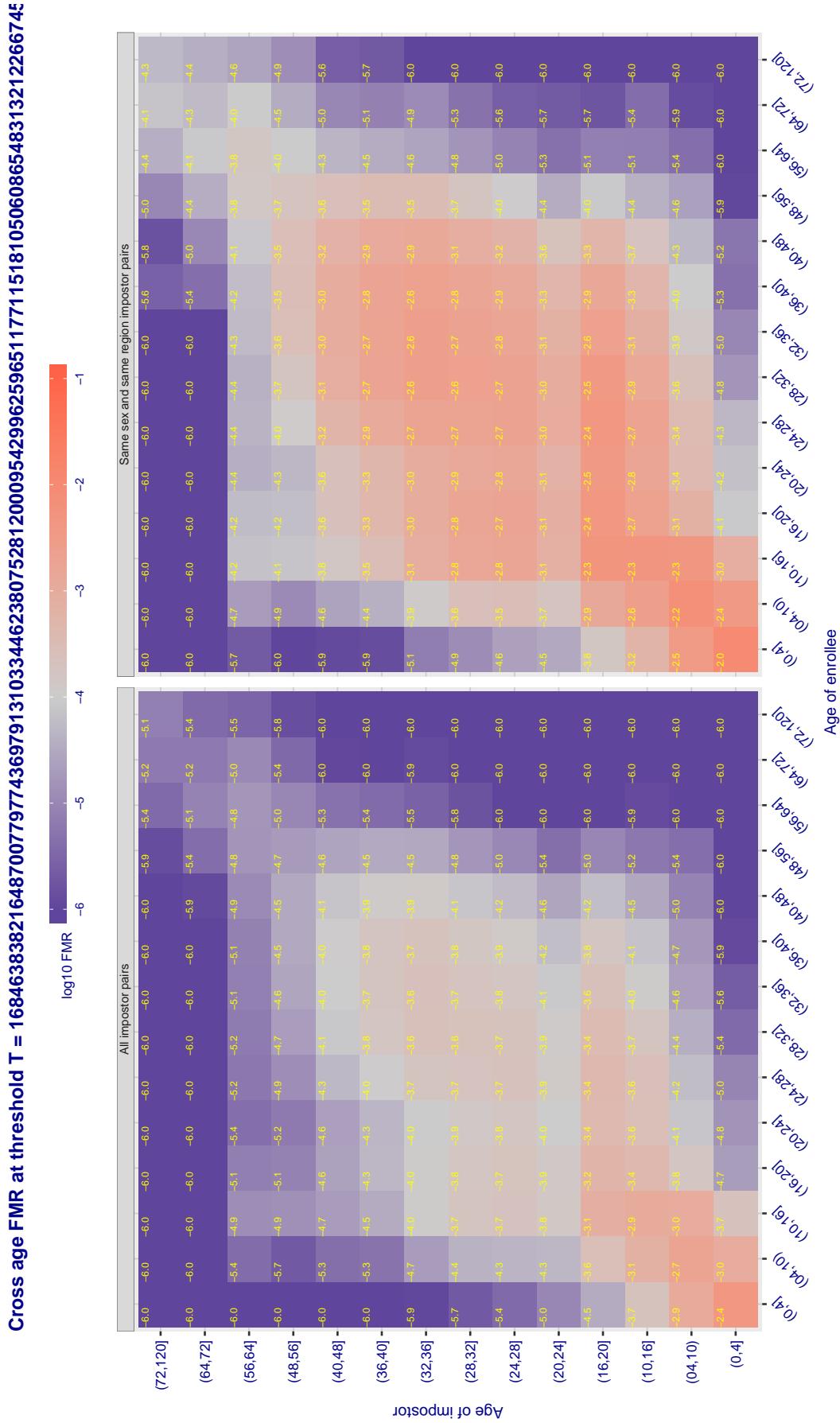


Figure 424: For algorithm nodeflux-001 operating on visa images, the heatmap shows false match observed over impostor comparisons of faces from different individuals who have the given age pair. False matches are counted against a recognition threshold fixed globally to give  $FMR = 0.001$  over all on the order of  $10^{10}$  impostor comparisons. The text in each box gives the same quantity as that coded by the color. Light colors present a security vulnerability to, for example, a passport gate.



**Figure 425:** For algorithm notiontag-000 operating on visa images, the heatmap shows false match observed over impostor comparisons of faces from different individuals who have the given age pair. False matches are counted against a recognition threshold fixed globally to give  $FMR = 0.001$  over all on the order of  $10^{10}$  impostor comparisons. The text in each box gives the same quantity as that coded by the color. Light colors present a security vulnerability to, for example, a passport gate.

Cross age FMR at threshold T = 1.997 for algorithm ntechlab\_006, giving FMR(T) = 0.0001 globally.

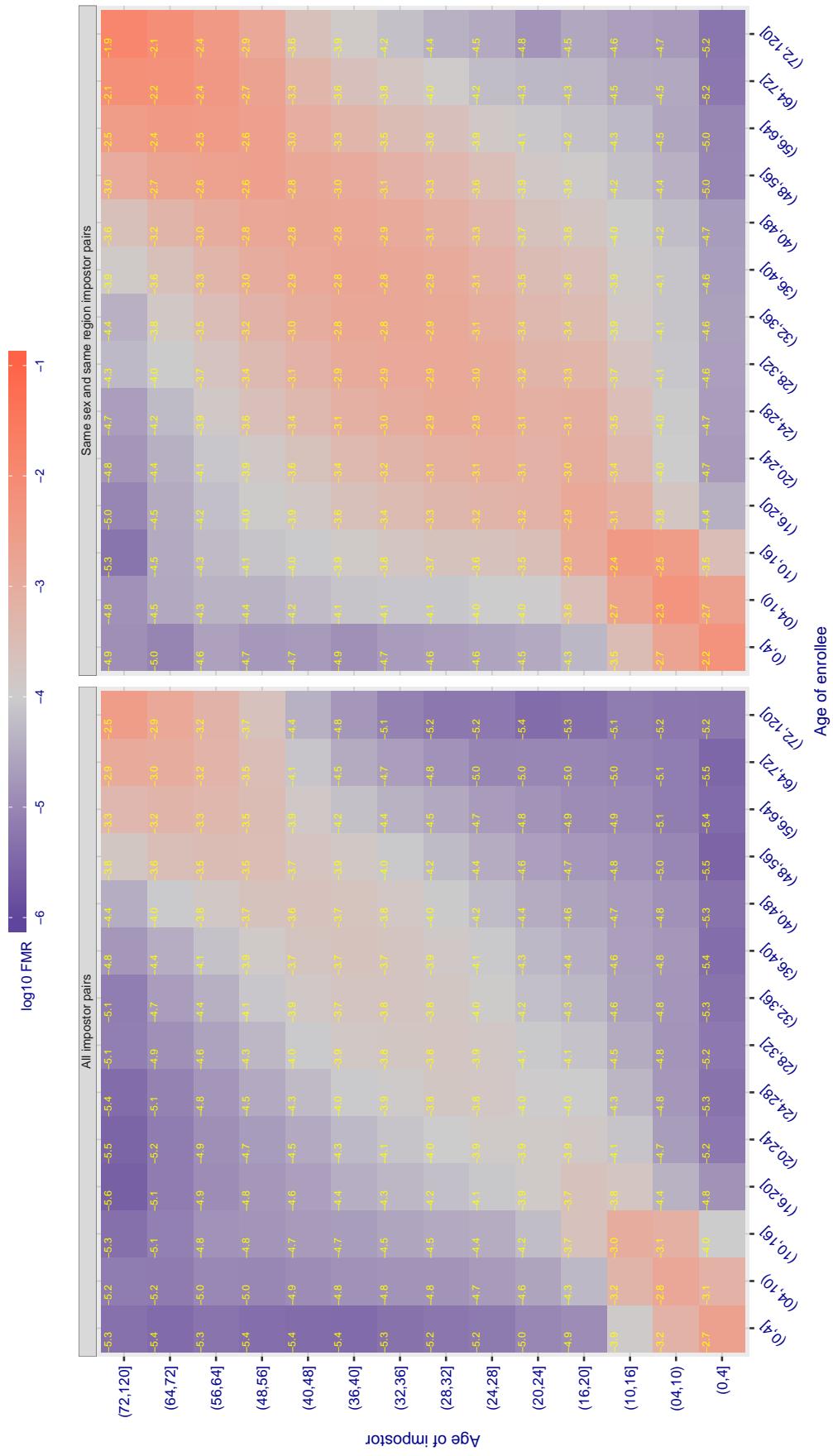
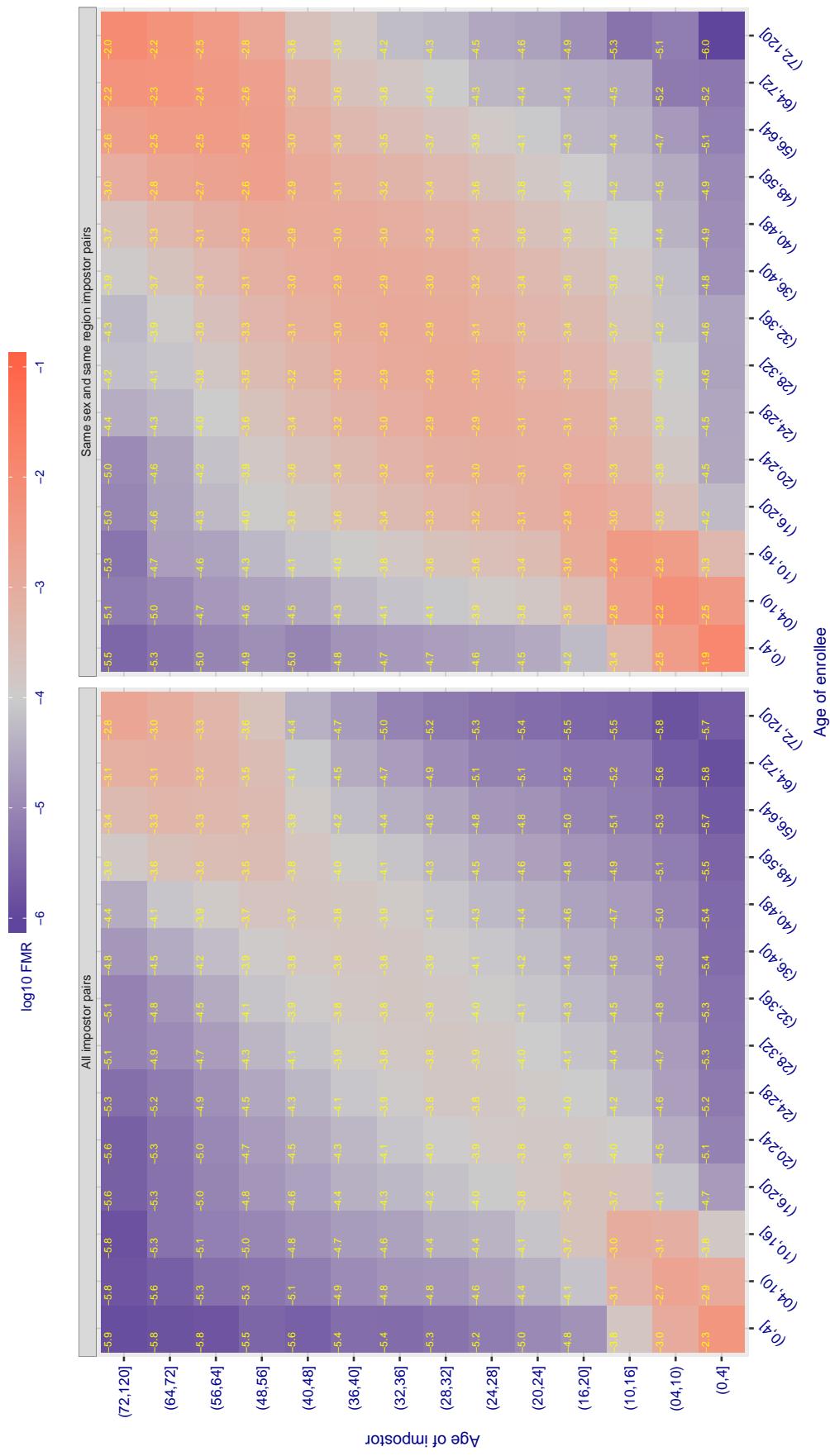
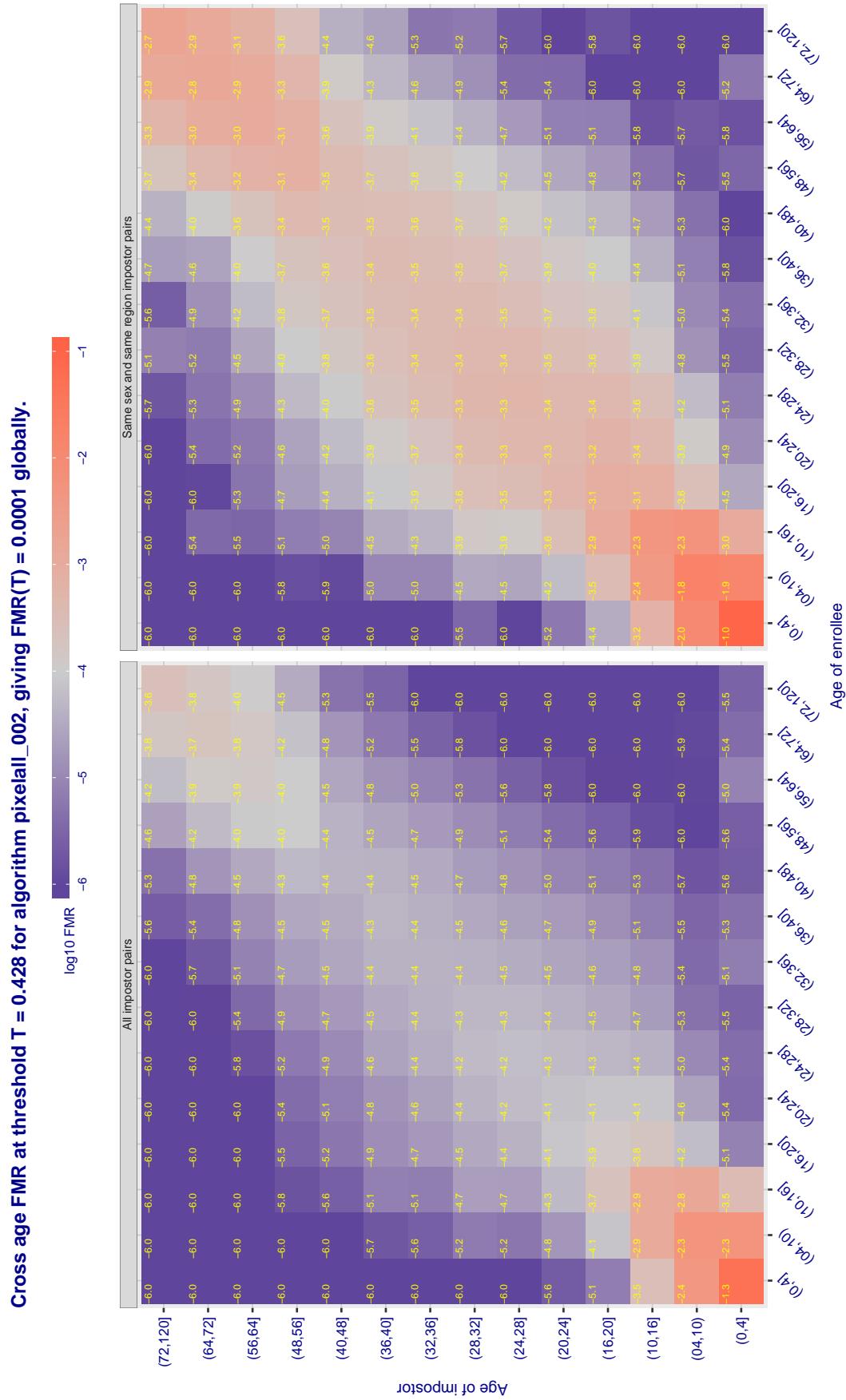


Figure 426: For algorithm ntechlab-006 operating on visa images, the heatmap shows false match observed over impostor comparisons of faces from different individuals who have the given age pair. False matches are counted against a recognition threshold fixed globally to give FMR = 0.001 over all on the order of  $10^{10}$  impostor comparisons. The text in each box gives the same quantity as that coded by the color. Light colors present a security vulnerability to, for example, a passport gate.

Cross age FMR at threshold T = 1.416 for algorithm ntechlab\_007, giving FMR(T) = 0.0001 globally.





**Figure 428:** For algorithm pixelall-002 operating on visa images, the heatmap shows false match observed over impostor comparisons of faces from different individuals who have the given age pair. False matches are counted against a recognition threshold fixed globally to give  $FMR = 0.001$  over all on the order of  $10^{10}$  impostor comparisons. The text in each box gives the same quantity as that coded by the color. Light colors present a security vulnerability to, for example, a passport gate.

Cross age FMR at threshold T = 0.337 for algorithm psl\_001, giving FMR(T) = 0.0001 globally.

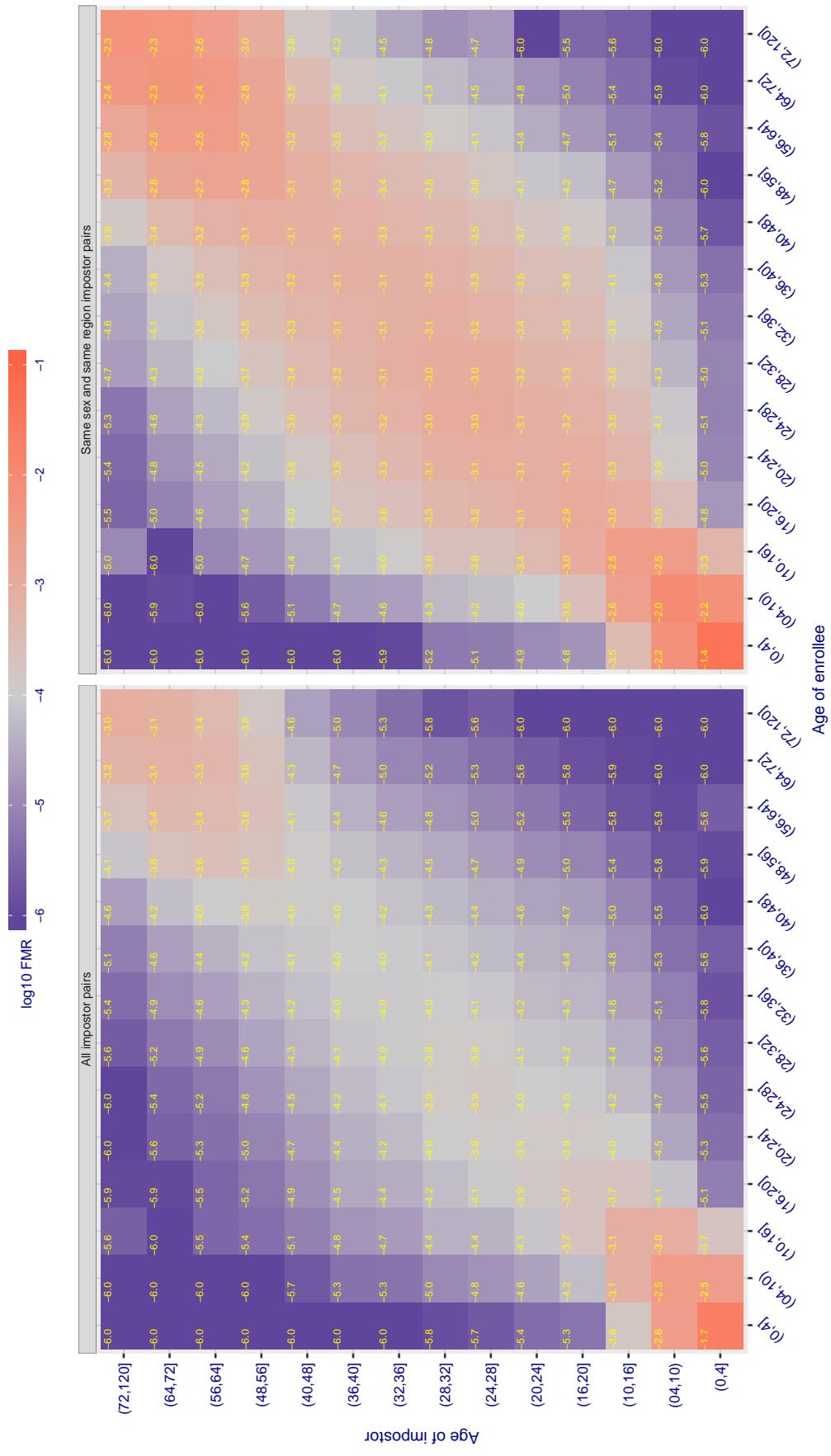
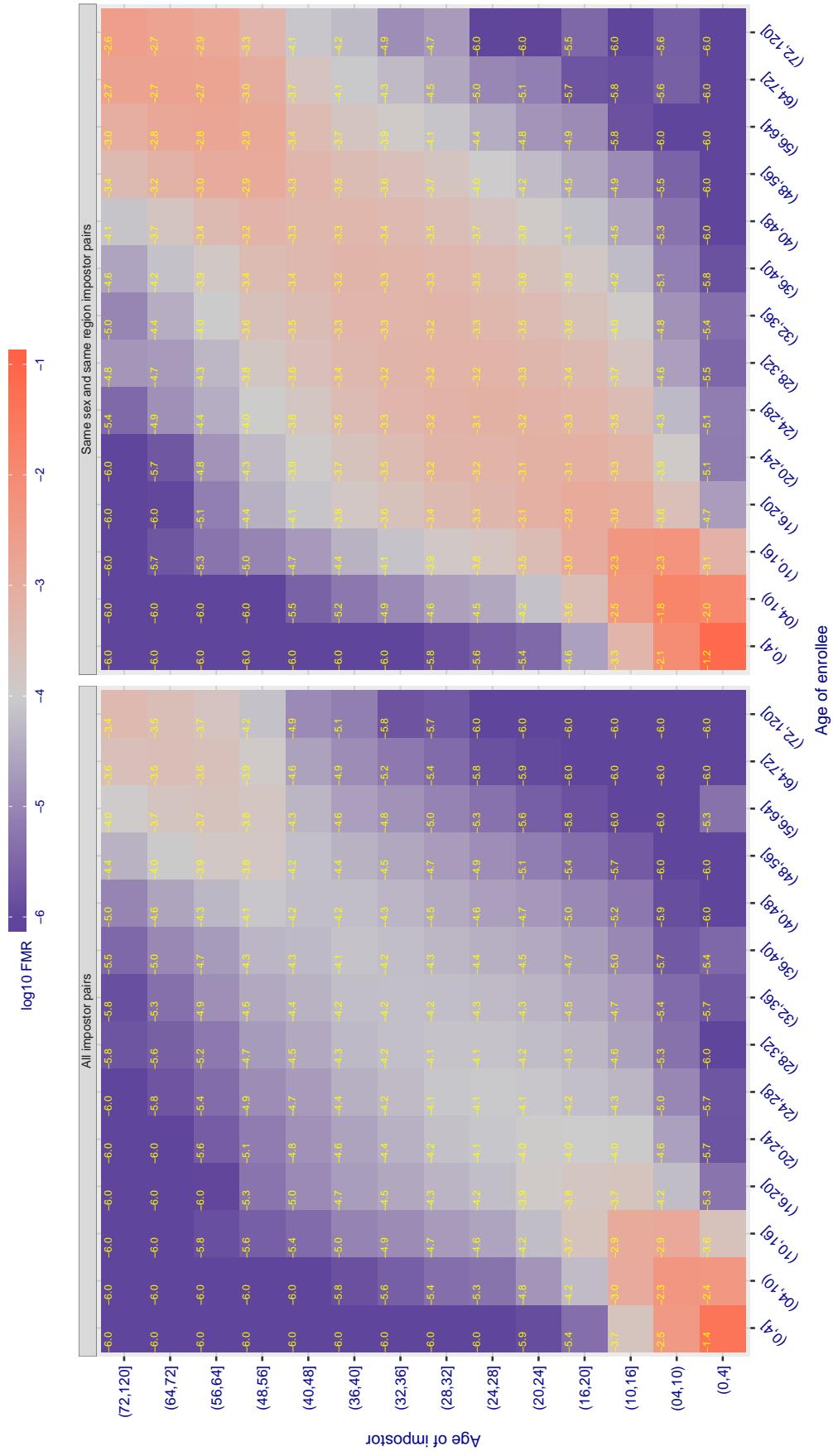
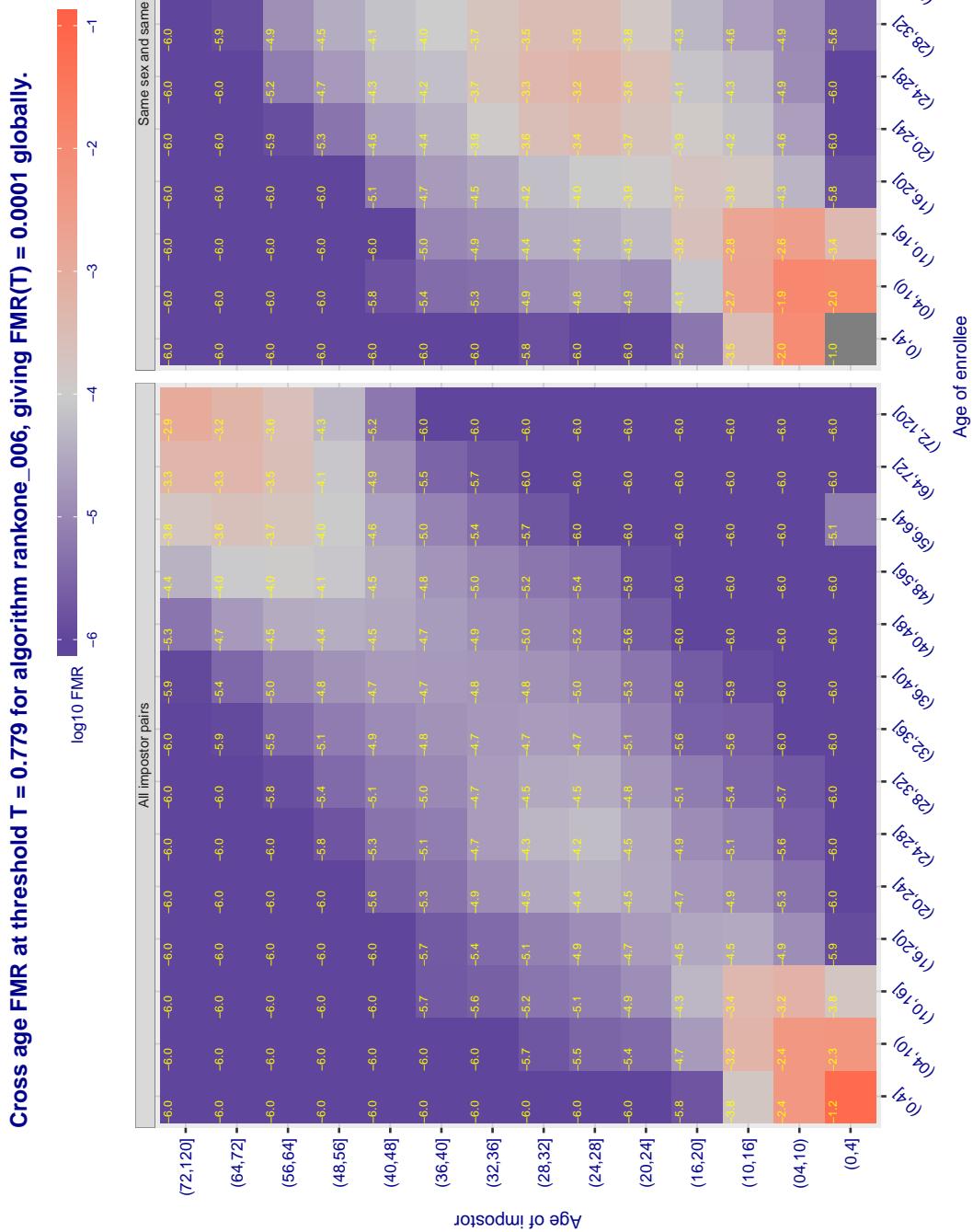


Figure 429: For algorithm psl\_001 operating on visa images, the heatmap shows false match observed over impostor comparisons of faces from different individuals who have the given age pair. False matches are counted against a recognition threshold fixed globally to give FMR = 0.001 over all on the order of  $10^{10}$  impostor comparisons. The text in each box gives the same quantity as that coded by the color. Light colors present a security vulnerability to, for example, a passport gate.

Cross age FMR at threshold T = 0.353 for algorithm psl\_002, giving FMR(T) = 0.0001 globally.





**Figure 431:** For algorithm rankone-006 operating on visa images, the heatmap shows false match observed over impostor comparisons of faces from different individuals who have the given age pair. False matches are counted against a recognition threshold fixed globally to give  $FMR = 0.001$  over all on the order of  $10^{10}$  impostor comparisons. The text in each box gives the same quantity as that coded by the color. Light colors present a security vulnerability to, for example, a passport gate.

Cross age FMR at threshold T = 0.661 for algorithm rankone\_007, giving FMR(T) = 0.0001 globally.

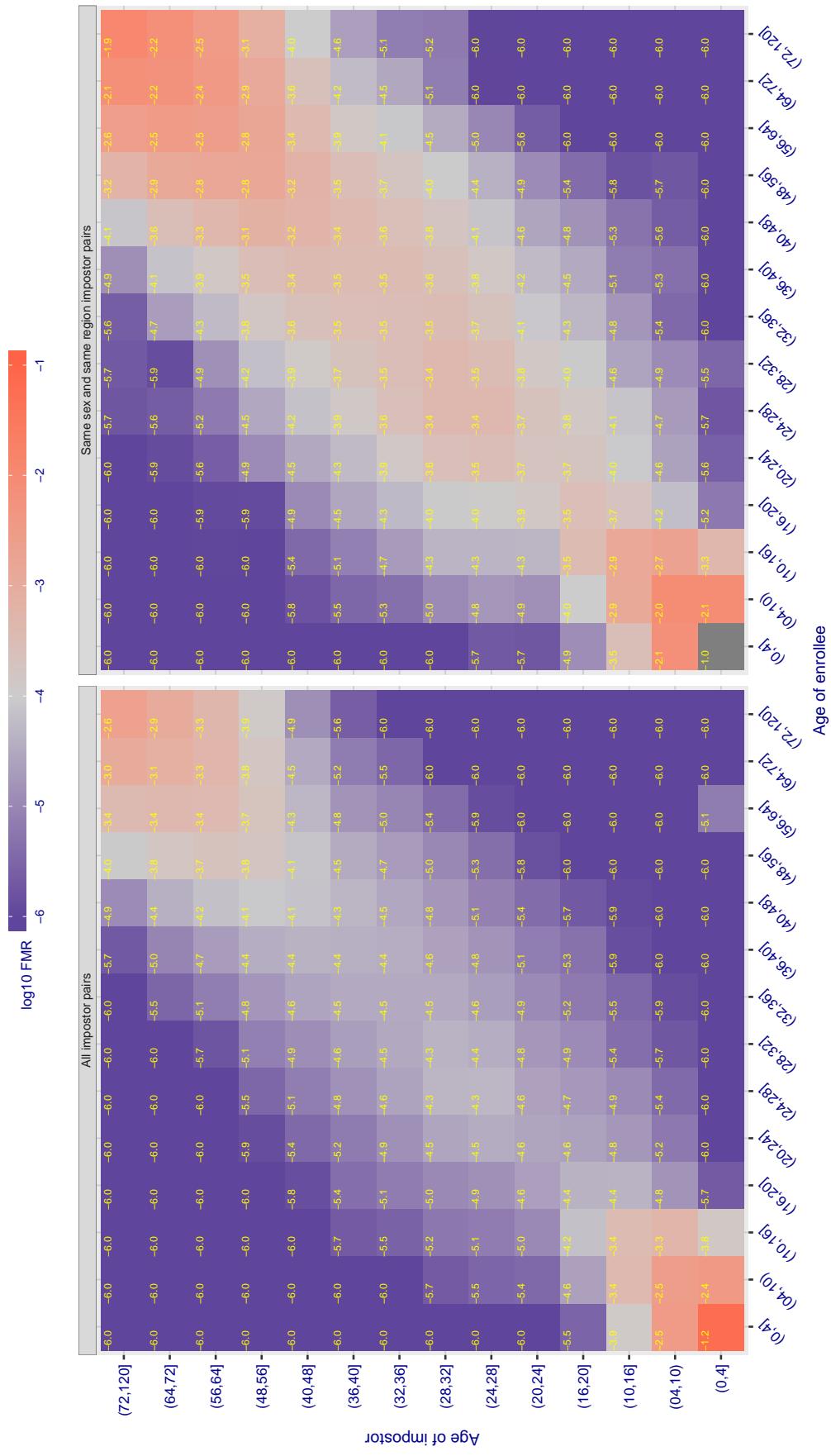


Figure 432: For algorithm rankone-007 operating on visa images, the heatmap shows false match observed over impostor comparisons of faces from different individuals who have the given age pair. False matches are counted against a recognition threshold fixed globally to give FMR = 0.001 over all on the order of  $10^{10}$  impostor comparisons. The text in each box gives the same quantity as that coded by the color. Light colors present a security vulnerability to, for example, a passport gate.

Cross age FMR at threshold T = 0.883 for algorithm realnetworks\_002, giving  $FMR(T) = 0.0001$  globally.

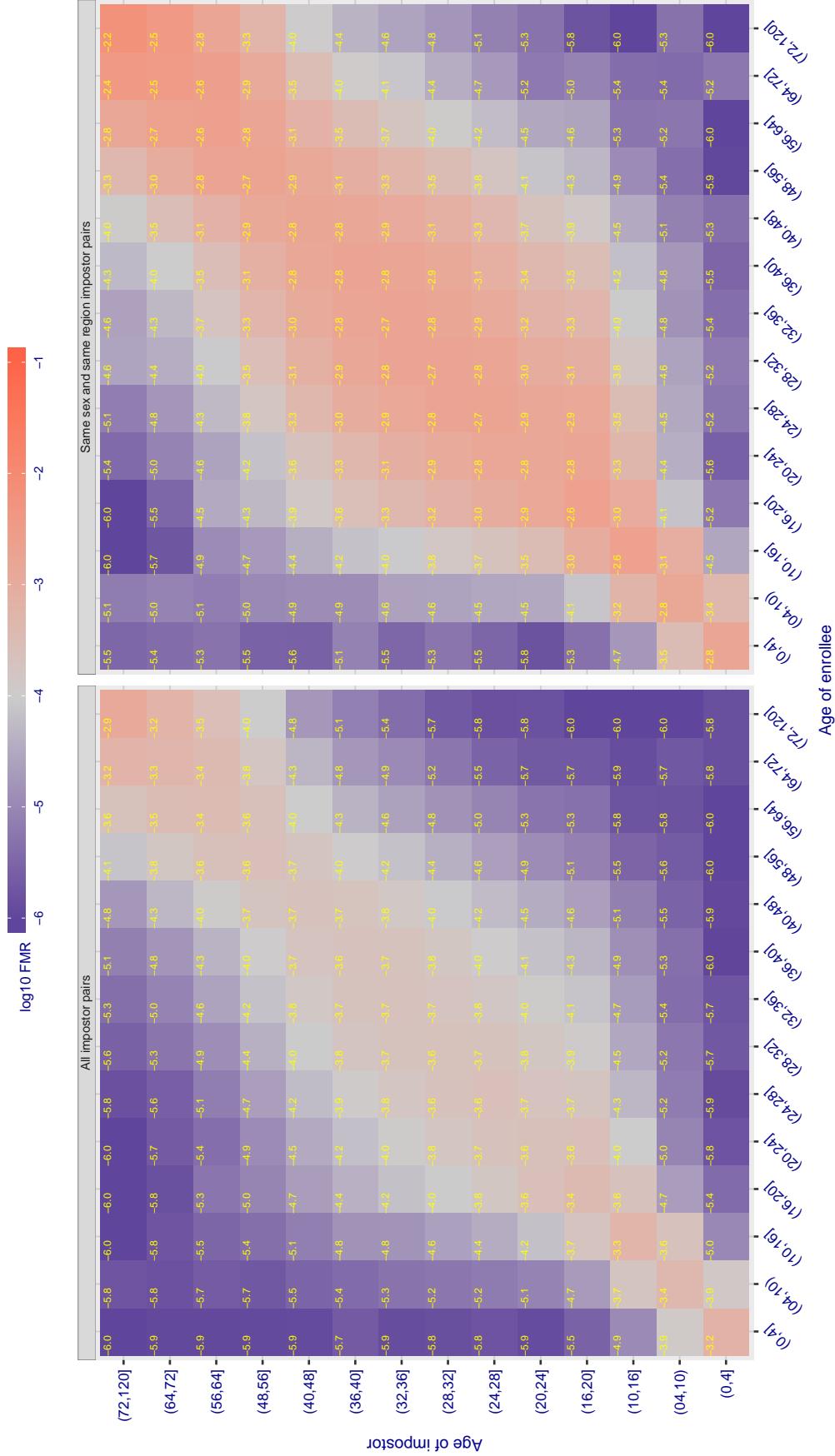


Figure 433: For algorithm realnetworks-002 operating on visa images, the heatmap shows false match observed over impostor comparisons of faces from different individuals who have the given age pair. False matches are counted against a recognition threshold fixed globally to give  $FMR = 0.001$  over all on the order of  $10^{10}$  impostor comparisons. The text in each box gives the same quantity as that coded by the color. Light colors present a security vulnerability to, for example, a passport gate.

Cross age FMR at threshold T = 0.886 for algorithm realnetworks\_003, giving  $FMR(T) = 0.0001$  globally.

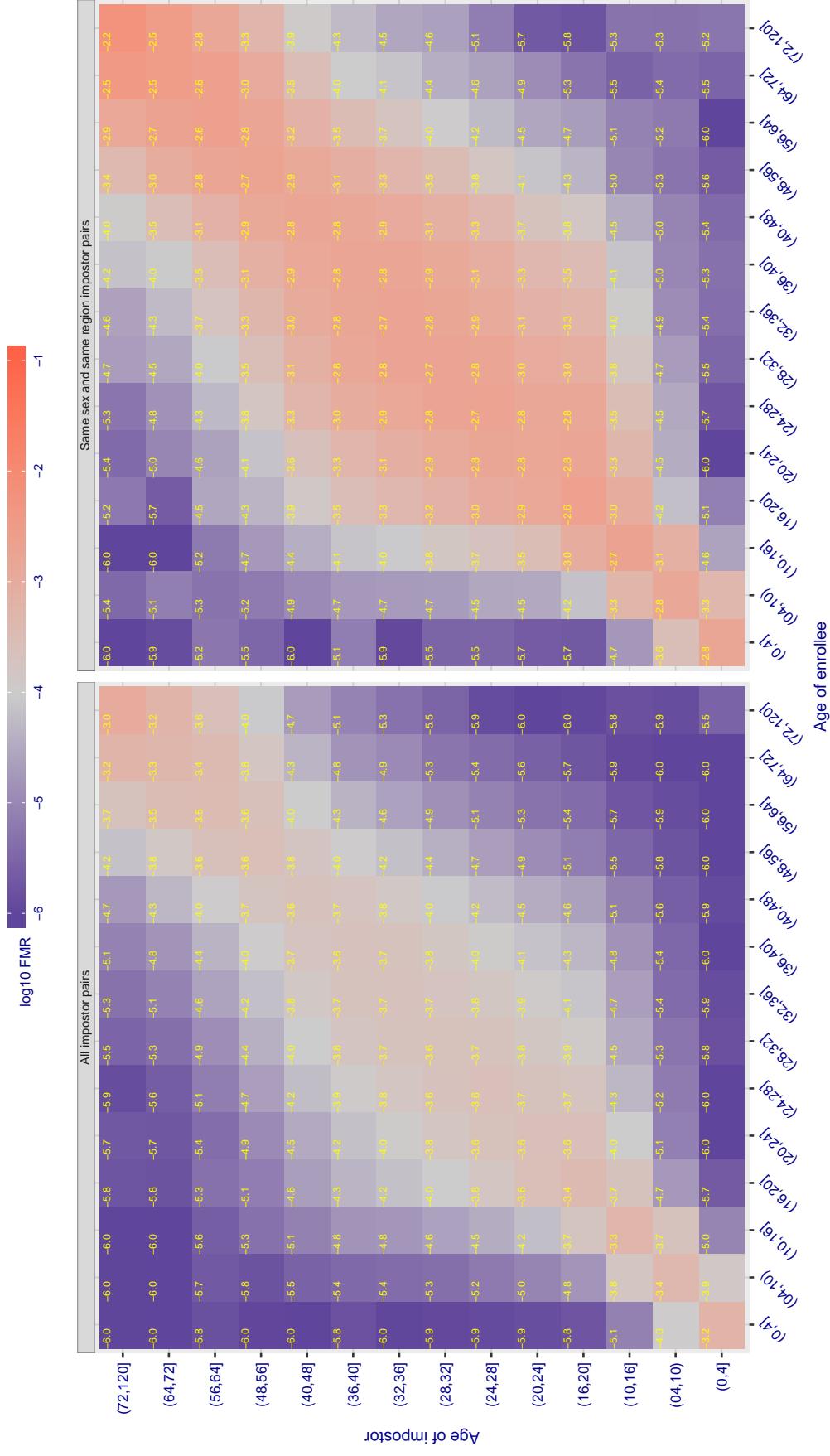


Figure 434: For algorithm realnetworks-003 operating on visa images, the heatmap shows false match observed over impostor comparisons of faces from different individuals who have the given age pair. False matches are counted against a recognition threshold fixed globally to give  $FMR = 0.001$  over all on the order of  $10^{10}$  impostor comparisons. The text in each box gives the same quantity as that coded by the color. Light colors present a security vulnerability to, for example, a passport gate.

Cross age FMR at threshold T = 70.373 for algorithm remarkai\_000, giving FMR(T) = 0.0001 globally.

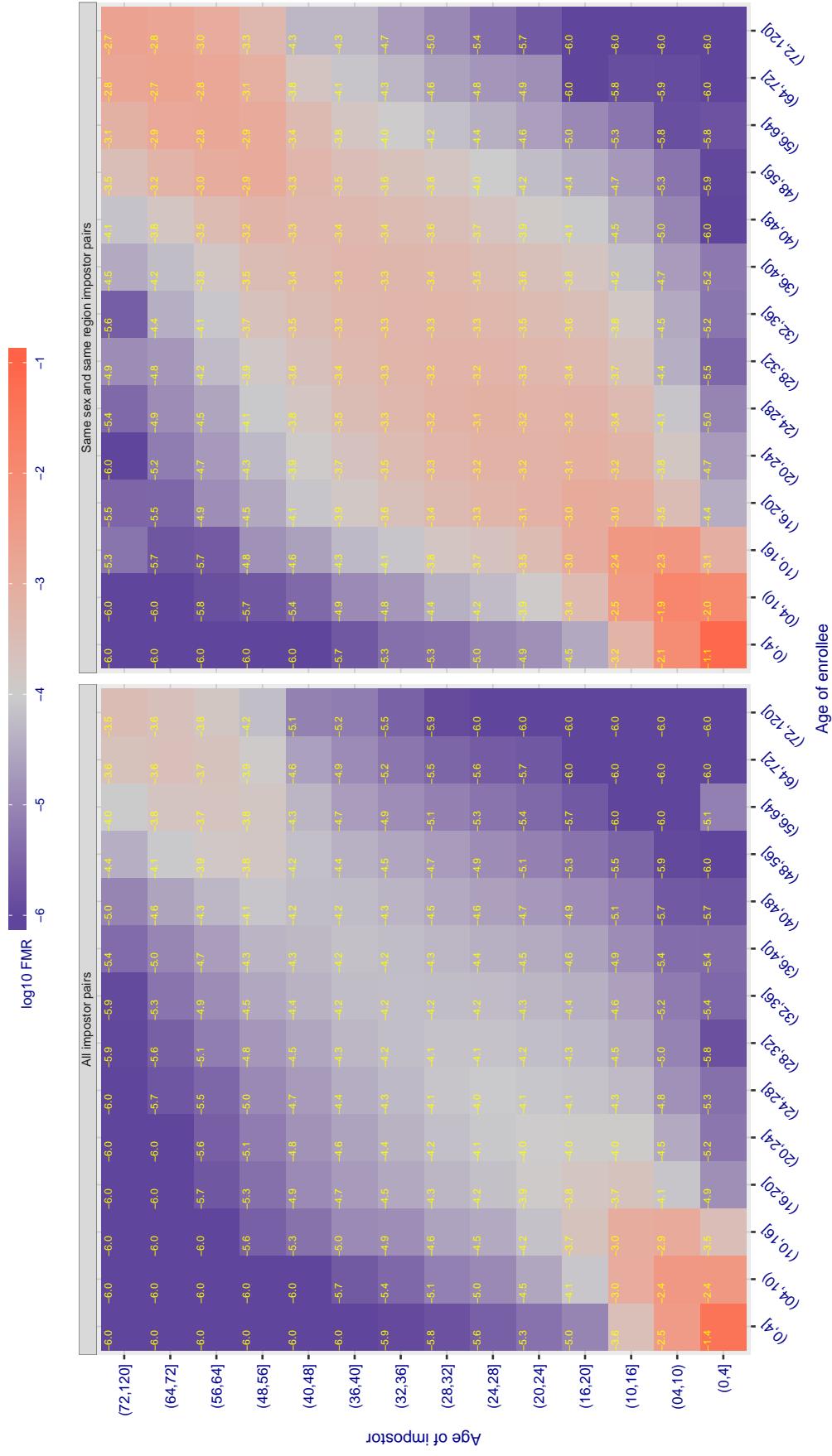
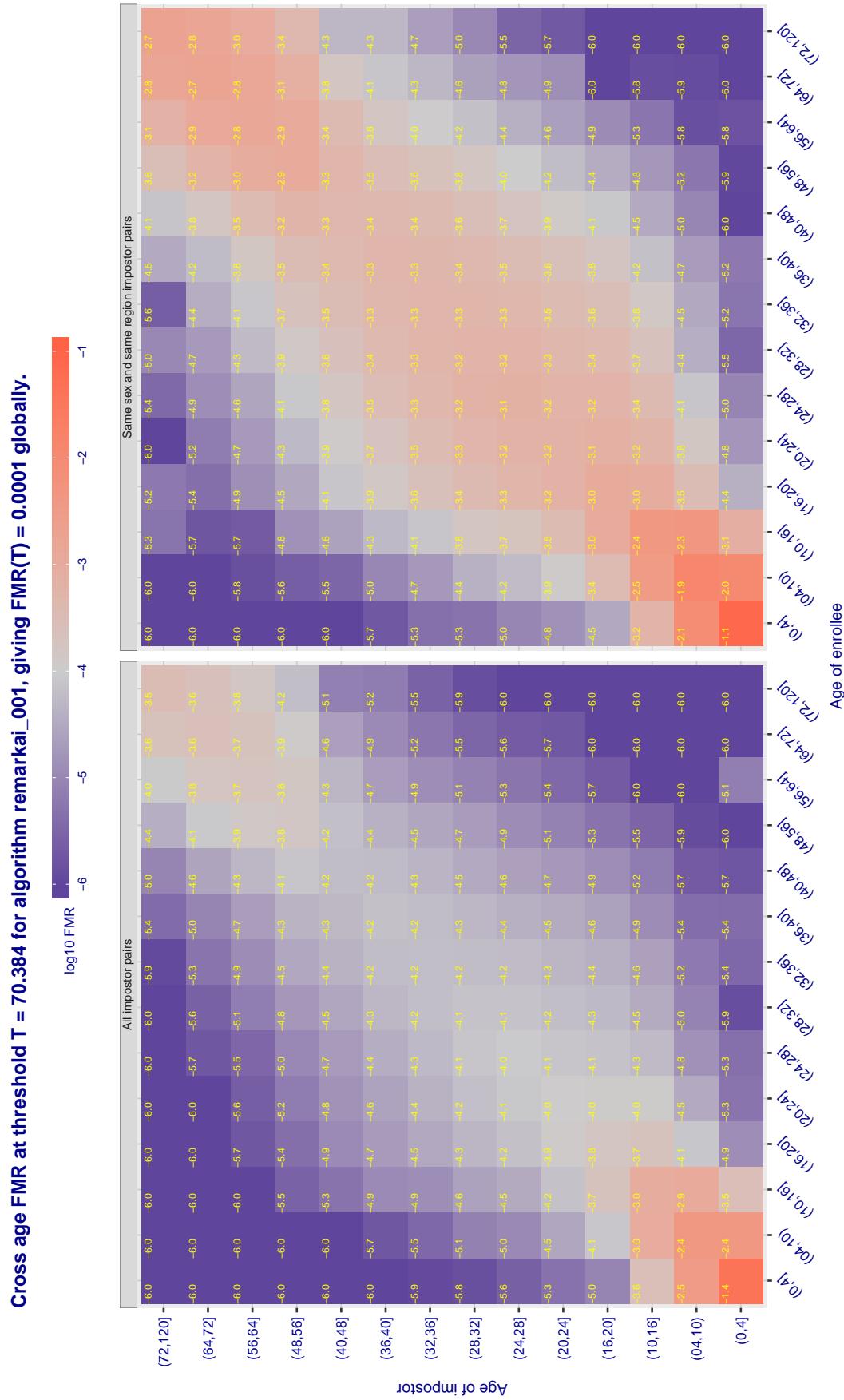
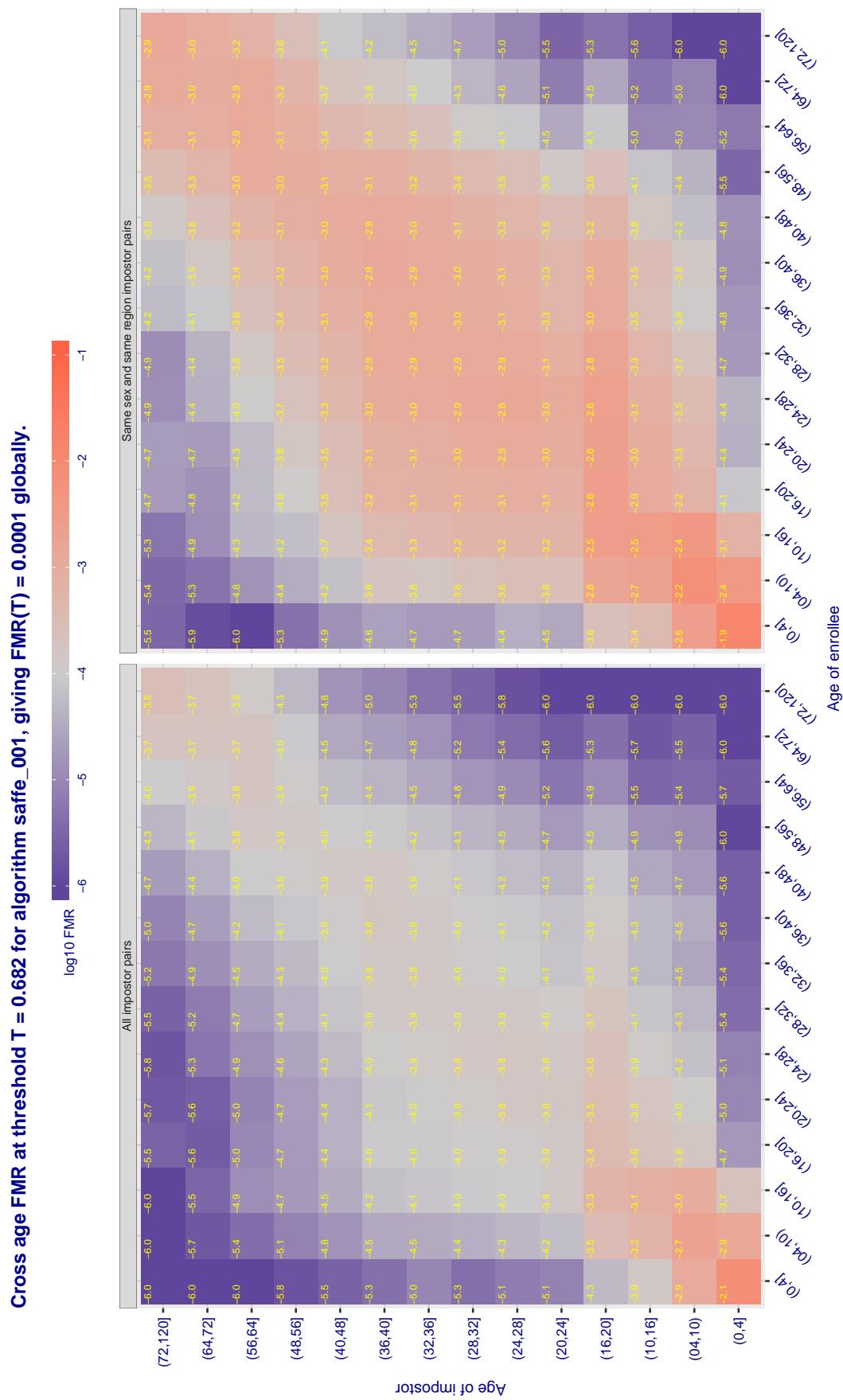


Figure 435: For algorithm remarkai-000 operating on visa images, the heatmap shows false match observed over impostor comparisons of faces from different individuals who have the given age pair. False matches are counted against a recognition threshold fixed globally to give  $FMR = 0.001$  over all on the order of  $10^{10}$  impostor comparisons. The text in each box gives the same quantity as that coded by the color. Light colors present a security vulnerability to, for example, a passport gate.



**Figure 436:** For algorithm *remarkai-001* operating on visa images, the heatmap shows false match observed over impostor comparisons of faces from different individuals who have the given age pair. False matches are counted against a recognition threshold fixed globally to give  $FMR = 0.001$  over all on the order of  $10^{10}$  impostor comparisons. The text in each box gives the same quantity as that coded by the color. Light colors present a security vulnerability to, for example, a passport gate.



**Figure 437:** For algorithm safe-001 operating on visa images, the heatmap shows false match observed over impostor comparisons of faces from different individuals who have the given age pair. False matches are counted against a recognition threshold fixed globally to give  $FMR = 0.001$  over all on the order of  $10^{10}$  impostor comparisons. The text in each box gives the same quantity as that coded by the color. Light colors present a security vulnerability to, for example, a passport gate.

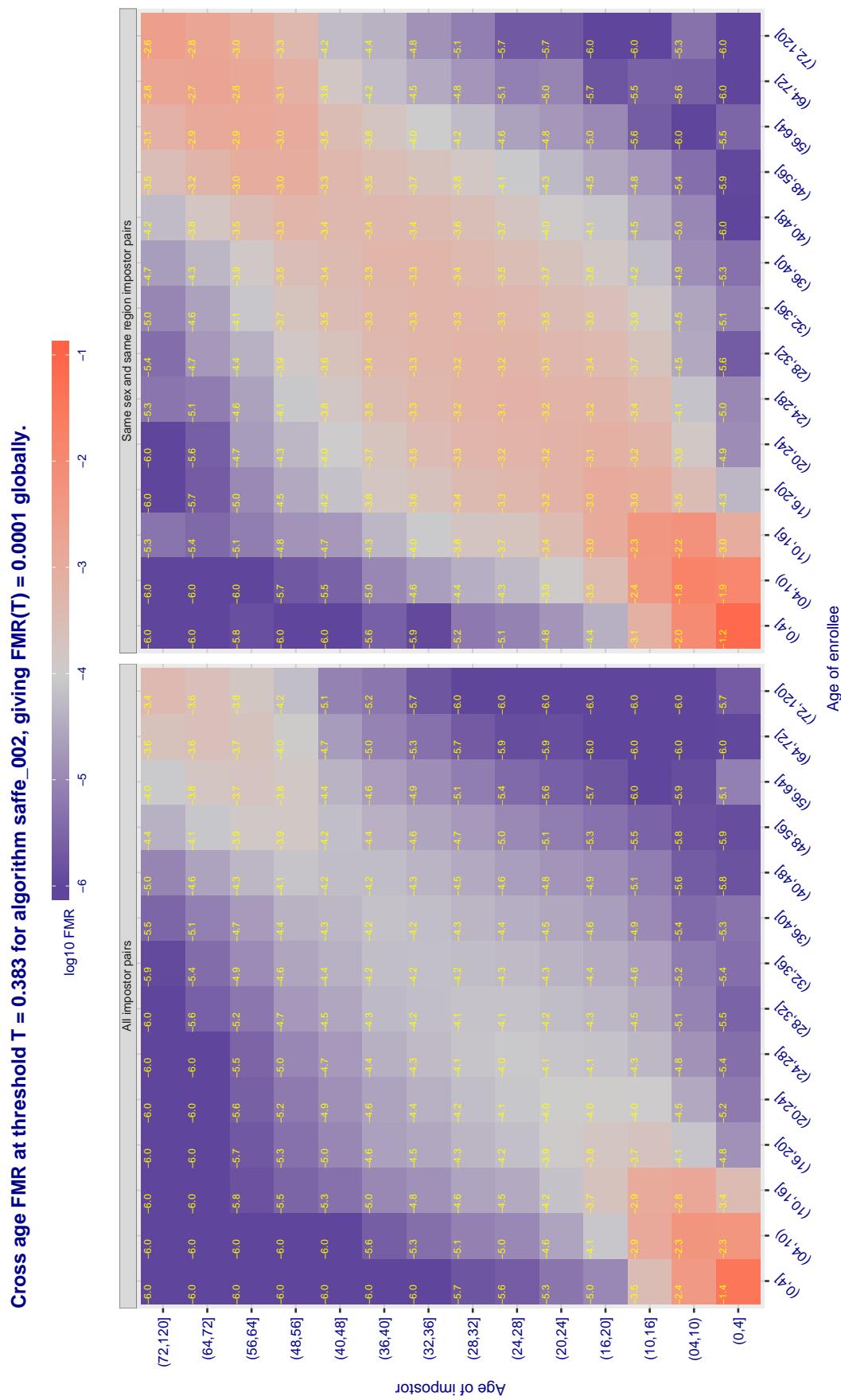


**Figure 438:** For algorithm saffe-002 operating on visa images, the heatmap shows false match observed over impostor comparisons of faces from different individuals who have the given age pair. False matches are counted against a recognition threshold fixed globally to give  $FMR = 0.001$  over all on the order of  $10^{10}$  impostor comparisons. The text in each box gives the same quantity as that coded by the color. Light colors present a security vulnerability to, for example, a passport gate.

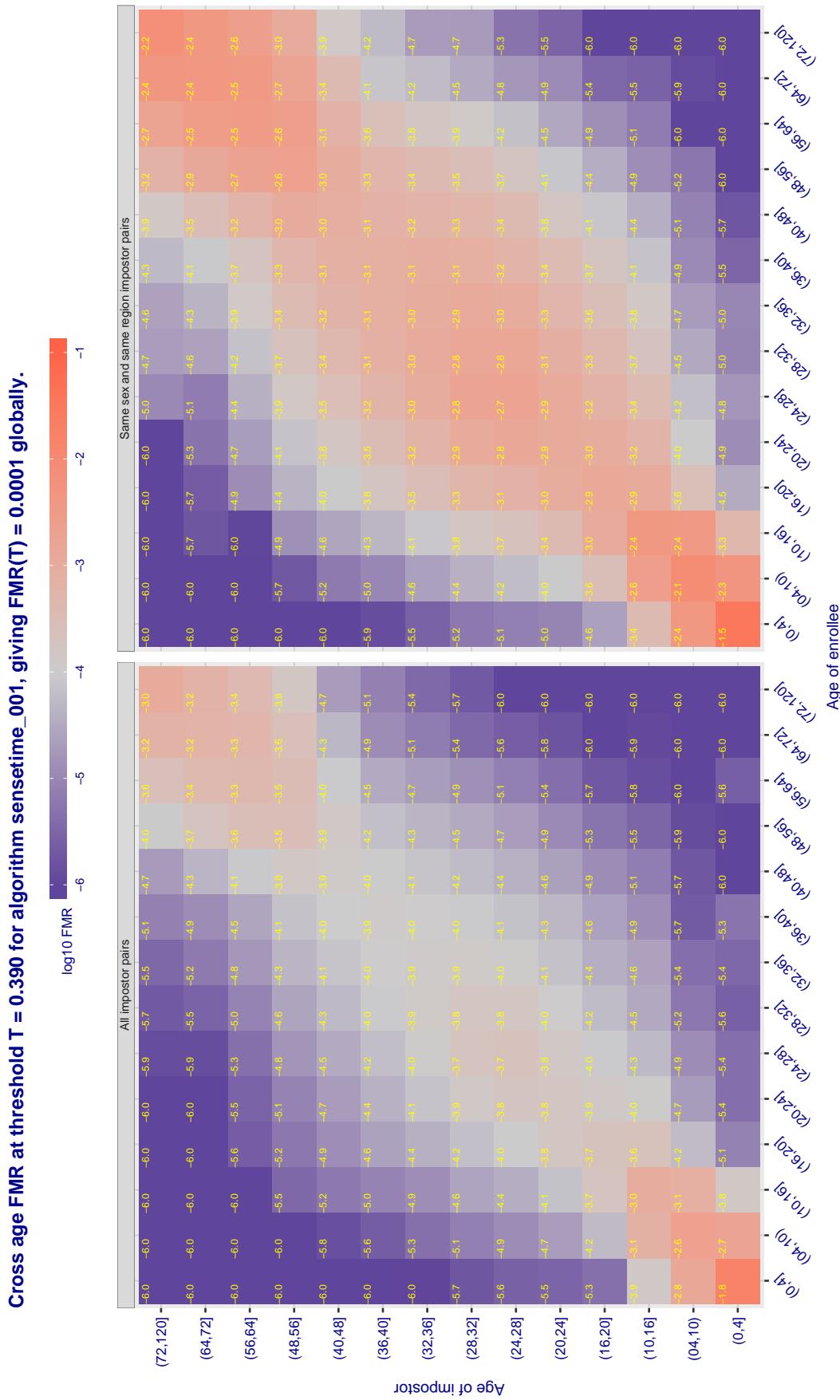


**Figure 439:** For algorithm sensetime-001 operating on visa images, the heatmap shows false match observed over impostor comparisons of faces from different individuals who have the given age pair. False matches are counted against a recognition threshold fixed globally to give  $FMR = 0.001$  over all on the order of  $10^{10}$  impostor comparisons. The text in each box gives the same quantity as that coded by the color. Light colors present a security vulnerability to, for example, a passport gate.

Cross age FMR at threshold T = 0.390 for algorithm sensetime\_002, giving FMR(T) = 0.0001 globally.

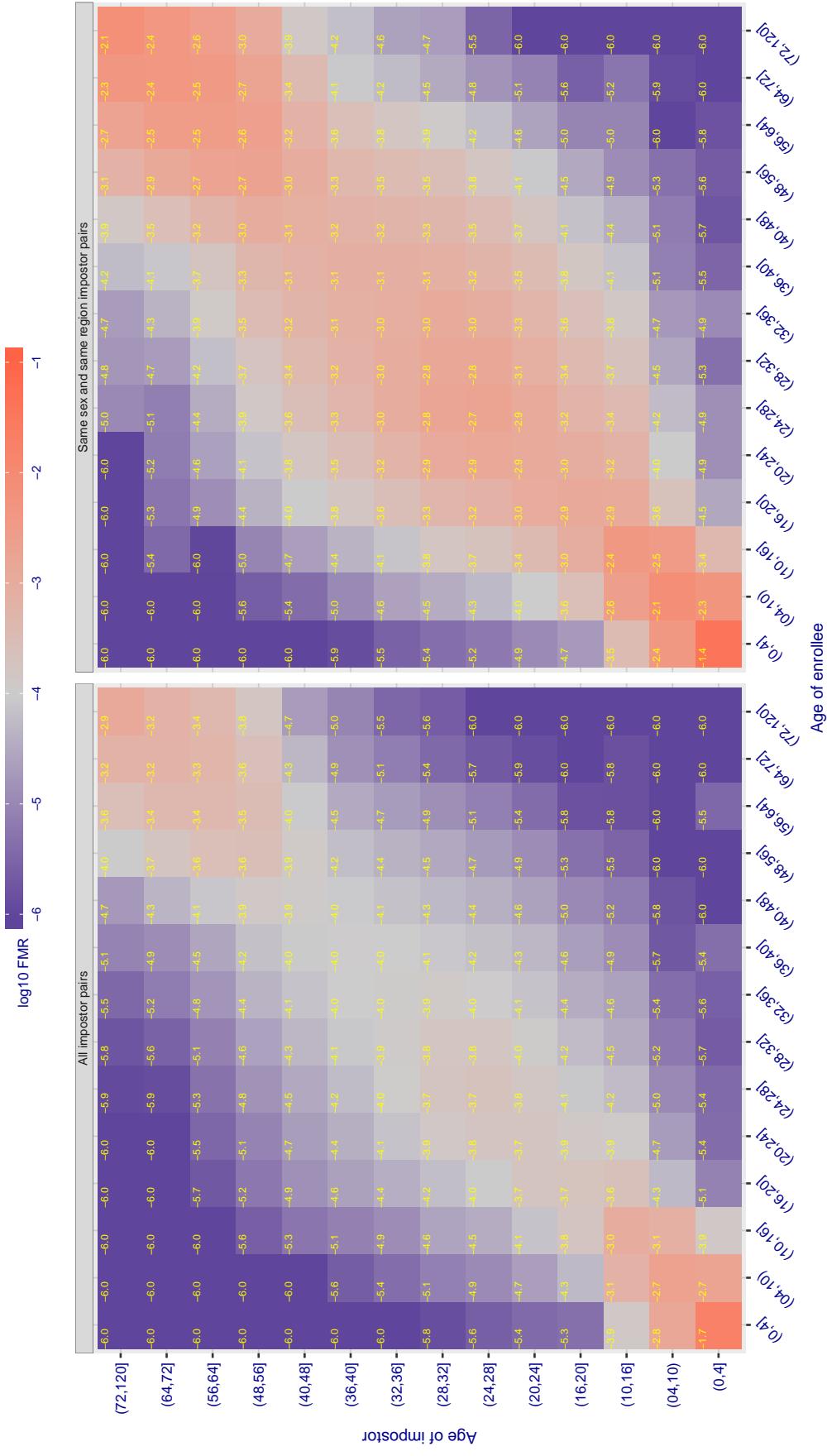


Figure 440: For algorithm sensetime-002 operating on visa images, the heatmap shows false match observed over impostor comparisons of faces from different individuals who have the given age pair. False matches are counted against a recognition threshold fixed globally to give  $FMR = 0.001$  over all on the order of  $10^{10}$  impostor comparisons. The text in each box gives the same quantity as that coded by the color. Light colors present a security vulnerability to, for example, a passport gate.

Cross age FMR at threshold T = 0.970 for algorithm shaman\_000, giving FMR(T) = 0.0001 globally.

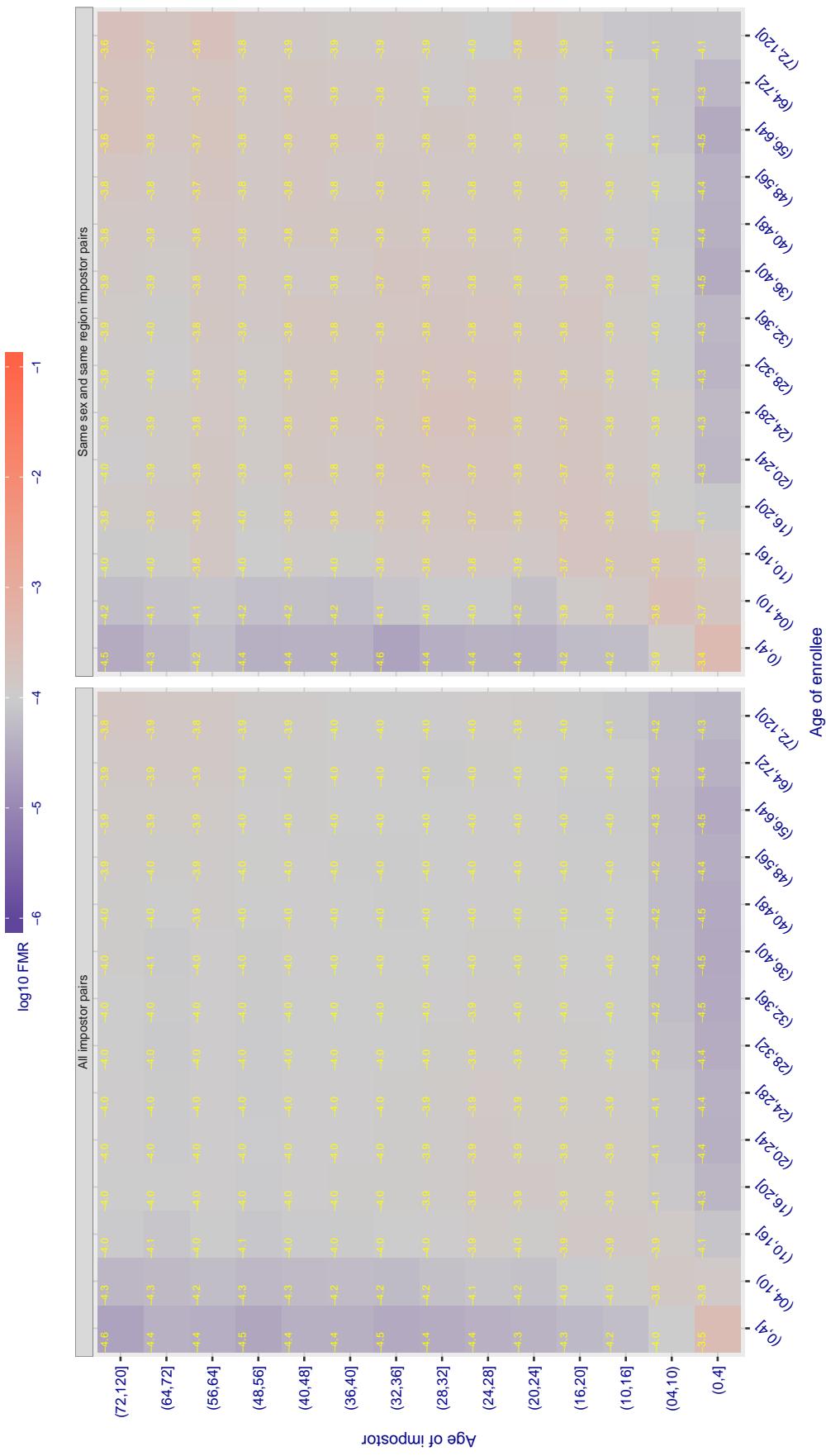
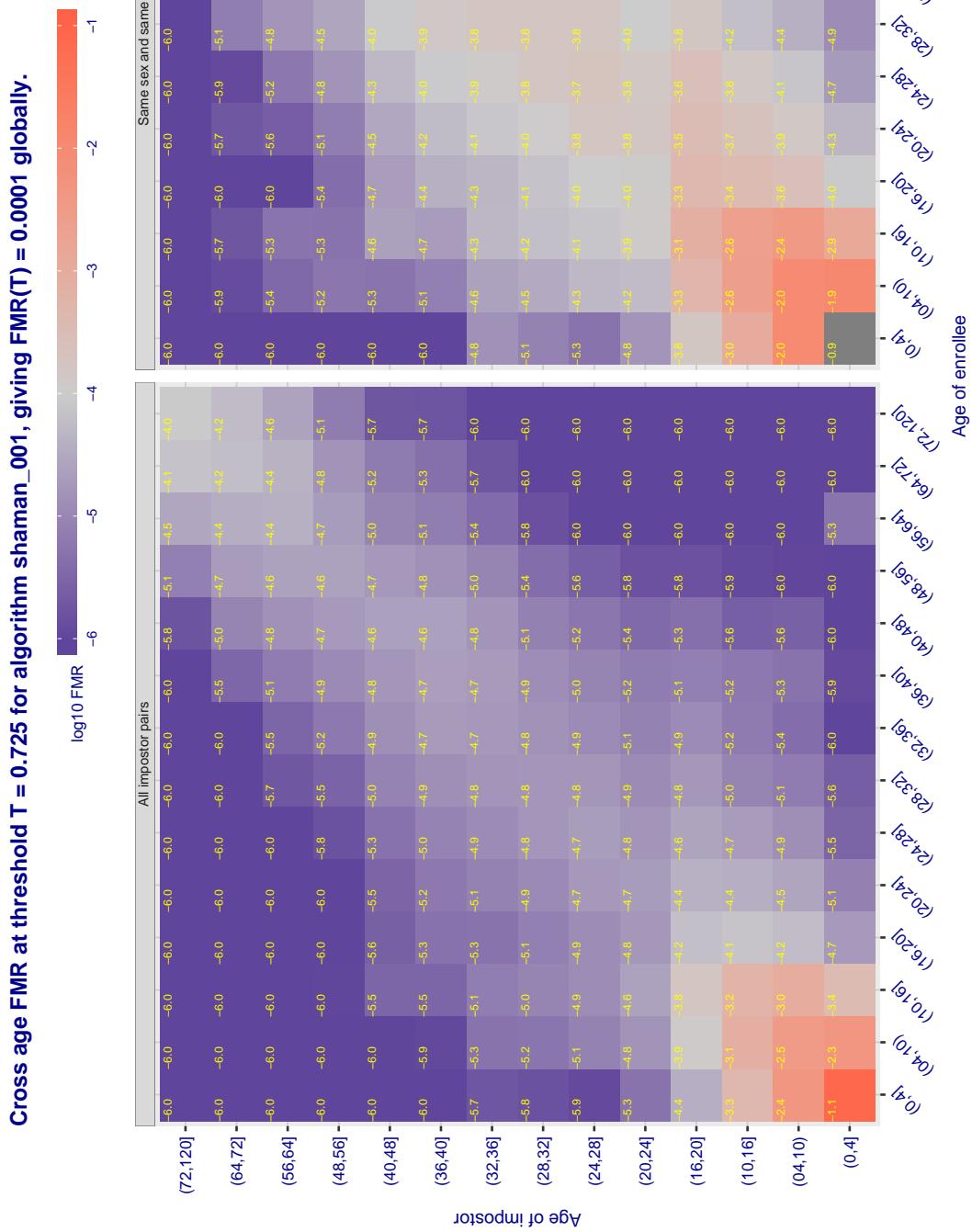
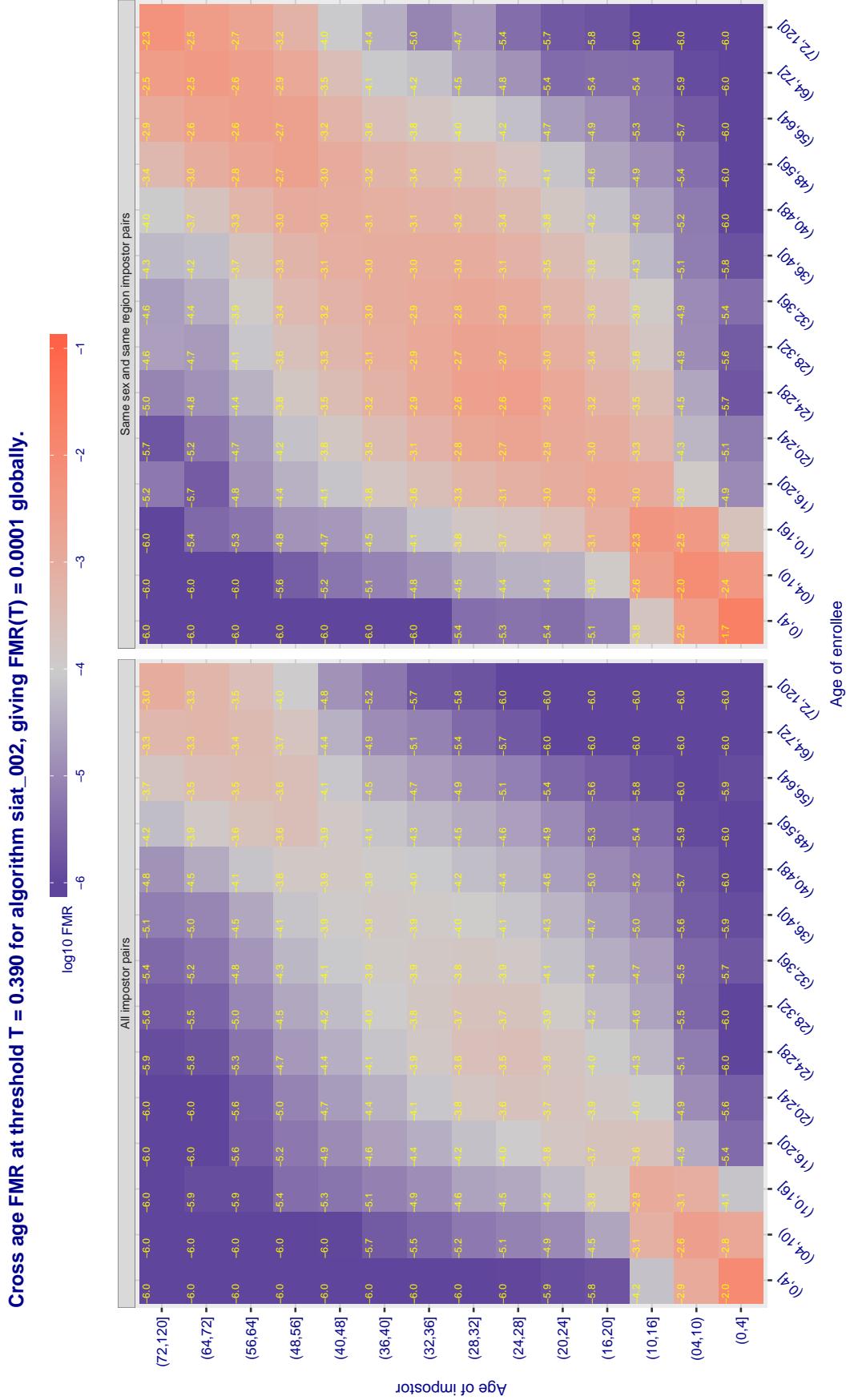


Figure 441: For algorithm shaman-000 operating on visa images, the heatmap shows false match observed over impostor comparisons of faces from different individuals who have the given age pair. False matches are counted against a recognition threshold fixed globally to give  $FMR = 0.001$  over all on the order of  $10^{10}$  impostor comparisons. The text in each box gives the same quantity as that coded by the color. Light colors present a security vulnerability to, for example, a passport gate.



**Figure 442:** For algorithm shaman-001 operating on visa images, the heatmap shows false match observed over impostor comparisons of faces from different individuals who have the given age pair. False matches are counted against a recognition threshold fixed globally to give  $FMR = 0.001$  over all on the order of  $10^{10}$  impostor comparisons. The text in each box gives the same quantity as that coded by the color. Light colors present a security vulnerability to, for example, a passport gate.



**Figure 443:** For algorithm siat-002 operating on visa images, the heatmap shows false match observed over impostor comparisons of faces from different individuals who have the given age pair. False matches are counted against a recognition threshold fixed globally to give  $FMR = 0.001$  over all on the order of  $10^{10}$  impostor comparisons. The text in each box gives the same quantity as that coded by the color. Light colors present a security vulnerability to, for example, a passport gate.

Cross age FMR at threshold T = 0.393 for algorithm siat\_004, giving  $FMR(T) = 0.0001$  globally.

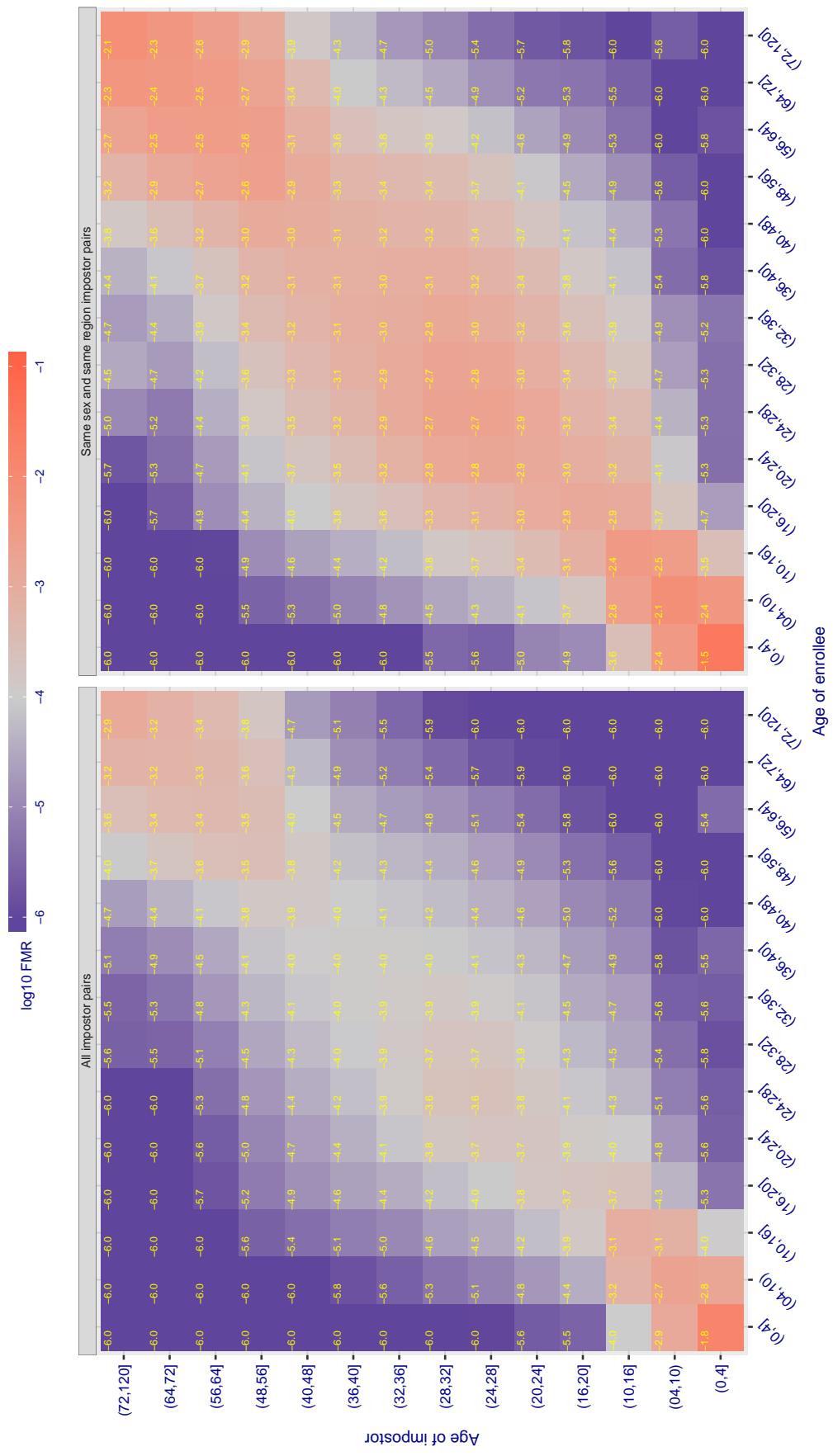


Figure 444: For algorithm siat\_004 operating on visa images, the heatmap shows false match observed over impostor comparisons of faces from different individuals who have the given age pair. False matches are counted against a recognition threshold fixed globally to give  $FMR = 0.001$  over all on the order of  $10^{10}$  impostor comparisons. The text in each box gives the same quantity as that coded by the color. Light colors present a security vulnerability to, for example, a passport gate.

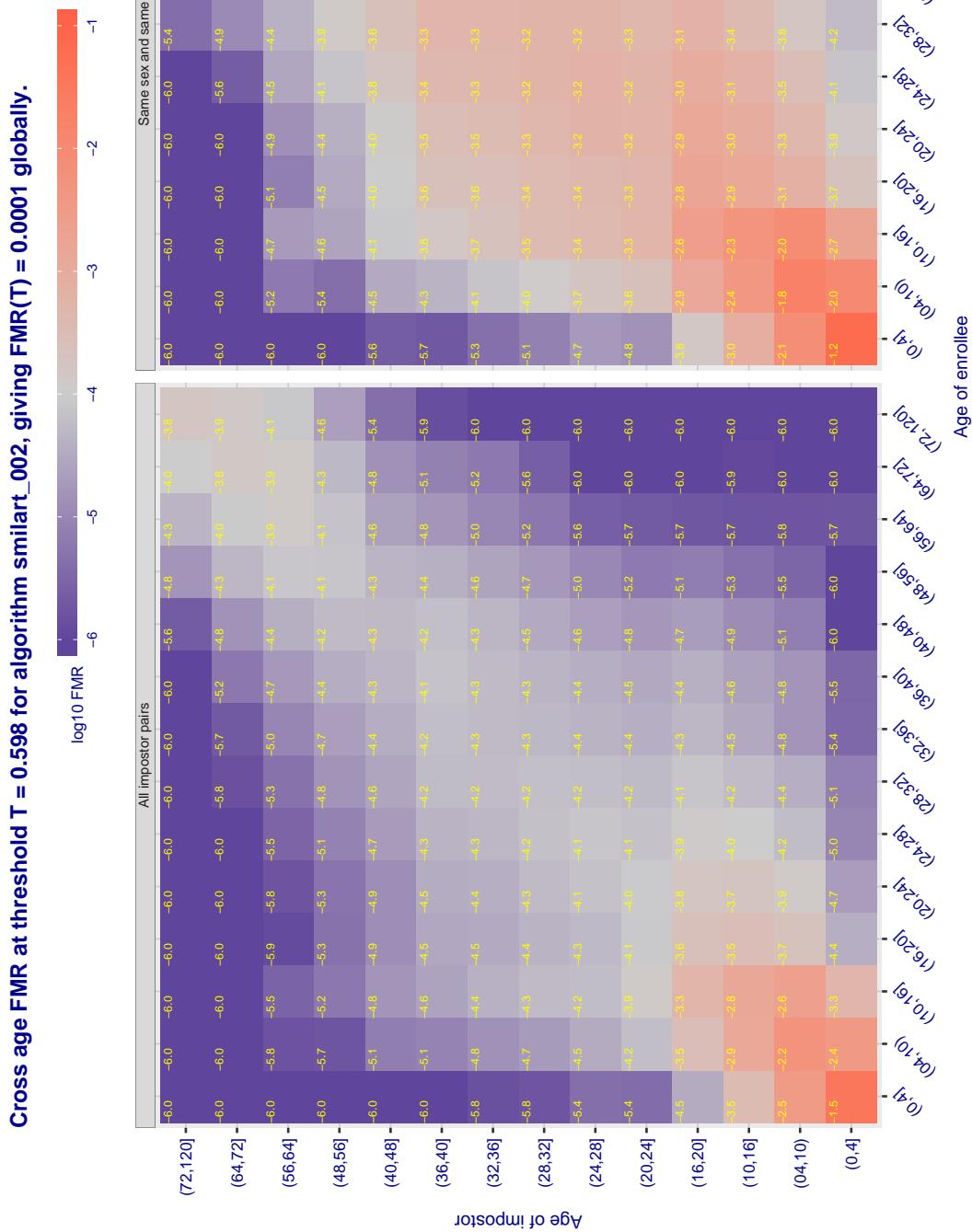


Figure 445: For algorithm *smilart-002* operating on visa images, the heatmap shows false match observed over impostor comparisons of faces from different individuals who have the given age pair. False matches are counted against a recognition threshold fixed globally to give  $FMR = 0.001$  over all on the order of  $10^{10}$  impostor comparisons. The text in each box gives the same quantity as that coded by the color. Light colors present a security vulnerability to, for example, a passport gate.

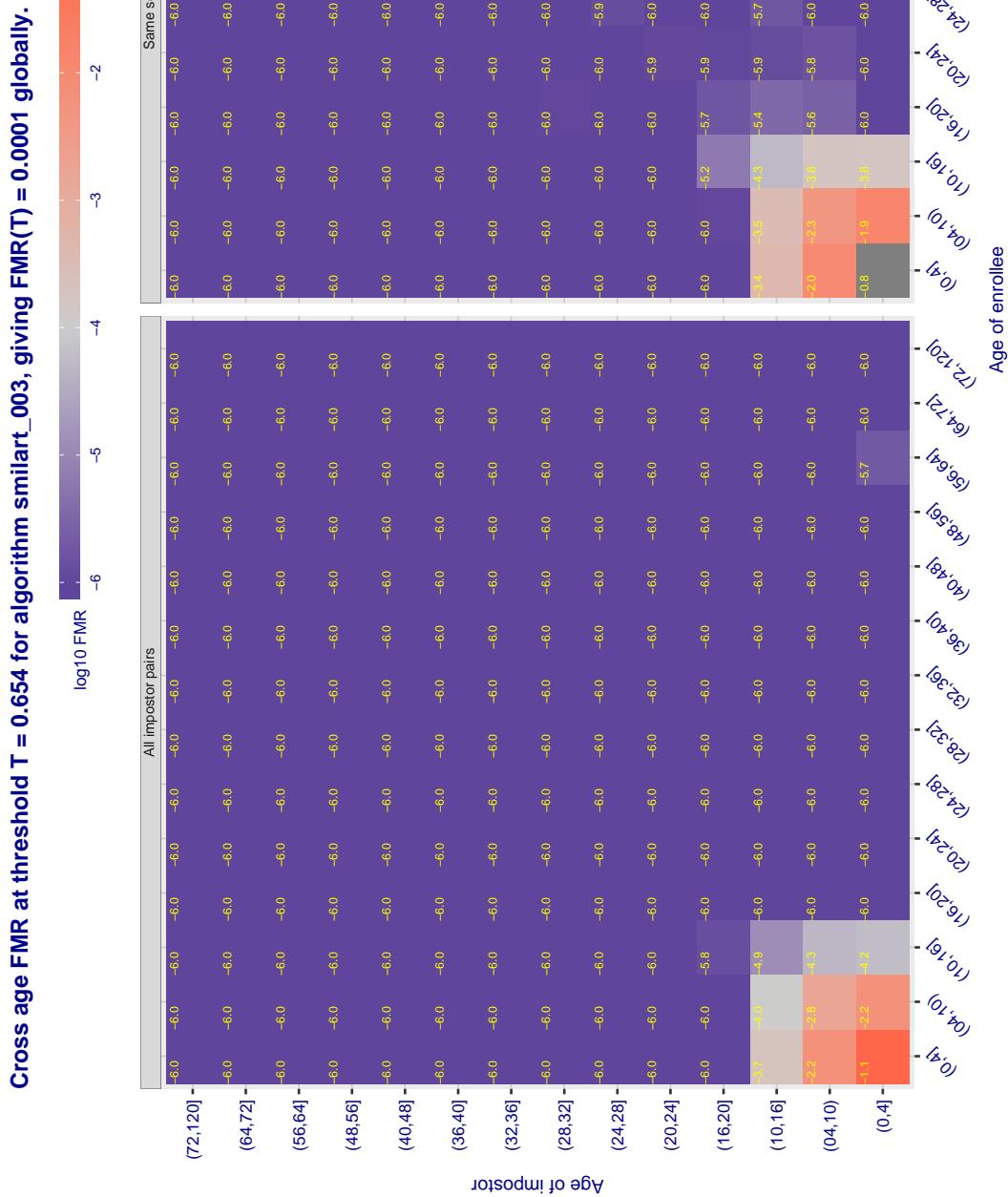


Figure 446: For algorithm *smilart-003* operating on visa images, the heatmap shows false match observed over impostor comparisons of faces from different individuals who have the given age pair. False matches are counted against a recognition threshold fixed globally to give  $FMR = 0.001$  over all on the order of  $10^{10}$  impostor comparisons. The text in each box gives the same quantity as that coded by the color. Light colors present a security vulnerability to, for example, a passport gate.

Cross age FMR at threshold T = 0.314 for algorithm starhybrid\_001, giving FMR(T) = 0.0001 globally.

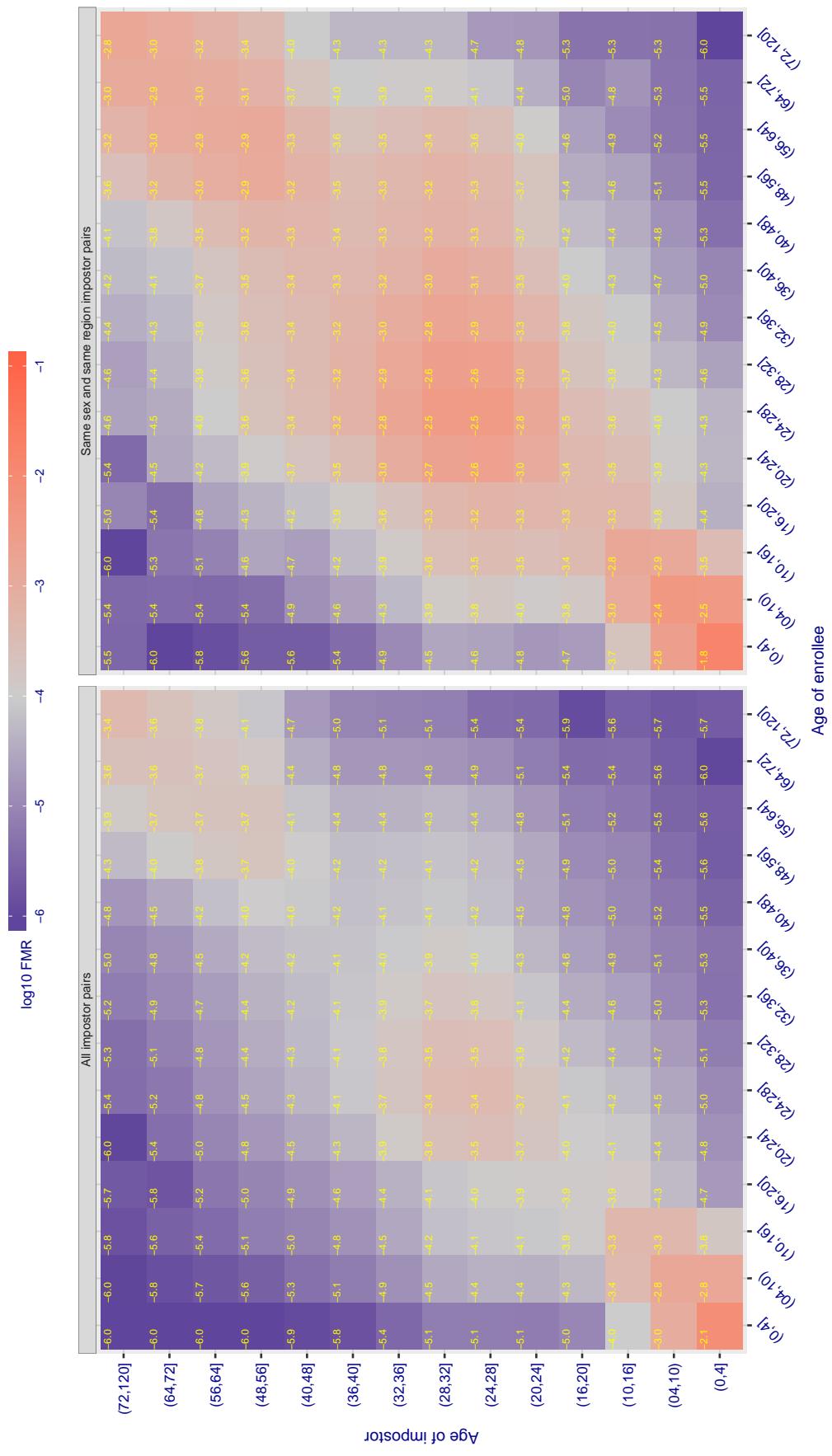


Figure 447: For algorithm starhybrid-001 operating on visa images, the heatmap shows false match observed over impostor comparisons of faces from different individuals who have the given age pair. False matches are counted against a recognition threshold fixed globally to give  $FMR = 0.001$  over all on the order of  $10^{10}$  impostor comparisons. The text in each box gives the same quantity as that coded by the color. Light colors present a security vulnerability to, for example, a passport gate.

Cross age FMR at threshold T = 0.221 for algorithm synthesis\_004, giving FMR(T) = 0.0001 globally.

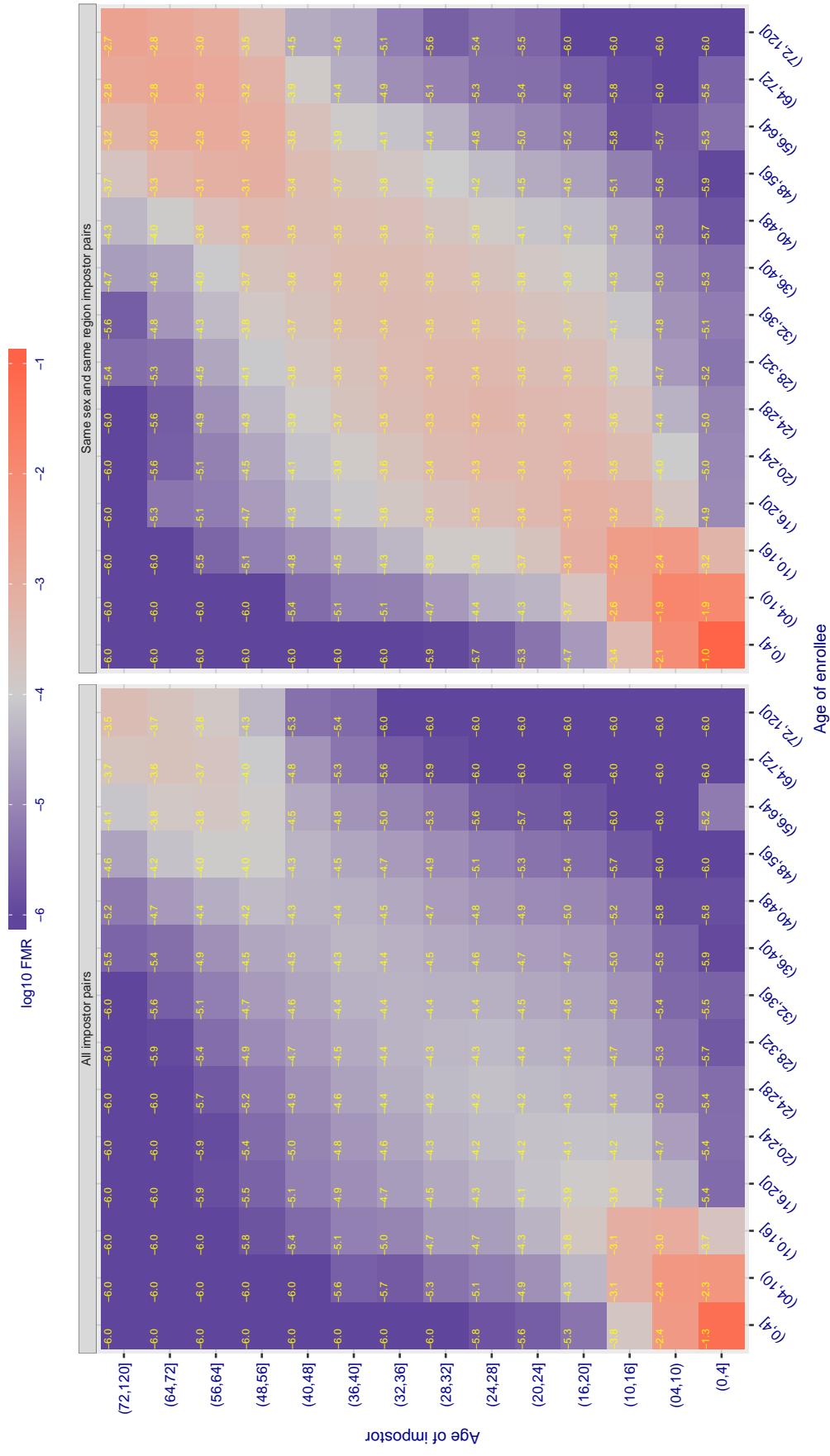


Figure 448: For algorithm synthesis-004 operating on visa images, the heatmap shows false match observed over impostor comparisons of faces from different individuals who have the given age pair. False matches are counted against a recognition threshold fixed globally to give FMR = 0.00 over all on the order of  $10^{10}$  impostor comparisons. The text in each box gives the same quantity as that coded by the color. Light colors present a security vulnerability to, for example, a passport gate.

Cross age FMR at threshold T = 0.356 for algorithm synthesis\_005, giving FMR(T) = 0.0001 globally.

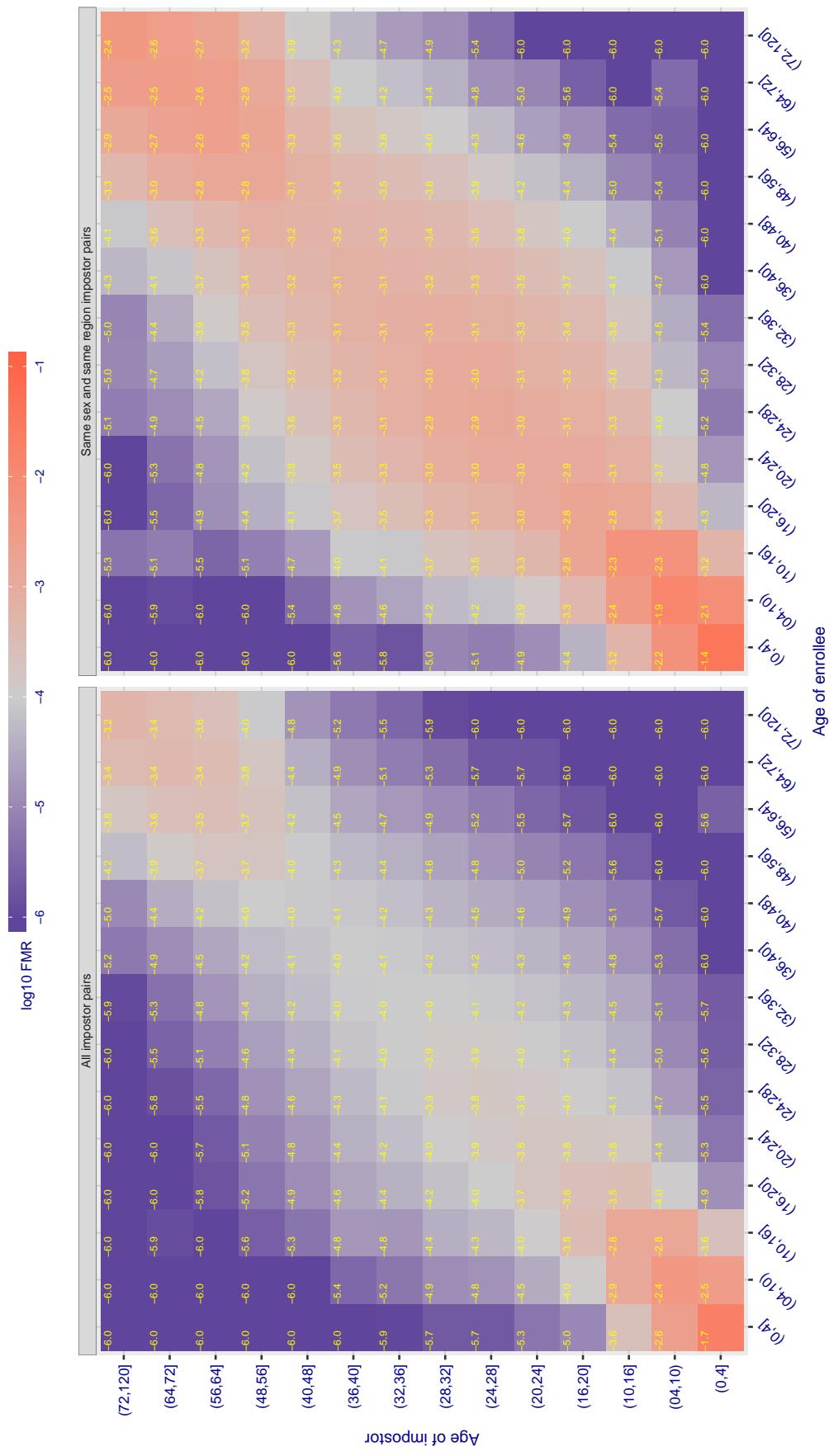


Figure 449: For algorithm synthesis-005 operating on visa images, the heatmap shows false match observed over impostor comparisons of faces from different individuals who have the given age pair. False matches are counted against a recognition threshold fixed globally to give FMR = 0.00 over all on the order of  $10^{10}$  impostor comparisons. The text in each box gives the same quantity as that coded by the color. Light colors present a security vulnerability to, for example, a passport gate.

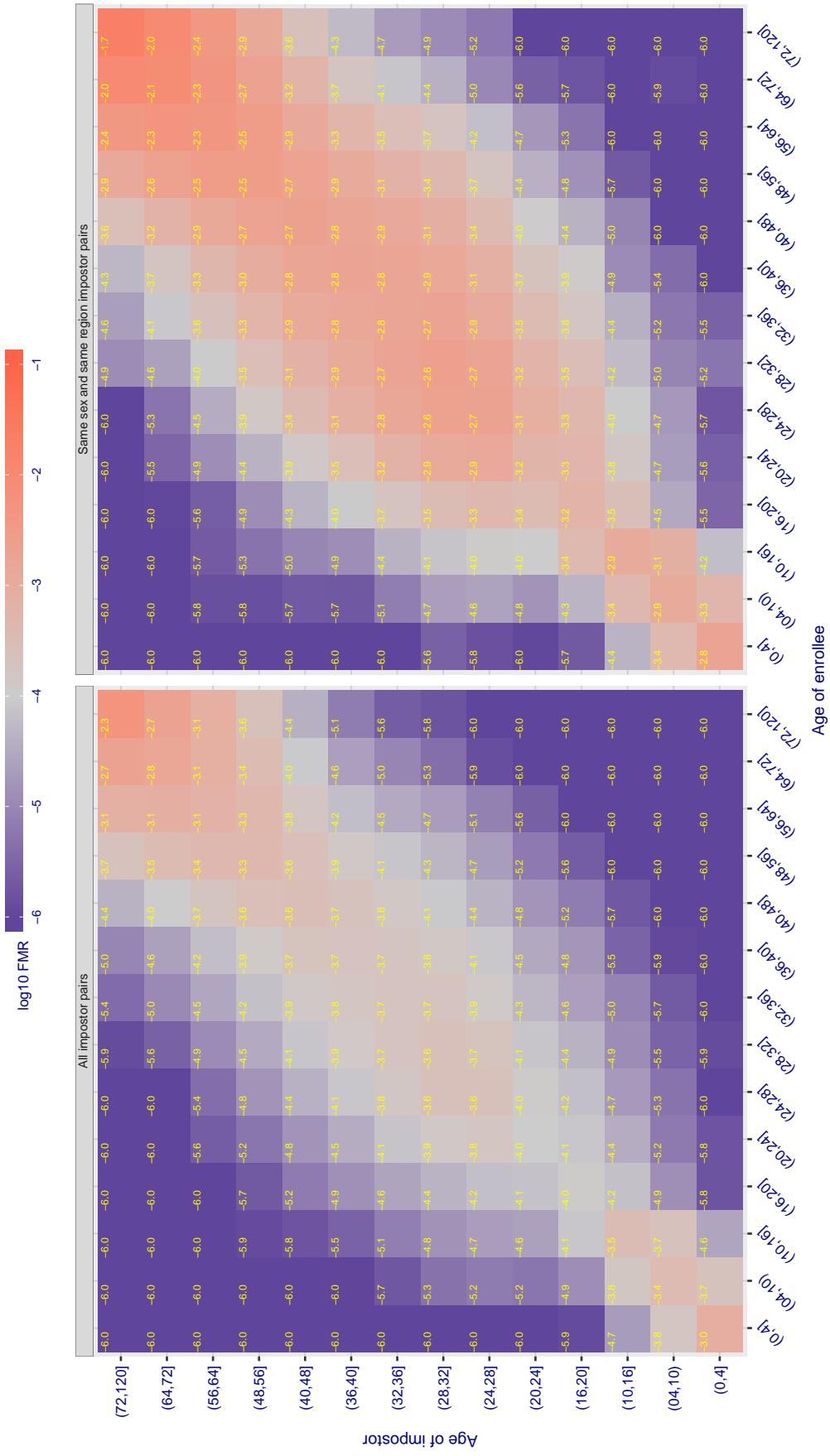
Cross age FMR at threshold T = 148.416 for algorithm tech5\_001, giving  $FMR(T) = 0.0001$  globally.

Figure 450: For algorithm tech5-001 operating on visa images, the heatmap shows false match observed over impostor comparisons of faces from different individuals who have the given age pair. False matches are counted against a recognition threshold fixed globally to give  $FMR = 0.001$  over all on the order of  $10^{10}$  impostor comparisons. The text in each box gives the same quantity as that coded by the color. Light colors present a security vulnerability to, for example, a passport gate.

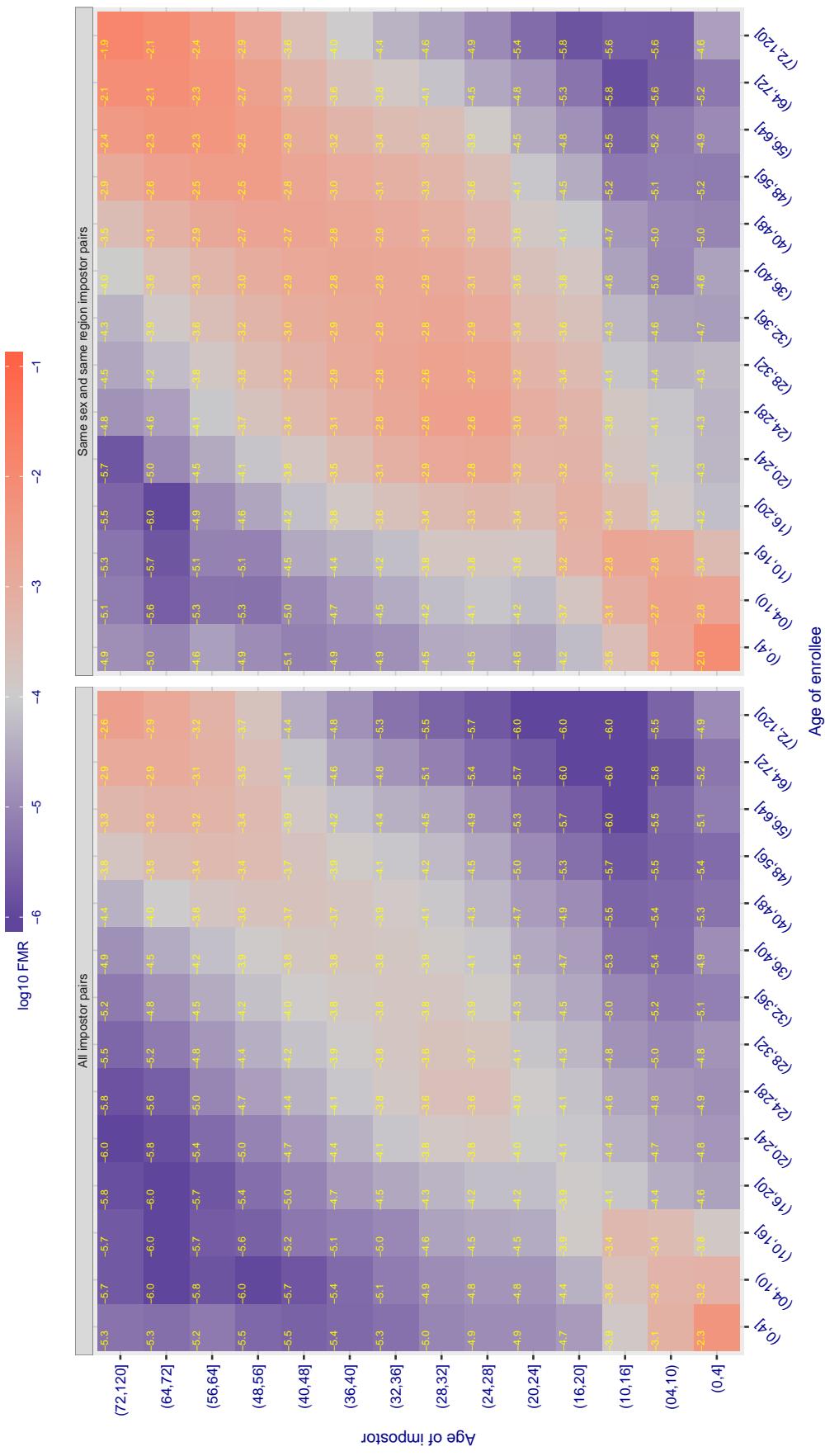
Cross age FMR at threshold T = 147.661 for algorithm tech5\_002, giving  $FMR(T) = 0.0001$  globally.

Figure 451: For algorithm tech5-002 operating on visa images, the heatmap shows false match observed over impostor comparisons of faces from different individuals who have the given age pair. False matches are counted against a recognition threshold fixed globally to give  $FMR = 0.001$  over all on the order of  $10^{10}$  impostor comparisons. The text in each box gives the same quantity as that coded by the color. Light colors present a security vulnerability to, for example, a passport gate.

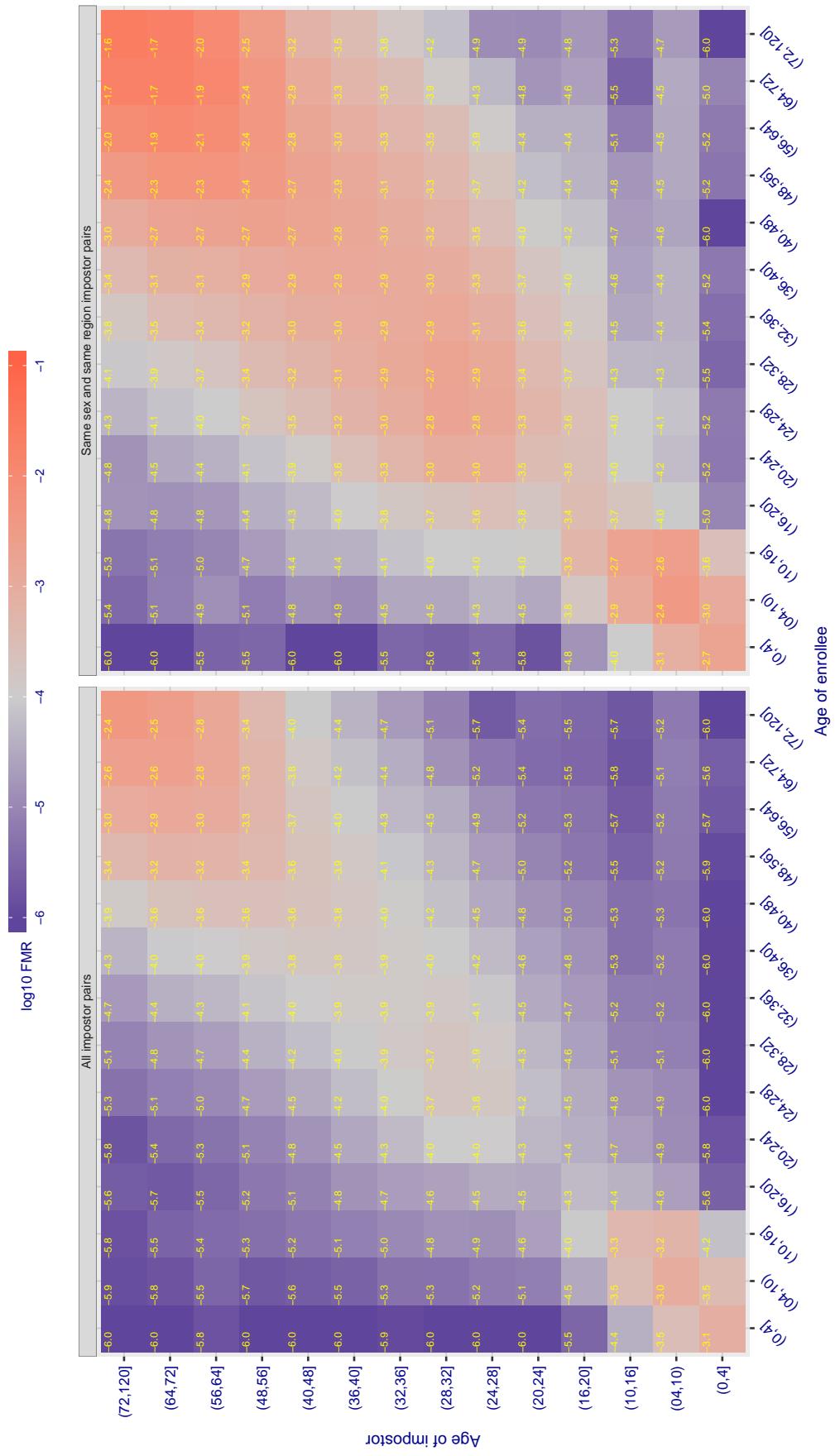
Cross age FMR at threshold T = 0.896 for algorithm tevian\_003, giving  $\text{FMR}(\text{T}) = 0.0001$  globally.

Figure 452: For algorithm tevian-003 operating on visa images, the heatmap shows false match observed over impostor comparisons of faces from different individuals who have the given age pair. False matches are counted against a recognition threshold fixed globally to give  $\text{FMR} = 0.001$  over all on the order of  $10^{10}$  impostor comparisons. The text in each box gives the same quantity as that coded by the color. Light colors present a security vulnerability to, for example, a passport gate.

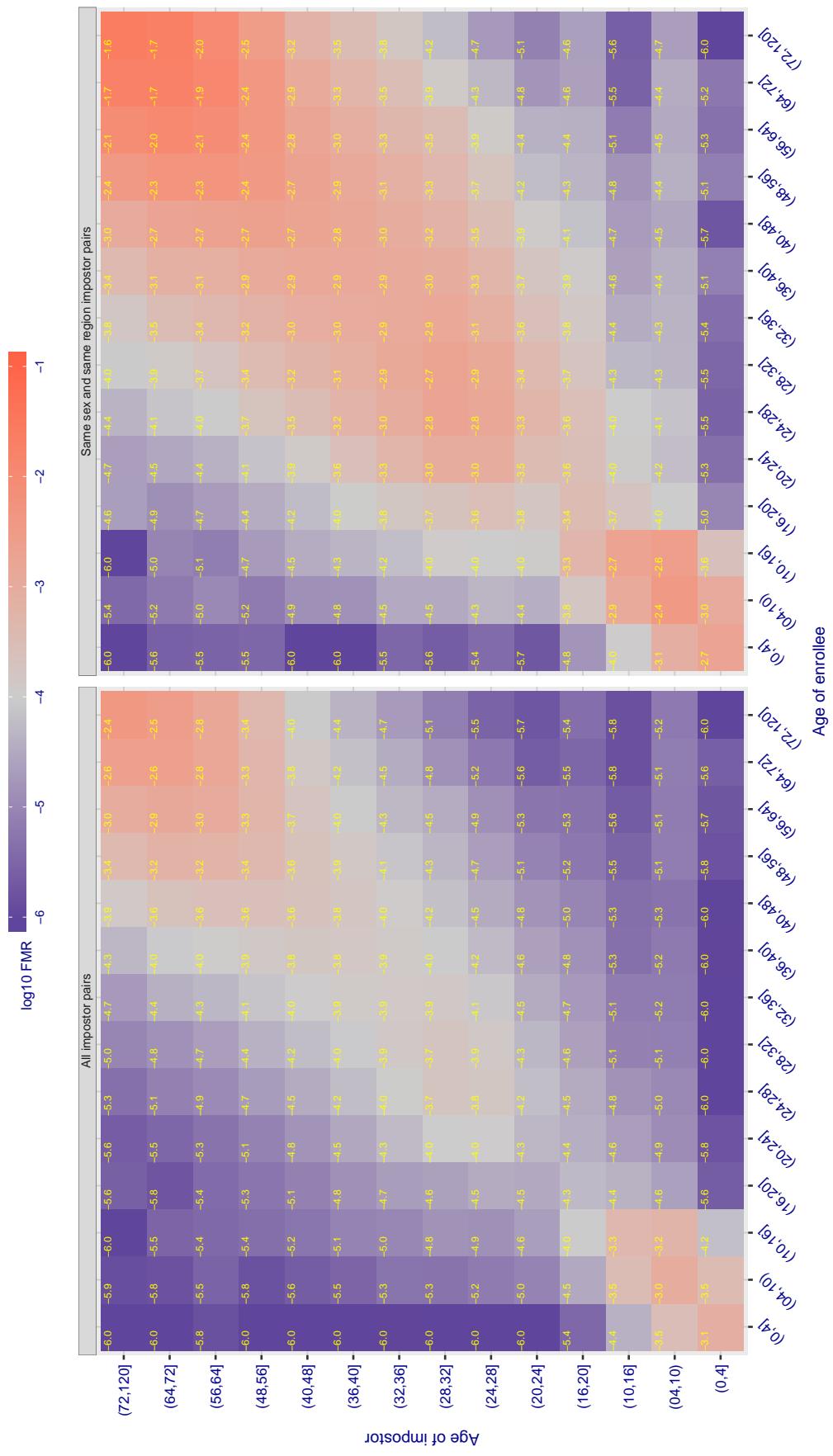
Cross age FMR at threshold T = 0.896 for algorithm tevian\_004, giving  $\text{FMR}(\text{T}) = 0.0001$  globally.

Figure 453: For algorithm tevian-004 operating on visa images, the heatmap shows false match observed over impostor comparisons of faces from different individuals who have the given age pair. False matches are counted against a recognition threshold fixed globally to give  $\text{FMR} = 0.001$  over all on the order of  $10^{10}$  impostor comparisons. The text in each box gives the same quantity as that coded by the color. Light colors present a security vulnerability to, for example, a passport gate.

Cross age FMR at threshold T = 151.011 for algorithm tiger\_002, giving FMR(T) = 0.0001 globally.

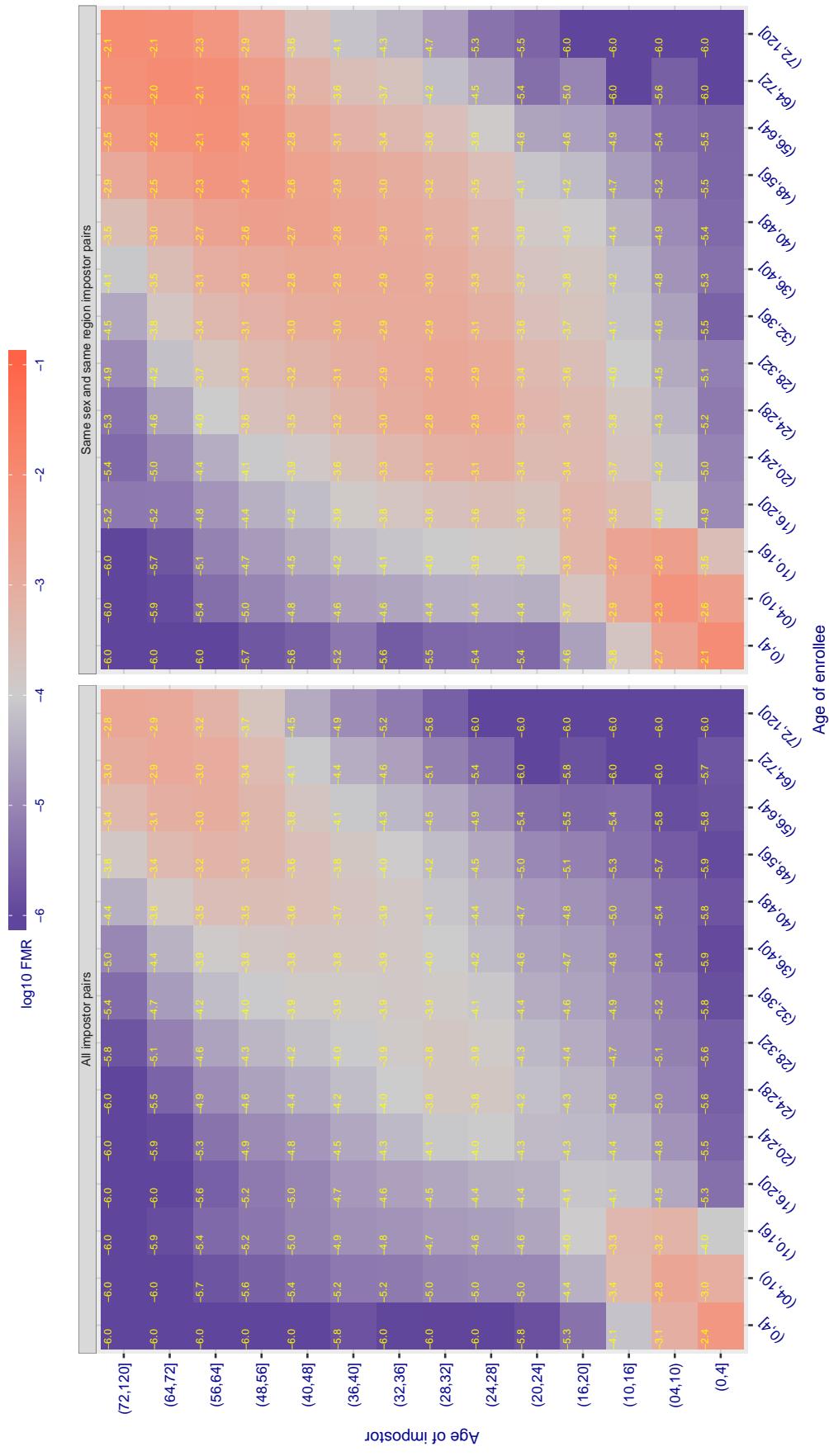
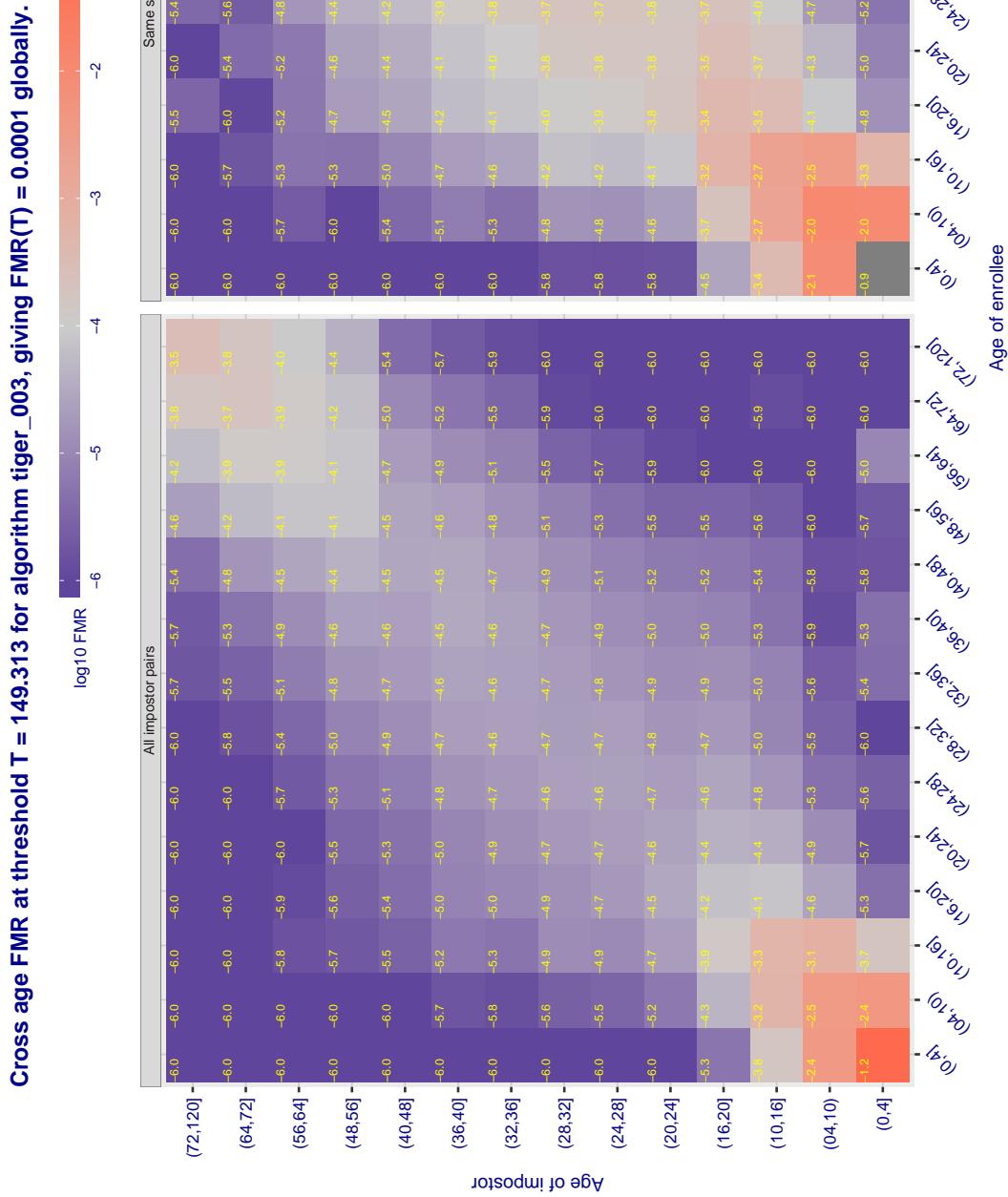


Figure 454: For algorithm tiger-002 operating on visa images, the heatmap shows false match observed over imposter comparisons of faces from different individuals who have the given age pair. False matches are counted against a recognition threshold fixed globally to give  $\text{FMR} = 0.001$  over all on the order of  $10^{10}$  impostor comparisons. The text in each box gives the same quantity as that coded by the color. Light colors present a security vulnerability to, for example, a passport gate.



**Figure 455:** For algorithm tiger-003 operating on visa images, the heatmap shows false match observed over impostor comparisons of faces from different individuals who have the given age pair. False matches are counted against a recognition threshold fixed globally to give  $FMR = 0.001$  over all on the order of  $10^{10}$  impostor comparisons. The text in each box gives the same quantity as that coded by the color. Light colors present a security vulnerability to, for example, a passport gate.

Cross age FMR at threshold T = 43.677 for algorithm tongyi\_005, giving FMR(T) = 0.0001 globally.

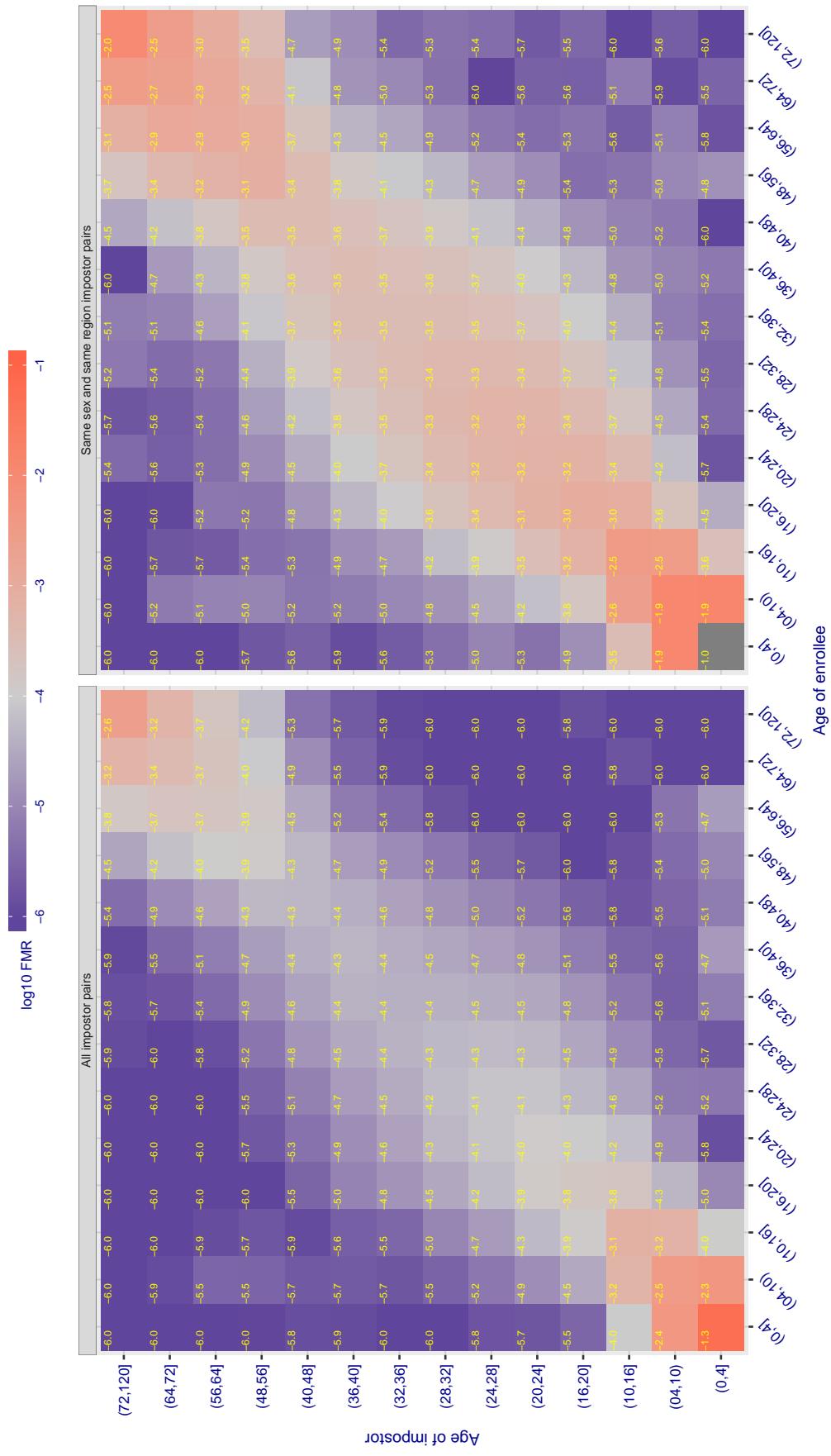
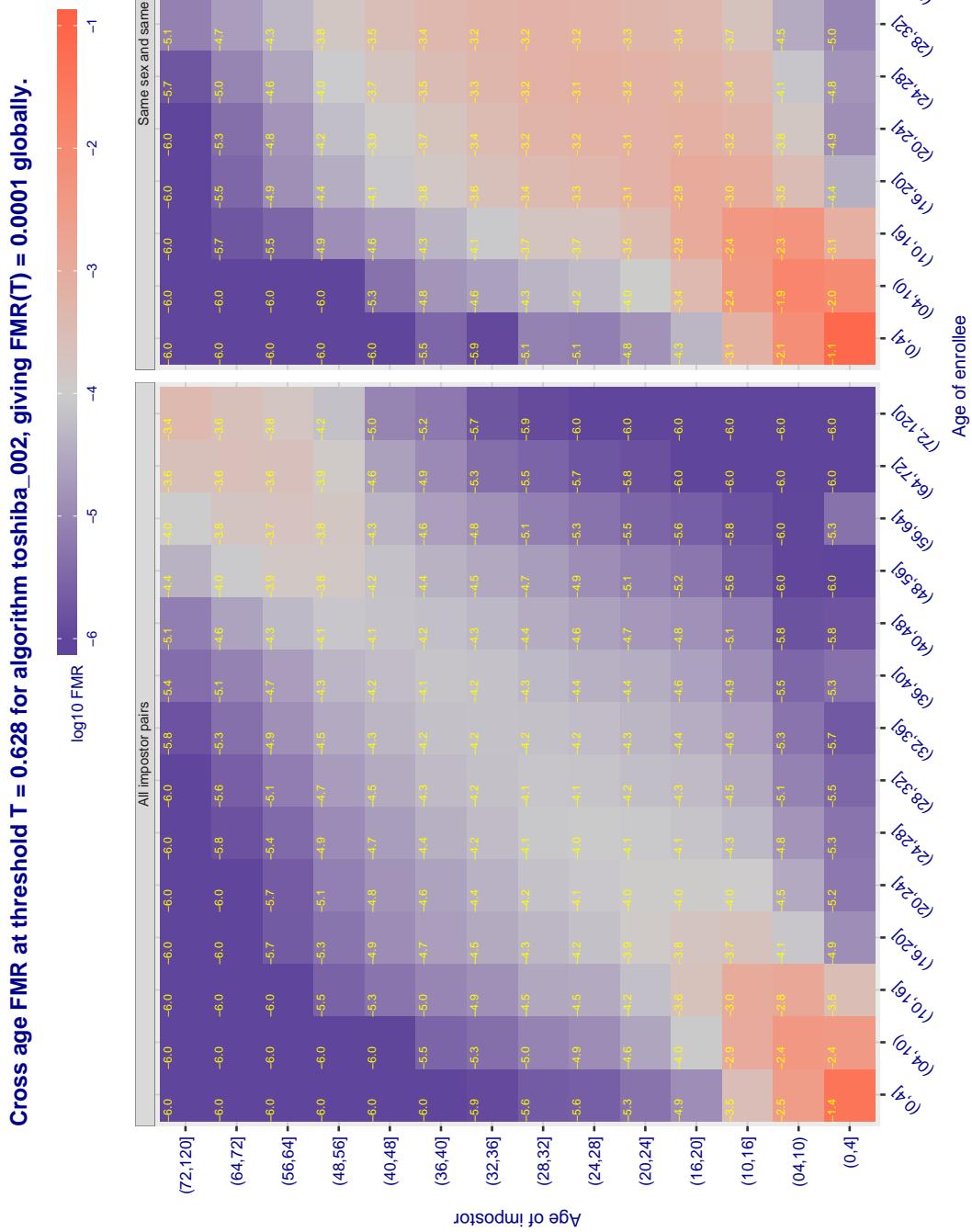
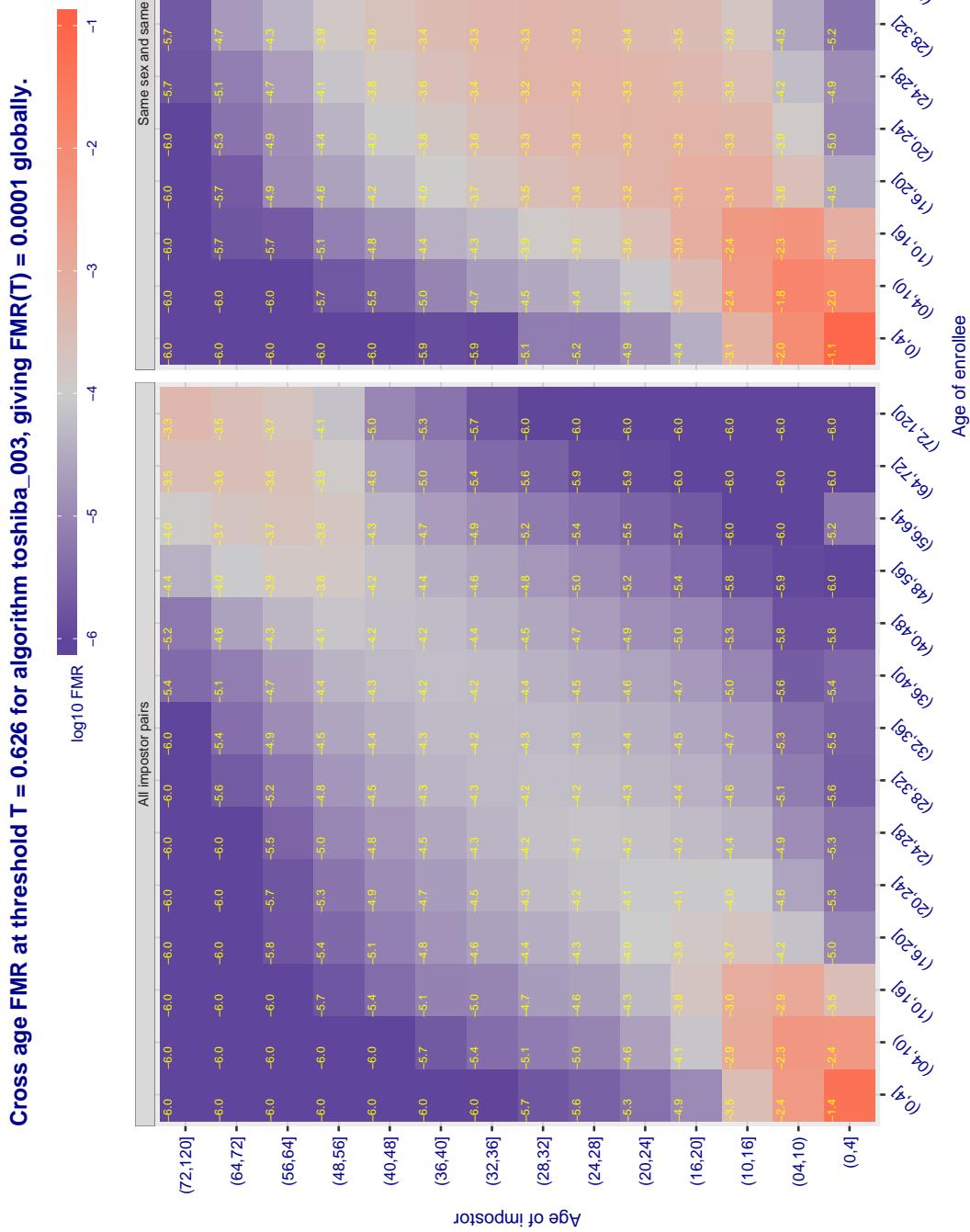


Figure 456: For algorithm tongyi-005 operating on visa images, the heatmap shows false match observed over impostor comparisons of faces from different individuals who have the given age pair. False matches are counted against a recognition threshold fixed globally to give FMR = 0.001 over all on the order of  $10^{10}$  impostor comparisons. The text in each box gives the same quantity as that coded by the color. Light colors present a security vulnerability to, for example, a passport gate.



**Figure 457:** For algorithm toshiba-002 operating on visa images, the heatmap shows false match observed over impostor comparisons of faces from different individuals who have the given age pair. False matches are counted against a recognition threshold fixed globally to give  $FMR = 0.001$  over all on the order of  $10^{10}$  impostor comparisons. The text in each box gives the same quantity as that coded by the color. Light colors present a security vulnerability to, for example, a passport gate.



**Figure 458:** For algorithm toshiba-003 operating on visa images, the heatmap shows false match observed over impostor comparisons of faces from different individuals who have the given age pair. False matches are counted against a recognition threshold fixed globally to give  $FMR = 0.001$  over all on the order of  $10^{10}$  impostor comparisons. The text in each box gives the same quantity as that coded by the color. Light colors present a security vulnerability to, for example, a passport gate.

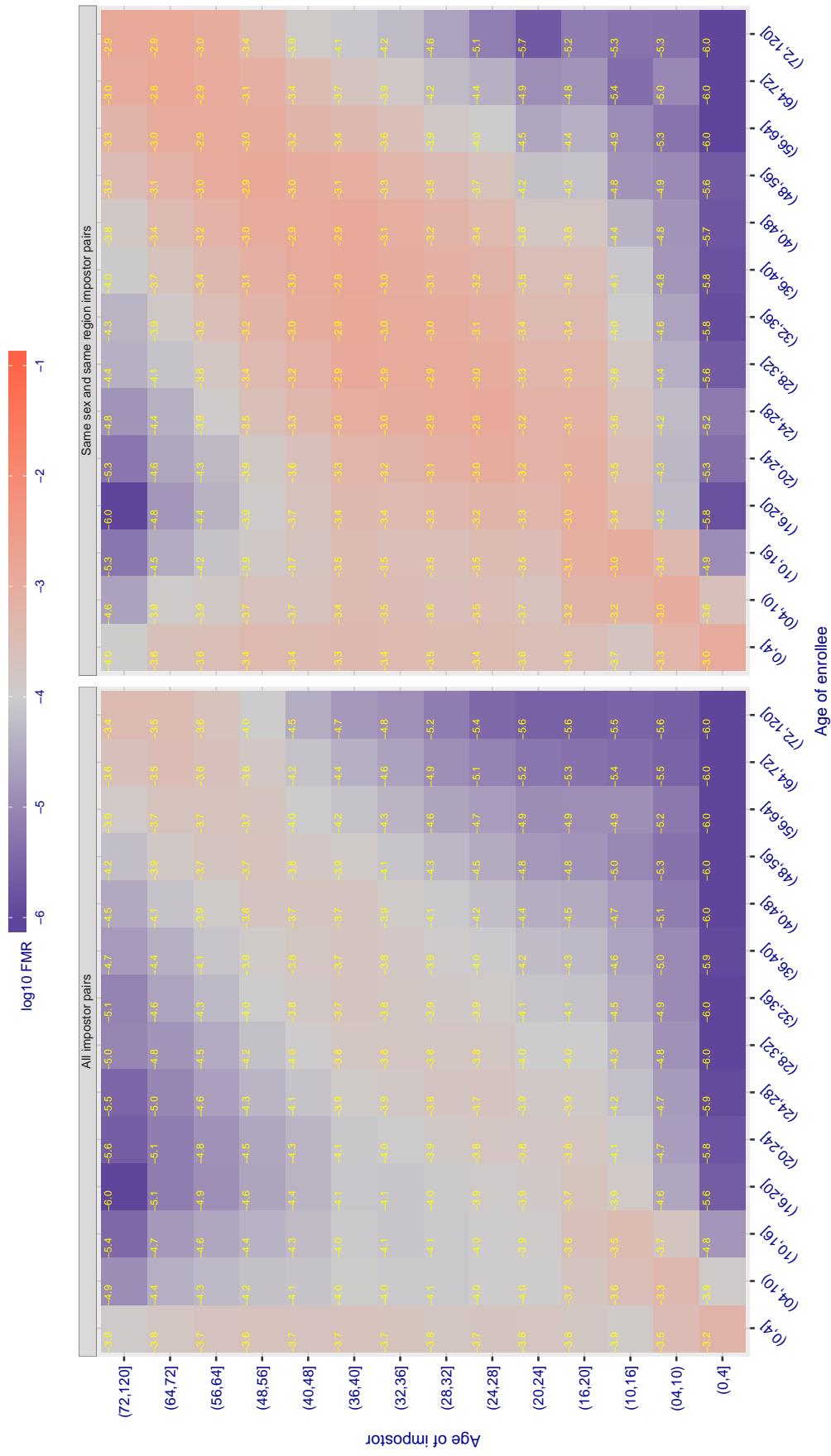
Cross age FMR at threshold T = 0.423 for algorithm vcog\_002, giving  $FMR(T) = 0.0001$  globally.

Figure 459: For algorithm vcog\_002 operating on visa images, the heatmap shows false match observed over impostor comparisons of faces from different individuals who have the given age pair. False matches are counted against a recognition threshold fixed globally to give  $FMR = 0.001$  over all on the order of  $10^{10}$  impostor comparisons. The text in each box gives the same quantity as that coded by the color. Light colors present a security vulnerability to, for example, a passport gate.

Cross age FMR at threshold T = 71.529 for algorithm vd\_001, giving  $\text{FMR}(\text{T}) = 0.0001$  globally.

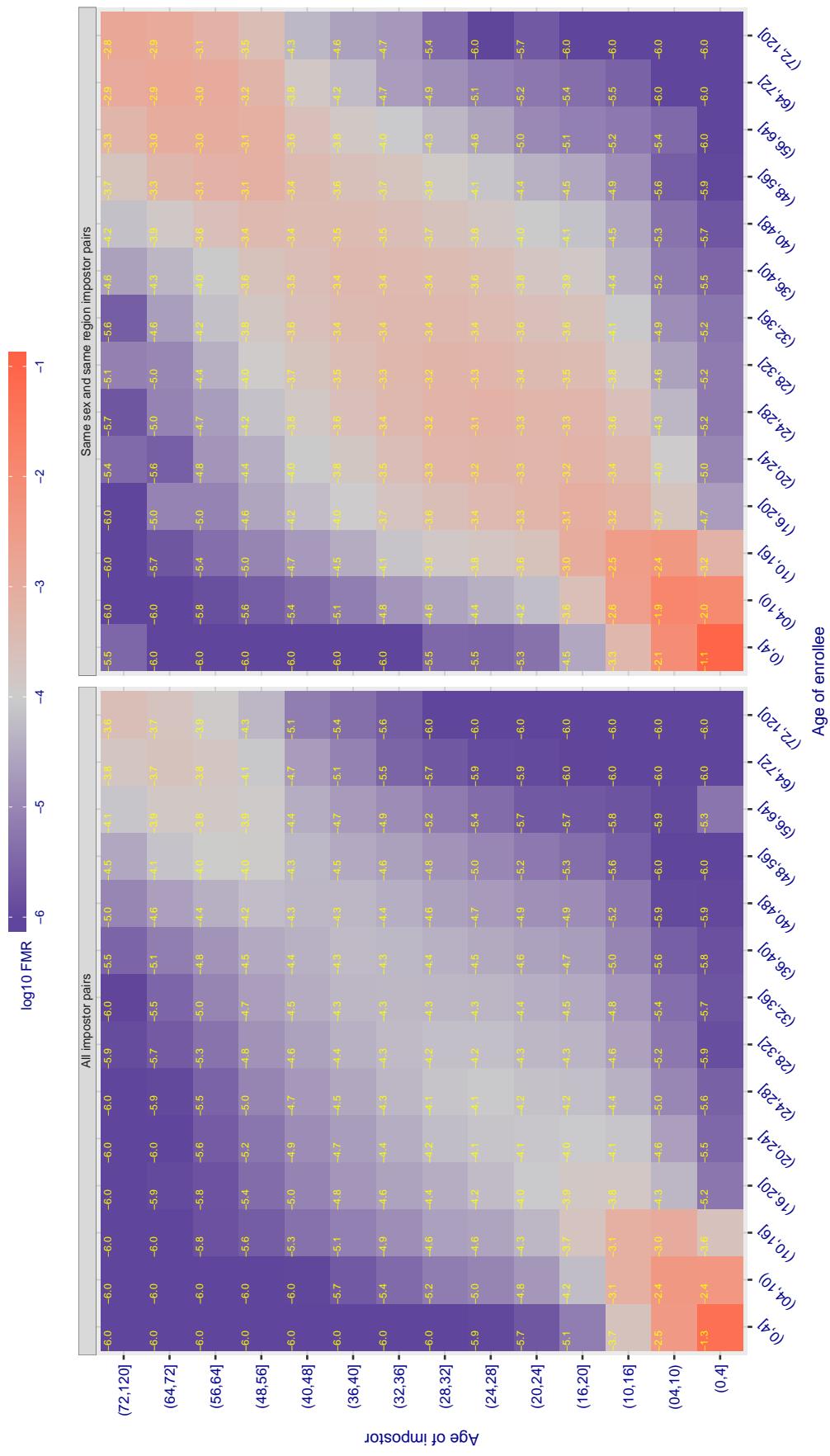
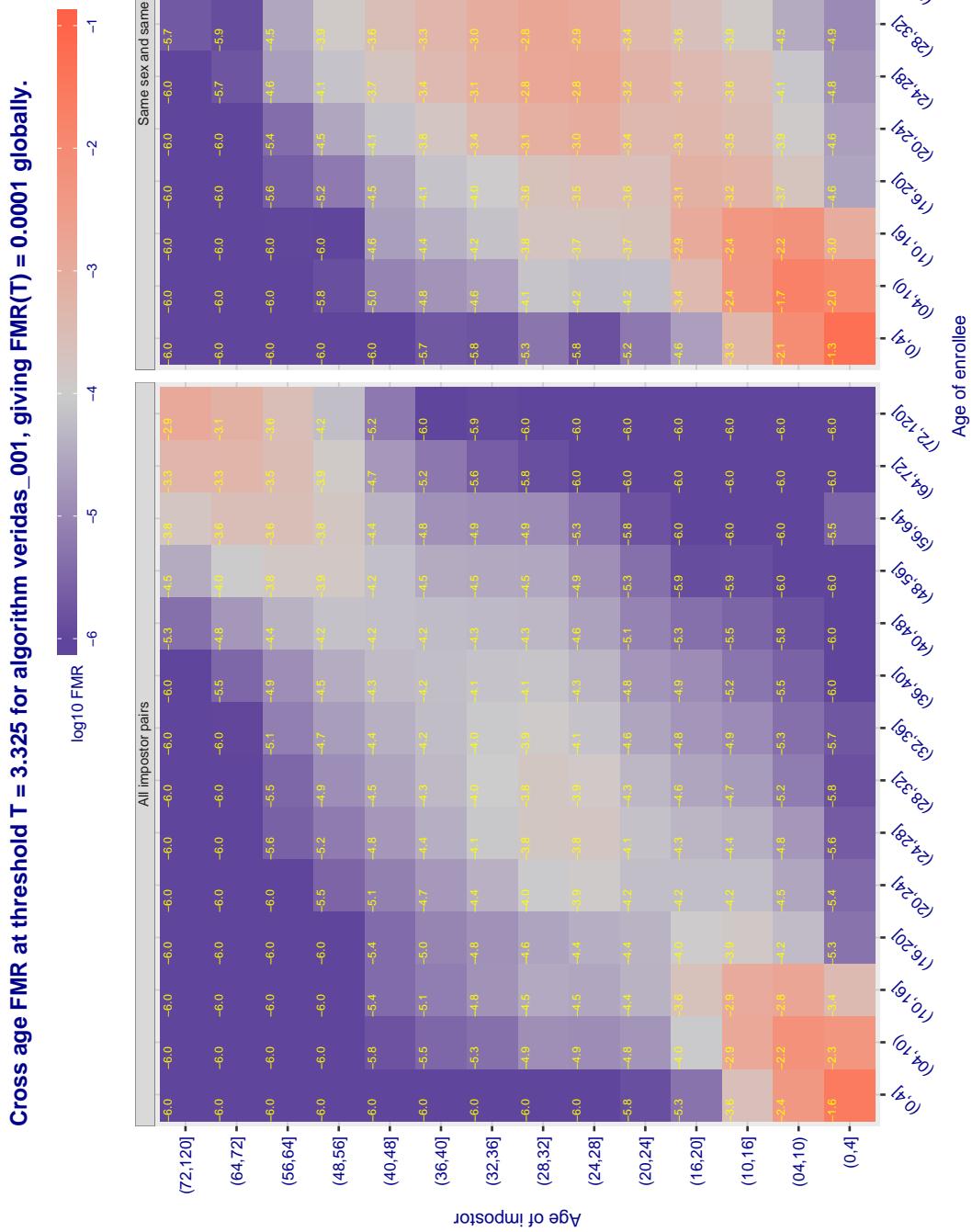
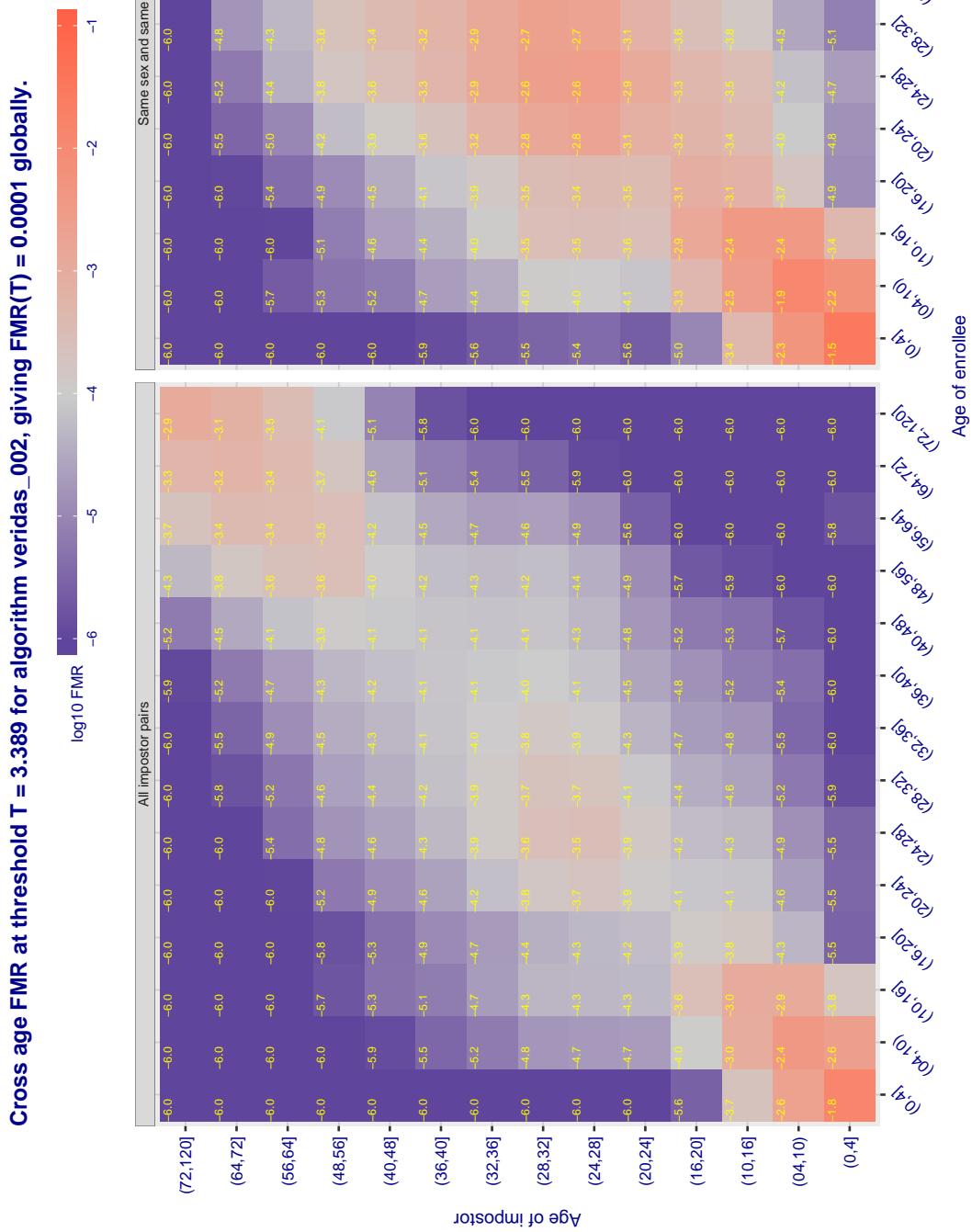


Figure 460: For algorithm vd\_001 operating on visa images, the heatmap shows false match observed over impostor comparisons of faces from different individuals who have the given age pair. False matches are counted against a recognition threshold fixed globally to give  $\text{FMR} = 0.001$  over all on the order of  $10^{10}$  impostor comparisons. The text in each box gives the same quantity as that coded by the color. Light colors present a security vulnerability to, for example, a passport gate.



**Figure 461:** For algorithm veridas-001 operating on visa images, the heatmap shows false match observed over impostor comparisons of faces from different individuals who have the given age pair. False matches are counted against a recognition threshold fixed globally to give  $FMR = 0.001$  over all on the order of  $10^{10}$  impostor comparisons. The text in each box gives the same quantity as that coded by the color. Light colors present a security vulnerability to, for example, a passport gate.



**Figure 462:** For algorithm veridas-002 operating on visa images, the heatmap shows false match observed over impostor comparisons of faces from different individuals who have the given age pair. False matches are counted against a recognition threshold fixed globally to give  $FMR = 0.001$  over all on the order of  $10^{10}$  impostor comparisons. The text in each box gives the same quantity as that coded by the color. Light colors present a security vulnerability to, for example, a passport gate.

**Cross age FMR at threshold T = 0.842 for algorithm videonetics\_001, giving FMR(T) = 0.00001 globally.**

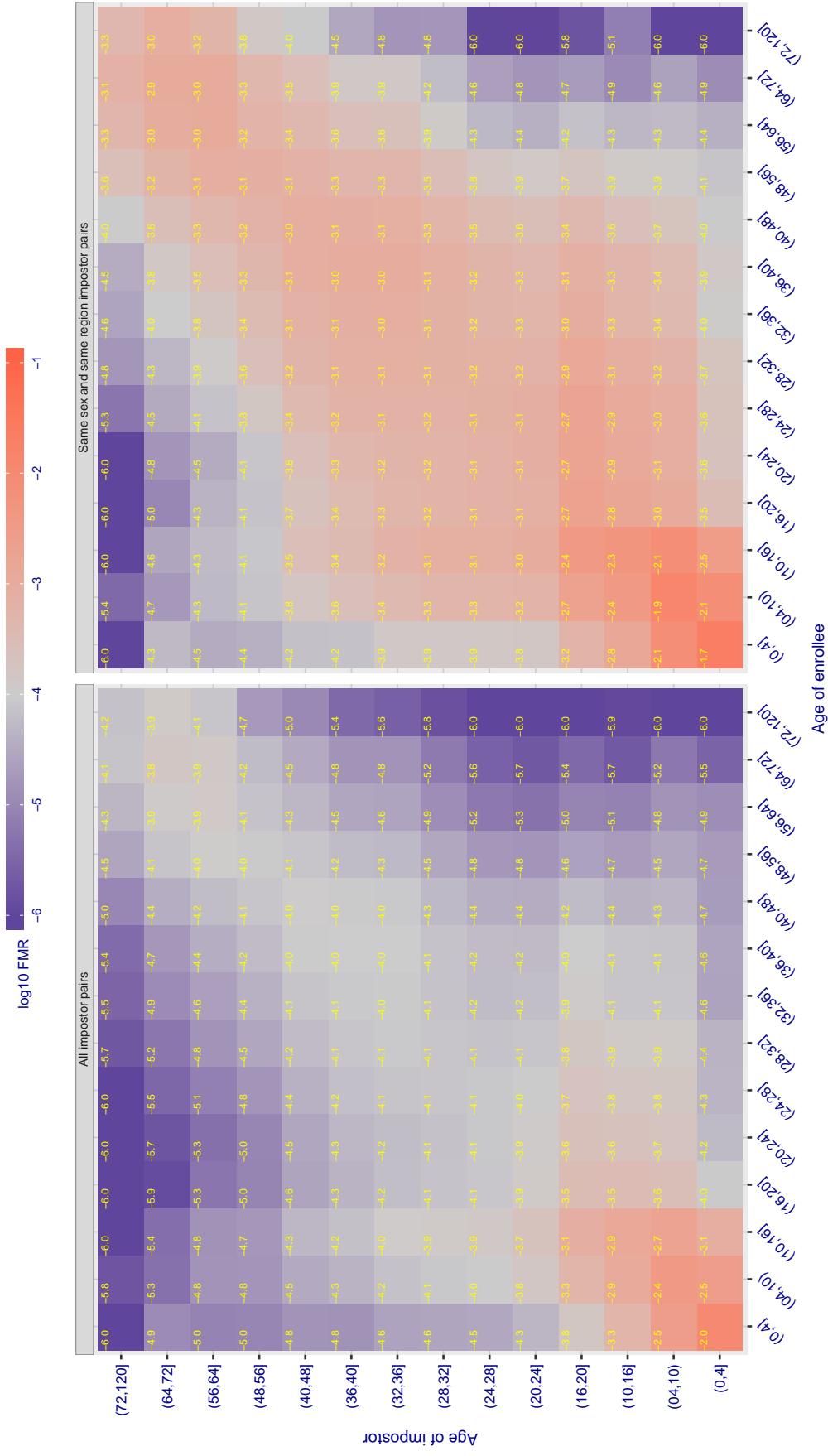


Figure 463: For algorithm videonetics-001 operating on visa images, the heatmap shows false match observed over impostor comparisons of faces from different individuals who have the given age pair. False matches are counted against a recognition threshold fixed globally to give FMR = 0.001 over all on the order of  $10^{10}$  impostor comparisons. The text in each box gives the same quantity as that coded by the color. Light colors present a security vulnerability to, for example, a passport gate.

Cross age FMR at threshold T = 3.057 for algorithm vigilantsolutions\_006, giving FMR(T) = 0.0001 globally.

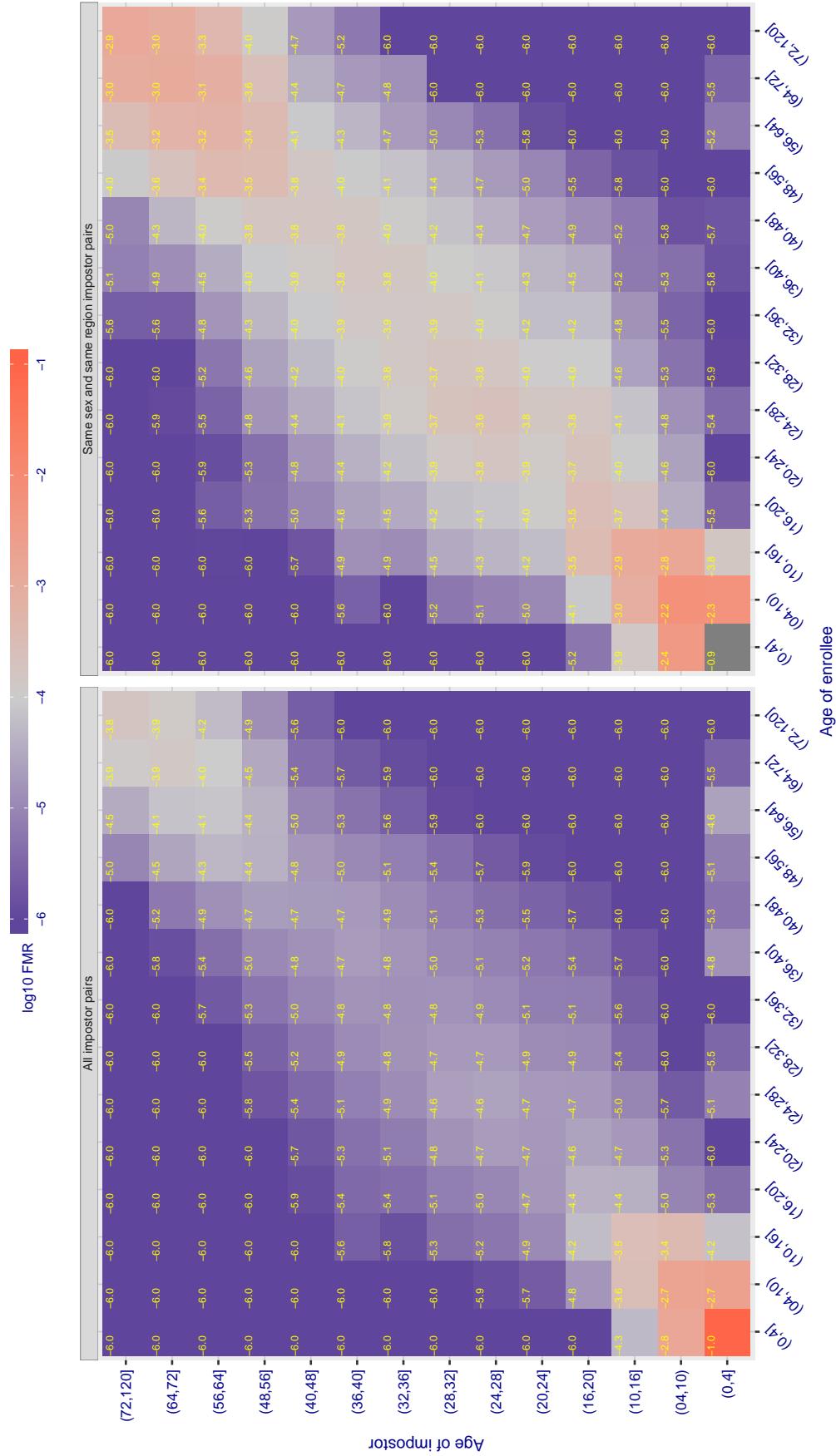


Figure 464: For algorithm vigilantsolutions-006 operating on visa images, the heatmap shows false match observed over impostor comparisons of faces from different individuals who have the given age pair. False matches are counted against a recognition threshold fixed globally to give FMR = 0.001 over all on the order of  $10^{10}$  impostor comparisons. The text in each box gives the same quantity as that coded by the color. Light colors present a security vulnerability to, for example, a passport gate.

Cross age FMR at threshold T = 0.432 for algorithm vion\_000, giving FMR(T) = 0.0001 globally.

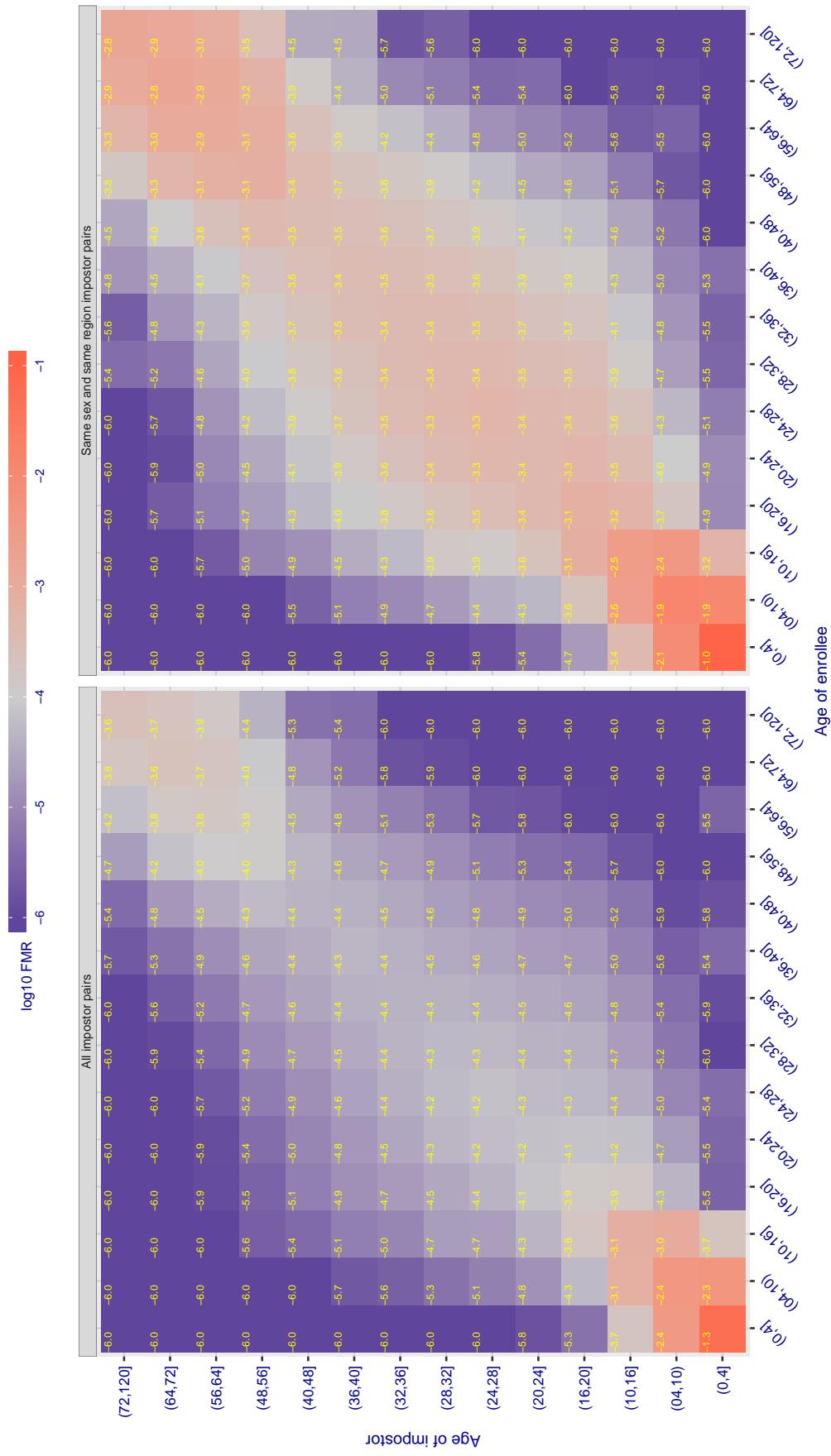


Figure 465: For algorithm vion-000 operating on visa images, the heatmap shows false match observed over impostor comparisons of faces from different individuals who have the given age pair. False matches are counted against a recognition threshold fixed globally to give  $FMR = 0.001$  over all on the order of  $10^{10}$  impostor comparisons. The text in each box gives the same quantity as that coded by the color. Light colors present a security vulnerability to, for example, a passport gate.

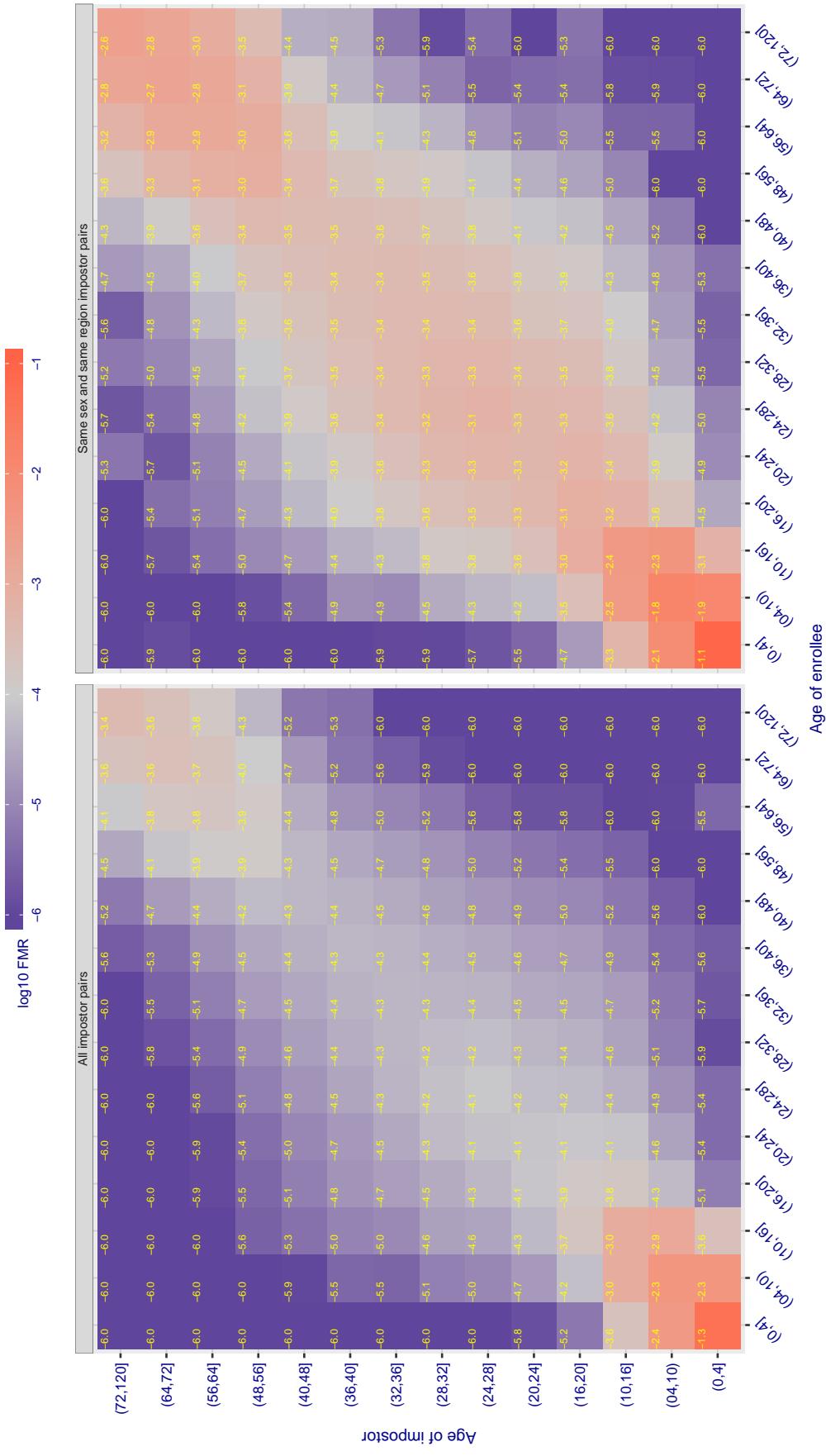
Cross age FMR at threshold T = 0.433 for algorithm visionbox\_000, giving  $FMR(T) = 0.0001$  globally.

Figure 466: For algorithm visionbox-000 operating on visa images, the heatmap shows false match observed over impostor comparisons of faces from different individuals who have the given age pair. False matches are counted against a recognition threshold fixed globally to give  $FMR = 0.001$  over all on the order of  $10^{10}$  impostor comparisons. The text in each box gives the same quantity as that coded by the color. Light colors present a security vulnerability to, for example, a passport gate.

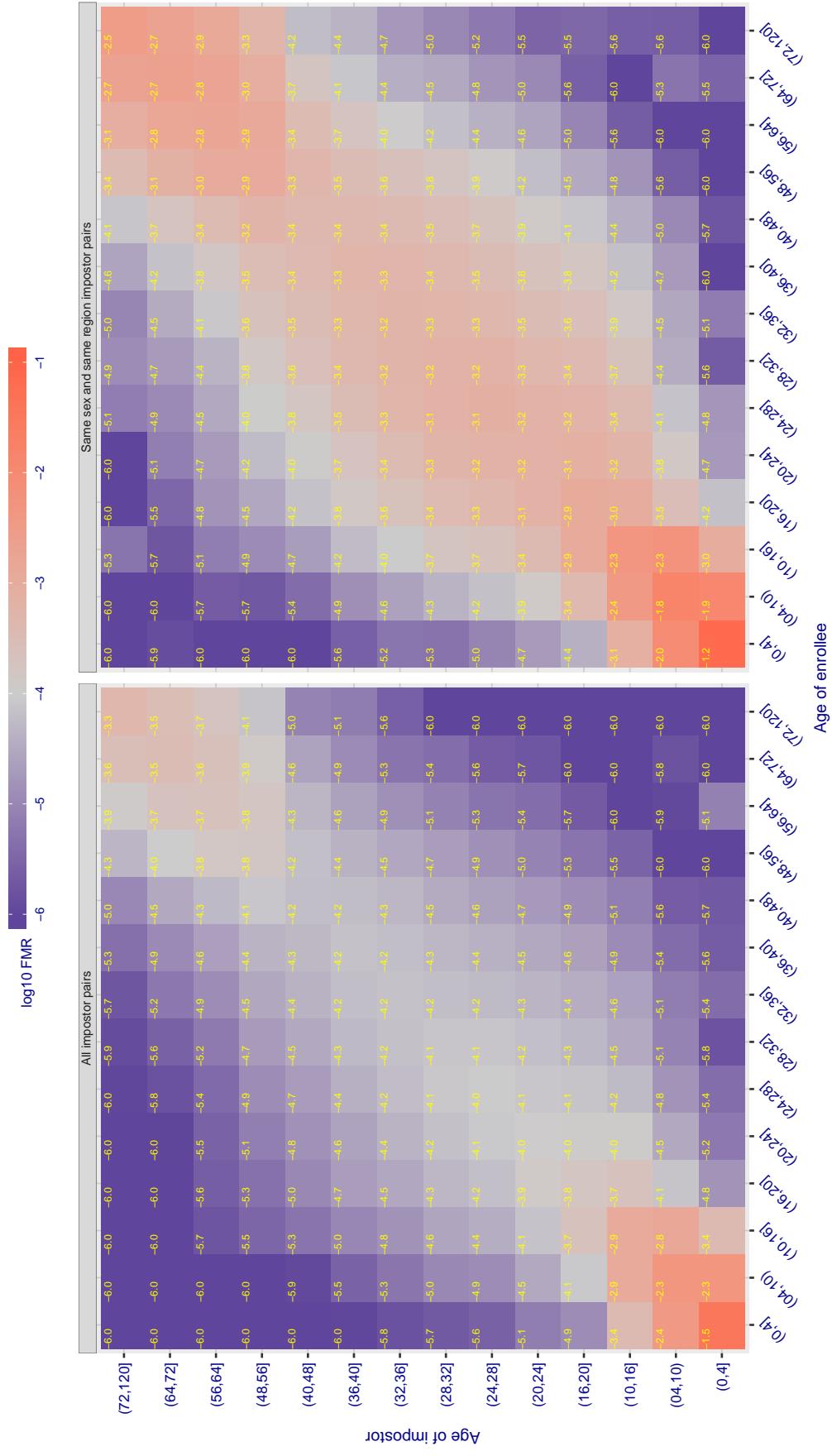
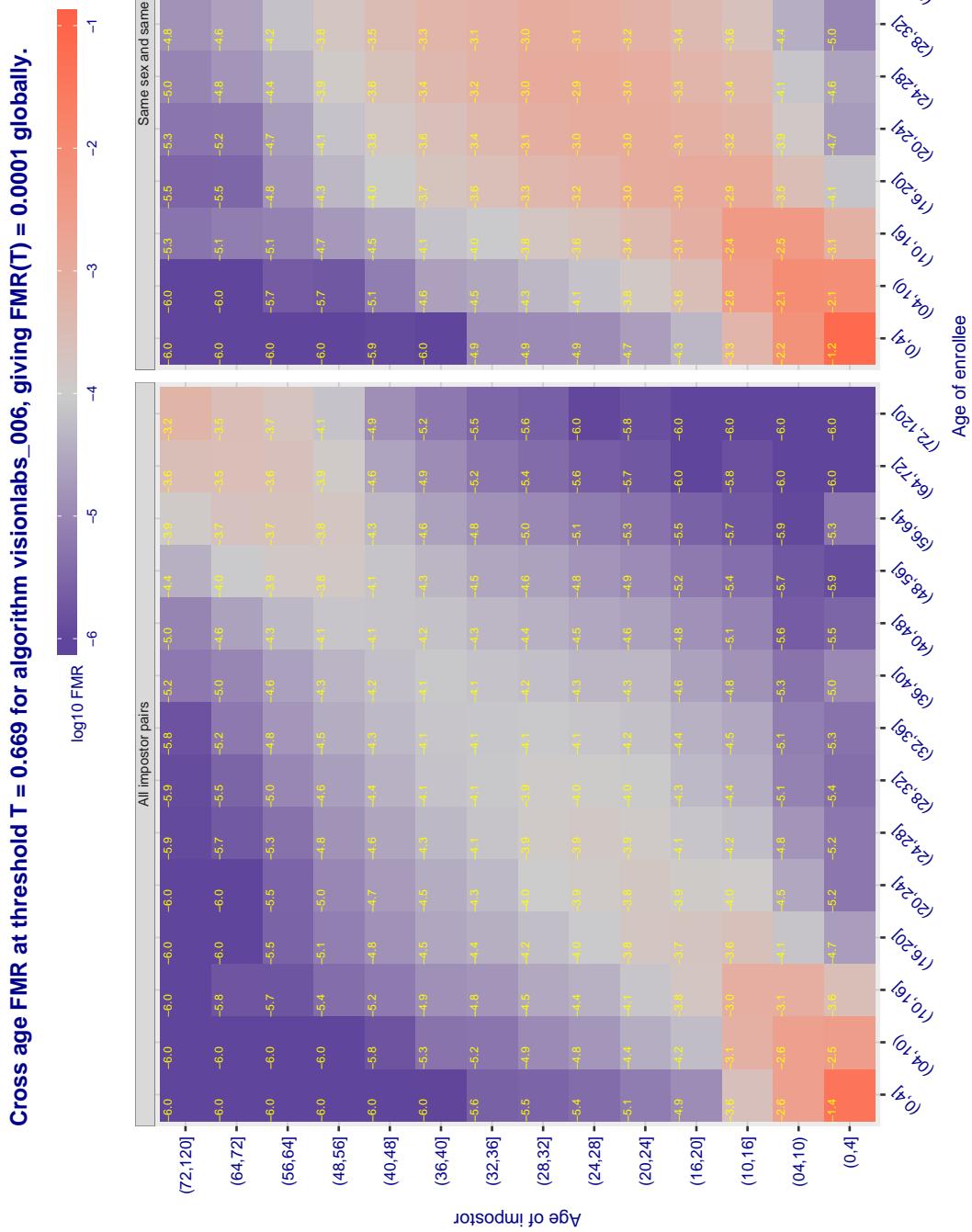
Cross age FMR at threshold T = 0.382 for algorithm visionbox\_001, giving  $FMR(T) = 0.0001$  globally.

Figure 467: For algorithm visionbox-001 operating on visa images, the heatmap shows false match observed over impostor comparisons of faces from different individuals who have the given age pair. False matches are counted against a recognition threshold fixed globally to give  $FMR = 0.001$  over all on the order of  $10^{10}$  impostor comparisons. The text in each box gives the same quantity as that coded by the color. Light colors present a security vulnerability to, for example, a passport gate.



**Figure 468:** For algorithm visionlabs-006 operating on visa images, the heatmap shows false match observed over impostor comparisons of faces from different individuals who have the given age pair. False matches are counted against a recognition threshold fixed globally to give  $FMR = 0.001$  over all on the order of  $10^{10}$  impostor comparisons. The text in each box gives the same quantity as that coded by the color. Light colors present a security vulnerability to, for example, a passport gate.

Cross age FMR at threshold T = 0.657 for algorithm visionlabs\_007, giving FMR(T) = 0.0001 globally.

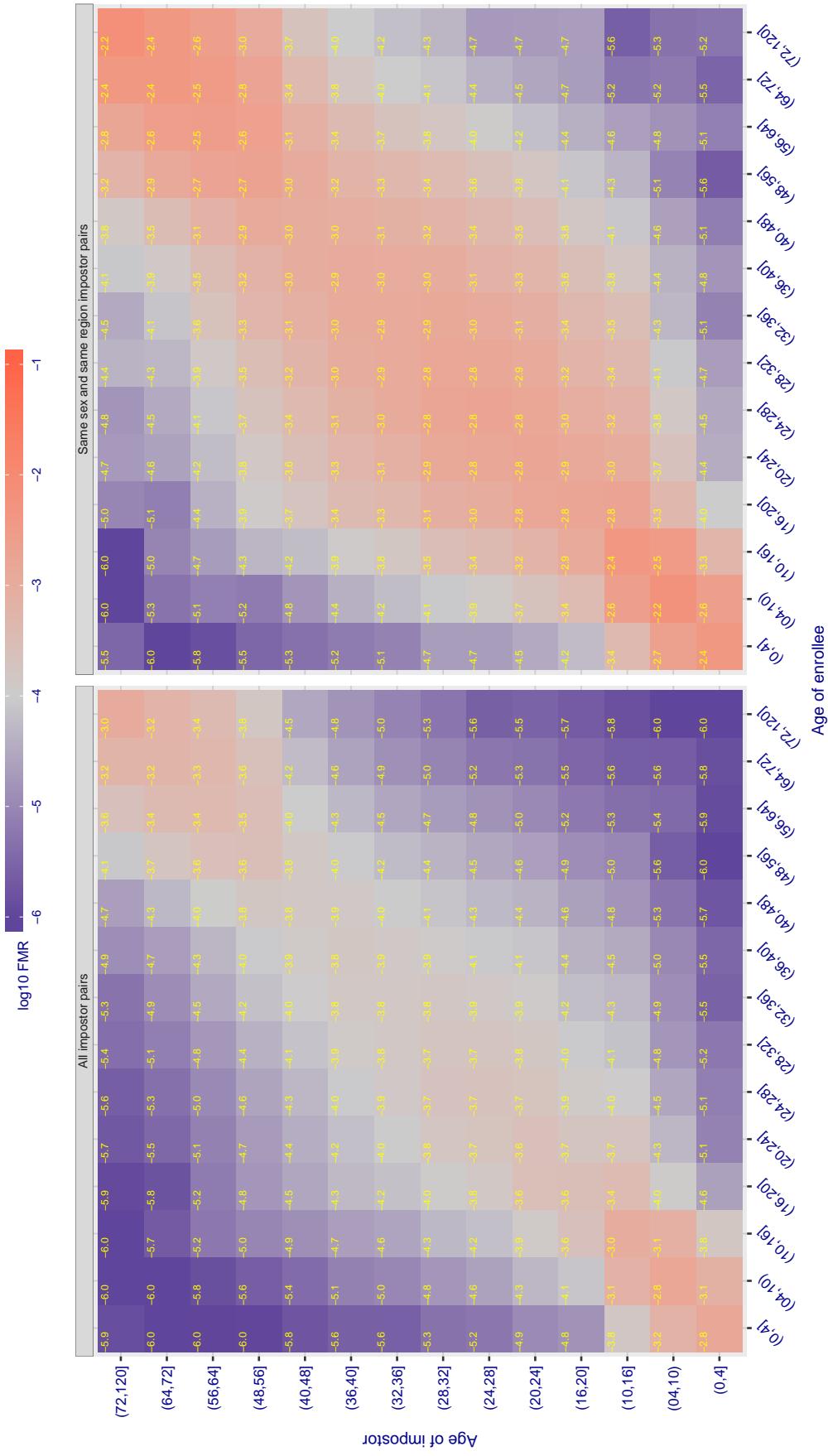


Figure 469: For algorithm visionlabs-007 operating on visa images, the heatmap shows false match observed over impostor comparisons of faces from different individuals who have the given age pair. False matches are counted against a recognition threshold fixed globally to give  $FMR = 0.001$  over all on the order of  $10^{10}$  impostor comparisons. The text in each box gives the same quantity as that coded by the color. Light colors present a security vulnerability to, for example, a passport gate.

Cross age FMR at threshold T = 995.398 for algorithm vocord\_006, giving FMR(T) = 0.0001 globally.

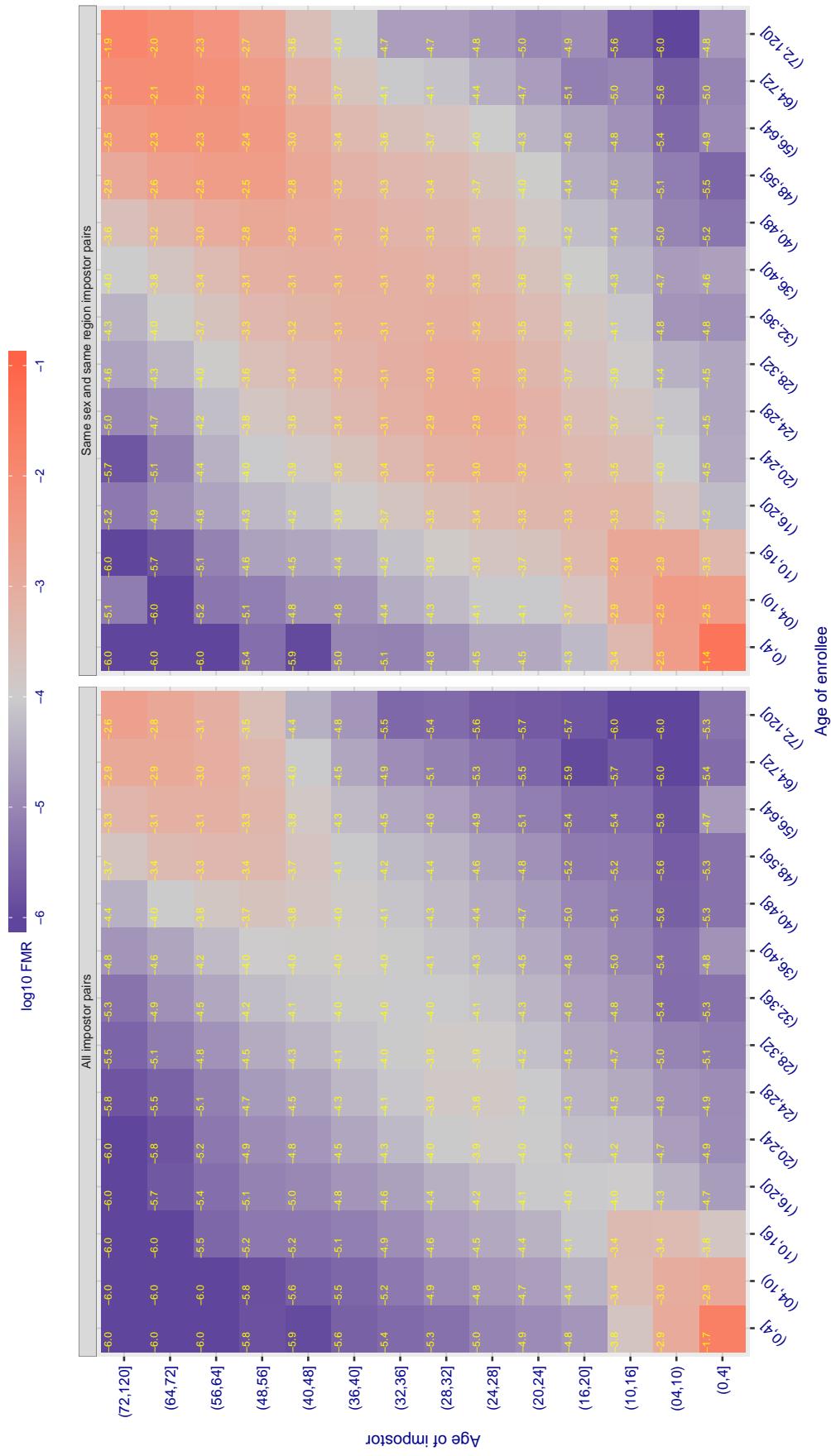
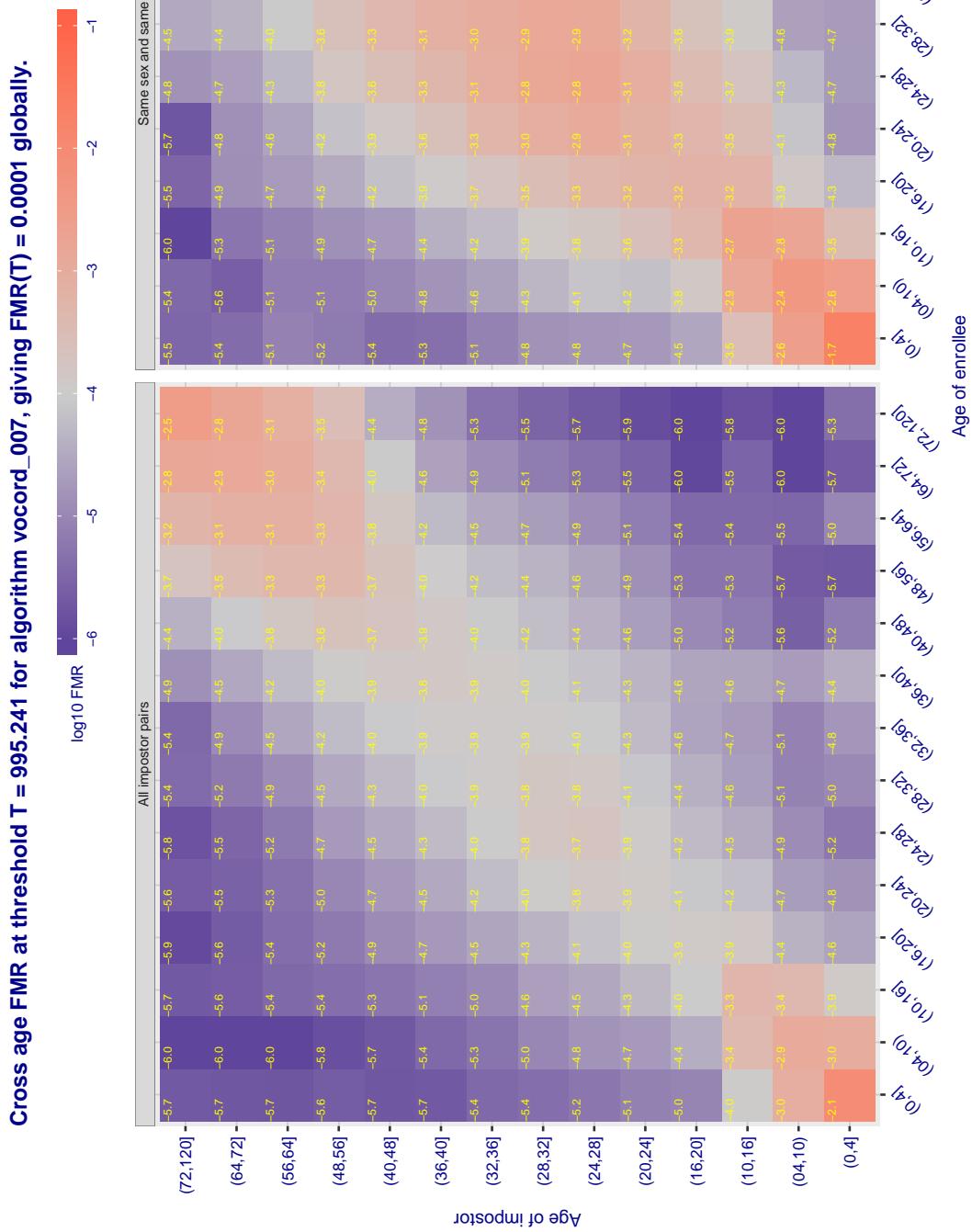


Figure 470: For algorithm vocord-006 operating on visa images, the heatmap shows false match observed over impostor comparisons of faces from different individuals who have the given age pair. False matches are counted against a recognition threshold fixed globally to give  $FMR = 0.00$  over all on the order of  $10^{10}$  impostor comparisons. The text in each box gives the same quantity as that coded by the color. Light colors present a security vulnerability to, for example, a passport gate.



**Figure 471:** For algorithm vocond-007 operating on visa images, the heatmap shows false match observed over impostor comparisons of faces from different individuals who have the given age pair. False matches are counted against a recognition threshold fixed globally to give  $FMR = 0.001$  over all on the order of  $10^{10}$  impostor comparisons. The text in each box gives the same quantity as that coded by the color. Light colors present a security vulnerability to, for example, a passport gate.

Cross age FMR at threshold T = 0.400 for algorithm winsense\_000, giving FMR(T) = 0.0001 globally.

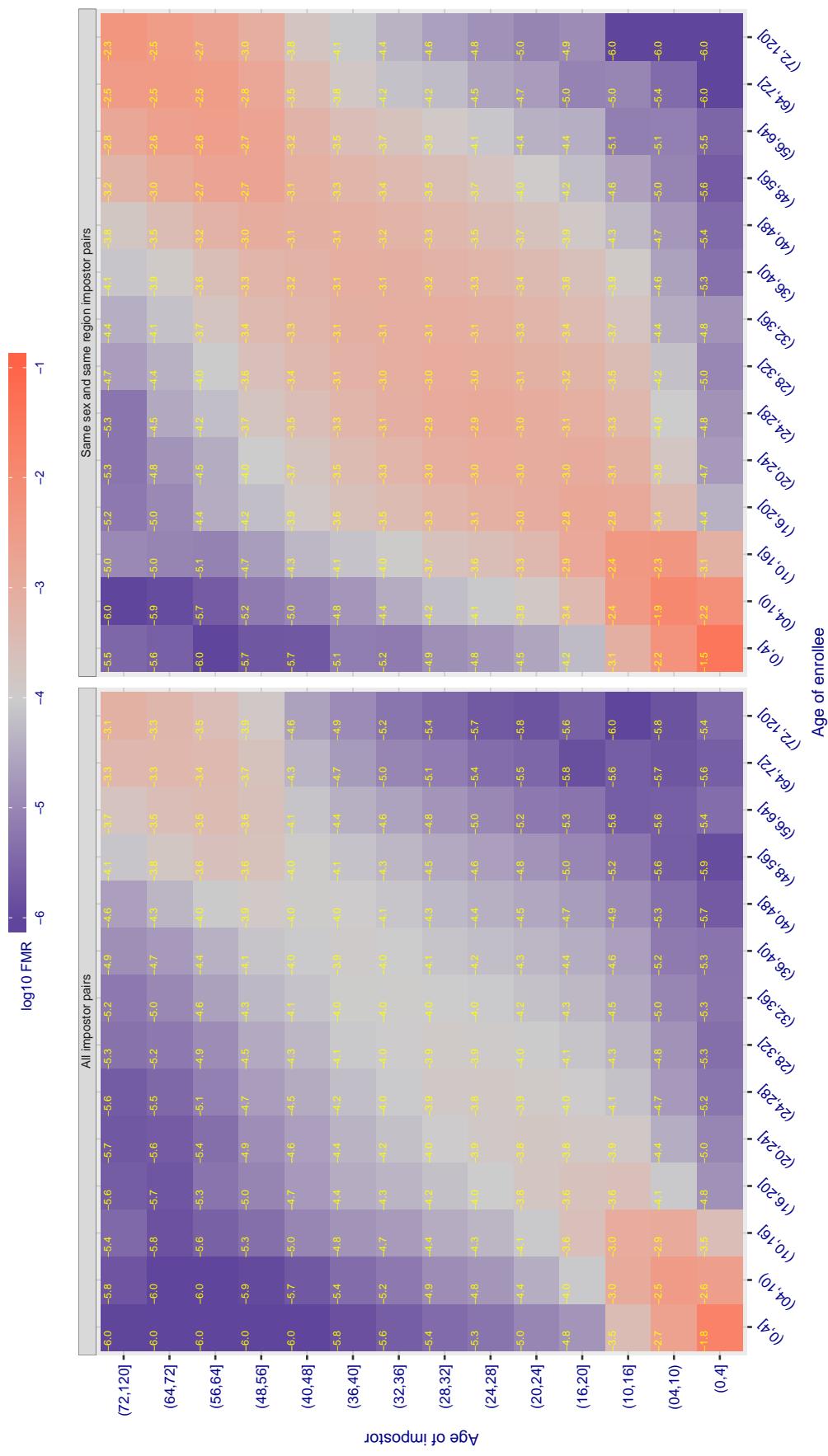
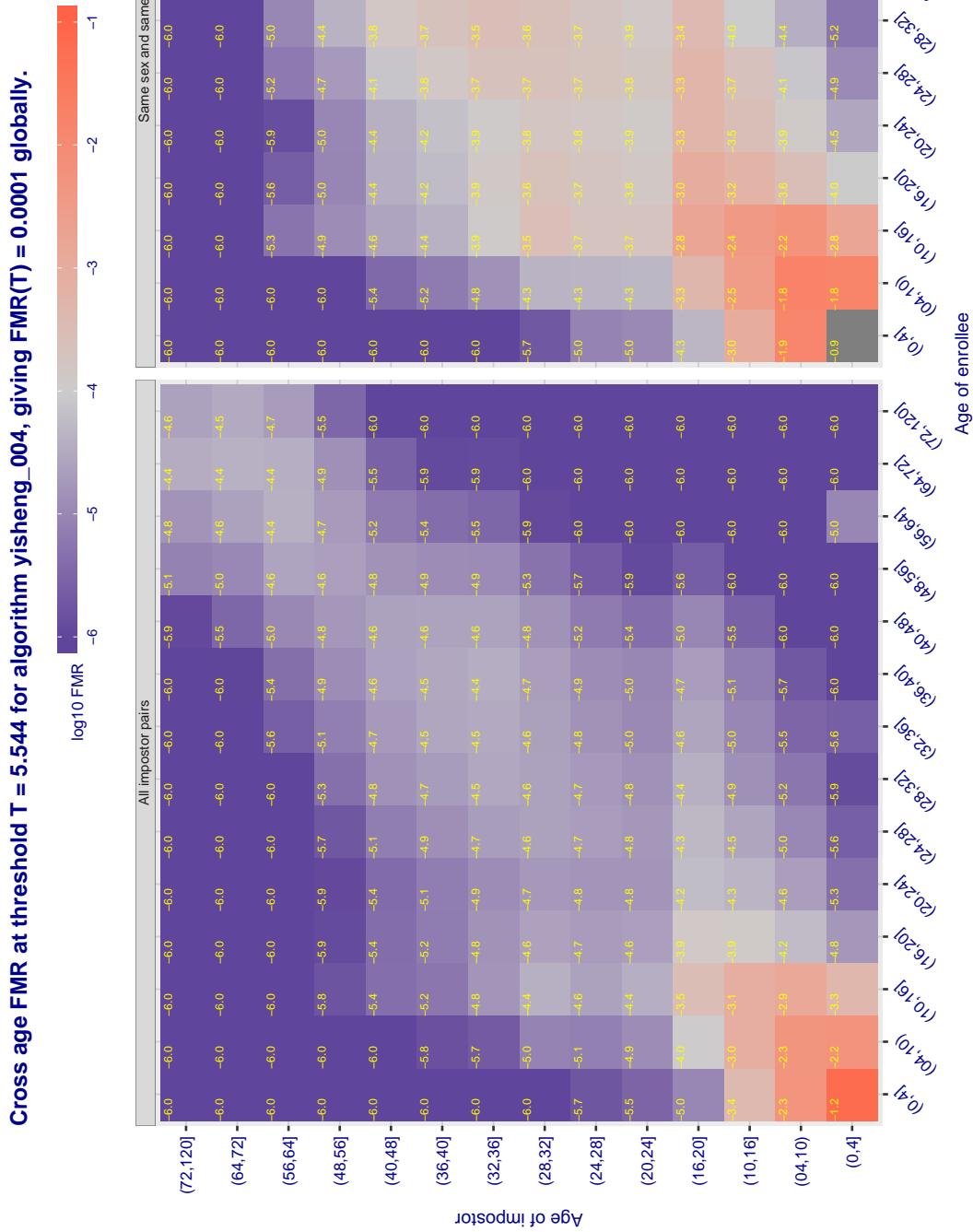


Figure 472: For algorithm winsense\_000 operating on visa images, the heatmap shows false match observed over impostor comparisons of faces from different individuals who have the given age pair. False matches are counted against a recognition threshold fixed globally to give FMR = 0.001 over all on the order of  $10^{10}$  impostor comparisons. The text in each box gives the same quantity as that coded by the color. Light colors present a security vulnerability to, for example, a passport gate.



**Figure 473:** For algorithm *yisheng-004* operating on visa images, the heatmap shows false match observed over impostor comparisons of faces from different individuals who have the given age pair. False matches are counted against a recognition threshold fixed globally to give  $FMR = 0.001$  over all on the order of  $10^{10}$  impostor comparisons. The text in each box gives the same quantity as that coded by the color. Light colors present a security vulnerability to, for example, a passport gate.

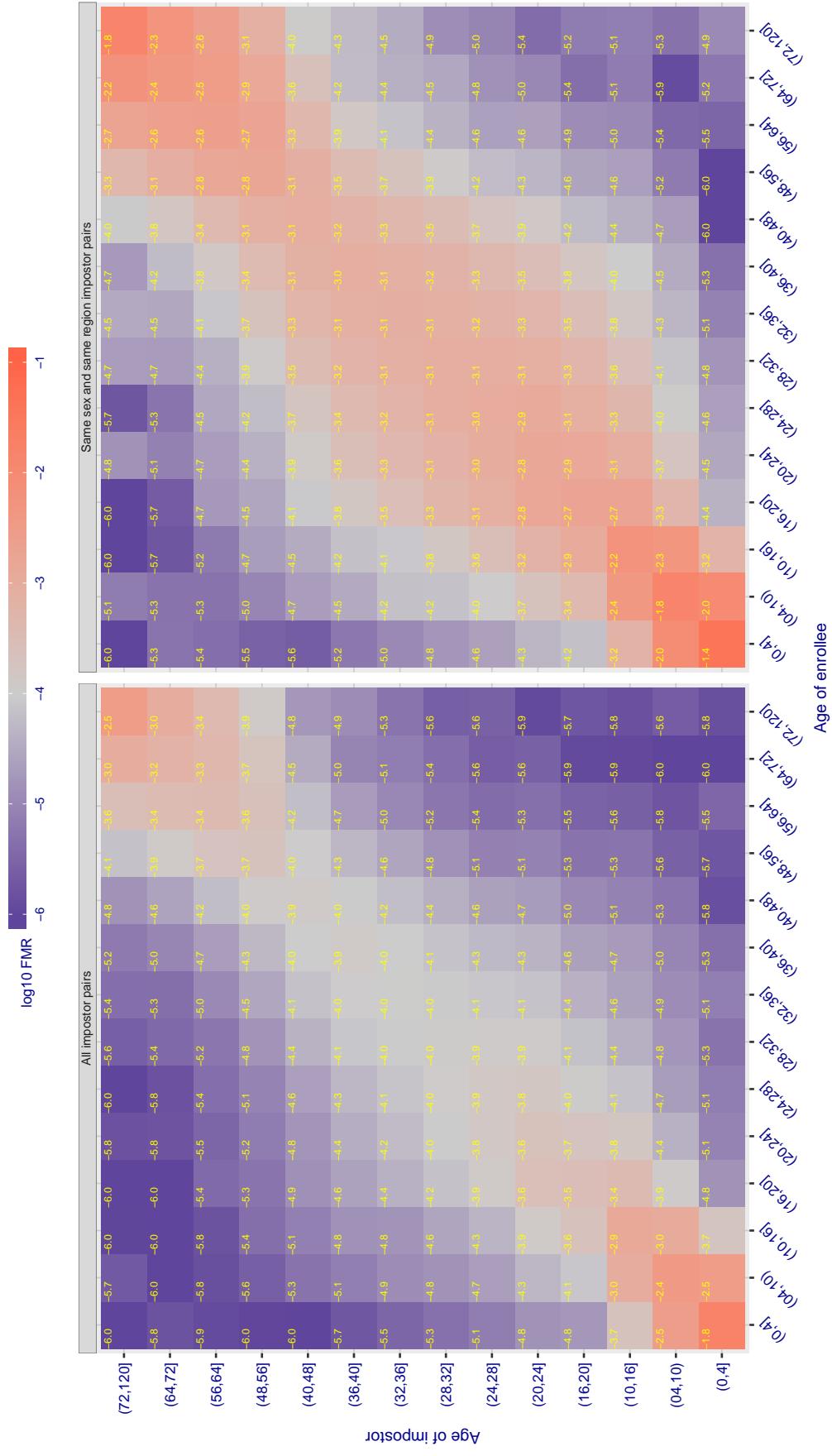
Cross age FMR at threshold T = 37.698 for algorithm yitu\_003, giving  $\text{FMR}(\text{T}) = 0.0001$  globally.

Figure 474: For algorithm yitu-003 operating on visa images, the heatmap shows false match observed over impostor comparisons of faces from different individuals who have the given age pair. False matches are counted against a recognition threshold fixed globally to give  $\text{FMR} = 0.001$  over all on the order of  $10^{10}$  impostor comparisons. The text in each box gives the same quantity as that coded by the color. Light colors present a security vulnerability to, for example, a passport gate.

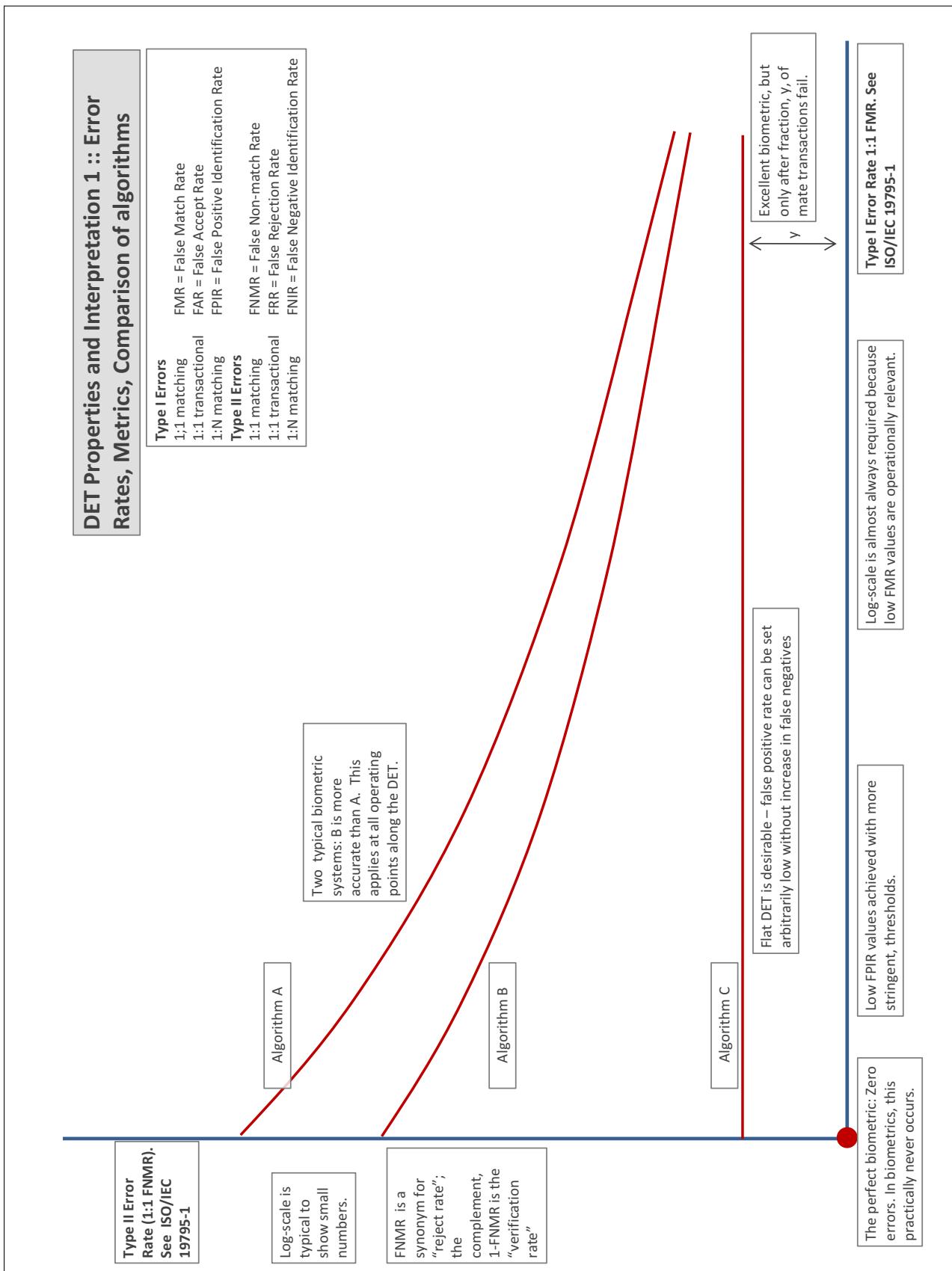
# Accuracy Terms + Definitions

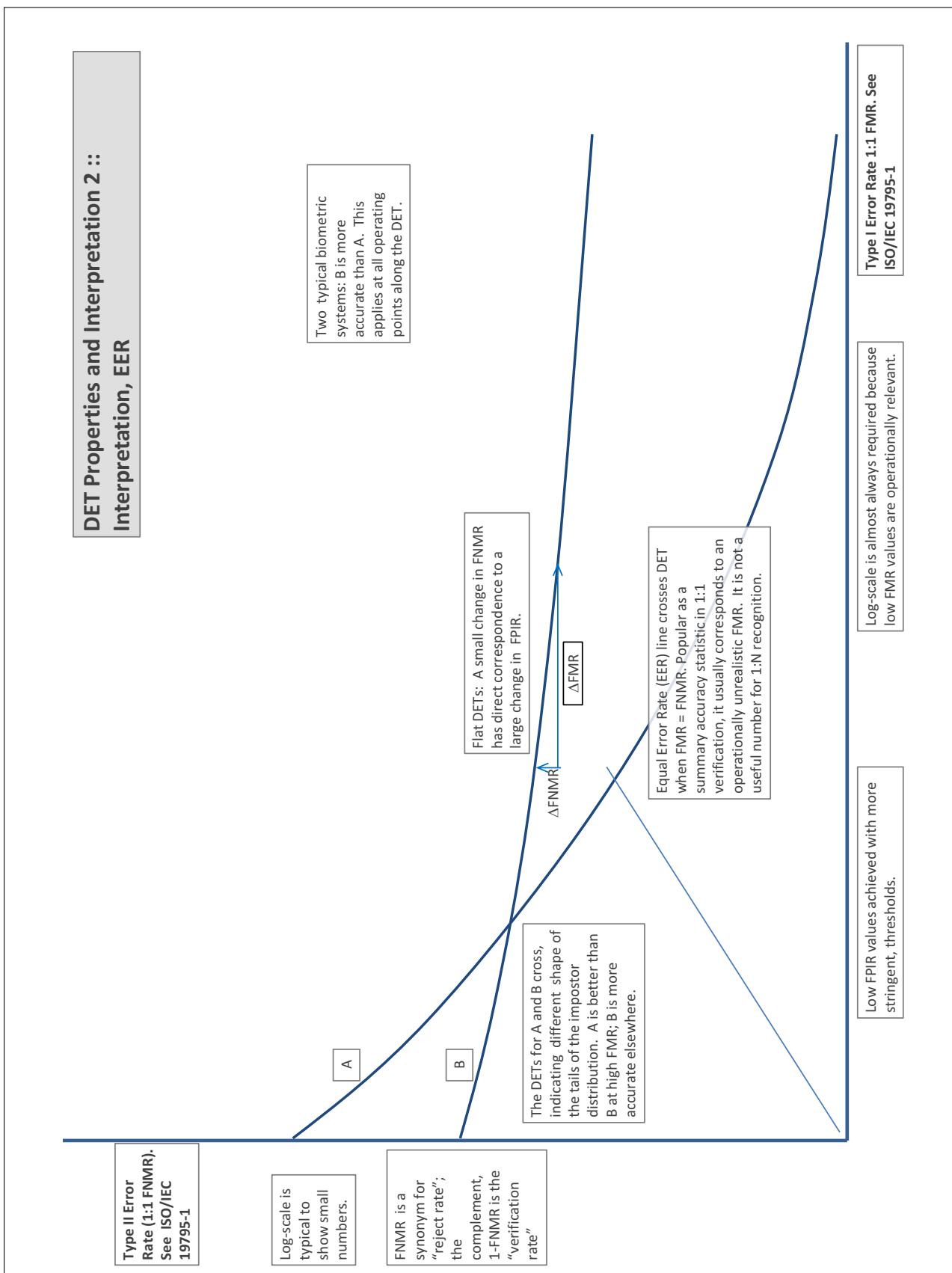
In biometrics, Type II errors occur when two samples of one person do not match – this is called a **false negative**. Correspondingly, Type I errors occur when samples from two persons do match – this is called a **false positive**. Matches are declared by a biometric system when the native comparison score from the recognition algorithm meets some **threshold**. Comparison scores can be either **similarity scores**, in which case higher values indicate that the samples are more likely to come from the same person, or **dissimilarity scores**, in which case higher values indicate different people. Similarity scores are traditionally computed by **fingerprint** and **face** recognition algorithms, while dissimilarities are used in **iris recognition**. In some cases, the dissimilarity score is a distance; this applies only when **metric** properties are obeyed. In any case, scores can be either **mate** scores, coming from a comparison of one person's samples, or **nonmate** scores, coming from comparison of different persons' samples. The words **genuine** or **authentic** are synonyms for mate, and the word **impostor** is used as a synonym for nonmatch. The words mate and nonmatch are traditionally used in identification applications (such as law enforcement search, or background checks) while genuine and impostor are used in verification applications (such as access control).

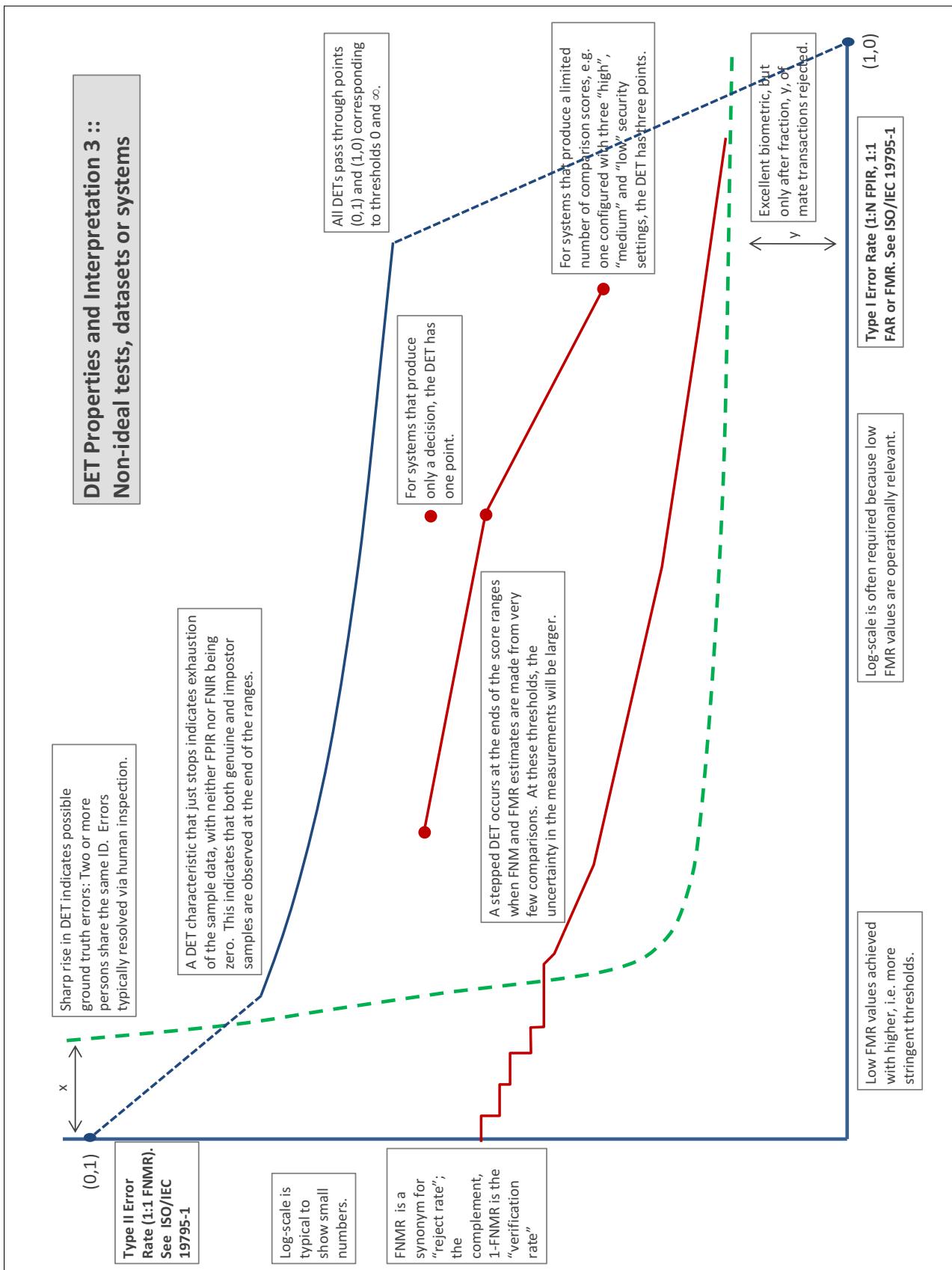
A **error tradeoff** characteristic represents the tradeoff between Type II and Type I classification errors. For verification this plots false non-match rate (FNMR) vs. false match rate (FMR) parametrically with T.

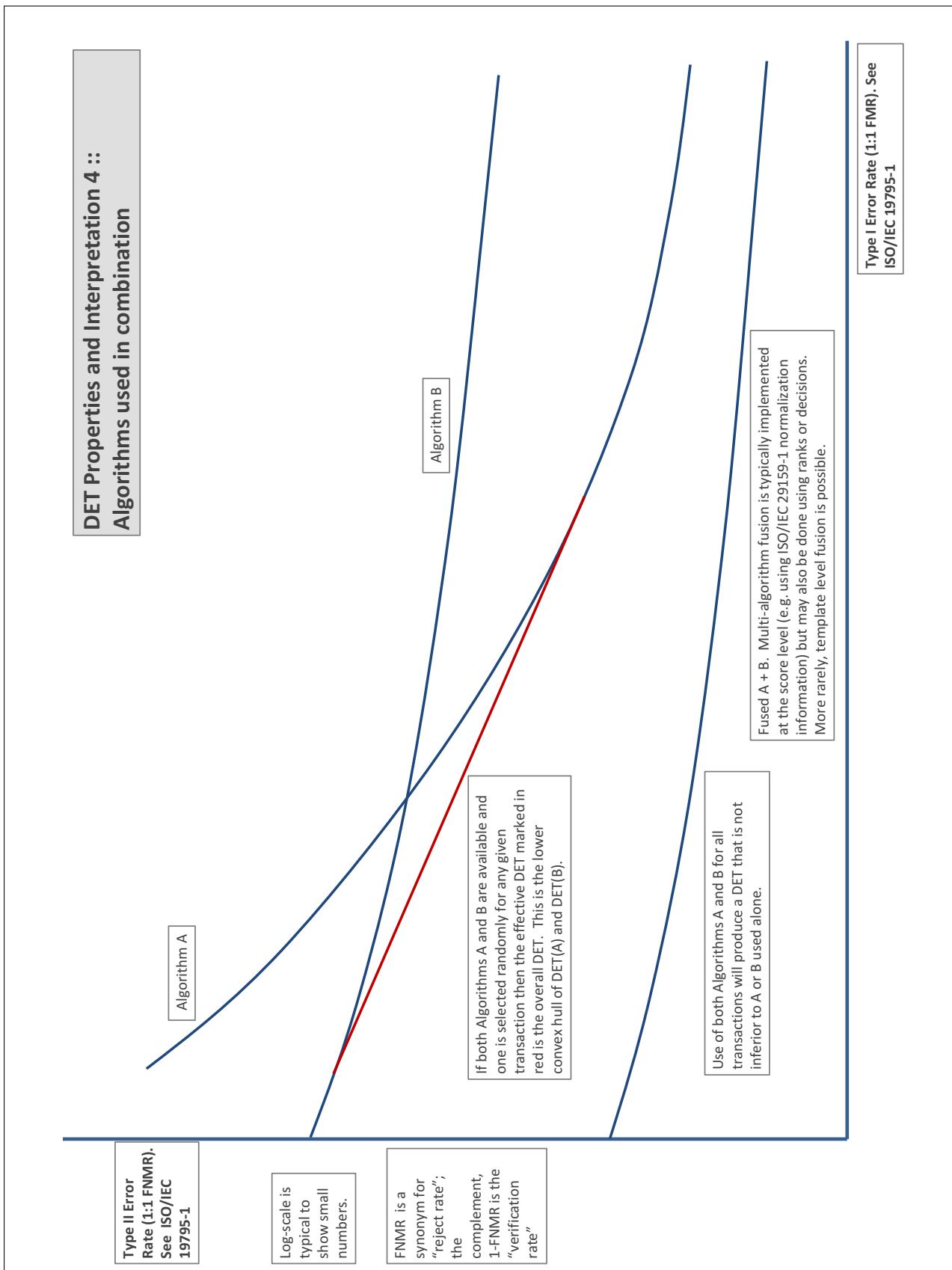
The error tradeoff plots are often called **detection error tradeoff (DET)** characteristics or **receiver operating characteristic (ROC)**. These serve the same function but differ, for example, in plotting the complement of an error rate (e.g.,  $TMR = 1 - FNMR$ ) and in transforming the axes most commonly using logarithms, to show multiple decades of FMR. More rarely, the function might be the inverse Gaussian function.

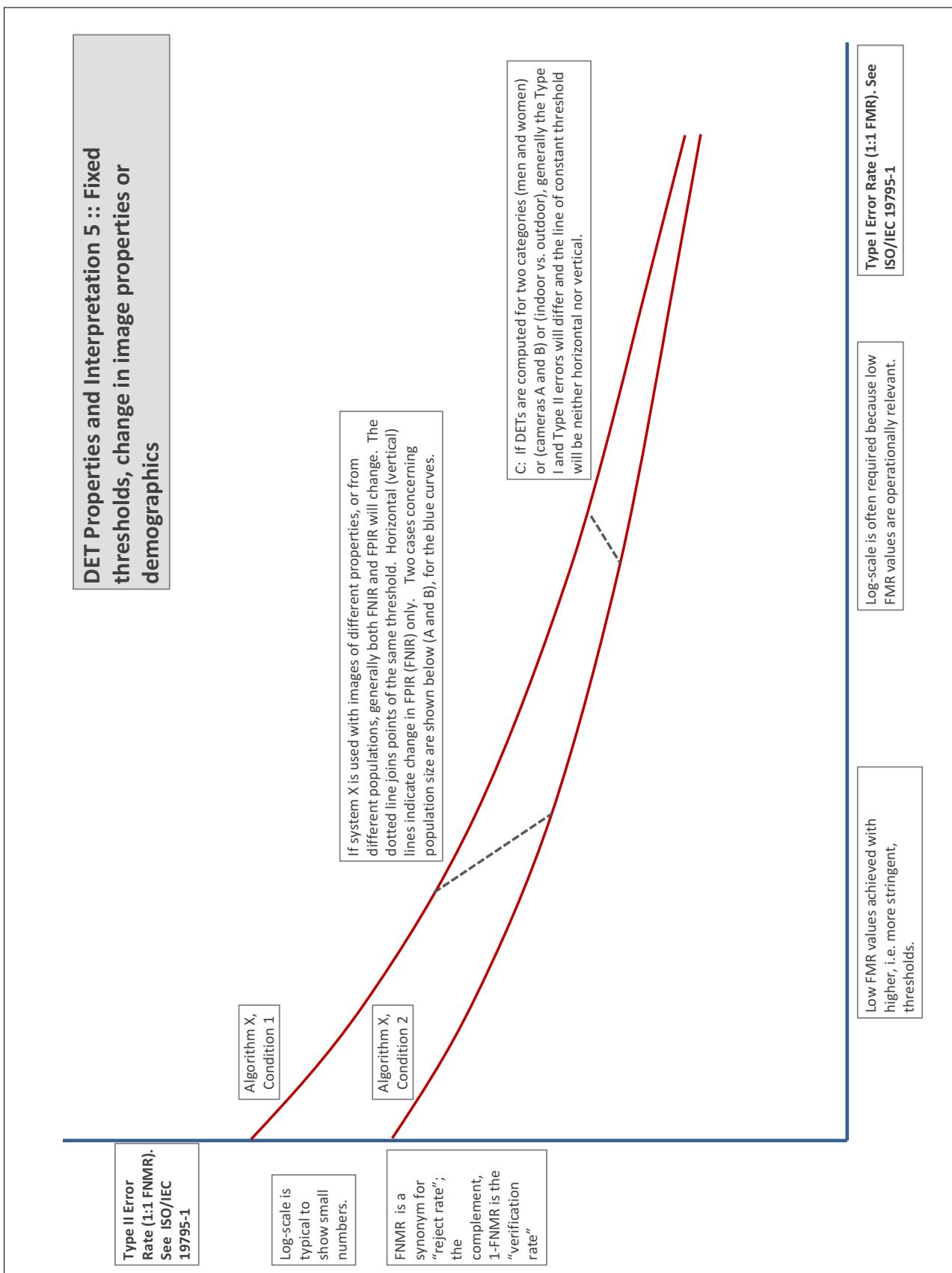
More detail and generality is provided in formal biometrics testing standards, see the various parts of [ISO/IEC 19795 Biometrics Testing and Reporting](#). More terms, including and beyond those to do with accuracy, see [ISO/IEC 2382-37 Information technology -- Vocabulary -- Part 37: Harmonized biometric vocabulary](#)











## References

- [1] P. Jonathon Phillips, Amy N. Yates, Ying Hu, Carina A. Hahn, Eilidh Noyes, Kelsey Jackson, Jacqueline G. Cavazos, Géraldine Jeckeln, Rajeev Ranjan, Swami Sankaranarayanan, Jun-Cheng Chen, Carlos D. Castillo, Rama Chellappa, David White, and Alice J. O'Toole. Face recognition accuracy of forensic examiners, superrecognizers, and face recognition algorithms. *Proceedings of the National Academy of Sciences*, 115(24):6171–6176, 2018.